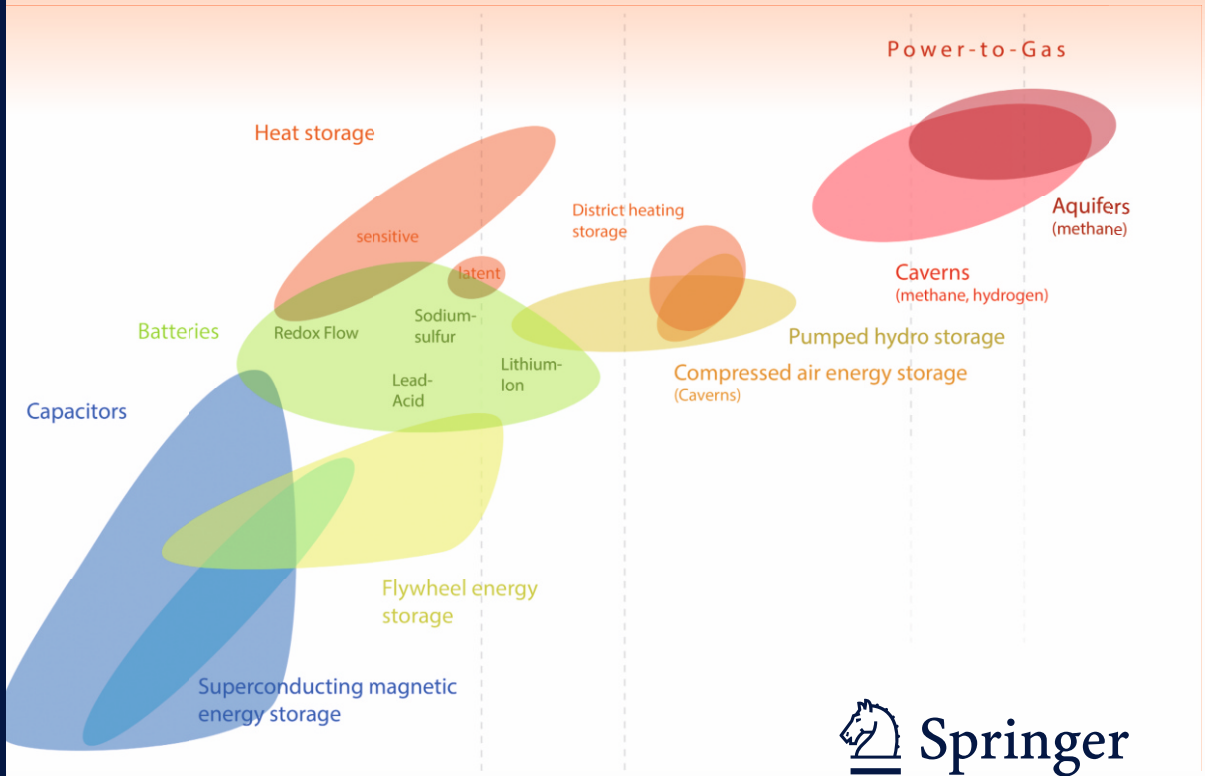
Michael Sterner · Ingo Stadler *Editors*

# Handbook of Energy Storage

## Demand, Technologies, Integration




Springer

Handbook of Energy Storage

Michael Sterner
Ingo Stadler
*Editors*

# Handbook of Energy Storage

Demand, Technologies, Integration

Translation of 2nd German edition Sterner, „Stadler Energiespeicher – Bedarf, Technologien, Integration“

Springer

*Editors*

**Michael Sterner**
University Regensburg
Regensburg, Germany

**Ingo Stadler**
TH Köln
Köln, Germany

Additional material to this book can be downloaded from
https://doi.org/10.1007/978-3-662-55504-0.

ISBN 978-3-662-55503-3 ISBN 978-3-662-55504-0 (eBook)
https://doi.org/10.1007/978-3-662-55504-0

© Springer-Verlag GmbH Germany, part of Springer Nature 2019
This work is subject to copyright. All rights are reserved by the Publisher, whether the whole or part of the material is concerned, specifically the rights of translation, reprinting, reuse of illustrations, recitation, broadcasting, reproduction on microfilms or in any other physical way, and transmission or information storage and retrieval, electronic adaptation, computer software, or by similar or dissimilar methodology now known or hereafter developed.
The use of general descriptive names, registered names, trademarks, service marks, etc. in this publication does not imply, even in the absence of a specific statement, that such names are exempt from the relevant protective laws and regulations and therefore free for general use.
The publisher, the authors and the editors are safe to assume that the advice and information in this book are believed to be true and accurate at the date of publication. Neither the publisher nor the authors or the editors give a warranty, express or implied, with respect to the material contained herein or for any errors or omissions that may have been made. The publisher remains neutral with regard to jurisdictional claims in published maps and institutional affiliations.

This Springer imprint is published by the registered company Springer-Verlag GmbH, DE part of Springer Nature.
The registered company address is: Heidelberger Platz 3, 14197 Berlin, Germany

This work is dedicated to our children and all the children of the world,
in the hope that they will be the first to live in a post-fossil fuel era.

# Preface to the English Edition

We are close to achieving clean, sustainable energy on a truly global scale. Wind and solar power have become the world's most affordable energy sources and have the potential to more than meet the energy demands of the planet, not just today but also in 2050 when the population is expected to reach 10 billion. But wind and solar are just two of the components of the transformation of our energy system. We also need infrastructure for flexible energy production and consumption, from high-voltage power lines to various forms of energy storage for power, gas, heating, and fuels. The good news is that the technology needed for a global clean-energy transition already exists. From wind, sun, water, air, and $CO_2$, today we can produce fertilizers, plastics, bulk chemicals, and fuels via Power-to-X (PtX).

Many have balked at the high costs of energy storage, but these critics fail to see the bigger picture. Locally generated energy can eliminate the need for billions of euros worth of fossil-fuel exports, and the unspent money can be invested in domestic renewable energy, in power-grid infrastructure, and in storage capacity, creating a well-developed and profitable clean energy business model. All we need now is the right kind of energy policies to promote it.

The Fridays for Future Movement is the most important youth movement since the 1960s. It is pushing the climate and energy transition topics to the top of the agenda. So they accomplish what we as Scientists for Future have tried for decades. And they add the necessary dimension because they have to experience and pay for the climate catastrophes that we have caused so far: they do not ask about technical feasibility or costs, they are demanding a planet from the older generation on which they can still live and survive. They ask for climate justice – and to act – right now!

Leading decision makers in every country must come to understand the importance of long-term planning beyond the immediate concerns of quarterly reports and legislative periods. In an age of alternative facts and fake news, this book is designed to provide a sound basis for rational policy discussions. For two things are crystal clear. First, there is no reason why we cannot meet the Paris climate target using current technology without resorting to experiments in geoengineering and CCS. Second, renewables and energy storage can break our dependence on fossil fuels and more fairly distribute labor and wealth creation in the energy sector. Of this, we have no doubt.

We were delighted by the positive response to the first edition of this book. Many individuals—from the industrial sector, the business world, politics, and society in general—have written to express their gratitude for a book that was timely, in-depth, and easy to understand. Now, thanks to this English language edition, we are pleased to bring our work to a much larger audience.

This would not have been possible without the expert translation provided by Lucais Sewell and Loren Marsh at WordSolid, to whom we are much indebted. The same goes for Gordon Taylor at Energy Policy UK who assisted us with many of the finer points.

We would also like to extend a heartfelt thanks to all the co-authors named in the chapters and the following students who worked tirelessly on both editions: Andreas Hofrichter, Andreas Lösing, Benjamin Lehmann, Bettina Vogl, Eric Dürselen, Florian Hüllen, Frank Strümpler, Henning Voss, Jens Fiedler, Leif Henning Möllmann, Lutz von Pidoll, Matthias Buchner, Moritz Falkenstein, Nicole Muggenthaler, Peter Gurka, Sebastian Zajac, Stefan Freundorfer, Thomas Estermann, Tristan Heiden. For their proofreading, Alexander Krajete, Bernd Stürmer, Robert Leinfelder, Wolfgang Köppel, and Ralf Steudel merit appreciative mention as well.

At Springer, Eva Hestermann-Beyerle, Birgit Kollmar-Thoni, Daniel Fröhlich, and Kenneth Quinn provided regular encouragement and marvelous editing. We also owe a great deal of thanks to all of our partners for lending us graphic materials and expertise, and for covering the translation costs.

Finally, and most importantly, we would like to thank our wives, Anne and Chrissi, whose unstinting support at home made this book better, as well as our children, Amalia, Clara, Elias, Enya, and Kira, whose future, like that of all of the world's children, we hope to make less uncertain with the ideas and knowledge provided in this book.

**Michael Sterner**
**Ingo Stadler**
Regensburg, Cologne; Germany, Europe, Planet Earth
Summer 2019

# List of Contributors


- **Franz Bauer (FENES OTH Regensburg)**

▶ Sects. 2.1, 2.2, 2.3, 2.4
▶ Sect. 8.1
▶ Sect. 9.3

- **Dr. Christopher Breuer (Westnetz GmbH)**

▶ Sect. 3.5

- **Dr. Marcus Budt (Fraunhofer UMSICHT)**

▶ Sect. 9.1

- **Dr. Eduardo Cattaneo (Hoppecke Batterien)**

▶ Sect. 7.6

- **Fritz Crotogino (KBB Underground Technology)**

▶ Sect. 8.4

- **Tim Drees (IAEW RWTH Aachen)**

▶ Sect. 3.5

- **Fabian Eckert (FENES OTH Regensburg)**

▶ Sects. 3.2, 3.3, 3.6, 3.7
▶ Sects. 4.2, 4.3, 4.6, 4.7
▶ Sects. 5.3, 5.5, 5.6
▶ Sects. 8.1, 8.3, 8.4, 8.5, 8.6, 4.7
▶ Sects. 11.4, 11.5, 11.6
▶ Sects. 13.1, 13.2, 13.3
▶ Sects. 14.1, 14.2, 14.3

- **Norman Gerhardt (Fraunhofer IWES)**

▶ Sects. 4.6, 4.7
▶ Sect. 14.1

- **Dr. Andreas Hauer (ZAE Bayern)**

▶ Sects. 10.1, 10.2, 10.3, 10.4, 10.5, 10.6, 10.7

- **Prof. Dr. Hans-Martin Henning (Fraunhofer ISE)**

▶ Sects. 4.5, 4.6, 4.7
▶ Sect. 5.5

- **Dr. Matthias Herrmann (Hoppecke Batterien)**

▶ Sect. 7.4

- **Dr. Götz Langer (Hoppecke Batterien)**

▶ Sect. 7.2

■ **Christian von Olshausen (sunfire GmbH)**
► Sects. 8.1, 8.6, 8.7
► Sect. 14.2

■ **Dr. Detlef Ohms (Hoppecke Batterien)**
► Sects. 7.1, 7.3

■ **Andreas Palzer (Fraunhofer ISE)**
► Sect. 4.5

■ **Dr. Bernhard Riegel (Hoppecke Batterien)**
► Sect. 7.6

■ **Dr. Niklas Rotering (Rotering Energy)**
► Sect. 3.4

■ **Prof. Dr. Ingo Stadler (CIRE TH Köln)**
► Sects. 6.1, 6.2, 6.3
► Sects. 7.5, 7.6
► Sects. 9.2, 9.3, 9.4
► Sects. 10.1, 10.2, 10.3, 10.4, 10.5, 10.6, 10.7
► Sects. 11.1, 11.2, 11.3, 11.4
► Sect. 13.1
► Sect. 14.1

■ **Prof. Dr.-Ing. Michael Sterner (FENES OTH Regensburg)**
► Sects. 1.1, 1.2, 1.3, 1.4
► Sects. 2.1, 2.2, 2.3, 2.4
► Sects. 3.1, 3.2, 3.3, 3.4, 3.5, 3.6, 3.7
► Sects. 4.1, 4.2, 4.3, 4.4, 4.5, 4.6
► Sects. 5.1, 5.2, 5.3, 5.4, 5.5, 5.6
► Sects. 8.1, 8.2, 8.3, 8.4, 8.5, 8.6, 8.7, 8.8, 8.9, 8.10
► Sects. 12.1, 12.2, 12.3, 12.4, 12.5, 12.6
► Sects. 13.1, 13.2, 13.3, 13.4
► Sects. 14.1, 14.2, 14.3

■ **Martin Thema (FENES OTH Regensburg)**
► Sects. 3.6, 3.7
► Sects. 8.2, 8.3, 8.4, 8.5, 8.6
► Sects. 12.1, 12.2, 12.3, 12.4
► Sect. 13.1
► Sects. 14.2, 14.3

■ **Tobias Trost (Fraunhofer IWES)**
► Sects. 5.2, 5.4
► Sect. 14.2

■ **Dr. Daniel Wolf (Home Power Solution GmbH)**
► Sect. 9.1
Figures: Franz Bauer, Martin Thema

# Contents


## I Meaning and Classification of Storage in the Energy Supply

1 **Energy Storage Through the Ages** ... 3
*Michael Sterner*
1.1 **100% Renewable Energy Before the Industrial Revolution** ... 4
1.1.1 Photosynthesis—Nature's Primary Way of Storing Energy ... 4
1.1.2 Wood, Peat, and Energy Crops—Using Stored Solar Energy ... 9
1.2 **Fossil Energy in the Fossil Age** ... 13
1.2.1 The Formation of Fossil Energy ... 13
1.2.2 Use and Emissions of Fossil Energy: Status Quo ... 15
1.3 **Transitioning to an Age of Renewables** ... 17
1.3.1 Climate Change and Resource Scarcity—the Drivers of a Global Energy Revolution ... 17
1.3.2 The Age of Renewable Energy is Only a Question of Time—Scenarios for Change ... 19
1.4 **Summary** ... 21
References ... 22

2 **Definition and Classification of Energy Storage Systems** ... 23
*Michael Sterner and Franz Bauer*
2.1 **Definition and Application** ... 24
2.2 **The Use of Storage Systems** ... 30
2.3 **Classification of Storage Systems** ... 33
2.3.1 Classification by Physical Energy Form ... 33
2.3.2 Calculation of Relevant Parameters ... 36
2.3.3 Temporal Classification ... 42
2.3.4 Spatial Classification ... 44
2.3.5 Economic Classification ... 45
2.4 **Summary** ... 46
References ... 47

## II Demand of Energy Storage

3 **Storage Demand in Power Supply** ... 51
*Michael Sterner, Christopher Breuer, Tim Drees, Fabian Eckert, Andreas Maaz, Carsten Pape, Niklas Rotering, and Martin Thema*
3.1 **Storage Demand and Surplus—Parameters and Definitions** ... 53
3.1.1 General Influence on the Storage Demand ... 53
3.1.2 Definition: Storage Demand ... 54
3.1.3 Distinction of Electricity Surplus with Respect to Markets and Networks ... 55
3.2 **Long-Term Scenarios of the Federal Environment Ministry** ... 56
3.2.1 Development of Primary, Final, and Usable Energy Demand ... 57
3.2.2 Development of the Electricity Mix ... 59

3.2.3 Effect of Minimum Generation and Import/Exporton the Storage Demand ..... 62
3.2.4 Effect of DSM on the Storage Demand ..... 64
3.2.5 Storage Deployment at 40%, 63%, and 85% Renewable Energies ..... 65
3.2.6 Abstract ..... 68
3.3 **"100% Renewable Electricity Supply," According to the Federal Environment Agency** ..... 69
3.3.1 Estimates on Power Consumption in 2050 ..... 69
3.3.2 Technical-Ecological Potential of Renewable Energies, Storage, and DSM ..... 71
3.3.3 Assumptions and Modeling of the 2050 Scenario ..... 75
3.3.4 Results for Storage Demand and Security of Supply ..... 78
3.3.5 Abstract ..... 86
3.4 **VDE-ETG Study on Market-Based Storage Demand** ..... 86
3.4.1 Methodology ..... 87
3.4.2 Assumptions for Modeling and Data Input ..... 89
3.4.3 Cross-Scenario Findings ..... 91
3.4.4 Findings of the 40% Scenario ..... 93
3.4.5 Findings of the 80% Scenario ..... 94
3.4.6 Findings of the 100% Scenario ..... 96
3.4.7 Summary ..... 97
3.5 **'Storage Roadmap' Study on Germany's Storage Requirements in the European Context** ..... 98
3.5.1 Methodological Approach ..... 98
3.5.2 Scenario ..... 100
3.5.3 Medium-Term Storage Simulation ..... 105
3.5.4 Long-Term Storage Simulation ..... 107
3.5.5 Significant Findings/Conclusions ..... 109
3.6 **Study of Network-Based Storage Requirements** ..... 110
3.6.1 Methodological Approach to Distinguishing Market and Network-Based Storage Requirements ..... 110
3.6.2 Case Study: PtG in Germany in 2022 with Delayed Network Expansion ..... 110
3.6.3 Minimal Storage Requirements in the European Network ..... 113
3.6.4 Summary ..... 114
3.7 **Comparison and Categorization of the Results** ..... 115
3.7.1 Comparison of the Results of the Three Studies ..... 115
3.7.2 Categorization of the Results in Comparison to Other Studies ..... 115
3.8 **Summary** ..... 132
References ..... 135

4 **Heating Supply Storage Requirements** ..... 137
*Michael Sterner, Fabian Eckert, Norman Gerhardt, Hans-Martin Henning, and Andreas Palzer*
4.1 **Basis and Objectives** ..... 139
4.2 **Development of Heating Requirements** ..... 139
4.3 **Development of the Heating Mix** ..... 140
4.3.1 Fossil Heating Supply ..... 140
4.3.2 Renewable Heating Supply ..... 141
4.4 **The Heating Sector Transition** ..... 142

4.4.1 Households ... 142
4.4.2 TIS ... 144
4.4.3 Manufacturing ... 145
4.5 **The Heating Sector Paradigm Shift** ... 146
4.5.1 An Example Transition: Crude Oil, Natural Gas,and Renewable Energy ... 146
4.5.2 Electricity as Primary Energy ... 146
4.6 **Storage Requirements in a Climate Goal Scenariofor the German Energy System in 2050** ... 147
4.6.1 Scenario Framework, Model, and Assumptions ... 147
4.6.2 Results for Storage Use in the Heating Area ... 148
4.7 **Surpluses, Storage Requirements,and Storage Potential** ... 151
4.7.1 Heating Sector Surpluses ... 151
4.7.2 Development of Storage Requirements ... 153
4.7.3 Storage Potential ... 155
4.8 **Summary** ... 160
References ... 162

5 **Storage Demand in the Transport and Chemical Sector** ... 165
*Michael Sterner, Fabian Eckert, Hans-Martin Henning, and Tobias Trost*
5.1 **Basics and Objectives in the Transport Sector** ... 167
5.1.1 Initial Situation and Developments in the Last Decades ... 167
5.1.2 Objectives in the Transport Sector ... 167
5.2 **Development of Mobility Needs** ... 169
5.2.1 Population Development ... 169
5.2.2 Development of Economic Performance ... 169
5.2.3 Spread of the Development of Mobility Needs for Passengerand Freight Traffic ... 169
5.3 **Development of Energy and Fuel Supply** ... 169
5.3.1 Developments in Passenger Traffic ... 171
5.3.2 Developments in Freight Traffic ... 172
5.3.3 Development of the Energy Mix in the Transport Sector ... 172
5.4 **Paradigm Change in the Transport Sector** ... 175
5.4.1 Electrification of Mobility via Batteries and Synthetic Fuels ... 175
5.4.2 Integration of Renewable Energiesas the Cornerstone of Mobility ... 178
5.5 **Storage Demands in the Transport Sector** ... 178
5.5.1 Storage Demand Today ... 178
5.5.2 Storage Demand in a Transport Sector Suppliedby 50% Renewable Energies ... 179
5.5.3 Storage Demand in the Study of the Fraunhofer ISE ... 181
5.5.4 Storage Study for the Agora Energy Transition ... 181
5.6 **Storage Demand in the Chemical Industry** ... 183
5.6.1 Resource Consumption Today and in 2050 ... 184
5.6.2 Necessary PtX Capacities for the Chemical Industry ... 184
5.7 **Summary** ... 185
References ... 187

# III Technologies for Energy Storage


6 **Electrical Energy Storage** ... 191
*Ingo Stadler*
6.1 **Capacitors—Supercaps** ... 192
6.1.1 Fundamental Features of a Capacitor ... 192
6.1.2 From Capacitor to Double-Layer Capacitor ... 195
6.1.3 Charging and Discharging ... 199
6.1.4 Losses, Efficiency, and Other Characteristic Values ... 205
6.1.5 Service Life ... 209
6.1.6 Applications ... 212
6.2 **Superconducting Electromagnetic-Energy Storage Systems** ... 214
6.2.1 Principles of Superconduction ... 214
6.2.2 Superconducting Electromagnetic Energy Storage (SMES) System ... 216
6.3 **Summary** ... 224
References ... 224

7 **Electrochemical Energy Storage Systems** ... 227
*Ingo Stadler, Bernhard Riegel, Detlef Ohms, Eduardo Cattaneo, Götz Langer, and Matthias Herrmann*
7.1 **Basic Principles** ... 230
7.1.1 Basic Physical Principles ... 230
7.1.2 Electrode Potential ... 232
7.1.3 Electrode Equilibrium ... 233
7.1.4 Nernst Equation ... 234
7.1.5 Electrochemical Reactions on Electrodes ... 235
7.1.6 Electrochemical Cells and Cell Reactions ... 235
7.1.7 Electrode and Cell Polarization ... 237
7.1.8 Side-Reactions ... 239
7.1.9 Energy and Efficiency ... 239
7.1.10 Types of Electrochemical-Energy Storage and Converters ... 240
7.1.11 Electrolyte ... 241
7.1.12 Cell Designs ... 242
7.1.13 Energy Storage Parameters ... 242
7.2 **Lead-Acid Batteries** ... 245
7.2.1 Design ... 245
7.2.2 Basic Reactions, Equilibrium, and Cell Voltage ... 247
7.2.3 Mole Balance and Storage Capacity ... 247
7.2.4 Discharging Characteristics ... 249
7.2.5 Side-Reactions ... 251
7.2.6 Charging Lead Batteries ... 255
7.2.7 Sealed Lead Batteries ... 257
7.2.8 Aging Mechanisms ... 259
7.2.9 Conclusion ... 260
7.3 **Nickel Batteries** ... 262
7.3.1 Conclusion ... 263
7.3.2 Nickel-Cadmium Batteries ... 263

7.3.3 Nickel Metal Hydride Batteries ... 277
7.3.4 Conclusion ... 279
7.4 **Lithium Batteries** ... 280
7.4.1 Operating Principle, Chemical Reactions, and Active Materials ... 281
7.4.2 Cell Voltage ... 283
7.4.3 Conclusion ... 286
7.4.4 Electrolyte and Electrochemical Stability Window ... 286
7.4.5 Other Cell Components ... 289
7.4.6 Conclusion ... 290
7.4.7 Electrode Material Conductivity ... 291
7.4.8 Conclusion ... 293
7.4.9 Designs and Application Areas ... 293
7.4.10 Operating Method and Typical Performance Characteristics ... 297
7.4.11 Conclusion ... 302
7.4.12 Outlook ... 302
7.5 **Sodium-Sulfur Batteries** ... 303
7.5.1 The Electrodes ... 303
7.5.2 The Electrolyte/Separator ... 304
7.5.3 The Heating System ... 305
7.5.4 Forms and Module Sizes ... 307
7.5.5 Charging and Discharging Process ... 308
7.5.6 Cycles, Capacities, and Service Life ... 311
7.5.7 Efficiency, Power, and Energy ... 311
7.5.8 Hazards and Safety ... 313
7.5.9 Conclusion ... 313
7.6 **Redox Flow Batteries** ... 314
7.6.1 Redox Flow Cell Design and Operation ... 314
7.6.2 Possible Material Pairings ... 318
7.6.3 Charging and Discharging Strategies ... 319
7.6.4 Energy Density, Power Density, and Efficiency ... 320
7.6.5 The Redox Flow Battery in Comparison ... 321
7.6.6 Service Life and Mechanisms that Shorten Service Life ... 322
7.6.7 Redox Flow Battery Application Areas ... 322
7.6.8 Recycling, Environmental Friendliness, and Safety ... 323
7.6.9 Conclusion ... 323
References ... 323

8 **Chemical Energy Storage** ... 325
*Michael Sterner, Franz Bauer, Fritz Crotogino, Fabian Eckert, Christian von Olshausen, Daniel Teichmann, and Martin Thema*
8.1 **Basics** ... 327
8.1.1 The C–H–O System as a Foundation for Energy Storage ... 327
8.1.2 Hydrogen as Energy Source ... 329
8.1.3 Hydrogen Production ... 333
8.1.4 Thermodynamics of Water Splitting ... 340
8.1.5 Electrolytic Conductivity ... 346
8.2 **Storing Technology Electrolysis** ... 352

8.2.1 Overview ... 352
8.2.2 Electrolysis Cell—Electrolysis Type ... 354
8.2.3 Electrolysis Block—Stack Design ... 359
8.2.4 Electrolyzers, Electrolysis Facilities, and Their Peripherals ... 360
8.2.5 Comparison of Different Electrolyte Technologies ... 362
8.2.6 Increasing Efficiency by Using Waste Heat ... 362
8.3 **Storing Technology-Methanationand Chemical Synthesis** ... 369
8.3.1 Overview of Methane as an Energy Source ... 369
8.3.2 $CO_2$ Sources for Power-to-X (PtX) ... 371
8.3.3 Chemical Methanation ... 373
8.3.4 Biological Methanation ... 380
8.3.5 Methanol Synthesis ... 388
8.3.6 FT Process ... 393
8.4 **Storage Media and Holding** ... 400
8.4.1 Gaseous Storage Media ... 400
8.4.2 Liquid Storage Media ... 413
8.4.3 Solid Storage Media ... 422
8.5 **Extraction Technologies** ... 425
8.5.1 Electricity Generation Using CHP Generation ... 426
8.5.2 Building Heating and Cooling Supply ... 433
8.5.3 Mobility and Transport ... 439
8.6 **The Storage System PtG** ... 441
8.6.1 The Beginnings of PtG ... 442
8.6.2 PtG Hydrogen ... 445
8.6.3 PtG Methane ... 447
8.6.4 Efficiency, Potentials, $CO_2$ Emissions, and Costs ... 453
8.6.5 Advantages and Disadvantages of Hydrogen and Methane ... 459
8.7 **The Storage System PtL** ... 461
8.7.1 PtL for Producing Fischer-Tropsch Liquid Fuels ... 463
8.7.2 PtL for Producing Methanol ... 463
8.7.3 Efficiency, Costs, and Early Markets ... 464
8.8 **Ocean Fuels as Further Development of PtG and PtL** ... 465
8.8.1 Raw Materials and Fuels from the Ocean—Issues of Potentialand Acceptance ... 466
8.8.2 Floating Wind Platform Option ... 469
8.8.3 Sail-Powered Energy Option ... 471
8.9 **$CO_2$ Reduction by Energy Systems PtG, PtL,and Ocean Fuels** ... 474
8.10 **Summary** ... 475
References ... 478

9 **Mechanical Energy Storage** ... 483
*Ingo Stadler, Franz Bauer, Marcus Budt, Eduard Heindl, and Daniel Wolf*
9.1 **Gaseous Media** ... 484
9.1.1 Compressed Air Energy Storage Power Plants ... 484
9.1.2 Renewable, Emissions-Free CAS Processes ... 492
9.1.3 Compressed Air Energy Storage Volumes ... 502
9.1.4 Conclusion ... 505
9.2 **Liquid Media** ... 506

9.2.1 Pumped-Storage Plants ... 506
9.2.2 Innovative Concepts for Storing Potential Energyin Liquid Media ... 510
9.3 **Solid Media** ... 533
9.3.1 Flywheel Storage Facilities ... 533
9.3.2 Mechanical Stored Energy Systems ... 546
9.4 **Summary** ... 556
References ... 557

10 **Thermal Energy Storage** ... 563
*Ingo Stadler, Andreas Hauer, and Thomas Bauer*
10.1 **Thermal Storage System Characteristics** ... 565
10.2 **Storage Technologies** ... 567
10.2.1 Sensible-Thermal Storage ... 567
10.2.2 Latent-Thermal Storage ... 568
10.2.3 Thermochemical-Thermal Storage ... 568
10.2.4 Thermophysical Properties and Material Requirements ... 571
10.3 **Thermodynamic Principles** ... 571
10.3.1 Thermal Energy ... 571
10.3.2 Heat Transfer ... 572
10.3.3 Thermal Insulation ... 573
10.4 **Sensible TES** ... 574
10.4.1 Storage Materials ... 574
10.4.2 Storage Systems Using Solid Storage Media ... 576
10.4.3 Storage Systems Using Liquid Storage Media ... 581
10.5 **Latent TES** ... 588
10.5.1 Characterization of Latent-Thermal Storage Materials ... 590
10.5.2 Latent-Thermal Storage Materials ... 591
10.5.3 Heat-Transfer Concepts ... 597
10.5.4 Conclusion ... 600
10.6 **Thermochemical-Energy Storage Systems** ... 601
10.6.1 Storage Materials for Thermochemical Processes ... 602
10.6.2 Designs ... 604
10.6.3 Conclusion ... 606
10.7 **Costs** ... 607
References ... 608

11 **Load Management as an Energy Storage System** ... 611
*Ingo Stadler and Fabian Eckert*
11.1 **Special Characteristics of Demand Response Compared to Other Energy Storage Systems** ... 615
11.2 **Demand Response in Households and Cross-Application Technologies** ... 616
11.2.1 Storage Heaters ... 616
11.2.2 Electric Hot Water Supply ... 618
11.2.3 Electric Cooling ... 620
11.2.4 Heating Circulation Pumps ... 623
11.2.5 Ventilation Facilities ... 624
11.2.6 Washing Machines, Clothes Dryers, and Dishwashers ... 625

11.3 **Industrial Applications of Demand Response** ... 626
11.4 **Summary of German and European Demand Response Potential** ... 630
11.4.1 Demand Response Potential in Germany ... 630
11.4.2 Demand Response Potential in Europe ... 630
11.4.3 Comparison of Various DSM Studies ... 631
11.5 **Developments and Trends** ... 632
11.5.1 Load Shedding Utilization in Industry ... 632
11.5.2 Future Technical and Economic Potential ... 632
11.5.3 Guaranteed Capacity and Renewable Energy Integration ... 633
11.5.4 Potential to Reduce Network Expansion and Annual Peak-Load ... 634
11.6 **Summary** ... 634
References ... 635

12 **Comparison of Storage Systems** ... 637
*Michael Sterner and Martin Thema*
12.1 **Overview of Technical and Economic Parameters** ... 640
12.2 **Application Areas Determined by Storage Capacity and Discharging Duration** ... 640
12.2.1 Electric-Energy Storage Systems—Capacitors and Coils ... 647
12.2.2 Electrochemical-Energy Storage Systems—Batteries ... 647
12.2.3 Mechanical-Energy Storage Systems—Pumped-Storage, CAS, and Flywheel Storage ... 648
12.2.4 Thermal-Energy Storage Systems—Thermal Storage ... 648
12.2.5 Chemical-Energy Storage Systems—Power-to-X (PtX) ... 649
12.2.6 Load-Management ... 650
12.3 **Comparison of Costs, Efficiency Levels, and Energy Densities** ... 650
12.3.1 Comparison of All Storage Systems by Cost, Efficiency, and Energy Density ... 650
12.3.2 Comparison of Electricity Storage Systems Costs by Cycle Duration ... 653
12.4 **Strengths, Weaknesses, and Stages of Development** ... 655
12.4.1 Energy-Storage System: Stages of Development ... 655
12.4.2 Strengths and Weaknesses of the Various Technologies ... 655
12.5 **Cost-Reduction Potential with Batteries and PtX** ... 656
12.5.1 Cost Trends and Potential with Lithium Batteries ... 656
12.5.2 Cost-Reduction Potential with PtG ... 662
12.6 **Future Potential and Public Acceptanceof Energy Storage Systems** ... 665
12.7 **Summary** ... 669
References ... 670

## IV Energy Storage Integration and Applications

13 **Storage Integration in Individual Energy Sectors** ... 675
*Michael Sterner, Ingo Stadler, Fabian Eckert, and Martin Thema*
13.1 **Integration in the Electricity Sector** ... 676
13.1.1 Function and Purpose of Storage in the Electricity Sector ... 676
13.1.2 Pumped-Storage Plants and Storage Power Plants ... 683
13.1.3 Flywheel Storage Facilities ... 695
13.1.4 Battery Power Plants ... 697
13.1.5 Decentralized Battery Storage Systems in Houses and Districts ... 699
13.1.6 Stand-Alone Networks with Renewable Energy and Storage Systems ... 708

13.1.7 Thermal Storage in Solar-Thermal Power Plants ... 721
13.2 **Integration in the Heating Sector** ... 725
13.2.1 Thermal Storage for Solar-Thermal Energy ... 726
13.2.2 Latent and Sorption Storage Systems in Buildings and Households ... 733
13.2.3 Forest-Wood Used as Chemical Storage for Heating Supply ... 736
13.3 **Integration in the Transportation Sector** ... 741
13.3.1 Biofuel Mixtures and the Use of Vegetable Oil ... 741
13.3.2 Integration of Hydrogen in the Transportation Sector ... 745
13.3.3 Integration of Flywheel Storage Systems in Short-Distance Public Transportation ... 747
13.4 **Summary** ... 749
References ... 752

14 **Storage Integration for Coupling Different Energy Sectors** ... 757
*Michael Sterner, Ingo Stadler, Fabian Eckert, Norman Gerhardt, Christian von Olshausen, Martin Thema, and Tobias Trost*
14.1 **Coupling of the Electricity and Heating Sectors** ... 758
14.1.1 Increasing the Flexibility of CHP Using Thermal Storage and Heating Networks ... 758
14.1.2 Integration of Electric Heat-Pumps Using Thermal Storage and Heating Networks ... 764
14.1.3 Integration of PtH Using Thermal Storage and Heating Networks ... 768
14.1.4 Battery Storage vs. Load Shifting vs. Thermal Storage—An Example ... 774
14.2 **Coupling of Power and Transport Sectors** ... 776
14.2.1 Electro-Mobility ... 776
14.2.2 Electric Fuels ... 780
14.3 **Coupling of the Power and Gas Sectors: PtG** ... 785
14.3.1 PtG in the Context of the Energy Supply System ... 785
14.3.2 Development of PtG in Germany and Neighboring Countries ... 788
14.4 **Summary** ... 801
References ... 803

**Supplementary Information** ... 805
Epilogue ... 806
Index ... 807

# Meaning and Classification of Storage in the Energy Supply

Contents

Chapter 1 Energy Storage Through the Ages – 3

Chapter 2 Definition and Classification of Energy Storage Systems – 23

# Energy Storage Through the Ages

*Michael Sterner*

**1.1 100% Renewable Energy Before the Industrial Revolution – 4**
1.1.1 Photosynthesis—Nature's Primary Way of Storing Energy – 4
1.1.2 Wood, Peat, and Energy Crops—Using Stored Solar Energy – 9

**1.2 Fossil Energy in the Fossil Age – 13**
1.2.1 The Formation of Fossil Energy – 13
1.2.2 Use and Emissions of Fossil Energy: Status Quo – 15

**1.3 Transitioning to an Age of Renewables – 17**
1.3.1 Climate Change and Resource Scarcity—the Drivers of a Global Energy Revolution – 17
1.3.2 The Age of Renewable Energy is Only a Question of Time—Scenarios for Change – 19

**1.4 Summary – 21**

**References – 22**

**Electronic supplementary material** The online version of this chapter (https://doi.org/10.1007/978-3-662-55504-0_1) contains supplementary material, which is available to authorized users.

© Springer-Verlag GmbH Germany, part of Springer Nature 2019
M. Sterner, I. Stadler (Eds.), *Handbook of Energy Storage*, https://doi.org/10.1007/978-3-662-55504-0_1

1

**Overview**

Human beings have relied on **stored energy** since time immemorial. The planet's **first mechanism for storing energy** arose two billion years ago. Photosynthesis captures **solar energy** in chemical bonds; it is a process on which **all life** depends. With the discovery of **fire** around one-and-a-half million years ago, early man learned to access this stored energy by burning wood. Only since **the Industrial Revolution** have humans used **fossil fuels**, which are the results of biomass produced millions of years ago, then subjected to geological processes. Today, the long-term objective is to utilize sustainable biomass storage, replicate it by technical means, and to develop new **storage technologies**.

This chapter is about the **history** of energy storage as it pertains to the **carbon cycle**. It begins with a natural energy storage system—**photosynthesis**—and examines its products **biomass**, peat, and **fossil fuels** before turning to storage technology in the **era of renewable energies**. It will also discuss how stored energy is used. This chapter focuses on natural biogenic and fossil energy storage. Other chapters are devoted to artificial storage technologies, including batteries, pumped-storage, and power-to-gas (PtG). Each begins with a short history of its respective technology.

## 1.1 100% Renewable Energy Before the Industrial Revolution

### ▪ The Sun—the Motor of Renewable Energy and Energy Storage

All natural energy—with the exception of deep geothermal energy, nuclear energy, and tidal power originates in the Sun. Before the Industrial Revolution, humans relied exclusively on energy from renewable sources. The most important source of energy during this time was biomass, such as wood, which ultimately owes its existence to stored solar energy. The use of wood as fuel goes back to the Stone Age, when it provided both heat for cooking and warmth, and also light and protection from wild animals. Another source of stored energy is peat, which human beings first used 2,000 years ago.

Human beings have used other forms of renewable energy as well: the Sun for solar drying, wind for sailing on rivers, lakes and oceans, and wind and water for milling and pumping. Wind and water energy are based on solar energy. The Sun generates high and low-pressure systems in the atmosphere, which creates wind and drives the hydrological cycle (evaporation and precipitation), producing rain which feeds the rivers. The warmth in the surface layers of the Earth is also, essentially, stored solar energy. But the largest share of energy use before the Industrial Revolution was stored solar energy in the form of biomass.

### 1.1.1 Photosynthesis—Nature's Primary Way of Storing Energy

All plant matter arises via photosynthesis and is thus stored as solar energy. In *oxygenic* photosynthesis, the radiant energy of the Sun is captured as chemical bond energy when water ($H_2O$) and carbon dioxide ($CO_2$) is converted into plant matter. A by-product is oxygen ($O_2$), which is needed for animal respiration and for burning stored biogenic and fossil energy (Fig. 1.1).

Photosynthesis mainly occurs in chloroplasts and has two basic steps [5, 8, 21]:

1. The creation of a redox potential by splitting water molecules into electrons, protons, and oxygen thanks to light reactions in pigment molecules.
2. The absorption, reduction, and synthesis of $CO_2$ into sugar and organic carbon bonds in light-independent reactions (Calvin cycle).

Photosynthesis is explained below using the example of glucose.

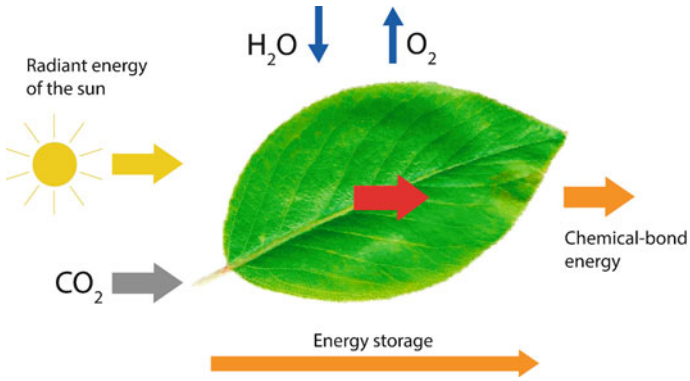



**Fig. 1.1** Photosynthesis: nature's storage of solar energy

### Water Splitting

Photosynthesis begins by splitting the water that plants draw from the soil and air into hydrogen and oxygen (Eq. 1.1). This light-dependent reaction takes place in two internal photosystems. In the first, energy is derived for splitting water and processing the $CO_2$. In the second, light energy ionizes the hydrogen, creating hydrogen ions (known as protons) and electrons. The by-product—oxygen—is returned to the atmosphere. As with photovoltaics (PVs), the energy of the absorbed photons is used to raise the energy levels of electrons, or in this case, pigment molecules known as chromophores. The sunlight absorbed by the plant (electromagnetic radiation energy $E_{ph}$) triggers three basic steps:

1. Transfer of electrons and protons to an intermediate $NADP^+$
2. Reduction of $NADP^+$ to NADPH (an electron carrier)
3. Preparation of ATP, an energy carrier necessary for the synthesis of $CO_2$.

$$12H_2O + E_{ph} \rightarrow 24(H) + 6O_2. \quad \textbf{(1.1)}$$

### Absorption, Reduction, and Synthesis of $CO_2$

Photosynthesis continues with a second light-independent reaction. This combines the hydrogen ions and electrons with carbon dioxide from the atmosphere, thus binding solar energy in a stable chemical form (Eq. 1.2). In the so-called Calvin cycle, $CO_2$ from the air is fixed in organic molecules (the $CO_2$ acceptor RuBP) within the chloroplasts. The resulting product is unstable and decomposes into two intermediate compounds, which the electrons from the NADPH reduce to a $C_3$ sugar. Then the modified $CO_2$ acceptor is regenerated in the final phase of the Calvin cycle with the help of the energy carrier ATP. The electron and energy carriers, NADPH and ATP, circulate internally between the light-dependent and light-independent reactions, maintaining the cycle.

The bond energy stored in carbon compounds is retained throughout the transformation to biomass food and fossil fuels, until it is released by oxidation in animals or artificial 'heat engines' (combustion engines and turbines), and the resulting $CO_2$ is returned to the atmosphere:

$$6CO_2 + 24(H) \rightarrow C_6H_{12}O_6 + 6H_2O. \quad \textbf{(1.2)}$$

### Gross and Net Photosynthesis

The total photosynthetic reaction can be represented as follows:

$$\text{Gross:} \quad 6CO_2 + 12H_2O + E_{ph} \rightarrow C_6H_{12}O_6 + 6O_2 + 6H_2O \quad \textbf{(1.3)}$$

$$\text{Net:} \quad 6CO_2 + 6H_2O + E_{ph} \rightarrow C_6H_{12}O_6 + 6O_2. \quad \textbf{(1.4)}$$

Depending on the plant type, photosynthesis results in a sugar with three or four carbon atoms. These carbon compounds supply the energy needed for the other plant processes

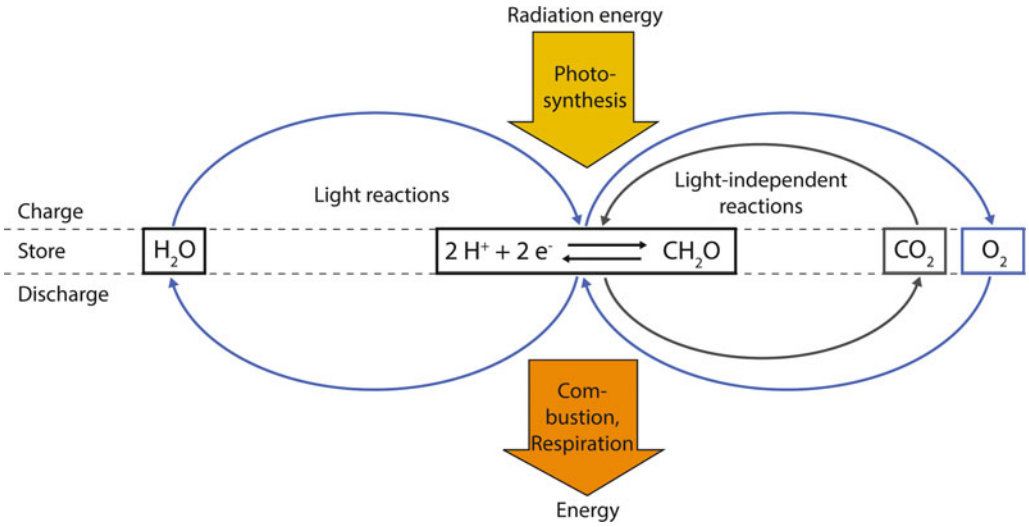



**Fig. 1.2** Closed cycle of photosynthesis (energy storage) and oxidation (energy use); based on data from [3]

and for building hydrocarbon chains. For example, glucose stores energy of 2.813 kJ/mol (0.78 kW h/mol).

Equation 1.2 can be simplified by dividing by six throughout to show the core reaction. It is represented in the C–H–O diagram and reveals the basic building block $[CH_2O]$ of the type of biogenic and fossil-based energy (▶ Sect. 8.1.1):

$$\text{Core equation:} \quad CO_2 + H_2O + E_{ph} \rightarrow [CH_2O] + O_2. \tag{1.5}$$

Photosynthesis reverses the oxidation involved in cell respiration. The latter uses oxygen produced by photosynthesis. $CO_2$ goes through a similar cycle, thus bringing the system full circle (Fig. 1.2).

Living beings harness much of the energy ingested as food to power their metabolism, with the balance used for growth and repairs. For example, adult male humans have a 'basal (resting) metabolic rate' of about 100 W (around 80 kcal/h). Both photosynthesis and respiration are redox reactions and obey the principles of electrochemistry (▶ Sect. 7.1).

## Efficiency

Photosynthetic efficiency is the chemical bond energy $E_{chem}$ divided by the annual global solar radiation $H_G$—the sum of direct, diffuse, and reflected radiation—reaching the plant's surface (Eq. 1.3). Efficiency can also be expressed using the variables chemical power $P_{chem}$ and global solar irradiation $E_G$. These result in the following:

$$\eta = \frac{P_{chem}}{E_G} = \frac{E_{chem}}{H_G}. \tag{1.6}$$

Photosynthetic efficiency depends on several things, including how much radiation energy can be absorbed by plants and the plant type or the metabolic system.

Global solar radiation can be absorbed, reflected, or transmitted. That which is absorbed depends on the spectrally selective characteristics of the plants. Under ideal conditions, their pigment molecules absorb only some 50% of the light they receive. In green plants, these selective absorbers are called chromophores, the part of a molecule responsible for color. They contain light-absorbing compounds such as chlorophyll a/b, carotinoids, and xanthophylle. So the shorter and more energy-intensive blue wavelengths are 'downshifted' to red light ($E_{ph} \leq 1.94$ eV) and excess energy escapes as waste heat. (Spectrally selective absorbers are also used in solar heat col-

lectors and PV cells.) Plants reflect most of the green light in the solar spectrum, which is why the human eye perceives them as 'green'. Another part of the solar radiation is transmitted.

### Sample Calculation of Theoretical Efficiency at the Molecular Level

To fix and transform $CO_2$, the ionization energy of at least eight 'red' photons is needed per molecule [3, 11]. Assuming a wavelength in the middle of the red spectrum of 680 nm, a photon (a quantum of solar radiation) with the Planck constant of $h$, of $6.626 \times 10^{-34}$ J·s, and the speed of light in a vacuum $c_0$ of $2.998 \times 10^8$ m/s has an energy of:

$$E_{\text{ph}} = h \cdot f = h \cdot \frac{c_0}{\lambda} = 2.92 \times 10^{-19}\,\text{J} = 1.82\,\text{eV}. \tag{1.7}$$

When multiplied by the Avogadro constant $N_A$ of $6.022 \times 10^{23}$ 1/mol, this results in a molar energy density of 176 kJ/mol (0.05 kW h/mol). For example, glucose contains 6 carbon atoms, so at least $6 \cdot 8 = 48$ photons are needed, producing a photon energy of 8.4 MJ/mol (2.4 kW h/mol). The calorific value of glucose is 2.8 MJ/mol (0.78 kW h/mol). The quotient of these values yields a theoretical maximum efficiency of 33%. In most cases, not 8 but 10 photons are necessary, lowering the efficiency to 26%. As only 50% of photons from the solar spectrum can be harnessed, this value is further reduced to 13%.

As with electrochemical-energy storage, photosynthesis stores energy at efficiencies significantly less than the theoretical due to a multitude of physical and electrochemical effects.

In the biological conversion process the theoretical efficiency cannot be reached. In practice, there are both optical and internal losses. When the energy-rich photons of the blue wavelengths are 'downshifted' to red wavelengths, large amounts of heat are lost. In addition, the plant needs energy to sustain itself. Studies to date differ as to the magnitudes of the various energy losses [1, 3, 11, 17, 21]. They differ mainly in their assumptions about reflection and absorption, and the losses in photochemical, biochemical, and physiological reactions. But it is agreed that plants can chemically store no more than 5% of solar energy (Fig. 1.3).

Indeed, the gross primary production efficiency is only 1 to 5%, depending on the plant type. From this, around 50% must be subtracted for the plant's respiration, yielding the net primary production (NPP) efficiency. So, in the end, only 0.5 to 2.5% of the solar energy is converted into chemical bond energy. In aquatic plants, photosynthesis is further limited by minerals dissolved in the water. For instance, the total photosynthetic efficiency for algae without any technical auxiliary systems is only 0.1% [24].

Although nature has optimized this storage process over millions of years, the efficiency is very low. However, much higher energy efficiencies can be achieved using artificial technologies such as photobiology, PtG, and power-to-liquid (PtL).

### Real Photosynthetic Efficiency at a Global Level

Assuming an annual average global solar radiation of $E_G = 167\,\text{W/m}^2$ on the global terrestrial surface area $A$ of $150 \times 10^{12}\,\text{m}^2$, of which $100 \times 10^{12}\,\text{m}^2$ is covered with vegetation, and a NPP of 2,200 EJ/a [2], the overall photosynthetic efficiency is given by:

$$\begin{aligned}\eta &= \frac{E_{\text{chem}}}{H_G} = \frac{\text{NPP}}{E_G \cdot A \cdot t} \\ &= \frac{2{,}200 \times 10^{18}\left(\frac{\text{W s}}{\text{a}}\right)\text{m}^2}{167\,\text{W} \cdot 100 \times 10^{12}\,\text{m}^2 \cdot 8{,}760\frac{\text{h}}{\text{a}} \cdot 3{,}600\,\frac{\text{s}}{\text{h}}} \\ &= 0.42\%. \end{aligned} \tag{1.8}$$

This value falls short of the ideal efficiency for land-based vegetation—2.5%—by a factor of 6.

#### ■ $CO_2$ Fixation of Plant Type $C_3$ or $C_4$

Selective breeding or the addition of nutrients and $CO_2$ can increase the productivity, and hence the energy storage efficiency, of plants. With regard to $CO_2$ fixation, there is a difference between $C_3$ and $C_4$ plants due to the

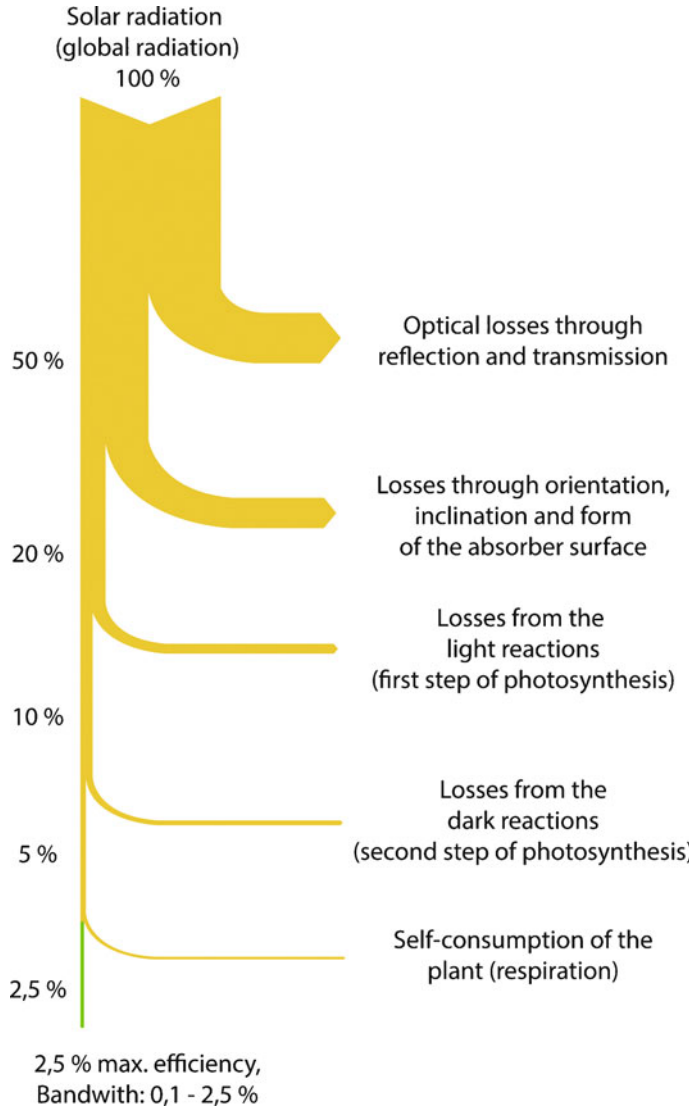



**Fig. 1.3** Sankey diagram of maximum photosynthetic efficiency—an example borrowed from [8]

bonding of carbon in the first step of the Calvin cycle:

| | |
|---|---|
| $C_3$ plants | bonding of three carbon atoms. For example, boreal grasses, rice, and wheat. |
| $C_4$ plants | bonding of four carbon atoms. For example, tropical grasses, corn, and sugar cane. |

$C_3$ plants close their receptors on hot days to prevent evaporation. During this time, the plant does not store energy. The secondary effect is known as photorespiration, when respiration occurs during energy use. $C_4$ plants are an evolutionary advance over $C_3$ plants. Due to their micro-biological structure, they use a minimum level of photorespiration and work better at higher temperatures and lower $CO_2$ concentrations. This produces more biomass in a shorter period of time than $C_3$ plants, and at higher photosynthetic efficiency.

The increase of $CO_2$ concentrations—e.g., through burning fossil fuels—fosters plant

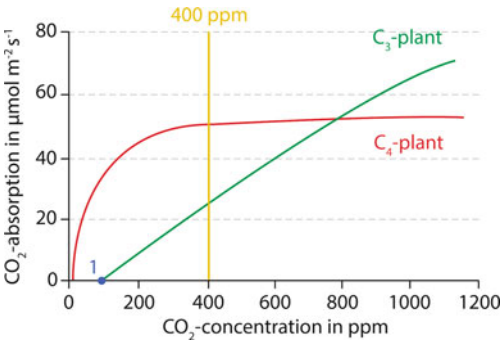



**Fig. 1.4** Dependence of photosynthesis on $CO_2$ concentration in the surrounding air for different plant types. In step 1 the plant absorbs as much $CO_2$ during energy storage as it uses for energy release (respiration). $CO_2$ concentration today (In 2015 the global monthly average surpassed the 400 ppm mark for the first time since records began)

growth to varying degrees. Figure 1.4 illustrates the difference between plant types. While the growth of $C_3$ plants increases with rising $CO_2$ concentrations, leveling off at around 1,000 ppm, its influence on $C_4$ plants is hardly noticeable. Relative to $C_4$ plants, $C_3$ plants can absorb more water in dry regions with higher $CO_2$ concentrations, increasing crop yield by 10–20%. It is unclear whether this $CO_2$ 'fertilization' will produce higher yields on a long-term basis as global warming and air pollution have complicated effects that are hard to calculate and have, so far, been largely neglected in discussions.

### Photosynthetic Energy Storage: The Basis of Life

Photosynthesis is a natural form of energy storage and, directly or indirectly, sustains all life on the planet. The first life forms on Earth were single-cell organisms called Archea, which appeared around 3.5 billion years ago, before oxygen was present in the atmosphere. Although they did not use photosynthesis, they contained the components for electron transport and cell respiration. These were the building blocks of what became anoxygenic photosynthesis and then, after sufficient quantities of atmospheric oxygen accumulated some two billion years ago, oxygenic photosynthesis. The first macroscopic life appeared 1.5 billion years ago, followed by dinosaurs around 235 million years ago, and humans some 200,000 years ago [5, 8].

Were natural photosynthesis to fail, life as we know it would disappear. Within 25 years, all higher life forms would have perished. Scientists have proposed that this explains the extinction of the dinosaurs some 65 million years ago. They argue that at the end of the Cretaceous period an asteroid impact in Mexico created a vast dust cloud that obscured the sun, strongly reducing photosynthesis [5].

Some of the first forms of life—organisms from the archaeal type strains—could produce methane gas from $CO_2$ and $H_2$; a capability also found in PtG technology (▶ Sect. 8.3).

## 1.1.2 Wood, Peat, and Energy Crops—Using Stored Solar Energy

The total yield of plant matter from solar energy is immense. The global NPP on land—less the energy used for respiration—amounts to some 60 Gt of organic carbon per year, ±10%, with around 60% above-ground and 40% below-ground (as roots and tubers) (Fig. 1.5).

Assuming that biomass has a gross calorific value (GCV) of 37 GJ/t, the global terrestrial stored energy is around 1,300 EJ ± 10% a year (34 Gt C $a^{-1}$ ± 10%) (Table 1.1). Researchers have estimated that up to one-half can be harvested on a sustainable basis [2]. However, that of food and raw materials (e.g., pulpwood) must be subtracted before the net bioenergy can be determined. According to [24], the sustainable bioenergy potential is 80–170 EJ/a, some 16 to 34% of the global primary energy need of 500 EJ/a.

In addition to the energy stored on land, energy is also captured by plankton and other aquatic plants. However, most aquatic biomass is used directly by consumers. Moreover, despite 70% of the Earth's surface being covered by oceans, the low efficiency of photosynthesis

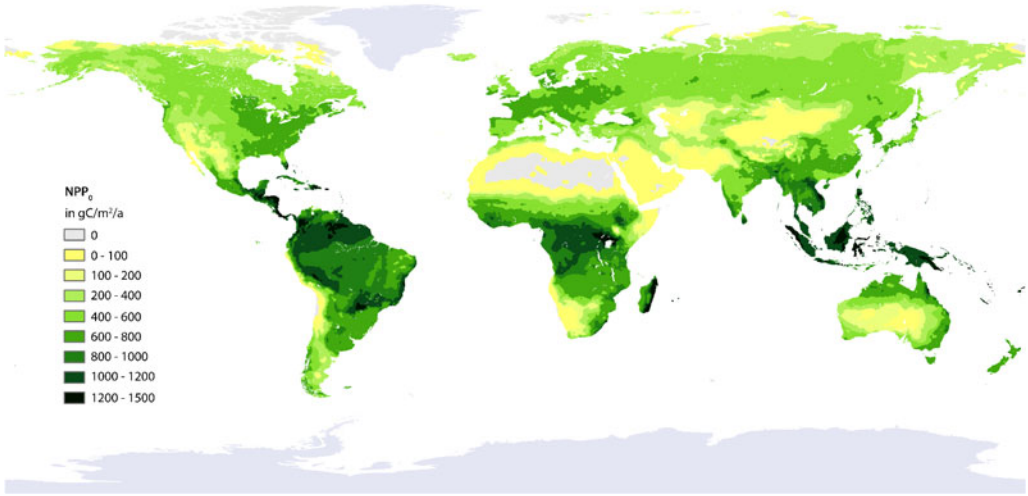



**Fig. 1.5** Global terrestrial NPP in 2000 by surface area. Globally, around 70% of available grasslands, 50% of savannas, 45% of boreal forests, and 27% of tropic forests are used for agriculture or timber harvesting [2, 14]. 100 g C $m^{-2}$ $a^{-1}$ corresponds to 1 t C $ha^{-1}$ $a^{-1}$, or 3.7 t $CO_2$ $ha^{-1}$ $a^{-1}$

**Table 1.1** Solar energy stored via photosynthesis as biomass and fossil energy for a global area covered by vegetation of $100 \times 10^{12}$ $m^2$. The global NPP (in t C $a^{-1}$) is converted to energy using a GCV of 37 GJ/t, with an uncertainty of at least $\pm 10\%$, following [2, 14]. The annual solar radiation energy and average power are calculated using a global annual average solar irradiance of $E_{SC} = 167$ W $m^2$

| | Solar energy | | Stored biomass, used energy | | |
|---|---|---|---|---|---|
| **Parameter** | **Energy in EJ** | **Output in TW** | **Energy in EJ** | **Output in TW[d]** | **Efficiency, solar to biomass** |
| Solar energy/ total NPP[a] | 526,651 | 16,700 | 2,200 | 70 | 0.42% |
| Above- ground NPP[b] | | | 1,300 | 41 | |
| Useable NPP | | | 650 | 21 | |
| Solar energy, or NPP, used in 2012[c] | 1.3 | 0.36 | 225 | 7 | |
| Global primary energy demand | | | 500 | 16 | |

[a] The planet's total surface area is $510 \times 10^{12}$ $m^2$ (51 billion ha), with 70.7% covered by oceans. The remaining land area totals $150 \times 10^{12}$ $m^2$. Of that, $100 \times 10^{12}$ $m^2$ is covered by vegetation. The solar energy received by this area is shown. For the solar energy received by the land area, this should be multiplied by 1.5.
[b] Above-ground share of plants that do not add carbon to the ground soil (root systems).
[c] Solar energy directly used in 2012 from PV plants (with an installed rated power of 100 GW), solar-thermal power-plants (2.6 GW), and solar heat (255 GW), taken from the *Global Status Report 2013* of the *Renewable Energy Policy Network*; NPP as biomass used for food, animal feed, raw materials in the industrial sector, and for energy.
[d] Expressed as the average power over the year.

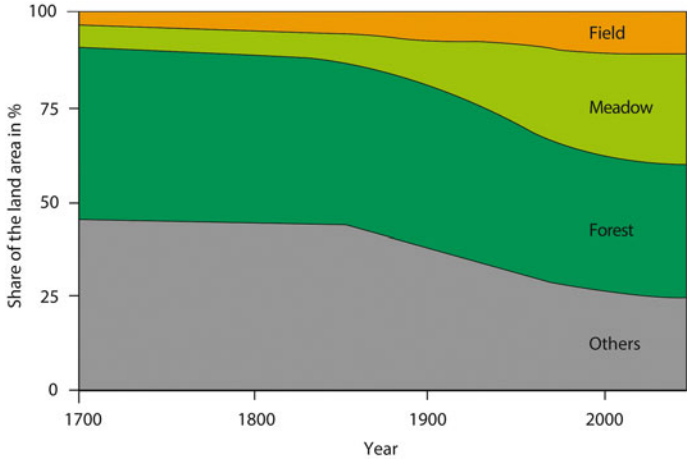



**Fig. 1.6** Land use changes through history. Forests are depleted along with their stored energy; data based on [12]

in water results in the absolute amount of stored energy being less than on land.

An example of the use (the 'discharge' process) of stored biomass is considered below.

### Wood—Sustainable Use

Biomass in the form of lignocellulose (wood) was the most used primary energy source from the Stone Age to the beginning of the Industrial Revolution. Between 1700 and 1850 around 180 million hectares of temperate forests were cleared to provide timber and create open land. This practice declined with the discovery and use of fossil fuels.

In the 19th century, forests covered just less than 50% of the Earth's surface. Since then, increasing deforestation and mechanized agriculture quickly depleted the forests, and today they cover only around a quarter of the Earth's surface (Fig. 1.6). About a third of existing forests are used for fire wood and timber products [12].

Three-and-a-half billion cubic meters of raw timber are cleared each year. Fifty percent is used as fire wood (solid wood and charcoal) and 50% as raw materials for secondary products, such as wood pulp for paper and books (25%), or lumber and furniture wood. The proportions vary greatly by continent. While in North America and Europe around 80% is used as timber, in Africa and Asia most is used as fire wood (Fig. 1.7) [13].

The amount of wood that grows each year exceeds the amount of wood cleared by a considerable amount. For instance, a 90% share of fire wood in Africa equals around 1% of wood growth on that continent [13]. As energy prices have risen, the demand for fire wood and timber has increased, leading to deforestation with possible negative effects.

Assuming that wood has an average calorific value of 900 MJ (2,250 kW h) per solid cubic meter (reflecting a mixture of hardwood and softwood), the planet's forests store around 29 EJ (8,100 TW h) a year of chemical energy, for a solar-to-wood storage annual average power of 925 GW.

In addition to energy, wood stores carbon from $CO_2$. Wood used in construction removes $CO_2$ from the atmosphere, often for long periods.

Before biomass was replaced by coal as the most widely used primary energy source in the 19th century, many sectors (such as the steel industry) relied on wood for fuel. One example is the German town of Iserlohn ('Iser' means iron and 'Lohn' means forest), where the steel industry experienced a boom fueled by wood from nearby Sauerland.

Even today, biomass is the most important primary energy for 2.6 billion people in over 60 countries. Two-thirds of the world's population use firewood as fuel for cooking and heating. But this use of wood is both inefficient (about

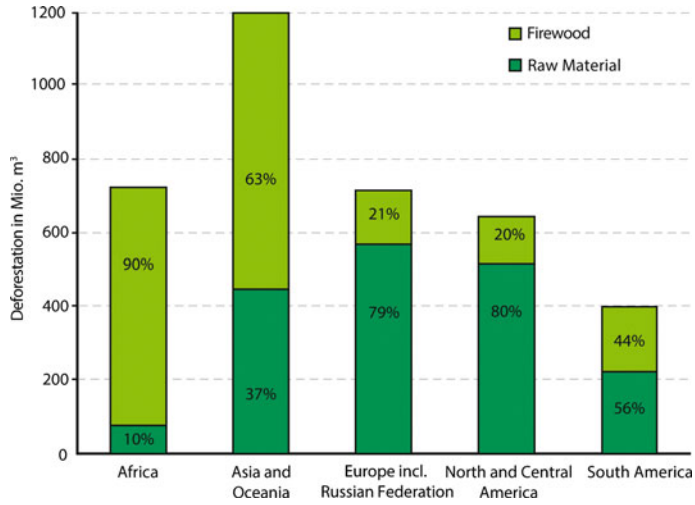



**Fig. 1.7** Wood from forests for fuel and raw materials in 2014; data based on [13]

5%) and the carbon monoxide it releases harms human health. Each year, around 1 million people die as a result of indoor air pollution from firewood. Moreover, the use of firewood and charcoal is often accompanied by logging and deforestation, which has negative effects on the micro-climate and on water and ground quality, contributing to global climate change [24]. Some alternatives to wood are the development of other renewable energies and the sustainable use of biomass, such as through improved cooking stoves, accompanied by measures promoting education and reforestation.

### Peat—Old Wood

When oxygen-rich biomass breaks down it turns into humus, which ultimately becomes soil. Peat, by contrast, consists of dead organic biomass formed from plant residues in waterlogged surroundings such as bogs. A precursor of brown coal, peat has a similar calorific value of about 20 MJ/kg (5.5 to 6 kW h/kg) when dry, with a high ash content. In the 18th and 19th centuries peat was used in power stations for electricity and heat. Today peat bogs are protected biotopes in Germany; only a few European countries (Finland, Ireland, and Estonia) still use peat as a significant energy source [6].

### Energy Plants for Transport and Animal Power

Without energy storage, our lives would not be possible. Our bodies are fueled by stored solar energy which we consume each day in the form of food. This is oxidized with oxygen inhaled from the air, resulting in carbon dioxide being exhaled, and producing an output power of around 100 watts.

The same processes occur in most animals. From when they were domesticated, animals have been used for mechanical power, such as for driving well-pumps and mills as well as for the transport of loads. For centuries, horses were man's main form of transportation. In India today, animal power—a form of renewable energy—is still widely used.

At one time, around a third of agricultural land was devoted to growing food for working animals. Today, now that the transport and industrial sectors require far more than one or two horsepower, available biomass would be unable to meet their fuel demands, despite fertilizers and industrial agribusiness. Yet simple estimates suggest that biomass in the form of plant oil could cover the fuel demands of tractors and machinery in agriculture and forestry. However in Germany, there is no organized market for pure plant oil.

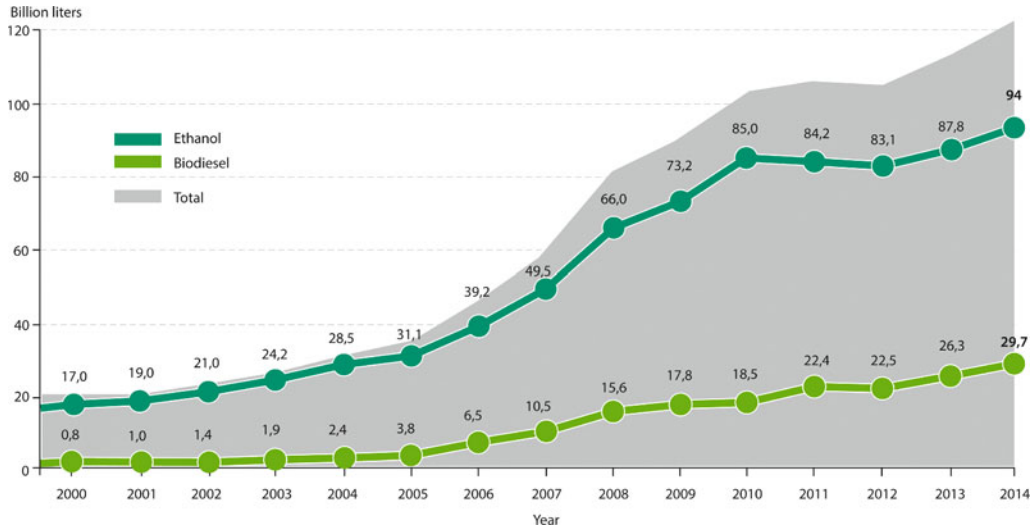



**Fig. 1.8** Global use of biofuels [9]

Biofuels made from energy plants can be used in cogeneration plants to produce electricity and heat. Today, almost all liquid biofuels are bio-ethanol (used in Otto engines) and biodiesel (used in Diesel engines), as Fig. 1.8 illustrates. However, the initial rise in usage has been slowed by strong price increases in agribusiness commodity markets and a changing political framework.

**Example**

In Germany, the average annual solar global irradiance is around 115 $Wm^{-2}$. In 2011, 910,000 ha of colza plants were used to produce biodiesel (with a yield of 2.6 million t) and colza oil (with a yield of 0.025 million t).

What is the areal output power achieved by biofuels? And what overall efficiency results from the capture of solar energy by, and the storage in, biofuels [9]?

Solution:

**Colza biodiesel:** – $37.1\,\mathrm{MJ/kg} = 10.3\,\mathrm{kW\,h/kg}$
**Colza calorific value:** – $37.6\,\mathrm{MJ/kg} = 10.4\,\mathrm{kW\,h/kg}$
**Colza agricultural land:** – $910{,}000\,\mathrm{ha} = 9{,}100{,}000{,}000\,\mathrm{m^2}$
**Hours per year:** – 8,760 h
**Biodiesel energy:** – $E_{\mathrm{Bio}} = 2.6 \cdot 10^9\,\mathrm{kg} \cdot 10.3\,\frac{\mathrm{kW\,h}}{\mathrm{kg}} = 2.7 \cdot 10^{10}\,\mathrm{kW\,h}$
**Colza energy:** – $E_{\mathrm{Raps}} = 0.025 \cdot 10^9\,\mathrm{kg} \cdot 10.4\,\frac{\mathrm{kW\,h}}{\mathrm{kg}} = 2.6 \cdot 10^8\,\mathrm{kW\,h}$
**Total energy:** – $E = 2.726 \cdot 10^{10}\,\mathrm{kW\,h} = 2.726 \cdot 10^{13}\,\mathrm{W\,h}$
**Output:** – $P_{\mathrm{Bio}} = \frac{E}{8{,}760\mathrm{h}} = 3.1 \cdot 10^9\,\mathrm{W}$
**Areal output:** – $\frac{P_{\mathrm{Bio}}}{A} = 0.34\,\frac{\mathrm{W}}{\mathrm{m^2}}$
**Efficiency:** – $\eta = \frac{P_{\mathrm{Bio}}}{P_{\mathrm{Solar}}} = \frac{0.34}{115} = 0.0030 = 0.30\%$

## 1.2 Fossil Energy in the Fossil Age

### 1.2.1 The Formation of Fossil Energy

With the invention of the steam engine in the 18th century and the Industrial Revolution that accompanied it, fossil energy sources such as coal, oil, and gas became increasingly important. Like carbonates such as limestone or dolomite, they were formed over millions of years via biochemical and geochemical reactions (Fig. 1.9):

- Hard coal and brown coal: dead organic biomass accumulates in anaerobic conditions in peat bogs, and under high pressures and temperatures over a geological time scale, becomes brown coal. This can eventu-

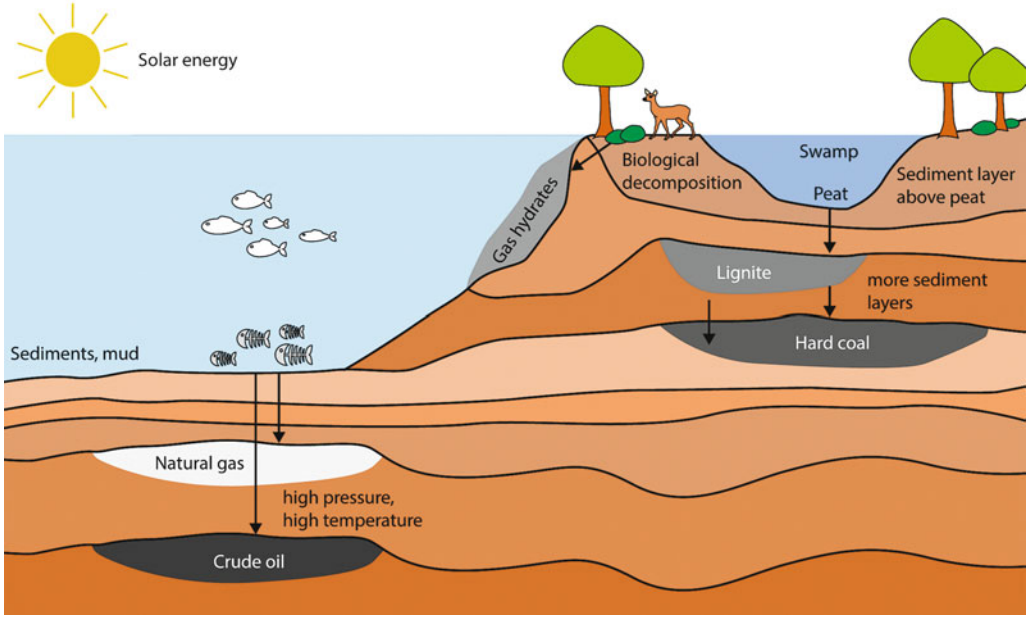



**Fig. 1.9** The formation of fossil fuels: dead biomass accumulated in anaerobic conditions in peat bogs and subjected to high pressure and temperatures over geological time becomes brown coal and then hard coal. Similarly, organic deposits on prehistoric ocean floors can turn into oil and natural gas

ally become hard coal, which is harder and has a higher-energy density.

- Oil: this forms in a similar way to coal. Dead plant and animal biomass (plankton, etc.) accumulates on the ocean floor over millions of years. When the ocean floor is subducted due to continental drift, these deposits are subjected to very high pressures and temperatures, and eventually become oil and natural gas, trapped in sedimentary rock. When this is impervious, they may form open reservoirs, and can be released by drilling. When the rock is porous, they can be released by first injecting water and chemicals at high pressure; a technique known as fracking. The extent of the environmental damage caused by fracking—such as minor earthquakes, groundwater pollution and other harmful consequences—is as yet unknown.
- Natural gas: this forms in a similar way to oil, and may be found with it [as 'associated' gas]. However, the geological conditions may also result in it being found alone.

Fossil fuels take millions of years to form but are consumed in an instant, relatively speaking. For instance, human beings consume as much energy from fossil fuel in a year as nature stores in three million years. As a result, reserves and supply are dwindling and peak oil production is looming.

## The Carbon Cycle

In an intact ecosystem, there is a closed carbon cycle between $CO_2$ and $O_2$. It consists of producers (1), consumers (2), and decomposers (3). This cycle regulates the carbon levels in the biosphere (Fig. 1.10).

The producers (plants) use solar energy to convert carbon dioxide and water into biomass (▶ Sect. 1.1.1). After the energy stored in biomass undergoes biological oxidation it can be used by consumers (people, animals, plants). Biological oxidation is the inverse of photosynthesis, in which organic mass is combusted by consumers using oxygen. Dead biomass is degraded aerobically by decomposers (soil organisms), which returns $CO_2$ to the atmosphere.

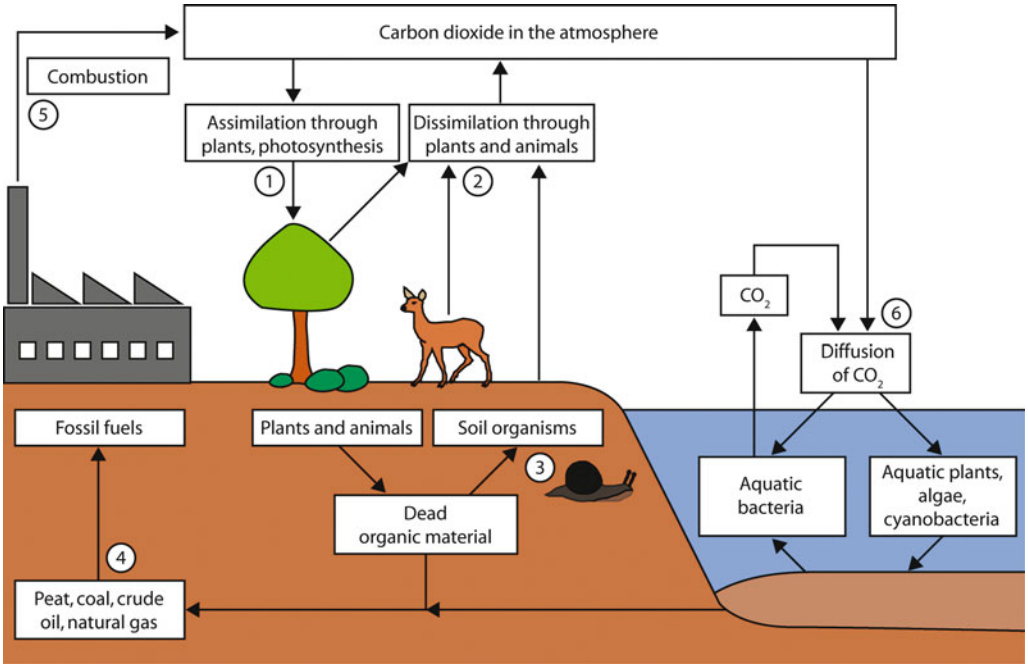



**Fig. 1.10** The carbon cycle: carbon that has been stored in fossil fuels over millions of years may be burned in seconds to form carbon dioxide ($CO_2$) and released to the atmosphere and the oceans

Fossil fuels (hydrocarbons) are formed from atmospheric $CO_2$. When after millions of years they are burned, $CO_2$ again enters the atmosphere. Although this is part of the carbon cycle, the $CO_2$ is released into the atmosphere in an instant, whereas absorption in biomass and the oceans takes several centuries, so that atmospheric levels rise, resulting in anthropogenic climate change (▶ Sect. 1.3.1).

### $CO_2$ Storage in the Oceans

As it is very water soluble, the oceans absorb some carbon dioxide from the atmosphere. Indeed, the oceans contain 50 times more carbon dioxide than the atmosphere. Between 1800 and 1995, some 120 Gt of carbon was absorbed by the oceans, which corresponds to around half of all $CO_2$ emissions from fossil fuels [3]. This has raised the acidity of the oceans, which threatens the existence of many marine organisms. Some carbon is fixed by algae, phytoplankton, and coral via photosynthesis, eventually forming reservoirs of oil and natural gas, and some as carbonates and hydrocarbonates. Scientists estimate that in 2011 the oceans absorbed $CO_2$ as follows: 1% as dissolved $CO_2$, 8% as carbonates ($CO_3^{2-}$), and 91% as hydrocarbonates ($HCO_3^-$).

## 1.2.2 Use and Emissions of Fossil Energy: Status Quo

### Three-Quarters of Global Primary Energy Comes from Stored Solar Energy

Setting aside nuclear energy, 88% of global primary energy demand is met by fossil energy (79%) and biogenic energy from photosynthesis (9%). These shares were determined using the 'substitution' method which, unlike the more common 'efficiency' method, does not understate the shares from wind, solar, and hydropower producing electricity. Figure 1.11 shows that hydropower (with electricity of 780 TW h/a) and nuclear energy (with heat of 2,480 TW h/a) are about equivalent.

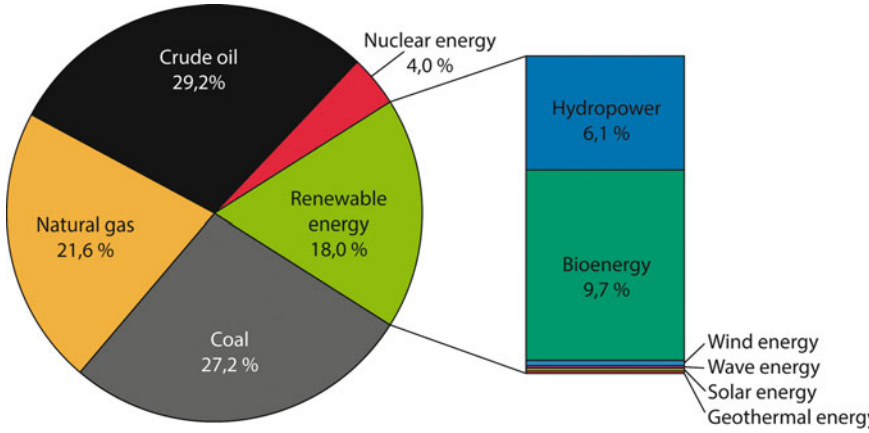



**Fig. 1.11** Share of global primary energy in 2014, measured by the 'substitution' method [7, 22]

Of the final energy consumption, only around 8% is taken directly from the environment. This illustrates the vital role of energy storage. As ever more renewable energy is harnessed, energy storage will retain this important role, although the types of storage may differ.

### Energy Sector $CO_2$ Emissions from Stored Fossil Energy

$CO_2$ emissions from burning fossil fuels have risen sharply over the past decades (Fig. 1.12). Although the $CO_2$ being emitted originally came from the atmosphere, the rate of release is immense. $CO_2$ captured over millions of years

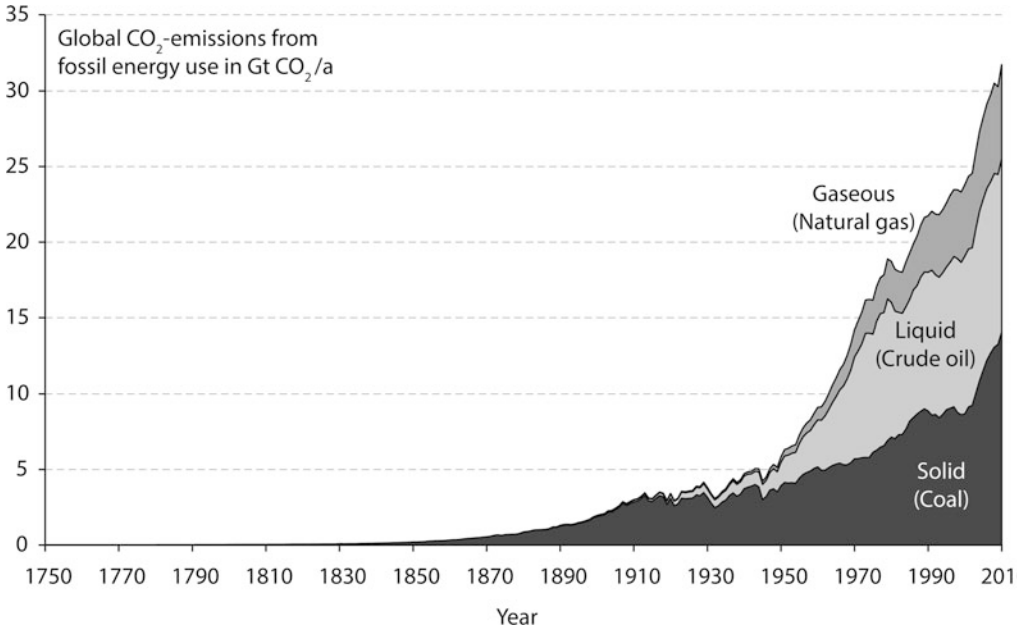



**Fig. 1.12** $CO_2$ emissions from fossil energy use, 1750–2014 [6]

is being released into the atmosphere at a very rapid rate (relative to geological time), causing the severe climate change observable today (▶ Sect. 1.3.1).

## 1.3 Transitioning to an Age of Renewables

### 1.3.1 Climate Change and Resource Scarcity—the Drivers of a Global Energy Revolution

Climate change and resource scarcity demand urgent action and are the prime drivers of a worldwide transition to renewable energies. Nuclear-related disasters may accelerate change in some countries, but all nations must face the challenge of ensuring the long-term security of energy supply.

The transformation of the energy supply consists of two basic components:

1. Increasing measures to reduce energy demand and increase energy efficiency.
2. Expanding the use of renewable energies.

#### Anthropogenic Climate Change—the Greatest Challenge for the Future

Two-thirds of all greenhouse gas emissions result from burning fossil fuels. Reducing their use and replacing them with renewable $CO_2$-free energy technologies is the goal of sustainable energy and climate policy action. There is no shortage of potential renewable energies. The challenge lies in providing supply security at different places and times when using weather-dependent energy sources. For this purpose in the medium- and long-term, energy storage is an absolute necessity.

The correlation of rising $CO_2$ levels and global warming was first demonstrated 120 years ago and has been confirmed many times since. By analyzing air-bubbles trapped in deep-drilled ice cores, scientists have been able to study $CO_2$ concentrations and air temperatures as far back as several hundred thousand years. Although the $CO_2$ concentrations have varied by only ±200 ppm (0.02%), the peaks and troughs correspond with the glaciations and 'interglacial' warm periods respectively.

Figure 1.13 shows that $CO_2$ concentration today is 400 ppm, which clearly exceeds the average of past millenia [5]. Given this concentration, a rise in average temperatures and the number of extreme weather events is to be expected. Indeed, both can be observed increasingly around the globe, even in places like Germany, which in recent years has experienced abnormally severe flooding and droughts. Europe's average yearly temperatures in 2002, 2003, 2006, 2007, and 2010 were above the 510-year average between 1500 and 2010 [4].

Climate change is also one reason for the worldwide flood of refugees. As rising temperatures have depleted supplies of fresh water and food and increased the number of severe storms and floods, many thousands have been forced to leave their homes and resettle in other regions. For instance, the crisis in Syria was preceded by a long period of drought displacing many from the country to the cities. Also, the West's military actions over the past two decades have been destabilizing the region, and these actions have been carried out primarily for the purpose of ensuring access to oil and gas. Alarmingly, forecasts for 2050 predicting military troops at national borders to stem a rising tide of refugees have already become reality today [13].

All proposals for solving the refugee crisis call for the preservation of local environments in addition to regional disarmament and peace. To achieve this, the nations of the world must abandon fossil fuels and take action to transform the energy supply. In essence, this means changing the forms of energy storage. Instead of relying on the energy stored in fossil fuels, new technologies suitable for storing renewable energy must be adopted. The use of renewables can help mitigate climate change while increasing supply security and regional autonomy.

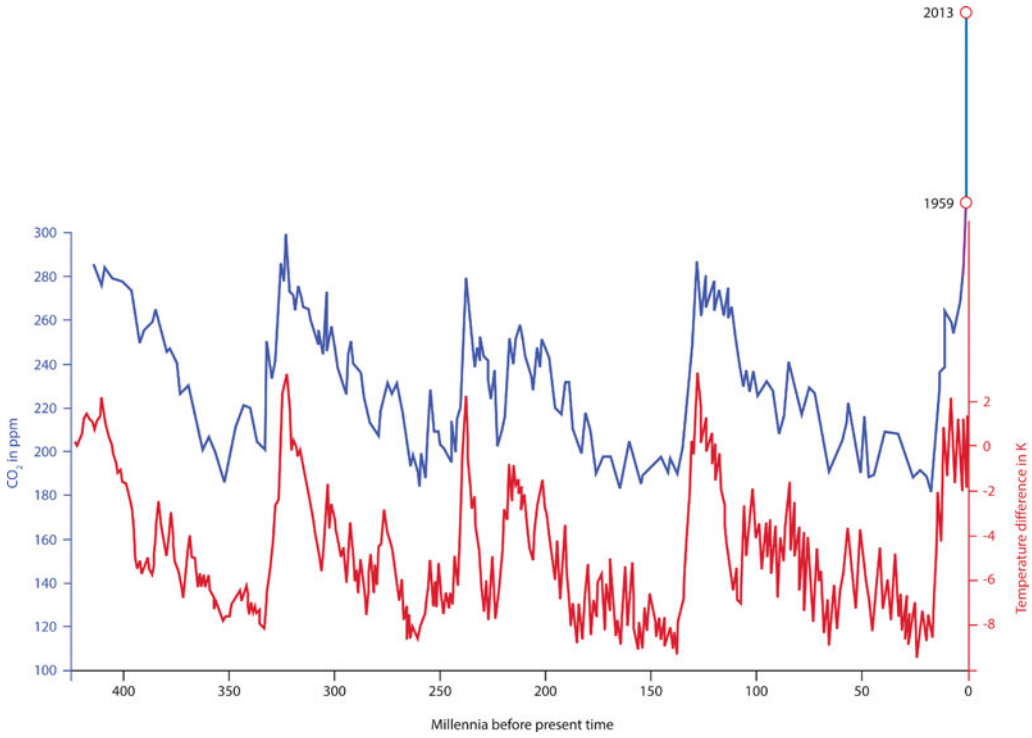



**Fig. 1.13** Correlation of temperature and $CO_2$ concentration in the Earth's atmosphere over millennia; data based on [7]

## Resource Scarcity—an Urgent Issue Independent of Climate Change

Anthropogenic climate change is not the only reason for a move to renewables. Stored fossil energies are being depleted at an extremely rapid rate. Even the addition of new chemically-extracted fossil fuels such as shale gas or shale oil cannot reverse this trend but only delay it temporarily. One study has dated the global peak of fossil and nuclear energy to the current decade [14] (Fig. 1.14).

The International Energy Agency (IEA) unintentionally provided evidence for potential resource scarcity when, in a recent forecast, they stated that future oil demand depends on "fields yet to be found" [2]. Their implicit assumption is that new reserves will continue to be discovered.

The oil and gas industry has pressed on with the extraction of unconventional fossil energies, such as tar sands oil, shale oil, and gas. As these have higher carbon footprints and are particularly harmful to the climate, it is only prudent to consider the end of the fossil age and draw some conclusions. Estimates of the remaining reserves of fossil energy vary widely, but sooner or later their extraction will become too costly in terms of money, energy, and in terms of the consequences for the climate.

If finding and deploying sustainable energy solutions is delayed, the risk of an abrupt supply shortage will increase, bringing with it price peaks along with political, societal, and economic instability.

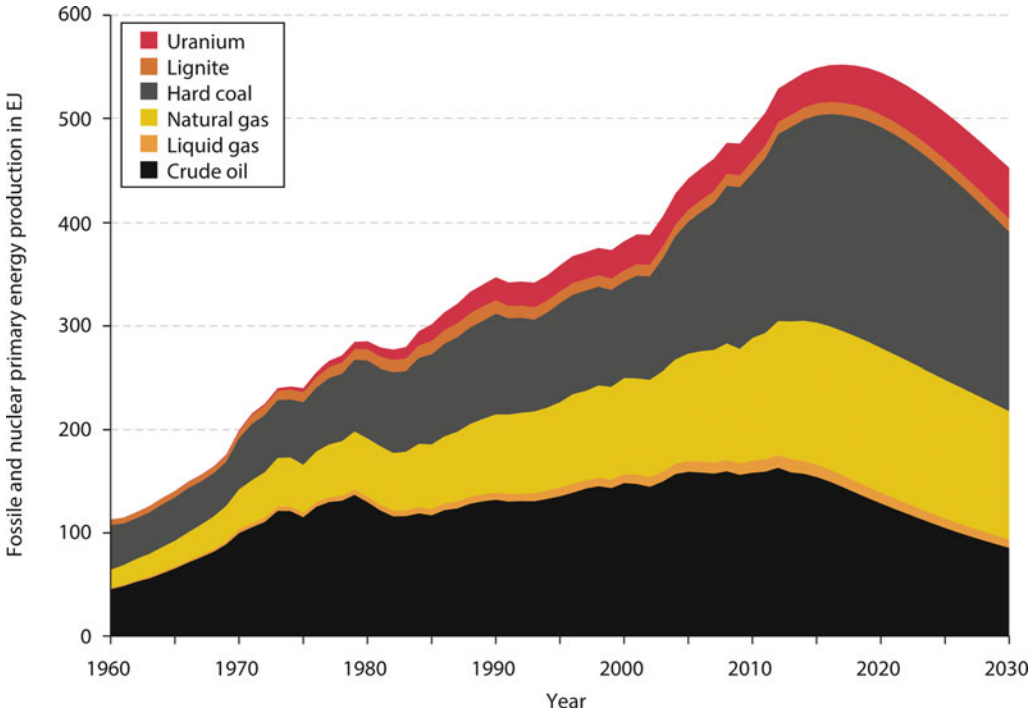



**Fig. 1.14** Global exploitation of oil, natural gas, liquid gas, hard coal, brown coal, and uranium, 1960–2030. (Source: EWG LBST 2014)

### 1.3.2 The Age of Renewable Energy is Only a Question of Time—Scenarios for Change

With dwindling fossil fuel resources and increasing climate change, energy supply security has become a global problem. Hence, Germany and other industrial countries are seeking to transform the energy system. Many studies present scenarios for future energy supply. This section presents global scenarios. Part II (Storage Demand) provides scenarios for Germany (▶ Chaps. 3, 4, and 5).

#### ▪ Scenarios for Returning to a Renewable Age

The 2010 Special Report on Renewable Energy Sources by the Intergovernmental Panel on Council Change argues that potential exists for a global energy transition [10]. Another study by the UNEP also came to this conclusion.

Figure 1.15 shows the evolution of primary energy supplies for the years 1850 to 2000 and a scenario for 2000 to 2100 produced by the UN, which depends on coal, oil, gas, nuclear

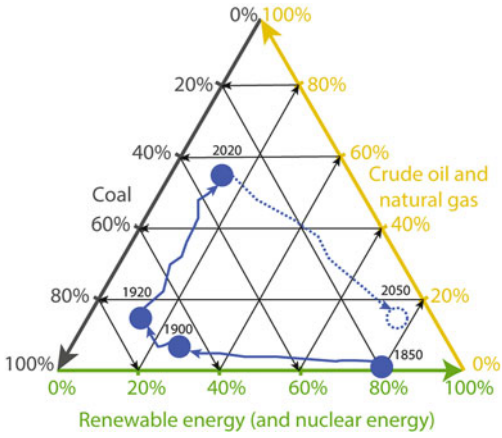



**Fig. 1.15** Evolution of primary energy supplies. (Source: UNEP 2000)

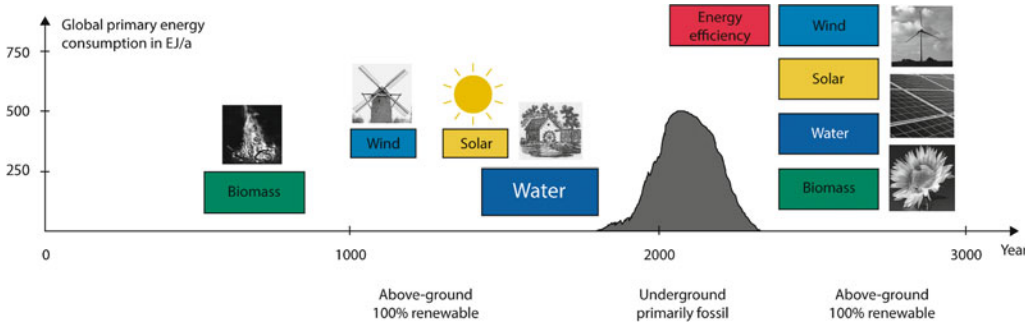



**Fig. 1.16** The beginning and end of the fossil age

energy, and renewables. More scenarios may be found in the climate change assessment reports issued by the IPCC.

For many thousands of years, biomass in the form of firewood was practically the only primary energy source used by human beings. Only as technology advanced did wind-energy, solar energy, and hydropower (mechanical and electrical) enter the mix. In the countries that lead the Industrial Revolution, above-ground renewable energies were displaced by underground depletable fossil energy sources (Fig. 1.16).

But every fossil fuel has a maximum rate of extraction. As global oil production slows, energy from solar, wind, water, and biomass will take over, as was the case before the fossil age. Recognizing this is crucial in discussions about transforming the energy system. And, with the world's population having already passed 7 billion, both energy efficiency and renewables will be essential for future energy security.

The energy resources people use depend on numerous factors. As income increases in developing countries, for instance, their inhabitants consume more liquid fuel and electricity but less firewood.

### Significance of Storage Despite the Decline of Stored Fossil Energy

A scenario simulated by the authors on a global energy transition [11] sheds some light on the role of intersectoral energy storage and the linking of different sectors to fulfill the targets of the Paris climate protection agreement. To reduce the mean global temperature rise significantly below 2 °C without biomass and CCS, a hard phase-out of fossil fuels and a massive expansion of renewable energy and cross-sectoral storage is necessary. The use of wind, hydro and solar energy in the form of electricity as 'primary energy' for power, heat, transport, and non-energetic use of fossil fuels will provide an energy efficient decarbonization. Due to almost no heat waste through the direct use of these renewable electricity resources in combination with storage, combustion engines in power plants, vehicles, and heating systems can be replaced efficiently until 2050 (Fig. 1.17). The core technologies for this kind of pure renewable transformation are wind, hydro, solar energy, e-mobility, heating pumps, CHP, and all kinds of power-to-X (PtX) energy storage links between all sectors. Using PtX, not only would the electricity storage problem be solved but renewable fuels would also be generated for transport segments that cannot use batteries. Furthermore, renewable fuels would be generated for the chemical industry, which currently depends fully on fossil oil and gas for plastics and fertilizers. As a result, the 2 °C goal can be reached without using millions of hectares for biomass, which provokes GHG emissions from land use, land use change, and forestry. Using uncertain and barely socially acceptable technologies like CCS or geoengineering can also be avoided. This 100% renewable scenario is technically doable and shows economic and social benefits in global energy transition.

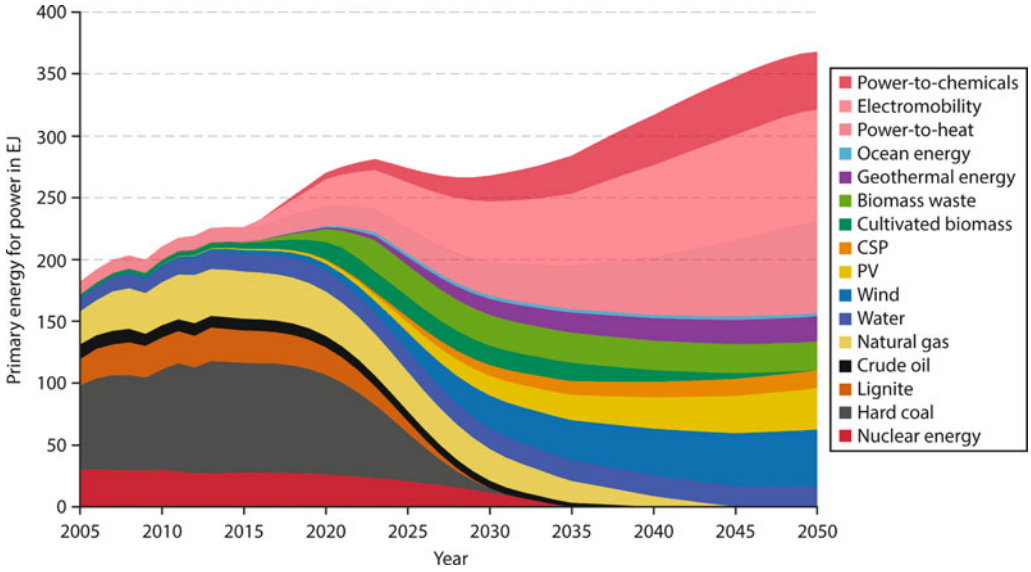



**Fig. 1.17** Own scenario for a global renewable energy transition by 2050, based on intersectoral energy storage and PtX without biomass and CCS [10]

## 1.4 Summary

- Throughout their existence human beings have **relied on sources of stored energy**. The key natural process for energy storage is **photosynthesis**, in which a reaction between water and $CO_2$ creates biomass, but the conversion efficiency is very low at 0.5–2.5%.
- For **many thousands of years** human beings had an **energy supply** that was **100%** renewable, based mainly on wood for energy and feed for animals, which provided transport and other forms of mechanical power.
- In the **Industrial Revolution** people turned to older forms of stored solar energy: biomass that had been transformed into **coal**, **oil**, **and natural gas**. Their use has since risen exponentially, leading to a corresponding release of fossil $CO_2$, which is the cause of **anthropogenic climate change**.
- Today fossil fuels dominate the global primary energy supply. But their **reserves** have entered **terminal decline**, which is why **other sources of energy** must be found as part of a transformation of the energy system.
- The **transformation of the energy system** consists of actions to increase **energy efficiency** and the harnessing of **renewable energies**. The more energy is saved and with increased use of hydropower, wind-energy, and solar energy, the less the dependence on stored fossil energy.
- The **return** to an energy supply based on renewable energies is **technically feasible**, **environmentally necessary**, and **economically beneficial *in the long-term***. The pillars of renewable energy supply are **wind and solar** energy. Storage technologies *and other mechanisms* needed for such a system already exist and will be described in detail in the following chapters.
- Alongside **classic forms of storage**, such as pumped-storage, batteries, and heat reservoirs, technologies that **emulate photosynthesis** will play an important role in the transformation of the energy system; especially in creating fuels for vehicle use from wind and solar energy.

## References


1. Adler S, Munk K (2000) Biochemie, Zellbiologie, Ökologie, Evolution. Spektrum Lehrbuch. Spektrum Akad. Verl, Heidelberg
2. Anton C (ed) (2013) Bioenergie: Möglichkeiten und Grenzen. Halle (Saale) (Stellungnahme)
3. Barber J (2009) Photosynthetic energy conversion: natural and artificial. Chem Soc Rev 38(1):185–196. https://doi.org/10.1039/B802262N
4. Barriopedro D, Fischer EM, Luterbacher J, Trigo RM, Garcia-Herrera R (2011) The Hot Summer of 2010: Redrawing the Temperature Record Map of Europe. Science 332(6026):220–224. https://doi.org/10.1126/science.1201224
5. Berg JM, Tymoczko JL, Stryer L, Gatto GJ (2013) Biochemie, 7th edn. Springer Spektrum, Berlin (Lehrbuch)
6. Boden TA, Marland G, Andres RJ (2009) Global, Regional, and National Fossil-Fuel CO2 Emissions. Oak Ridge
7. BP (2013) Statistical review of world energy. BP, London
8. Campbell NA, Kratochwil A, Lazar T, Reece JB (2009) Biologie, 8th edn. Pearson Studium – Biologie. Pearson Studium, München [u.a.]
9. Deutschland, Fachagentur Nachwachsende Rohstoffe (2012) Basisdaten Bioenergie Deutschland, 2012. Aufl. nachwachsende-rohstoffe.de. Fachagentur Nachwachsende Rohstoffe, Gülzow-Prüzen
10. Edenhofer O, Pichs Madruga R, Sokona Y (2012) Renewable energy sources and climate change mitigation. Special report of the Intergovernmental Panel on Climate Change. Cambridge University Press, New York
11. Edwards G, Walker D (1983) C3, C4. Mechanisms, and cellular and environmental regulation of photosynthesis. Blackwell Scientific Publ, Oxford
12. FAO (2012) State of the world's forests, 2012. Food and Agriculture Organization of the United Nations, Rome
13. FAOSTAT (2013) FAOSTAT Forestry Data. FAOSTAT – Statistical Division of the Food and Agriculture Organization of the United Nations. http://faostat.fao.org/site/630/default.aspx. Accessed 3 Sept 2013
14. Haberl H, Erb KH, Krausmann F, Gaube V, Bondeau A, Plutzar C, Gingrich S, Lucht W, Fischer- Kowalski M (2007) Quantifiying and mapping the human appropriation of net primary production in earth's terrestrial ecosystems. PNAS 104(31):12942–12947
15. IEA (2012) World Energy Outlook 2012. Paris
16. Mihajlovic-Wachter C, Caduff C, Burg Tv (2008) Ökologie/Ethik. Zwei wichtige Aspekte im Unterricht, 2nd edn. Fuchs, Rothenburg
17. Munk K (2008) Taschenbuch der Mikrobiologie. Thieme, Stuttgart
18. NOAA (2013) Trends in Atmospheric Carbon Dioxide. Recent Global CO2. http://www.esrl.noaa.gov/gmd/ccgg/trends/global.html (Created 08.2013)
19. Paappanen T, Leinonen A (2005) Fuel Peat Industry in EU. Brussels
20. Petit JR, Jouze J, Raynaud D, Barkov NI, Barnola J-M, Basile I, Bender M, Chappellaz J, Davisk M, Delaygue G, Delmotte M, Kotlyakov VM, Legrand M, Lipenkov VY, Lorius C, Pepin L, Ritz C, Saltzmank E, Stievenard M (1999) Climate and atmospheric history of the past 420,000 years from the Vostok ice core, Antarctica. Nature 1999(399):429–436
21. Purves WK, Sadava D, Held A, Markl J (eds) (2011) Purves Biologie, 9th edn. Spektrum Akad. Verl, Heidelberg
22. REN21 (2014) Renewables 2014 Global Status Report
23. Sterner M, Bauer F (2016) Weltweit Null-Emissionen bis 2050. Szenarien zur globalen Dekarbonisierung auf Basis erneuerbarer Energien, Sektorenkopplung und Energiespeicher ohne negative Emissionen, Biomasse und CCS
24. Sterner M, Schmid J (2009) WBGU Gutachten – zukunftsfähige Bioenergie und nachhaltige Landnutzung. In: Faulstich M, Mocker M (eds) Biomasse & Abfall. Emissionen mindern und Rückstände nutzen. Dorner PrintConcept GmbH, Sulzbach-Rosenberg, pp 23–38
25. WBGU (2008) Climate Change as a Security Risk. Springer, Berlin, Heidelberg, New York
26. WBGU (2008) Welt im Wandel: Sicherheitsrisiko Klimawandel. Springer, Berlin
27. Zittel W (2013) Fossile und Nukleare Brennstoffe. Die künftige Versorgungssituation. Fossil and Nuclear Fuels – the Supply Outlook, Berlin

# Definition and Classification of Energy Storage Systems

*Michael Sterner and Franz Bauer*

**2.1 Definition and Application – 24**

**2.2 The Use of Storage Systems – 30**

**2.3 Classification of Storage Systems – 33**
2.3.1 Classification by Physical Energy Form – 33
2.3.2 Calculation of Relevant Parameters – 36
2.3.3 Temporal Classification – 42
2.3.4 Spatial Classification – 44
2.3.5 Economic Classification – 45

**2.4 Summary – 46**

**References – 47**

**Electronic supplementary material** The online version of this chapter (https://doi.org/10.1007/978-3-662-55504-0_2) contains supplementary material, which is available to authorized users.

© Springer-Verlag GmbH Germany, part of Springer Nature 2019
M. Sterner, I. Stadler (Eds.), *Handbook of Energy Storage*, https://doi.org/10.1007/978-3-662-55504-0_2

2

**Overview**

**Energy supply** always requires **energy storage—either as an intrinsic property or as additional system**. It is an intrinsic property of solid, liquid, and gaseous fuels, although less so of water-borne heat, but not of electricity. So to meet variable demands and supplies, heat and electricity networks usually require additional storage systems. When they are added to an energy network, should they be viewed as 'suppliers' or as 'consumers'? Who is responsible for covering the costs of storage systems? To categorize storage systems in the energy sector, they first need to be carefully defined.

This chapter **defines** storage as well as storage systems, describes their **use**, and then classifies storage systems according to temporal, spatial, physical, energy-related, and economic criteria.

## 2.1 Definition and Application

### ■ Definitions

Clear terminology is required to accurately describe and categorize the range of energy storage systems.

**Definition**

A **storage unit** is a facility or container to stock, store, and preserve goods.

**Definition**

An **energy storage** is an energy technology facility for storing energy in the form of internal, potential, or kinetic energy. An energy storage system performs three processes: **charging** (loading), **storing** (holding), and **discharging** (unloading). These processes are physically implemented by energy converters (charging and discharging), storage units (holding), and peripherals. A complete facility, including all of these components, is called an **energy storage system**.

**Definition**

An **energy carrier** is a material that stores energy. It is found in the storage unit of an energy storage system.

Figure 2.1 illustrates the definition of an energy storage system whose most important parameters are described in ▶ Sect. 2.3.2. In purely scientific terms, the storage unit, or simply the container that stores the energy carrier, is the (energy) storage system. In addition, energy converters are required for charging, discharging, and operating the peripherals. Together these units compose an energy storage system, which is also commonly called simply a storage system. In this book, the term 'energy storage' is sometimes used instead of the longer term, 'energy storage system', to refer to a facility combining all three processes.

### ■ 'Loading and Unloading' vs 'Charging and Discharging'

In general usage, stores are often described as being subject to 'loading' and 'unloading'. However, in academic discussions, and within this book, these processes are called 'charging' and 'discharging'.

### ■ Extent of the Energy Storage System

The three processes of charging, storing, and discharging need not be linked with any specific medium, device, or location. The network energy carrier can differ from the storage medium, which may be accessed via a heat exchanger. The three processes may be performed within a single device, or by three separate devices. The former must be in a single location, but the latter need not.

With batteries and capacitors, the three processes are performed within a single device, hence in a single location. Electrical energy is converted and stored chemically on the electrodes or in the active material and double layer. Battery storage systems are composed of battery cells or battery packs (storage units), power electronics (energy converter) for charging as

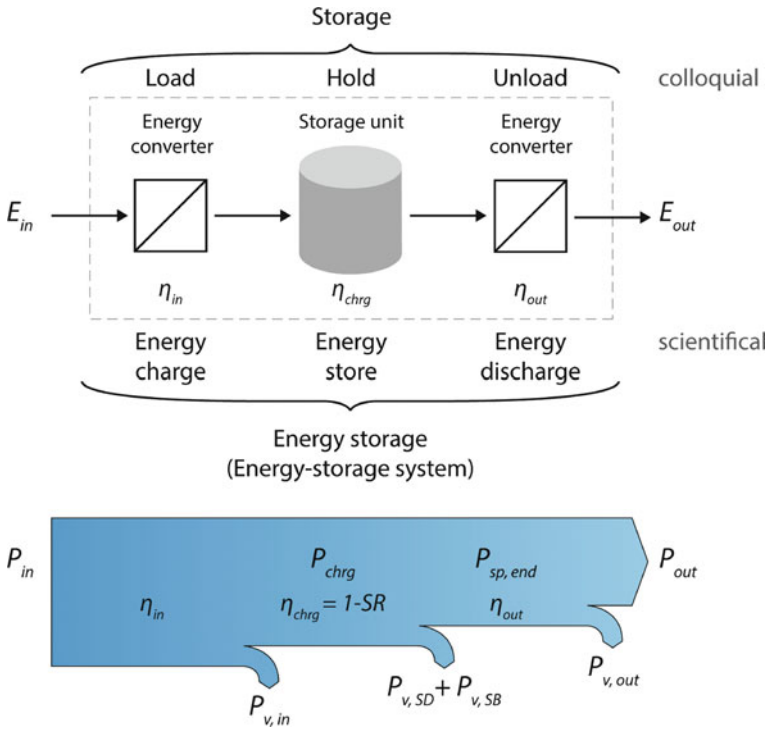



**Fig. 2.1** Energy storage system definition based on the triad of charging (loading), storing, and discharging (unloading), as well as the essential physical dimensions. A facility system includes all three of these components. As a result, energy storage can also be called an energy storage system (which are also commonly called storage systems)

well as discharging, and a battery management system (peripheral). The complete system is called an energy storage facility.

In a pumped-storage plant, the three processes are performed by three separate devices, but in a single location. Thus, charging is performed by an electric motor-driven pump that moves water from a lower reservoir to an upper reservoir. The upper reservoir stores 'potential' energy, the amount depending on the quantity of water and the difference in elevation between the upper and lower reservoirs. Discharging is performed by water from the upper reservoir flowing down through a turbine connected to an electric generator, and so to the lower reservoir. Thus, pumps and turbines are 'energy converters', which form an energy storage system with the upper and lower reservoir and ancillary units.

For a power-to-gas (PtG) energy storage system, the electrolysis and methanation plant used for charging, the gas storage tank (storage unit), and the gas-fired (heat and) power plant used for discharging (both energy converters), may all be in different geographical locations.

The power rating, the energy capacity, and the 'round-trip' efficiency of an energy storage system all depend primary on those of the three processes, whether performed in a single device or three separate devices.

### Energy Storage System Subcategories

Energy storage systems may be divided into primary and secondary energy storage systems, as well as sectoral and cross-sectoral energy storage systems. The definition of sector coupling is also crucial here.

2

**Definition**

**Primary energy storage systems** are energy storage systems that are charged and discharged only once.

**Definition**

**Secondary energy storage systems** are energy storage systems that may be charged and discharged multiple times.

Primary energy storage systems include energy carriers with intrinsic storage, such as solid, liquid, and gaseous fuels, in coal dumps, oil tanks, and gas vessels. In the case of fossil fuels, the stored energy originates from the Sun via photosynthesis, producing biomass which, over very long periods of time, is transformed into primary energy carriers. These can be discharged only once. They are burned in power and heating plants, and are used to power transport vehicles. Similarly, primary (or 'disposable') batteries, which are assembled from 'energetic' chemicals, can also be discharged only once.

Secondary energy storage systems are 'rechargeable'. They include electrical devices such as capacitors and inductors, electrochemical devices such as secondary (or rechargeable) batteries, kinetic energy devices such as flywheels, potential energy systems such as pumped-storage plants, compressed air energy storage systems (CAES), and chemical storage systems holding gases or liquids (hydrogen or hydrocarbons) in tanks or underground caverns. All these can be charged multiple times with renewable energies such as biomass (from photosynthesis), biogas (from anaerobic digestion), renewable fuels (from renewable PtG and power-to-liquid, or PtL, plants), and discharged multiple times with appropriate technologies.

**Definition**

**Sectoral energy storage systems** are energy storage systems used in only one energy sector. With these storage systems, both charging and discharging occurs in the same sector.

**Definition**

**Cross-sectoral energy storage systems** are energy storage systems that may be used in more than one energy sectors, and in one or both directions, thereby linking two or more sectors. Charging and discharging do not necessarily occur in the same sector.

**Definition**

**Sector coupling** connects the electricity, heating, and transportation sectors with the 'non-energetic consumption of fossil raw materials' (especially in the chemical industry) using energy storage systems and energy converters. Renewable electricity is typically used as a primary energy source to decarbonize the other sectors.

When discussing energy storage systems, the division into the subcategories of sectoral and cross-sectoral is significant. The following is a detailed examination of this important distinction. Energy storage systems are essential for sector coupling, because this is not feasible without energy storage.

### ■ Sectoral Energy Storage Systems: Electricity Storage Systems, Heat Storage Systems, Fuel Storage Tanks, and Gas Storage Tanks

Examples of sectoral energy storage systems are pumped-storage plants (electricity sector), thermal storage units (heat sector) and gaseous, and liquid fuel tanks (transport sector). Such energy storage systems are integrated via networks into larger systems, but only for end users in the same energy sectors. However, gas storage tanks and caverns can be used by end users via sector linking in all three sectors (electricity, heat, and transport).

**Electricity storage systems** include those that store electrical energy directly; for example, electrostatically (in capacitors) or electromagnetically (in inductors) (▶ Chap. 6). However, electrical energy may also be converted into another form, such as electrochemical

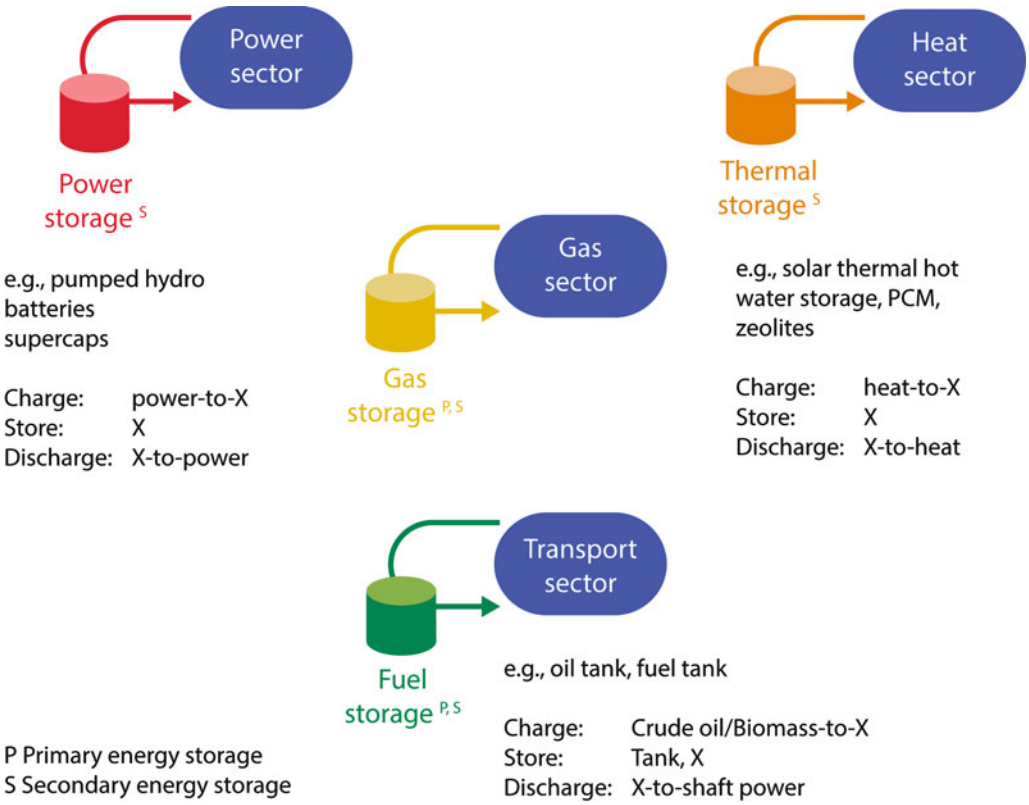



**Fig. 2.2** Definition of sectoral energy storage systems using electricity storage facilities, heat storage systems, liquid fuel tanks, and gas tanks as examples

(in secondary batteries), thermal (in high-temperature stores), kinetic (in flywheels), potential (in pumped-storage and CAES), and chemical (in synthetic fuel plants, such as PtG and PtL). Upon discharging the storage system, electrical energy is available again, albeit reduced by the round-trip efficiency (Fig. 2.2).

### Example of Electricity Storage: Pumped-Hydro Storage (PHS)

**Charging:** – electrical energy is converted into mechanical stored (potential) energy by pumping water from a lower reservoir to an upper reservoir.
**Storing:** – the amount of potential energy stored is determined by the accessible water volume in the upper reservoir and the height difference between this and the lower reservoir.
**Discharging:** – the potential energy of the water is converted into rotational (kinetic) energy by a turbine, which drives a generator producing electricity.

**Heat storage systems** store heat using sensible, latent, or thermochemical heat storage (▶ Chap. 10). As with electricity storage facilities, the energy stored can be converted back into heat, again with losses that reduce the efficiency (Fig. 2.2).

### Example of Heat Storage: Solar-Thermal Plant

**Charging:** – solar radiation heats solar collectors containing (typically) a circulating water-glycol mixture. The heat in this liquid is then transferred via a heat exchanger to water in a storage tank.
**Storing:** – the heat is stored as sensible heat in buffer storage units (water tanks) with a temperature difference between the heated water and the cold water.
**Discharging:** – the thermal energy of the heated water may be transferred directly or via a heat exchanger. This may be used for space heating, producing domestic hot water (DHW), or for process heating, for example in breweries.

**Storage systems for fuels** store chemical energy in the form of hydrocarbons or other energy carriers (▶ Chap. 8). For conventional fuels, the original production process is photosynthesis (▶ Sect. 1.1.1). For synthetic renewable fuels, the production process that mimics photosynthesis is PtG or PtL. The charging and discharging of storage tanks and caverns is done with pumps or compressors (◘ Fig. 2.2). Finally the chemical energy in the fuels is converted into thermal and mechanical energy, in heating systems and combustion engines. Therefore, such fuels can act as cross-sectoral storage systems.

**Example of Fuel Storage: Fuel Storage Tanks and the Use of Crude Oil for Transport**

**Charging:** – the fuel is pumped into a fuel tank. The fuel has previously been charged with solar energy by photosynthesis, collected as biomass or crude oil, and then processed into fuel.
**Storing:** – the fuel stored in the tank is an energy carrier containing chemical binding energy.
**Discharging:** – the fuel is transferred from the tank into an engine, where it is converted into thermal and mechanical energy.

### ▪ Cross-Sectoral Energy Storage Systems: PtG, Power-to-Heat—PtH, PtL, Power-to-Chemicals—PtC, Power-to-X—PtX, and Electric Vehicles

A classic example of a cross-sectoral energy storage system is (night) storage heaters that link 'off-peak' electricity to the heat sector. A modern version is called PtH. Here, heat pumps and resistance heaters convert (primarily) wind and solar electricity, but also balance energy (gray electricity) into heat. For the electricity sector, PtH systems are almost always end users. Although conversion of low-grade heat back to power is possible, e.g., via organic Rankine cycle (ORC) plants, the thermodynamic efficiency is low and are rarely economically feasible (◘ Figs. 2.3 and 2.4). The reconversion of heat out of PtH is also called power-to-heat-to-power (PtHtP).

PtG technology has unique attributes. In principle, it is a charging technology, using water electrolysis to produce hydrogen (▶ Sect. 8.2), and optionally, combining it with carbon dioxide to synthesize methane (▶ Sect. 8.3). However, the gas is an energy carrier that can be stored and transported in the gas infrastructure, and used by all three energy sectors (▶ Sect. 2.3).

The electricity sector can use PtG synthesis plants as part of an electricity storage system. After the gas has been made and stored, it may be discharged and converted via gas-to-power devices, such as gas-fired power plants (◘ Figs. 2.3 and 2.4). Thus a proportion of the original electricity, less conversion losses, is returned to the electricity sector (◘ Fig. 2.2).

The electricity and heat sectors can be linked by PtG synthesis plants and burning the resulting gas in boilers, CHP plants, etc. (◘ Figs. 2.3 and 2.4).

The electricity and transport sectors can be linked by synthesizing fuels in **PtG, PtL**, or more generally, PtF plants. The synthetic fuels, or 'e-fuels', can be stored in tanks and caverns for later use. Their main advantage is the use of existing infrastructure and technology: pipelines, tanks, filling stations, and motors.

The electricity and transport sectors can also be linked by electric vehicles; currently only in one direction, although in principle, in both directions. In the former case, electric vehicles act as end users, but in the latter case, with so-called 'Vehicle-to-Grid' (V2G) technology, their batteries could act as storage systems for the electricity sector.

### ▪ Sector Coupling, PtX, and PtC

Linking the electricity sector to other sectors is typically called sector coupling. The definition of this term is derived from the definition of cross-sectoral energy storage systems.

PtX is a general term covering PtH, PtG, PtL, and PtC (▶ Chap. 5). ◘ Figure 2.4 shows the various possible links. For the sake of simplicity, the non-energetic consumption of fossil raw materials sector (for example, production of plastics, fertilizers, etc.) which is separately

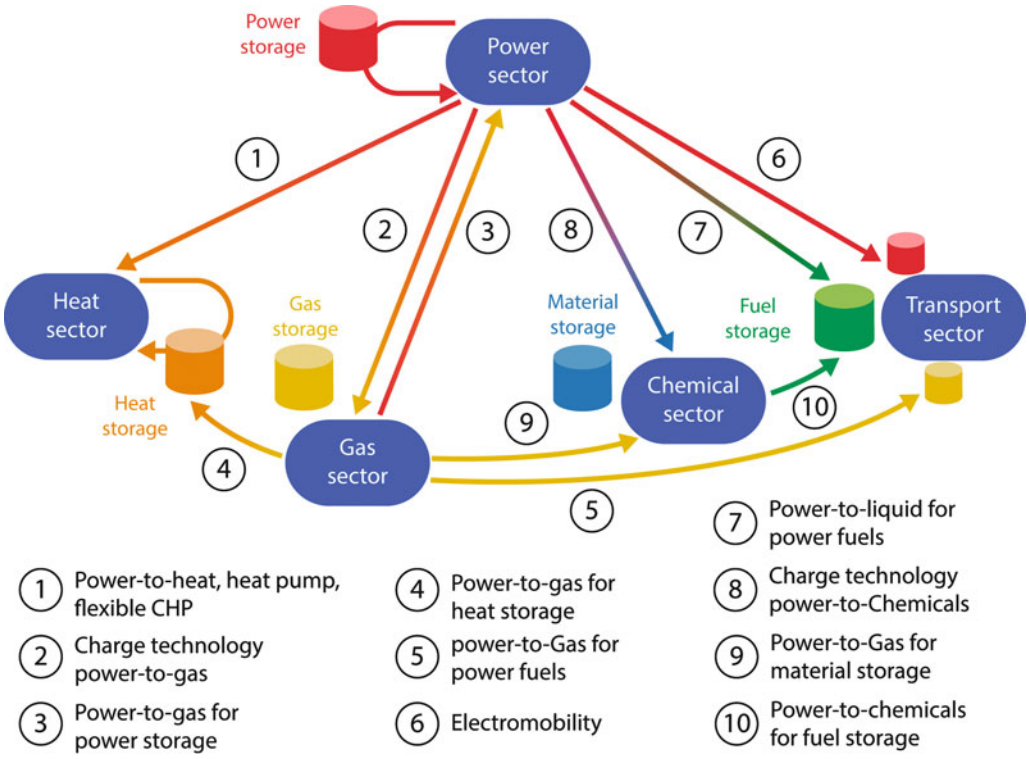



**Fig. 2.3** Examples of cross-sectoral energy storage systems respectively sector coupling, including those using PtH, combined heat and power (CHP), heat pumps, PtG, electric vehicles, PtC, and PtL. All processes which use electricity as primary energy can also be called PtX

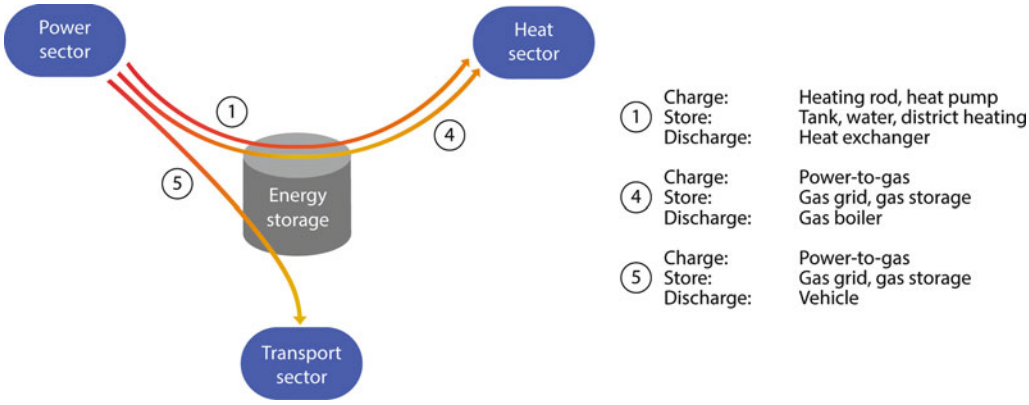



**Fig. 2.4** Examples of cross-sectoral energy storage systems. PtH (1): links the electricity and heat sectors by electrical resistance heaters or heat pumps, with or without heat storage; PtG for heating (4): links the electricity and heat sectors with PtG for charging existing gas storage tanks and gas-fired boilers for discharging; PtG for fuels (5): links the electricity and transport sectors with PtL, power-to-fuel (PtF) for charging, and heat engines for discharging

accounted for in energy balances is called the 'chemical sector' in the illustration.

In principal, the production of raw materials for the chemical industry using PtC could also be viewed as a storage process if the use of renewable energy sources for that purpose frees stored fossil energy in the form of natural gas, oil, or coal for other energy-related applications (▶ Sects. 8.6 and 13.3). These units could as well provide positive and negative reserve capacity in the electricity sector or be used for load-management. In fact, all of these technologies could provide additional flexibility for balancing fluctuations of supply and demand in the electricity sector.

In Germany, there are plans to replace the concept of end users with a concept of final energy release calculated uniformly across all sectors. This would economically facilitate the transfer of energy from sector to sector without doubling or tripling the release. This concept is particularly relevant in the case of network congestion. Network congestion results in compensation payments in the billions for unused renewable electricity (feed-in management), and for balancing that energy afterwards (redispatch). Designing the storage infrastructure and the electricity network infrastructure in parallel, therefore, seems to make good sense.

### ▪ Combinations of Charging, Storing, and Discharging

Table 2.1 shows possible combinations of charging, storing and discharging processes.

### ▪ PtC as an Energy Conversion Process

PtC technology is not discussed in detail because it is usually regarded as an energy conversion technology. However, the production of chemical compounds could also be viewed as part of an energy storage system. Such PtC plants could be subject to load-management, providing reserve capacity for balancing fluctuations of supply and demand in the electricity sector.

## 2.2 The Use of Storage Systems

The purpose of energy storage systems is to balance supply and demand temporally (over time). They complement energy networks, which are for balancing supply and demand spatially (across space).

**Example**

The use of electricity storage facilities is often used as an argument against expanding electricity networks. This argument is, however, not valid because the two perform different functions:

**Electricity network:** – **spatial balancing**
**Electricity storage systems:** – **temporal balancing**

Local intermediate storage of electricity at the location of electricity generation or consumption could help relieve network shortages if its use benefits the network, and it is not market-driven. But electricity storage systems are not a substitute for spatial balancing.

However PtG has unique attributes: electricity can be shifted in time by storing the resulting gas in the gas infrastructure, and shifted in space by transporting it over the gas network.

Energy storage systems can be used to balance fluctuations—absorbing surpluses and making up deficits (supply gaps or shortages). Balancing these is important for heat supply. The output of solar-thermal plants rarely matches the demand for hot water or space heat. Hot water (buffer) tanks can absorb surpluses and then make up deficits at a later time (in the evening or at night). The effective 'storage capacity' of such tanks is determined mainly by their volume and heat losses.

Electricity networks can also benefit from energy storage systems. They can supply positive and negative reserve power capacity and balancing energy to the electricity network (reserve markets and supply balancing). This can avoid curtailing the output of wind and solar farms, thus increasing the use of environmentally-friendly energy.

**Table 2.1** Examples of energy storage and conversion technologies and their applications

| Storage class | Storage technology | Charging | Storing | Discharging | For the electricity sector | For the heating sector | For the transport sector |
|---|---|---|---|---|---|---|---|
| **Sectoral** | | | | | | | |
| Electric | Capacitors | Direct | Electric field | Direct | Electricity storage, short-term | – | Recuperation, short-term electricity storage |
| | Inductors | Direct | Magnetic field | Direct | Electricity storage, short-term | – | – |
| Electrochemical | All batteries except redox flow | Integrated electrochemical conversion | electrode or active material | Integrated electrochemical conversion | Electricity storage, short and long-term | – | – |
| | Redox flow battery | Pump, cell | Tank, chemical compounds | Pump, cell | Electricity storage, short and long-term | – | – |
| Chemical | Fuel storage tank | Pump, photosynthesis | Tank, fuel, cavern | Pump, burner, engine | – | Fuel storage tank | Fuel storage tank |
| Mechanical | Pump-storage plant | Pump, engine | Upper reservoir, water | Turbine, generator | Electricity storage, short and long-term | – | – |
| | Compressed air energy storage system | Compressor, engine | Cavern, pipe, heat storage system | Turbine, generator | Electricity storage, short-term | – | – |
| | Stored-energy storage system | Pump, engine | Movement of granite, rock | Turbine, generator | Electricity storage, short and long-term | – | – |
| | Flywheel energy storage system | Engine | Rotational energy | Generator | Electricity storage, short-term | – | – |
| | Elastic-energy storage system | Mechanical work | Stored energy | Mechanical work | Electricity storage, short-term | – | Emergency brake in case of vehicle power failure |

**Table 2.1** (Continued)

| Storage class | Storage technology | Charging | Storing | Discharging | For the electricity sector | For the heating sector | For the transport sector |
|---|---|---|---|---|---|---|---|
| Thermal | Hot water tank | Heat exchanger | Tank, water | Heat exchanger | – | Heat storage | – |
| | Latent-heat storage | Heat exchanger | Phase-change materials (PCM) | Heat exchanger | – | Heat storage | – |
| | Thermochemical storage | Chemical energy conversion | Zeolites, tanks | Chemical energy conversion | – | Heat storage | – |
| **Cross-sectoral** | | | | | | | |
| Electrochemical | Electric vehicles batteries | Power electronics, integrated electrochemical process | Electrode | Electric vehicles, hybrid | Load-management | – | Energy supplier |
| Chemical | PtG electricity | Electrolysis, methanation | Gas network, gas storage system | CCGT, gas turbine | Electricity storage, long-term | – | – |
| | PtG heating | Electrolysis, methanation | Gas network, gas storage system | Gas-fired boiler | Load-management | Heating supplier | – |
| | PtG mobility | Electrolysis, methanation | Gas network, gas storage system | Gas vehicle, car | Load-management | – | Fuel supplier |
| | Hydrocarbons | Photosynthesis | Biomass, fossil energy, gas storage system | Combustion technology | Electricity storage | Heating supplier | Fuel supplier |
| Thermal | PtH | Heating element, heat pump | Tank, water, heating network | Heat exchanger | Load-management | Heating supplier | – |
| | Absorption heat storage | Heating element, heat pump | Zeolites, etc., tank | Heat exchanger | Load-management | Heating supplier | – |
| Mechanical | Drive system | Engine | flywheel (kinetic energy) | | Load-management | – | Drive |
| | Brake energy recovery | | flywheel (kinetic energy) | Generator | Load-management | – | Brake |

Moreover, the storage systems used with conventional electricity generation can also be used for renewable energies. Pumped-storage plants, compressed air energy power plants, and electric storage heaters have long been used to shift 'electricity surpluses' at night to meet peak loads during the day. This allows nuclear and coal power plants to operate at constant 'base' loads, which gives the maximum economic efficiency and the simplest operation without load changes. That in turn reduces specific $CO_2$ emissions per kW h of electricity. However it also increases the ecologically harmful nuclear and fossil wastes released into the environment. Even if these power plants produce lower specific emissions when operating at maximum efficiency, using storage systems to increase their output still produces greater total emissions.

The geopolitical purpose of energy storage systems is to ensure security of supply. Yet supply still relies, to a large extent, on energy stored as biogenic and fossil energy (▶ Chap. 1). Therefore, Germany and other countries keep very large strategic reserves of oil and natural gas. The latter also allows the supply of gas, imported predominantly from Russia and Norway, to be decoupled from demands related to seasonal fluctuations (winter/summer). They can also cover peaks in electricity demand by supplying gas to gas-fired power or CHP plants.

One example is the Etzel storage facility in Lower Saxony, southwest of Wilhelmshaven. It currently includes 62 underground caverns with a geometric volume of 38 million $m^3$. Of these, 23 are used for crude oil, with a storage capacity of over 10 million $m^3$ (10 billion liters, 63 million US barrels). They hold the strategic oil reserves of Germany and other European nations. In addition, they are used for temporary storage of natural gas imports and to cover consumption peaks. Currently, 39 of the Etzel caverns can store natural gas with a 'working' volume of around 3.5 billion N $m^3$, amounting to approximately 4% of Germany's annual gas consumption (◘ Fig. 2.5).

The German caverns are salt domes over 250 million years old, and very well-suited for oil and gas storage. In total, the German oil reserves could meet the nation's demand for 90 days. In addition, the total underground gas storage capacity is equivalent to 217 TW h, which is about 25% of Germany's annual gas consumption of approximately 900 TW h.

#### ▪ Categorization of Energy Supply Storage Systems

Energy storage systems can be categorized as primary and/or secondary for each link in the energy conversion chain from the Sun to useable energy (◘ Fig. 2.6). The Sun is a very long-term and safely distant fusion reactor, the radiation from which drives biomass production, as well as wind and water cycles.

The conclusion is obvious: without energy storage systems, energy supply is not feasible. Energy storage systems are essential elements of our energy system.

## 2.3 Classification of Storage Systems

Besides defining and categorizing energy storage systems, classifying them allows them to be compared effectively (▶ Chap. 12). Several approaches to classification will be discussed. This section classifies them according to their characteristics and application areas, which offers important insights. (◘ Fig. 2.7).

### 2.3.1 Classification by Physical Energy Form

It is common practice to classify energy storage systems according to the physical form of energy stored. The following are the basic forms of stored energy:

- Electrical energy, including electrical power as well as electrostatic or electromagnetic energy.
- Chemical energy, including molecular binding energy.

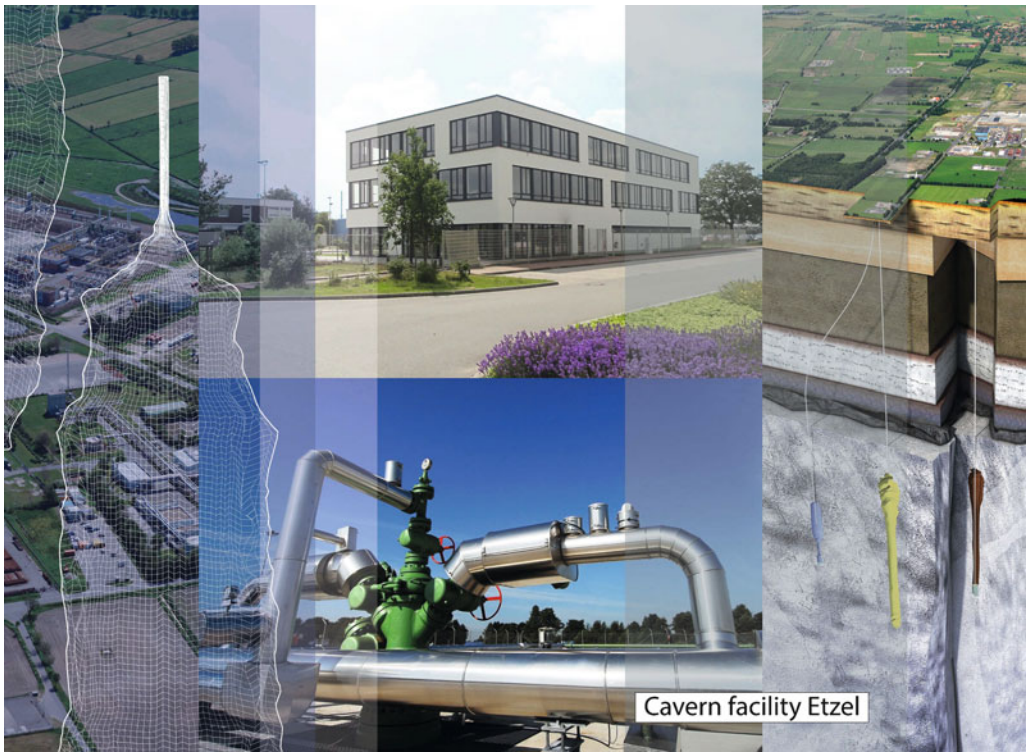



**Fig. 2.5** The Etzel storage facility southwest of Wilhelmshaven, with 23 crude oil caverns and 39 gas caverns, is the largest German storage facility for strategic oil and gas reserves (Source: IVG Caverns GmbH)

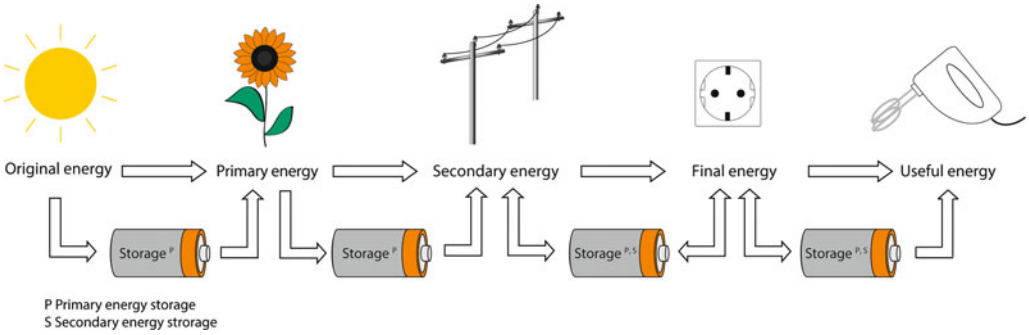



**Fig. 2.6** Categorization of energy storage systems in the energy conversion chain

- Mechanical energy or kinetic and potential energy.
- Thermal energy for heating and cooling.

These four energy forms themselves can be broken down into significant subgroups.

For example, mechanical-energy storage systems include the subgroup of potential energy storage systems such as pump-storage plants (PSP), as well as the subgroup of kinetic energy storage systems such as flywheels.

In electrochemical-energy storage systems such as batteries or accumulators, the energy is stored in chemical form in the electrode materials, or in the charge carriers in the case of redox flow batteries. As a result, they are

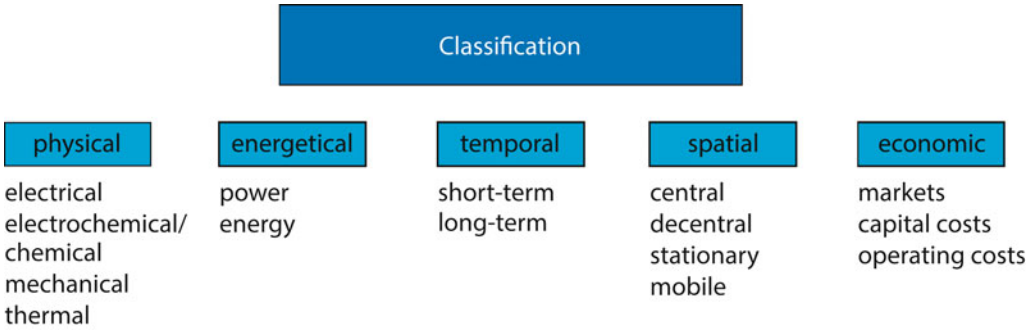



**Fig. 2.7** Classification of energy storage systems

a subgroup of chemical-energy storage systems. However, this subgroup is so large that an entire chapter in this book (▶ Chap. 7) is dedicated to them as a separate class of storage systems, which are in addition to the four energy forms.

Another subgroup is electromagnetic energy storage systems. This form of electric-energy storage uses an alternating electromagnetic field.

There is no such thing as a purely magnetic energy storage system. This is because there are no magnetic charges. Magnetism is caused by moving electric charges. It exerts its effects on moving electric charges as well. As with the theory of relativity, only the relative motion of electric charges is relevant here. In electromagnets, these moving electric charges are the moving electrons in a current-carrying conductor (coil). In permanent magnets, they are the atomic ring currents produced by the orbit of electrons around the atomic nucleus together with the electrons' spin [4]. It is, however, still common to call these magnetic-energy storage systems, even though these are always electromagnetic-energy storage systems. However, they are counted as electric-energy storage systems due to their physical characteristics.

Since this classification by energy form is the most common and convenient one used, it is used to structure Part III (Storage System Technologies, ▶ Chap. 12).

- **Electricity Storage Systems (Electromagnetic Storage Systems, Electrostatic Storage Systems)**

Electricity storage systems store energy in electrostatic fields, such as bi-layer capacitors, and in magnetic fields, such as superconducting coils. They are exclusively secondary energy storage systems.

Electricity as direct current can be stored electrostatically using capacitors. These often have two layers, hence the name double-layer capacitors (so-called *supercaps*). Electricity as alternating current can be stored in electromagnetic fields using coils (inductors). The magnetism is caused by, and affects, moving electric charges, which are electrons moving in a current-carrying coil. Maintaining these fields without an external energy supply to offset standing losses requires a very low internal resistance (ideally near zero). So electromagnetic energy stores rely on superconductors and are named accordingly (superconducting magnetic-energy storage, SMES).

Another type of electromagnetic storage uses permanent magnets. In this case, the moving electric charges are electrons orbiting the nucleus, together with their spin, producing atomic ring currents [4].

Storage systems that store electric energy directly, using electrostatic and electromagnetic technologies, are discussed under electricity storage systems in ▶ Chap. 6.

### Chemical Storage Systems

Chemical storage systems contain primary or secondary energy converted into energy carriers with high energy-densities. They include gases such as hydrogen, natural gas, windgas, biogas, liquids such as methanol, ethanol, gasoline, kerosene, and diesel and solids, such as biomass, coal, ethylene, and propylene.

Charging involves either a natural process (photosynthesis) or a technical process (PtG, PtL). The resulting energy carriers may be stored in tanks or caverns. Discharging typically involves combustion processes and the conversion of thermal energy into mechanical or electric energy. Fuels such as hydrogen can also be converted via a fuel cell into electric energy. Individual components and complete systems of this kind are presented in ▶ Chap. 8.

### Mechanical Storage Systems

Mechanical storage systems exploit the energy stored in gaseous, liquid, or solid media due to their position (potential), speed (kinetic), or thermodynamic state (pressure). They include CAES, pumped-storage plants, flywheels, mechanical stored energy, and springs. They are predominantly used to store secondary energy and are described in more detail in ▶ Chap. 9.

### Thermal Storage Systems

Thermal-energy storage systems are secondary energy storage systems that store heat. They can be grouped by the technology used:

- Sensible-heat storage systems store energy within a medium, changing in temperature before and after charging, which can be 'felt'. This is multiplied by the heat capacity and mass of the medium to determine the amount of energy stored. Sensible-heat storage systems, such as hot water tanks, are found in almost every home and require adequate thermal insulation.
- Latent-heat storage systems store energy without the medium changing in temperature, which cannot be 'felt'. Charging and discharging involves changing the state of the medium, as in PCM, and using the resulting enthalpy. In buildings, latent-heat storage systems can store and release heat with small temperature swings, and have low standing losses.
- Thermochemical heat storage systems use thermoreversible chemical reactions. The storage system is charged by an endothermic reaction, absorbing the resulting enthalpy. This is then discharged by an exothermic reaction.

Thermal-energy storage systems are described in more detail in ▶ Chap. 10.

### Electrochemical Storage Systems

In electrochemical-energy storage systems, such as batteries or accumulators, the energy is stored in chemical form in the electrode materials, or in the case of redox flow batteries, in the charge carriers.

While electrochemical storage systems could be seen as a subgroup of chemical-energy storage systems, they are sufficiently distinct from the four energy forms above to be covered in a separate chapter (▶ Chap. 7).

## 2.3.2 Calculation of Relevant Parameters

### Relevant Physical and Energetic Parameters for Storage Systems

The physical parameters of various storage systems can also be compared. These determine which are appropriate for various specific purposes. ◘ Table 2.2 shows a selection of relevant parameters. Others include the number of cycles (cycle life) per day, week, or year, the storage filling level, and the *reaction* time (access time). With batteries, the depth of discharge (DOD) and state of charge (SOC) are also important.

These performance and energy parameters also determine the technical benchmarks for energy storage systems [2].

They are divided among the three energy storage processes: charging (converting energy), storing (holding energy), and discharg-

ing (converting energy). In the following discussion, these parameters are categorized and defined in terms of power, energy, and other criteria.

### ■ Power Parameters

The charging power $P_{\text{chrg}}$ (or supplied power $P_{\text{sup}}$ or loading power $P_{\text{load}}$) of a storage system is equal to the energy supplied and stored $E_{\text{chrg}}$ per charging time $t_{\text{chrg}}$ (Eq. 2.1). Similarly, the discharging power $P_{\text{dischg}}$ (or consumed power $P_{\text{cons}}$ or unloading power $P_{\text{unload}}$) is equal to the energy consumed and discharged per discharging time (Eq. 2.2). Both powers are expressed in watts (W).

$$P_{\text{load}} = P_{\text{chrg}} = \frac{dE_{\text{chrg}}}{dt} = \left.\frac{E_{\text{chrg}}}{t_{\text{chrg}}}\right|_{E=\text{const}}, \tag{2.1}$$

$$P_{\text{unload}} = P_{\text{dischg}} = \frac{dE_{\text{dischg}}}{dt} = \left.\frac{E_{\text{dischg}}}{t_{\text{dischg}}}\right|_{E=\text{const}}. \tag{2.2}$$

A number of power losses may occur across the entire storage cycle (Fig. 2.1). The charging efficiency of the energy storage system $\eta_{\text{chrg}}$ determines the charging power losses $P_{V,\text{echrg}}$ (Eq. 2.3). Similarly, the discharging efficiency $\eta_{\text{dischg}}$ determines the discharging power losses $P_{\text{Vdischg}}$ (Eq. 2.7).

In addition, the storage efficiency $\eta_{\text{st}}$ determines the storage losses $P_{V,\text{st}}$ (Eq. 2.4). These losses are, in turn, determined by the self-discharge and stand-by power losses (see Eqs. 2.5 and 2.6). Both depend on the energy storage duration, also called the storage duration $t_{\text{st}}$. This is the period of time the stored energy is 'held'. If an energy storage system did not 'hold' the energy, it would simply consist of two energy conversions. It would then cease to function as an energy storage system that shifts energy over time. In general, energy storage systems cannot keep the level of stored energy constant over the storage duration $t_{\text{st}}$. This is because of self-discharge due to internal processes or external factors. These losses are called the self-discharge power losses $P_{V,\text{SD}}$. They are particularly significant with short-term storage systems such as batteries, flywheel storage systems, or warm-water storage facilities. With storage cycles lasting over a month, or as along as a year, these losses may significantly exceed the charging and discharging losses. Long-term storage systems, such as gas storage systems, tend to have low self-discharge power losses. In addition, stand-by power losses $P_{V,\text{SB}}$ occur over the time the energy is stored. These losses are caused by peripherals (such as battery management systems) required to ensure the energy system can be loaded or unloaded without delay. These losses also include the energy supplied to facility peripherals guaranteeing the energy storage system's constant availability,

$$P_{V,\text{in}} = P_{\text{in}} - P_{\text{st,start}}, \tag{2.3}$$

$$P_{V,\text{st}} = P_{V,\text{SD}} + P_{V,\text{SB}} = \left.\frac{dE_{V,\text{st}}}{dt_{\text{st}}}\right|_{P_{\text{in}},P_{\text{out}}=0}, \tag{2.4}$$

$$P_{V,\text{SD}} = \left.\frac{dE_{V,\text{SD}}}{dt_{\text{st}}}\right|_{P_{\text{in}},P_{\text{out}}=0}, \tag{2.5}$$

$$P_{V,\text{SB}} = \left.\frac{dE_{V,\text{SB}}}{dt_{\text{st}}}\right|_{P_{\text{in}},P_{\text{out}}=0}, \tag{2.6}$$

$$P_{V,\text{out}} = P_{\text{st,end}} - P_{\text{out}}. \tag{2.7}$$

The power gradient PG (or 'ramp rate') of an energy storage system is equal to the charging or discharging power per unit of time. This is an important attribute of storage systems used to balance fluctuations in energy supply and demand. It is expressed as %/minute of the maximum power (Eq. 2.8),

$$\text{PG} = \frac{dP}{dt}; \text{with } P = P_{\text{chrg}} \text{ or } P_{\text{dischg}}. \tag{2.8}$$

### ■ Energy Parameters

The overall capacity of an energy storage system $E$ is the total energy that it can absorb ($E_{\text{st,start}}$), hold ($E_{\text{st,max}}$), or release ($E_{\text{st,start}}$). It may be expressed in Joules (J) or in Watt-hours (W h).

**Table 2.2** Summary of relevant energy storage system parameters

| Parameter | Unit[a] | Meaning |
|---|---|---|
| Power | | |
| Power $P$ | W | Power as energy per unit of time |
| Charging power $P_{\mathrm{chrg}}$ (also supplied power $P_{\mathrm{sup}}$) | W | Charging power (loading power) as energy/work/heat per unit of time |
| Discharging power $P_{\mathrm{dischg}}$ (also consumed power $P_{\mathrm{cons}}$) | W | Discharging power (unloading power) as energy/work/heat per unit of time |
| Charging power losses $P_{V,\mathrm{chrg}}$ | W | Power losses caused by energy conversion for charging |
| Storage power losses $P_{V,\mathrm{st}}$ | W | Power losses from self-discharge and in the stand-by state over the storage (holding) period $t_{\mathrm{st}}$ |
| Stand-by power losses $P_{V,\mathrm{SB}}$ | W | Power losses in the stand-by state over the storage (holding) period $t_{\mathrm{st}}$ |
| Self-discharge power losses $P_{V,\mathrm{SD}}$ | W | Power losses from self-discharge over the storage (holding) period $t_{\mathrm{st}}$ |
| Discharging power losses $P_{V,\mathrm{dischg}}$ | W | |
| Power density $p$ | W/kg, W/m$^3$ | Usable power per unit of mass or volume |
| Power gradient PG | W/s | Power-related charging and discharging speed (loading and unloading speed) |
| Energy | | |
| Energy $E$, work $W$ (energy quantity, storage system capacity) | W h | Usable energy content of a storage system |
| Energy density $e$[b] | W h/kg, W h/m$^3$ | Usable quantity of energy per unit of mass or volume |
| Stored energy $E_{\mathrm{st,start}}$ (energy content as energy $E$, work $W$, heat $Q$, maximum value as storage capacity) | W h | Stored energy in the energy storage system (energy content) for the maximum value (storage capacity) $E_{\mathrm{st,max}}$ |
| Remaining energy $E_{\mathrm{st,end}}$ | W h | Remaining energy in the energy storage system after the storage duration $t_{\mathrm{st}}$ (stored energy minus losses after self-discharge and stand-by) |
| Energy to be stored or supplied $E_{\mathrm{chrg}}$ (or $E_{\mathrm{sup}}$) | W h | Energy to be stored or supplied in an energy storage system (loading process) |
| Storage losses $E_{V,\mathrm{st}}$ | W h | Losses from self-discharge and in the stand-by state over the storage (holding) period $t_{\mathrm{st}}$ |
| Self-discharge losses $E_{V,\mathrm{SD}}$ | W h | Losses from self-discharge over the storage (holding) period $t_{\mathrm{st}}$ |
| Stand-by losses $E_{V,\mathrm{SB}}$ | W h | Losses from self-discharge in the stand-by state over the storage (holding) period $t_{\mathrm{st}}$ |
| Discharged or dischargeable energy $E_{\mathrm{dischg}}$ ($E_{\mathrm{cons}}$) | W h | Discharged or dischargeable energy from an energy storage system (discharging process) |

**Table 2.2** (Continued)

| Parameter | Unit[a] | Meaning |
|---|---|---|
| Time and efficiency | | |
| Efficiency $\eta$ | 1 (%) | Efficiency of an energy conversion or storage process |
| Charging efficiency $\eta_{\mathrm{chrg}}$ | 1 (%) | Efficiency of the charging energy conversion process |
| Storage efficiency $\eta_{\mathrm{st}}$ | 1 (%) | Efficiency of the storage process (holding the stored energy) |
| Discharging efficiency $\eta_{\mathrm{dischg}}$ | 1 (%) | Efficiency of the discharging energy conversion process |
| Overall efficiency $\eta_{\mathrm{over}}$ of a storage cycle with the storage duration $t_{\mathrm{st}}$ | 1 (%) | Efficiency of the entire energy storage process of a cycle with the storage duration $t_{\mathrm{st}}$ |
| Self-discharge rate SR | 1 (%)/day, 1 (%)/week, 1 (%)/month | Proportion of stored energy lost by self-discharge over a time period |
| Charging duration $t_{\mathrm{chrg}}$ | s | Duration of the charging process (loading process) |
| Storage duration $t_{\mathrm{st}}$ | s | Duration that the energy is actually stored or held |
| Discharging duration $t_{\mathrm{dischg}}$ (E/P ratio) | s | Duration of the discharging process (unloading process); also called the E/P ratio |

[a] The SI units (cubic) meter, kilogram, second, with Joule and Watt are preferred. Other units such as Watt-hour may also be used.
[b] Gravimetric density is important for all storage media—solids, liquids, and gasses. Volumetric density can be especially important for gasses.

The term 'capacity' is used in different ways in the fields of physics, engineering, and economics:

1. For the capacity $C$ of a component equal to the quotient of the charge $Q$ and the voltage $U$ ('capacity of a capacitor')
2. For the charge $Q$ of a battery cell, battery pack, or battery
3. For the power $P$ of a power plant ('capacity market')
4. For the energy $E$ that can be 'produced' by a storage system (storage capacity)

Only the first usage is valid in physics. But since the term storage capacity is commonly applied to energy storage systems, it is also used that way in this book.

Like power, the energy within the storage cycle can also be calculated and defined. At the start of the storage cycle, a quantity of energy is stored in the energy storage system $E_{\mathrm{st,start}}$ (Eq. 2.9). This quantity is determined by the supplied energy to be charged $E_{\mathrm{chrg}}$ or $E_{\mathrm{sup}}$ multiplied by the charging efficiency $\eta_{\mathrm{chrg}}$. Due to energy conversion losses, $E_{\mathrm{chrg}}$ exceeds $E_{\mathrm{st,start}}$ (Eq. 2.11). The quantity of energy still stored at the end of the storage process before discharge is $E_{\mathrm{st,end}}$ (Eq. 2.10). This differs from the quantity of energy stored $E_{\mathrm{st,start}}$ because of self-discharge losses ($E_{V,\mathrm{SD}}$) and stand-by losses ($E_{V,\mathrm{SB}}$) during storage (temporal shifting of the energy, 'holding' the energy). These energy losses during holding determine the storage losses $E_{V,\mathrm{st}}$ (Eq. 2.12). The storage losses do not include the charging and discharging losses. As a result, the storage duration $\Delta t$ or $t_{\mathrm{st}}$ determines the power losses caused by the energy losses $E_{V,\mathrm{SD}}$ (Eq. 2.13) and $E_{V,\mathrm{SB}}$ (Eq. 2.14).

2

At the end of the storage cycle, additional losses occur during discharging. These losses are determined by the storage system's discharging efficiency $\eta_{\text{dischg}}$. This means that the dischargeable or discharged $E_{\text{dischg}}$ is smaller than $E_{\text{st,end}}$ (Eq. 2.15).

$$E_{\text{st,start}} = E_{\text{in}} \cdot \eta_{\text{in}}, \tag{2.9}$$

$$\begin{aligned} E_{\text{st,end}} &= E_{\text{st,start}} - E_{V,\text{st}} \\ &= E_{\text{st,start}} - E_{V,\text{SB}} - E_{V,\text{SD}}, \end{aligned} \tag{2.10}$$

$$\begin{aligned} E_{\text{in}} &= \int_{t=0}^{t_{\text{in}}} P_{\text{in}}(t) \cdot dt \\ &= P_{\text{in}} \cdot t_{\text{in}}|_{P=\text{const}} = \frac{E_{\text{st,start}}}{\eta_{\text{in}}}, \end{aligned} \tag{2.11}$$

$$\begin{aligned} E_{V,\text{st}} &= E_{V,\text{SD}} + E_{V,\text{SB}} \\ &= E_{\text{st,start}} - E_{\text{st,end}} \\ &= P_{V,\text{st}} \cdot t_{\text{st}}|_{P_{\text{in}},P_{\text{out}}=0}, \end{aligned} \tag{2.12}$$

$$\begin{aligned} E_{V,\text{SD}} &= E_{\text{st,start}} - E_{V,\text{SB}} \\ &= P_{V,\text{SD}} \cdot t_{\text{st}}|_{P_{\text{in}},P_{\text{out}}=0}, \end{aligned} \tag{2.13}$$

$$\begin{aligned} E_{V,\text{SB}} &= E_{\text{st,start}} - E_{V,\text{SD}} \\ &= P_{V,\text{SB}} \cdot t_{\text{st}}|_{P_{\text{in}},P_{\text{out}}=0}, \end{aligned} \tag{2.14}$$

$$\begin{aligned} E_{\text{out}} &= \int_{t=0}^{t_{\text{out}}} P_{\text{out}}(t) \cdot dt \\ &= P_{\text{out}} \cdot t_{\text{out}}|_{P=\text{const}} \\ &= E_{\text{st,end}} \cdot \eta_{\text{out}}. \end{aligned} \tag{2.15}$$

The energy density of a storage system is the capacity divided by the volume or mass. It is an important attribute for evaluating energy storage systems. It is expressed as a volumetric energy density $e_V$ in kW h/m$^3$ or as a gravimetric energy density $e_m$ in kW h/kg (Eq. 2.16).

$$e_m = \frac{E_{\text{st}}}{m}, \; e_V = \frac{E_{\text{st}}}{V}. \tag{2.16}$$

**Comparison of Various Energy Densities**

The following compares the volumetric energy densities of various storage systems, taken from [3] and [5].

Electric storage systems (low-energy density)

| | |
|---|---|
| Double-layer capacitor: | 10 kW h/m$^3$ |
| Superconducting magnetic coil: | 3 kW h/m$^3$ |

Chemical storage systems (high-energy density)

| | |
|---|---|
| Hydrogen: | 400 kW h/m$^3$ (at 300 K and 200 bar) |
| Methane: | 1,200 kW h/m$^3$ (at 300 K and 200 bar) |
| Gasoline: | 10,000 kW h/m$^3$ |

Electrochemical storage systems (medium-energy density)

| | |
|---|---|
| Lead battery: | 70 kW h/m$^3$ |
| Lithium-ion battery: | 300 kW h/m$^3$ |

Mechanical storage systems (very low-energy density)

| | |
|---|---|
| Potential energy (pumped-storage with 540 m): | 1.5 kW h/m$^3$ |
| Potential energy (Huntorf CAES with store at 70 bar): | 20 kW h/m$^3$ |
| Kinetic energy (a steel flywheel at 5,000 revolutions/min): | 20 kW h/m$^3$ |

Thermal storage systems (medium-energy density)

| | |
|---|---|
| Sensible heat (water with $\Delta T = 80$ K): | 93 kW h/m$^3$ |
| Latent heat (water-steam at 1 bar and 373 K): | 627 kW h/m$^3$ |
| Thermochemical storage systems: | 200–500 kW h/m$^3$ |

## ■ Efficiency and Time Parameters

The efficiency $\eta$ of any technology or system is defined by its benefit to cost ratio [7]. The benefit of an energy storage system is the capacity to balance supply and demand temporally, fv, to hold or temporally shift energy that can be

used at the end of the process as discharged energy $E_{\text{dischg}}$. The effort of an energy storage system is the energy used $E_{\text{chrg}}$. Because the storage process includes charging (loading), storing (holding), and discharging (unloading), the efficiency of an energy storage system is determined by:

- The charging efficiency level (or loading efficiency level) $\eta_{\text{chrg}}$,
- The storage efficiency level $\eta_{\text{st}}$,
- The discharging efficiency level (or unloading efficiency level) $\eta_{\text{dischg}}$.

The product of these three is the overall (or round-trip or 'total') efficiency $\eta_{\text{over}}$ of the energy storage system (Eq. 2.17). This is defined by the ratio of the energy discharged $E_{\text{dischg}}$ to energy charged $E_{\text{chrg}}$:

$$\eta_{\text{over}} = \eta_{\text{chrg}} \cdot \eta_{\text{sp}} \cdot \eta_{\text{dischg}} = \frac{E_{\text{dischg}}}{E_{\text{chrg}}}. \quad \textbf{(2.17)}$$

The charging and discharging processes, and any losses during storage, are expressed by power. When these vary, the energy may be determined by integrating the power over time. However, when these are constant, the energy is the product of the process power and time.

The charging efficiency $\eta_{\text{chrg}}$ is the ratio of the energy stored $E_{\text{st,start}}$ to the energy charged $E_{\text{chrg}}$, which may be expressed as a dimensionless number or as a percentage (Eq. 2.18). If the charging process is composed of several sub-processes, then the charging efficiency is the product of the efficiencies of these subprocesses:

$$\eta_{\text{chrg}} = \frac{E_{\text{sp,start}}}{E_{\text{chrg}}}. \quad \textbf{(2.18)}$$

The storage system efficiency $\eta_{\text{St}}$ is determined by the ratio of the energy remaining in the energy storage system $E_{\text{st,end}}$ after the storage duration $t_{\text{st}}$ to the energy stored at the start $E_{\text{st,start}}$ (Eq. 2.20). This efficiency should not be confused with the overall efficiency $\eta_{\text{over}}$ of a storage cycle. In addition, the storage efficiency $\eta_{\text{St}}$ can also be determined using the self-discharge rate SR, defined by the ratio of the self-discharge losses $E_{V,\text{SD}}$ after the storage duration $t_{\text{st}}$ to the energy charged $E_{\text{st,start}}$ (Eq. 2.19). With sensible-heat storage systems, self-discharge is determined by the thermal resistance of the insulation and the temperature intervals between the storage medium and the environment. With pumped-storage plants, self-discharge occurs because of evaporation in the upper reservoir. With batteries, it is due to internal electrochemical processes.

$$\begin{aligned} \text{SR} &= \frac{E_{V,\text{SD}}}{E_{\text{st,start}}} = \frac{\int_{t=0}^{t_{\text{st}}} P_{V,\text{SD}} \cdot dt}{E_{\text{st,start}}} \\ &= \left. \frac{P_{V,\text{SD}} \cdot t_{\text{st}}}{E_{\text{st,start}}} \right|_{P=\text{const}}. \end{aligned} \quad \textbf{(2.19)}$$

$$\begin{aligned} \eta_{\text{sp}} &= \frac{E_{\text{st,end}}}{E_{\text{st,start}}} = 1 - \frac{E_{V,\text{st}}}{E_{\text{st,start}}} \\ &= 1 - \text{SR} - \frac{E_{V,\text{SB}}}{E_{\text{st,start}}}. \end{aligned} \quad \textbf{(2.20)}$$

Equation 2.21 defines the discharging efficiency $\eta_{\text{dischg}}$: the ratio of the energy discharged $E_{\text{dischg}}$ to the remaining energy stored in the storage system $E_{\text{st,end}}$ after the storage duration $t_{\text{st}}$:

$$\eta_{\text{out}} = \frac{E_{\text{dischg}}}{E_{\text{st,end}}} = \frac{E_{\text{dischg}}}{\eta_{\text{st}} \cdot E_{\text{st,start}}}. \quad \textbf{(2.21)}$$

The charging duration $t_{\text{chrg}}$ (also loading duration) of a storage system in s, and min or h is equal to the energy supplied and charged $E_{\text{chrg}}$ divided by the charging power $P_{\text{chrg}}$ (Eq. 2.22):

$$t_{\text{chrg}} = \frac{E_{\text{chrg}}}{P_{\text{chrg}}}. \quad \textbf{(2.22)}$$

The storage duration $t_{\text{st}}$ is the duration that the energy is actually stored or held in the energy storage system. In practice, this duration is measured and then used to determine the quantity of storage losses (Eq. 2.23):

$$t_{\text{st}} = \frac{E_{V,\text{st}}}{P_{V,\text{st}}}. \quad \textbf{(2.23)}$$

The unloading or discharging time $t_{\text{dischg}}$ is the time it takes to unload a storage system. Similar to the charging time, it is determined by the

quotient of the consumed, dischargeable energy $E_{\text{dischg}}$ and the discharging power $P_{\text{dischg}}$. This is also termed the E/P ratio ('energy-to-power') or W/P ratio ('word-to-power'). It is almost always based on the maximum discharging power (Eq. 2.24):

$$t_{\text{dischg}} = \frac{E_{\text{dischg}}}{P_{\text{dischg}}}. \tag{2.24}$$

The discharging duration is the most important attribute for the *temporal classification* of the energy storage systems discussed in this section.

Another important parameter is the cycle number $z$ (frequency of use). This determines how often the storage content $E_{\text{st}}$ of an energy storage system is used over a certain period of time (e.g., day, year) (Table 2.2). Often, the full-load cycles for a storage system are given. This is the number of complete charging and discharging processes in an energy storage system ($E_{\text{st,max}}$) over a certain period of time. Some long-term storage systems, such as gas storage systems, have only one full-load cycle per year. Short-term storage systems such as capacitors have several thousand full-load cycles over the same period. When used for ensuring voltage quality, they are cycled several times a second. But in general, energy storage systems are not completely charged or discharged during a cycle. Instead, they are partially cycled. These partial cycles can be accumulated and converted to 'equivalent full-load cycles'. This allows different energy storage systems to be more effectively compared. The cycle number also has a direct influence on the service-life of an energy storage system.

There are two kinds of service-life; service-life over time and cycle life. The service-life over time $t_{\text{cal}}$ is the technical service-life of an energy storage system, including its peripherals. The cycle life $z_{\text{max}}$ is the energy storage system's maximum number of cycles. With battery storage systems, the end of service-life is defined as a percentage of the maximum SOC or storage content $E_{\text{st,max}}$. To ensure long service-life, batteries are cycled only within a certain range of charge. This is because full-load cycling entails deep-discharging, and reduces service-life.

**Example of the Goldisthal Pump-Storage Plant**

This pump-storage plant exploits the potential energy of an upper reservoir net volume of 12 million $m^3$ and an average drop-height of 301.65 m, giving a nominal storage capacity $E_{\text{St}}$ of 9,864 MW h. When pumping (charging), the power of the four pump-turbine units is $P_{\text{chrg}} = 4 \cdot 257 = 1{,}028\,\text{MW}$ and their efficiency is $\eta_{\text{chrg}} = 87\%$. When generating (discharging), the power of the four pump-turbine units $P_{\text{dischg}} = 4 \cdot 269\,\text{MW} = 1{,}076\,\text{MW}$ and their efficiency $\eta_{\text{dischg}} = 92\%$. Hence, the overall (round-trip) efficiency $\eta_{\text{over}}$ is 80% [1].

If the pumped-storage plant is charged at a constant power of $P_{\text{chrg}} = 100\,\text{MW}$ with an assumed charging efficiency $\eta_{\text{chrg}} = 87\%$ for one hour, then the water level of the upper storage reservoir is raised, with an increase in the stored energy of 87 MW h.

The self-discharge of pumped-storage plants by evaporation is usually low. If this is ignored, then with a discharging efficiency $\eta_{\text{dischg}} = 92\%$, the stored potential energy of 87 MW h can be converted into electric energy of 80 MW h.

Using the above efficiencies, and again ignoring self-discharge losses, the pumped-storage plant has the following maximum charging and discharging durations:

$$t_{\text{chrg}} = \frac{E_{\text{sp}}}{P_{\text{chrg}} \cdot \eta_{\text{chrg}}} = \frac{9{,}864\,\text{MW h}}{1{,}028\,\text{MW} \cdot 0.87} = 11\,\text{h},$$

$$t_{\text{dischg}} = \frac{E_{\text{sp}} \cdot \eta_{\text{sp}} \cdot \eta_{\text{dischg}}}{P_{\text{dischg}}} = \frac{9{,}864\,\text{MW h} \cdot 1 \cdot 0.92}{1{,}076\,\text{MW}} = 8.4\,\text{h}.$$

## 2.3.3 Temporal Classification

Analyzing how long storage systems can supply energy requires them first to be grouped together in terms of their discharging durations $t_{\text{dischg}}$ (E/P ratios). They are usually divided

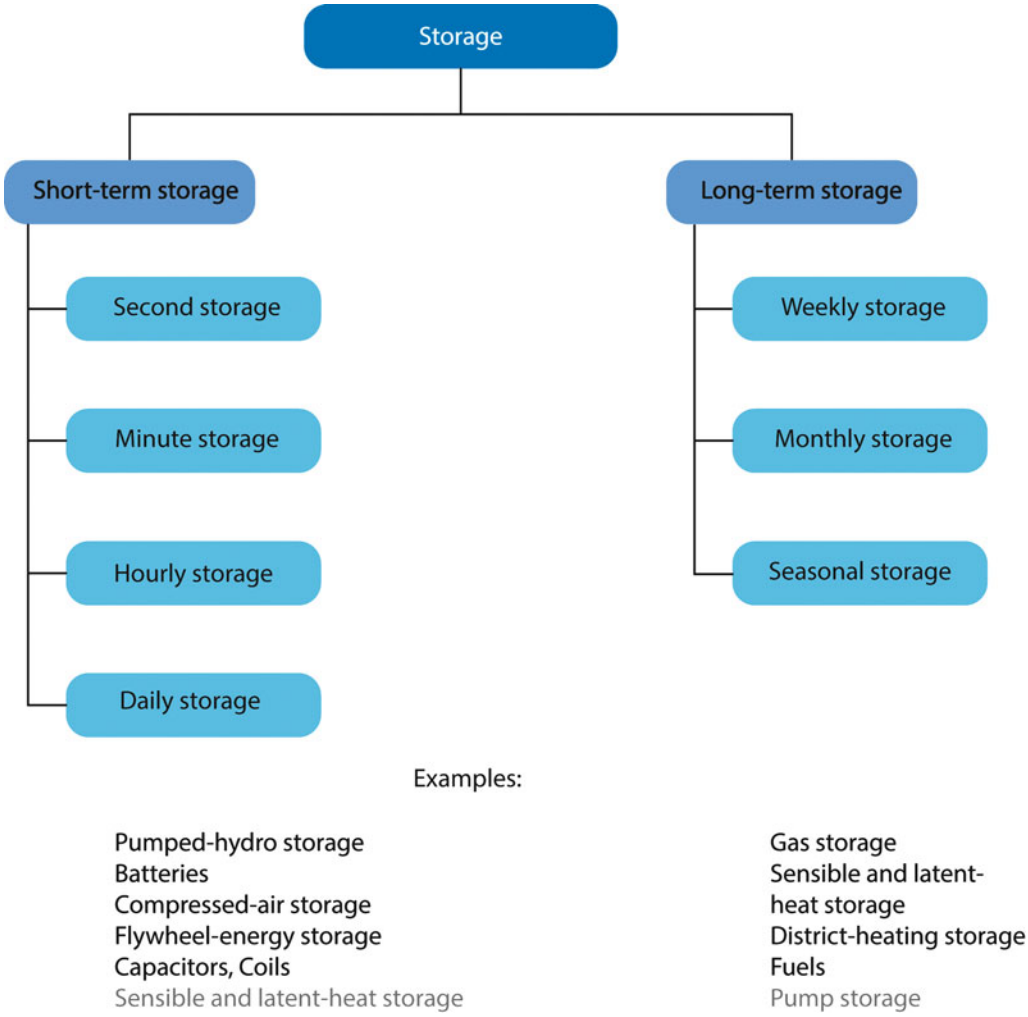



**Fig. 2.8** Classification of short and long-term storage systems

into short or long-term storage systems. The term 'medium-term storage system' is sometimes used, but storage systems defined in this way differ little from short-term storage systems. As a result, the term is not used here. Short and long-term storage systems are classified and categorized using more precise units of time in Fig. 2.8.

### Short-Term Storage Systems (Seconds, Minutes, Hours, Days)

Short-term storage systems store energy for periods, ranging from a few nanoseconds to an entire day ($t_{\mathrm{dischg}} \leq 24\,\mathrm{h}$), but most short-term storage systems are designed for hourly or daily storage. In the electricity sector, they usually have an E/P ratio ranging from one to ten hours, as well as high cycle-numbers and cycle-efficiency levels. These characteristics make them particularly well-suited for balancing short-term fluctuations in the electricity network.

**Example**

Short-term storage systems fall into the following categories:

- For storage over seconds: flywheels, superconducting electromagnetic energy storage systems, bi-layer capacitors, and batteries.
- For storage over minutes: batteries and sensible-heat storage systems.
- For storage over hours: batteries, pumped-storage plants, CAES, and sensible-heat storage systems.
- For storage over days: batteries, pumped-storage plants, CAES, and sensible-heat storage systems.

#### ■ Long-Term Storage Systems (Weeks, Months, Seasons, Years)

Long-term storage systems hold energy for periods ranging from many days or weeks to several months or years ($t_{\mathrm{dischg}} \geq 24\,\mathrm{h}$). They are used to balance seasonal fluctuations in energy supply due to, for example, lengthy periods without wind, low water levels for hydropower, or long dark periods. They typically feature high E/P-ratios, high storage-capacities with low storage loss, and low cycle numbers and cycle-efficiency levels.

**Example**

Long-term storage systems fall into the following categories:

- Weekly storage systems: PSP, cavern and aquifer storage systems, and sensible-heat storage systems.
- Monthly storage systems: storage water, cavern and aquifer storage systems (porous storage), and sensible-heat storage systems.
- Yearly storage systems: storage water, cavern and aquifer storage systems (porous storage), and sensible-heat storage systems.

Except for a few pumped-storage plants and stored water hydropower facilities in Norway and the Alps, most long-term storage systems use oil and gas in underground caverns and aquifer stores. Beyond their standard use as strategic reserves, they can also be used for fuels synthesized with renewable energies in PtG or PtL plants.

Like storage duration, cycle numbers, storage dynamics, and storage stability are essential characteristics in temporal classification. Here, the service-life or cyclical lifespan as well as the charging and discharging power gradients PG are key factors.

### 2.3.4 Spatial Classification

Another approach to storage system classification is spatial, based on [6]. This divides storage systems either between centralized and decentralized storage systems, or between fixed and mobile storage systems.

#### ■ Centralized Storage Systems

Centralized storage systems are large, typically fixed units such as PSP or oil and gas caverns. They have geological and topological requirements that can be a disadvantage.

#### ■ Decentralized Storage Systems

Decentralized storage systems are small, modular, distributed storage units. They are well-suited to the decentralized character of renewable energy systems. Examples include house battery storage systems at photovoltaic (PV) facilities or accumulators at base stations. They do not require specific environmental conditions, but with larger storage systems of this kind there are very limited economies of scale. In addition, multiple decentralized storage systems can be controlled from a single point, for example in a 'virtual' power plant.

#### ■ Dual-Use Storage Systems

Some storage systems can also perform a dual function:

- After their use for mobility, the batteries of electric cars can supply power to homes or other stationary applications (second life), such as with V2G systems.
- Hot water tanks in homes or district heating networks can be retrofitted with electric heating (resistance heater, electric heat pump) for storing surplus wind or solar electricity.
- In addition to their original functions, such as balancing supply in the electricity sec-

tor or supporting mobility in the transport sector, many energy storage systems can perform an additional function for the electricity network at a marginal cost. This increases their cost-effectiveness.

#### Fixed Storage Systems

Fixed storage systems are tied to a specific location. They are primarily central storage systems such as PSP, cavern storage systems, aquifers, or mechanical stored energy systems, but they also include decentralized storage systems such as CAES. Central fixed storage systems often cannot be located where the energy is generated and used. This is the disadvantage with these systems, because the transportation of electricity, heat, or fuel results in transmission losses.

#### Mobile Storage Systems

Mobile storage systems such as batteries or fuel tanks can be placed at particular locations for short or long periods.

### 2.3.5 Economic Classification

The costs of energy storage systems may be compared based on their application areas, service-lifetimes (cycle numbers), and stages of development. Several parameters are relevant for economic classification.

#### Capital Costs

One important parameter is the specific investment cost $k_0$ (also $I_0$ or CAPEX, which refers to capital expenditure). These are one-time costs incurred by storage system construction and start-up. They are based on the installed power (€/kW) or the installed storage system capacity (€/kW h) (Eq. 2.25).

It is common to combine these two; when charging and discharging power, $P_{\text{chrg}}$ and $P_{\text{dischg}}$ are independent of storage system capacity $E_{\text{over}}$. Overall investment $k_{\text{over}}$ at start-up includes both:

$$k_0 = \frac{k_{\text{over}}}{P_{\text{dischg}}}; \quad \text{or} \quad k_0 = \frac{k_{\text{over}}}{E_{\text{sp}}}. \qquad (2.25)$$

Cost factors vary from one storage system technology to another. The capital costs of battery storage plants are primarily determined by the energy capacity (€/kW h). For PtG, the capital costs depend mainly on the powers of the charging and discharge units (€/kW), of which the latter may already exist, whereas the cost of storage capacity (€/kW h) is relatively low.

#### Operating Costs

The second important economic parameter is operating costs, or operational expenditure (OPEX). These are the costs that result from operating a storage system (for example purchasing of electricity, maintenance, insurance). They are based on the amount of converted energy (€/kW h), and can be divided among fixed operating costs (personnel, maintenance, insurance, etc.) and variable operating costs (purchasing of electricity or fuel, replacement parts, etc.).

For example, the fixed operating costs are based on the personnel costs of operating a facility independent of its capacity utilization. They are often assumed to be 1 to 5% (roughly 2%) of the investment costs. However, the variable operating costs of a storage system may be based on the output energy.

#### Annuity Investment Costs

Annuity investment costs are a common economic indicator for energy storage systems. They are calculated from the following parameters:

- Investment costs $k_0$ for charging and discharging in €/kW and storage system capacity in €/kW h
- Service-life $t_{\text{serv}}$ in years
- Capital interest (imputed interest) $i$ in 1/year (or %/year)
- Annual fixed operating costs $k_{\text{fix}}$ in €/kW/year and €/kW h/year
  These are often taken as 1–5% of the investment costs.

Service lives vary widely, from three to ten years (currently) for battery systems to up to 80 years or more for PSP. With improved battery man-

agement system software, and more precisely, defined applications, battery service-life in the future could be extended to up to 20 years. This is the goal of a project initiated by Samsung and Younicos AG, which is described in ▶ Sect. 13.1.

Capital interest (and also imputed interest) is determined by general economic conditions (key interest rates, interest rate policy) and investors' expectations for returns. Rates between 5 and 15% are common depending on interest rate policy and the risk assessed by investors, banks, and entrepreneurs. In the energy sector, 10% is the usual rate.

The annuity factor $a$ in 1/years is calculated from the capital interest and the service-life (Eq. 2.26):

$$a = \frac{i \cdot (1+i)^{\left(\frac{t_{\text{serv}}}{\text{years}}\right)}}{(1+i)^{\left(\frac{t_{\text{serv}}}{\text{years}}\right)} - 1}. \tag{2.26}$$

The annuity investment costs $k_a$ in €/kW/year can then be easily determined (Eq. 2.27):

$$k_a = k_0 \cdot a \ + k_{\text{fix}}. \tag{2.27}$$

If annual revenues exceed this annuity, then in general, the investment is worthwhile.

**Battery Power Plant Example**

A large battery power plant is planned to be used as a short-term storage system ($t_{\text{dischg}} < 1$ h) in reserve markets (balancing energy) with a storage capacity of $E_{\text{over}} = 10$ MW h and a discharging power of $P_{\text{dischg}} = 10$ MW for a 110 kV network node.

It is assumed that lithium-ion cells can be purchased for $k_0 = 200$ €/kW h and the power electronics they require for $k_0 = 180$ €/kW. The facility is planned to be amortized over ten years at an expected capital interest of 10%. The fixed operating costs are assumed to be 2% of the investment costs. This means the overall investment is $k_{\text{over}} = (2 + 1.8)$ million € $= 3.8$ million €, the fixed operating costs are $k_{\text{fix}} = 3.8$ million € $\cdot\, 0.02/10$ MW $= 7.6$ € kW$^{-1}$ years$^{-1}$, and the specific investment is $k_0 = 3.8$ million €/10 MW $= 380$ €/kW.

According to Eq. 2.28, the annuity investment costs then are:

$$k_a = 380\,\frac{€}{\text{kW}} \cdot (0.16275 + 0.02)\,\frac{1}{\text{a}} = 69\,\frac{€}{\text{kW} \cdot \text{a}} = 69\,\frac{\text{T€}}{\text{MW} \cdot \text{a}} = 69\,\frac{\text{M€}}{\text{GW} \cdot \text{a}}. \tag{2.28}$$

If annual revenues on the reserve markets exceed these annuity investment costs combined with the variable operating costs of, for example, the purchase of electricity, then investment in the battery power plant would be profitable and economically feasible.

Additional economic considerations vary widely depending on the storage system's specific application and market area. For this reason they are not included in this chapter. More detailed discussions of economic considerations are, however, included in the other chapters where relevant.

## 2.4 Summary

- A **storage** unit is a facility or container to stock, store, and preserve goods.
- An **energy storage system** is an energy technology facility for storing energy serving the following three purposes: **charging**, **storing**, and **discharging** or loading, holding, and unloading.
- An **energy carrier** is a material that stores energy.
- Primary energy storage systems are charged and discharged a single time. Secondary energy storage systems may be charged and discharged many times.
- **Sector coupling** connects the electricity, heating, transportation, and chemical sectors using renewable electricity as a primary energy source to decarbonize the other sectors. Also termed PtX, sector coupling is infeasible without energy storage systems,

and is by definition basically equivalent to cross-sectoral energy storage.

- Energy storage systems are divided into sectoral and cross-sectoral energy storage systems: **Sectoral energy storage systems** are used exclusively in only one of the three energy sectors of electricity, heat, and transportation. They function in both directions. **Cross-sectoral energy storage systems** are used to link energy sectors. They typically link the electricity sector to the heat and transportation sectors in a single direction. Examples include PtG, PtH, PtL, PtC, heat pumps, and electric vehicles.
- Energy storage systems are primarily used to **temporally balance** energy supply and demand. They generally do not compete with energy networks responsible for **balancing spatial** supply and demand.
- There are several approaches to classifying energy storage systems. The most common approach is **classification** according to physical form of energy and basic operating principle: electric (electromagnetic), electrochemical/chemical, mechanical, thermal.
- The technical benchmarks for energy storage systems are determined by physical **power and energy measures**. Storage capacity, energy density, charging and discharging power, level of efficiency, and discharging duration are the most important measures.
- Based on their discharging durations, energy storage systems can also be divided into **short-term storage system**s (up to a day) and **long-term storage systems** (up to several years).
- **Investment costs** for storage, charging or discharging technologies are given either in terms of power in €/kW or of capacity in €/kW. To calculate annuity investment costs, **fixed costs** are assumed to be **2%** of investment costs.

## References

1. Dünkel W (2006) Pumpspeicherwerk Goldisthal – 1.060 MW-Kavernenkraftwerk. Kassel (Bericht – Exkursion in das Pumpspeicherwerk Goldisthal/ Thüringer Wald)
2. Emele L (2011) Techno-Ökonomischer Vergleich von Erneuerbarem Methan mit anderen Stromspeichertechnologien. Universität Kassel (Master Thesis)
3. Feddeck P (2001) Thermochemische Speicher. Eggenstein-Leopoldshafen
4. Neyer A (2013) Magnetismus. Grundlagen der Elektrotechnik. TU, Dortmund
5. Ortloff F (2011) Speicherung von regenerativ erzeugter elektrischer Energie in der Erdgasinfrastruktur
6. Sauer D (2011) Energiespeichersysteme. RWTH Aachen, Aachen
7. VDI (2003) VDI Richtlinie 4661: Energiekerngrößen – Definitionen, Begriffe, Methodik. Beuth Verlag, Berlin

# Demand of Energy Storage

Contents

Chapter 3 Storage Demand in Power Supply – 51

Chapter 4 Heating Supply Storage Requirements – 137

Chapter 5 Storage Demand in the Transport and Chemical Sector – 165

# Storage Demand in Power Supply

*Michael Sterner, Christopher Breuer, Tim Drees, Fabian Eckert, Andreas Maaz, Carsten Pape, Niklas Rotering, and Martin Thema*

**3.1 Storage Demand and Surplus—Parameters and Definitions – 53**
3.1.1 General Influence on the Storage Demand – 53
3.1.2 Definition: Storage Demand – 54
3.1.3 Distinction of Electricity Surplus with Respect to Markets and Networks – 55

**3.2 Long-Term Scenarios of the Federal Environment Ministry – 56**
3.2.1 Development of Primary, Final, and Usable Energy Demand – 57
3.2.2 Development of the Electricity Mix – 59
3.2.3 Effect of Minimum Generation and Import/Export on the Storage Demand – 62
3.2.4 Effect of DSM on the Storage Demand – 64
3.2.5 Storage Deployment at 40%, 63%, and 85% Renewable Energies – 65
3.2.6 Abstract – 68

**3.3 "100% Renewable Electricity Supply," According to the Federal Environment Agency – 69**
3.3.1 Estimates on Power Consumption in 2050 – 69
3.3.2 Technical-Ecological Potential of Renewable Energies, Storage, and DSM – 71
3.3.3 Assumptions and Modeling of the 2050 Scenario – 75

**Electronic supplementary material** The online version of this chapter (https://doi.org/10.1007/978-3-662-55504-0_3) contains supplementary material, which is available to authorized users.

© Springer-Verlag GmbH Germany, part of Springer Nature 2019
M. Sterner, I. Stadler (Eds.), *Handbook of Energy Storage*, https://doi.org/10.1007/978-3-662-55504-0_3

3.3.4 Results for Storage Demand and Security of Supply – 78
3.3.5 Abstract – 86

**3.4 VDE-ETG Study on Market-Based Storage Demand – 86**
3.4.1 Methodology – 87
3.4.2 Assumptions for Modeling and Data Input – 89
3.4.3 Cross-Scenario Findings – 91
3.4.4 Findings of the 40% Scenario – 93
3.4.5 Findings of the 80% Scenario – 94
3.4.6 Findings of the 100% Scenario – 96
3.4.7 Summary – 97

**3.5 'Storage Roadmap' Study on Germany's Storage Requirements in the European Context – 98**
3.5.1 Methodological Approach – 98
3.5.2 Scenario – 100
3.5.3 Medium-Term Storage Simulation – 105
3.5.4 Long-Term Storage Simulation – 107
3.5.5 Significant Findings/Conclusions – 109

**3.6 Study of Network-Based Storage Requirements – 110**
3.6.1 Methodological Approach to Distinguishing Market and Network-Based Storage Requirements – 110
3.6.2 Case Study: PtG in Germany in 2022 with Delayed Network Expansion – 110
3.6.3 Minimal Storage Requirements in the European Network – 113
3.6.4 Summary – 114

**3.7 Comparison and Categorization of the Results – 115**
3.7.1 Comparison of the Results of the Three Studies – 115
3.7.2 Categorization of the Results in Comparison to Other Studies – 115

**3.8 Summary – 132**

**References – 135**

**Overview**

Energy storage systems (in the past as well as today) are one significant part in the energy supply. The following three chapters describe how **storage demand** will develop in the future for the **electricity**, **heat**, and **traffic sectors**, as well as for non-energetic consumption of fossil resources (the **chemical industry**). ▶ Chapter 3, the core section on storage demand, makes clear how and why the **electricity sector** is the **nucleus** of the energy supply of all sectors and why it creates **essential bridges** between electricity, heat, and transport sectors, as well as with the chemical industry.

If planned electricity network expansion takes place and flexibilities in generation and consumption are fully exploited, the demand for **electricity storage**, according to present estimates, will only reach a significant scale at **60–80% shares of renewable energy** in the power supply. **Network expansion** has a great impact on the storage demand, as well as **flexible power generation** in power plants, **combined heat and power (CHP)**, and flexible consumption via **demand-side management (DSM)**. Four **studies** in the context of storage demand and the role of energy storage systems for flexibility are comprehensively addressed. The authors and the co-authors were themselves participants in these studies, which will be complemented by ongoing research. A meta-study summary of the main results is shown in ▶ Sect. 3.7, and these results are compared with seven **further studies**.

## 3.1 Storage Demand and Surplus—Parameters and Definitions

### 3.1.1 General Influence on the Storage Demand

#### ■ Surplus vs. Need for Flexibility vs. Storage Demand

The term storage demand is mainly associated with a surplus of electrical power which stems from renewable energies. The common belief is that renewable energies are in themselves a good thing, but that they do not work without adequate storage. A high share of renewable energies can be integrated into the power supply system without further installation of storage due to a great number of flexibility options, which can, if used in the right way, significantly reduce the amount of storage demand.

As energy storage is, in many cases, the most expensive option to smooth out fluctuations, it will not be of great importance until the share of renewable energies on the power market has reached a very high level. By storing and extracting (charging and discharging), it temporally shifts electricity generation, and by doing so, balances demand and supply in the grid. A combination of DSM and flexibility of conventional power generation also provides this temporal shift so this task does not have to be accomplished exclusively by storage. The influence these flexibility options have on the need for storage is significant. Their instability feed-in along with the structure of conventional and renewable power plants affects the storage demand. For example, feed-in from wind and photovoltaic (PV) power systems are subject to strong fluctuations and, therefore, unpredictable. Because of its flexibility, energy storage can compensate for forecasting errors on a short-term scale. In addition to generation systems, the grid has a major impact on the amount of storage needed; it provides spatial balance just as storage does in terms of time. It is for this reason that these two technologies can basically coexist in every system (▶ Chap. 2). The power supply system ensures balance between demand and supply at all times within and across borders of marketing areas. This balance is determined by how these market areas are defined.

#### ■ Parameters for the Storage Demand

The following parameters are drivers for an increased surplus storage demand.

- Generation:
  - High rate of expansion of renewable energies (RE)

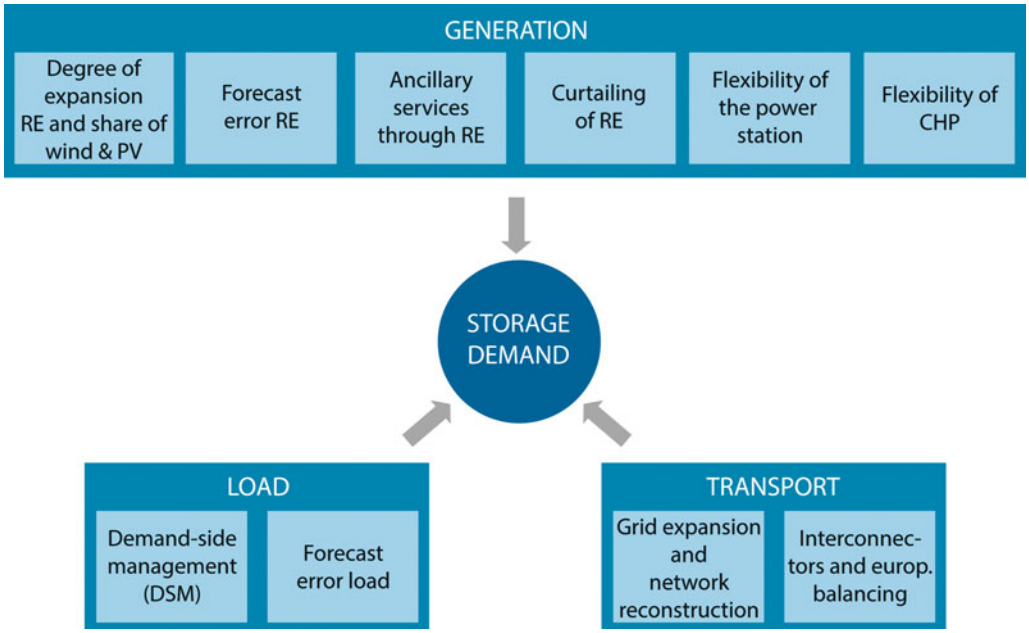



**Fig. 3.1** Parameters for the storage demand

- High shares of fluctuating RE e.g., wind and PVs
- High forecasting errors in RE and load
- Stagnation or increase of the number of 'must-run' power plants (plants for ancillary services or CHP)
- Inflexible conventional thermal power plants

- Distribution:
  - Delay in grid expansion and conversion (distribution and transmission network level)
  - No additional cross-border interconnections to the rest of Europe
- Consumption:
  - Rigid power demand
  - No DSM in power markets (mainly operating reserved)

The following factors decrease surplus and the amount of storage needed.

- Generation:
  - Usage of flexible power plants and generation facilities (retrofit of conventional power plants, usage of flexible CHP, construction of flexible thermal power plants, flexible biogas plants, flexible control of wind and PV plants)
  - Improvements in forecasts for renewable energies and load
  - Reduction of the number of must-run plants (ancillary services provided by renewable energies, flexibilization of existing CHP connected to heat networks)
- Distribution:
  - Grid reinforcement and expansion on all levels including regional and cross-border
  - Additional cross-border interconnections to the rest of Europe
- Consumption:
  - Usage of flexible loads (DSM)
  - Transferring DSM to power markets (mainly operating reserve)

Fig. 3.1 depicts these main parameters.

### 3.1.2 Definition: Storage Demand

A definition of the term storage demand can be derived from these considerations:

**Definition**

Electrical energy storage demand in order to balance fluctuations in generation is a result of surplus and shortages when powering residual load (excess and deficit), after consideration of all primary balancing and flexibility options.

### ■ Clarification about the Definition

In this context, the term residual load is of great importance:

**Definition**

Residual load is the amount of power needed minus feed-in of renewable energies. It is divided into surplus and shortage if feed-in consists exclusively of renewable energies.

Along with storage, the following points are major measures of balance or flexibility options.

- Measures of transfer and distribution:
  - Grid expansion in distribution and transmission networks to eliminate network bottlenecks.
  - Grid conversion (e.g., installation of voltage-regulated distribution transformer).
  - Improving voltage stability (e.g., management of reactive power by AC-converters).
  - Cross-border interconnections to the rest of Europe.
- Measures of generation:
  - Flexibilization of thermal power plants.
  - Flexibilization of renewable energy plants.
  - Flexibilization of CHP by using heat storage.
  - Improving reliability of forecasts for wind and PV plants.
  - Using the flexibility provided by a pan-European power generation cluster.
  - Reduction of must-run plants by having renewable energies take over ancillary services.
  - Curtailment of renewable power plants and compensation by thermal plants or gas turbines, respectively.
- Measures of consumption:
  - Making load more flexible by DSM, especially industrial and new applications (E-Mobility, heat pumps, air-conditioning, etc.).
  - Improving forecasts of load.

These measures are prior-ranking flexibility options if they are economical and/or locally accepted. Generally, many of these flexibility options decrease total costs of power supply more than energy storage systems would. Nevertheless, there is more to energy transition than just technological and economical aspects.

Surplus, shortages, storage demand, and the need for flexibility are correlated, as shown in these simplified equations (Eqs. 3.1 and 3.2).

$$\begin{aligned}&\text{Residual load (surplus and shortages)}\\&= \text{load} - \text{renewable feedin}\\&= \text{need for flexibility}\end{aligned} \tag{3.1}$$

$$\begin{aligned}&\text{Need for storage}\\&= \text{need for flexibility}\\&\quad - \text{priorranking flexibility options.}\end{aligned} \tag{3.2}$$

## 3.1.3 Distinction of Electricity Surplus with Respect to Markets and Networks

### ■ Energy Markets vs. Power Markets

When referring to power supply, balance of generation ('energy market') has to be distinguished from ancillary services such as 'power markets' (▶ Sect. 13.1).

Within market segments there may be a surplus which has its cause in either the energy market (energy cannot be integrated into market) or the network itself. These kinds of energy surplus are distinct from one another according to what they are based on:

- Market-based surplus is a result of a higher generation rather than consumption of

electricity. It leads to 'negative electricity prices', when:
  - The residual load is negative and the supply of renewable energies is higher than the demand.
  - Power plants feed-in at the wrong time or more than they are expected to do.
- Network-based surplus results from overloading the network or a bottleneck in the transmission network, in which case, feed-in is not possible at some nodes. This may happen if contracts were made on the market that cannot be fulfilled at that point of time for physical reasons, such as grid restrictions or network bottlenecks because of power plant failures or grid disturbances. The immediate consequence is curtailment, which means the closure of wind and PV plants. Other power plants, may be turned on or off in the course of redispatch (congestion management).

By using storage it is possible to feed-in surplus that otherwise would have been impossible to integrate into the market. In addition, renewable energy that would have had to be curtailed because of a bottleneck in the transmission network (network-based storage demand) can be integrated.

In this context there is always talk of negative electricity prices and 'oversupply of renewable energy', however, the amount of energy curtailed in 2011 is ca. 0.4 TW h resp. 0.7 per mille of the gross electricity consumption in Germany of 600 TW h [10]. Even though it is strongly dependent on the weather and there is an increasing trend in this relatively small amount, there will be less surplus in electricity after grid expansion and conversion because surplus is mainly network-based. From an economical point of view, grid expansion and conversion make more sense than installing storage. However, it seems, that storage is more socially accepted than grid expansion.

#### The Storage Demand in Germany in the Course of Energy Transition

In order to be able to calculate the storage demand in Germany, it is essential to know how the development of power consumption, on the one hand, and fluctuating feed-in from renewable energies on the other will develop. Furthermore, the influence of the above-named parameters and flexibility options are crucial. It is impossible to make a prediction about the exact amount of storage needed in the course of energy transition because of a great number of variables and uncertainties. A prediction of that kind would depend very much on assumptions being made. Therefore, a trend and a conclusion shall be derived from analyzing and synthesizing various studies on the subject. Since only the balance of generation is shown in 'Langfristszenarien des BMU' (Long-Term-Scenario of the Federal Environment Ministry), the UBA study and the VDE-ETG study, only market-based surplus can be determined. It is significantly more difficult to estimate network-based surplus. Trends will be taken into account in ▶ Sect. 3.5. Following that, in ▶ Sect. 3.7 there is a contrasting juxtaposition and further interpretation on the basis of six more studies.

## 3.2 Long-Term Scenarios of the Federal Environment Ministry

For several years, the Federal Environment Ministry has been launching a number of studies to analyze the expansion of renewable energies. They aim to find out how the federal government's climate and energy goals can be reached. The last long-term studies were launched by a consortium of the German Aerospace Center (DLR), the Fraunhofer Institute for Wind Energy and Energy System Technology (IWES) and the Engineering Office for New Energies (IfNE). They were published in 2012 under the name of 'Langfristszenarien und Strategien für den Ausbau der erneuerbaren Energien in Deutschland bei Berücksichtigung der Entwicklungen in Europa und global' (long-term scenario for the expansion of renewable energies in Germany in consideration of developments in Europe and global developments) [25].

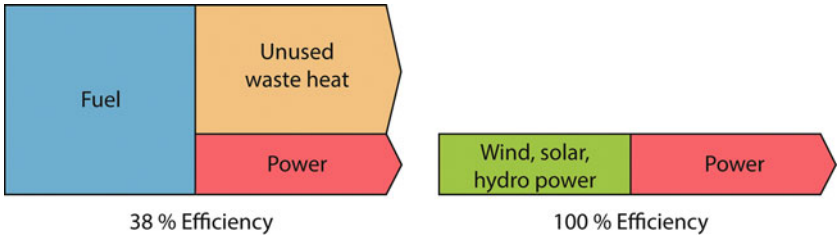
### 3.2.1 Development of Primary, Final, and Usable Energy Demand

#### ▪ Leap in Efficiency Based on Direct Generation of Electricity in Wind, Solar, and Water Plants

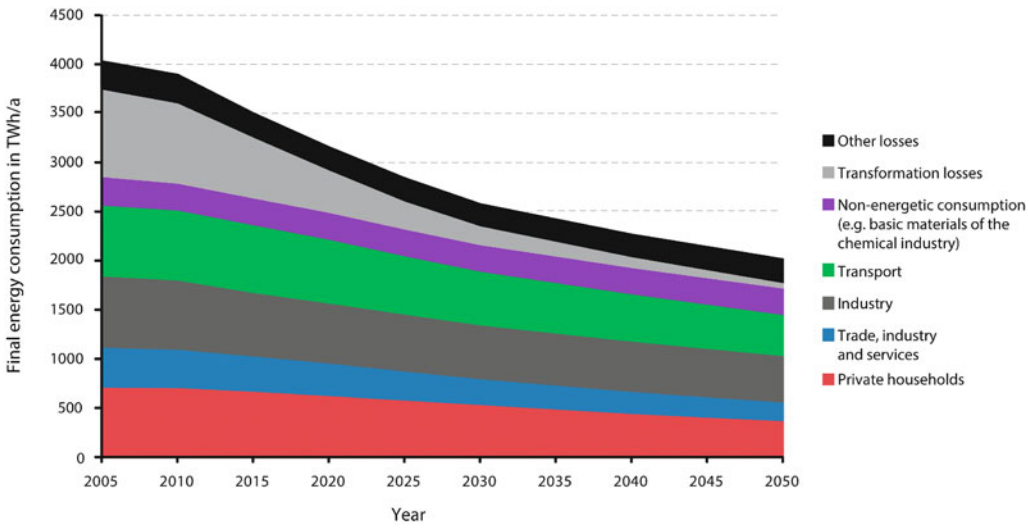
By using energy provided directly by wind, solar, or water plants, waste heat production of conventional thermal power plants can be avoided, which leads to a major leap in efficiency. In proportion to the amount of power provided by these three sources the volume of greenhouse gases emitted by the usage of fossil fuels will decrease. ◘ Figure 3.2 illustrates this link using, as it is commonly done, the efficiency method to calculate primary energy [22].

#### ▪ Primary and Final Energy Across all Sectors

The savings of primary energy that were made possible by replacing conventional power plants with direct power generation is reflected on the balance sheet. In the basic scenario, until 2050, total final energy consumption in the three sectors of electricity, heat, and traffic will decline by almost 50% in comparison to the reference year 2010 (◘ Fig. 3.3). That means 7,267 PJ/a (2,019 TW h/a) will be all that is left from 14,044 PJ/a (3,901 TW h/a). Other crucial factors are efficiency improvements in the




◘ **Fig. 3.2** Efficiency gain by direct power generation from wind, sun, and water [37]




◘ **Fig. 3.3** Development of power consumption decided by sectors and consumption in the process of conversion (total = primary energy), (NE: non-energetic consumption, e.g., synthetics or fertilizers in chemical industry [25])

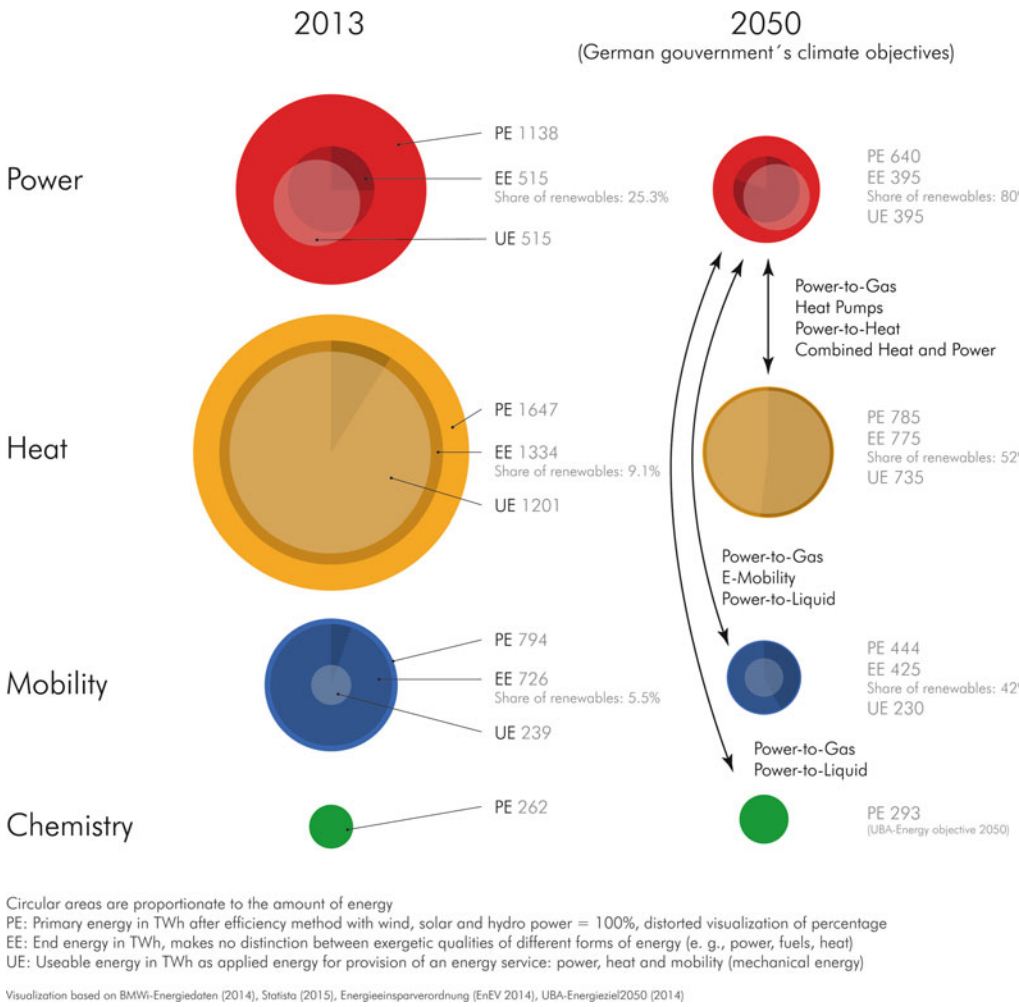



**Fig. 3.4** The power sector as the core of future energy supply. Primary, final, and usable energy without non-energetic consumption according to scenario 2011 A from Langfristszenarien des BMU for 2010 and 2050

heat and transport sector, also in relation to the power sector:

- Expansion of cogeneration of heat and electricity (CHP)
- Expansion of heat pumps
- Measures of energy efficiency in the heat sector (mostly reconstruction and building standards)
- Expansion of e-mobility
- Measures of energy efficiency in the transport sector

As shown in Fig. 3.4, that makes the power sector the core of energy supply.

1. Power sector:
   - Efficiency improvements based on direct power generation and the expansion of CHP will reduce the amount of waste heat, and consequently, primary energy by more than 50%.
   - Electricity demand (final energy = usable energy, ca. 515 TW h) will be reduced in the power sector (ca. 390 TW h) but will increase in total, including electricity demands for heat (ca. 95 TW h) and transport (ca. 150 TW h), to some 635 TW h.

- New interconnections to the heat sector (CHP, heat pumps) and the transport sector (e-mobility and electricity fuels) will be established.

2. Heat sector:
   - Efficiency improvements based on reconstruction and more efficient building standards will reduce the demand for primary, final, and usable energy by half.
   - The interconnection to the power sector via heat pumps; power-to-heat (PtH) and CHP will be crucial.
3. Transport sector:
   - Traffic volume for passenger transport will almost remain static but increase for freight transport.
   - Meanwhile, usage of e-mobility will lead to greater efficiency increases, which is why the need for primary energy in total will be reduced by half, the need for final energy will decrease, and the usable energy consumption will remain static.
   - In the future, the interconnection between transport and electricity via e-mobility and electricity fuels will play a major role for mobility.

#### Important Explanations of Depictions of Primary, Final, and Usable Energy

The calculation of primary energy is done by using the efficiency method, which has the advantage of rating power from wind, PV, and water plants as 100% primary energy without losses. The downside is a somewhat distorted picture in the comparative proportional representation.

The substitution method is superior in this regard. It calculates the amount of fossil primary energy substituted by energy from wind, PV, and water plants and therefore represents all sources of primary energy commensurately.

There is no differentiation between forms of final energy (electricity, combustible, fuel) with regard to exergy. Usable energy is depicted for reasons of comparability, because the form of chemical and thermal energy is inherently different from the form of mechanical and electrical energy. Usable energy is a more neutral way of comparing forms of energies that otherwise would be compared one-to-one. At least in that way a direct comparison of the electricity and transport sector is possible to a large extent.

Usable energy is the target energy, meant to fulfil needs for energy services such as electricity, heat or cooling, and locomotion (mechanical energy). In the power sector, final energy is equivalent to usable energy. In the heat sector, the conversion into usable energy is not loss-free (e.g., combustion or heat transfer), which is why a degree of utilization is included in the calculation: 90% in 2010 and 95% in 2050.

In the transport sector, usable energy is mechanical energy, propelling the axle. Conventional combustion engines (gasoline, diesel, natural gas, biofuels) cause a lot of efficiency losses, which are taken into account when calculating the degree of utilization: 20% in 2010 and 30% in 2050. Usable energy for fuel cell vehicles (FCV) using hydrogen as fuel in 2050 was calculated with a 60% degree of utilization.

Developments in the heat and transport sector will be looked at more closely in ▶ Chaps. 4 and 5.

### 3.2.2 Development of the Electricity Mix

#### Electricity Demand

Despite all future efficiency improvements for electrical appliances, electricity demand will remain static after a slight decline (Fig. 3.5). Efficiency gains will be compensated by a higher degree of electrification in all areas and by the linking of the power sector with the heat and transport sector.

#### Present Electricity Mix

Figure 3.5 shows the electricity mix for 2010:

- Ca. 378 TW h (61%) fossil energy
- Ca. 141 TW h (23%) nuclear energy
- Ca. 105 TW h (17%) renewable energy

Eight-three percent of a total of 622 TW h gross electricity generated in Germany comes from

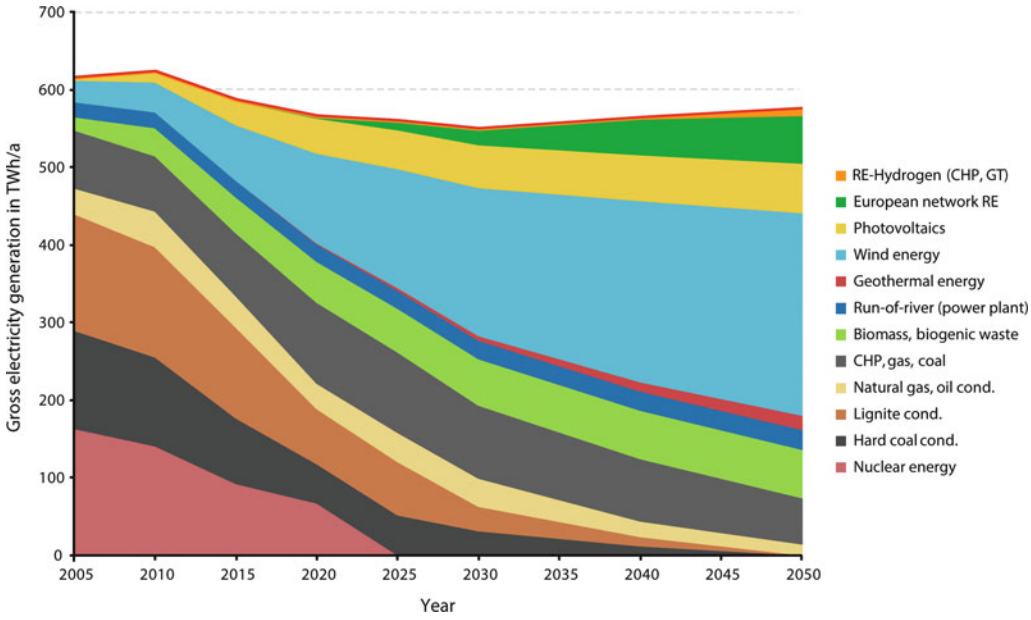



**Fig. 3.5** Composition of gross electricity generation. The red line marks the total. In 2022 the nuclear phase-out of Germany will take place, which explains the distortion of the average between 2020 and 2025. (GT = gas turbine, Cond. = condensing power plant) [25]

fossil or nuclear sources. The present gross value includes vertical grid load along with self-consumption of power plants, but does not cover the power generation of German Rail and industrial self-provision (partially via CHP). In 2013 the share of renewable energy was already at 25%, and thus supplied one-quarter of electricity demand in Germany [2].

The primary energy consumption in the power sector is calculated using the efficiency method, ca. 1,430 TW h. The respective degree of efficiency for fossil power plants (on average ca. 38 in 2010 –61% in 2050) and nuclear ones (notional 33%) is used to calculate primary energy consumption. For electricity directly generated from wind, sun, or water which does not take a calorific value as basis, primary energy is calculated with a degree of efficiency of 100%. This means 1 kW h of final energy is equivalent to 1 kW h primary energy.

### Future Electricity Mix

In the future, mainly wind and solar energy will play key roles in power generation (Fig. 3.5). Until 2020 expansion of renewable energies will not only compensate for the missing nuclear power generation but also for the decline in fossil power generation. In this scenario, fossil fuels are being used far more intensively for power generation via CHP than is the case today. It is for this reason that $CO_2$ emissions will decrease until the power sector is virtually emission-free in 2050. With this perspective in mind, in the long-term, renewable energies will contribute 489 TW h to a total of 574 TW h (85%) gross electricity generation.

### Installed Capacity vs. Gross Electricity Shares

In the course of expanding direct power generation from wind, sun, and water, the need for fossil energy sources is declining and so is the utilization of fossil-fueled power plants. By using coal or natural gas as energy storage and, thus, being an 'extraction-technology', these conventional plants were able to feed-in constantly and as required. This is why their shares in gross electricity generation were always very large in comparison to installed capacity. Matters are different with wind and solar energy:

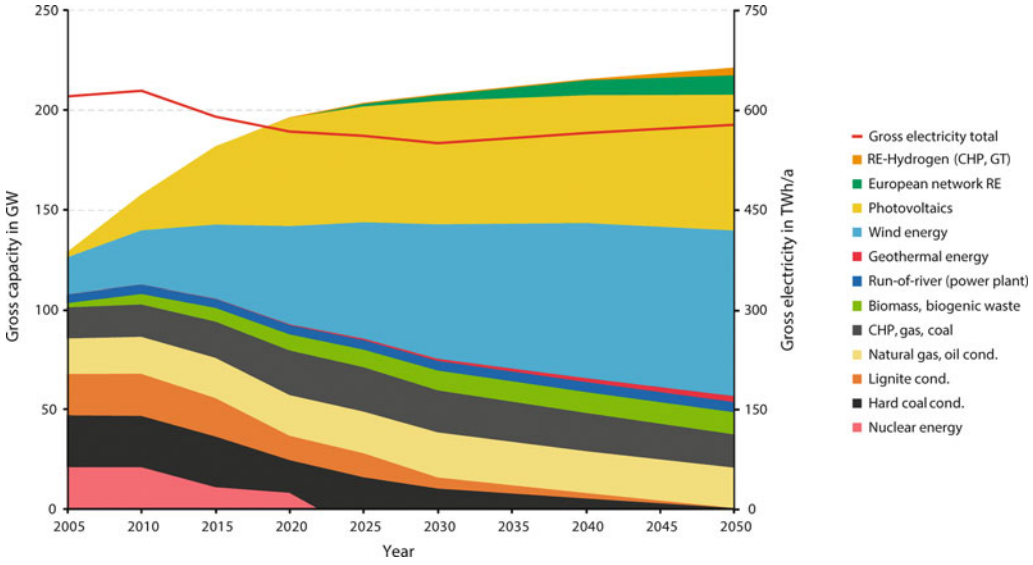



**Fig. 3.6** Installed capacity in power plant stock vs. gross power generation (*red line*). Wind becomes an essential pillar. Installed capacity of wind plants will draw level with PVs at some point in the middle of the century. The capacity of the German power plant stock will increase from today's ca. 150 GW to some 225 GW in 2050, while power consumption will remain almost static at ca 600 TW h/a (*red line*) [25]

their average utilization is 1,800–3,000 full-load hours (h) for onshore, 3,500–4,000 h for offshore wind plants, and 700–1,100 h for PVs. In order to supply the same amount of energy with wind and solar plants as with fossil-fueled ones, greater output capacities will be necessary.

As Fig. 3.6 shows, a higher installed capacity is needed in order to supply an electricity demand, which is approximately identical to today's, because of the decline of fossil-fueled power plants in favor of wind and solar plants which, for meteorological reasons, feed in only a small number of full-load hours.

The significant difference between full-load hours of installed capacities and the amount of energy generated can be seen by comparing Figs. 3.5 and 3.6.

### Dynamic Simulation to Determine Power Surplus and Storage Demand

These annual values of installed capacities and amounts of energy do not provide any information on the situation concerning the grid and the power trade, which is essential for the storage demand. It is for that reason that models were developed in the study to simulate feed-in from renewable energies and power consumption with a temporal resolution of one hour and a spatial resolution of seven by seven km. In this way, information about power surplus and the need for flexibility options such as storage can be gathered.

Figure 3.7 shows a snapshot of a simulation of feed-in from fluctuating wind and solar energy at a share of some 40% renewable energies. It also depicts the amount of residual load, which is crucial for the economic and technological deployment of conventional power plants and storage.

When considering residual load (load minus feed-in) only, the conclusions below can be drawn.

1. Conventional power plants will have to face the following challenges as their utilization declines:
   - Technological requirements for shorter maintenance, minimum operating periods, and higher power gradients for short run-up and run-down times will increase.

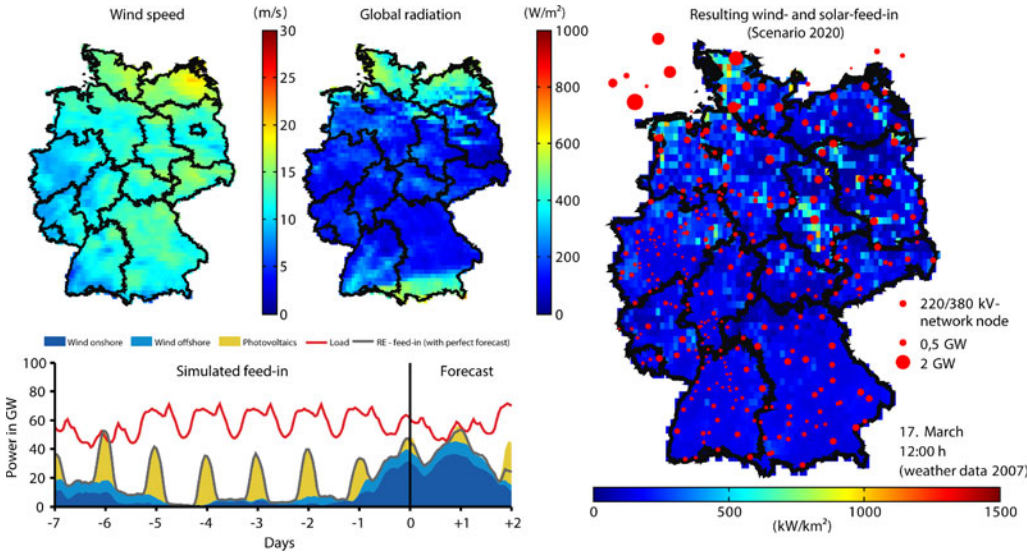



**Fig. 3.7** Fluctuating feed-in from wind and solar plants in a scenario of ca. 40% renewable energies (according to scenario 2011 A, that will be in 2020). The *top left* shows a prognosis for wind velocity, and the top right for solar global irradiation. This data was provided by the German Meteorological Service (GMS). The chart on the *lower left* shows power requirements (load) and simulations of feed-in from wind and solar plants based on meteorological data. Using this, residual load can be calculated. The *right-hand side* chart shows aggregated feed-in from wind and solar power into their respective 110 kV hubs [25]

- Economic pressure will increase because invested assets cannot be used while profit margins have to be gained.

2. Fluctuations in the grid will increase significantly:
   - Load fluctuations in the range of GW will become the norm. They will increase requirements for network operation.
   - Despite the huge expansion of renewable energies, the maximum power plant capacity to cover the annual peak-load (technical security of supply) is barely declining.
   - The need for flexibility options, such as energy storage, to balance feed-in from renewable energies will arise.

The following are parameters for power plant deployment modeling:

- Regional feed-in from non-controllable renewable energies (wind, PV) and their respective forecasts
- Non-controllable load and load forecast with regard to the region
- Possibility of DSM (e-mobility, heat pumps, air-conditioning, and households)
- Electricity transmission in the regional network model—not yet applied in the study (results based on ideal grid expansion)
- Deployment of power plants (condensing power plants, CHP, biomass, pump-storage plants—PSP)
- Deployment of energy storage (pump-storage, power-to-gas—PtG, etc.)

The results in ▶ Sect. 3.2, ▶ Chaps. 4, and 5 were derived from this model.

### 3.2.3 Effect of Minimum Generation and Import/Export on the Storage Demand

#### Effect of Minimum Generation of Power Plant Stock—Must-Run

In this scenario, it is already possible to (over-) supply the whole of Germany with renewable

**Table 3.1** Need for technical minimum generation in conventional power plants [17]

| Aspect | Criterion for minimum generation/function | Resulting minimum effective power generation in GW |
|---|---|---|
| (n-1)-security (failure protection) | Securing flexibility potential<br>Shift of generation up to 7 GW | 3 GW from standing idle plants (market-based) |
| Short-circuit power | Sufficient short-circuit power at network nodes and branches | (–) (if drawn from the European compound) |
| Voltage stability | Supply of reactive power in times of strong winds and low-load | 4–8 GW |
| | Supply of reactive power in times of weak winds and high load | 16–20 GW |
| Controlling system balance | Securing system balance in times of insecure and deranged operating conditions | 8–25 GW |

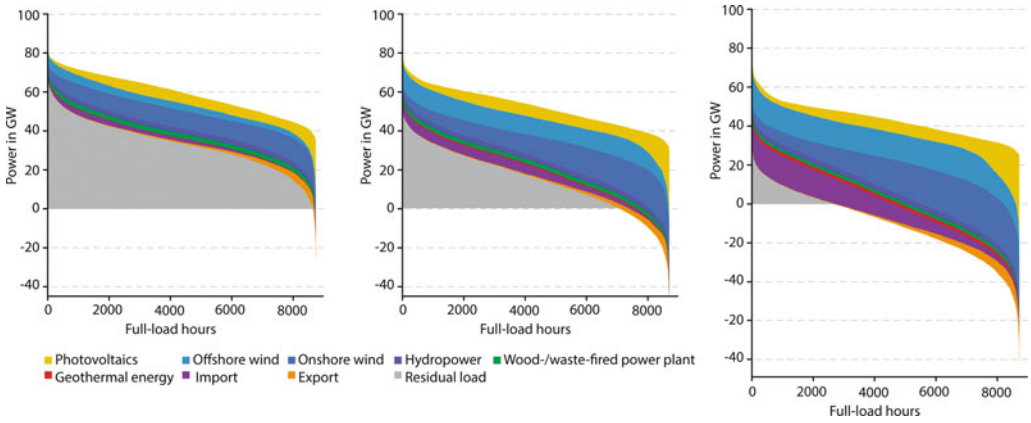



**Fig. 3.8** Effect of must-run capacities and import/export on electricity surplus (ideal grid expansion provided) shown by means of an annual load duration curve for 2020 (40% RE), 2030 (63% RE), and 2050 (85% RE) [26]

energy in a couple of days and weekends in spring or summer in the year 2020. The crucial factor for the amount of power surplus is the minimum generation of conventional power plants to ensure system stability and supply of heat via heat networks (must-run-units).

Today's need for technical minimum generation in the conventional power plant stock was determined in a study carried out by the FGH [17] and can be seen in Table 3.1.

In addition to these value figures, which cannot simply be added up, there is a certain minimum generation from CHP plants. The resulting need for must-run-units on this scale is an obstacle for a system containing strongly fluctuating renewable energies. If the need for must-run-capacities does not decline and there is a delay in grid expansion, there will be significant power surplus when, in 2020, the share of renewable energies is at 40%. This becomes clear when drawing a line at 20 or 30 GW in Fig. 3.8.

These 'gray' surpluses, on the other hand, make measures of balance such as energy storage necessary. They are called gray because renewable energy could still be integrated, but the source of energy is mainly fossils. The actual amount of minimum generation is expected to

decrease because of flexibilization of CHP and the provision of ancillary services by renewable energies.

#### Effect of Import and Export

Power imports and exports via cross-border AC and DC interconnections have a balancing effect on fluctuations in feed-in and, therefore, decrease power surplus and storage demand. In 2030, transmission capacities are estimated to have reached 11.7 GW on AC and 13.8 GW on HVDC lines. By 2050 another 17.6 GW of bipolar DC lines will be installed.

As shown in the section for 2050 (Fig. 3.8), imports and exports will still not be able to fully compensate for strong fluctuations when the shares of renewable energies are very high.

### 3.2.4 Effect of DSM on the Storage Demand

#### Technical Potential for DSM

Today's rigid demand for power can be made more flexible by DSM. Every kW h that can be 'consumed' is temporally shifted, and can be part of the extraction unit of an energy storage system. In ▶ Chap. 11, a more detailed explanation is given of how DSM can work as energy storage.

Intelligent control of load, including cost signals and forecasts, is indispensable if DSM is to be integrated into balancing groups, power, and energy markets. Intelligent control will be taken care of by IT and communications technology ('smart grid' and 'smart meter'). Furthermore, legal foundations have to be adjusted to fully realize the potential. Data protection has to be taken into account as well. The required power measurements and peak-load restrictions for industrial companies are already established. For households, standard load-profiles will apply, which will only be valid if the number of households is greater than 100–150. That is why, at this point, no appropriate DSM is possible for households.

According to the Dena-Grid Study II [14], households are able to make the greatest contribution to load balancing in a positive as well as in a negative sense. In private households, these mainly consist of storage heating, electric heat-pumps, cooling and freezing devices, washing machines, and dryers. Together, this is a technical potential of more than 30 GW to consummate power surplus on a short-term scale (negative contribution). On the other hand, households can potentially 'provide' more than 10 GW (positive contribution), which they do by turning off and thus temporally shifting consumption to a point of time when a smaller load or more power is in the grid. Figure 3.9 shows the technical potential of DSM in 2015, based on the Dena-Grid Study II [14], without taking the economic framework into account.

#### Economic DSM Potential

The economic potential is much smaller in all three sectors because huge investments are required in business and the industrial sector, while households have to make sacrifices as far as comfort is concerned.

Because of this, the Dena-Grid Study II predicts an economic potential of 3.3 GW for the industrial sector and 0.8 GW for business in 2020, which will mainly be traded on the control power market. For households the potential is estimated to be 1.5 GW [14].

Due to efficiency improvements, these potentials are bound to decline in the long run. New electrical loads, such as e-cars, heat pumps or electrolyzers for electricity fuels, have more potential for DSM. Their integration requires obligatory DSM, since they could impair network stability if they were to consume power all at the same time.

#### Relation Between DSM and Storage Demand

Simulation of power supply shows that DSM is an alternative worth considering, as it is able to reduce the energy storage demand. Figure 3.10 compares the contribution of DSM in 2020, 2030, and 2050.

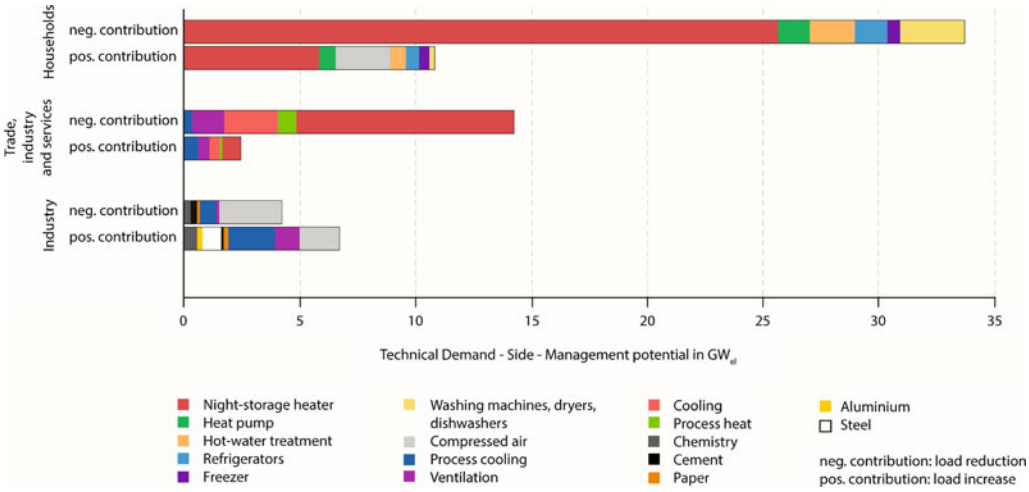



**Fig. 3.9** Technical potential for DSM in 2015, based on the Dena-Grid Study II [14, 25]

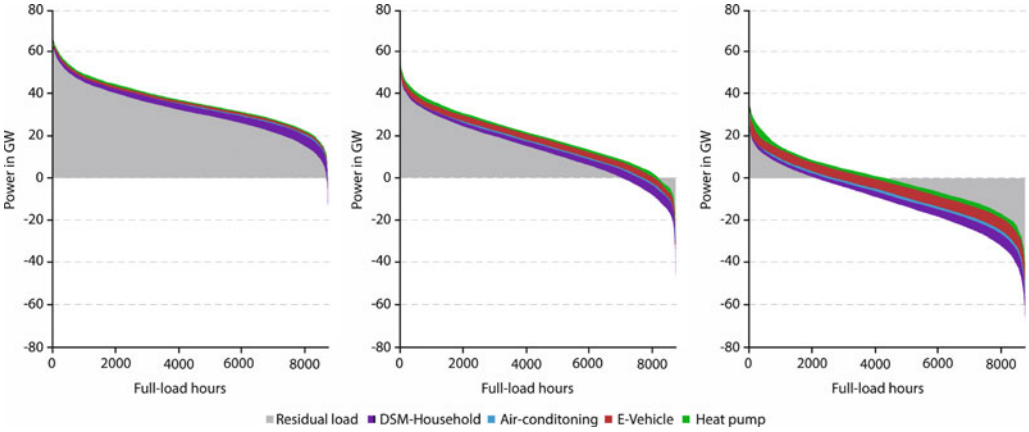



**Fig. 3.10** Effect of DSM on electricity surplus, based on an ideal grid expansion, shown by means of an annual load duration curve for 2020 (40% RE), 2030 (63% RE), and 2050 (85% RE) [25]

In 2020, mainly storage heating and hot water preparation will be used in DSM households. If the modeled potential, as described above, is fulfilled, DSM will almost fully compensate for the power surplus that is left after import/export, always assuming small must-run capacities.

At some point between 2030 and 2050, electric vehicles, heat pumps, and intelligent loads will catch up in terms of DSM, and it will not be possible to integrate all power surplus.

### 3.2.5 Storage Deployment at 40%, 63%, and 85% Renewable Energies

#### Storage Deployment in 2020: 40% Renewable Energies in the Electricity Mix

Fig. 3.11 shows the simulated deployment of the German power plant stock in 2020 after all previously described measures of import/export, DSM, and additional storage have been

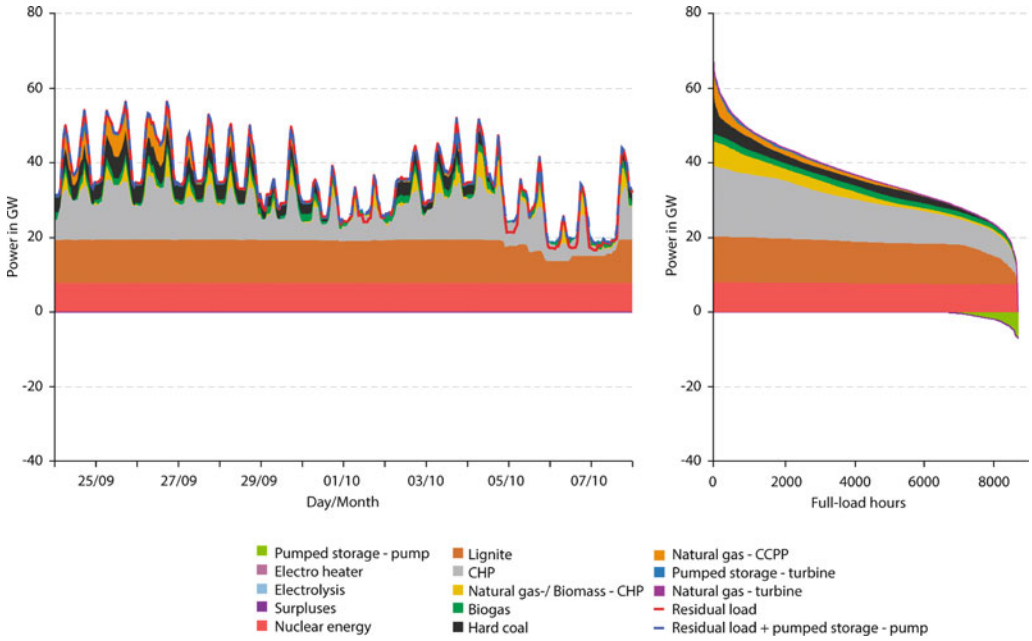



**Fig. 3.11** Deployment of power plant and storage deployment in the scenario year 2020 at 40% renewable energies [25]

taken into account. Today's storage consists of pump-storage power from the German balancing group (PSW Germany, PSW Vianden Luxembourg, and PSW Ilwerke Austria) and the compressed air storage (CAS) Huntorf. It is a conservative assumption that no new pump-storage projects will be able to be realized until 2020, but even without them, 40% of renewable energies can be integrated into power generation, provided that grid expansion has been sufficient and that the above mentioned measures have been taken.

The deployment of storage will mainly take place on a short-term basis—specifically on pre-existing pumped-hydro storage (PHS), which along with balance of generation, will be traded on reserve markets as operating reserve. All 3.7 TW h/a pumped-hydroelectricity are exclusively 'gray'. This means that renewable energies have no share in the electricity mix of the storage system. With regard to the model assumptions, the need for long-term storage does not exist in this scenario. If an ideal grid expansion is realized and power plants are used fully flexibly, there is no need for additional storage.

### ▪ Storage Deployment in 2030: 63% Renewable Energies in the Electricity Mix

As a result of the further expansion of renewable energies after 2020, and the associated increase in fluctuation, requirements on the conventional power plant stock and the flexibilization of CHP will be very high. Therefore, the expansion of heat storage for CHP-systems is of great importance. Figure 3.12 exemplarily shows the course of load over a period of two weeks.

Along with heat storage, 5.9 TW h/a pumped-hydroelectricity will be deployed, assuming that all projects known to be in planning today will be completed. Thirty-one percent of

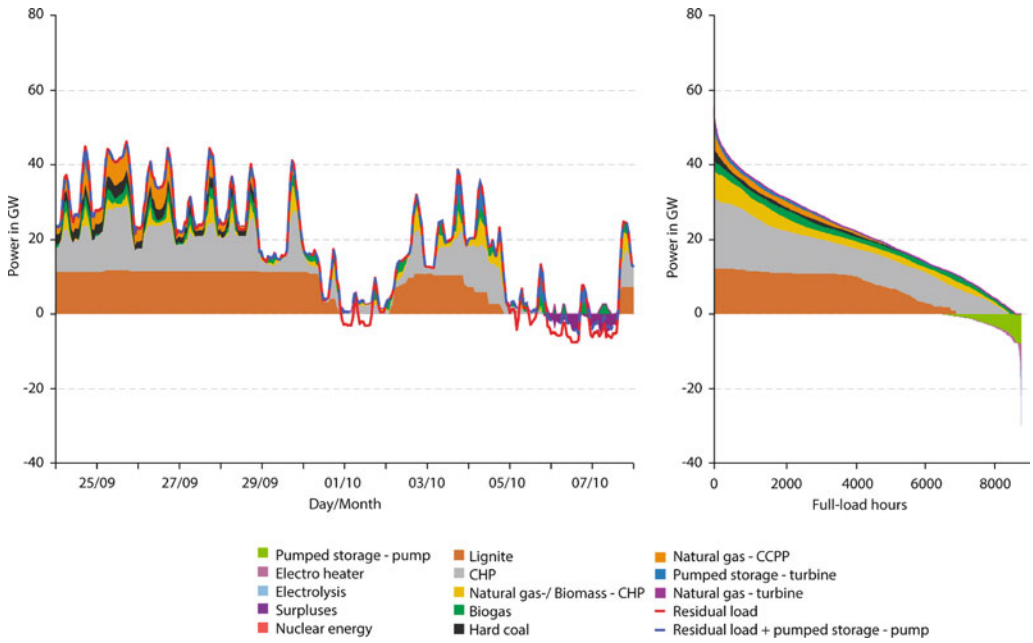



**Fig. 3.12** Deployment of power plant and storage deployment in the scenario year 2030 at 63% renewable energies [25]

this pump currently have a renewable source, which means one-third of it serves the integration of renewable energies. Indirectly, it encourages integration by reducing the amount of must-run-units and increasing utilization of CHP, thus creating more flexibility in the whole system.

Surplus can almost fully be integrated by using heat and short-term storage. There will not be much further surplus for PtH and long-term storage, such as PtG at 63% renewable energies in the electricity mix.

### ■ Storage Deployment in 2050: 85% Renewable Energies in the Electricity Mix

In 2050, long-term storage will be used to its full extent and be of significant importance in achieving climate objectives and objectives concerning the expansion of renewable energies (Fig. 3.13). At 85% renewable energies and ideal grid expansion, its utilization will be economically acceptable. Utilization of short-term storage will be very good also. The share of renewable energies in the pump is currently between 85 and 87%, which equals 8 TW h and, therefore, surmounts values from 2020 and 2030 significantly. In this high-percentage scenario, PtH will supply the demand for heat on a GW-scale in times of very high electricity surplus due to the weather.

### ■ Storage Demand Resulting from Operating Reserve

Another indicator of the storage demand is the need for operating reserve. It is part of ancillary services and balances the system on a short-term scale in cases of power plant outages or forecasting errors. According to the simulations, the need for secondary power will increase only slightly from today's ca. ±2 to

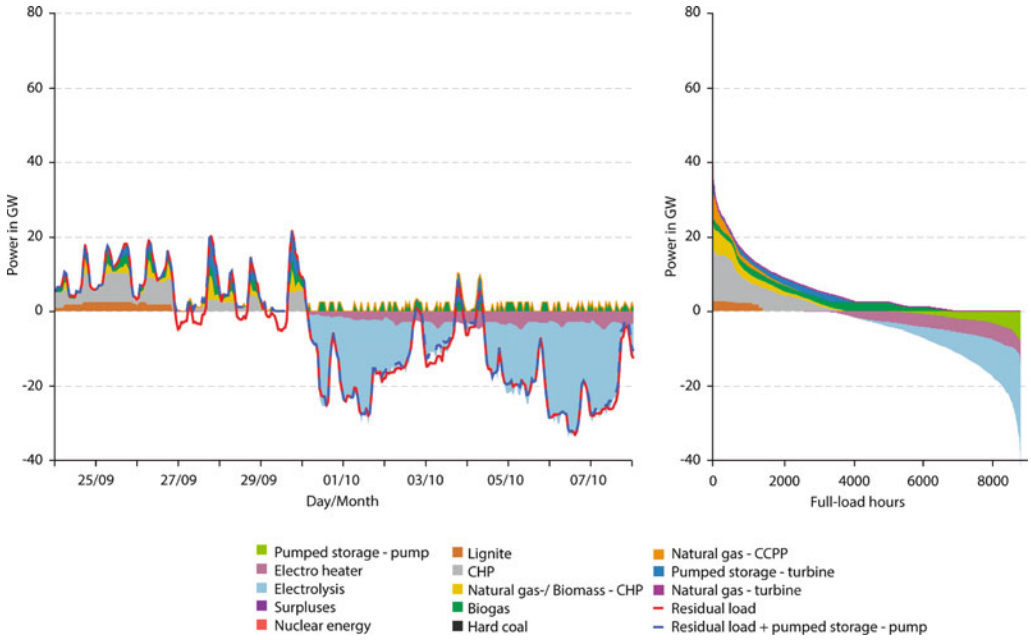



**Fig. 3.13** Deployment of power plant and storage in the scenario year 2050 at 85% renewable energies [25]

±2.2 GW until 2020 and 2030. To a certain extent, the same applies for minute-reserve, which will, mainly on the positive side, increase slightly from ca. 2 to 4 GW until 2020, but then remain static. The primary operating reserve market is of easily manageable size with only ±600 MW, and no factor for the storage demand.

Generally, the need for operating reserve is closely interrelated with forecasting quality of wind, PVs, and load, which will continue to improve over time. Therefore, storage demand for renewable energy systems equal the amount of conventionally provided ancillary services, such as operating reserve replaced by renewable energies [25].

## 3.2.6 Abstract

On the basis of the essential assumptions (ideal grid expansion in Germany, flexibility of CHP, AC and DC interconnections to adjoining European control areas, transmission network level only), the following statements are made on surplus and storage demand by Langfristszenarien des BMU:

### 3.2.6.1 Conclusion

- As soon as **2020**, **renewable energies will be able to (over-)supply** the whole of Germany within a couple of days in spring and summer. The decisive factor for electricity surplus is the amount of **minimum generation** for **ancillary services** and **power generation connected** to **heat supply** (must-run-units).
- If the demand for must-run capacity remains static and grid expansion is delayed further, expansion of renewable energies to 40% in 2020 will lead to **significant electricity surplus**. However, the actual need for must-run capacity will decrease in the course of the **flexibilization** of CHP and the

ancillary services being taken over by renewable energies.

- The storage demand resulting from **operating reserve** equals the amount of conventionally provided ancillary services, such as operating reserve replaced by renewable energies. The main influence on storage demand is **improving forecasting quality of wind, PVs, and load**.
- **Electricity imports and exports** will diminish fluctuations from wind and solar energy and, therefore, **reduce** storage demand.
- **DSM** has a **diminishing** effect.
- At **40%** renewable energies in 2020, only short-term storage in the form of **pumped-hydro** will be deployed. Renewable energies will have no share in the pump current. There will be **no need for additional storage**.
- At **63%** renewable energies in 2030, **additional short-term storage** will be needed, which can be provided by pumped-hydro projects now in planning. Pump current will be 31% renewable. **Heat storage** will be needed to make CHP more **flexible**. PtH and long-term storage systems, such as PtG, will not be frequently deployed.
- To achieve climate goals in the power sector by increasing the share of renewable energies to **85%** by 2050, **short-term as well as long-term storage** is needed. Long-term storage such as PtG will be in use to its full extent. The electricity mix in pumped-hydroelectricity will consist of 87% renewable energies. **Heat storage** and **PtH** play an essential role in heat supply and provide well utilized flexibility for the power sector.

## 3.3 "100% Renewable Electricity Supply," According to the Federal Environment Agency

In order to find out if it is possible to fully supply Germany with renewable energies in 2050, the Federal Environment Agency has, in cooperation with the Fraunhofer IWES Kassel, launched a study in which the federal government's goals concerning energy transition and climate protection are being tested for feasibility [42]. This study will be examined below, focusing on electricity surplus and storage demand.

### 3.3.1 Estimates on Power Consumption in 2050

#### 3.3.1.1 Framework Conditions and Overview

- **Demographic and Economic Framework Conditions**

The study is based on the assumption that living conditions and the Federal Republic's status as highly developed industrial country with corresponding economic structure and demand for mobility, will not have changed by 2050. Neither will the usage pattern.

The population is expected to decline from 82 M today to 72 M in 2050. There will be a slight increase in life expectancy and in birthrate and immigration, which is similar to today.

An average GDP growth of 0.7% until 2050 is assumed to be the economic development in which, due to the continuation of former trends, the share of services is increasing.

Furthermore, it is (very conservatively) assumed that the best technology on today's market is deployed without significant enhance-

**Table 3.2** Presupposed power consumption in 2050 including ohmic line losses and transformation losses [42]

| | |
|---|---|
| Final energy consumption (electricity) | 468 TW h |
| Households | 105 TW h |
| Business, trade, services | 90 TW h |
| Industrial sector | 201 TW h |
| Transport | 72 TW h |
| Transformation consumption | 8 TW h |
| Net power consumption | 476 TW h |
| Line losses | 30 TW h |
| Total power consumption | 506 TW h |

ments until 2050. Quite optimistically, on the other hand, fulfilment of efficiency potential until 2050 is presupposed.

The analysis of load coverage and storage demand in 2050 is based on power consumption of households, business, trade and services (GHD), the industrial sector, and power for transport. The reference years for data input are 2005 and 2008.

#### ▪ Presupposed Power Consumption in 2050

Table 3.2 recapitulates all assumptions concerning power consumption in 2050. Despite ongoing electrification of heat and traffic, total power consumption will be less than what it is today (ca. 600 TW h/a).

From 2005 until 2050, the total amount of final energy for electricity, heat, and transport will be reduced by more than 50% in this scenario. Along with this significant reduction of final energy, the substitution of fossil fuels by electric energy sources will be observed in all sectors. While barely reaching 27% in 2005, the percentage of electricity in final energy consumption will increase up to more than 50% in 2050. Electricity will be the core of energy supply in this scenario as well (▶ Sect. 3.2.1).

### 3.3.1.2 Derivation of Saving Potential and Development by Sectors

#### ▪ Power Consumption of Private Households

Ambitious efficiency goals have been set for power consumption of private households. Thus, electricity is supposed to fully replace fuels, while final energy consumption will decrease from 760 TW h in 2005 to 105 TW h in 2050.

Households need heat (space heating and hot water) as well as power (lighting and electric appliances).

With regard to space heating, it is assumed that the average area-specific need for usable energy will decline from 144 kW h $m^{-2}$ $a^{-1}$ today, to ca. 26 kW h $m^{-2}$ $a^{-1}$. By increasing the annual renovation rate to 3.3% and further raising standards for new construction, a complete restructuring of existing buildings is to be achieved which, in turn, will help to meet the aforementioned goal concerning the decline in energy consumption. The residual need for heating power of 101 TW h will be supplied by solar energy (5%) and electric heat-pumps (95%, i.e., 31 TW h electricity plus 65 TW h environmental heat) working with an annual COP of 3.1.

The need for hot water will not change until 2050, because the usage pattern is not expected to change. Cutbacks are only estimated to be made in heat storage and distribution. As in the case of space heating, the need for water-heating power will mostly be met by electric heat-pumps and solar-thermal devices and, thus, leave only the small amount of 5.6 TW h to be supplied by electricity.

The study is based on the assumption that all peripheral devices for generation and distribution of hot water and space heating are state-of-the-art. Comfortable indoor climate will be created by ventilation systems with heat recovery, which circumvent high energy

losses caused by aeration. Their power consumption is negligible compared to the energy they save. Another important factor are heating circulation pumps which will consume only 3.6 TW h/a instead of 8.5 TW h/a after considerable efficiency improvements.

Using illuminants of the highest efficiency level will minimize power consumption for lighting from 12 (2005) to 2 TW h. Electricity needs of domestic appliances, and information and communication devices can also be decreased by efficiency improvements such as the replacement of gas by electric stoves and avoidance of stand-by losses. In this scenario, a cutback of 25% to 63.5 TW h/a can be realized.

- **Power Consumption in the Industrial Sector and in Business, Trade, and Services**

In the industrial sector, energy demand can be divided up into mechanical energy, space heating, and process heating, which makes up the largest portion. It will be possible to reduce energy demand for process heating by 42% per year to 50 TW h by measures such as heat recovery. The remaining demand for process heating will be supplied by electricity, CHP of biogas plants, or other energy sources. More efficient and demand-oriented facilities can reduce the need for mechanical energy, as well as the need for lighting, by two-thirds. Space heating will almost entirely be based on electric heat-pumps.

In conclusion, despite an increase in production by more than one-third, final energy demand will be reduced from 674 (2005) to 498 TW h/a (2050), with renewable energies contributing 41%.

In the business, trade, and services sector, despite additional power requirements for cooling by ventilation and air-conditioning, an estimated 60% of the final energy consumption may fall away. Because of efficiency improvements in lighting, space heating, mechanical energy, and process heating, the amount of energy needed will be reduced from 406 to 171 TW h/a, with more than 60% being provided by the power sector.

- **Transport**

Today, ca. 22 TW h electricity in the transport sector almost exclusively power rail vehicles. The expansion of e-mobility will cause the relevance of electricity in the transport sector to increase significantly. This prediction is based on the assumption that, in 2050, half of all passenger kilometers will be completed electrically and, thus, will cause an additional power demand of 50 TW h.

## 3.3.2 Technical-Ecological Potential of Renewable Energies, Storage, and DSM

### 3.3.2.1 Potential of Renewable Energies

The assumptions made about the expansion of renewable energies greatly affect the storage demand. In this section, the basic technical-ecological potentials of renewable energies will be examined more closely. PVs and wind energy have been identified as essential pillars.

- **PVs**

Relevant factors for the PV potential are its efficiency and space availability. In this study, average efficiency is conservatively estimated to be 19%. As far as the amount of space is concerned, all rooftops, facade surfaces, and noise barriers are regarded as potential. With conversion areas not taken into account, the total usable area is 1,620 $km^2$, on which a capacity of 275 GW can be installed, which in turn produces 248 TW h/a at 900 full-load hours.

- **Onshore Wind Energy**

Plant technology (mainly the rotor-generator-ratio, hub height) and usable area are crucial factors for wind power, in much the same way

as for PV plants. In the study, ca. 1% of the total surface area of Germany can be regarded as technical-ecological potential, because there were no other evaluations at that point of time. The UBA study is based on the assumption that power density for onshore wind power plants is at around 16.6 MW/km$^2$, which results in a conservative potential of 60 GW. Until 2050, more efficient and higher plants will generate 180 TW h/a at 3,000 full-load hours.

A newer IWES study came to the conclusion that 2% of the national territory are technical-sustainable potential, on which a capacity of 198 GW can produce 390 TW h/a at 2,000 h/a [9].

### Offshore Wind Energy

On the high seas, winds blow constantly, more often, and are stronger, which is the key advantage of offshore wind energy compared to onshore. Limiting factors are maintenance on the sea and connections to the shore. Owing to the absence of reliable studies, an estimation concerning installed capacity was made based on Langfristszenarien des BMU (▶ Sect. 3.2). Taking increasing water depth into account, 45 GW at 4,000 h/a have the potential of generating 180 TW h/a. This means that onshore power generation is equal to offshore.

A recent IWES study for Foundation Offshore confirms an energy potential of 258 TW h/a for an installed capacity of 54 GW operating 4,778 h/a on all presently usable areas in the North and Baltic Sea [31].

### Hydropower

In Germany, the potential hydropower is, except for small hydropower, almost fully tapped with 5.6 GW and 24 TW h/a (as of 2011, [7]). Natural rivers are not expected to drive large-scale hydropower plants. Only modernization and expansion of existing plants and new construction of small capacity plants have the potential to increase power capacity and energy gain. In 2050, the technical-ecological potential is an installed capacity of 5.3 GW, which will generate 24 TW h.

### Deep Geothermal Energy

From our present point of view, deep geothermal energy is only marginally important for power supply in Germany (Table 3.3). The total amount of electricity it generated in 2013 is 24 GW h, which is 0.007% of the annually power consumption across Germany [42]. The advantages of these plants are their ability to meet base-load requirements because of their high utilization of more than 7,500 full-load hours. An additional advantage is that that heat generation is linked to power generation. If heat usage is disregarded, there is a large potential of 312 TW h/a. As for further restrictions, there is the matter of area development from an ecological angle and regional planning which, when taken into account, reduces the technical-ecological potential in 2050 to some 50 TW h/a generated by the installed capacity of 6.4 GW. Twenty-five percent self-consumption of the plant is already included.

### Biogenic Rest and Waste Materials

As far as biomass is concerned, only biomass from waste materials is analyzed because power generation from energy crops is in competition with food production, but is not necessarily greenhouse gas neutral and can have other negative impacts on the environment such as on monocultures. The biomass potential of forests, due to natural regeneration and regrowing wood, is left to material use and not taken into account in the UBA study for power generation. There are always rest and waste materials when processing food and animal feed. They are the potential source of 202 TW h/a thermal energy. Biogas contributes some 40 TW h/a, which equals 23 TW h/a if fed into and distributed by the gas grid, and converted into electricity in gas or steam power plants with an efficiency of 57%.

**Table 3.3** Technical-ecological potential of renewable energies in 2050 compared to 2011, based on conservative estimates from the UBA, cf. [7, 42]

| | 2011 | | 2050 (100% scenario) | |
|---|---|---|---|---|
| | Installed capacity in MW | Energy in TW h | Technical-ecological power potential in GW | Technical-ecological energy potential in TW h |
| PVs | 25 | 19.3 | 275 | 248 |
| Onshore wind | 29 | 48.3 | 60 | 180 |
| Offshore wind | 0.2 | 0.6 | 45 | 180 |
| Hydropower | 4.4 | 18.1 | 5.2 | 24 |
| Deep geothermal energy | 0.008 | 0.02 | 6.4 | 50 |
| Biomass from waste | 1.7 | 5.0 | Gas-fueled power generation as required | 23 |
| Total | 60.3 | 91.3 | 392 | 705 |

■ **Abstract**

Table 3.3 compares today's installed capacity and energy sources with the technical-ecological potential calculated for renewable energies. They have the potential to supply German power demand by themselves.

### 3.3.2.2 Potentials of Storage Systems

As in the VDE-ETG study (▶ Sect. 3.4), in the UBA study, short-term storage consists exclusively of PSP, which balance fluctuations in power generation on a daily basis. As for long-term storage, chemical storage systems using hydrogen or methane from PtG will be examined more closely.

■ **PSP**

Functionality, implementation, and the pros and cons of PSP are described in ▶ Chap. 9 and ▶ Sect. 13.1. Today, there is pumped-hydro with an extraction rate of 6.6 GW and a storage capacity of 40 GW h in Germany. The study is based on the assumption that storage capacity will increase by 0.33 GW due to repowering (modernization of existing plants) and 1.645 GW due to new construction of PSP (Atdorf, Einöden, and Blautal). Because of uncertainties of feasibility and unforeseeable environmental risks, the potential of other locations or new concepts, like using mines as PSP, are not taken into account. In total, turbine power is expected to increase from today's 6.6 to 8.6 GW, and storage capacity from 15 GW h to ca. 55 GW h.

■ **Cavern and Porous Storage Facilities**

Functionality, implementation, and the pros and cons of PtG and gas storage are described in ▶ Chap. 8 and ▶ Sect. 14.3. Cavern storage is suited for methane and hydrogen while porous storage can only hold methane.

Table 3.4 shows the estimated storage capacities for methane (natural gas, windgas) and hydrogen. The potential of porous storage facilities equals the now existing gas storage capacity of 217 TW h. Further potentials are not expected.

Today, cavern storage facilities with a process gas volume of $V_n = 7{,}816\ \mathrm{Mm^3}$ are in use,

**Table 3.4** Capacities of all German cavern and porous storage facilities in 2050, cf. [42]

| Maximum usable process gas | Cavern storage $V_n$ in $Mm^3$ | Porous storage $V_n$ in $Mm^3$ | Total $V_n$ in $Mm^3$ | Total $E_{th}$ in TW h |
|---|---|---|---|---|
| Hydrogen | 36,800 | 0 | 36,800 | 110.4 |
| Methane | 36,800 | 13,600 | 51,400 | 514.0 |



another 7,366 $Mm^3$ are already under construction or in the planning stage. With technical and ecological restrictions taken into account, the further potential is an estimated 400 cavern storage facilities until 2050, which means a duplication of process gas volume to 36.8 $Gm^3$. More detailed information on gas storage systems, their functionality and their potential, can be found in ▶ Sect. 8.4.

Where energy storage is concerned, there could be a capacity of 110 TW h in the form of hydrogen and 514 TW h in the form of methane on hand. These storage capacities exceed future needs by far. Potentials for gas storage for today and in the future are derived separately in ▶ Sect. 8.4.

### 3.3.2.3 Potential of DSM

DSM can be seen as virtual storage; it performs the same task by temporally shifting the demand, and thus contributes to balancing fluctuations in energy systems dominated by renewable energies (▶ Chap. 11). This service is almost always cheaper than 'pure energy storage' and, therefore, preferred to minimize costs for the integral system.

There are large potentials in the industrial sector, and in business, trade and services, and households [23, 36, 44], as listed below.

- Industrial sector:
  - Chloric-alkali electrolysis
  - Paper manufacturing
  - Cement manufacturing
  - Refrigeration supply
- Business, trade, and services:
  - Cold storages, grocery stores
  - Refrigeration supply and air-conditioning
  - Hot water supply
  - Storage heating
- Households:
  - Laundry, drying, dish washing
  - Refrigeration and freezing
  - Electric heat-pumps
  - Hot water supply
  - Storage heating
  - Air-conditioning

In the UBA study, the greatest potentials are seen in electric heat-pumps, air-conditioning, electric vehicles, and energy-intensive loads in the industrial sector.

#### ▪ Heat Pumps

In this study, it is assumed that heat demand is mostly supplied by heat pumps with buffer storage in all sectors (▶ Sect. 3.3.1.2). These buffer storages provide a large 'virtual' storage capacity of 44 TW h/a in the form of heat storage, which can be used, to a large extent, as DSM between the power and heat sector. Since heat pumps are supported by solar-thermal devices in the power range of 2 to 200 kW, their DSM potential is usually between November and February.

#### ▪ Air-Conditioning

Air-conditioning can easily be integrated into DSM in correlation with PV plants, as it is only necessary when the Sun shines intensely. In these cases, latent-heat accumulators (PCM-devices) and ice storage technologies are used (▶ Chap. 10). A large share of energy demand (28 TW h/a) can be used to balance feed-in fluctuations.

#### ▪ Electric Mobility

Vehicles are not being used most of the day (stationary vehicles). Plug-in hybrids and purely

electric vehicles are, up to a certain point, flexible concerning the point of time of recharge, which is why they are so well-suited for storing surpluses ('grid-to-vehicle', or 'G2V'). The reverse ('vehicle-to-grid', or 'V2G'—making the vehicle a complete electricity storage with a bidirectional connector) will not be examined because car manufacturers have not taken that path, and it would reduce durability of the accumulators. The study presupposes that all power demand of electric vehicles (50 TW h/a) is integrated into DSM.

#### ■ Industrial Sector

Power consumption for industrial processes in the chemical industry (chlorine), pit-and-quarry industry (cement), steel production and process heat, or compressed air generation is estimated to be some 50 TW h/a. In the scenario, half (1.5 GW) of the technical potential of positive minute-reserve provision (3 GW) is being realized. Further potentials are not taken into account, which makes it a conservative assumption.

#### ■ Others

Another concept is the deployment of cooling and freezing devices in trade or washing machines, dishwashers, and dryers in households. These potentials are not included in the UBA study.

## 3.3.3 Assumptions and Modeling of the 2050 Scenario

### 3.3.3.1 The 'Region's Network' Scenario

For the simulation of future power supply, different scenarios are possible. One of them is the fusion of European grids into one, in which all potentials of renewable energies and storage systems are realized. As an alternative, German power supply could work on the basis of decentralized stand-alone power systems, which balance generators and consummators locally as far as possible.

The middle course would be the so-called 'region's network', in which all German regions are interconnected as tightly as possible, and the individual region supplies power demand by reciprocally exchanging renewable energy with others. In this scenario, only a very small amount of energy has to be imported. Security of supply is guaranteed by co-operation between these regions.

#### ■ Electricity Generation and Storage

In the region's network scenario, the majority of potentials of renewable energies named in ▶ Sect. 3.3.2 are realized and matched with storage potentials. Only half of the PV potential is realized, and biogas from waste biomass is only used for peak loads and as a reserve. It is for this reason that, in this scenario, the biomass potential is not realized in the power sector, but mainly provides a substitution for fossil fuels in transport and in the industrial sector. The potential of storage is fully made use of.

Arising surplus is primarily exchanged between regions and secondarily consumed by DSM, as required. Only then, if need be, is storage deployed; mainly pump-storage because of their great efficiency, and after having realized their short-term storage potential, long-term storages, such as PtG, including gas storage. Short-term as well as long-term storage, in combination with gas turbine or combined-cycle plants, represent peak load and reserve plants. Additionally, methane or hydrogen can be used as electricity fuels in transport or in the industrial sector. This leaves only a very small amount of electricity unaccounted for.

Table 3.5 shows the degree to which the technical-ecological potential of renewable energies and energy storage is used in the region's network scenario.

#### ■ Heat Production and Refrigeration

Since, due to efficiency improving measures, heat demand has decreased, it is almost possible to completely supply it by heat pumps, in combination with solar-thermal plants. In some regions, concepts to use waste heat from CHP, geothermal plants or seasonal solar-thermal

**Table 3.5** Overview of potential realization of renewable energies and energy storage in the region's network scenario. Adapted from [42]

| | Technical-ecological potential 2050 | | Region's network scenario | |
|---|---|---|---|---|
| | Power in MW | Energy in GW h | Power in MW | Energy in GW h |
| PVs | 275,000 | 24,800 | 120,000 | 104,000 |
| Onshore wind | 60,000 | 180,000 | 60,000 | 170,000 |
| Offshore wind | 45,000 | 180,000 | 45,000 | 177,000 |
| Hydropower | 5,200 | 24,000 | 5,200 | 22,000 |
| Deep geothermal energy | 6,400 | 50,000 | 6,400 | 50,000 |
| Biomass from waste | As required | 23,000 | 23,300 | 11,000 |
| Short-term storage | 8,600 | 55 | 8,600 | 55 |
| Long-term storage | As required | 514,000 (methane)<br>110,400 ($H_2$) | 44,000 | As required |

storage will be applied. Process heat will be supplied by gas from PtG or waste heat.

In the course of climate change, an increase in cooling demand is expected, which can be supplied by adequate concepts (Sun screen, energy saving cooling and ventilation engineering, and air-conditioning) of DSM.

#### ▪ Transport

In the scenario, half the cars are powered electrically. This increases electricity demand, while at the same time decreasing $CO_2$ emissions and fuel demand. Electricity demand for rail transport increases as well.

#### ▪ Energy Distribution

The German grid is integrated into a pan-European transmission network. Hydrogen or methane from waste material biomass or PtG can be fed into the existing natural gas grid. Additionally, gas can be temporarily stored in porous or cavern storage facilities for seasonal balance.

### 3.3.3.2 Modeling and Simulating the Scenario

#### ▪ Approach of the Model

Energy balances are, in most cases, created and discussed exclusively on an annual basis and are, therefore, uninformative when it concerns dynamics and stability of a system. To gather useful insights into this, a simulation with great spatial and temporal resolution is necessary. This simulation is based on meteorological and load data from the years 2006–2009. This makes it possible to take weather extremes, which occur throughout the years, such as Kyril (the storm that raged in Germany in January 2007) into account, and thus make results more universally valid. Temporal resolution is one hour, spatial resolution is $14 \cdot 14\,km^2$ for wind, PVs, and heat pumps. Renewable power generation, behavior of storages, and the load as well as DSM potential of the load can be observed in the simulation.

#### ▪ Model Structure and Methodology

Figure 3.14 shows the structure of the SimEE-modell and also its method of function, which has been created in MATLAB. Points 1, 2, and, 3 represent 'measuring points' for residual load for the figures shown in ▶ Sect. 3.3.4.2. The base-load equals the total demand including losses. Loads in e-mobility, heat pumps and air-conditioning are not included because they are being used as DSM. Hence, the base-load can be calculated from historic load-profiles. Some of the heat demand and the charging

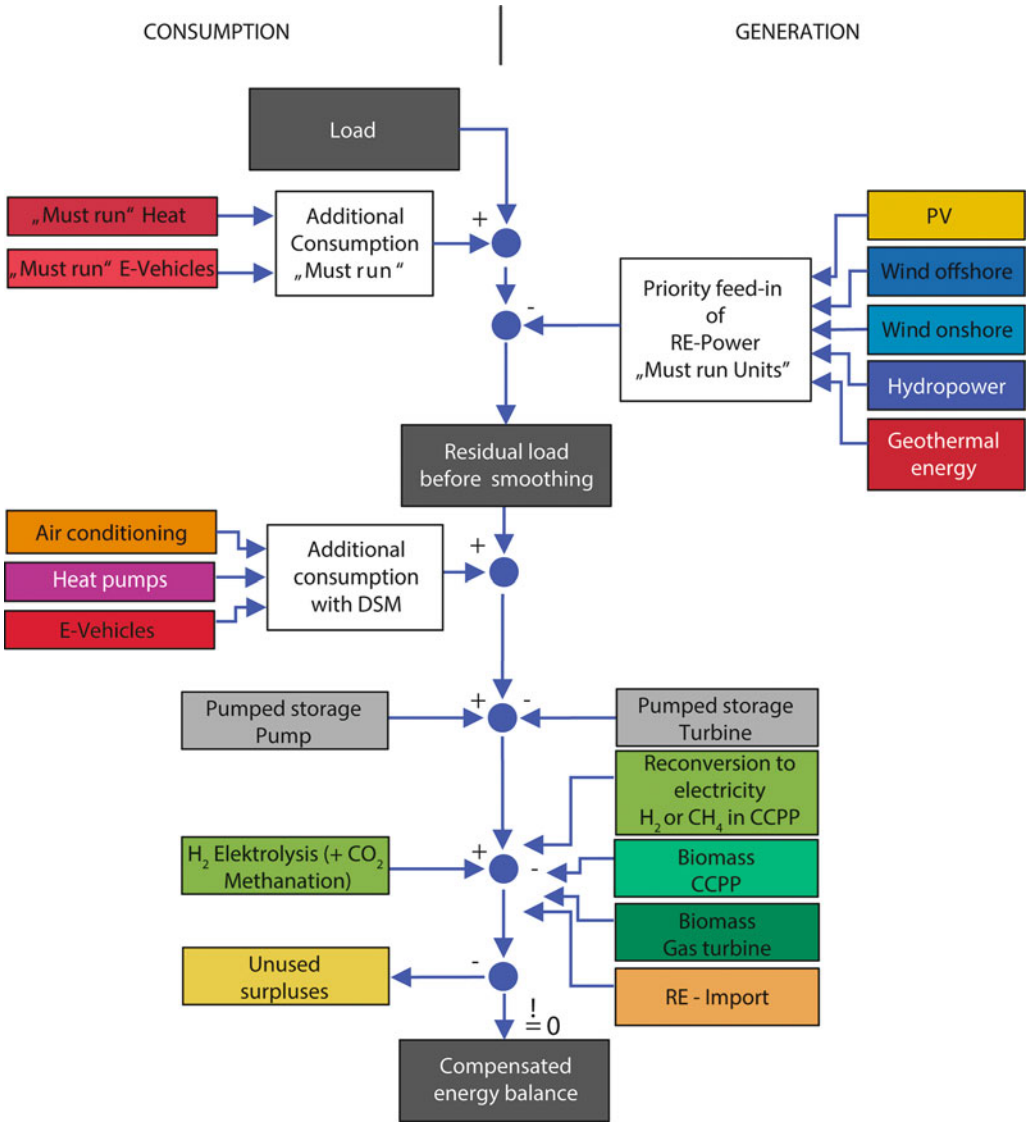



**Fig. 3.14** Structure of the SimEE-modell by the Fraunhofer IWES for the UBA study [42]

of electric vehicles is independent of the feed-in situation on the grid. Therefore a certain amount of power must be provided at all times. These must-run shares of electric vehicles and heat pumps have been taken into account. The residual load consists of the base-load minus feed-in from wind, PV hydropower, and geothermal plants. Depending on the situation, the residual load can be greater than zero (load > renewable feed-in) or smaller than zero (load < renewable feed-in).

DSM using electric vehicles, heat pumps, and air-conditioning is mainly applied in times of negative residual load. The adaption of controllable loads optimizes the synchronization of overall load and power generation. Having fully made use of this potential, pump-storage is deployed as short-term storage and PtG as

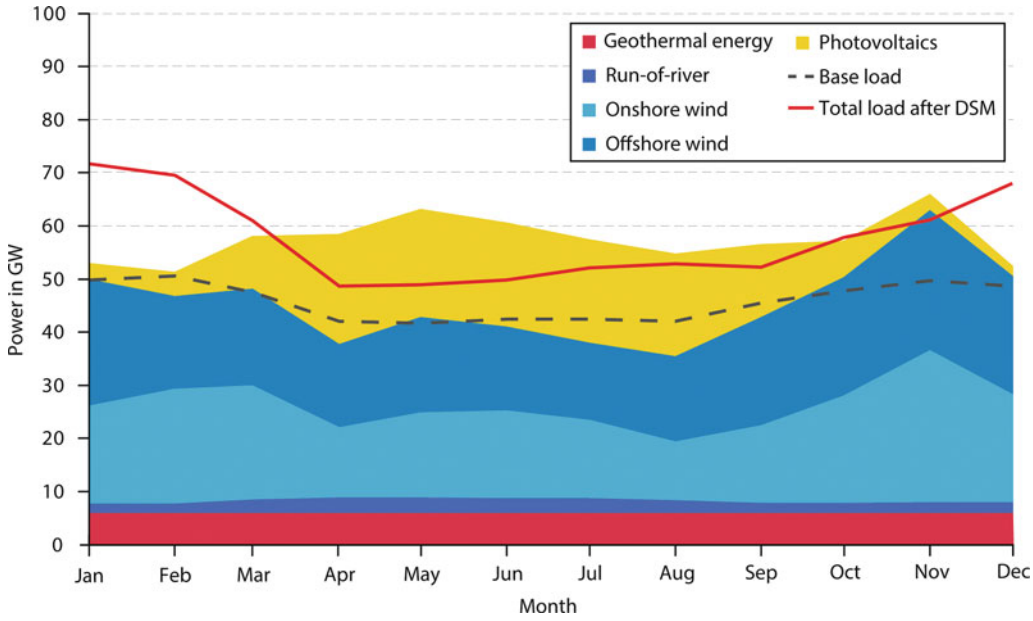



**Fig. 3.15** Monthly average of feed-in from renewable energies based on the meteorological years 2006–2009 [42]

long-term storage. Gas turbines and combined cycle power plants supply remaining deficits using gas from waste biomass and PtG.

A small amount of renewable power imports from the European network compound will remain. Very little surplus electricity will be curtailed because PtG capacities, which would have to be installed, are not worthwhile from an ecological and energetic point of view.

## 3.3.4 Results for Storage Demand and Security of Supply

### 3.3.4.1 Feed-In Behavior of Renewable Energies Throughout the Years

Feed-in from renewable energies is weather-dependent and, therefore, fluctuates with changing seasons over several years. Figure 3.15 shows these fluctuations for the scenario on the basis of a monthly average of feed-in from renewable energies based on meteorological data from 2006–2009. Despite considerable fluctuations of individual energy sources, the monthly average of total feed-in is approximately 50–60 GW. Wind and solar energy complement each other very well over the seasons. According to the weather, feed-in from PVs is greater in summer, while feed-in from wind is greater in winter. The latter coincides nicely with an increased power demand in this season.

Other studies also show this effect and have found the ideal mixture-ratio of installed capacities of wind power and PVs to be some 60:40. Provided there is an ideal grid, this combination reduces fluctuations in Germany and Europe to a minimum, and maximizes balancing effects [19, 21, 29].

The results are detailed below.

PVs:

- On an hourly average, a maximum of ca. 52 GW of a total of 60 GW (87%) installed capacity can be reached. The monthly average is ca. 40 GW and the annual average is ca. 20 GW.
- Despite considerable monthly fluctuations, the annual electricity generation is approximately the same.

Onshore wind:
- On average per hour, a maximum of ca. 80 GW of a total of 120 GW (67%) installed capacity can be reached. The monthly average is ca. 25 GW and the annual average is ca. 20 GW.
- Monthly generation fluctuates strongly by the year.
- Annual generation fluctuates significantly, but tends to follow similar patterns over the years. Generation is greater in winter than in summer.

Offshore wind:
- On average per hour, a maximum of ca. 42 GW of a total of 45 GW (93%) installed capacity can be reached. The monthly average is ca. 35 GW and the annual average is ca. 20 GW.
- The winter–summer tendency of onshore wind is also noticeable for offshore wind, although it is possible to generate the same amount of energy with 25% less installed capacity.
- Annual fluctuations are less pronounced than for onshore wind and PVs: Offshore wind is regarded as the most constant energy source of these three.

Hydropower:
- On average per day, a maximum of ca. 3.2 GW of a total of 5.2 GW (62%) installed capacity can be reached. The annual average is ca. 2.2 GW and a continuous average is ca. 1.5 GW.
- Contrary to common expectations, feed-in from hydropower is not constant over the year but fluctuates by the day and the season; e.g., over the thawing period during spring and early summer.

Deep geothermal energy:
- Geothermal electricity generation is constant at 5.8 GW.
- An advantage is its independence of the weather and its predictable power generation. A disadvantage is its high costs which, however, are not taken into consideration in this study.

In addition to this stochastic evaluation, a more detailed simulation including DSM and storage deployment in an hourly resolution is required. Only then is the full extent to which surpluses and deficits have to be balanced becomes apparent.

As an example, Fig. 3.16 shows a month of December with little feed-in from wind because of a two week calm period, while, in contrast, Fig. 3.17 shows a sunny August. It is clearly evident that in 2050, renewable energies, with the help of DSM, will be able to supply the electricity demand. However, there will be times in which the deployment of storage is inevitable. In the first days of December, surpluses will be stored via long-term storage and used during the 14 days of calm. In August, DSM will be able to match electricity demand to PV feed-in peaks at noon.

Figure 3.17 also highlights those extreme feed-in peaks from PVs and even more extreme gradients when peaks of wind and PVs coincide, e.g., on 14/15 August in the year given in the example.

### 3.3.4.2 Evaluation of the Residual Load as an Indicator for Surpluses and Shortages

Residual load is the difference between renewable feed-in and load (see definition in ▶ Sect. 3.2). The UBA study distinguishes between three kinds of residual loads:

1. Difference between base-load and renewable feed-in without flexibility options and conversion of biomass to electricity (residual base-load), as shown in Fig. 3.18. In base-load, the overall load is included except for flexible deployment of air-conditioning, e-mobility, and heat pumps as DSM (point 1 in Fig. 3.14).
2. Difference between overall load and renewable feed-in, including DSM power consumers but excluding PHS as shown in Fig. 3.19 (point 2 in Fig. 3.14).

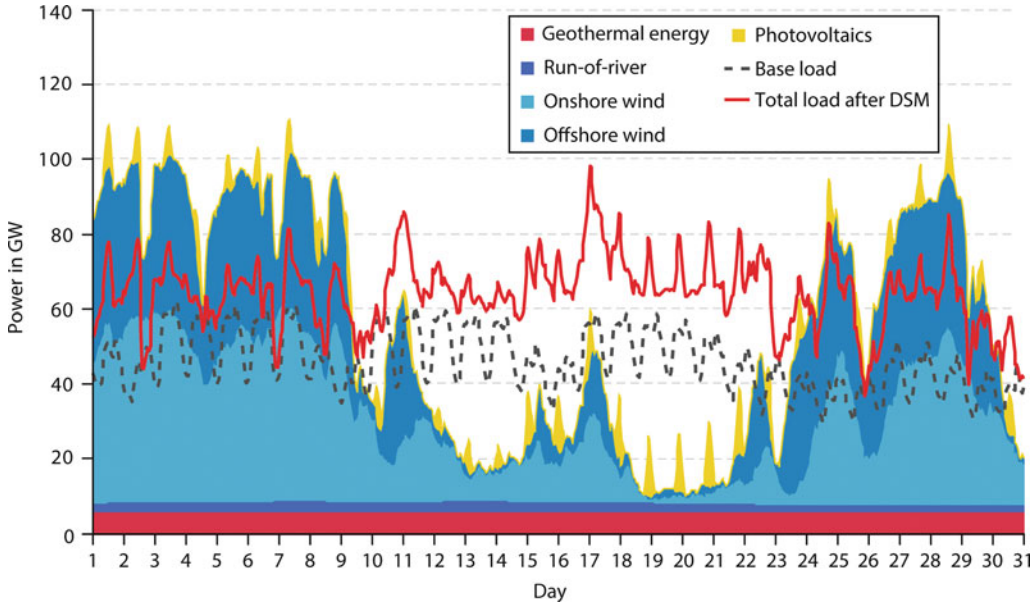



**Fig. 3.16** Feed-in from renewable energies and electricity demand (*red line*) with DSM (*dashed red line*) for December 2050 based on meteorological data from 2007. Several weeks with no wind justify the demand for long-term storage and seasonal balance [42]

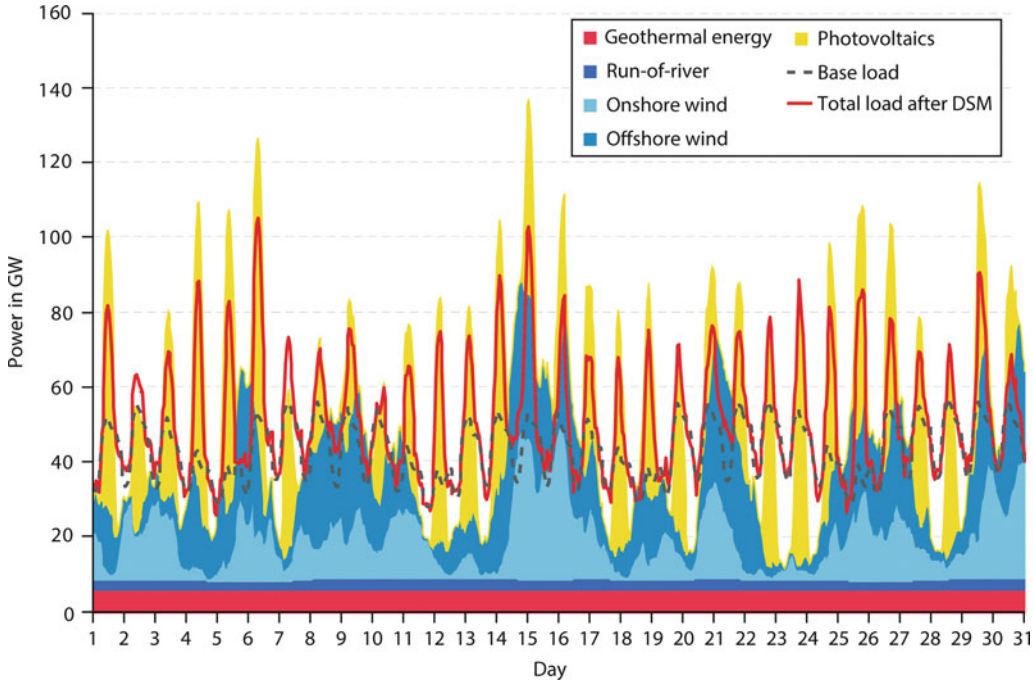



**Fig. 3.17** Feed-in from renewable energies and electricity demand (*red line*) with DSM (*dashed red line*) for December 2050 based on meteorological data from 2007. Daily peaks in feed-in from PVs justify the demand for short-term storage and daily balance [42]

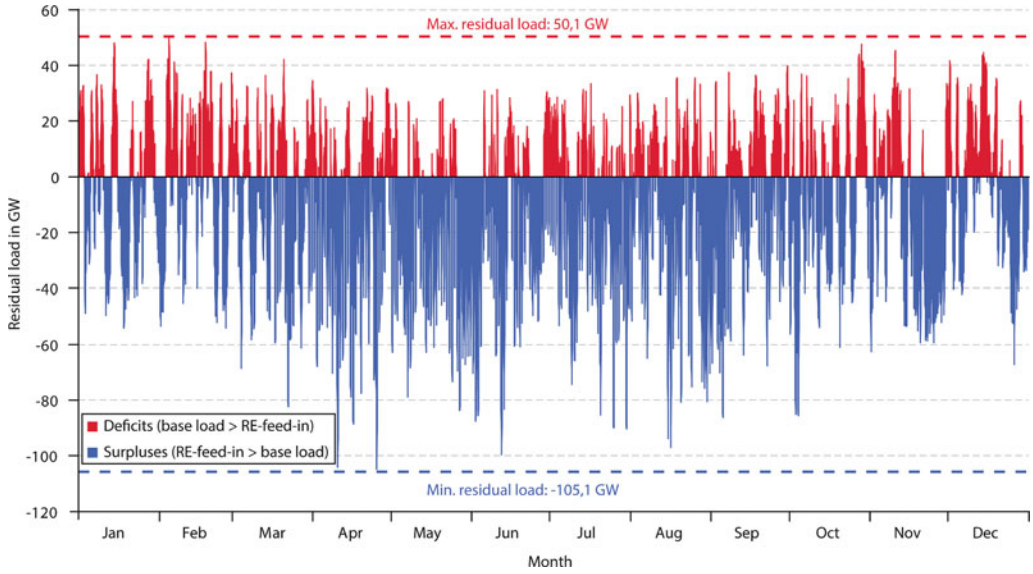



**Fig. 3.18** Residual base-load—without deployment of DSM (heat pumps, air-conditioning, e-mobility) and PHS [42]

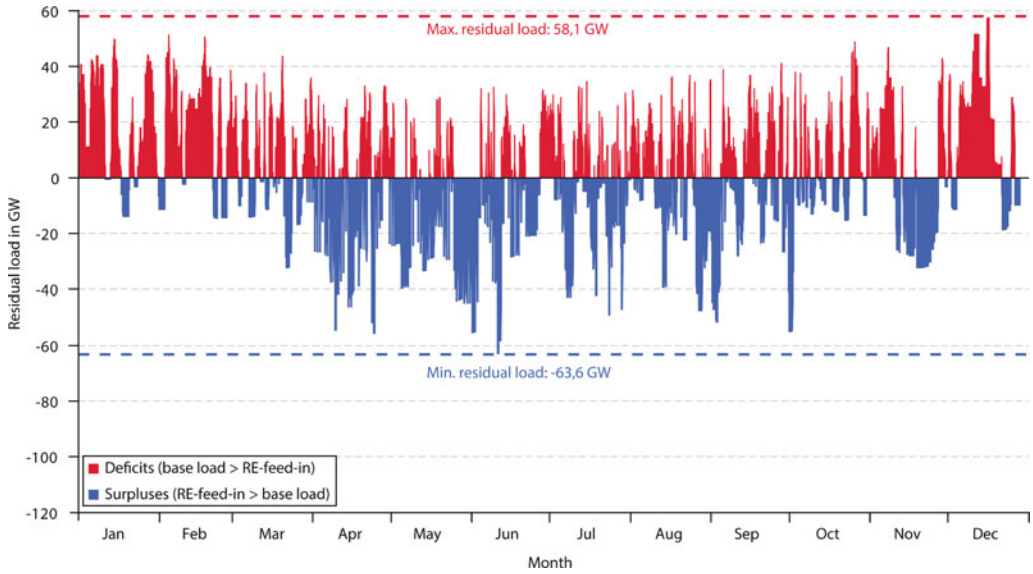



**Fig. 3.19** Residual overall load with deployment of DSM (heat pumps, air-conditioning, e-mobility) without PHS [42]

3. Residual overall load with DSM and PHS as shown in Fig. 3.20 (point 3 in Fig. 3.14).

These figures show these different residual loads using the example of the meteorological year 2009.

Figure 3.18 shows the extreme deflections of the system: hourly surpluses reach up to 105 GW (blue), and deficits reach up to 50 GW. Without DSM and energy storage, up to 150 TW h surplus energy is generated in

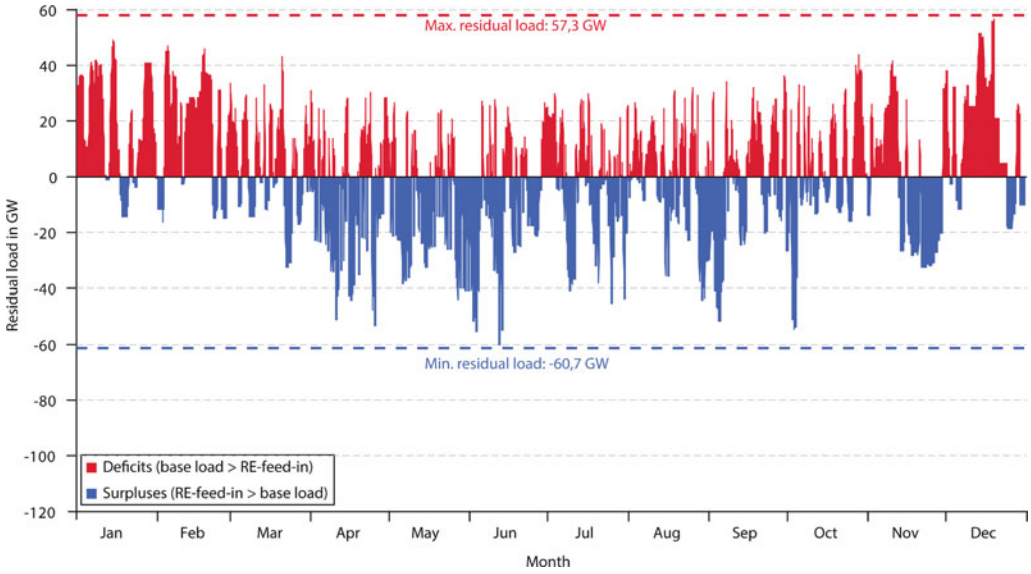



**Fig. 3.20** Deployment of PHS to balance residual overall load with deployment of DSM (heat pumps, air-conditioning, e-mobility) [42]

the Federal Environmental Agency's 100% scenario.

The deployment of new, flexible consumers (heat pumps, air-conditioning, and e-mobility) via DSM will make the integration of almost half (ca. 65 TW h of 150 TW) the surpluses possible and smooth out the deficit curve (Fig. 3.19). This result underlines the importance of DSM (▶ Chap. 11) in its function as energy storage.

### 3.3.4.3 Storage Deployment in a 100% Renewable Power Supply

Great heat storage capacities will be needed and will be used in DSM. For this reason, pure electricity storage via pumped-hydro on a short-term scale and PtG on a long-term scale will be examined in the following.

#### ▪ Deployment of Pumped-Hydro as Short-Term Storage

The complete potential of pump-storage in the German control area, as described in ▶ Sect. 3.3.2.2, is made use of in Fig. 3.20. By comparing this figure to Fig. 3.19, one can see the smoothing effects of short-term storage: maximal deficits are reduced by ca. 1 to 57.3 GW, while maximum surpluses are reduced by ca. 3 to 60.7 GW. At the same time, their balancing effects on the residual overall load is very limited because of their small storage capacities.

The injection and withdrawal rate of PHS is 8.6 GW; they store an average of 8.0 TW h and extract 6.0 TW h. This results in annual full-load hours of ca. 910 h resp. 700 h and 2.0 TW h in losses.

#### ▪ Deployment of PtG as Long-Term Storage

Only a fraction of the potential of long-term storage (gas storage) presented in ▶ Sect. 3.3.2.2 is necessary in a 100% renewable power supply system. In terms of long-term storage, the UBA study distinguishes renewable hydrogen from renewable methane. In both cases, 99% of all surpluses are stored. By curtailing 1% surplus energy, electrolysis capacity can be reduced to 64% (44 GW) of the maximum surplus capacity. Storing this remaining percent would cause a disproportionate technical and financial expenditure.

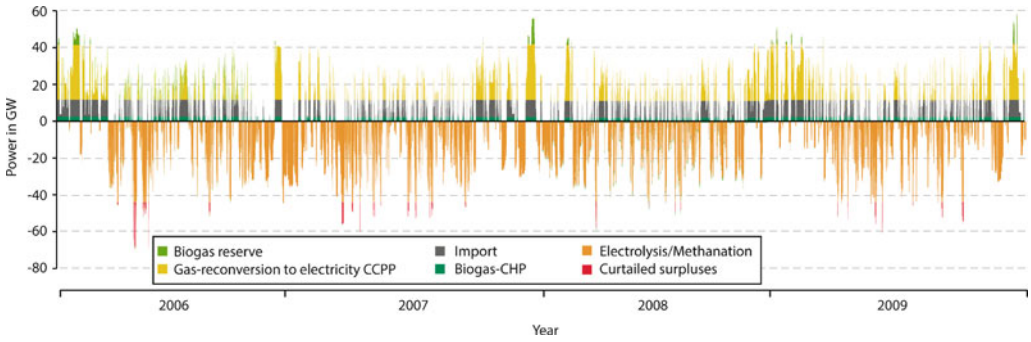



**Fig. 3.21** Deployment of PtG as long-term storage and for supplying residual deficits via little renewable imports and flexible biogas plants over the meteorological years 2006–2009 [42]

The hydrogen variant's overall efficiency of PtG (44 GW electrolysis and 30.4 GW reconversion to electricity via combined cycle plants) is somewhere near 42%. It will thus be possible to supply 100% of the overall load; electricity imports of less than 5% of the overall power demand in 2050 (6.9 GW) are taken into account. Additionally, flexible reconversion of biogas (17.5 GW gas turbines as reserve and 2.5 GW flexible cogeneration plants) supply peak demand.

The methane PtG variant's overall efficiency is 35% and, therefore, less than in a pure hydrogen system because of the additional step of methanation. On the plus side, there are significantly smaller technical and financial expenditures for a pure hydrogen infrastructure because no adaption of the presently existing natural gas grid and gas power plants is necessary. Additional losses are compensated for by electricity imports amounting to 6% (9.3 GW) of the power consumption in 2050. Analogous to the hydrogen variant, peak-load reserve and power supply in times of deficits are provided by imports, biogas in flexible cogeneration plants, and extraction of renewable gas (Fig. 3.21).

In Fig. 3.22, the fill level curve of the necessary gas storage volume is shown in terms of energy (in TW h). If gas storage is filled with 40 TW h at the beginning of the simulation, it will never run empty. The maximum necessary storage capacity is 75 TW h and, therefore, far less than the presently available gas storage capacity of 217 TW h (ca. 35%), or than the technical-ecological potential of 514 TW h (ca. 15%). In addition, the significant decline of heat demand will reduce gas sales, and thereby create free capacities in gas storage. The storage minimum is 10 TW h. The seasonal character of long-term storage is obvious: energy for winter is mostly stored in the months of summer.

In the UBA scenario, PtG plants with a storing power of $P_{in} = 44$ GW and combined cycle plants with an extraction power of $P_{out} = 28$ GW are deployed. As shown in Fig. 3.23, the utilization rate of PtG plants in terms of storing time is ca. 2,060 h (24%) and extraction time of combined cycle plants is ca. 1,230 h (13%).

### Evaluation of the Energy Balance

Figure 3.24 shows average power generation and consumption based on the installed capacity and utilization according to the meteorological years of 2006–2009.

Wind energy generates the largest energy share. Because of a greater number of full-load hours, offshore plants, in spite of a smaller installed capacity (45 GW), play a role just as important as onshore wind (60 GW). Since plants on facades and in unsuited locations lower the amount of average full-load hours to 870 h, the contribution of PVs is smaller, despite an installed capacity of 120 GW.

The installed capacity of geothermal power (6.4 GW) and run-of-river plants (5.2 GW) may be the smallest of all, but because of their great number of full-load hours of 8,000 h/4,300 h, they supply almost half/a third




**Fig. 3.22** Fill levels of gas storages over the meteorological years 2006–2009 [42]

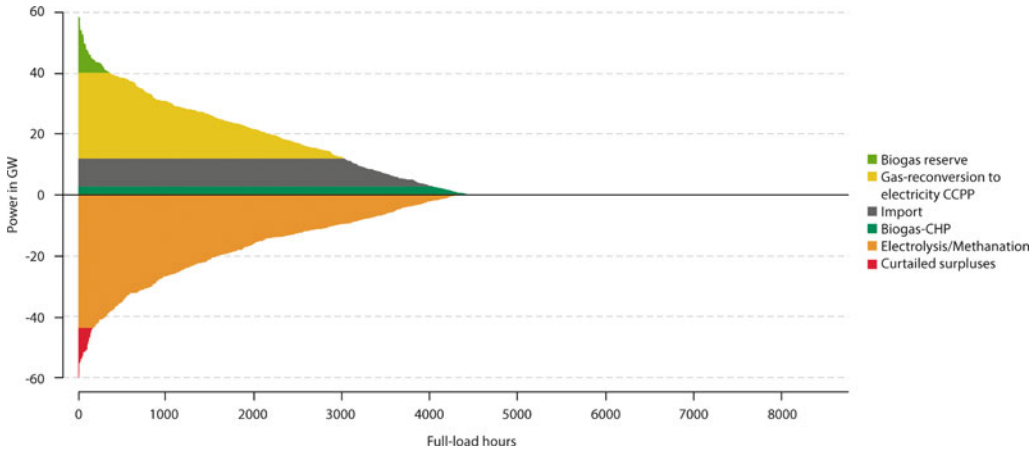



**Fig. 3.23** Annual load duration curve of the remaining residual load in the variant renewable methane from PtG and combined cycle plants, biogas, and power imports [42]

of what PVs generate. Biogas from waste biomass is of importance for security of supply. It is deployed along with CHP to supply peak-load demands via reserve power plants. Their utilization of ca. 500 h is accordingly small.

In total, renewable energies with an installed overall capacity of ca. 260 GW provide an average of 534 TW h/a. In addition, there is also the extraction of storages (pumped-hydro 6.0 TW h/a and combined cycle plants

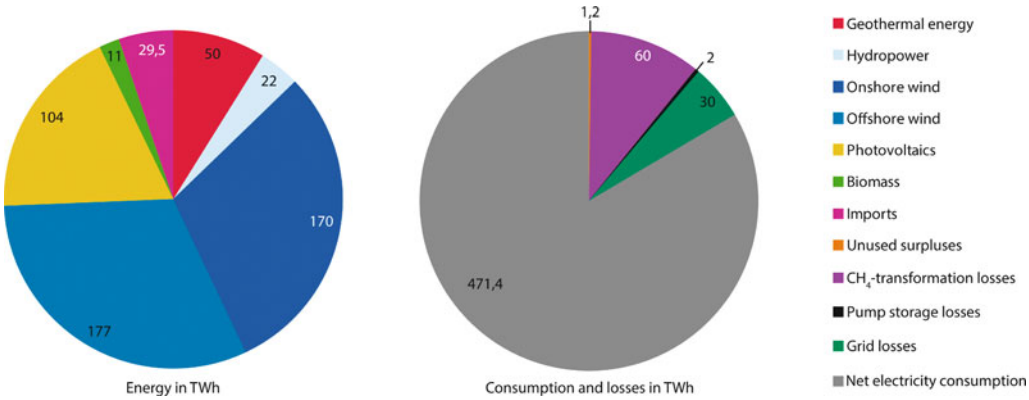



**Fig. 3.24** Energy balances of generation and consumption in the UBA scenario—variant renewable methane [42]

PtG 38 TW h/a) and electricity imports of 23 TW h/a.

On the other hand, there are power consumption (557 TW h/a), losses in the storage systems (pumped-hydro 2 TW h/a, and PtG 59 TW h/a), as well as losses in the grid (30 TW h/a) and a small amount (1 TW h/a) of unused surpluses.

### Results Concerning the Security of Supply—Ensured Power

The UBA study shows that a sufficient amount of ensured power can be supplied to all of Germany at any given time. Energy storage helps to provide an uninterrupted power supply, even during extended periods of little wind and insolation.

### Balance of Power Gradients

Power gradients are the increase or decrease of feed-in power per unit of time. Since these power gradients strongly increase with a higher installed capacity of wind and solar power, operating reserve and ensured power supplied by storage and reserve power plants will grow ever more important.

The highest occurring positive gradients of residual load (increasing residual load because of decreasing feed-in) were all in the time between 3 pm and 5 pm in the range of 17–24 GW/h. Since their occurrence is related to PVs and the decline of solar altitude, they can easily be integrated into planning. A phenomenon similar to this can be seen in the morning hours, when the highest negative power gradients occur. They are in the same range as the positive ones.

The amounts of these gradients can easily be predicted, because they are subject to the position of the ecliptic. A decline of these gradients can be reached by intensifying the expansion of PV plants facing east or west. A balance such as this requires flexible plants which allow a quick start-up. For positive gradients of residual load, these are gas turbine plants; for negative gradients, these are PtG plants (electrolyzers). They can both be started up or shut down in no time and thus ensure the necessary balance.

### Provision of Control Power

Power gradients of load and generation which are not foreseeable are being absorbed by operating reserve. Possible options are pumped-hydro plants, combined cycle plants, gas turbines, PtG plants, and controllable loads including heat storage via DSM. From a technical point of view, these plants can provide sufficient positive and negative operating reserve because there is enough power plant capacity. Thus, security of supply and network stability are ensured at any given time, even in a 100% scenario, such as the region's network scenario.

### 3.3.5 Abstract


- In 2050, it is **technically and ecologically possible** to supply all three energy sectors (**power, transport, and heat)** with **renewable energies exclusively**.
- The **technical potentials** of onshore wind (ca. 390 TW h), offshore wind (ca. 260 TW h), and PVs (ca. 250 TW h) add up to a total of ca. 900 TW h, and are therefore capable of **supplying** not only electricity demands but also energy for heating and individual mobility.
- The **heat demand** can **be supplied** completely **electrically** by measures of **energy efficiency** and the **coupling of power and heat sector**.
- Despite massive over-installation of wind and PV plants (together 225 GW), a remaining **thermal power plant compound** (*back-up*) in the order of **two-thirds** of the annual peak-load (60 GW) is required.
- The **security of supply**, which characterizes Germany's power supply of today, can be ensured at any time; even when power supply is exclusively based on renewable energies. Storage and reserve power plants provide sufficient ensured power, operating reserve, and reserve energy.
- When feeding-in, **wind and solar energy** complement each other very well on a **seasonal** scale. The **ideal ratio** is **60:40**, at which their fluctuations cancel each other out in the most optimal way.
- A functioning system is based on **grid expansions** and **infrastructural measures** for **DSM** (smart meter and smart grid).
- The **farthest-reaching and most effective measure** is the **integration of the heat sector**: great potentials of DSM are realized via air-conditioning (ca. 28 TW h) and heat pumps and storage (ca. 44 TW h). Additionally, there is the controlled charging of electric vehicles and the deployment of batteries (ca. 50 TW h). Thus, it can be said that DSM plays a decisive role for a power supply based on 100% renewable energies. Almost half the surpluses (ca. 65 TW h of 150 TW h) can be integrated, while the deficit curve is smoothed out significantly.
- The technical-ecological potential of **pumped-hydro** (short-term storage), 0.055 TW h, is realized to its full extent. This is enough to **smooth the load curve**, but decidedly **insufficient** when it comes to meeting the storage requirements in a power supply consisting of 100% renewable energies.
- Only **15%** of the technical-ecological potential of long-term storages (gas storage) is needed in the **renewable methane variant**: 75 of 514 TW h. When considering a **pure hydrogen system**, 110 TW h **cavern storage** is necessary, 80% or 85 TW h of which is being utilized.
- **Curtailment of 1%** surplus energy allows a reduction of PtG power to 64% of the maximum surplus power. Storing this remaining percent would cause a disproportionate technical and financial expenditure.
- A **pan-European electricity network** provides potential of further **cost-optimization** and offers the possibility to make the system more flexible.


## 3.4 VDE-ETG Study on Market-Based Storage Demand

So far, two studies have been considered in ▶ Sects. 3.2 and 3.3 respectively, which either do not take costs for storage into account or assume an ideal grid expansion in Germany. This section focuses on a study which reflects both costs and grid restrictions.

In 2012, the Power Engineering Society (ETG), a part of the Association for Electrical, Electronic & Information Technologies (VDE), published the interdisciplinary developed study 'Energy Storages for the Energy Transition' [45]. It includes an analysis of the impact energy storage has on the electrical energy system in a reference scenario and three future scenarios, each of which represent a cer-

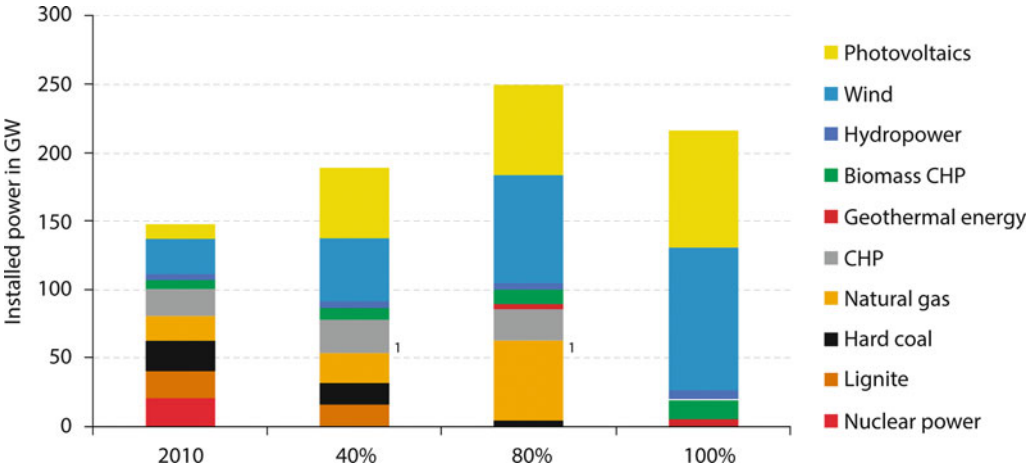



**Fig. 3.25** Installed power plant capacities according to the ETG-VDE study. Footnote 1: if necessary, further construction of gas power plants is required to guarantee supply with ensured power [45]

tain level of integration of renewable energies into the energy system.

The reference year is 2010 (17% renewable energies, and renewable capacities as of the beginning of 2010). The long-term expansion goal of renewable energies of 80% (80% scenario, year 2050), but also the short-term expansion goal of 40% (40% scenario, years 2020–2025), as well as an outlook on an expansion goal of 100% (100% scenario), exceeding the 'Energy Concept 2050', will be looked at. An outline of installed generation capacities is given in Fig. 3.25 for each scenario.

With the level of fluctuation in generation being as high as described, the German electricity system has to face huge technical challenges, which concern system stability, security of supply, the expansion of transmission and distribution networks, as well as the central issue of balancing generation and consumption. Balancing of this sort requires flexibility in the power supply system, which can generally be guaranteed by energy storage, flexible thermal power plants, flexible loads (DSM), and controllable renewable power plants.

Thus, the study is concerned with how great the storage demand is when it comes to balancing future electricity systems in which renewable energies are predominant, while taking flexibility of remaining thermal power plants and the readiness to make feed-in from renewable energies more flexible into account.

### 3.4.1 Methodology

Figure 3.26 shows an overview of the methodology of the VDE-ETG study. Each starting point is a scenario in which power plant capacities and consumption are defined. This allows, among other things, the calculation of residual load. Every alternative represents a different possibility of storage expansion which, by comparison, provides information on the utility of energy storage.

In concurrence with ▶ Chap. 2, a preceding VDE-ETG study, 'Energy Storage in Electricity Systems with High Shares of Renewable Energies' [43] from 2009, which is the basis for the VDE-ETG study discussed in this section, divides storage technologies into two groups:

- Short-term storage with high cycle-efficiency (≥75%) but little storage capacity, such as pumped-hydro, CAS, batteries, and DSM (heat storage)
- Long-term storage with little cycle-efficiency (≤40%) to date, but great storage capacity, such as chemical storage in hydrogen or methane PtG.

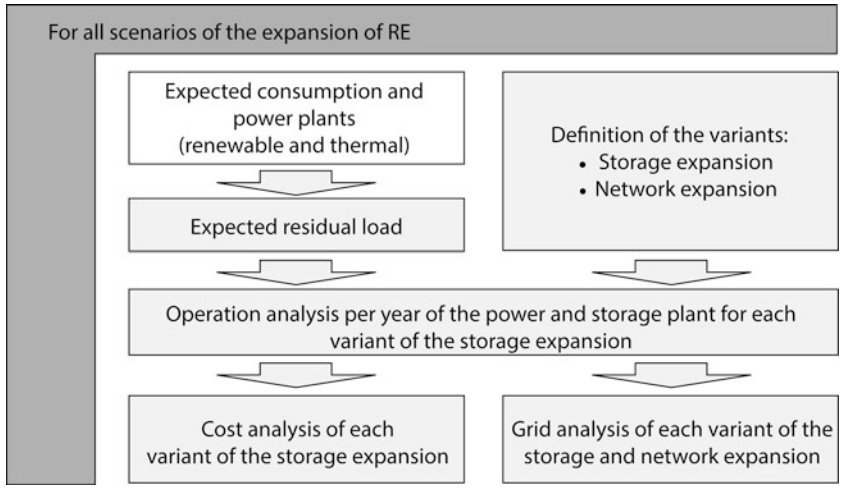



**Fig. 3.26** Overview of the methodology of the VDE-ETG study [45]

For this reason, the Energy Storages for the Energy Transition study abstracts storage technologies and examines the storage demand for the electricity system separately for short-term and long-term storage. In the study, representative values for cycle efficiency and storage capacity have been applied to examine the following alternatives:

- Alternative A: thermal power plants and the curtailment of renewable generation provide the flexibility needed for balancing generation and consumption. No new storages will be added to the presently existing ones.
- Alternative B: flexibility will be provided by thermal power plants and newly constructed short-term storages. The extent of the new additions will be adapted to the actually usable potential (full addition).
- Alternative C: flexibility will be provided by thermal power plants and by a full addition of long-term storages.
- Alternative D: flexibility will be provided by thermal power plants and by a full addition of short-term and long-term storages.
- Alternative E: flexibility will be provided by thermal power plants and a storage compound consisting of short-term and long-term storages with half the storing power of Alternative D.

All new constructions described in each alternative are additions to existing German PHSs in 2010. In total, the pump performance is at 7.2 GW, turbine output is at 8.2 GW, and storage capacity is at 48 GW h.

The central part of the analysis is the simulation of power plant and storage compounds operating over the year. This simulation is based on an established method developed by the RWTH Aachen University. When fed the residual load curve, its output is the cost optimized deployment of storage and power plants for every hour of a given year. Other significant results of this stage of the analysis are used storage capacity, curtailed renewable generation, primary energy consumption, and $CO_2$ emissions.

The curve of renewable feed-in is calculated using the Fraunhofer IWES' well-tried model, which is based on expectations of renewable energy plants installed in the future, their geographical spread, and high-resolution meteorological data. Future installations will be made as described in Langfristszenarien des BMU for 2010 (▶ Sect. 3.2); all meteorological data is provided by the DWD's (GMS) COSMO-EU model.

Cost analysis is based on a detailed storage model, and refers to the evaluation of results provided by a simulation of operation over the year using the same results to calculate in-

vestments and operating costs for storage and power plants, as well as the overall electricity production costs. The RWTH Aachen's model for long-term and short-term storage compounds takes usage-dependent durability and, additionally (in case of life-sized dimensioning), admissible withdrawal rates into account.

An increasing grid expansion of German transmission networks has been examined for all scenarios of alternatives A, D, and E using a method similar to the one which was used to determine the need for storage expansion. The increasing expansion is represented by five different grid models. Since this is a current subject of research (▶ Sect. 3.6) and there are (in parts) new insights, this part of the VDE-ETG study is not presented in the following sections.

## 3.4.2 Assumptions for Modeling and Data Input

Every study, including the VDE-ETG study, Energy Storages for the Energy Transition [45], makes assumptions and uses data input, the knowledge of which allows the interpretation and contextualization of its results. They will be presented in the following sections.

### 3.4.2.1 General Assumptions

- The future storage demand is essentially determined by its balancing function. Further storage functions, such as providing operating reserve, power quality, congestion management, voltage and grid stability, supply quality, and even island networks, are merely additional functions and of lesser importance when concerning the demand for power and energy. They will therefore be disregarded in this subsection but examined more closely in ▶ Sect. 13.1.
- Short-term storage is characterized by a cycle efficiency of 80% and an E/P-ratio (energy-to-power) of 5 W h/W; the model used to describe long-term storage has a cycle efficiency of 40% and unlimited storage volume.
- Future storage and power plant deployment for reasons of (energy-economical) balancing will be controlled by today's principles of the electricity markets, which results in non-static minimal electricity production costs.
- The study only examines the power supply system. Interconnections to other energy systems, such as transport, heating, and the supply with natural gas, will be left out, save for the analysis of short-term and long-term storage, CHP plants, and demand-dependent power consumption of electric heat-pumps, electrical vehicles, and air-conditioning.

### 3.4.2.2 Assumptions Made to Determine the Residual Load

- The study examines curves with an hourly resolution.
- Annual curves have to be complete in order to include annual cycles of weather-dependent energy sources such as wind and sun, on the one hand, and situations relevant for design such as prolonged times of low winds or storms, on the other. The study is based on the meteorological year 2007, which includes both extremes. Other meteorological years might lead to slightly different results.
- The data input for expected generation power and load is based on the almost annually updated data framework in 'Langfristszenarien 2010' [27], which is a recognized basis for energy-economic development of the power sector.
- Generation and load are not exactly presented as done in Langfristszenarien 2010 because renewable power imports from the European power system and large-scale deployment of electrolysis powered by solar or wind energy with the aim to produce chemical fuels to substitute natural gas, such as hydrogen or methane, are not taken into account.
- Since this study is focused on the German storage demand, which is dependent on the

expansion of renewable energies in Germany, a 'Germany-only' system is examined; imports and exports of power for balancing the German system are disregarded.
- In the simulation of operation over the year, CHP plants (biomass and fossil) are deployed flexibly up to a certain degree. They are regarded as heat-controlled, but able to reduce their power output, assuming supplemental firing.
- The load curve, disregarding grid losses, electric vehicles, air-conditioning, and heat pumps, has been adapted from the ENTSO-E's load duration curve of 2007. The curve concerning electric vehicles, air-conditioning, and electric heat-pumps was calculated on the basis of the time series of heat and mobility demand, taking only actual usage into account.
- The 100% scenario was derived from the 80% scenario in a simplified manner, by leaving power consumption at the same level and upscaling renewable generation to 100%.

#### 3.4.2.3 Assumptions Made Concerning the Simulation of Operation over the Year

- To determine storage requirements for the annual operations simulation, the electricity network was initially considered as a 'copper plate' (point model). The study assumed that the electricity network's requirements neither necessitated the use of power plants and storage, nor prevented the use of power plants and storage. As a result, the study assumed a level of network expansion adequate for the transmission system as determined by network analyses. With the exception of reserve power, the study also assumed that technical alternatives were available for providing system services.
- In addition, the study assumed national supply security. This means that there are always an adequate number of power plants available in Germany to cover consumer load, and to meet transmission system operators' requirements for reserve at all times. The power station portfolio was therefore only partly an input parameter. It was also partly the result of this study.
- Additional power plants may be required to ensure supply security besides those included in the 2010 BMU long-term scenarios. This study assumed that the gas power plants included in the 2010 BMU long-term scenarios, as well as those required for discharging long-term storage, were implemented as combined cycle power plants. It also assumed that all additional gas power plants required to ensure supply security were implemented as gas turbines.
- Reserve power provided to transmission system operators by power plants and storage is not available for balancing functions. As a result, the amount provided must be taken into account when calculating storage requirements. The amount was determined here by using a standard probabilistic method that took into account renewable energy feed-in forecast errors, as well as power plant outages.

#### 3.4.2.4 Cost Analysis Assumptions

- The fuel prices assumed in the annual operations simulation are based on the 2010 BMU long-term scenarios.
- Annuity investment costs were determined based on a uniform calculated interest rate of 9%, and on amortization over the service life of the power plant, renewable energy facility, or storage.
- The power plant and renewable energy facility investment costs assumed in the cost analysis were based on the 2010 BMU long-term scenarios, adjusted as required using empirical data from past RWTH Aachen energy sector studies.
- The investment and operational costs for storage assumed in the cost analysis were based on the VDE-ETG study, 'Energy Storage in Power Supply Systems with a High

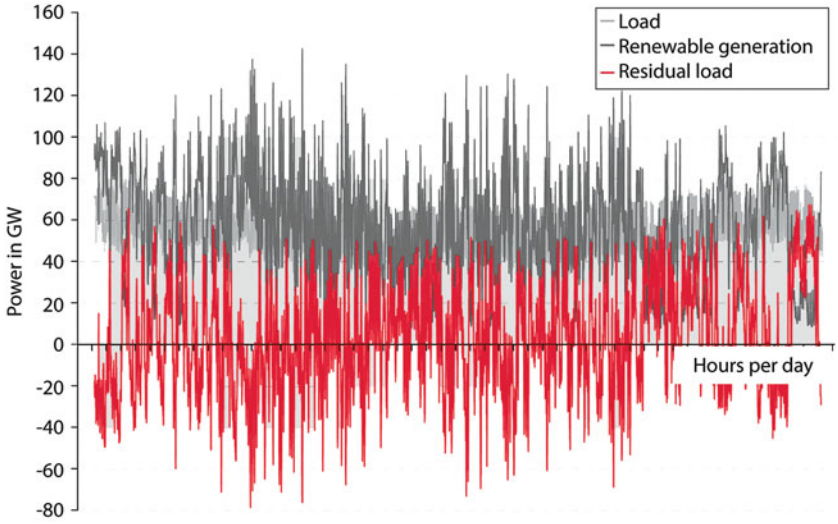



**Fig. 3.27** Residual load in the 80% scenario [45]

Share of Renewable Energy Sources', adjusted as required using additional empirical data from RWTH Aachen and OTH Regensburg.

- The cost analysis assumed a storage mix with an overall efficiency level approximating the levels generally assumed for short-term and long-term storage. Short-term storage was defined as a mix of load-management, pumped-storage plants, compressed air energy storage (CAES), and various battery technologies. The costs assumed for long-term storage were based on chemical storage using hydrogen. If the costs of modifications to the gas infrastructure are ignored, these costs in general do not vary significantly from those of chemical storage using methane.

## 3.4.3 Cross-Scenario Findings

### 3.4.3.1 Increase the Flexibility of Power Supply System Facilities

Expansion of renewable energy facilities in the future will require increased power supply system flexibility on both the generation and consumer sides. From reviewing the various ways this has been studied, it is apparent that these flexibility requirements could always be met by the rest of the power station portfolio, by curtailing renewable energy feed-in, or by short and long-term storage.

In the past, the power supply system relied extensively on fossil energy. Fluctuations occurred primarily on the demand side. As the use of renewable energy increases, fluctuations on the supply side will increase as well. As a result, flexibility requirements in the electrical energy system will increase together with the use of renewable energy. These requirements can be determined by performing a statistical analysis of residual load, and met in a variety of ways.

Figure 3.27 shows a graph of load, renewable energy generation (excepting biomass), and the resulting net balance of residual load for the 80% scenario. The pattern here is obvious: as the share of renewable energy grows, volatility rises, the average falls, and the number of hours with generation surpluses in the residual load increases.

In the 100% scenario, required over-installation of renewable energy power caused generation surpluses of up to 80 GW. The maximum residual load was reduced by up to

**Table 3.6** Comparison of various 80% scenario versions; curtailment without accounting for network congestion and network operations [45]

| | Reduced storage portfolio (version E) | Storage for 100% renewable energy use (version D) |
|---|---|---|
| Short-term storage (Charging/discharging capacity/storage capacity) | 14 GW/14 GW/70 GW h | 28 GW/26 GW/140 GW h |
| Long-term storage (Charging/discharging capacity/storage capacity) | 18 GW/18 GW/7 TW h | 36 GW/29 GW/8 TW h |
| Quantity of renewable energy from wind energy and PV facilities curtailed | 0.4 TW h/year | 0 TW h/year |
| Annuity investment costs for storage | 3 billion euros/year | 5.1 billion euros/year |

approximately 10 GW, or 12.5% in comparison with 2010. The power range expanded significantly.

Flexibility was required in both the short-term area (less than one day), and the long-term area (more than one day). In all the versions of cycle efficiency and storage capacity discussed above (A to E), these flexibility requirements in the short and long-term areas could always be met by the flexible use of fossil fuel power plants and CHP facilities, by using short and long-term storage, or by curtailing renewable energy.

### 3.4.3.2 Avoid Designing Storage for Generation Peaks

Renewable energy peaks are rare but large. Curtailing them is generally more cost-efficient than designing storage charging capacity for these peak values. Further research is required to determine the optimal ratio of generation capacity, storage, and curtailing.

Because renewable energy full-load hours are limited, even in the 40% scenario the 2010 BMU long-term scenarios included an installation of wind energy and PV facilities exceeding the peak-load of around 80 GW, and with a total power amounting to 98 GW. In the 80% scenario the total was 144 GW, and in the 100% scenario 191 GW of PV and wind energy facilities were installed. But an analysis of the resulting residual load indicated that large renewable energy generation peaks were relatively rare (Fig. 3.27). The 80% scenario generated maximum surpluses of around 50 GW, and maximal deficits of around 70 GW.

Dimensioning the storage portfolio to eliminate the curtailing of renewable energy resulted in annuity investment costs of around 5.1 billion euros (Table 3.6). If storage capacity was reduced to approximately half the original storage charging capacity, for example, then annual curtailments of about 400 GW h (around 1% of total annual electricity consumption) of renewable energy from wind energy and PV facilities is required.

This was, however, offset by a 2.1 billion euro reduction in annual storage portfolio investments. In addition, despite the reduction in capacity, energy throughput in long-term storage was not significantly reduced. The result was significantly lower energy throughput costs and improved cost efficiency.

These results demonstrate that designing storage for renewable energy generation peaks makes little sense. Further research is required to determine the optimal ratio of energy capacity, storage, and curtailing, as well as of charging and discharging capacity.

## 3.4.4 Findings of the 40% Scenario

### 3.4.4.1 Make Thermal Power Plants and Renewable Energy Feed-In Management Cost-Efficient

With a 40% share of renewable energy, short and long-term storage were not required to ensure stable power supply. Use of the thermal power station portfolio together with marginal curtailing of renewable energy feed-in were adequate for providing the required flexibility.

With a 40% share of renewable energy, adding further storage increased electricity generation costs (Fig. 3.28). In addition, under the assumed conditions, storage served less to integrate renewable energy and typically more to optimize the use of thermal power plants. This led to a 'perpetuation' of feed-in from fossil fuel power plants with the associated consequences (▶ Sect. 5.5.4.2). The investment costs for addition storage also exceeded the reduction in variable electricity generation costs. The latter are primarily fuel costs, which were marginal under the conditions assumed.

Among the alternative versions studied (A to E), electricity generation costs were lowest in version A. In this version, flexibility required by the power supply system for balancing generation and consumption was provided by marginally curtailing wind and PV renewable energy generation to around 260 GW h per year (about one-tenth of a percent of renewable energy generation) or biomass generation to around 539 GW h per year. It was also provided by using thermal power plants, as well as by curtailing heat-oriented, fossil fuel fired CHP facilities.

The quantities of renewable energy from wind, PV, and biomass referred to here only include curtailments required to balance generation and consumption. The figures do not account for curtailments caused by inadequate transmission systems and distribution network expansion.

### 3.4.4.2 Renewable Energy Requires Only Limited Storage

If renewable energy covers 40% of gross electricity consumption, then under the assumed conditions, negative residual load (i.e., a surplus situation where renewable energy generation exceeds consumption) occurs in only around 44 of the 8,760 hours in a year. This means that, in the short-term, storage will be used less to store renewable electricity, and typically more to optimize the use of thermal power plants.

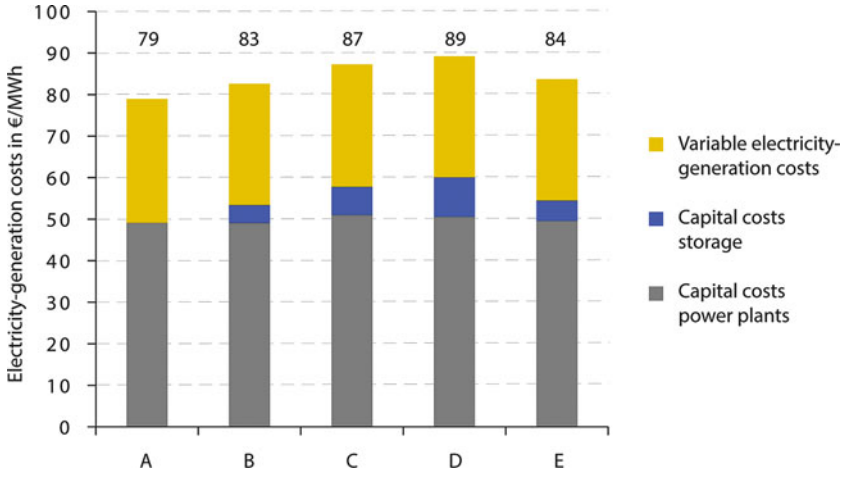



**Fig. 3.28** Forty percent scenario: electricity generation costs in various versions [45]

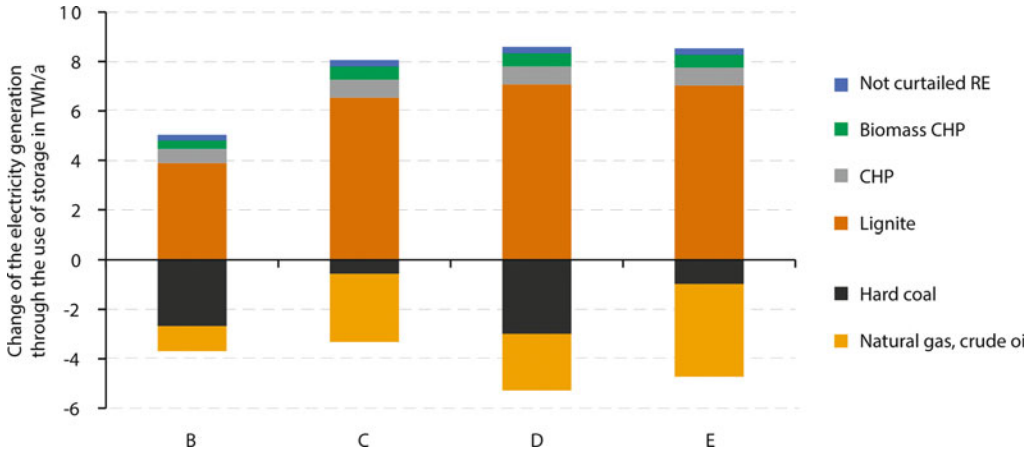



**Fig. 3.29** Forty percent scenario: shifting of electricity generation due to additional storage [45]

In the 40% scenario, total surplus energy generation amounted to only 0.26 TW h per year under the assumed conditions. This is equivalent to only one-tenth of a percent of total renewable energy generation, demonstrating that, with the network expansion planned, very little storage is required. But the peak negative residual load was relatively high, reaching 9.8 GW for an hour. The analysis here assumed that CHP facilities can be shut down when there are generation surpluses.

Due to this assumption, almost no renewable energy storage was required in the 40% scenario. As is currently the case, a 40% share of renewable energy storage is primarily used to optimize the use of thermal power plants by leveling residual load. This then allows cheaper power plants, so-called base-load power plants, to be used for generation. In this scenario, storage discharging (unloading) capacity was not necessarily required because the capacity provided by conventional power station portfolio was adequate.

Figure 3.29 illustrates the change in renewable energy generation in the additional storage versions studied (versions B to E) according to the annual operations simulation of the power plant and storage portfolio. In this figure, positive values can be interpreted as increases in generation and charging, and negative values as decreases in generation and discharging. This means that the use of storage in the 40% scenario typically resulted in a perpetuation of cheaper lignite coal power plants, and a marginalization of gas or hard coal power plants.

## 3.4.5 Findings of the 80% Scenario

### 3.4.5.1 Use Long- and Short-Term Storage for Climate Protection

With a 40% share of renewable energy, short and long-term storage was not required from a climate-protection perspective under the conditions assumed. At a renewable energy share of 80% or above, use of storage in the regular electricity market resulted in about a 10% reduction of $CO_2$ emissions beyond the 85% reduction in total power supply system emissions achieved in 1990.

With a 40% renewable energy share, short and long-term storage was only rarely used to charge renewable electricity. Instead, it was typically used to optimize the use of thermal power plants. The result was increased electricity generation by thermal, fossil fuel power plants to cover storage losses (with cycle efficiency levels at 40% for long-term storage and 80% for short-term storage), as well as a marginaliza-

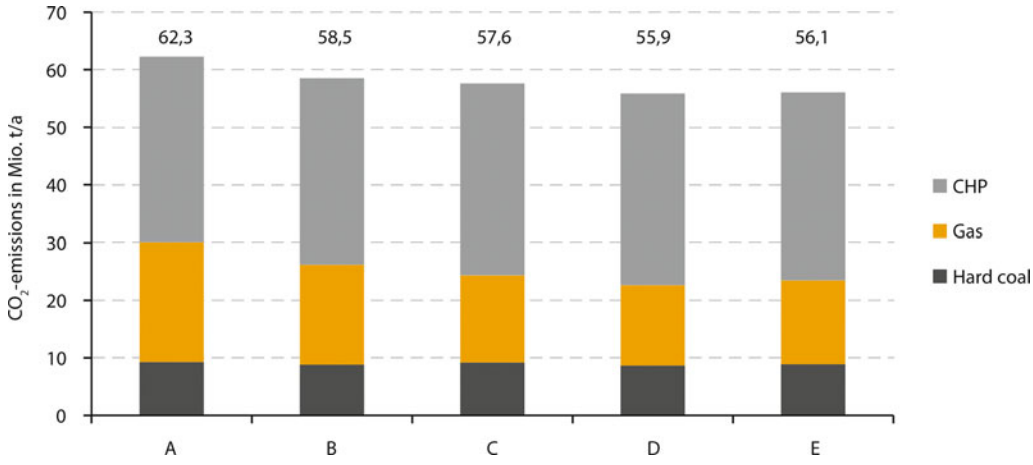



**Fig. 3.30** Eighty percent scenario: emissions [45]

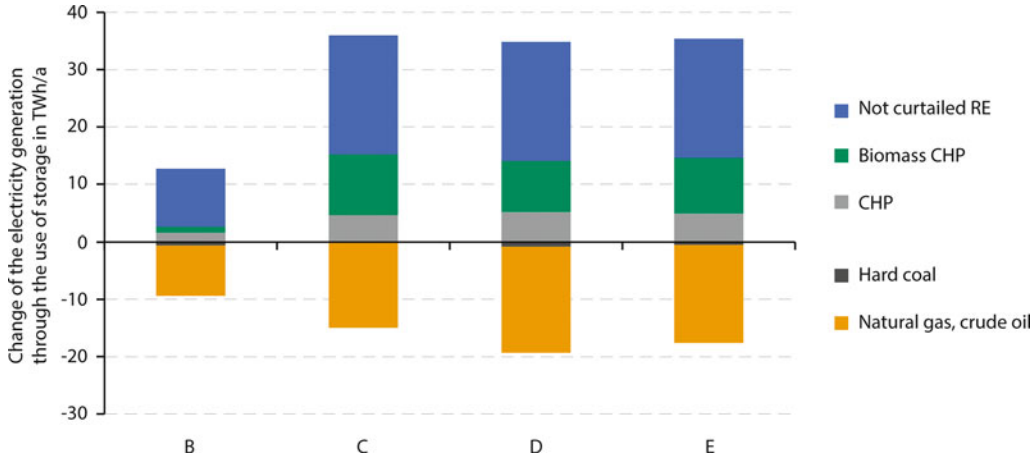



**Fig. 3.31** Eighty percent scenario: shifting of electricity generation due to additional storage [45]

tion of gas or hard coal power plants in favor of lignite coal.

Using storage to economically optimize the use of thermal power plants resulted in up to 1.8% more $CO_2$ emissions than in version A, in which there was no additional storage (see versions B to E in Fig. 3.30), with a 40% share of renewable energy. With an 80% share of renewable energy (Fig. 3.30), storage reduced $CO_2$ emissions by up to 10%. This was in addition to the significant reductions achieved by increased use of renewable energy. This is because storage charges renewable electricity in significant quantities at an 80% share of renewable energy, and replaces fossil gas electricity when discharging (Fig. 3.31).

### 3.4.5.2 Combining Short and Long-Term Storage with Curtailing is Recommended

With an 80% share of renewable energy, under the conditions assumed for 14 GW or 70 GW h (five hours) of short-term storage, about 18 GW or 7.5 TW h (17 days) of long-term storage was required in addition to the storage available today. This relatively large additional requirement was primarily the result of considering

Germany as a stand-alone system, and ignoring cross-border flows. If Germany were considered to be part of the larger European grid system, then significantly smaller storage capacity would probably be required.

The 2010 BMU long-term scenarios assumed that there are specific expansion goals for renewable energy in the 80% scenario. Assuming this generation portfolio without additional storage (version A), about 30 TW h or about 7% of renewable energy was curtailed. This means that version A did not meet the renewable energy share goal of 80% of gross electricity consumption, and yielded only a 73% share of renewable energy.

These results demonstrate that dimensioning storage capacity to fully exploit renewable energy by charging during all generation peaks (version D) apparently makes little sense. Instead, a combination of storage and renewable energy curtailing is preferable (version E). If half of the theoretically required short and long-term storage capacity is assumed, then under the conditions assumed, less than 1% of renewable energy would had to be curtailed.

In version E, short-term storage was expanded to a power of 14 GW and a capacity of 70 GW h. This is equivalent to approximately twice the pumped-storage plant capacity available today. To calculate short-term storage costs, a storage portfolio, including battery storage (especially lead-acid, lithium-ion, and sodium sulfur batteries), CAES, and load-management was assumed to be in place.

Long-term storage with a power of 18 GW has a discharging duration of about 17 days. This means that only very large storage capacities can be considered here, and that energy storage costs must be quite low to ensure the result is cost-efficient. For this reason, in Germany, only storage systems based on PtG are considered. Suitable energy carriers here are hydrogen and methane gas. They can be stored in dedicated caverns (mainly hydrogen), or in the existing gas network, and in gas storage (mainly methane gas). Reconverting hydrogen or methane gas to electricity requires gas power plants, decentralized CHP facilities, or fuel cell systems. Energy consumption in long-term storage (about 16 TW h per year) is very low in comparison to current gas consumption in Germany (around 850 TW h per year), falling under 2%. The calculated costs for storage assumed chemical storage using hydrogen. If costs for modifications to the gas infrastructure are ignored, in general these costs do not vary significantly from those of chemical storage using methane gas.

Taking into account potential reductions in storage technology costs, the estimated annuity investment costs for the storage portfolio would be around three billion euro. Long-term storage costs represent about 75% of these costs. The costs of discharging units for long-term storage (such as gas power plants, fuel cells, or CHP) are not included in storage costs. They are included, instead, in the costs for the power plant portfolio.

### 3.4.6 Findings of the 100% Scenario

If the share of renewable energy is increased from 80 to 100%, then three times the amount of short and long-term storage are required in the storage portfolio. Electricity generation costs increased by about 19%. This final increase in the share of renewable energy by 20% was more expensive than the increase by 63% in 2010 from 17 to 80%.

Table 3.7 shows the installed storage powers and capacities.

Increasing the share of renewable energy by 20% to full renewable generation meant expanding the storage portfolio as well. As a result, short-term storage power and capacity was 2.5 times higher, and long-term storage power and capacity was 3.5 times higher than in the 80% scenario.

Energy storage costs here played a decisive role, accounting for about 25% of electricity generation costs. The costs of discharging units for long-term storage were included in the power plant portfolio costs. The costs of modi-

**Table 3.7** Comparison of the 80% and 100% scenarios [45]

| | 80% scenario (version E) | 100% scenario (version D) |
|---|---|---|
| Short-term storage (Charging/discharging capacity/storage capacity) | 14 GW/14 GW/70 GW h | 36 GW/35 GW/184 GW h |
| Long-term storage (Charging/discharging capacity/storage capacity) | 18 GW/18 GW/7 TW h | 68 GW/42 GW/26 TW h |
| Annuity investment costs for storage | 3 billion euros/year | 12 billion euros/year |

fications to the gas infrastructure for long-term storage with hydrogen as well as the costs for methanation with PtG were excluded.

### 3.4.7 Summary

- The interdisciplinary VDE-ETG study made certain assumptions that limit the usefulness of its results in specific areas. In particular, the exclusion of the German energy system's **European neighbors**, the assumption of **full CHP flexibility**, and the exclusion of **network restrictions** were **critically important assumptions**. Despite these simplifications, some relevant conclusions can still be drawn from the study.
- The energy system will require renewable energy to be more flexible in the future. The ability to **curtail** facilities when surpluses occur over extremely short time periods is essential to ensure safe and cost-effective operation of the generation system with a high share of renewable energy. The absolute volume of curtailments amounted to nearly **one-tenth of a percent** of renewable energy production. **Designing storage** for **generation peaks makes little sense** from both a technical and economic point of view.
- In the short-term (with a renewable share of around 40%), **increasing the flexibility** of the **thermal power plant portfolio** is the **most attractive flexibility option**. This is because balancing effects result in lower storage requirements when the entire European energy system is considered. Even the results for Germany as a stand-alone system demonstrate that additional storage cannot cover its own capital costs when CHP facilities are used flexibly. Since the increase requires little additional hardware, the costs for increasing flexibility, as described in the study, are negligible compared to the costs of storage.
- With a renewable share of **40%**, **additional short and long-term storage is not required** if the thermal power plant portfolio's flexibility is also increased, as assumed. Storage is used less to integrate renewable energy, and more to optimize the use of thermal power plants. As a result, electricity generation from gas and hard coal power plants is reduced in favor of cheaper but more $CO_2$-intensive **lignite coal electricity generation**. The use of storage, therefore, increases **$CO_2$ emissions** by 1.8%.
- Without additional storage, the **80% scenario** becomes a 73% scenario. An electricity sector without energy storage generates **10%** more $CO_2$ emissions than a system with energy storage. It is therefore possible to achieve **high shares of renewable energy without storage**, particularly if extensive balancing is taken into account. High shares of renewable energy are also **necessary to protect the environment, as well as to meet** renewable energy **expansion goals**.
- Additional **storage was required** in scenarios with shares of renewable energy on the order of 80%. A **combination of short and long-term storage** generally seems to

be a **reasonable** solution. The 80% scenario yielded a requirement of 14 GW or 70 GW h (five hours) of additional short-term storage, and 18 GW or 7.5 TW h (17 days) of new requirements for long-term storage. But the assumptions made should be kept in mind when considering these results. Storage requirements could be significantly lower when the larger European grid system is considered as well.

- Although increasing the share of renewable energy to 100% is technically feasible, it presents a challenge. The German generation system would become very volatile. It would cause hourly average **generation surpluses** of **up to 80 GW**, while the maximum residual load was minimally reduced to only about 67 GW.
- Increasing the share of renewable energy from **80 to 100% tripled storage requirements**. Electricity generation costs increased by about 19% in comparison with the 80% scenario. Energy storage costs accounted for about 25% of electricity generation costs. In Germany, long-term storage for energy volumes in the order of 30 TW h would be required. Considering Europe as a whole, cross-regional balancing effects may make it easier to attain a 100% share of renewable energy.

## 3.5 'Storage Roadmap' Study on Germany's Storage Requirements in the European Context

Since the studies on storage requirements discussed in ▶ Sects. 3.3 and 3.4 focused on Germany, balancing effects in the European electricity generation and transmission system were not considered as a flexibility option.

The 'Storage Roadmap' project produced a study that considers these effects in addition to other flexibility options. The study was supported by BMWi federal funding, and conducted from 2011 to 2014 by a consortium, including the Fraunhofer Institute for Wind Energy and Energy System Technology (IWES), the Institute of Power Systems and Power Economics (IAEW) of RWTH Aachen, and the Foundation for Environmental Energy Law [30].

The electricity exchange between market areas was determined using a Europe-wide simulation of the use of generation facilities, storage, and load-management. A detailed model of the generation and demand situation for the majority of the countries in the ENTSO-E network was also used. Network restrictions in the medium-term were determined in detail using a downstream AC power flow. In considering the long-term, only the limited exchange capacities between market areas were taken into account in power plant use planning. But since adequate network expansion was assumed up to this time within the market areas, over the long-term, network congestion within market areas was not considered.

The energy sector analyses for the medium-term with 26% and 37% shares of renewable energy in Europe, or 45–50% and 69% shares in Germany, are generally by IAEW. Analyses of long-term storage requirements with a 82% share of renewable energy in Europe and 88% in Germany are by IWES. The Foundation for Environmental Energy Law produced a legal study and assessment of storage law at the same time (as the energy sector analyses), the results of which can be found in [30]. The following discussion first examines the methodical approach taken by this study. A description of the scenarios and their results follows. The discussion then concludes with a description of the relevant findings in the context of the previously discussed studies.

### 3.5.1 Methodological Approach

The project's modeling approach applied various part models sequentially. The energy sector simulation for the European electricity generation system took into account the over-

lap between the heating and transport sectors. The goal of optimization was to meet electricity demand at minimum total economic cost, with marginal conditions defining the European electricity generation system taken into account. Modeling of the electricity system in the medium-term was scenario-based. Modeling over the long-term also included the option to expand thermal power plants, short and long-term storage, or transmission capacity within the model. Here, as well, the goal of optimization was to meet electricity demand at minimum total economic cost. Capacity expansion was factored in to load coverage costs by taking into account annuity investment costs. The following is a brief, step-by-step description of the procedure followed by the study.

#### 3.5.1.1 Renewable Energy Time Series

Relying on detailed modeling using historical weather data, the study realistically simulated wind and solar energy fluctuations, gradients, and smoothing effects. Modeling of renewable energy electricity generation was initially performed for the entire area studied for a grid with a mesh size of 7 km. Using information on existing facilities as well as expansion modeling, taking into account renewable energy resources and suitable areas, the model incorporated the replacement of old renewable energy facilities or the addition of new ones. The study also took into detailed account technical developments such as increases in the system efficiency level (PV), or larger hub heights with reduced rotor-specific nominal power (f). Historical weather data for 2011 from the German Weather Service's COSMO-EU model [3, 4], as well as radiation data from Meteosat satellites [6, 34] were used as input data for the physical models of the renewable energy facilities. This was then used to generate electricity generation time series broken down by hour for the various technologies in each weather model area. Finally, this data was aggregated as input data for load flow simulations, taking into account regionalized electricity demand in residual load time series at each high-voltage network node. A second aggregation of all the time series within a market area yielded the input data required for planning upstream power plant utilization or expansion. Under real conditions, only inexact forecast renewable energy feed-in data was available for power plant use planning. The result was imperfect power plant utilization, with intraday trade or balancing power required to balance deviations between forecasted and actual residual load. These conditions are reflected in the model by taking into account artificial time series forecasts for wind energy and PV feed-in, as well as electricity demand for all scenario years. In addition, for long-term storage management, a long-term residual load forecast was taken into account. For this purpose statistics were generated based on a time series over many years for renewable energy feed-in and load, with weekends and holidays taken into account in the case of load.

#### 3.5.1.2 Economic Simulation for Storage in the Medium-Term

To determine Germany's storage requirements in the medium-term, a multi-step simulation of the electricity generation system took into account influences on market behavior and network operations. The first step of the economic simulation for storage [15] was an integral market simulation of the European electricity generation system. This step determined the minimum cost of (i.e., economically optimal) power plant utilization to cover demand and provide balancing reserve, given the technical limitations for electricity generation and transmission. Both existing storage and additional storage projects were taken into account in the market simulation. The savings that resulted also determined the benefits of the storage projects studied for the electricity market.

Since all European electricity markets were considered to have unlimited transmission capacities with no congestion within each market area, the resulting load and feed-in situation could result in transmission system congestion. Transmission congestion was then dealt with by modifying power plant utilization by means of so-called *redispatch*. The network operations

simulation took this process into account by determining hourly power flows in both base-load situations as well as congestion situations based on power plant utilization determined by the market. The European transmission network model applied here was based on public, freely-available data.

Next, the study simulated the actions of transmission system operators in network operations to relieve transmission congestion. The redispatch measures available included adjusting the use of conventional, thermal power plants, as well as the use of storage. The goal of load flow optimization here was to minimize transmission congestion, the number of interventions, and redispatch costs [16]. This method produced a reliable network usage situation for each hour studied.

This multi-step simulation allowed the overall benefits of technology-dependent storage projects to be determined from both a market and network point of view. These benefits consist of reductions in electricity generation costs as well as redispatch costs. Renewable energy facility curtailments may be reduced as well. The resulting cost savings for the electricity generation system are also assigned to storage. The overall benefits are then compared with the required investments and operating costs to determine the economically viable level of storage expansion.

#### 3.5.1.3 European Power Plant Use and Optimized European Expansion Planning in the Long-Term

As power plant use is optimized and renewable energy expanded, the analysis of long-term storage requirements determined how hourly electricity demand can be met at a minimal cost in comparison with the studies discussed above. The analysis took into account existing renewable energy facilities, including storage water-power facilities. The required thermal power plant, storage, and transmission capacities between market areas determined the integrated optimization for a calendar year.

#### 3.5.1.4 Germany Examined in Detail

The optimized electricity generation system defined by European expansion planning was then examined in detail for Germany. The goal was to account for additional aspects such as balancing power requirements, forecast errors, and power plant flexibility. The previously determined expansion planning capacities were used in this step. These capacities include additional storage, seasonal storage filling levels, and import and export time series from upstream European expansion planning. The approach taken here was to add additional electricity storage in steps, with the goal of reducing electricity generation costs. Finally, the economically optimal level of storage expansion that resulted was interpreted as the 'storage requirement' for the overall system's economic optimization.

### 3.5.2 Scenario

Reliably estimating storage requirements means taking into account balancing effects caused by the energy generation system network in Europe. Although the focus was on an analysis of Germany's storage requirements, as shown in ◘ Fig. 3.32, the Storage Roadmap simulations took into account the majority of the ENTSO-E network.

As in the 2010 and 2011 long-term scenarios (▶ Sects. 3.2 and [24, 26]), the model accounted for renewable energy from solar-thermal power plants in North Africa. Although the study concentrated on the electricity sector, as in ▶ Sect. 3.3, it also took into account cross-sectoral electricity applications such as electro-mobility, electric heat-pumps, or air-conditioning.

#### 3.5.2.1 Assumptions

For Germany and Europe, the generation system was generally based on the 2011 long-term scenarios [26]. These scenarios reflect a restructuring of the generation system to reduce the



**Fig. 3.32** Area of study including North Africa [30]

use of coal, while expanding the use of renewable energy and natural gas generation. Since there has been rapid development in the renewable energy sector in recent years, some assumptions have been modified or replaced with new data.

### Electricity Demand and Expansion of Renewable Energy

Assumptions concerning the development of electricity demand in Germany were based on the German federal government's energy concept [13], which predicted a reduction in electricity demand by 25% by 2050 (10% by 2020, 15% by 2030) in comparison with 2008. In addition, the study took into account new consumers that facilitate efficient energy sector coupling and can significantly contribute to integrating renewable energy. These included electric heat-pumps, air-conditioning, and electro-mobility. Figure 3.33 and Table 3.1 show the development of electricity consumption and consumer demand.

With various conditions assumed, the simulation focused on those years when the share of renewable energy in German electricity consumption was at 45–50%, 69%, and 88%. Due to changes in the EU's national action plans and some unexpected increases in renewable energy, the BMU's 2011 long-term scenarios (Figs. 3.33 and [26]) have been partially modified to reflect these new conditions.

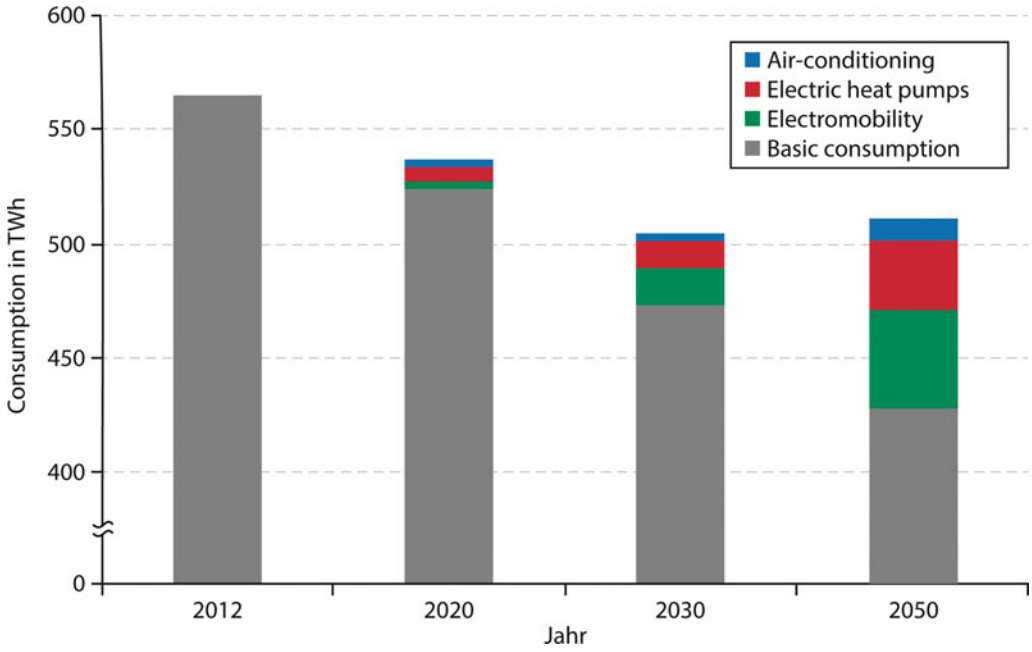



**Fig. 3.33** Development of electricity consumption (Flex$^+$) including new consumers: air-conditioning, electric heat-pumps, and electro-mobility [30]

**Table 3.8** Development of basic electricity consumption and new consumer requirements between 2020 and 2050

| TW h/year | 2020 | 2030 Flex$^-$ | 2030 Flex$^+$ | 2050 |
|---|---|---|---|---|
| Basic electricity consumption | 524 | 473 | 473 | 427 |
| Electro-mobility | 1 | 0 | 10 | 26 |
| Electric heat-pumps | 7 | 11 | 11 | 30 |
| Air-conditioning | 2 | 4 | 4 | 10 |
| ∑ New consumers | 10 | 15 | 35 | 66 |

## Power Plant Portfolio

Energy transition's success heavily depends on increasing the power plant portfolio's flexibility. The study considered two sensitivity scenarios for the year with a 37% share of renewable energy in Europe: one scenario with low flexibility (*Flex*$^-$), and the other high flexibility (*Flex*$^+$).

The following assumptions were made:

- Higher flexibility will reduce conventional power plant power and time minimums.
- Biogas facilities will increasingly be used flexibly by gas storage or additional capacity.
- CHP facilities will increasingly be equipped with thermal storage. Greater PtH capacity was also presumed. The study examined scenarios with both high and low flexibility.

## Storage Costs

The cost efficiency or economic necessity of electricity storage depends primarily on investment costs, as well as technical parameters such as efficiency and cycle life. The study distinguished costs for storage power and costs for storage capacity. Assumptions similar to [18] were used for model calculations.

Figure 3.34 shows an example of cost assumptions for the technologies studied with six-hour and 200-hour storage.

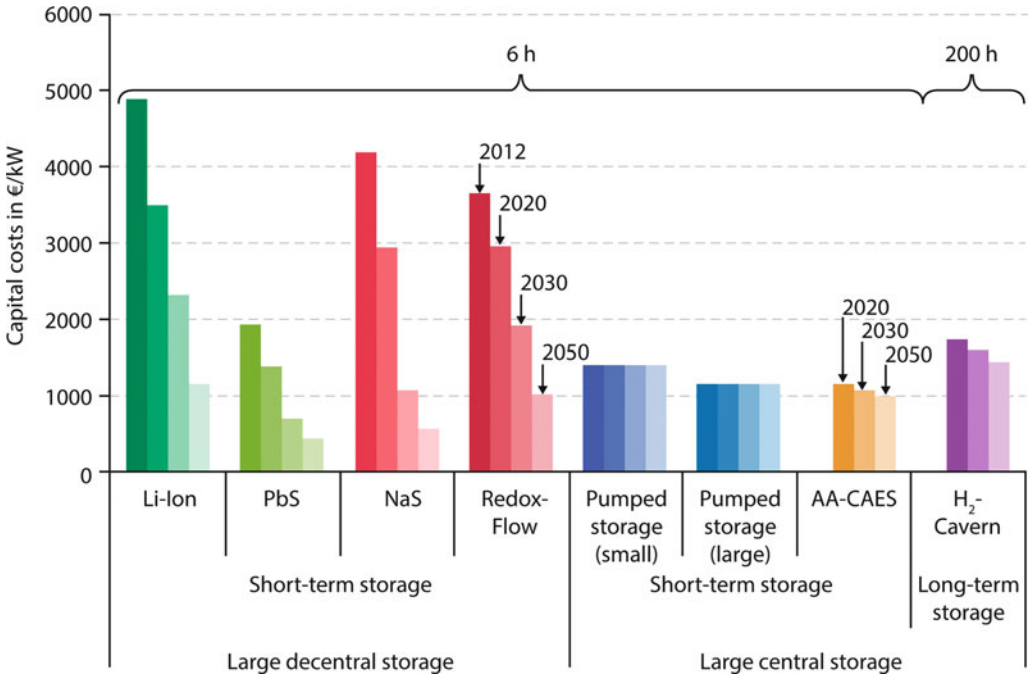



**Fig. 3.34** Comparison of investment costs for short and long-term storage for the years 2012, 2020, 2030, and 2050 [30]

### Load-Management

Load-management offers considerable potential for smoothing residual load. Residual load in turn can be sold for profit on the electricity market (▶ Chap. 11). In addition, load-management offers high connection capacities. As electro-mobility, electric heat-pumps, and air-conditioning become more prevalent, load-management could reduce power plant utilization. Starting with the medium-term scenario, night storage heating and electric heating for hot water decline. For electro-mobility, in the medium-term, only 20% of the power plant portfolio is expected to participate in load-management. Higher flexibility (60%) is expected only in the long-term. The integration of thermal storage would allow flexible use of electric heat-pumps (▶ Sect. 4.1).

Despite the high connection capacity of 108 GW for load-management applications in the 82% scenario, due to technical, time-of-day, and seasonal restrictions, only a maximum of 26.7 GW could be used. This means that due to technical and economic factors, the theoretically large potential can in reality only be utilized to a limited extent at any time.

In the future, PtH will also significantly influence storage requirements. Therefore, it can be assumed that CHP facilities will be equipped with thermal storage as well as electrode boilers. In the long-term, it is assumed that PtH will provide 14 GW of additional flexibility potential.

### Network Expansion Assumptions

The European transmission network model includes all existing connections in 2010. For the scenarios studied, it has been expanded to account for network development plans (NDPs).

In the scenario with a 26% share of renewable energy in Europe, all of the measures in the 2013 NDP [1], as well as the 2012 ten-year plan (TYNDP) for Europe, have been implemented. For the medium-term scenario (at around 2030) with a 37% European share of renewable energy, delayed (the Network-version)

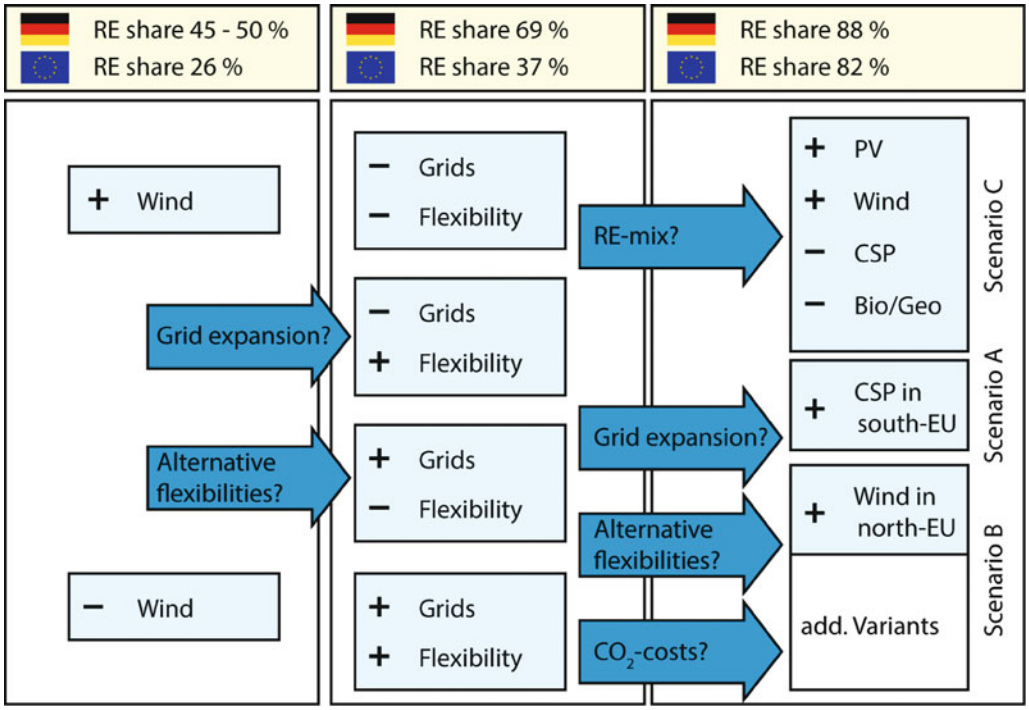



**Fig. 3.35** Overview of the various scenarios in each of the time periods studied, as well the sensitivity scenarios considered [30]

as well as completed (the Network+ version) network expansion, including all the measures of the NDP and TYNDP, were studied separately. Completed network expansion was used as the basis for the long-term scenario, which also included additional transmission capacity optimization, where required. As in the studies above, the basis used was decisive for storage requirements.

A complete description of assumptions can be found in ▶ Sect. 4.2 of the final report of the Storage Roadmap study [30].

### 3.5.2.2 Overview of Scenarios

The Storage Roadmap study examined the effect of various measures on storage requirements in the medium and long-term. The study included various sensitivity calculations, illustrating in detail the effects of such factors, such as delayed wind energy facility expansion by 2020 and delayed network expansion by 2030. In addition, the study examined the influence of load-management, flexible CHPs, and flexible power plants in various combinations. By around 2020, the study assumed a share of renewable energy in Germany of 45–50%, and in the EU of 26%. By around 2030, the study assumed a share of renewable energy in Germany of 69%, and in Europe, of 37%.

The long-term analysis studied three different scenarios: A, B, and C. Given actual developments, scenario C is considered the most likely; especially since the development of solar-thermal power plants in Europe has failed to meet expectations. Therefore, this scenario will be analyzed in detail together with only the most important findings from scenarios A and B. Scenarios A and B are similar to the BMU long-term scenarios from [26].

Due to falling prices for PV energy and wind power, on economic grounds, other technologies such as solar-thermal power plants, bioenergy, and geothermal energy seems to have limited potential for expansion. Figure 3.35

presents an overview of the scenarios studied and the effects of various measures. Other sensitivity scenarios studied include various combinations of renewable energy, $CO_2$ certificate costs, network expansion, and alternative flexibility options.

### 3.5.3 Medium-Term Storage Simulation

In order to demonstrate the economic benefits of additional electricity storage and assess the resulting storage requirements, an analysis of the generation situation and its effects on the transmission network was performed first.

#### 3.5.3.1 Results of the Generation Situation

For the medium-term, the scenario with a share of renewable energy in Germany of 45–50% and in the EU of 26% was considered first. In this scenario, expanded onshore wind energy capacity and reduced electricity generation from natural gas and hard coal (scenario Wind+) resulted in slight variations in electricity generation in Germany. Surplus generation was mainly exported to neighboring countries.

When the assumed renewable energy expansion is increased to a share of 68–70% in Germany and 37% in Europe, the effects on electricity generation were greater. Most of the renewable energy feed-in came from on and offshore wind energy facilities. The remaining demand was met with thermal power plants using brown coal, hard coal, and natural gas.

If network expansion was accelerated by adding transmission capacity to foreign countries (the Network+ scenario), generation rose slightly in Germany. Scenarios with increased flexibility (Flex$^+$) led to larger changes in the generation structure because, in these cases, flexibility options were used on both the demand side and the generation side. However, this was accompanied by decreased use of established flexible power plant technologies and storage such as pumped-storage. So, for these scenarios with higher flexibility, lower requirements for new storage in the electricity market can be assumed.

Especially where there was a share of renewable energy of 68–70% in Germany, most of the energy came from on and offshore wind energy facilities, primarily concentrated in the north of the country. This means that many situations placed heavy north-to-south transport requirements on the transmission network that could cause network congestion (▶ Sect. 3.4).

#### 3.5.3.2 Results of Congestion in the Transmission Network

To ensure secure network operations with a growing share of renewable energy, the study simulated network security under the given transport requirements. When expansion projects from the NDP were taken into account, the results of the network operations simulation demonstrated that the assumed network infrastructure was generally adequate for the new network utilization situation in these generation scenarios.

With a 45–50% share of renewable energy in Germany, expansion of the north-to-south connections with three HVDC transmission lines meant that generation at the levels determined for the electricity market required only limited intervention. At close to 60 million euros per year, the resulting redispatch costs were also quite low. This scenario primarily focused on local transmission network congestion, not systemic congestion. So presuming that the planned HVDC transmission lines are in use, with a 45–50% share of renewable energy in Germany, apparently no expansion of electricity storage is required when only the network is considered.

In the scenario with a 69% share of renewable energy in Germany, a reduction in the thermal power plant portfolio accompanied by an expansion in wind energy facilities caused larger changes in the network utilization situation. The results for this time period also demonstrated that the number of measures required and the costs incurred generally increased. With delayed network expan-

sion (Netw-), congestion situations occurred primarily at wind energy facility network connection points on the German coast and along the north-to-south lines.

In comparison, network expansion planned for 2030 had a positive effect on redispatch costs and quantities, resulting in a 30% reduction in costs in the Flex$^+$ Network+ scenario.

#### 3.5.3.3 Results for Additional Storage Requirements

To determine storage requirements in the energy generation system, the economic benefits of typical storage projects were calculated. Here, an additional 300 MW of pumped-storage capacity was assumed, as well as a PtG facility with a 1.2 GW capacity. The utilization of the electricity generation system was determined for these scenarios by using an updated market simulation, as well as by taking account of the additional storage projects. The two short-term scenarios with lower shares of renewable energy yielded limited savings. These ranged under 1 million €/GW per year with additional pumped-storage.

For the scenarios with a 37% share of renewable energy in Europe, additional PtG facilities yielded limited savings because of the low level of efficiency. In comparison, pumped-storage yielded savings of up to 4 million €/GW per year at best. This is, however, still very low compared to overall system costs. The scenario with higher flexibility (Flex$^+$) yielded even lower potential savings with additional storage capacity. In sum, the results indicated that expanding electricity storage in the European electricity generation system would yield only limited generation cost savings.

But electricity storage could reduce costs and offer economic benefits. This is because integrating storage into network operations through transport tasks in the opposite operational direction can relieve strain on the network. Here, storage with temporally decoupled feed-in must be distinguished from storage with spatially decoupled feed-in. Pumped-storage can offer only a few hours of temporal decoupling, and is mainly found in the south behind the current congestion area. In addition, in network operations, storage offers the greatest potential in locations where renewable energy feed-in is curtailed over a relatively large number of hours. This means that adding PtG facilities makes good sense, since the existing gas infrastructure's gas network can be used to decouple feed-in temporally as well as spatially [15].

PtG facilities in network operations have been found to relieve strain on the network and, therefore, reduce costs. However, the use of alternative flexibility options also influences the potential of additional storage in network operations. As a result, only limited cost savings could be realized using additional PtG facilities in the scenario with accelerated network expansion and high flexibility (Flex$^+$ Network+). In addition, PtG facilities improved the integration of renewable energy in the electricity system, thereby reducing the necessity to curtail renewable energy.

#### 3.5.3.4 Cost/Benefit Analysis

To assess the economic potential of additional storage capacity, the savings achieved were compared with the required investments and operating costs (Fig. 3.36). The assessment also took into account that more renewable energy could be integrated.

The comparison demonstrated that, under the given conditions, none of the storage versions studied were economically beneficial. This was due to limited cost savings in the electricity market, as well as low requirements for greater storage flexibility. Balancing in the European generation system, priority use of load-management and flexible CHP facilities were already available as flexibility options.

In addition, given the assumed expansion projects, the network infrastructure was largely adequate for the shares of renewable energy studied. As a result, electricity storage such as PtG offered an advantage exclusively in the area of spatial decoupling. Even with a high renewable energy share of 37% in Europe, electricity storage did not offer economic benefits exceeding its costs.

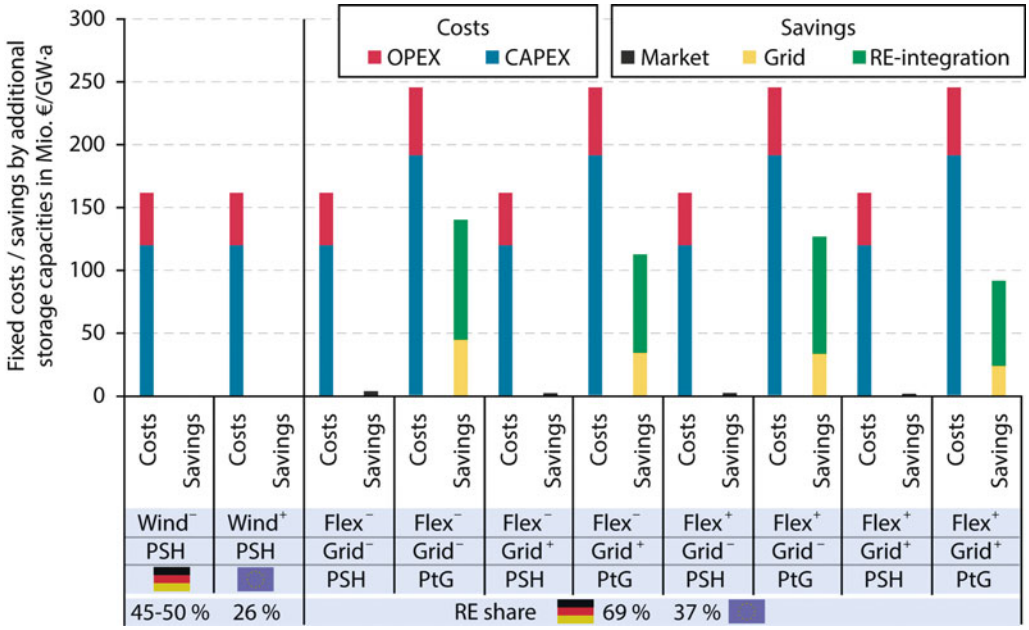



**Fig. 3.36** Cost efficiency of various additional storage versions [30]

It should also be noted that only temporary congestion situations caused transmission network restrictions. As a result, implementing further improvements in the electricity network could mean additional electricity storage is no longer cost-efficient.

## 3.5.4 Long-Term Storage Simulation

The long-term storage simulation assumed an 88% share of renewable energy in Germany, and an 82% share in Europe.

### 3.5.4.1 Results of European Expansion Optimization

The following sensitivity scenarios were studied for the long-term scenario: load-management, network expansion, gas turbines and combined cycle power plants, batteries with various capacities, and PtG.

The results demonstrated that, over and above the TYNDP European NDP, network expansion and cross-border interconnectors no longer had a significant influence on storage requirements. The results in ▶ Sect. 3.8 and Fig. 3.37 support the same conclusion.

Another significant finding was that comprehensive exploitation of load-management potential provided adequate network flexibility. This means that no (scenario B), or low (scenario C; 5.5 GW), additional flexible short-term storage—especially batteries—were required.

Short-term storage requirements increased only when 50% or more of assumed load-management potential from new consumers such as heat pumps, air-conditioning, and electro-mobility was exploited. In fact, requirements increased significantly when these consumers were firmly integrated.

In scenario C with high additional PV, electricity storage requirements of at least 5.5 GW and, at most, 19.2 GW with inflexible electricity consumption resulted in Germany. Despite the use of load-management potential in Europe, the required storage capacity amounted to 66 GW. In the inflexible scenario, the result was

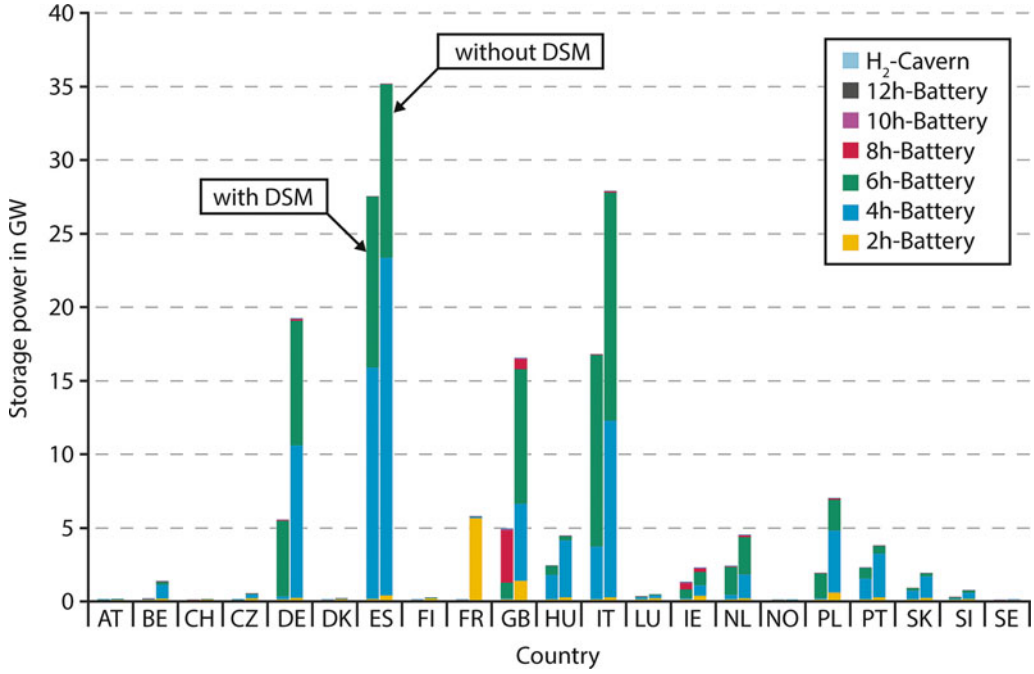



**Fig. 3.37** Forty percent scenario: shifting of electricity generation due to additional storage [30]

130 GW. The wide range is striking, confirming what the comparison of various studies in ▶ Sect. 3.7 indicated; that storage requirements depend heavily on the measures implemented to increase flexibility in the electricity system. Load-management is particularly decisive here.

Figure 3.37 shows installed storage capacity in all the countries studied with both comprehensive utilization and no utilization of load-management potential.

The renewable energy mix also affected requirements. Base-load renewable energy, such as geothermal or solar-thermal power plants with storage or biogas facilities, significantly reduced electricity storage requirements. But since electricity generation costs are (and will remain) lower for electricity from PV and wind power facilities than from base-load renewable energy (with the exception of hydropower, which is limited in potential), cost savings with these facilities exceed the costs of additional storage.

In all the scenarios studied, unexploited renewable energy surpluses amounted to less than 1.3% of German electricity generation from renewable energy, i.e., less than 6.1 TW h of around 456 TW h. Unexploited electricity surpluses in Europe occurred primarily in countries on the edge of the network; for example, in Italy, Spain, and the United Kingdom.

### 3.5.4.2 Results of the Detailed Study of Germany

The study considered in detail, using sensitivity analysis, how forecast error, balancing power requirements, and power plant portfolio restrictions affect economically determined storage requirements in Germany.

Additional electricity storage was added to the storage requirements determined for Europe in steps under the altered conditions, and then total system costs compared. The savings achieved by avoiding the addition of gas turbines as well as lower fuel consumption were also compared to the costs of additional storage.

In scenario B above, no additional electricity storage was required because, among other

reasons, load-management in Europe was fully exploited. In the altered sensitivity analysis, adding even 0.5 GW of battery storage dramatically lowered costs. This is because the availability of lower-priced primary balancing power (PBP) reduced fuel costs. Optimized costs for additional short-term storage expansion were achieved at 2 GW. The result was savings of around 700 million euros/year, amounting to 6.5% of total system costs.

In scenario C, the simulation results indicated that 5.5 GW of storage is required in Europe when a fully flexible electricity system is assumed, and that cost savings due to the use of storage for balancing power are low. But it was also shown that increasing storage capacity by an additional 3 GW did somewhat reduce costs. As a result, the economically optimal level of storage capacity amounts to 8.5 GW.

### 3.5.5 Significant Findings/Conclusions

- A **key finding** of the Storage Roadmap study is that **flexibility options** will be crucial to the electricity system in the future. They have a **direct influence on renewable energy integration**, and **reduce electricity storage requirements**. This means that, given adequate electricity network expansion, **renewable energy expansion** to meet medium-term goals **does not depend on adding electricity storage**.
- The following **factors** have a **strong effect** on the **timing and quantity** of demand for additional **electricity storage**: renewable energy expansion, increased CHP flexibility, network expansion or upgrading, and integration of load-management measures.
- If **new consumers** such as heat pumps, air-conditioning, and electro-mobility are **not used** for **DSM**, then **more short-term storage** with storage durations ranging from two to four hours is required. **With no DSM** at all, **short-term storage** with **storage durations of four to six hours is required**.
- If **PV is added** progressively, then in one scenario with inflexible electricity consumption, the resulting **electricity storage requirements** were at least **5.5 GW**, and at most **19.2 GW**. Despite the use of load-management potential in **Europe**, the **storage capacity** required was still **66 GW**. In the **inflexible scenario**, the result was **130 GW**. This wide range illustrates that storage requirements heavily depend on implementing measures to increase flexibility in the electricity system, and in particular, on load-management.
- **The earlier alternative flexibility options** are fully functional, and **the later** additional **electricity storage** is **required**. In contrast, **inadequately implementing** these measures means **increased storage requirements** for **electricity trade**, relieving **network congestion**, and **integrating renewable energy**.
- **Very high shares of wind and PV power over the long-term will result in higher storage requirements**. In all the scenarios and sensitivity analyses studied, the integration of the European electricity system and high system flexibility resulted in very low renewable energy surpluses ranging from 0.2 to 1.3%.
- Given the **alternative flexibility options** assumed here, **additional electricity storage** in the **European electricity generation system** yielded only **minimal generation cost savings**.
- If **expansion** of the **transmission network is delayed**, then **energy transition goals** can **only be met at a higher economic cost**. Even with **higher shares of renewable energy**, the assumed **expansion of the European electricity network** in the medium-term **is adequate**. Over the long-term, optimized expansion planning calls for only minimal expansion of the transmission network in Europe.
- Under the assumed conditions, **PtG** is **not economical** with very **high shares of renewable energy**. **But adding** PtG **still makes** good **sense**, because the **existing**

**gas infrastructure** can be used to **balance renewable feed-in temporally** as well as **spatially**. PtG facilities in **network operations** have been found to **relieve strain** on the network as well as to **reduce renewable energy curtailment**, and therefore to **reduce costs**.

- In the scenario with an **over 90% share of renewable energy**, **long-term storage** is required. Here **PtG** is the **only alternative currently available** for **balancing seasonal fluctuations**. In addition, use of the **gas network** could **replace** use of **fossil energy carriers** in the **chemical industry**, **transportation**, and **heating** sectors.
- Besides **balancing generation**, **increased demands** on the **electricity system** also resulted in **higher storage requirements**. These requirements were caused by **demand for balancing power**, in turn caused by renewable energy **feed-in forecast errors**, as well as by the **suspension of thermal power plants** to **provide system services**. **Short-term storage** is a particularly **economical alternative** in this case.
- **Decreasing electricity storage costs** are a **crucial requirement** for its economical use in the future. In addition, **policy initiatives** to **integrate storage technologies are required**. In order to adequately **ensure energy storage planning security** in the future, the **legal framework** should be **technology-neutral** and **flexible**.

## 3.6 Study of Network-Based Storage Requirements

The studies described in ▶ Sects. 3.2, 3.3, 3.4, and 3.5 made significant progress towards determining storage requirements as well as the principal causal relations. Having demonstrated energy storage's relevant market and network-based potential, the following uses the example of a case study to examine storage requirements on the network and system side when network expansion is significantly delayed.

Market-based surpluses may occur when existing energy cannot be financially integrated into the market. But they can also occur at network nodes due to congestion in the transmission network. In both of these cases, storage can be used to charge surplus energy on the market or relieve congestion in the electricity network. The latter generates network-based storage requirements. As suggested in ▶ Sect. 3.5, the question then becomes how high network-side requirements for PtG facilities will be if regional congestion is considered.

### 3.6.1 Methodological Approach to Distinguishing Market and Network-Based Storage Requirements

The methodological approach taken here was based on the Storage Roadmap study's approach (▶ Sect. 3.5). To estimate network-based storage requirements caused by severely delayed network expansion, for example, the approach used a model of the European transmission network based on previously determined levels of generation facility and storage utilization. The model simulated load flows in normal as well as disrupted operations. It also identified network security breaches.

Finally, it simulated required redispatch, as well as required modifications in feed-in from conventional and renewable power plants. The model also took into account flexible use of thermal power plants and renewable energy facilities as well as storage. These methods could then be used to reduce renewable energy feed-in curtailing requirements, for example.

### 3.6.2 Case Study: PtG in Germany in 2022 with Delayed Network Expansion

The following applies the methodological approach described in ▶ Sect. 3.6.1 to an example case study. The discussion examines the poten-

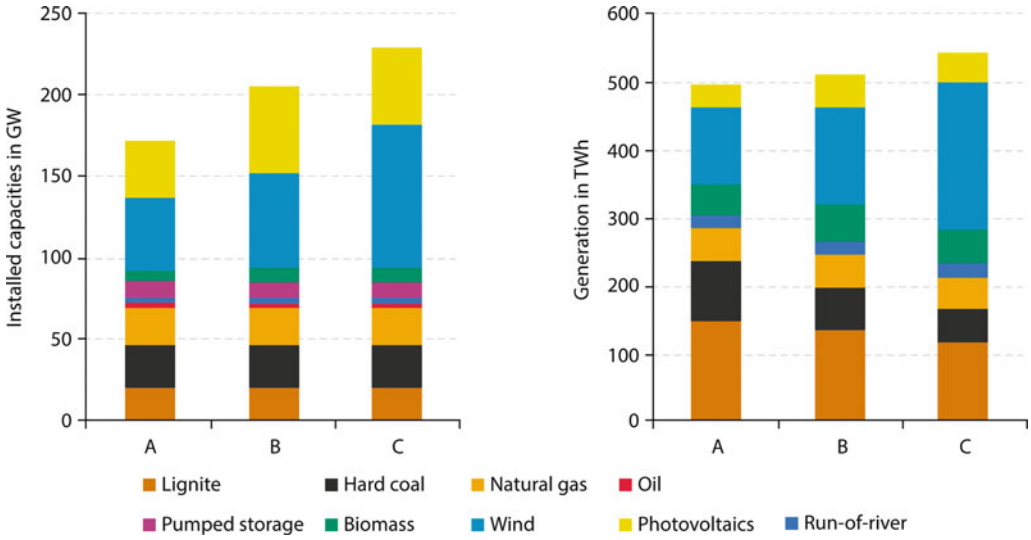



**Fig. 3.38** Installed capacities and resulting electricity generation in Germany in the three scenarios studied [12]

tial of facilities based on PtG technology in the electricity generation and transmission system. It also considers the most appropriate locations for PtG facilities [11].

### Future Scenarios Studied

To determine the effect of PtG facilities on the electricity generation system, the case study examined three different possible future developments of the generation system, which could take place by the year 2022. All renewable energy scenarios are based on the Nation Renewable Action Plans (NREAP) of the European Union (EU). The installed capacities in Germany were adjusted within the scenario framework to align with the transmission network operators' 2011 NDP.

The renewable energy share of German electricity generation varies from 44% in the scenario '44% RE', to 52% in the scenario '53% RE', to 61% in scenario '61% RE'. Figure 3.38 shows the installed capacities as well as the resulting electricity generation. The study assumed that the total installed capacity for PtG facilities was 4 GW.

Although renewable energy achieved high market penetration, especially in the 62% RE scenario, only marginal market-side shut-downs of renewable energy such as wind power were observed. Shut-downs may be required in situations where feed-in from renewable energy significantly exceeds the load, and additional energy exports abroad to integrate the energy into the market are excluded. As Fig. 3.39 shows, only 2.9 TW h per year of renewable energy facility generation was shut down in the 61% RE scenario.

### Market-Based PtG Facility Potential

Due to the assumed efficiency of 60% and a future gas price for the scenario of 31.6 €/MW h (3.2 cents/kW h), PtG facilities could economically produce hydrogen with a spot market electricity price below 19 €/MW h (1.9 cents/kW h). Although the facilities in the 44% RE scenario were used in only 55 hours per year due to low spot market prices, in the '52% RE' scenario their use increased to 363 hours per year. As a result of very low market prices, in part, in the 61% RE scenario, use of the facilities even reached 1,016 hours per year (Fig. 3.40). Generally, the facilities were used in times of low spot market prices, i.e., typically in times of low or even negative residual load.

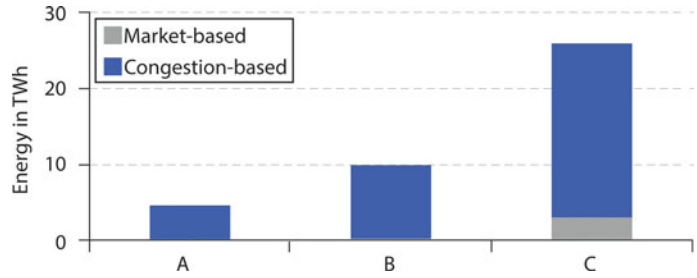



**Fig. 3.39** Wind energy shut-downs due to market prices and network congestion [12]

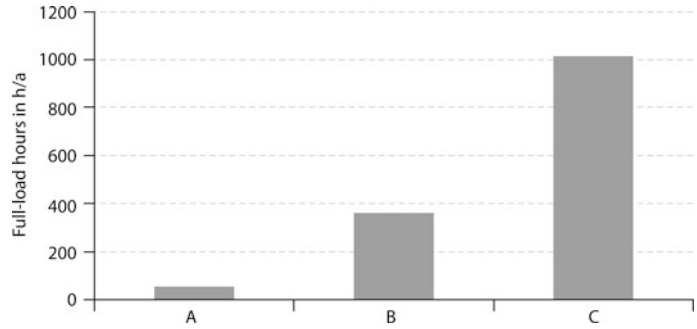



**Fig. 3.40** Market-side full-load hours for PtG facilities [12]

### Slow Expansion Results in Significant Congestion

Hourly network operations simulations were performed for all three scenarios, based on the determined market-side power plant utilization. These simulations also took into account the delayed network expansion assumed in the scenarios. The results indicated significant congestion in parts of the transmission network (for example in the north-to-south and east-to-south connections).

Taking into account the assumed installed capacity of 4 GW, PtG facilities were then uniformly distributed across all locations in the German transmission network to identify favorable locations, and the congestion-based use of the facilities, which were determined according to the methodology applied. If exclusively location-independent incentive instruments are developed to promote PtG facilities, this pattern of distribution could result in reality as well.

PtG facility shut-downs due to network congestion were reduced, i.e., price-driven utilization times. Shut-downs occurred in southern, central, and western Germany.

In contrast, PtG facilities in northern and eastern Germany were often activated to avoid congestion in the transmission network, as well as in part to prevent wind power facility shut-downs (Fig. 3.41).

### Significance of Location for Facility Assessment

Based on uniform distribution and the determined location-specific facility use, the next step identified the locations where network-side activation was particularly frequent. The study identified eight particularly favorable locations; three in southeastern Germany and five in northern Germany (Fig. 3.41). Facilities were then concentrated at these locations with a total capacity of 500 MW at each location. The assessment of PtG facilities at these favorable locations in another network operations simulation indicated that optimal positioning of PtG facilities can relieve transmission network congestion, as well as prevent renewable energy feed-in shut-downs at a large-scale. In northern Germany, electricity surpluses clearly resulted from wind energy. In southern Germany, they resulted from simultaneously high

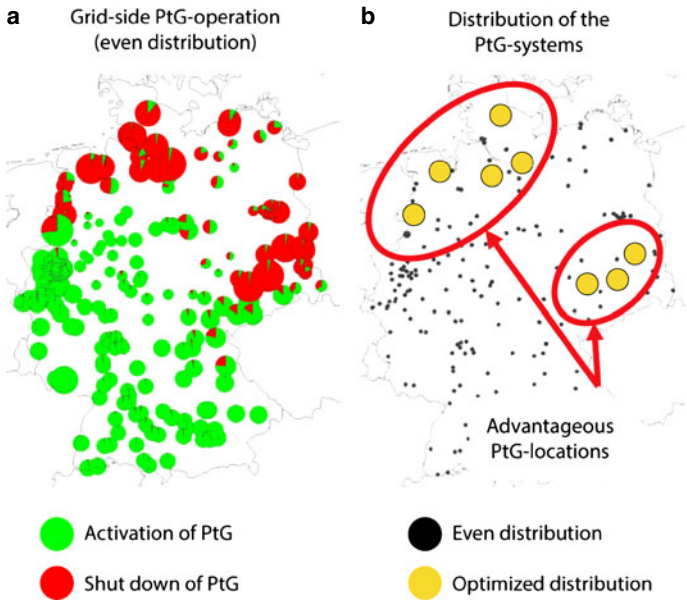



**Fig. 3.41** Network-side use (**a**) and distribution (**b**) of PtG facilities. **a** shows the resulting redispatch of PtG facilities due to network congestion for the 61% RE scenario. *Green circles* indicate shut-downs (reduction in demand for PtG facilities at the location). *Red circles* indicate PtG facility activations (increase in demand) [12]

feed-ins from wind energy facilities and lignite coal power plants. These plants are on the network because of low wholesale prices that still cover costs.

### ▪ High Utilization in the North, Low Utilization in the South

To assess the influence of positioning, the study determined average PtG facility full-load hours in the 61% RE scenario for various German states (Fig. 3.42). Since all facilities were activated at the same spot market price, market-driven use for all facilities was identical and independent of the location chosen.

In the case of uniformly distributed positioning, network congestion reduced PtG facility use in Bavaria and North Rhine-Westphalia. These PtG facilities were shut down to avoid connection overloads. This led to an average facility use of less than 300 hours per year in Bavaria; a very low figure.

Although facilities in the south had low utilization times because of their location, PtG facilities in northern and eastern Germany were activated for many additional hours per year because of transmission network congestion. The result was high average facility use in these areas. Precise positioning at favorable locations amplified this effect. Optimal distribution resulted in 2,000 to 2,500 full-load hours per year at facilities in Saxony-Anhalt, Saxony, and Schleswig-Holstein. This means that PtG facilities at these favorable locations could be optimally exploited in network operations to relieve transmission network congestion.

It should be emphasized that PtG facility use resulting from network congestion heavily depends on future network expansion. This is because network expansion could relieve local network congestion, significantly reducing congestion-based PtG facility potential.

## 3.6.3 Minimal Storage Requirements in the European Network

The case study presented above demonstrates that short and long-term storage may be required for various reasons. But in all cases, the goal should be to assess storage or future storage requirements from the point of view of the entire European system. This means taking its

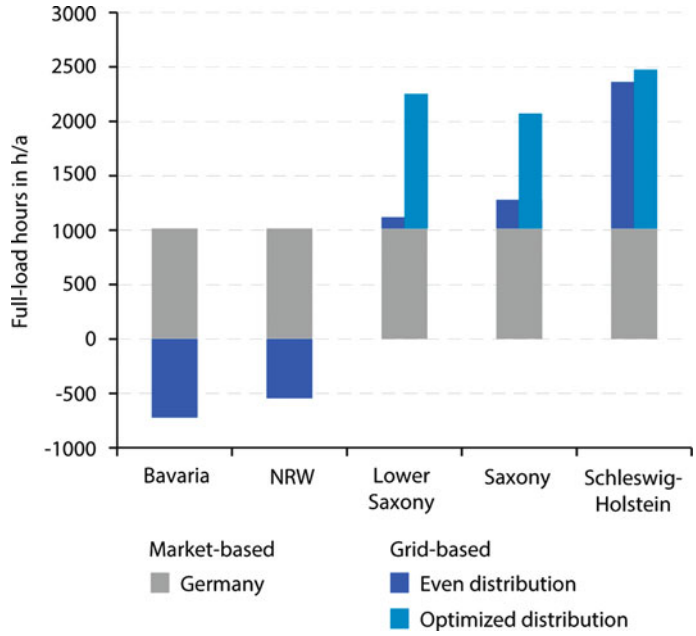



**Fig. 3.42** Potential full-load hours for facilities in various regions with various facility distributions; market-based use is uniform across Germany because of identical spot market electricity prices, but PtG facilities in Bavaria and North Rhine-Westphalia created additional congestion in network operations and, therefore, experienced network-based shutdowns. In northern and eastern Germany, by contrast, PtG facilities were activated to relieve network congestion [12]

effects on the electricity markets into account, as well as the transmission network.

Compared with expanding excessively large generation and storage capacities at a great cost, further European domestic market integration as well as expansion of regional and European transmission capacities are expected to result in significant economic advantages. Although a certain level of self-reliance or regional balancing of load and generation may be desirable from a geopolitical point of view, previous studies have shown that network expansion and cross-regional balancing are the most cost-effective alternatives available today.

### 3.6.4 Summary

- The effect of feed-in from wind energy and PV facilities on storage capacity is largely a function of forecast accuracy. In addition, **expansion of the transportation network** is a significant factor in relieving congestion. As a result, **market-based** and **congestion-based storage requirements** must be carefully distinguished.
- A case study examined **PtG facility potential** with significantly delayed network expansion in a scenario for the year 2022, and identified **favorable facility locations**.
- The potential of PtG is heavily-**dependent on the share of renewable energy** in the electricity generation system. The technology offers little significant market-based potential in the short and medium-term. But with a **60%** or higher share of renewable energy in German electricity generation, there is a significant increase in resulting electricity surpluses.
- PtG facilities could be **operated using surplus electricity** (for example, from wind power facilities) that could otherwise not be used without PtG facilities. But the technology cannot cost-effectively exploit all electricity surpluses. As a result, short-term shut-downs of wind energy facilities may be necessary.
- Where PtG facilities are **located** has a **significant effect** on the technology's eco-

nomic benefits. Facilities at **favorable locations** can **reduce transmission network congestion** as well as power plant utilization interventions (redispatch). But **poorly located facilities** (for example, in Bavaria or North Rhine-Westphalia) can significantly **increase** the **costs of stable transmission network operations**. This means that poorly located facilities are used less in network operations, reducing their cost efficiency.

- PtG facility **full-load hours** producing renewable gas vary widely at various locations, as well as in the various scenarios studied. A high number of full-load hours cannot be achieved at inappropriate locations and in scenarios with a low share of renewable energy. But up to **2,500 full-load hours per year** were achieved in scenarios with a high share of renewable energy and facilities at **appropriate locations**.
- Today, most **electricity surpluses** are **network-based**. Once **electricity network expansion eliminates congestion**, with a 50% share of renewable energy, **market-based storage requirements will be low**.
- Starting with a **60 to 80%** share of renewable energy, PtG facilities are expected to offer **considerable operational potential**.
- The **advantage** of using PtG to store renewable energy is that the energy can be stored as well as **transported over the gas network**. In the medium-term, the efficiency and cost-effectiveness of PtG facilities prevent them from being used to economically avoid or replace extensive **electricity network expansion**. The facilities **can only complement** that expansion.
- Using generation and storage facilities to strengthen **national supply, security** should be compared with cheaper options such as expanding **European transmission capacities** and exploiting synergies within the **European domestic market**.

## 3.7 Comparison and Categorization of the Results

### 3.7.1 Comparison of the Results of the Three Studies

The studies discussed differ in terms of the questions they consider as well as their modeling assumptions. As a result, only limited comparisons can be drawn. ◘ Table 3.9 provides an overview of the key questions, assumptions, and results of the three studies.

### 3.7.2 Categorization of the Results in Comparison to Other Studies

In addition to the research discussed thus far (the BMU long-term scenarios, the UBA 100%, and the VDE-ETG study), there are further studies which are partly based on these that used similar methods and yielded similar results.

#### 3.7.2.1 DIW Study—'Electricity Storage as a Central Element of Renewable Energy Electricity Integration'

- **Background, Methodology, and Assumptions**

The study, 'Electricity Storage as a Central Element of Renewable Energy Electricity Integration (StoRES—Storage for Renewable Energy Sources)', was conducted by the German Institute for Economic Research (DIW) in Berlin on behalf of the BMU for the years 2022, 2023, and 2050 [32]. The methodology and assumptions were based extensively on the VDE-ETG study (▶ Sect. 3.4) and the UBA study (▶ Sect. 3.3). The scenario design was based on the BMU

**Table 3.9** Comparison of the results of the studies considered

| | BMU long-term scenarios | | VDE-ETG study |
|---|---|---|---|
| Key question | Climate protection through renewable energy | Technical implementation of energy transition | Storage requirements with high shares of renewable energy |
| Author institute | DLR, Fraunhofer IWES, IfNE | UBA, Fraunhofer IWES | IAEW (RWTH Aachen), ISEA (RWTH Aachen), Fraunhofer IWES, ESEM (TU Karlsruhe), FENES (OTH Regensburg) and others |
| **Assumptions** | | | |
| Network expansion in Germany | Complete (copper plate) | Complete (copper plate) | |
| Import/export | (40%) net transfer capacities from 2011, (63%) 11.7 GW AC, 13.8 GW DC (85%) 11.7 GW AC, 31.4 GW DC | $H_2$ scenario: 5% of electricity demand $CH_4$ scenario: 6% of electricity demand | Focus on German storage requirements, i.e., assumes neither imports nor exports of electricity to balance the German system |
| Power plant and CHP flexibility | Standard | Flexible biogas facilities: gas turbine-CHP 2.5 GW and biogas reserve power plants GuD 17.5 GW | Heat-oriented CHP, electricity reduction by additional firing possible |
| *Must-run* (minimum generation) | None | None | None |
| Load-management | (40%): HH 1.1 GW, HP 2.7 GW, AC 2.5 TW h per year, EM 20% of all vehicles (63%): HH 1.25 GW, HP 4.7 GW, AC 5 TW h per year, EM 40% of all vehicles (85%): HH 1.3 GW, HP 7.3 GW, AC 10 TW h per year, EM 60% of all vehicles | (100%): manufacturing 1.5 GW; completely flexible: HP 44 TW h per year, AC 28 TW per year, EM 50 TW per year | Not accounted for |
| **Surpluses and storage requirements** | | | |
| 40% share of renewable energy (around 2020) | 3.7 TW h (pumped-storage) | – | Surpluses 0.26 TW h |
| 63% share of renewable energy (around 2030) | 5.9 TW h (pumped-storage) | – | – |
| 80–85% share of renewable energy (around 2050) | 8.0 TW h (pumped-storage) | – | Surpluses 30 TW h |
| 100% share of renewable energy (around 2050) | – | 8.0 TW h (pumped-storage) 90.5 TW h (PtG) 1.2 TW h (unused surpluses) | – |

**Table 3.9** (Continued)

| | BMU long-term scenarios | | VDE-ETG study |
|---|---|---|---|
| **Short-term storage utilization** | | | |
| 40% share of renewable energy (around 2020) | PSW around 8.7 GW<br>Compressed air 0.32 GW<br>Thermal storage | – | 7.2 GW @ 48 GW h (version A) |
| 63% share of renewable energy (around 2030) | PSW around 12.2 GW<br>Compressed air 0.32 GW<br>Thermal storage | – | – |
| 80–85% share of renewable energy (around 2050) | PSW around 12.2 GW<br>Compressed air 0.32 GW<br>Thermal storage | – | 14 + 7.2 GW @ 70 + 48 GW h capacity (version E) |
| 100% share of renewable energy (around 2050) | – | PSW 8.6 GW @ 55 GW h capacity, charging electricity: 8.0 TW h, discharging electricity: 6.0 TW h<br>Thermal storage | 36 GW @ 184 GW h capacity (version D) |
| **Long-term storage utilization** | | | |
| 40% share of renewable energy (around 2020) | None | – | None |
| 63% share of renewable energy (around 2030) | Not applicable | – | – |
| 80–85% share of renewable energy (around 2050) | Not applicable | – | 18 GW @ 7 TW h capacity (version E) |
| 100% share of renewable energy (around 2050) | Not applicable | PtG<br>$H_2$ version: 44 GW @ 85 TW h, charging electricity: 90.5 TW h, discharging electricity: 38.1 TW h<br>$CH_4$ version: 44 GW @ 75 TW h, charging electricity: 90.5 TW h, discharging electricity: 31.6 TW h<br>Thermal storage | 68 GW @ 26 TW h capacity (version D) |

Key: HH = households, HP = heat pumps, AC = air-conditioning, EM = electro-mobility.

long-term scenarios (by 2050) (▶ Sect. 3.2), as well as the NDP (basis for 2022 and 2023) in addition to other sources. Three alternative scenario were considered:

1. Implementation of the German federal government's energy and climate policy goals (only 2022 A)
2. Increased expansion of renewable energy and gas power plants—main scenario in the NDP (2022 B and 2023 B)
3. Additionally increased expansion of renewable energy and gas power plants

The methodology also included a detailed assessment of residual load determined by sepa-

rately considering short-term storage with batteries (two hours) and pumped-storage (eight hours), as well as by distinguishing between flexible or inflexible biomass and minimum generation power plants.

#### Results

Due to the similarity in methodology and assumptions, the results of the VDE-ETG study and the UBA study were essentially identical:

- Assuming flexible biomass electricity generation, no minimum electricity generation, extensive power plant flexibility, and renewable energy facility take-over of system services, electricity surpluses were low (the same assumptions and results of the VDE-ETG study). Only 471 surplus hours resulted in the 2032 scenario year.
- An inflexible system (strict biomass electricity generation and 20 GW must-run capacity) resulted in significantly more surpluses than a flexible system. In scenario B 2032, a flexible system generated 4.4 TW h in surpluses, equivalent to 2% of maximum electricity generation from wind and PV. In an inflexible system, the surpluses amounted to 18% of this reference value.
- The surplus calculations overestimated the effects of inflexible power plants, network restrictions, import and export, simple upscaling of individual wind and PV time series, spatial distribution of wind and PV, and other flexibility options such as PtH.
- Gradients increased together with renewable energy (similar to the UBA study).
- Practically no additional storage was required with unlimited curtailments. Instead, significant quantities of renewable energy was not used. In scenario 2032 B alone, there was 15% of annual wind and PV electricity generation.
- Designing the system to fully integrate all surpluses was inefficient from both a technical and economical point of view; utilization was too low to allow cost-effective operation. Curtailing 1% of surpluses in the scenario year 2032 reduced required storage capacity from 74 to 38 GW in an inflexible system, or from 41 GW to zero in a flexible system (similar to the VDE-ETG and UBA studies).
- With curtailment of renewable energy generation realistically set at 1%, daily and seasonal storage expansion begins in 2050, or in an inflexible system, in 2022 (Table 3.10).
- Hourly storage (lithium-ion battery storage with a discharging duration of two hours) could not benefit the system because many surpluses lasted longer than two hours, and assumed annuity investment costs were higher than for pumped-storage (eight hours).
- Long-term storage in the form of monthly storage (500 hours) such as PtG is required in a flexible system starting in 2050, and in an inflexible system with a high rate of renewable energy expansion starting in 2020.
- Import and export, reducing minimum electricity generation, increasing conventional and biomass-based power plant flexibility (for example biogas storage), and CHP using thermal storage dramatically reduced electricity sector storage requirements (identical with the BMU long-term scenarios and VDE-ETG study results).
- Future storage requirements cannot be assessed or determined using individual weather years. Achieving reliable results requires taking several years at a time into account (as in the UBA study).

### 3.7.2.2 NOW Study: 'Integration of Wind-Hydrogen Systems into the Energy System'

#### Background, Methodology, and Assumptions

On behalf of the National Organization of Hydrogen and Fuel Cell Technology (NOW), a consortium including PLANET GbR, FH Lübeck, Fraunhofer ISI, IEU at FH Stralsund, and KBB Underground Technologies GmbH conducted an in-depth study on the integration of PtG into the energy system [41].

**Table 3.10** Electricity storage expansion in GW (averages for all simulations) for battery storage, pumped-storage, and PtG in various scenarios with curtailment of renewable energy generation realistically set at 1% of surpluses. The figures shown from the DIW studies do not take into account storage requirements for system services, or storage requirements for thermal storage used to increase CHP and thermal electricity generation flexibility [32]

| Scenario year | 2022 A (federal government goals) | 2022 B (NDP main scenario) | 2022 C (progressive RE expansion) | 2032 B (NDP main scenario) | 2050 (BMU long-term scenarios) |
|---|---|---|---|---|---|
| **Flexible system**: no minimum electricity generation (must-run), flexible biomass electricity generation using thermal storage, and biogas storage among other methods | | | | | |
| Battery storage as hourly storage for two hours | 0 | 0 | 0 | 0 | 0 |
| Pumped-storage as daily storage for eight hours | 0 | 0 | 0 | 1 | 9 |
| PtG as monthly storage for 500 hours | 0 | 0 | 0 | 0 | 7 |
| **Inflexible system**: no minimum electricity generation (must-run), flexible biomass electricity generation using thermal storage, and biogas storage among other methods | | | | | |
| Battery storage as hourly storage for two hours | 0 | 0 | 0 | 0 | 0 |
| Pumped-storage as daily storage for eight hours | 4 | 12 | 19 | 24 | 21 |
| PtG as monthly storage for 500 hours | 0 | 0 | 7 | 14 | 40 |

The study focused on hydrogen as a component of PtG (▶ Chap. 8), and on the implementation of PtG hydrogen systems in 2030 from a technical and economic point of view. Storage requirements were also a crucial issue in this study.

The modeling approach simplified surpluses to wind surpluses exclusively in two zones within Germany, with limited network expansion (the northeast zone and northwest zone). In the study, adequate infrastructure expansion allowed hydrogen to be utilized as fuel for transportation and electricity reconversion. The study examined all the technologies required such as hydrogen storage in caverns (▶ Sect. 8.4). The study also performed a system analysis and drew conclusions from the results. The electricity volumes and installed capacity for 2030 in the moderate scenario were based on the BMWi's 2011 energy scenarios [33]. The ambitious scenario was based on the 2012 BMU long-term scenarios discussed in ▶ Sect. 3.2. Nearly 50% of installed wind capacity was generated in the two zones.

The electricity market in the study was based on the Fraunhofer ISI model PowerACE. The electricity network was highly simplified as a copper plate in two zones, similar to the regions in the Dena Grid Study II [14]:

- Northwest zone: North Sea, Schleswig-Holstein, Hamburg, Bremen, and northwestern Lower Saxony
- Northeast zone: Baltic Sea, Mecklenburg-Western Pomerania, Brandenburg, and Berlin

The most important network expansion assumptions that significantly affected the results were:

**Table 3.11** Wind surpluses in TW h per year in the NOW study covering two zones in northern Germany in 2020 and 2030 scenario years [41]

| | | Northwest zone | | Northeast zone | |
|---|---|---|---|---|---|
| Scenario | Network expansion | Moderate | Ambitious | Moderate | Ambitious |
| 2020 | 25% Dena II | 0 | 0 | 0 | 0 |
| | 12.5% Dena II | 0.5 | 0.9 | 0 | 0 |
| 2030 | 50% Dena II | 0.002 | 3.8 | 0 | 0 |
| | 25% Dena II | 8.1 | 26.5 | 0 | 0 |

- No restrictions within each zone (copper plate), and a 3 GW transmission capacity between the two zones.
- Transmission capacity to neighboring zones was limited: only a quarter of the network expansion in the Dena Grid Study II was implemented by 2020, and only half by 2030. Past delays in network expansion were used to justify these assumptions.
- No expansion beyond 2011 levels in Net Transfer Capacity (NTC), i.e., in import and export to Germany's neighboring countries.

#### Results

These assumptions produced the following results for these moderate and ambitious scenarios:

- There was no wind energy surplus in either zone in 2020 with the network expansion assumed (25% of forecasted network expansion in the Dena Grid Study II). The network expansion was assumed to be reduced by half, from 25 to 12.5% generated wind surpluses between 0.5 TW h per year (moderate) and 0.9 TW h per year (ambitious).
- Higher renewable energy feed-in and reduced load in 2030 generated 0.002 TW h per year of wind surpluses in the northwest zone in the moderate scenario, and 3.8 TW h per year in the ambitious scenario with 50% of the network expansion assumed in Dena II, and 8.1 TW h per year (moderate) and 26.5 TW h per year (ambitious) with a quarter of the network expansion assumed in Dena II. There were no significant wind surpluses in the northeast zone, since 90% of installed offshore wind capacity was assumed in the North Sea.

Table 3.11 summarizes these results.

The critical difference from the studies considered in ▶ Sects. 3.2 to 3.4 is the fundamentally different network expansion assumptions for Germany. If network expansion is massively delayed or not implemented at all in energy transition, as assumed in the NOW study, then significant surpluses will result in the electricity system from 2020.

Another remarkable limitation of these results is that, besides network expansion, the NOW study includes no other forms of flexibility. Significantly lower surplus volumes result when realistic flexibility assumptions are made regarding thermal power plants, CHP, load-management, import and export with European neighbors, and short-term storage use.

Finally, the issue of the energy source used for producing hydrogen is not addressed. Possible solutions to this problem are presented in ▶ Chap. 7 and ▶ Sect. 8.8.

### 3.7.2.3 SRU Special Assessment—'Ways to 100% Renewable Energy Electricity Generation'

#### Background, Methodology, and Assumptions

The German Advisory Council on the Environment (SRU) published a study on electric-

ity transition in 2011, investigating the technical viability and costs of electricity generation purely from renewable energy [35]. The study also considered whether bridging technologies are required, and what steps should be taken to achieve climate-friendly electricity generation.

The study developed four scenarios, each with an electricity consumption of 500 TW h and 700 TW h:

1. Self-reliance—national self-sufficiency
2. Net self-reliance alongside exchange with Denmark and Norway
3. Maximum 15% net imports from Denmark and Norway
4. Maximum 15% net imports from Europe and North Africa (similar to *Desertec*)

These target scenarios were calculated in hourly intervals by the DLR, and were also simulated in the BMU long-term scenarios. Therefore, the results are virtually identical to the results of these two studies.

The assumption for network expansion within the regions and across the German states significantly affected storage requirements. The DLR model, called REMix, bundled renewable energy feed-in for each German state into just one point (point model—national copper plate), varying only the transmission capacities between the states with distribution losses taken into account. The scenarios feature very high installed offshore wind capacity, and very high transmission capacities to Denmark and Norway.

Three storage technologies were studied for the year 2050:

- Pumped-storage (efficiency 80%, investment costs 1,600 €/kW, storage capacity 0.05 TW h, no expansion in Germany, but conversion of storage water-power facilities in Norway to pumped-storage)
- CAES (efficiency 80%, investment costs 280 €/kW, technical potential of storage capacity 3.5 TW h, 1.5 TW h actually used)
- PtG (hydrogen, efficiency 49%, investment costs 1,500 €/kW)

Other flexibility options such as integrating the heating sector using PtH or heat pumps were not considered.

### Results for Storage Requirements

The study demonstrated that, in principal, potential renewable energy in Germany and Europe is adequate for full supply. It also demonstrated that supply can be technically assured in each hour by integrating the appropriate transportation and storage capacities, and that networking with Scandinavia and Europe is cheaper than nationally self-sufficient electricity supply. Costs could also be reduced by reducing electricity consumption, i.e., by increasing energy efficiency (Table 3.12).

The use of pumped-storage was very limited because system services used 6 of the 7 GW of assumed pumped-storage capacity. In comparison with the other studies, CAES was only significant in the SRU study, where it was used for short-term storage. Battery storage was mainly used for short-term storage in the other studies.

Battery storage was not taken into account by the SRU study because its "overall potential as long-term energy storage at the required scale of storage capacity" in comparison with other forms of storage was "determined to be rather low" [36].

Similarly, Scandinavian hydropower and the European-North African network were used for long-term storage in the SRU scenario, while in the other studies, PtG was used for long-term storage. For this reason, the SRU scenario's approach included an installed offshore wind capacity at almost twice the level of onshore wind capacity. In contrast, in the other studies, cheaper onshore wind power was used. For example, the onshore wind power capacity of 33 GW was assumed for the year 2050 by the 2011 study in scenario 1.a was actually already exceeded in 2013. The assumed capacity of 25 GW in scenario 1.b kept it at 2010 levels.

The key finding of the SRU study regarding storage requirements was that integrating Scandinavian hydroelectric power and storage water-power facilities using extremely high transmission capacities in the double-digit gi-

**Table 3.12** Results of the four SRU scenarios for storage requirements (surpluses, storage utilization) with electricity generation purely from renewable energy in Germany, and with an electricity consumption of 500 TW h (version A). DK = Denmark, NO = Norway, FLh = full-load hours. Values are rounded to two or three places [35]

| | National self-sufficiency | Self-reliance with 15% exchange with DK and NO | Maximum 15% net imports from DK and NO | Maximum 15% net imports from Europe and North Africa[a] |
|---|---|---|---|---|
| Installed fluctuating capacities in GW | | | | |
| PV | 86 | 41 | – | – |
| Wind on land | 33 | 40 | 25 | 28 |
| Wind at sea | 73 | 73 | 73 | 73 |
| Transmission capacity *P* in other countries in GW or 'network length'/in GW km | | | | |
| Denmark *P* | 0 | 42 | 47 | 53 |
| Norway *P* | 0 | 46 | 50 | 116 |
| 'Network length'/in the network Germany–Denmark–Norway | 0 | 53,195 | 58,701 | 103,745 |
| 'Network length'/in other countries (Europe and North Africa) | 0 | 0 | 0 | 848,247 |
| Surpluses in Germany and storage losses | | | | |
| Curtailed surpluses after import and export and storage utilization[b] in TW h | 53 | 0.2 | 0.5 | 0.1 |
| Maximum surplus power in GW | 181 | 101 | 45 | 71 |
| Storage losses in TW h | 17 | 1.6 | 2.0 | 4.7 |
| Storage utilization—pumped-storage in Germany | | | | |
| Charging power in GW | 0.5 | 1.2 | 0.5 | 0.8 |
| Energy charged in TW h | 1.2 | 1.0 | 1.1 | 1.5 |
| Utilization (charging) in FLh | 2,400 | 830 | 2,200 | 1,880 |
| Discharging power in GW | 0.5 | 1.2 | 0.5 | 0.8 |
| Energy discharged in TW h | 1.0 | 0.8 | 0.9 | 1.2 |
| Utilization (discharging) in FLh | 2,000 | 670 | 1,800 | 1,500 |
| Storage utilization—CAES in Germany | | | | |
| Charging power in GW | 32 | 18 | 19 | 21 |
| Energy charged in TW h | 51 | 5.7 | 7.0 | 16 |
| Utilization (charging) in FLh | 1,600 | 320 | 370 | 760 |
| Discharging power in GW | 32 | 18 | 19 | 21 |
| Energy discharged in TW h | 34 | 4.3 | 5.2 | 12 |

**Table 3.12** (continued)

| | National self-sufficiency | Self-reliance with 15% exchange with DK and NO | Maximum 15% net imports from DK and NO | Maximum 15% net imports from Europe and North Africa[a] |
|---|---|---|---|---|
| Utilization (discharging) in FLh | 1,060 | 240 | 275 | 570 |
| Storage utilization—PtG (hydrogen) in Germany | | | | |
| Charging power in GW | 0 | 0 | 0 | 0 |
| Discharging power in GW | 0 | 0 | 0 | 0 |

[a] The simulation was based on only every second hour. The results may vary from other figures based on every hour. In addition, the figures found in the study's tables differ from those found in the text.
[b] Surpluses in Germany (copper plate) with linking abroad that were curtailed after the use of storage.

gawatt range resulted in marginal or practically 'no storage requirements' in Germany. In addition, the SRU study found that under the assumed conditions, linking abroad is more cost-efficient.

The costs included the conversion and expansion of storage water-power facilities in Norway (84 TW h of storage capacity with a maximum filling level of 80 TW h and a minimum filling level of 14 TW h) and Sweden (34 TW h of storage capacity) into the double-digit gigawatt range to pumped-storage, as well as the expansion of the electricity networks in these countries.

### 3.7.2.4 Fraunhofer IWES Study—'The Energy Transition Business Model'

#### Background, Methodology, and Assumptions

Building on the BMU long-term scenarios, the UBA study, the BMU Storage Roadmap, and other sources, the Fraunhofer Institute for Wind Energy and Energy System Technology in Kassel developed The Energy Transition Business Model—An Answer to the Energy Transition Costs Argument [19]. This study extended the period of energy transition to the year 2050 and expanded it to the areas of heating and transportation. Investments for technologies such as wind and PV were offset against savings in fuel costs for fossil and nuclear energy facilities. Using this approach, the study demonstrated that, even with conservative assumptions (no increase in fuel costs and $CO_2$ damage costs), investments in energy transition could yield inflation-adjusted returns of 2.3%. If real price increases based on NEP 2014 [8] or the BMU climate protection scenario 2050 [27] are assumed, then the returns increased to 4 to 6.7%.

In addition to scientifically refuting the common argument that energy transition is expensive, the study also calculated cross-sectoral storage requirements in a transition scenario. Assuming full supply from renewable energy using 915 TW h from wind and PV electricity and 85 TW h from other renewable energy sources (▶ Sect. 3.3.2.1, UBA study on potential renewable energy sources in Germany), 335 TW h were used in the classical electricity sector, 300 TW h in the heating sector (75% of heating requirements covered by heat pumps in addition to PtH), and 120 TW h in the transportation sector for electric motors (electromobility and overhead cable trucks).

Two-hundred-and-thirty-five TW h of electricity storage was required for the cross-sectoral technology PtG. Here, the technology

**Table 3.13** Requirements for energy storage, utilization, and investment costs in the year 2050 in the Fraunhofer IWES study, The Energy Transition Business Model; pumped-storage is not included [19]

| Technology | Installed 2050 capacity in GW | 2050 storage capacity in GW h | Utilization in full-load hours | 2011 investment costs in €/kW | 2050 investment costs in €/kW |
|---|---|---|---|---|---|
| Battery parks (eight hours) | 10 | 80 | Around 1,000 | 1,934 | 435 |
| PtG | 78 | Not applicable | Around 3,000 | 2,000 | 750 |
| PtH | 23 | Not applicable | Around 5,000 | 100 | 100 |

was used to meet requirements for electric fuels and gas heating, as well as to secure electricity supply using gas power plants.

#### Results for Storage Requirements

In addition to classical pumped-storage with a utilization of about 1,000 full-load hours (which the study did not expand beyond its current capacity), the energy storage requirements were the following, as detailed in Table 3.13.

The PtG charging power of 78 GW was very high. This was due to additional electricity demand from the heating and transportation sectors, as well as to the high total power of 430 GW of fluctuating renewable energy capacity required (180 GW onshore wind, 50 GW offshore wind, and 200 GW PV in an economically optimal mix). This study used battery parks to meet short-term storage capacity requirements. These were on a similar scale as additional capacity in the other studies. The same is true for PtH.

These results are very similar to those of the UBA study, in which significantly more ambitious energy efficiency goals resulted in lower storage requirements and installed storage capacity.

### 3.7.2.5 Fraunhofer ISE Study—'The German Energy System in 2050'

#### Background, Methodology, and Assumptions

The Fraunhofer Institute for Solar Energy Systems (ISE) in Freiburg developed a model similar to the one used by Fraunhofer IWES to simulate and mimic the total system. The study, 'The German Energy System in 2050', analyzed both electricity storage requirements as well as storage requirements in the heating sector. In addition, the model took into account the transportation sector using fixed shares of various energy carriers (electricity, synthetic fuels, fossil energy). It also took into account the industrial sector's energy requirements for process heat [21, 28, 29].

The objective was always to minimize total costs while meeting climate protection goals at the same time. The study considered the electricity and heating sectors in detail. ▶ Chapters 4 and 5 discuss the study's modeling assumptions and results for heating sector storage requirements at greater length.

One perspective was a climate protection scenario in the REMod-D model where the $CO_2$ reduction goal was 80 to 85% in comparison to 1990, and the total installed renewable energy capacity was 452 GW: 150 GW onshore wind, 38 GW offshore wind, 259 GW PV, five GW hydropower, and a flexible biomass capacity with an energy potential of 335 TW h. Seven GW from hard coal, three GW from lignite coal power plants, and 215 TW h from natural gas remained in the fossil mix.

Previous studies of the REMod-D explored three other perspectives. Unfortunately in those studies, only the electricity and heating sectors were considered. These previous modeling versions resulted in calculations for three different 100% scenarios without imports, but with various levels of building renovation and installed renewable energy capacities. In these

**Table 3.14** Three 100% scenario versions for the electricity and heating sectors. In all versions, installed hydropower capacity was 5 GW and available bioenergy 50 TW h. Imports and the share of fossil energy were fixed at zero. In all versions, electricity demand remained constant at 500 TW h [21, 28, 29]

| | RetrofitMax | Medium | REMax |
|---|---|---|---|
| PV capacity in GW | 182 | 205 | 262 |
| Wind on land in GW | 170 | 170 | 200 |
| Wind at sea in GW | 75 | 85 | 85 |
| Reduction of heating demand due to building renovation compared to 2010 | Minus 40% | Minus 50% | Minus 68.2% |

scenarios, $CO_2$ emissions compared to 1990 were fully reduced (Table 3.14).

#### Results for Storage Requirements in the Electricity Sector

Battery parks, pumped-storage (constant, no expansion), PtG (electrolysis and methanation to produce methane, no hydrogen), and centralized as well as decentralized thermal storage (partly in heating networks) were used. Table 3.15 summarizes the results for storage with links to the electricity sector.

In terms of the results for batteries and PtG, the study came to the same conclusions as the Fraunhofer IWES study, The Energy Transition Business Model, with the exception that renewable gas was reconverted to electricity primarily by using decentralized CHP. In addition, gas heat pumps or gas-fired condensing boilers were used as discharging technologies, and fuel-based processes were used in the industrial sector or commerce were supplied with 420 TW h. The additional costs for gas heat pumps compared to gas-fired condensing boilers are not always feasible in buildings with high flow-temperatures and low heating requirements. As a result, in the climate protection scenario, gas-fired condensing boilers were used in place of gas heat pumps. This was because all buildings suited to heat pumps already have electric heat-pumps.

It is striking that gas storage capacities and discharging capacities for PtG increased significantly in the 100% scenario for electricity and heating in comparison to the climate protection scenario for all energy sectors. In addition, centralized thermal storage requirements varied with renovation levels and the use of gas heat pumps. But since heating requirements were essentially constant, thermal storage requirements were determined by the building renovation rate.

### 3.7.2.6 BMU Study—'Flexibility and Storage Options'

#### Background, Methodology, and Assumptions

Another BMU study, 'Systematic Comparison of Flexibility and Storage Options in the German Electricity System to Integrate Renewable Energy, with an Analysis of Relevant Framework Conditions (Flexibility Options)', examined the effects of various flexibility options on storage requirements [5].

The study posited increasing shares of renewable energy from 40 to 100% in the scenario years 2020, 2030, and 2050 using an electricity market model (PowerFlex) and a European network model. The results were intended to assess flexibility and storage options in terms of their costs, as well as in terms of their potential capacity to reduce greenhouse gasses and integrate renewable energy.

#### Results for Flexibility Requirements and Electricity Surpluses

The following were the initial results from the study assessing residual loads for flexibility and storage requirements:

**Table 3.15** Storage requirements in the climate protection scenario for all sectors (electricity, heating, transportation, and the industrial sector), as well as for three Fraunhofer ISE Freiburg scenarios for 100% reduction of $CO_2$ emissions in the electricity and heating sectors. There were no buffer storage connections to micro-CHP and to electric or gas heat pumps [21, 28, 29]

| | Climate protection scenario (85% $CO_2$ reduction) | Scenarios for 100% reduction of $CO_2$ emissions in the electricity and heating sectors | | |
|---|---|---|---|---|
| Scenario | | RetrofitMax | Medium | REMax |
| Short-term storage | | | | |
| Battery storage TW h | 0.078 | 0.068 | 0.055 | 0.052 |
| Pumped-storage TW h | 0.060 | 0.060 | 0.060 | 0.060 |
| Long-term storage | | | | |
| PtG charging units (electrolysis capacity and methanation) in GW | 61 | 48 | 64 | 87 |
| Gas storage capacity in TW h | 12 | 66 | 62 | 78 |
| Combined cycle power plant discharging units and gas turbines in GW | 39 | 68 | 71 | 74 |
| Centralized CHP discharging units in GW | 25 | 17 | 13 | 13 |
| Micro-CHP discharging units in GW | 0 | 0.03 | 0.04 | 0.05 |
| Gas heat pump discharging units (100% scenarios) or gas-fired condensing boilers (climate protection scenario) in GW (thermal capacity) | 29 | 0 | 48 | 103 |
| Central thermal storage in millions of $m^3$ | 25 | 91 | 68 | 49 |

- Even in the 100% scenario, back-up power plant requirements sank to only 65 GW (similar to the VDE-ETG study).
- Real renewable energy surpluses (not system-driven surpluses caused by must-run, etc.) were negligible in the 40% scenario, and only were relevant starting with a renewable energy share of 60%, which increased exponentially (similar to the BMU long-term scenarios).
- With a renewable energy share of 60%, electricity surpluses (without use of flexibility options) of about 6 TW h occurred, and deficits of about 5 TW h occurred.
- In the 100% scenario, electricity surpluses (without use of flexibility options) on the order of 80 TW h occurred, and deficits of about 75 TW h occurred.

### 3.7.2.7 Agora Study—'Electricity Storage in the Energy Transition'

#### Background, Methodology, and Assumptions

The Agora study, 'Electricity Storage in the Energy Transition' [29], examined how much additional storage would reduce total system costs in an existing, functioning electricity system for the years 2023, 2033, and for a time with a renewable energy electricity share of 90% (around 2050).

FENES OTH Regensburg conducted the study in collaboration with IAEW and ISEA RWTH Aachen as well as ef.Ruhr (TU Dortmund) for the think-tank Agora Energiewende. The study focused on areas relevant to storage requirements which have been ignored by other studies, such as storage requirements due to system services, storage requirements in the distribution network, and storage requirements in the context of all energy sectors and flexibility options.

The study made the following assumptions:

- Share of renewable energy:
  - 2023: 43% in Germany, 23% in Europe
  - 2033: 60% in Germany, 40% in Europe
  - Long-term: 90% in Germany, 60% in Europe
- Network expansion and market areas:
  - Unchanging market areas
  - Full network expansion within the market areas
  - Variation in interconnectors between the market areas for 2023–2033
- Alternative flexibility options:
  - Variation in load-management and flexible power plants for 2023–2033
  - No individual consideration of many new electricity consumers such as electro-mobility, heat pumps, air-conditioners, or power-to-x (PtX) for transportation and the chemicals industry
- Power plant portfolio, electricity demand, and existing pumped-storage:
  - Based on the 2012 NDP and the ten-year plan (TYNDP) for Europe
  - Existing pumped-storage remained
  - Fixed and paid-for gas power plants to cover annual peak-load

Using the definitions in ▶ Chap. 2, the study divided electricity storage into two classes, regardless of technology: short-term and long-term storage. Battery power plants based on lithium-ion technology were used for short-term storage. PtG in combination with hydrogen and methane was used for long-term storage. The assumed technical and economic parameters are similar to those in ▶ Chap. 12 and are described in the study.

Newly installed electricity storage capacity in both classes was varied for different time-frames: short-term storage ranged from 0 to 36 GW, long-term storage from 0 to 16 GW.

The models applied are basically identical to the models in the VDE-ETG study (▶ Sect. 3.4) and the Storage Roadmap (▶ Sect. 3.5). Details regarding investment and fuel costs, installed renewable energy capacity, conventional power plants in Europe, and other assumptions can be found in [41].

The study's key findings are presented and illustrated below.

### General Premise

Because of the fixed gas power plants and alternative flexibility options assumed, it was not possible to optimize flexibility option expansion including electricity storage. This limitation of the methodology significantly reduced economically-driven requirements for new electricity storage in all the scenarios.

### Findings on Medium-Term Electricity Storage Requirements at the Transmission Network Level in the Time-frame from 2023 to 2033

- From the electricity market perspective, additional storage was not necessarily required in the medium-term as long as the European transmission network was only marginally expanded, and other flexibility options within the European market areas were activated, even with delays.
- In the 2030s, slightly expanding long-term storage (around three GW) was economically viable if European transmission network expansion was largely deferred. The activation of other flexibility options was delayed, and storage costs improved favorably.
- Additional electricity storage perpetuated base-load share in residual load. Given the assumed emission certificate prices (27 to 45 €/t $CO_2$), this could slightly increase electricity generation from (lignite) coal

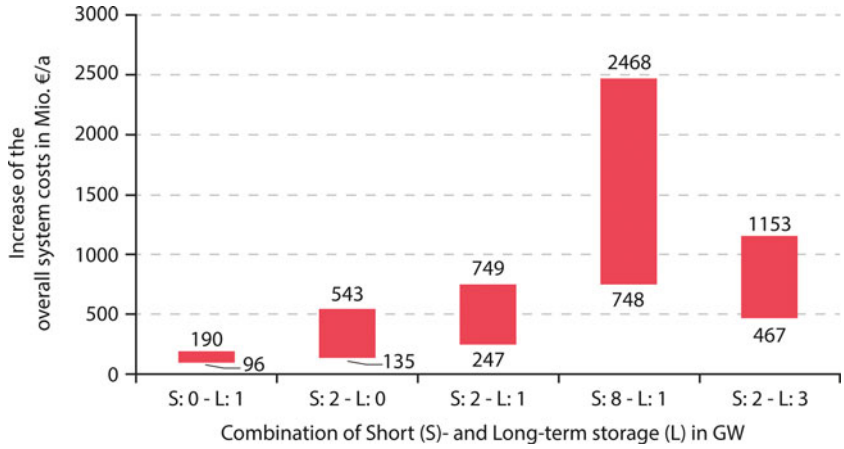



**Fig. 3.43** Additional costs and savings from new electricity storage expansion in various short and long-term storage (S and L) versions of the 43%/22% inflexible scenario for the year 2023 in millions of euros per year [39]

power plants at the expense of gas power plant generation. In the scenarios studied, electricity storage on the electricity market integrated only very little additional quantities of renewable energy electricity generation in the medium-term.

These findings were based on simulations of medium-term scenarios for 2023 and 2033 in two versions. The first version assumed full utilization of cross-border interconnectors and new load-management potential as described in ▶ Sect. 3.5 (flexible scenario). The inflexible scenario assumed a ten-year delay in utilization of flexibility options because, for example, of realistic public acceptance issues.

Figure 3.43 shows that the use of new electricity storage never reduced total system costs in Germany in any of the scenarios.

The use of long-term storage, such as PtG at up to three GW below the assumed premises, resulted in cost-reductions only in the inflexible scenario for the year 2033. Other storage combinations also produced results below the limit for cost-efficiency (Fig. 3.44).

In other cases, the electricity storage investment costs affected costs so dramatically that they caused additional electricity system costs for balancing generation alone.

Currently, flexibility options available in the electricity system are adequate to efficiently integrate renewable energy until the early 2020s. With full network expansion in the market areas, renewable energy surpluses would remain relatively low even until 2033; 1.6% of renewable energy in the inflexible scenario and 0.3% in the flexible scenario.

Additional available flexibility options leveled residual load, improved base-load power plant utilization, and reduced peak-load power plant requirements. Due to the economic advantages of coal power plants which, despite the rise in $CO_2$ emission certificate prices (in 2023 at 27 €/t and in 2033 at 45 €/t) remained ahead of low-carbon gas power plants in the merit order, using flexibility options for balancing generation alone did not result in reduced levels of $CO_2$-intensive electricity in the German electricity mix.

### Findings on Long-term Electricity Storage Requirements at the Transmission Network Level (90%/60%)

Even in the assumed system, including many other flexibility options and shares of renewable energy to match, electricity storage always reduced total system costs over the long-term if storage costs favorably improve.

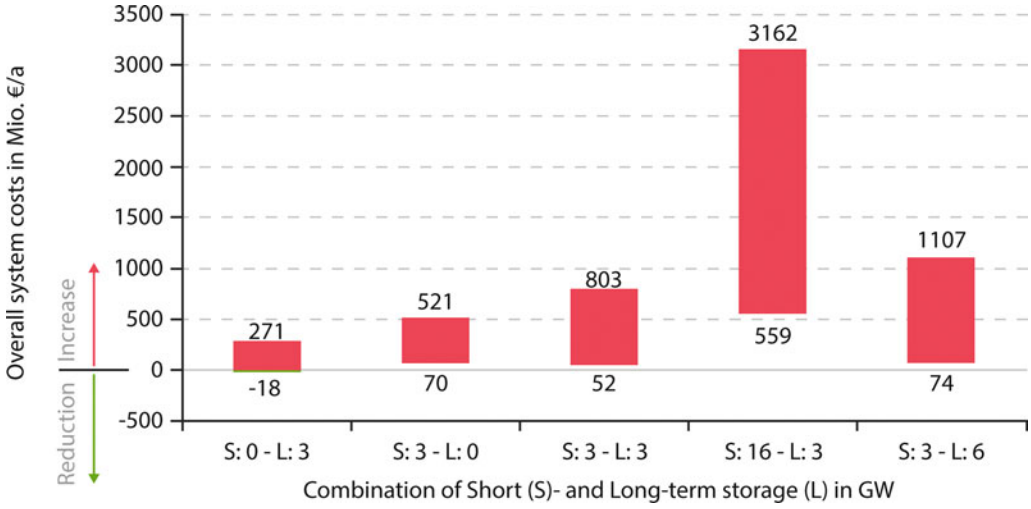



**Fig. 3.44** Additional costs and savings from new electricity storage expansion in various short and long-term storage (S and L) versions of the 60%/40% inflexible scenario for the year 2033 in millions of euros per year [39]

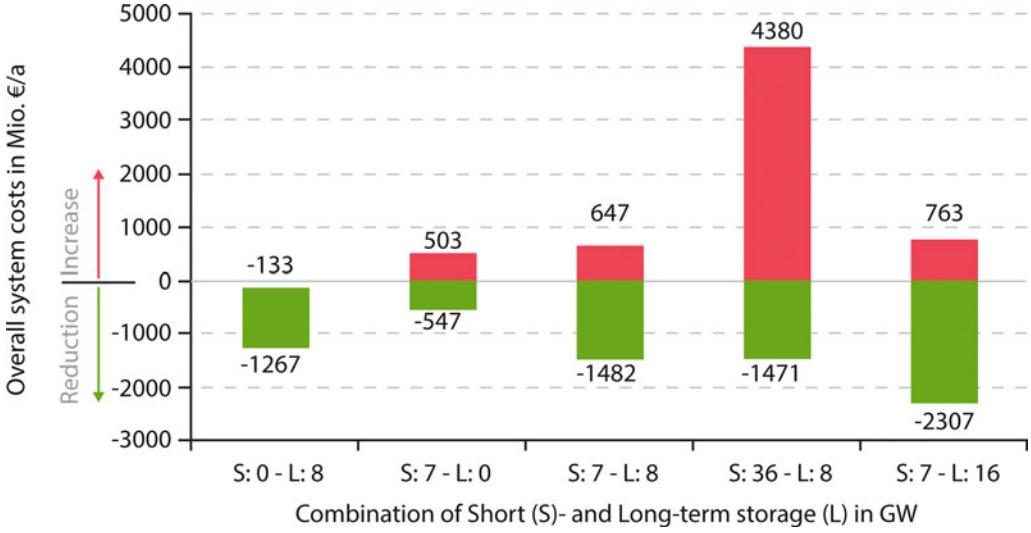



**Fig. 3.45** Additional costs and savings from new electricity storage expansion in various short and long-term storage (S and L) versions of the 90%/60% inflexible scenario for a long-term horizon (for example the year 2050) in millions of euros per year [39]

- Short-term storage faces greater competition from other flexibility options than long-term storage. This could reduce system costs over the long-term, even if storage costs do not favorably improve.

Over the long-term, with very high renewable energy shares in Germany and Europe, all of the storage versions studied resulted in reduced system costs (Fig. 3.45).

The greatest savings were achieved with an installed capacity of 16 GW for long-term storage and 7 GW for short-term storage. In addition, in these scenarios very large renewable energy surpluses could be completely integrated; only 3% remained unused. Because these small

energy volumes conceal very high capacities, capturing these surpluses with additional electricity storage was very expensive. In addition, the storage installations they required were not economical due to low operating times.

New electricity storage also had a beneficial effect on guaranteed capacity: it replaced the conventional power plant portfolio's guaranteed supply and, therefore, the power plants themselves in combination with renewable energy generation. By allowing greater integration of renewable energy, and as a result, reducing fuel consumption, new electricity storage could result in major savings.

In particular, the use of long-term storage such as PtG was an option with 'no regrets'; even with conservative assumptions, the 8 GW assumed would result in reduced costs. In addition, renewable energy curtailing was reduced from 7.2 to 5%, integrating an additional 11.5 TW h of renewable energy electricity.

With exclusive use of 7 GW of short-term storage in contrast, curtailing of renewable energy surpluses could only be limited to 6.2%. Short-term storage faced strong competition from alternative flexibility options for short-term surpluses because they generally required lower investment costs. As a result, the versions with a higher share of long-term storage were notably more cost-effective. This was due to seasonal load-shift potential and their ability to absorb large surplus volumes.

- **Findings on Electricity Storage Requirements at the Transmission Network Level (90%/60%)**
- In specific cases at the low-voltage level of the transmission network, storage use could delay or prevent network expansion, resulting in cost savings.
- Storage can only prevent network expansion when used to benefit the network. Storage use driven by the electricity market could even cause transmission network expansion in particular situations.

At the transmission network level, only battery storage operated to serve the network was studied. The goal was to determine the storage capacity required to minimize network expansion and network conversion costs. The study focused on the low and medium-voltage network because, at higher voltage levels, battery storage capacity would have to be very large. This would make it a poor competitor to network expansion and conversion.

Using an example network, the cost effects of battery storage use benefitting the network were compared with the following flexibility options:

- Conventional network expansion
- Technical modifications to connection guidelines (elimination of the 2% and 3% voltage criteria)
- Use of controllable local network transformers (CLNT)

Eliminating conventional network expansion and relying exclusively on battery storage was not cost-effective in any of the scenarios studied. Available network capacities were generally only adequate to integrate renewable energy surpluses for a few years. In addition, network expansion created additional operating reserves that could be used for further renewable energy expansion.

Expanding CLNT could entirely exhaust existing network operating reserves, especially in regions with high renewable energy expansion capacity. Technical modifications to connection guidelines would have a similar effect.

As a result, battery storage requirements in the low-voltage network should be estimated at a relatively low level. With a required storage capacity of 2,100 MW h, using battery storage as a substitute for network expansion resulted in a storage requirement of about 700 MW.

In specific cases, among the measures available, use of battery storage at the low-voltage network level could be a cost-efficient option to strengthen the network. This was particularly true when voltage problems and operating resource overloads occurred simultaneously.

Here, it was crucial that storage was used to benefit the network. 'Benefiting the network' means maintaining network load

through the use of energy storage. If battery storage was market-driven—for example, house battery storage systems used to maximize self-consumption, or on the electricity market—then it could even cause higher network expansion requirements in the transmission network, e.g., if it charges in times of electricity shortages, or if it discharges in times of electricity surpluses.

To avoid these critical network situations as well as additional network expansion, dynamic operation in both network-driven and market-driven modes is recommended (▶ Sect. 13.1).

- **Findings on Electricity Storage Requirements for System Services**
  - From a technical point of view, battery storage was particularly well-suited to supplying PBP. As battery prices fall in the future, using battery storage to provide PBP could be economically viable.
  - Energy storage could provide additional system services, increasing its cost efficiency.
  - Electricity storage could replace conventional power plants and contribute to guaranteed capacity.

- **Findings on Markets for Battery Storage and PtG Beyond the Electricity Market**
  - Battery storage in decentralized applications will develop independently from the electricity market, and establish itself over the long-term in Germany and internationally. The decisive markets are, therefore, new and existing PV facilities, as well as electro-mobility.
  - Parts of mobility that cannot be electrified as well as the chemical industry are the main markets for PtX in the form of synthetic fuels and electricity-generating basic materials. This is because there are few alternatives based on renewable energy available here, and the revenues for stored energy on these markets are higher than on the electricity market.
  - The markets for energy storage beyond the electricity sector result in higher electricity demand as well as increased availability of flexibility in the electricity generation system. Beyond their actual proper uses, these storage systems could provide additional services on the electricity market at a marginal cost.

- **Select Policy Recommendations and Outlook**
  - With renewable energy shares of electricity generation being over 90% in Germany and over 60% in Europe, more energy storage for decarbonization will be required in all markets and sectors. Ensuring storage will be on the market by this time requires technology and market development in the years before, as well as commercialization of storage to decrease costs. Revenues from the $CO_2$ certificate trade could be used to finance programs required for this purpose. Ensuring energy storage will be fully utilized requires research and development to achieve storage integration. It also requires standardizing energy storage.
  - As with all flexibility options, it is reasonable to expect that energy storage applications will not lead to higher $CO_2$ emissions by increasing the use of electricity from fossil power plants. This is especially crucial for electro-mobility and synthetic fuels, which could reduce $CO_2$ emissions in the transportation sector.
  - The development and implementation of flexibility options will not succeed if based purely on economic criteria. A wide spectrum of flexibility options could compensate for a lack of cost-effective options due to limited public acceptance.

The results demonstrate that a paradigm shift to renewable energy generation is within reach, and that energy storage can facilitate that shift. Energy storage is vital for replacing fossil power plants and guaranteeing continued supply security in energy transition. Assuming high shares of renewable energy, the use of electricity storage reduces system costs by saving fossil resources and integrating renewable energy surpluses.

## 3.8 Summary

This chapter closes with a review of the results on electricity surpluses from the studies discussed. This is followed by a conclusion summarizing their findings. Figure 3.46 provides a convenient summary of the results.

- **Storage requirements—general**
- After all **flexibility options** with priority have been taken into account, **storage requirements** result from **surpluses** with over-supply of **residual load**, and **deficits** with under-supply of **residual load** (consumption minus renewable energy feed-in). This means that flexibility requirements are greater than storage requirements.
- **Network expansion** in Germany, **import and export**, **flexible power plants**, **CHP**, and **DSM** are the flexibility options that have the **greatest effect** on storage requirements.
- The **electricity network**'s function is to **spatially balance** surpluses and deficits. **Storage**'s function is **temporal balancing**. As a result, **competition** between storage and the electricity network is generally **excluded**.
- Today, most **surpluses** are **network-based**. They practically disappear once electricity networks are expanded and transmission congestion is eliminated. Network expansion and increased power plant and CHP flexibility result in new, **market-based storage requirements** only above a renewable share of **60 to 80%**. With extensive interconnector expansion for import and export in Europe, these requirements occur only above a **renewable energy share** in electricity consumption of **80 to 95%**.
- Ensuring storage will be on the market by this time **requires technology and market development** in the years before, as well as **commercialization** of storage.

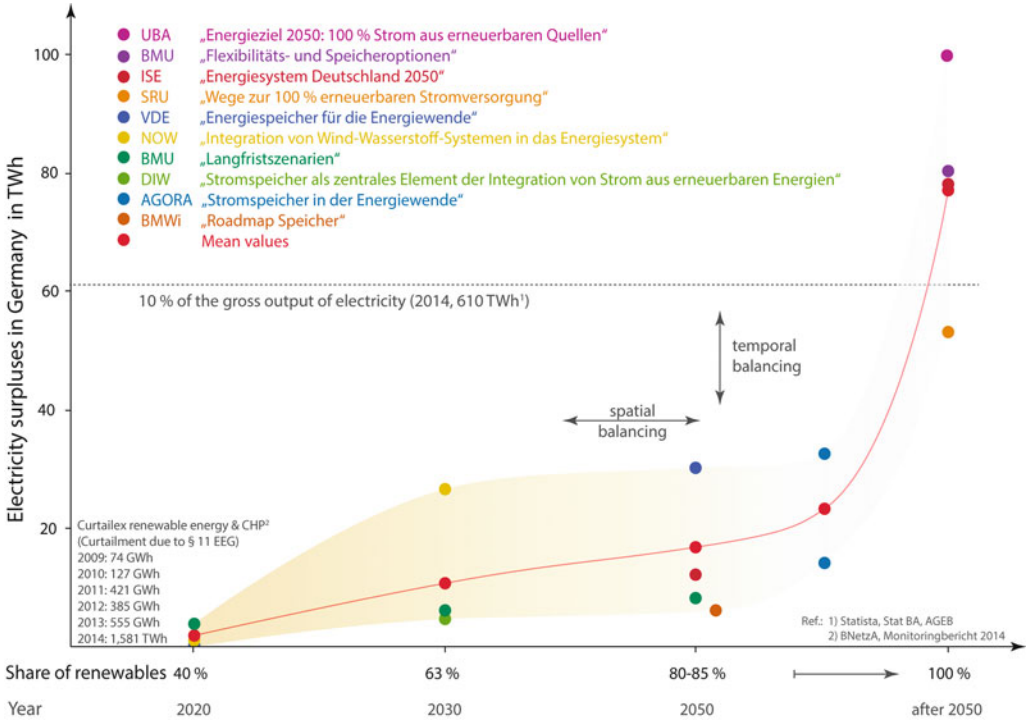



**Fig. 3.46** Electricity surplus estimates (flexibility and storage requirements) until 2050 [38]. Data from [5, 11, 12, 19, 20, 25, 28–30, 32, 35, 40–42, 45]

- German use of **Scandinavian hydropower capacity** dramatically **reduces storage requirements** in Germany. This however requires **converting storage water facilities** to pumped-storage, **increasing transmission capacity**, and **network expansion within Scandinavia**.
- To **refinance** itself, storage can provide **system services** independently from the electricity market, while also participating on **balancing power markets**.
- Storage requirements for **system services** are very limited due to the size of the market. These requirements will be further reduced by improved wind, solar radiation, and load **forecasts**, as well as by renewable energy participation on **balancing power and reserve markets**.
- Increasing quantities of **thermal storage** will be required to increase CHP flexibility, as well as for electricity storage in the heating sector using PtH and electric heat-pumps.
- **Location is decisive** for **network-based surplus storage**. Favorable locations are in regions with high wind feed-in, such as **northern and eastern Germany**, where high full-load hours can also be achieved. In other regions, market-driven storage use could even be the cause of transmission network expansion. The result is network-driven energy storage shut-offs negatively impacting the storage's cost-effectiveness.
- In addition, **transmission network restrictions** are caused by **temporary congestion** that could be eliminated by taking steps to improve the electricity network. This would also **reduce** the **cost-effectiveness of electricity storage**.
- In the **transmission network**, storage use may, in specific cases, delay or **prevent network expansion**, resulting in **cost savings**. But in these cases, **storage must be used to benefit the network**.
- Future storage requirements cannot be determined using individual **weather years**. Achieving reliable results requires taking **several weather years at a time into account**.

### Storage requirements—renewable energy share of around 40%

- At shares of 40% or above, with full power plant flexibility and network expansion, German **electricity demand can be 100% met** for short periods using renewable energy. If **higher minimum generation** as well as heat-oriented, **fixed** fossil, and biogenic **CHP** (*must-run*) are retained in an **inflexible system**, it will result in **significant surpluses**. Considered in the European context, it will result in lower surpluses in Germany.
- In the short-term, the **most economically attractive flexibility option** is to increase thermal power plant portfolio flexibility using CHP, network expansion across Europe, and load-management. Given this flexibility, **no additional storage requirements** are expected with a renewable energy share of 40%.
- In this time-frame, **additional storage** is used less to integrate renewable energy, and more to **optimize the use of thermal power plants**. This results in **increased $CO_2$ emissions**.
- In the **transmission network**, storage use may, in specific cases, **prevent network expansion**, resulting in **cost savings**.

### Storage requirements—renewable energy share of around 60%

- Given planned network expansion, market-driven surpluses that could be integrated with **short-term storage** occur at renewable energy shares between **40% and 60%**. For **long-term storage**, the shares are between **60% and 80%**. In **inflexible systems** with fixed power plants and CHP but no network expansion, surpluses occur at shares above **30% or 40%**.
- Above these shares, storage also **integrates significant quantities** of renewable energy, leading to a perpetuation of gray electricity as well as higher total system $CO_2$ emissions.

### Storage requirements—renewable energy share of around 80%

- At a renewable energy share of 80% or above, both **short and long-term storage** is required to **avoid** massive renewable energy **curtailing** and **achieve climate protection goals**. In the single-digit GW range, **storage use** is **cost-effective**.
- By absorbing renewable energy and **reducing** fossil fuel use, short and long-term storage reduce **$CO_2$ emissions** in the electricity sector.

### Storage requirements—renewable energy share of 100%

- With full renewable energy generation, **energy storage** is **critical** for supply security.
- Storage requirements **increase** by a **factor of two to four between 80% and 100%**. Long-term storage in particular expands significantly. The energy storage's share of **electricity generation costs** is about **20 to 30%**.
- Despite massive over-installation of wind and PV, **back-up capacity requirements** (long-term storage discharging capacity: gas power plants) **are not much lower** than they are today (60 to 70 GW or about 80% of annual peak-load). This figure is even higher when power plant and power facility non-availability is taken into account.
- In all studies, **gas storage capacity** available today is more than **adequate** for long-term storage requirements using **PtG**, with maximum storage use ranging from 30 to 40%.

### Storage use in the energy system transition

- **Electricity** will play an increasingly important role in the future as **primary energy** for the heating and transportation sectors.
- Renewable energy **integration requires** greater electricity system **flexibility**.
- The **electricity mix** determines the **ecological benefits** of **storage**. The **framework conditions** and **area of application** determine the **economic** benefits of **storage**.
- If low-cost, **$CO_2$-intensive lignite coal electricity generation** remains in the electricity system together with low shares of renewable energy feed-in, **additional flexibility options** such as network expansion, load-management, and energy storage systems perpetuate coal electricity's use and will result in **higher $CO_2$ emissions**.
- With increasing shares of renewable energy, **residual load** (consumption minus renewable generation) becomes **increasing volatile**, the **gradients** become **steeper**, and the **surpluses become larger**.
- The **cheapest**, and **most efficient measure** to **integrate storage** is to integrate the **heating sector** into the electricity sector using load-management, PtH, heat pumps, heating networks, and thermal storage.
- Due to its **higher efficiency** and **lower costs**, **short-term storage** will be used before long-term storage. But unlike **long-term storage**, its **capacity** is usually **quite limited**. Among short-term storage options, if costs continue to decrease, **battery parks** with a discharging duration from **one to four hours** will be preferable to **pumped-storage** with a **discharging duration of six to eight hours**.
- Marginal renewable energy **curtailment** (for example **1%**) makes **sense** from both **a technical and economic** point of view. **Storage capacity** could be **reduced by 30 to 40%**, **reducing costs** significantly. Unlimited curtailment eliminates storage requirements, but it also means that renewable energy share targets cannot be met, and that climate protection goals are not achieved. As a result, a **combination** of marginal **curtailment** and **energy storage** is recommended.
- The advantage of using **PtG** to store energy is that the **energy** can be **stored** as well as **transported** over the **gas network**. This **expands** the **electricity network**.
- Using generation and storage facilities to maintain **national supply security** should be compared with **cheaper** options, such as **expanding European transmission capac-**

**ities** and exploiting **synergies** within the **European domestic market**.

- **Full renewable energy generation** is **achievable** as well as **rational** from a **technical**, **ecological**, and **economic** point of view. Sustainable renewable energy potential is adequate. **Wind** and **PV** will become **fundamental pillars** of the system. To cancel out their fluctuations, the best capacity ratio of wind to PV is 60 to 40.
- By **linking** the **electricity sector** with **heating**, **cooling**, **transportation**, and **the chemical industry**, primary wind and PV energy **can be stored** across sectors in all physical forms. The result is higher installed wind, PV, and PtG capacities. **Electricity sector thermal storage requirements** are determined by the **building renovation rate**, as well as by the use of other **heating options** such as heat pumps.

## References

1. 50Hertz Transmission GmbH, Amprion GmbH, EnBW Transportnetze GmbH, TenneT TSO GmbH (2012) Netzentwicklungsplan Strom 2012 (Entwurf der Übertragungsnetzbetreiber)
2. Agora Energiewende (2013) Die Energiewende im Stromsektor 2013: Erzeugung, Verbrauch, Erneuerbare Energien und CO2-Emissionen. Agora Energiewende, Berlin
3. Baldauf M, Seifert A, Förstner J, Majewski D, Raschendorfer M, Reinhardt T (2011) Operational Convective-Scale Numerical Weather Prediction with the COSMO Model: Description and Sensitivities. MonWeaRev
4. Baldauf M, Seifert A, Förstner J, Majewski D, Raschendorfer M, Reinhardt T (2011) Operational Convective-Scale Numerical Weather Prediction with the COSMO Model: Description and Sensitivities. MonWeaRev
5. Bauknecht D, Koch M, Tröster E et al (2013) Systemischer Vergleich von Flexibilitäts- und Speicheroptionen im deutschen Energiesystem zur Integration der erneuerbaren Energien und Analyse entsprechender Rahmenbedingungen. Berlin (Vortrag zur Fachtagung „Aktuelle Vorhaben zum Klimaschutz und zur Umsetzung der Energiewende")
6. Blanc P, Gschwind B, Lefèvre M, Wald L (2011) The HelioClim project: Surface solar irradiance data for climate applications. Remote Sensing
7. BMU (2012)) Erneuerbare Energien in Zahlen. Nationale und internationale Entwicklung, 2012. Bundesministerium für Umwelt, Naturschutz und Reaktorsicherheit, Berlin
8. BNetzA (2013) Genehmigung des Szenariorahmens zum NEP/O-NEP 2014. Bonn
9. Bofinger S, Callies D, Scheibe M, Saint-Drenan YM, Rohrig K (2011) Potentiale der Windenergienutzung an Land. Kassel
10. Bömer J, Döring M, Beestermöller C (2013) Abschätzung der Bedeutung des Einspeisemanagements Abschätzung der Bedeutung des Einspeisemanagements nach §11 EEG und §13 Abs.2 EnWG. Auswirkungen auf die Windenergieerzeugung in den Jahren 2010 und 2011. Berlin
11. Breuer C, Drees T, Echternacht D, Linnemann C, Moser A (2011) Identification of Potentials and Locations for Power-to-Gas in Germany. 6th International Renewable Energy Storage Conference Eurosolar, Berlin
12. Breuer C, Drees T, Echternacht D, Linnemann C, Moser A (2012) Standorte und Potenziale für Power-to-Gas. E/m/w Zeitschrift Für Énerg Markt Wettbew 2012(4)
13. Das Energiekonzept der Bundesregierung 2010 und die Energiewende 2011
14. DENA (2011) dena-Netzstudie II. Berlin
15. Drees T, Pape C, Breuer C, Gerhardt N, Sterner M, Moser A (2012) Mittelfristiger Speicherbedarf und geeignete Standorte im Übertragungsnetz. VDE-Kongress 2012, Stuttgart
16. Eickmann J, Drees T, Sprey J, Moser A (2013) Optimizing Storages for Transmission System Operation. 8th International Renewable Energy Storage Conference and Exhibition, Berlin
17. FGH (2012) Studie zur Ermittlung der technischen Mindesterzeugung des konventionellen Kraftwerksparks zur Gewährleistung der Systemstabilität in den deutschen Übertragungsnetzen bei hoher Einspeisung aus erneuerbaren Energien. Mannheim (Abschlussbericht)
18. Fuchs G, Lunz B, Leuthold M, Sauer DU (2012) Technologischer Überblick zur Speicherung von Elektrizität. Überblick zum Potential und zu Perspektiven des Einsatzes elektrischer Speichertechnologien. Institut für Stromrichtertechnik und Elektrische Antriebe (ISEA), RWTH, Aachen (Im Auftrag der Smar Energy for Europe Platform GmbH (SEFEP), http://www.sefep.eu/activities/projects-studies/Ueberblick_Speichertechnologien_SEFEP_deutsch.pdf )
19. Gerhardt N, Sandau F, Zimmermann B, Pape C, Bofinger S, Hoffmann C (2014) Geschäftsmodell Energiewende. Eine Antwort auf das „Die-Kosten-der-Energiewende"-Argument. Herkulesprojekt Energiewende, Kassel
20. Henning H-M, Palzer A (2012) 100% Erneuerbare Energien für Strom und Wärme in Deutschland
21. Henning H-M, Palzer A (2014) A comprehensive model for the German electricity and heat sector in a future energy system with a dominant contribu-

tion from renewable energy technologies – Part I Methodology. Renew Sustain Energy Rev 30:1003–1018. https://doi.org/10.1016/j.rser.2013.09.012
22. IEA (2012) World Energy Outlook 2012. OECD Publishing, Paris
23. Klobasa M (2007) Dynamische Simulation eines Lastmanagements und Integration von Windenergie in ein Elektrizitätsnetz auf Landesebene unter regelungstechnischen und Kostengesichtspunkten. ETH Zürich, Zürich (Diss. Nr. 17324 Wiss)
24. Nitsch J, Pregger T, Scholz Y, Naegler T, Sterner M, Gerhardt N, Papa C, Wenzel B (2010) Langfristszenarien und Strategien für den Ausbau der erneuerbaren Energien in Deutschland bei Berücksichtigung der Entwicklung in Europa und global (Leitstudie 2010)
25. Nitsch J, Pregger T, Sterner M, Wenzel B (2012) Langfristszenarien und Strategien für den Ausbau der erneuerbaren Energien in Deutschland bei Berücksichtigung der Entwicklung in Europa und global. Bundesmin. für Umwelt Naturschutz und Reaktorsicherheit, Berlin (Schlussbericht BMU – FKZ 03MAP146)
26. Nitsch et al (2012) Leitstudie 2011. Langfristszenarien und Strategien für den Ausbau der erneuerbaren Energien in Deutschland bei Berücksichtigung der Entwicklung in Europa und global. Berlin
27. Öko-Institut e.V. (2013) BMU Klimaschutzszenario 2050, Rahmendaten. Berlin ((unveröffentlicht))
28. Palzer A, Henning H-M (2013) A Future German Energy System with a Dominating Contribution from Renewable Energies: A Holistic Model Based on Hourly Simulation. Energy Technol. https://doi.org/10.1002/ente.201300083
29. Palzer A, Henning H-M (2014) A comprehensive model for the German electricity and heat sector in a future energy system with a dominant contribution from renewable energy technologies – Part II: Results. Renew Sustain Energy Rev 30(0):1019–1034. https://doi.org/10.1016/j.rser.2013.11.032
30. Pape C, Gerhardt N, Härtel P, Scholz A, Schwinn R, Drees T, Maaz A, Sprey J, Breuer C, Moser A, Sailer F, Reuter S, Müller T (2014) Roadmap Speicher. Bestimmung des Speicherbedarfs in Deutschland im europäischen Kontext und Ableitung von technisch-ökonomischen sowie rechtlichen Handlungsempfehlungen für die Speicherförderung. Kassel (Kurzzusammenfassung)
31. Rohrig K, Richts C, Bofinger S, Jansen M, Siefert M, Pfaffel S, Durstewitz M (2013) Energiewirtschaftliche Bedeutung der Offshore-Windenergie für die Energiewende. Kassel (Kurzfassung)
32. Schill W-P (2013) Stromspeicher als zentrales Element der Integration von Strom aus erneuerbaren Energien (StoRES – Storage for Renewable Energy Sources). Erste Ergebnisse im DIW Wochenbericht 34-2013, Berlin
33. Schlesinger M, Lindenberger D, Lutz C (2010) Energieszenarien für ein Energiekonzept der Bundesregierung Projekt Nr. 12/10, Basel, Köln, Osnabrück, Berlin
34. Solar Radiation Data (2013) Einstrahlungsdaten. Paris
35. SRU (2011) Wege zur 100% erneuerbaren Stromversorgung. Erich Schmidt, Berlin (Sondergutachten)
36. Stadler I (2006) Demand Response. Nichtelektrische Speicher für Elektrizitätsversorgungssysteme mit hohem Anteil erneuerbarer Energien. dissertation.de, Berlin (Als Manuskript gedruckte Habilitationsschrift)
37. Sterner M, Schmid J, Wickert M (2008) Effizienzgewinn durch erneuerbare Energien
38. Sterner M, Jentsch M (2011) Energiewirtschaftliche und ökologische Bewertung eines Windgas- Angebotes. Kassel (Gutachten für Greenpeace Energy)
39. Sterner M, Moser A, Thema M, Eckert F, Schäfer A, Drees T, Rehtanz C, Häger U, Kays J, Seack A, Sauer DU, Leuthold M, Stöcker P (2014) Stromspeicher in der Energiewende. Untersuchung zum Bedarf an neuen Stromspeichern in Deutschland für den Erzeugungsausgleich, Systemdienstleistungen und im Verteilnetz. Berlin (Studie)
40. Sterner M, Thema M, Eckert F, Moser A, Schäfer A, Drees T, Rehtanz C, Häger U, Kays J, Seack A, Sauer DU, Leuthold M, Stöcker P (2014) Stromspeicher in der Energiewende. Untersuchung zum Bedarf an neuen Stromspeichern in Deutschland für den Erzeugungsausgleich, Systemdienstleistungen und im Verteilnetz. Berlin (Studie)
41. Stolzenburg K (2013) Large Wind-Hydrogen Plants in Germany: The Potential for Success. Results from the study: Integration von Wind-Wasserstoff-Systemen in das Energiesystem – presented at IRES 2013. Berlin
42. UBA (2010) 2050: 100% erneuerbarer Strom. Energieziel 2050. Umweltbundesamt, Dessau- Roßlau
43. VDE (2009) Energiespeicher in Stromversorgungssystemen mit hohem Anteil erneuerbarer Energieträger. http://www.vde.com/de/fg/ETG/Arbeitsgebiete/V1/Aktuelles/Oeffentlich/Seiten/Energiespeicherstudie-Ergebnisse.aspx. Accessed 29 Dec 2013
44. VDE ETG (2012) Demand Side Integration. Lastverschiebungspotenziale in Deutschland; ein notwendiger Baustein der Energiewende; Gesamttext. VDE-ETG, Frankfurt am Main (VDE-Studie)
45. VDE ETG (2012) Energiespeicher für die Energiewende. Frankfurt am Main

# Heating Supply Storage Requirements

*Michael Sterner, Fabian Eckert, Norman Gerhardt, Hans-Martin Henning, and Andreas Palzer*

**4.1 Basis and Objectives – 139**

**4.2 Development of Heating Requirements – 139**

**4.3 Development of the Heating Mix – 140**
4.3.1 Fossil Heating Supply – 140
4.3.2 Renewable Heating Supply – 141

**4.4 The Heating Sector Transition – 142**
4.4.1 Households – 142
4.4.2 TIS – 144
4.4.3 Manufacturing – 145

**4.5 The Heating Sector Paradigm Shift – 146**
4.5.1 An Example Transition: Crude Oil, Natural Gas, and Renewable Energy – 146
4.5.2 Electricity as Primary Energy – 146

**4.6 Storage Requirements in a Climate Goal Scenario for the German Energy System in 2050 – 147**
4.6.1 Scenario Framework, Model, and Assumptions – 147
4.6.2 Results for Storage Use in the Heating Area – 148

**Electronic supplementary material** The online version of this chapter (https://doi.org/10.1007/978-3-662-55504-0_4) contains supplementary material, which is available to authorized users.

© Springer-Verlag GmbH Germany, part of Springer Nature 2019
M. Sterner, I. Stadler (Eds.), *Handbook of Energy Storage*, https://doi.org/10.1007/978-3-662-55504-0_4

**4.7 Surpluses, Storage Requirements, and Storage Potential – 151**
4.7.1 Heating Sector Surpluses – 151
4.7.2 Development of Storage Requirements – 153
4.7.3 Storage Potential – 155

**4.8 Summary – 160**

**References – 162**

**Overview**

Unlike the electricity sector, heating and cooling storage requirements have attracted little public attention. This is because these storage requirements have generally already been met, and will not change significantly in the future. In the electricity sector by contrast, there will be a significant shift from primary energy storage to electricity and final energy storage.

Both sectors have remarkably high storage requirements. Almost all households have thermal buffers. The same is true of renewable energy heating systems such as pellet heating, geothermal, or solar-thermal systems. Some households with liquid gas or oil heating even have two storage units: a fuel tank and a thermal buffer. Exceptions include heating systems with upstream storage such as district heating or gas storage. In the future, integration of the electricity and heating sectors by combined heat and power (CHP) generation, heat pumps, power-to-heat (PtH), and power-to-gas (PtG) will facilitate the use of renewable energy, and lead to a paradigm shift.

Relying on results from various studies, this chapter examines the development of heating supply in Germany and the resulting thermal storage requirements. The chapter's later sections provide surplus and storage potential estimates. Cooling requirements are included as 'process cooling' under 'process heat', and as 'air-conditioning' over 'room heating'. It is primarily integrated into electricity demand.

## 4.1 Basis and Objectives

### ■ Basis of the Analysis

To consider renewable energy's contribution to heating supply and storage requirements, the discussion relies on the BMU's (German Federal Ministry for the Environment, Nature Conservation and Nuclear Safety) long-term scenarios [9] (just as it did in ▶ Chap. 2), as well as the Fraunhofer ISE energy scenario for all sectors. The latter describes a viable target system presented in hourly intervals and takes climate protection guidelines into account [6, 11, 12]. In addition, other studies were analyzed, such as the Fraunhofer IWES study [10].

The discussion begins with an analysis of long-term scenarios in ▶ Sects. 4.2 to 4.3. The study examined various scenarios in light of the federal government's goals. The results discussed here come from Scenario 2011 A. In this scenario, the energy generation transition process in Germany resulted in a reduction of greenhouse gas emissions by 80% between the years 1990 and 2050.

### ■ Heating Sector Goals

The German federal government has set the following basic defining goals for the heating sector:

- Reduce heating requirements by 20% between 2008 and 2020.
- Reduce primary building heating requirements by 80% between 2008 and 2050.
- Increase the share of renewable energy in the heating sector's final energy consumption by 14% by 2020.
- Increase the share of renewable energy in gross final energy consumption by 18% by 2020, 30% by 2030, 45% by 2040, and 60% by 2050.

In addition, the federal government determined that:

- CHP generation should be promoted.
- The heating requirements of new buildings should be reduced by gradually implementing zero-energy building standards.
- The renovation rate in older buildings should be increased from 1 to 2% per year by implementing the renovation roadmap.
- Existing buildings should be climate-neutral by 2050.

## 4.2 Development of Heating Requirements

In Germany, heating and cooling requirements in 2010 were about 1,430 TW h. This means

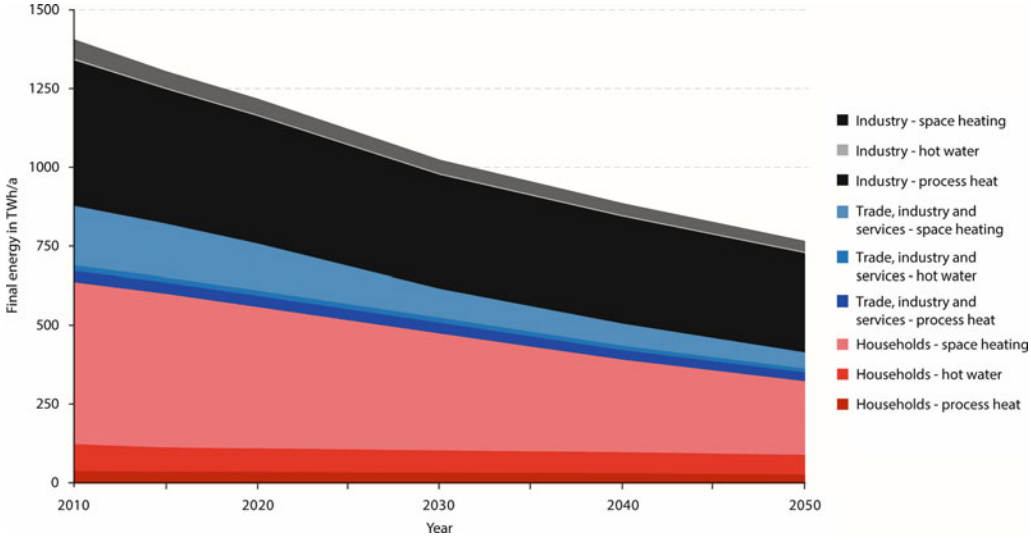



**Fig. 4.1** Development of heating requirements (final energy) from 2005 to 2050 in the household, manufacturing, and trade, industry, and services (TIS) sectors [9]

that, in comparison to the electricity and transportation sectors, the highest requirements were for this sector (▶ Sect. 3.2).

Heating demand can be generally divided among three different application areas:

- Room heating
- Hot water
- Process heat

Efficiency measures are expected to most effectively reduce heating requirements in the room heating area. This is because the average energy requirements for new buildings are below 40 kW h $m^{-2}$ $a^{-1}$. This is significantly below today's average of around 150 kW h $m^{-2}$ $a^{-1}$. In addition, better insulation will consistently reduce heating requirements in existing buildings.

Hot water requirements in contrast can only be reduced by about 25%. This is because useful energy for hot water is not expected to change in the future. Here, higher efficiency will be achieved by increasing the efficiency of generation and distribution. It is a similar for process heat. Useful energy will remain at similar levels to today, meaning final energy requirements can only be reduced by 30%. Efficiency options in this area have already been implemented. The result is that, in contrast to room heating, no reductions are expected (Fig. 4.1).

The greatest potential for reducing heating consumption by 2050 is in the TIS sector:

| | |
|---|---|
| TIS: | minus 67% |
| Households: | minus 47% |
| Manufacturing: | minus 27% |

In total, this would reduce heating requirements in Germany by 45%, with a reduction down to 780 TW h in 2050.

## 4.3 Development of the Heating Mix

### 4.3.1 Fossil Heating Supply

Today, heating supply comes almost entirely from fossil energy carriers. In this scenario, this changes to a mix of fossil and renewable energy (Fig. 4.2).

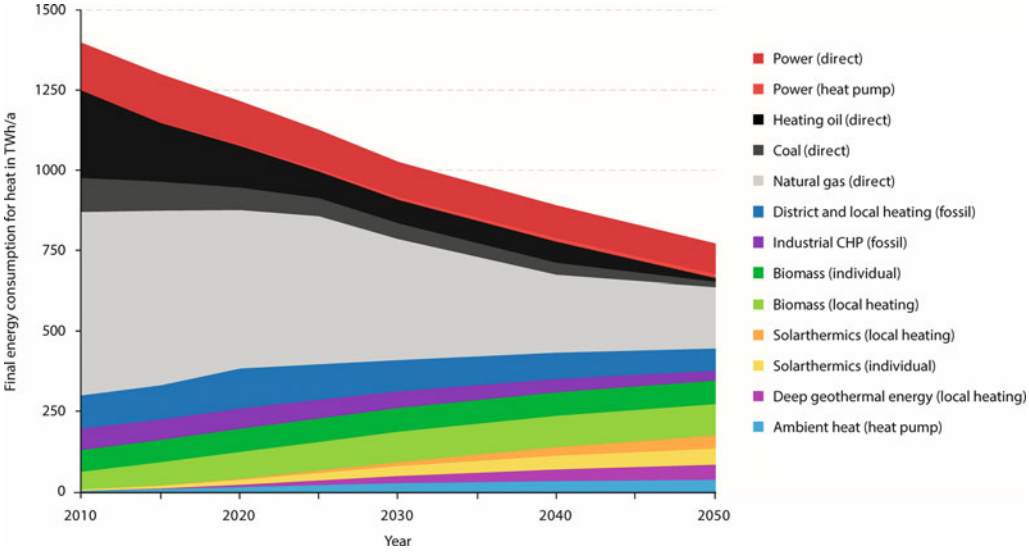



**Fig. 4.2** Final energy for heating including electricity-based heating supply (heat pumps, night storage heating). According to [9]

The fossil share of the heating mix will remain high in the future because local and district heating from CHP generation will still rely primarily on fossil energy carriers, and process heat cannot be entirely supplied by renewable energy. Technically feasible temperature-levels with solar-thermal energy, geothermal energy, and CHP waste heat are often inadequate for these purposes. In certain cases, direct heating supply using renewable electricity can be used to meet demand at even the highest temperatures. Since manufacturing will still require high temperatures, in the future natural gas consumption for process heat supply will remain at the same levels as today. Over the long-term, renewable methane from PtG facilities could be used as a natural gas substitute.

The share of direct crude oil and coal heating will fall nearly to zero, while natural gas, which is the relatively low-carbon energy carrier, will continue to be used in the future. The gas infrastructure is compatible with renewable energy and, therefore, sustainable. For the short-term, biogas can be used by applying the same methods and technologies. In the long-term, fossil gas will also be generated using PtG.

### 4.3.2 Renewable Heating Supply

The absolute renewable energy share of heating supply will triple from today's level of 136 to 366 TW h per year by 2050. Due to a low final energy demand of around 780 TW h, the relative share will increase by a factor of five from today's level of around 11% to around 50%.

As in many other countries, biomass will remain the largest source of renewable energy. Renewable raw materials will play a crucial role in individual heating and for energy communities. Wood heating systems (pellets, woodchips, logs) will be essential for the renewable energy heating supply. With natural regeneration as well as improved forest utilization and forest management, wood heating has significant potential for growth (▶ Sect. 13.2). The contribution of biogas and biogenic waste in CHP will also increase in the future. The scenario assumed increased expansion of solar collectors. Currently, photovoltaic (PV) is growing faster. In principal, solar-thermal energy and PV complement one another in heating supply. For the primary heating supply, solar-thermal facilities together with thermal storage could meet the

bulk of heating demand. Additionally, electricity surpluses from PV facilities could provide heat for existing thermal storage using heating rods and electric heat-pumps. There are, therefore, many methods of bridging the gaps between the electricity and heating sectors, by using CHP and heat pumps in particular, as these gain importance.

Individual facilities will dominate the heating supply until 2030, when adequate expansion of local and district heating networks will permit the use of all forms of renewable energy heating supply. As is typical of electricity generation, over the long-term, these network-connected facilities are expected to exceed the number of individual facilities. But since it is difficult to predict technical and cost developments here, the share of solar collectors, heat pumps, and biomass-based CHP facilities may vary from expectations.

Another factor to be considered from 2020 is the use of older, inefficient facilities, such as small biomass heating systems in particular. Until that time, installation of new facilities based on renewable energy in newly built buildings and the use of fossil fuels will be the decisive factors is decarbonizing the heating sector.

## 4.4 The Heating Sector Transition

The combination of reduced demand (▶ Sect. 4.2) and increasing renewable energy shares in the heating mix (▶ Sect. 4.3) will allow the heating sector to be completely transitioned in the household, in the TIS sectors, and in manufacturing as well.

The study 'Interaction of Renewable Energy Electricity, Heating, and Transportation' outlines the decarbonization of the heating sector by 2050, with detailed roadmaps for each sector [10]. The study describes three phases:

| | |
|---|---|
| Phase I: | reduction of system temperatures (2012–2025) |
| Phase II: | increased flexibility and heat pump expansion (2025–2035) |
| Phase III: | use of PtH and sector coupling (2035–2050) |

Using the simulation results, measures and milestone for achieving climate protection and energy goals were identified in each phase, and then briefly described for each sector.

The assumptions concerning the development of heating requirements and the heating mix are very similar to those in ▶ Sects. 4.2 and 4.3. Detailed information about the simulation methodology can be found in [10]. Led by Fraunhofer IWES in Kassel, the study was the first to examine the cost-optimized expansion of renewable energy and heating technologies. The study described this expansion in detail by year.

### 4.4.1 Households

In 2012, primary energy requirements for heating in German households amounted to 553 TW h. The potential for savings in this area is very high (▶ Sect. 4.2). Extensive renovations of existing buildings, strict requirements for new buildings, and increased ambient heat use with heat pumps could reduce primary energy requirements by around 70% by 2050.

The heating transformation will result in extensive storage potential for fluctuating electricity volumes. There are five milestones for households in this transition (◘ Fig. 4.1).

- **Reduction of System Temperatures (2012–2025)**

The first phase, 'reduction of system temperatures2', includes two milestones:

1. System temperatures are reduced in district heating networks and buildings. In addition to energetic renovation, widespread use of low-temperature heating systems such as underfloor and wall heating accelerates the use of decentralized electric heat-pumps with low system temperatures. Use of less effective direct electric heating such as night storage heating is reduced.
2. Reducing system temperatures requires greater use of heat pumps and higher annual heat pump performance factors. Since electricity is primary energy, new buildings should be outfitted exclusively with electric heat-pumps (▶ Sect. 4.5.2). In existing

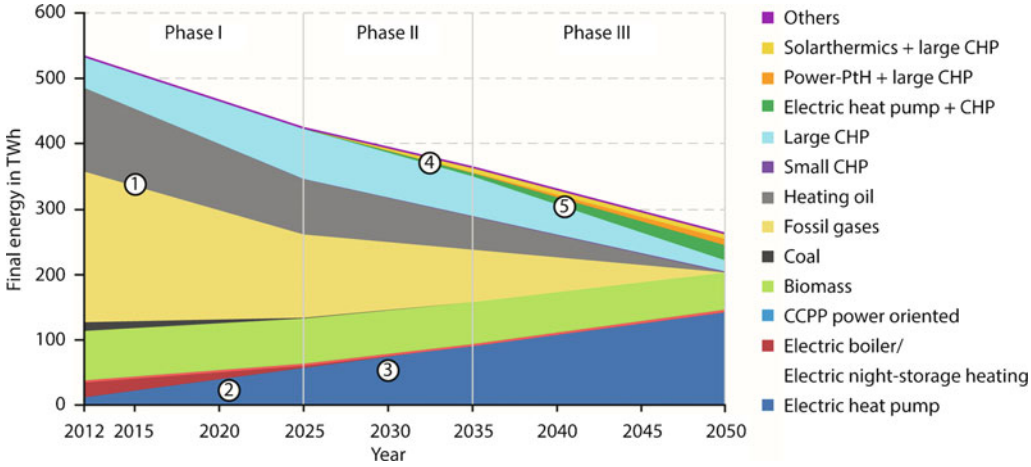



**Fig. 4.3** Transition of household sector heating requirements by 2050, phases and milestones [10]

buildings, first oil boilers and then gas-fired boilers should be replaced by heat pumps. For homes in rural areas or older buildings, woody biomass is the energy carrier of choice.

### Increased Flexibility and Heat Pump Expansion (2025–2035)

Since thermal storage is a cost-effective flexibility option, the second phase, 'increased flexibility and heat pump expansion', relies on increased flexibility in the electricity system. This phase includes the following milestones:

3. From 2025 to 2035, renewable energy expansion will require increased flexibility options. This will include thermal storage as well as hot water tanks, for example. The use of building envelopes is also essential. They allow efficient buildings to provide storage capacity for periods ranging from a day to a week.
4. The fourth milestone focuses on reducing system temperatures in district heating networks to under 80 °C. This would allow the currently dominant fossil energy carriers, natural gas and hard coal, to be replaced by large centralized electric heat-pumps, solar-thermal facilities, and large CHP primary based on renewable energy. Securing new heating sources for heat pumps such as waste water, brine, and waste heat from data centers or manufacturing areas, etc., is also essential.

### Use of PtH and Sector Coupling (2035–2050)

The introduction of energy sector coupling (▶ Chap. 14) dominates the third and last phase of heating transition in the household sector.

5. From the year 2035 to 2050 in particular, electricity surpluses will dramatically increase due to wind and solar electricity. Cheaper storage options in the heating sector will result in increased reliance on PtH using heat pumps with a performance factor above 2.5 and heating rods in district heating. This will proportionally reduce CHP utilization.

### Overall Assessment

In this scenario, after the transition in 2050, household room heating supply will be three-quarters building-dependent and one-quarter network-dependent (Fig. 4.3). Decentralized electric heat-pumps will be the primary energy suppliers, and will meet 53% of heating demand. Biomass in the form of solid biomass (wood) and gaseous biomass (biogas) will be the primary heating sector energy carrier in rural regions and for older buildings (22%).

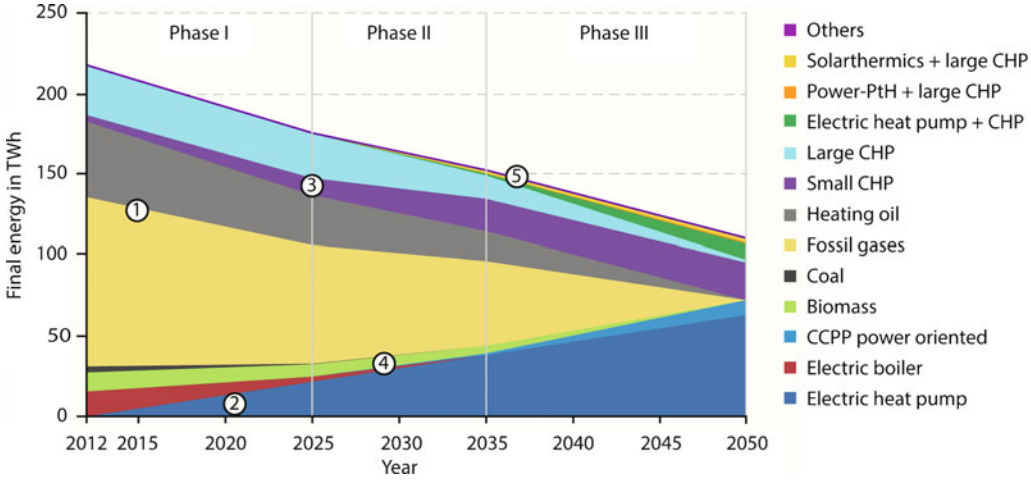



**Fig. 4.4** Transition of TIS sector heating requirements by 2050, phases and milestones [10]

Another 24% of heating will be supplied over the network using district heating with CHP, electric heat-pumps, and solar-thermal energy, as well as by a combination of CHP and electro-mobility.

The paradigm shift in the energy balance outlined in ▶ Sect. 4.5.2 produces one unexpected result. Primary energy requirements will be exceeded by room heating energy requirements. This is because the efficiency method (▶ Sect. 1.2.2) considers wind, solar, and hydropower electricity as 100% primary energy, and because heat is used from geothermal energy, water, ice storage, and air which are not considered primary energy. Electricity demand for decentralized electric heat-pumps accounts for 26% of household primary energy requirements, even though it meets over 50% of total heating demand.

## 4.4.2 TIS

The three transition phases for households also applies to non-residential buildings in the TIS sector. There are also five milestones for reducing primary energy requirements by 74%, from 236 TW h to about 60 TW h by 2050 (Fig. 4.4).

1. Low-temperature heating systems as well as heat pumps in existing buildings are crucial for eliminating oil and gas boilers in office and retail buildings.
2. Reducing flow-temperatures below 60 °C increases heat pump efficiency. Primarily brine-to-water heat pumps with performance factors above four should be used.
3. In a decentralized form, as mini CHP plants, CHP can play an important role in this sector by flexibly serving a range of heating profiles.
4. Operation of the CHP will be electricity-oriented (▶ Sect. 14.1). They will also be equipped with adequate thermal storage to still operate while decoupled from heating. In addition, surpluses from wind power in warmer periods will be integrated using flexible heat pumps with thermal storage, as well as CHP with heating rods. The use of woody biomass will be shifted to supplying older buildings in the household sector, as well as to supplying process heat in manufacturing.
5. As with households, in the last phase, the importance of PtH using heating rods increases in comparison to heat pumps in the TIS sector. District heating requirements can be adequately met using a combination of CHP and heat pumps.

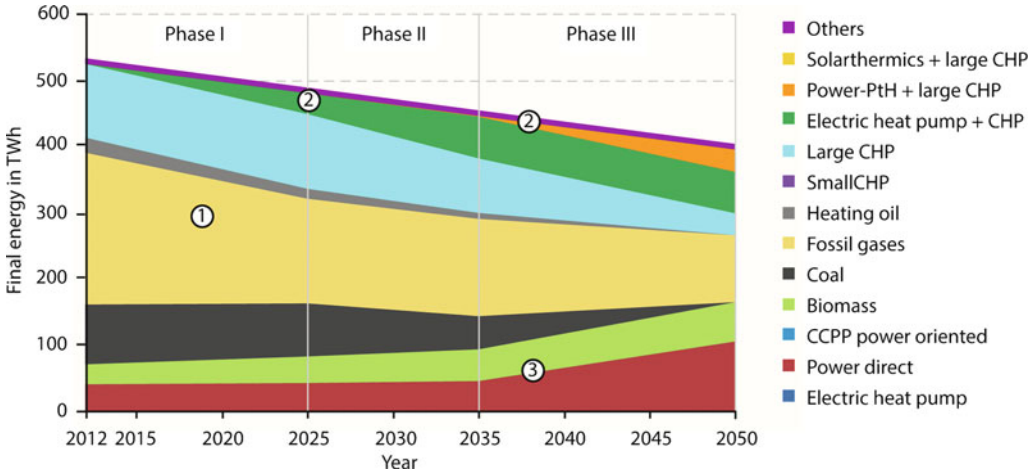



**Fig. 4.5** Transition of manufacturing sector heating requirements by 2050, phases and milestones [10]

In 2050, 57% of final energy requirements will be met using decentralized heat pumps, 21% using CHP, and 9% using district heating. Heating supply will be 86% building-dependent, and 14% network-dependent using stand-alone or heating networks.

### 4.4.3 Manufacturing

The manufacturing sector is fundamentally different from the other two sectors, because room heating is of secondary importance, and higher temperatures for process heat are essential. But with primary energy requirements of around 530 TW h per year, this sector is still a critical factor in achieving climate protection goals. By taking the following measures, primary energy requirements can be reduced (in three phases) to around 350 TW h (Fig. 4.5).

#### Improve Efficiency

In the first phase, switching technologies to improve efficiency is central.

1. Heat pumps are used for process heat at low-temperature ranges, as well as for room heating. In addition, coupled CHP use can replace direct fossil fuel combustion. This reduces coal and crude oil requirements.

#### Reduce Fossil Energy Carrier Use

The second milestone is achieved in phases two and three.

2. First, and strictly on economic grounds, direct use of electricity in electrode boilers is forced to temperatures ranging up to 500 °C. Then, starting in 2035, larger renewable energy surpluses are integrated using PtH facilities. This allows fossil energy carriers such as natural gas to be replaced to provide process heat at the upper temperature-range.

#### Increase the Use of PtH

As in the other two sectors, the third phase is primarily focused on renewable energy fluctuations and sector coupling.

3. Direct use of electricity for process heat at the upper temperature-range relying on PtH is reduced. Hot water is produced using heat pumps, and steam using large CHP power plants. Direct use of electricity in coupled with PtH-CHP or heat pump CHP is reduced together with the use of large CHP.

Starting in 2025, the use of coal for manufacturing heat can be eliminated. Natural gas can be partially replaced as well, but it will remain a significant factor until 2050, meeting

a quarter of final energy requirements. Woody biomass use will double to a share of 15%. Renewable electricity will be the primary energy carrier in manufacturing.

## 4.5 The Heating Sector Paradigm Shift



As in the electricity sector, there will be a paradigm shift in the heating sector. The use of fossil heating carriers will be dramatically reduced by 2050. At the same time, shares of renewable energy will dramatically increase. This will be the result of increased efficiency due to energetic renovation in private households, as well as more efficient use for processes in manufacturing. In addition, a large portion of fossil fuels will be replaced by renewable energy from decentralized facilities such as solar facilities, biomass heating, and heat pumps, or from network-connected facilities such as biomass, geothermal energy or solar-thermal facilities.

### 4.5.1 An Example Transition: Crude Oil, Natural Gas, and Renewable Energy

The development of coal, crude oil, and natural gas in the last century is an example of a heating energy carrier transition. In the beginning of the 20th century, particularly in urban areas, biomass was first replaced by coal, then by cheaply available crude oil. Crude oil was then replaced by natural gas in the 1960s and 1970s. Heating sector companies kept up with these changes, and are currently preparing themselves for future structural changes (Fig. 4.6).

In the past, single energy carriers were used to supply heating: first wood, then coal, then oil and gas. Today and in the future, a broader spectrum of energy carriers will be used. In addition to those already mentioned, the range will include solar-thermal energy, geothermal energy, biogas, windgas, solar gas, and all other direct and indirect uses of renewable electricity relying on PtH.

### 4.5.2 Electricity as Primary Energy

By turning renewable electricity into primary energy, the electricity system's paradigm shift will also link the electricity and heating sectors, requiring the use of storage. This will be in addition to the links that have already been established, i.e.:

- Electric heating: electricity used for process heating
- Heat storage stoves: electricity used for room heating

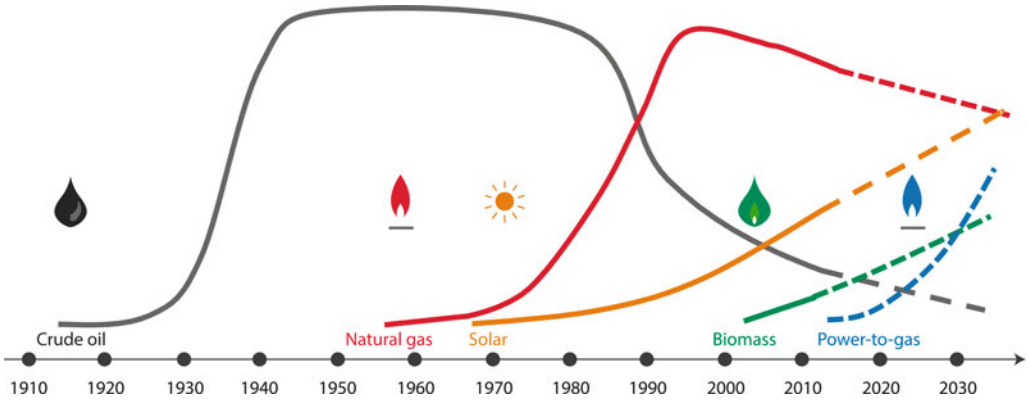



**Fig. 4.6** Structural changes in heating supply using Viessmann-Gruppe as an example [13]

- CHP generation: fossil fuels more efficiently used by coupling electricity and heating supply

Other new links will be added:

- Electric heat-pumps: electricity used to efficiency supply ambient heat from the air, the ground, or liquids in combination with heat and cold storage
- PtH: electricity surpluses used in heating networks and thermal storage by means of electric resistance heaters and electric heat-pumps
- PtG: electricity in the form of gas used in the heating sector (primarily process heating), in gas heat pumps, and in CHP.

Seamlessly merging the electricity and heating sectors together will have significant effects on storage requirements in the electricity sector (▶ Chap. 3), offer enormous potential for integrating renewable energy (▶ Sect. 14.1), and provide a conveniently economical option for energy generation design (▶ Chaps. 10 and 11). The following section of this chapter explores this paradigm shift in-depth. In addition, it provides a 'heating transition roadmap' for all heating sectors including storage requirements.

**PtH**

PtH is an energy system that directly or indirectly generates heat from electricity with optional use of thermal storage, thereby linking the electricity and heating sectors. Direct use with electric resistance heating (heating rods, boilers, electro-boilers) is generally distinguished from indirect use with electric heat-pumps (hot water heat pumps, heat pumps for heating or cooling, high-capacity heat pumps).

In combination with thermal storage, both kinds of use offer potential for storing renewable energy surpluses, as well as for providing cost-effective flexibility to the electricity sector by linking the heating sector to other sectors.

## 4.6 Storage Requirements in a Climate Goal Scenario for the German Energy System in 2050

In addition to the studies on storage requirements within a purely renewable energy electricity sector (▶ Chap. 3), the Fraunhofer ISE study, 'The German energy system in 2050', quantified electricity sector storage requirements as well as heating sector storage requirements, with full implementation of linking the electricity and heating sectors [7].

This ongoing study examined installed renewable energy technology at a similar cost and scale to the UBA and the VDE storage studies reviewed in ▶ Chap. 3. It included research into a German energy system with a majority share of renewable energy. The study used an hourly time grid and real weather data to determine storage requirements for electricity and heating [6, 7, 11, 12].

### 4.6.1 Scenario Framework, Model, and Assumptions

The REMod-D model assumes cost-based optimization across the entire German energy system, with a particular focus on the electricity and heating system in 2050. The model's goal is to reduce total energy-driven $CO_2$ emissions by 85% in comparison to 1990, as well as to minimize total costs for all components. The model includes the following components, each at a share determined by the optimization.

- **Generation:**
  - Renewable sources:
    - PV
    - Wind on land
    - Wind at sea
    - Hydropower (not part of the optimization since potential is very limited)
    - Biogas
    - Solar-thermal energy
    - Remaining conventional steam power-plants (brown and hard coal). This is not

part of the optimization, but is based on remaining power plants set at fixed levels based on the power plant decommissioning schedule
- Discharging from gas storage:
  - Gas and steam power plants
  - Centralized CHP plants
  - Decentralized district heating plants (DHP)
  - Gas heat pumps
  - Gas-fired condensing boilers

- **Storage:**
  - Battery storage
  - Gas storage (hydrogen, natural, and synthetic methane)
  - Pumped-storage (not part of the optimization but set at fixed levels since potential is very limited)
  - Centralized thermal storage
  - Decentralized thermal storage

- **Consumption:**
  - Electricity
  - Low-temperature heating (room heating, hot water)
  - Fuels for processes in trade and manufacturing
  - Transportation

Unlike the electricity sector studies, the ISE study accounts for all parameters relevant to the heating sector, such as the level of energetic renovation in existing buildings or thermal storage capacity. The study calculated results for various versions to define a system that would meet German climate protection goals while still keeping the use of fossil energy carriers at low levels. Energetic building renovation reduced existing building heating consumption by 50% in comparison with today's levels.

Installed renewable energy capacity included 168 GW from wind energy facilities on land and 33 GW from those at sea, and required an installed PV facility capacity of 166 GW.

In addition, the results indicated that electric heat-pumps would be the dominant technology for supplying low-temperature heating. This is because heat pumps are the most efficient system for heating supply. It is also because they provide negative balancing power, i.e., they can absorb electricity surpluses flexibly over time. This makes them particularly useful for linking the electricity and heating sectors. They can be even more useful here if used in combination with thermal storage, allowing electricity-oriented operation (▶ Sect. 14.1).

### 4.6.2 Results for Storage Use in the Heating Area

In the selected climate goal scenario with a total reduction of energy-driven $CO_2$ emissions of 85% compared to 1990, installed wind and PV capacity was so high that surpluses were adequate for PtG operation producing renewable gas (▶ Chap. 8). In addition, electricity surpluses were stored in thermal storage using load-management and PtH.

The total annual costs for this energy system were determined to be about 200 billion euros. These costs are roughly the same as the costs of today's energy system, based on fossil energy carriers which cost around 220 billion euros. Figure 4.7 shows the climate goal scenario simulation results for generation, storage use, and consumption.

Heating sector storage requirements here can be divided between large centralized thermal storage, smaller decentralized thermal storage, and gas storage for methane.

#### Centralized Thermal Storage

Centralized thermal storage with a storage capacity of 641 GW h was required. Centralized thermal storage was charged with 15 TW h per year from electricity surpluses using PtH, and with 43 TW h per year using centralized CHP, large heat pumps in heating networks, or centralized solar-thermal facilities. Storage-discharging supplied 45 TW h per year to cover heating load. The rest became storage and network losses.

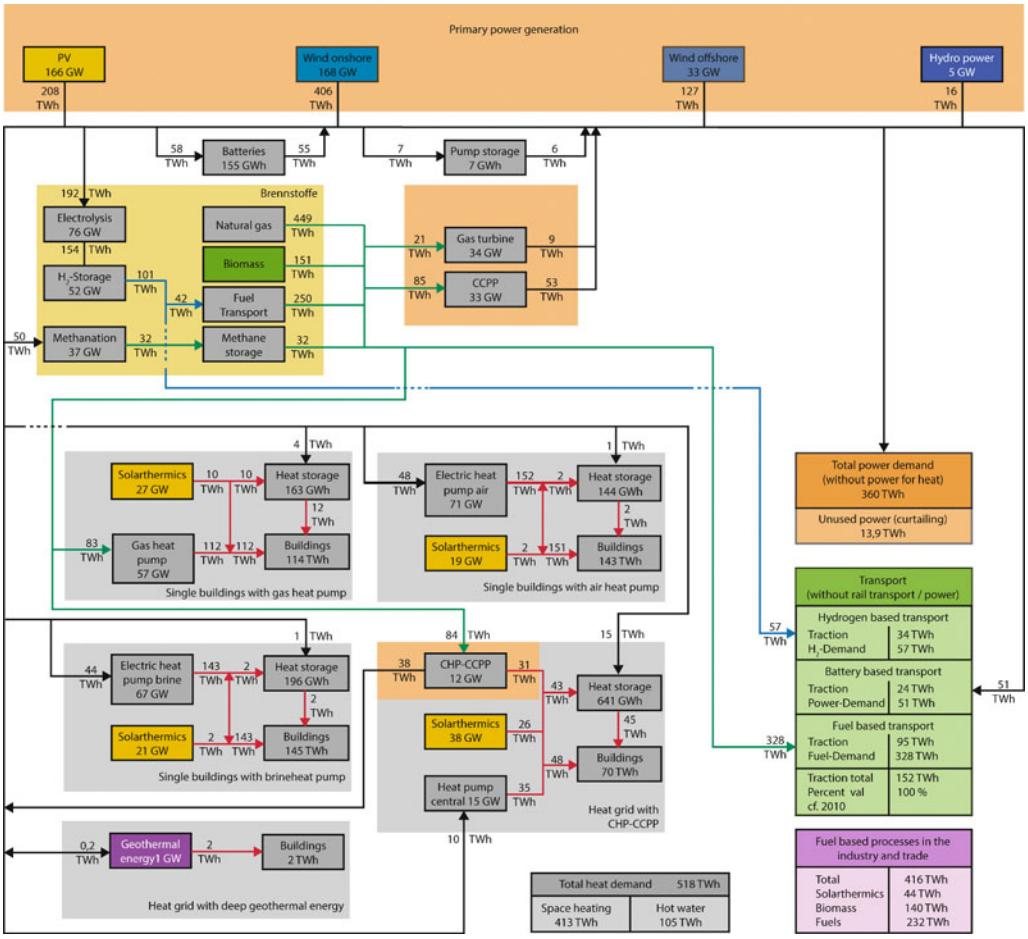



**Fig. 4.7** Results of the climate goal scenario for Germany's energy system in 2050. In addition to battery and pumped-storage, gas storage was required for renewable methane. Thermal storage was essential to meet climate protection goals. It was charged with flexible CHP, heat pumps, solar-thermal energy, and PtH (electric heaters) [7]

## Decentralized Thermal Storage

Electric heat-pumps, gas-fired facilities, and smaller solar-thermal facilities combined with decentralized storage covered heating load for buildings not served by heating networks. Thermal storage was essential here, because electric heat-pumps balanced renewable energy electricity surpluses. This means that their operation was not demand-driven, but as far as possible, was supply-driven; that is, it was electricity-oriented.

Solar-thermal facilities require thermal storage right from the start. In contrast, gas heat pumps or gas-fired condensing boilers fed with biogas, windgas, or solar gas can be used as required, and as a result do not feed into decentralized thermal storage.

Like centralized thermal storage, decentralized thermal storage also absorbs electricity surpluses using PtH. As a result, total decentralized thermal storage charging amounted to 20 TW h per year, with 16 TW h per year discharged to cover heating load. The remaining energy was provided by the relevant heating technologies, and proportionally by solar energy.

## Gas Storage—Methane Storage

The third type of storage used in the heating sector in this study was methane storage. In

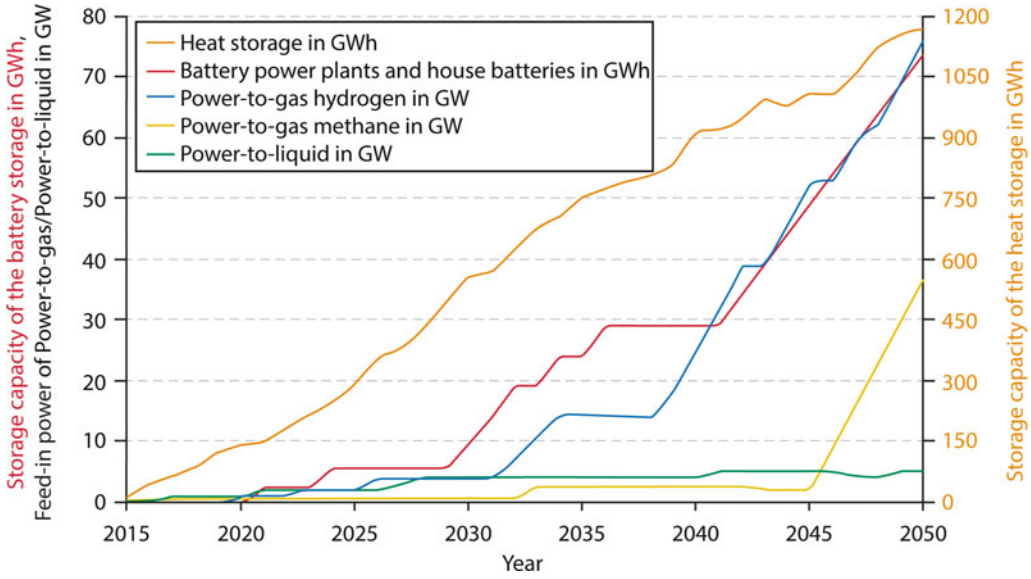



**Fig. 4.8** Development of various storage technologies by 2050 according to a climate goal scenario. The greatest storage requirements are for thermal storage used as short-term storage, followed by stationary battery storage, PtG (hydrogen, methane), and PtL. This demonstrates that thermal storage will be vital to the energy transition process [5]

addition to the gas infrastructure already in existence today, the model also calculated storage capacity for methane with PtG facilities. This gas storage was required for both the electricity and heating sectors, and was filled with windgas and solar gas.

Total PtG facility feed-in amounted to 32 TW h per year, requiring a storage capacity of 12 TW h. This amounts to 4.2% of the 280 TW h of gas storage capacity available today. The existing gas infrastructure was used to discharge the storage, meaning that gas was used in both the electricity and heating sectors.

### Dependence of PtG as Well as Gas Storage Requirements on $CO_2$ Goals

Another key result was that requirements for windgas and solar gas used in the system as long-term storage depended heavily on energy-driven $CO_2$ emissions goals.

When $CO_2$ emissions were reduced by 80% compared to the reference year (1990), the electricity and heating sectors required only small quantities of synthetic fuels. These fuels were, however, still necessary for individual motorized transport.

But together with biomass and existing fossil energy-carriers, there were still adequate fuels available for the energy system to supply electricity and heating, complementing fluctuating renewable energy. This changed if energy-driven $CO_2$ emission reduction goals were set higher.

### Necessity of PtG at a National Level with $CO_2$-Emissions Reduction Goals of 85% and Above

With $CO_2$ emissions reduction goals of 85% and above—at least at a purely national level—the transition from wind and solar energy to synthetic energy carriers using PtG was vital to meet demand in all consumption sectors at all times.

This means that the required installed charging power for PtG increased at a disproportionate rate with the demand for synthetic fuels. This is because these conversion chains are associated with comparably low efficiency levels (Fig. 4.8).

**Table 4.1** Overview of storage requirements and storage use in the heating sector with an energy system based on an 85% reduction in $CO_2$ emissions in Germany (PtH; PtG) [6, 7, 11, 12]

| | Centralized thermal storage | Decentralized thermal storage | Gas storage ($H_2$ and $CH_4$) |
|---|---|---|---|
| Storage capacity | 25 million $m^3$ water | Around 8 million 800 liter units | 12 TW h |
| Total charging | 58 TW h/year | 20 TW h/year | 154 ($H_2$) and 32 ($CH_4$) TW h/year |
| Electricity surpluses | 15 TW h/year (PtH) | 6 TW h/year (PtH) | 186 TW h/year (PtG) |
| Centralized CHP plus heat pumps and centralized solar-thermal energy | 43 TW h/year | – | – |
| Decentralized electric heat-pumps with solar-thermal energy | – | 4 TW h/year | – |
| Decentralized solar-thermal energy with gas heat pump facilities | – | 10 TW h/year | – |
| Biomass | – | – | 335 TW h/year |
| Discharging (heating sector only) | 45 TW h/year | 16 TW h/year | 167 TW h/year (including fossil gas) |
| Gas heat pumps | – | – | 83 TW h/year |
| CHP | – | – | 84 TW h/year |

#### Table Overview of Storage Requirements in the Heating Sector

Table 4.1 gives an overview of the results of the 85% scenario for storage requirements and storage use. It shows storage capacity requirements for a system based primarily on renewable energy, as well as quantities of energy charged and discharged per year.

#### Development of Thermal Storage Requirements

Figure 4.8 shows the development of thermal storage compared to other energy storage options such as battery storage, PtG (hydrogen, methane), and power-to-liquid (PtL).

The development demonstrates that thermal storage used as short-term storage could be an essential component of a successful and cost-effective energy transition. This form of storage, as well as stationary battery storage, will be in demand as short-term storage. PtG with hydrogen then becomes essential in the medium-term. In the final phase of the transformation, beginning in 2040, PtG with methane will also be in high demand. There is also a growing, yet relatively constant, demand for PtL for long-distance transportation (aviation, shipping, etc.) (▶ Chap. 5).

But overall, thermal storage will have the greatest importance among energy storage options. In the scenario year 2050, its storage capacity exceeded that of battery storage or PtG by a factor of 15.

## 4.7 Surpluses, Storage Requirements, and Storage Potential

### 4.7.1 Heating Sector Surpluses

Electricity sector surpluses are different from heating sector surpluses. Use of PV and wind obviously results in electricity surpluses, and these have been recognized as a challenge. But

surpluses in the heating sector have not been adequately considered. The energy carrier for heating is usually stored solar energy in the form of oil, coal, gas, or biomass.

### Solar Energy Surpluses

Current renewable energy surpluses result almost exclusively from solar-thermal energy in times when thermal storage is full. On days with high solar radiation and little heating demand—i.e., primarily in summer—solar circuits in solar facilities come to a standstill once storage is full. As a result, the temperature of the heat-carrying liquid in the collector rises dramatically to around 200 °C, causing it to vaporize. The medium's volume therefore expands, thus increasing pressure. The pressure is then absorbed by a membrane expansion vessel (MEV) to protect the solar facility from damage. As solar radiation decreases, temperatures in the collector falls, and the gas condenses. The result is that pressure as well as temperatures in the facility fall. So this mechanism protects against damage, but surpluses are neither stored nor used. One solution to this problem would be to use thermal storage at a large scale, such as for ice storage, to store heat in the phase-change of water using solidification and melting energy. Another option would be to devise a method to feed the heat into the heating network. This could also function as a buffer (▶ Chap. 10).

### Surpluses from Electricity-Oriented CHP and Biogas Production

Most biogas facilities generate electricity on-site from the gas they produce. The heat generated from this process is rarely used, and as a result, released into the atmosphere. This is typically because there is no demand for heat on-site; i.e., no heat-sink. Even if there is demand in winter, in summer the heat cannot be used. Seasonal-thermal storage could, in principal, fill these temporal gaps in demand (▶ Chap. 10). Another option is to distribute the energy over energy networks: either by feeding the heat into heating networks for distribution, or by producing biogas to feed into the gas network for distribution. The biogas could alternatively also be put in gas storage. Ideally biogas should be reconverted to electricity in DCHP using heat.

Another solution to the heat-sink problem on-site is to use micro-gas connections to carry raw biogas to satellite CHP. Located several kilometers away from the biogas facilities, these CHP would then feed the heat into larger heat-sinks or the heating network. Pilot projects exploring mobile latent-heat storage are also currently underway. Here, trucks are used to transport biogas heat to heat-sinks [2].

Facilities that produce electricity from conventional gas or solid fuels such as wood or coal could follow the example of biogas facilities. In the industrial CHP area some CHP are purely 'electricity-oriented', partially due to electricity generation incentives. These CHP either cool heat down over time or feed it into a heating network. One common way to increase energy efficiency is to use a portion of CHP waste heat—or industrial process waste heat in general—at suitable temperatures to generate electricity again.

### Use of Surpluses from Nuclear and Coal Power Plants

CHP generation has never been used to exploit waste heat from nuclear power plants. This is because the quantities of heat involved are very large, and because they occur in locations where there is no suitable heating demand. For a variety of reasons, such as lack of public acceptance, district heating networks have also never been used at nuclear power plants.

Instead, starting in the 1960s to 1980s, an early form of linking between the electricity and heating sectors was implemented to improve nuclear power plant capacity utilization: night storage heating. This significantly increased power plant and network utilization during the night. Figure 4.9 shows the development of normalized electricity consumption over the period of a day. In France, a similar approach resulted in a heavily electricity-based heating supply. In Belgium, the approach was used to illuminate expressways at night.

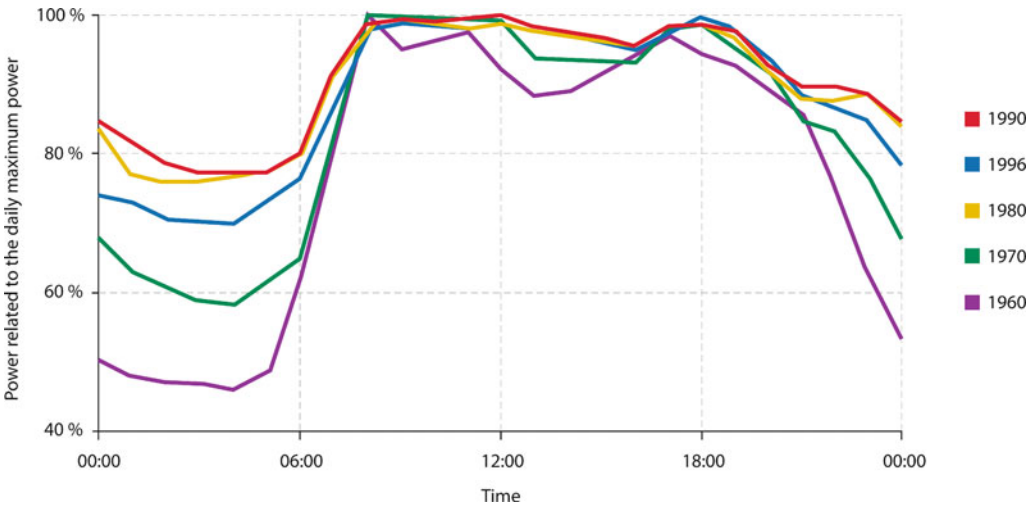



**Fig. 4.9** Development of the normalized daily load-profile in Germany from 1960 to 1996

The goal in each of these cases was to integrate 'electricity surpluses' from fossil and nuclear electricity generation. For this reason, there are still negative connotations associated with night storage heating. From a technical point of view, existing night storage heating in households and TIS with an installed capacity of around 35 GW offers the most load-management potential in Germany (▶ Sect. 3.1 and ▶ Chap. 11).

## 4.7.2 Development of Storage Requirements

### Storage Requirements for Crude Oil, Coal, and Gas

With less crude oil and coal heating, fuel storage tank requirements for heating supply will decline as well. Table 4.2 shows the anticipated development of various heating carriers from 2010 to 2050 [9]. Use of crude oil and coal will decline the most, but natural gas will decline significantly as well. As a result, the market for oil and coal storage will be smaller. Gas storage remains a significant factor because it is required by CHP, and because it is compatible with renewable gas (biogas, windgas, solar gas).

### Storage Requirements for Linking Electricity and Heating: CHP

If CHP heating is not located at the same place as heating demand, then heating networks are required. If CHP heating and heating demand do not occur at the same time, then thermal storage is required.

Heating networks alone provide a certain buffer. But temperature changes tend to increase heating network maintenance costs. As a result, public utilities irregularly and only partially exploit the network buffer capacities of one to two hours.

As CHP flexibility increases, thermal storage for CHP becomes increasingly essential. This is because CHP flexibility requires transitioning from previously standard heat-oriented operations, to electricity-oriented operations decoupled from heating. The options here include sensible and latent-heat storage. Storage capacity is often limited by location availability and cost efficiency. Storage design also varies depending on location and other individual factors [4]. Thermal storage is essential; particularly with very high CHP heating capacity use in relation to annual peak-load in the heating network. In these cases, greater available flexibility could exhaust even extensive storage potential. Due to these uncertainties in technical

**Table 4.2** Development of fossil energy and CHP demand in the heating sector [9]

| TW h | 2010 | 2020 | 2030 | 2050 |
|---|---|---|---|---|
| Gases (manufacturing/process gas) | 583 | 504 | 385 | 81 |
| Crude oil | 277 | 132 | 74 | 13 |
| Coal | 107 | 69 | 49 | 14 |
| CHP | 106 | 127 | 99 | 70 |
| Manufacturing CHP | 68 | 64 | 52 | 30 |



design and case-by-case cost efficiency, it is difficult to predict specific CHP storage requirements apart from general trends (Table 4.2).

### Storage Requirements for Linking Electricity and Heating: PtH and Electric Heat-Pumps

The use of electricity is differentiated by its application.

PtH (for example, heating rods, electro-boilers, resistance heating, large heat pumps) is defined as an electric heat generator in a bivalent or hybrid system containing at least one heat generator based on a chemical energy carrier.

This means that monovalent electric heat generators such as night storage heating or decentralized electric heat-pumps are not defined as PtH. PtH provides essential flexibility for CHP. But combined with storage, it may further reduce CHP utilization, and therefore compete with CHP. Depending on the overall system's cost efficiency, it may be appropriate to design thermal storage, either for PtH or as a CHP facility. For process heat at high temperatures, currently no storage is used for CHP or PtH. From a technical point of view, it is currently not required to supplement existing thermal inertia in the heating system. In the future, however, it may become essential (▶ Chap. 11 and ▶ Sect. 14.1).

Existing buffer storage already typically offers adequate capacity for the use of PtH in the household area. Even if PtH here requires no additional storage, thermal storage in combination with a relatively cost-efficient, oversized PtH capacity could still be used over the long-term to integrate feed-in peaks from wind and PV, and to improve the relationship between PtH and PtG. Figures 4.15 and 4.16 show precise numbers for charging power in the GW range, as well as feed-in durations (around one to six hours) from thermal storage for PtH.

Because it requires a heat exchanger, thermal storage for monovalent electric heat-pumps results in efficiency losses. This is in contrast to exclusive use of underfloor heating or building mass. Because of the coefficient of performance (COP, see ▶ Sect. 8.5), to use this flexibility option, very large amounts of storage in comparison to the volume of electricity that can be shifted are required. The specific dimensions would be determined by individual economic factors. In the area of proprietary electricity generation using PV, there is an incentive to considerably increase thermal storage temperatures. Although higher temperature gradients result in reduced storage efficiency, increased shares of proprietary electricity could also result. Different outcomes could be achieved by modifying the legal framework for proprietary electricity generation. In the night storage heating area, thermal storage capacity in existing facilities is adequate. Unlike heat pumps, at a suitable scale, its 100% efficiency makes it a viable option for electricity loads as well.

### Storage Requirements for Solar Facilities

Thermal storage requirements for solar facilities are difficult to quantify. One factor is solar-thermal energy expansion. In Ger-

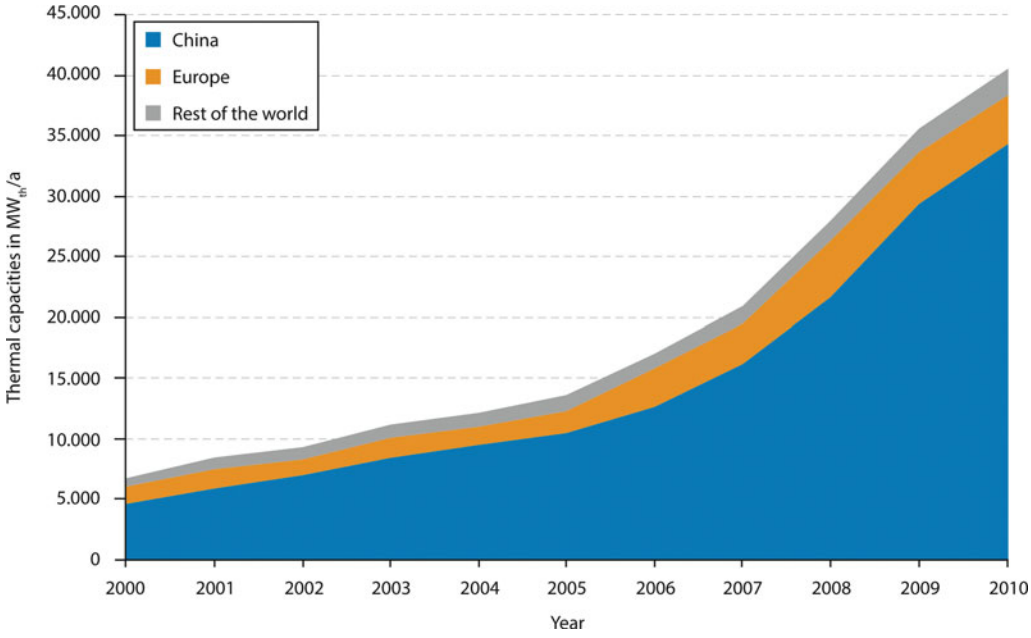



**Fig. 4.10** Global annual solar collector expansion from 2000 to 2010. According to [14]

many the annual expansion rate has dropped in recent years, while in Asia the market is growing (Fig. 4.10). Solar-thermal energy expansion in Germany will lead to a small increase in thermal storage requirements in the area of hot water generation, but to a large increase in thermal storage requirements in the area of heating support. Network-connected systems closely resembling Danish heating networks are a promising option for the future. But for solar-thermal energy in particular, large seasonal storage is crucial (▶ Chap. 10). In contrast to Asia where many new systems are being installed, future market developments in Germany remain uncertain.

An IEA scenario foresees growth by a factor of ten in the solar facility market by 2050 (Fig. 4.11). In addition to solar energy for room heating and hot water, applications for low-caloric process heat and cooling (solar cooling; for example, using ice storage) will gain in importance [8]. Storage requirements will grow at a similar rate as solar facility expansion in all segments except process heat.

### 4.7.3 Storage Potential

Unlike electricity which is easily transported and distributed, heat supply in the heating sector is usually locally limited and coupled with storage, or at least with the thermal mass of the heating system and with heating distribution. This is because generation and consumption are slower than with electricity, and because heat distribution is limited by heat loss. The following discussion examines storage potential in heating sector supply using renewable energy.

#### ▪ Sensible-Heat Storage System Potential

Existing sensible-heat storage systems in individual buildings are usually combined with a boiler. Their primary function is to prevent frequent burner cycling. Except in the case of PtH with PV, these storage volumes are practically irrelevant when considering intermediate storage for renewable energy. In addition, sensible-heat storage systems are used with thermal solar facilities. Storage in single-

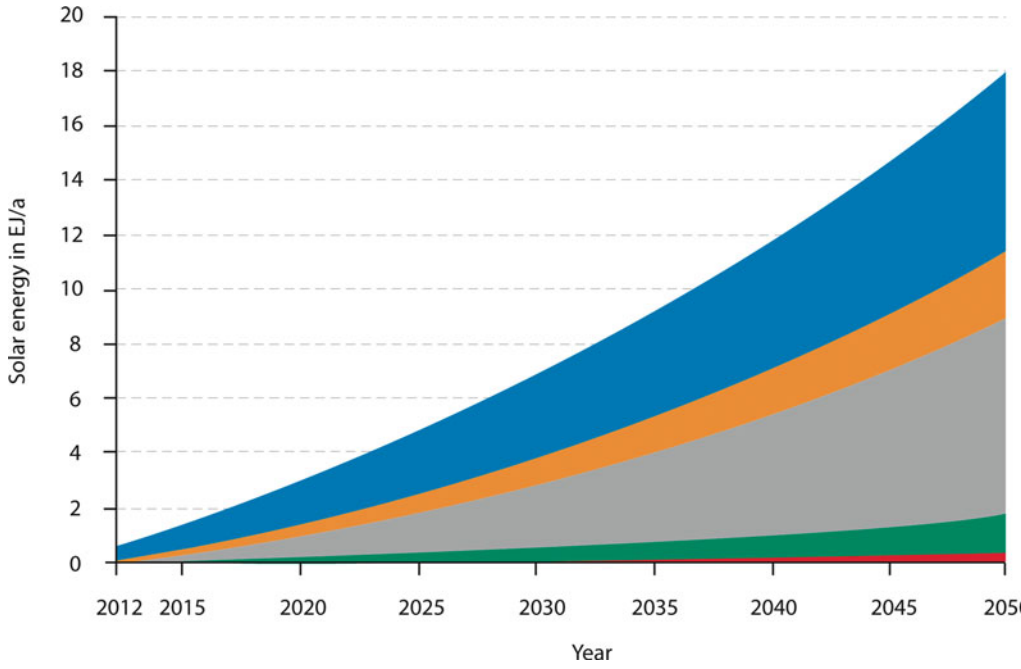



**Fig. 4.11** IEA roadmap for solar facility or thermal storage expansion [8]

family houses typically range from around 200 liters for facilities purely used for hot water, to between one and two $m^3$ of water for solar-thermal facilities used for both hot water and heating support. Combined with heat pumps, this type of storage could be increasingly important in the future. This is because it would permit electricity-oriented heat pump operation.

Large thermal storage systems are still uncommon in heating networks in Germany. However, the 2012 CHP law provides incentives for expanding storage in district heating networks in Germany.

**Example**

The Mannheim power plant is an example of district-heating storage. The power plant has a steel water tank with the following parameters:

- Height 36 m
- Diameter 40 m
- Storage volume 43,000 $m^3$, heatable to 98 °C
- Storage capacity 1,500 MW h
- Charging and discharging capacity 250 MW

This storage provides both electricity generation flexibility and heating in combination with the Rhine-Neckar area district heating network.

With very large storage volumes, depressurized thermal storage (under 100 °C) is more economical. A more expensive option with temperatures up to 130 °C is hydraulic integration into German heating networks. Pressurized storage (above 100 °C, cascaded coupling with metal cylinders) offers more freedom from a technical point of view. But it is significantly more expensive, and therefore limited in total volume.

**Example**

Currently in Denmark—with heating network temperatures significantly below 100 °C—there is considerable expansion of large thermal storage facilities with quantities of water ranging from 1,000 $m^3$ to over 100,000 $m^3$ in storage volume. Some are designed as deep ponds. These storage systems are linked to heating networks, allowing flexible charging—depending on elec-

tricity prices—with heat from CHP facilities, heat from large electric heat-pumps operated by low-cost electricity surpluses from wind energy, or heat from large solar-thermal facilities.

Building mass can also function basically as a kind of sensible-heat storage system (▶ Chap. 10). By increasing temperatures by 1–2 °C, this potential can be exploited with acceptable losses and no reduction in comfort. The economic potential here is especially significant for decentralized applications such as electric heat-pumps, or mini and micro-CHP.

### Latent and Thermochemical Heat Storage Potential

Latent-heat storage's advantage is that it can charge and discharge heat at a constant temperature. With thermochemical heat storage, heat can be stored over long time periods with practically no loss. Both storage technologies are currently used primarily for special applications, and are not a significant factor for storing large quantities of energy in the energy system (▶ Chap. 11).

In the form of phase-change materials (PCM) integrated into building mass, latent-heat storage could potentially be used to heat or cool rooms in the future. Combined with air-conditioners, it could function as storage for fluctuating electricity volumes using load-management without compromising comfort. Another form of latent-heat storage is ice storage. Here, cooling from melting is used to thermally charge the storage and heat from freezing is used to discharge it. The technologies used for charging and discharging are heat exchanges in combination with heat pumps and solar collectors.

If cost-effective systems are developed, thermochemical storage could also be used for long-term storage in buildings—for example in combination with solar-thermal facilities. But due to the large investment costs and low cycle numbers, further research and development is required to ensure cost efficiency.

### PtG, Gas Storage, and CHP or Gas Heat Pump Potential

The form of heat storage used most commonly today is closely linked with the main heating energy carrier: natural-gas storage. Caverns and porous storage systems can store biogas, windgas, or solar gas, and have enough capacity to hold about a sixth of Germany's annual heating demand: 217 TW h of chemically stored energy compared to 1,430 TW h of thermal energy demand (▶ Sects. 3.3 and 8.4). CHP or gas heat pumps are used to discharge gas storage.

### Potential of PtH Depending on the Penetration of Electric Heat-Pumps

PtH could play a significant role in linking the electricity and heating sectors. As a result, detailed temporally resolved heat load-profiles are required to quantitatively estimate storage potential. ◘ Figure 4.12 shows forecast heat load-profiles for the year 2050 from studies conducted by IWES Fraunhofer in Kassel [10]. The forecasts also used the BMU long-term scenarios [9] to predict development of heating demand (▶ Sect. 3.2).

PtH, when used as a bivalent element in a hybrid system, allows thermal storage to integrate renewable energy electricity surpluses. Storage of electricity and heat using this bivalent storage method is valuable because these facilities can provide negative as well as positive balancing capacity over the short-term. PtH facilities contribute to positive balancing power by exiting the network when renewable energy electricity feed-in is low, and providing electricity when there are shortages. Another option is to start up CHP facilities, provide balancing power by feeding in electricity, and store heat in bivalent thermal storage.

Theoretically, the heat load-profiles considered in ◘ Fig. 4.12 result in a very large potential capacity for PtH, ranging from about 200 GW in winter, to about 50 GW in summer. Due to low investment costs of about 100 €/KW, PtH is especially useful for exploiting high generation peaks occurring in rela-

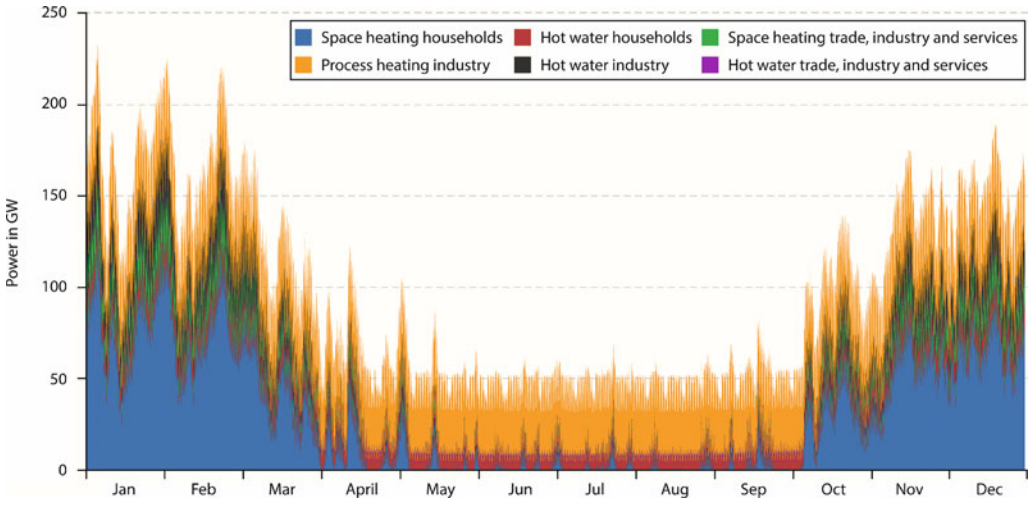



**Fig. 4.12** Heat load-profiles over all sectors in the year 2050 according to the 2012 BMU long-term scenarios [3]

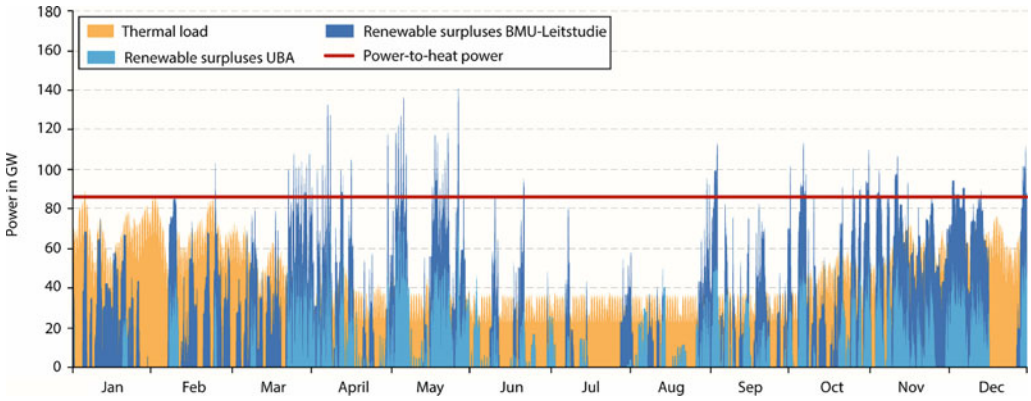



**Fig. 4.13** Heating load and PtH capacity in the optimistic scenario for 2050 compared to electricity surpluses from the 2010 BMU long-term scenarios and the UBA study [3]

tively few hours annually. But the use of PtH only makes sense in bivalent heating systems because, at lower temperature-ranges, significantly more efficient alternatives such as electric heat-pumps are available. As shares of renewable energy in the electricity mix rise, these alternatives become increasingly important.

The German Heat Pump Association's 2011 industry forecast predicts the development of the heat pump market until 2030 in conservative and optimistic scenarios [1]. The conservative scenario assumes delayed modernization in the areas of building renovation and heating system renewal. This resulted in high heating loads. The optimistic scenario, in contrast, assumes that heating modernization will accelerate and that renovation rates will increase. Fraunhofer IWES extended both developments until 2050, so that in the optimistic scenario, around 50% of heating demand in the hot water and heating areas for households and trade was met by decentralized electric heat-pumps. By comparison, this figure was only around 12% in the conservative scenario. In addition, large heat pumps were used in the district heating network instead of electro-boilers in the opti-

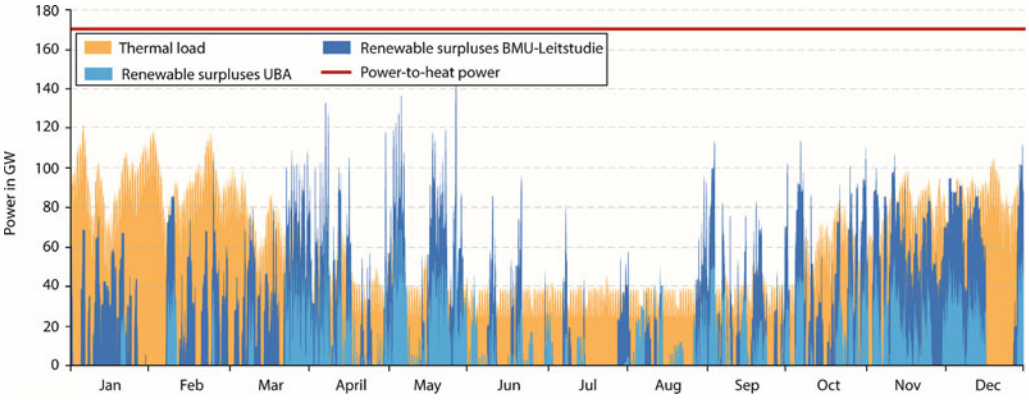



**Fig. 4.14** Heating load and PtH capacity in the conservative scenario for 2050 compared to electricity surpluses from the 2010 BMU long-term scenarios and the UBA study [3]

mistic scenario. In summer, a sensitivity analysis showed that solar-thermal energy used for process heat below 100 °C, room heating and hot water could further reduce the potential of PtH. The rest of the discussion concerns the optimistic scenario.

Figure 4.13 shows renewable energy surpluses from the studies presented in ▶ Chap. 3 (the 2010 BMU long-term scenarios; the scenario with full renewable energy supply for electricity, heating, and transportation, and the UBA study with 100% heat pumps and nearly passive house standards), as well as the heating load from the optimistic scenario for 2050. As discussed in the study by Fraunhofer IWES, with a relatively low share of heat pumps in the year 2050 in the heating sector, PtH's potential capacity was 169 GW in winter (including heat pumps). This was based on the highest heating load to ensure supply security, with decentralized heating rods used as buffer storage. But the highest heating load would not be required simultaneously in all locations in Germany. Also, in the conservative scenario many heating systems that could integrate large PtH capacities remained.

Electricity surpluses, heating load, and PtH capacity for the conservative scenario are also illustrated in Fig. 4.14. With a large share of heat pumps (in district heating as well) and consequently high buffer storage use, PtH's potential capacity was 86 GW (including heat pumps) [3].

Almost without exception, PtH was capable of integrating all electricity surpluses. Exhausting this potential depends on the margin conditions of electricity market design, alternative renewable energy heating sources such as electric heat-pumps or solar-thermal energy, and the development of building renovation. In combination with PtH as an element of bivalent heating, thermal storage will also play an essential role by absorbing electricity surpluses.

Figures 4.15 and 4.16 show the contribution of PtH as a bivalent heating element combined with various heating technologies and decentralized heat pumps in various heating sectors. The figures show the results of the optimistic scenario for typical low heating load situations (summer nights), as well as for typical high heating load situations (winter days).

If large numbers of solar-thermal energy facilities in Germany are taken into account, then regardless of installed heating capacity, PtH potential was 38 GW in summer when used as a bivalent heating element. Assuming representative levels of storage for the individual application areas in 2050, then 69 GW h or 0.07 TW h of electricity capacity could still be stored or after deducting solar-thermal feed-in 184 GW h or 0.18 TW h. This application of PtH allowed a large portion of energy to be im-

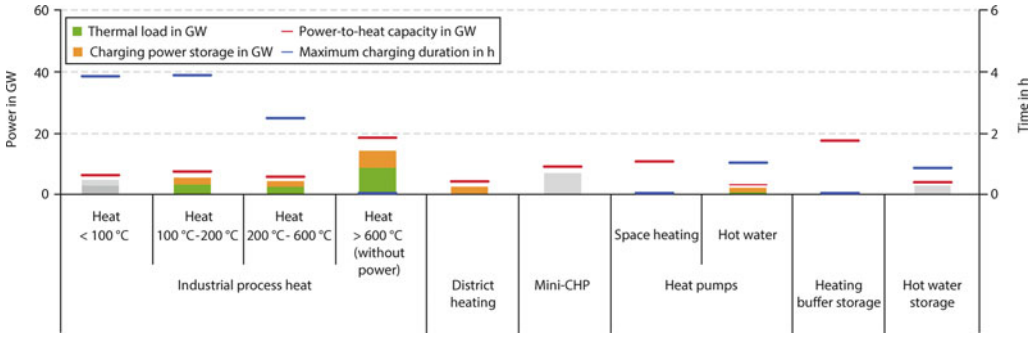



**Fig. 4.15** Heating load, thermal storage charging capacity, PtH capacity, and maximum charging durations in the optimistic scenario for typical low heating load situations (summer nights) in 2050. The parameters were: direct potential heating load supply using PtH without storage (*blue bars*, average over 12 hours), required thermal storage charging capacity for PtH (*red bars*, average over 12 hours), installed PtH charging capacity (*green points*), and maximum thermal storage charging duration using PtH in relation to the *red bars* (*yellow points*). If heating load was met with solar-thermal energy, then the bars are *gray* [3]

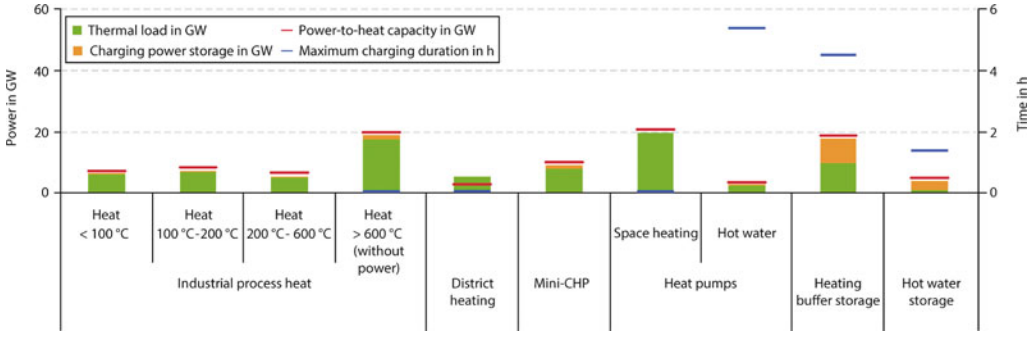



**Fig. 4.16** Heating load, thermal storage charging capacity, PtH capacity, and maximum charging durations in the optimistic scenario for typical high heating load situations (winter days) in 2050. The parameters were: direct potential heating load supply using PtH without storage (*blue bars*, average over 12 hours), required thermal storage charging capacity for PtH (*red bars*, average over 12 hours), installed PtH charging capacity (*green points*), and maximum thermal storage charging duration using PtH in relation to the *red bars* (*yellow points*). If heating load was met with solar-thermal energy, then the bars are *gray* [3]

mediately used for heating without any storage requirements. With load-management, the energy could also be used to serve the system.

In summer, the largest loads expected were for process heat and hot water. In winter, low-temperature heating for room heating added to the load. Low-load situations at night in summer (average over 12 hours) resulted in a minimum charging capacity of 25 GW, or 20 GW when solar-thermal energy was deducted. In this case electricity surpluses were immediately integrated and utilized in the heating sector. High-load situations during the day resulted in a maximum charging potential of 82 GW in winter. The various possible charging durations were heavily-dependent on the specific application and specific load [3].

## 4.8 Summary

- **Low-temperature heating requirements** (room heating, hot water) **will fall** significantly in the future. **Energetic renovation** of existing buildings is essential, but imple-

mentation of **energy efficiency measures** in TIS also has significant potential.

- The existing heating demand will increasingly be met by **renewable energy** in the future. **Electric heat-pumps** (ambient heat) will play an increasingly important role. Solar-thermal energy, geothermal energy, biomass, and PtG coupling of the electricity, gas, and heating sectors using CHP and gas heat pumps will also be essential. Despite the reduction in heating demand, **storage requirements** in the heating sector are expected to **increase overall**. This is because higher shares of renewable energy require increased temporal balancing.
- In the household, TIS, and manufacturing sectors, energy transition will require **electricity** to become the **primary energy carrier** for heating supply.
- As a result, **cross-sectoral energy storage** such as PtH and electric heat-pumps **including thermal storage will be essential** in the future.
- **Thermal storage** will allow the heating sector **to cost-effectively absorb fluctuations** in an **electricity sector based on renewable energy**.
- To pave the way, **system temperatures must be reduced** by applying strict efficiency standards and transitioning to technologies **that allow electricity-based heating supply**.
- **CHP generation** will remain a crucial technology in all sectors. **High flexibility** can be achieved with this technology through **electricity-oriented operation** using heating networks and thermal storage **decoupled from heating in hybrid combination** with peak-load boilers and electric heating.
- In all sectors, **electric heat-pumps** will increasingly be used to provide **hot water**.
- Because **heat pumps** will be more widespread and the ambient heat they produce is not considered primary energy, household sector **final energy requirements** for room heating will exceed **primary energy requirements**.
- The use of **woody biomass** will be shifted from the **TIS sector to supplying older buildings in the household sector** and process heat in manufacturing.
- For process **heat at the upper temperature-range**, **direct electricity use** will allow **fossil energy carriers** to be **replaced** by renewable energy.
- Starting in 2025, the **use of coal** for manufacturing heat can be eliminated. **Fossil and renewable gas** will, however, **remain essential** here over the long-term.
- The **paradigm shift** in the heating sector will rely primarily on a range of heating supply options beyond oil and gas. The **coupling** and **convergence** of the **electricity and heating sectors** will be decisive here. It will also result in the following changes:
  - Increased **CHP flexibility**, including:
    - Transitioning from heat-oriented operation to electricity-oriented operation decoupled from heating.
    - Expansion and utilization of centralized and decentralized **thermal storage** for this purpose.
  - Activation of **PtH** and **electric heat pump** potential as a flexibility option using:
    - Decentralized **electric heat-pumps** in household thermal buffers.
    - Centralized **electric heat-pumps** for **heating networks** and **thermal storage**.
    - Short-term: centralized **electric heaters** (electric resistance heating) in heating networks.
    - Long-term: centralized **electric heaters** in **manufacturing** for high-temperature **process heat**.
    - Decentralized **electric heaters** in household thermal storage in combination with PV.
  - Expansion of **heating networks** to utilize centralized **CHP** and **large heat pumps**.
  - Renewable energy electricity potential for **process heat**.

- Renewable electricity will increasingly supply electricity-based, high-temperature process heat.
- Flexible process heat applications will offer opportunities for providing **balancing power**.
- In combination with **PtH**, **PtG** can provide access to renewable energy for process heat.

- Using the potential of **PtG**:
  - More than **half** of German **households** have a **gas connection**, allowing even rental apartments to be supplied with renewable energy heating without major on-site conversions.
  - Renewable gas can be used in **gas heat pumps**, **CHP**, and **gas boilers** for high-temperature process heat.
  - Renewable gas can be efficiently used in **bivalent** and **hybrid applications** such as gas heat pumps, CHP, or gas boilers in combination with a simple heating rod, a large electric heat pump, or an electroboiler.
- Regarding **storage requirements**, various trends can be identified:
  - Despite decreasing heating demand, **thermal storage demand** will **increase** due to the use of renewable energy as well as electricity-oriented, heat-decoupled CHP.
  - At the same time, an **increasingly important** factor will be the **integration** of the **heating sector** with the electricity sector through coupling and convergence.
  - Through this process, **thermal storage** will **become crucial** for the **electricity sector**. This is because it can make thermal generation in the **electricity sector more flexible**.
  - Additional energy demand in summer for **cooling** and **air-conditioning** could create a new demand for **cold storage**, ideally in the form of combined heat and cold storage; for example, with ice storage.
  - **Surpluses** from thermal energy and CHP could be exploited using **heating networks** and **thermal storage**.
  - **Heating sector storage potential** in the form of thermal and gas storage is **very large**, and could be exploited using various charging technologies such as CHP, PtH, and PtG.
  - Among the energy storage options, **thermal** storage's function is the most important for energy transition. The **storage capacity required here exceeds electricity and fuel storage requirements** in the other energy sectors **by a wide margin**.

## References


1. BWP (2013) BWP-Branchenstudie 2013. Szenarien und politische Handlungsempfehlungen. Daten zum Wärmepumpenmarkt bis 2012 und Prognosen bis 2030. Berlin
2. Deckert M, Binder S, Hornung A (2013) Mobiler Latentwärmespeicher auf dem Prüfstand – Wärme nimmt Fahrt auf. Bwk Vdi-springer-verlag 65(9):34–37
3. Gerhardt N (2013) Potentialanalyse für Power-to-Heat. 3. DI-Fachkonferenz Energiespeicher für die Energiewende 2013, Mainz
4. Gores S, Harthan R, Hermann H, Loreck C, Matthes FC (2013) Perspektiven der Kraft-Wärme-Kopplung im Rahmen der Energiewende. BMU Studie, Berlin
5. Henning H-M, Palzer A (2015) System- und Kostenentwicklung einer Klimaschutzkompatiblen Transformation des deutschen Energiesystems. bis 2050. Freiburg (Sektor- und Energieträgerübergreifende, modellbasierte Untersuchung zur schrittweisen Reduktion energiebedingter CO2-Emissionen durch Energieeffizienz und den Einsatz Erneuerbarer Energien von heute bis zum Jahr 2050)
6. Henning H-M, Palzer A (2014) A comprehensive model for the German electricity and heat sector in a future energy system with a dominant contribution from renewable energy technologies – Part I Methodology. Renew Sustain Energy Rev 30:1003–1018. https://doi.org/10.1016/j.rser.2013.09.012
7. Henning H-M, Palzer A (2015) System- und Kostenentwicklung einer Klimaschutzkompatiblen Transformation des deutschen Energiesystems. bis 2050. Freiburg (Sektor- und Energieträgerübergreifende,

modellbasierte Untersuchung zur schrittweisen Reduktion energiebedingter CO2-Emissionen durch Energieeffizienz und den Einsatz Erneuerbarer Energien von heute bis zum Jahr 2050)
8. IEA (2013) Technology Roadmap Solar Heating and Cooling 2050. Paris
9. Nitsch J, Pregger T, Sterner M, Wenzel B (2012) Langfristszenarien und Strategien für den Ausbau der erneuerbaren Energien in Deutschland bei Berücksichtigung der Entwicklung in Europa und global. Bundesmin. für Umwelt Naturschutz und Reaktorsicherheit, Berlin (Schlussbericht BMU – FKZ 03MAP146)
10. Norman Gerhardt, Fabian Sandau, Angela Scholz, Henning Hahn, Patrick Schumacher, Christina Sager, Fabian Bergk, Claudia Kämper, Wolfram Knörr, Jan Kräck, Udo Lambrecht (2015) Interaktion EE-Strom, Wärme und Verkehr. Analyse der Interaktion zwischen den Sektoren Strom, Wärme/Kälte und Verkehr in Deutschland in Hinblick auf steigende Anteile fluktuierender Erneuerbarer Energien im Strombereich unter Berücksichtigung der europäischen Entwicklung. Ableitung von optimalen strukturellen Entwicklungspfaden für den Verkehrs- und Wärmesektor, Kassel
11. Palzer A, Henning H-M (2013) A Future German Energy System with a Dominating Contribution from Renewable Energies: A Holistic Model Based on Hourly Simulation. Energy Technol. https://doi.org/10.1002/ente.201300083
12. Palzer A, Henning H-M (2014) A comprehensive model for the German electricity and heat sector in a future energy system with a dominant contribution from renewable energy technologies – Part II: Results. Renew Sustain Energy Rev 30(0):1019–1034. https://doi.org/10.1016/j.rser.2013.11.032
13. Reuter M (2013) Power-to-Gas: Biological methanization; first at a municipal sewage plant. 8th International Renewable Energy Storage Conference, Berlin
14. Weiss W, Mauthner F (2012) Solar Heat Worldwide – Markets and Contributions to the Energy Supply 2010. Solar Heating and Cooling Programme, Gleisdorf, Österreich

# Storage Demand in the Transport and Chemical Sector

*Michael Sterner, Fabian Eckert, Hans-Martin Henning, and Tobias Trost*

**5.1 Basics and Objectives in the Transport Sector – 167**
5.1.1 Initial Situation and Developments in the Last Decades – 167
5.1.2 Objectives in the Transport Sector – 167

**5.2 Development of Mobility Needs – 169**
5.2.1 Population Development – 169
5.2.2 Development of Economic Performance – 169
5.2.3 Spread of the Development of Mobility Needs for Passenger and Freight Traffic – 169

**5.3 Development of Energy and Fuel Supply – 169**
5.3.1 Developments in Passenger Traffic – 171
5.3.2 Developments in Freight Traffic – 172
5.3.3 Development of the Energy Mix in the Transport Sector – 172

**5.4 Paradigm Change in the Transport Sector – 175**
5.4.1 Electrification of Mobility via Batteries and Synthetic Fuels – 175
5.4.2 Integration of Renewable Energies as the Cornerstone of Mobility – 178

**Electronic supplementary material** The online version of this chapter (https://doi.org/10.1007/978-3-662-55504-0_5) contains supplementary material, which is available to authorized users.

© Springer-Verlag GmbH Germany, part of Springer Nature 2019
M. Sterner, I. Stadler (Eds.), *Handbook of Energy Storage*, https://doi.org/10.1007/978-3-662-55504-0_5

**5.5 Storage Demands in the Transport Sector – 178**
5.5.1 Storage Demand Today – 178
5.5.2 Storage Demand in a Transport Sector Supplied by 50% Renewable Energies – 179
5.5.3 Storage Demand in the Study of the Fraunhofer ISE – 181
5.5.4 Storage Study for the Agora Energy Transition – 181

**5.6 Storage Demand in the Chemical Industry – 183**
5.6.1 Resource Consumption Today and in 2050 – 184
5.6.2 Necessary PtX Capacities for the Chemical Industry – 184

**5.7 Summary – 185**

**References – 187**

**Overview**

In the **transport sector**, energy transition is still **in its beginnings**: shares of renewable fuels are at **5%** and are, with the exception of a small percentage in electrical rail transport, almost entirely restricted to **biofuel**. The transport sector, i.e., road, air, shipping, and rail traffic, consumes around 30% of all final energy in Germany and its **dependency** of over 90% on **petroleum** is still **very high**. As a result, its shares in greenhouse gas emissions are at 20%.

The **necessary structural change** in mobility, based on energy transition, is closely linked to the question of **operating energy** and of **energy storage** also. Aside from vehicles directly powered by wind or solar energy, mobility without storage is not possible: fuel tanks in cars, gas stations, and airplanes are omnipresent.

The focus of the considerations on storage demand in the transport sector is on the question of how these **storages** can be used with renewable energies via **bio** and **synthetic fuels**, and on the question of how much storage is necessary for these new drive technologies, such as **e-mobility**. Before this, mobility needs today and in future need to be examined.

In the **chemical sector**, the situation is very much alike: there is a great dependency on fossil resources, and decarbonization is inevitable to achieve ambitious climate goals. The structural change to convert and store renewable electricity as primary energy via **power-to-X** (PtX) represents a storage demand. First estimates will conclude this chapter.

## 5.1 Basics and Objectives in the Transport Sector

### 5.1.1 Initial Situation and Developments in the Last Decades

As a result of energy transition, the transport sector is affected by structural change just like the power and heat sectors. Dependency on the energy carrier oil is most prominent in the transport sector. It is a inherent characteristic of mobility—except for the low powers for traffic via overhead electrical wires—to rely on mobile or stationary energy storage.

Oil-based fuels have been the energetic basis of the transport sector for decades, with a share of 90% of its final energy consumption in 2016 (Fig. 5.1). The constant growth of the transport sector is compensated for by increases in efficiency of drive technologies, which lead to the final energy consumption remaining almost static (sufficiency). While there was a noticeable change of technology from gasoline to diesel over the past few decades, small amounts of biofuels and natural gas joined the mix from the year 2000 and onwards. Apart from gas and diesel fuels, fuels for air traffic in particular have significant shares. In 2016, biofuels supplied some 4% (29.7 TW h) of the final energy consumption. The share of electricity is 1.4% (11.4 TW h), which mostly powers rail traffic.

These numbers illustrate the great challenges facing the transport sector in relation to sustainable energy supply and usage. Motorized individual transport in particular, which caused some 56% of final energy consumption in the transport sector in 2010, is facing structural changes [9]. In view of the this, the deployment of alternative fuels, drive technologies, and other measures to reduce $CO_2$ emissions will be discussed and resolved on a national and international level.

### 5.1.2 Objectives in the Transport Sector

The federal government has, following its energy concept, set ambitious energy and climate protection goals for the transport sector, such as reducing final energy consumption by 10% by 2020 and by 40% by 2050, as compared to the reference year 2005. In addition, the 'National Electromobility Development Plan' is to be realized and, thereby, the number of electric vehicles increased to 1 million by 2020 and 6 million by 2030 [4].

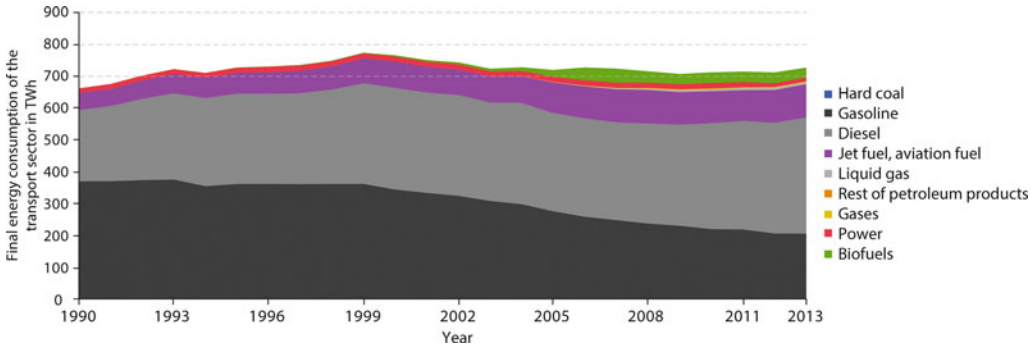





**Fig. 5.1** Final energy consumption in Germany between 1990 and 2016 in TW h, listed by energy carriers [2]

These plans are flanked by the European Commission's goals, according to which the transport sector's greenhouse gas emissions have to be reduced to 40% of the amount at 1990 by 2050 [5], as well as by self-commitment of isolated branch associations. The International Air Transport Association (IATA), for instance, has a goal towards $CO_2$-neutral growth from 2020 onwards [7]. These self-commitments are, however, controversial, because they did not always prove effective in the past, especially within the auto-industry.

For this reason, objectives were set using EU-levels which limit the average $CO_2$ emissions of the automobile manufacturer's models to 95 g $CO_2$-equivalent per km. In addition, the EU Commission targets a quota of ca. 5% for biofuels and 2.5% for synthetic fuels (power-to-gas—PtG, power-to-liquid—PtL, [6]).

**Definition**

Synthetic fuels are energy carriers, produced electric energy by electrolysis of water and, optionally, synthesis (PtG and PtL) and is used in transport. E.g., hydrogen, methane (windgas), methanol, and Fischer-Tropsch fuels (wind diesel, wind kerosene).

In addition to these general objectives concerning fleet consumption, fuel mix, and drive technologies, the federal government is further planning the implementation of a sustainable mobility and fuel strategy, according to the leitmotif 'away from oil'. It includes these following key points concerning energy carriers (energy supply), infrastructure (transport and storage), and drive technologies (energy efficiency) [3]:

- Climate objectives and energy carriers:
  - Personal road traffic and rail traffic will be closely connected to climate objectives and renewable energies.
  - Workable concepts for the future, which mainly resort to biofuels and synthetic fuels (biokerosene, PtL, renewable liquefied natural gas—LNG) are to be developed for transport modes with currently a high dependency on oil and high requirements to the energy carrier's energy densities (air, shipping, cargo, machines).
  - The current goals related to energies in the transport sector is for it to be diversified and broadened with alternative fuels, in order to reduce dependency on fossil energy carriers.
- Drive concepts:
  - Innovative drive technologies are to be established.
  - Efficiency of combustion engines are to be increased.
- Infrastructure:
  - Traffic flow is to be optimized.
  - Infrastructure for alternative fuels, such as hydrogen, is to be set up.

In order to achieve these goals, measures will have to be taken in all areas of mobility, which can be divided into the following categories:

- Passenger traffic
- Freight traffic

And also:

- Road traffic
- Rail traffic
- Shipping traffic
- Air traffic

Every area and combination of areas imposes requirements on energy carrier, infrastructure, drive technology, and (consequently) on energy storage.

## 5.2 Development of Mobility Needs

The question of energy storage is closely connected to the one of mobility needs. According to the study 'The Future of Mobility' by the Institute for Mobility Research (IFMO), mobility needs depend on two main factors. These are demographic development and the development of economic performance [8].

### 5.2.1 Population Development

Demographic change can be observed in all areas of life, and consequently affects mobility as well. Increasing urbanization leads to a lower mobility demand for people in the countryside and imposes higher requirements on urban logistics and infrastructure. Intermodality, meaning the changing of different transport modes, will be used more frequently [12]. In addition to a concentration of population in metropolitan areas, the share of elders, who have different mobility needs compared to young people, increases. Among young people, a certain change in mentality can be observed: the car loses its significance as a status symbol compared to other lifestyle attributes, such as cell phones. The demand for personal vehicles decreases, while the popularity of other concepts, such as car sharing, increases. All of this, and increasing mobility requirements, which underlie a growing ecological awareness, causes the majority of studies to come to the conclusion that personal mobility needs will almost remain static.

### 5.2.2 Development of Economic Performance

Economic performance, as a measure for the amount of produced and consumed goods in a national or global economy, is tightly linked to freight traffic. Even though it also influences income development, and thus passenger traffic, the interconnection between economy and traffic can be seen most clearly in freight traffic. Strong economic growth is reflected in an increased freight traffic volume. Most examinations are based on this very trend.

### 5.2.3 Spread of the Development of Mobility Needs for Passenger and Freight Traffic

Alongside the IFMO study, there are a large number of further research findings which predict the development of passenger and freight traffic (Table 5.1). When comparing these results directly, the tendencies of future traffic volumes appear very similar to one another. All in all, freight traffic volume is expected to increase significantly, while passenger traffic will, in most cases, remain static.

## 5.3 Development of Energy and Fuel Supply

Findings from the BMU long-term scenarios concerning freight and passenger traffic will be used in the same way they were used in the pre-

**Table 5.1** Forecast of the development of traffic volume in freight and passenger transport in the future. Passenger traffic volume in bn passenger kilometers. [8, 10, 11, 13, 20]

| Studies | 2010 | 2020 | 2030 | 2050 |
|---|---|---|---|---|
| DLR, IWES, IFNE (2012): BMU—Langfristszenarien 2011 | 1,129 | 1,153 | 1,147 | 1,053 |
| WWF Deutschland (2009): Modell Deutschland Klimaschutz bis 2050—Referenzszenario | 1,093[a] | 1,111 | 1,104 | 1,023 |
| WWF Deutschland (2009): Modell Deutschland Klimaschutz bis 2050—Innovationsszenario | 1,090[a] | 1,101 | 1,087 | 998 |
| Prognos AG, EWI, GWS (2010): Energieszenarien für ein Energiekonzept der Bundesregierung—Referenzszenario | 1,106[a] | 1,123 | 1,115 | 1,046 |
| Prognos AG, EWI, GWS (2010): Energieszenarien für ein Energiekonzept der Bundesregierung—Zielszenarien | 1,104[a] | 1,112 | 1,098 | 1,019 |
| Öko-Institut, DLR, ISI (2012): Renewbility II—Basisszenario | 1,178[a] | 1,281[a] | 1,385 | – |
| Öko-Institut, DLR, ISI (2012): Renewbility II—Klimaschutzszenario | 1,137[a] | 1,160[a] | 1,183 | – |
| IFMO (2010): The Future of Mobility. Scenarios for the Year 2030—Global Dynamics | 1,120[a] | 1,143[a] | 1,166[a] | – |
| IFMO (2010): The Future of Mobility. Scenarios for the Year 2030—Matured Progress | 1,115[a] | 1,082[a] | 1,050[a] | – |
| Freight traffic volume in bn tonne kilometer: | | | | |
| DLR, IWES, IFNE (2012): BMU—Langfristszenarien 2011 | 624 | 798 | 888 | 912 |
| WWF Deutschland (2009): Modell Deutschland Klimaschutz bis 2050—Referenzszenario | 634[a] | 775 | 869 | 1,033 |
| WWF Deutschland (2009): Modell Deutschland Klimaschutz bis 2050—Innovationsszenario | 635[a] | 779 | 876 | 1,047 |
| Prognos AG, EWI, GWS (2010): Energieszenarien für ein Energiekonzept der Bundesregierung—Referenzszenario | 675[a] | 777 | 876 | 1,053 |
| Prognos AG, EWI, GWS (2010): Energieszenarien für ein Energiekonzept der Bundesregierung—Zielszenarien | 675[a] | 781 | 882 | 1,067 |
| Öko-Institut, DLR, ISI (2012): Renewbility II—Basisszenario | 648[a] | 819[a] | 990 | – |
| Öko-Institut, DLR, ISI (2012): Renewbility II—Klimaschutzszenario | 654[a] | 837[a] | 1,021 | – |
| IFMO (2010): The Future of Mobility. Scenarios for the Year 2030—Global Dynamics | 595[a] | 725[a] | 884[a] | – |
| IFMO (2010): The Future of Mobility. Scenarios for the Year 2030—Matured Progress | 588[a] | 643[a] | 704[a] | – |

[a] Figures calculated based on the study.

vious chapters concerning storage demand in the power and heat sector.

In addition to these DLR, IWES, and IfnE studies, there are other significant studies concerning mobility which are presented in Table 5.1. Some studies assume, rather conservatively, that energy supply will continue to be dominated by conventional energy carriers,

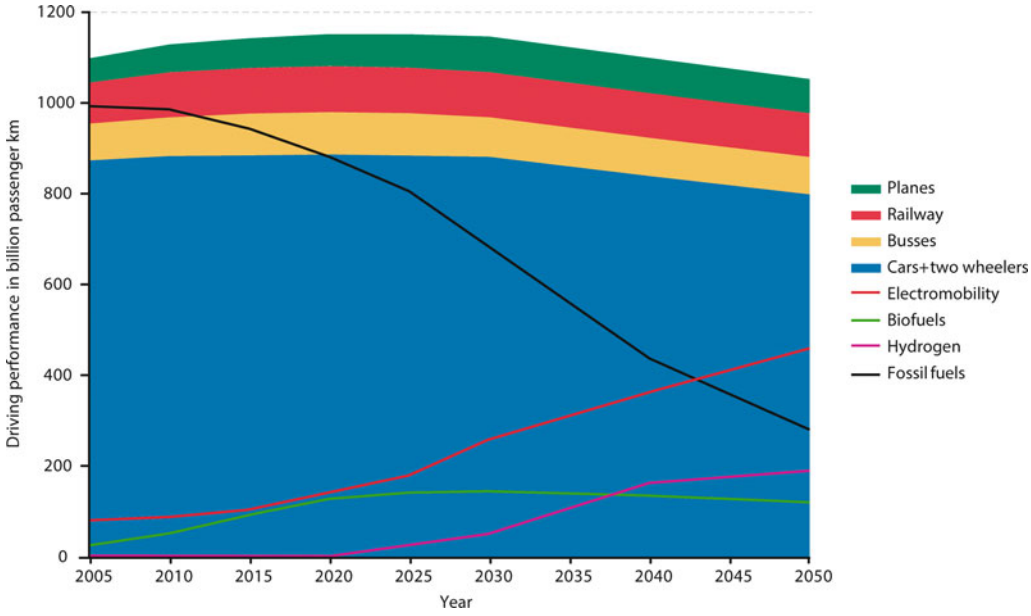



**Fig. 5.2** Development of passenger traffic volume, listed by categories and energy sources

while others predict a progressive change of the transport sector, based mainly on e-mobility. The selected BMU long-term scenarios represent the middle course [11].

### 5.3.1 Developments in Passenger Traffic

Figure 5.2 shows the developments of traffic volume in passenger transport and the energy mix in Germany between 2005 and 2050. While passenger traffic volume tends to increase, final energy consumption remains almost static for the time examined because of efficiency improvements.

The energy mix shows a significant decline of fossil fuels. They are substituted by renewable electricity and renewable fuels to ever higher degrees. The paradigm change of 'electricity becoming primary energy' also takes place in passenger traffic. Even though only rail traffic is powered electrically today, an electrification of traffic via hybridization is expected in the future. In the end, this electrification will also catch on in machines, and also in long-distance and air traffic using synthetic fuels.

In this scenario, the number of electrically driven vehicles increases according to the goals set for 2020 (1 M) and 2030 (6 M) to 16 M in 2040 and 22 M in 2050. In the latter case, it was assumed that 80% of hybrid car mileage and 60% of hybrid bus mileage is powered by renewable electricity.

Synthetic fuels, such as hydrogen, PtG, and PtL, will increase in importance from 2030 onwards and surpass biofuels in the long-run, because their potential is greater and there is less competition concerning land use. Biofuels are, nevertheless, an important link because, until 2030, they are the only option that can provide a relevant amount of renewable fuels with high-energy density. They can be used to power air traffic, non-electrified rail traffic, buses, and machines. A change of aviation fuel requires global adaption of infrastructure and fuel supply, because aircrafts are only used nationally to a very limited degree.

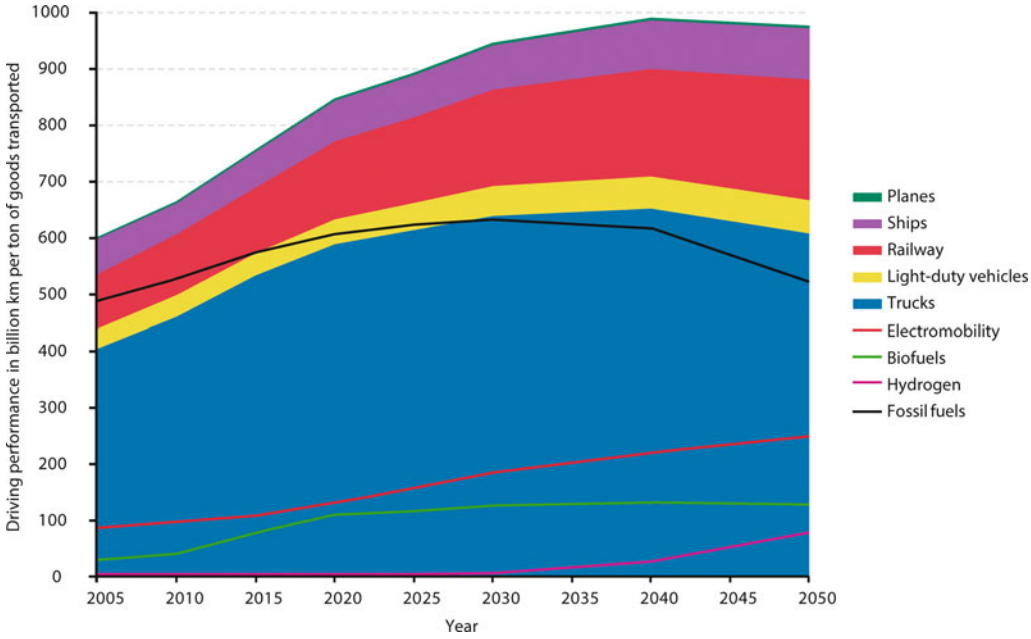



**Fig. 5.3** Development of freight traffic volume, listed by categories and energy sources

### 5.3.2 Developments in Freight Traffic

As proven within numerous scenarios in Table 5.1, freight traffic volume will continue to increase. BMU long-term scenarios are based on the assumption that sufficiency will take effect; that is, that strong growing mobility needs will, in the medium-term, be limited by efficiency improvements, which leads to the forecast that these needs will increase by 58% by 2030, and 62% by 2050 [11].

Figure 5.3 shows a forecast of the development of freight traffic volume in Germany between 2005 and 2050, with truck traffic growing fastest. This growth can only be reduced by the usage of more efficient vehicles and hybridization between 2040 and 2050. Another option is to put freight traffic on rails instead of roads, which increases the importance of rail traffic. In 2010, it was powered 90% electrically and, according to the scenario, it will be 96% electric in 2050. Hybridization of trucks was assumed to be 30% complete, and light commercial vehicles were assumed to be 50% complete by 2050.

Unlike passenger traffic, freight traffic will be dependent on fossil fuels as main energy carriers for decades. Even though it can be assumed that, in shipping traffic, there will be a change from marine diesel oil to LNG, the dependency on fossil fuels will remain. For rail traffic specifically, there is the possibility of integrating renewable energies via electricity as 'fuel', because electrification is almost complete in that field. There are similar approaches to power truck traffic via overhead electrical wires, which in turn would make power current electrification of road infrastructure necessary. For the main part of freight traffic, the only remaining options to reach climate-neutrality are bio and synthetic fuels.

### 5.3.3 Development of the Energy Mix in the Transport Sector

#### ▪ Fossil Energy Carriers

The introduction of renewable energies in the fuel area will be the most complicated of all

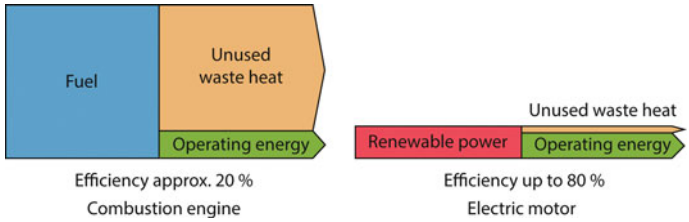



**Fig. 5.4** Efficiency improvements because of e-mobility [15]

three energy sectors, because this sector is characterized by combustibles with high-energy densities. As a result, dependency on fossil fuels will remain for an extended period of time, and can only be reduced by measures of energy efficiency applied at the driving end and with consumers, intermodality, and traffic optimization. As can be seen in Fig. 5.5, the importance of gasoline is declining in the long run, as is the importance of other fossil fuels because of efficiency improvements and substitution.

## E-Mobility

There are a number of options for the substitution of fossil fuels. Greatest efficiency gains will, without a doubt, be due to e-mobility, since an electric drive's efficiency is at 70–80%, which is three to four times better than a conventional combustion drive's efficiency (which is 20–30%). This results in an expectedly lower final energy consumption (Fig. 5.4). However, this efficiency boost is only possible, if directly generated renewable energy from wind, solar, or hydropower plants is used. The usage of fossil electricity is not expedient, because efficiency losses of conventional power plants will cancel out the efficiency boost of e-mobility.

The strong decline of final energy consumption of 40% between 2010 and 2050 that can be seen in Fig. 5.5 is mainly based on e-mobility. Those shares of electricity in mobility, which are already significant today, are power rail traffic.

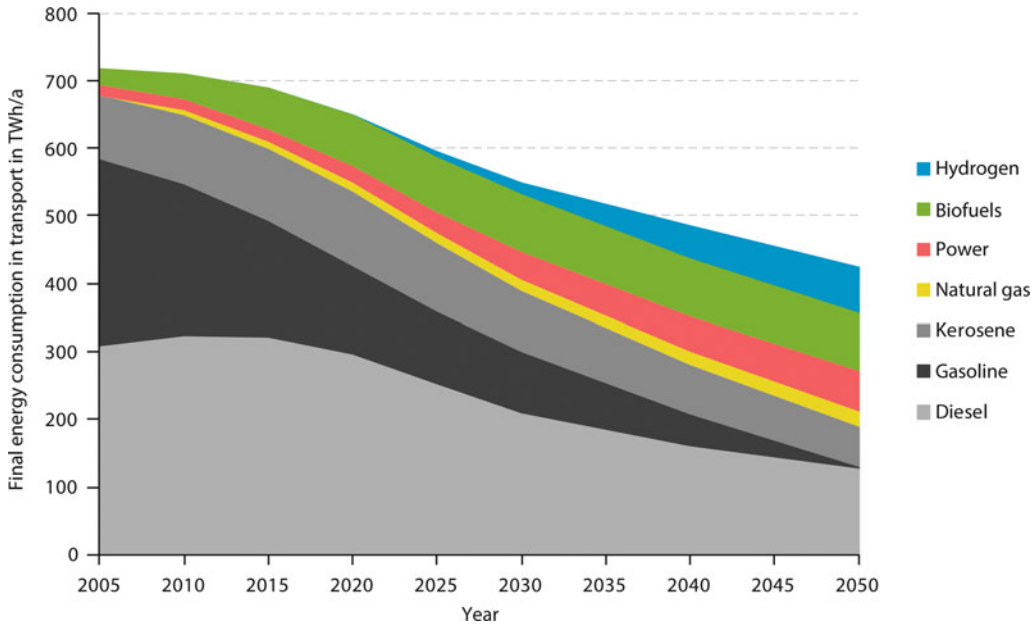



**Fig. 5.5** Development of final energy consumption in transport in the BMU Leitszenarien [11]

### Bio and Synthetic Fuels

Fuels with high-energy densities are needed as a supplement for e-mobility in the long-distance traffic sector of individual transport, for machines as well as for air, shipping, and freight traffic. The integration of biofuels is especially easy, because they can be used in conventional engines. They do make an important contribution, but the sustainable potential of biofuels is limited. While it suffices to substitute fossil fuels in agriculture, it is too small to supply significant shares of the German or global fuel demand [19].

The introduction of E10 to individual mobility predominantly failed because of lack of acceptance from the general public (food-versus-fuel debate). In addition to the aspect of land availability, there is no definitive scientific answer to the question of climate impacts of biofuels. It is mainly direct and indirect land usage changes because of the cultivation of energy crops that massively influence climate impacts of biofuels.

As the potential of biofuels is limited, and electric vehicles are not suitable for all purposes because of their small range and the low-energy density of their batteries, synthetic fuels will play an important role in the traffic of the future. It is for this reason that technologies which can produce these synthetic fuels, such as PtG and PtL, will be essential in order to reach $CO_2$ reduction goals.

In the examined scenario, hydrogen was regarded as electricity fuel. In order to use hydrogen, new infrastructures and adequate drive technologies are necessary, as well as electrolyzers, which do not exist as yet. It can be assumed that only from 2030 on, hydrogen will be used comprehensively for that reason. Alternatively, hydrogen can be processed to a gas substitute or to liquid fuels and used in the existing infrastructure and in drive technologies (▶ Sect. 8.3).

### Overall Shares of Renewable Energies

Today's shares of 5.4% of renewable energies in the transport sector will increase to 14% (90 TW h) in 2020. From 2030 onwards, a quarter of the energy mix will be renewable, and from 2050 onwards, half the energy consumed in the transport sector will be supplied by renewable energies (210 TW h).

In the year 2050, 70% of individual transport will be able to be powered using renewable energy; at 50%, electric vehicles are the mainstay, while bio and synthetic fuels reduce the need for fossil fuels in long-distance transport. In order to carry out climate protection and realize a system change, it will be necessary to draw up to 44 TW h for electric vehicles and 87 TW h for synthetic fuels from the power sector every year. This will result in 50 GW additional need for installed renewable capacities, which will mostly be supplied by wind energy. This additional need is to be provided for by the power sector and can be regarded as storage demand for the transport sector.

These numbers seem very large, but they have to be put into perspective with regard to today's fuel consumption. The following sample calculation shows how great the constant fuel consumption in German gas stations is, compared to the consumption of combustibles in the power and heat sector.

**Which amount of power is constantly being applied to German gas stations?**

Every year, some 600 TW h of electrical energy is consumed, with power fluctuating between 40 and 80 GW in the German electricity system. These numbers are comparable to those of the transport sector. When dividing the annual fuel consumption of 700 TW h by 8,760 h, and thus assuming base-load qualities over the whole year, the result is a constantly applied power of 80 GW.

**Which amount of power is controlled by a refueling driver?**

A simple comparison of a dispenser and a diesel generator illustrates the great energy density of compact fossil fuels in daily use.

In a common gas station, 0.5 liters of fuel can be drawn from the dispenser per second. Gasoline has a calorific value of 9 kW/L, diesel



**Fig. 5.6** Refueling of a car vs. power and heat generation with the same amount of energy. The power flow of a dispenser is between 16 and 18 GW, and thus, equivalent to a cogeneration plant of the 6–7 MW class. (Source: Kzenon, fotolia and Petair, fotolia)

10 kW/L. Thus, the following calculation provide the answer:

**Gasoline:** – $P_{\text{Gasoline}} = 0.5\,\frac{\text{L}}{\text{s}} \cdot 9\,\frac{\text{kW h}}{\text{L}}\,\frac{3.600\,\text{s}}{\text{h}} = 16.2\,\text{MW}$,

**Diesel:** – $P_{\text{Diesel}} = 0.5\,\frac{\text{L}}{\text{s}} \cdot 10\,\frac{\text{kW h}}{\text{L}}\,\frac{3.600\,\text{s}}{\text{h}} = 18\,\text{MW}$.

This means that the driver controls a 16–18 MW power flow when refueling (Fig. 5.6).

Provided with this power flow, a diesel cogeneration plant with an electrical power of 6–7 MW and a thermal output of 8–9 MW could supply 12,000–14,000 households with electricity at 0.5 kW mean power and 1,600–1,800 households with heat at an average demand of 5 kW.

## 5.4 Paradigm Change in the Transport Sector

Just like in the heat sector, a paradigm change is currently taking place in mobility: the connection of the power and transport sectors, verbalized as 'hybridization' and 'electrification' of mobility with new drive concepts, energy storage, and synthetic fuels. In addition, the integration of renewable energies will be an important feature of mobility.

Being one of the most important segments in the transport sector, motorized individual transport in particular has to make a significant contribution to sustainable mobility development. Today, the German car market is almost exclusively made up of conventional combustion engine vehicles. In addition to gasoline and diesel fuels which are mainly used, bio and synthetic fuels (especially in the form of admixtures), liquefied petroleum gas (LPG), and natural gas (compressed natural gas—CNG) will be used. However, it is e-mobility that plays the key role in climate protection and energy efficiency.

### 5.4.1 Electrification of Mobility via Batteries and Synthetic Fuels

▶ Section 14.2 describes the connection of the power and transport sector using examples and key points.

- **Electricity as Primary Energy—Electrification of Drive Trains and Infrastructure**

So far, only rail traffic is electrified to a large degree, however there is further potential. An almost complete electrification of railroads with renewable energy will make rail traffic the greatest electricity consumer in Germany, and

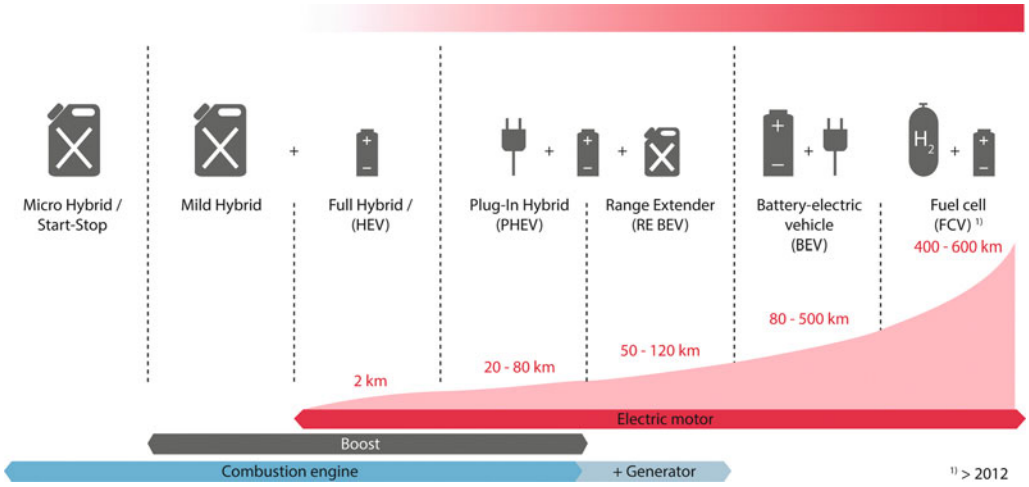



**Fig. 5.7** Electrification of the drive train from combustion to electric engine, examplified by a car [14]

thus a critical element of the integration of renewable energies. Intelligent coupling of rail traffic, local transport, and car sharing offers will make sustainable long-distance passenger transport on the basis of renewable energies possible. Freight traffic on rails is very efficient and should, therefore, be expanded. As shown in ▶ Sect. 5.3.2, freight traffic is continuously increasing, which makes its interlocking with truck and shipping traffic extremely important for energy transition. This has a relieving effect on freight traffic volume on the road, increases the overall efficiency, and decreases dependency on fossil energy carriers. Expansion (not demolition) of existing railway capacities and a high level of utilization, which can be ensured by intelligent logistics, are a prerequisite [12].

Truck traffic is almost exclusively dependent on fossil or biogenic fuels. Recent studies show the potential of electrification of truck traffic via overhead electrical wires. In the course of energy transition, power lines, which can be integrated into the motorway infrastructure, will be necessary to a vast extent. The VDE (the association for Electrical, Electronic, and Information Technologies) suggests building ducts in which power lines can run alongside the motorway. By doing so, the motorway can partially be electrified via overhead electrical wires or inductive charging units [18].

This approach also solves the range problem of e-mobility in cars. Today's state-of-the-art purely electrically powered vehicles have a range of only 200–300 km because of a limited battery capacity. In addition, it is batteries which cause the largest pool of costs in battery electric vehicles (BEV). However, they also have significant advantages compared to conventional combustion vehicles:

- When using renewable electricity, efficiency is three to four times greater.
- BEVs cause less emissions of fine particles and noise.
- Contrary to mobile usage of combustibles, it is (in principle) possible to capture $CO_2$ and use waste heat accumulating when converting combustibles into electricity for BEVs.
- A BEV can be used as electricity storage via uni- or bidirectional charging and discharging.

For the future, an increasing diversification of drive concepts in road traffic is expected, with electrification and hybridization proceeding gradually, as shown in Fig. 5.7:

- **Micro-hybrid:** automatic start-stop is already integrated into most models today. In

times of stand still the combustion engine is turned off and the rest of the vehicle is powered by electricity from the battery only. The battery can optionally be recharged by brake energy recovery.

- **Mild-hybrid:** the vehicle has an electric drive, which complements the combustion drive. In most cases, both drive trains are connected in parallel.
- **Full-hybrid:** a full-hybrid vehicle can be powered, both purely electrically and purely by combustion, which is why this system is also called parallel hybrid. Still, the combustion engine is primarily used. Brake energy and combustion energy feed into the battery, which makes these vehicles more efficient than conventional ones. It is nevertheless powered almost exclusively by the previously tanked fuel, and therefore, in most cases by fossil energy.
- **Plug-in hybrid:** the plug-in hybrid is the first one to actually couple the power and transport sector, because it is possible to charge the vehicle's batteries externally with a plug. Most routes are short-distance and can be driven purely electrically in a plug-in hybrid vehicle. The flexibility to drive long-distances remains because the battery can be recharged by the combustion engine. For this reason, this type of vehicle satisfies both needs: emission-free short-haul routes and unlimited long-distance mobility. This hybrid is very similar to the full-hybrid and its drive trains can be connected in parallel or serial.
- **Electric vehicle with *range extender*:** there is a smooth transition between plug-in hybrids and electric vehicles with range extenders. Electric vehicles with range extenders are often constructed as serial hybrids. This means it is driven purely electrically and, when required, a small combustion engine in combination with a generator can recharge the battery.
- **BEV:** there is no combustion engine in a purely electric vehicle. It is powered exclusively electrically. Its range is limited by battery capacity and it is 'refueled' electrically only by charging units or the exchanging of the batteries.
- **Fuel cell vehicles (FCV) and synthetic fuels:** the vehicle is powered by electricity only, as the cold combustion of hydrogen and oxygen to water provides electrical energy. Hydrogen is produced by the electrolysis of water beforehand, and is distributed and stored as gas or liquid in hydrogen tanks.

A charging infrastructure, which is explained in ▶ Sect. 14.2, will be needed for plug-in hybrids, electric vehicles with range-extenders, and BEVs. Great challenges, which have to be faced in this context, are high investment costs for the development and also current costs for the operation of the charging infrastructure.

Similar to how there is no existing infrastructure for e-mobility, there is none for the distribution of hydrogen for FCVs. An infrastructure for hydrogen can either be realized in a central or in a decentralized way. When deploying the central option, electricity is converted into hydrogen, which is stored and then brought to gas stations via pipelines or trucks. In other cases, electricity instead of hydrogen is transported to a local decentralized electrolyzer at the gas station and converted before the hydrogen can be stored and filled in tanks. In addition to the technical expenditure of hydrogen mobility, the financial expenditure is tremendous, which is why it has not made the breakthrough yet and leaves other synthetic fuels such as windgas and PtL as real options.

### Synthetic Fuels

Along with hydrogen, which is the most efficient electricity fuel for mobility, there are other gaseous and liquid fuels produced through renewable energies that will be of significance. The disadvantage of a missing hydrogen infrastructure and unavailable FCVs can be compensated for by gas mobility on the basis of renewable gas. The existing transport and storage capacities of the natural gas grid can be

used for renewable methane, produced via PtG, and its distribution. In addition, there are already more than 900 natural gas filling stations in Germany. The electricity fuel windgas in the form of methane has the same characteristics as natural gas and is, therefore, completely compatible with the natural gas infrastructure, including gas stations and mature, cost-efficient drive technology (▶ Sect. 8.3). The volumetric energy density of methane is greater than that of hydrogen by a factor of three, which reduces the need for storage space. In addition to gas mobility in road traffic for cars and trucks, gas, as an energy carrier low in $CO_2$ with a high-energy density, will be of importance to shipping traffic in the form of LNG so that emission limits in ports can be met. The necessary LNG terminals are also state-of-the-art.

In the future, liquid synthetic fuels from wind and solar energy will contribute significantly to the coupling of the power and transport sector. Electricity as a primary energy for diesel or kerosene will pave the way for renewable electricity into air traffic and power machines, such as construction, agricultural, and forestry vehicles. When deploying PtL in the transport sector, the existing gas stations and distribution methods can be used to their full extent, which leaves only very few adaptions to be made.

### 5.4.2 Integration of Renewable Energies as the Cornerstone of Mobility

In addition to the essential component 'electrification of mobility', the increasing importance of biofuels, which support e-mobility and synthetic fuels, is becoming evident.

Generally, there are different renewable options for different vehicle concepts, which are presented in the matrix ◘ Fig. 5.8. Said matrix also shows trends which may change according to developments of technologies/markets in the future.

## 5.5 Storage Demands in the Transport Sector

Similar to the storage demands in the heating sector, storage demands in the transport sector are very difficult to predict. There are only a small number of studies, and the issue is (to a large extent) still subject to research. Nevertheless, a particular development in storage demand within the transport sector is presented and calculated for a purely renewable energy system in the following.

### 5.5.1 Storage Demand Today

For a considerable amount of time, there has been an enormous storage demand in mobility in the form of fossil fuels, which also includes the admixture of biofuels. While biofuels and synthetic fuels can use similar storages, there is a new storage demand in e-mobility.

- **Fossil Fuels**

The monthly demand for gasoline or diesel is more or less constant over the year. Contrary to the power or heat sector, there is (so far), no need for a seasonal balance in the transport sector, which makes consumption easily plannable. This in turn makes the design of stocking capacities easy and allows the production of fuels to constantly follow their consumption. In refineries and pipeline terminals, fuels are stored only for a short period of time before their consumption. These conventional storages consist of aboveground tanks made out of steel or below-ground storages such as caverns or aquifers, as described in detail in ▶ Sect. 8.4.2.

After the refinery, further energy storages are needed in order to use these fuels:

- Fuel trucks and tankers are needed for distribution to gas stations for road, rail, shipping, and air traffic
- Mobile tanks of road and rail vehicles, machines, ships, and aircrafts

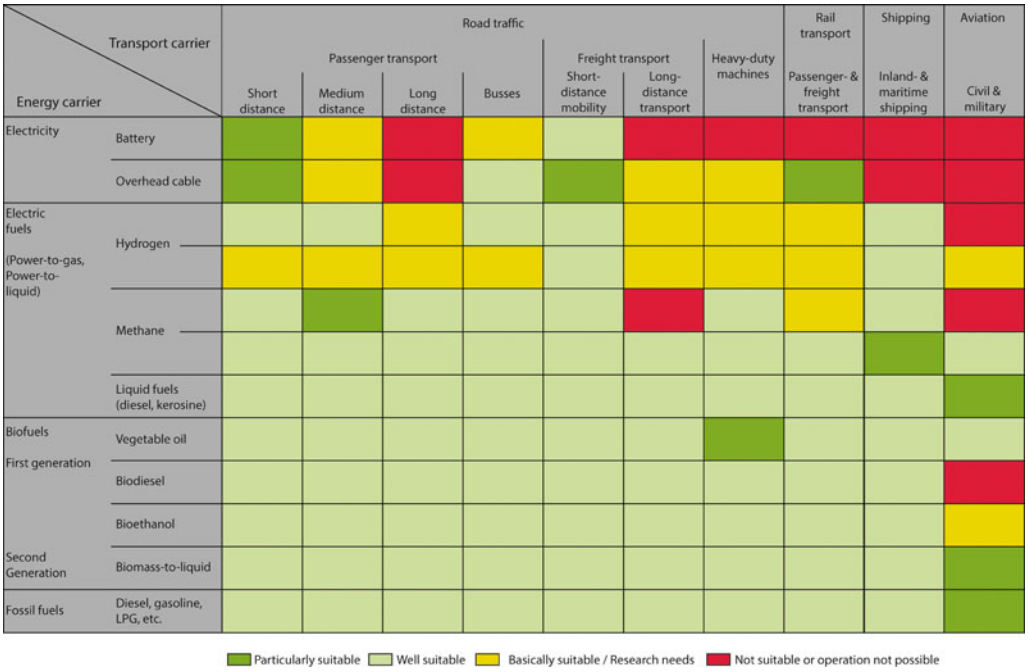



**Fig. 5.8** Matrix: vehicle—alternative energy

### Biofuels

In Germany, oilseeed rape is mostly harvested from July onwards, and can then either be stored as oil seed as oil or, after transesterification, as biodiesel (▶ Sect. 8.4.2.3). In 2010, up to 26.4 TW h biodiesel was produced. When storing biodiesel at a calorific value of 10.3 kW h/m$^3$ and a density of 880 kg/m$^3$, a storage volume of up to 2.91 Mm$^3$ is necessary to store a year's production. A similar volume is needed for rape oil. In order to store the oil seeds only, a storage capacity of 6.51 Mt is necessary, when assuming a good yield of 2.8 T per hectare and year.

It is very difficult to do such a calculation for bio-ethanol, because different plants with different times of harvest and different yields per hectare are used, and because large parts of bioethanol are imported.

## 5.5.2 Storage Demand in a Transport Sector Supplied by 50% Renewable Energies

According to the basis scenario in [11], around half of transport services will be supplied by renewable energies by 2050. Table 5.2 breaks down the development of the four energy carriers; fossil fuels, biofuels, synthetic fuels generated from surplus power or electricity fuel plants, and electricity for electric traction.

### Storage Demand for Conventional Fuels

In the future, fossil fuels will be stored in the same way as today, while the necessary storage capacity will decrease according to the decline of their significance.

**Table 5.2** Development of the final energy consumption in the transport sector in Germany from 2010 to 2050 [11]

| | 2010 | | 2050 | |
|---|---|---|---|---|
| | Final energy in TW h/a | Shares | Final energy in TW h/a | Shares |
| Fossil fuels (gasoline, diesel, kerosene, gases) | 685 | 93% | 212 | 50% |
| Biofuels (bio-ethanol, biodiesel, and BTL) | 36 | 4.9% | 83 | 20% |
| Synthetic fuels (hydrogen, windgas, wind diesel) | 0 | 0% | 67 | 16% |
| Electricity (e-mobility) | 16 | 1.6% conventional, 0.5% renewable | 60 | 14% (purely renewable) |



### Storage Demand for Biofuels

The production of biofuels depends very much on the biomass' time of harvest and requires different storage capacities and technologies, according to the process step. The storing of energy crops containing sugar for the production of ethanol may also lead to losses of substance, because biological processes such as respiration have an enhancing effect on dry matter loss. Biogas can be stored in existing gas storages when used as fuel. If biofuels, such as biomass-to-liquid (BTL), are integrated into refinery processes, the existing mineral oil infrastructure can be used as storage.

### Storage Demand for Synthetic Fuels

The need for long-term gas storage, such as caverns or porous storage, for hydrogen or methane made from PtG results from electricity surpluses in the grid (▶ Chap. 3). Additionally, the natural gas infrastructure will be needed for pure wind or solar fuels. If hydrogen is integrated directly into refinery processes (e.g., hydrocracking), there is no additional storage demand. This is so, because in the existing infrastructure, integration is possible on the fossil path.

### Storage Demand for Electric Drives

Similar to the storage demand for synthetic fuels, the storage demand for e-mobility is tightly connected to the power sector. In the short-term, the electric vehicle's batteries can be used for demand-side management (DSM), and in the long-term, they represent a small storage capacity for the power-grid. In different examinations until 2050, e-mobility is integrated into and connected to the power sector via its storage demand. However, absolute amounts are small, as shown in the following sample calculation.

**Storage Capacity After Complete Electrification of all Vehicles in Germany**

There are currently up to 42 M vehicles in Germany. A storage capacity amounting to ten times the pumped-hydro storage (PHS) in Germany would be created if all these vehicles were to be exchanged by BEVs with a storage capacity of 20 kW h, 50% of which are approved exclusively for electricity storage.

$$W_{42\text{M BEVs}} = 42 \times 10^6 \text{ vehicles} \cdot 10 \frac{\text{kW h}}{\text{vehicle}} = 420 \text{ GW h}.$$

### 5.5.3 Storage Demand in the Study of the Fraunhofer ISE

▶ Section 4.4 details a study by the Fraunhofer Institute for Solar Energy Systems (ISE), which examines a mostly renewable energy system in the future. It contains a greatly simplified model of the transport sector, in which the mileage of all vehicles, including air traffic, is the same as mileage today. This results in an energy demand today and in the model of 137 TW h, which is used purely exergetically to move vehicles. This energy is allocated to the used drive technologies based on the following assumptions:

- **Fossil fuels:** forty percent of mileage is still powered by conventional combustion engines and fossil fuels. This basically corresponds to heavy-duty and air traffic.
- **BEVs:** thirty percent of mainly urban short-distance routes are driven by BEVs.
- **Synthetic fuels:** thirty percent are driven by vehicles with fuel cells and electric engines on the basis of hydrogen.

All this results in the amounts of energy shown in ◘ Fig. 4.7.

BEVs supply 30% of the traction energy (41 of 137 TW h). At an assumed efficiency of 75% for charging, discharging, and electric drive, this requires a total of 55 TW h to drive these vehicles. At an average of one charge cycle per day, these vehicles represent an energy storage with a capacity of up to 150 GW h. An underlying assumption is that the German vehicle stock of 42 M, 12.6 M of which are BEVs, provide an average storage capacity of 12 kW h per vehicle.

This 40% of traction energy (ca. 55 TW h) provided by synthetic fuels relies on 150 TW h of hydrogen from wind and solar energy in electricity fuel plants:

- Eighty-two TW h/a of which are for driving FCVs.
- The other 68 TW h/a are converted into the electricity fuel methane.

In order to balance the demand for hydrogen for vehicles and supply of electricity from renewable energies, a hydrogen storage in the order of 20 TW h/a is necessary.

### 5.5.4 Storage Study for the Agora Energy Transition

▶ Section 3.7.2.7 contains results concerning electricity storage demand from the storage study completed by 'Agora Energy Transition' of FENES, IAEW, ISEA, and ef. Ruhr. In the same study, the storage demands for the transport sector and for the chemical industry were also estimated on the basis of a complete decarbonization because of the climate in those three sectors.

#### 5.5.4.1 Assumptions Concerning the Development of PtX

The numbers this estimate is based on originates from a study by the German Federal Ministry for the Environment concerning the decarbonization of Germany. In this study, the federal government's goals are to reduce greenhouse gas emissions by 90–95% by 2050 [17]. Based on this, two scenarios are presented in [1, 16].

1. Progressive: for the upper end of the bandwidth, a progressive development of PtX technology and its deep integration into the markets is assumed, because of its necessity for reaching climate protection goals.
2. Conservative: for the lower end of the bandwidth of the development tendencies, it is assumed that the federal government's goals remain unchanged, which leaves PtX as one flexibility option amongst others.

In order to determine the storage demand in Germany, in addition to knowing each energy sector's consumption separately, it is important to be aware of technical parameters of PtX and its temporal development. Furthermore, the potential of renewable energies described in ▶ Chap. 3 plays a profound role.

**Table 5.3** Assumptions concerning PtX (representative for PtG) for the examined reference years 2023, 2033, and 2050, which is the year associated with 90% renewable energies (RE)

| | | 2023 | 2033 | 90% RE |
|---|---|---|---|---|
| Efficiency in % | Hydrogen | 65–70 | 70–75 | 78–84 |
| | Methane | 58–60 | 68–70 | 77–79 |
| Full-load hours in h | | 4,000 | 5,000 | 6,000 |



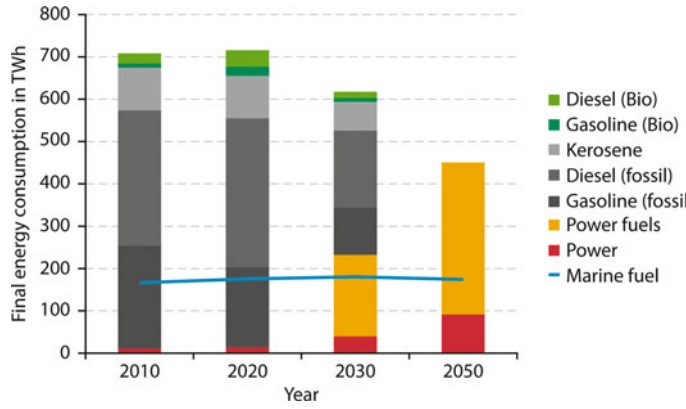



**Fig. 5.9** Final energy consumption in TW h/a of the transport sector between 2010 and 2050; biological and fossil fuels will be substituted by synthetic fuels in the course of decarbonization of the transport sector [17]

**Definition**

PtX means the transformation of resources and primary energy in the form of electricity into energy carriers, such as heat, cold, products, fuels, or other resources. PtX is an umbrella term for PtG, PtL, power-to-fuels (PtF), power-to-chemicals (PtC), power-to-product (PtP), and also power-to-heat (PtH).

The bandwidth of efficiency shown in Table 5.3 follows the respective pressures of hydrogen and methane storage, which in turn depend on the energy service to be provided (▶ Sect. 8.6.4.2). Efficiency improvements are mainly due to the deployment of high-temperature electrolysis (HTES) (▶ Sect. 8.2.2.3), which is still subject to research and development. Additionally, further improvements are expected because of new materials and a deeper understanding of the reactions and processes taking place.

Assumptions made concerning plant usage are based on the usage of renewable electricity, which will supply ever higher shares of the overall power consumption (▶ Chap. 3). Renewable energy sources which have not been tapped to date are also included (▶ Sect. 8.8).

### 5.5.4.2 Energy Demand of a Decarbonized Transport Sector

In the energy storage study for Agora Energy Transition as well as in others, it is assumed that a paradigm change in the transport sector towards e-mobility and synthetic fuels will take place (▶ Sect. 5.4). While in the scenarios of the BMU pilot study 2011 (▶ Sect. 5.5.2) renewable energies are assumed to supply only 50%, this study and [17] assume that they will supply 100%.

This means that by 2050 fossil and biological fuels will be substituted by synthetic fuels from PtX (Fig. 5.9). It is because of the high degrees of utilization of renewable energies in e-mobility that the final energy demand is significantly lower in 2050 than in the preceding years. The energy demand for ships, which

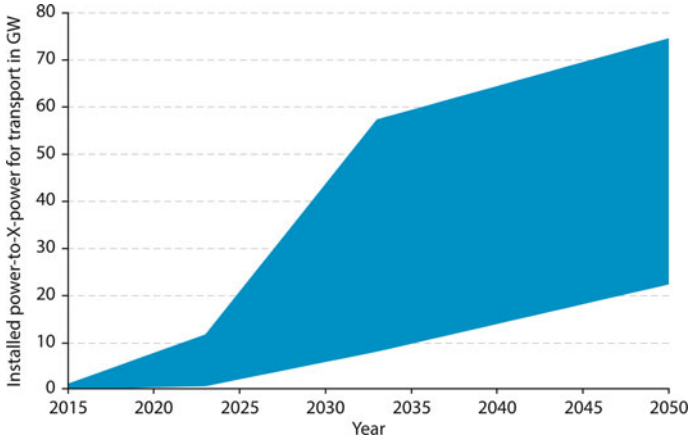



**Fig. 5.10** Bandwidth of the possible development of PtX capacities for the transport sector between 2015 and 2050, as in [16]

would further increase the storage and energy demand, is included separately. However, it is not taken into account in the Agora storage study.

#### 5.5.4.3 Necessary PtX Capacities for the Transport Sector

The storage demand and, therefore, the necessary PtX capacities for the transport sector can be determined using assumptions concerning technical parameters of PtX (▶ Sect. 5.5.4.1) and final energy consumption in the transport sector (▶ Sect. 5.5.4.2).

The upper end of the bandwidth is calculated using the maximum values from Fig. 5.9. Furthermore, it is assumed that PtX technology will develop in time for PtX to be used to supply the enormous demand. In addition to the assumptions made in [17] half the amount of biofuels is substituted by synthetic fuels, because the expansive usage of biofuels hits the wall of sustainable biomass potential (▶ Chap. 3).

For the lower end of the bandwidth, a conservative value, which is 3% lower than the upper end of the bandwidth in 2023, is 15% lower in 2033 and 30% lower in 2050, and is set for each reference year. Figure 5.10 shows a possible development of PtX capacities until 2050 with linear interpolation between the reference years.

## 5.6 Storage Demand in the Chemical Industry

In addition to decarbonizing the power, heat, and transport sectors, it is also regarded as imperative to do so in the chemical industry by replacing fossil resources with renewable ones. Since it is cheapest to provide renewable energies from wind or solar energy in the form of electricity, the transformation of electricity to precursors via PtX is an effective option. This results in an additional storage demand.

Right now, the demand for fossil fuels in the chemical sector is relatively small compared to the energy sectors. However, there is a significantly greater efficiency potential in the energy sectors than there is in the chemical industry. Additionally, some energy services, such as e-mobility or electric heat-pumps, can be provided by renewable electricity, which will lead to a strong decrease of primary energy demand (▶ Sect. 3.2.1).

For non-energetic consumption of fossil resources, an increase of 30% (0.7% per year) is predicted for 2050, because the increasing resource efficiency of production will be more than canceled out by Germany's growing economic performance [17].

### 5.6.1 Resource Consumption Today and in 2050

In 2009, the consumption of natural gas, mineral oil, and coal for material use made up 4% (18.4 Mt) of the overall demand for fossil resources [17]. Besides that, 2.7 Mt renewable resources were consumed, which equals 237 TW h if put into energetic use.

Of the above-named fossil resources, petroleum derivatives and natural gas can be replaced by renewable methane, hydrogen or methanol from PtG/PtL, by producing synthesis gas from $H_2$ and $CO_2$. By means of synthesis processes, this synthesis gas is transformed to higher-valence hydrocarbons (alkenes, paraffin waxes, polymers), which in turn are the base for a number of different chemical raw materials. This makes numerous applications, such as the production of alcohols, synthetics, and lubricants, as well as cosmetics and medicine, accessible to wind and solar energy. Another option is the synthesis of hydrogen and nitrogen to fertilizers, which have been produced in an electricity-based electric arc process before the Haber-Bosch process was used (▶ Sect. 8.1).

Shares of coal that is used today can be substituted with renewable resources (mainly ligneous biomass). ◘ Table 5.4 shows the non-energetic consumption in the chemical industry in a greenhouse gas neutral Germany, as in [17].

**◘ Table 5.4** Non-energetic consumption of renewable resources in chemical industry in a greenhouse gas neutral Germany in 2050, as in [17]

| Energy carrier | | Amount in Mt |
|---|---|---|
| Renewable resource | | 3.6 |
| Renewable resource | Methane | 18.3 |
| | Charcoal | 0.1 |
| **Total** | | **22** |

### 5.6.2 Necessary PtX Capacities for the Chemical Industry

The need for renewable resources in the chemical sector and, thus, the necessary storage capacity for PtX can be deduced from ◘ Table 5.4. Energy demand makes up 96% or 282 TW h of the overall demand which will be supplied by renewable methane (PtG). The other 4% are renewable resources and, therefore, almost climate-neutral.

For the years 2023 and 2033, [16] assumes the growth to be a linear one between 2009 (237 TW h) and 2050 (282 TW h). Comparable to the transport sector (▶ Sect. 5.5.4), the storage demand is within a bandwidth, the limits of which are deduced from a conservative and a progressive development: in 2023, 0.5–5% of all chemical resources will be produced renewably, in 2033 it will be 5–30%, and in 2050 it will be 30–96%.

The electrical energy demand needed to produce the above-named percentages of renewable resources results from the efficiency of PtX for the respective reference years (▶ Sect. 5.5.4.1).

The demand for renewable electricity for decarbonization can be determined to be 350 TW h/a, if an average efficiency of 80% is assumed for PtX and hydrogen is assumed to be used as the starting material of many chemical products.

Using the number of full-load hours, respective capacities can be determined, which allows the calculation of the development potential of PtX in the chemical industry (◘ Fig. 5.11).

Three-hundred-and-fifty TW h of electricity corresponds to about half of the German gross power consumption. How this enormous amount of energy is to be provided, is a question that cannot be answered yet. Considering climate change however, the necessity of decarbonization becomes clear (▶ Chap. 1). In this area, new approaches have to be found, such as those described in ▶ Sect. 8.8 (usage of remote

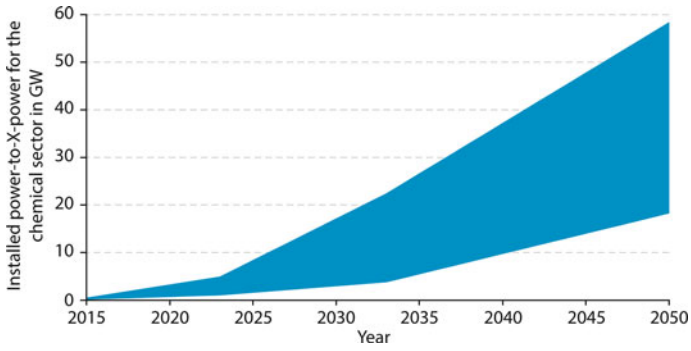



**Fig. 5.11** Bandwidth of the development of PtX capacities in the chemical industry [16]

hydropower, geothermal energy, and offshore wind power).

Along with the results concerning storage demand in the power and transport sector (▶ Sects. 3.7.2.7 and 5.5.4.3) the necessary PtX capacities in Germany can be calculated for the reference years as shown in Table 5.5. Necessary measures for the development of this technology is outlined in ▶ Chaps. 8, 12, 13, and 14.

## 5.7 Summary

In order to achieve the ambitious goals in the transport sector as well as cross-sectoral goals concerning climate and energy policy, there are a **huge number of technologies and energy carriers** available to choose from. Across all transport carriers, it is very important to **increase the drive's efficiency** in order to reduce final energy consumption until 2050 by 40% of the amount needed in 2005. It is only possible to reduce the average $CO_2$ emissions of car registrations to **95 g** by 2021 if the drive train is **progressively electrified**. In **air and shipping traffic, national solo actions are not possible** because of the persistent, international fuel infrastructure. The following developments are expected in particular:

- **Mobility Demand**
  - **Passenger traffic volume** remains almost **static**, and is mostly based on demographic change.
  - **Freight traffic volume increases significantly** and is tightly **connected to economic developments**; efficiency improvements are canceled out by the increased demand.
- **Energy Mix**
  - It is expected that **drive concepts will grow more diverse** in the road traffic of the fu-

**Table 5.5** Bandwidth of the necessary installed capacity of PtX in the power, transport, and chemical sector for the reference years 2023, 2033, and 2050 [16]

| | Installed capacity of PtX in GW | | | | | |
|---|---|---|---|---|---|---|
| | 2023 | | 2033 | | 2050 | |
| | Min | Max | Min | Max | Min | Max |
| Power sector | 0 | 0 | 0 | 0 | 0 | 8 |
| Transport sector | 0.8 | 12 | 8.1 | 57 | 22 | 75 |
| Chemical sector | 1 | 4.9 | 3.7 | 22 | 18 | 59 |
| **Total** | **1.8** | **17** | **12** | **80** | **41** | **141** |

ture, with a step-by-step **electrification of the drive train**.
- The **basis of energy carriers**, which is mostly fossil fuels today, is **gradually being expanded**, which will lead to a **tighter interlocking and stronger integration of the power and transport sector**.
- **Fossil energy consumption**, especially **gasoline**, will decline significantly; **Kerosene** for air traffic and **diesel** for freight traffic and machinery will **remain almost static**.
- **E-mobility on the basis of renewable energy** leads to the most notable **efficiency gains**.
- **Biofuels** are important in the areas of **machines, long-distance mobility**, and **air traffic**, but their **potential is too small** to supply the entire fuel demand.
- **Synthetic fuels** will become **crucial** for reaching climate goals and are of special importance to **freight traffic, machines, shipping, and air traffic**.
- The **introduction of renewable energies** to the fuel area will be the **greatest challenge** in comparison with the other energy sectors.

## Paradigm Change

- **Electricity** will become **primary energy**, including within the transport sector.
- Electrification of mobility is effected by the **hybridization** and **synthetic fuels**.
- The gradual **hybridization of the drive train** from micro-hybrid to fully electrical vehicles is not limited to **cars**, but includes **trucks** and **buses via overhead wires** as well as the **expansion of electric rail traffic**.
- **Biofuels** will, in spite of second and third generations, **not suffice** to meet the fuel demand, and therefore should **be used strategically only**.
- **Synthetic fuels** will surpass the limited potential of biofuels and represent **another form of electrification** of the transport sector.
- E-mobility and **hydrogen** require **new infrastructures** for transport and distribution.
- There is a **renewable alternative or concept for every kind of drive**.

## Storage Demand in the Transport Sector

- **Conventional storage demand** will decrease as **fossil energy carriers decline**, because a growing amount of **ambient energy** will be directly fed into transport via **'solar'**, **renewable mobility**, and an **electrification of drive trains**.
- **Biofuels** will require **storage capacities** unless the combustible is directly integrated into mineral oil infrastructure.
- **Electric vehicles** can efficiently provide a **huge percentage of traction energy** with **renewable electricity**. If 30% of the traffic volume is provided by BEVs, the amount of electricity needed is (depending on design) about 60 TW h/10% of today's gross power consumption. Thus, **power consumption will not increase significantly** because of the introduction of e-mobility. Assuming one charging cycle per day, a storage demand in the form of a battery capacity of about 150 GW h will arise.
- It is virtually **mandatory to coordinate the charging of BEVs with renewable energy supply** to **avoid** additional **grid load** and **grid expansion**. If integrated into **DSM**, all electric vehicles together will provide a **useful system flexibility** for the **power sector** in the middle and long-run. This flexibility can, therefore, **decrease the short-term storage demand**.
- **Synthetic fuels** are needed as **substitutes for fossil fuels**, which are in use for applications with high requirements to energy density. Supplying 40% of the energy needed in transport, an **enormous additional electricity demand** amounting to about 150 TW h will arise.
- The contribution of direct and indirect usage of electrical energy as fuel for **climate protection** is mainly subject to the increas-

ing **power generation from renewable energies** in the power sector.

- If the **transport sector is completely decarbonized by 2050**, there is an **additional demand for renewable electricity** for synthetic fuels which results in an additional **PtX capacity amounting to 22–75 GW**, depending on the power source.

### Storage Demand in the Chemical Industry

- The **decarbonization of the chemical industry** will require the **transition of fossil to renewable resources**.
- **Today**, the **non-energetic consumption of fossil resources for material use makes up 4%** of the overall deposits of fossil combustibles and resources.
- The **sustainable potential of biomass is not sufficient** to form the basis of resources needed for the chemical industry.
- The **transformation of cheap and area efficient wind and solar energy** to chemical resources **via PtX** will become **necessary in the course of decarbonization**.
- If the **growth in chemical industry remains at 0.7%/a**, the **power demand for PtX may** increase **up to 350 TW h at an installed capacity of ca. 60 GW**. This is around **half of Germany's power consumption**.
- The **supply of additional electricity** for PtX is a **challenge for which first approaches have been found**.
- **PtX and PtG are not** only **mere electricity storage technologies**, they are **also needed in the transport and chemical sector**. For these reasons, it seems that the introduction of these technologies is mandatory.

## References

1. Agora Energiewende (2013) Die Energiewende im Stromsektor 2013: Erzeugung, Verbrauch, Erneuerbare Energien und CO2-Emissionen. Berlin
2. Arbeitsgemeinschaft Energiebilanzen e.V. (2012) Auswertungstabellen zur Energiebilanz für die Bundesrepublik Deutschland 1990 bis 2011. Berlin (Berechnungen auf Basis des Wirkungsgradansatzes)
3. BMVBS (2013) Die Mobilitäts- und Kraftstoffstrategie der Bundesregierung (MKS). Energie auf neuen Wegen, Berlin
4. BMWi, BMU (2010) Energiekonzept für eine umweltschonende, zuverlässige und bezahlbare Energieversorgung. Berlin
5. EU (2011) Weißbuch. Fahrplan zu einem einheitlichen europäischen Verkehrsraum – Hin zu einem wettbewerbsorientierten und ressourcenschonenden Verkehrssystem. Brüssel
6. EU (2014) A policy framework for climate and energy in the period from 2020 to 2030. Brussels
7. IATA (2009) Carbon-Neutral Growth by 2020. Bold Industry Commitment on Environment, Kuala Lumpur
8. ifmo (2010) Zukunft der Mobilität. Szenarien für das Jahr 2030 ; zweite Fortschreibung, 1st edn. BMW Verlag, München (ifmo-Studien)
9. Kalinowska D, Krähe M, Rumpke C (eds) (2012) Verkehr. Energie. Klima. Alles Wichtige auf einen Blick, 1st edn. Deutsche Energie-Agentur GmbH (dena), Berlin
10. Kirchner A, Matthes FC (2009) Modell Deutschland. Klimaschutz bis 2050: Vom Ziel her denken. Endbericht der WWF Deutschland Studie, Berlin, Basel
11. Nitsch J, Pregger T, Sterner M, Wenzel B (2012) Langfristszenarien und Strategien für den Ausbau der erneuerbaren Energien in Deutschland bei Berücksichtigung der Entwicklung in Europa und global. Bundesmin. für Umwelt Naturschutz und Reaktorsicherheit, Berlin (Schlussbericht BMU – FKZ 03MAP146)
12. Pehnt M, Sterner M, Gerhardt N, Lambrecht U (2012) Fahrplan Energiewende
13. Schlesinger M, Lindenberger D, Lutz C (2010) Energieszenarien für ein Energiekonzept der Bundesregierung Projekt Nr. 12/10. Basel, Köln, Osnabrück, Berlin
14. Steiger W (2012) Rahmenbedingungen zukünftiger Mobilität - Strategie des Volkswagenkonzerns. VDI Bezirksgruppe Ingolstadt 2012/13 in Kooperation mit der Hochschule Ingolstadt AutoUni/VDI Braunschweiger Bezirksverein e.V., Ingolstadt (Seminarreihe)
15. Sterner M, Schmid J, Wickert M (2008) Effizienzgewinn durch erneuerbare Energien – der Primärenergiebeitrag von erneuerbaren Energien. Brennst Wärme Kraft 2008(06):60 (Springer VDI Verlag)
16. Sterner M, Thema M, Eckert F, Moser A, Schäfer A, Drees T, Rehtanz C, Häger U, Kays J, Seack A, Sauer DU, Leuthold M, Stöcker P (2014) Stromspeicher in der Energiewende. Untersuchung zum Bedarf an neuen Stromspeichern in Deutschland für den

Erzeugungsausgleich, Systemdienstleistungen und im Verteilnetz. Berlin (Studie)
17. UBA (2014) Treibhausgasneutrales Deutschland im Jahr 2050, Dessau-Roßlau. http://www.umweltbundesamt.de/publikationen/treibhausgasneutrales-deutschland-im-jahr-2050-0
18. VDE ETG (2011) Stromübertragung für den Klimaschutz. Potenziale und Perspektiven einer Kombination von Infrastrukturen. VDE-Studie, Frankfurt am Main (Gesamttext)
19. WBGU (2008) Welt im Wandel: Zukunftsfähige Bioenergie und nachhaltige Landnutzung. WBGU, Berlin (Hauptgutachten 2008)
20. Zimmer W (2013) RENEWBILITY II Szenario für einen anspruchsvollen Klimaschutzbeitrag des Verkehrs. Umweltforschungsplan des Bundesministeriums für Umwelt, Naturschutz und Reaktorsicherheit Nachhaltige Mobilität und Immissionsschutz. Öko-Institut e.V, Freiburg

# Technologies for Energy Storage

Contents

Chapter 6 Electrical Energy Storage – 191

Chapter 7 Electrochemical Energy Storage Systems – 227

Chapter 8 Chemical Energy Storage – 325

Chapter 9 Mechanical Energy Storage – 483

Chapter 10 Thermal Energy Storage – 563

Chapter 11 Load Management as an Energy Storage System – 611

Chapter 12 Comparison of Storage Systems – 637

# Electrical Energy Storage

*Ingo Stadler*

**6.1 Capacitors—Supercaps – 192**
6.1.1 Fundamental Features of a Capacitor – 192
6.1.2 From Capacitor to Double-Layer Capacitor – 195
6.1.3 Charging and Discharging – 199
6.1.4 Losses, Efficiency, and Other Characteristic Values – 205
6.1.5 Service Life – 209
6.1.6 Applications – 212

**6.2 Superconducting Electromagnetic-Energy Storage Systems – 214**
6.2.1 Principles of Superconduction – 214
6.2.2 Superconducting Electromagnetic Energy Storage (SMES) System – 216

**6.3 Summary – 224**

**References – 224**

**Electronic supplementary material** The online version of this chapter (https://doi.org/10.1007/978-3-662-55504-0_6) contains supplementary material, which is available to authorized users.

© Springer-Verlag GmbH Germany, part of Springer Nature 2019
M. Sterner, I. Stadler (Eds.), *Handbook of Energy Storage*, https://doi.org/10.1007/978-3-662-55504-0_6

**Overview**

The **technologies** used for energy storage are **highly diverse**. The third part of this book, which is devoted to presenting these technologies, will involve discussion of **principles** in **physics**, **chemistry**, **mechanical engineering**, and **electrical engineering**. However, the **origins** of energy storage lie rather in **biology**, a form of storage that is referred to as 'chemical-energy storage'. **Solar energy** is stored in the form of chemical compounds in **hydrocarbons** that **release energy** when **combusted**. The **fossil potential** of chemical-energy storage systems is **dwindling**, however, the sustainable potential for **biomass** is **limited** (see ▶ Chaps. 1 and 2).

To achieve clean energy transition, **electricity** will become an increasingly important **primary energy source**. The mainstays will be **wind and solar energy**; this fact emerges clearly from the scenarios used to determine storage demand (▶ Chaps. 3 and 5). Because these sources are utilized most economically by generating electricity, **directly storing** energy from these sources in the form of **electrical energy** is an obvious choice.

This chapter will investigate direct electrical energy storage in **capacitors** and **inductors**. This chapter explains the physical and electrical principles underlying both types of energy storage, derives various characteristic values, and describes their function and possible applications.

## 6.1 Capacitors—Supercaps

Energy storage in a capacitor is based on maintaining an electric field in which energy is stored. This section describes the fundamental features of the electric field, including the basic values describing the field. This is followed by a description of a capacitor in general with a subsequent consideration of the special features of the double-layer capacitor.

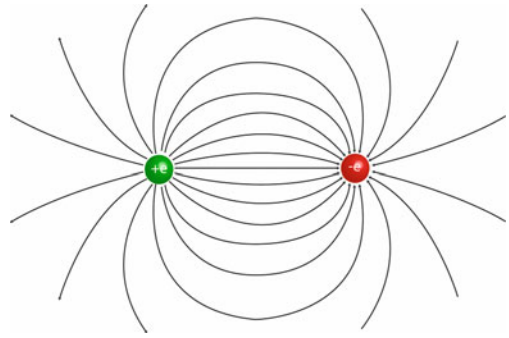



**Fig. 6.1** The electric field $E$ between two charges

### 6.1.1 Fundamental Features of a Capacitor

#### The Electric Field

The French physicist Charles Augustin de Coulomb (1736–1806) studied the force effects of charges. He determined that electrical charges with the same sign repel each other while electrical charges without the same sign attract. Charges thus exert a force on one another and force lines are used to illustrate this effect by indicating the value and direction of the force in space. As a whole, they describe the electric field $E$ (Fig. 6.1).

By definition, the field lines start on positive charges and end on negative charges. $e$ denotes the elementary charge,

$$e = 1.602 \times 10^{-19}\,\mathrm{C}, \tag{6.1}$$

which refers to the smallest possible charge quantity. A + or − symbol indicates the polarity or the sign. The C in Eq. 6.1 is the unit of charge, named after the physicist Coulomb:

$$1\,\mathrm{C} = [\mathrm{A\,s}] = 1\ \text{coulomb}. \tag{6.2}$$

The force exerted by the charges increases with an increasing number of charges; that is, it is proportional to the quantity of charge. However, the force declines as the distance from the charges increases. The electric field is therefore

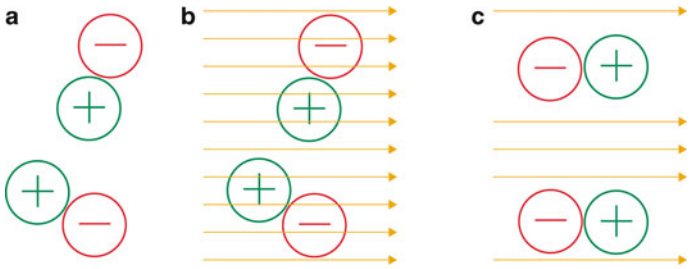



**Fig. 6.2** **a** Dipole in space, **b** effect of an external electric field, **c** aligned dipoles which weaken the external electric field

defined as follows:

$$\vec{E} = \frac{\vec{F}}{Q} = \left[\frac{\mathrm{V\,A\,s}}{\mathrm{m \cdot C}}\right] = \left[\frac{\mathrm{V}}{\mathrm{m}}\right]. \tag{6.3}$$

The unit volt [V] in Eq. 6.3 refers to the electrical voltage $U$:

$$U = \left[\frac{\mathrm{J}}{\mathrm{C}}\right]. \tag{6.4}$$

It indicates the energy of each charge and, therefore, characterizes the potential work done by each unit of charge. Accordingly, it can be considered to be the cause of the current.

### ▪ Material Dependency—Dielectrics

The propagation of the electric fields and the force per charge associated with this propagation are dependent on the material. Of special importance in this regard are non-conducting materials; that is, materials with high resistance, which are also referred to as dielectrics. These materials weaken electric fields by forming dipoles. A dipole refers to a pair of charges which can be displaced or aligned but which are otherwise stationary. This means that they cannot move freely and there is no flow of current as a result. If an external electric field acts on the dipoles, they align themselves and generate an 'opposing field' in the process, which counteracts the original external field (Fig. 6.2).

The influence exerted on the field by the dielectric material is taken into account using a parameter called the permittivity $\varepsilon$ (from the Latin word 'permittere'—allow, let through). The permittivity is made up of two factors:

$$\varepsilon = \varepsilon_0 \cdot \varepsilon_r = 8.854 \times 10^{-12}\,\frac{\mathrm{A\,s}}{\mathrm{V\,m}} \cdot \varepsilon_r. \tag{6.5}$$

$\varepsilon_0$ is the absolute permittivity, relative to a vacuum. It describes to some extent the permeability of the vacuum to electric fields. The factor $\varepsilon_r$ is a dimensionless parameter. This means that the permittivity of materials for electric fields is always a multiple of that for a vacuum. $\varepsilon_r$ is the relative permittivity and has a value greater than, or equal, to 1. Some values for $\varepsilon_r$ are shown in Fig. 6.3.

The permittivity is linked to the electric field by the electric flux density:

$$D = \frac{Q}{A} = \left[\frac{\mathrm{A\,s}}{\mathrm{m}^2}\right]. \tag{6.6}$$

The flux density $D$ is the charge displacement for a certain area in space that was generated by the charges of the 'original field'. The complete relationship is shown in Eq. 6.7:

$$D = \varepsilon_0 \varepsilon_r E = \varepsilon E. \tag{6.7}$$

### ▪ Capacity C

The charge storage is expressed by the capacitance:

$$C = \frac{Q}{U} = \left[\frac{\mathrm{A\,s}}{\mathrm{V}}\right] = 1\ \text{farad}. \tag{6.8}$$

This indicates the relationship between the charge $Q$ and the voltage $U$. The capacitance is also used to describe capacitors, the circuit elements used to store electrical charge. It should be noted here that capacitance is associated not only with capacitors but it is also present in overhead lines and cables, and anywhere that different voltages are separated by a non-conducting material.

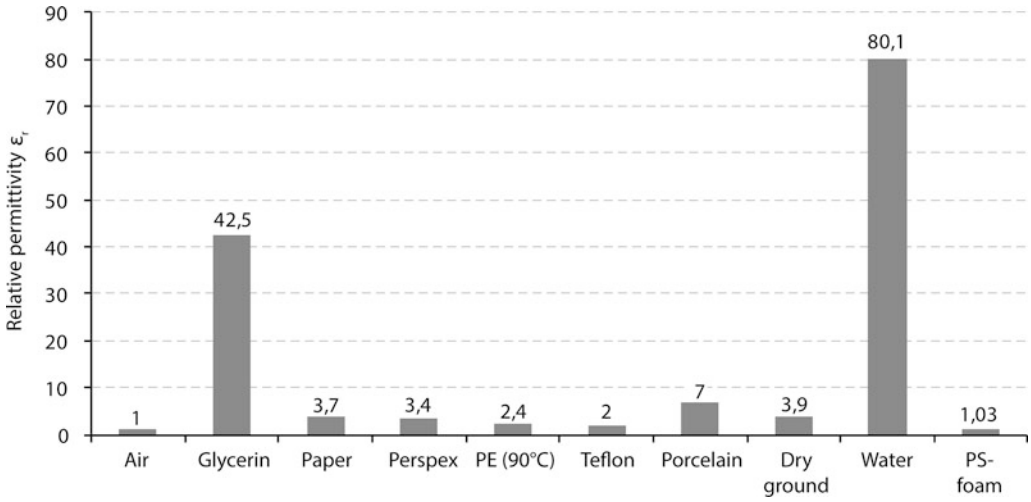



**Fig. 6.3** Values for the relative permittivity of selected materials

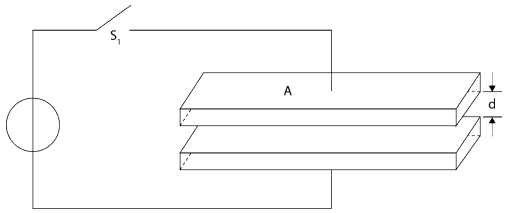



**Fig. 6.4** The parallel plate capacitor made up of two plates of area $A$, separated by distance $d$, connected to a power supply via a switch $S_1$

## Capacitors

A capacitor is an arrangement of two opposing electrodes that are separated by a non-conducting material. The physical relationships are explained using the example of a parallel plate capacitor (Fig. 6.4).

The charge $Q$ is first determined using the electric flux density $D$:

$$Q = \int_A D\,da = D \cdot A. \tag{6.9}$$

The electrical voltage $U$ is then determined using the electric field $E$:

$$U = \int_0^d E\,dx = E \cdot d. \tag{6.10}$$

If the edge effects can be ignored ($A \gg d$), a parallel plate capacitor becomes a homogeneous arrangement. This means that for Eqs. 6.9 and 6.10, there are linear relationships. When both equations are substituted into Eq. 6.11, this produces:

$$C = \frac{DA}{Ed}. \tag{6.11}$$

This allows the electric flux density as defined by Eq. 6.7 to be inserted. This produces the capacitance of the parallel plate capacitor:

$$C = \frac{E\varepsilon A}{Ed} = \varepsilon\frac{A}{d}. \tag{6.12}$$

The capacitance of the parallel plate capacitor increases according to Eq. 6.12 as the electrode surface increases and the electrode separation distance decreases. It must be noted here that this is an ideal capacitor and both ohmic and inductive properties of the plates, the leads, and the non-conducting material are not taken into account.

## Energy Stored in a Capacitor

The energy stored in a capacitor is supplied to the capacitor by a power supply. During charging, there is a flow of current to the capacitor.

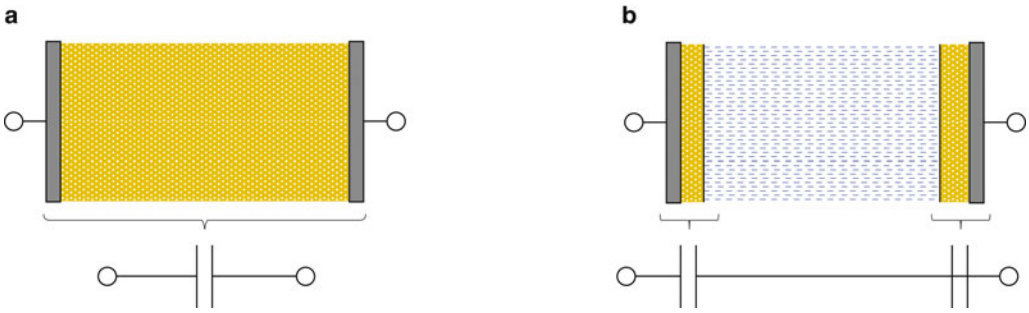



**Fig. 6.5** **a** The 'traditional' capacitor, electrode – dielectric material – electrode; **b** the supercapacitor, electrode – dielectric layer – electrolyte – dielectric layer – electrode

The switch $S_1$ in Fig. 6.4 is closed. The capacitor is charged, with current $i$ and voltage $u$ being time-dependent variables. The change in the energy content $dW$ over a small time interval $dt$ produces:

$$dW = u \cdot i\,dt. \tag{6.13}$$

In this equation, $i \cdot dt$ corresponds to the change in the charge that leads to a change in the voltage $du$:

$$i \cdot dt = C \cdot du. \tag{6.14}$$

For Eq. 6.13, therefore, this yields:

$$dW = C \cdot u \cdot du. \tag{6.15}$$

For the energy content of the capacitor, this yields:

$$W = \int_0^U C \cdot u \cdot du = C \left[\frac{1}{2}u^2\right]_0^U = \frac{1}{2}CU^2. \tag{6.16}$$

The voltage $U$ in this equation is the power supply voltage; that is, the voltage that was applied to the capacitor.

### 6.1.2 From Capacitor to Double-Layer Capacitor

Electrical energy is also stored in a double-layer capacitor by separating charges on two electrodes in an electric field. The essential difference here is the type of non-conducting material used and the arrangement of the individual capacities. Furthermore, the capacitance of the double-layer capacitor is made up of two capacitances:

$$\left[\begin{array}{c}\text{Capacitance of the}\\ \text{supercapacitor}\end{array}\right] = \left[\begin{array}{c}\text{double-layer}\\ \text{capacitance}\end{array}\right] + \left[\begin{array}{c}\text{pseudo-}\\ \text{capacitance}\end{array}\right].$$

The double-layer capacitance makes up about 90% of the overall capacitance and the pseudocapacitance makes up about 10% [22]. The capacitance therefore is not produced solely by the double-layer. The term supercapacitor (or supercap) is therefore desirable. The difference between the traditional capacitor, which is also referred to as an electrostatic capacitor, and the supercapacitor is clarified in Fig. 6.5.

#### 6.1.2.1 Double-Layer Capacitors

If an electrode is immersed in an electrolyte (an electrolyte is a substance that, as an aqueous solution, conducts electricity better than pure water [18]), a chemical reaction occurs that results either in the loss of electrons from the electrode into the solution or uptake of electrons from the solution into the electrode. Both cases generate a potential difference (potential is the capacity to have something compared to a reference value; in this case a voltage potential $\phi$ in V). In the first case (the loss of electrons), the elec-

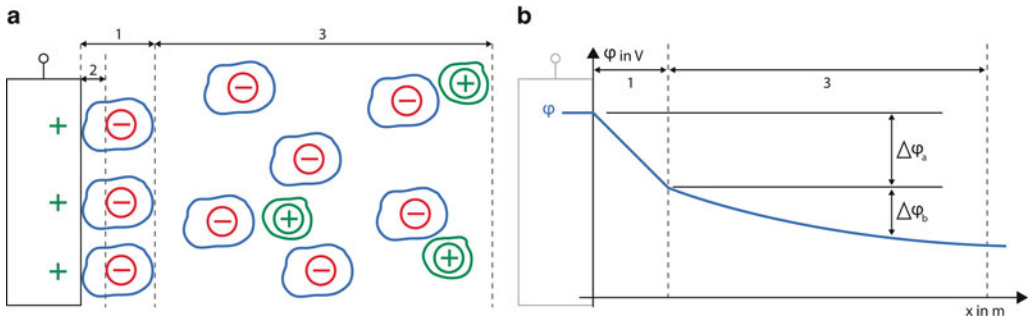



**Fig. 6.6** **a** Solvated electrons in the rigid (1) and diffuse (3) double-layer. (2) shows the inner Helmholtz plane; **b** the change in the electrical potential in the rigid and diffuse double-layer. $\phi_a$ is the linear potential drop in the rigid double-layer and $\phi_b$ is the exponential potential drop in the diffuse double-layer



trode develops a positive charge compared to the solution (the electrolyte). The electrons released from the electrode undergo hydration in the electrolyte. This process involves particles dissolved in water (the electrons in this case) becoming enveloped by water molecules due to attractive forces [18]. The enveloped electrons now attempt to get as close as possible to their opposing charges (the positive electrode). They are kept a certain distance from the electrode as a result of their hydration sheath. This is the electrochemical or Helmholtz double-layer, named after its discoverer, Hermann von Helmholtz (1821–1894).

The arrangement of the solvated electrons, referred to subsequently as anions, depends on the thermal movement of the molecules. In this way, the rigid double-layer was initially replaced by the diffuse double-layer. According to the model developed by Otto Stern (1888–1969), the actual arrangement of the electrochemical double-layer is made up of both the rigid and the diffuse-layer. The double-layer capacitance is accordingly made up of the electrode (positive charge), the non-conducting material with the radius of the solvation sheath, and the electrons (negative charge bearers) in the solvation sheath.

### 6.1.2.2 Pseudocapacitance

The second capacitance that contributes to the overall capacitance of the supercapacitor is the pseudocapacitance (Fig. 6.7). Neutral molecules from the electrolyte, water dipoles, or corresponding ions are adsorbed by the electrode as a result of van der Waals forces (forces between molecules that link them to one another in solids and liquids [1]). This can subsequently lead to a redox reaction (the transition of an electron from one material or one species to another material [1]). This also contributes to the capacitance. Because this is a chemical reaction, however, this contribution to the overall capacitance is referred to as pseudocapacitance.

### 6.1.2.3 Determining the Capacitance

The capacitance of a double-layer is produced almost exclusively by the rigid Helmholtz plane for a concentrated electrolyte solution (high number of dissolved electrons in the electrolyte). With a solvation sheath radius of about 0.2 nm and an $\varepsilon_r$ of 80.1 for the solvation sheaths, most of which are made up of water according to [9], this produces a specific capacitance of about 355 µF/cm$^2$ for each individual capacitance in Fig. 6.5b. The actual capacitance values are, however, in the order of 5–50 µF/cm$^2$ [9]. This are two major reasons for this:

The alignment of the dipole is affected by the solvated ions. This leads to a value for $\varepsilon_r$ that is actually only between six and 30 [9].

The overall capacitance for the rigid Helmholtz plane is made up of the capacitance of the inner and the outer Helmholtz planes combined. They, therefore, form a series cir-

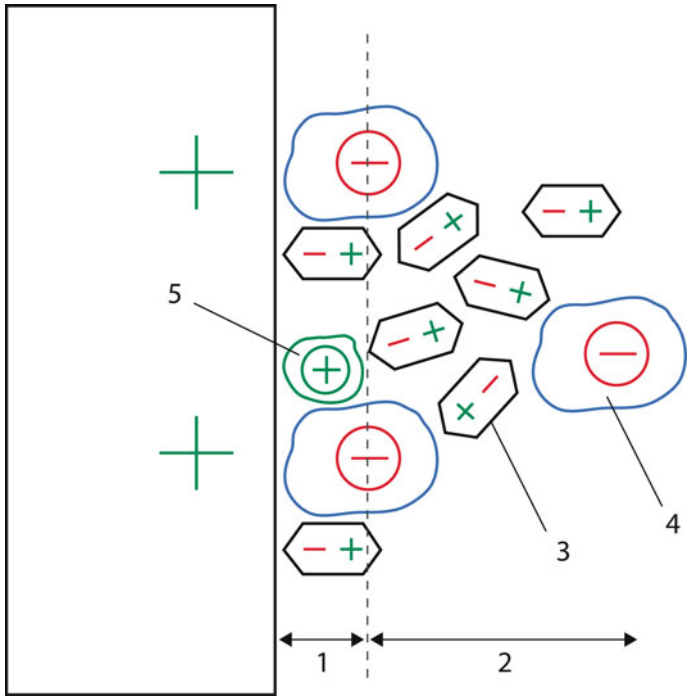



**Fig. 6.7** The electrochemical double-layer, divided into the (1) inner and (2) outer Helmholtz planes, (3) water dipoles, (4) solvated ions (electrons), (5) adsorbed ion

cuits made up of two capacitances. The overall capacitance is described by Eq. 6.17.

$$\frac{1}{C_{\text{tot}}} = \frac{1}{C_1} + \frac{1}{C_2} + \ldots + \frac{1}{C_n}. \qquad \textbf{(6.17)}$$

This overall capacitance $C_{\text{tot}}$ is less than the smallest individual capacitance. Because the double-layer involves two capacitances in a series circuit, Eq. 6.17 can also be expressed in the following way:

$$C_{\text{tot}} = \frac{C_{\text{inner}} \cdot C_{\text{outer}}}{C_{\text{inner}} + C_{\text{outer}}}. \qquad \textbf{(6.18)}$$

Nevertheless, supercapacitors do have high capacitance values. This is due in part to the electrode material used. A very porous activated carbon is used in this example. It has the property of forming, not a smooth, but a rather 'bumpy' surface structure which creates a very large surface area. For the simplest case of a series circuit, this produces four capacitances of which two capacitances form a double-layer, and both double-layers together in turn form the capacitor.

A larger surface area has a positive effect on the capacitance (Eq. 6.12). For the capacitance $C$, which depends on the surface area $A$ and the distance $d$ between two surfaces, this means an increase in the surface area leads to an increase in the capacitance. Activated carbon also has very good adsorption properties which leads to a high pseudocapacitance (Fig. 6.8). One gram of activated carbon has a surface area of 300–2,000 $m^2$ [11].

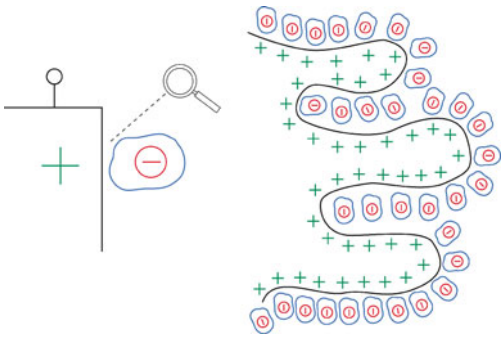


**Fig. 6.8** Surface structure of the activated carbon electrode

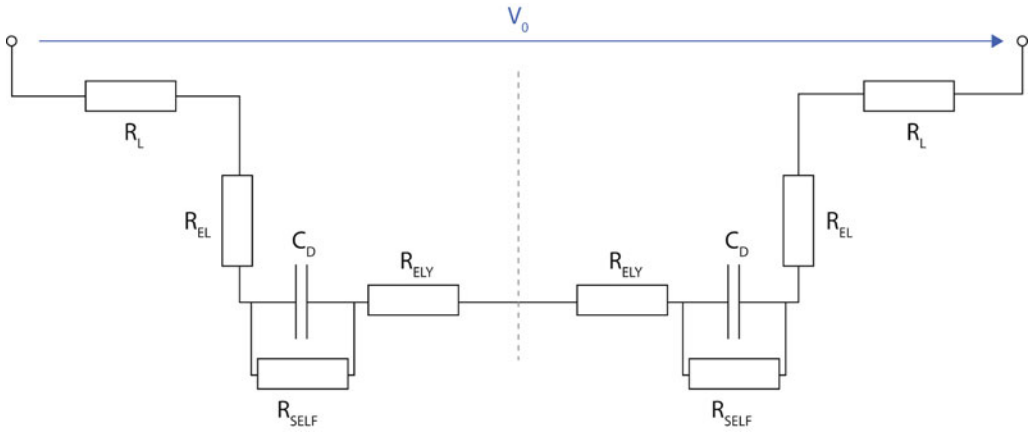



**Fig. 6.9** Equivalent circuit of the supercapacitor. $R_L$ – lead resistance, $R_{EL}$ – electrode resistance, $C_D$ – double-layer capacitance, $R_{ELY}$ – electrolyte resistance, $R_{SELF}$ – phase transition resistance (self-discharge), *dashed line* – separator

Figure 6.9 shows the equivalent circuit of the supercapacitor with its ohmic losses in the leads, the electrodes, and the electrolytes. The resistance $R_{SELF}$ represents the transition resistance which is responsible for self-discharge (▶ Sect. 6.1.4).

### 6.1.2.4 Structure

Like other capacitors, supercaps have a multi-layered or coiled structure. Rolling up several layers to form a cylinder produces a considerably larger surface area, which has a positive effect on the capacitance (Eq. 6.12). Capacitors can be poled. In this case, the side that forms the negative pole is labeled with a minus sign. Figure 6.10 shows three capacitors for electronic applications. Each of the capacitors shown in the figure is less than 5 cm in size. Note that the middle capacitor in Fig. 6.10, a supercap, has a capacitance of 10 F. This capacitor has a capacitance that is $4.5 \times 10^6$ greater than that of the impulse capacitor shown in the left of the figure, even though they both have approximately the same physical size.

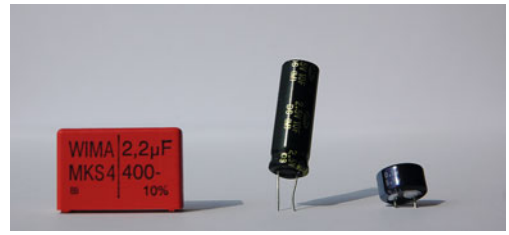



**Fig. 6.10** Various capacitors, from left to right, impulse capacitor 2.2 µF, *supercap* 10 F, *supercap* 0.1 F

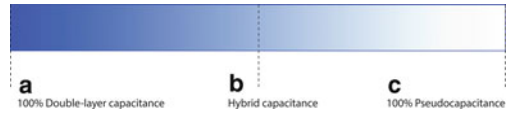



**Fig. 6.11** Schematic for the classification, **a** pure double-layer capacitance, **b** hybrid capacitance, **c** pure pseudocapacitance

#### ▪ Family Structure

The supercapacitor family can be classified on the basis of the underlying storage principle. There are three groups: pure pseudocapacitors, pure double-layer capacitors, and the hybrid capacitors that combine the two storage principles (Fig. 6.11).

A capacitor can be classified on the basis of Fig. 6.11. A capacitor with a pure double-layer capacitance would be located to the far left in Fig. 6.11 under a. A capacitor that uses both storage technologies (double-layer and pseudocapacitance) would be located right in

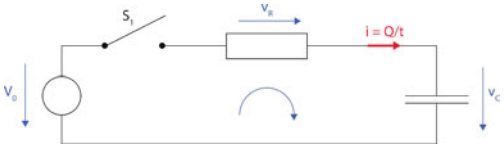



**Fig. 6.12** Simplified equivalent circuit for charging a capacitor. The *curved arrow* indicates the mesh circuit

the middle at b. Both are, however, considered members of the supercapacitor family. There is accordingly a large number of possible combinations – for example, hybrid capacitors can be made up of 70% double-layer capacitance and 30% pseudocapacitance [1, 7, 8, 11–13, 18, 22].

## 6.1.3 Charging and Discharging

Supplying energy to a capacitor is described as charging, while the withdrawal of energy from a capacitor is referred to as discharging. The following section describes the mathematics and behavior of the charging and discharging of capacitors and supercapacitors.

### 6.1.3.1 Charging a Capacitor

According to Fig. 6.12, the capacitor is made up of the ohmic resistance $R$ and the capacitance $C$. The resistance $R$ includes all lead resistances as well as the ohmic fraction of the capacitor.

To charge the capacitor, the switch $S_1$ in Fig. 6.12 is closed at an arbitrary time $t$. The power supply now creates a separation of charge in the capacitor. In the process, electrons move from the upper plate to the lower and current flows $i(t)$. The current changes over time. However, the electrons do not move from the upper plate through the non-conducting material to the lower plate. Instead, they flow through the outer circuit, through the power supply. With each separated charge, a charge pair forms, which in turn forms an electric field as described in ▶ Sect. 6.1.2.1. When the capacitor is fully charged, all charges are separated. There is no further displacement or movement of the charge and the current $i(t)$ is therefore 0. The value is only approximately zero, however. In actual fact, the capacitor can never be fully charged and there is always charge being displaced, even if this is a very small quantity.

#### ■ Change in the Charging Voltage

The change in the capacitor voltage $u_c(t)$ can be determined using the mesh equation. If switch $S_1$ in Fig. 6.12 is closed, for the selected mesh circuit

$$u_R + u_c(t) = U_0 \text{ then applies.} \tag{6.19}$$

The time-dependent voltage $u_R$ through the resistance $R$ can be described by the current $i(t)$, the charge current, which is the same at every point in the closed circuit. The current becomes:

$$i_c = C\frac{du_c}{dt}. \tag{6.20}$$

This now produces the following relationship for Eq. 6.19:

$$RC\frac{du_c}{dt} + u_c(t) = U_0. \tag{6.21}$$

Equation 6.21 is a first-order non-homogenous linear differential equation. The solution for this differential equation is:

$$u_c(ce) = U_0\left(1 - e^{-\frac{t}{\tau}}\right). \tag{6.22}$$

Equation 6.22 assumes that the voltage on the capacitor can assume, at most, the value of the source voltage $U_0$, but never actually reaches this value. The change in the voltage is produced by the change in the exponential function that depends on the time $t$ and on a parameter $\tau$ which is the time constant:

$$\tau = RC = \left[\frac{\text{V}}{\text{A}} \cdot \frac{\text{A s}}{\text{V}}\right] = [\text{s}]. \tag{6.23}$$

The time constant $\tau$ determines the charging time for the capacitor. The change, the shape of the curve, and the rise time for the charging voltage are determined by the term inside the bracketed expression in Eq. 6.22:

$$1 - e^{-\frac{t}{\tau}}. \tag{6.24}$$

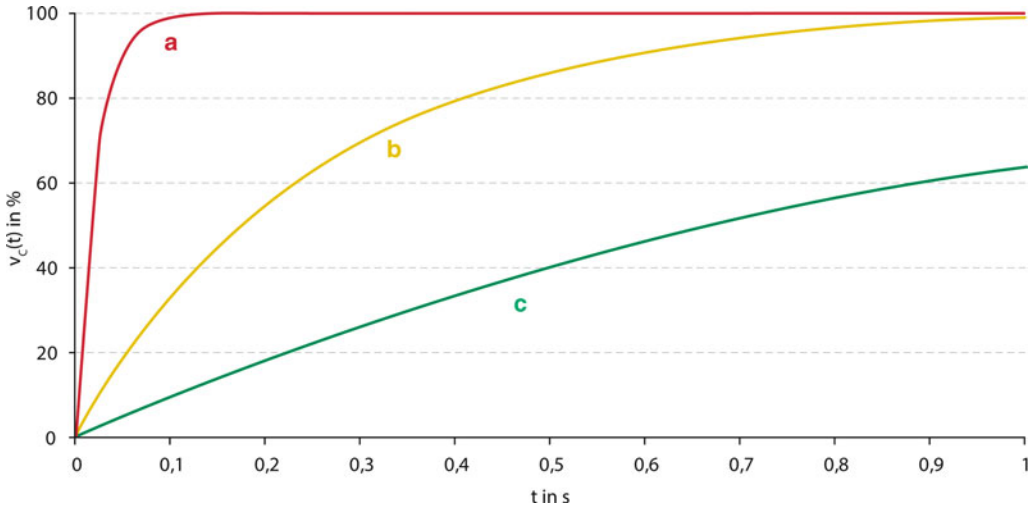



**Fig. 6.13** Capacitor voltage during charging, **a** $\tau = 0.02\,\text{s}$, **b** $\tau = 0.25\,\text{s}$, **c** $\tau = 1\,\text{s}$

For $t$ equals $\tau$, this produces a value of 0.63. The capacitor voltage consequently reaches 63.2% of the source voltage $U_0$ after time $\tau$. Equation 6.24 is shown for different values for $\tau$ in Fig. 6.13. The particular voltage values are produced by multiplying by the maximum possible voltage in each case.

As shown in Fig. 6.13a, the capacitor is fully charged after 0.1 s, whereas for case b, up to one second is required. In all three cases, the capacitance is kept constant and the resistance $R$ is varied, where in case a) it has the smallest and in case c) the highest value. $R$ in case a having the smallest value and case c the highest. Consequently, a low resistance appears desirable because it allows rapid charging. A low resistance leads, however, to a high current $i(t)$, which under some circumstances can lead to excessive temperatures or even destruction of the conductor or the capacitor.

#### ▪ Change in the Charge Current

The charge current of the capacitor is determined using Eqs. 6.20 and 6.22 to give:

$$i_c(t) = \frac{U_0}{R} e^{-\frac{t}{\tau}}. \tag{6.25}$$

The charge current also changes exponentially but has the following special feature: If the switch in Fig. 6.12 is closed, the current $i_c(t)$ for $\lim_{t\to 0}$:

$$\lim_{t\to 0} i_c(t) = \lim_{t\to 0} \frac{U}{R} e^{-\frac{t}{\tau}} = \frac{U}{R}. \tag{6.26}$$

The charge current is limited only by the resistance $R$ shortly after the switching process. Unlike the voltage $u_c(t)$, the current can jump. If there is no other resistance for current limitation in the charging circuit, $R$ in Eq. 6.25 corresponds only to the low ohmic resistance of the capacitor. This can generate large charge current peaks (Fig. 6.14).

Only as the electric field increases or the capacitor current increases does the current reduce, converging on zero. Thus, for the capacitor in the charged state, there is a very high resistance.

### 6.1.3.2 Discharging a Capacitor

To discharge a capacitor, it is separated from the source and connected to a resistor using switch $S_2$ (Fig. 6.15). The resistor can be viewed as a consumer or load. Strictly speaking, this must be referred to as the impedance $Z$, a combination of the elements $R$, $L$, and $C$. To simplify the examination of the discharge behavior, however, it is assumed that this is a purely ohmic resistance.

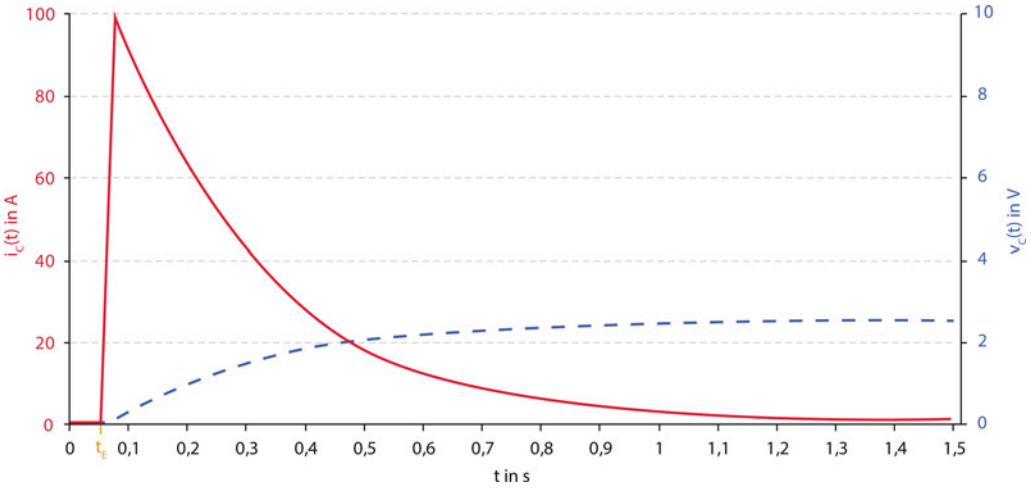



**Fig. 6.14** Charge current for the capacitor after switching on at time point $t_E$. The *dashed line* represents the voltage $u_c(t)$

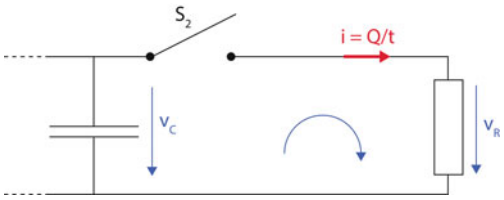



**Fig. 6.15** Equivalent circuit for discharging a capacitor. The *curved arrow* indicates the mesh circuit

If the switch $S_2$ in Fig. 6.15 is closed, the separated charges return to their corresponding counter charges through the resistor. The consequence is a current flow through the load, which in this case is $R$. The voltage that drives the current originates from the electric field of the capacitor. With each charge that is returned, the electric field in the capacitor is reduced. The capacitor voltage correspondingly decreases. When all charges have been returned, the capacitor has shifted from its charged state Fig. 6.16b back to its original state Fig. 6.16a. Again, a minimum residual field or residual voltage is present.

### Change in the Discharge-Voltage

To describe the discharge-voltage, the mesh equation (Kirchhoff's second law) is postulated from the circuit in Fig. 6.15:

$$u_c = u_r \leftrightarrow u_c - u_r = 0. \tag{6.27}$$

The voltage $u_r$ across the load resistance is expressed by the current as defined in Eq. 6.20. Taking into account Eq. 6.27, this yields the following homogeneous linear first-order differential equation:

$$u_c - RC\frac{du_c}{dt} = 0. \tag{6.28}$$

After separating the variables, the solution to the differential equation is:

$$u_c(t) = U_A e^{-\frac{t}{\tau}}. \tag{6.29}$$

The voltage $U_A$ corresponds to the capacitor voltage at time point $t = 0$ at which the switch $S_2$ is closed. This is the voltage that was charged to the capacitor prior to discharging. Equation 6.29 corresponds to a falling exponential function that has the initial value $U_A$. Again, a consideration of the threshold for $t \to \infty$ indicates that, although the capacitor voltage moves towards zero, this value is never actually achieved. A small residual voltage is always present:

$$\lim_{t\to\infty} u_c(t) = \lim_{t\to\infty} U_A e^{-\frac{t}{\tau}} = u_c(t) \to 0. \tag{6.30}$$

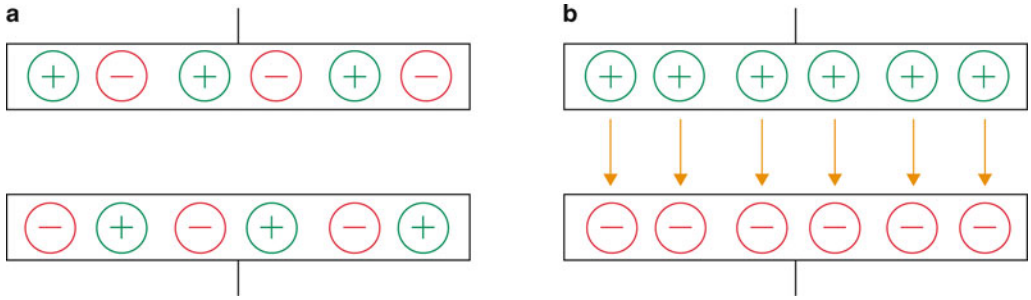



**Fig. 6.16** **a** The uncharged capacitor with the charges randomly distributed, **b** the charged capacitor with the *arrows* indicating the electric field



The time constant $\tau$ corresponds to that from Eq. 6.23. Again, the load resistance $R$ for the specified capacitance $C$ has a critical influence on the discharging behavior, which can be seen in Fig. 6.17.

### Discharge-Current

The discharge-current is produced by applying Eq. 6.20 to the discharge-voltage, Eq. 6.29:

$$i_c(t) = -\frac{U_A}{R} e^{-\frac{t}{\tau}}. \tag{6.31}$$

The discharge-current differs from the charge current in Eq. 6.25 only in the negative sign. There is also a jump in the current here. The current can be limited by increasing the resistance but this leads to a longer discharge time thanks to the higher time constant $\tau$ (Fig. 6.18).

## 6.1.3.3 Charging and Discharging Behavior of Supercapacitors

### Charging Behavior of a Supercapacitor

After applying a voltage to the terminals of the capacitor, the voltage acts on the charges in the metal and the ions in the electrolyte. This causes a displacement in the charge that produces a negative charge on one electrode and a positive charge on the other electrode. Both electrodes attract their corresponding counter

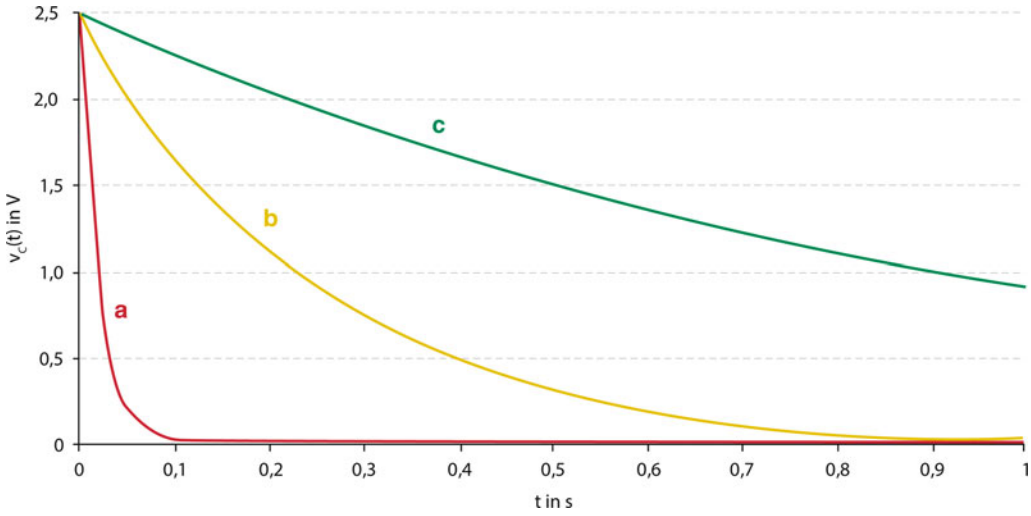



**Fig. 6.17** Capacitor voltage during discharge, **a** $\tau = 0.02$, **b** $\tau = 0.25$, **c** $\tau = 1$

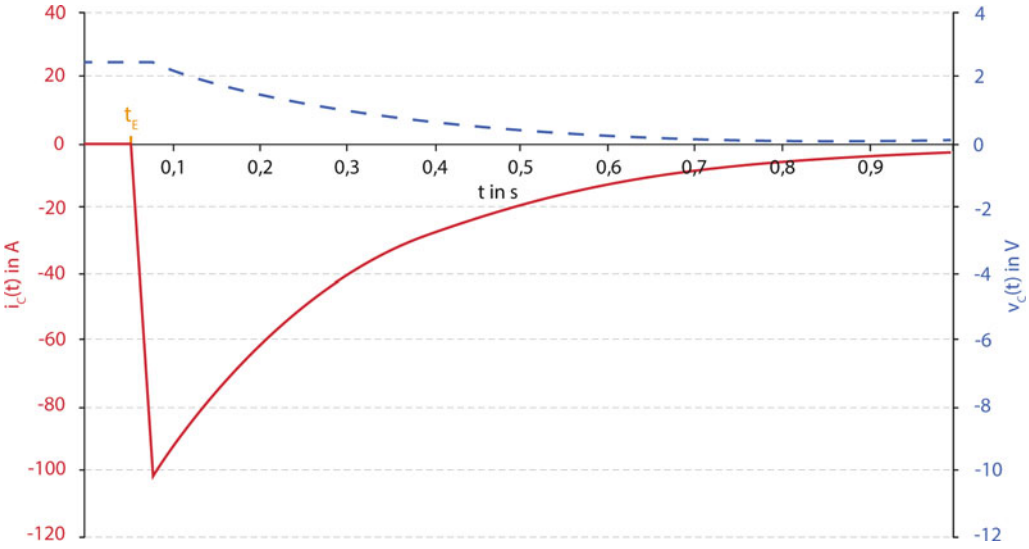



**Fig. 6.18** Change in the discharge-current: The *dashed line* corresponds to the discharge-voltage, $t_E$, at the moment of switching

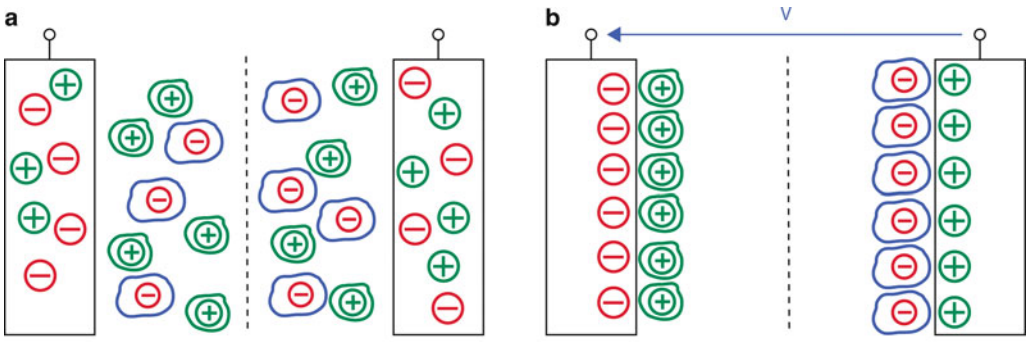



**Fig. 6.19** **a** The uncharged supercapacitor, **b** the charged supercapacitor after applying a voltage

charges in the electrolyte, meaning that the negative electrode (cathode) attracts cations while the positive electrode (anode) attracts the anions. The opposing charges accumulate in the inner and outer Helmholtz plane in front of the electrodes as a result of the solvation sheath. This produces an electric field in which the electrical energy is stored (Fig. 6.19).

The charging behavior of a supercapacitor differs in two aspects from that of a traditional capacitor. To illustrate these differences requires a closer examination of the equivalent circuit (Fig. 6.20).

The capacitance of the supercapacitor is formed from a number of individual capacitances that are located after the particular lead resistance of the electrode. The network also includes many small transition resistances in the Helmholtz plane and the electrolyte. The further the capacitance is located from the terminals, the greater the time constant $\tau$. This leads to the downstream capacitances discharging slower than the upstream capacitances. This produces a slight deviation in the charging curve from the ideal capacitance and a prolongation of the charging time.

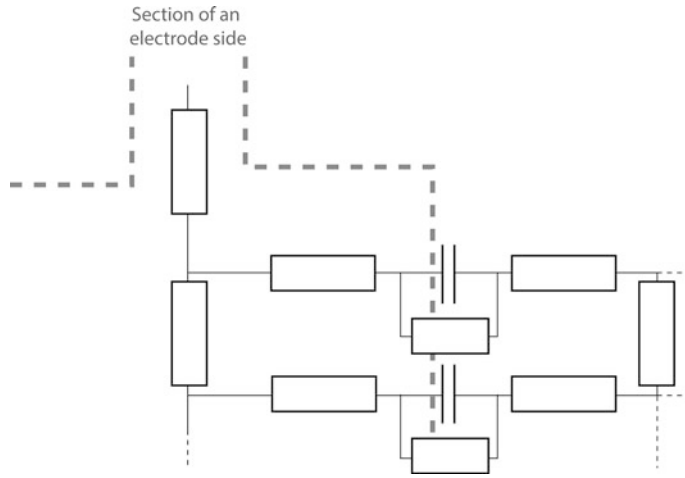



**Fig. 6.20** Expanded equivalent circuit of a supercapacitor, single electrode

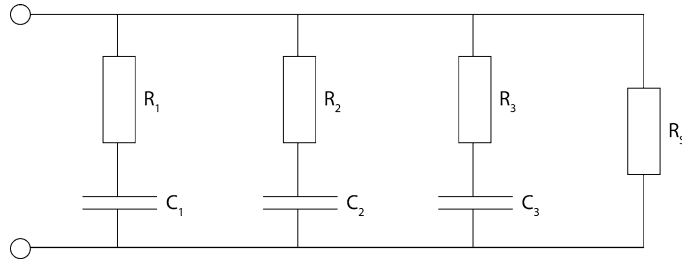



**Fig. 6.21** Simplified equivalent circuit adapted from the 'three-branch model' (see [6]). Each capacitance $C$ has a greater time constant $\tau$ than the previous one, $\tau_1 < \tau_2 < \tau_3$. The resistance $R_{SE}$ describes the self-discharge



## Rapid Charging Processes

If a supercapacitor is rapidly charged or discharged, a considerable voltage difference can develop once the charging or discharging process is completed. The expanded equivalent circuit from Fig. 6.20 or the simplified equivalent circuit from Fig. 6.21 are used by way of explanation (there are several equivalent circuit diagrams available for supercapacitors based on the objectives of the modeling).

The simulated process is shown in Fig. 6.22. The supercapacitor is connected to the power supply at time point 0 and charged. At time point $t_1$, the power supply is removed and the terminals of the capacitor remain open. The actual voltage curve drops as a result of the recharging. Between time point $t_2$ and time point $t_3$ the capacitor is discharged. From this point the voltage would have to remain at the discharge value, but as a result of recharging, the voltage increases again.

Rapid discharging by connecting a load resistance leads to the capacitance $C_1$ being the first to discharge completely. The voltage that can be measured at the terminals is 0 at this point because a mesh made up of load resistance $R_V$, $R_1$, and $C_1$ does not produce a voltage when 'discharged'. $C_1$ is the only 'power supply'. After removing the load, a voltage is once again measured. This is the result of recharging the capacitances with one another. Because the last capacitances are only slowly and incompletely discharged, the charges are redistributed. This means that $C_1$ is partly recharged by $C_2$ and $C_3$. This process can also occur during charging. Rapid charging would lead to only $C_1$ being completely charged. After removing the charging voltage, $C_1$ would re-

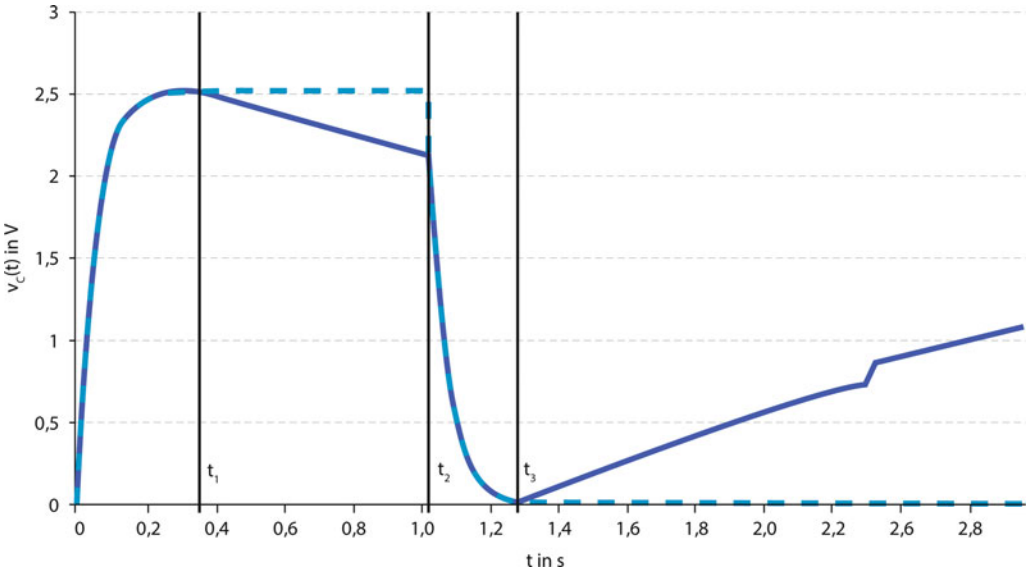



**Fig. 6.22** Simulated charging and discharging curves; $t_1$ is the end of the charging, $t_2$ is the start of the discharging, $t_3$ is the end of the discharging

lease part of the charge to $C_2$ and $C_3$. As a result, there is a voltage drop at the terminals.

### Actual Charging/Discharging Curves

Figure 6.23 shows complete charging and discharging of a supercapacitor of size 10 F to a voltage of 2.5 V. The capacitor is charged through a resistance from a power supply and then discharged through the same resistance. The voltage peaks at each of the switch time points result from 'switch bounce'. The contacts of the mechanical switch do not close fully but instead remain slightly separated and then close again until a conducting contact junction is produced. This can lead to high-voltage jumps. The charge current is limited to 2.5 A due to the step input.

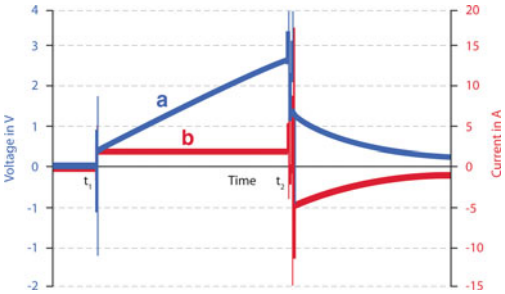



**Fig. 6.23** Charging/discharging-curve of a supercapacitor 10 F, 2.5 V, **a** voltage, **b** current, axis scale 1 V/div, 5 A/div. $t_1$ indicates the start of charging and $t_2$ indicates the start of discharging. The bounce effect can be seen at each of the switching times

## 6.1.4 Losses, Efficiency, and Other Characteristic Values

In a real capacitor, energy cannot be stored for an unlimited period. The energy provided upon discharging is less than the energy supplied to the capacitor. The following section discusses the losses that arise as well as the resultant efficiency.

### Causes of Energy Losses in a Real Capacitor

When considering the capacitor as a real element in a circuit, the resistance of the terminals, the electrodes, and the electrolyte must be taken into account. The inductance of the connecting leads and the conductance of the di-

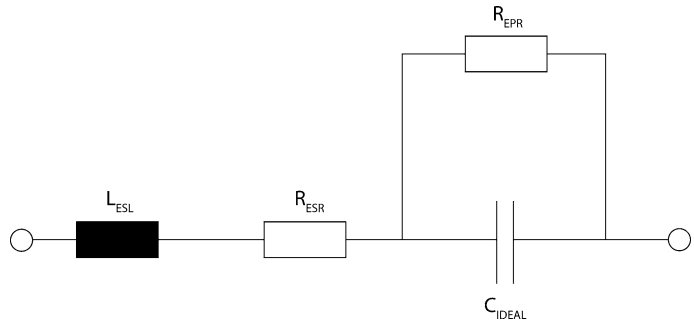



**Fig. 6.24** Equivalent circuit for a capacitor adapted from DIN EN 60384-1 [5], $L_{ESL}$: *Equivalent Series Inductivity*, $R_{ESR}$ *Equivalent Series Resistance*, $R_{EPR}$ *Equivalent Parallel Resistance*



electric material must not be neglected when considering a real capacitor.

There are energy losses occurring at all these points during charging, discharging, and storage. Heat is released in the resistance of the lead and the electrodes as a result of the current. Similarly, the movement of ions in the electrolyte and the chemical reactions release heat. The conductivity of the dielectric material causes the capacitor to discharge, which is referred to as self-discharge. The current flow causes heat losses in the dielectric material. An equivalent circuit standardized in accordance with DIN 60384-1 is used to illustrate the situation (Fig. 6.24).

The losses caused by inductive properties are represented by $L_{ESL}$. The values for the ohmic resistance of the lead, electrode, electrolyte, and the dielectric material are summarized in $R_{ESR}$. The resistance $R_{EPR}$ represents the discharge-resistance of the dielectric that is used to illustrate the self-discharge. The actual capacitance of the capacitor is indicated as the ideal capacitance $C_{IDEAL}$.

### Self-Discharge

Self-discharge describes the loss of stored energy in a capacitor without external interference and without an external load being connected. If the terminal or open-circuit voltage (OCV) of a charged capacitor is measured at time point $t_1$ and this measurement is repeated at a later time point $t_2$, the voltage at time point $t_2$ will be less than that at time point $t_1$, even though there is no load connected.

The cause is the finite resistance of the dielectric, represented by the resistance $R_{EPR}$ in Fig. 6.24. Only the dielectric or the dielectric layer prevents the separated charges from being exchanged and this maintains the electric field. Because this is not infinitely large, however, current can flow through the dielectric which leads to an exchange of charge. An electric field is thus generated and the energy stored in it is converted to heat.

To maintain the charge in the capacitor, current is required to keep the otherwise declining voltage of the capacitor at a constant value. This value can be found in specification sheets. Thus, for example, for a supercapacitor of size 10 F, after a period of 72 hours at 25 °C, a current of 0.03 mA is required to maintain the cell voltage of 2.7 V [16].

It is not possible to generalize about the energy losses here because the self-discharge current is not constant and depends on factors such as the cell temperature, cell voltage, previous charging/discharging cycles, and the preceding charging/discharging behavior. A typical curve for the voltage during self-discharge is shown in Fig. 6.25.

### Determining Energy Loss

A generally applicable determination of losses proves difficult because the relationships are non-linear. Even using the internal resistance of the capacitor to determine the losses using the power dissipation varies depending on the load and external influences. One option for determining the internal resistance (combining the resistance $R_{ESR}$ and $R_{EPR}$) is provided by DIN

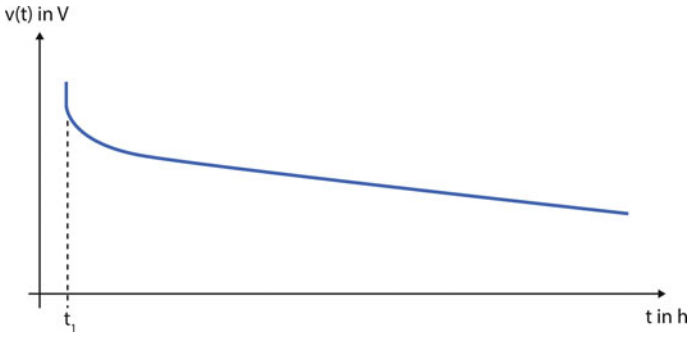



**Fig. 6.25** Exemplary curve showing the capacitor voltage during self-discharge. The capacitor is operating without a load from time point $t_1$ onwards

62391-1 4.5.5. 'Calculation of the Internal Resistance'.

Another option for determining the losses is using the energy balance. In accordance with the principle of the conservation of energy, the energy supplied to the capacitor corresponds to the sum of the stored energy, or the energy that can be discharged again, respectively, and the energy loss. The difference between the supplied energy $E_{zu}$ and the withdrawn energy $E_{ab}$ therefore represents the energy loss $E_v$ (Eq. 6.32):

$$E_v = E_{zu} - E_{ab}. \tag{6.32}$$

Once again, a generally applicable result cannot be derived because the energy losses are highly dependent on external influences and the load. The results are different following short and fast-charging, a short storage period, and rapid discharging compared to when the capacitor is slowly charged and the energy is stored over a long period.

### Efficiency

The efficiency $\eta$ is determined by the ratio of the withdrawn energy and the supplied energy. The calculation, using Eq. 6.33, is carried out by forming the integral between the total nominal voltage of the capacitor and half this value, which is the area of the most frequent operation [25]:

$$\eta = \frac{E_{ab}}{E_{zu}} = \frac{\int_{U_N}^{0.5U_N} U \cdot I dt}{\int_{0.5U_N}^{U_N} U \cdot I dt}. \tag{6.33}$$

The specifications from the manufacturer provides very little in the way of information about the efficiency. It is usually stated as being > 90% [26].

### Experimental Results in Determining the Efficiency

In an experiment to determine the efficiency of double-layer capacitors, the energy losses of 40 capacitors of size 1,500 F at 2.7 V were examined at different constant charging/discharging currents. The voltage was varied between 1.7 V and 105 V. A mean efficiency of 95.8% was determined (see [27] and Fig. 6.26).

### Energy Density

The energy density describes the quantity of energy stored per unit of mass. The volumetric energy density:

$$\frac{\text{Energy}}{\text{Volume}} = \left[\frac{\text{W}}{\text{m}^3}\right] \tag{6.34}$$

and the gravimetric energy density relative to the mass:

$$\frac{\text{Energy}}{\text{Mass}} = \left[\frac{\text{W}}{\text{kg}}\right] \tag{6.35}$$

are differentiated. The energy density for a capacitor can be derived from the energy of the electric field. In Eq. 6.13 the current $i$ is expressed by:

$$i = \frac{dQ}{dt}. \tag{6.36}$$

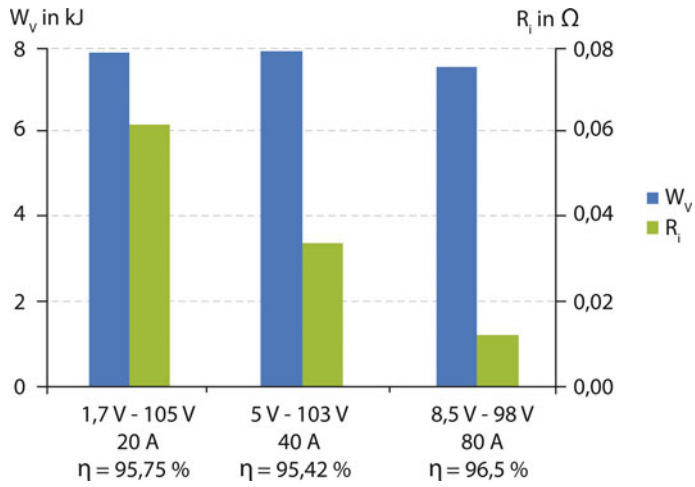



**Fig. 6.26** Efficiency, energy losses, and internal resistance of supercapacitors (experimental result). Author's figure based on values from [27]. For 20 A: $\eta = 95.7\%$, $W_v = 7{,}908\,\mathrm{J}$, $R_i = 61.6\,\mathrm{m\Omega}$; for 40 A: $\eta = 95.42\%$, $W_v = 7{,}985\,\mathrm{J}$, $R_i = 33\,\mathrm{m\Omega}$; for 80 A; $\eta = 96.5\%$, $W_v = 5{,}376\,\mathrm{J}$, $R_i = 12.3\,\mathrm{m\Omega}$

6

Thus, taking Eq. 6.36 into account yields the following expression:

$$dW = \frac{dQ}{dt} u dt = u dQ. \tag{6.37}$$

The voltage in Eq. 6.37 can be substituted in the case of a parallel plate capacitor according to Eq. 6.3 by the electric field strength. This yields:

$$dW = E \cdot d dQ. \tag{6.38}$$

In Eq. 6.38, $d$ corresponds to the distance between the electrodes. The change in the charge $dQ$ also causes a change in the electrical displacement flux density $D$. It can therefore be expressed in the following form:

$$dQ = A dD. \tag{6.39}$$

In Eq. 6.39 $A$ represents the plate area. Inserting Eq. 6.39 in Eq. 6.38 produces:

$$dW = EA \cdot d dD. \tag{6.40}$$

$A \cdot d$ corresponds to the volume ($V$). This yields the following expression for the energy density:

$$\frac{dW}{V} = \int E dD. \tag{6.41}$$

According to Eq. 6.41, for the parallel plate capacitor with an area $A$ and plate distance $d$ for the integration limits from 0 to $D$:

$$\frac{W}{V_{\mathrm{ol}}} = \varepsilon_0 \varepsilon_r E^2. \tag{6.42}$$

The energy density is often specified in W h/kg in data sheets. It is calculated using the capacitive energy as defined in Eq. 6.43:

$$\frac{W}{V} = \frac{1}{2} \frac{C \cdot U^2}{3{,}600\,\mathrm{s} \cdot m}. \tag{6.43}$$

In this equation, $m$ corresponds to the mass of capacitance in kg.

### Power Density

The power density is the energy density with respect to time. It is defined for supercapacitors based on DIN EN 62391-2: the power density indicates the electrical power that can be transferred per unit of mass (or volume) of a capacitor. The greater the power density, the greater the current that can be effectively withdrawn [4].

The power density can be determined using the following equation given in the DIN standard:

$$P_{\mathrm{d}} = \frac{1}{2} \frac{(U - U_6 + U_e) \cdot I}{m}. \tag{6.44}$$

The parameters in the above equation are defined as follows:

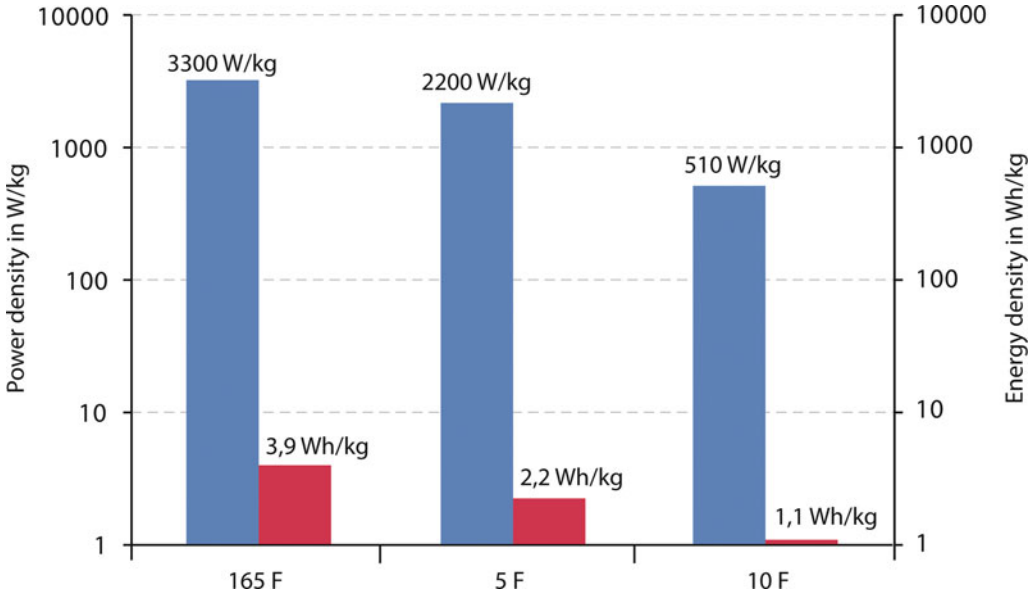



**Fig. 6.27** Power/energy density of supercaps, 65 F (industrial, rail vehicles, automobiles), 5 F (electronic equipment), 10 F (smart electricity meters, PC backup). The axis scale is logarithmic

$P_d$ – the specific power per mass in W/kg
$U$ – the charging voltage in V
$U_6$ – the drop in voltage in V at 20% ($0.2\,U$) of the charging voltage
$U_e$ – 40% ($0.4U$) of the charging voltage in V
$I$ – the discharge-current in A
$R_d$ – the internal resistance in Ω
$m$ – the mass of the capacitor in kg [4]

The discharge-current is specified using $U_6$ with the help of the internal resistance $R_d$:

$$I = \frac{U_6}{R_d}. \tag{6.45}$$

The internal resistance is determined using the direct current measuring method as defined by IEC 62391-1-1, 4.6.2. Like the energy density, the power density can be specified relative to either volume or mass. Typical characteristic values for the power density and the energy density are stated for three different supercapacitors in Fig. 6.27.

### ▪ Typical Characteristic Values

Other typical characteristic values that can often be found in the data sheets provided by manufacturers are shown in Table 6.1.

## 6.1.5 Service Life

The service life of a capacitor describes the change over time in certain characteristic values relative to their specific nominal value or baseline value at the start of use. For a capacitor, this refers specifically to the reduction in the capacitance $C$ and the increase in the internal resistance $R_{ESR}$ (Fig. 6.24). If a certain value is reached after a particular period has elapsed, this is referred to as the end of the service life. Because aging is highly dependent on the operating temperature, manufacturers indicate a service life for a maximum temperature. For capacitance $C$, a reduction in the capacitance by 20% is assumed to define the end of the service life. The necessary dimensioning capacitance $C_L$ is determined using Eq. 6.46:

$$C_L = k_L \cdot C_{Nom}. \tag{6.46}$$

The factor $K_L$ is dimensionless. For the reduction indicated above of 20%, $K_L$ is 0.8. For the increase in the internal resistance, an increase

**Table 6.1** Typical characteristic values for supercapacitors

| Frequently stated specifications | Explanation | Typical values |
|---|---|---|
| Operating temperature (ambient temperature) | Optimal temperature, working temperature | −40 to +70 °C |
| Capacitance tolerance | Percentage deviation from the nominal capacity | ± 20% -70% |
| Capacity reduction | Drop in the capacitance compared to the baseline value | About 20% |
| Mass | Weight of the capacitor | A few g to several kg |
| Cell voltage (nominal value) | Voltage at the capacitor | 2.5 to 160 V |



of 100% of usually specified:

$$R_L = R_{\mathrm{ESR}} + R_{\mathrm{ESR}} \cdot k_L . \qquad (6.47)$$

A reduction in these characteristic values is associated with a reduction in the storage capacity. This does not mean, however, that the capacitor no longer functions once it has reached these values.

### Causes of Aging

Aging is induced by chemical changes in the capacitor materials (conductor, electrolyte, dielectric, separators, housing, insulation film). The following factors lead to a reduction in the capacitance:

- Increase in the internal resistance $R_{\mathrm{ESR}}$
- Increase in the electrode resistance
- Evaporation of the electrolytic fluid
- Decomposition of the contact material (e.g., activated carbon), and change in the electrolyte due to chemical reactions
- Reduction in the insulation effect of the dielectric material, which corresponds to the reduction in the parallel resistance $R_{\mathrm{EPR}}$ (Fig. 6.24)

The increases in the resistance in particular have negative effects because they lead to elevated temperatures during operation. This results on the one hand in increased losses, and on the other hand, in further damage to the capacitor. As a result of the reduction in the parallel resistance, the self-discharge increases.

### Mechanisms that Shorten the Service Life

Aging of the capacitor is primarily caused by the temperature, the voltage, the electrical loading conditions, and the mechanical loads. Exceeding the permitted cell voltage in particular can lead to damaging the electrolyte in double-layer capacitors. However, the temperature of the capacitor exerts the greatest influence. This is the sum of both the ambient temperature and the internal temperature of the capacitor. This leads to the question of which processes can cause a temperature increase.

### Temperature Influences

The capacitor is affected from the outside by the ambient temperature, which is generally not a factor that is readily influenced and, therefore, it is essential to ensure adequate cooling.

The capacitor also heats up because of energy losses in the resistors. Delayed polarization generates heat in the dielectric material because the dipoles only align with a finite speed and cannot readily adapt to changes in the field conditions (as a result of charging or discharging). For the capacitance value, Eq. 6.48 applies for most dielectrics [7]:

$$C(t_x) \approx C_{20} \cdot (1 + \alpha_{20} \cdot [t_x - 20\,^{\circ}\mathrm{C}]) . \qquad (6.48)$$

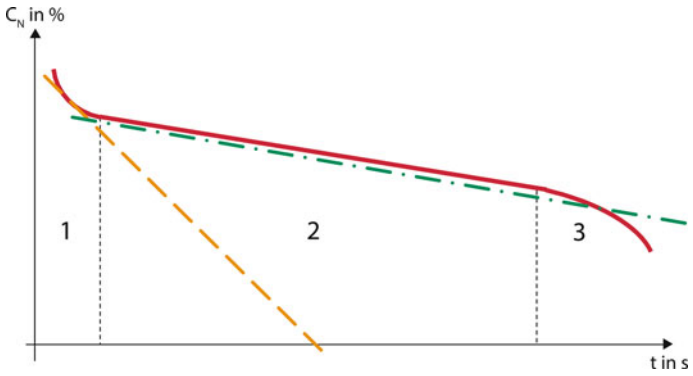



**Fig. 6.28** Change in the capacitance (*solid line*) due to aging, *area 1*: exponential reduction, *area 2*: linear reduction, *area 3*: natural exponential reduction, *dashed line*: erroneous approximation, *dotted line*: correct approximation

$C_{20}$ corresponds to the capacitance at a temperature of 20 °C. The temperature coefficient $\alpha_{20}$ with the unit 1/K describes the change in the capacitance with temperature. High loading conditions and frequent and rapid charging or discharging lead to increased heating of the capacitor. The heating depends particularly on the number of and intervals between the charging and the discharging cycles.

### ■ Breakdown

An increase in the capacitor voltage is simultaneously associated with an increase in the field strength within the capacitor. If the maximum permitted field strengths for the dielectric are exceeded, this can lead to breakdown. This means that an electron avalanche, a type of short-circuit, is forced through the dielectric as a result of the increased field strength. This current flow leads to increased heating, even to the extent that the dielectric is destroyed at the site where the breakdown occurred.

### ■ Determining the Service Life

The service life of a capacitor is dependent on many factors. To be able to define a precise time frame for the aging process requires knowing all influencing parameters. Because this is very unlikely, standardized procedures are used to estimate the service life to ensure comparability.

The service life of a supercapacitor can be determined by approximating a straight line on the service-life curve. The rated values specified by the manufacturer upon reaching the service life according to Eqs. 6.46 and 6.47 yield different results. Based on empirical values, it can be assumed that the capacitance reaches its limit rather than the internal resistance [14]. The typical curve for the reduction in the capacitance is shown in Fig. 6.28.

The decline in the capacitance occurs in three stages. In the first stage, there is an exponential fall in the capacitance shortly after the first use. This stage is unsuitable for the calculation, being short compared to the useful life, and can be disregarded (Fig. 6.28, Sec. 1). The second stage is characterized by a linear reduction in the capacitance and this interval is used to estimate the expected service-life (Fig. 6.28). In the third stage there is again an exponential reduction, making this stage also unsuitable for calculating the service life.

### ■ Approximation Method for Estimating the Service Life

The capacitance at the start of the use $C_A$ is first measured. This can also be found in the data sheet supplied by the manufacturer. It is recommended, however, to determine it metrologically because of tolerances [15]:

$$C_A = i\frac{dt}{du}. \tag{6.49}$$

With the measurement during charging, $i$ corresponds to the charge current, $dt$ to the charging time, and $du$ to the change in the voltage at the capacitor. After a time interval $\Delta t$ the capacitance is measured again ($C_E$). This time

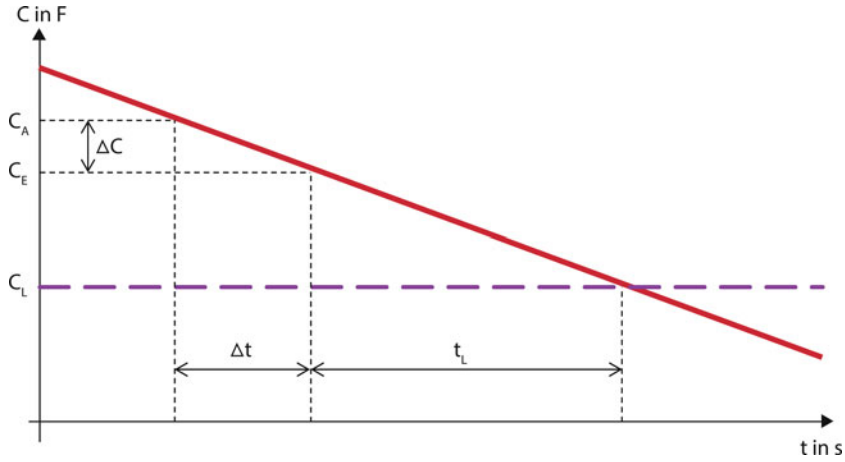



**Fig. 6.29** *Straight line* used to determine the service life of the supercapacitor, $C_A$: initial capacitance, $C_E$: final capacitance, $C_L$: service-life limit, $\Delta C$: change in capacitance, $\Delta t$: delay between measurements, $t_L$: service life

interval should be sufficiently long enough because, otherwise, the method will produce an erroneous approximation [15]. The line corresponds to the approximation of the exponential decline in the capacitance. If the measurement period that has been selected is long enough, this produces an approximation that corresponds to the long-term course (see dashed line in Fig. 6.28).

The capacitance value for the limits of the service life $C_L$ as defined by Eq. 6.46 is determined using the capacitance values $C_A$ and $C_E$ (Fig. 6.29). The service life $t_L$ is determined using:

$$t_L = \Delta t \frac{(C_E - C_L)}{C_A - C_E}. \qquad (6.50)$$

This method is only valid if the required conditions, specifically the temperature, are met. The more the future behavior of the capacitor deviates from these conditions, the less precise the prognosis for the service life [15]. The service life of a supercapacitor in the upper power range (several 100 F) as used for industrial applications lies in the range of ten years.

### 6.1.6 Applications

The first developments in the field of supercapacitors started in the 1960s, driven primarily by the two manufacturers, General Electric and Sohio. Larger production runs began in 1978 when Panasonic launched the Goldcap. The capacitance values at this time were still in the farad range. The market has grown steadily since this time and is now serviced by about 40 major manufacturers (see Fig. 6.30 and [28]).

Supercapacitors have a high power density and should therefore be considered power storage systems rather than energy storage systems. They are able to provide large amounts of power within a limited time frame. Capacitors are therefore suitable for providing starting energy in the transport sector (rail transport and automobiles), for ensuring reliability for power supply systems, and for bridging or compensating for short-term load fluctuations. Figure 6.31 shows the areas in which supercapacitors are used.

#### ▪ Use in Wind Turbines

In some operational situations, the rotor blades of wind turbines have to be rotated out of the wind or the angle of attack of the rotor has to be adjusted when wind speeds are high to prevent

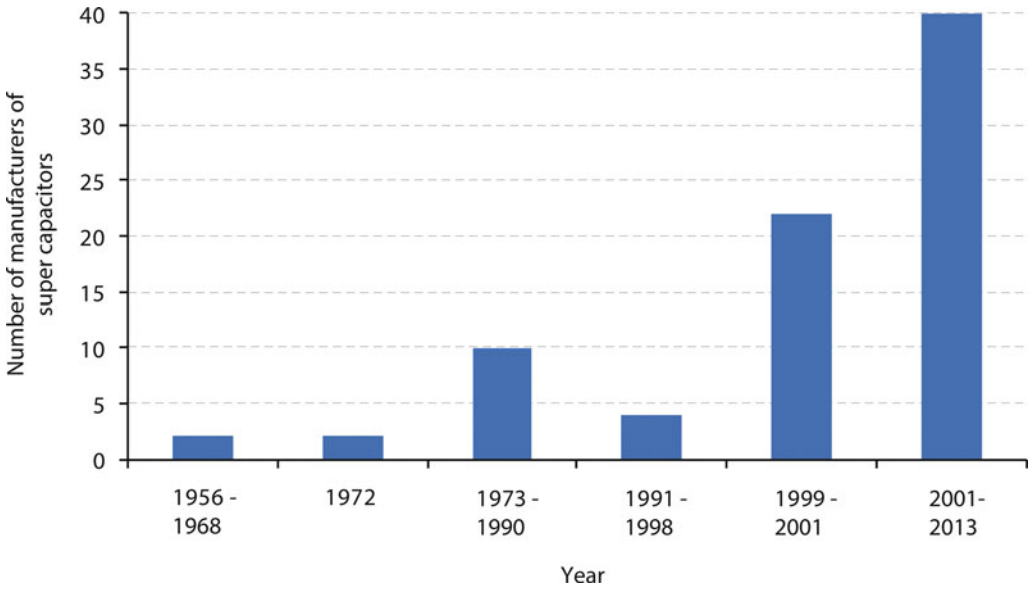



**Fig. 6.30** Number of major manufacturers of supercapacitors from 1956 to 2013

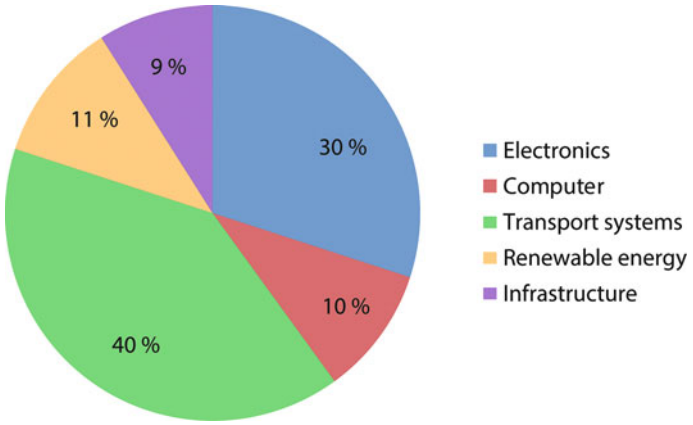



**Fig. 6.31** Market share for supercapacitors according to areas of use for 2012; author's figure adapted from [28]

damage to the turbine. This is done using electrical motors and requires very high power to be applied within a short period, which can be provided by a supercapacitor (Fig. 6.32). Because capacitors have a short delay time compared to batteries, they are very suitable for carrying out such tasks, particularly in wind turbine generator systems that are difficult to access such as offshore systems. Supercapacitors are already in use in more than 20,000 wind turbine generator systems. The dimensioning is based on a service life of about 15 years or 500,000 to 1,000,000 charging/discharging cycles [17].

### Use in the Transport Sector

In rail vehicles, supercapacitors can be used to provide braking energy, which is referred to as recuperation (Fig. 6.33). When rail vehicles brake, the previous kinetic energy,

$$E_{\text{kin}} = \frac{1}{2} m v^2, \tag{6.51}$$

is converted irreversibly into heat, and is therefore lost to subsequent use. This can happen, if, for example, a rail vehicle weighing 100 t traveling at a speed of 100 km/h releases a total of



**Fig. 6.32** Supercapacitor for supplying power for rotor blade adjustment in the center of the hub of a wind turbine [17]

38.58 MJ of heat energy when decelerating to 0 km/h.

Instead of converting this energy to heat, with recuperation it is fed into a storage system from which it is later released when the vehicle accelerates again. The properties of a double-layer capacitor, that is, high power density with a comparably small size allowing for rapid charging and discharging because of the high current-carrying capacity, are very useful in this situation. Recuperation enables energy savings of up to 30% [2]. This system of using braking energy can also be taken advantage of in road traffic for fuel cell buses or electric or hybrid vehicles.

## 6.2 Superconducting Electromagnetic-Energy Storage Systems

Superconduction, in which the ohmic resistance of a material tends to zero and therefore almost completely vanishes, was discovered for the first time in 1911. The Dutch physicist Heike Kamelingh Onnes, who worked mostly on the liquefaction of gases, noticed this phenomenon in mercury. Previous development has been aimed primarily at identifying superconductors with a higher transition temperature. Some important discoveries in the history of superconductors are shown in Fig. 6.34 [23].

### 6.2.1 Principles of Superconduction

This section describes the functional principle of a **s**uperconducting **m**agnetic-**e**nergy **s**torage (SMES) system. Superconduction itself will first be explained followed by a description of an SMES.

Superconductors are divided into two groups referred to as type I and type II. They differ specifically in their behavior in magnetic fields. While type I superconductors exclude a magnetic field almost completely apart from a thin surface layer on its interior (Meissner-

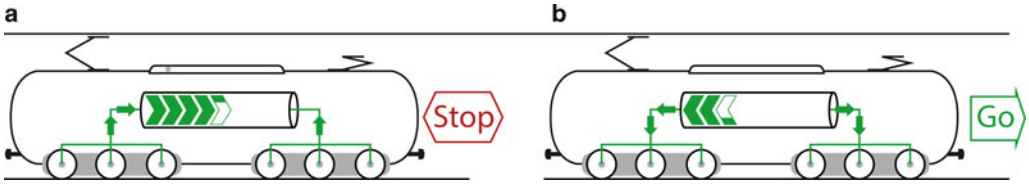



**Fig. 6.33** Recuperation, **a** kinetic energy is sent to the supercapacitor during deceleration, **b** stored energy is provided for acceleration

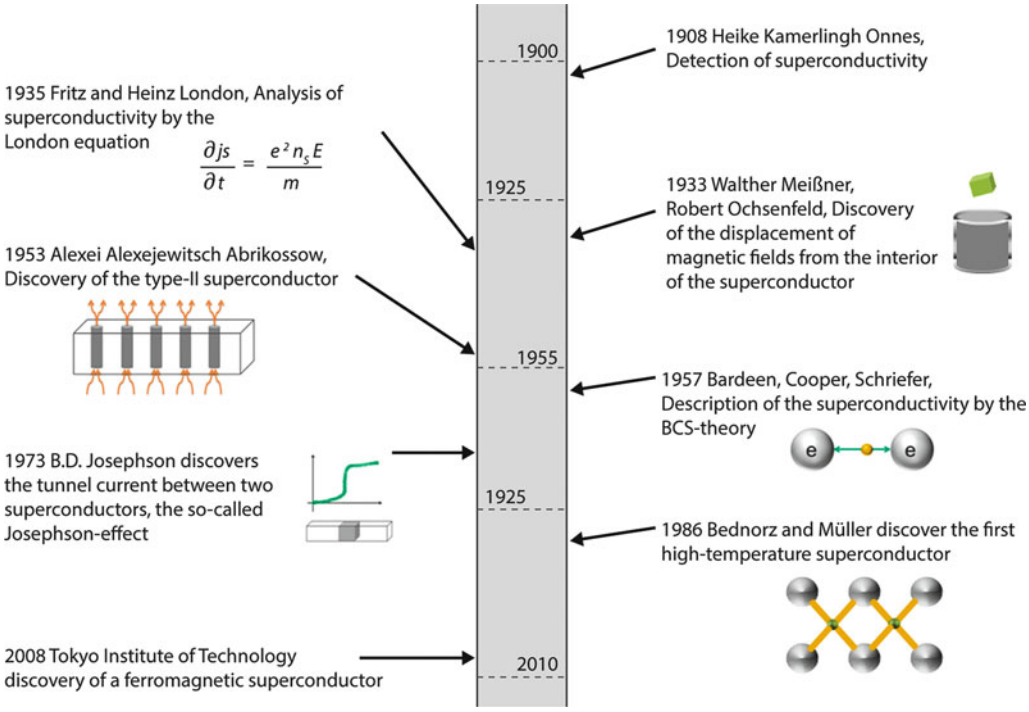



**Fig. 6.34** History of superconductors (author's figure based on [23])

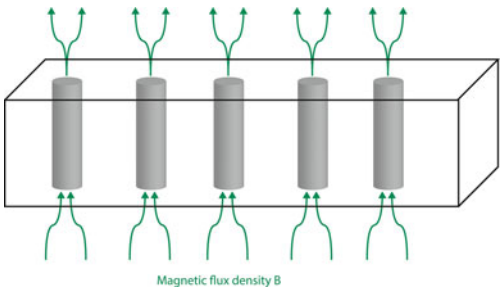



**Fig. 6.35** Magnetic flux lines in type II superconductors

Ochsenfeld effect), in type II superconductors a magnetic field penetrates the superconductor in magnetic flux lines above a certain critical magnetic flux density $B_{Oc}$ (B critical) (Fig. 6.35).

The behavior of type I superconductors is described using the BCS theory (formation of Cooper pairs), while that of type II superconductors is not yet fully understood but it is assumed that Cooper pairs are also formed in this type of superconductor [3].

### From Normal Conduction to the Superconducting State

When a metal is in a state of normal conductivity, in an electric field accelerated, negatively charged electrons generate interactions with the shells of the atomic nucleus as they move through the crystal lattice of the metal. These interactions are collisions with the shells of the atomic nuclei and lead to the metal conductor heating up as well as reducing the number of freely mobile electrons, which in turn leads to a reduction in the current. This process is referred to as the ohmic resistance of the conductor. In the state of normal conductivity, some of the electrical energy is converted to heat and this is referred to as the ohmic loss (Fig. 6.36).

In the superconducting state, electrons form pairs known as Cooper pairs. The total momentum of these Cooper pairs is 0. On the

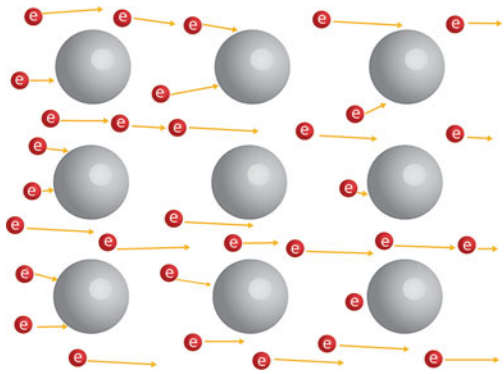


**Fig. 6.36** The ohmic conduction mechanism

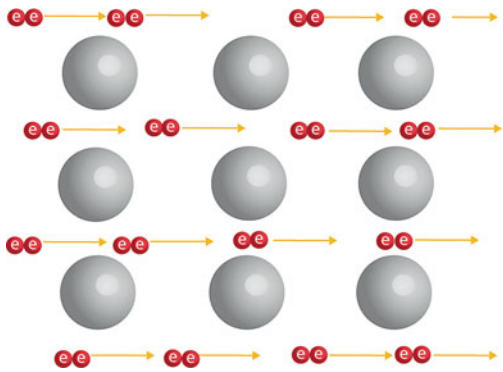


**Fig. 6.37** Cooper pairs in the superconducting state

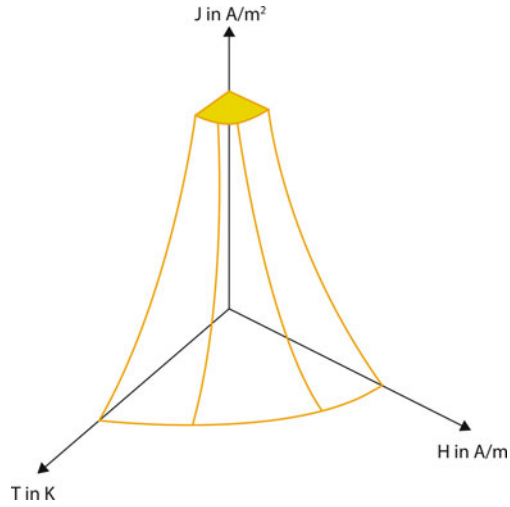



**Fig. 6.38** Boundary conditions for the superconducting state

The superconduction depends on the energy-state of the Cooper pairs. The addition of too much energy leads to a loss in superconductivity due to a change in the momentum. Three parameters play a special role here:

- Current
- Magnetic flux density
- Temperature

They represent boundary conditions and their maximum value must not be exceeded. This produces a function for the superconduction that depends on these three parameters (see Fig. 6.38 and [3]).

basis of experimental results, it is assumed that all Cooper pairs have a single quantum state. The electrons in pairs, therefore, form a unit that correspond in all their physical properties.

Because the momentum of a Cooper pair is 0, this must also apply to the entire Cooper pair mass. This excludes any interactions with the crystal lattice; that is, with the atomic nuclei, because any interactions such as collisions would affect the momentum. This momentum would then not equal zero, which would lead to the Cooper pair decaying and, therefore, the collapse of the superconducting state. As such, there is no interaction with the crystal lattice in the superconducting state and no ohmic losses as a result. The electrons move as a Cooper pair through the crystal lattice of the conductor material without making any contact; this state is a lossless displacement of charge (Fig. 6.37).

### 6.2.2 Superconducting Electromagnetic Energy Storage (SMES) System

An SMES system is made up essentially of a superconducting coil, a cryogenic cooling system, and an inverter, if applicable, because an SMES can only be operated with direct current. Coil protection plays an important role here.

Exceeding the thresholds indicated above would lead to immediate collapse of the super-

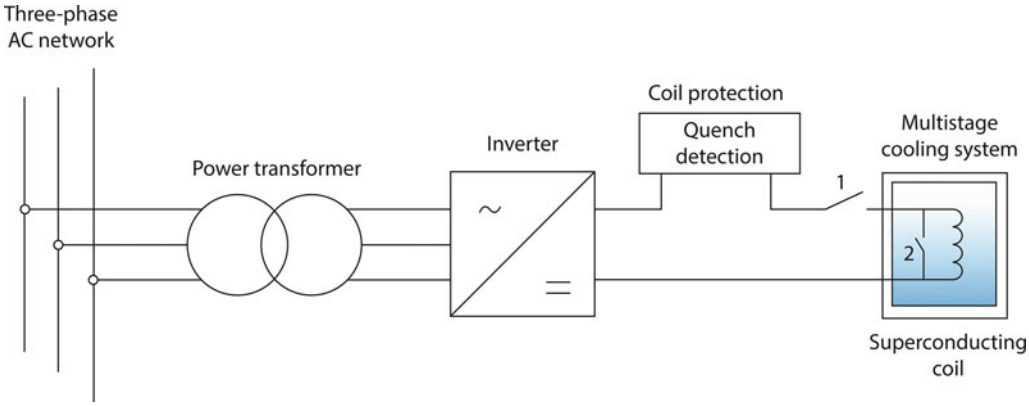



**Fig. 6.39** System architecture of an SMES

conduction and transition to the ohmic conducting state. This process is referred to as quench protection. A current that can be easily managed in the superconducting state would, according to

$$P_v = I^2 \cdot R \tag{6.52}$$

lead to immediate heating of the conductor as a result of the abrupt development of ohmic resistance. This can lead to energy losses, damage, and even to destruction of the conductor or the coil. Coil protection, known as quench detection, is therefore essential. This must detect the beginning of the quench and promptly protect the conductor or the coil from heating up too much.

The first protective mechanism involves designing the superconductor as a composite conductor. The superconductor itself is surrounded by an additional coating of a highly conductive metal. In the case of a fault (that is, the occurrence of a quench), the current is transmitted by the parallel metal conductor and excess heating is reduced. It is possible, in principle, to dimension the composite conductor such that if quenching occurs, the conductor does not heat up excessively and external protective circuitry is not required.

The consequences are, however, an increase in the conductor volume and a reduction in the effective current density in the conductor. This would lead to higher costs, a greater volume, and thus also to reduced efficiency. This method is therefore considered less desirable.

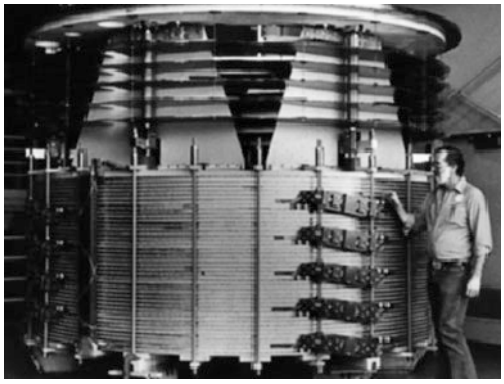


**Fig. 6.40** Superconducting 30 MJ coil from the Los Alamos National Laboratory [21]

A more advantageous approach is switching to an external resistor. Most of the magnetic energy is converted to heat energy, not in the superconductor, but rather outside it with the composite conductor only having to transport the increased current during the switch-over phase. The overall structure of an SMES system is shown in Fig. 6.39.

The key element for energy storage in a magnetic field is the coil or inductor (Fig. 6.40). Its properties and size can be determined using the law of induction.

If there is a change in the current in a conductor loop, this causes a change in the mag-

netic flux $\varphi$. This generates a voltage that counteracts the change in flux, and thus also its proportional current change. This process is referred to as induction or induced voltage. Because the current generates the voltage directed against it, this is also referred to as self-inductance. The link between the magnetic flux change and induced voltage is described by the law of induction:

$$u_l = \frac{d\varphi}{dt}. \tag{6.53}$$



Because the magnetic flux $\varphi$ is generated by current, the induced voltage is ultimately dependent on the change in current and the geometric arrangement and material of the coil or the conductor arrangement. Thus, the following applies for the induced voltage:

$$u_l = L\frac{di}{dt}. \tag{6.54}$$

The parameter $L$ is referred to as the inductance:

$$[L] = \frac{\mathrm{V\,s}}{\mathrm{A}} = 1\,\mathrm{H} = 1\ \text{Henry}. \tag{6.55}$$

By substituting Eqs. 6.53 and 6.54, the following is obtained for $L$:

$$L = \frac{d\varphi}{di}. \tag{6.56}$$

The inductance is, however, not only proportional to the change in flux but also to the number of turns $N$ of the coil; that is, the number of conductor loops that are penetrated by the same magnetic flux. If a non-ferromagnetic material is used, Eq. 6.56 can also be written as:

$$L = N\frac{\varphi}{i}. \tag{6.57}$$

The magnetic flux is produced by the flux density and the area $A$ penetrated by the magnetic flux:

$$\varphi = B \cdot A. \tag{6.58}$$

Thus, for Eq. 6.57:

$$L = N\frac{B \cdot A}{i}. \tag{6.59}$$

The flux density itself is generated in turn by the magnetic field strength and the permeability $\mu_0\mu_r$:

$$B = \mu_0\mu_r H. \tag{6.60}$$

$H$ is the magnetic field strength, which is also referred to as the magnetic excitation. Ultimately, this parameter includes the current that induces the magnetic field. $\mu_0\mu_r$ takes into account the magnetic material properties. In this case, $\mu_0$ is the magnetic field constant that indicates the magnetic conductivity of the vacuum. The magnetic conductivity properties of all other materials are a multiple of $\mu_0$, and therefore the factor $\mu_r$, which has no unit, is added. To simplify the calculation, the two are merged to form a combined factor:

$$\mu = \mu_0\mu_r. \tag{6.61}$$

The magnetic field strength $H$ is determined using Ampere's law:

$$\oint \vec{H}\,d\vec{s} = \Theta. \tag{6.62}$$

Ampere's law states that the sum of all magnetic field strengths along a closed enveloping surface produces the electrical magnetomotive force $\Theta$. $\Theta$ is the sum of all currents that flow through this closed surface. Assuming that the route elements $d\vec{s}$ and $\vec{H}$ have the same direction and $\Theta = N \cdot i$, Eq. 6.62 can be written as follows:

$$\oint \vec{H}\,d\vec{s} = \oint H\,ds = Hl = Ni. \tag{6.63}$$

Substituting Eq. 6.60 into Eq. 6.59 and taking into account Eq. 6.61 produces the following:

$$L = N\frac{\mu \cdot H \cdot A}{i}. \tag{6.64}$$

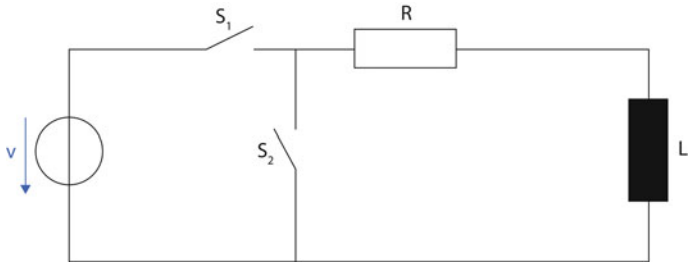



**Fig. 6.41** *RL* circuit represented as a simplified equivalent circuit for the coil with two switches

After solving the simplified Ampere's law Eq. 6.63 for $H$ and inserting it into Eq. 6.64, the inductance $L$ can be expressed as:

$$L = N^2 \frac{\mu A}{l}. \tag{6.65}$$

The expression contained in this equation,

$$\Lambda = \frac{\mu A}{l} \equiv \text{Material size} \cdot \frac{\text{Area}}{\text{Length}},$$

is similar to the conductance $S$. Therefore, this expression is also referred to the magnetic conductance $\Lambda$. The inductance is therefore also determined from the magnetic conductance and the number of turns in the quadratic equation:

$$L = N^2 \cdot \Lambda. \tag{6.66}$$

### Energy Storage

The energy stored in the magnetic field of the coil is determined using the simplified equivalent circuit for the coil.

The ohmic resistor $R$ in Fig. 6.41 represents the lead resistance of the coil. After closing the switch $S_1$ at time point $t_1$, the $RL$ circuit is supplied with electrical energy $W_{el}$ from the power supply up to time point $t_2$. This can be determined by integrating the power:

$$W_{el} = \int_{t0}^{t1} iu dt = \int_{t0}^{t1} iu_r dt + \int_{t0}^{t1} iu_l dt. \tag{6.67}$$

The first integral corresponds to the energy supplied by the power supply. The second integral determines the electrical energy that is irreversibly converted to heat in the ohmic resistor. The energy stored in the magnetic field of the coil is determined in the third integral. Taking into account Eq. 6.54, this becomes:

$$W_{coil} = \int_{t0}^{t1} iL \frac{di}{dt} dt = L \int_{i0}^{i1} i\, di = \frac{1}{2} L [i^2]_{i_0}^{i_1}. \tag{6.68}$$

Once the energy has been transferred by the power supply, switch $S_1$ is opened and switch $S_2$ is closed. The energy stored in the magnetic field is converted to heat by the current linked with it in the resistance $R$. The energy storage is therefore only of very short duration.

Most of the stored energy can no longer be discharged to the load network that supplied the energy because of these losses. However, if the coil is a superconducting coil, the resistance $R$ is no longer present below the transition temperature. The current could be stored virtually indefinitely until it is withdrawn. This is referred to as a continuous current. This current would generate a magnetic field around itself in the coil, which would be displaced out of the superconductor depending on the type of superconductor, or it penetrates through it in magnetic flux lines [3, 10].

### The Charging Process

During the charging process, the switch $S_1$ in Fig. 6.41 is closed and switch $S_2$ is opened. A current flows from the network through the inverter and through the coil. Although the coil itself in the superconducting state no longer has ohmic resistance, the leads, the inverter, and

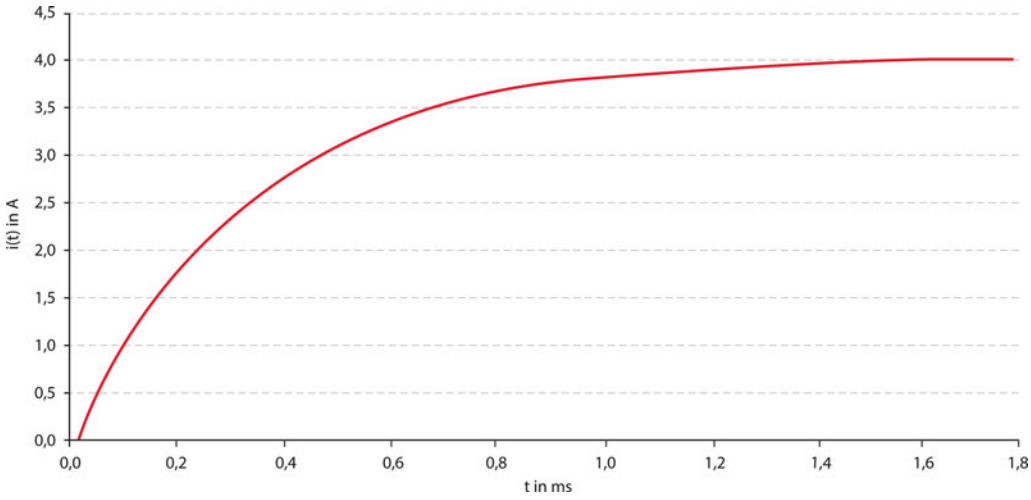



**Fig. 6.42** Charge current for a coil

the entire supply network, from which the coil is charged, still has resistance. When considering the charging process, all ohmic resistance values in Fig. 6.41 are combined in $R$. After setting up the mesh equation,

$$u(t) = u_r + u_L \tag{6.69}$$

applies for the $RL$ circuit.

The following inhomogeneous first-order differential equation is produced from this as a result:

$$u(t) = i(t)R + L\frac{di}{dt}. \tag{6.70}$$

This differential equation is used to generate a function that describes the change in the current or the voltage during the charging process. Solving the differential equation for the current $i(t)$ yields:

$$i(t) = i_0\left(1 - e^{-\frac{t}{\tau}}\right). \tag{6.71}$$

$\tau$ is the time constant that is dependent on the resistance and the inductance of the coil:

$$\tau = \frac{L}{R}; \quad [\tau] = \text{s}. \tag{6.72}$$

This produces an exponentially increasing current, the behavior of which is dependent on the geometric and material properties of the coil. The behavior is shown in Fig. 6.42.

A magnetic field is generated in the coil. Switch $S_2$ is then closed, the coil is short-circuited, and switch $S_1$ is opened. The coil is therefore separated from the network. The lead resistance is no longer relevant and the inductance $L$ of the coil is all that remains. This means that the resistance in Eq. 6.71 tends to zero. For the change in the current, this yields:

$$i(t) = \lim_{R\to 0} i_0\left(1 - e^{-\frac{t}{\tau}}\right) = \lim_{R\to 0} i_0\left(1 - e^{-\frac{Rt}{L}}\right) = 0. \tag{6.73}$$

The change in the current over time is thus 0. Accordingly, the current maintained by the magnetic field can, in theory, flow indefinitely. The electrical energy remains stored in the magnetic field [7, 8].

### ▪ Discharging Process

For the discharging process, at time point $t_x$, at which the stored energy is delivered to the network or the load, switch $S_2$ in Fig. 6.41 is opened and switch $S_1$ is closed.

The inductance is no longer short-circuited but instead linked to the network through the

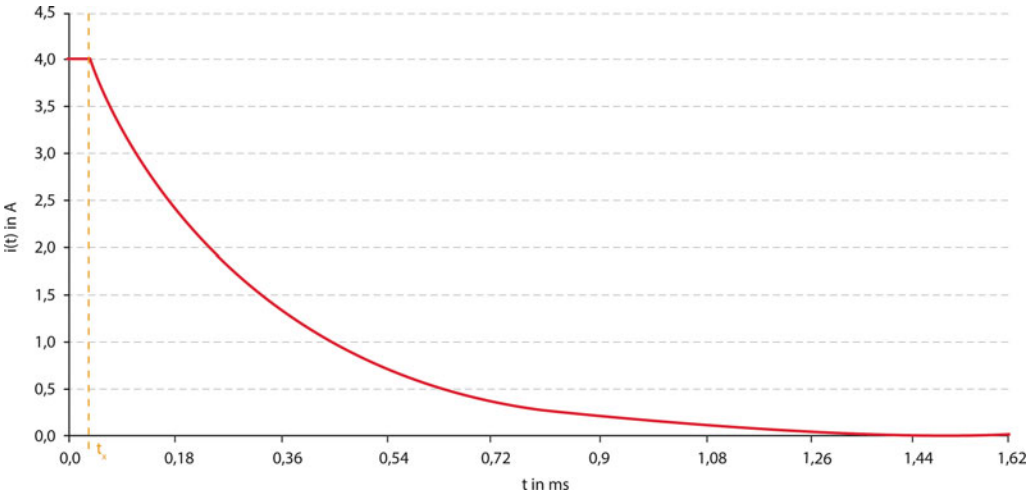



**Fig. 6.43** Change in the current during discharging of a coil

inverter. Both lead and network resistance is therefore present and the current flows back into the network through the inverter. The behavior of the discharging process is produced by Eq. 6.71. The current in Eq. 6.71 has a negative value because of the negative voltage. The current therefore drops exponentially from a previously attained initial value (Fig. 6.43).

The magnetic field of the inductor decays in the process. If it is of an adequate size, the coil acts like a DC voltage source [19].

SMES systems can store electrical energy directly just like capacitors with no further conversion required. In an SMES system itself, no chemical conversion processes are needed to store energy and there is no mechanical wear as a result of moving components.

The service life and the number of charging/discharging cycles are therefore very high. The service life of an SMES is about 30 years and the number of cycles is more than 1 million. Partial discharging is also readily possible [19].

### 6.2.2.1 Efficiency and Losses of SMES

Even if the ohmic resistance disappears, an SMES system is still not without losses.

Every SMES requires a control system to control the charging and discharging. A stable temperature is also important for an SMES to ensure that it remains below the transition temperature. The energy required for this control leads to losses. The DC voltage for operating

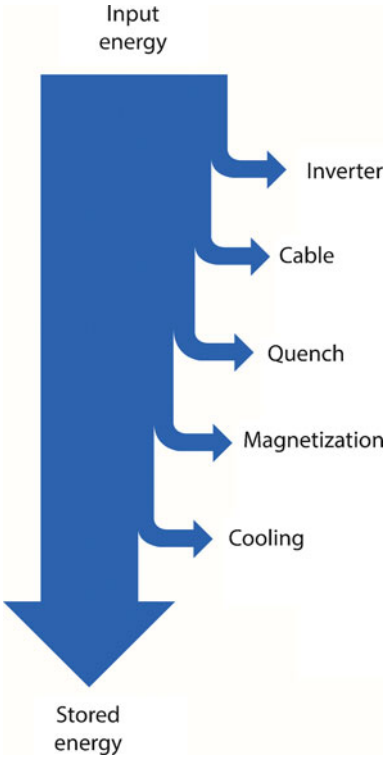



**Fig. 6.44** Energy losses in the SMES

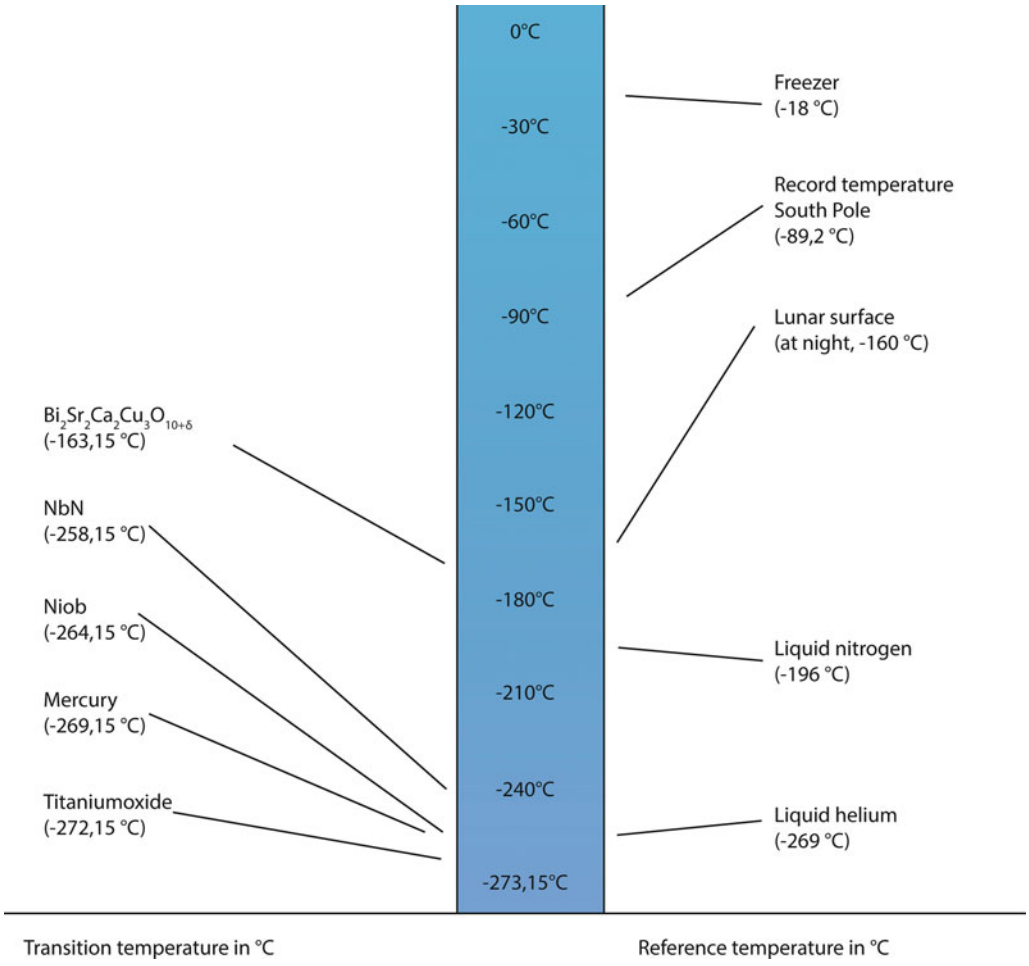



**Fig. 6.45** Transition temperature of various superconductors compared to other characteristic temperatures

the SMES also requires an inverter, which is again associated with losses. Because not all the leads in the SMES system are superconducting, there are ohmic losses in all the input and output leads.

Furthermore, superconductors have alternating field losses that are referred to as hysteresis losses on the basis of the magnetic field changes [24].

The most important losses of all are, however, thermal losses. Because the superconductor itself must be kept below its transition temperature during operation, continuous cooling is required to compensate for heat flow generated by the temperature gradient between the ambient temperature and the coil temperature. The cooling system must also counteract the heating that results from the change in the magnetic field during charging and discharging.

Figure 6.44 shows the losses that result during charging and discharging.

Because the thermal losses are proportional to the temperature-difference, current superconductor research is focused on finding conductors with the highest possible transition temperatures. The temperature-level of some superconductors is shown in Fig. 6.45.

Considerable progress was achieved when the transition temperature of −196 °C was exceeded because this allows more cost-effective

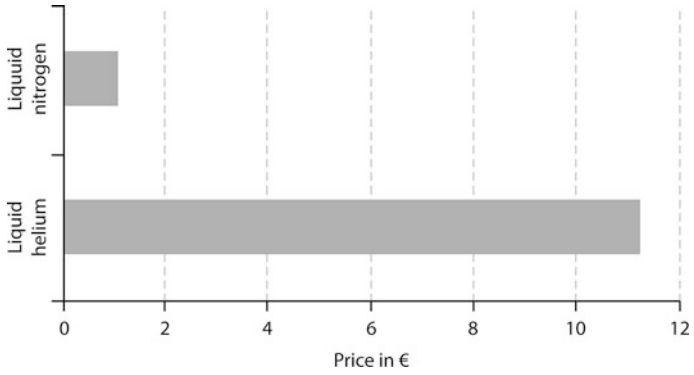



**Fig. 6.46** Price difference between liquid helium and liquid nitrogen

liquid nitrogen to be used for cooling instead of expensive liquid helium. Figure 6.46 shows the price difference between the two liquid coolants, nitrogen (boiling temperature −196 °C) and helium (−269 °C), for a volume of 300 liters [24].

### 6.2.2.2 Possible Applications for SMES System

SMES do not currently play a role in energy storage. Because of their high-power density combined with a very low-energy density, SMES are defined as power storage systems rather than as energy storage systems.

**Table 6.2** Cost analysis for electromagnetic storage systems from the NEDO Organization [20]

| | |
|---|---|
| System 110 MW/15 kW h | 690 USD/kW |
| System 100 MW/500 kW h | 1,970 USD/kW |

SMES have the advantage of direct energy-storage with no rotating parts and no chemical processes required to convert the energy. This is counteracted, however, by very high costs and considerable thermal losses. Table 6.2 shows the result of a Japanese cost analysis from 2009.

Possible applications would therefore include use for:

- Short-term storage
- Network stabilization or safeguarding of voltage quality
- Securing the power supply in stand-alone power systems
- Uninterruptible power supply (UPS)

Major storage systems for network applications are currently still in the development phase. In contrast, small SMES systems for voltage stabilization are already in use. A summary of the possible uses is shown in Table 6.3.

**Table 6.3** Current situation for SMES technology for 2002 [21]

| Storage use | Voltage quality | System stability | Peak load-leveling |
|---|---|---|---|
| Status quo | Different storage systems in operation | Demonstration model | Theoretical approaches |
| Empirical data | Problems with the output power | Still insufficient empirical data | Long-term study required |
| Developmental trend | In production | Production and search for customers | None |
| Problem | SMES costs | Cost optimization required | Costs too high |

## 6.3 Summary

- The key role that will be played by **electricity** in the energy supply systems of the future is highlighted throughout this book. Accordingly, the subject of energy storage needs to be considered with a view to **purely electrical systems**.
- There are two components in electrical engineering that can store energy: **capacitors** and **coils**. This chapter concentrated on discussing features of importance for energy storage: namely, the features of **supercapacitors** and **superconducting coils**.
- Avoiding the conversion of electrical energy into other forms of energy has the advantage of avoiding **potentially high conversion losses**. However, this is offset by the disadvantage of **extremely low energy densities**—both in terms of volume and weight—and **exorbitantly high costs**. For this reason, these two systems are only used at present in **niche segments**.



## References


1. Atkins PW (2007) Physikalische Chemie, 4th edn. VCH, Weinheim [u. a.]
2. Bombardier Transportation (2009) EcoActive Technologies. MITRAC Energy Saver, Zürich
3. Buckel W (1994) Supraleitung. Grundlagen und Anwendungen, 5th edn. VCH, Weinheim [etc.]
4. Deutsches Institut für Normung e.V (2007) Elektrische Doppelschichtfestkondensatoren zur Verwendung in Geräten der Elektronik – Teil 2 (DIN EN 62391-2). Beuth Verlag, Berlin
5. DIN (2010) DIN EN 60384-1:2010-05;VDE 0565-1:2010-05. Festkondensatoren zur Verwendung in Geräten der Elektronik – Teil 1: Fachgrundspezifikation (IEC 60384-1:2008 + Corrigendum 2008); Deutsche Fassung EN 60384-1:2009
6. Faranda R (2010) A new parameters identification procedure for simplified double layer capacitor two-branch model. Electr Power Syst Res 80(4):363–371. https://doi.org/10.1016/j.epsr.2009.10.024
7. Führer A, Heidemann K, Nerreter W (2011) Grundgebiete der Elektrotechnik, Arnold Führer; Klaus Heidemann; Wolfgang Nerreter, 9th edn. vol 2. Hanser, München
8. Hagmann G (2006) Grundlagen der Elektrotechnik. Das bewährte Lehrbuch für Studierende der Elektrotechnik und anderer technischer Studiengänge ab 1. Semester, 12th edn. AULA-Verl, Wiebelsheim (mit 4 Tabellen, Aufgaben und Lösungen)
9. Hamann CH, Vielstich W (2005) Elektrochemie, 4th edn. Wiley-VCH, Weinheim
10. Kathke M (1999) Supraleitung. Eine Einführung. Aachen
11. Lippold B (2013) Aktivkohle. http://www.chemie.de/lexikon/Aktivkohle.html. Accessed 24 Oct 2013 (Chemie.de Informationsservice GmbH)
12. Lippold B (2013) Permittivität. http://www.chemie.de/lexikon/Permittivit%C3%A4t.html. Accessed 24 Oct 2013 (Chemie.de Informationsservice GmbH)
13. Lott J (2001) Einsatz des Doppelschichtkondensators als Zusatzspeicher im Elektrofahrzeug. Fortschritt-Berichte VDI Reihe 21, Elektrotechnik, vol 307. VDI-Verl, Düsseldorf
14. Technologies M (2009) Product Guide. Maxwell Technologies BOOSTCAP Ultracapacitors, San Diego CA
15. Technologies M (2013) Application Note. Life Duration Estimation, San Diego CA
16. Technologies M (2013) Datasheet HC Series Ultracapacitors. San Diego CA
17. Technologies M (2013) Ultracapacitor usage in pitch control system. San Diego CA
18. Mortimer CE, Müller U (2010) Chemie. Das Basiswissen der Chemie, 10th edn. Thieme, Stuttgart
19. Neupert U (2009) Energiespeicher. Technische Grundlagen und energiewirtschaftliches Potenzial. Fraunhofer-IRB-Verl, Stuttgart
20. Nomura S, Shintomi T, Akita S, Nitta T, Shimada R, Meguro S (2010) Technical and Cost Evaluation on SMES for Electric Power Compensation. Ieee Trans Appl Supercond 20(3):1373–1378. https://doi.org/10.1109/TASC.2009.2039745
21. Norris B, Symons P, Schoenung S, Hassenzahl W, Knoxville K (2002) Handbook of Energy Stoage for transmission or Distribution Applicaitons. California
22. Schmidt VM (2003) Elektrochemische Verfahrenstechnik. Grundlagen, Reaktionstechnik, Prozessoptimierung. Wiley-VCH, Weinheim
23. Schwaiger F, Sailer B, Glaser J, Meyer H-J (2002) Supraleitfähigkeit. Strom eiskalt serviert. Chemie unserer Zeit, Mainz
24. Simon O (1999) Einsatz eines supraleitenden magnetischen Energiespeichers zur Kompensation von Netzrückwirkungen. Fortschritt-Berichte VDI Reihe 21 Elektrotechnik, vol 268. VDI-Verl, Düsseldorf
25. van de Bossche P, van Mulders F, Verbruggel B, Omar N, Culcu H, van Mierlo J (2013) The Cell versus the System. Standardization challenges for electricity storage devices, Stavanger

26. WIMA (2013) Anwendung von WIMA Doppelschicht-Kondensatoren. http://www.wima.de/DE/supercap_applic.htm. Accessed 24 Oct 2013 (WIMA Spezialvertrieb elektronischer Bauelemente GmbH & CO.KG)
27. Yonghua C (2010) Assessments of Energy Capacity and Energy Losses of Supercapacitors in Fast Charging–Discharging Cycles. Ieee Trans Energy Convers 25(1):253–261. https://doi.org/10.1109/TEC.2009.2032619
28. Zogbi D (2013) Supercapacitors the Myth, the Potential and the Reality. http://www.ttiinc.com/object/me-zogbi-20130403.html. Accessed 24 Oct 2013 (tti Inc)

# Electrochemical Energy Storage Systems

*Ingo Stadler, Bernhard Riegel, Detlef Ohms, Eduardo Cattaneo, Götz Langer, and Matthias Herrmann*

**7.1 Basic Principles – 230**
7.1.1 Basic Physical Principles – 230
7.1.2 Electrode Potential – 232
7.1.3 Electrode Equilibrium – 233
7.1.4 Nernst Equation – 234
7.1.5 Electrochemical Reactions on Electrodes – 235
7.1.6 Electrochemical Cells and Cell Reactions – 235
7.1.7 Electrode and Cell Polarization – 237
7.1.8 Side-Reactions – 239
7.1.9 Energy and Efficiency – 239
7.1.10 Types of Electrochemical-Energy Storage and Converters – 240
7.1.11 Electrolyte – 241
7.1.12 Cell Designs – 242
7.1.13 Energy Storage Parameters – 242

**7.2 Lead-Acid Batteries – 245**
7.2.1 Design – 245
7.2.2 Basic Reactions, Equilibrium, and Cell Voltage – 247
7.2.3 Mole Balance and Storage Capacity – 247
7.2.4 Discharging Characteristics – 249
7.2.5 Side-Reactions – 251
7.2.6 Charging Lead Batteries – 255
7.2.7 Sealed Lead Batteries – 257
7.2.8 Aging Mechanisms – 259
7.2.9 Conclusion – 260

**Electronic supplementary material** The online version of this chapter (https://doi.org/10.1007/978-3-662-55504-0_7) contains supplementary material, which is available to authorized users.

© Springer-Verlag GmbH Germany, part of Springer Nature 2019
M. Sterner, I. Stadler (Eds.), *Handbook of Energy Storage*, https://doi.org/10.1007/978-3-662-55504-0_7

**7.3 Nickel Batteries – 262**
7.3.1 Conclusion – 263
7.3.2 Nickel-Cadmium Batteries – 263
7.3.3 Nickel Metal Hydride Batteries – 277
7.3.4 Conclusion – 279

**7.4 Lithium Batteries – 280**
7.4.1 Operating Principle, Chemical Reactions, and Active Materials – 281
7.4.2 Cell Voltage – 283
7.4.3 Conclusion – 286
7.4.4 Electrolyte and Electrochemical Stability Window – 286
7.4.5 Other Cell Components – 289
7.4.6 Conclusion – 290
7.4.7 Electrode Material Conductivity – 291
7.4.8 Conclusion – 293
7.4.9 Designs and Application Areas – 293
7.4.10 Operating Method and Typical Performance Characteristics – 297
7.4.11 Conclusion – 302
7.4.12 Outlook – 302

**7.5 Sodium-Sulfur Batteries – 303**
7.5.1 The Electrodes – 303
7.5.2 The Electrolyte/Separator – 304
7.5.3 The Heating System – 305
7.5.4 Forms and Module Sizes – 307
7.5.5 Charging and Discharging Process – 308
7.5.6 Cycles, Capacities, and Service Life – 311
7.5.7 Efficiency, Power, and Energy – 311
7.5.8 Hazards and Safety – 313
7.5.9 Conclusion – 313

**7.6 Redox Flow Batteries – 314**
7.6.1 Redox Flow Cell Design and Operation – 314
7.6.2 Possible Material Pairings – 318
7.6.3 Charging and Discharging Strategies – 319
7.6.4 Energy Density, Power Density, and Efficiency – 320
7.6.5 The Redox Flow Battery in Comparison – 321
7.6.6 Service Life and Mechanisms that Shorten Service Life – 322

7.6.7 Redox Flow Battery Application Areas – 322
7.6.8 Recycling, Environmental Friendliness, and Safety – 323
7.6.9 Conclusion – 323

**References – 323**

**Overview**

Direct storage of electrical energy using capacitors and coils is extremely efficient, but it is costly and the storage capacity is very limited. Electrochemical-energy storage offers an alternative without these disadvantages. Yet it is less efficient than simple electrical-energy storage, which is the most efficient form of electricity storage.

Batteries and accumulators are forms of electrochemical-energy storage. Electrochemical systems use electrodes connected by an ion-conducting electrolyte phase. In general, electrical energy can be extracted from electrochemical systems. In the case of accumulators, electrical energy can be both extracted and stored. Chemical reactions are used to transfer the electric charge.

Two categories of electrochemical-energy storage are low-temperature batteries such as lead, nickel, and lithium batteries, and high-temperature batteries such as sodium-sulfur batteries. Two further categories are batteries with external storage such as redox flow batteries, and those with internal storage (the majority of batteries).



## 7.1 Basic Principles

Before describing the most common battery technologies, this section outlines the basic principles of the thermodynamic and chemical processes used by all the technologies. The electrochemical processes are too complex to be described here in detail, and have been somewhat simplified.

### 7.1.1 Basic Physical Principles

Energy storage in batteries uses charge carriers collected and released by reduction and oxidation processes. Their flow creates an electric current $i(t)$:

$$i(t) = \frac{dQ}{dt}. \tag{7.1}$$

An electron (or proton with the charge $Q$ [A s = Coulomb = C]) has an elementary charge of $e = 1.602177 \times 10^{-19}$ C. The Faraday constant is derived from the elementary charge $e$ and the Avogadro constant $N_A = 6.0221415 \times 10^{23}$ mol$^{-1}$:

$$F = e \cdot N_A = 9.648534 \times 10^4 \cdot \mathrm{C} \cdot \mathrm{mol}^{-1}. \tag{7.2}$$

With $n_{e^-}$ electrons released, a charge quantity of

$$Q = n_{e^-} \cdot F = \int i(t)dt \tag{7.3}$$

is transported.

The quantity of released electrons $n_{e^-}$ is calculated by using stoichiometry and reaction equations. In the reactions on the anode and cathode sides, ions are converted in each reaction process. As a result, electrons are collected or released. To balance the charge, some protons are also collected or released. This means that the number of transferred electrons is proportional to the mass of material on the electrode. Faraday's first law of electrolysis establishes an equivalence between the quantity of deposited material and the quantity of electric charge.

With a reduction reaction:

$$\vartheta_E + ze^- \rightarrow \vartheta_p \tag{7.4}$$

where the stoichiometric factors $\vartheta_E$ and $\vartheta_p$ stand for the reactant or product of the reaction. Multiplying by the valence $z$ results in the charge quantity:

$$Q = n_E \cdot z \cdot F = n_{e^-} \cdot F = \int i(t)dt. \tag{7.5}$$

The potential difference $U = \Delta\varphi = \varphi_{\mathrm{cathode}} - \varphi_{\mathrm{anode}}$ is used to calculate the work required to transport the charge quantity between the cathode and anode per mole of reactions:

$$w_{\mathrm{el}} = -z \cdot F \cdot U \ \left[\mathrm{J} \cdot \mathrm{mol}^{-1}\right]. \tag{7.6}$$

For a more detailed explanation, see ▶ Sect. 7.1.2. If the work is carried out reversibly

at a constant temperature and pressure, then it is equivalent to the implementable chemical reaction, and as a result, to the free reaction enthalpy:

$$\Delta G_R : w_{el} = \Delta G_R \left[\mathrm{J \cdot mol^{-1}}\right]. \quad (7.7)$$

Changes in temperature, for example, result in unintended irreversible processes within the chemical reactions. Because of the heat effect, usable reaction enthalpy $\Delta H_R$ at reaction entropy $\Delta S$ will then be lower than free reaction enthalpy $\Delta_R G$. As a result:

$$\Delta G_R = \Delta H_R - T \cdot \Delta S. \quad (7.8)$$

If $\Delta G_R < 0$ then $w_{el} < 0$. This is called a galvanic cell discharge process where power is released. But if $\Delta G_R > 0$ and as a result $w_{el} > 0$, it is called an electrolysis cell discharge process and power is absorbed. The charging process can only be forced by applying an external voltage (▶ Sect. 7.1.6). In addition, $\Delta G_R$ depends on the reactants, and therefore varies:

$$\Delta G_R = \Delta G^0 + R \cdot T \cdot \ln\left(\prod_{i=1}^{n} a_i{}^{\vartheta_i}\right). \quad (7.9)$$

Here $\Delta G^0$ is the reaction enthalpy under standard conditions ($p = 1\,\mathrm{bar}$; $T = 298.15\,\mathrm{K}$; $c_i = 1\,\mathrm{mol/L}$; $a_i = 1$), and so the standard free reaction enthalpy. In addition, $R$ stands for the gas constant where $R = 8.3145\,\mathrm{J/(mol \cdot K)}$, $T$ for temperature in Kelvin, and $a_i$ for reactant activity $i$ in mol/L. $\vartheta_i$ is the stoichiometric coefficient for educts $< 0$ and products $> 0$.

The activity is also the thermodynamic measure for the effectiveness or efficacy of a substance I:

$$\alpha_i = \gamma_i \cdot c_i. \quad (7.10)$$

This means that the activity coefficient $\gamma$ is a dimensionless correction-coefficient dependent on the substance i. An 'ideally' diluted solution is one where the distance between ions is very large and their interaction negligibly small. This results in an activity coefficient of $\gamma = 1$, so that the activities of the substance concentrations $c_i$ are given by:

$$c_i = \frac{n_i}{V}\,[\mathrm{mol \cdot dm^{-3}}]. \quad (7.11)$$

Here $n_i$ stands for the quantity of dissolved material and $V$ for the volume of solution. If the reaction system is in chemical equilibrium, this results in what is termed the mass-action or equilibrium constant $K_c$ in Eq. 7.11. As the name suggests, in this state the concentrations of all reactions remain constant. This is because the bonds resulting from the chemical reactions are made and broken at the same speed. This process describes a dynamic equilibrium where the net external reaction has been halted. As a result:

$$\Delta G^0 = -R \cdot T \cdot \ln(K_c). \quad (7.12)$$

The equilibrium voltage $U^0$ is calculated by equating it with Eq. 7.6 under standard conditions:

$$\frac{\Delta G^0}{z \cdot F} = -U^0. \quad (7.13)$$

If Eq. 7.6 is used in Eq. 7.7, and Eq. 7.13 in Eq. 7.9, the result is the general Nernst equation where $U$ is the Nernst potential:

$$U = U^0 + \frac{R \cdot T}{z \cdot F} \cdot \ln\left(\prod_{i=1}^{n} a_i{}^{\vartheta_i}\right). \quad (7.14)$$

See also the discussion in ▶ Sect. 7.1.4.

The standard equilibrium voltage $U^0$ is calculated from the difference between the standard single potentials $\varphi^0$ of the two electrodes:

$$\varphi^0_{\mathrm{cathode}} - \varphi^0_{\mathrm{anode}} = U^0. \quad (7.15)$$

The electrode potentials are listed in reference books, and depend on the reduction process of the electrode. The potential of a reference hydrogen electrode (RHE) is used as a convenient reference. Under standard conditions, it reaches a value of zero.

### 7.1.2 Electrode Potential

All electrochemical processes involve a transfer of charge between areas with equivalent physical and chemical characteristics (phases). The inner electric potential is the quantity of energetic change that accompanies a change in the phase's electric charge. The inner electric potential $\varphi$ is defined by the electric work $W_{el}$ required to transport a positive charge to a phase from an infinite distance (Fig. 7.1),

$$W_{el} = z \cdot F \cdot \varphi. \tag{7.16}$$

Here $z$ represents the valence and $F$ the Faraday constant.

The difference of inner electric potential between two phases in contact (phase boundary) is called the Galvani potential. If the two phases in contact are metallic, then the difference is also called the Volta potential. Because the potentials of various metals vary by temperature, thermocouples are used to measure the temperature.

When an electrical conductor is immersed in an electrolyte solution, a potential difference is also created at the phase boundary. A system consisting of several phases (metal and electrolyte) facilitating the exchange of charges is called an electrode. In everyday speech, sometimes only the metal submerged is called the electrode. This is misleading; an electrode is defined by the entire multi-phase system created by the contact of the electric conductor (for example, a metal) with the ion conductor in the electrolyte solution.

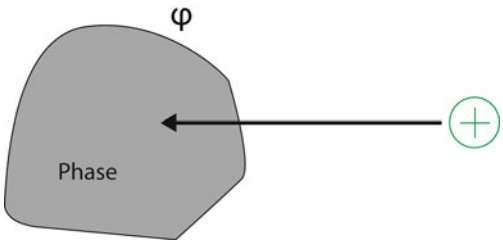



**Fig. 7.1** Inner electric potential

Electrodes are termed ion electrodes or redox electrodes depending on the way the charge carrier (ions or electrons) penetrates the boundary.

There are also two types of ion electrodes. The second type of ion electrode is an electrode where the charge is transferred through more than one boundary. This is the case when, for example, a low-solubility salt is deposited on the metal surface. These electrodes are also sometimes called multiple electrodes (in contrast to 'simple' electrodes with only one boundary). Since the electrochemically active material remains stationary, these kinds of electrodes are frequently used in accumulators.

Electrodes are also termed homogenous or heterogeneous depending on whether the reactants and products are in the same phase (Fig. 7.2).

Insertion electrodes (for example in lithium ion cells) are a special case. Here a foreign ion is embedded in a crystal grid. This creates phase areas defined by the gradient of embedded foreign ions. Across these areas, potential may vary within the phase.

If two electrodes in contact with the same electrolyte are combined, a measurable potential difference between these electrodes is the result. An example of a simple ion electrode is a system with a metal submerged in an aqueous solution containing the same metal ions. This allows the ions in the metal grid to cross the phase boundary into the electrolyte phase (oxidation of the metal). The result is a negative charge in the metal grid. In addition, the ions from the electrolyte phase can move into the metal grid (reduction), giving the metal phase a positive charge.

The chemical properties of the metal and of the metal ions it interacts with in the electrolyte solution create a certain potential difference across the phase boundary. This potential difference varies with various metals. Base metals tend to dissolve quite easily. The result is a negative charge in the metal phase, hindering the process. This was called solution pressure by early electrochemical researchers. Voltage se-

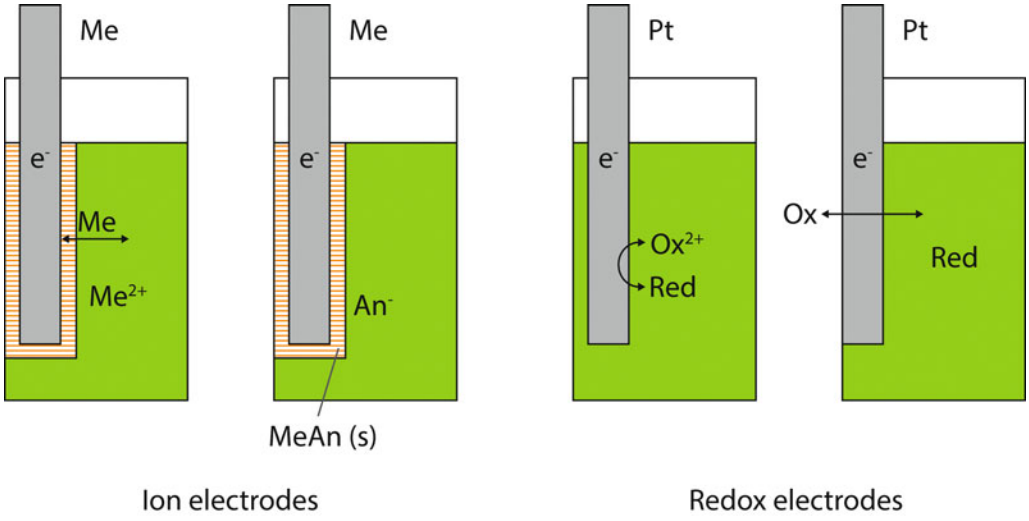



**Fig. 7.2** Ion and redox electrodes

ries for various metals were then compiled by observation.

To understand electrodes in accumulators, this concept of potential must be expanded to apply to all electrodes. But to produce potential series for electrodes, the concentration of electrochemical components must be taken into account.

Chemical thermodynamic formulas are applied to determine the reactivity of the various materials used to create the potential difference.

The reactivity is determined by the chemical potential $\mu$ of the ions used, as defined in Eq. 7.17. The differential quotient of free enthalpy $G$ is thermodynamically determined by the quantity of component materials at a constant temperature $T$ and pressure $p$.

$$\mu_i = \left(\frac{\partial G}{\partial n_i}\right)_{T,p}. \tag{7.17}$$

### 7.1.3 Electrode Equilibrium

When no electric current flows through an electrode, there is equilibrium between the electrochemical reaction partners. A difference in potential in the phases results in a potential difference across the phase boundary.

Assuming constant pressure and temperature, according to chemical thermodynamics, equilibrium is reached when the free reaction enthalpy is zero. With electrochemical reactions, this process is more complex. Electrochemical equilibrium is reached on the electrode when the chemical driving force is compensated exactly by the phase boundary potential. Seen from the outside, no reaction can then be observed and the electric current is zero. Partial reactions (back and forth reactions, dynamic equilibrium) may however continue internally at a certain rate. But these reactions must cancel each other out in total, neutralizing all partial currents.

The concentrations of materials active in the electrochemical equilibrium state are called the equilibrium concentrations. The potential is called the equilibrium electrode potential. If an electrical current is applied or facilitated by creating a power-circuit, then the electrode is polarized and no longer in electrochemical equilibrium. Its potential deviates from the equilibrium value, and the concentrations change.

### 7.1.4 Nernst Equation

An electrode's potential in the electrochemical equilibrium state is determined by the concentration of electrode components and defined by the Nernst equation. To formulate the Nernst equation, i.e., the dependence of the electrode potential on the concentrations, the electrode reaction must be determined first.

In the example below, an electrode has been chosen that allows the material in a reduced form (Red) to be converted to an oxidized form (Ox). The reaction formula is structured so that the oxidized form of the redox pair is on the right side:



$$\mathrm{Red} \underset{\text{Reduction}}{\overset{\text{Oxidation}}{\rightleftarrows}} \mathrm{Ox}^{z+} + ze^{-}. \tag{7.18}$$

The electrode potential is then determined as follows:

$$U = U^0 + \frac{RT}{zF} \ln \frac{c_{\mathrm{Ox}}}{c_{\mathrm{Red}}}. \tag{7.19}$$

For the reactants involved here, the general gas constant is $R$ (around 8.314 J/(K mol), the Faraday constant is $F$ (around 96,500 s A/mol), the charge exchanged per formula reaction according to the reaction formula is $z$, the standard electrode potential is $U^0$, and the equilibrium concentrations is $c$.

In the general formulation of the Nernst equation, the logarithmic term contains the concentrations $a$ of the components. The product of the equilibrium concentrations on the side of the oxidized form of the redox pair is in the numerator. The product of the equilibrium concentrations on the side of the reduced form of the redox pair is in the denominator. The electrode reaction's stoichiometric coefficients appear as exponents:

$$U = U^0 + \frac{RT}{zF} \cdot \ln \left( \frac{\prod_i a_{\mathrm{Ox},i}^{n_i}}{\prod_i a_{\mathrm{Red},i}^{n_i}} \right). \tag{7.20}$$

Strictly speaking, instead of concentrations the so-called activities (effective concentrations) and fugacities should be used, and these should be measured in relation to a standard state. A dimensionless quotient in logarithmic terms then results. In practice, activities and fugacities are approximated by using measures of concentration (mole fraction or mol/ltr) and pressure.

As a result, the logarithmic term's value reflects the deviation between the electrode potential and the so-called standard state. With a thermodynamically defined standard state, the components' activities are equal to one. The standard state indicated here is not associated with any particular temperature.

In practice, it is difficult to determine the conditions where all components are in the standard state. Nevertheless, these standard electrode potential values are useful for purposes of comparison. These values are often given for a temperature of 25 °C.

If the gas is a thermodynamically ideal gas, then with a gaseous reactant, this approximates the standard state. That means that the gas's behavior obeys the ideal gas equation, and the interaction between the particles is negligible. A pressure of 1 atm = 1.01325 bar is also assumed. With condensed (solid, liquid) materials, the standard state is the state of the pure material.

The potentials of individual electrodes can only be measured in comparison to other electrodes. As a result, the so-called hydrogen electrode is often used as a reference electrode. The RHE is based on the heterogeneous electrochemical equilibrium reached between the hydrogen ion concentration in an electrolyte solution, and the gaseous hydrogen above this solution on an inert metal:

$$\mathrm{H_2} \underset{\text{Reduction}}{\overset{\text{Oxydation}}{\rightleftarrows}} 2\mathrm{H}^{+} + 2e^{-}. \tag{7.21}$$

The electrode equilibrium is, therefore, also defined by hydrogen oxidation or reductive hydrogen separation. For the purposes of measurement, sheet platinum modified to enlarge

the surface is used as an inert metal:

$$U_H = U_H^0 + \frac{RT}{2F} \ln\left(\frac{a_{H^+}^2}{a_{H_2}}\right) = U_H^0 + \frac{RT}{F} \ln\left(\frac{a_{H^+}}{\sqrt{a_{ph_2}}}\right). \quad (7.22)$$

The standard electrode potential of the hydrogen electrode $U_H^0$ is 0 by definition. The definition of the standard conditions requires a state where all reactants involved have an activity (effective concentration $a$ or fugacity $a_p$) of 1. For the hydrogen electrode, this means that the gaseous hydrogen's behavior conforms to that of an ideal gas and has a pressure of 1 atm = 101,325 Pa. It also means that the solution has 1 mol/ltr of hydrogen ions, and that their activity coefficient is 1. This precise state cannot be achieved in reality. But the standard hydrogen electrode is still useful as a well-defined reference.

In practice, more convenient reference electrodes are used to measure potentials such as $Hg/HgO/OH^-$ in alkaline electrolytes and $Hg/Hg_2SO_4/SO_4^{2-}$ in acid/water electrolytes. As Eq. 7.22 indicates, the RHE's potential is directly related to the pH value of the solution. With insertion electrodes (for example metal oxide electrodes from lithium cells), charging and discharging cause the concentrations of the embedded material to change continually. The electrode's state of charge (SOC) can be directly determined from the potential.

### 7.1.5 Electrochemical Reactions on Electrodes

Electrochemical reactions occur during charge exchange (redox reaction). The quantity of material is proportional to the quantity of charge converted.

Mole is the unit used to measure the quantity of material. A mole of a material contains $6.022 \times 10^{23}$ particles (Avogadro constant). When the term mole is applied to electric charge, it refers to a charge quantity of 96,485 A s. This charge quantity is called the Faraday constant $F$. Oxidation processes are called anodic reactions, and reduction processes called cathodic reactions.

A chemical redox reaction can be formulated for every electrode process. The charge converted in an electrochemical process is determined by the quantity of material $n$ (number of moles) and the valence $z$ of charges converted per mole:

$$q = z \cdot F \cdot n. \quad (7.23)$$

For polyvalent ions, multiple valences must be taken into account. Instead of molar mass, what is called the equivalent mass of a material is frequently given. This is determined by the molar mass divided by the valence change in a material (Table 7.1).

### 7.1.6 Electrochemical Cells and Cell Reactions

If several electrodes are combined, then an electrochemical chain or cell is created whose cell voltage then can be measured. The potentials of the individual electrodes can be measured by using an additional reference electrode that can be exposed to electricity while remaining constant. Theoretically, it is only possible to measure the voltage between phases of identical materials. In practice, metal/metal transfers to the measurement instrument must also be taken into account (Fig. 7.3).

The chain or cell voltage is determined by the sum of the potential differences, and measured by the connection phase difference:

$$U = \varphi^{\mid} - \varphi^{\mid'}. \quad (7.24)$$

In 1780, Glavani first observed the voltage differences between various metals connected by an electrolyte. The observation was the result of experiments studying the effects of static electricity on biological materials. Galvani observed the electrical effects of various metals when brought into contact with a frog's

**Table 7.1** Characteristic material properties

| Material | Atomic or molar weight | Standard electrode potential at 25 °C | Valence change | Melting point | Density | Electrochemical equivalents | | |
|---|---|---|---|---|---|---|---|---|
| – | g | V | – | °C | g/cm³ | A h/g | g/A h | A h/cm³ |
| $H_2$ | 2.01 | 0 | 2 | – | – | 26.59 | 0.037 | – |
| Li | 6.94 | −3.01 | 1 | 180 | 0.54 | 3.86 | 0.259 | 2.06 |
| Na | 23.0 | −2.71 | 1 | 98 | 0.97 | 1.16 | 0.858 | 1.14 |
| Mg | 24.3 | −2.38<br>−2.69, alk | 2 | 650 | 1.74 | 2.20 | 0.454 | 3.8 |
| Al | 26.9 | −1.66 | 3 | 659 | 2.69 | 2.98 | 0.335 | 8.1 |
| Ca | 40.1 | −2.84<br>−2.35, alk | 2 | 851 | 1.54 | 1.34 | 0.748 | 2.06 |
| Fe | 55.8 | −0.44 | 2 | 1,528 | 7.85 | 0.96 | 1.04 | 7.5 |
| Zn | 65.4 | −0.76<br>−1.25, alk | 2 | 419 | 7.14 | 0.82 | 1.22 | 5.8 |
| Cd | 112.4 | −0.40 | 2 | 321 | 8.65 | 0.48 | 2.10 | 4.1 |
| Pb | 207.2 | −0.13 | 2 | 327 | 11.34 | 0.26 | 3.87 | 2.9 |



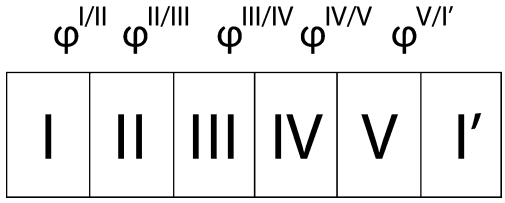



**Fig. 7.3** Phase scheme of an electrochemical cell

leg. The voltages triggered muscle contractions, which he at first misunderstood as 'animal electricity'. These observations allowed the later formulation of an electrochemical voltage series for metals, categorized as 'base' metals and 'precious' metals by Volta and Ritter. The discovery also laid the groundwork for the invention of galvanic electricity sources and electrochemical-energy storage.

Potential differences, i.e., measurable voltages, can also occur between chemically equivalent electrodes if the concentrations of the materials involved differ. These are called concentration cells.

A cell's electrodes are called anodes (oxidation) or cathodes (reduction) depending on the reaction that occurs there. As a result, the positive electrode of an accumulator is an anode during charging and a cathode during discharging. The terms anode and cathode are coupled with the reactions that occur. They are not synonyms for electrode polarity as often assumed.

With complete cells as with electrodes, the voltages in a state without current applied are distinguished from the voltages in a state with current applied. In a state without current, it is called the open-circuit voltage (OCV). When current is applied, the battery's clamping voltage varies from its OCV (cell polarization).

To formulate the cell reaction with current applied, it is assumed that the same charge quantity flows through both electrodes. The chemical equation for the sum reaction is formulated so that the charges created and consumed on the electrodes cancel each other out (electroneutrality principle).

The cell reaction is frequently formulated so that it equals a discharge of the chain with the

pole connected. The free reaction enthalpy that results in the chemical formulation of the reactions (Gibbs free energy, $\Delta G_R$) is normally negative for the discharge. In contrast to the convention in other fields, in chemical thermodynamics, all variable changes are formulated from the perspective of the system studied. This means that energy, or free enthalpy removed from the system, assumes a negative value.

The relationship between the free reaction enthalpy and the cell voltage ($U$) is:

$$\Delta G_R = -z \cdot F \cdot U. \quad \textbf{(7.25)}$$

In this equation, $F$ is the Faraday constant and $z$ is the charge converted in the reaction. The valence $z$ and the change in molar Gibbs energy (free reaction enthalpy) $\Delta G_R$ are always determined by the quantity of material of the formula reaction according to the reaction equation determined (see Hess's Law of chemical thermodynamics).

If the pole of a cell is connected, i.e., the cell is discharged, then the electrode reactions and (by their combination) the cell reactions continue until equilibrium is achieved ($\Delta G_R = 0$, $U = 0$). At the same time, the concentrations of the materials involved change, balancing the potentials of the electrodes. This state would also be reached by a purely chemical process of the cell components at the end of the reaction.

For the sake of simplicity, the reactions are assumed to occur under constant external conditions, e.g., isothermally and isobarically. The energetic changes during the reaction can be calculated from the material constants. Here exothermal (heat-releasing) reactions are distinguished from endothermal (heat-absorbing) reactions.

The pole of an electrochemical cell is sometimes called the cathode or anode. These terms are, however, misleading because they refer only to partial reactions (the cathodic reaction is reduction, the anodic reaction is oxidation). But in an accumulator, the direction of the reactions change depending on whether it is charging or discharging. As a result, the terms positive pole and negative pole should be used instead.

### 7.1.7 Electrode and Cell Polarization

Electrochemical reactions are composed of many partial processes. These include transport processes such as diffusion or migration, adsorption, crystallization, and transfer processes. As with friction in mechanical processes, these processes require that the energy thresholds inhibiting the reaction are exceeded first. With electric current, these obstructions function like resistance, changing the potentials of the electrodes or the voltage of the electrochemical cells. Such deviations from the equilibrium potential or the equilibrium cell voltage are termed electrode or cell polarization.

In simple terms, these changes can be understood as electric resistance in an electric current. By their nature, the physical phenomena that produce polarization have various time dependencies. As a result, polarization resistance should be considered a complex resistance with no exact parallel in electrical engineering. Circuit diagrams are, therefore, of only limited use here. Among other things, these dependencies are the basis for fv (EIS). EIS is used to study electrochemical phenomena in batteries, and covers a large frequency range from just a few μHz to around 100 kHz.

The main polarization phenomena with battery electrodes are:

- Activation polarization
- Diffusion polarization
- Crystallization polarization
- Adsorption polarization

Simple ohmic polarization caused by the limited electric conductivity of the cell components or electrolytes also plays a role here. In addition, the concentrations of the reaction partners can vary from location to location during the cell reaction, resulting in additional polarization (concentration polarization).

These processes can be described mathematically using various models. Activation polarization is crucial here. It basically determines the obstacles that result when the charge car-

rier is activated through the electrode's phase boundary. Energetic analysis of the partial reactions (back and forth reactions in establishing equilibrium) results in the Butler-Volmer equation, which can be used to formulate the anodic and cathodic partial reactions. This equation establishes a relationship between the polarization $\eta$ and the cathodic or anodic current density:

$$i = i_0 \cdot \left\{ \exp\left[ \frac{\alpha \cdot z \cdot F}{RT} \cdot (U - U_0) \right] - \exp\left[ -\frac{(1-\alpha) \cdot z \cdot F}{RT} \cdot (U - U_0) \right] \right\}. \quad (7.26)$$

Here $J$ and $J_0$ are the current density or the exchange current density determined by the electrode surface $A$, $\alpha$ the symmetry factor (which determines how quickly the back and forth reactions cancel each other out), $z$ the number of electrons, $F$ the Faraday constant, $U$ and $U_0$ the electrode or equilibrium potential, $R$ the general gas constant, and $T$ the absolute temperature.

The back and forth reactions that result in dynamic electrochemical equilibrium at the electrode can also be considered as anodic or cathodic partial currents. In electrochemical equilibrium (with no current detectable from outside), the two partial currents are equal in magnitude. The magnitude of these partial currents is then called the exchange current density. If the partial currents are very large, even with no current detectable from outside the electrode may change dramatically (passivation, shape-change, dendrite deposits, etc.).

As indicated by the Butler-Volmer equation, the size of the partial currents depends on the relation of the electrode potential to the equilibrium potential (Fig. 7.4).

With high polarization, the current-voltage curve for the partial reactions takes on a logarithmic form across a wide range. This logarithmic form is used to describe the battery processes in mathematical form. The straight line that results on a semi-logarithmic scale is called the Tafel line (Fig. 7.5).

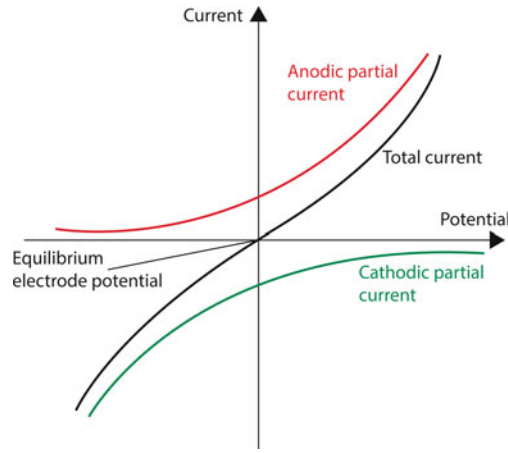



**Fig. 7.4** Current-voltage curve

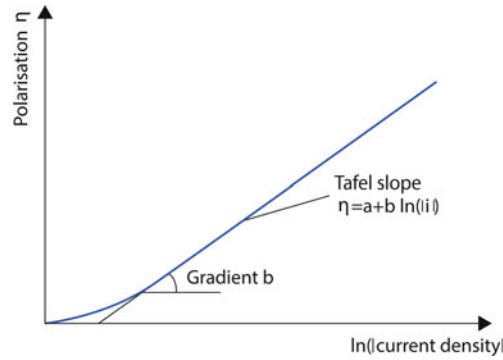



**Fig. 7.5** Tafel line

If the concentrations of the reactant materials sink dramatically when current is applied, then the reaction speed at the electrode surface depends on the speed that the reactants move by diffusion from the surrounding solution to the reaction zone. In this case, the reaction is considered diffusion controlled. Similarly, how fast the products that result from the reaction move away may also limit reaction speed (Fig. 7.6).

The electrode's reaction zone is typically considered as a three-dimensional structure with the reaction occurring on a boundary, whose size far exceeds the geometrical cross-sectional area of the electrode. The presence of pores and micro-structures also increases the electrochemical reaction surface.

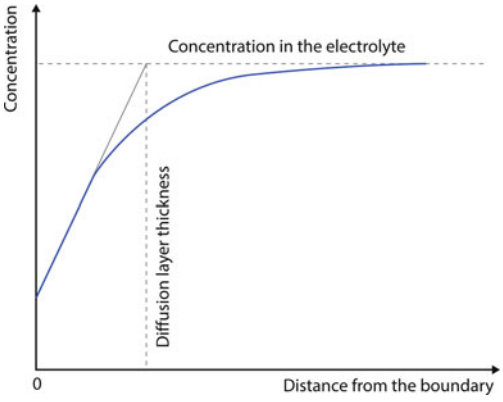



**Fig. 7.6** Concentration at an electrode with current applied

### 7.1.8 Side-Reactions

At a certain electrode potential, other processes involving the cell components may occur besides the actual electrode reaction. For example, in aqueous electrolytes, hydrogen or oxygen may be produced at the electrodes before the charging process is completed. This may be caused by the depletion of the reaction components when the accumulator is close to fully charged. These reactions reduce energy storage efficiency.

Other side processes in the cells result in chemical changes in the reactants that may affect the reactivity of the components. Change processes in the electrodes are partially caused by such chemical changes. These include chemical changes that result from the components' limited stability (for example electrolyte decomposition, reactions with additional components, corrosion, etc.).

### 7.1.9 Energy and Efficiency

Discharging electrochemical cells converts chemically stored energy into electric energy. The free enthalpy (Gibbs energy) of the cell reactions produces the energy converted to electricity.

The relation of cell voltage to free reaction enthalpy determines the electrical values' relation to chemical thermodynamic relationships:

$$G = G(T, p), \tag{7.27}$$

$$dG = \left(\frac{\partial G}{\partial T}\right)_{p=\text{const}} dT + \left(\frac{\partial G}{\partial p}\right)_{T=\text{const}} dp, \tag{7.28}$$

$$dG = -SdT + Vdp. \tag{7.29}$$

The following applies for isothermal and isobaric relationships:

$$\Delta_R G = \Delta_R H - T\Delta_R S, \tag{7.30}$$

$$\Delta_R G = -zFU_0. \tag{7.31}$$

An advantage of electrochemical-energy storage over thermal processes is that it is an isothermal process. As a result, it is not dependent on the conversion efficiency of the Carnot limit (e.g., a thermal engine).

Various criteria determine the efficiency of energy storage in batteries.

The ampere hours efficiency (A h efficiency) is derived from the amount of electricity that can be removed from the battery compared to the amount of electricity used to charge the battery. Since a portion of the electricity is typically consumed by side-reactions, the efficiency level is always less than one. The reciprocal value is also often called the charging factor (ampere hours charged that permit a certain quantity of charge to be removed from the battery). With cells that exclude side-reactions (e.g., lithium cells), theoretically the A h efficiency should be one.

The A h efficiency depends on the current-strength used for charging and discharging, the voltage window (shut-off voltage), and the charging process (with constant current — or CC — $I$, $UI$ characteristic curve, etc.). The same applies when considering the energy.

Efficiency levels depend heavily on the accumulator's operating method, and can only be compared under defined conditions.

Another parameter particularly relevant for fuel cells (electrochemical converters) is the

thermodynamic efficiency of the electrochemical reaction. This is determined by the relation between free reaction enthalpy and reaction enthalpy (observed as an isothermal process under constant pressure; or similarly, the relation of free energy to change in internal energy as an isothermal process at constant volume).

### 7.1.10 Types of Electrochemical-Energy Storage and Converters



Electrochemical storage and energy converters are categorized by several criteria. Depending on the operating temperature, they are categorized as low-temperature and high-temperature systems. With high-temperature systems, the electrode components or electrolyte are functional only above a certain temperature. These systems include solid oxide fuel cells (SOFC) and sodium batteries (sodium nickel chloride and sodium-sulfur).

Primary batteries (single-charging of chemical energy) are also distinguished from secondary batteries or accumulators (repeated complete or at least nearly complete electric-charging) based on their functionality. With both of these, cell component quantity determines the volume of stored energy (Faraday's law). They are combined storage systems and energy converters. In practice, both functions are somewhat compromised as a result.

Since fuel cells are not electrochemical storage systems and function solely as converters of chemical energy to electric energy, they are excluded from the discussion. In addition to the fuel cell stack itself, external storage is required for the reactants. Oxidation components are typically not required, as long as there is adequate ambient air.

Combined with water electrolyzers, hydrogen fuel cells are considered complex storage systems. In recent years, there have been significant advances in the development of proton exchange membranes (PEM) and SOFC fuel cells (solid oxide fuel cells). In addition, other types such as alkaline fuel cells (as for the Apollo program), phosphoric acid electrolyte fuel cells (PAFC), and molten-carbonate fuel cells (MCFC) have been developed. Experiments with direct use of other fuels such as hydrogen (for example hydrazine, methanol, and formic acid) have so far been unsuccessful. But reformers that extract hydrogen from other reactants could theoretically be used instead.

So-called flow cells function similarly to fuel cells. They were developed for stationary use in particular. Reaction component conversion takes place in a cell stack consisting of electrodes and—with separated electrolyte chambers—a membrane. Electrolyte solutions containing the reactants in a dissolved form flow through the components. In contrast to fuel cells, here the reactants can be converted in both directions. This means that energy can be converted into chemical changes (concentration changes of the electrolytes), or chemical energy converted into electric energy. The quantity of energy is determined by the volume of external storage.

In addition to these basic types of energy systems, there are special types that combine electrode forms. These include metal-air cells (for example, zinc-air), where the reaction at the oxygen electrode (or air electrode) is equivalent to the reaction in a fuel cell. These systems are sometimes referred to as semi-fuel cells, because no storage is required for one of the components (oxygen). When functioning as an accumulator, electrochemically charging the cells is technically complex. Due to the high potential level, oxygen separation can lead to corrosion of the electrode materials, causing the zinc electrode to undergo geometrical changes (shape-change) as well as passivation. As a result, some have proposed mechanically regenerating the cells (external-charging or repasting the zinc electrode).

Another special case is bilayer or super capacitors. Here, the storage of energy does not rely on any chemical process. As with capacitors, the bilayer is simply recharged. In contrast to conventional capacitors familiar from electrical engineering, here the electrode surface

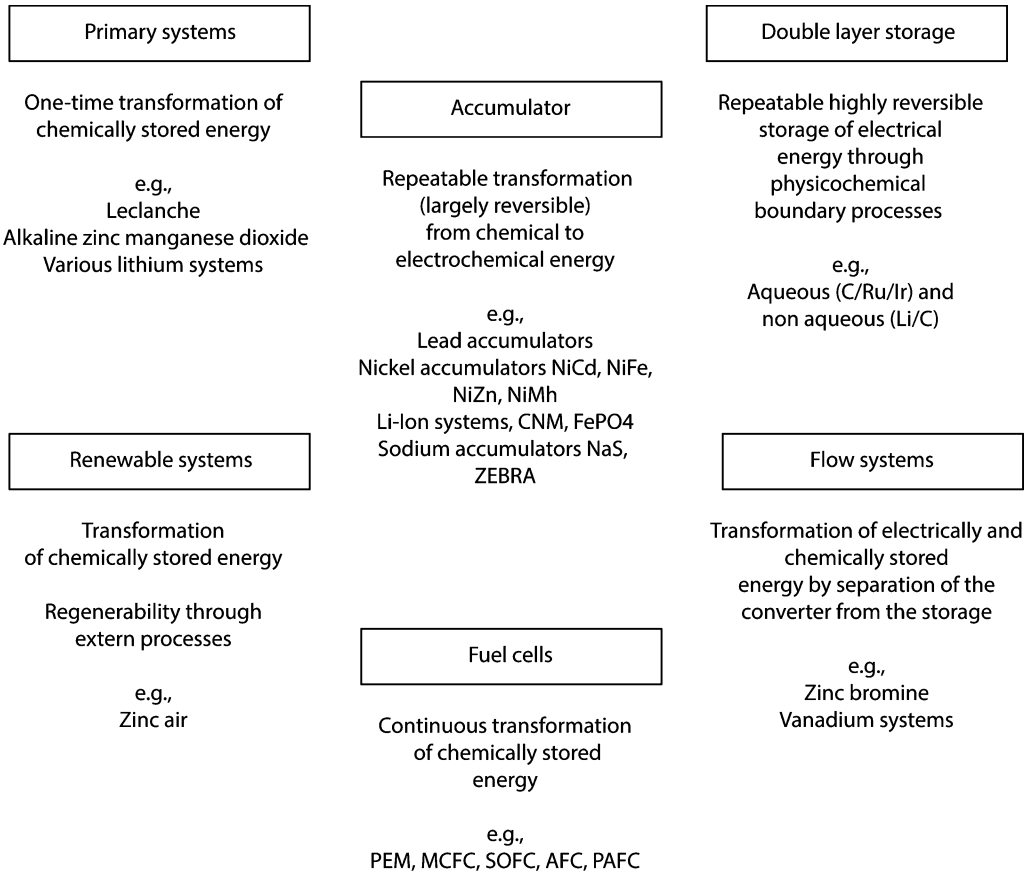



**Fig. 7.7** Types of electrochemical-energy storage

has been increased by the type and design of the material. In addition to a purely electrostatic effect, the charging process also includes sorption processes on the electrode materials. The result is comparably high electrical capacities. Super capacitors are discussed together with purely electrical storage in ▶ Chap. 6. The advantages of super capacitors are their high-specific capacities and good reversibility. A drawback is their low-energy densities, which are significantly below those of conventional electrochemical storage (Fig. 7.7).

### 7.1.11 Electrolyte

An important component of galvanic cells is the electrolyte solutions in which the electrodes are submerged, or with which they are in contact. Unlike an electrical conductor, electrolytes are composed of an electrolyte matrix (usually a solvent with a sufficiently high dielectric-constant) and electrolyte salts, i.e., charged ions disassociated in the solvent. This allows the charge carriers to move quite freely, resulting in high conductivity. Electrolyte solutions are always electrically neutral, i.e., they must always contain an equal number of positive (cations) and negative (anions) ions. There are also electrolytes in the form of polymers or gels that function on the same principle.

The electrical conductivity of electrolytes is significantly lower than that of metals. In addition, it is heavily-dependent on temperature and concentration. Aqueous electrolytes are an exception. Here, a charge transfer mech-

**Table 7.2** Overview of common electrolytes

| Electrolyte | Temperature range [°C] | Example | Range of specific conductivity $\Omega^{-1}\,cm^{-1}$ |
|---|---|---|---|
| Aqueous electrolyte | −40 to 80 | Ni/Cd, Ni/MH | $15 \times 10^{-1}$ |
| Non-aqueous, inorganic electrolyte | −40 to 150 | Li systems | $2 \times 10^{-2}$ to $10^{-1}$ |
| Molten salts | | BZ | $\sim 10^{-1}$ |
| Polymer electrolyte | 0 to 150 | Lithium cells | $10^{-7}$ to $10^{-4}$ |
| Organic electrolyte | −20 to 150 | Lithium cells | $2 \times 10^{-2}$ to $10^{-1}$ |
| Inorganic solid electrolyte | > 300 | Na/S, Na/$NiCl_2$ | $10^{-8}$ to $10^{-5}$ |

7

anism using hydrogen bonds results in high electrical conductivity without requiring the ions to change location. The result is a conductivity about three times higher than with other ions. Organic electrolytes and solid electrolytes offer far less conductivity than aqueous systems. Their conductivity is also heavily-dependent on temperature. Use of these electrolytes is one reason for high operating-temperature requirements (high-temperature batteries, SOFC) (Table 7.2).

### 7.1.12 Cell Designs

Batteries and cells differ in design. Since batteries can either be sealed or vented, one criterion is how the energy storage is separated from the environment. The terms for these two designs vary by battery type. Vented batteries can equalize the pressure with the environment in the gas-phase.

A critical factor with accumulators is the operating method. When aqueous accumulators are charged, a certain amount of overloading may be required. This results in consumption of the electrolytic water, which must then be refilled at regular intervals. In these cases, the cells are either open or vented. Additional features (for example plugging for gas recombination, central degassing, water refill systems, etc.) may also be added to allow these battery systems to function like sealed systems.

Depending on their design, cells are called prismatic cells (preferable to the term rectangular), round cells (cylindrical), or pouch cells (cell units wrapped in foil). The design partly determines the heat exchange capacity.

Cells can be combined in modules and batteries or used as single cells (for example, in frames, trays, etc.). In recent years, a number of requirements have been introduced that can only be met by very compact, high-energy density batteries.

### 7.1.13 Energy Storage Parameters

The most important parameters for energy storage are the voltage curve and the energy content. The voltage curve is determined by the difference between the electrode potentials, and therefore by the kind of electrodes used. Charging and discharging process voltage limits must be determined separately for each individual system.

The energy storage's energy content is determined by the quantity of material used (Faraday's law) and the voltage curve during discharging. With batteries, the measure used is called A h capacity. Unlike how the term is used in electrical engineering, here, capacity means the charge quantity that can be stored in a battery. It should be kept in mind that the extractable capacity depends on the load cur-

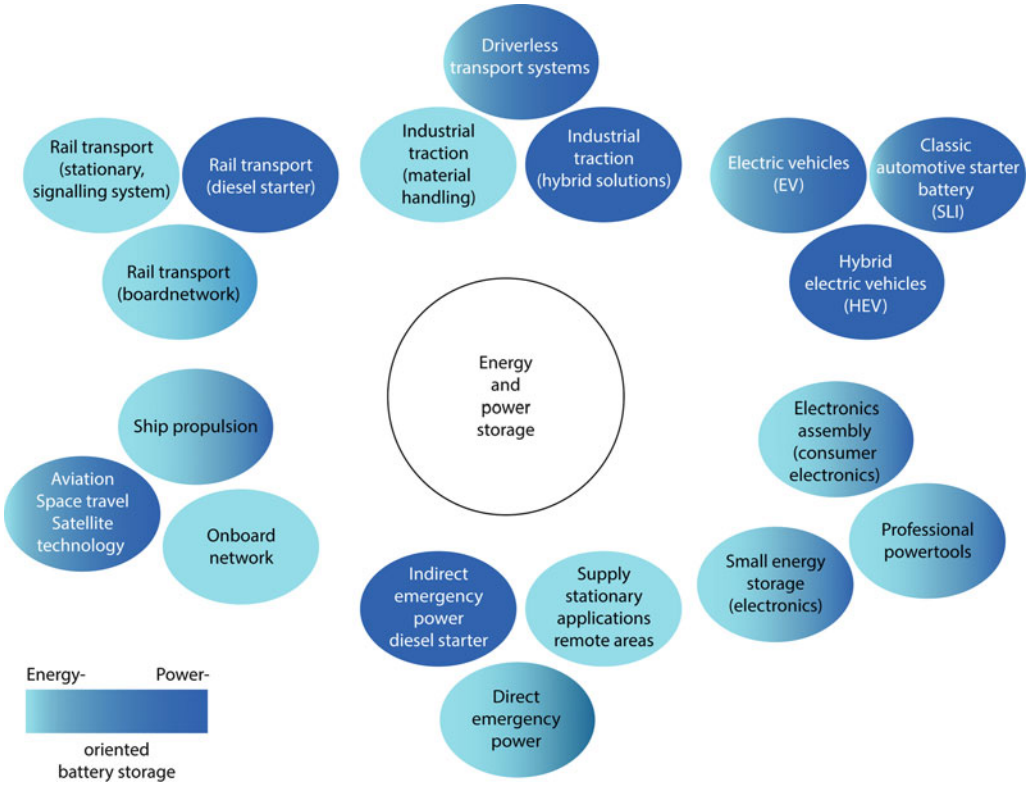



**Fig. 7.8** Battery systems and their application areas

rent, the discharge end criterion (for example the cut-off voltage), and the discharging conditions.

An important criterion in practice is also the power that can be extracted from the battery (Fig. 7.8). This depends on the cell design, and is typically limited by the manufacturer as required. Because of electrochemical processes, this quantity is dynamically determined by the battery's state (for example, SOC).

A cell has an internal resistance determined by the battery's resistance and external conditions. This is calculated using pulse measurements (voltage changes during discharging or charging with adequate pulse height) or impedance measurements (overlapping low-level signals from alternating current electricity or voltage, frequency-dependent or at a fixed measuring frequency).

To compare batteries, the parameters are related to weight (specific energy, specific power) or volume (energy or power density). Comparison is often difficult, because it depends on whether the comparison is on the cell, battery, or system level, and which components are taken into account. Particularly when comparing power data, the experimental conditions for the comparison must be described in detail (Table 7.3).

The relationships between the power and energy parameters are often presented in what is called a Ragone chart. Here the specific power and specific energy (each related to weight) of various batteries are plotted on a logarithmic scale. The usefulness of the chart depends on how accurately the measurements listed in the chart reflect the characteristics of the batteries (inclusion of the weight of all components of

**Table 7.3** Overview of common battery systems

| Secondary batteries (accumulators) | Negative | Positive | Cell reaction | Temp.[a]/ electrolyte | $E$ [V] | g/A h | A h/kg |
|---|---|---|---|---|---|---|---|
| Lead-acid | Pb | $PbO_2$ | $Pb + PbO_2 + 2H_2SO_4 \rightarrow 2PbSO_4 + 2H_2O$ | RT, acidic | 2.1 | 8.32 | 120 |
| Edison (nickel-iron) | Fe | NiOOH | $Fe + 2NiOOH + 2H_2O \rightarrow 2Ni(OH)_2 + Fe(OH)_2$ | RT, alkal. | 1.4 | 4.46 | 224 |
| Nickel cadmium | Cd | NiOOH | $Cd + 2NiOOH + 2H_2O \rightarrow 2Ni(OH)_2 + Cd(OH)_2$ | RT, alkal. | 1.35 | 5.52 | 181 |
| Silver-zinc | Zn | AgO | $Zn + AgO + H_2O \rightarrow Zn(OH)_2 + Ag$ | RT, alkal. | 1.85 | 3.53 | 283 |
| Nickel-zinc | Zn | NiOOH | $Zn + 2NiOOH + 2H_2O \rightarrow 2Ni(OH)_2 + Zn(OH)_2$ | RT, alkal. | 1.73 | 4.64 | 215 |
| Nickel hydrogen | $H_2$ | NiOOH | $H_2 + 2NiOOH \rightarrow 2Ni(OH)_2$ | RT, alkal. | 1.5 | 3.46 | 289 |
| Nickel metal hybrid | MH | NiOOH | $MH + NiOOH \rightarrow M + Ni(OH)_2$ | RT, alkal. | 1.35 | 6.50 | 206 |
| Silver-cadmium | Cd | AgO | $Cd + AgO + H_2O \rightarrow Cd(OH)_2 + Ag$ | RT, alkal. | 1.4 | 4.41 | 227 |
| Zinc/chlorine | Zn | $Cl_2$ | $Zn + Cl_2 \rightarrow ZnCl_2$ | RT, acidic | 2.12 | 2.54 | 394 |
| Zinc/bromine | Zn | $Br_2$ | $Zn + Br_2 \rightarrow ZnBr_2$ | RT, acidic | 1.85 | 4.17 | 239 |
| Li/manganes-dioxide | Li | $MnO_2$ | $Li + MnIVO_2 \rightarrow MnIVO_2\,(Li+)$ | RT, org. | 3.5 | 3.50 | 286 |
| Li/iron-disulfide | Li(Al) | $FeS_2$ | $2Li(Al) + FeS_2 \rightarrow Li_2FeS_2 + 2Al$ | HT, inorg. | 1.73 | 3.50 | 285 |
| Li/iron-monosulfide | Li(Al) | FeS | $2Li(Al) + FeS \rightarrow Li_2S + Fe + 2Al$ | HT, inorg. | 1.33 | 2.99 | 345 |
| Sodium-sulfur | Na | S | $2Na + 3S \rightarrow Na_2S_3$ | HT, $\beta$-$Al_2O_3$ | 2.1 | 2.65 | 377 |
| Sodium/nickel chloride | Na | $NiCl_2$ | $2Na + NiCl_2 \rightarrow 2NaCl + Ni$ | HT, $\beta$-$Al_2O_3$ | 2.58 | 3.28 | 305 |

[a] RT = room temperature; HT = high-temperature.

a battery, such as the tray, for example, control technology, etc.). The comparison should actually be based on discharging data measured at a constant power. However, the discharging data is frequently measured using constant-current discharging, and then converted. There is another difficulty when partially charged batteries are considered. Using the Ragone chart with systems such as fuel cells, flow batteries, or metal-air cells requires taking into account the external reactant storage in the comparison as well. For these reasons, cross-system comparisons using Ragone charts are of limited use, and should be relied on less than commonly thought.

## 7.2 Lead-Acid Batteries

The lead sulfuric acid system was invented 150 years ago, and is still one of the best-known electrochemical systems. In its first form, it consisted of sheets of lead rolled together. The active mass layer was produced by charging and then reversing the polarity (Gaston Planté, 1859). The first electrodes with an electrode grid and active mass paste followed (Camille Faure, 1881). Industrial production began at the end of the 19th century (Henri Tudor, 1887). Later improvements in lead batteries were closely linked to developments in plastics. Newly invented plastics were used to improve separator materials, electrode casings, and battery containers. Lead batteries with low water consumption (low-maintenance batteries) have been manufactured in America since 1935 with electrode grids made out of lead-calcium alloys instead of lead-antimony alloys. At the end of the 1950s, 'dry-cell batteries' using gelled electrolyte were developed for the commercial market by the company Sonnenschein. Batteries with the electrolyte absorbed in glass-fiber mats (Gates Rubber Corporation, Cyclon spiral cell) joined these so-called sealed batteries in 1972.

Today, the lead battery is the most commonly used form of storage for applications outside the consumer sector. Lead batteries have been perfected over this 150-year history for their primary applications as starter batteries, electric drive batteries, and stationary batteries for emergency electricity supply.

At the beginning of this century, lead-acid battery storage became increasingly important for network-connected applications in the local ($\approx$ 10 kW h) and decentralized ($\approx$ 1 MW h) sectors. For local applications, these facilities can be operated as stand-alone systems or as network-connected systems. They are frequently used in connection with renewable energy generation. Specially designed stationary lead batteries are used for these applications.

### 7.2.1 Design

A lead battery cell is composed of the following electrochemical chains connected in series: $Pb/PbSO_4/H_2SO_4(aq)$, $H_2SO_4(aq)/PbSO_4/PbO_2/Pb$. Each of these electrochemical chains consists of an electrode of the second kind, forming a half-cell. The electrodes are in turn composed of a collector (for example a grid) and the active mass. The electrode collector is made of a lead alloy. The active mass of the positive electrode is made of lead-dioxide. The active mass of the negative electrode is made of porous sponge lead (Table 7.4). Both electrodes are completely submerged in the electrolyte (diluted sulfuric acid). To increase mechanical stability and avoid short-circuits, a separator is placed between the electrodes. Higher capacities can be achieved by connecting the chains in parallel and expanding the electrodes.

**Table 7.4** Active mass characteristics

| | | Positive active mass | Negative active mass |
|---|---|---|---|
| Surface (BET[a]) | $m^2/g$ | 3–5 | 0.5–0.7 |
| Pore size distribution | µm | 0.3–1 | 1–4 |
| Porosity | % | 50–55 | 55–60 |
| Specific resistance | $10^{-6}\ \Omega$ m | 200 | 2 |

[a] BET: the **B**runauer-**E**mmett-**T**eller analytical method uses experimental data to determine the specific surface-based on mass.

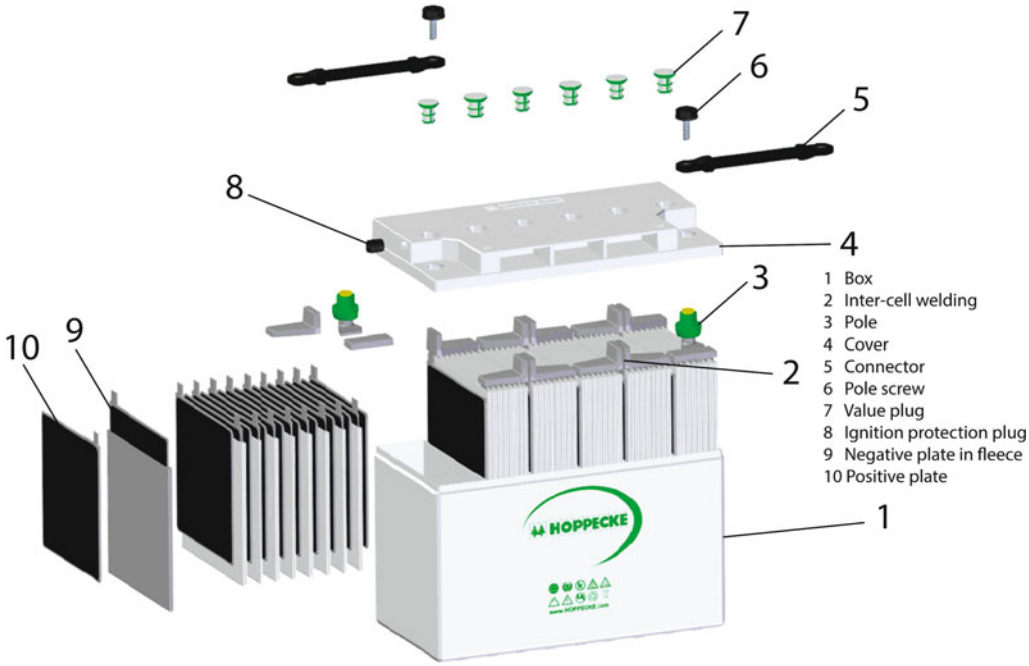



**Fig. 7.9** Battery design (exploded view)

The cell container is made exclusively of plastics such as polypropylene (PP), styrene-acrylonitrile, and acrylonitrile-butadiene-styrene. Transparent materials are particularly useful with stationary applications. They allow the cells to be easily inspected. This also allows convenient monitoring of the acid level, gassing, incipient dendrite deposits, or quantity of active material in the sludge chamber.

Waste material such as active mass sludge is often collected in a sludge chamber between the container bottom and the bottom edge of the plate set. The area above the plate set is filled in with what is called head lead, i.e., the bridges between the electrodes connected in parallel and the pole fastened to it (Fig. 7.9).

The cells are classified by application area and positive electrode type. Large-surface, grid, and tube electrodes are the most popular kinds. As a result, batteries are often referred to as large-surface (Planté plate), grid plate (flat plate), or armored plate (tubular plate).

With large-surface electrodes, a soft-lead collector up to 10 mm thick is cast in the form of a radiator grill with close-mesh slats. Using a special formation process, a 200 µm thick $PbO_2$ layer is created on this greatly enlarged collector surface.

The most common are grid electrodes. Using a pasting process, the initially inactive mass is applied to the lead-grid meshwork of the collector. This is then converted into an active mass over several different manufacturing steps.

Modern tube electrodes use a tube sleeve made of sulfur-stabilized polyester. This has a polyacrylic resin coating with an outer diameter of up to 10 mm extending to the neighboring tubes. The sleeve stretches to the bulge of the spine grid's head lead. The bulge holds the spines that taper to about 3 mm in diameter. Each is connected to a tube. Each tube has a spine in the middle stretching its entire length. It is completely surrounded by active mass, which is in turn fixed in place by the tube sleeve.

The first two kinds of electrodes are primarily used for power-oriented applications. The

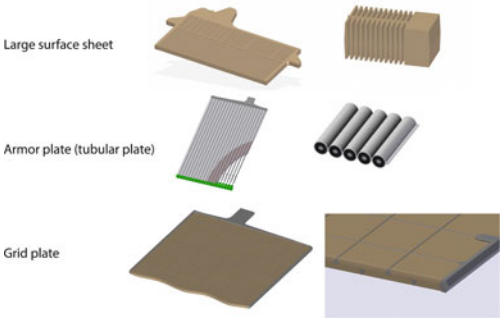



**Fig. 7.10** Electrode forms: large-surface, tube, and grid electrodes

tube sleeve design is ideal for cyclically stable lead cells. This is because surrounding the spine with fixed active mass can significantly reduce the production of sludge. Figure 7.10 illustrates the various forms of positive electrodes.

### 7.2.2 Basic Reactions, Equilibrium, and Cell Voltage

By separating the two half-cells, the central chemical reactions can be isolated:

$$PbO_2 + 3H^+ + HSO_4^- + 2e^- \leftrightarrow PbSO_4 + 2H_2O, \quad (7.32)$$

$$Pb + HSO_4^- \leftrightarrow PbSO_4 + H^+ + 2e^-. \quad (7.33)$$

The cell reaction of the complete cell is a synproportionation from elementary non-valent lead and tetravalent lead to the level of bivalent lead. This is the result of adding the individual reactions in the half-cells. The mole balance is given by the complete reaction:

$$Pb + PbO_2 + 2H^+ + 2HSO_4^- \leftrightarrow 2PbSO_4 + 2H_2O \quad (7.34)$$

$$207\,g + 239\,g + 2 \cdot 98\,g \leftrightarrow 2 \cdot 303\,g + 2 \cdot 18\,g.$$

Here, the forward discharging reaction corresponds to the reverse-charging reaction. The formulas also demonstrate that the electrolyte functions as an ion conductor and takes part in the reaction itself (Fig. 7.11). This dual function of the electrolyte links its concentration or acid density with the degree of conversion of the electrodes or the battery's SOC. Since the change in density also affects the battery's voltage, the quantity of charge that can be discharged depends on the current as well. This is called Peukert's law (▶ Sect. 7.2.4).

An electric current is only possible when electron conduction in the electrodes and the external consumer is completed by ion conduction in the electrolyte to form a circuit. The transfers at the boundaries of the electrodes to the electrolyte are described by the chemical reactions given above.

The chemical reactions at both electrodes occur during the solution phase. The individual steps of the reaction is the activation reaction itself. But the transport of the ion species $Pb^{2+}$ and $HSO_4^-$ as well as dissolution and capture are also part of the activation reaction. In ▶ Sect. 7.2.3, overvoltages are assigned to each individual step of the complete reaction (Fig. 7.12)

The system's voltage in an unloaded condition can be calculated by using the free reaction enthalpy of the reaction partners and the Nernst equation. For acid densities between 1.20 and 1.30 g/cm$^3$, it can be very accurately estimated by using an empirical formula [1] (valid for acid densities at 25 °C):

$$U_0\,[\mathrm{V}] = \text{acid density}\,\left[\mathrm{g/cm^3}\right] + 0.84. \quad (7.35)$$

The relationship between sulfuric acid density at 25 °C, its molality (temperature-independent), and the OCV $U_0$ (temperature coefficient of +0.20 mV/K [3], i.e., nearly temperature-independent) are illustrated in Fig. 7.13.

### 7.2.3 Mole Balance and Storage Capacity

In the complete reaction in Eq. 7.34, a mole conversion occurs with 642 g of reactants us-

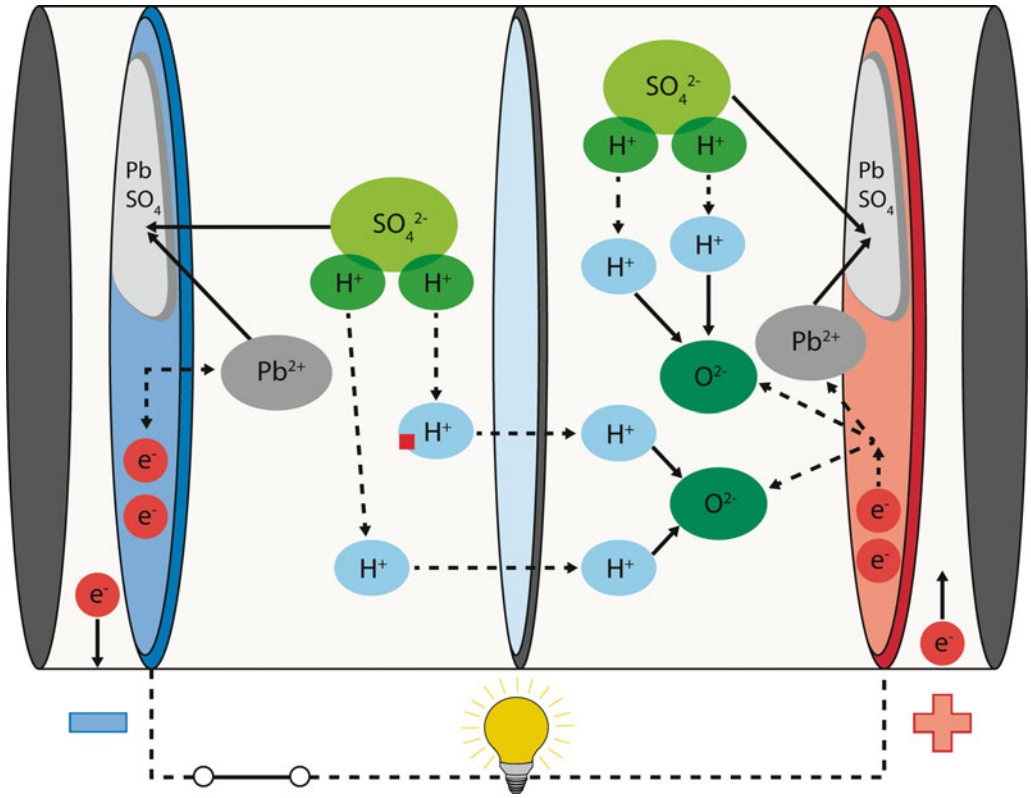



**Fig. 7.11** Cell discharging reaction

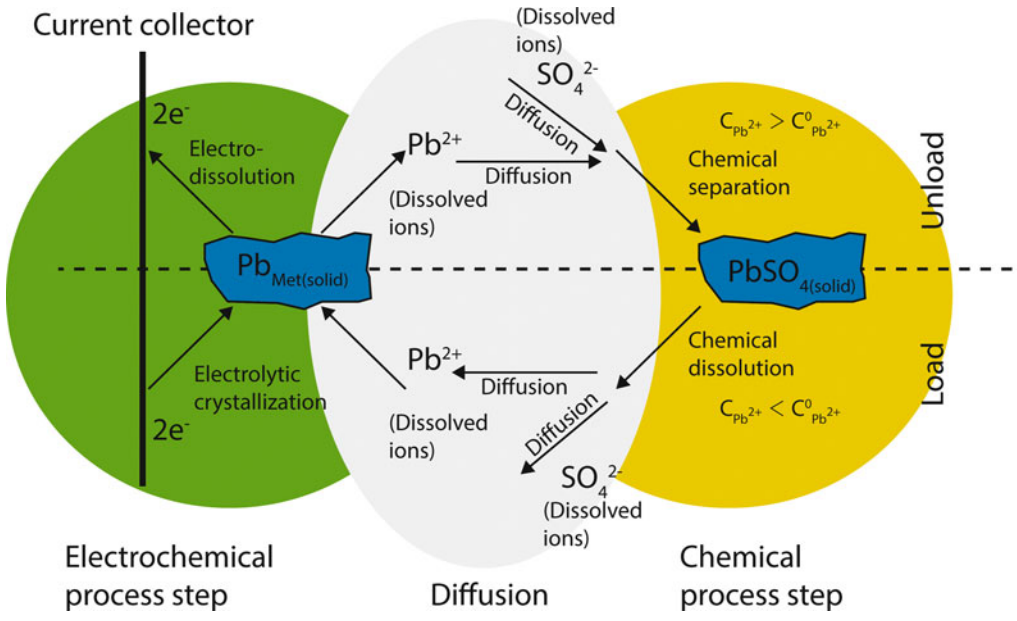



**Fig. 7.12** Individual chemical reaction steps (for a negative electrode, in this instance)

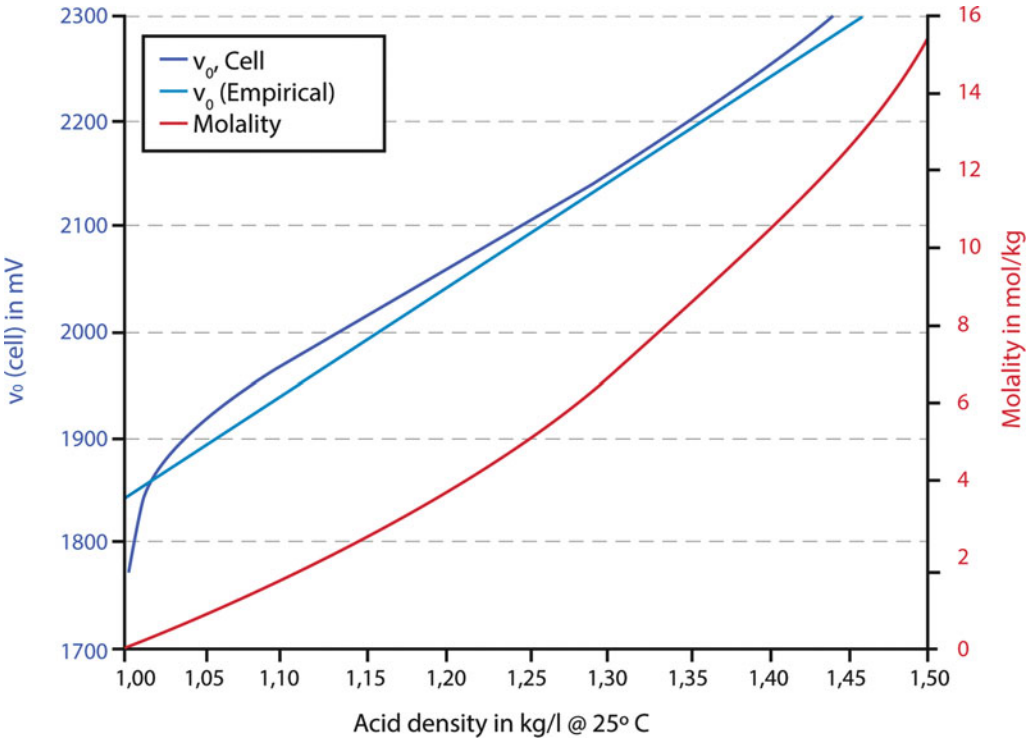



**Fig. 7.13** Acid density, Cell Voltage and molaity, OCV

ing two moles of electrons. This is equivalent to a charge quantity of $2 \cdot 96{,}500\,\mathrm{A\,s} = 53.6\,\mathrm{A\,h}$. The ideal energy content requires a moderate discharging voltage of 1.92 V:

$$53.6\,\mathrm{A\,h} \cdot 1.92\,\mathrm{V}/0.642\,\mathrm{kg} = 160\,\mathrm{W\,h/kg}.$$

But the ideal energy content can never actually be achieved:

- Because the actual system must include active components (grid, head lead, pole, battery housing, separators, water to dilute the sulfuric acid).
- Because in an actual system the active components cannot be fully charged (mass efficiency, acid consumption).

The actual energy content of a lead battery is therefore between 25 and 40 W h/kg. A lead battery's extractable quantity of charge under real conditions is called its capacity. The nominal capacity can be measured by discharging the battery under standard conditions (for example, 20 °C, discharge over twenty hours, 1.8 V/cell final discharge-voltage with starter batteries) (Table 7.5).

### 7.2.4 Discharging Characteristics

When current is applied, there is a voltage drop across the resistances of all cell components. It must also be taken into account that the reaction speed is forced on the chemical reaction. But it can only be forced on the reaction if additional activation energy ($Q \cdot \Delta U$) is available for charge movement (charge $Q$). This additional voltage $\Delta U$ is termed overvoltage. Unlike the voltage drop, it is not linear to the current at the ohmic resistances. All voltage drops and overvoltages are largely determined by the current-strength, the temperature, and the acid density. The activation reaction is described by the Butler-Volmer equation (Eq. 7.26). With large

**Table 7.5** Charge content

| One ampere hour consumes during discharging, and generates during charging | | |
|---|---|---|
| Pb | $PbO_2$ | $2H_2SO_4$ |
| 3.86 g | 4.46 g | 3.66 g |
| **… generates during discharging, and consumes during charging** | | |
| $2PbSO_4$ | $2H_2O$ | |
| 11.315 g | 0.672 g | |
| **… decomposed during overloading** | **and generates electrolysis gases** | |
| $H_2O$ | $H_2$ | $O_2$ |
| 0.336 g | 0.037 g = 0.418 L[a] | 0.299 g = 0.209 L[a] |

[a] At 0 °C, 1 bar.



overvoltages, the Butler-Volmer equation's second term (the reverse reaction) can be ignored, and the equation analytically solved for the overvoltage. The straight line that results on a semi-logarithmic scale is called the Tafel line.

Overvoltage is primarily an empirically measurable quantity that can be separated from the purely ohmic voltage drop, for example in impedance measurements. However, the causes of overvoltage can be explained by the various physical and chemical phenomena in the complete reaction's individual steps (Fig. 7.12). Overvoltages and ohmic voltage drops together result in the deviation of measured voltage from OCV when current is applied. This is also called polarization. Table 7.6 lists the most important factors contributing to polarization in a cell.

When discharging with CC, the effect of the various voltage drops can be shown in a simple graph (Fig. 7.14). The voltage drop in the OCV as well as the depth of discharge (DOD) results from the electrolytes' participation in the chemical reaction. This is a decisive difference between lead sulfuric acid systems and NiCd, (NiMH), Na-NiCl, and lithium ion systems.

In addition to the voltage drop caused by the internal resistance of the cell, the change in concentration of the electrolyte and the diffusion of the active sulfate ions limits the maximum capacity of lead cells. The capacity's resulting dependence on current has been formulated by Peukert:

$$I^{pc} \cdot t = \text{const.} \qquad \textbf{(7.36)}$$

The Peukert coefficient pc has a value between 1 and 2. If the coefficient is 1, then the discharging time (capacity) is independent of the current. For lead batteries, the coefficient is around 1.3. The smaller the coefficient, the better the battery performs with high-capacity applications. But since the coefficient is not universally applicable, the capacity's dependence on current with various battery cell types must be provided by the manufacturer. Figure 7.15 shows an example of the capacity's dependence on current.

This illustration also indicates the terminology typically used for the capacity of lead batteries. The specifications for discharging time are also given in the index. The ten-hour capacity $C_{10}$ indicates the capacity that can be extracted with a current of $I_{10}$. According to the configuration data shown in Fig. 7.15, the three-hour capacity up to a final discharge-voltage of 1.8 V/cell is $C_3 = 140$ A h. The current is then $I_3 = 46.7$ A.

The dependence on the final discharge-voltage is also included in Fig. 7.15. The capac-

**Table 7.6** Overvoltages in a lead accumulator

| Description | Cause | Time constant |
|---|---|---|
| Ohmic voltage drop | Ohmic resistance, collector + electrolyte + active mass | – |
| Inductive voltage drop | Battery construction's inductance | – |
| Activation overvoltage | Charge carriers require activation energy to be activated through the electrode/electrolyte boundary | Ms to seconds, determined by the bilayer capacity |
| Diffusion overvoltage | Uneven distribution of the ions involved in the reaction | 15–60 minutes to several days with sealed cells |
| Reaction overvoltage | Inhibited upstream or downstream reactions | – |
| Concentration overvoltage | Diffusion and reaction overvoltage combined | 15–30 min |
| Crystallization overvoltage | Delayed crystallization formation; for example, voltage delay when discharging | Seconds to minutes |

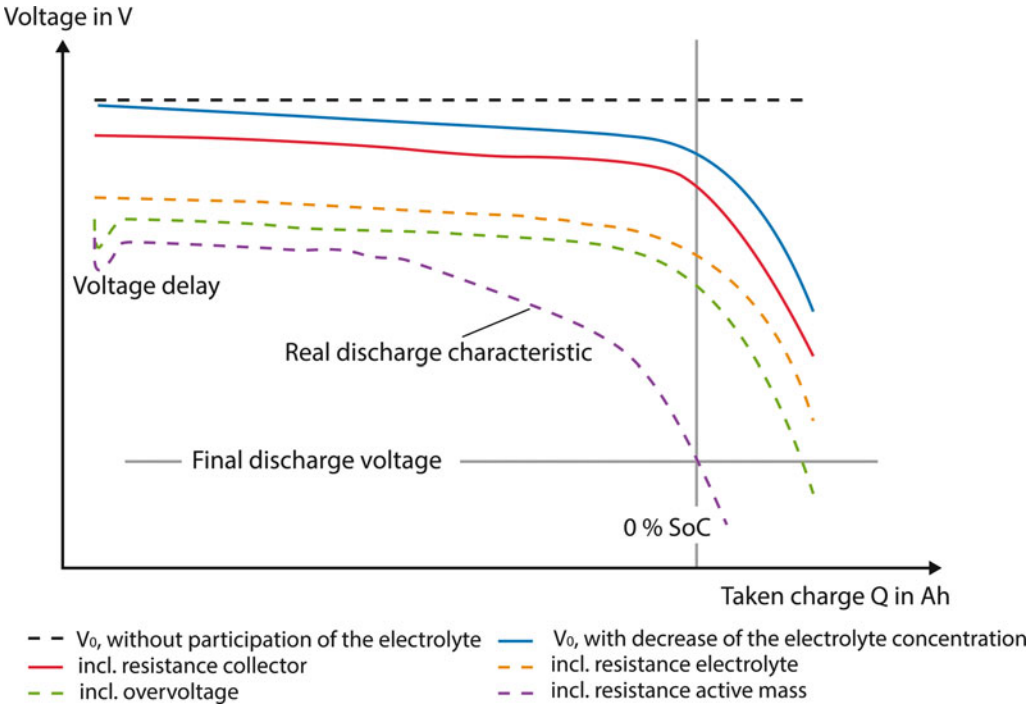



**Fig. 7.14** Discharging characteristics with discharging at a CC

ity's dependence on temperature is, however, omitted. In addition, the capacity of lead cells increases by about 0.6% for each degree the temperature is increased.

### 7.2.5 Side-Reactions

The side-reactions in Eqs. 7.32 and 7.33 are unfortunately not the only reactions that oc-

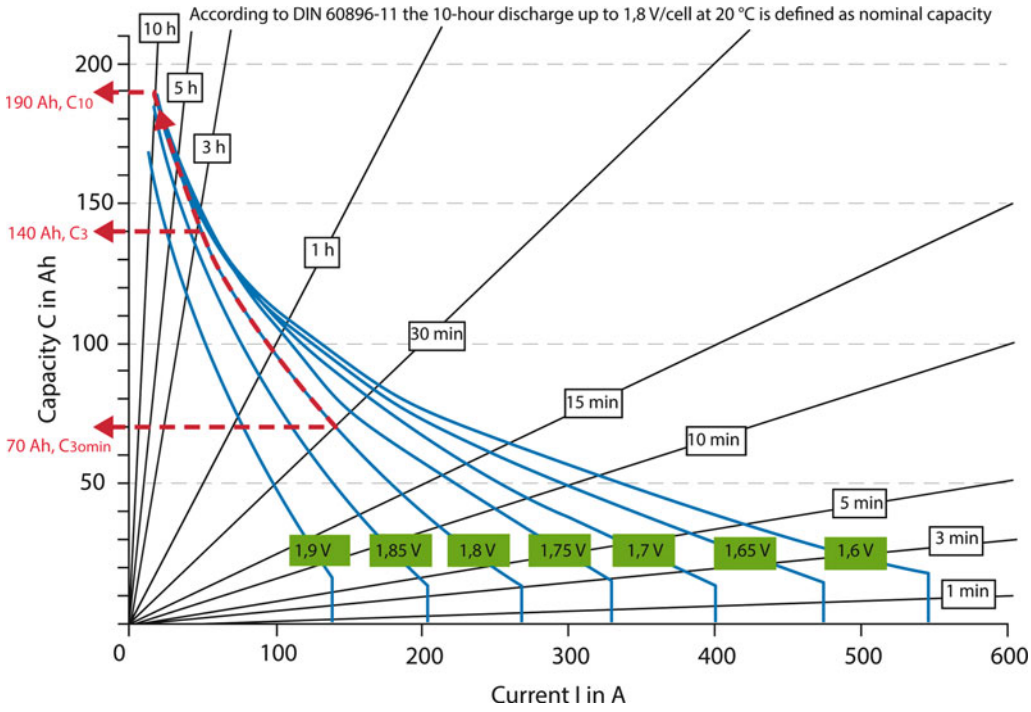



**Fig. 7.15** Configuration data for lead-acid cells

cur in lead sulfuric acid systems. There are also side-reactions at both electrodes. These reactions occur practically parallel to the main reaction. During the charging procedure, they divert a portion of the electricity. In the case of an open external power-circuit, they discharge the electrodes (self-discharge). The circuit diagram in Fig. 7.16 shows all the 'resistances' described in the last section that contribute to voltage drop, as well as the side-reactions that occur parallel to the main reaction. The diode connected in front of the side-reactions allows the current to flow in only a single direction. Side-reactions are not necessarily directly linked. As a result, they can be studied separately in the positive and negative half-cells. In fact, they lead to different self-discharge rates at the positive and negative electrodes. Articles [4] and [32] provide a good overview.

### Negative Electrode

The side-reactions' most significant effect is hydrogen formation,

$$Pb + H^+ + HSO_4^- \leftrightarrow PbSO_4 + H_2, \quad \textbf{(7.37)}$$

that is independent of voltage, acid density, temperature, and pressure. It is catalyzed by foreign materials in the system. Antimony plays a particularly important role here, because it is usually contained in the collectors of vented batteries as an alloy component. During the battery's service life, the release of antimony by corrosion can accelerate the speed of hydrogen formation to a point where the negative electrode can no longer be fully charged (see antimony poisoning in the chapter on ageing phenomena). With a hydrogen content above 4%, hydrogen formation can lead to an explosion. Hydrogen formation is therefore one reason that battery facilities require ventilation [6].

The second significant side-reaction at the negative electrode is oxygen reduction:

$$Pb + \frac{1}{2}O_2 + H^+ + HSO_4^- \leftrightarrow PbSO_4 + H_2O. \quad \textbf{(7.38)}$$

It is limited by the transport of oxygen to the electrode. The diffusion speed of oxygen in diluted sulfuric acid is very low. This means that

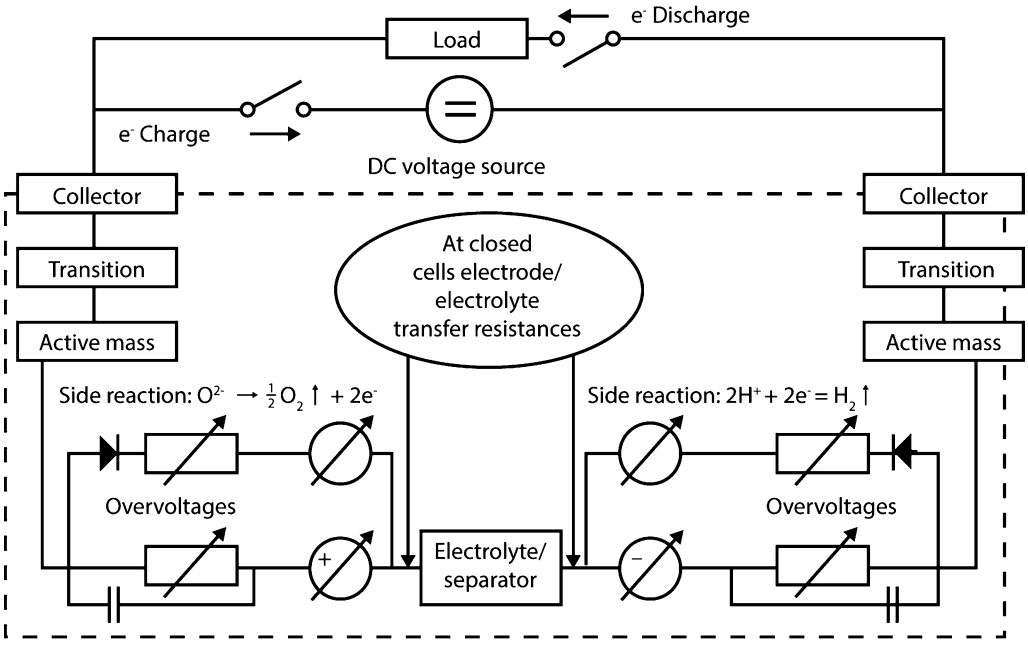



**Fig. 7.16** Circuit diagram

the importance of oxygen reduction in vented lead batteries is secondary. But in sealed batteries, there are gas channels between the electrodes within the immobilized sulfuric acid. Here the diffusion speed of oxygen is very high. As a result, in sealed batteries, oxygen reduction is the most significant side-reaction at the negative electrode. This is discussed in detail in the section on sealed batteries.

### ■ Positive Electrode

Oxygen formation,

$$PbO_2 + H^+ + HSO_4^- \leftrightarrow PbSO_4 + H_2O + \frac{1}{2}O_2, \quad \textbf{(7.39)}$$

is the most significant side-reaction in vented batteries as well as sealed batteries at the positive electrode. This reaction is catalyzed by impurities as well (for example, Co). In sealed batteries, oxygen diffuses to the negative electrode where it is reduced (see the discussion about the oxygen electron-hole recombination cycle in ▶ Sect. 7.2.7). Combined with hydrogen, oxygen creates combustible oxyhydrogen gas (please take safety precautions and take care of ventilation requirements).

### ■ Grid Corrosion

Unlike the complete reaction between the two half-cells (Eq. 7.34), this corrosion reaction occurs at the positive electrode when idle:

$$PbO_2 + Pb + 2H^+ + 2HSO_4^- \leftrightarrow 2PbSO_4 + 2H_2O. \quad \textbf{(7.40)}$$

The lead comes from the collector, and the electrons are absorbed by this highly oxidized form of tetravalent lead, i.e., in the lead-dioxide of the active mass. The reaction only occurs when the diluted sulfuric acid can penetrate the pores of the active mass and reach the location of the corrosion reaction. But if a thick $PbO_2$ corrosion layer is created during overcharging or float charging, then a reaction can only occur with transport through the solid. $H_2O$ is transported through the $PbO_2$ layer, and $PbO_2$ results at the $Pb/PbO_2$ boundary. Layer formation is promoted by the structural similarity of certain modifications of Pb, PbO, and $PbO_2$.

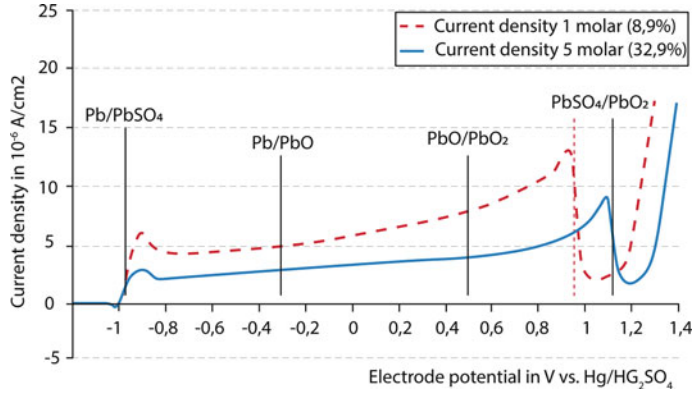



**Fig. 7.17** Corrosion related to voltage [9, 17]



This is the formula for the complete reaction:

$$Pb + 2H_2O \leftrightarrow PbO_2 + 4H^+ + 4e^-. \quad \textbf{(7.41)}$$

But the alloy components of the collector (for example antimony) are oxidized as well:

$$5PbO_2 + 2Sb + 6H^+ + 6HSO_4^- \leftrightarrow (SbO_2)_2SO_4 + 5PbSO_4 + 6H_2O. \quad \textbf{(7.42)}$$

In contrast to lead sulfate, antimony-bearing sulfate is highly soluble at high acid-densities. As a result, a portion is dissolved and then, again, reduced to metallic antimony at the negative electrode. This in turn results in catalytically accelerated hydrogen formation at the negative electrode (antimony poisoning).

The corrosion rate is heavily-dependent on the voltage, the acid density [17, 31], the grid alloy type, the foreign materials (chloride ions, for example), and the temperature. Gird corrosion is assumed to follow the Arrhenius equation. As a result, a 10 °C increase in temperature would be expected to double the rate of corrosion (empirical formula). The rate of corrosion is higher at low-acid densities than at high acid-densities. At low-acid densities, antimony used as an alloy component inhibits corrosion. Figure 7.17 clearly demonstrates the corrosion rate's dependence on voltage. The corrosion rate is lowest with low-charging polarization and highest with low-discharging polarization (for example due to impurities). As a result, batteries should be kept idle as little as possible and regularly recharged, or when holding a charge, kept at a low-polarization voltage.

An additional result of grid corrosion is an increase in the volume of the positive grid. This is because corrosion products have a higher volume than the original products. Mechanical seals are used on the battery pole in industrial batteries for this reason. They allow the positive collector to expand without destroying the battery container. A short-circuit caused by an enlarged positive collector is a common design flaw, particularly with start batteries.

### ■ Oxidization of Organic Substances

Organic substances that come into contact with the positive active mass are oxidized:

$$PbO_2 + \text{organic substance} + H^+ + HSO_4^- \leftrightarrow PbSO_4 + H_2O + CO_2. \quad \textbf{(7.43)}$$

These substances include organic impurities as well as organic compounds that are part of the design, particularly in the separators. As a result, ribs are used on the separators to increase the distance to the positive active mass.

When the separators are made of PVC, chlorine results from their decomposition. The oxidization of chloride ions and chlorine to perchloric acid ($HClO_4$) is especially significant, because perchloric acid at concentrations above 200 mg/L significantly increases corrosion of the positive collector components. In addition, chloride ions in non-desalinated water can be oxidized to produce perchloric acid. This is an-

other reason why lead accumulators are always filled with fully desalinated water [44].

#### ■ Additional Side-Reactions

Less significant side-reactions at the positive electrode include oxidation of hydrogen, or the formation of peroxosulfuric acid ($H_2S_2O_8$). No further discussion is required here about metals such as iron that are oxidized at the positive electrode ($Fe^{2+} \rightarrow Fe^{3+} + e^-$) and reduced at the negative electrode ($Fe^{3+} + e^- \rightarrow Fe^{2+}$), increasing the battery's self-discharge rate.

### 7.2.6 Charging Lead Batteries

Charging is an essential feature of a secondary cell. Chemically, it is the reverse of the lead-acid battery discharging reaction in Eq. 7.34. A variety of charging regimes are used for charging, with the current, voltage, or power of the charger kept constant. According to DIN 41772 [5], the phases are referred to by *I*, *U*, and *W*. A complete regime is, for example, a IoUoIa charging, where 'o' stands for 'switch-over' and 'a' for 'switch-off'. The charging duration is a critical factor, because unless a second battery is available, the device powered by the battery is idle during the charging time.

As discussed in ▶ Sect. 7.2.4, the level of charging efficiency is determined by voltage drop. As a result of voltage drop, higher voltages are required for charging than can be discharged. During the charging reaction, speed is determined by the dissolution of lead sulfate crystals and the transport of $Pb^{2+}$. ◘ Figure 7.18 demonstrates this effect as overvoltage increases. Besides voltage efficiency, another factor is that lead-acid batteries must also be charged with a larger quantity of charge than can be extracted from them. This is called the charging factor. Both reduce energy efficiency. The additional electricity charged is used by the side-reactions. The electrolysis reaction uses most of the electricity (decomposition to $H_2$ and $O_2$). In vented batteries, this has the positive effect by homogenizing the electrolyte. Homogenization is especially important in tall cells. This is because, during discharging, sulfuric acid is used in variable degrees by the active mass. As a result, it is also variably consumed in different areas of the collector. In the upper area of the cell, more sulfuric acid is used. This results in a lower density during discharge. In the lower area of the cell, the precise opposite occurs. This means that during charging, highly concentrated sulfuric acid escapes through the pores of the active mass and 'falls' down onto the electrode surface. The result may be a very high sulfuric acid density in the lower cell area. In contrast, the sulfuric acid density in the upper electrode area (and over the electrodes) only changes significantly when the so-called gassing voltage of 2.4 V/cell is exceeded. If an insufficiently charged and, therefore, stratified cell is allowed to sit idle, then the sulfuric acid densities at various heights becomes equal. This is caused by diffusion as well as by the different potentials (Nernst equation) correlating to the sulfuric acid densities at different cell heights. These differences in potential are short-circuited by the electrode, resulting in greater sulfate formation in the lower electrode area than in the upper electrode area. It also means that after storage, the distribution of concentrations reflects the distribution of sulfate in the electrodes.

Equalizing the acid density by overloading results in lower charging efficiency. Here, the most valuable form of energy (electric energy) is used to force the simple process of homogenization. Intentional overloading also increases water consumption and temperatures in the battery, resulting in a shorter service life. Solutions offered by manufacturers to this problem with cyclic batteries is the use of pulse charging or air injected beneath the electrodes to achieve homogenization. These solutions increase efficiency and shorten the charging duration.

Charging efficiency is also heavily-dependent on temperature. At higher temperatures, the speed-determining reaction steps in the dissolution of lead-sulfate and diffusion of $Pb^{2+}$ occur more quickly. As a result,

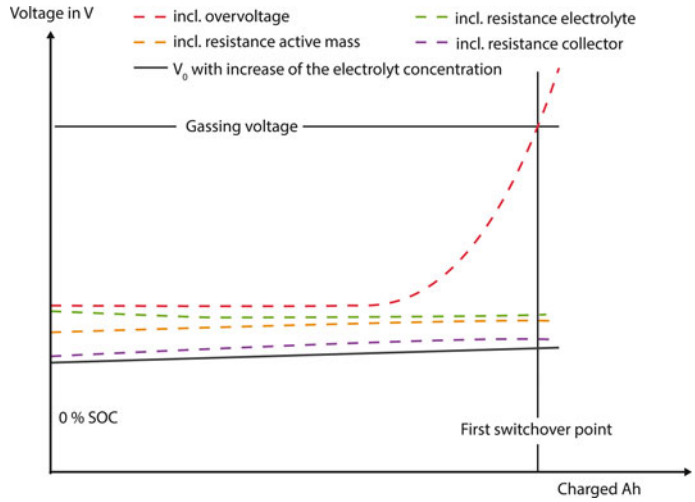



**Fig. 7.18** Charging characteristics with charging at a CC



the battery can be charged at lower voltages. The standard voltage correction assumed is −4 mV/°C. Since charging efficiency depends on temperature, lower charging voltages must be used at higher temperatures to avoid battery overload. For the same reason, higher charging voltages must be used to compensate for this effect at lower temperatures. If temperatures vary significantly within the battery, then cells in lower-temperature areas may still be only partially charged when cells in high-temperature areas are already overcharged. As a result, homogenous temperature distribution is required to ensure long and uninterrupted use of the battery.

In sulfated batteries, the step in the lead sulfate dissolution that determines speed is crucial. This is because in that step, the lead sulfate crystals have become so large that they can only be dissolved with adequately high overvoltage. A small current must then be applied to prevent irreversible sulfation. An alternative is deep-discharging followed by recharging. Here, the sulfate crystals are dissolved in the deep-discharging state with its corresponding low-acid density. This is because the crystals' solubility increases as the acid density falls.

Another temperature issue with charging is that part of the energy lost during charging is converted into heat energy. This in turn heats the battery. As a result, temperatures are directly determined by the charging regime. A simple method of calculating the quantity of energy converted into heat is to use the difference between the actual voltage and the OCV of the reaction. Multiplying this by the current applied to the reaction results in the actual heat output. At the start of charging, the charging reaction occurs (Eq. 7.34) with an OCV of, for example, 2.04 V (according to Eq. 7.35 corresponding to an acid density of 1.20 g/cm$^3$). Charging occurs with 50 A at 2.2 V. The actual heat power for one cell is therefore $(2.2 - 2.04\,\text{V}) \cdot 50\,\text{A} = 8\,\text{W}$. When reversible heat is included, in reality the heat power is even larger. That is because reaction entropy decreases in the lead cell charging reaction (Eq. 7.34), releasing additional heat. This can be taken into account by using a thermal OCV that is always 68 mV less than the real OCV. At the end of charging, the electricity is used almost entirely by the electrolysis reactions (Eqs. 7.37 and Eq. 7.39), and the electrolysis reaction's OCV is 1.23 V. The charging current would be at 10 A and the voltage at 2.5 V. The actual heat power is therefore $(2.5 - 1.23\,\text{V}) \cdot 10\,\text{A} = 12.7\,\text{W}$. Heat energy is produced by the integration of heat power. Because charging currents are high, heat power at the start of charging is high. The heat power further in-

**Table 7.7** Comparison of sealed batteries and vented batteries

| Advantages | Disadvantages |
|---|---|
| Low water loss | Higher investment costs |
| No water refilling required | Water loss results in capacity loss |
| Acid cannot be drained | Increased voltage spread |
| Position not a factor for installation | |
| Acid-layering can be prevented | |
| Longer cycle life | |

creases because of the high-voltage difference, especially when the electricity is used by the electrolysis reaction. As a result, charging current must be reduced if a large portion is used by the gas formation reaction. This is the case when the voltage reaches around 2.4 V/cell.

### 7.2.7 Sealed Lead Batteries

In lead batteries, hydrogen and oxygen gassing side-reactions result in water loss from the electrolyte. Regularly refilling the individual cells in a lead battery means high maintenance costs, especially if the battery facilities are distributed over a wide area or difficult to access. Without refilling, maintenance is required only at infrequent intervals (Table 7.7).

Catalyzed electron-hole recombination of the resulting hydrogen and oxygen to produce water can be achieved using an external recombinator [14]. The water can then be fed back into the battery container.

An internal electron-hole recombination cycle can be forced by creating paths of diffusion through the electrolyte, and containing the gas by sealing the cell with an overpressure valve. This allows the oxygen produced at the positive electrode during the charging reaction to follow the diffusion paths. It can then be used in an exothermic reaction (Eq. 7.38) at the negative electrode. As a result, the negative electrode's potential is not pushed strongly negative during the charging reaction by continual oxidation. If the negative electrode's potential is moderate, then the hydrogen formation side-reaction uses only a small amount of electricity. Figure 7.19 illustrates the resulting oxygen electron-hole recombination cycle.

To ensure that hydrogen formation at the negative electrode is not greatly increased by antimony poisoning, the collectors are made of a lead-calcium-tin alloy. The diffusion paths remain open if the electrolyte is fixed in a gel or an AGM (adsorptive glass mat). Diffusion paths are created when fissures develop in the gel or when the adsorptive glass mat is not fully saturated with electrolyte. Fixing the electrolyte also permits lead batteries to be used in any position. In addition, fixed electrolyte significantly decreases potential hazards during transport, installation, and operation compared with vented batteries.

The overpressure valve that seals a lead cell retains electrolyte gases in the cell, prevents oxygen in the atmosphere from penetrating the interior of the cell, and relieves internal overpressure.

Relieving internal overpressure results in a loss of hydrogen and oxygen (= water). Corrosion of the positive collector lead in the reaction described by Eq. 7.41 also consumes water. This means that water loss is inevitable, and cannot be avoided by refilling the cell. Water loss also results in higher acid densities. Water loss increases together with the charging voltage and temperature. The decrease in water levels means more gas channels are formed. As a result, more oxygen is transported. This in turn

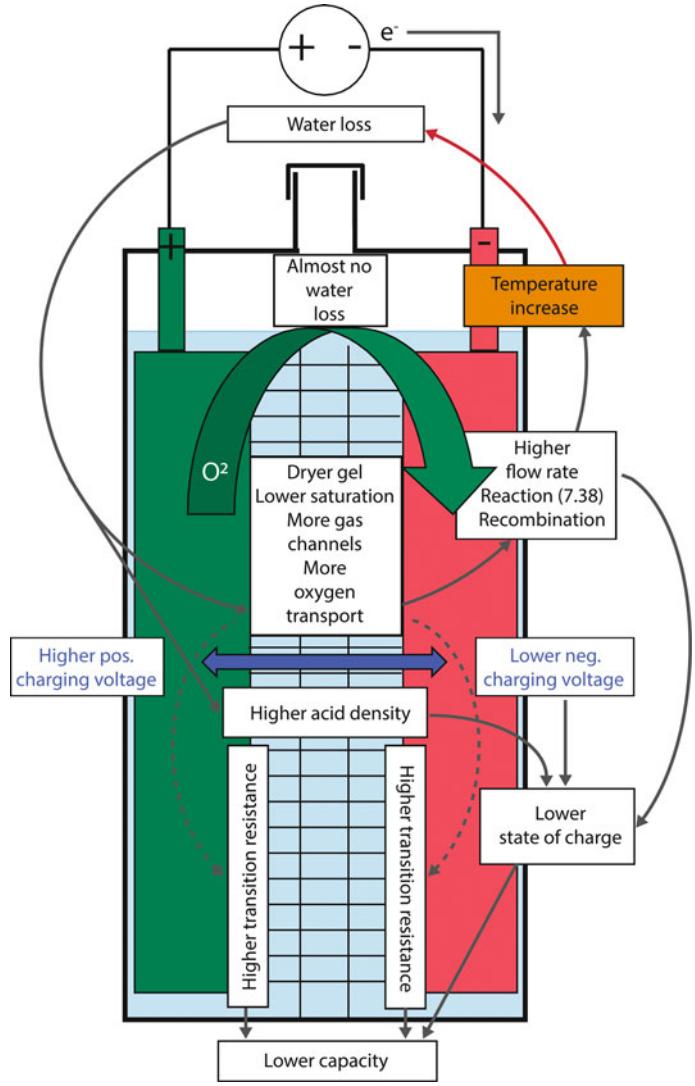



**Fig. 7.19** $O_2$ electron-hole recombination cycle and mechanisms in a sealed lead-acid cell

reduces the negative electrode's charging voltage. An effective electron-hole recombination cycle and a lower negative electrode charging voltage reduce water consumption, but also reduce the negative electrode's SOC. Water loss increases transfer resistance between electrode and electrolyte. Increased transfer resistance and the negative electrode's reduced SOC result in lower cell capacity.

The exothermal electron-hole recombination reaction in Eq. 7.38 increases the cell's temperature. In extreme cases, severely elevated cell temperatures can result in severely elevated water loss. Since water loss also causes the cell temperature to increase, there is a feedback effect (Fig. 7.19). This is called thermal runaway. Thermal runaway is more common with older cells, where water levels have already fallen too low. Additional boundary conditions that contribute to thermal runaway are high-charging voltages, inadequate heat extraction, and high ambient temperatures. Higher cell temperatures may eventually soften the cell housing. Since the cell housings in AGM batteries bulge

under plate set pressure, thermal runaway may cause severe bulging in the side walls.

Since new sealed cells have various saturation levels, their cell voltages during charging with constant battery voltage (for example, with float charging) are distributed across a wider range compared to vented batteries. As Fig. 7.19 shows, cells with higher electrolyte saturation levels have higher negative voltages and a lower recombination efficiency. These cells lose more water, and so become indistinguishable from cells with lower saturation within a few months.

When the negative electrode is discharged by the oxygen cycle, the negative electrode side-reactions are coupled with the positive electrode side-reactions:

$$i_{O_2} + i_{corr} = i_{recom} + i_{H_2}, \qquad \textbf{(7.44)}$$

according to the reactions in Eqs. 7.37, 7.38, 7.39 and 7.41.

This means that changes at the positive electrode (increased corrosion) cause changes at the negative electrode (hydrogen formation). But since the opposite is not the case, additional electricity consumed by a side-reaction at the negative electrode does not influence the positive electrode. This additional electricity consumption can therefore only be sustained by self-discharging the negative electrode. As a result, the negative electrode's SOC may fall, even during charging. Additional side-reactions at the negative electrode include:

- Increased hydrogen formation due to impurities.
- Penetration of ambient oxygen through leaks, or of acid from neighboring cells.

In gel cells, acid-layering is largely prevented from affecting performance. But layering may affect the performance of AGM cells. This effect cannot be measured directly, but is determined instead from the distribution of the sulfate in the electrodes. Since layering in sealed cells cannot be removed by simple electrolyte circulation, it must be prevented by the design and by using appropriate materials.

An appropriately designed AGM separator with a high fine fiber content and manufactured with high set pressure can be used to prevent layering. The advantages of AGM batteries manufactured with high set pressure include reduced transfer resistance between electrode and electrolyte, and longer cycle life. In effect, material tightly pressed on the flat positive electrode prevents the formation of active mass sludge like a tube sleeve.

The gradual discharge of the negative electrode described above is dramatically accelerated by antimony poisoning. As a result, lead-antimony alloys are not used for sealed battery collectors. Instead, lead-calcium-tin alloys are used. Lead-tin alloys, or pure, refined lead can also be used with the appropriate manufacturing processes. These collector materials may vary in terms of their corrosion characteristics and the extent of grid growth with lead-antimony alloys (there is more extensive grid growth with lead-calcium alloys). But it is nevertheless essential to prevent the formation of passivation layers between the grid and active mass (called the antimony-free effect) by adding tin, for example.

### 7.2.8 Aging Mechanisms

A crucial factor with secondary batteries is service life. A battery's service life is partially determined by time. But it is primarily determined by the loads placed on the battery and the way the battery is operated. Besides time, other important factors include DOD, temperature, charging procedure, average SOC, and performance demands (current level). Framework conditions such as the electrolyte filling level, temperature distribution, and insulation resistance between the cells are also crucial. The most important parameter for aging is the extractable charge. As a result, capacity tests are always performed as part of the service life test. Figure 7.20 shows the results for capacity in various service life tests. The service life is defined as the time from storage start-up to

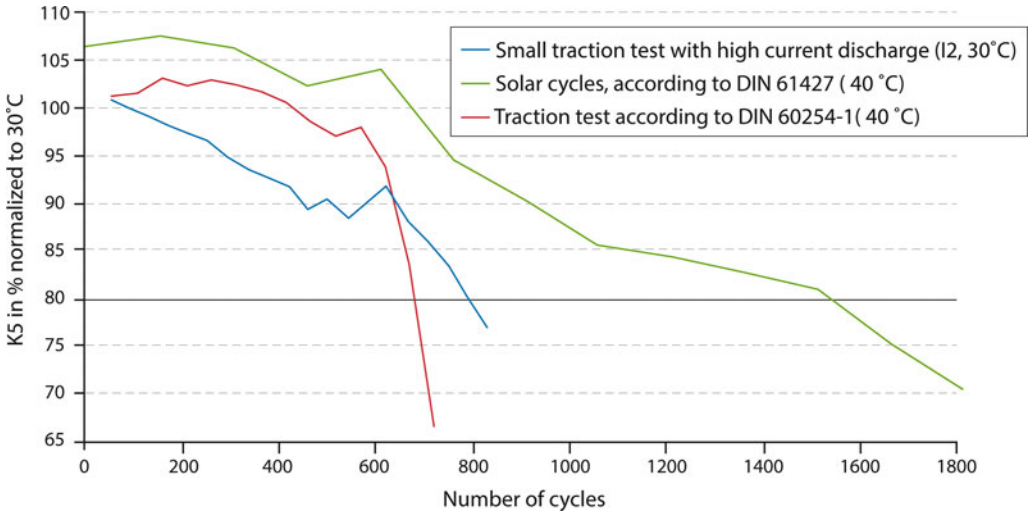



**Fig. 7.20** Capacity results with three different cycle regimes for a sealed 50 A h block battery

storage failure. According to DIN 43539/Part 4, service life ends when storage capacity falls below 80% of rated capacity.

The aging mechanisms that reduce capacity are determined by how the battery is operated. Figure 7.20 shows how identically designed batteries perform in different service life tests. Some of these are traction cycles with high current at room temperature, and with moderate current at higher temperatures. Others are cycles with lower DOD which, during charging, may only reach a partial SOC. These cycles therefore simulate 'solar battery' use. In this case, the traction cycles' higher DOD is clearly more degrading. With traction cycles, increased temperature has a greater effect on aging than high- discharging current density.

The aging mechanisms are also mutually-dependent (Table 7.8). For example, grid corrosion results in increased resistance within the grid, which in turn increases the unequal distribution of electricity. This has a considerable effect on the charging electrode elements located farther from the electricity collector. Due to inadequate charging, significant quantities of sulfate are found on the electrode (sulfatation) when the battery is opened for inspection.

The primary causes of battery failure depends on the application area. Ageing in starter batteries and stationary batteries is primarily due to corrosion. Greater demands are also now placed on starter batteries because of the growing importance of automobile electrical systems. As a result, starter batteries are increasingly in cyclic use. That means they frequently cycle through partial states of charge. This is particularly the case in cars with a start-stop function. These batteries typically age due to mass degradation or sulfatation. The situation with stationary batteries is similar, because they are increasingly used as active energy storage in local networks (in combination with, for example, a photovoltaic facility — PV facility). Batteries in cyclical use in electric cars age mainly due to mass degradation. Increasing lead battery service life requires avoiding these causes of aging as much as possible.

### 7.2.9 Conclusion

- The **lead sulfuric acid battery** was invented 150 years ago, and today, is perhaps one of the **best-known electrochemical-energy storage systems**.
- These are primarily used as **starter batteries**, **electric drive batteries**, and **sta-**

**Table 7.8** Aging mechanisms in lead batteries. A complete summary of mechanisms can be found in [31]

| Mechanism | Description | Result | Cause |
|---|---|---|---|
| Corrosion of the positive collector | Corrosion of the positive grid. The head lead also corrodes, allowing corrosion products to fall between the electrodes | Ohmic resistance increases, the collector breaks, and there is bad contact between the collector and the active mass. With armored plates, the sleeves may break open | High-charging voltage, high-temperatures, high perchloric acid content, low-acid densities, inappropriate collector alloys |
| Grid formation | The volume of corrosion products exceeds the volume of original products | Short-circuit between the electrodes | All causes of corrosion, inappropriate grid alloys |
| Active mass failure | A part of the (often positive) active mass peels off and falls into the sludge chamber. Active material may also get stuck to the negative electrode or between the electrodes and the separator (charging combs) | Capacity loss, short-circuit | Mechanical stress with cycling, high-current densities during discharge, high-charging voltages i.e., intensive gassing, deep-discharging, polarity reversal |
| Dendrite deposits | Small 'lead finger' deposits where seed crystals are lacking; may lead to perforation of the separator | Short-circuit between the electrodes | High-current densities during discharge, low-acid densities, deep-discharging |
| Sulfatation of the positive and negative electrodes | Formation of large lead sulfite crystals (hard lead sulfate) that cannot be converted, even with extended charging | Reduced capacity, reduced acid density | Long idle times, inadequate charging, partial states of charge, high acid-density, acid-layering |
| Water loss | Particularly with sealed batteries, water loss results in irreversibly reduced capacity | Negative sulfatation due to increased electron-hole recombination electricity, increased acid density, layering, thermal runaway | High-charging voltage, high-temperatures, impurities |

**tionary batteries for emergency electricity supply**.

- For stationary applications, these lead batteries can be operated as stand-alone systems or as network-connected systems. They are frequently used in connection with **renewable energy generation**. Specially designed stationary lead batteries are used for these applications.
- Lead batteries typically have a **long service life**. Operating conditions that accelerate aging should be avoided as much as possible. This requires:
  - Correct dimensioning of the battery or the application.
  - Never deep-discharging.
  - Avoiding long idle periods in deep states of charge.
  - Timely removal of electrolyte layering.
  - Use of a charging process with only moderate overload (water loss).
  - Adjusting the charging voltage to the temperature.
  - Maintaining cell temperatures between 20 °C and 45 °C.

## 7.3 Nickel Batteries

Beginning in the late 19th century, scientists began investigating new forms of electrochemical storage with a higher-energy density and greater reliability than conventional lead batteries. At almost the same time, Jungner and Edison invented an alkaline battery using a nickel oxyhydroxide/nickel hydroxide electrode. These advances paved the way for nickel-cadmium and nickel-iron batteries. Unlike lead accumulators, these batteries have a low-rated voltage of only 1.3 V. Although a low-rated voltage has drawbacks, an advantage is that practically no aging and corrosion processes occur in alkaline electrolytes. As a result, the cells have a very long service and cycle life. These cells are also extremely reliable, even when used improperly (abuse tolerance). The addition of steel housing made these batteries even more robust. Due to their high, nearly constant electrolyte concentration, these cells are also suited for use at very low-temperatures.

A small number of alternatives to the nickel oxyhydroxide/nickel hydroxide electrode have been developed for the positive electrode of alkaline batteries. These include silver/silver oxide electrodes and manganese-dioxide electrodes. These are typically used in primary cells, frequently combined with a zinc electrode. They are usually limited to use in primary cells because the silver electrode's high-oxidation power degrades the separator, and because of the complexity of the $MnO_2$ electrode's mechanism. Zinc electrodes also present difficulties, because the zinc hydroxide's high solubility promotes dendrite deposits. It also leads to passivation and deformation of the zinc electrode. These electrodes are, nevertheless, common in special batteries; for example in button cells or for high-performance and military applications.

Air electrodes are a special case. In combination with a zinc electrode, they can be used to produce light primary batteries. These were first developed as hearing aid batteries, and to power cameras (Polaroid system). In recent decades, there have been numerous attempts to design a rechargeable version of this system. The goal of these efforts was to leverage the enormous energy densities that the system can achieve as a result of the voltage curve, and because no storage is required on the air side. In addition, zinc is a conveniently available and environmentally-friendly material. All of these factors have driven the search for a zinc-air system to power vehicles or for use as stand-by batteries. But the complexity of the problem has proven intractable (air electrode, dendrite deposits, shape-change, zinc electrode passivation and poor cycle stability, system open to the environment, etc.).

As a result, predominantly cadmium and zinc electrodes as well as electrodes using hydrogen storage alloys are used as negative electrodes in alkaline electrolytes. Compressed hydrogen electrodes are also popular for high-tech applications (aerospace, military). In the past, nickel oxyhydroxide/nickel hydroxide electrodes were also combined with iron electrodes. But these nickel/iron cells have serious disadvantages in terms of cycle life, gassing properties, energy efficiency, and self-discharging. For these reasons, they have virtually disappeared from use. Aluminum electrodes (primary or mechanically regenerated) are also extremely rare.

Table 7.9 provides a general overview of the specifications for various battery systems.

Figure 7.21 shows a comparison of potentials and overcharge reactions (hydrogen or oxygen formation).

The positive electrode's potential is in the range of oxygen separation. This means that, as a side-reaction, it competes with charging and oxygen-release from the nickel oxyhydroxide is thermodynamically possible. Additives in the paste can mitigate this effect.

The nickel-zinc cell's higher voltage compared to other systems is primarily a result of the negative electrode's potential. But because this potential is in the range of hydrogen separation, the zinc electrode has a strong tendency to self-discharge. That tendency must be countered kinetically. The same is true for primary

**Table 7.9** Overview of nickel batteries

| System | $U_G = -zF\Delta G_{298}$ in V | $U_H = -zF\Delta H_{298}$ in V | $\Delta H/\Delta G$ in % | Theoretical special energy W h/kg | Practical special energy W h/kg | Practical energy density W h/L |
|---|---|---|---|---|---|---|
| Ni/$H_2$ | 1.31 | 1.51 | 115.3 | 379 | 50 | 60 |
| Ni/MeH | 1.31 | 1.35 | 103.0 | 213 | 60 | 150 |
| Ni/Cd | 1.29 | 1.44 | 111.6 | 209 | 50 | 100 |
| Ni/Zn | 1.72 | 1.88 | 109.0 | 324 | 70 | 130 |

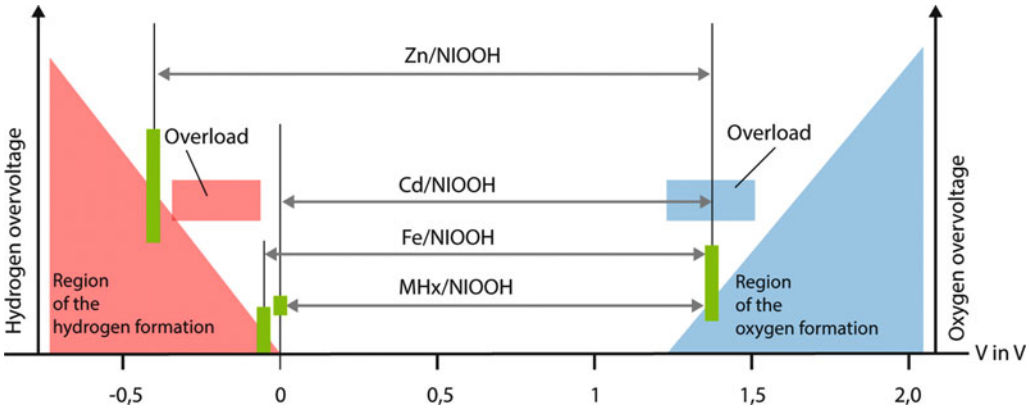



**Fig. 7.21** Potentials and overload reactions compared

cells (alkaline zinc-manganese dioxide system). Previously common additives (such as mercury) have been replaced with others to minimize the impact on the environment.

### 7.3.1 Conclusion

- **Nickel batteries** were developed to meet the need for electrochemical storage with a **higher-energy density and greater reliability** than conventional lead batteries.
- Nickel batteries have a **low-rated voltage** of only around 1.3 V.
- Practically no aging and corrosion processes occur in alkaline electrolytes. As a result, these cells have **a long service life**.
- Nickel batteries are suited for **use at low-temperatures**.
- Nickel batteries include a range of different kinds of batteries. For practical applications, **nickel-cadmium and nickel metal hybrid batteries** are the most common. These batteries are discussed in the following section.

### 7.3.2 Nickel-Cadmium Batteries

Nickel-cadmium accumulators are alkaline batteries. Energy is stored by converting nickel hydroxide into nickel oxyhydroxide at the positive electrode, where the nickel undergoes a formal change of metal valence state from +2 to +3. During charging, at the negative electrode the cadmium-hydroxide (cadmium with a valence of +2) is converted to metallic cadmium (valence 0). The reactants and reaction products are in a solid aggregate state that

is typically insoluble in the alkaline electrolyte, which is a potassium hydroxide solution. The rated cell voltage is around 1.3 V.

The composition of the electrodes and the electrolyte, as well as the design of the electrodes and cells, vary by application. The theoretical energy content of a Ni/Cd system is about 210 W h/kg.

#### 7.3.2.1 Cells

The cell's passive components (metal leads, etc.) are typically made of nickel or nickel-plated steel. For the cell housing, in addition to plastics such as polyolefins (PP, PE), polyamide, and polyethersulfone, steel is also used.

The cell design can either be vented (degassing vent) or sealed (overpressure valve/safety valve/rupture disk, partly hermetic cells).

Figure 7.22 illustrates an alkaline cell using an FNC cell as an example.

- **Chemical Reactions**

Negative electrode:

$$\mathrm{Cd} + 2\mathrm{OH}^- \underset{\text{charge}}{\overset{\text{discharge}}{\rightleftarrows}} \mathrm{Cd(OH)_2} + 2e^-, \quad \textbf{(7.45)}$$

Positive electrode:

$$2\mathrm{NiOOH} + 2\mathrm{H_2O} + 2e^- \underset{\text{charge}}{\overset{\text{discharge}}{\rightleftarrows}} 2\mathrm{Ni(OH)_2} + 2\mathrm{OH}^-, \quad \textbf{(7.46)}$$

Cell:

$$\mathrm{Cd} + 2\mathrm{NiOOH} + 2\mathrm{H_2O} \underset{\text{charge}}{\overset{\text{discharge}}{\rightleftarrows}} \mathrm{Cd(OH)_2} + 2\mathrm{Ni(OH)_2}. \quad \textbf{(7.47)}$$

The resulting equilibrium cell voltage is 1.30 V at room temperature. The following specific charges for the reactants are given by Faraday's law:

**$Ni(OH)_2$:** – 0.289 A h/g,
**$Cd(OH)_2$:** – 0.366 A h/g.

#### 7.3.2.2 Positive Electrode

The reactions presented here are simplifications of the actual processes involved. Even after over a hundred years of use, some aspects of the reactions in these cells are still not completely understood. As a result, only a few selected aspects will be discussed here.

Unlike nickel hydroxide, nickel oxyhydroxide is a conductor of electricity. But this conductivity is inadequate to ensure low internal resistance. As a result, conductive additives in the electrode mass or active materials embedded in an electrically conductive electrode matrix are required. Otherwise, electrochemical cycling is limited to thin layers.

The electrode reaction requires hydrogen ion intercalation in the nickel hydroxide's grid structure. The active nickel hydroxide is in what is termed a $\beta$-modification. Strictly speaking, the reversible reaction depends on hydrogen ion intercalation:

$$\beta\text{-NiOOH} + \mathrm{H}^+ + e^- \underset{\text{charge}}{\overset{\text{discharge}}{\rightleftarrows}} \beta\text{-Ni(OH)}_2. \quad \textbf{(7.48)}$$

The nickel hydroxide develops a layer structure allowing the intercalation of other ions (Fig. 7.23).

As a result, the potential of the positive electrode is formally determined by the Nernst equation:

$$E = E^0 + \frac{R \cdot T}{F} \cdot \ln\left(\frac{a_{\mathrm{NiOOH}} \cdot a_{\mathrm{OH}^-}}{a_{\mathrm{Ni(OH)_2}} \cdot a_{\mathrm{H_2O}}}\right), \quad \textbf{(7.49)}$$

with $E^0 = 0.49\,\mathrm{V}$.

Through aging and overlap, the $\beta$-$Ni(OH)_2$ may be converted with less active modifications. These correlations can be shown in what is termed a Bode plot.

Since the reactants are solid materials that crystallize separately, the potential is only essentially dependent on the pH level of the electrode. In addition, since the negative electrodes are similarly dependent on the pH level, as long as the electrode mechanisms remain the

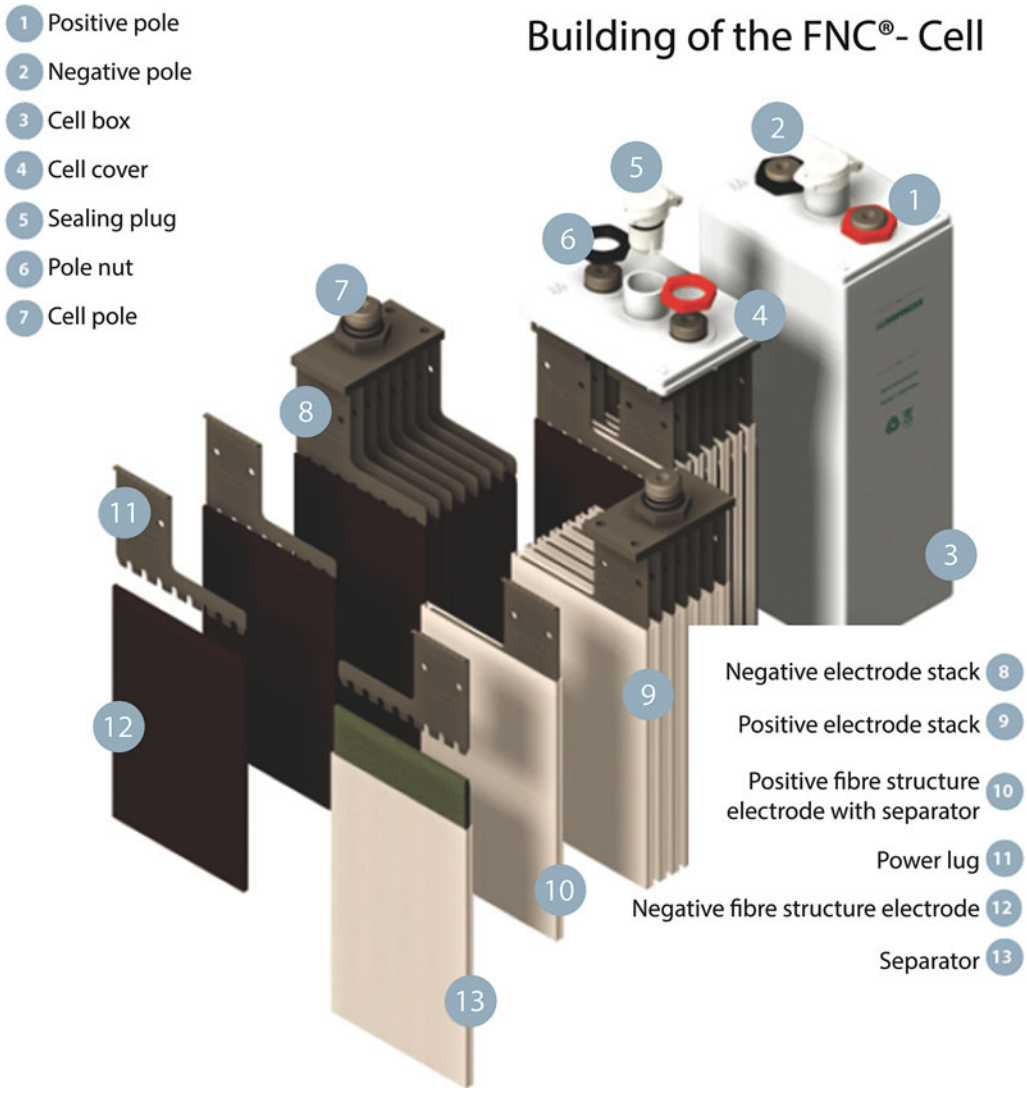



**Fig. 7.22** Fiber nickel-cadmium (FNC) cell design

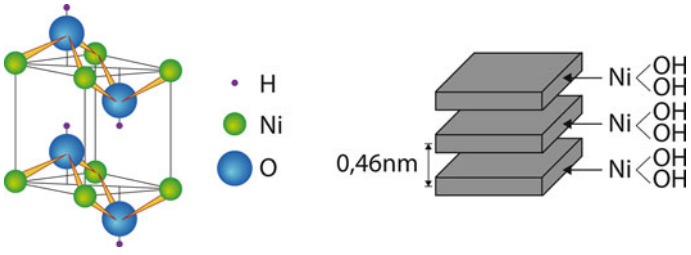



**Fig. 7.23** Nickel hydroxide layer structure

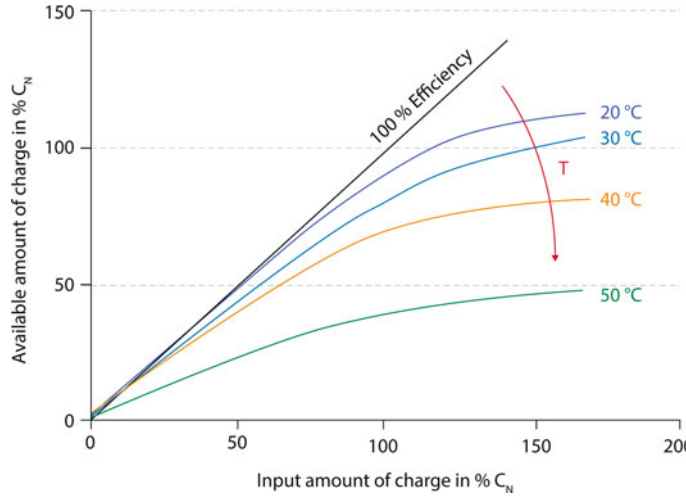



**Fig. 7.24** Charging efficiency curve



same, the effect of the pH level is in large part-compensated by the cell voltage. As a result, the cell voltage as well as the internal resistance of nickel-cadmium cells is heavily-dependent on the cell's SOC. This is an advantage, because it means the cell can be easily charged or discharged across all states of charge. The disadvantage is that voltage measurements are not useful for determining the cell's SOC.

Most alkaline cells are designed so that the positive electrode's capacity limits the discharge of the entire cell. The cell is positively limited because the dischargeability (extractable capacity) of the negative electrode depends more on the discharging current than the positive electrode. As a result, the cell's SOC is about equal to the positive electrode's SOC. A more detailed analysis (such as for sealed cells or special operating states) is beyond the scope of the present simplified overview.

With cycling of the nickel hydroxide/nickel oxyhydroxide electrode, electrolyte components ($Li^+$, $K^+$ ions) are also embedded. These changes are partially irreversible, and alter the volume of the electrode through swelling.

Due to the small difference between the electrode potential of the nickel hydroxide conversion and the oxygen formation potential, oxygen coverage of the surface and oxygen separation occur before the conversion is complete. A result of these processes is that the entire volume of electricity applied is not used for the conversion of the nickel hydroxide. This means that, depending on the battery type and application, an excess charge of up to 20% is required to achieve a full SOC. The difference between the nickel hydroxide conversion potential and the oxygen separation potential falls as the temperature increases. At temperatures above 50 °C, oxygen separation dominates (Fig. 7.24).

At the same time, the nickel oxyhydroxide's chemical stability falls. As a result, the cell's self-discharge increases dramatically. A range of additives in the positive electrode and the electrolyte can improve chargeability and charge retention. The idea here is to increase the charge (in mA h/g) that can be practically achieved during operation. Additives that increase the electrical conductivity of the electrode materials (for example nickel powder and cobalt) are suited for this purpose. By improving the charged nickel oxyhydroxide's chemical stability, oxygen separation is inhibited. Premature oxygen-release when charging can be curbed by increasing the oxygen overvoltage. In addition, additives are used to limit electrode material swelling (volume change).

A special characteristic of the positive electrode is that the nickel hydroxide may occur

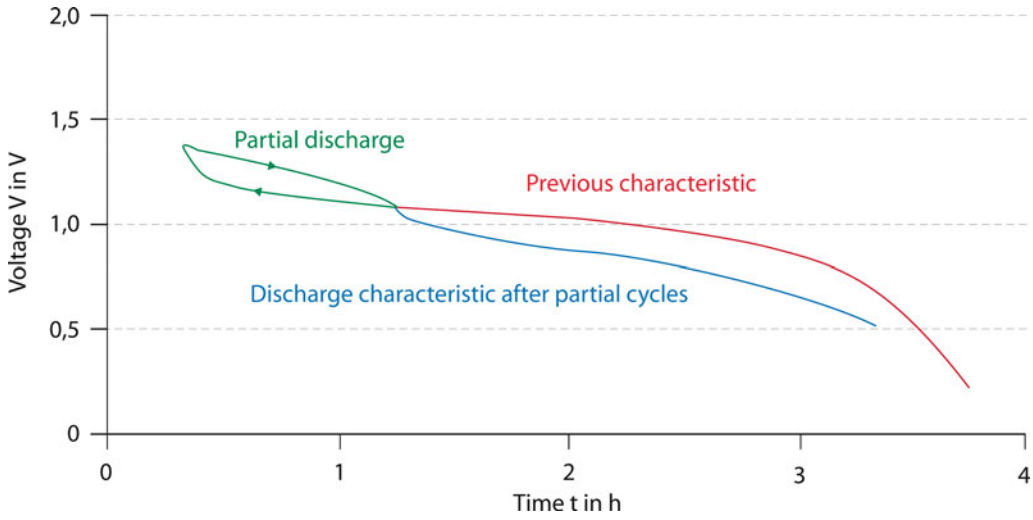



**Fig. 7.25** Changes in the discharge-curve after partial cycles

in several crystal modifications with a range of chargeabilities. These determine the ageing mechanisms (Bode plot).

With extended, continual overcharging, subsequent polarization is temporarily stronger during discharge. This is also a result of chemical changes in the positive electrode (voltage depression and lazy battery effect).

The memory effect is a similar phenomenon, which is particularly significant with sealed nickel-cadmium cells. Here, after partial discharges, there is a voltage drop at the same place on the discharging curve during the next charging. This problem can be eliminated by fully discharging once or several times (Fig. 7.25). The causes of this effect are assumed to be in the negative electrode or in the electrolyte boundary at the electrodes. Despite intensive research, some aspects of this mechanism are still not understood.

With cycling, the electrode material particle layers near the surface (electrolyte interface) are chemically changed when current is applied. As a result, the surfaces and inner volumes of the particles have different phase compositions. Since the electrode's potential is determined by the phase boundary state, cycling may result in hysteresis. This state remains for an extended period, even after the current has been shut off. If the current is interrupted during charging or discharging, the potential at the electrode will vary depending on the direction the current was applied. This increases the difficulty of determining the SOC during cyclic operation by measuring the potential.

### 7.3.2.3 Negative Electrode

The negative electrode is defined by the cadmium/cadmium hydroxide equilibrium. The potential compared to the SHE is −0.81 V. Nickel-plated steel is also used for the leads.

After the electrode is fully charged, overcharging hydrogen is formed. Hydrogen separation is severely inhibited at the cadmium surface, making the potential extremely negative. As a result, cell voltage increases dramatically at the end of charging. With open industrial cells, this allows charging at a constant voltage (CV) with no additional electronic limiting (IU charging). When a given voltage is reached, the current drops off. The gasses produced during overcharging in open, ventilated cells are released through an opening (gas-permeable cell plug; for example a porous barrier to protect against flashback and central gassing systems). This allows the surplus energy that cannot be absorbed by the cell during overcharging to be diverted by the release of hydrogen and oxygen.

Since the resulting gas mixture is flammable, the gasses released must be discharged (ventilation) from the battery or battery compartment during operation. Generally, the quantity of gas is minimized by using the appropriate loading process and a low-charging voltage. Due to electrolyte decomposition, gas formation entails compensating for water loss. This requires regular maintenance or an automatic (or semi-automatic) water refill system. As with lead accumulators, cell accessories can be used to recombine the gases. To estimate the quantity of gas released, the portion of oxygen formed that is then reduced at the negative electrode must also be taken into account.



With gas-tight cells (round cells or prismatic cells; for example electronics applications or vehicle applications), overcharging produces an internal oxygen cycle. The oxygen produced at the positive electrodes is transferred to the negative electrodes. The transfer is achieved by special battery design, or by using the electrolyte. The oxygen is then reduced at the negative electrode so that practically no hydrogen is released. This minimizes internal cell pressure. Since surplus energy remains in the cell during overcharging, temperatures increase at the end of charging. This increase in temperature can be used with gas-tight cells to determine when charging is complete. The electrodes can also be designed to allow long-term, fully sealed cell operation. The charging curve of these cells differs from that of open cells. With sealed cells, due to oxygen recombination, the electrode potential is not negative at the end of charging. The cell voltage initially rises only slightly at the end of charging. Since cell voltage in a nickel-cadmium system has a negative temperature gradient (reaction entropy), an increase in cell temperature actually results in a decrease in cell voltage. Many chargers use the voltage inflection point or resistance inflection point to determine when charging is complete.

As with all metal electrodes, the conversion mechanism includes a solution phase. As a result, metal separation tends to occur at thermodynamically optimum points in the crystal grid. This process coarsens the crystal structure, reducing the specific surface area. Separator additives are used to slow or prevent this process. Use of carriers containing nickel (or nickel additives) can also result in the formation of intermetallic phases between cadmium and nickel. These reduce battery cyclability.

#### 7.3.2.4 Electrolyte

These cells use an alkaline electrolyte. This electrolyte is a potassium hydroxide solution (KOH). Concentrations of 20% with a lye density of 1.19 g/cm$^3$ are common. Potash lye is a highly corrosive liquid. Contact with the skin results in severe chemical burns and should be strictly avoided. Protective gear (protective eyewear and gloves) is required when working with open cells.

The electrolyte may absorb carbon dioxide when exposed to the air. This elevates the level of carbonate, reducing conductivity and increasing the resistance of the cells. As a result, open cells are typically sealed with a plug. The plug is designed to allow the escape of gasses released during charging.

Since water is decomposed during open cell operation, the concentration of the electrolyte changes (electrolyte concentration can be estimated by measuring the density). Maintenance is required to refill the battery with deionized water. These cells have removable plugs or hinged lid plugs for this purpose.

The cell reaction consumes virtually no electrolyte. As a result, these cells can be operated with very small quantities of electrolyte (immobilized electrolyte). This is the case with compact cells and gas-tight cells. In general, these cells' current capacity is only marginally dependent on the SOC. As a side-reaction of the charging process, oxygen formation (as discussed above) is heavily-dependent on the temperature and electrolyte. The use of lithium hydroxide or sodium hydroxide additives (ternary electrolyte) improves the positive electrode's chargeability at higher temperatures.

Concentrated electrolyte solutions are used for special low-temperature applications. In practice, the cells can be operated up to the triple point in the KOH/$H_2O$ phase diagram

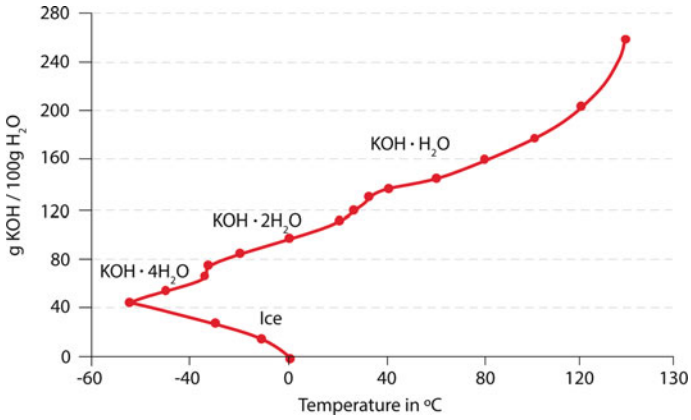



**Fig. 7.26** Use of electrolyte solutions for low-temperature applications [12]

(about −50 °C) with some loss of capacity and performance (Fig. 7.26). Use of higher electrolyte concentrations increases the usable capacity, but reduces the cycle life.

### 7.3.2.5 Technologies for Alkaline Cells

Nickel-cadmium batteries are manufactured in a variety of designs. The most important technologies used here include pocket-plate electrodes, sinter electrodes, fiber structure electrodes, and foam electrodes. These electrodes differ widely in terms of their composition and characteristics. Tubular pocket technology first developed by Edison is no longer used because it is too costly.

#### ▪ Pocket-Plate Cells

With pocket-plate technology, the electrochemically active materials are applied to perforated metal strips. The strips are connected by fixing rails, creating the electrodes. This mechanically sturdy design is an advantage. Manufacture of the electrodes is highly automated, and typically, both electrodes are manufactured using this technology. The electrodes are separated by separators, and sometimes by spacers as well. The spatial capacity of the electrodes can be varied depending on the strip form. To ensure adequate contact among the active components, electrically conductive materials must be added. Carbon (carbon black and graphite) and nickel powder are used for this purpose. Carbon as well as nickel, iron, or iron oxide are used in the negative electrode (Fig. 7.27).

A drawback of using carbon is that it converts to carbonate over time. This reduces the electrolyte's conductivity, requiring that the lye be changed. Because of the greater thickness of the electrodes, these cells are often used for low or moderate loads. These cells are very common in stationary applications (emergency electricity supply) and the railroad sector (starter batteries and emergency electricity supply). They perform well over a wide range of temperatures.

#### ▪ Sinter Cells

Very high-specific cell loads require excellent contact among the active components. With sinter electrodes, contact is facilitated by a carrier plate (usually a perforated plate) sintered with nickel powder on both sides. Using chemical and electrochemical processes, this metallic sinter layer is then filled with active components (for example nickel hydroxide precipitates from nickel nitrate solutions). This complex process results in reliable electrodes that are used in high-performance cells designed for a range of applications. Besides the high cost, a disadvantage of these electrodes is the sinter structure's sensitivity to mechanical stress caused by volume change during cycling. In addition, nitrate solution residue may increase self-discharge (Fig. 7.28).

To keep costs low, sinter electrodes today are only used as positive electrodes in many

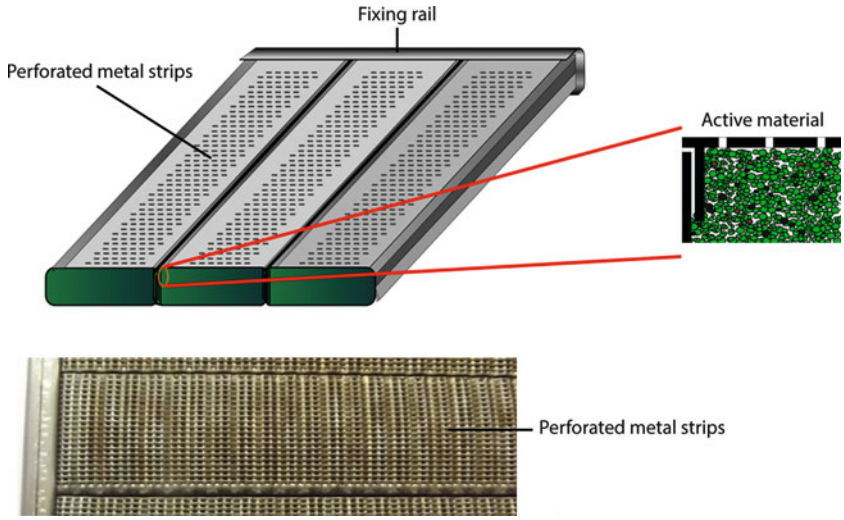



**Fig. 7.27** Pocket-plate cell design

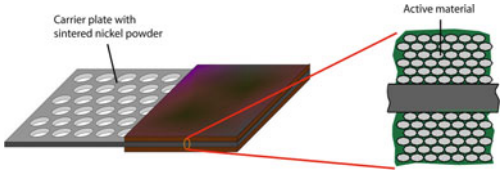



**Fig. 7.28** Example of a sinter cell

cells. Cadmium electrodes are manufactured as plastic bonded (extruded) electrodes. With these electrodes, the electrode material is applied to a carrier (perforated plate, metal mesh, etc.) together with a polymeric organic binder. The electrode thickness is usually limited.

Sinter-sinter cells are typically used for aeronautic and military applications. Combination sinter-plastic bonded electrodes are also used for demanding applications (the railroad and automotive sectors or stationary applications) (Fig. 7.29).

### Fiber Structure Electrodes

Fiber structure electrodes were introduced in the 1980s as an alternative to conventional structures. With these electrodes, the active material is inserted in a conductive substrate made of nickel-plated plastic fiber. This substrate has a felt-like structure with a high-fiber density. This effectively fixes the electrochemically active components, facilitates contact between them, and allows compensation for volume change during cycling. The result is cells with an extremely long service life suited for a wide range of applications. Since the form and thickness of the carrier structure is highly variable, the cells can be designed to maximize either capacity or energy. This allows the cells to be designed for a wide variety of applications to suit a customer's specific needs. Additional advantages of these cells include fast-charging and reliable operation at both high and low-temperatures. These cells are used for both stationary and mobile applications (the railroad sector and driverless transport systems). They are also used in the aerospace sector.

### Technologies for Sealed Cells

The development of mobile electric and electronic devices combined with the spread of electric drive technologies has driven demand for sealed batteries that can be operated in any position. Because of their excellent characteristics, engineers then developed alkaline batteries with gas-tight cells. These cells typically have a very compact design suited for applications where space is limited.

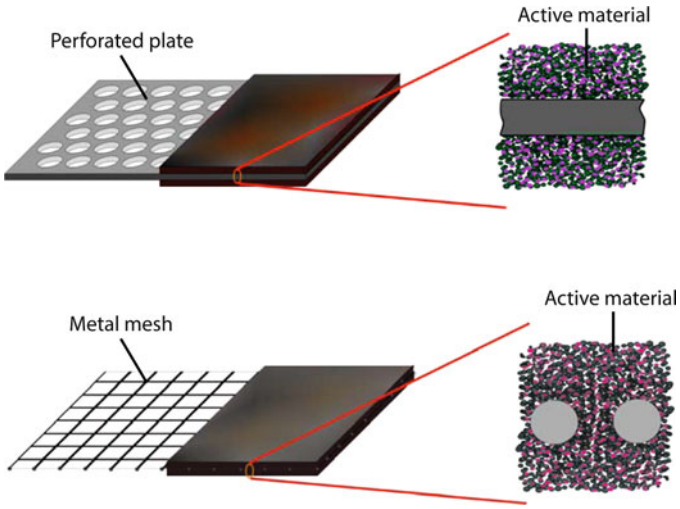



**Fig. 7.29** Sinter-sinter cell

Bonded plastic or sinter structure electrodes may be used in these cells. Fiber structure technology can also be used in gas-tight cells (vehicle drive systems and aerospace). Electrodes-based on nickel foam are another option. Open nickel foams are produced using nickel plating of foamed polymer (polyurethane for example). The foam's organic core is thermally removed, leaving behind a highly conductive nickel structure.

Gas-tight sealed cells are built in both cylindrical and rectangular designs (often called prismatic cells). They are also designed as small button cells. The cylindrical cells are very cheap, and like primary cells, produced in large quantities. The cylindrical geometry's mechanical stability is also an advantage when pressure changes in the cells. The disadvantage of these cells is that, with high-current loads, heat dissipation through the cylinder's shell is limited.

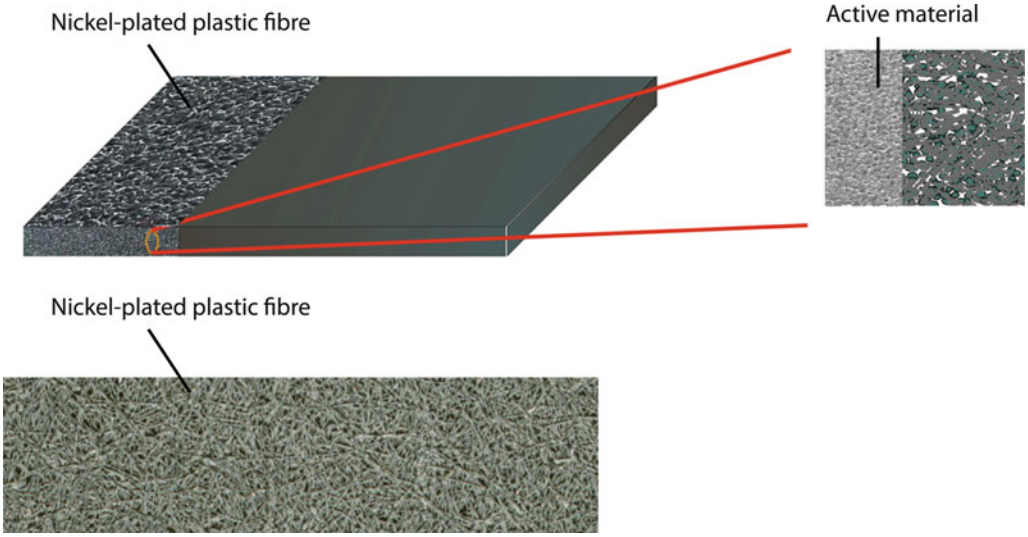



**Fig. 7.30** Fiber tsructure electrodes

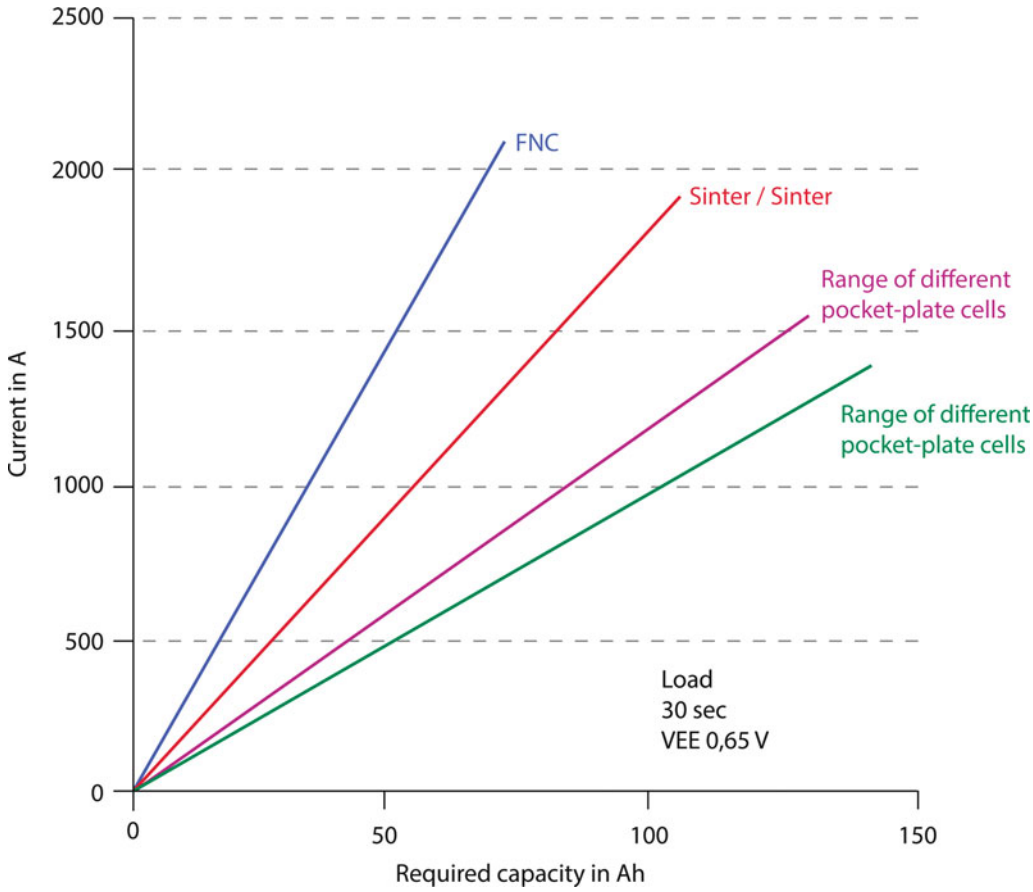



**Fig. 7.31** Required capacity compared with current load capacity and technology used

The surface to volume ratio is lower than with rectangular cells.

With gas-tight nickel-cadmium cells or nickel metal hydride cells, the ratio between the two electrode capacities must be carefully dimensioned to take into account both charging and discharging reserves. With cells used in electronics applications, for environmental reasons (recycling) the nickel-cadmium system has recently mostly been replaced by nickel metal hydride or lithium cells.

### 7.3.2.6 Nickel-Cadmium Cell Characteristics

Battery cycle life depends on load profile (cycle depth and current-strength). The quantity of current put through a battery across its entire service life (with FNC about 3,000 times the rated capacity) falls as the cycle capacity increases. Ambient temperature has an even greater effect. Capacity is limited by the positive electrode, and the positive electrode's ageing mechanisms depends on temperature (Arrhenius equation: about an 8–12 K increase in temperature accelerates aging by a factor of two). As a result, thermostatic control may increase service life. This is especially true with batteries bearing high-current loads, but it is also true for a range of other batteries.

There are a number of different factors in choosing a cell technology. For example, the goal may be a certain battery size (capacity) with a particular profile (current requirement) and a defined charging time. Since battery size

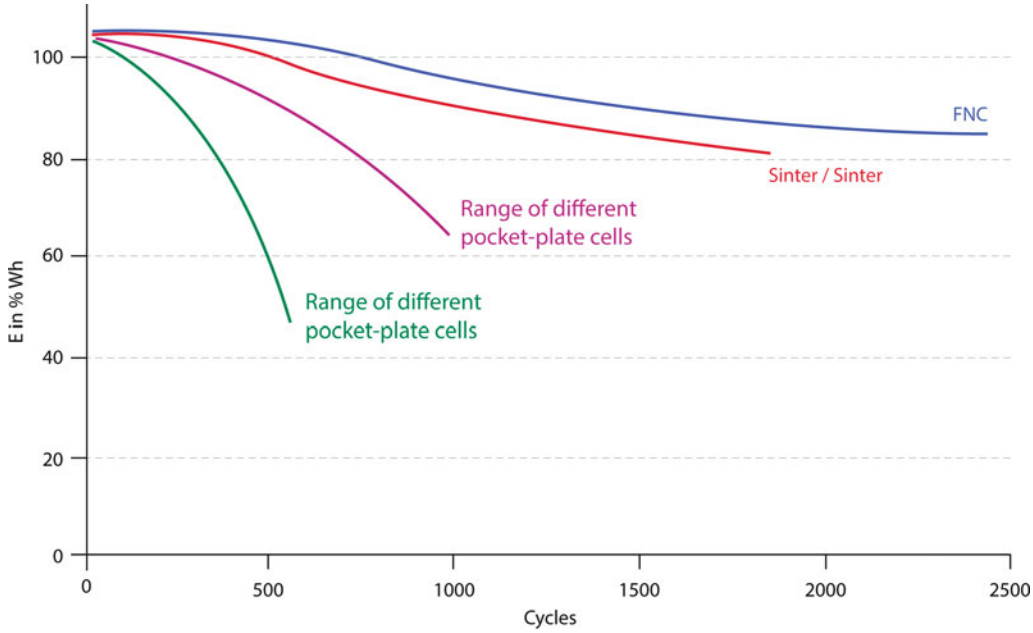



**Fig. 7.32** Cycle life for different technologies

affects facility investment costs, choosing the right system is a difficult process that also requires taking into account lifecycle costs (peripherals, service, and service life) (Figs. 7.31 and 7.32).

### 7.3.2.7 Designs and Application Areas

The majority of nickel-cadmium cells in use today have an open design. With gas-tight designs such as the RECOM design, oxygen formed at the negative electrode during charging is entirely recombined. There are also partial solutions (for example the Hoppecke FNC-A design) that recombines only a portion of the oxygen (Fig. 7.33).

External electron-hole recombination facilities and semi- or fully-automatic water refill systems are required for maintenance-free operation.

The charging characteristics of these cells differ from those illustrated in Fig. 7.34 (CC charging).

Industrial cells are typically manufactured in sizes ranging from a few A h to 2,000 A h in

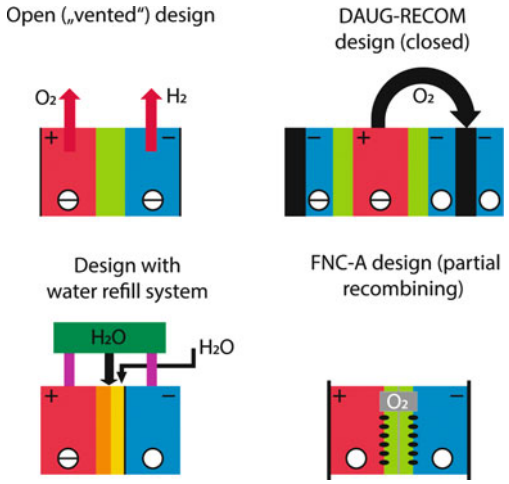



**Fig. 7.33** Various nickel-cadmium cell designs

different load classes: *L* (low, discharge times above several hours), *M* (medium, discharge times of about an hour), *H* (high, discharge times less than an hour), *X* (extreme, short-term loads with very high-current levels; for example, diesel starters). The loading currents follow the same scheme, but are designed to suit the appli-

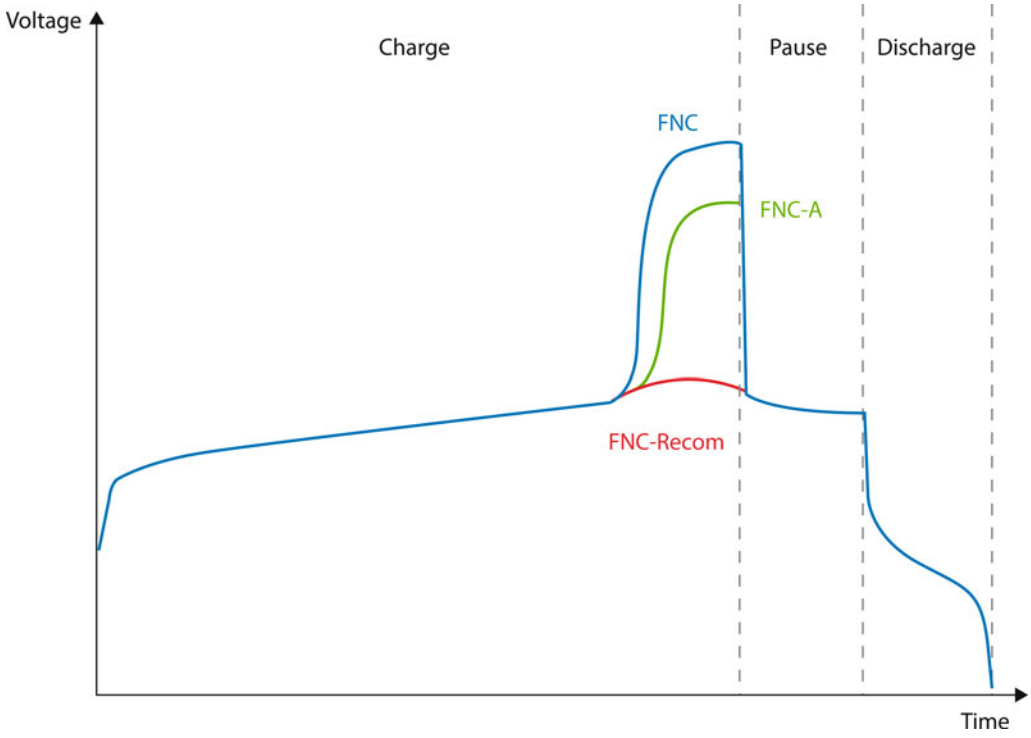



**Fig. 7.34** Nickel-cadmium cell charging characteristics



cation. Depending on the load type, the cells' internal resistance (pulse resistance) ranges from 20–100 mΩ A h (i.e., a 200 A h cell typically has an internal resistance below 1 mΩ). In practice, battery cells can be connected in series or parallel (Figs. 7.35 and 7.36).

Depending on the application area, battery cells are mounted on troughs or carriers, or on special frames. Recently, the trend is to develop and manufacture complete battery systems (including charging and control technology).

Nickel-cadmium batteries have a very long service and cycle life, a high-current capacity, and perform well over a wide temperature-range. Another advantage of these cells is their tolerance to operational disruptions such as deep-discharging and overcharging (abuse tolerance). Unlike other battery chemistries, nickel-cadmium batteries can be stored in practically any SOC without causing irreversible changes or damage.

The batteries are used in many applications in what is termed stand-by parallel operation (stationary use, railway sector, etc.). Here, they are also operated at a constant charging voltage (float charging). To avoid overcharging and the risks of thermal overheating, the charging voltage is typically adjusted to the ambient temperature. The specific adjustment depends on the cells' type and operating method (overvoltage and gas formation). For thermodynamic reasons, a nickel-cadmium battery's equilibrium cell voltage has a negative temperature coefficient. Since the temperature may rise when current is applied, a constant charging voltage may cause the current to rise even further if not corrected (Fig. 7.37).

With stand-by parallel operation (UPS applications), the float charging voltage is set to minimize water consumption across the entire temperature-range. If the charging voltage falls or the primary electricity supply fails, the bat-

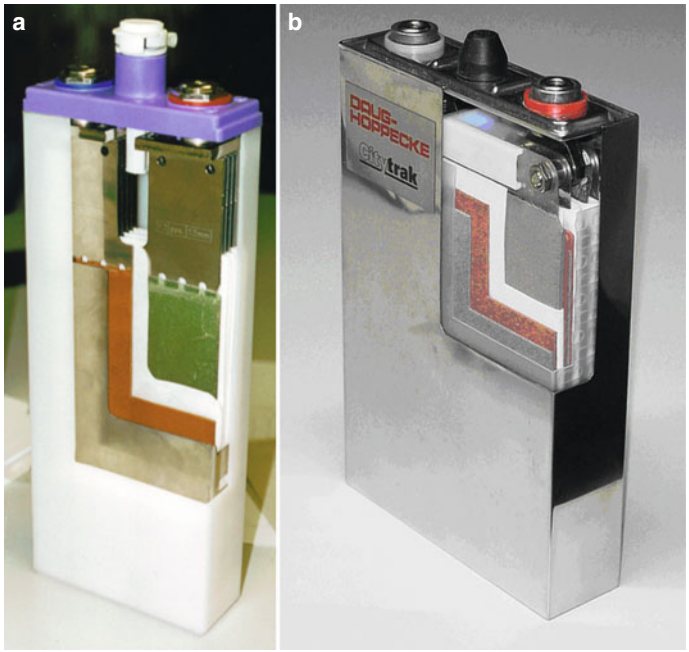



**Fig. 7.35** **a** FNC-A industrial cell, **b** gas-tight FNC-RECOM cell



**Fig. 7.36** FNC-cells for a range of applications

tery can immediately take over supply for all connected consumers.

In some cases a boost charge process is also used. After being connected to a load, the battery is first charged at an increased charging voltage and then charged at a lower maintenance-charge voltage.

With driverless transport vehicles, the battery must automatically recharge in a very short time once a defined quantity of charge has been extracted (for example, 30% of the rated capacity). For this purpose, very high-charging currents (up to 2.5 times the numerical rated capacity in A h) are used. Charging is considered complete when the charging current at a CV falls below a certain threshold value. Using this process, alkaline batteries can continually power automatic vehicle for months at a time.

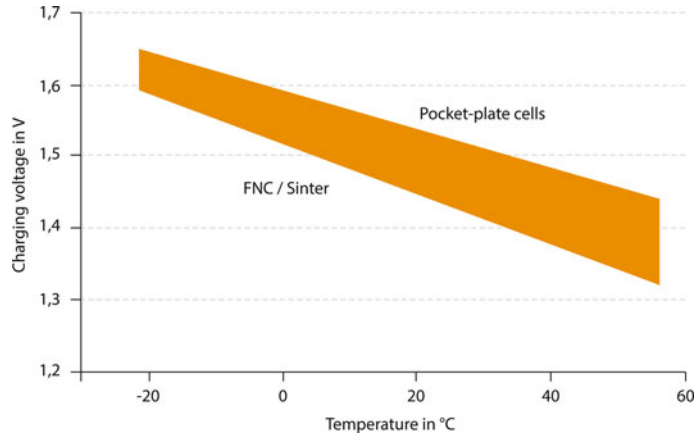



**Fig. 7.37** Temperature-compensated charging voltage with float charging






**Fig. 7.38** Battery for driverless transport systems

### 7.3.2.8 Water Decomposition During Charging

In stationary facilities in particular, there is a certain amount of overcharging of the cells. The following overload reactions occur:

$$2OH^- \rightarrow \frac{1}{2}O_2 + H_2O + 2e^-, \quad (7.50)$$

$$2H_2O + 2e^- \rightarrow H_2 + 2OH^-. \quad (7.51)$$

This reaction consumes electrolyte water:

$$H_2O \rightarrow \frac{1}{2}O_2 + H_2. \quad (7.52)$$

According to Faraday's law, 1 A h decomposes 0.335 ml of water. At 298 K and a pressure of 0.101 MPa, there is around 0.448 L of precipitated hydrogen at the negative electrode, and 0.224 L of precipitated oxygen at the positive electrode.

Water loss may vary if it escapes the cell as steam together with the gasses. It may also vary if inhibited by means such as partial internal or external electron-hole-recombination, additives, or cell sealing mechanisms.

### 7.3.2.9 Conclusion

- Energy is stored by converting **nickel hydroxide into nickel oxyhydroxide** at the positive electrode, where the nickel undergoes a formal change of metal valence state from +2 to +3. During charging, at the negative electrode, the **cadmium hydroxide** (cadmium with a valence of +2) is converted to **metallic cadmium** (valence 0).
- Nickel-cadmium batteries have a **very long service and cycle life**, a **high-current** capacity, and can be operated over a **wide temperature-range**.
- Nickel-cadmium batteries are **relatively tolerant to operational conditions, such as deep-discharging and overcharging**.
- Unlike other battery technologies, nickel-cadmium batteries can be stored **in practically any SOC** without causing irreversible changes or damage.

## 7.3.3 Nickel Metal Hydride Batteries

The need for higher power and energy densities prompted scientists to explore alternative electrode combinations. The use of compressed hydrogen as the reactant at the negative electrode led to the development of special high-performance batteries. These are, however, too costly for general applications. Philips began researching reversible hydrogen storage using special metal alloys in the 1960s. The results led to a nickel metal hydride battery system suited for high-performance applications. This system is widely used in consumer electronics. It is also used to store energy in the Toyota Prius hybrid car.

Nickel metal hydride batteries are, in many ways, similar to gas-tight nickel-cadmium batteries. These similarities include their voltage, long service life, and reliability. The positive electrode, separation method, and electrolyte are also basically the same. The most important difference is the negative electrode. This is where the hydrogen stored in the alloy is converted. In simple terms, the cell reaction is a hydrogen shuttle mechanism that results in a very compact cell.

### 7.3.3.1 Chemical Reactions

Negative electrode:

$$\mathrm{M(H) + OH^- \underset{\text{charge}}{\overset{\text{discharge}}{\rightleftarrows}} M + H_2O + e^-} \quad \textbf{(7.53)}$$

Positive electrode:

$$\mathrm{NiOOH + H_2O + e^- \underset{\text{charge}}{\overset{\text{discharge}}{\rightleftarrows}} Ni(OH)_2 + OH^-} \quad \textbf{(7.54)}$$

Cells:

$$\mathrm{M(H) + NiOOH \underset{\text{charge}}{\overset{\text{discharge}}{\rightleftarrows}} M + Ni(OH)_2} \quad \textbf{(7.55)}$$

The resulting equilibrium cell voltage is 1.30 V at room temperature.

### 7.3.3.2 Negative Storage Electrode

A range of alloys for hydrogen storage have been developed for other uses. The absorption of hydrogen in these alloys should be viewed as a physicochemical process. (This is not the case for other hydrides in chemistry. But these hydrides are not relevant to the present discussion.) Thermodynamic equilibrium is reached between the activity (concentration) of the hydrogen in the metal lattice and the pressure of the hydrogen in the area around the storage alloy. A range of metals and alloys can be used as storage alloys. They vary by storage capacity (hydrogen per unit of weight of the alloy), as well as by the pressure range or temperature range required to allow the storage or release of hydrogen. Hydrogen's equilibrium pressure increases together with the temperature and concentration of dissolved hydrogen. This causes the pressure in NiMH cells to change during cycling (Fig. 7.39).

These storage alloys can be used in batteries if they allow hydrogen exchange at a working temperature under ambient pressures, and if the exchange is largely reversible. These include $AB_2$ type Laves phases and type $AB_5$ nickel-lanthanum alloys ($LaNi_5$). In place of pure lanthanum, a composite metal more easily extracted from rare-earth metals is used (lanthanum group elements) (Fig. 7.40).

The alloy composition is varied to optimize storage capacity, power capacity, working temperature-range, service life, and cost. Storage capacities ranging from 300–350 mA h/g are given for the popular $AB_5$ alloys (this is equivalent to a storage capacity of about one hydrogen atom per metal atom in the alloy). The presence of oxygen or high-electrode potentials may destroy the alloy. Boundary layers are formed, resulting in increased polarization. Alloy additives such as cobalt, aluminum, manganese, etc., improve the alloy's characteristics. In the future, the development of crystalline superstructures and the use of other alloy elements are expected to deliver even higher energy densities.

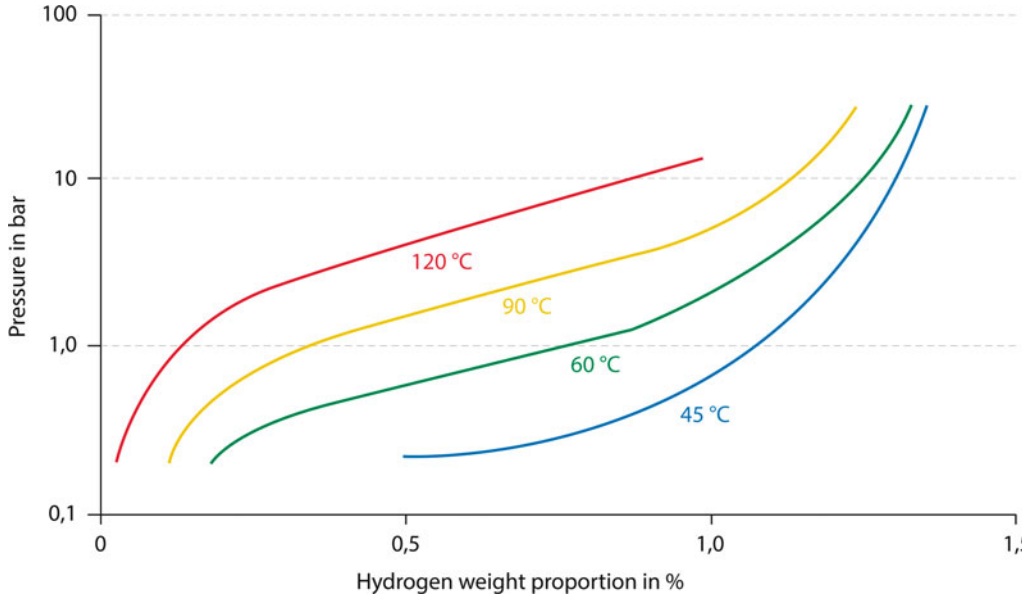
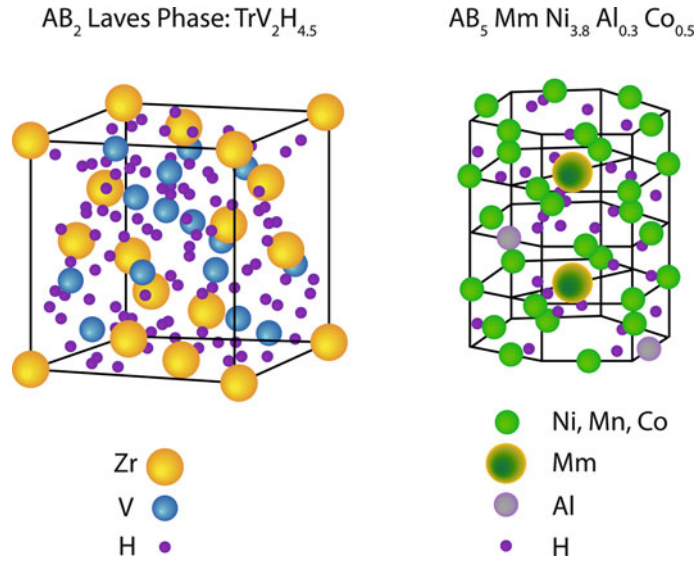



**Fig. 7.39** Typical isothermal profile of $AB_5$ storage alloys

**Fig. 7.40** $AB_2$ and $AB_5$ Laves phases




The electrochemical reactions occur at the boundary between the storage alloy and the electrolyte. As a result, hydrogen transport must arise from the alloy bulk phase to the surface during charging or discharging. At low temperatures (particularly below −10 °C), the hydrogen's mobility in the alloy is considerably reduced. As a result, the electrodes' electrochemical load capacity falls. These electrodes are also large in size compared to the positive electrode.

The electrodes are manufactured as plastic-bonded electrodes. Perforated plates, nickel foams, or nickel meshes are used as carriers.



**Fig. 7.41** Hoppecke nickel metal hydride module 75 A h/10 cells

The cells are produced in a prismatic rectangular design or a round cell design. They are sealed during operation.

#### 7.3.3.3 Applications

With the first nickel metal hydride cells, the drawback was increased self-discharge. But by using special separators and electrode components, self-discharge was reduced. Today, these cells have excellent charge retention characteristics, and remain charged even after long storage periods.

Unlike nickel-cadmium cells, there is no significant voltage increase once they are fully charged. This is because the charging and overcharging process at the negative electrode does not change. Since the oxygen reaction can continue essentially unchecked, the conditions resemble those in sealed nickel-cadmium cells with full oxygen electron-hole-recombination.

The increase in temperature, or the voltage inflection point during charging with limited current, can be used to determine when the cells are fully charged. Large batteries are usually thermally monitored or electronically limited during charging.

The advantages of these cells is the significantly higher energy and power densities, the avoidance of toxic cadmium, and the low final charging voltage for a full charge. The SOC among cells can be balanced in larger batteries by monitored charging within the battery unit. The cells can be designed for limited tolerance to deep-discharging (and even polarity reversal). Since the cells have practically no soluble electrode components, the risk of dendritic short-circuits is minimal. As a result, the cells have a very long cycle life. These characteristics make the cells an excellent fit for hybrid drive system applications (Figs. 7.41, 7.42 and 7.43).

As with nickel-cadmium cells, available capacity falls together with the positive electrode's cyclability. In addition, the storage alloys are prone to corrosion processes. With gas-tight cells, electrolyte depletion may occur in the separator (increased electrode porosity and water decomposition during overcharging).

### 7.3.4 Conclusion

- Nickel metal hydride batteries were designed for **high-performance applications**.
- These batteries are widely used **in consumer electronics** and **to store energy in hybrid cars**.
- The most important difference between these batteries and nickel-cadmium batteries is the **negative electrode**. This is where hydrogen stored in the alloy is converted. In simple terms, the cell reaction is a **hydrogen shuttle mechanism**. This allows the cells to be **very compact**.
- The advantages of nickel metal hydride batteries are the **significantly higher energy and power densities**, the **avoidance of toxic cadmium**, and the **low final charging voltage** for a full charge.
- Nickel metal hydride battery cells contain practically **no soluble electrode components**. As a result, the risk of dendritic short-circuits is minimal. This also means the cells have a **very long cycle life**.

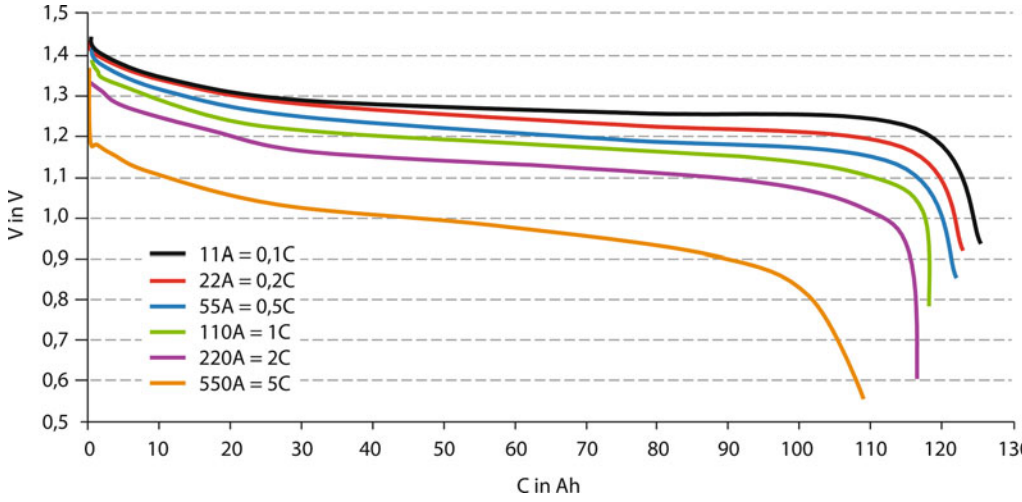



**Fig. 7.42** NiMH industrial cell characteristics



**Fig. 7.43** 25 kW h NiMH hybrid drive battery system for buses

## 7.4 Lithium Batteries

Lithium ion batteries use a range of different cell chemistries. In lithium ion batteries, during discharge the negative electrode functions as a source of lithium ions (Li ions), and the positive electrode as a sink. The electrolyte separates the transport of Li ions from the transport of electrons. If metallic lithium is used for the negative electrode, then the cell voltage results from the difference between the electrochemical potential of the positive electrode material and the lithium (negative electrode). The Li ions resulting from the reaction $\mathrm{Li} \rightarrow \mathrm{Li}^{+} + e^{-}$ are transported through the electrolyte to the positive electrode. The electrons flow through the exterior power-circuit to supply electrical energy.

Lithium batteries, therefore, fall into two categories; systems with metallic lithium and systems without. Lithium ion cells are systems where the Li ions can be embedded in the positive and negative electrode materials (as solids). This means that metallic lithium is not used for the negative electrode in lithium ion cells.

Lithium batteries first appeared in the early 1970s. Since then, a range of different electrode materials have been developed and tested. The diversity of materials used for the electrodes and electrolyte in the lithium system makes it quite unlike the lead-acid system, for example.

The system was developed in stages. Early research focused primarily on Li metal systems [40]. The $\mathrm{Li}/(\mathrm{CF})_n$, and later, the $\mathrm{Li}/\mathrm{I}_2$ systems were then developed, as well as the $\mathrm{Li}/\mathrm{MnO}_2$ system popular for consumer applications. The $\mathrm{Li}/\mathrm{Ag}_2\mathrm{V}_4\mathrm{O}_{11}$ system was also used for medical applications such as implanted defibrillators.

With rechargeable lithium batteries, the processes that occur when the material system discharges must be reversible in the other direction. Research on this problem also began in the early 1970s [40]. One solution is a system that

uses a lithium aluminum compound (LiAl) as the material for the negative electrode, and iron sulfide or vanadium oxide ($Li_xV_2O_5$) as the material for the positive electrode.

At practically the same time, research began on intercalation of electrochemically active materials in electrically conductive host materials such as ($TaS_2$) [40]. The material, titanium sulfide ($TiS_2$), seemed to hold the most promise for use in energy storage applications. The crystal structure of this material forms in layers, allowing the Li ions to easily embed themselves in the free space between the layers. In addition to $TiS_2$, similar compounds such as $MoS_2$, $LiVS_2$, and $LiCrS_2$ were developed. The first large rechargeable lithium cell prototypes and commercial products used metallic lithium or LiAl compounds for the negative electrode, and materials such as $TiS_2$ or $MoS_2$.

After John B. Goodenough demonstrated that the compound lithium cobalt oxide ($LiCoO_2$) could be used as an electrochemically active material for the positive electrode, SONY achieved a major breakthrough in the early 1990s. By combining a $LiCoO_2$ electrode with a negative electrode containing carbon, rechargeable lithium ion cells could be produced and marketed on a large scale for the first time. Since then, millions of these batteries have been produced for portable consumer electronics applications (for example, computers, mobile phones, and cameras) [9, 40]. Using $LiCoO_2$ instead of $TiS_2$ resulted in significantly higher cell voltages. In addition, a significant advantage of negative electrodes containing carbon is that, unlike metallic lithium, they do not form dendrites with metal separation.

The storage used in consumer applications typically has a rated capacity of up to several hundred milliampere hours. Rechargeable secondary lithium ion batteries for industrial applications are typically large-format lithium ion cells with a rated capacity of around 10 to 100 ampere hours. In these large-format lithium ion cells, newer materials have been developed for the positive electrode. Typical examples are transition metal oxides such as $LiNi_aMn_bCo_{1-a-b}O_2$ in a variety of stoichiometries. For a detailed description of developments in lithium battery cell chemistry, see Whittingham's survey article [40] or other listed reference sources [2, 9].

Extensive further research on lithium ion cell chemistry is still required, and it remains a focus of current research and development. It can be expected that new materials will be developed for electrodes and electrolytes in particular.

The following sections provide an introduction to rechargeable lithium ion cells. The emphasis here is on large-format cells. The data, measurements, and performance characteristics given for cells in ▶ Sects. 7.4.9 and 7.4.10 apply to commercially available, large-format cells. However, these figures are provided only for the purpose of illustrating the typical behavior of lithium ion cells. Since manufacturers are constantly modifying the design and characteristics of these cells, see the manufacturer's technical specifications for detailed, updated information.

### 7.4.1 Operating Principle, Chemical Reactions, and Active Materials

Energy storage in rechargeable lithium ion cells is based on the reversible insertion and removal of Li ions in active materials by electrochemical redox reactions. The insertion of Li ions in the host grid is called intercalation. The active materials are also called intercalation compounds, and the electrodes are called intercalation electrodes. The term insertation is also sometimes used in this context. Intercalation can occur at the positive or negative electrode. Since the $Li^+$ ion has a small radius of about 0.068 nm, $Li^+$ can easily be intercalated in certain structures. This is the case with graphite for example, where the layers are separated by a distance of $\sim$ 3.35 nm. The active material is reduced or oxidized when the Li ions are intercalated or deintercalated. If metallic lithium is used for the

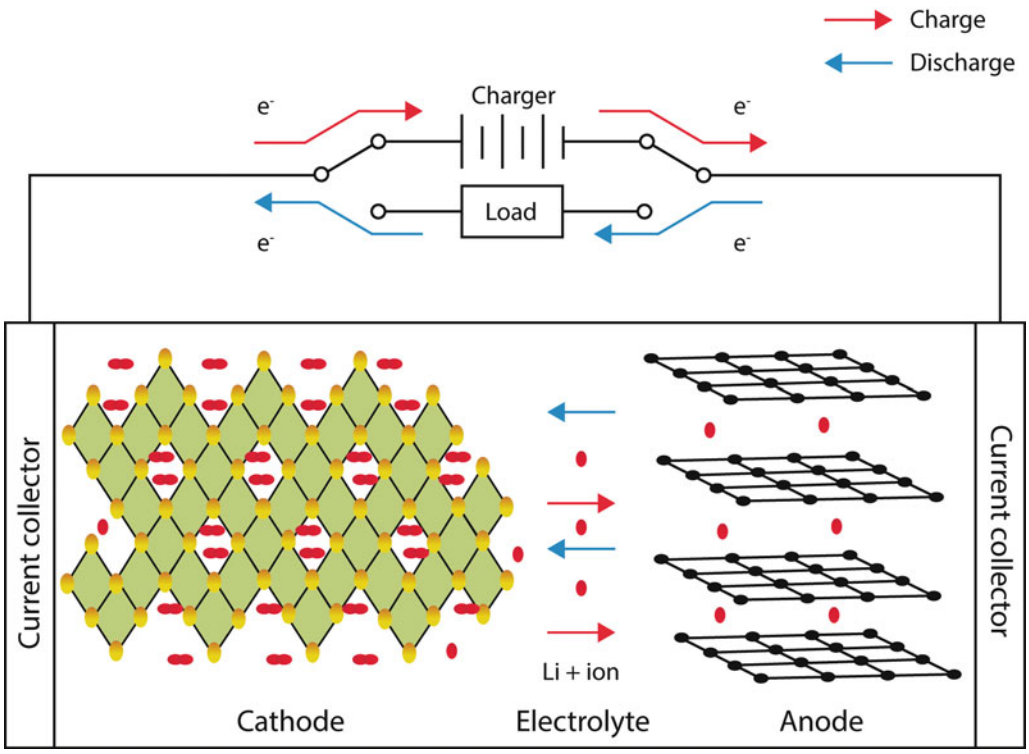



**Fig. 7.44** Basic design and operation of a lithium ion cell. Lithium ions are reversibly intercalated in the active material of the positive and negative electrodes. The external circuit carries the flow of electrons. The positive and negative electrodes are separated by the electrolyte (ion conductor)

negative electrode, then the Li ions are separated and dissolved at a metallic electrode.

Figure 7.44 shows the basic design of a lithium cell. The positive and negative electrodes are connected by an ion-conducting electrolyte. The separator serves as an electrical insulator, preventing direct contact between the two electrodes (electrical short-circuit). The electrodes are electrically connected to the consumer by an external circuit.

During charging and discharging, the electrochemical reactions occur at the electrode active materials. These reactions can be illustrated by using the following system as an example: transition metal oxide ($Li_xMeO_2$, Me; for example, Co, Mn, Ni)/electrolyte/graphite ($C_6$).

During charging, the positive electrode active material is oxidized, raising the transition metal's oxidation number to one (in the example here from $Me^{III}$ to $Me^{IV}$), and releasing an electron into the external circuit. Li ions are deintercalated from the host grid and released into the electrolyte, where they are transported to the negative electrode (Fig. 7.44). Reduction occurs at the negative electrode. The Li ions are transferred from the electrolyte to the active material (graphite) and intercalated there. Electrons flow through the external circuit to the negative electrode, resulting in charge neutrality (Fig. 7.44). For each intercalated Li ion, one electron is assigned to the graphite.

The following equations describe the chemical reactions in simplified form.

Positive electrode:

$$Li_x^{I}Me^{III}O_2 \leftrightarrow xLi^+ + xe^- + Me^{IV}O_2. \quad \textbf{(7.56)}$$

Negative electrode:

$$xLi^+ + xe^- + C_6 \leftrightarrow Li_x^{I}C_6^{-I}, \quad \textbf{(7.57)}$$

where $x$ is between zero and one. When metallic lithium is used, the Li ions are separated at the anode.

During discharging, the processes at the electrodes occur in reverse. This allows the exterior power-circuit to supply electrical energy. The Li ions are deintercalated at the negative electrode. After being transported to the positive electrode, they are intercalated in the active material there. As a result, the electrons from the negative electrode are fed into the exterior power-circuit. The positive electrode active material is reduced. The negative electrode active material is oxidized.

### 7.4.2 Cell Voltage

To achieve the highest cell voltage possible, the positive electrode active material's redox pair must have the highest possible standard potential in comparison to the negative electrode. High-capacity results from maximizing the number of Li ions that can be intercalated in the material. The following criteria determine an active material's effectiveness in a lithium ion cell:

- High-specific energy density (in W h/kg)
- Reversible and fast-acting intercalation reaction
- Good electric and ionic conductivity
- Thermal stability
- Structural stability with Li ion intercalation
- Electrochemical stability

Another factor is mechanical stress caused by volume change in the active material during Li ion intercalation and deintercalation. If this stress is excessive, it can cause individual fragments of the electrode material to separate and flake off. This may damage the cell irreparably. Similarly, Li ion intercalation and deintercalation may lead to phase-change in the active material [2, 9]. In addition, the choice of active materials for lithium ion cells must take into account material and production costs, natural reserves, environmental friendliness, and toxicity. For example, the chemical element cobalt is significantly rarer and more expensive than manganese or iron. Ideally, these materials should, therefore, be used instead of cobalt.

With a redox potential of −3.05 V (compared to the SHE), lithium has the most negative standard potential of all the materials suitable for use as a negative electrode. Together with its very high-specific capacity of around 3,800 A h/kg, these characteristics make lithium the ideal material for use as a negative electrode. But the metallic Li electrode's tendency to form dendrites prevents use as a negative electrode in rechargeable batteries. Dendrite formation means that tree-like or needle-shaped Li structures are formed on the electrode surface when Li ions separate from the electrolyte. Li ion separation results in capacity loss, reducing the service life and cyclability of the cell. If the dendrites penetrate the separator connecting the positive and negative electrodes, then the cell short-circuits. Another problem with lithium is its high reactivity to water or residual moisture in the cell components.

Due to their low redox potentials, in place of metallic lithium, carbons in powder form (such as graphite) can be used as negative electrodes. Amorphous carbons and other modifications also may be viable alternatives. Carbons differ in terms of their degree of crystallinity, particle size, morphology, porosity, purity, degree of compression, graphite source (natural, synthetic), and so on. Graphite's redox potential is about 50–300 mV (vs. $Li^+/Li$). The maximum theoretical capacity is 372 A h/kg, with intercalation up to $LiC_6$. Compared to metallic lithium, graphites are significantly safer and have a higher electrochemical reaction reversibility. Mechanical stress at a volume change of ∼ 12% [42] can be tolerated by its excellent layer structure without causing cell damage.

Table 7.10 shows the redox potentials of several applicable active materials in comparison with $Li^+/Li$, as well as typical figures for maximum usable specific capacity of the electrode [9, 40]. Besides

**Table 7.10** Redox potentials and maximum usable specific capacity for several applicable active materials

| Active material | Potential vs. Li/Li$^+$ [V] | Maximum usable specific capacity [A h/kg] | Comments |
|---|---|---|---|
| $Li_xCoO_2$ | 3.9 | 130–150 | $x$: 0.5–1 |
| $LiNi_{1-a-b}Mn_aCo_bO_2$ | ~ 3.8 | 150–190 | E.g., $a = 0.33$, $b = 0.33$ |
| $LiNi_{0.8}Co_{0.15}Al_{0.05}O_2$ | 3.8 | ~ 190 | |
| $LiFePO_4$ | 3.4 | 150–160 | |
| $Li_xMn_2O_4$ | 4.1 | 100–120 | $x$: 0–1 |
| Graphite | 0.05–0.3 | Theor. 372 | Neg. electrode |
| $Li_4Ti_5O_{12}$ | 1.55 | ~ 150 | Neg. electrode |

7

$LiCoO_2$ as discussed above, materials for the positive electrode include other layered oxides such as $LiNi_{1/3}Mn_{1/3}Co_{1/3}O_2$ and $LiNi_{0.8}Co_{0.15}Al_{0.05}O_2$, compounds with a spinel structure such as $LiMn_2O_4$, or compounds with an olivine structure (for example $LiFePO_4$). The titanate compound $Li_4Ti_5O_{12}$ (spinel structure) is a suitable material for the negative electrode.

As Table 7.10 shows, the maximum usable specific capacity ranges from 110–190 A h/kg. The maximum usable voltage is limited to $< 4.5$ V (vs. Li$^+$/Li). As described above, most commercially available cells use graphites or other carbon compounds as negative electrodes. The resulting mean cell voltages for the systems listed in Table 7.10 are, therefore, determined by the redox potential of the positive electrode minus an average potential of ~ 200 mV (graphite electrode). For example, the mean voltage for the $LiFePO_4$/graphite system is 3.2 V. A special feature of lithium ion cells is that, during charging and discharging, the lithium is not oxidized or reduced by the processes at the intercalation electrodes. The Li ions are reversibly intercalated or deintercalated. As a result, the redox potential of the lithium (Li$^+$/Li) is not used for calculating the cell voltage.

Figure 7.46 graphs the potentials at both electrodes during discharge. The electrode potentials are shown relative to the redox potential of Li$^+$/Li (at 0 V). The system used in the example is $LiFePO_4$/graphite. The discharge capacity is incremented (given in arbitrary units). During discharge (Li ion intercalation in $LiFePO_4$), the positive electrode's potential falls. As Fig. 7.45 shows, the mean potential for $LiFePO_4$ is ~ 3.4 V (*vs.* Li$^+$/Li). When the Li ions deintercalate from the graphite ($LiC_6$ as intercalated form), the negative electrode's potential gradually increases. The difference between the two curves at the electrodes (the dotted line in Fig. 7.45) determines the discharge-curve. For the example system $LiFePO_4$/graphite shown here, the result is a mean cell voltage of 3.2 V (Table 7.10). The same procedure can be followed to determine the electrode potentials during the charging phase. The stability window shown in Fig. 7.45 indicates the potential range for commonly used liquid electrolytes. For a more detailed explanation, see the section on electrolytes (▶ Sect. 7.4.4).

Figure 7.46 shows the discharging curves for various active material systems. The active materials' redox potentials determine the cell voltages that result. The maximum cell voltage was achieved by $LiMn_2O_4$ (~ 3.9 V); the lowest in the system $Li(Ni,Mn,Co)O_2/Li_4Ti_5O_{12}$ at 2.3 V. Another special feature of lithium ion cells is how the cell voltage varies in relation to the cell's SOC (Fig. 7.46). The $Li(Ni,Mn,Co)O_2$/C system's cell voltage con-

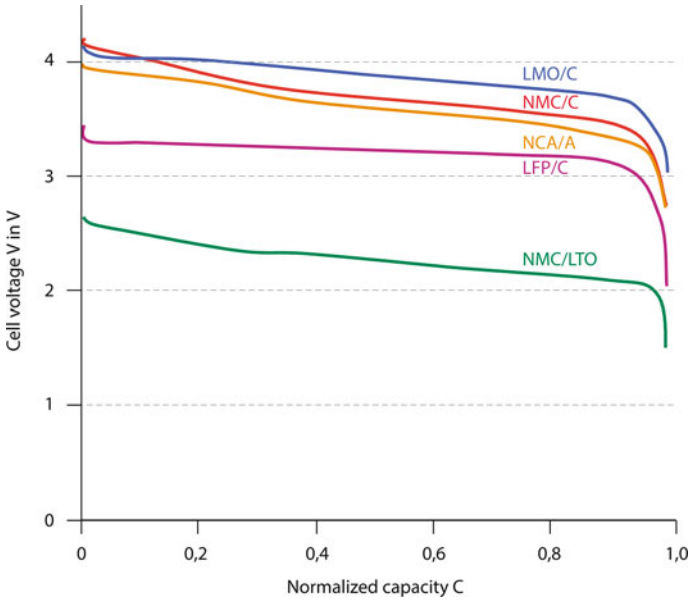



**Fig. 7.45** Charge-discharge curves for various active material systems with $LiMn_2O_4$ (LMO), $LiFePO_4$ (LFP), $Li(Ni,Co,Al)O_2$ (NCA), $Li(Ni,Mn,Co)O_2$ (NMC), carbon (C), and $Li_4Ti_5O_{12}$ (LTO)

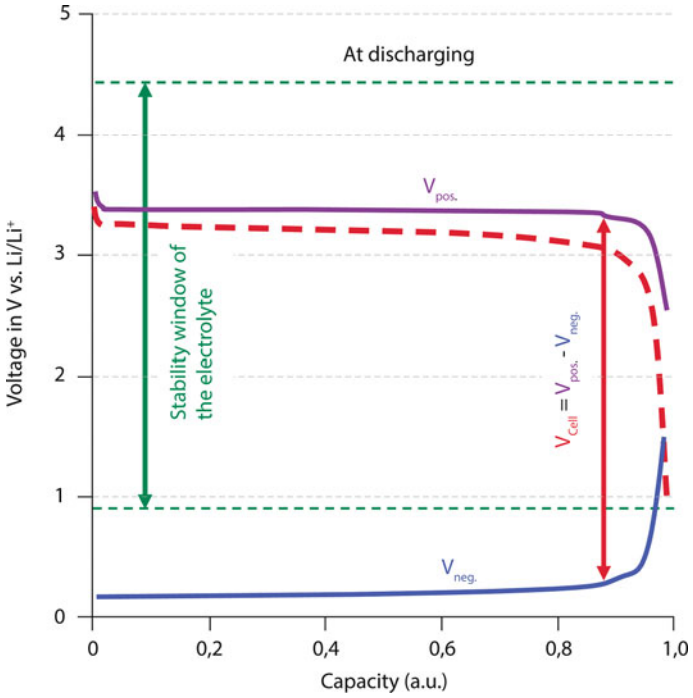



**Fig. 7.46** Graph of electrode potential at the positive ($V_{pos.}$) and negative ($V_{neg.}$) electrode during discharge using $LiFePO_4$/graphite as an example system. The difference (the dotted line) determines the cell voltage discharge curve. The potential range within which the electrolytes used in lithium ion cells are electrochemically stable are also indicated

stantly increases. In contrast, the $LiFePO_4$/C system has a plateau-like curve with a substantial constant cell voltage range. Thermodynamic considerations can explain this behavior (▶ Sect. 7.1).

Since the positive electrode active materials are also in powder form, their characteristics in terms of particle size and morphology, porosity, purity, degree of compression, composition, and so on, vary. Further discussion on this topic can be found in the section on electrode design (▶ Sect. 7.4.4).

For detailed discussions of the individual active materials, the electrochemical processes at the electrodes, and structural specifics, see the sources cited in the bibliography (for example [40, 42]).



### 7.4.3 Conclusion

- Energy storage in rechargeable lithium ion batteries is based on the reversible insertion and removal of Li ions in active materials by electrochemical redox reactions. This is called intercalation.
- A variety of compounds can be used as active materials in the positive and negative electrodes. As a result, lithium ion cells vary in terms of their cell voltage and specific capacity.
- In modern large-format cells, layered oxides (such as $Li(Ni,Mn,Co)O_2$), spinel structures (such as $LiMn_2O_4$), or **transition metal phosphates/olivine structures** (such as $LiFePO_4$) are typically used in the positive electrode. Graphites and amorphous carbons are frequently used in the negative electrode.
- Typical figures for the practically usable specific capacity of the (positive) active materials range from 110 to 190 A h/kg; typical cell voltages range from 2.3–3.9 V.

### 7.4.4 Electrolyte and Electrochemical Stability Window

Liquid, solid, or polymer electrolytes can all, in principal, be used in lithium batteries. Li systems can, therefore, also be categorized by the electrolyte used. Scientists speak of lithium ion polymer cells, or lithium ion cells, with liquid electrolyte, for example.

Liquid electrolytes are typically organic solvents with a conducting salt dissolved in it. Because lithium is a reducing agent that reduces hydrogen ions to hydrogen, aqueous electrolytes cannot be used. The electrolyte solutions must be aprotic, i.e., electrolytes that do not split off protons (= hydrogen ions). In place of organic solvents, ionic liquids can also be used. These liquids are salts that remain liquid even at room temperature. In polymer electrolytes, the conducting salt is aggregated in macromolecules or embedded in a polymer matrix. Liquid electrolytes can also be embedded. (Since polymer is an electrical insulator as well as dimensionally stable, a separator is not required. Because of its high internal resistance (poor ion conductivity), it only allows low-discharging currents compared to liquid electrolytes. Gel electrolytes can be used at room temperature. Solid electrolytes can be used at temperatures of around $> 60\,^{\circ}C$).

Some polymers such as polyvinylidene fluoride (PVdF), polyacrylonitrile, and polyethylene glycol are described here as examples [13, 21]. The ion conductivity of polymer electrolyte is frequently inadequate at room temperature. Alternative solid electrolytes are, for example, ion-conducting glasses. In general, various electrolytes can also be mixed to combine the individual materials' different benefits. Intensive research on polymer as well as other solid electrolytes, or ionic liquids, continues [13] or [41].

**Table 7.11** Physical characteristics of frequently used non-aqueous solvents (EC – ethylene-carbonate, PC – propylene carbonate, DMC – dimethyl-carbonate, DEC – diethyl-carbonate, EMC – ethylmethyl-carbonate, LiPF6 – lithium hexafluorophosphate) [20, 41]

| Solvent | Viscosity (cP) | Dielectric constant | Melting temperature [°C] | Boiling temperature [°C] | Flash point [°C] |
|---|---|---|---|---|---|
| EC | 1.9 (40 °C) | 89.8 | 36.4 | 248 | 160 |
| PC | 2.5 | 64.9 | −48.8 | 242 | 132 |
| DMC | 0.59 | 3.1 | 4.6 | 91 | 18 |
| DEC | 0.75 | 2.8 | −74.3 | 126 | 31 |
| EMC | 0.65 | 3.0 | −53 | 110 | 0…23 |

Because of their practical relevance, only liquid electrolytes are discussed in what follows. The electrolyte transports the Li ions. Conducting salts dissolve easily when the solvent has a high dielectric-constant $\varepsilon$ and the solvents are dipolar. In addition, a low grid energy between the conducting salt's cation and anion facilitates its dissociation. Table 7.11 lists several common solvents together with their physical characteristics. With its high dielectric-constant of $\sim 89.7$, ethylene-carbonate (EC) is one example of a suitable solvent with good solubility for conducting salts.

When the Li ions can move easily in the solvent and electrostatic interaction with its anion is low, high ion mobility results. This can be easily demonstrated by observing the movement of Li ions in the electrolyte solution when an external electric field $E$ is applied. The electrical power, together with a frictional force proportional to the speed v in the opposite direction, both act on the ions (see Stokes' drag). In a steady state, a balance of forces results in:

$$q \cdot E = 6 \cdot \pi \cdot r \cdot v \cdot \eta \tag{7.58}$$

where $q$ is the ion's electric charge, $\eta$ is the dynamic viscosity of the electrolyte solution, and $r$ is the radius of the particle. In addition, the mobility $u$ of the ions is determined by:

$$u = \frac{|v|}{|E|} = \frac{q}{6\pi\eta r}. \tag{7.59}$$

The ion mobility of the Li ions is, therefore, high when the dynamic viscosity of the electrolyte solution is low. The viscosity of liquids in relation to temperature can be approximated using this simple formula, with $a$ and $b$ as constants $(a, b > 0)$:

$$\eta(T) = a \exp(b/T). \tag{7.60}$$

As the temperature $T$ increases viscosity decreases, facilitating ion mobility.

In comparison to other solvents such as dimethyl-carbonate (DMC), diethyl-carbonate (DEC), and ethyl methyl carbonate (EMC), the EC discussed above has a comparably high viscosity (Table 7.11), and so a low ion mobility. To obtain a high dielectric-constant together with low viscosity, organic solvent mixes are used. The mixing ratios are determined by the application area.

The use of organic electrolytes is determined by the lower temperature limit (solidification) and upper temperature limit (vaporization or decomposition). Table 7.11 also lists the melting and boiling temperatures of the solvents discussed here. Since electrolyte solution melting and solidification temperatures depend on the mixing ratio, these must be determined separately or looked up in phase diagrams.

For example, an EC-based electrolyte (the melting temperature of EC is around 36.4 °C, i.e., it is solid at room temperature) can only be used in combination with a solvent with a lower melting point, such as DEC or EMC

at temperatures above around −20 °C. In contrast, the upper temperature limit for lithium ion cells is, in practice, not determined by the solvent mixture's evaporation point. Instead, it is primarily determined by the conducting salt or other components and side-reactions (▶ Sect. 7.4.10.5).

Conducting salts with good solubility and electrochemical stability are, for example, lithium perchlorate ($LiClO_4$), lithium hexafluorarsenate ($LiAsF_6$), and lithium hexafluorphosphate ($LiPF_6$). Their ion conductivities are in the range of a few mS/cm, and depend on the solvent used with the salt. Gradually increasing the conducting salt concentration – starting at a very low concentration – also increases the conductivity. This is because the increased numbers of disassociated ions in the electrolyte solution results in an increased number of charge carriers. But if the concentration is increased even further, the conductivity falls. At higher concentrations, interaction among the ions increases, leading to reduced conductivity. As a result, conducting salt concentrations are typically ∼ 1 mol/L. Despite its sensitivity to water, $LiPF_6$ is very commonly used as a conducting salt because of its other excellent characteristics.

To determine the electrochemical stability of an electrolyte, measurements are typically compared with those taken from an inert reference electrode. To determine the electrochemical stability of an electrolyte more exactly or more precisely for a particular application, these measurements must be compared with those taken from the surfaces of the active materials used with the electrolyte in the lithium cell. But comparing these measurements to those from electrodes made of active materials is significantly more complex. This is because additional influences and processes, such as the actual reversible redox reactions, passivation effects, etc., must also be taken into account.

The ideal electrolyte would be electrochemically stable in a range of around 0–5 V (vs. $Li^+/Li$), i.e., in a range covering all relevant electrode potentials (▶ Sect. 7.4.1). Organic solvents (with the conducting salts above) are stable within a range of ∼ 1 to ∼ 4.5 V [13, 41]. New electrolytes are currently being developed with higher conductivities that remain electrochemically stable, even at higher voltages.

As a result, what is termed the electrochemical voltage window is limited by the electrolyte's oxidation potential $E_{Ox}$ and the reduction potential $E_{Red}$. Figure 7.45 graphs these two potentials. Since they limit the cell voltage, they also limit the areas of application. (The oxidation potential of around 4.5 V is linked to the highest occupied molecular orbital, and the reduction potential of around 1.0 V is linked to the lowest unoccupied molecular orbital.)

If the redox potentials of the active materials (for example $LiFePO_4$, $Li(Ni,Mn,Co)O_2$) fall within the electrochemical voltage window and the cell is used within this window, then irreversible decomposition of the electrolyte through reduction or oxidation is largely avoided.

Because of the strongly reductive or oxidative effects of the active materials, in reality, the phases' thermodynamic stability when side-by-side is not primarily due to the electrolyte's stability when in contact with the electrodes. It is rather due to chemical passivation of the active material surfaces.

If carbon electrodes are used as negative electrodes, then the redox potential lies outside the electrochemical stability window of the organic solvents discussed above (around 1–4.5 V). As a result, the electrolyte is reduced at the negative electrode because of its low potential. With the solvent EC, this occurs at a potential of around 0.9 V (vs. $Li^+/Li$). The electrolyte partially decomposes each time the cell is charged, or generally whenever the electrode potential is outside the stability window. Over the long-term, this results in large losses in capacity. In addition, solvated Li ions are also intercalated together with Li ions during charging. This causes bulging of the active material layer. When individual layers of the active material peel off as a result, it is termed exfoliation. Since this reduces the reversibility of the cell to a few cycles, carbon electrodes are not suitable for use in these cells.

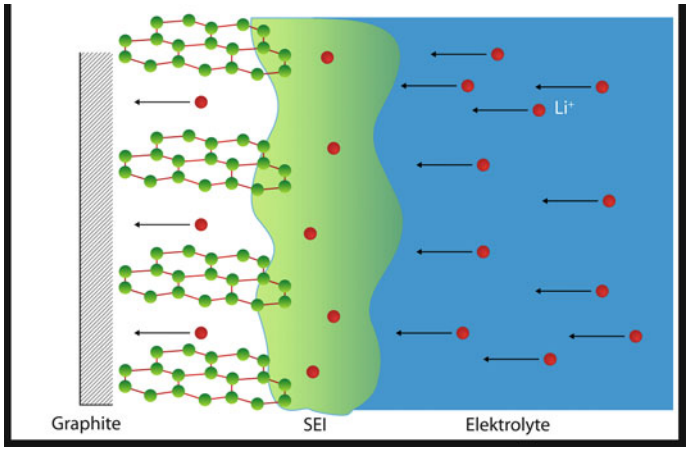



**Fig. 7.47** Illustration of SEI intermediate layer formation due to the decomposition of EC-based electrolytes

The decomposition products of some solvents (EC, for example) form a stable lithium-ion conducting passivation layer on the anode surface which permits reversible operation of lithium ion cells. The layer formed is termed a solid electrolyte interface (SEI). Figure 7.47 illustrates how this layer is formed. The SEI layer is permeably only by Li ions. This intermediate layer protects the negative electrode from intercalation by other solvated Li ions, and the electrolyte from further decomposition. It is created during the first charge.

In contrast, the solvent PC decomposes at a low electrode potential (around 0.5 V vs. $Li^+/Li$). Its layer formation behavior is therefore inferior. Besides providing protection, the intermediate layer also increases ion conduction resistance. Solid body diffusion determines the diffusion of Li ions through the SEI layer. Solid body diffusion can vary considerably from liquid diffusion. The SEI layer's ion conduction resistance is related to the cell's internal resistance. In addition, the layer's thermal and chemical stability must be taken into account. Research has shown that the intermediate layer's thickness gradually increases together with service life. As a result, it increases the internal resistance of the cell [41].

If active materials with redox potentials within the electrochemical stability window are used for the negative electrode, then no SEI layer is formed (for example, $Li_4Ti_5O_{12}$ with 1.55 V (vs. $Li^+/Li$)). (When $Li_4Ti_5O_{12}$ is used for the negative electrode, the higher redox potential at 1.55 V (vs. $Li^+/Li$) results in a lower cell voltage. Another result is reduced energy density. It is necessary, therefore, to strike a balance between higher-energy-density or stability/longer service life, and lower internal resistance of the negative electrode.) This means that these materials have the advantage of increasing the cell's service life, but the disadvantage of reducing the usable specific energy density.

Less is known about intermediate layers considered as passivation layers on the active materials of the positive electrode. Unlike the formation of SEI on carbon negative electrodes, the formation and influence of these layers on conductivity mechanisms has not been studied in detail. They are currently a focus of research.

### 7.4.5 Other Cell Components

The electrodes are electrically separated by a separator that must, at the same time, allow ions to flow freely. Microporous plastic foils made of polyolefins, such as polyethylene (PE) and PP, or in a multi-layer structure are suitable materials. When polymer electrolyte is used, polymer can also be used as a separator.

The plastic foils are typically 20–30 μm in thickness with a porosity of around 40%. At

cell temperatures above 130–150 °C, the plastics mentioned above (PE and PP) soften, sealing the pores of the separator. This in turn interrupts the flow of ions. This mechanism is termed shut-down. If a small local short-circuit occurs (for example due to a foreign particle) or the cell temperature rises to ∼ 130 °C, this shut-down function may prevent the cell from being charged or discharged again. If the temperature rises above 150 °C, then the separator melts entirely and contracts, removing the electric insulation between the positive and negative electrodes.

Separator thickness, porosity, form stability, and rigidity can be varied to achieve various cell characteristics. For example, a thinner separator can have the advantage of increasing the cell's energy density. But a certain minimum thickness is required to prevent dendrite formation on the positive electrode when there is metallic separation at the negative electrode (for example during overcharging). Other requirements such as chemical resistance and reasonable manufacturing costs must also be taken into account. Newer separators are frequently made with meshes and membranes, or produced with a ceramic coating. Because these materials are form-stable over a wide temperature-range, there is no shut-down mechanism.

Besides adequate mechanical rigidity, the collector must have good wettability and adhesion to the electrode materials, adequate chemical and electrochemical stability (ideally between 0 and 5 V vs. $Li^+$/Li), good electrical conductivity, and moderate material and manufacturing costs. In addition, alloying between the electrode and collector materials cannot be permitted. Aluminum is used on the positive electrode side, and copper on the negative electrode side. The collectors are designed as foils with a thickness of 10–30 µm. The surfaces are frequently subjected to wet-chemical pretreatment or even coated to achieve the precise surface quality required, as well as to improve adhesion and electric contact. The electrode potentials and possible onset of corrosion must be taken into account when considering the electrochemical stability of collector materials placed in contact with the electrolyte. Corrosive conducting salts may dissolve aluminum, and at higher potentials, local pitting corrosion may occur. Pitting corrosion results in cell damage [21, 41]. Aluminum is thermodynamically unstable, and its oxidation potential is 1.39 V vs. $Li^+$/Li. Aluminum only gains stability by forming a natural passivation layer during cell operation. Depending on the conducting salt used and the electrode potential applied, the electrolyte can be decomposed during the first charging-discharging cycle when the electrolyte comes into contact with the aluminum collector. Since decomposition causes a passivation layer to form that completely covers the aluminum surface, stable operation of the cell is maintained. This process prevents deep corrosion. This applies to all the salts described in the section on electrolytes [21]. The electrolyte (or in particular the conducting salt) used determines whether this stable layer forms during the first cycle, and must be considered separately.

If copper is used as an electricity collector for the negative electrode, the copper oxidizes and dissolves at very low cell voltages (around $< 1$ V). This is because the potentials at the negative electrode during deep-discharging of the cell may exceed the redox potential of copper. As a result, copper ions enter the solution. When the cell is charged again, copper is deposited on the negative electrode. This reduces the electrode's permeability to Li ions, meaning a part of the original electrode material is no longer electrochemically active. As the cell continues to operate, this leads to increased Li metal separation with dendrite formation (risk of short-circuit) and loss of capacity.

### 7.4.6 Conclusion

- Liquid, solid, or polymer electrolytes or combinations of these electrolytes can all, in principal, be used in lithium batteries.

- Liquid electrolytes composed of a conducting salt and organic, aprotic solvents are typically used.
- **$LiPF_6$** is very commonly used as a conducting salt because of its excellent characteristics. Choosing an organic solvent requires finding an optimal balance between a high dielectric-constant for good conducting salt solubility, and a low viscosity for good ion conduction.
- **EC/DEC/EMC** mixtures are frequently used. At room temperature, the ion conductivity of polymer electrolytes or other solid electrolytes are often inadequate.
- Plastic materials (often PE and PP) as well as other meshes are used as separator materials. Separators may have a single layer or multi-layer structure, or be partly coated.
- Electricity collectors made of aluminum are used on the positive electrode side, and copper collectors on the negative electrode side. The collectors are designed as thin foils.

### 7.4.7 Electrode Material Conductivity

Compared to electrodes in lead-acid batteries and alkaline systems, the intercalation electrodes used in lithium ion cells (for example $LiCoO_2$, $LiFePO_4$, and graphite) are what are termed continuum electrodes. The redox reaction occurs in the active material volume. After moving from the electrolyte into the active material, the Li ions must then move to their sites in the grid. Both the ionic conductivity (Li ions) of the electrolyte and the electrodes, as well as the electrical conductivity of the electrodes and electricity collectors, are factors in this process. The ion conductivity of the SEI solid formed must also be taken into account (▶ Sect. 7.4.4). This means that the mobility and diffusion of Li ions in liquids as well as solids are important considerations.

In addition, the electrochemically active materials used are composed of individual particles. To ensure electrical contact between the individual active particles, these are mixed with a conductive material (a good electrical conductor) such as carbon, for example. This also improves electrical contact with the electricity collector. The electrode materials are held together by what are termed binders. As a result, most electrodes used in lithium ion cells should be viewed as complex, porous, composite materials.

The diffusion of condensed materials (solids and liquids) is generally caused by the transposition of atoms or ions due to random thermal motion. Transposition process kinetics depend on temperature, and are described by the Arrhenius equation. For liquids, several simple models are used. As already discussed in ▶ Sect. 7.4.1, these include Stokes' drag law for the laminar flow around a sphere. Solid diffusion can be attributed to various mechanisms. Due to their small radius, Li ions can easily diffuse through grid interstices. Li ion mobility is determined by the solid's structure, binding characteristics, and possible defects. Depending on the diffusion path created in the crystal, structures with tunnels aligned in a single direction (1D), with layers (2D), and with tunnels aligned in three directions (3D, with nodes) may result. $LiFePO_4$ exhibits a typical 1D structure, $Li(Ni,Mn,Co)O_2$ and $LiCoO_2$ a layer structure (2D), and $LiMn_2O_4$ a typical 3D structure. This explains the diffusion coefficient listed in ◘ Table 7.12. If Li ions can easily diffuse between the layers (2D) (as with $LiCoO_2$), then diffusion coefficients at the highest range between $10^{-10}$ and $10^{-8}$ $cm^2/s$ result. This also explains why Li ions can easily diffuse parallel to the graphite layers. To realistically describe diffusion in structures such as these, crystallographic anisotropy of the Li ion diffusion constants (for example, tunnel with $LiFePO_4$) as well as the effects of grain boundaries and micro-structures must be taken into account.

Comparison of these diffusion coefficients with those of the electrolytes demonstrates that Li ion diffusion into the active materials is significantly lower. As a result, it may be determined by speed. There are a range of options

**Table 7.12** Summary of the diffusion coefficients and electrical characteristics for some materials used in lithium ion cells [28, 39]

| Components | Diffusion coefficient $D$ ($cm^2/s^{-1}$) | Electrical conductivity ($S\,cm^{-1}$) | Band gap (eV) |
|---|---|---|---|
| $LiCoO_2$ | $10^{-10}$…$10^{-8}$ | $\sim 10^{-4}$ | 0.5–2.7 |
| $LiFePO_4$ | $10^{-15}$…$10^{-10}$ | $\sim 10^{-9}$ | 0.3–1 |
| $LiMn_2O_4$ | $10^{-11}$…$10^{-9}$ | $\sim 10^{-6}$ | 0.28–2.2 |
| Carbon (graphite, MCMB, fiber) | $10^{-12}$…$10^{-7}$ | Graphite: $\sim 10^{3}$ | – |
| Electrolyte (conducting salt $LiPF_6$) | $\sim 10^{-6}$ | – | – |
| Aluminum | – | $\sim 3 \times 10^{5}$ | 0 |
| Copper | – | $\sim 6 \times 10^{5}$ | 0 |



for influencing diffusion. One option is to dope the material. This approach alters the (electrical) band structure to facilitate Li ion diffusion. Another option is to shorten the diffusion path by reducing particle size as well as altering particle morphology and form (for example, a flattened form). This can be demonstrated by using a simplified model. First, assume a cube with an edge length of one unit of length (LE). The surface area of the cube is then 6 $LE^2$. If the cube is split into two, then the surface area is 8 $LE^2$. If the original cube (edge length of 1 LE) is split into eight equal parts (8 cubes), then the total surface area is 12 $LE^2$. Similarly, the effect of particle form can be understood by comparing the surface area to the volume ratio of a sphere with that of an octahedron. These simplified models demonstrate that the ratio of surface area to volume can be changed by altering particle size or particle form. A larger surface area and shorter diffusion paths (several smaller particles instead of one large particle) facilitate charge exchange and diffusion.

But a larger surface area can also be a disadvantage if multiple passivation layers are formed. This is because passivation layers may act as diffusion barriers (ionic resistance). Many aspects of these approaches are still not well understood.

If active materials containing carbon are used, then SEI formation on the negative electrode side must also be taken into account. Since it has a lower diffusion coefficient than the active material, it increases (ionic) resistance. In addition, Li ion intercalation in graphite is a special case. There are several intercalation stages, which are seen as small plateaus in the OCV curve (see the behavior with $LiFePO_4$, ▶ Sect. 7.4.1 and Fig. 7.45). But with non-graphite (amorphous) carbons, no intercalation stages are observed. Interestingly, amorphous phases have poorer electrical conductivity than the graphite phase, but better diffusion characteristics. As a result, diffusion can be precisely adjusted by varying the percentages of graphite phase and amorphous phase (carbon black). This approach can also be used with positive electrode active materials, because adding grain boundaries results in practically amorphous phases.

Compared to graphite in the negative electrode or in metallic electricity collectors (Al, Cu), the materials used on the positive electrode side (oxide, spinel, phosphate) have a conductivity which is several orders of magnitude lower. Table 7.12 lists some figures for these materials. In addition, these materials are semi-conductors. This means that their conductivity is thermally activated. There are various approaches here also. These include doping the active material particles to increase conductivity, coating the electrode particles to increase

electrode conductivity, and reducing particle size (analogue diffusion). The most effective approach is to coat the active material particles in the sub-micrometer to nanometer range (for example with carbon). Here, particle size is reduced at the same time as the conductive coating is applied. This improves the electrical contact of the particles while largely avoiding electrically insulating inactive material.

Due to how the materials are manufactured, there is currently no way to effectively vary the particle size or morphology and the coating independently. As a result, it is not possible to confidently attribute the mechanisms involved solely to electric and ionic conductivity. More generally, the effects of grain boundaries and active material structural changes—such as reversible phase transformations—must also be taken into account. There are therefore two aspects here that must be considered separately: whether the electrical characteristics of the active material are altered (for example by doping) on their own, or whether the conductivity of the electrode (made of active material, conductivity additive, binder, coating) overall is altered by varying particle size and morphology.

### 7.4.8 Conclusion

- The electrodes used in lithium ion cells are typically composed of active materials and materials such as carbon and binders that improve conductivity. As a result, the most common electrodes used should be viewed as complex, porous, composite materials. In addition, electrical conductivity and diffusion (for Li ions) vary considerably among the individual cell components. Varying the particle size and applying a conductive coating may, for example, affect electrode conductivity, and therefore optimize cell performance. The following factors must be taken into account when considering lithium ion cell behavior and internal resistance [28]:
  - Charge transfer
  - Liquid diffusion in the electrolyte (ionic)
  - Solid diffusion in the active material and SEI (ionic)
  - Electrical conductivity (active material, conductivity additives, electricity collectors, binder additives)
  - Boundary surface effects (electrolyte/electrode, active material/conductivity additives, active material/electricity collector, conductivity additives/electricity collectors)

### 7.4.9 Designs and Application Areas

Large-format lithium ion cells are generally produced in round, prismatic, or coffee bag designs. Cells with a capacity over 40 A h are only available in prismatic or pouch form. In addition to these designs, button cells are also produced. These are used for lower-capacity applications, such as watches or as back-up batteries in electronic circuitry.

Lithium ion cells are sealed air-tight. There is no direct contact between the cell interior and the external environment. Depending on the rated capacity, several electrode pairs are stacked together, or one electrode pair is wound and coiled (see [4] and Fig. 7.48). In general, the positive and negative electrodes are dimensioned to ensure the negative electrode's capacity exceeds the positive electrode's capacity. This prevents overcharging of the negative electrode during charging.

In round cells, the electrode stack (coil) is placed in metal housing. The external poles are either located on one side or on opposite sides. The electrode stack and the poles are electrically insulated from the housing by a separator layer. Figure 7.49 shows the basic design.

Round, small-format lithium ion cells with normal capacities are produced in the usual sizes for device batteries. Round large-format cells have special dimensions. Table 7.13 describes two examples of each kind.

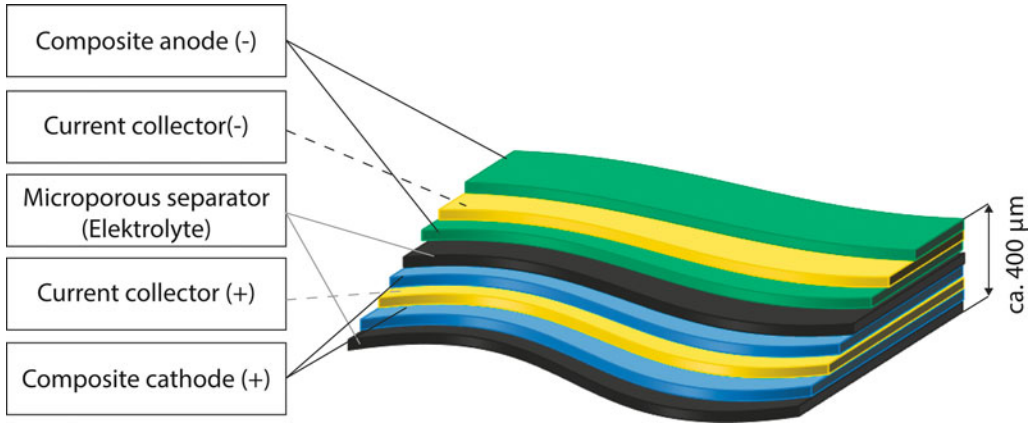



**Fig. 7.48** Electrode stack design in a lithium ion cell



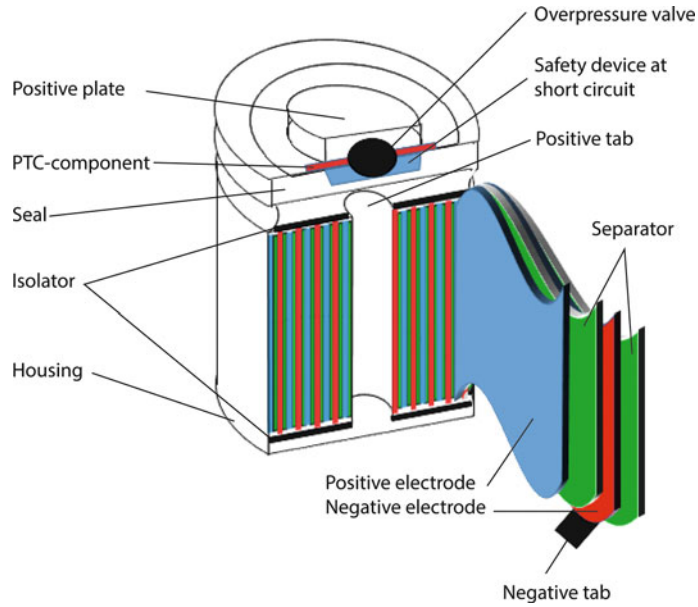



**Fig. 7.49** Basic round cell design: the essential components are labeled

The advantage with this design is that it is relatively easy to integrate a safety vent into the housing and to integrate a current interrupting device to protect against short-circuits. In addition, the metal housing makes cylindrical cells relatively robust. The shell is used as a cooling surface. At higher currents or lower exterior temperatures in particular, there can be a negative effect on temperature distribution. The constructional design of the electrodes (coil) results in an axisymmetric temperature profile in the cell with substantial temperature gradients. This causes internal resistance to vary from place to place in the cell. It also dramatically alters the cell interior. Space within the battery is wasted because the cylindrical form prevents several cells from being stacked seamlessly together.

In prismatic cells, the electrodes are wound in coils or several electrode pairs are divided by separator layers and stacked one on top of the other. The individual separator layers are placed between the electrodes, or a single layer is used in a $z$-fold assembly. The individual

**Table 7.13** Summary of typical lithium ion battery sizes

| Description | Diameter (mm) | Height (mm) | Rated capacity (A h) |
|---|---|---|---|
| AAA | 10.3 | 45 | < 1 |
| 18650 | 18 | 65 | Around 2 |
| Large-format | 55 | 220 | Around 40 |
| Large-format | 40 | 145 | Around 7 |




**Fig. 7.50** Basic prismatic cell design. The most important components are labeled

electrode pairs are wired in parallel to increase capacity. The individual electrode pairs are also connected within the cell housing by collector lugs. The lugs are connected by welding and joining, or are connected by another connection process. The external poles are electrically insulated from one another. Steel or aluminum alloys are used for the housing. Plastics are also sometimes used. Figure 7.50 shows the basic design. The external poles are usually both on one side. Capacities typically range from ∼ 10 A h to a few hundred A h. The dimensions of a cell with a rated capacity of 20 A h (mass 0.68 kg) are for example 90 mm × 148 mm × 27 mm (H × L × D). Depending on the design, the metal housing is typically around 0.7 mm thick.

The rugged metal housing is one advantage of this design. Another advantage is the larger cooling area compared to cylindrical cells. Since the electrode stack is significantly wider than it is thick, there is a smaller temperature gradient in the cell volume. As a result, the temperature distribution is more even. In addition, the geometrical form allows space within the battery to be more efficiently exploited in the battery system design. Compared to pouch designs (discussed below), a drawback of these cells is lower-energy density at the cell level. If metal housing is used, its mass reduces the usable energy density. With plastic housings, after several years of use moisture may penetrate the cell interior or the plastic may no longer provide an adequate barrier. But little research has been devoted to these problems (aging of plastics or their welded connections). Moisture penetration may result in irreparable damage or accelerate the aging of the cell.

The pouch form is also often called the coffee bag design. Here the electrode stack design is like prismatic cells. The most important difference is the shell. The shell is a plastic-laminated aluminum foil bag (typical foil thickness of around 150 μm). The external poles are either located on one side or on opposite sides. Figure 7.51 shows the basic design. Rated capacities typically range from ∼ 10 A h to around 100 A h. The dimensions of a cell with a rated capacity of ∼ 40 A h are, for example. 220 mm × 210 mm × 11 mm (H × L × D, weight ∼ 1.1 kg).

In comparison to prismatic designs, the reduced mass of the housing here is a major advantage. This is because no solid metal housing is required. The design allows a higher specific energy density to be achieved with a given cell chemistry. The use of space is basically just as efficient as in prismatic cells. In addition, the housing's low mass means its heat capacity is lower. This allows the cell to be cooled more easily. A drawback of this design is its lower mechanical durability (aluminum foil bag). The shell is also sealed with what are termed heat seal joints. These joints may be less effective as barriers, and allow moisture exchange with the environment. Around the seal seams, damage to the laminate or seal seam may allow the




**Fig. 7.51** Basic coffee bag cell design

electrolyte to come into contact with the moisture in the air (irreversible decomposition of the electrolyte, hydrofluoric acid formation).

### Electrode Design and Dimensions

The various kinds of electrodes used in lithium ion cells all feature basically the same design. Because of their particle structure, they are porous. There are two types of porosity; porosity accessible to the electrolyte and closed porosity. As discussed above, the electrode material includes a composite material which is made of active material (positive or negative), conductivity additives, and a binder material. The binder material keeps the active material particles together. The conductivity phase electrically connects the individual active material particles. This increases the electrical conductivity of the electrode (▶ Sect. 7.4.7). Chemically stable fluoropolymers such as PVdF are often used as binder materials.

Electrode material is applied to the electricity collectors using a coating process. The original materials in powder form (active material, binder, additives) are first mixed in a solvent to create a homogenous dispersion. This is then applied using a spraying process, or other suitable process. Electrode layer thickness typically ranges from several tens of μm to about 100 μm. For active materials containing a PVdF binder, often the solvent *N*-methyl-2-pyrrolidone (NMP) is used. In addition, intensive research on alternative water-based binder systems continues. After coating, a drying step follows to remove the solvent. Since the electrolytes used are often sensitive to water, use of water is an important factor in the drying step. In addition, some active materials tend to age when exposed to moisture. As a result, particularly critical process steps in cell manufacture are performed in what are termed dry rooms, or in an inert gas atmosphere. For information on material synthesis design and active material manufacturing, see the relevant reference literature [18, 35].

The performance characteristics of the cell may be altered by varying the particle form, the proportions, and the porosity produced with compressed electrode materials (calendaring during manufacture). These are important factors when producing electrodes for high-current capacity cells or high-performance cells with higher porosity, smaller electrode layer thickness, or smaller particle sizes (▶ Sect. 7.4.7). This results in a larger contact surface between the electrolyte and active material, facilitating Li ion charge transfer into, or out of, the active material. It also shortens the diffusion paths, or conductivity paths, into the active material. But since these benefits reduce the specific mass distribution (electrode mass per collector surface), they also reduce the energy density of the cell. To optimize the energy density of the cells, a lower porosity and large electrode layer thickness is required. This increases the specific mass distribution in comparison to electrodes optimized for high

**Table 7.14** Comparison of typical performance characteristics for a high-energy and a high-current cell using the Li(Ni,Mn,Co)$O_2$/C as an example (pouch design, nominal cell capacity ~ 50 A h, manufacturer's specifications; the comparison is provided as an illustration of a cell design with typical parameters)

| Characteristic | High-performance cell | High-energy cell |
|---|---|---|
| Maximum charging current (constant) | 3C | 2C |
| Maximum charging current (pulse < 10 s) | 5C | 3C |
| Maximum discharging current (constant) | 12C | 5C |
| Maximum discharging current (pulse < 10 s) | 15C | 8C |
| Specific energy density (W h/kg) | 150 | 180 |
| Cell mass (g/A h) | ~ 25.7 | ~ 21.3 |
| Typical applications | For example, HEV | For example, EV |

currents. As a result, a cell optimized for energy density has less electrode and collector surface area than a high-current cell with nominally the same rated capacity. Typical performance characteristics for a high-energy and a high-current cell of a Li(Ni,Mn,Co)$O_2$/C system are given as an example in Table 7.14 (nominal cell capacity: ~ 50 A h). High-performance cells can handle significantly higher charging and discharging currents. They can handle even higher charging and discharging currents over a short period, i.e., for pulse loads.

For example, the discharging current (charging current) over a short period can be as high as 15C (5C) ($x$C indicates $x$ times the module capacity; for example, charging: C = 50 A h → 5C = 250 A). A permitted constant discharging current of > 5C is typically used to distinguish high-performance cells from high-energy cells. But high-performance cells require a higher cell mass per A h. For example, in hybrid cars, fast-charging lithium ion batteries are required for storing brake energy with recuperation, so high-performance cells are used. But in (purely) battery-driven electric cars (EV), high-energy cells are used.

Using the figures from ▶ Sect. 7.4.1, the maximum energy density of Li(Ni,Mn,Co)$O_2$ (3.8 V; ~ 170 A h/kg) is ~ 650 W h/kg. But according to Table 7.14, the practical energy density of a Li(Ni,Mn,Co)$O_2$/C cell is 150 W h/kg or 180 W h/kg. This is because cell weight includes both active as well as passive components. As a result, there is a discrepancy between theoretical energy density and practically available energy density with all battery systems.

## 7.4.10 Operating Method and Typical Performance Characteristics

### 7.4.10.1 Charging and Discharging Lithium Cells

Depending on the cell chemistry used, every lithium ion cell can only be safely operated within certain voltage limits. The upper voltage limit is equivalent to the voltage at a 100% SOC, and the lower voltage limit equivalent to the voltage at 0% SOC. Whatever the cell chemistry used, the voltage limits set by the manufacturer must be followed. Deep-discharge of a cell results in electrode damage (for example copper dissolution) and electrolyte decomposition, as well as (possibly) to cell thermal runaway (when charged again). Cell overcharging also results in irreparable damage. It may cause strongly exothermic decomposition of the electrode materials, electrolyte decomposition, and other reactions affecting a range of cell components.

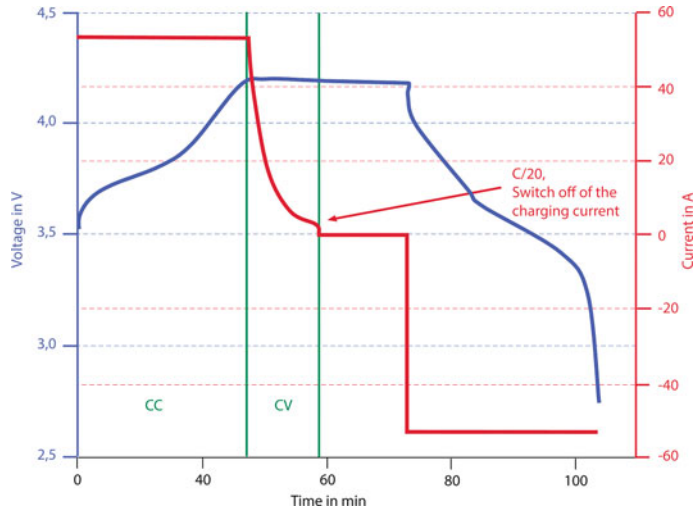



**Fig. 7.52** Typical charging and discharging cycle for a lithium battery. Charging and discharging with CC includes both a CC phase and a CV phase. The CV voltage of the cell is equivalent to the charging end voltage specific to the system. The minimum charging current required to end the CV phase and the discharging end voltage must also be specified. A $Li(Ni,Mn,Co)O_2/C$ system is used here as an example: rated capacity 53 A h, charging and discharging current 53 A (or one hour of current), charging end voltage 4.2 V, CV phase cut-off current C/20

To determine cell capacity or test cell behavior, often what is termed a CCCV charge combined with a Constant Current (CC) discharge are used. Charging is divided into two charging phases: CC charging and Constant Voltage (CV) charging. Figure 7.52 illustrates this charging process using the $Li(Ni,Mn,Co)O_2/C$ system (rated capacity 53 A h) as an example. Charging begins with CC (in this example, one hour of current, 53 A). Depending on the cell chemistry used and other conditions such as temperature and internal resistance, a cell voltage results that then increases constantly as the cell's SOC rises. In the example, charging with CC is continued until a specific voltage typical for the system—here 4.2 V—is achieved. This is called the charging end voltage. This voltage depends on the system used.

Then the cell voltage is maintained at the level of the charging end voltage. During the CV phase, the charging current gradually falls (Fig. 7.52). Charging ends when a specific number is reached; for example, a current of $I = C/20$. In the illustration, an idle phase follows after the charging phase. Next comes CC discharging (to determine the capacity, for example). Here, the cell is discharged with CC until a cell voltage typical for the specific system—termed the discharging end voltage—is reached. Figure 7.52 illustrates discharging at a current of 53 A with a discharge end voltage of 2.75 V.

In conclusion, lithium ion cells should only be operated within the voltage limits permitted by the cell chemistry used. This means that safe operation of lithium ion cells requires monitoring the voltage of each cell, and containing cell voltage within the permitted voltage range specified.

### 7.4.10.2 Discharging Characteristics

Fig. 7.53a shows the typical discharging characteristics of a $Li(Ni,Mn,Co)O_2/C$ system. Some of these characteristics require further explanation. The graph shows cell voltage compared with extracted capacity. The discharging rate (C-rate) or discharging current was also varied. Discharge curves for C-rates from C/5 to 3C are shown. The cell was always discharged with CC. Capacity is normalized to the cell's

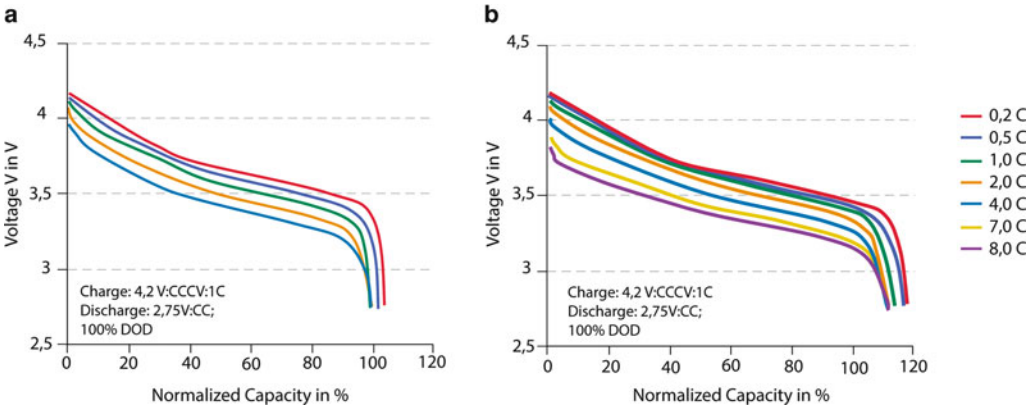



**Fig. 7.53** **a** Discharging characteristics of a lithium ion cell (high-energy cell), **b** discharging characteristics of a high-performance cell (CCCV charging): current rate 1C, up to 4.2 V; CC discharging: 2.75 V, DOD 100%)

rated capacity at a C-rate of one. Constantly decreasing cell voltage as the cell discharges is a typical feature of the $Li(Ni,Mn,Co)O_2$/C system used in the example (▶ Sect. 7.4.1). Since, with this system, the relationship between cell voltage and SOC is unambiguous, the cell's SOC can easily be determined by measuring the cell voltage. (By way of comparison, with the $LiFePO_4$/C system the cell's SOC cannot be determined from the cell voltage alone.)

The relationship between cell voltage and extracted capacity is almost exactly the same with higher discharge rates, but with offset voltage levels. The only discrepancy is at the beginning of discharging. Here, the cell voltage decreases more rapidly because of overvoltage. If the cell is operated outside the permitted range, i.e., discharged at $>$ 3C as in the example shown, the cell voltage drops precipitously. The mean cell voltage decreases as the discharging rate increases. The charged and extracted quantity of charge depends on the C-rate. The precise relationship must be determined separately for each individual cell chemistry and cell design.

The battery in the example is a typical high-energy cell. Figure 7.53b shows the discharging characteristics of a high-performance cell. The discharging curves demonstrate that the relationship between cell voltage and state of discharge with discharging currents up to 8C is constant. Even at these high-current rates, the cell voltage does not collapse. This means that the cell has a high-current capacity. Similarly, the usable capacity shown on the $x$-axis depends on the current rate (C-rate) used.

Figure 7.53 also demonstrates that a cell can only be operated within the charging and discharging current limits determined by its design. If these maximum permitted currents are exceeded, the cell voltage may collapse. Potential differences can occur that result in electrode potentials outside the permitted voltage window (stability window). This can cause irreparable damage to the cell. As a result, charging and discharging currents must be monitored and contained within the specific permitted current range. To ensure safe operation, monitoring is required with both continuous operation and pulse loads.

### 7.4.10.3 Temperature Characteristics

Discharging characteristics also include temperature characteristics. Temperature characteristics must be determined separately depending on the system and electrolyte used. Figure 7.54 uses a Li(Ni,Mn,Co)O2/C system cell as an example. The cell was discharged at a CC (1C-rate) at temperatures of −20, −10, 0, 20, and 45 °C. Using a temperature of 20 °C as a reference, the illustration demonstrates that extracted capacity clearly increases

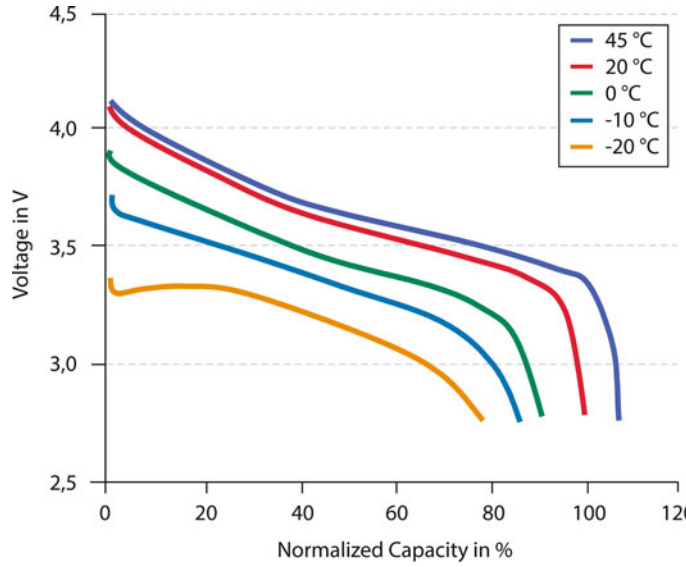



**Fig. 7.54** Discharging characteristics of a lithium ion cell (high-energy cell) compared to temperature (CCCV charging): current rate 1C, up to 4.2 V; CC discharging: 2.75 V, DOD 100%



at higher temperatures, and significantly decreases at temperatures below 20 °C. The mean cell voltage decreases as the temperature decreases. At temperatures below −10 °C, the discharging curve changes, indicating a significant collapse in voltage.

These characteristics can be explained by considering the viscosity of the electrolyte. Viscosity falls at lower cell temperatures, reducing ion mobility and increasing internal cell resistance. With constant discharging current, this leads to a dramatic voltage drop. This means that the discharge end voltage is reached faster. As a result, the full capacity of the cell cannot be exploited. Other effects include reduced electrode material conductivity, kinetic inhibition, and orientation polarization effects. Clearly the performance characteristics of the cell are largely determined by temperature. Monitoring cell temperature and maintaining it in the permitted range is, therefore, crucial.

### 7.4.10.4 Service Life and Self-Discharge

Lithium ion cell service life and aging are typically determined in relation to service life over time, or to cycle life. They, therefore, describe changes in the cell's condition over a period of time or over a number of cycles. Changes in the cell's condition are usually measured in terms of the cell's capacity loss. The relevant external factors are the following.

- Aging over time: temperature and SOC
- Cycle life: charging and discharging rate, temperature, SOC, and DOD

These external factors are called stress factors. In addition, the loss in usable capacity can also be determined in relation to time, number of cycles (or charge put-through), and the stress factors listed above. Figure 7.55 uses the Li(Ni,Mn,Co)$O_2$/C system as an example to show the relation of cell capacity to number of cycles for various DOD (one hour of charging and discharging current). A cell's end of life is typically defined as when the usable capacity of the cell falls to 80% of the initial capacity. The effect of DOD here is obvious. With other active material systems, the relationships and the resulting service lives differ.

Lithium ion cells typically have a very low self-discharge rate. Capacity loss per year at room temperature is in the range of < 3% (with an average SOC), but at high temperatures it can rise to 15%. Since self-discharge generally increases as storage temperature and SOC increase, cell storage temperature and SOC are

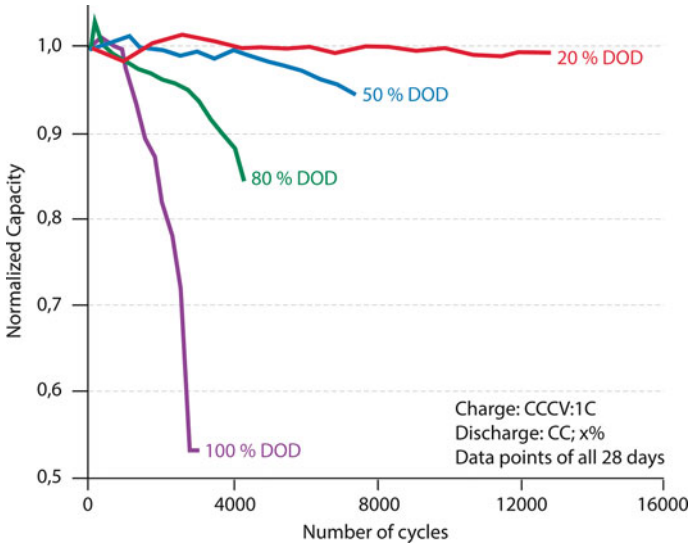



**Fig. 7.55** Relation of capacity to number of cycles for various DOD using the Li(Ni,Mn,Co)$O_2$/C system as an example (room temperature, one hour of charging and discharging current, various DOD)

key factors for these cells. If lithium ion cells are stored over long periods while monitored by electronics powered by the cells themselves, then the electricity consumption of the monitoring electronics must be taken into account together with the cell's own self-discharge.

At the electrode level, loss of contact between the active material particles is one factor in aging. The contacts are broken due to mechanical stress caused by volume change during Li ion intercalation and deintercalation. This results in a loss of electrochemically active material, as well as possibly an increase in internal resistance. Another factor is the continued growth of the SEI layer, increasing the internal resistance of the cell. If fissures develop within the SEI intermediate layer, when the SEI layer is formed again lithium is gradually consumed, and the concentration of charge carriers is reduced. A final factor is the successive separation of the transition metal ions (layered oxides) by the electrolyte. For further discussion of aging, consult the extensive list of sources cited in the bibliography [18].

### 7.4.10.5 Lithium Ion Cell Safety

Research on the safety of lithium ion cells is ongoing, and much work remains before any definitive conclusions can be reached. The following analysis explores several key aspects.

The thermal decomposition of the positive electrode materials is frequently a focus with the safety of lithium ion cells. Studies on this subject demonstrate that, depending on the material, decomposition occurs at temperatures ranging from 150–250 °C. Thermally initiated decomposition releases heat that then further accelerates the decomposition of the active material. This is termed thermal runaway. If oxygen is released during decomposition—as with transition metal oxides currently under consideration—an enormous amount of heat may be produced (unlike $LiFePO_4$, for example, which releases no oxygen).

But for a complete picture, other factors such as the thermal stability of the negative electrode, the electrolyte or other cell components must also be taken into account. In addition, boundary conditions determined by cell design and potential manufacturing or assembly errors also play a role.

The separators are designed to remain stable up to temperatures of about 130–150 °C. The upper temperature limit for the use of an electrolyte is determined primarily by the thermal stability of the conducting salts found in the solution, and by the side-reactions. The most commonly used conducting salts begin to decompose at temperatures of around 100 °C. Since chemical reactions accelerate at higher

temperatures (Arrhenius equation), higher cell temperatures increase the reaction between the electrolyte and, for example, $LiC_6$. This in turn increases SEI layer formation (increased internal resistance). It can also result in gas formation and cell bulging. In addition, at temperatures of > 70 °C, the SEI passivation layer decomposes more rapidly. Since these reactions are generally exothermal, heat is released and the cell's temperature rises. If a lithium ion cell is thermally well-insulated, the heat released may trigger thermal runaway.

At lower temperatures (around −30 to 20 °C), the separation of solvent components by freezing is usually reversible. But SEI decomposition reactions and other side-reactions at higher temperatures are irreversible. As a result, the permitted operational temperature-ranges for EC-based electrolytes typically range from −20 °C to around 50 °C/60 °C. If abnormal operating conditions lead to the cell being opened, highly flammable components such as DMC, DEC, and EMC may pose a serious risk (Table 7.7). New electrolytes are increasingly mixed with additives that hinder decomposition reactions and reduce flammability.



## 7.4.11 Conclusion

- The **performance characteristics** of lithium ion cells depend heavily on the **cell chemistry** as well as the **electrode and cell design**. They are categorized as **high-performance or high-energy cells**. Lithium cells must be **monitored and controlled** (for example by a battery management system) to ensure safe operation. The following variables must be monitored carefully:
  - The individual cell voltage
  - The maximum permitted charging and discharging current limits
  - The cell temperature
- Operating lithium ion cells **outside the permitted limits** may pose a **serious safety hazard**.
- To ensure a **long service life**, the **SOC** of a lithium ion cell should ideally range **between 30 and 70%**. High-temperatures may cause high states of charge to reduce the cell's service life. As a result, they should be avoided.

## 7.4.12 Outlook

Lithium ion cells remain a focus of current research and development. Although a lithium ion cell service life of several hundred cycles and several years (for example < 5 years) is acceptable for consumer applications, they are inadequate for many industrial applications. These applications require higher current capacity and faster charging capacity, as well as improved energy density, service life, and safety. For example, fast-charging batteries are required for storing brake energy with recuperation in hybrid cars. Service lives > 10 years are required for storage in electricity networks.

Engineering lithium ion technologies for these purposes will require significant scientific and technical advances. Improving the high-current capacity of large-format lithium cells will also require a better understanding of the relationship between material synthesis, electrode design (particle size, morphology, distribution, porosity, and composition), and performance characteristics (current rates and internal resistance).

To increase energy density (specific capacity and redox potentials), new positive and negative electrode active materials are currently under development. Examples include transition metal phosphates (high-voltage olivine, around 5 V vs. $Li^+/Li$) such as $LiMnPO_4$, $LiCoPO_4$, or $LiNiPO_4$, hyperstoichiometric layered oxides $Li_{1+\delta}(Ni,Mn,Co)O_2$, new manganese spinels, and mixtures of various active materials. Use of these new compounds also requires new electrolytes that can cover the range of redox potentials in this electrochemical voltage window.

Due to their high-specific capacities, silicon and tin alloys as well as silicon-carbon compos-

ite materials may be appropriate for the negative electrode. Since Li ion intercalation and deintercalation result in enormous volume expansion, use of these materials also requires effectively compensating for mechanical stress.

Currently, electrolyte additives are a focus of research. What are termed shuttle mechanisms may be used to improve safety. After a certain cell voltage is reached, the voltage is prevented from increasing further by the onset of a reversible reaction of the additive. Alternatively, when a certain voltage is reached, the onset of additive polymerization increases the internal resistance. This in turn causes cell shutdown. Additives are also used to improve SEI formation stability. Polymer, or other solid electrolytes, could be considered as replacements for liquid electrolytes as well. This would eliminate the risk of electrolyte leakage and possibly avoid the need for a classical separator. Due to their high internal resistance, their use so far has been limited. Alternatives are currently under study.

## 7.5 Sodium-Sulfur Batteries

Sodium-sulfur accumulators are high-temperature batteries. They operate at temperatures above 300 °C [34].

Figure 7.56 shows a sodium-sulfur accumulator with a cylindrical design. The negative electrode is located in the cell's interior. At operating temperatures, it is immersed in liquid sodium. Within the cylindrical, ceramic, and $Na^+$ ion-conducting solid electrolyte made of doped sodium aluminum oxide (also called $\beta$-alumina ($\beta$-$NaAl_{12}O_{17}$)), there is a metal cylinder shaped like a test tube with a hole at the bottom. This metal cylinder, therefore, separates the solid electrolyte from the sodium electrode. The metal cylinder is called a safety insert, and is formed so that there is a controlled flow of liquid sodium from the interior. After losing its valence electron, sodium as a positive ion can diffuse through the crystal lattice vacancies of the solid electrolyte. This is because metallic sodium is oxidized to $Na^+$ during the discharging process.

If the ceramic separator breaks, an internal short-circuit results. The safety insert limits the flow of sodium so that the heat produced can escape, and thermal runaway is prevented [16, 33].

In the outer part of the cell, the positive electrode is composed of graphite felt immersed in liquid sulfur contained in a cathode container.

All cells are placed in thermally insulated containers with integrated heating and cooling. A battery management system separate from the battery system is required to regulate the temperature.

### 7.5.1 The Electrodes

NaS accumulators must be operated at high temperatures to ensure the sodium and sulfur as well as the sodium polysulfide produced are always in liquid form. Generating adequate energy flow between the electrodes requires exceeding the solidification temperatures of all these materials. Of these materials, the sodium polysulfides have the highest melting points. This is particularly true for those with up to three S atoms in the negative ion. Their optimal operating temperature is 320 °C. Because of its high grid energy, $Na_2S_2$ has an even higher melting point. As a result, it should not be allowed to form, i.e., discharging must be stopped before it can form [16].

Compared to other batteries, the liquid state of the electrode materials results in a higher cycle life [10, 11].

Since sodium is a highly reactive alkaline metal, particularly in combination with water, it must be securely protected from contact with the environment in a metal container. The second active component, liquid sulfur, is contained in the outer areas of the cell. Sulfur is an electrical insulator in both liquid and solid states. To ensure good electrical conductivity, it is impregnated with graphite felt. Besides electron transport, the felt structure also serves to

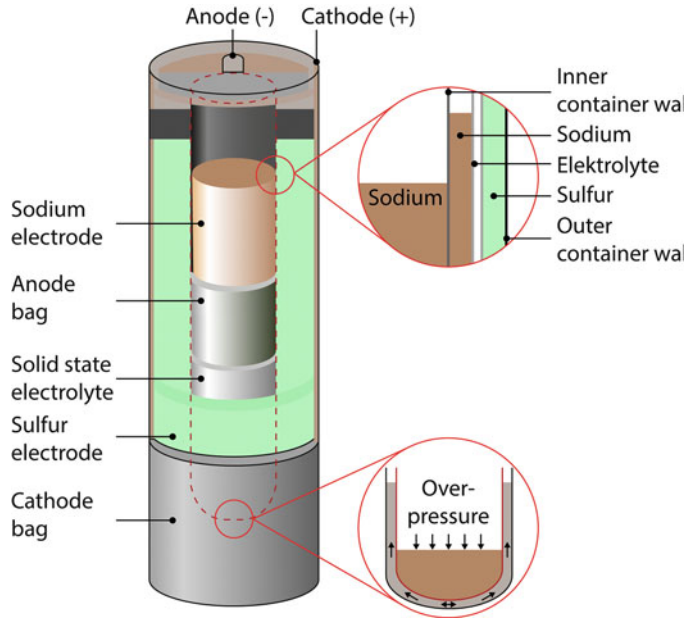



**Fig. 7.56** Sodium-sulfur accumulator design



separate the sodium polysulfide produced during discharging from the outer surface of the solid electrolyte. This means that, in combination with the safety insert, the graphite felt prevents a spontaneous chemical reaction if the ceramic solid electrolyte breaks [33].

### 7.5.2 The Electrolyte/Separator

The separator divides the anode and cathode into electrically and spatially isolated electrochemical elements (Fig. 7.57). In the case of the NaS system, the separator divides the sodium on the negative electrode from the sulfur on the positive electrode. With this system, the separator must be exclusively permeable to cations for converting chemical into electrical energy (and vice versa). The NaS system separator is made of ceramic. The primary component of the ceramic solid electrolyte is highly Na-ion conductive $\beta$-alumina ($NaAl_{12}O_{17}$). It resembles unglazed ceramic in appearance, and is ion-conducting at temperatures above around 300 °C.

This electrolyte permits a sodium ion conduction of 0.2 to ~ 0.4 S/cm. It simultaneously serves as an electron insulator, providing electrical insulation ranging from $1 \times 10^{14}$–$1 \times 10^{15}$ Ω cm [16, 34, 43].

The composition of the beta-alumina group of oxides is typified by alternating densely and loosely packed layers. The loosely packed layers are called conductive surfaces. These allow free mobility of the sodium cations in an electrical field. In these layers, the portion of oxide ions is low. The densely-packed layers are called spinel blocks. They are composed of layers of oxygen ions paired with aluminum ions. They are located at the octahedrally or tetrahedrally coordinated grid sites. In the $\beta$-alumina group, there are two clearly distinct crystal structures in a hexagonal array. The two crystal structures differ in terms of their chemical stoichiometry, as well as the sequence of oxygen ion arrays bordering the conductive surfaces [19, 30].

Figure 7.58 gives a general idea of the relationships between the molecules and their arrangement.

The spinel blocks are connected by the conductive surfaces. As Fig. 7.58 shows, mobile

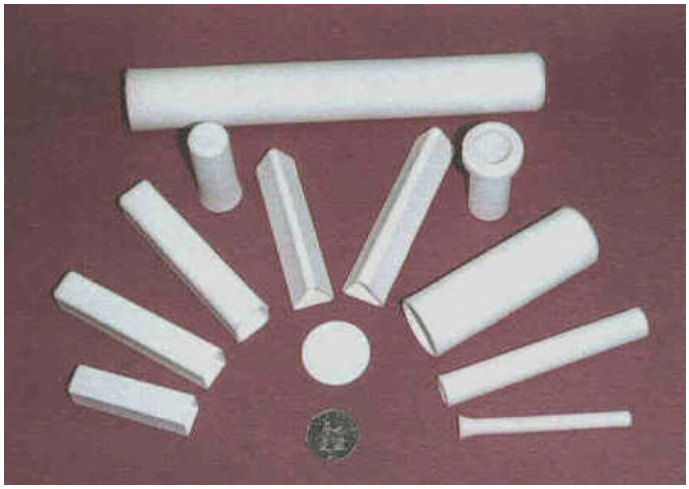


**Fig. 7.57** Ceramic solid electrolyte design from Ionotec

sodium ions diffuse through the conductive layers perpendicular to the C-axis [19].

Because of its sodium ion-conducting characteristics, the separator is used as a membrane in NaS batteries. Here it resembles a cylindrical cup filled with liquid sodium. During discharge, sodium is oxidized to $Na^+$. This can then diffuse through the ceramic into the cathode holder containing the sulfur [16, 34]. Ceramic has a high compressive strength of 2,000–4,000 MPa, and a high-resistance to corrosion and wear. As a result, it can tolerate the significant stresses in NaS batteries [43].

### 7.5.3 The Heating System

To maintain the required operating temperature of 320–350 °C, a heating system is a crucial component of these batteries (see Figs. 7.59

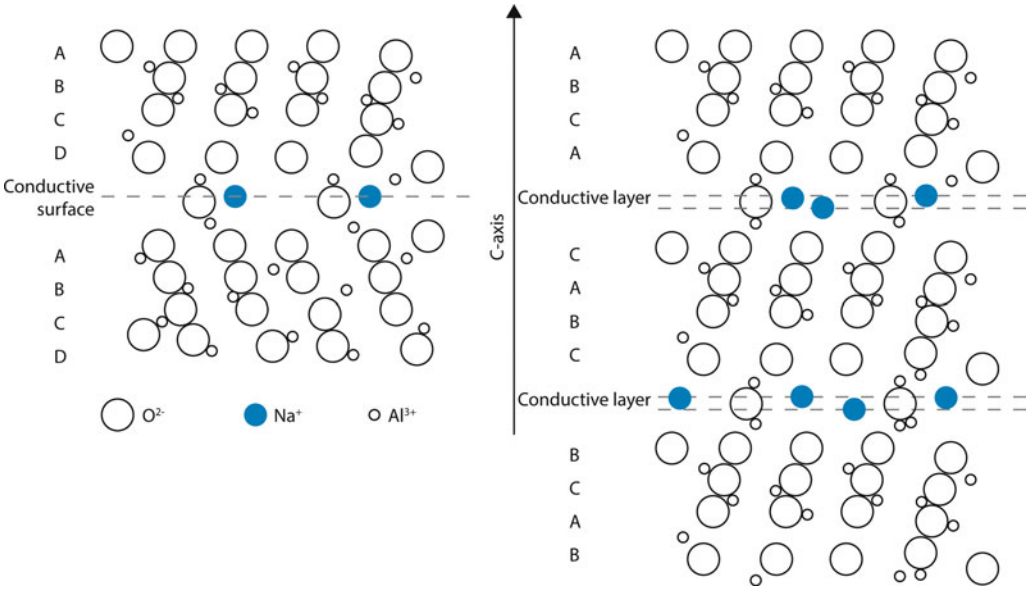



**Fig. 7.58** Atomic layers in $\beta$-alumina $NaAl_{12}O_{17}$

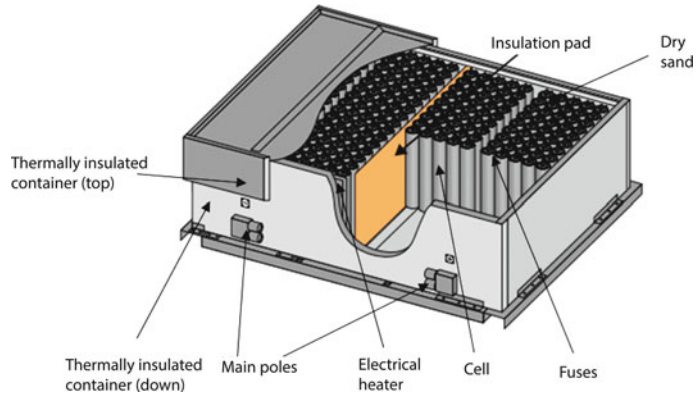



**Fig. 7.59** Basic design of a battery module



and 7.60). The battery's internal resistance is lowest within this temperature range. If the temperature falls, performance or efficiency falls dramatically. Crystallization of the polysulfide salts also results [36]. In active use, reaction heat in a high-temperature battery is adequate to maintain the optimal operating temperature. But a heating system is essential for maintaining the temperature in idle phases. As a result, high-temperature batteries always include a battery management system. This system is separate from the battery, and compensates for thermal loss during idle periods by controlling an internal or external heating mechanism. When in operation, the battery's temperature may also rise to levels where active cooling is required. Thermal sensors are used to monitor the temperature and control whether heat is applied or removed [34].

Some modalities must be considered for thermal sensor positioning. They must not cause a short-circuit between the cells or cell groups, and the sensor position should not allow the measuring location to shift during operation.

Sensor placement should also take into account that the sensors cannot be accessed once the battery has been completed and thermally insulated. If a sensor malfunctions, the battery must be cooled down and opened. This is a time-consuming and expensive process [8, 14, 33, 34].

Another important aspect of the heating system is thermal insulation. The individual cylindrical cells are typically collected in an evacuated module. Thermal insulation keeps thermal losses low, and maintains the operating temperature during idle phases. This allows quick access to the storage system when electricity is in demand.

Because large amounts of energy are required to maintain operating temperatures during idle phases, sodium-sulfur accumulators

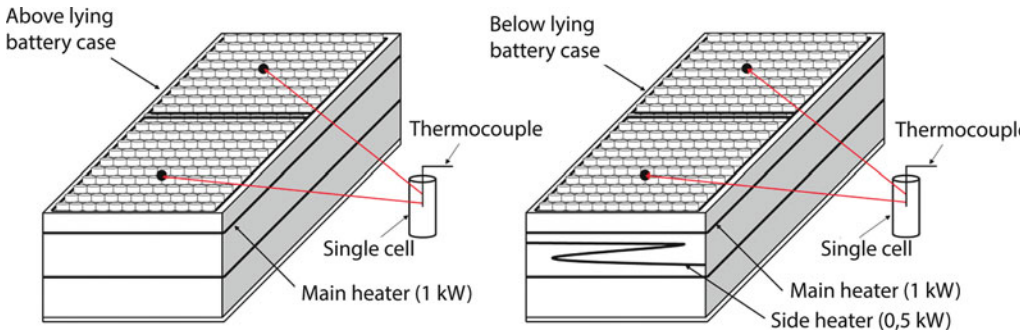



**Fig. 7.60** Basic heat system design




**Fig. 7.61** One MW NaS storage block from Younicos AG in Berlin

are best-suited for short-term energy storage [16, 33].

### 7.5.4 Forms and Module Sizes

Battery modules are composed of individual cells connected in parallel and series. These modules themselves can then be connected in series or parallel to achieve the electrical characteristics required. The firm NGK offers a load-leveling module and a power quality module. The main differences between the two modules are the order of the cells inside the module and their safety systems [26, 37]. The cells inside a NaS module are cylindrical. With an average diameter of 90.5 mm and height of 542 mm, each cell weighs about 5.3 kg. The average discharging voltage of each cell is about 1.93 V with a discharging duration of about six hours [26].

The modules are stored connected together in a block system. Figure 7.61 illustrates a typical block system. Here, twenty 50 kW modules are connected together to produce one MW of power.

Various sizes of storage blocks are used. Power can be further increased by connecting storage blocks together [22].

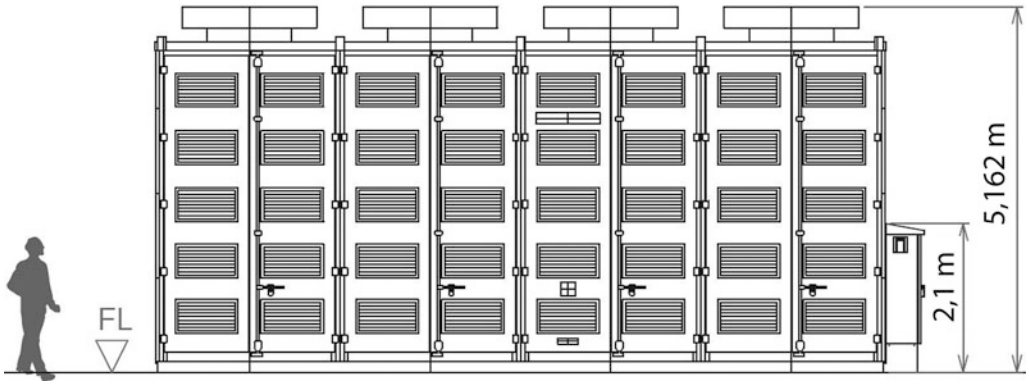



**Fig. 7.62** Basic design of a two MW block






**Fig. 7.63** 34 MW NaS storage block system

Figures 7.62 and 7.63 show NaS systems in various sizes.

The two MW block shown in Fig. 7.62 is around 5.1 m high and around 10.3 m long. The block is composed of two 1,000 kW blocks, each weighing 86 tons. But even storage blocks with a capacity of 12,000 kW h are not among the largest NaS systems [22].

Connecting seventeen two MW NaS blocks together results in a rated power of 34 MW and a total energy of 204 MW h.

The system shown in Fig. 7.63 feeds the energy into a 154 kV high-voltage network. This is the largest NaS system installation to date. Connected to a 54 MW wind park, including 34 wind turbines, the system is used to balance power fluctuations [22].

### 7.5.5 Charging and Discharging Process

Low electrochemical self-discharge is typical of NaS cells. The batteries self-discharge only over very long storage periods without any charging or discharging. But to maintain a 20 kW h battery at operating temperatures, for example, around 100 W of heating capacity is required. This is termed thermal self-discharge.

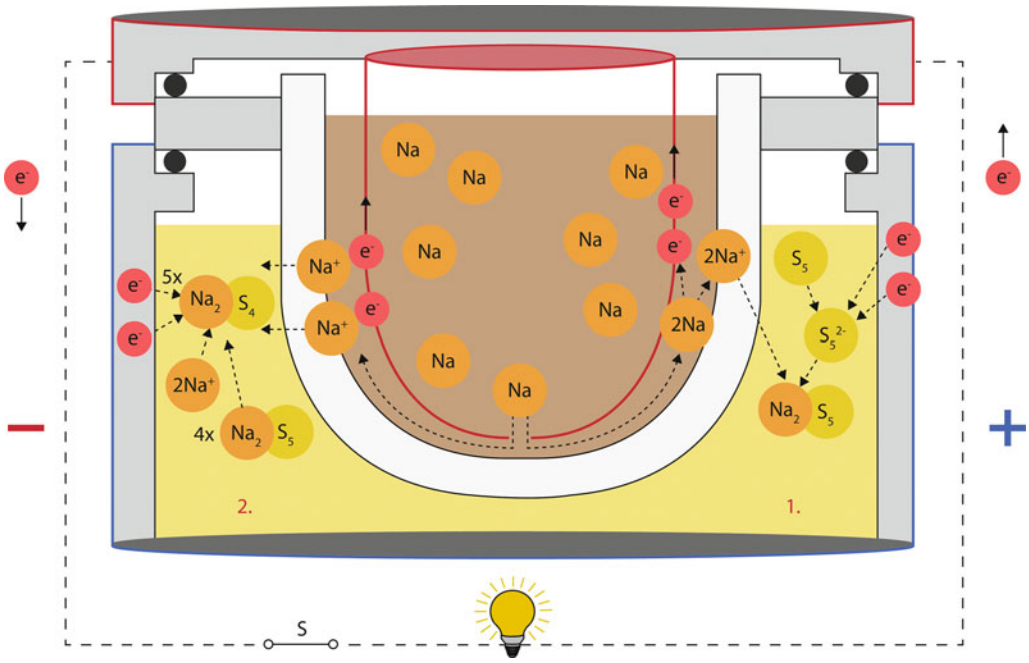



**Fig. 7.64** Reactions in a NaS cell

If this is included in electrochemical self-discharge, then the self-discharge is actually very high [26].

During discharge, metallic sodium is oxidized to $Na^+$. The sodium ions can then diffuse through the ceramic electrolyte to the positive electrode, compensating for the charge of the polysulfide anions formed from the sulfur there.

The electrons from the sodium electrode that reach the sulfur electrode through the external circuit reduce the elemental sulfur. As a result, $Na_2S_5$, for example, is formed [16, 34].

The following is a (highly simplified) equation for the first discharging step (Fig. 7.64):

$$2Na + 5S \xrightarrow{\text{discharge}} Na_2S_5. \qquad \textbf{(7.61)}$$

Liquid pentasulfide is disassociated into ions in the melt. This reaction mechanism is described in detail in [36].

In a charged state, the cell's OCV is about 2.08 V. As long as adequate elementary sulfur remains, the voltage stays at 2.08 V.

Because of its high operating-temperatures, a NaS cell's OCV cannot be determined beyond the benchmarks established by the electrochemical voltage series. Instead, they must be calculated using the Nernst equation [20]:

$$E = E^0 + \frac{RT}{zF} \ln \frac{c_{Ox}}{c_{Red}}, \qquad \textbf{(7.62)}$$

$E$ – Electrode potential
$E^0$ – Standard electrode potential
$R$ – Universal or molar gas constant $R = 8.31447\,J \cdot mol^{-1} \cdot K^{-1} = 8.31447\,C \cdot V \cdot mol^{-1} \cdot K^{-1}$
$T$ – Absolute temperature [K]
$z$ – Number of transferred electrons
$F$ – Faraday constant $F = 96{,}485.34\,C \cdot mol^{-1} = 96{,}485.34\,J \cdot V^{-1} \cdot mol^{-1}$
$c$ – Redox pair activity (Red → Reducer, Ox → Oxidizer)

The Nernst equation determines the redox pair's electrode potential in relation to concentration.

The state changes and the voltage falls after around 65% discharge. This is due to the low levels of sodium and sulfur remaining after extensive discharge. This means that sodium

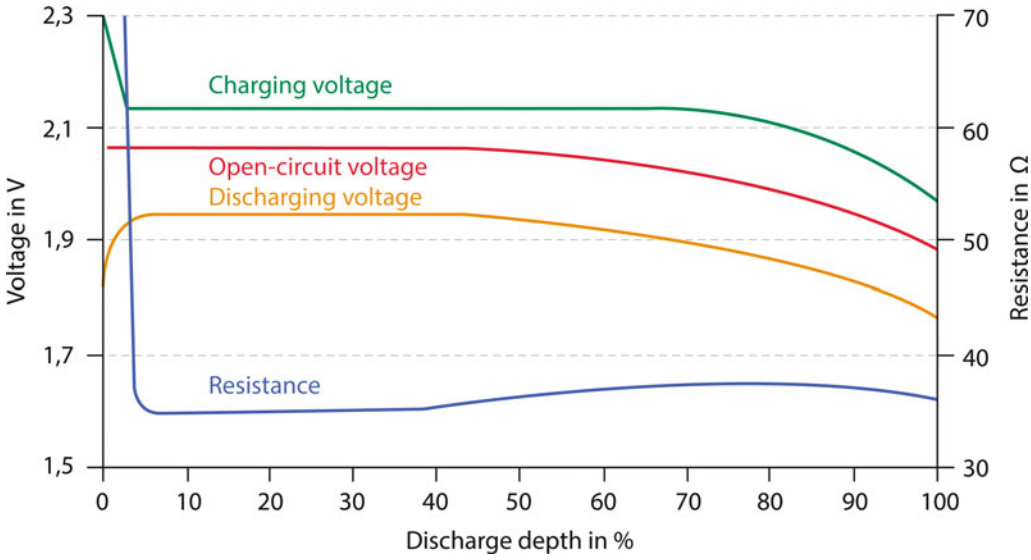



**Fig. 7.65** OCV and cell voltage during charging and discharging of an A08 cell

tetrasulfide $Na_2S_4$ is formed first [11, 16, 34]. The reaction equation here is:

$$4Na_2S_5 + 2Na \xrightarrow{\text{discharge}} 5Na_2S_4. \qquad (7.63)$$

At this stage of the discharging process, the cell voltage falls to around 1.9 V.

Further reduction of sulfur by sodium causes the cell voltage to continue to fall. Because of the low sulfur content in the system, only sodium trisulfide $Na_2S_3$ can be formed. This reduces the cell voltage to around 1.78 V.

If discharging is continued even further, then the accumulator is damaged by deep-discharging. The formation of sodium disulfide $Na_2S_2$ has devastating consequences for NaS cells. Since the internal resistance rises dramatically at this stage, significant thermal loss and thermal stress may result for the cell. Manufacturers stop charging with the earlier formation of sodium trisulfide to extend accumulator service life. This is achieved by interrupting the discharging process at a DOD of 70% [16, 34].

### ■ Electrical Operating Limits and Problems with Charging and Discharge Processes

Figure 7.65 graphs the charging, open-circuit, and discharging voltages. The blue line is the internal resistance.

When current is applied, the cell voltage falls. This is due to the ohmic voltage drop in the electron and ion-conducting elements. The internal resistance has virtually no relation to the SOC. It increases significantly when the accumulator is fully charged, because sulfur on the positive electrode limits conductivity.

Given of the high-resistant state of NaS cells when fully charged, they can be connected either in series or parallel. Active cell voltage balancing stabilizes the cell voltage, even if the cell internal resistance varies due to manufacturing tolerances.

A rapid increase in resistance indicates a full SOC. This means that the accumulator can be charged with a CC until a rapid increase in resistance, and until a charging end voltage of 2.12 V. If NaS systems are connected in parallel, then at the end of charging, current flows only through those strings that are not fully charged. Connecting several cells in series presents a problem. If a cell has already reached a 100% SOC but the overall string voltage has not reached the interrupting voltage of 2.12 V, then a drastic reduction in sodium ion concentration may cause dielectric flashover in the fully charged cell.

Dielectric flashover can destroy the ceramic solid electrolyte. This problem can be elimi-

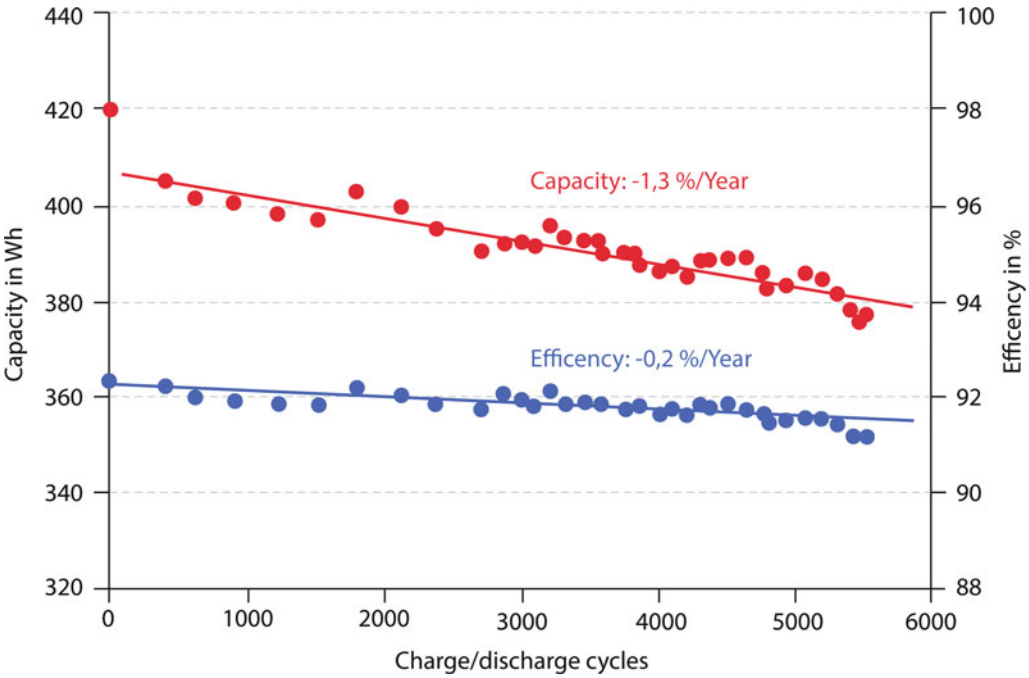



**Fig. 7.66** NaS battery capacity and efficiency

nated by installing module voltage metering and a bypass mechanism to prevent current from flowing to the already charged modules.

In addition, manufacturers specify upper charging and discharging current limits to prevent the separators from overheating. In the NaS system, most ohmic resistance comes from electrolyte resistance. As a result, excessive charging currents may cause sodium dendrite formation [7, 34].

### 7.5.6 Cycles, Capacities, and Service Life

Manufacturer specifications from NGK Insulators indicate an expected service life of 15 years. The cell can be discharged 2,500 times to a 100% DOD over this time. If the cell is consistently discharged to 90%, then the number of charging cycles increases to 4,500. If a NaS system is discharged to 65% of its potential DOD, then the number can reach 6,500 cycles. Some sources cite a number of charging cycles exceeding 10,000. But this can only be achieved with minimal discharging of < 20%. Sodium-sulfur accumulators are very sensitive to deep-discharging, and are almost never discharged to 100%. Drastic reductions in sodium and sulfur levels lead to the formation of sodium disulfide. Because of sodium-sulfide's high melting-point, this should be avoided [22, 29].

Figure 7.66 shows the number of charging and discharging cycles in a service life test. Capacity falls by 1.3% per year. Efficiency falls by about 0.2% per year.

### 7.5.7 Efficiency, Power, and Energy

Several factors determine the efficiency of a NaS battery. In all batteries, losses are caused by internal resistance. In addition to ohmic losses due to internal resistance, in sodium-sulfur accumulators there are also thermal losses from maintaining the operating tem-

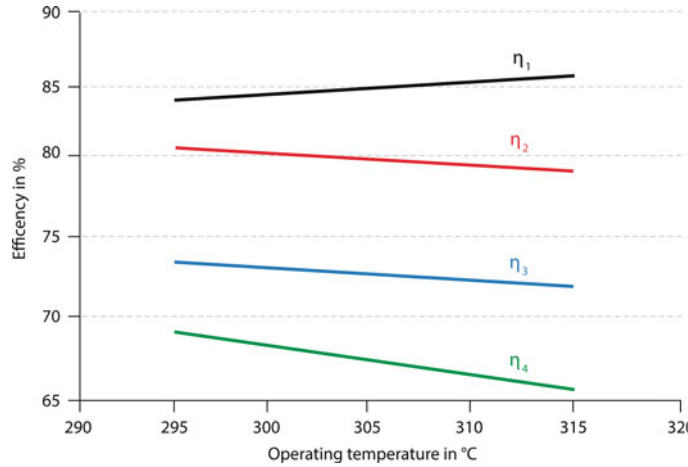



**Fig. 7.67** Efficiency in relation to operating temperature



perature. An accumulator's efficiency is determined by the operating current [7, 29]:

$$\eta = \frac{U_0 - I_E \cdot R_i}{U_0 + I_L \cdot R_i}, \tag{7.64}$$

$U_0$: – OCV
$I_E$: – Discharging current
$I_L$: – Charging current
$R_i$: – Internal resistance

At an operating temperature of around 300 °C, a NaS facility's efficiency is about 85%. After power inversion and deduction of thermal heating in idle phases, the realistic efficiency is about 75% [29].

The energy density of NaS accumulators is about 218 W h/kg. The power density of NaS accumulators is about 200 W/kg.

Figure 7.67 details the efficiency of a 100 kW module.

Efficiency is shown in relation to temperature. The upper graph $\eta_1$ shows the battery's electrochemical efficiency. The lower graph $\eta_2$ shows the energetic efficiency, taking into account heating losses. The two graphs, $\eta_1$ and $\eta_2$, only consider the direct current side.

The function $\eta_3$ shows the accumulator's daily efficiency with heating losses and power inversion losses taken into account. An efficiency of 95% was assumed for the inverter. The last function $\eta_4$ shows the weekly efficiency. Heating losses are taken into account with the assumption that there are no cycles on two days of the week. Graphs $\eta_3$ and $\eta_4$ consider the alternating current side.

The illustration demonstrates that increased operating temperatures only increase the purely electrochemical efficiency. Graphs $\eta_2$, $\eta_3$, and $\eta_4$ fall as the temperature increases.

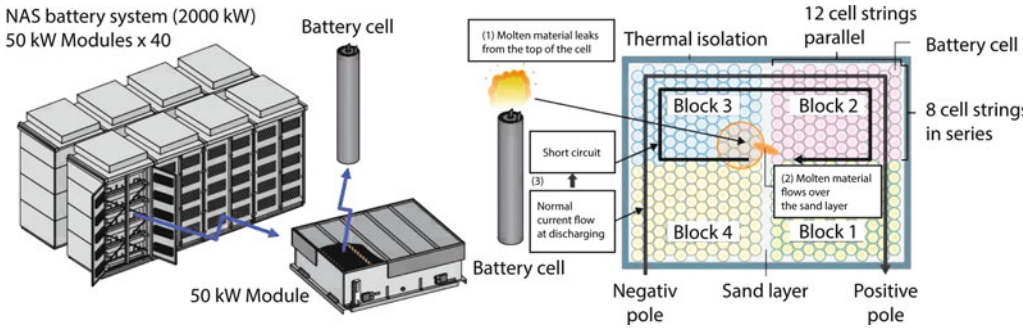



**Fig. 7.68** Basic design of a NaS battery system and cell arrangement

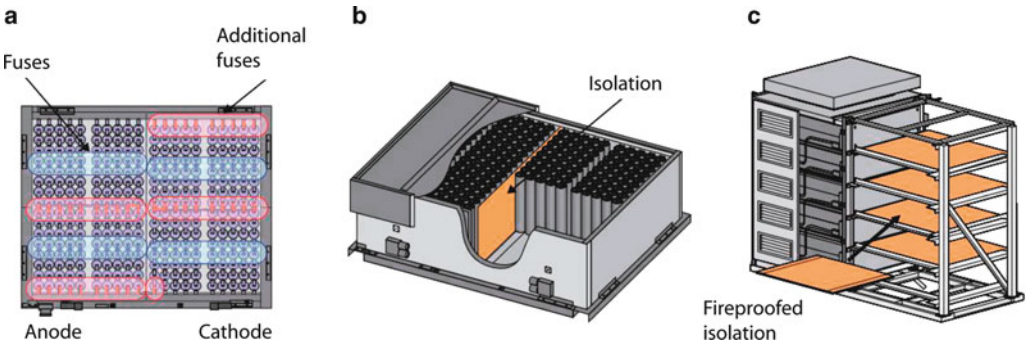



**Fig. 7.69** **a–c** NaS system safety measures

The illustration also shows that $\eta_1$ is primarily affected by the module's internal resistance, which falls as the temperature increases. But the electrical heating system strongly affects the efficiencies $\eta_{2-4}$.

For increasing overall efficiency, the key factors are the design or manufacture of the thermally insulated container and the permitted operating temperature.

## 7.5.8 Hazards and Safety

With sodium-sulfur accumulators, operational safety is a major challenge. In an accident, instant reactions among the liquid components can result in temperatures well over 1,000 °C.

A well-known example of a NaS accumulator accident occurred in September 2011 when a large 2,000 kW storage block caught fire. The cause of the fire was a defective NaS cell. A fracture within the cell caused the liquid electrode materials to leak, resulting in a short-circuit in the neighboring block (Fig. 7.69). Since there was no limiting fuse installed between the cells, the short-circuit current continued to flow and heat the system. The result was that a large number of cells were destroyed and set on fire. The fire then spread across the entire module. Since the fire and molten electrode materials destroyed the shells of the modules above and below as well, the fire spread across the entire storage block [23, 24].

After the cause of the fire had been determined, a number of safety measures were put in place to prevent chain reactions [23, 24]. Fuses were installed between the cells to break short-circuit current (Fig. 7.69a). In addition, insulation was placed between the cell blocks to contain a short-circuit caused by liquid sodium (Fig. 7.69b). The insulation was designed to ensure that fireproof plates were placed above and below the module to prevent fire from spreading.

## 7.5.9 Conclusion

Sodium-sulfur accumulators are **high-temperature batteries** with an operating temperature of around 320 °C. This high operating-temperature also determines the battery's special characteristics:

- The cells are placed in thermally insulated containers and require heating and cooling.
- The electrode materials, **sodium**, **sulfur**, and **sodium polysulfide, are in liquid form**, and the **separator** is made of **ceramic**.
- Since **sodium** is highly reactive with water, it must be protected from contact with the environment in a **metal container**.
- During operation, **current heat** is adequate to maintain the optimal operating temperature. The **heating system** is required in idle phases.

- This also determines the **efficiency**: the battery itself has a **low self-discharge rate**. But over **long idle periods**, electric heating causes the battery to discharge at an **unusually high rate**.

## 7.6 Redox Flow Batteries

All the batteries considered above are simultaneously charging, storage, and discharging units. There is another type of battery with external storage, allowing power and energy to be dimensioned independently from one another: the redox flow battery.



### History

Energy storage using redox pairs was discovered in the mid-20th century. This was immediately followed by the development of redox flow batteries. In 1970 at the Lewis (Glenn today) Research Center, the American space agency NASA developed a cell using this technology with the electrolyte pair iron titanium. Iron(III) chloride ($FeCl_3$) was used as an oxidizing agent and titanium chloride ($TiCl_2$) as a reducing agent in alkaline electrolytes. To increase efficiency, after further research, L. Thaller replaced the titanium with chrome [38] but this caused two problems. The first was that an ion-selective membrane was required, making the cell significantly more expensive. The second was that, to ensure the reactions continued smoothly, this membrane could not be bonding. The design and operating principles described in US patent 3996064 'Electrical Rechargeable Redox Flow Cell' from 1976 are still valid today. Cells with a pure vanadium solution were first proposed in 1978. They were then developed at the University of New South Wales by Maria Skyllas-Kazakos in the 1980s, and patented in Australia in 1986. US patent 4786567 in 1988, as well as numerous scholarly publications, made the vanadium redox flow battery (VRFB) internationally known. The pure VRF cell led to the development of the vanadium bromide cell and is still the most common cell type today. This cell has an energy density twice that of the VRF cell. To distinguish them from the rechargeable redox cells invented in the mid-1950s that 'chemically' recharged the active masses, these cells are termed 'electrically' rechargeable. Scientists immediately recognized the system's potential for storing electrical energy from PV and wind power facilities (load shifting), as well as for peak-shaving, load-leveling, or uninterruptible power supply (UPS).

### 7.6.1 Redox Flow Cell Design and Operation

The voltaic cell of a redox flow battery is separated into two half-cells by the membrane. The electrolytes that store the energy are pumped through the cell in two separate circuits connected by the membrane. Ion exchange occurs through the membrane. The ion exchange membrane used depends on the redox flow battery (RFB) type. It is made either of a microporous separator that allows all ions to pass through, or a selective anion or cation exchange membrane that prevents the electrolytes from mixing. Perfluorinated, sulfonated, ion-selective Nafion® type 115 and 117 membranes are used. In recent years, modified Nafion variants such as Nafion/$SiO_2$ or the sandwich-like 'SPEEK' membrane (sulfonated poly(tetramethyldiphenyl) ether ketone) have also been used in VRF batteries. From an electrotechnical point of view, the actual reactions of reduction and oxidization (i.e., electron release and electron absorption) occur at the electrodes [33].

Because of the electrochemical voltage window, the electrodes are usually made of graphite and placed in aqueous liquid electrolyte. To maximize the specific power, graphite felts with large specific surface areas are used as electrodes. The large-area electrodes made of carbon or graphite felt do not actively participate in the electrochemical reaction. They function solely as electricity collectors in the electron transfer between the oxidized or reduced ions

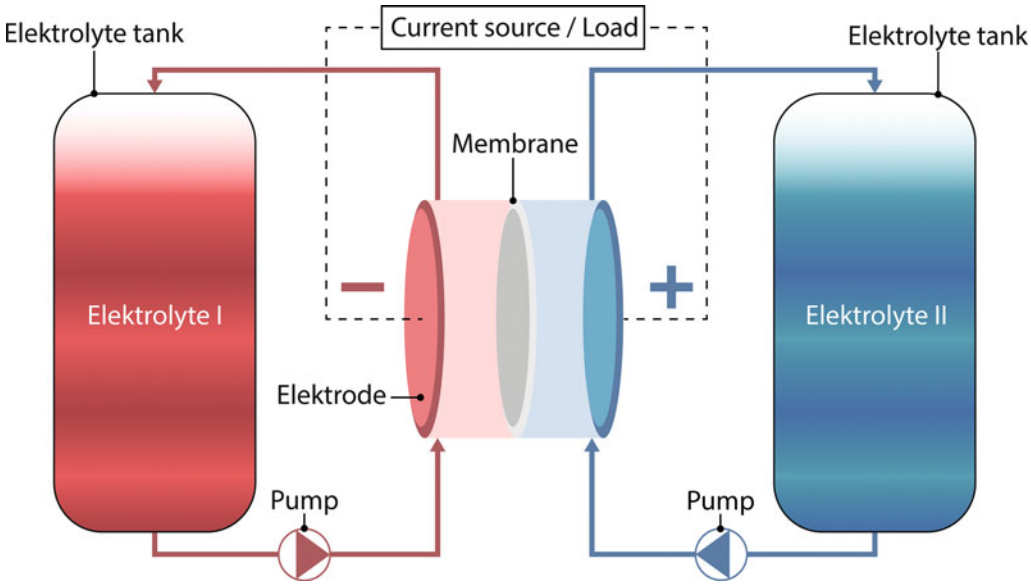



**Fig. 7.70** Technical design of a redox flow battery

of the redox pairs (electrolytes). The graphite felt is thermally bonded and placed in a bipolar conducting polyethylene substrate filled with carbon. Liquid electrolytes composed of salts dissolved in a solvent are used for the actual reaction partners (the active masses or species). Inorganic or organic acids can be used as solvents. The battery's energy density is primarily determined by the electrode density and cell voltage. The electrolytes are stored in two separate tanks outside the cell. This means that the redox flow cell is the only kind of electrochemical-energy storage that allows the dimensioning of energy quantity and power independently from one another. RFB peripherals include pumps, tubes, valves, heat exchangers, and electrolyte tanks. All parts in contact with the electrolytes must be resistant to sulfuric acid, or have a coating resistant to sulfuric acid. In most RFB facilities, the peripheral components are standard products that can be used for other applications as well. The electrolyte tubes must be able to withstand thermal cycling without developing leaks. Operational disruptions in RFB facilities are commonly caused by electrolyte loss through leakage. The battery management system is an essential component of the control electronics. The cell is charged by manually filling the tanks or by applying an external current. The cell voltage determined by the Nernst equation is 1.0–2.2 V. As with fuel cells, the individual cells can be connected in series in a stack with the electrodes functioning as bipolar electrodes (Fig. 7.72). The liquid electrolyte is then supplied in parallel. As with other batteries, the individual stacks can be connected in parallel or series to achieve the combination of capacity and voltage required. This means that the redox flow cell, in some ways, resembles a fuel cell in its design, but it has an accumulator in its electrochemical reversibility. As already indicated, the most important characteristic of this technology is that it allows energy and power to be dimensioned independently from one another. This is achieved by separating the energy converter and the storage medium [25]. The quantity of electrolytes determines the quantity of energy stored. The size of the active electrode surfaces determines the power. Figure 7.70 shows the technical design of a redox flow battery.

The redox flow cell is basically an accumulator where reduction (electron absorption)

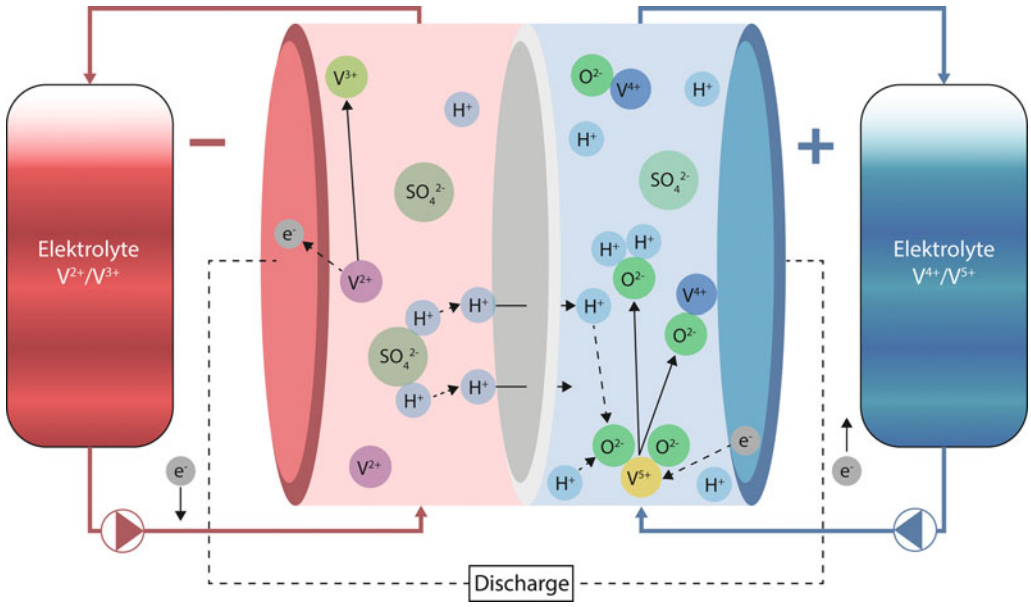



**Fig. 7.71** Reactions in the half-cells

occurs between the electrodes and through the membrane in one half-cell, and oxidation (electron release) in the other half-cell. It stores electrical energy in the form of chemical compounds. Figure 7.71 outlines the reactions using the pure vanadium redox flow cell as an example.

The following are the reactions in the half-cells.

Catholyte:
$$\mathrm{VO_2^+ + 2H^+ + e^- \rightarrow VO^{2+} + H_2O} \quad (7.65)$$
$$\left(\mathrm{V^{5+} + e^- \rightarrow V^{4+}}\right)$$

Anolyte:
$$\mathrm{V^{2+} \rightarrow V^{3+} + e^-} \quad (7.66)$$

Complete reaction:
$$\mathrm{V^{2+} + VO_2^+ + 2H^+ \leftrightarrow V^{3+} + VO^{2+} + H_2O.} \quad (7.67)$$

Potential:

$$U = U^0 \cdot \frac{R \cdot T}{z \cdot F} \cdot \ln\left\{\left(\frac{c_{\mathrm{VO_2^+}} \cdot \gamma_{\mathrm{VO_2^+}} \cdot c_{\mathrm{2H^+}} \cdot \gamma_{\mathrm{2H^+}}}{c_{\mathrm{VO^{2+}}} \cdot \gamma_{\mathrm{VO^{2+}}}}\right) \cdot \left(\frac{c_{\mathrm{V^{2+}}} \cdot \gamma_{\mathrm{V^{2+}}}}{c_{\mathrm{V^{3+}}} \cdot \gamma_{\mathrm{V^{3+}}}}\right)\right\}. \quad (7.68)$$

**Electrolyte:** – 1.5 M $VSO_4$ in 2 M $H_2SO_4$
**Membrane:** – Nafion (*perfluorosulfonic acid membrane*) or modified Nafion
**Electrodes:** – Carbon felt electrode

In the vanadium cell discharging process, first the sulfuric acid dissociates on the anode side in the aqueous electrolyte solution. This means that the sulfuric acid molecules decompose into ions, releasing protons. The protons are then transported through the membrane to the cathode side half-cell where they attach themselves to the oxygen ions. As a result, water ($H_2O$) is formed. Besides water, an oxygen compound ($VO^{2+}$) is formed from the vanadium ion ($V^{4+}$). During the charging process, the same reactions occur in reverse.

▶ Section 4.4.1 describes the electrochemical principles and indices in detail. The equilibrium condition of an individual cell or theoretical OCV $V_{oc}$ can then be determined by entering the chemical equations for the reactions into the Nernst equation.

The general form of the Nernst equation is:

$$U = U^0 + \frac{RT}{zF} \ln \frac{c_{\mathrm{Ox}}}{c_{\mathrm{Red}}}, \quad (7.69)$$

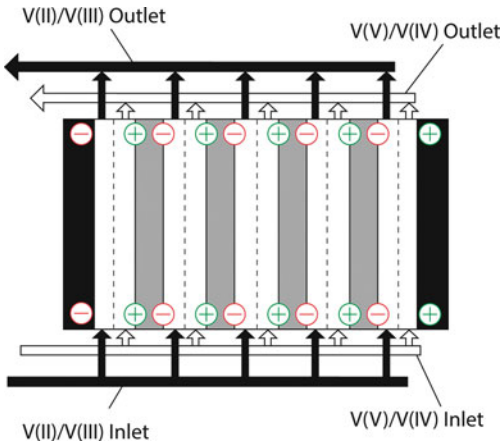



**Fig. 7.72** Redox flow cells connected in series. The *dotted line* is the membrane. The *dark electrodes* are the monopolar electrodes, and the *light electrodes* are the bipolar electrodes. The *dark arrows* in and out represent the circulation of bi- or trivalent vanadium, and the *light arrows* in and out represent the circulation of tetra- or pentavalent vanadium

where $U$ is the Nernst potential, $U^0$ the equilibrium voltage, $R$ the gas constant with $R = 8.3145\,\mathrm{J/(mol \cdot K)}$, $T$ the temperature, $z$ the valence, and $F$ the Faraday constant. The quotient of the oxidizing and reducing agent concentrations must also be determined.

As a general rule:

$$\begin{aligned} \text{Catholyte:}\quad & K^n \rightarrow \mathrm{K}^{n+1} + e^- \quad \text{(charging)} \\ & K^{n+1} + e^- \rightarrow \mathrm{K}^n \quad \text{(discharging)}, \end{aligned} \tag{7.70}$$

$$\begin{aligned} \text{Anolyte:}\quad & A^n + e^- \rightarrow \mathrm{A}^{n-1} \quad \text{(charging)} \\ & A^{n-1} \rightarrow \mathrm{A}^n + e^- \quad \text{(discharging)}. \end{aligned} \tag{7.71}$$

Fig. 7.72 shows the basic design of a redox flow stack composed of five cells connected in series.

Using only one element with oxidation states of +2, +3, +4, and +5 in both electrolytes for the redox pair solved most of the major problems associated with earlier pure vanadium cell designs. This prevents complications such as deposits and dendrite formation. These can destroy the membrane or cause a short-circuit, destroying the entire cell. In addition, vanadium ions are only transported as intended during battery discharge. This means that the battery retains its total capacity in later charging cycles. Processes that result in electrolyte contamination are also avoided, making the redox flow cell a very robust cell with a long service life. A drawback is that the energy density is limited by the limited solubility of vanadium pentoxide in sulfuric acid. During discharging, pentavalent vanadium is converted into tetravalent vanadium in the catholyte. This then reacts with oxygen to form divanadyl cations ($VO^{2+}$). An operating temperature between 20 °C and 30 °C is maintained to prevent further divanadyl cation reaction with the solid vanadium pentoxide. If the temperature exceeds 40 °C, then the reaction is determined by the concentration and the length of time the battery is idle. Vanadium ion concentration in the electrolyte ranges from 0.1–10 mol/L. Ideally the concentration should be 2–3 mol/L. In water or in acids dissolved in water, vanadium pentoxide results at temperatures over 40 °C and concentrations over 1.6 mol/L. Vanadium pentoxide formation is irreversible and has negative repercussions, clogging and damaging the cell. Replacing aqueous solutions with ionic solutions prevents this process. Increased vanadium concentrations in the electrolyte result in increased energy densities. The operating temperature can then also exceed 40 °C, resulting in higher power densities. This is because ionic liquids have higher melting and boiling points than water and aqueous solutions. The chemical characteristics of ionic liquids include other advantages such as chemical stability, improved chemical conductivity, lower vapor pressure, and higher thermal stability. The selection criteria for electrochemically active redox species are listed below.

- Solubility of the oxidized and reduced species in the electrolyte.
- High reversibility and fast reaction kinetics of the redox pairs in both the charging and discharging directions; if possible, avoidance of multi-step processes.

- Stability of the electrolyte during oxidation or reduction of the active redox materials, for example, to avoid potential water decomposition.
- Does not require the use of complex, heavy ions.

The requirements for the ion-selective membrane are as follows:

- High ion conductivity for select anions or cations depending on the system.
- Minimizes cross-diffusion of ions between the catholyte and anolyte areas.
- Chemical and mechanical stability in the operating temperature-range.
- Minimal reduced conductivity and ion selectivity due to aging processes caused by cyclic operation.



## 7.6.2 Possible Material Pairings

Besides the pure vanadium redox flow cell previously described in ▶ Sect. 7.5.1, there are other types of cells with various other material pairings. This section describes those types.

### ■■ Iron Chrome Redox Flow Cell

Catholyte: $Fe^{3+} + e^- \rightarrow Fe^{2+}$ **(7.72)**

$U^0 = 0.77\,\text{V vs. NHE}$

Anolyte: $Cr^{2+} \rightarrow Cr^{3+} + e^-$ **(7.73)**

$U^0 = -0.41\,\text{V vs. NHE}$

Complete reaction: $Cr^{2+} + Fe^{3+} \leftrightarrow Cr^{3+} + Fe^{2+}$ **(7.74)**

**Standard equilibrium voltage:** – $U^0 = 1.18\,\text{V}$
**Electrolyte:** – 1 M $CrCl_3$ on the negative side $FeCl_2$ in 2 M HCl on the positive side
**Electrodes:** – 3.15 mm carbon felt (with traces of Pb and Au separation as catalysts on the Cr side to make the chrome reaction reversible)
**Membrane:** – Ion exchange membrane series CD1L from Ionics Inc. in Watertown, Ma

Side-reaction on the CR (negative) side:

$\rightarrow H_2;\ U^\theta = 0\,\text{V vs. NHE}$ **(7.75)**

### ■■ Polysulfide Bromide Redox Flow Cell

Catholyte: $Br_2 + 2e^- \rightarrow 2Br^-$ **(7.76)**

Anolyte: $S_4^{2-} \rightarrow 2S_2^{2-} + 2e^-$ **(7.77)**

Complete reaction: $S_4^{2-} + Br_2 \leftrightarrow 2S_2^{2-} + 2Br^-$ **(7.78)**

**Standard equilibrium voltage:** – $U^\theta = 1.5\,\text{V}$
**Electrolyte:** – $NaS_2$/NaBr

### ■■ Vanadium Bromine Redox Flow Cell

Catholyte: $Br_3^- + 2e^- \rightarrow 3Br^-$ **(7.79)**

Anolyte: $V^{2+} \rightarrow V^{3+} + e^-$ **(7.80)**

Complete reaction: $V^{2+} + Br_3^- \leftrightarrow V^{3+} + 3Br^-$ **(7.81)**

**Standard equilibrium voltage:** – $U^0 = 1.3\,\text{V}$
**Electrolyte:** – $VCl_3$-HCl/NaBr-HCl

Hybrid flow systems function on the same principle as redox flow batteries, except that one of its electroactive components (Zn) is deposited in solid form at the anode.

### ■■ Zinc-Bromine Cell

Catholyte: $Br_3^- + 2e^- \rightarrow 3Br^-$ **(7.82)**

Anolyte: $Zn \rightarrow Zn^{2+} + 2e^-$ **(7.83)**

Complete reaction: $Zn + Br_3^- \leftrightarrow Zn^{2+} + 3Br^-$ **(7.84)**

**Standard equilibrium voltage:** – $U^\theta = 1.8\,\text{V}$
**Electrolyte:** – $ZnBr_2$/$ZnBr_2$

### ■■ Zinc-Cerium Cell

Catholyte: $2Ce^{4+} + 2e^- \rightarrow 2Ce^{3+}$ **(7.85)**

Anolyte: $Zn \rightarrow Zn^{2+} + 2e^-$ **(7.86)**

Complete reaction: $Zn + 2Ce^{4+} \leftrightarrow Zn^{2+} + 2Ce^{3+}$ **(7.87)**

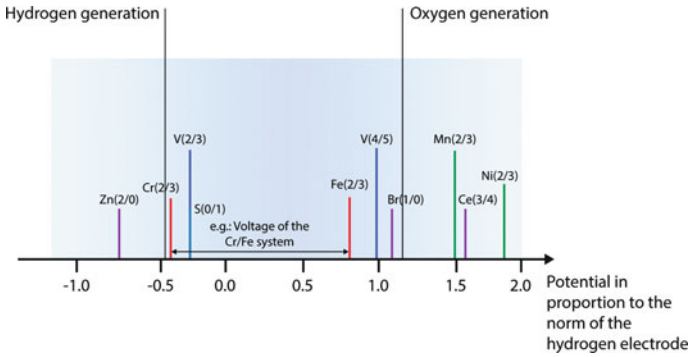



**Fig. 7.73** Potential material pairings [15]

**Standard equilibrium voltage:** – $U^{\theta} = 2.4\,\mathrm{V}$
**Electrolyte:** – $CH_3SO_3H/CH_3SO_3H$

Figure 7.73 lists the potential redox pairings.

## 7.6.3 Charging and Discharging Strategies

Because of their technical characteristics (deep-discharge capability and very high cycle life), charging and discharging strategies are relatively unimportant with redox flow cells. This clearly separates these energy storage systems from other electrochemical storage systems. Since their service life and cycle life depend on it, the strategies are essential with lead accumulators and lithium ion accumulators.

A facility's SOC can be easily monitored by measuring the OCV. Figure 7.74 shows the cell OCV as a function of the module's SOC. Operating a redox flow facility requires a battery management system. This system measures the temperature-level, voltage, and current in order to maintain the cell at the optimal operating point.

### ▪ Current-Voltage Characteristic

Activation overvoltage is highest at low currents. At high currents, a diffusion overvoltage $U_{\chi}$ results if the electrochemical reactions occur faster than reactants are supplied. In the range of ohmic losses, the relation is practically linear. At a particular SOC of the cell, cell resistance and overvoltage $U_{\eta}$ can be experimentally determined from the current-voltage values in the linear range.

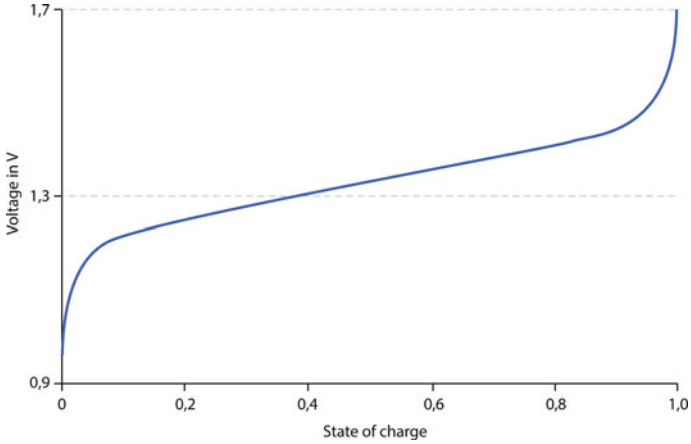



**Fig. 7.74** VRF cell idle voltage vs. SOC

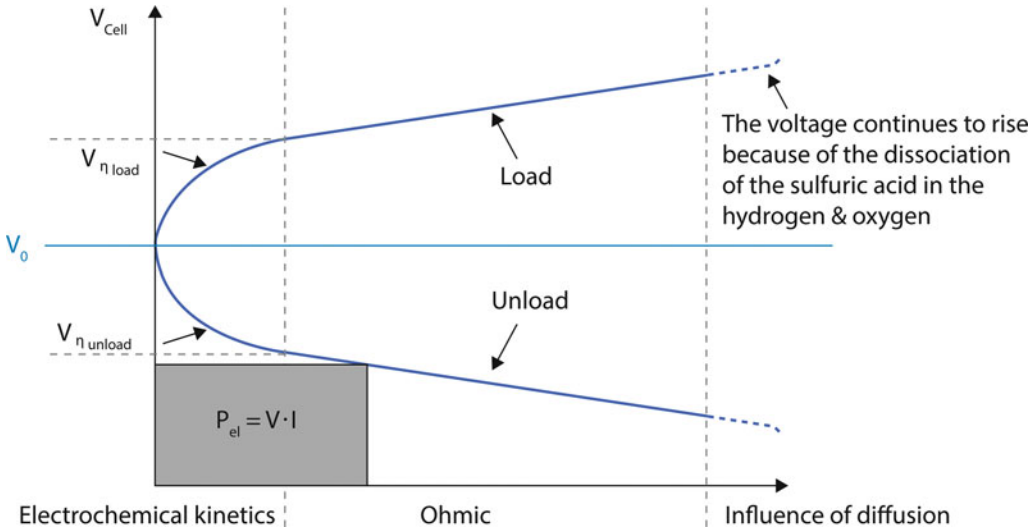



**Fig. 7.75** Current-voltage characteristic

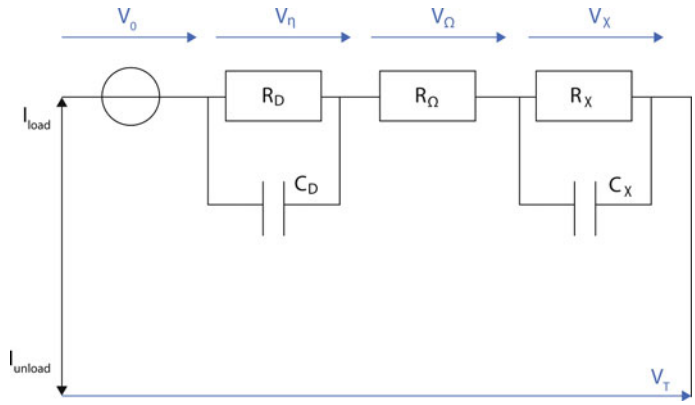



**Fig. 7.76** Redox flow cell circuit diagram

Figure 7.75 shows the current-voltage characteristic.

### Circuit Diagram

Fig. 7.76 shows a highly simplified circuit diagram of a redox flow cell. The diagram includes a RC element and an ohmic resistance. The RC element of the diffusion and equilibrium processes must also be taken into account. Although it may be negligible when the cell is operated at optimum temperatures, resistance increases considerably when temperatures fall.

$R_D$ stands for the activation resistance of the electrode reaction charge transfer, and $C_D$ for bilayer charging. $R_\Omega$ stands for ohmic resistance. In the RC element of the diffusion and equilibrium processes, the temperature-level affects the resistance. The diffusion process affects the capacity.

## 7.6.4 Energy Density, Power Density, and Efficiency

The electrical efficiency of a redox flow cell is relatively high at around 90%. But if losses from peripherals such as pumps are taken into account, the efficiency is only 70–80% (Table 7.15). As already discussed, energy

**Table 7.15** Comparison of RFB system parameters [15]

| System | Cell voltage [V] | Current density [mA/cm$^2$] | A h efficiency [%] | Energy efficiency [%] |
|---|---|---|---|---|
| Fe/Cr | 1.03 | 6.5 | 81 | 66 |
| Bromine/polysulfide | 1.53 | 60 | 90 | 67 |
| Vanadium/vanadium | 1.70 | 80 | 90 | 72–81 |
| Vanadium/bromine | 1.70 | – | – | 80 |

density and power can be scaled independently from one another. Energy density depends solely on the electrolyte's solubility in the liquids. Power depends solely on the how the individual stacks are wired together. But capacity is determined by the size of the tank.

There are two central factors that cause reduced RFB energy efficiency.

1. Parasitic currents along the electrolyte tubes connected in parallel
   This is an ion current connected in parallel to the electric wiring of the bipolar electrodes. This shunt current results in energy losses between 3 and 5%. It also increases the risk of metallic dendrite formation along the electrolyte tubes, which can lead to clogging. In addition, concentration gradients of the electroactive species can cause cell component corrosion. To solve this problem, thinner electrolyte tubes are used, increasing resistance. As a result, faster ion flow with higher pressure differences is required. This then increases the energy requirements of the peripherals.
2. Pump-power
   Pump-power is required to circulate the electrolyte. Using tubes of a larger diameter to reduce pump-power increases shunt current.

As a result, these two factors reducing efficiency can only be optimized by finding a compromise between them.

### 7.6.5 The Redox Flow Battery in Comparison

In comparison to other electrochemical battery technologies, the redox flow battery has the following advantages.

- Simple, modular cell design
- Suited for large storage capacities
- Very long service life because the electrodes do not react and, therefore, do not degenerate
- Separate energy conversion and storage allows flexible dimensioning of energy and power
- Separate storage of electrolyte liquids (anolyte and catholyte) effectively prevents self-discharge This means that self-discharge is limited to reactants within the cell itself
- Short reaction time of under 100 ms
- Low maintenance costs
- Environmentally-friendly
- Fast-charging by changing the electrolyte (not possible with accumulators)

The redox flow battery has, however, the following disadvantages.

- Relatively low energy and power density
- Peripherals are required, increasing energy consumption, and as a result, reducing system efficiency

- Branch current (bypass current) reduces efficiency
- Uniform current conditions are required in the cell; in large cells in particular, uneven current conditions may produce by-products such as gases, and destroy the cell stack
- Difficulties sealing the cells and cell stack
- Reduced cell voltage due to reactant mixing during discharging
- Concentration and purity of the redox pairs difficult to maintain



### 7.6.6 Service Life and Mechanisms that Shorten Service Life

There is currently relatively little data on the service life of redox flow cell central reaction units or electrolytes. In principal, there should be no structural changes of the individual components with the current cell types (vanadium). The assumption is that, as a result, the service life is quite long. For pure vanadium cells, manufacturers give a cycle life above 13,000. For the other electrolyte and cell types, the cycle life is estimated at 10,000 if the cells are operated in a SOC ranging from 20–80%. This means that among all accumulator types, the service life of the redox flow cell is one of the longest. Mechanisms that shorten service life, such as cell destruction by dendrite formation, can be virtually eliminated if the cells are handled and operated correctly. But the long service life of a redox flow cell using aqueous solutions is severely compromised when operated at low or excessively high-temperatures, for example. If the concentration of electrolyte in the liquid is incorrect, this may also shorten the service life.

### 7.6.7 Redox Flow Battery Application Areas

There are currently plans to use redox flow systems in the following application areas.

1. For balancing load-peaks and voltage support
   Pure vanadium redox flow cells and zinc/bromine cells are already in use in this area, particularly in the USA and Japan.
   - The Japanese energy utility, Kansai Electric Power Corporation, has used redox flow batteries for around 20 years for load-peak balancing.
   - Since 2004, the Pacific Corporation in Utah, USA, has used vanadium technology for load-peak balancing to stabilize its supply network. The vanadium redox flow batteries used in Utah have a power of 250 kW and an energy quantity of 2 MW h.
   - The ZBB Energy Corporation and the California Energy Commission each operate energy storage facilities with a capacity of 2 MW h to compensate for load-peaks of up to 1.5 MW.
   - In County Donegal in Ireland, a portion of the electricity generated by a wind park is temporarily stored in a 2 MW/12 MW h vanadium redox flow cell, and then fed into the network after a time delay [27].
2. For supplying reserve capacity and balancing energy
   Increasing use of decentralized generation facilities will also increase the demand for reserve capacity and balancing energy. Redox flow cell technology could also be used locally to meet or compensate for a portion of these energy requirements.
3. As back-up/UPS systems for emergency electricity supply and to operate stand-alone networks
   Surplus wind energy on King Island (Australia) is temporarily stored in a redox flow cell (200 kW/800 kW h) and then fed into the network as required. A vanadium redox flow cell there also powers a stand-alone network that supplies 1,800 people with electricity [27].
4. As storage for electro-mobility
   An advantage of using redox flow batteries for electro-mobility instead of lithium

ion batteries is that it would reduce charging times considerably. When the cell's electrolyte is depleted or discharged, the electrolyte liquid could be drained at a service station and then replaced with charged liquid. The process would then be similar to refueling with gas or diesel fuel. The drained electrolyte liquid could then be recharged electrically at the service station and sold to another customer. The process would therefore be reversible and regenerative. Compared to ion technology, the greatest disadvantage of these cells is the low energy densities. This reduces how far the car could be driven before refueling. Currently, a redox flow cell could power a car for only about a quarter of the distance that a lithium battery can [25].

### 7.6.8 Recycling, Environmental Friendliness, and Safety

The electrolyte can be either internally (by the charging process) or externally (by the recycling process) completely regenerated without requiring any vanadium losses. If the cell is improperly handled or damaged in an accident, the vanadium poses few risks. But the sulfuric acid (solvent) and vanadium dust that may be produced by drying or fire could cause significant problems.

### 7.6.9 Conclusion

- A unique feature of redox batteries is that the **storage container and the reaction cell are spatially separated**. As a result, almost any combination of energy and power can be achieved with this battery type.
- The technology is **highly developed**, but there are **many unanswered questions** that are still being investigated.
  - **Improved materials** could result in an efficiency of up to 90%.
  - Significantly lower resistance **electrodes** made of **carbon fibers** could be used in these cells.
  - Scientists are also researching the use of **cheaper materials** to **reduce facility costs**.

## References

1. Berndt D (1986) Bleiakkumulatoren, 11th edn. VDI-Verlag, Düsseldorf
2. Besenhard JO (1999) Handbook of battery materials. Wiley-VCH, Weinheim, New York
3. Bode H (1977) Lead-acid batteries. A Wiley-Interscience series. Wiley, New York
4. Bullock KR (1982) Self-Discharge in Acid-Starved Lead-Acid Batteries. J Electrochem Soc 129(7):1393. https://doi.org/10.1149/1.2124172
5. DIN (1979) DIN 41 772: Halbleiter-Gleichrichtergeräte. Beuth Verlag, Berlin
6. DIN (2011) DIN EN 50272-2 - Sicherheitsanforderungen an Batterien und Batterieanlagen – Teil 2: Stationäre Batterien; Deutsche Fassung EN 50272-2:2001. Beuth Verlag, Berlin
7. Dustmann C-H (1991) Zukunftschancen für Hochenergiebatterien. Batterien und Akkumulatoren
8. Eck G (1990) High temperature storage battery (European Patent 19880117185)
9. Ellis BL, Lee KT, Nazar LF (2010) Positive Electrode Materials for Li-Ion and Li-Batteries. Chem Mater 22(3):691–714. https://doi.org/10.1021/cm902696j
10. Engel KM (2005) Natrium-Batterien
11. Eulitz C-M, Scheuermann S, Thier H-J (1965) Brockhaus ABC Chemie. F.A. Brockhaus, Leipzig
12. Falk SU, Salkind AJ (1969) Alkaline storage batteries. The Electrochemical Society series. Wiley, New York
13. Goodenough JB, Kim Y (2010) Challenges for Rechargeable Li Batteries. Chem Mater 22(3):587–603. https://doi.org/10.1021/cm901452z
14. Hoppecke (2013) Rekombinationssystem für stationäre Batterien. http://www.hoppecke.de/produkte/zubehoer/aquagen_r_premium_top. Accessed 4 Sept 2013 (Hoppecke)
15. Jossen A, Weydanz W (2006) Moderne Akkumulatoren richtig einsetzen, 1st edn. Ubooks, Neusäß (36 Tabellen)
16. Kiehne H-A (2003) Batterien. Grundlagen und Theorie, aktueller technischer Stand und Entwicklungstendenzen, 5th edn. Kontakt & Studium, vol 57. Expert, Renningen (mit 51 Tabellen)
17. Lander JJ (1956) Further Studies on the Anodic Corrosion of Lead in H[sub 2]SO[sub 4] Solutions. J Electrochem Soc 103(1):1. https://doi.org/10.1149/1.2430227

18. Linden D (1995) Handbook of batteries, 2nd edn. McGraw-Hill, New York
19. Lu X, Lemmon JP, Sprenkle V, Yang Z (2010) Sodium-beta alumina batteries: Status and challenges. JOM 62(9):31–36. https://doi.org/10.1007/s11837-010-0132-5
20. Merck (2009) Produktinformationsbroschüre: Materials for Li-ion batteries and double-layer capacitors. Darmstadt
21. Moosbauer DJ (2010) Elektrochemische Charakterisierung von Elektrolyten und Elektroden für Lithium-Ionen-Batterien – Entwicklung einer neuen Messmethode für elektrochemische Untersuchungen an Elektroden mit der EQCM. http://epub.uni-regensburg.de/18757/. Accessed 4 Sept 2013 (Dissertation)
22. NGK (2009) Energy Storage System for Reducing CO2 Emissions. Hannover
23. NGK (2012) Cause of NAS Battery Fire Incident, afety Enhancement Measures and esumption of Operations. http://www.ngk.co.jp/english/news/2012/0607.html. Accessed 3 Oct 2013 (NGK Insulator, L.T.D)
24. NGK (2012) NGK Will Implement NAS® Battery Safety Enhancement Measures and Meticulous Quality Assurance in an Effort to Restore Confidence and Expand Business. http://www.ngk.co.jp/english/csr/pdf/csr2012_04.pdf. Accessed 19 Dec 2013 (NGK Insulator, L.T.D)
25. Noak J (2009) Verbesserte Redox-Flow-Batterien für Elektroautos. http://www.fraunhofer.de/de/presse/presseinformationen/2009/09/redox-flow-batterie-fuer-elektroautos.html. Accessed 3 Oct 2013 (PI 16.09.2009. Fraunhofer-Institut für Chemische Technologie ICT)
26. Novacheck F, Himelic J (2011) Sodium Sulfur Battery Energy Storage And Its Potential To Enable Further Integration of Wind (Wind-to-Battery Project). CO, Denver
27. Oertel D (2008) Energiespeicher – Stand und Perspektiven
28. Park M, Zhang X, Chung M, Less G, Sastry AM (2011) A review of conduction phenomena in Li-ion batteries
29. Pohl C, Kriebs K (2006) Prüfung von wirtschaftlichen Einsatzmöglichkeiten einer NaS-Batterie
30. Röhr C (2013) Chemie der Metalle. Oxide und Hydroxide. Universität Freiburg
31. Ruetschi P (2004) Aging mechanisms and service life of lead–acid batteries. J Power Sources 127(1):33–44. https://doi.org/10.1016/j.jpowsour.2003.09.052
32. Rüetschi P, Angstadt RT (1958) Self-Discharge Reactions In Lead-Acid Batteries. J Electrochem Soc 105(10):555. https://doi.org/10.1149/1.2428662
33. Rummich E (2009) Energiespeicher. Grundlagen, Komponenten, Systeme und Anwendungen. expert-Verl, Renningen (mit 22 Tabellen)
34. Schöpe F, Karden E, Küssel R (1997) Batteriemanagementsysteme für Elektrostraßenfahrzeuge. FAT-Schriftenreihe. Fat Frankfurt/m (132)
35. Sopicka-Lizer M (2010) High-energy ball milling. Mechanochemical processing of nanopowders. Woodhead Publishing in materials. Woodhead Publishing; CRC Press, Oxford, Boca Raton
36. Steudel RSY (2013) Polysulfide chemistry in sodium-sulfur batteries and related systems–a computational study by G3X(MP2) and PCM calculations
37. Tanka K (2013) Recent Sodium Sulfur Battery Applications in Japan. Nagoya
38. Thaller L (1976) Electrically Rechargeable Redox Flow Cell (US Patent 3996064)
39. Valoen LO, Reimers J (2005) Transport Properties of LiPF6-Based Li-Ion Battery Electrolytes. Kanada
40. Whittingham S (2004) Lithium Batteries and Cathode Materials. New York
41. Xu K (2004) Nonaqueous Liquid Electrolytes for Lithium-Based Rechargeable Batteries. Chem Rev (10):4243–4886
42. Zhang W-J (2011) A review of the electrochemical performance of alloy anodes for lithium-ion batteries. J Power Sources 196(1):13–24. https://doi.org/10.1016/j.jpowsour.2010.07.020
43. Zimmermann UD (2013) Oxidkeramik – Aluminiumoxid (Al2O3). Der bekannteste oxidkeramische Werkstoff. http://www.ceramtec.de/werkstoffe/aluminiumoxid/. Accessed 2 Oct 2013 (CeramTec GmbH)
44. ZVEI (2011) Merkblatt des ZVEI Nr. 3. Anforderungen an Elektrolyt und Nachfüllwasser für Bleibatterien

# Chemical Energy Storage

*Michael Sterner, Franz Bauer, Fritz Crotogino, Fabian Eckert, Christian von Olshausen, Daniel Teichmann, and Martin Thema*

**8.1 Basics – 327**
8.1.1 The C–H–O System as a Foundation for Energy Storage – 327
8.1.2 Hydrogen as Energy Source – 329
8.1.3 Hydrogen Production – 333
8.1.4 Thermodynamics of Water Splitting – 340
8.1.5 Electrolytic Conductivity – 346

**8.2 Storing Technology Electrolysis – 352**
8.2.1 Overview – 352
8.2.2 Electrolysis Cell—Electrolysis Type – 354
8.2.3 Electrolysis Block—Stack Design – 359
8.2.4 Electrolyzers, Electrolysis Facilities, and Their Peripherals – 360
8.2.5 Comparison of Different Electrolyte Technologies – 362
8.2.6 Increasing Efficiency by Using Waste Heat – 362

**8.3 Storing Technology-Methanation and Chemical Synthesis – 369**
8.3.1 Overview of Methane as an Energy Source – 369
8.3.2 $CO_2$ Sources for Power-to-X (PtX) – 371
8.3.3 Chemical Methanation – 373
8.3.4 Biological Methanation – 380
8.3.5 Methanol Synthesis – 388
8.3.6 FT Process – 393

**Electronic supplementary material** The online version of this chapter (https://doi.org/10.1007/978-3-662-55504-0_8) contains supplementary material, which is available to authorized users.

© Springer-Verlag GmbH Germany, part of Springer Nature 2019
M. Sterner, I. Stadler (Eds.), *Handbook of Energy Storage*, https://doi.org/10.1007/978-3-662-55504-0_8

**8.4 Storage Media and Holding – 400**
8.4.1 Gaseous Storage Media – 400
8.4.2 Liquid Storage Media – 413
8.4.3 Solid Storage Media – 422

**8.5 Extraction Technologies – 425**
8.5.1 Electricity Generation Using CHP Generation – 426
8.5.2 Building Heating and Cooling Supply – 433
8.5.3 Mobility and Transport – 439

**8.6 The Storage System PtG – 441**
8.6.1 The Beginnings of PtG – 442
8.6.2 PtG Hydrogen – 445
8.6.3 PtG Methane – 447
8.6.4 Efficiency, Potentials, $CO_2$ Emissions, and Costs – 453
8.6.5 Advantages and Disadvantages of Hydrogen and Methane – 459

**8.7 The Storage System PtL – 461**
8.7.1 PtL for Producing Fischer-Tropsch Liquid Fuels – 463
8.7.2 PtL for Producing Methanol – 463
8.7.3 Efficiency, Costs, and Early Markets – 464

**8.8 Ocean Fuels as Further Development of PtG and PtL – 465**
8.8.1 Raw Materials and Fuels from the Ocean—Issues of Potential and Acceptance – 466
8.8.2 Floating Wind Platform Option – 469
8.8.3 Sail-Powered Energy Option – 471

**8.9 $CO_2$ Reduction by Energy Systems PtG, PtL, and Ocean Fuels – 474**

**8.10 Summary – 475**

**References – 478**

**Overview**

Purely **electrical** energy storage technologies are **very efficient**, however they are also very expensive and have the smallest **capacities**. **Electrochemical**-energy storage reaches higher capacities at smaller costs, but at the expense of efficiency. This pattern continues in a similar way for **chemical-energy storage**. In terms of capacities, the limits of batteries (accumulators) are reached when low-loss long-term storage is of need. Chemical-energy storage and stocking fulfills these requirements completely. The storing itself may be subject to significant efficiency losses, but, from today's point of view and in combination with the existing gas and fuel infrastructure, it is the **only** national **option** with regards to the **long-term storage of renewable energies**.

Chemical-energy storage is the **backbone** of today's conventional energy supply. Solid (wood and coal), liquid (mineral oil), and gaseous (natural gas) **energy carriers** are 'energy storages' themselves, and are stored using different technologies. In the course of energy transition, chemical-energy storage will be of **significant importance**, mainly as long-term storage for the power sector, but also in the form of **combustibles and fuels** for transport and heat. Not only are conventional storing technologies discussed within this chapter, but a detailed explanation is also given about the storage of renewable energies in the form of gaseous (power-to-gas, PtG) and liquid (power-to-liquid, PtL) energy carriers for electricity, heat, chemicals, and in the form of synthetic fuels.

## 8.1 Basics

### 8.1.1 The C–H–O System as a Foundation for Energy Storage

The three crucial elements of the chemical energy industry—and therefore of chemical storage—are Carbon (C), Hydrogen (H), and Oxygen (O) .

Figure 8.1 shows the chemical structure of organic compounds as well as their combustion products. The connecting lines between oxygen, hydrogen, and carbon have to be divided according to the ratio of the material's composition. This figure shows the three elements and the related compounds of interest for the energy industry:

- $H_2O$ and $CO_2$ as combustion products, as well as all of their mixtures, which can be found on the line of combustion products between these two compounds.
- $CH_2O$ as representative for biomass (sugar: $C_6H_{12}O_6$) and its dehydration products. peat, lignite, stone coal, and anthracite on the carbonization line between $CH_2O$ and C.
- Gaseous and liquid hydrocarbons, thus methane, liquid gases, gasoline, diesel kerosene, and waxes are, in order of their increasing chain length, strung between $CH_4$ and $CH_2$ (representing an infinitely long hydrocarbon chain).
- All alcohols (not depicted), which are, because of their hydroxyl group, located to the right of their respective hydrocarbon.
- The energy content and, thus, the storage potential of a substance increase with its proximity to the HC axis of hydrocarbons, and decrease with a growing rate of oxidation and the proximity to oxygen.

#### Fossil Energy Industry and Biomass Usage are a One-Way Street

The major movement in this system is the one from left to right by combustion of stored chemical compounds. Figure 8.2 shows the most important correlations in the chemical energy industry: processes of the fossil energy industry are characterized by the combustion of hydrocarbons and coal, i.e., their oxidation and their transition into combustion products. It becomes obvious that the fossil energy industry only moves from left to right. The reduction of the global biomass stock, mainly in the form of unsustainable deforestation of rainforests, as well as the exploitation of peat, follow the

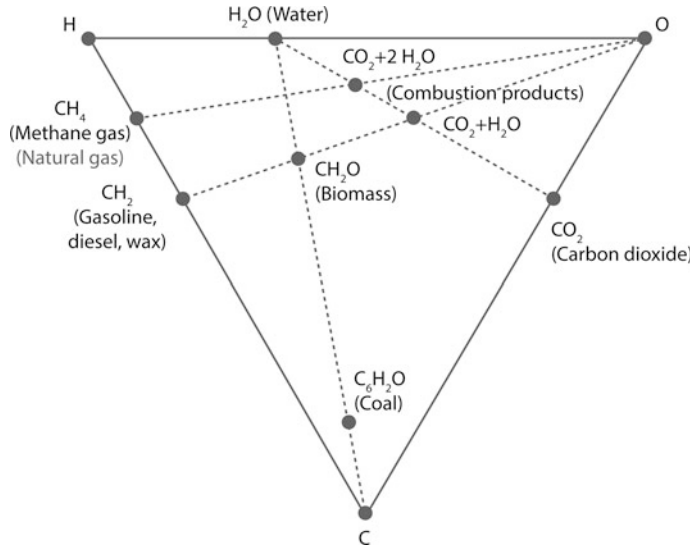



**Fig. 8.1** Structure of the fossil system with the elements carbon, hydrogen and oxygen [49]

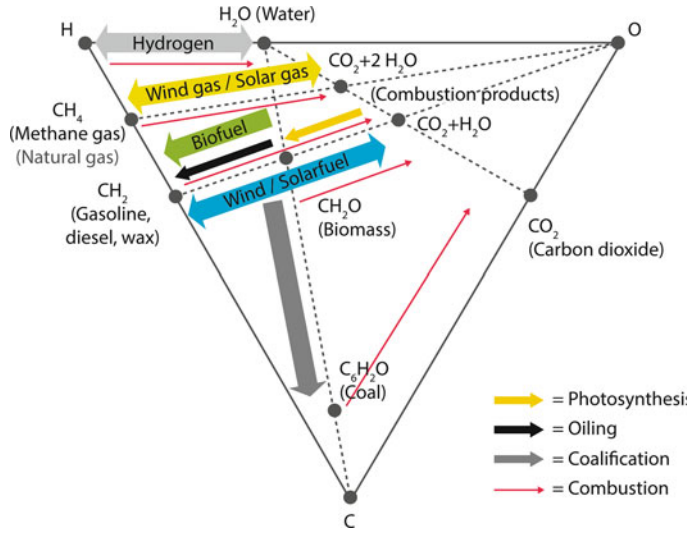



**Fig. 8.2** Natural photosynthesis and its imitation using water electrolysis and synthesis for energy storage and for closing the carbon cycle [49]

same principle and consequently increase the amount of $CO_2$ in the atmosphere.

## Natural and Artificial Photosynthesis Close the Carbon Cycle

The only natural countermovement or alternative to the fossil energy industry is photosynthesis. Powered by solar energy, it produces biomass, and thus an energy containing a starting point for fossil energy carriers that moves away from combustion products. However, its volume is much too small to supply the demand of energy carriers humanity has. This bottleneck is the reason why biogenic hydrocarbons and biogenic coal from hydrothermal carbonization (dark-gray arrow, which is also called biochar) cannot represent a solution to supplying the demand for chemical energy carriers.

In order to overcome this bottleneck, the concept of hydrogen economy (light-gray arrow) came up. This is a most important ability which refers to the production of chemical energy carriers by electrolysis, working inde-

pendently of photosynthesis. This has made it possible to transform the one-way street of combustion into a closed cycle without biogenic processes.

Since, because of storage and transportation issues, it is not possible to adapt all applications which, so far, were powered by hydrocarbons to hydrogen, concepts for synthetic hydrocarbons have emerged recently (yellow arrow: wind/solar methane, windgas, PtG; blue arrow: PtL).

Existing gas storage capacities and gas power plants can be used via PtG, and thus provide sufficient long-term storage, which is a problem today in the power-grid (▶ Chap. 3). This also creates an option for supplying the future storage demand in the heat sector (▶ Chap. 4). Air traffic and terrestrial long-distance transport in particular depend on the higher-energy density of liquid hydrocarbons (▶ Chap. 5). This higher-energy density is based, firstly, on the greater molecule-specific calorific value, and secondly, on the liquid or solid state of aggregation (gasoline, diesel, kerosene, and paraffin waxes).

#### ▪ Wind and Hydropower, Solar, and Geothermal Energy as the Only Energy Options

In order to actually close the carbon cycle, it is essential that the energy needed for the technically recreated photosynthesis is provided by carbon-free energy carriers, such as wind power, solar energy, hydropower, or geothermal energy. All other options which include the usage of carbonaceous energy carriers, such as fossil energy or biomass, would not close the cycle because losses in the processes lead to higher $CO_2$ emissions. Nuclear energy, low in $CO_2$, is not to be taken into consideration because it creates yet unsolved waste and security problems, leading to incalculable follow-up costs. From today's point of view, the transformation of the remaining renewable, carbon-free energy sources is the cheapest option to closing the carbon cycle, which makes water electrolysis the crucial technical component for this option.

The volume of gases is always given in standard cubic meter $m^3_n$

**Definition**

A standard cubic meter is a unit of volume for gases. It is used for the comparison of gas quantities at different temperatures and pressures.

Gases are compared in their physical standard conditions at $T_n = 273.15\,\mathrm{K} = 0\,^\circ\mathrm{C}$.

### 8.1.2 Hydrogen as Energy Source

#### ▪ Discovery and Deposit

Hydrogen was discovered and described for the first time in 1766 by the English physician and chemist Henry Cavendish, when researching metals and acids. In 1787, the French chemist Antoine de Lavoisier proved in an experiment that the mass of all reactants remains the same in chemical reactions. In the course of his research he discovered oxyhydrogen, the existence of which he proved in the aforementioned experiment. In further experiments he transformed oxyhydrogen into water which, for him, was the crucial reason for giving it the name 'hydrogen'. Its name and its symbol H is based on the Latin word 'hydrogenium' ('water producer'), or the ancient Greek term 'hydor gignomai' ('becoming/creating water') [90].

Hydrogen is the lightest gas and is listed first in the periodic table of elements. The most common isotope consists of one proton and one electron. Hydrogen is colorless and odorless and is rarely found in its pure form in nature due to it being highly reactive and, therefore, forming many chemical bonds. Hydrogen is part of almost all organic compounds in nature, and is part of chemical compounds, such as hydrocarbons and, of course, water. The Earth's crust consist of ca. 50% hydrogen, which makes it the most common element on the Earth [131].

**Table 8.1** Important parameters of hydrogen [38]

| | |
|---|---|
| Gas density | 0.0899 kg/m$^3$ |
| Molar mass | 2.0158 kg/mol |
| Critical point | $T = 33.19\,\text{K}$, $p = 13.15\,\text{bar}$, $\rho = 0.03012\,\text{kg/L}$ |
| Triple point | $T = 13.956\,\text{K}$, $p = 0.072\,\text{bar}$ |
| Boiling point at 1 bar | $T = 20.39\,\text{K}$, $\rho = 0.07079\,\text{kg/L}$ |
| Specific heat capacity $c_p$ at 25 °C and 1 bar | 14.3 kJ kg$^{-1}$ K$^{-1}$ |
| Thermal conductivity $\lambda$ at 25 °C and 1 bar | 0.1861 W m$^{-1}$ K$^{-1}$ |
| Specific low calorific value at 0 °C and 1 bar | 3.0 kW h/m$^3$ or 33.4 kW h/kg |
| Specific high-calorific value at 0 °C and 1 bar | 3.55 kW h/m$^3$ or 39.5 kW h/kg |
| Production cost of fossil hydrogen | 4 ct/kW h or 1.34 €/kg (in 2014) |
| Production cost of renewable hydrogen | 25–30 ct/kW h or 8–10 €/kg (in 2014) |

8

### Properties

Hydrogen is highly flammable and much lighter than air. It has a very large ignition range from 4.0–77% at an ignition temperature of 560 °C, which means it is highly reactive and not problem-free in relation to safety. Hydrogen cylinders are marked with red shoulders. It is possible that gas escaping at a high velocity ignites itself. Its 33.3 kW h/kg make hydrogen the gas with the highest gravimetric energy-density, under standard conditions, however, its volumetric energy density of 3 kW h/m$^3$ is only one-third that of natural gas. This puts hydrogen at the bottom of the list of chemical energy carriers [38]. Important characteristics of hydrogen can be found in Table 8.1.

### Advantages and Disadvantages as an Energy Source

The comparative advantages and disadvantages of hydrogen as an energy source are listed below.

Advantages:

- Endless supply since it is the most common element on Earth.
- Sustainable production from renewable electricity, solar-thermal energy, and biomass.
- Clean combustion producing only water.
- Highest gravimetric energy density of all gasses.
- Practically insoluble in water.
- High-efficiency exceeding 'cold' combustion in fuel cells since it is not dependent on the Carnot limit.
- Can be used flexibly in all areas including electricity, heating, and transport.
- No technical or economical restrictions since hydrogen can be flexibly converted into other energy sources.

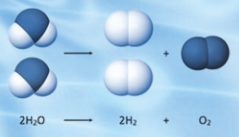
Disadvantages:

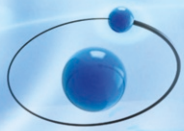
- Since hydrogen is a very small atom, it diffuses extremely easily and may cause embrittlement of pipes and tanks.
- Extremely combustible because of its very large ignition range.
- Difficult to burn in conventional gas power stations because of its high flame velocity.
- Energy density is higher with hydrogen than batteries or pumped-storage, but lower than with hydrocarbons.
- Since hydrogen is found exclusively in compounds and cannot be 'mined' easily like other raw materials, hydrogen production is energy-intensive—for example, with an efficiency ranging from around 54 to 84% using water electrolysis.

# HYDROGENICS

SHIFT **POWER** | **ENERGIZE** YOUR WORLD







Hydrogenics: shifting power to renewable hydrogen

www.hydrogenics.com

Today, hydrogen is primarily used as a material in the chemical industry, and as an energy source, but only to a very limited extent for fuel in the aerospace sector [44]. Hydrogen has enormous potential as a replacement for fossil fuels. But since hydrogen is currently produced almost exlusively using fossil hydrocarbons, replacing conventional fuels with hydrogen makes little sense until hydrogen is renewable. Various renewable hydrogen storage systems are described in detail in ▶ Sect. 8.6.1.

#### The Chicken or the Egg

The challenge of using hydrogen as an energy source is currently a chicken or the egg dilemma. Without an infrastructure there are very few consumers, but without consumers there is little infrastructure. If there are no hydrogen filling stations, then consumers do not purchase hydrogen vehicles. In addition, vehicles driven purely by hydrogen cost over €100,000, and are therefore far too expensive for the average consumer. Technical problems aside, these costs will only fall if the vehicles are mass produced. But since there are no consumers, building a hydrogen infrastructure is not ecomonical. Integrating hydrogen methanation may be a solution. This entails additional costs and a loss in efficiency, but would make hydrogen available using the existing natural gas infrastructure as well as for gas applications in all energy markets.

### 8.1.3 Hydrogen Production

Hydrogen's high-energy density is its greatest advantage compared to other storage technologies. But this high level of chemical energy is also required to produce hydrogen from water or other materials, and is determined by the laws of thermodynamics. As a result, the energy source used and the efficiency of its production are decisive technical and energetic factors when comparing hydrogen to other technologies.

#### Overview of Hydrogen Production

Hydrogen can be produced in a variety of ways (◘ Fig. 8.3). Besides water electrolysis with its special relevance for energy storage, thermal processes are also standard. Photolytic processes are still in the early phases of research. Electric, thermal, and chemical energy as well as electromagnetic radiation energy (light energy from photons) can be used as an energy source.

Although fossil energy sources dominate hydrogen production, exlusive use of renewable energy could make hydrogen production climate-neutral. As a result, this chapter focuses on water electrolysis. The following section briefly describes the principle methods of producing hydrogen.

#### Global Hydrogen Production and Consumption

At an industrial scale, currently hydrogen is chiefly produced using steam reformers. In this process hydrocarbons with a high hydrogen percentage such as methane or methanol are reformed. Other conversion processes, such as chlor-alkali electrolysis or coal gasification, use fossil source materials [9, 116].

Annually, about 20 billion $m^3$ of hydrogen is produced in Germany. Worldwide, about 500 billion $m^3$ or about 50 million tons is produced, amounting to about 2% of global primary energy consumption [9, 40, 112]. Across the world, hydrogen is produced almost exclusively from fossil hydrocarbons:

- Natural gas (48%)
- Liquid hydrocarbons (30%)
- Coal (18%)
- Water electrolysis (4%)

Hydrogen consumption worldwide is difficult to quantify. This is because large quantities are produced and consumed on-site at chemistry parks, and as a result, not included in statistics [112]. Hydrogen is often directly reused as a component in synthesis gas. Worldwide, synthesis gas is used for [9]:

- ∼ 51% for ammonia production
- ∼ 35% crude oil refineries for hydrogenation processes
- ∼ 8% for methanol production

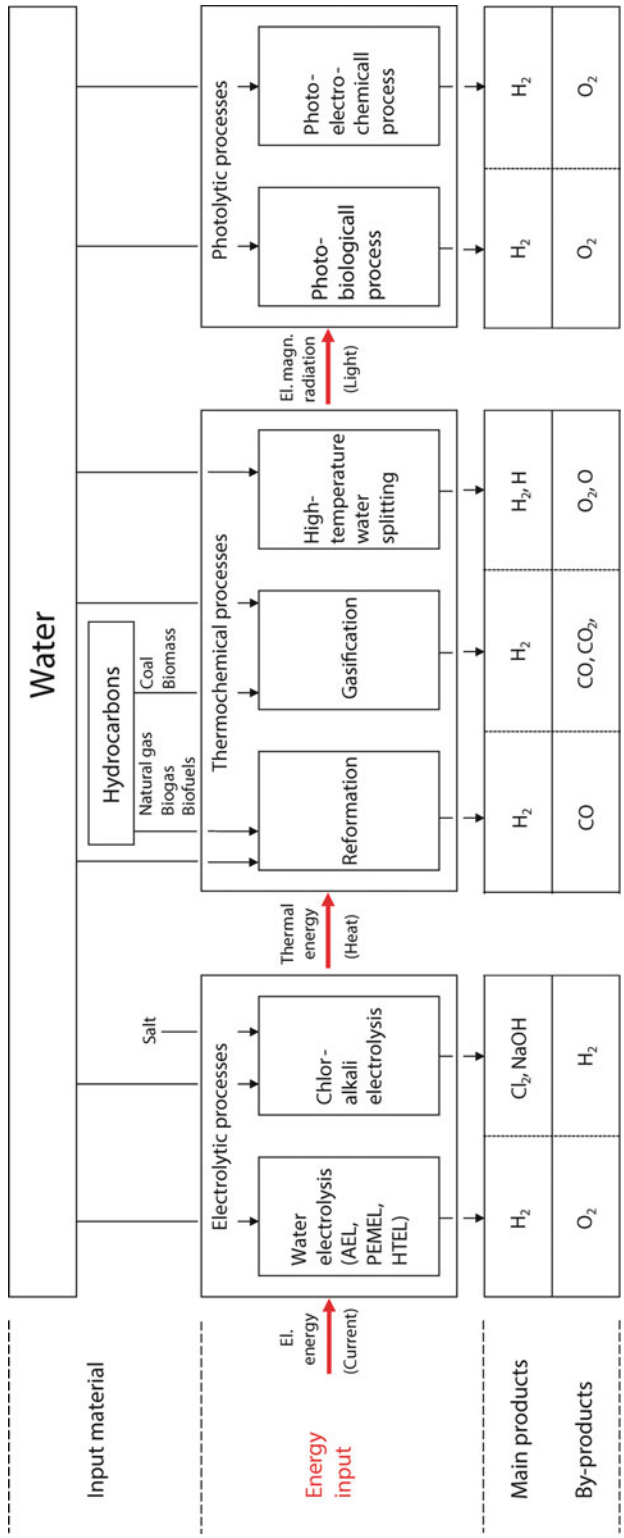



**Fig. 8.3** Various methods of producing hydrogen

Like synthesis gas, hydrogen itself is also used primarily for these three applications. According to [40], in 2010 hydrogen was used for the following applications:

- ~ 45% for producing ammonia (fertilizers).
- ~ 46% in crude oil refineries for reducing and hydrogenating long-chain hydrocarbons to produce gasoline, diesel, or kerosene (for example for hydrocracking and hydrodesulfurization).
- ~ 4% to produce methanol (for example, for use as a basic chemical material).
- ~ 2% in metal production and processing (for example, in metallurgy as a shielding gas for welding and cutting).
- ~ 1% in the electronics industry (for example, for semi-conductor manufacture).
- ~ 1% in the food industry (for example, for hydrogenating liquid oils to solid fats, e.g., vegetable oil to margarine).
- ~ 1% in other processes (for example, hydroformylation, also called oxo-synthesis, or as a cooling agent for large synchronous generators in conventional power plants).

Hydrogen is conventionally produced primarily by reforming natural gas. This is because at 1 €/kg, the production costs with this process are by far the lowest. In comparison, the cost of hydrogen from renewable energy currently ranges from 6 to 10 €/kg. As a result, external costs incurred by fossil $CO_2$ are a key factor in determining the economic viability of renewable hydrogen.

### 8.1.3.1 Electrolytic Processes

#### Water Electrolysis

Discovered over 200 years ago, electrolytic water splitting is, in principal, not a new technology. But in the context of energy storage using PtG and PtL, it has become a crucial core component of chemical-energy storage.

The discovery of the voltaic pile in 1799—basically the first reliable, continuous electricity source—led to the first experiments with electrolysis. The electrolysis process uses electric currents to produce a redox reaction. This principle was discovered in 1800 by the scientist Johann Wilhelm Ritter (1776–1810) in Germany and, at the same time, by William Nicholson, Anthony Carlisle, and William Cruickshank in England.

Ritter demonstrated that odorless, galvanic hydrogen and oxygen were produced by decomposing water. In his forward to Ritter's article, the journal's publisher and Ritter's former teacher Johann Heinrich Voigt described the gas mixture produced by electrolysis as 'life air', or flammable air that, when ignited, released heat, light, and water. Voigt hypothesized that the "warming and shining element of sunshine" was in the gases or in the forces that they released (J. W. Ritter in [125]). This reasonable hypothesis was based on the observation that oxyhydrogen reactions release heat and radiation energy like the Sun. In addition, Voigt had previously recognized that this process plays a role in photosynthesis:

> After observing the vesicle columns (electrolysis) in fig. 3 (Fig. 8.4 left), it seems probable that a very similar process causes plants to grow. Of the sunshine so essential to vegetation, the warming element is perhaps in the Earth, and the shining part in the air. These elements are equivalent to the powers in silver and zinc in a voltaic battery. The device in fig. 3 (Fig. 8.4) clearly suggests that the rising vesicle of flammable gas comes from the Earth where there is water from rainfall. This produces quantities of materials that nourish the plant and cause it to grow. These are then deposited where they are required …

The reversal of oxyhydrogen reactions by water electrolysis using solar energy is, therefore, a process that imitates nature.

This first experiments in 1800 resulted in the discovery of the three principal water electrolysis processes still used today. These are described in detail in ▶ Sect. 8.2:

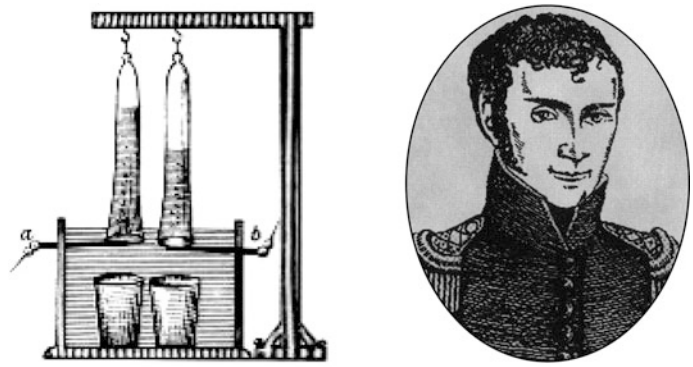


**Fig. 8.4** The first alkaline electrolyzer (experiment by Johann Wilhelm Ritter in 1800) proving that hydrogen and oxygen were produced in a ratio of 2:1

1. Alkaline electrolysis (AEL)
2. Membrane electrolysis or acid electrolysis (proton exchange membrane) PEMEL
3. High-temperature electrolysis (solid oxide electrolysis) HTES or SOEL

8

#### ■ Production as a By-Product of Chlor-Alkali Electrolysis

Chlorine is a very common basic chemical produced by chlor-alkali electrolysis using electricity and brine. If salt (sodium chloride) is dissolved in the water of an electrolysis system, chlorine, in addition to hydrogen, is produced. The electrolysis of aqueous sodium chloride produces combustible chlorine gas. As with water electrolysis, this means that the products must be separated at the moment they are produced. As a result, in a chlor-alkali electrolysis cell the anode compartment and cathode compartment are separated. The cells are connected in series in a cell room, and supplied with salt solution in parallel. They consume enormous quantities of electricity, which must often be supplied by dedicated, high-voltage lines (for example 220 kV).

Three chlor-alkali electrolysis processes have been developed. The diaphragm process came first, but was then replaced by the amalgam process because it required extensive cleaning. This amalgam process, however, works with mercury, resulting in toxic mercury contamination of the air and water. As a result, new materials were developed, beginning in the 1970s, that led to the membrane process.

Figure 8.5 shows a ThyssenKrupp Electrolysis GmbH facility of this type in Marl, Germany.

In the membrane process, 31% salt brine is separated from water using a cation exchanger membrane. The membrane is permeable to sodium ions, but not to chloride ions and hydroxide ions. When current is applied, chlorine gas is produced at the anode and hydrogen gas at the cathode. The gasses are then separately collected. The remaining hydroxide ions combine with the sodium ions to produce 33% sodium hydroxide. This is used as a by-product (Eq. 8.1):

$$2H_2O(l) + 2NaCl(aq) \rightarrow 2NaOH(l) + H_2(g) + Cl_2(g) \quad E^0 = -2.19\,V. \tag{8.1}$$

Worldwide, 45 million tons of chlorine are produced each year. An enormous quantity of hydrogen is, therefore, also produced as a by-product—around 14 billion $m^3$ or 3% of global hydrogen production. This hydrogen is either integrated in the chemical park where it is produced or not used at all [38, 112].

### 8.1.3.2 Thermochemical Processes

#### ■ Production from Natural Gas or Biomethane Using Steam-Reforming

The most common process worldwide for producing hydrogen is steam-reforming using fossil natural gas or low boiling point crude oil fractions (naphtha). In principal, this process can also use biomass. Fermentation of biomass



**Fig. 8.5** Vestolit GmbH chlor-alkali electrolysis facility in Marl, Germany with an annual production capacity of 237,000 tons sodium hydroxide and 210,000 tons of chlorine. The facility was designed by ThyssenKrupp Electrolysis GmbH (previously the electrolysis division of ThyssenKrupp Uhde GmbH), Dortmund (source: ThyssenKrupp Electrolysis GmbH)

such as corn, grass, or manure results in a biogas composed of methane gas and $CO_2$. Hydrogen can be produced from the methane gas using steam-reforming.

Carbon monoxide and hydrogen are produced from natural gas and water vapor in a gas-fired tubular oven (Eq. 8.2). The reactor contains a nickel catalyst. The natural gas is first desulfurized to prevent deactivation of the catalyst. The catalytic reaction is highly endothermic, and occurs at 800 to 900 °C and 20 to 40 bar. The overall process is allothermal [38]:

$$CH_4(g) + H_2O(g) \rightarrow CO(g) + 3H_2(g)$$
$$\Delta H_R^0 = +206\,kJ/mol. \quad \textbf{(8.2)}$$

In a further step, the carbon monoxide can then be converted to carbon dioxide with water vapor and a cobalt oxide or iron(II) oxide catalyst at 250 to 450 °C. The carbon dioxide can then be converted into more hydrogen. This homogenous, water-gas shift reaction is exothermic (Eq. 8.3). The reactor is designed and constructed to ensure that the reactor's kinetics and equilibrium are properly balanced. The carbon dioxide is washed out from the resulting gas mix under pressure with cold water. This leaves only the pure, water-insoluble hydrogen behind.

$$CO(g) + H_2O(g) \rightarrow CO_2(g) + H_2(g)$$
$$\Delta H_R^0 = -41.2\,kJ/mol. \quad \textbf{(8.3)}$$

Figure 8.6 shows a fired steam reformer designed by ThyssenKrupp Industrial Solutions AG (previously Uhde GmbH).

### ■ Production from Coal or Solid Biomass Using Gasification and Pyrolysis

Using pyrolysis (smoldering and degassing) in an airtight vessel, hydrocarbons can be decomposed by heat alone into coke (practically pure carbon), pyrolysis oil, and hydrogen-rich pyrolysis gas. Pyrolysis is also part of the gasification process. But oxygen, or air, is also supplied at one point in the process (partial oxidation). This allows the heat required to decompose the hydrocarbons to be produced by their own combustion. There are four steps in gasification:

1. Drying the hydrocarbons at about 200 °C.
2. Pyrolysis at 200–500 °C.
3. Oxidation: during partial combustion, the temperature increases up to 2,000 °C and parts of the hydrocarbons are decomposed into light gas components (CO, $H_2$, $H_2O$, $CO_2$ and $CH_4$).
4. Reduction: most of the synthetic gas components are produced by reducing CO and



**Fig. 8.6** Neste Oil Oyj steam-reforming facility in Porvoo, Finnland, with an annual hydrogen production capacity of 153,000 N $m^3$/h. The facility was designed by ThyssenKrupp Industrial Solutions AG (previously Uhde GmbH), Dortmund (source: ThyssenKrupp Industrial Solutions AG)



$H_2O$ (the Boudouard reaction in Eq. 8.4 and the homogenous water-gas shift reaction in Eq. 8.3):

$$C(s) + CO_2(g) \rightarrow 2CO(g)$$
$$\Delta H_R^0 = 159.9\,kJ/mol, \quad (8.4)$$
$$C(s) + H_2O(g) \rightarrow CO(g) + H_2(g)$$
$$\Delta H_R^0 = 118.5\,kJ/mol. \quad (8.5)$$

In addition, the heterogeneous water-gas shift reaction (Eq. 8.3) and the methane reaction (Eq. 8.6) occur during gasification. In this last reaction, carbon and hydrogen are converted to methane. Increasing the pressure results in a higher methane content:

$$C(s) + 2H_2(g) \rightarrow CH_4(g)$$
$$\Delta H_R^0 = -87.5\,kJ/mol. \quad (8.6)$$

Depending on the reactor type (fixed bed reactor, fluidized bed reactor, or entrained flow gasifier), gasification occurs at temperatures ranging between 800 and 1,500 °C at pressures ranging from 1 to 80 bar. The gas conversion rate ranges from 75 to 80%.

The resulting raw gas is converted to synthetic gas by gas purification. Using gas preparation (water-gas shift reaction to increase the hydrogen content, and $CO_2$ separation using absorption or wash-out), this is then processed to produce hydrogen [106].

Using this method, hard coal or lignite coal can be converted to fossil hydrogen. The best-known example in Germany is 'town gas', which is produced using water vapor and air as gasification agents. Town gas is a poisonous mixture of carbon monoxide and hydrogen. For many years, it was used as fuel in street lighting, to heat buildings, and for ovens.

On the same principle, hydrogen can also be produced by biomass gasification. Here, biomass is mechanically shredded (for example into woodchips), dried at 200 °C, and then gasified, cleaned, and prepared as hydrogen in a reactor.

Hydrogen can also be produced by pyrolyzing biomass. After being dried and shredded, woody biomass is decomposed at 400 to 450 °C and around 35 bar in a sealed container into coke and pyrolysis gas. The coke is then finely ground and again gasified to CO. The synthetic gas can then be prepared as hydrogen [124].

Besides the technical and economic restrictions, unlike water electrolysis, the biomass process depends on the availability and sustainable potential of biomass.

### ▪ Production Using Thermochemical Water Splitting with Concentrated Solar Energy

Concentrated solar-thermal energy in the form of high-temperature heat can be used in a va-

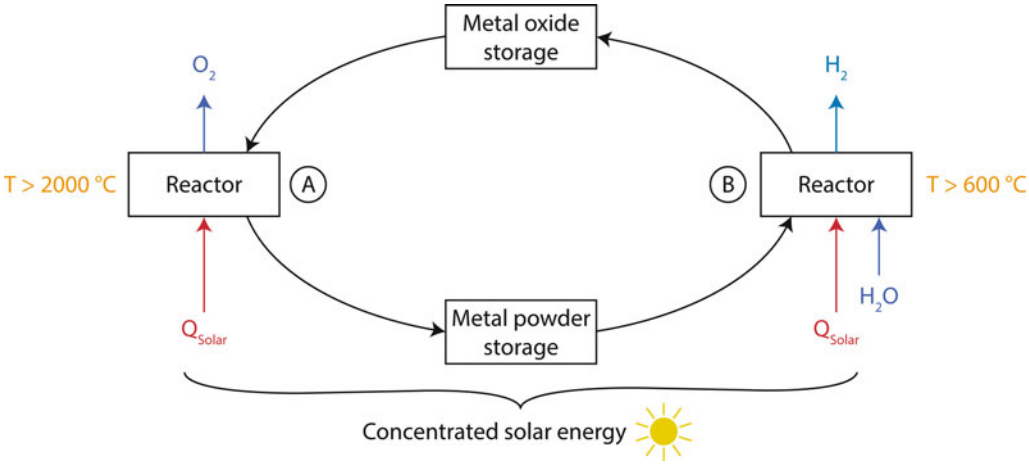



**Fig. 8.7** Operating principle of thermochemical water splitting in a two-step thermal cycle process

riety of ways to produce hydrogen. If no connection to the electricity network is available or the connection is prohibitively expensive, then using electricity from solar-thermal energy power plants for water electrolysis is a reasonable alternative. In addition, high-temperature heat can be used in steam electrolysis (▶ Sect. 8.2.2.2).

But since high-caloric heat is a driver of thermochemical cycle processes, it can also be used for thermochemical water splitting. At extremely high temperatures of 3,300 K, water vapor and hydrogen occur in the same concentrations at equilibrium. This means that, at these temperatures, water can be decomposed to hydrogen and oxygen solely by applying heat. But this approach is not technically feasible because the oxyhydrogen reaction causes the hydrogen to recombine back with the oxygen to form water vapor, and there are no materials that can selectively separate the hydrogen at these temperatures [131].

As with photosynthesis, which is also a difficult process to achieve in a single step (see ▶ Sects. 1.1 and 8.1.3.3), it makes sense to divide the process of water splitting using high-temperature heat into two-steps. This significantly reduces the temperature levels required. With this approach, metal oxides are selectively reduced and oxidized in a two-step thermal cycle process at temperatures ranging from 600 to 1,200 °C. These metals also function as catalysts. Ideally they remain unaltered and can be recycled. The high-temperature heat $Q$ for this process is produced by solar-thermal energy collectors. Figure 8.7 illustrates this process:

- In the first step, metal oxides such as zinc-oxide or iron oxide are reduced to metal powder using the concentrated solar heat $Q$. The metal oxides are, at the same time, dissociated into pure metal and oxygen. The metal is cooled, separated, and collected for the second step.
- In the second step, the metal reacts with water vapor to form hydrogen and metal oxide. The metal powder oxidizes. As a result, oxygen is extracted from the water vapor, leaving behind pure hydrogen. The solar heat $Q$ is required in this step to maintain the reaction.

The reactions with zinc-oxide are (Eqs. 8.7 and 8.8):

$$2\mathrm{ZnO(s)} \xrightarrow{\text{heat } Q} 2\mathrm{Zn(s)} + \mathrm{O_2(g)}, \tag{8.7}$$

$$2\mathrm{Zn(s)} + 2\mathrm{H_2O(g)} \rightarrow 2\mathrm{ZnO(s)} + 2\mathrm{H_2(g)}, \tag{8.8}$$

and with iron oxide (Eqs. 8.9 and 8.10):

$$\mathrm{Fe_3O_4(s)} \xrightarrow{\text{heat } Q} 3\mathrm{Fe(s)} + 2\mathrm{O_2(g)}, \tag{8.9}$$

$$3Fe(s) + 4H_2O(g) \rightarrow Fe_3O_4(s) + 4H_2(g). \quad (8.10)$$

Besides zinc and iron, other materials such as $H_2SO_4$ can also be used.

The thermochemical water splitting process is still in the early phases of research.

#### 8.1.3.3 Photolytic Process

For many years, researchers in biology have attempted to achieve photosynthesis in a single step. Similarly, there have also been many attempts to produce hydrogen using a photolytic process. This is because a photolytic process could make the chemical-catalytic production and other syntheses of hydrogen significantly more efficient from a biological and bioelectrochemical point of view. Although many approaches appear promising, this charging technology is still in its infancy. Extensive research is still required to develop an economical process with long-term reliability.



- **Production from Water Using a Photobiological Process with Micro-Organisms and Light Energy**

Photosynthetic micro-organisms such as green algae or cyanobacteria can split water into hydrogen and oxygen in light reactions. Using the special enzyme hydrogenase, the $H^+$ protons and $e^-$ electrons can be converted into pure hydrogen. Hydrogenases are microbial metal proteins that function as catalysts. They have mono-iron, di-iron, or nickel-iron at their catalytic sites, and are sensitive to oxygen. Depending on the strain of bacteria used, the hydrogenase composition and the internal processes in photosystem I and II (or in the hydrogen catalysis) differ [2].

Micro-organisms are basically similar to plants. Plants also use photosynthesis to split water with light energy, store hydrocarbons, and release oxygen. The difference is that micro-organisms release hydrogen instead of oxygen. Compared to other processes, this process is very slow. It is, nevertheless, a very promising avenue of research.

- **Production from Water Using a Photoelectrochemical Process with Special Semi-conductors**

Besides research on bio-inspired catalyst materials, special semi-conductors have been developed that can generate adequate voltage from sunlight for water splitting. In terms of current technology, this could be described as a photovoltaic (PV) and electrolysis cell combined in one. This photoelectrochemical system uses electromagnetic radiation energy to directly dissociate water into hydrogen and oxygen. Similar to PV cells, the various semiconductors are sensitive to various bandwidths and various areas of the spectrum.

The advantage of this method of producing hydrogen is that it is a very compact process with a wider choice of operating temperatures ranging from 0 °C to very high temperatures. The challenges include developing appropriate process-optimized materials, minimizing internal resistance losses, improving long-term stability despite corrosion, increasing the energy yield, and reducing system costs using advanced manufacturing technologies [15].

### 8.1.4 Thermodynamics of Water Splitting

Carbon-neutral methods of producing hydrogen are generally based on water electrolysis. As a result, this chapter focuses primarily on water electrolysis. ▶ Section 7.1 describes the electrochemical principles in detail. These principles are only briefly summarized here as they relate to water electrolysis.

#### 8.1.4.1 Complete Reaction and Maximum Efficiency

- **Complete Reaction**

The following is the complete equation for water electrolysis:

$$2H_2O(l) \xrightarrow{\text{el. energy}} 2H_2(g) + O_2(g). \quad (8.11)$$

The energy required by water splitting is determined by the Gibbs-Helmholtz equation:

$$\Delta H_R = \Delta G_R + T \cdot \Delta S_R, \tag{8.12}$$

Here $\Delta H_R$ is the usable reaction enthalpy, $\Delta G_R$ the free reaction enthalpy or Gibbs potential, $T$ the temperature in Kelvin, and $\Delta S_R$ the change in entropy. $\Delta H_R$ is the gross calorific value, or GCV (upper calorific value), of hydrogen, and $\Delta G_R$ the lower calorific value. The following are the standard conditions for one mole of hydrogen:

$$\Delta H_R^0 = 285.83 \frac{\text{kJ}}{\text{mol}}, \tag{8.13}$$

$$\Delta G_R^0 = 237.13 \frac{\text{kJ}}{\text{mol}}. \tag{8.14}$$

The zero in the index of the physical dimension indicates normal conditions are assumed: a temperature of $T = 298.15\,\text{K}$ (25 °C) and a pressure of $p = 1{,}013\,\text{hPa}$ (1 bar).

### ■ Decomposition Voltage and Theoretical Efficiency

Electrolytes are typically aqueous solutions of salts, acids, and leaches. The voltage required for their electrolysis is determined by Faraday's two laws:

1. The quantity of material deposited from the electrolyte $n$ is proportional to the charge $Q = I \cdot t$ flowing through the conductor:

$$n = k \cdot I \cdot t. \tag{8.15}$$

2. The same charge $Q$ always results in the same quantity of material deposited in different electrolytes:

$$k = \frac{1}{z \cdot F}. \tag{8.16}$$

Therefore, the quantity of material $n$ is:

$$n = \frac{I \cdot t}{z \cdot F} \tag{8.17}$$

and the charge $Q$.

$$Q = n \cdot z \cdot F \tag{8.18}$$

in A s or Coulomb (C) with:

$k$ – Electrochemical equivalent of the electrolyte,
$z$ – Number of electrons exchanged (with water splitting $z = 2$),
$F$ – Faraday constant derived from the elementary charge and the Avogadro constant: $F = 96{,}485\,\text{A s mol}^{-1} = 26.8\,\text{A h}$,
$I$ – Current-strength in the electrolyte,
$t$ – Duration of current flow.

The electrical energy required for decomposition $W_{el}$ is defined as follows:

$$W_{el} = U \cdot Q = U \cdot I \cdot t. \tag{8.19}$$

If the electrical energy $W_{el}$ is equated to the reaction enthalpy $\Delta G_R$ from Eq. 8.14 and the equation resolved for the voltage, when Faraday's law for $n = 1$ mole is integrated into the equation, the result is the theoretical minimum decomposition voltage, or reversible cell voltage:

$$U_{rev} = \frac{\Delta G_R^0}{n \cdot z \cdot F} = \frac{237.2\,\text{kJ}}{1\,\text{mol} \cdot 2 \cdot 96{,}486\,\text{A} \cdot \text{s/mol}} = 1.23\,\text{V}. \tag{8.20}$$

Since, however, due to the entropy $\Delta S_R$ the actual energy used is higher, the thermoneutral decomposition voltage is:

$$U_{th} = \frac{\Delta H_R^0}{z \cdot F} = \frac{285.9\,\text{kJ}}{1\,\text{mol} \cdot 2 \cdot 96{,}486\,\text{A} \cdot \text{s/mol}} = 1.48\,\text{V}. \tag{8.21}$$

These numbers reflect the thermodynamic efficiency, which is equivalent to the maximum attainable efficiency of water electrolysis when the water is in liquid form.

Table 8.2 presents all the values for water splitting in a two-phase system and in a gas-phase reaction.

Figure 8.8 shows the temperature dependencies of the various parameters. It should be noted that entropy rises together with temperature, and that the efficiency falls together with

**Table 8.2** Values for water splitting (based on [84])

| | Two-phase system: water in liquid form (25 °C, 1 bar) | Gas-phase reaction: water in gaseous form (100 °C, 1 bar) |
|---|---|---|
| Gibbs potential $\Delta G$ | 237.13 kJ/mol | 228.57 kJ/mol |
| Bonding enthalpy $\Delta H$ | 285.83 kJ/mol | 241.82 kJ/mol |
| Thermodynamic efficiency | 83.0% | 94.5% |
| Reversible cell voltage | 1.23 V | 1.18 V |
| Thermoneutral decomposition voltage | 1.48 V | 1.25 V |
| Reversible voltage temperature dependency | −0.85 mV/K | −0.23 mV/K |
| Thermoneutral voltage temperature dependency | 0 | 0.046 mV/K |



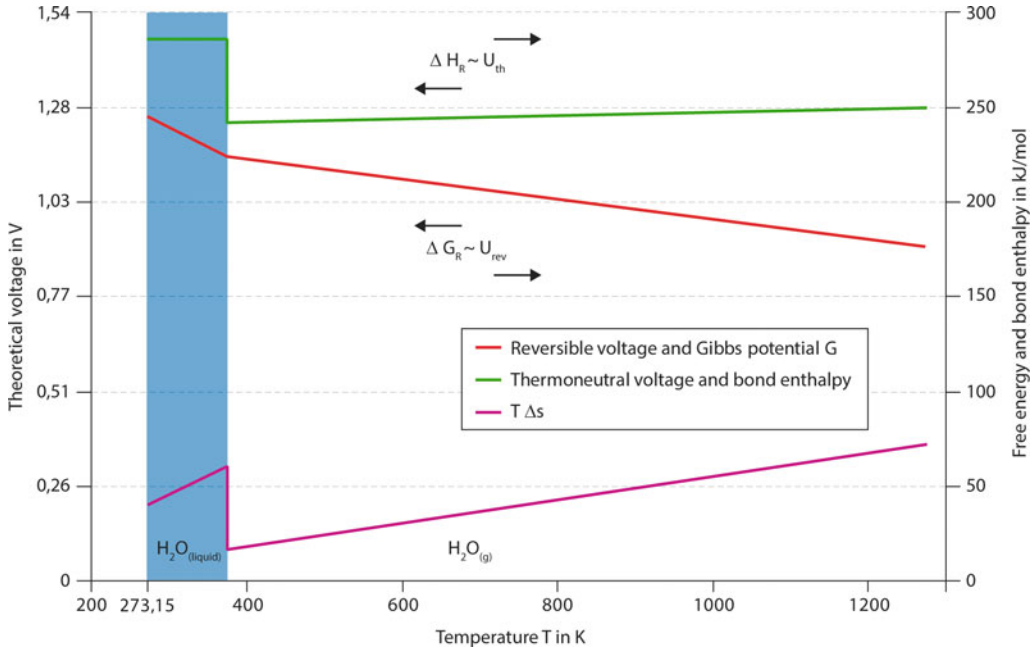



**Fig. 8.8** Temperature dependencies of standard parameters

the temperature. As a result, the ideal temperature for water (steam) electrolysis ranges from around 373 to 400 K. In practice it is, of course, technically difficult to maintain these ideal conditions. These effects are the topic of the next section.

### 8.1.4.2 The Nernst Equation and Additional Losses

The Nernst equation describes the relationship between the electrode potential and the concentrations of the materials involved in the

reaction. Using this equation, the change in free enthalpy $\Delta G_R$ and the open-circuit voltage (OCV) $U_0$ (also written as $\Delta E$ for electromotive force in older texts) can be computed for any redox reaction.

The Nernst equation is analyzed in detail in ▶ Chap. 7. The discussion in this section applies the equation specifically to water electrolysis:

$$\Delta G_R = \Delta G_R^0 + R \cdot T \cdot \ln\left(\prod_{i=1}^{k} \{a_i\}^{\nu_i}\right), \tag{8.22}$$

$$\Delta U = \Delta U^0 + \frac{R \cdot T}{z \cdot F} \cdot \ln\left(\prod_{i=1}^{k} \{a_i\}^{\nu_i}\right) \tag{8.23}$$

with:

$R$ – Molar gas constant $R = 8.31451\,\mathrm{J\,mol^{-1}\,K^{-1}}$,
$\{a_i\}$ – Activity of a material $i$ in relation to standard activity,
$\nu_i$ – Stoichiometric coefficient of the material $i$ (products +, educts –).

In 1889, Walther Hermann Nernst proved that two half-cells containing the same element with a single charge but in different concentrations produce a cell voltage of $U = 0.059\,\mathrm{V}$ per power of ten difference in concentration. Between half-cells with a double charge, the cell voltage is reduced by half. These voltages apply at a standard temperature of $T = 298.15\,\mathrm{K}$.

For electrolysis, by converting the natural logarithm to the common logarithm ($\ln(x) = \ln(10) \cdot \log_{10}(x)$), Eq. 8.23 becomes:

$$\begin{aligned} U &= U^0 + \frac{0.059\,\mathrm{V}}{z} \cdot \log_{10}\left(\frac{c_{Ox}}{c_{Red}}\right) \\ &= U^0 + \frac{0.059\,\mathrm{V}}{z} \cdot \left[\log_{10} c_{Ox} - \log_{10} c_{Red}\right]. \end{aligned} \tag{8.24}$$

### Reaction at the Cathode

A chemical redox reaction can be formulated for every electrode process. At the cathode, assimilation of an electron ($z = 1$) results in hydrogen:

$$\underbrace{H^+ + e^-}_{\text{oxid. components}} \rightarrow \underbrace{\frac{1}{2}H_2}_{\text{red. components}}. \tag{8.25}$$

Since the hydrogen immediately escapes, there is only a minimal change in concentration. In addition, for hydrogen formation at 25 °C the standard electrode potential $U_H^0$ is by definition equal to zero (RHE—reference hydrogen electrode, or alternatively, SHE—standard hydrogen electrode), and is used as the reference for all other electrode potentials.

The change in concentration of the oxidized components is equivalent to the change in proton or hydrogen ions. Applying the definition for pH value (an abbreviation for the Latin phrase, 'potentia Hydrogenium', or the potential of hydrogen), $\mathrm{pH} = -\log_{10}([H^+])$, the resulting potential at the cathode is:

$$\begin{aligned} U &= 0 + 0.059\,\mathrm{V} \cdot (\log_{10}([H^+]) - 0) \\ &= -0.059\,\mathrm{V} \cdot \mathrm{pH}. \end{aligned} \tag{8.26}$$

### Reaction at the Anode

At the anode, release of an electron produces oxygen as follows:

$$\underbrace{\frac{1}{2}H_2O}_{\text{oxid. component}} \rightarrow \underbrace{\frac{1}{4}O_2 + H^+ + e^-}_{\text{red. components}}. \tag{8.27}$$

The standard normal potential for oxygen formation is:

$$U^0 = +1.23\,\mathrm{V}. \tag{8.28}$$

The concentration of water remains basically constant, and is calculated into the standard normal potential. As with the cathode, the concentration of the resulting gases can be ignored.

As a result:

$$U = 1.23\,\mathrm{V} - 0.059\,\mathrm{V} \cdot \mathrm{pH}. \tag{8.29}$$

The sum of the electrode potentials derived from Eqs. 8.26 and 8.28 is the theoretical minimum decomposition voltage, and it is identical to Eq. 8.20.

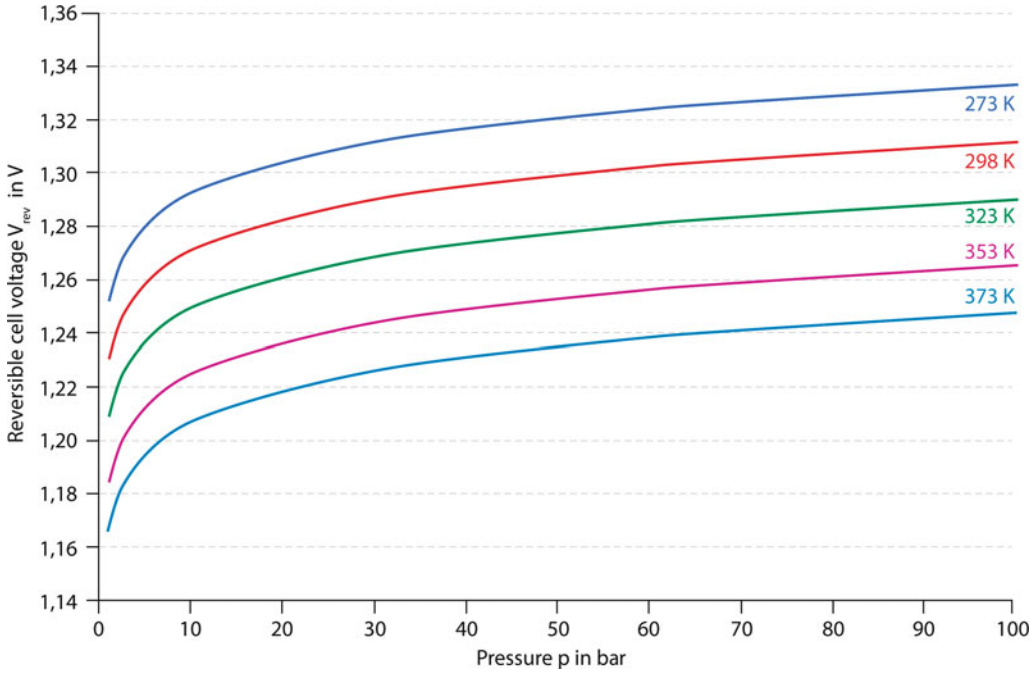



**Fig. 8.9** Effect of operating pressure on reversible cell voltage (minimum decomposition voltage) with water splitting at various temperatures

The effect of pressure on cell voltage at a constant temperature can be determined using the Nernst equation in Eq. 8.23:

$$U_{\mathrm{rev},p} = U_{\mathrm{rev}} + \frac{3 \cdot R \cdot T}{4 \cdot F} \cdot \ln\left(\frac{p}{p_0}\right). \quad \textbf{(8.30)}$$

Figure 8.9 applies this equation at various temperatures. The higher the operating temperature, the lower the cell voltage. But the cell voltage increases logarithmically as the pressure increases.

### Kinetic Effects and Voltage-Drops in Electrolysis Cells

As with batteries, kinetic effects that cause voltage-drops in the cell also occur with electrolysis. Like friction in engineering mechanics, partial processes such as diffusion, migration, or adsorption of the charge carriers cause 'friction losses' detectable by voltage-drops. In addition to the minimum decomposition voltage $U_{\mathrm{rev}}$, these 'overvoltages' at the cathode, anode, and possibly at the diaphragm or membrane, must also be take into account with water electrolysis. When the charge carriers are activated, these overvoltages appear as polarization losses at the boundary between the electrodes and electrolytes. They depend on the electrode material and the gasses produced (Fig. 8.10).

In addition, there are irreversible losses that depend on the current density, and as with all electrical systems, ohmic losses caused by the circuit's internal resistance. As a result, in reality the actual cell voltage $U_{\mathrm{cell}}$ ranges from 1.5 to 2.0 V and is given by [6]:

$$U_{\mathrm{cell}} = U_{\mathrm{rev}} + I \cdot (R_{\mathrm{A}} + R_{\mathrm{K}}) + U_{\mathrm{El,A}} + U_{\mathrm{El,K}} + U_{\mathrm{G,A}} + U_{\mathrm{G,K}} + U_{\mathrm{D}} + |\eta_{\mathrm{A}}| + |\eta_{\mathrm{K}}| \quad \textbf{(8.31)}$$

with

$I(R_{\mathrm{A}} + R_{\mathrm{K}})$ – ohmic voltage drop at the electrodes—linearly—dependent on the current-strength,

$U_{\mathrm{El,A}} / U_{\mathrm{El,K}}$ – ohmic voltage drop in the electrolyte—linearly-dependent on the current-strength,

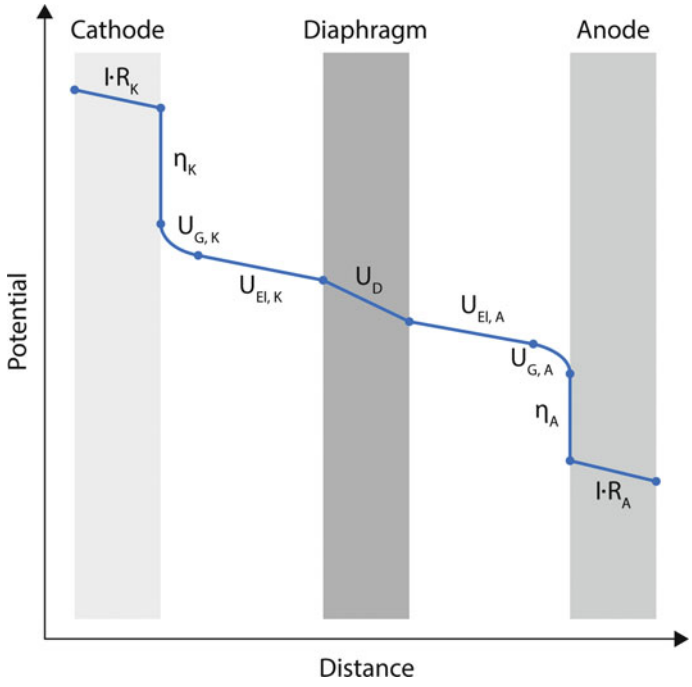



**Fig. 8.10** Voltage-drops in an electrolyte cell [6]

$\eta_A$ – overvoltage at the anode—logarithmically-dependent on the current-strength,
$\eta_K$ – overvoltage at the cathode—logarithmically-dependent on the current-strength,
$U_{G,A}/U_{G,K}$ – voltage drop caused by gas-bubble formation between the electrodes and the diaphragm—linearly-dependent on the current-strength,
$U_D$ – ohmic voltage drop in the diaphragm—linearly-dependent on the current-strength.

The ohmic losses at the electrodes can be minimized by ensuring that they are in good contact and by reducing the formation of oxide layers.

The voltage drop in the electrolyte can be reduced by minimizing the distance between the electrodes as much as possible and increasing the electrolytic conductivity. The overvoltages at the anode and cathode can be reduced by thermal activation, i.e., by increasing the electrolyte temperature, or by catalytic activation of the electrodes.

Gas-bubble formation between the electrodes and the diaphragm produces an electrolyte-gas mixture with a significantly lower conductivity than pure electrolyte. In addition, gas-bubbles on the electrodes reduce the active surface area. To minimize gas-bubble losses, gas-permeable electrodes should be used where possible. This allows product gasses on the reverse side of the electrode to move away more quickly.

The ohmic losses $U_D$ occur only in cells with a diaphragm or membrane. They play a crucial role when the electrodes are placed directly on the diaphragm (membrane) [6].

In a simplified form, the overall efficiency with all specific losses taken into account can be formulated as:

$$\eta_{ges} = \frac{U_{rev}}{U_{cell}}. \qquad \textbf{(8.32)}$$

Figure 8.11 shows the cell voltage's dependency on current density, the minimum decomposition voltage $U_{rev}$, and the voltage loss shares. At high current-densities, due to thermal losses cell cooling is required.

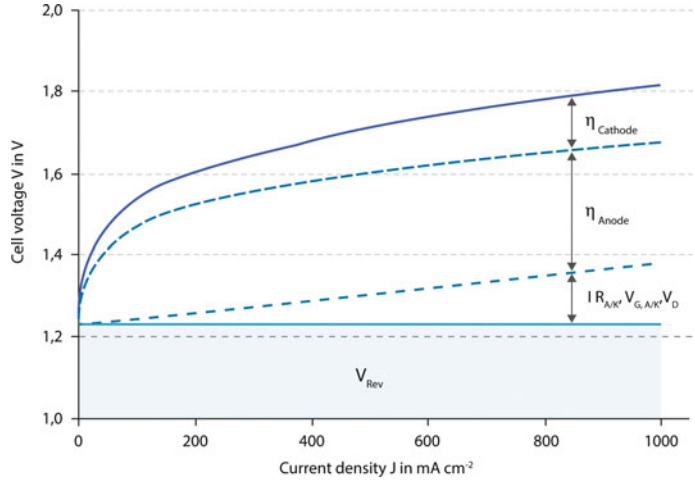



**Fig. 8.11** Cell voltage compared to current density [96]



### 8.1.5 Electrolytic Conductivity

With electrolysis, various charge carriers enable current flow. Here electrical conductivity must be carefully distinguished from electrolytic conductivity. In metals, electrons enable electricity transport. With electrolytic conductivity, ions are transported in melts or solutions of salts, acids, or leaches. An electrolyte dissolved in a suitable solvent forms solvated ions or hydrogenated ions with water.

The force driving this process is the energy released by the formation of molecular solvent shells around the ions. If this energy is not at least as large as the cohesive force of the electrolyte (with salts this is equivalent to the grid energy), then no dissolution takes place. All electrochemical processes are determined by specific laws and formulas. The following section focuses on only a selection of the most important relationships discussed in [75].

#### 8.1.5.1 From Ion Transport to Electrical Current Flow

■ **Calculating Ion Forces**

For every electron absorbed, an electron is shed. Although these two processes are physically separated at the cathode and anode in electrochemical reactions, one still cannot occur without the other. The formation of electrically charged particles in water enables electrolyte solutions to conduct electricity. If neutral molecules are formed, no flow of electricity can be detected.

This demonstrates that an electrolyte's capacity to transport electricity depends on the transport of solvated ions. Driven by the electric field, the ions accelerate to a certain speed. This constant transport speed $\vec{v}$ is reached after a brief starting process, and is primarily determined by the Stokes drag force $\vec{F}_R$ [47]:

$$\vec{F}_R = 6 \cdot \pi \cdot \eta \cdot r_I \cdot \vec{v} \tag{8.33}$$

with

$\eta$ – viscosity of the surrounding medium,
$r_I$ – radius of the solvated ion.

The electrical force $\vec{F}_{el}$ acting on the ion is given by:

$$\vec{F}_{el} = n_e \cdot e_0 \cdot \vec{E} \tag{8.34}$$

with

$n_e$ – equivalent number (also $z$): number of ions (or electrodes) that are exchanged,
$e_0$ – elementary electric charge $1.602 \times 10^{-23}$ J/K,
$\vec{E}$ – electric field force.

The maximum transport speed $\vec{v}$ of the solvated ions is reached when the electrical force and frictional force are in equilibrium:

$$\vec{v} = \frac{z \cdot e_0 \cdot \vec{E}}{6 \cdot \pi \cdot \eta \cdot r_I}. \tag{8.35}$$

Equation 8.35 demonstrates that for specific $\eta$ and $E$ values, every ion type has a characteristic transport speed determined by the ion charge and the radius of the solvated ions. The associated ion mobility will be discussed below.

### Calculating Charges in Electrolyte

For clarity, the following discussion considers a binary electrolyte solution ($A^+ + B^-$), i.e., an electrolyte that contains only one type of anion and one type of cation:

$$AB \rightarrow A^+ + B^-. \tag{8.36}$$

The current $I$ that in a specific time $\Delta t$ can pass through a control field $A$ perpendicular to the direction of motion is determined by the sum of the negative and positive charges. Equations 8.37 and 8.38 give the quantity $N$ of cations (superscript '+' sign) or anions (superscript '–' sign) that in the time $\Delta t$ can be transported through a cross section $A$:

$$N^+ = \gamma^+ \cdot c \cdot N_A \cdot A \cdot v^+ \cdot \Delta t, \tag{8.37}$$

$$N^- = \gamma^- \cdot c \cdot N_A \cdot A \cdot v^- \cdot \Delta t \tag{8.38}$$

with

$y^+, y^+$ – stoichiometric coefficient of the anions and cations
$c$ – concentration
$N_A$ – Avogadro constant $6.022 \times 10^{23}\,1/\text{mol}$.

The partial charges $\Delta Q^+$ or $\Delta Q^-$ can be calculated from the ion charge $z^{\pm} \cdot e_0$ and number of ions $n$ that pass through field $A$:

$$\Delta Q^+ = z^+ \cdot e_0 \cdot N^+ = z^+ \cdot e_0 \cdot \left(\gamma^+ \cdot c \cdot N_A \cdot A \cdot v^+ \cdot \Delta T\right), \tag{8.39}$$

$$\Delta Q^- = z^- \cdot e_0 \cdot N^- = z^- \cdot e_0 \cdot (\gamma^- \cdot c \cdot N_A \cdot A \cdot v^- \cdot \Delta T). \tag{8.40}$$

Using the Faraday constant $F = e_0 \cdot N_A$, the charge $\Delta Q$ can be determined:

$$\Delta Q = \Delta Q^+ + \Delta Q^- = F \cdot A \cdot \left(z^+ \cdot \gamma^+ \cdot c \cdot v^+ + z^- \cdot \gamma^- \cdot c \cdot v^-\right) \cdot \Delta t. \tag{8.41}$$

### Calculating Ion Mobility, Current-Strength, and Ohmic Resistance in Electrolyte Solutions

Applying the law of electric charge $\Delta Q = I \cdot \Delta t$ results in Eq. 8.42 for electric current-strength:

$$I = F \cdot A \cdot \left(z^+ \cdot \gamma^+ \cdot c \cdot v^+ + z^- \cdot \gamma^- \cdot c \cdot v^-\right). \tag{8.42}$$

To determine ohmic resistance in an electrolyte solution, the electric mobility $u^+$ for cations and $u^-$ for anions are used. In physical chemistry, ion mobility is defined as the traveling speed of ions of a certain type in water in an electric field of 1 V/m. As noted above, this mobility depends on the size, charge, and hydrate shell, as well as its other interactions with the solvent. It is usually in the order of around $5 \times 10^{-8}\,\text{m}^2/(\text{V} \cdot \text{s})$. The exceptions are $OH^-$ and $H_3O^+$ with mobilities four and seven times higher [119].

If the speed in Eq. 8.42 is replaced by $v = E \cdot u$, the result is:

$$I = F \cdot A \cdot E \cdot \left(z^+ \cdot \gamma^+ \cdot c \cdot u^+ + z^- \cdot \gamma^- \cdot c \cdot u^-\right). \tag{8.43}$$

If then the electric field strength $E = U/l$ is replaced by the voltage $U$ and the length of the conductor $l$, the result is:

$$I = F \cdot \frac{A}{l} \cdot \left(z^+ \cdot \gamma^+ \cdot c \cdot u^+ + z^- \cdot \gamma^- \cdot c \cdot u^-\right) \cdot U. \tag{8.44}$$

The electric resistance $R$ can be determined by resolving this equation, which results in Eq. 8.45:

$$R = \frac{1}{F \cdot \frac{A}{l} \cdot \left(z^+ \cdot \gamma^+ \cdot c \cdot u^+ + z^- \cdot \gamma^- \cdot c \cdot u^-\right)}. \tag{8.45}$$

### Summary

Electrolytic conductivity is determined by:

- The number of charge carriers (concentration)

- The charge per ion (charge number)
- The traveling speed of the ions in the liquid (the faster they travel, the greater the conducitivity)

Electric resistance is increased by factors that hinder mobility. These factors include interionic attraction forces, viscosity of the electrolyte solution, and ion solvation. Increasing the temperature reduces the influence of these factors, and therefore reduces the electric resistance [75]. All values required to achieve successful results can be determined precisely and accurately by applying the formulas derived here.

Conductivity is crucial for water electrolysis. With AEL, for example, conductivity is increased by adding potassium hydroxide (KOH) (▶ Sect. 8.2.2.1).



### 8.1.5.2 Specific and Molar Conductivity

Typically, using the specific resistance $\rho$ or specific conductivity $\kappa$ for calculations is more practicle. This is because these values can be determined independently from the cross-sectional field and the length.

In addition, electrical conductivity is a characteristic value for the behavior of electrolyte solutions. As with specific resistance, it is defined as the conductivity of a cube with an edge length of 1 cm using Eq. 8.46 [47]:

$$\frac{1}{\rho} = \kappa = F \cdot c \cdot \left(z^+ \cdot \gamma^+ \cdot u^+ + z^- \cdot \gamma^- \cdot u^-\right) \tag{8.46}$$

with $R = \rho \cdot \frac{l}{A}$

with $\rho = \frac{1}{\kappa}$.

According to Eq. 8.46, the conductivity is, therefore, proportional to the concentration of the dissolved salt. But this is valid only for electrolyte solutions at infinite dilution, because up to this point, it has been assumed that ions in the solution can move entirely independently from one another. To take this effect into account, the molar conductivity $\Lambda_m$ is used:

$$\Lambda_m = \frac{\kappa}{c}. \tag{8.47}$$

Dividing $\Lambda_m$ by the equivalent number $n_e$ (or also $z$) results in the equivalent conductivity $\Lambda_{eq}$. The equivalent number is defined by the charge-carriers exchanged in the electrochemical reaction. Also termed the electromagnetic significance, it is calculated using the following equation:

$$n_e = z^+ \cdot \gamma^+ = z^- \cdot \gamma^-. \tag{8.48}$$

This is then used to determine the equivalent conductivity $\Lambda_{eq}$:

$$\Lambda_{eq} = \frac{\Lambda_m}{n_e}. \tag{8.49}$$

According to Eq. 8.47, molar conductivity does not depend on concentration. But the Debye-Hückel-Onsager theory states that more negative ions are found near positive ions than elsewhere, and vice-versa. As a result, each ion is surrounded by a cloud of opposite ions. These then create a field that impedes mobility. The strength of this field increases together with the concentration. Therefore, increasing the concentration increases the likelihood of interionic interactions, because the quantity of dissolved particles increases. ◘ Figure 8.12 illustrates these effects in simplified form.

In real solutions, electrostatic attraction forces between solvated particles and friction among solvated particles cause the molar conductivity or equivalent conductivity to fall as the concentration increases. This means that ion mobility falls as the concentration increases, and that electrical conductivity begins again to fall once a maximum level has been reached. As a result, there is an approximately linear relationship between specific conductivity and concentration only at low concentrations. According to Debye-Hückel-Onsager, non-linear effects increase in significance as the concentration increases.

Molar conductivity and equivalent conductivity can be assumed to be independent from

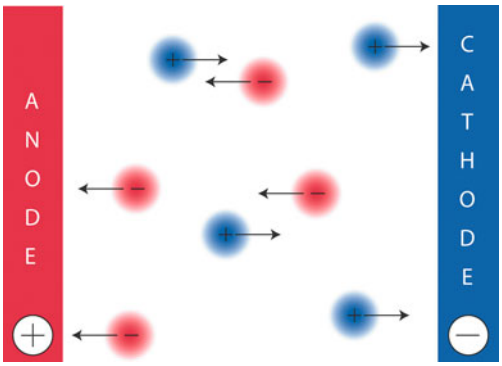



**Fig. 8.12** Ion transport in strong electrolyte solutions with solvate shells [47]

concentration only at infinite dilution. This is only the case with ideal solutions where the concentration $c$ is near zero. At the end of the 19th century, Friedrich Kohlrausch formulated an empirical law determining the relationship of concentration to molar conductivity in strong electrolytes (Kohlrausch's square root law; see [45]):

$$\Lambda_m = \Lambda_m^0 - k_c \cdot \sqrt{c} \tag{8.50}$$

with

$\Lambda_m^0$ – molar limiting conductivity,
$k_c$ – empirical constant.

Kohlrausch also demonstrated that the molar limiting conductivity $\Lambda_m^0$ can be described as the sum of the individual ions' contributions:

$$\Lambda_m^0 = F \cdot \left(\gamma^+ \cdot u^+ + \gamma^- \cdot u^-\right). \tag{8.51}$$

According to the Debye-Hückel-Onsager theory, the empirical constant $k_c$ for a strong electrolyte can be defined as 1.1 with $T = 298\,\mathrm{K}$ (for example, NaCl, HCl, KOH) using Eq. 8.52 [74]:

$$k_c = 0.229 \cdot \Lambda_m^0 + 60.20. \tag{8.52}$$

This constant also depends on the temperature, the molar limiting conductivity of the electrolyte, the dielectric constants, and the viscosity of the solvent. This equation is only valid for diluted solutions with concentrations below 0.01 mol/L.

There is currently no accepted formula for concentrated solutions. In principal, theory increasingly deviates from reality as the concentration increases. Experimental measurements are required to achieve relatively accurate results for electrolyte solutions at higher concentrations (▶ Sect. 8.1.5.3).

Unlike in strong electrolytes, in weak electrolytes dissociation in the solvent is incomplete. Weak electrolytes include Brönsted acids and bases (for example $CH_3COOH$ or $NH_3$). The conductivity depends on the level of dissociation (level of deprotonation) $\alpha$, which is determined by the ratio of the number of particles in the solution to the total number of particles. This is the reaction seen in Eq. 8.53:

$$KA + H_2O \rightleftharpoons K^+ + A^- \tag{8.53}$$

with

**KA** – non-protonated electrolyte,
**$K^+$** – cations,
**$A^-$** – anions.

Since it is abundantly available, the concentration of water can be assumed to be a constant. As a result, the acid strength or equilibrium constant $K_S$ is defined by:

$$K_s = \frac{c\left(K^+\right) \cdot c\left(A^-\right)}{c(KA)}. \tag{8.54}$$

The dissociation level is defined so that the concentration $c$ for an acid in a state of equilibrium is given by:

$$\left[K^+\right] = \alpha c,\ \left[A^-\right] = \alpha c \text{ and } [KA] = (1-\alpha)c. \tag{8.55}$$

If deviations of the activity coefficient from one are ignored, then the acid-constant $K_s$ can be approximated as:

$$K_s = \frac{\alpha^2 c^2}{(1-\alpha)c} = \frac{\alpha^2 c}{1-\alpha}. \tag{8.56}$$

If an acid is at infinite dilution, then what is called complete deprotonation results. This means that even weak electrolytes can be practically completely dissociated if the dilution is high enough. If this is the case, then the molar conductivity is equivalent to the limiting conductivity $\Lambda_m^0$. To calculate the actual molar conductivity $\Lambda_m$ at a dilution that is not infinite requires taking into account the level of dissociation. This is because only a fraction of the molecules are dissociated into ions:

$$\Lambda_m = \alpha \cdot \Lambda_m^0. \tag{8.57}$$

If Eq. 8.57 is solved for the level of dissociation and Eq. 8.56 then applied, the result is Ostwald's dilution law:

$$K_s = \frac{(\Lambda_m)^2}{(\Lambda_m^0 - \Lambda_m) \cdot \Lambda_m^0} \cdot c. \tag{8.58}$$

This law is a special case for the law of mass-action, which determines the ratio of activities of products and educts of a chemical reaction in chemical equilibrium. To be absolutely accurate, activities should be used in the calculations instead of concentrations. But the resulting difference is negligible.

These formulas also produce increasingly inaccurate results with larger margins of error as the concentration increases. With concentrated solutions, it makes better sense to measure the resistance. This process is described in the following section [3].

### 8.1.5.3 Measuring Electrolytic Conductivity

Usually, electrolytic conductivity is determined by experimental measurements. This is because the variables discussed in ▶ Sect. 8.1.5.2 are often difficult to calculate or to determine. Using experimental methods, measurements for electrolyte solutions of all kinds can be determined with a relatively small margin of error.

Here two electrodes of highly conductive material such as platinum, carbon, graphite, or stainless steel are dipped in the electrolyte solution. Then the voltage applied and the resulting current through the cell are measured

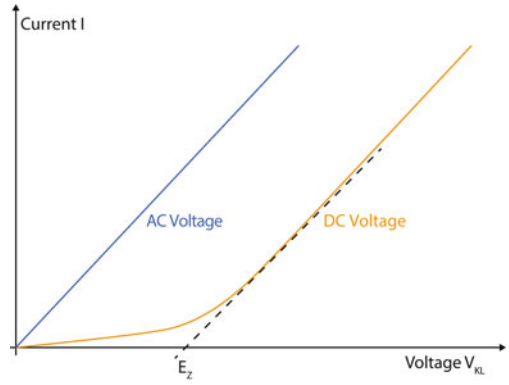



**Fig. 8.13** Characteristic current-voltage curve of an electrolyte cell with AC and DC voltage. The measurements are accurate only with alternating current

and recorded. According to Ohm's law, for the resistance $R$ [23]:

$$R = \frac{U}{I}. \tag{8.59}$$

The inverse of the resistance $R$ is the conductivity $G$ or the conductivity value:

$$G = \frac{1}{R} = \frac{I}{U}. \tag{8.60}$$

As with a capacitor (▶ Chap. 6), the specific resistance $\rho$ or the specific conductivity $\kappa$ is determined by taking into account the cell constant $C = l/A$. This is typically determined by taking a calibration measurement using a solution for which the conductivity is already known:

$$\rho = \frac{1}{\kappa} = \frac{R}{C} = \frac{R \cdot A}{l} \tag{8.61}$$

with

$l$ – plate separation,
$A$ – plate surface area.

If DC voltage is applied, then as predicted by Ohm's law, no linear relationship is observed (Fig. 8.13).

Applying direct current results in a build-up of charges at the electrodes (polarization). This also results in substance conversion through

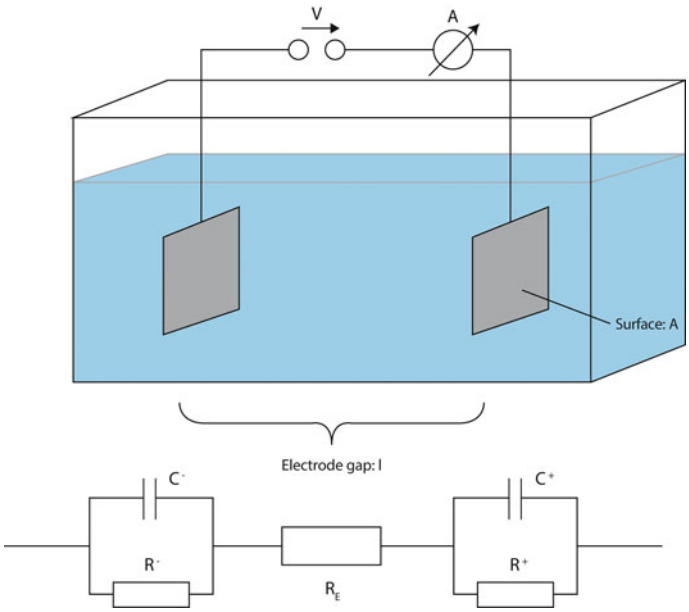



**Fig. 8.14** Circuit diagram of a cell for measuring conductivity

electrolysis, distorting the conductivity measurements.

The electrodes can be represented in a circuit diagram of an electrolyte cell as a parallel connection between a non-linear resistance ($R^+$ *and* $R^-$) and a bilayer capacity ($C^+$ and $C^-$) at the phase boundary between the electrolyte solution and electrode. The ohmic resistance of the electrolyte solution $R_E$ is connected in parallel (Fig. 8.14).

For the purposes of measurement, the electrode resistances must be eliminated. To avoid electrode reactions, a stationary AC voltage (1,000 to 4,000 Hz) is applied [74]. As with a capacitor, the bilayer is then recharged at the same rate as the AC voltage. At higher frequencies, the capacity functions as a short-circuit, and the current is determined solely by the ohmic resistance of the electrolyte solution. This allows the current to flow without requiring a charge transfer at the phase boundary.

As shown in Fig. 8.13, AC voltage measurements produce a linear curve, as expected. In addition, here, $E_z$ is the decomposition voltage required with DC voltage. If this voltage is exceeded, then the electrode potentials are exceeded and there is a significant current flow. As the frequency and electrode surface area are increased, the polarization resistances referred to above drop. The least effects are observed with electrodes of platinized platinum [54].

In practice, conductivity meters are often used to determine conductivity. Conductivity meters measure the current-strength and voltage $U$, and then automatically calculate and display the conductivity value or conductivity. Here the measurement area is critical. Larger measurement areas require meters that are very expensive. This problem can be solved by using a meter with a Wheatstone bridge circuit. The bridge circuit consists of four resistances. Two are connected in series, and then in parallel (Fig. 8.15).

Two of the resistances are known, a third is variable, and the fourth resistance is determined by the conductivity of the electrolyte solution being tested. This is placed in a container—the conductivity cell—with two electrodes of platinum, silver, graphite, or materials with similar characteristics. The cell is then connected to the bridge, and the resistance or conductivity of the solution determined by alignment. The bridge is aligned when the ammeter or oscilloscope reads zero. In the circuit

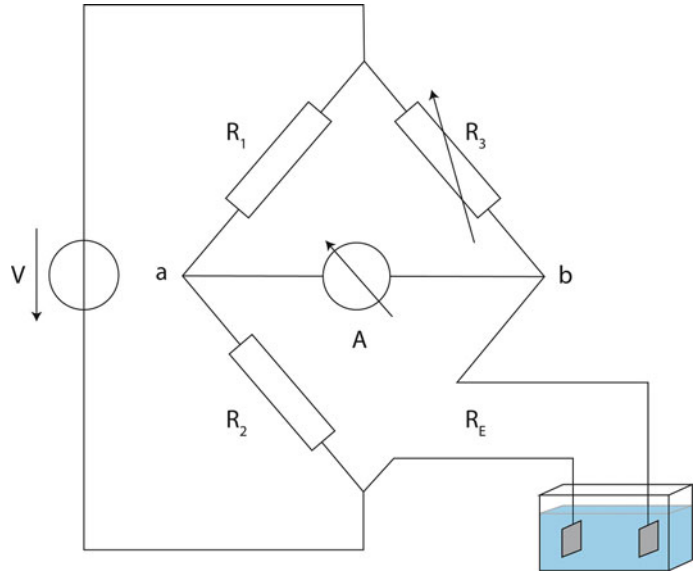



**Fig. 8.15** Wheatstone bridge circuit for determining conductivity



shown here, that means there is no current between the nodes a and b:

$$R_E = \frac{R_2}{R_1} \cdot R_3 \qquad (8.62)$$

with

$R_1$, $R_2$ – fixed resistances,
$R_3$ – variable, adjustable resistance.

Using this measurement, the conductivity value or specific conductivity can then be determined with Eq. 8.61.

## 8.2 Storing Technology Electrolysis

### 8.2.1 Overview

#### The Water Electrolysis Processes

Three water electrolysis processes, relevant from a technical point of view, are currently available. They differ considerably in terms of their function, operating conditions, and stage of development:

- AEL
- Membrane electrolysis or acid electrolysis (proton exchange membrane) PEMEL
- HTES or SOEL

Generally, a distinction is made between depressurized electrolysis, atmospheric electrolysis, and pressurized electrolysis.

#### Atmospheric Electrolysis

The advantages of atmospheric electrolysis (Fig. 8.16) are simple; robust facility design, comparably easy control, and a large load-range from under 20% utilization to full utilization. Scientists have extensive operational experience with these facilities, and capital costs are significantly lower than with pressurized electrolysis. But since the maximum reasonable current density with atmospheric operation (0.02 to 0.05 bar overpressure) limits stack capacity, large quantities of space are required. In addition, a complex gas-drying process and an initial compression step are disadvantages of this system. An upstream gas container at atmospheric pressure is required to avoid constant activation and deactivation of the compressor.

#### Pressurized Electrolysis

Pressurized electrolysis (Fig. 8.17) typically uses a system pressure of 30 bar, with testing facilities using pressures up to 120 bar. This allows the facility to be directly coupled with many industrial applications, which often use

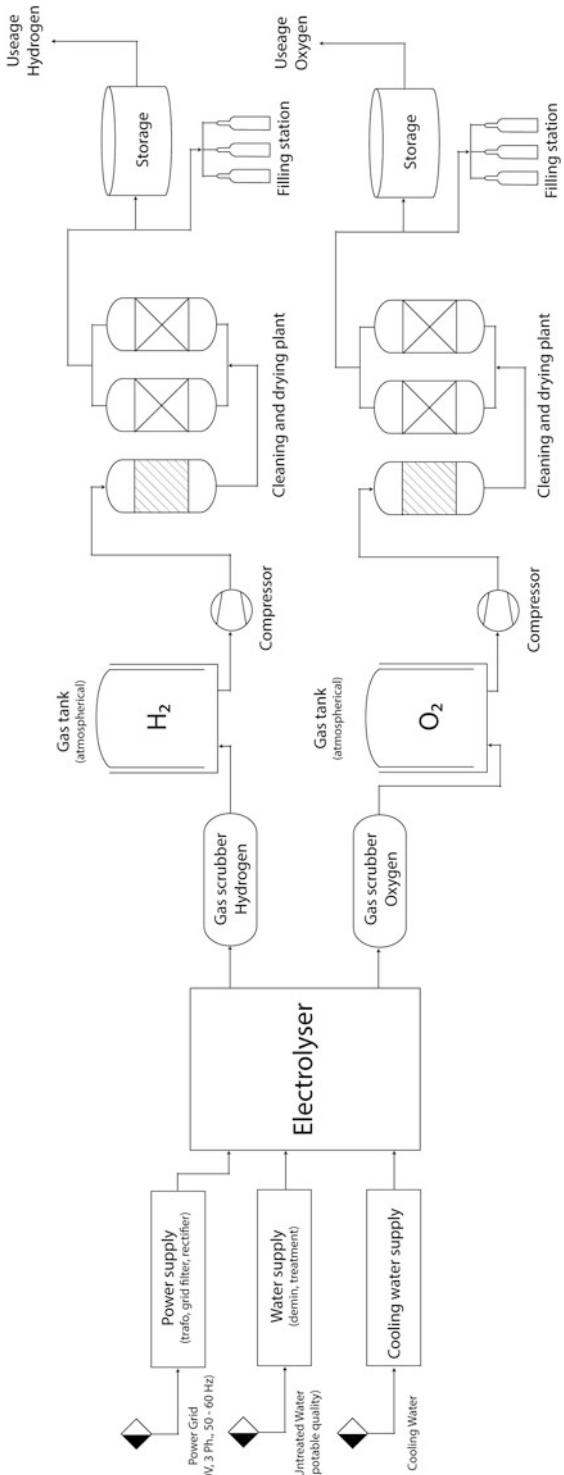



**Fig. 8.16** Atmospheric electrolysis facility design [129]

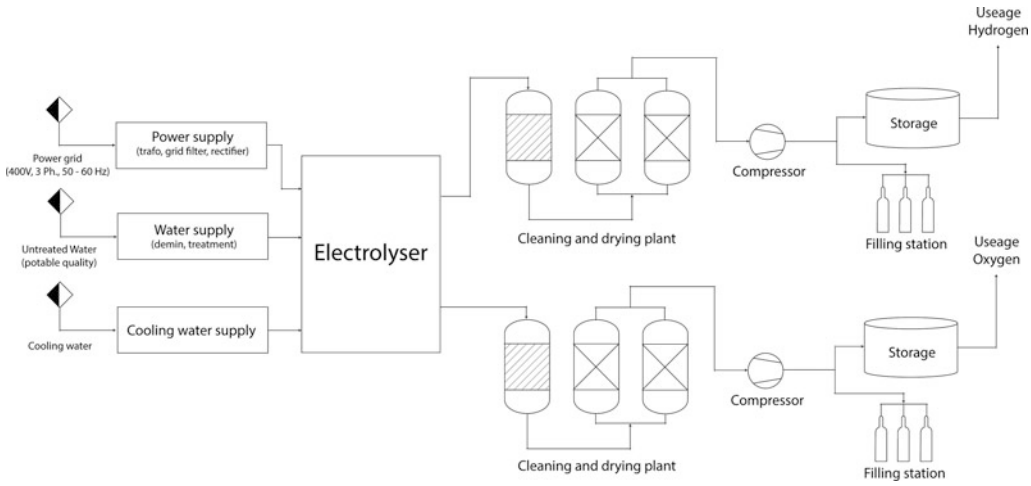



**Fig. 8.17** Pressure electrolysis facility design [129]

8

low pressures. The increased pressure significantly reduces the size of the facility and eliminates the precompression steps. This in turn reduces capital costs. But higher capital costs for the pressure eletrolyzer, higher maintenance costs, and extensive safety technology requirements offset these advantages. In addition, at pressures over 10 bar, the usable load range is only from 30 to 100%. This can be a disadvantage, particularly if the facility is operated with fluctuating renewable energy [129].

To produce usable product gasses with electrolysis, a large number of electrolyte cells (▶ Sect. 8.2.2) must be connected in series to make electrolysis blocks or stacks (▶ Sect. 8.2.3). These stacks are then placed in electrolysis facilities (▶ Sect. 8.2.4) and embedded in various peripheral systems ensuring safe and efficient operation. The following sections discuss these sub-systems in detail.

## 8.2.2 Electrolysis Cell—Electrolysis Type

### 8.2.2.1 AEL

AEL is a proven process that has been applied at an industrial scale for many years. Because they require reliably constant power, most existing facilities have been built near large power plants. For example, the world's largest depressurized electrolysis power plant is at the Aswan Dam in Egypt with a rated power of 156 MW and a hydrogen production rate of 33,000 $m^3$/h. Scientists have extensive experience with this technology, and it is commercially available. But for use in combination with fluctuating renewable energy, significant improvements are required in dynamic operation, operation under pressure, and efficiency.

#### ▪ Operating Principle

Figure 8.18 shows the basic design and operation of an alkaline electrolyzer cell. Adding 20 to 40% by weight potassium hydroxide (KOH) to water which circulates through the two half-cells separated by an ion-conducting membrane to increases its conductivity. This decreases the internal resistance of the cell and increases its efficiency. Porous, large surface-area electrodes are placed near the membrane on either side. Voltage is then applied to the electrodes. Under ideal conditions, the voltage should be equal to or larger than the decomposition voltage of water, or 1.23 V. As a result, in the cathode reaction (Eq. 8.63) the water on the cathode-side is split into atomic hydrogen and hydroxide ions ($OH^-$):

$$2H_2O(l) + 2e^- \rightarrow H_2(g) + 2OH^-. \quad \textbf{(8.63)}$$

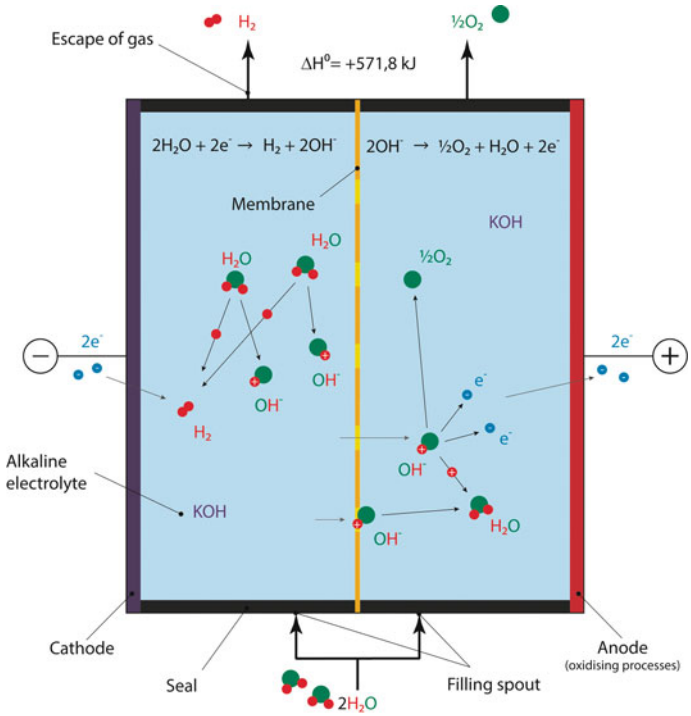



**Fig. 8.18** Operating principle of AEL

Since the resulting protons react to form $H_2$ molecules that rise and are then separated from the electrolyte, the hydroxide ions diffuse through the membrane and react in the anode reaction (Eq. 8.64). Here, they shed electrons to become water and atomic hydrogen:

$$2OH^- \rightarrow \frac{1}{2}O_2(g) + H_2O(l) + 2e^-. \quad \textbf{(8.64)}$$

The resulting oxygen molecules are separated from the electrolyte as well, and then released. The water consumed is refilled by the water supply. For the complete reaction (Eq. 8.65), in each half-cell, two electrons are required. These electrons are transported through the closed circuit that includes the current source:

$$H_2O(l) \rightarrow H_2(g) + \frac{1}{2}O_2(g). \quad \textbf{(8.65)}$$

The cell-frame seals the cell from the environment, insulates the electrodes from each other, and holds the membrane. With low loads, the current created by the rising gas-bubbles, for the most part, ensures electrolyte circulation and homogenous charge-carrier distribution. With higher loads, the electrolyte must be actively recirculated, consuming additional energy.

### 8.2.2.2 Membrane Electrolysis (PEM, PEMEL)

Membrane electrolysis, or PEM electrolysis (PEM stands for proton exchange membrane), was developed from fuel cell technology and is based on the inverse processes of a fuel cell. It is better-suited than AEL to dynamic operation, even under pressure. But up to this point, it has only been tested in smaller facilities.

#### ▪ Operating Principle

A PEM electrolysis cell (Fig. 8.19) is composed of a proton exchange membrane (PEM) typically connected on both sides to the electrodes in the membrane electrode assembly (MEA). A solid polymer electrolyte (SPE) such as Nafion is placed on the electrodes. This highly porous material facilitates the flow of current from the bipolar plates to the electrode.

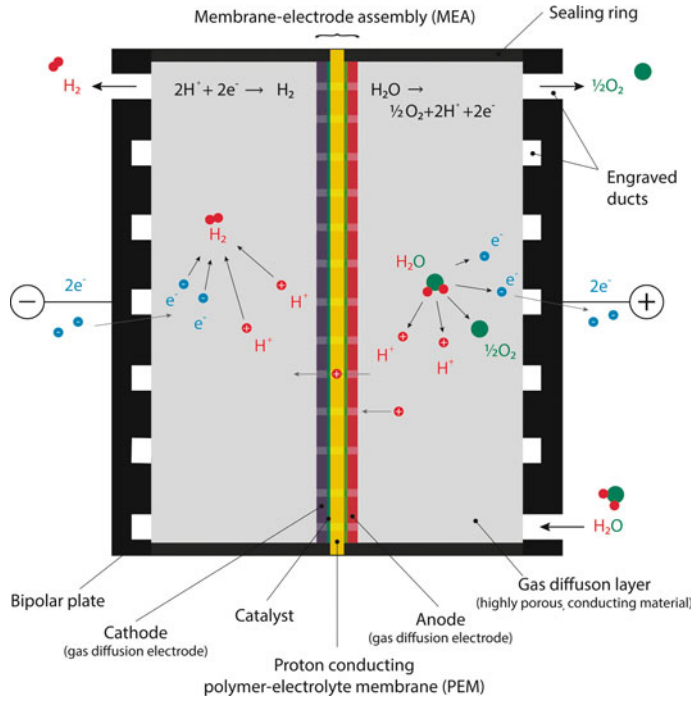



**Fig. 8.19** Operating principle of membrane electrolysis

It also ensures that water is transported to the electrode, and that product gasses are transported away from the electrode.

Depending on the stack design, the bipolar plates are engraved with channels that carry water to the electrode and transport product gasses away. In addition, these channels ensure that the current density in the electrolyte is evenly distributed.

This means that the operating principle of PEM electrolysis fundamentally differs from that of AEL. Water is fed to the anode, where in the anode reaction (Eq. 8.66) it is split into atomic oxygen and two protons with the decomposition voltage of water applied:

$$H_2O(l) \rightarrow \frac{1}{2}O_2(g) + 2H^+ + 2e^-. \quad \textbf{(8.66)}$$

The oxygen combines to form $O_2$ molecules and is then released. The protons diffuse through the membrane to the cathode, where in the cathode reaction (Eq. 8.67), they react with two electrons to form hydrogen:

$$2H^+ + 2e^- \rightarrow H_2(g). \quad \textbf{(8.67)}$$

This means that only the anode-side half-cell is immersed in water. In theory, the cathode-side half-cell exclusively contains hydrogen. In practice, the humidity in this half-cell remains high. But compared with AEL, the hydrogen produced still contains far fewer impurities. With AEL, residues in part from the alkaline electrolyte must be washed out.

### 8.2.2.3 HTES

HTES of steam, or steam electrolysis, splits water vapor instead of liquid water. This means that the energy required for the phase-change from a liquid to gaseous state does not need to be supplied during electrolysis by electricity. Instead the water can be evaporated externally, for example, by using waste heat from industrial processes. This reduces electrical energy requirements by about 16%. In addition, some of the energy required to split the water into oxygen and hydrogen is supplied by high-temperature heat ranging from around 850 to 1,000 °C. As a result, the cell voltage can be reduced by more than 0.5 V, compared to PEMEL

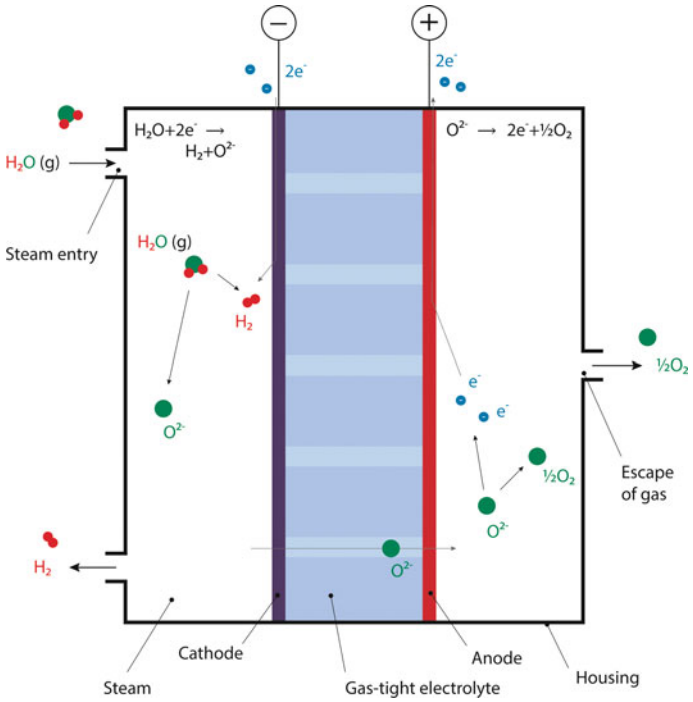



**Fig. 8.20** Operating principle of HTES

and AEL, to under 1 V, greatly improving electrical efficiency.

HTES also has two other important applications:

1. Besides water vapor, $CO_2$ can also be reduced to CO. This means that synthetic gas for PtG and PtL could be generated directly from $H_2O$ and $CO_2$ using electrolysis.
2. The components are, in practice, reversible, i.e., a HTES could be used as a fuel cell or an electrolyzer without modification. This means that utilization and efficiency increase at locations with fluctuating energy supply (see ▶ Sects. 8.2.5 and 8.5.1.1).

Both have been proven in practice, and are currently being developed for industrial use. But in the following discussion, the focus is on normal steam electrolysis. Although the physical properties differ, the same principles apply to $CO_2$ electrolysis.

### ■ Operating Principle

The operating principle of HTES is based on reversing the reaction in a solid oxide fuel cell (SOFC). The two half-cells are separated by an $O_2$ ion-conducting solid electrolyte with the electrodes placed on either side (Fig. 8.20).

The cathode side is supplied by superheated steam which reacts with two electrons to form hydrogen and $O_2$ ions (Eq. 8.68 cathode reaction). The hydrogen is extracted and the $O_2$ ions diffuse through the electrolyte to the anode. There, they shed electrons in the anode reaction (Eq. 8.69) to form oxygen:

$$H_2O + 2e^- \rightarrow H_2 + O^{2-}, \qquad \textbf{(8.68)}$$

$$O^{2-} \rightarrow 2e^- + \frac{1}{2}O^{2-}. \qquad \textbf{(8.69)}$$

The overall reaction equation is:

$$H_2O \rightarrow H_2 + \frac{1}{2}O_2. \qquad \textbf{(8.70)}$$

### ■ Reversible Electrolysis/fuel Cell (rSOC)

A 2014 project (▶ Sect. 14.2.2.4) demonstrated that using the same components for HTES and using it as a high-temperature cell (▶ Sect. 8.5.1.1) was both theoretically possible and practically feasible. Called a reversible solid

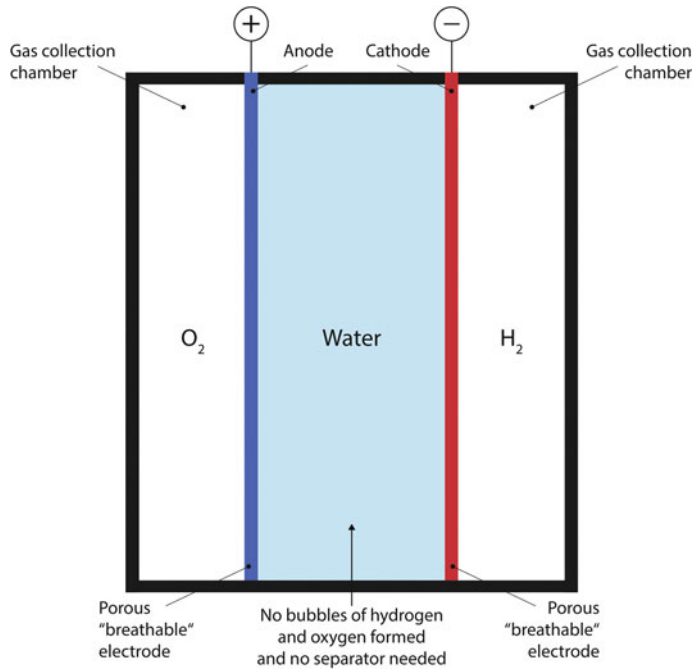



**Fig. 8.21** Functional schematic of the membrane-less electrolysis



oxide cell (rSOC), this technology is currently being developed for industrial applications.

The thermodynamic principles of the various operating methods are described in ▶ Sects. 8.1.4 and 8.5.1. In practice, this technology combines four advantages.

1. Higher utilization than stand-alone charging or discharging facilities.
2. Reversibility does not significantly increase the capital costs of these facilities.
3. By linking the electricity and chemical networks and their associated inputs and outputs, unlike batteries, this technology is not dependent on a fixed relationship between charging and discharging. As a result, these facilities can be operated to take the best advantage of electricity prices.
4. The facilities use low-cost energy carriers when generating electricity, and produce high-value chemical molecules when consuming electricity. As a result, costs and revenues can be optimally balanced.

Because this technolgoy allows more freedom andincreases energy efficiency, economic simulations using rSOC generate better numbers than those using stand-alone electrolyzers or fuel cells. The first prototypes and field tests will determine how long this technology will take to reach the industrial market.

### 8.2.2.4 Membrane-less Electrolysis

Conventional water electrolysis converts water into bubbles of hydrogen and oxygen gas that are then swept away and collected outside of the electrolysis cell [57]. The newly developed membrane-less electrolysis avoids the formation of bubbles and directly converts water into the bulk gases.

#### ▪ Operating Principle

This approach effectively employs an aqueous liquid acid or alkaline cell with porous, 'breathable' electrodes. Electrolytic water splitting occurs at the surface of the electrodes, with the generated gases passing directly through the electrodes into a gas collection chamber. Like in any electrolysis cell, hydrogen is created at the cathode electrode, oxygen at the anode electrode. Figure 8.21 shows the functional schematic of the membrane-less electrolysis.

The porous electrodes are based on gas-permeable, water-impermeable materials. Their surface areas are very high. Membranes are usu-

ally needed to keep the hydrogen-bubbles from mixing with the oxygen-bubbles, to avoid the creation of explosive oxyhydrogen gas. The lack of a membrane enables the operation of breathable-electrode electrolyzers at lower-current densities than conventional electrolyzers. As lower-current densities favor high energy-efficiencies, breathable-electrode electrolyzers can operate at a stack efficiency of more than 90% (Fig. 8.11). As a consequence, the voltage drops in the cell are also reduced (Fig. 8.10).

By using high-pressure electrolyzers at pressures of 100–900 bar, the need for hydrogen compressors can be eliminated. Currently, the highest pressure that has been achieved in a PEM electrolyzer is 350 bar using thick and densely-packed PEMs to maintain low rates of gas crossover. Thickening PEMs also reduces their conductivity and thus the conversion efficiency [19]. Membrane-less electrolysis cells are expected to be capable of generating 3.0 pure hydrogen at pressures above 300 bar without a decline in their inter-electrode conductivity or energy efficiency. The first test series has been started, but long-term tests have to prove the overall concept and durability of these new electrolysis cells.

Another feature of the breathable-electrode technology that derives from the absence of a diaphragm is its ability to operate at temperatures above 110 °C. Commonly used diaphragms degrade or fail at temperatures higher than 110 °C. However, operating in the range of 110–250 °C is particularly attractive in water electrolysis, because catalytic efficiency and performance increases non-linearly with temperature (Fig. 8.9). The hydrogen production rate of a cell can, therefore, be amplified by allowing the cell to heat itself up to a higher operating-temperature [67]. Then thermal management becomes simpler, as cooling devices like chillers may be not be necessary or decrease in scale.

Membrane-less electrolysis units can be operated also with intermittent currents of renewable energy sources. Sudden increase in bubble volume in conventional water electrolyzers may crumble the catalyst, drive the liquid electrolyte out of the cell, or even create a potential burst hazard. In contrast, in a breathable-electrode, newly-formed gas directly joins a body of existing gas behind the electrode. In this large body with bulk gas, intermittent increases in gas generation can be buffered. Membrane-less electrolyzers can handle 25-fold increases in current and intermittent overloads in seconds. Therefore, this new technology shows many advantages versus the standard cell designs; but as for any new technology—durability and upscale has to be proven in field.

### 8.2.3 Electrolysis Block—Stack Design

Since the gas production rates of individual electrolyte cells are limited, the number of cells must be increased for larger capacities. For this purpose, several cells are connected together in a filter press design to produce a stack. With this design, the stack can be either monopolar or bipolar.

#### ▪ Monopolar Stack Design

In a monopolar filter press design, the individual cells are connected in parallel. As a result, the system voltage is low when current levels are high. The advantage of this design is that defective cells can be removed from the stack without significantly effecting the function of the other cells (Fig. 8.22).

#### ▪ Bipolar Stack Design

Bipolar stack design (Fig. 8.23) is used to increase the system voltage or terminal voltage of the stack and thereby reduce the input current.

Here plates are placed between the half-cells facing the anode on one side and the cathode on the other. These plates are called bipolar plates. Using this method, the individual cells can be directly connected in series to form a stack. But the behavior of this stack depends on all the individual cells it contains. If one of the cells fail, then the whole stack must be shut down. This results in higher maintenance costs.

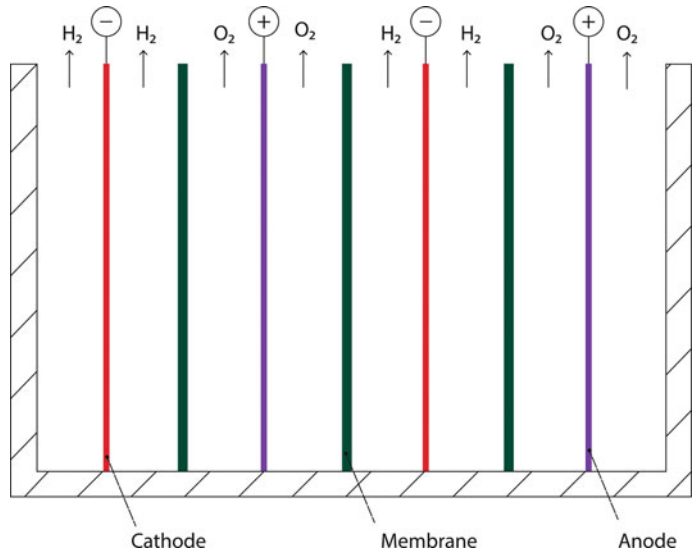



**Fig. 8.22** Basic monopolar stack design



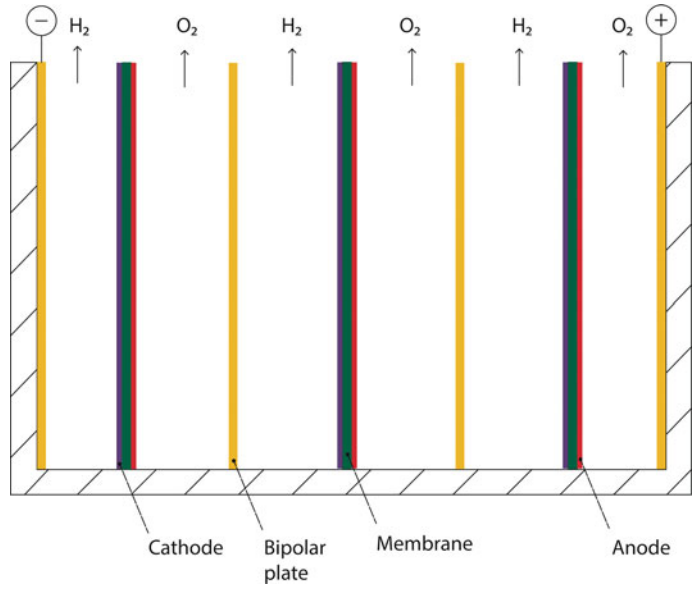



**Fig. 8.23** Basic bipolar stack design

### 8.2.4 Electrolyzers, Electrolysis Facilities, and Their Peripherals

The stacks described above are the core systems in all electrolysis facilities. Here, the term 'electrolyzer' principally refers to the device that produces the product gasses, hydrogen and oxygen, from electrical energy and water using 'electrochemical water decomposition' [16]. As described in ▶ Sect. 8.2.1, to operate a complete facility, a number of peripheral systems are required. These peripheral systems are connected upstream and downstream from the stack, or serve the system as a whole [16]. In principal, many sub-systems are the same with alkaline and PEM electrolysis. They differ primarily by the design of the cells, but also because PEM electrolysis does not require an electrolyte cir-

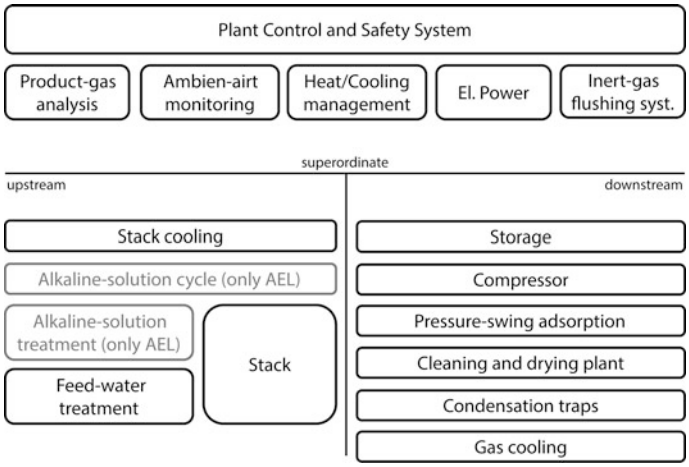



**Fig. 8.24** Electrolysis facility components: sub-systems connected upstream, subsystems connected downstream, and subsystems that serve the system as a whole are grouped separately in the diagram

cuit and leach preparation. Figure 8.24 provides an overview of electrolysis facility components. These components are explained in detail in the following sections.

### 8.2.4.1 Upstream Facility Components—Water and Leaches

Feed water is supplied by a facility component in the stack using reverse osmosis, for example. About 0.8 liters of water is required to produce a standard cubic meter of hydrogen. This prevents harmful ions and suspended solids from contaminating the leach supply, which is the next step. In this step, the water levels in the leach circuit decreased by the electrolyte are replenished. The leach circuit circulates through the stack, as well as the gas separator for the hydrogen and/or oxygen product gasses. At the same time, the circuit serves to cool the cell. The effective thermal power removed can be reused in other process steps (▶ Sect. 8.2.6).

### 8.2.4.2 Downstream Facility Components—Gas Preparation

The product gas is separated by the gas separators in the electrolyte circuit, or with PEM electrolysis directly removed from the stack. Using gas aftercooling and condensate separators, the product gas is cooled down to a point where the electrolyte remaining in the gas can be condensed out and returned to the electrolyte circuit. As a result, the components described below are protected against aggressive condensation to optimize operation.

To purify the product gasses, in a cleaning and drying system, first the remaining oxygen is recombined with hydrogen in a catalyst cartridge to form water and water vapor. This water is then cooled, condensed, and separated, resulting in a hydrogen purity of 99.9% by volume. This level of purity is also called hydrogen 3.0, with the numeral before the decimal standing for the number of nines in the percent, and the numeral after the decimal standing for the last number after the nines.

To achieve an even higher purity of 99.999% by volume (hydrogen 5.0), the residual water can be further reduced using pressure swing adsorption.

Using a gas compressor and intermediate storage, the volume of the product gas can be reduced and the gas maintained at a defined pressure level.

### 8.2.4.3 Facility Components Serving the Entire System—Energy, Materials, Control, and Regulation Systems

For safe operation, the facility must be supplied with an inert gas such as nitrogen. This is so

that, when required to prevent an explosion, a flushing system can flush all gas-carrying components in the facility with inert gas.

The electrical input power $P_{in}$ is required primarily by the power electronics used to operate the electrolyzer. A smaller portion amounting to an annual average below 10% is used for self-consumption to supply the facility's auxiliary systems. Compressed air supply is only required if some facility components such as valves have a pneumatic design. Electric systems are a more efficient alternative here.

The thermal management system regulates heating and cooling requirements for the electrolyte circuit, gas cooling, water condensation, gas purification, and compression.

A product gas-analysis system and an ambient air monitoring system are essential components of an electrolysis facility as they are critical for safety. Sophisticated, standardized technology monitors the characteristics of the product gasses and ambient air, identifying potential hazards early on.

A control and safety system for the entire facility serves as a process control system in normal operation. It also monitors for errors and notifies the facility operator. Using this system, the operator can check the operational status of individual components, monitor operation, and react to errors.

## 8.2.5 Comparison of Different Electrolyte Technologies

This section compares the electrolyte technologies discussed above. Table 8.3 compares these technologies and their characteristics side-by-side.

## 8.2.6 Increasing Efficiency by Using Waste Heat

Compared to other storage technologies, with water electrolysis, efficiency and utilization is fairly low (▶ Chap. 12). But its efficiency can be increased by using waste heat, which also increases the economic efficiency of operating the facility. The following section discusses the design of the components required, the integration options, and the consequences for the facility as a whole.

### 8.2.6.1 Basic Principles

Water electrolysis produces process waste heat that can be integrated into heat cycles. Waste heat is also produced by various industrial processes. Utilizing this heat is often cheap and technically straightforward. Still, most waste heat is simply released into the atmosphere by cooling systems.

Utilizing the waste heat of an electrolysis facility could increase its overall efficiency, as well as improve its economic efficiency and reduce its $CO_2$ footprint (▶ Sect. 8.2.6.4).

Because heat must be constantly drawn off from the electrolysis facility, waste heat can only be integrated into a heat cycle if the heat can still be constantly extracted. As a result, choosing the best heat-sink with hybrid operation using fluctuating wind and solar energy is a challenge. One solution is to install an additional cooling system to remove excess waste heat when required.

Besides hydrogen and oxygen, waste heat is a product of electrolysis that can be exploited for further use (Fig. 8.25). But because of the low-temperature levels, a portion of the waste heat cannot be used. The same applies during facility start-up.

### 8.2.6.2 Basic Principles of Design and Basis of Calculations

There are essentially three main components required to utilize electrolysis waste heat:

- A thermally insulated piping system to transport the heat.
- A coolant pump to circulate the heating fluid.
- A heat exchanger to transfer the heat.

Because these components have a strong reciprocal effect on each other, optimization is

**Table 8.3** Technical comparison of electrolyzers

| | AEL | | PEMEL—membrane electrolysis (proton exchange membrane electrolysis) | | HTES of steam | |
|---|---|---|---|---|---|---|
| **Electrolyte** | Liquid | KOH | Solid | Membrane | Solid | Ceramic |
| Operating temperature in °C | 40–90 | | 20–100 | | 700–1,000 | |
| Pressure in bar | 1–30 | | 30–50 | | Around 30 | |
| **Reactions** | | | | | | |
| Cathode reaction | $2H_2O + 2e^- \rightarrow H_2 + 2OH^-$ | | $2H^+ + 2e^- \rightarrow H_2$ | | $H_2O + 2e^- \rightarrow H_2 + O^{2-}$ | |
| Charge-carrier | $OH^-$ | | $H^+$ | | $O^{2-}$ | |
| Anode reaction | $2OH^- \rightarrow \frac{1}{2}O_2 + H_2O + 2e^-$ | | $O^{2-} \rightarrow \frac{1}{2}O_2 + 2e^-$ | | $O^{2-} \rightarrow 1/2O_2 + 2e^-$ | |
| Efficiency level in % | 62–82 | | 67–82 | | 65–82 | |
| **Stack design** | | | | | | |
| Design | Bipolar, filter press | | Filter press | | No commercial products available | |
| Active cell area | 0.1–4 $m^2$ | | 10–750 $cm^2$ | | Up to 100 $cm^2$ | |
| Current density in A/$cm^2$ | 0.2–0.45 | | Up to 2.5 | | 0.3–3.0 | |
| Cell voltage in V | $< 2.4$ | | $< 2.2$ | | | |
| Cells per stack | Up to 700 | | $< 120$ | | | |
| System design | Leach circuit (KOH) Power electronics Gas separators, gas scrubbing, compression, refining | | Similar to AEL, simple system design, pressure-resistant design | | Currently still in planning, coupled with a HT source | |
| Hydrogen production rate in $m^3/h$ | 1–760 | | 0.01–30 | | Currently largest facility: 5.7 $m^3/h$ at 18 kW | |
| Electrical power | 5 kW–3.4 MW | | 0.5–160 kW | | | |
| Idle times incl. overhaul in h/a | 20–30 | | 10–20 | | N/a | |
| Energy in kW $h_{el}/m^3$ $H_2$ | 4.5–7.0 | | 4.5–7.5 | | 3.2 0.6 kW $h_{th}/m^3$ $H_2$ | |
| Partial-load range in % | 20–100 | | 0–100 | | N/a | |
| Power density in W/$cm^2$ | Up to 1.0 | | Up to 4.4 | | | |
| Capital costs $I_0$ in €/kW, as of 2014 | 800–1,500 | | 2,000–6,000 | | | |
| Construction, delivery | 10% $I_0$ | | 10% $I_0$ | | | |
| Maintenance, operation, insurance | 4% $I_0$ per year | | 4% $I_0$ per year | | | |

**Table 8.3** (Continued)

| | AEL | PEMEL—membrane electrolysis (proton exchange membrane electrolysis) | HTES of steam |
|---|---|---|---|
| Advantages | Inexpensive to produce and to buy, extensive operational experience, proven technology | Simple design and process technology since no electrolyte circuit is required, low overvoltages by using stainless steel catalysts | Cell voltage with water vapor is lower than with liquid water, at higher temperatures heat can be supplied as an energy input; for example, from chemical synthesis |
| Disadvantages | Complex leach cleaning required, not designed for dynamic operation | Extensive material requirements, expensive materials | Separating hydrogen and water steam at high temperatures may be a problem |



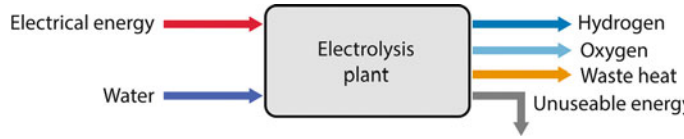



**Fig. 8.25** Waste heat as an additional product of an electrolysis facility

crucial for their effective design. The individual components use long-proven, cutting-edge technology.

### ▪ Piping System

The piping system transports the fluid that stores the energy in the form of (waste) heat. Good insulation is critical for keeping thermal losses low. The designs and materials used for piping systems vary widely. Some systems contain single-insulated pipes, and others contain two pipes for feed and return enclosed in sheath insulation. The latter system uses less insulation material and saves space. Keeping the two pipes close together also reduces thermal losses during transport. But high capital costs are a disadvantage of this system.

Piping system dimensioning affects volumetric flow, and as a result, flow speed.

The mass flow of the fluid $\dot{m}_{\mathrm{Fl}}$ depends on the waste heat of electrolysis $\dot{Q}_{\mathrm{FL}}$ and the temperature differential between the feed and return pipes $\Delta T_{\mathrm{Fl}}$ (Eq. 8.71):

$$\dot{m}_{\mathrm{Fl}} = \frac{\dot{Q}_{\mathrm{El}}}{c_{p\,\mathrm{Fl}} \cdot \Delta T_{\mathrm{Fl}}} \tag{8.71}$$

with

$c_{p,\mathrm{Fl}}$ – specific thermal capacity at constant pressure (usually water at 4.182 kJ kg$^{-1}$ K$^{-1}$).

The choice of pipe width (diameter nominal, or DN) and the resulting surface area $A_{\mathrm{Ri}}$ directly affect the volumetric flow $\dot{V}_{\mathrm{Fl}}$ and the resulting flow speed $c_{\mathrm{Fl}}$:

$$\dot{m}_{\mathrm{Fl}} = \dot{V}_{\mathrm{Fl}} \cdot \rho_{\mathrm{Fl}} = A_{\mathrm{Ri}} \cdot c_{\mathrm{Fl}} \cdot \rho_{\mathrm{Fl}} \tag{8.72}$$

with

$\rho_{\mathrm{Fl}}$ – fluid density (usually water at 1 kg/L).

Reducing the pipe width has the advantage of reducing the system's material and space requirements. The disadvantage is increased flow speed. A flow speed of about 0.8 to 2.0 m/s can be assumed as standard.

Thermal losses are essential in determining a piping system's efficiency. Thermal losses are determined by the piping system's temperature differential and its thermal resistance. The thermal resistance is the result of:

- Heat transfer resistance from the fluid to the interior wall of the pipe.
- Heat-conduction resistance of the individual pipe layers $R_{RS}$.
- Heat transfer resistance of the exterior wall of the pipe to the soil $R_E$.
- Interaction between the feed and return pipes $R_{VR}$.

Since it has a negligible effect and is complex to calculate, the heat transfer resistance at the inner wall of the piping system can be ignored.

The heat-conduction resistance of a pipe $R_{RS}$ depends on the geometrical dimensions as well as the materials used and their conductivities $\lambda_1$, $\lambda_2$. These can be calculated using Eq. 8.73, as here for a pipe with two layers:

$$R_{RS} = \frac{1}{2 \cdot \pi} \cdot \left( \frac{\ln \frac{d_{a1}}{d_{i1}}}{\lambda_1} + \frac{\ln \frac{d_{a2}}{d_{a1}}}{\lambda_2} \right). \quad (8.73)$$

Besides the heat conductivity of the soil $\lambda_E$, the laying depth $h_m$ and the external diameter of the pipe used $d_{a2}$ determines the heat-conduction resistance $R_E$ as shown in Eq. 8.74:

$$R_E = \frac{1}{2 \cdot \pi \cdot \lambda_E} \cdot \ln \frac{4 \cdot h_m}{d_{a2}}. \quad (8.74)$$

The interaction between the feed and return pipes $R_{VR}$ also significantly contributes to the piping system's thermal losses (Eq. 8.75). The axial-center distance between the feed and return pipes $a$ also has an additional effect:

$$R_{VR} = \frac{1}{2 \cdot \pi} \cdot \frac{1}{2 \cdot \lambda_E} \cdot \ln \left( 1 + \frac{4 \cdot h_m^2}{a^2} \right). \quad (8.75)$$

The effective average temperature $T_m$ is the last value required to determine the piping system's thermal losses $Q_{RS}$ (Eq. 8.76). This temperature is calculated using the average temperature of the feed pipe $T_{Vl}$ and the return pipe $T_{Rl}$ as well as the temperature of the soil $T_E$,

$$T_m = \frac{T_{Vl} + T_{Rl}}{2} - T_E. \quad (8.76)$$

The previous equations result in the thermal losses of the piping system $Q_{RS}$, where the total length of piping $l$ in the system is also taken into account (Eq. 8.77):

$$Q_{RS} = \frac{T_m \cdot l}{R_{VR} + R_E + R_{RS}}. \quad (8.77)$$

### Coolant Pump

The coolant pump is the source of the coolant volumetric flow. It also compensates for pressure losses in the piping system and heat exchanger.

Current energy losses caused by irreversible processes (for example friction) in the piping system manifest themselves as pressure losses $\Delta p_{VRS}$. These pressure losses can be confidently estimated from the known dimensions ($l_{RS}$, $d_{RS}$) and characteristics of the piping system. They are partially determined by the piping system's surface properties $\lambda_{Rau}$ at the inner wall and the number of elbow joints used $\sum \xi$. The squared fluid flow speed $c_{Fl}$ is also required for the calculation (Eq. 8.78):

$$\Delta p_{VRS} = \left( \lambda_{Rau} \cdot \frac{l_{RS}}{d_{RS}} + \sum \xi \right) \cdot \rho_{Fl} \cdot \frac{c_{Fl}^2}{g}. \quad (8.78)$$

This equation is valid only for incompressible fluids. This is often the case since water is usually used as a coolant.

The piping system pressure loss level $H_{VRS}$ is calculated directly from the pressure losses, and is a key parameter for determining pump design (Eq. 8.79):

$$H_{VRS} = \Delta p_{VRS} \cdot \frac{\rho_{Fl}}{g}. \quad (8.79)$$

Pressure losses affect the heat exchanger in two ways:

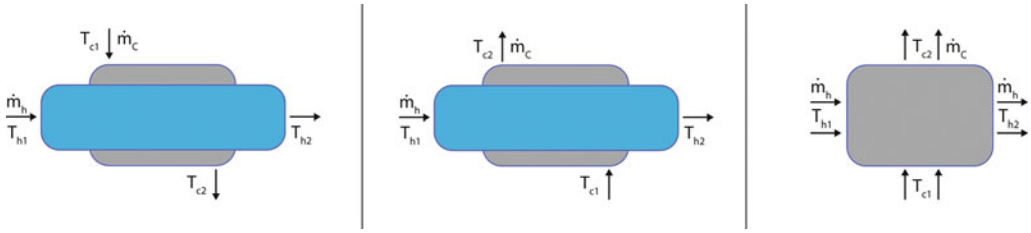



**Fig. 8.26** Various types of flow control in heat exchangers (recuperators): c = cold fluid, h = hot fluid

- When pressure losses are too low, laminar flow occurs within the heat exchanger, increasing thermal losses.
- But if pressure losses are very high, the load on the coolant pump is also higher, leading to higher energy consumption.

8

Precisely and scientifically calculating the pressure losses in the heat exchanger is a highly detailed and complex process. As a result, it is omitted here. Pressure loss levels can be provided by the manufacturer, or they can be estimated based on the power, operating principle, and size of the heat exchanger used.

The overall pressure loss $\Delta p_{V,\mathrm{ges}}$ is calculated from the pressure loss in the piping system $\Delta p_{V,\mathrm{RS}}$ and the heat exchanger $\Delta p_{V,\mathrm{WT}}$:

$$\Delta p_{V\,\mathrm{ges}} = \Delta p_{V\,\mathrm{RS}} + \Delta p_{V\,\mathrm{WT}}. \qquad \textbf{(8.80)}$$

Together with the overall pressure loss $\Delta p_{V,\mathrm{ges}}$, the volumetric flow required $V_{\mathrm{Fl}}$ and the coolant pump's efficiency $\eta_{\mathrm{P}}$ determine the coolant pumps' electrical power consumption $P_{\mathrm{el,P}}$:

$$P_{\mathrm{elP}} = \frac{\dot{V}_{\mathrm{Fl}} \cdot \Delta p_{V\,\mathrm{ges}}}{\eta_{\mathrm{P}}}. \qquad \textbf{(8.81)}$$

Since the facility's pressure level is relatively low, it does not greatly affect the choice of pump.

### Heat Exchanger

The heat exchanger transfers the energy stored in the heating fluid in the form of waste heat from electrolysis to a cooler medium; the heatsink. This process requires a range of devices. The operating principle and design of these devices may vary considerably. Currently, there are three basic heat exchanger designs:

- Regenerators: the heat is transferred to a storage medium and released at a later time.
- Fluid mixture: the hot fluid is directly mixed with another fluid in order to warm it.
- Recuperators: the heat is fed to a partition that immediately transfers it to a cold fluid.

The most common design is the recuperator. With this design, the flow control can be divided into three main categories (Fig. 8.26).

The various types of flow control have various characteristics as well as different advantages or disadvantages depending on the application. Compared with the uniflow principle, using the counterflow principle significantly reduces the amount of surface area required to transfer the heat. In addition, using a counterflow heat exchanger allows the hot fluid to be cooled to a lower level (Fig. 8.27). This is especially useful with waste heat from an electrolysis facility, because the temperature levels are not very high with some electrolysis processes.

Figure 8.27 graphs the temperature curves of the hot and cold fluids with the uniflow principle and the counterflow principle.

For the sake of simplicity, it can be assumed that, in an ideal heat exchanger, the overall heat flow $Q$ released by the hot fluid is absorbed by the cold fluid. The heat capacities $c_{\mathrm{p,h}}$, $c_{\mathrm{p,c}}$ of the fluids are also key factors (Eq. 8.82). Here the symbol c stands for the cold fluid and h for the hot fluid:

$$\dot{Q} = \dot{m}_{\mathrm{h}} \cdot c_{p\,\mathrm{h}} \cdot \Delta T_{\mathrm{h}} = \dot{m}_{\mathrm{c}} \cdot c_{p\,\mathrm{c}} \cdot \Delta T_{\mathrm{c}}. \qquad \textbf{(8.82)}$$

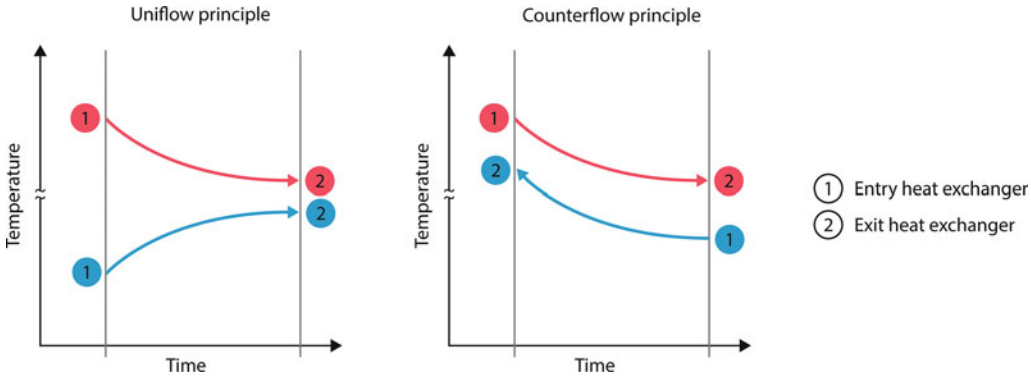



**Fig. 8.27** Temperature curves in heat exchangers using the uniflow principle and the counterflow principle

The temperature differentials $\Delta T_h$, $\Delta T_c$ can be determined from the input temperature $T_{h,1}$, $T_{c,1}$ and the output temperature $T_{h,2}$, $T_{c,2}$ of the heat exchanger (Eqs. 8.83 and 8.84):

$$\Delta T_h = T_{h2} - T_{h1}, \tag{8.83}$$

$$\Delta T_c = T_{c2} - T_{c1}. \tag{8.84}$$

With many applications, the same fluid is used for the hot and cold circuit, meaning they also have the same thermal capacity.

But the mass flows in the cold and hot circuits still differ. As a result, the average temperature-difference is determined logarithmically $\Delta T_{log}$ using Eq. 8.85:

$$\Delta T_{log} = \frac{\Delta T_h - \Delta T_c}{\ln \frac{\Delta T_h}{\Delta T_c}}. \tag{8.85}$$

A key parameter is the heat transfer surface area $A$ required by the heat exchanger (Eq. 8.86). This parameter largely determines the size and price of the heat exchanger:

$$A = \frac{Q}{k \cdot \Delta T_{log}}, \tag{8.86}$$

with

$k$ – heat transfer coefficient.

Precisely calculating the pressure losses $\Delta p_{WT}$ is a highly complex process. These calculations also vary depending on which principle the heat exchanger design uses. The pressure losses can be roughly calculated using Eq. 8.87:

$$\Delta p_{WT} = \sum \xi \cdot \frac{\rho_{Fl}}{2} \cdot c^2, \tag{8.87}$$

with

$\rho_{Fl}$ – Fluid density,
$\sum \xi$ – Geometric design,
$c$ – Speed of the fluid in the heat exchanger.

### 8.2.6.3 Integrating Waste Heat

Waste heat from electrolysis retained after losses in the piping system and heat exchanger can be fed into a range of heating systems or heat cycles. Three factors primarily determine how waste heat is integrated:

- The electrolysis process used or the normal temperature-level.
- Proximity of the site to a suitable heat input.
- The integration options at the facility site.

The electrolysis processes described in ▶ Sect. 8.2.2 vary widely in terms of their temperature ranges and levels of development (Table 8.4).

AEL is the most common and most economical process, but it also has the lowest temperature-range. As a result, application and integration options for the waste heat are limited. In general, the temperature level of the electrolysis should be significantly higher than the temperature level of the heat cycle. The other criterion is the proximity of the facility

**Table 8.4** Temperature levels and stages of development for three common electrolysis processes

| Electrolysis process | Temperature range | Level of development |
|---|---|---|
| AEL | 40–90 °C | High |
| PEM electrolysis | 20–100 °C | Medium |
| HTES | 700–1,000 °C | Low |

**Table 8.5** List of possible heat-sinks for waste heat from electrolysis facilities

| Integration option | | Temperature level |
|---|---|---|
| District heating | Feed | 90–130 °C |
| | Return | 55–80 °C |
| Local heating | Feed | 70–100 °C |
| | Return | 55–70 °C |
| Public facilities | | Varies by facility |
| Manufacturing | | > 100 °C |

site to a suitable heat input. Transport over long distances entails high capital costs and additional transport losses.

These two factors significantly limit the technically and economically feasible options for exploitating waste heat.

The integration options at the facility site primarily determine which heating system is supplied by waste heat from electrolysis. Table 8.5 lists examples of heat-sinks.

Since alkaline or PEM electrolysis are currently the most common, Tables 8.4 and 8.5 together demonstrate that typically only feed-in into the heating network returns is feasible.

Exceptions may be public facilities or similar consumers with large heating requirements for whom the temperature level is of secondary importance. Examples include swimming pools, hospitals, or manufacturing sites in close proximity requiring heat at low-temperature levels.

### 8.2.6.4 Effects of Waste Heat Utilization

#### Increase in Overall Efficiency

When waste heat from electrolysis is used, the overall efficiency of the facility significantly increases.

The efficiency of the electrolysis facility without waste heat use is $\eta_{\text{without}}$, where consumption is defined as the electrical energy fed in $P_{\text{el,in}}$, and as the output the energy content of the hydrogen produced. This output is determined by the hourly production of hydrogen $\dot{m}_{\text{H}_2}$ and its GCV $H_{s_{\text{H}_2}}$ (Eq. 8.88):

$$\eta_{\text{without}} = \frac{\dot{m}_{\text{H}_2} \cdot H_{s_{\text{H}_2}}}{P_{\text{el,in}}}. \tag{8.88}$$

The efficiency is heavily-dependent on the electrolysis technology used, the level of pressure, and the size of the facility (Table 8.3).

The usable process waste heat $\dot{Q}_{\text{use}}$ exceeds the thermal losses in the piping system $\dot{Q}_{\text{RS}}$ and the coolant pump's electrical power consumption $P_{\text{el,P}}$. This means that, as shown in the Sankey diagrams in Fig. 8.28, the overall efficiency $\eta_{\text{with}}$ of the electrolysis can be increased (Eq. 8.89):

$$\eta_{\text{with}} = \frac{\dot{m}_{\text{H}_2} \cdot H_{s_{\text{H}_2}} + \dot{Q}_{\text{use}} - \dot{Q}_{\text{RS}}}{P_{\text{el,in}} + P_{\text{el,P}}}. \tag{8.89}$$

The Sankey diagrams in Fig. 8.28 clearly demonstrate an increase in electrolysis facility efficiency.

#### Economic Efficiency

Three factors primarily determine the economic efficiency of waste heat use:

- The number of full-load hours per year.
- The source of electricity used by the electrolysis.
- The quantity of heat fed in per year.

The quantity of heat fed in per year $W$ is determined by Eq. 8.90 from the heat power $\dot{Q}_{\text{use}}$ and the full-load hours of the electrolysis $t_{\text{FLS}}$:

$$W = \dot{Q}_{\text{use}} \cdot t_{\text{FLH}}. \tag{8.90}$$

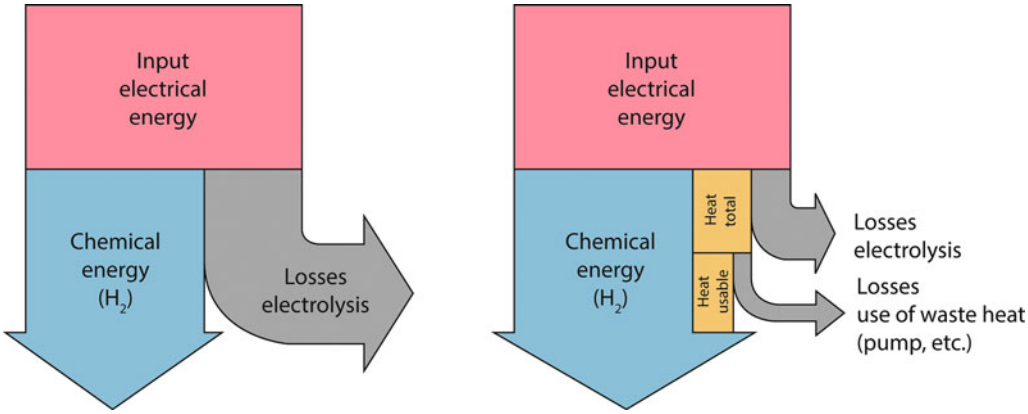



**Fig. 8.28** Sankey diagrams for an electrolysis facility with and without waste heat use

Waste heat use revenues vary with the rate of compensation for heat, which ranges from three to 15 ct/kW h. If renewable electricity is used by the electrolysis, then the waste heat that results is also renewable energy. This qualifies it for German subsidies (EEG, KWKG).

The revenues calculated from the quantity of heat $W$ multiplied by the rate of compensation are offset by the costs for the piping system, the coolant pump, and the heat exchanger. Since these components use cutting-edge, well-developed technologies, the capital costs are low. Operating costs for these components are also low.

A facility's economic efficiency can be improved by developing a coherent heat use concept that includes synergetic utilization on-site. The decision to use waste heat should be based on the individual parameters of the sepcific project. But studying this option makes good sense, because internally consuming or selling waste heat as a by-product can improve efficiency and boost revenues.

## 8.3 Storing Technology-Methanation and Chemical Synthesis

### 8.3.1 Overview of Methane as an Energy Source

#### 8.3.1.1 Overview

In a second step using $CO_2$, electrolytically produced hydrogen can be converted to gaseous or liquid hydrocarbons. The technologies most commonly used in this step are:

- Methanation
- Methanol synthesis
- Fischer-Tropsch process (FT process)

Since only small quantities of hydrogen can currently be integrated into the energy infrastructure, processing hydrogen further at a higher cost makes good sense. The technologies listed above allow hydrogen to be stored, transported, and used more easily.

This is then a solution to the chicken or egg dilemma described in ▶ Sect. 8.1.2.

**Table 8.6** Key characterstics of methane

| Methane | $CH_4$ |
|---|---|
| Gas density at 0 °C and 1.013 bar | 0.7175 kg/m$^3$ |
| Molar mass $M$ | 16.043 kg/kmol or 16.043 g/mol |
| Critical point | $T = 190.555$ K, $p = 45.99$ bar, $\rho = 0.162826$ kg/L |
| Triple point | $T = 90.68$ K, $p = 0.1174$ bar |
| Boiling point at 1.013 bar | $T = 111.63$ K, $\rho = 0.4226$ kg/L |
| Specific heat capacity $c_p$ at 0 °C | 2.156 kJ/(kg K) |
| Thermal conductivity $\lambda$ at 25 °C and 1 bar | $338.9 \times 10^{-4}$ W/(m K) |
| Specific low calorific value at 0 °C and 1.013 bar | 9.97 kW h/m$^3$ or 13.9 kW h/kg |
| Specific high calorific value at 0 °C and 1.013 bar | 11.0 kW h/m$^3$ or 15.12 kW h/kg |
| Production cost of fossil methane | Around 2.5 ct/kW h (high calorific value, import) |
| Production cost of renewable methane (windgas) | Around 4–50 ct/kW h |

8

### Methanation Types

There are two types of methanation:

- Chemical methanation—or thermochemical"=catalytic methanation, or catalytic hydrogenation of CO or $CO_2$.
- Biological methanation.

**Chemical methanation**

the term 'catalytic methanation' is often used as a synonym for (thermo)chemical methanation. But since biological methanation is based on the same principle and enzymes intrinsically contain catalysts, for clarity, (thermo)chemical methanation should be distinguished from biological methanation. In addition, thermochemical processes usually occur at temperatures above 700 to 800 °C, which is not the case with mathanation. For this reason catalytic, thermochemical methanation is termed 'chemical methanation'.

## 8.3.1.2 Natural Gas as an Energy Source

Natural gas is mainly methane. It is used energetically for energy supply and as a material in the chemical industry. In this area, natural gas is used as the basis for a range of chemical source materials. For example, methane can be converted to higher chain hydrocarbons such as methanol using a synthesis process. Methanol also has a wide spectrum of applications in the chemical industry. In 2008, Germany imported a total of around 1,000 TW h of natural gas, 3% of which was used in the chemical industry [104].

Methane is the simplest compound in the alkane group, and has the molecular formula $CH_4$. Alkanes are also called paraffins, or saturated hydrocarbons. Alkanes consist only of carbon and hydrogen atoms. All bonds are single bonds. Alkanes are non-polar compounds, and as a result, do not mix or mix only very little with polar compounds such as water.

Compared to other hydrocarbons, methane and all alkanes are relatively chemically inert. But the gas still has excellent properties as a fuel (Table 8.6).

Methane is a gas at room temperature. Methane's boiling point is about −161 °C and its melting point about −183 °C [75]. Its gravimetric energy density is 13.9 kW h/kg, about three times lower than that of hydrogen (33.3 kW h/kg). But its volumetric energy density is over three times higher than that of

**Table 8.7** Sources of $CO_2$ used on educt for methanation and other syntheses

| Source | Designation/category | Example process |
|---|---|---|
| Atmospheric $CO_2$ | Green carbon | Separation from the air using electrodialysis or adsorption |
| Biogenic $CO_2$ | Green carbon | Separation from biogas |
| Fossil $CO_2$ | Black carbon | Separation from flue gases in (for example) power plants, cement, and steel production |
| $CO_2$ recycling | Green carbon | Combustion of climate-neutral gas (biogas and windgas) in gas power plants, then separation from the flue gas, then recycling of the $CO_2$ for energy storage |

hydrogen, making it an excellent energy source and storage medium.

Methane has the following advantages:

- Good characteristics as a combustion gas or energy source/storage medium.
- High volumetric energy density (factor of three compared to hydrogen).
- Chemically inert, especially in comparison to other hydrocarbons.
- Convertible to higher chain hydrocarbons.
- Extensive existing infrastructure for energy transport and energy storage.

Its disadvantage is its comparably low gravimetric energy density (factor of a 1/3 compared to hydrogen).

### 8.3.2 $CO_2$ Sources for Power-to-X (PtX)

Various storage technologies such as PtG, PtL, and power-to-chemicals (PtC) require $CO_2$ as an educt-gas. The following is a list of the typical sources of this gas (Table 8.7).

If no fossil $CO_2$ is released by the process, then the use of $CO_2$ in the process is climate-neutral overall. It should also be noted that fossil power plants do not become $CO_2$-neutral by using $CO_2$ (green washing). This is because the $CO_2$ after use (carbon capture and use—CCU) in the storage process is released again into the atmosphere by energetic use. In addition, $CO_2$-rich gasses, for example, from biomass are better-suited as sources than flue gas from power plants. This is because, with these gasses, less energy is required to separate the $CO_2$ [49, 107].

The following discusses the advantages and disadvantages of each of these sources. The integration of $CO_2$ sources into PtG storage systems is discussed in ▶ Sect. 8.6.3.

#### ■ Biogenic $CO_2$ from Biogas Treatment Plants

Biogas is about 60% methane and 40% $CO_2$. To feed biogas into the gas network, the $CO_2$ must be separated from the methane to raise it to natural gas quality levels. The $CO_2$ remaining after biogas treatment is cheap and climate-neutral. This is because it is normally not reused, and because it was previously extracted from the atmosphere by plant photosynthesis.

In 2010, less than 100 biogas treatment plants produced around 280 million $m^3$ of biomethane. Assuming a PtG system efficiency of 60%, the $CO_2$ separated by these plants could theoretically be used to store 3.1 TW h of electricity surpluses in the form of methane. The goal of current energy policy is to feed in 6,000 million $m^3$ of biomethane by 2020. This is unlikely due to the cost, but it can still be assumed that around 2,600 million $m^3$ of biomethane will be fed in, which is equivalent to a conversion of 29 TW h of electricity surpluses [117].

#### ■ Biogenic $CO_2$ from Raw Biogas

Another way of using biogenic $CO_2$ is by using raw biogas. The advantage here is that the

$CO_2$ does not need to be separated. The hydrogen from electrolysis is mixed directly with biogas in a reactor where it reacts with the surplus $CO_2$. The resulting methane composed of biomethane from the biogas facility and methane from the Sabatier reaction can then be raised to adequate quality levels and fed into the natural gas network. In contrast with fixed conversion to electricity on-site to meet base-load demand, this allows flexible use of biogenic gas in storage and power plants. If the residual load is positive, i.e., the feed-in of renewable energy is lower than the load, then the biogas can be converted to electricity on-site without using electrolysis. If the residual load is negative, i.e., the available renewable energy exceeds demand, then after electrolysis and methanation, the methane can be fed into the natural gas network for storage. Currently there is no CHP generation at biogas facilities. In 2010 in Germany, 13.3 TW h of electricity was fed in using district heating plants. Assuming an efficiency of 37% and the biogas composition as described above, this is equivalent to 2,400 million $m^3$ of $CO_2$ potential. Taking into account that electricity surpluses are not always available, in the future the overlap between biogas facility operating hours and surpluses will be about one in four. For 2020, this results in a theoretical potential to absorb 10 TW h of electricity surpluses. If biogas facilities are expanded in the future, then by 2050 a potential to absorb 18 TW h of electricity surpluses can be assumed [117].

### Other Biogenic $CO_2$ Sources

$CO_2$ produced as a waste product of other processes in compost facilities, for example, can also be economically used for methanation. Two important processes here are bio-ethanol production and $CO_2$ separation at sewage treatment plants. In 2010, these processes used 300 or 250 million $m^3$ $CO_2$ to methanize 4 or 5 TW h of electricity surpluses. Since yield per hectare and the use of bio-ethanol in the transportation sector will increase, by 2020 the potential is estimated to be 17 TW h [117]. Other potential $CO_2$ sources include biomass gasification processes that convert lignocellulosic plants to synthesis gas (see ▶ Sects. 8.1.3 and 8.3.6).

### $CO_2$ Separation from Air

Use of $CO_2$ directly from air is a convenient option. Combined with a CCS process, it could result in lower levels of $CO_2$ in the air. But separation from the air is expensive and technically difficult. As a result, other $CO_2$ sources are preferred. There are a range of processes currently available [107, 117]:

- Adsorption on solids
- Absorption in solution liquids
- Condensation in cryogenic processes
- Separation from air using membranes

The first German PtG pilot facility in Stuttgart (▶ Sect. 14.3.2) used separation from air by adsorption in solution liquids (electrodialysis), demonstrating that the concept is technically feasible [107].

An advantage is that $CO_2$ can be extracted independent of the location. With hydrogenation syntheses, location is often a limiting or determining factor. Recent research advances indicate that the costs for this process will fall, increasing its economic efficiency. As a result, this $CO_2$ source could play a decisive role in the future. Other reasons are that biogenic and fossil $CO_2$ have limited potential, and there are some regions with no $CO_2$ sources at all.

### $CO_2$ from Power Plants or Manufacturing Facilities

Power plants and manufacturing facilities produce large quantities of $CO_2$. They offer enormous potential for mathanation and other syntheses. Power plants can be replaced by renewable energy, but the steel and cement industry, for example, will continue to rely on cheap fossil energy sources with high-energy densities. These industries will therefore emit $CO_2$ unless the energy system is converted to hydrogen across the board, which is unlikely to occur anytime soon (▶ Sect. 8.6.5). There are also processes that produce $CO_2$ as a waste product regardless of their energy source. But unlike

biogenic $CO_2$, these $CO_2$ sources are not decentralized.

In the steel industry, 142 TW h of electricity surpluses could be methanized using current $CO_2$ emissions. In the cement industry, there is 77 TW h of potential. Since the $CO_2$ content of the emissions from both sectors is lower than from a biogas facility, for example, the emissions must be treated, which is difficult and costly [117]. As a result, integrating PtG into a biogas facility is a better option.

Power plants are not considered as $CO_2$ sources. This is because, in the short-term, no green washing of $CO_2$-intensive power plants is planned, and in the long-term, the electricity sector will be entirely decarbonized. In addition, processing the waste-gas of power plants would increase their primary energy consumption by 20 to 44% [117]. That would mean that a portion of the $CO_2$ emissions separated would actually be produced by the increased energy consumption required to separate $CO_2$. This is clearly a paradox. It could only have a net benefit if the $CO_2$ was stored for thousands of years, or used to produce a solid material, preventing it from entering the atmosphere.

In 2009, the chemical industry also produced 15.6 million tons of $CO_2$ [117].

#### ■ $CO_2$ Recycling/Oxy-Fuel Concept

$CO_2$ recycling refers to a closed carbon cycle (▶ Chap. 1). After combustion of renewable methane using the extraction technologies described in ▶ Sect. 8.5.1, the $CO_2$ is separated from the flue gas and then recycled using methanation. If pure oxygen produced as a by-product of electrolysis is used for the combustion of the methane at the correct stoichiometric ratio, then the $CO_2$ can be relatively easily separated since only $CO_2$ and water result from the combustion. This is significantly more difficult in practice than in theory [107]. ▶ Section 8.6.3 explains how extraction technology, electrolysis, and methanation could be successfully integrated into the power system.

#### ■ Electricity Surpluses

PtG facilities are used when there is negative residual load. As a result, the best $CO_2$ sources are of little use when there are no electricity surpluses in the German system. Due to efficiency losses with the PtG storage system, renewable energy should, as a rule, be consumed directly and only used to produce methane in times of surpluses or network congestion. ▶ Chapter 3 describes in detail when and where electricity surpluses occur and how they can be stored. ◘ Table 8.7 shows the surplus forecast for 2020.

The roles of various $CO_2$ sources in the entire PtG system are described in detail in ▶ Sect. 8.6.3. These roles also apply with all other syntheses.

### 8.3.3 Chemical Methanation

In 1902, the French chemist, Paul Sabatier, published his discovery of the catalytic conversion of $CO_2$ respectively CO and hydrogen to methane. This chemical reaction is, as a result, called the Sabatier reaction.

#### ■ The CO Methanation Breakthrough

The industrial breakthrough of CO methanation came during the oil crisis of the 1970s when oil prices spiked rapidly. Since natural gas prices were coupled with oil prices, natural gas energy prices spiked drastically at the same time.

The dramatic increase in energy prices significantly slowed the economies of the industrialized nations. This led to a large-scale roll-out of nuclear energy, as well as the founding of the International Energy Agency (IEA) in Paris.

The agency's goal was to produce synthetic natural gas (SNG) from coal (also called substitute natural gas). Because it was very cheap compared to other energy sources, lignite coal was primarily used. It was also used because the industrialized nations had large domestic supplies of this coal, and its price was unaffected by swings in the prices of crude oil and natural gas [49].

**Table 8.8** $CO_2$ emissions in millions of tons and potential electricity surpluses in TW h for PtG (times when $CO_2$ production and surpluses overlap at a potential maximum of 100% and at 25%)

| | 2010 | | | 2020 | | |
|---|---|---|---|---|---|---|
| | $CO_2$ emissions in million $m^3$ | Storable electricity surpluses in TW h (25% time overlap) | Storable electricity surpluses in TW h (100% time overlap) | $CO_2$ emissions in million $m^3$ | Storable electricity surpluses in TW h (25% time overlap) | Storable electricity surpluses in TW h (100% time overlap) |
| Electricity surpluses | – | 0.1 | 0.1 | – | 0.26 | 0.26 |
| $CO_2$ from biogas flue gas electricity | 2,400 | 10 | 10 | 3,480 | 14.5 | 14.5 |
| $CO_2$ from biogas treatment plants | 187 | 0.775 | 3.1 | 1,730 | 7.25 | 29 |
| Bio-ethanol | 300 | 1.25 | 5 | 1,020 | 4.25 | 17 |
| Sewage treatment plants | 250 | 1 | 4 | 250 | 1 | 4 |
| Steel industry | 8,400 | 35.5 | 142 | As in 2010 | | |
| Cement industry | 4,600 | 19.3 | 77 | | | |

This meant that SNG was produced at an industrial scale from lignite coal using CO methanation. The gas mixture produced had a relatively low methane content. It was first treated and then fed into the gas network.

### The $CO_2$ Methanation Breakthrough

Various studies conducted in the 1990s and 2000s in Germany demonstrated that the renewable energy system would require large quantities of storage in the future, and that these requirements would be met either by storage water-power facilities in Scandinavia or by hydrogen caverns [103, 121].

Despite its early discovery in France in 1902, using $CO_2$ methanation with energy technology was only studied much later. As with CO methanation, this is because cheaply available resources made it unnecessary. In the 1970s and 1980s, the SolChem concept of chemical-energy storage for solar energy using $CO_2$ was developed in the USA [22, 71]. In the 1990s, Japan built the first chemical $CO_2$ methanation facility under laboratory conditions. Japan is a densely populated country with limited domestic resources, and as a result, was researching liquefied natural gas (LNG) power plants [48, 133]. Germany began to consider $CO_2$ methanation in the early 2000s in relation to fuel cells [94]. Building on solar methanol and biomass gasification research, in 2006, Michael Specht at the Center for Solar Energy and Hydrogen Research in Stuttgart studied the application of the Sabatier reaction to energy storage in Germany [5, 107].

Independently, in 2007, Jürgen Schmid and Michael Sterner at the Institute for Solar Energy Supply Technology in Kassel invented a system that coupled electricity and gas. Using Specht's research, these scientists then jointly developed the PtG concept. This significantly contributed to breakthroughs related to $CO_2$ methanation for energy storage between 2009 and 2011 (▶ Sect. 8.6.1 and [101, 127]). Sterner and Schmid's further research demonstrated the use of $CO_2$ methanation in the context of energy transition [79, 107, 118].

Today, $CO_2$ methanation is considered a crucial component of sustainable, comprehensive energy systems. These systems couple the electricity and gas networks to relieve the electricity networks. They also integrate the heating and transport sectors.

The early stages of PtG research are described in detail in ▶ Sect. 8.6.1.

### 8.3.3.1 Basic Principles

#### ▪ Chemical Reactions

In chemical methanation, two reversible equilibrium reactions occur [61]:

- The water-gas shift reaction
- CO methanation

The first chemical reaction separates the very weakly reactive $CO_2$, and precedes the methanation reaction itself (Eq. 8.91). In principal, direct hydrogenation of the $CO_2$ is also an option, but it is rarely used [94]:

$$H_2 + CO_2 \rightarrow CO + H_2O \quad \Delta H_R^0 = 41\,\text{kJ/mol}. \tag{8.91}$$

The second chemical reaction is the main reaction that hydrogenates the CO (Eq. 8.92). The equation for CO methanation is:

$$3H_2 + CO \rightarrow CH_4 + H_2O$$
$$\Delta H_R^0 = -206\,\text{kJ/mol}. \tag{8.92}$$

As a result, the complete reaction for $CO_2$ methanation is Eq. 8.93:

$$4H_2 + CO_2 \rightarrow CH_4 + 2H_2O$$
$$\Delta H_R^0 = -165\,\text{kJ/mol}. \tag{8.93}$$

The Sabatier reaction in the reverse direction is known as steam-reforming from natural gas, and is the most common process for producing hydrogen (▶ Sect. 8.1.3.2). The precise mechanisms of carbon oxides methanation are described in detail in [94]. The complete reaction (Eq. 8.93) is highly exothermic. As a result, reliable thermal management to remove the energy released is crucial for maintaining the methanation reaction in the proper temperature-range, and for shifting the reaction equilibrium towards methane. Catalysts are used to reduce the high reaction temperatures otherwise required. Paul Sabatier and Jean-Baptiste Senderens discovered in 1902 that various materials such as nickel, ruthenium, rhodium, platinum, iron, and cobalt accelerate the reaction. Nickel was, and remains, the first choice for this process due to its good availability, selectivity, and activity in the reaction, as well as its low price. All catalysts are highly sensitive to gas impurities and trace substances. They are especially sensitive to sulfur in compounds such as $H_2S$ or COS as well as to organic sulfur, chlorine, and heavy metals. Since these impurities deactivate the catalysts, chemical methanation requires excellent gas treatment [61, 94]. The operating pressure and operating temperature vary by the reactor concept used. Low temperatures and high pressures are preferable from a thermodynamic point of view [61]. Temperatures typically range from around 200 to 600 °C and pressures from around 20 to 80 bar. The process temperature must not fall below 200 °C to avoid the formation of the catalyst poison nickel tetracarbonyl [58]. A range of reactors have been experimentally tested in pilot and demonstration projects. Currently, the largest known reactor for $CO_2$ hydrogenation is a MW-class, a two-zone MAN reactor operating at pressures ranging from 5 to 10 bar and at temperatures ranging from 200 to 350 °C under normal conditions. In stand-by mode, the reactor is maintained at operating temperatures (▶ Sect. 14.3)

### $CO_2$ Source Requirements for Chemical Methanation

With chemical methanation, there are two primary $CO_2$ source requirements: the source must have a certain level of purity, and the source must supply the quantity of gas required in the time-frame required. The purity of the $CO_2$ source is crucial, because contaminants such as sulfur degrade the catalysts and may at some point deactivate the reactor. The methanation reaction further increases these purity requirements. This is because the admixture of $H_2$ reduces the volume fraction of the minor components such as the sulfur compounds. Then, once the reaction begins, one part methane is produced from five parts eductgases, of which one part is the impure $CO_2$ (Eq. 8.95). The remaining minor components, as a result, encounter fewer hydrogen and $CO_2$ parts. The concentrations of impurities increase as the gas flow passes through the catalyst bed, and the catalysts' limits may be exceeded.

If the $CO_2$ is separated using a pressure swing absorption (PSA) facility or amine scrubbing, then the use of flue gas from biogas facilities for energy crops is an excellent choice. In addition, the $CO_2$ is directly absorbed by the crops using photosynthesis, meaning the carbon cycle is closed.

### Waste Heat Utilization

Using high-temperature waste process heat can significantly improve the efficiency, cost-effectiveness, and carbon footprint of methanation. Waste heat is also produced by the alkaline or proton exchange membranes (PEM) electrolysis unit upstream. This heat can be used by a low-temperature heat-sink (▶ Sect. 8.2.6). As a result, an overall heat concept should be developed for both the low-caloric waste heat from electrolysis and the high-caloric waste heat from methanation. The synergies of this concept must be optimized for each individual location.

The waste process heat can be used for a range of applications:

- Supplying steam for HTES (▶ Sect. 8.6.4).
- Internal process heat (gas treatment).
- Electricity generation (ORC process) for internal (electrolysis and self-supply) or external use.
- Integration of heat-sinks (district heating, local heating).

The most convenient use is for the internal heat demands of the entire facility. Energy in the form of heat is required for a wide range of technical and chemical processes. One example is the processing of educt and product gases, which ideally should occur synchronously. When waste heat is produced by methanation, it can be used to regenerate the scrubbing fluid loaded with $CO_2$ from amine scrubbing. Here as well, thermal storage can be used to temporally buffer the waste heat. This is just one example among many. With biogas facilities the heat can be used to heat fermenters, sanitize waste, or process other substrates.

But the waste heat produced is also at temperatures sufficient to generate electricity. Theoretically a conventional steam turbine system, an ORC process, or a Kalina process could be used for this purpose. Even greater efficiency could be achieved by vaporizing feed water and using the steam for HTES as in PtL facilities. This technology is still in experimental development, but would increase efficiency by about 20% (▶ Sect. 8.7).

Waste heat could also be fed into district or local heating. But heat extraction should always be synchronized and coupled with heat production. As a result, intermittent operation using wind and solar electricity surpluses poses a challenge. If operation is continuous, then the heat must be consistently drawn off from the facility at all times throughout the year. Since some heat-ssinks cannot consistently draw off heat in the summer, this would cause the methanation facility to shut down at these times.

## 8.3.3.2 Reactor Concepts

In principal, methanation is a special form of the FT process with virtually no risk of chain-growth. As a result, the reactor concepts also

closely resemble those using the FT process (▶ Sect. 8.3.6.2).

### Drawing off Waste Heat—Preventing Hotspots

Chemical methanation releases large quantities of energy in the form of heat. All reactor concepts require highly reliable heat extraction. Otherwise, hotspots may form in the reactor.

**Definition**

A hotspot is selective overheating of the catalyst within the reactor at a specific location.

Overheating causes the reaction equilibrium to shift towards the educt-gas. This may deactivate or even permanently damage the catalyst. In both cases, the reactor ceases to operate properly.

### Flexible Operation

Reactor concepts must also allow flexible operation. In the future, methanation facilities will be used in PtG facilities to absorb and balance fluctuations in the electricity network caused by wind and solar facilities. As a result, these reactors must allow dynamic operation at different load points.

Molten salts and water vapor, for example, are used to maintain the reactor at a constant temperature. In addition, thermal losses from convection and radiation while in stand-by mode must be covered. Auxiliary electric heat and adequately thick reactor insulation have been successfully used for this purpose in experimental reactors. The mass of the catalyst bed also effects start-up time.

Pre-rinsing and post-rinsing of the reactor during start-up and shut-down also slow the system down. To ensure that the reactor starts up in operational conditions safe for the catalyst, it must be pre-rinsed with hydrogen before use. In addition, to avoid damage to the catalyst no harmful residual gases can remain in the reactor after use. For this purpose the reactor is filled with hydrogen in stand-by mode, or kept in an inert atmosphere. These internal operational times mean the reactor has start-up and shut-down gradients (also called ramps) that make operation with fluctuating wind and solar energy a challenge.

### Processes in Use and in Development for Chemical Methanation of $CO_2$

There are various reactor concepts for implementing chemical methanation. They are described in detail in the sub-chapter on the FT process in ▶ Sect. 8.3.6.2. From a purely theoretical point of view, homogenous temperature distribution makes the fluidized bed process inappropriate for the two-step process of $CO_2$ methanation, in which different temperatures for $CO_2$ splitting and for CO methanation are an advantage. But there is no experimental data to substantiate this assumption.

The concepts currently in use differ considerably from those tested in the laboratory by stage of development, catalyst used, and basic design. The following discussion focuses on two reactor concepts:

- Fixed bed reactor (in use and in development)
- Three-phase reactor (in development)

### Fixed Bed Reactor

The fixed bed reactor is the most established reactor concept. The process can be designed using a single step or several steps. The gas quality required by DVGW G 260 can only be achieved using a several-step process with gas treatment connected to a single-step process [24]. The catalyst is placed as a fill between pipes or plates.

Reactor designs vary widely. The thermal management systems used vary as well. The educt-gas streams over the catalyst and is converted to the product gas. The heat produced is drawn off by a coolant in the pipe or plate (◘ Fig. 8.29).

The standard fixed bed reactor design is the pipe-bundle reactor, which is described in ▶ Sect. 8.3.6.2. A process currently commercially available is the TREMP process from the company Haldor Topsoe (Topsoe's recycle methanation process) composed of three

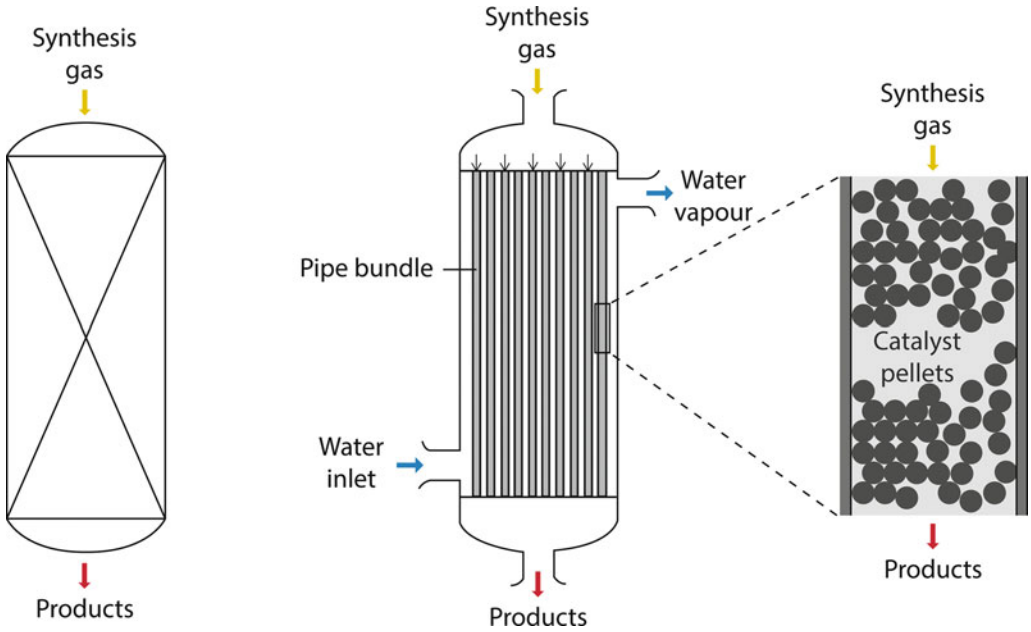



**Fig. 8.29** Reactor design and detail of catalyst filling in a pipe-bundle reactor [87]

adiabatic fixed bed reactors (Fig. 8.30). Only a portion of the educt-gas is used in each reactor. Temperatures in the reactors range from 250 to 700 °C. The pressure range goes up to 30 bar and decreases from reactor to reactor (Table 8.9). To limit hotspots, a portion of the gas mixture is recycled in the first reactor. After passing through all three reactors, the reaction heat is decoupled, usually to generate high-pressure steam [61, 86].

The stability of the catalyst in stationary operation with CO methanation has been shown to exceed 8,000 hours in long-term tests. The stability of the catalyst with $CO_2$ methanation using highly variable wind and solar electricity over the long-term has yet to be determined.

The TREMP process has several significant advantages:

- Potential recycling of superheated, high-pressure steam that can be directly fed into a steam turbine.
- Energy savings due to a high recycling rate, i.e., most of the synthesis gas is used per cycle, which otherwise would have to be fed back into the cycle incurring energy losses.
- Stable and high reactivity over a wide range of temperatures (250 to 700 °C) using a mix of various catalysts.

Other notable methanation processes, some commercially available, are the Lurgi process, the Linde process, the RMP process, the MAN processes, and the HICOM process from the company Davy. All are basically tube-bundle reactors [61]. The advantage of these reactors is that the pressure and resulting volumetric flow can be controlled in each tube or in the tube-bundle as a whole, ensuring that the reaction occurs evenly. The difficulties include thermal management as well as preventing hotspots and hot zones.

There also experimental plate reactors, where the catalyst is placed between the plates as a solid filling. These reactors should have better thermal characteristics than pipe-bundle reactors, but this has yet to be proven in long-term stability tests. Although fixed bed reactors have been in use for over a century, there are still important questions about the characteristics of pipe-bundle and plate reactors (currently

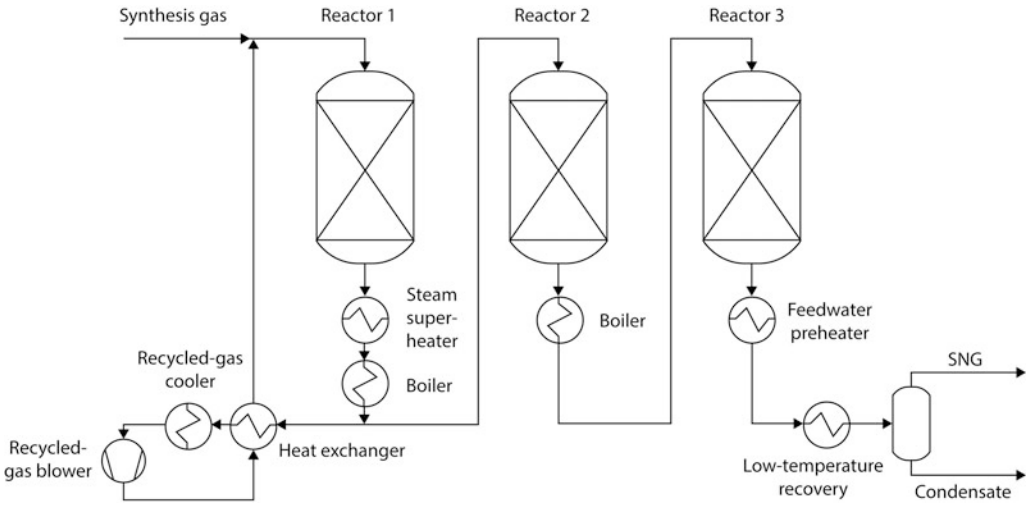



**Fig. 8.30** Basic design of a TREMP process from Haldor Topsoe, Sweden [61, 86]

**Table 8.9** Operating parameters of a CO methanation reactor using the TREMP process from Haldor Topsoe, Sweden in March, 1979 (ADAM I) [61]

| | Educt-gas | Reactor 1 input | Reactor 1 output | Reactor 2 output | Reactor 3 output | SNG |
|---|---|---|---|---|---|---|
| Temperature in °C | | 300 | 604 | 451 | 303 | 23 |
| Pressure in bar | 27.3 | 27.2 | 27.1 | 27.05 | 27.0 | 27.0 |
| Gas in $m^3/h$ | 535 | 1,416 | 1,255 | 348 | 334 | 119 |
| Gas composition in % | | | | | | |
| $H_2$ | 65.45 | 36.88 | 20.96 | 8.10 | 1.77 | 3.11 |
| CO | 9.84 | 4.28 | 1.17 | 0 | 0 | 0 |
| $CO_2$ | 8.96 | 6.13 | 4.46 | 2.07 | 0.95 | 1.67 |
| $CH_4$ | 11.30 | 28.12 | 37.44 | 44.36 | 47.28 | 82.95 |
| $N_2O$ | – | 19.19 | 29.82 | 38.84 | 43.06 | 0.10 |
| $N_2$ | 4.4 | 5.41 | 6.15 | 6.64 | 6.93 | 12.16 |

under study at a range of institutions, including ZSW Stuttgart, the Engler-Bunte Institute (EBI) Karlsruhe, the Max-Planck Institutes, the TU Munich, and the FAU Nürnberg-Erlangen) as follows:

- Reaction characteristics.
- Alternating operation with base-loads, partial-loads, and peak loads.
- Start-up and shut-down processes.
- Stability of the process and the catalysts.
- Reactor design and design structure to optimize flow over the catalyst bed.

The fundamental principles and parameters of reactor design are described in [51].

### Three-Phase Reactor

The three-phase reactor was first tested in the 1970s [61]. The technology was then studied again in the early 2010s by the DVGW research

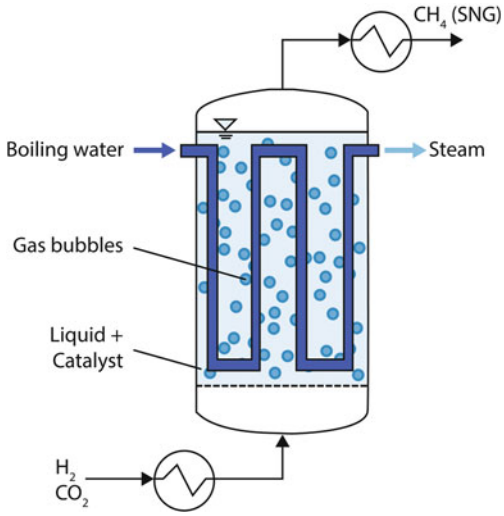



**Fig. 8.31** Three-phase reactor for methanation by the DVGW EBI in Karlsruhe



center at the EBI of the Karlsruhe Institute for Technology. Unlike the pipe-bundle reactor, this reactor concept is still entirely in the research and development phase.

All three phases are present in the reactor: solid (catalyst), liquid (reactor liquid), and gas (hydrogen and $CO_2$) (Fig. 8.31). The educt-gas flow enters the liquid from below and then rises through it as bubbles. The catalyst in powder form is held in suspension in the liquid. A suspension is formed by finely distributing small particles of a solid material in a liquid so that they float in it. Hydrogen and $CO_2$ dissolves in the suspension as it passes through it, and then reacts with the catalyst particles suspended in the liquid. The liquid does not participate in the reaction, and serves only to draw off the heat. Since the catalyst particles are suspended directly in the liquid itself, the risk of hotspot formation is minimal. The reaction occurs at 300 °C and 20 bar [46].

As a result, methanation using a three-phase reactor has significant advantages in terms of heat extraction and control. In addition, it can also be applied flexibly with dynamic operation. Because of its high liquid content, this reactor has a high mass. This means that short interruptions in operation can be buffered and the temperature can be maintained for a short time at the required level. An external supply of heat can also be applied with little difficulty. But these advantages are offset by certain difficulties. These include maintaining the temperature of the liquid stable and upscaling the experimental technology to industrial levels. In addition, cold-starting the reactor is relatively energy-intensive.

#### ▪ Operating Mode and Conversion Rates

All reactors can be operated either in once-through mode or full-conversion mode. In once-through mode, the synthesis gas is fed through the reactor a single time and is, as far as possible, completely converted. The residual gases are thermally recycled or integrated into the process. In full-conversion mode, the residual gases are treated and fed again into the reactor to achieve the highest conversion rate possible.

A disadvantage of chemical methanation—regardless of the reactor concept—is that in continuous operation, the methane content of the product gas currently peaks at about 95%. To subsequently increase the methane content so that the product gas qualifies as a replacement gas for natural gas according to DVGW G 260, a downstream membrane process must be applied [134].

An alternative is to use biological methanation instead of chemical methanation. As described in the next section, this process results in higher methane content levels in the reactor itself, even when the flow rates are lower.

### 8.3.4 Biological Methanation

Biological methanation is also called methanogenesis. It was discovered in the 16th century by the Italian physicist Alessandro Volta while researching the flammability of marsh gas. He called the gas it produced 'burning air' [7, 78].

### Classification of Methanogenesis in Biology

Like chemical methanation, biological methanation is based on the conversion of hydrogen and $CO_2$ to methane. Here, the conversion is performed by organisms from the Archaea domain, previously also called archaebacteria or primordial bacteria. They are among the oldest forms of life on Earth.

The Archaea kingdom was the first domain of life, and date back three or four billion years. Archaea's modern classification was established in the 1970s by Carl Woese based on the sequencing analysis of the ribonucleic acid 16Sr-RNA. This molecule performs vital functions in the cell [115].

Based on this new classification, the five biological domains of animals, plants, protists, fungi, and bacteria were reduced to three domains:

- Bacteria
- Archaea
- Eukarya

The Archaea are grouped into three phyla; the Euryarchaeota, Crenarchaeota, and Korarcheaota. The Euryarchaeota are the most important for biological methanation, and include the methogen group.

### Occurrence in Nature

The Archaea existed at a time when the Earth's atmosphere contained no oxygen. They use hydrogen and $CO_2$ to produce methane; an essential component of their metabolism. Since they are generally anaerobic, they cannot live in oxygen. As oxygen appeared in the Earth's atmosphere, they gradually migrated to places where there is no oxygen.

Their natural habitat is in the deep sea, in what are called black smokers. Black smokers are hydrothermal vents in the seabed at depths ranging from around 2,000 to 4,000 m. At these depths, the water pressure ranges from around 200 to 400 bar. The hot water released from the black smokers raises the temperature of the ocean in their vicinity to around 350 °C. Since the vents release large quantities of gases and minerals, such as sulfur compounds together with thermal water into the ocean, the pH level of the ocean in their vicinity is between 4 to 8. Only highly resistant micro-organisms can tolerate these harsh conditions. Archaea bacteria produce methane using methanogenesis in this environment. The robustness of these bacteria is technically useful for methanation [62]. Archaea are also found in other habitats such as volcanoes, sewage treatment plans, soil, or the digestive tracts of ruminants.

The flexibility these organisms need to survive is also technically useful for energy storage. In the absence of hydrogen and $CO_2$, these bacterial strains 'hibernate' until the educt-gases are available again. Unlike with chemical methanation, this process occurs in biological methanation as a consequence of the bacteria's inability to store energy and without any pressure applied [63].

## 8.3.4.1 Basic Principles

Like chemical methanation, biological methanation uses catalysts. The difference is that the catalysts are packed in enzymes, and that the reactions occur in living organisms (the bacteria). The example in Fig. 8.32 shows these kinds of bacteria in a bio-reactor from the company Electrochaea GmbH.

### Advantages and Disadvantages Compared to Chemical Methanation

This conversion process adapted from nature has a range of advantages compared to chemical methanation [85]:

- Methane content exceeding 98% with low reactor load (low gas-flow rate) and using a single conversion step without gas treatment.
- Low process temperatures ranging from around 40 to 60 °C vs. 200 to 600 °C.
- Low process pressures ranging from around 1 to 3 bar vs. 5 to 80 bar.
- Low purity requirements for the educt-gases carbon monoxide and hydrogen.
- Fast and flexible load alternations without pre-rinsing and post-rinsing with nitrogen.

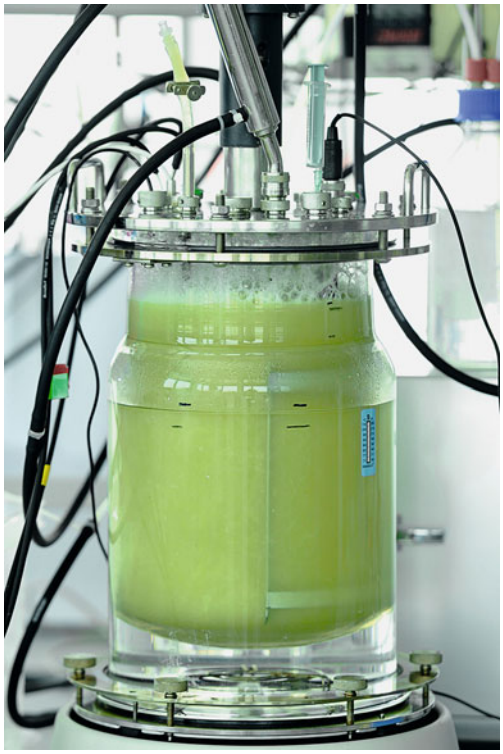


**Fig. 8.32** Stirrer tank reaktor for biological methanation with Archaea-micro-organisms (Source: Electrochaea GmbH)

- Small facilities in decentralized concepts at kW scale technically practicle and feasible.

But these advantages are offset by disadvantages, primarily due to using living bacteria strains that reproduce, consume, become inactive, and die out:

- Constant feeding of the bacteria required (similar to fertilizer).
- Waste water recycling and treatment also possibly required.
- Poor solubility of hydrogen in aqueous solutions, or energy consumption required to insert gas (around 1% of the product gas as electrical energy: for example 2 kW h per $m^3$ reactor volume at 200 kW h methane gas per hour).
- Upscaling to large facility levels not as easy as with chemical methanation, which has a better time-volume yield than biological methanation; currently biological methanation is limited by its dimensioning to the single-digit MW range that can only be exceeded using a modular design.

### Biological Reactions

The basic process is a reduction of $CO_2$ by integrating several $H_2$ molecules from formaldehyde and methanol using a formate step (salts) to form $CH_4$.

The operating principle of the methanogenesis process is illustrated in Fig. 8.33.

A hydrogenase participates in each of the four reduction process steps illustrated in Fig. 8.33. This means that hydrogen functions as an electron donor in each step. A range of cofactors with a variety of functions accompany this process. They can be categorized as follows:

| | |
|---|---|
| C1 carriers: | for example methanofuran (MFR), tetrahydromethanopterin ($H_4$MPT). |
| Electron donors: | for example coenzyme B (CoB), F420. |
| Catalysts: | for example F430. |

C1 carriers are cofactors that bind with the carbon (C) from the $CO_2$ in the course of the process. The term electron donor applies to particles such as F420 that can shed electrons. But the factor F430 functions solely as a catalyst.

The first step of methanogenesis uses a MFR dehydrogenase to bind $CO_2$ to MFR and then reduce it to the formyl group. It is then translocated to $H_4$MPT and finally reduced by F420 with two further steps in the methyl group. Methyltransferase is used to translocate the $H_4$MPT groups to CoM–S–$CH_3$. Then the methyl coenzyme M reductase is used to reduce the methyl group to methane.

The resulting by-product CoM–S–S–CoB can be converted to coenzymes M and B using hydrogenase. These can then be reused in the methanogenesis cycle [10, 25, 76].

Michael Hermann Bott and Rudolf Kurt Thauer have determined the reaction rates for

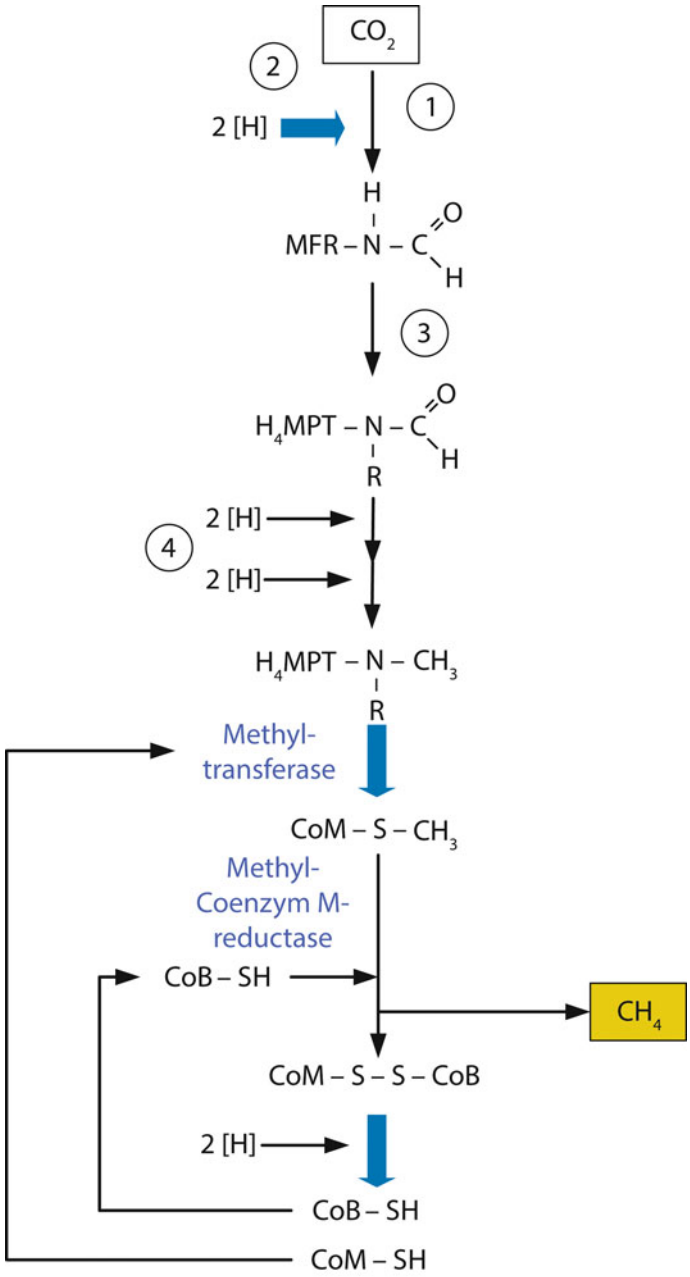



**Fig. 8.33** Methanogenesis from $CO_2$ [76]. The individual process steps and their colors are the following. *Black arrow*: reactions catalyzed by soluble enzymes. *Blue arrow*: reactions catalyzed by membrane-bound enzymes that facilitate the transport of particles from one side of the cell membrane to the other. (*1*) MFR dehydrogenase (enzyme that oxidizes its substrate. This occurs at the acceptor by a catalysis of proton translocation). (*2*) Hydrogenase (▶ Sect. 8.1.3.3). (*3*) Formyltransferase (enzyme that catalyzes the translocation of a methyl group from a donor to an acceptor). (*4*) Electron donor

various methanogenic bacteria in batch experiments [13]. A single bacteria strain called a pure culture was used in each of these experiments. In all the experiments, an ideal mixture of gas was fed a single time into a pressure vessel. Methane formation was measured as the pressure was reduced (Table 8.10). There were significant differences in methane formation among the various pure cultures.

The rates of formation ranging up to 96 liters of methane per liter of pure culture per day demonstrate an effective conversion rate

**Table 8.10** Methane formation rates with different bacteria strains (pure cultures) [91]

| Strain | Growth density [mg protein/liter] | Rate of $CH_4$ formation [nmol/(min·mg protein)] | Rate of $CH_4$ formation [μmol/(min·liter (culture))] | Rate of $CH_4$ formation [mg/(min·liter (culture))] | Rate of $CH_4$ formation [ml/(min·liter (culture))] | Rate of $CH_4$ formation [liter/(day·liter (culture))] |
|---|---|---|---|---|---|---|
| Methanobacterium thermoautotrophicum | 500 | 6,000 | 3,000 | 48 | 66 | 96 |
| Methanobrevibacter aboriphilus | 500 | 840 | 420 | 6.7 | 9.0 | 13.4 |
| Methanospirillum hungatei | 180 | 220 | 40 | 0.64 | 0.8 | 1.27 |
| Methanosarcina barkeri | 170 | 150 | 26 | 0.41 | 0.6 | 0.82 |

8

equivalent to a specific continuous power of around 40 kW/m$^3$ of fermenter volume [91].

Other processes resulted in methane formation rates of up to 540 liters per day and per liter culture, equivalent to a thermal power of 250 kW per m$^3$ [62].

### Gas Purity and Gas Quality

The educt-gas $CO_2$ can be obtained from the sources described in ▶ Sect. 8.3.1. But unlike with chemical methanation, no treatment of the $CO_2$ or of the hydrogen produced from the electrolyte is required. This is because most of the additives provide minerals required for bacterial growth [50, 85].

With the correct facility design, these organisms can be used to generate product gas with a methane content of around 97% by volume. About 1% by volume of hydrogen and about 0.5% by volume of $CO_2$ remains in the product gas (Fig. 8.34). In other experiments, using an educt-gas of 80% hydrogen and 20% $CO_2$ resulted in the following product gas qualities in a single step [85]:

Laboratory experiments:

- 98.9% $CH_4$
- 0.6% $CO_2$
- 0.5% $H_2$

Pilot plant with a reactor volume of 1 m$^3$:

- 98% $CH_4$
- 2% $CO_2$
- < 0.1% $H_2$

Gas quality levels defined by the DVGW for replacement gas can be obtained by using biological methanation with low volumes or low reactor utilization and without additional gas conditioning or treatment [24].

Biological methanation is a promising technology. Challenges include supplying the gases required (especially hydrogen), the amount of energy required for that supply, and upscaling the technology. In addition, the technology is typically limited by its time-volume yield. The higher the methane formation rate compared to the time-volume yield as well as to the energy required for stirring and the process engineering, the more efficient and cost-effective the facility can be.

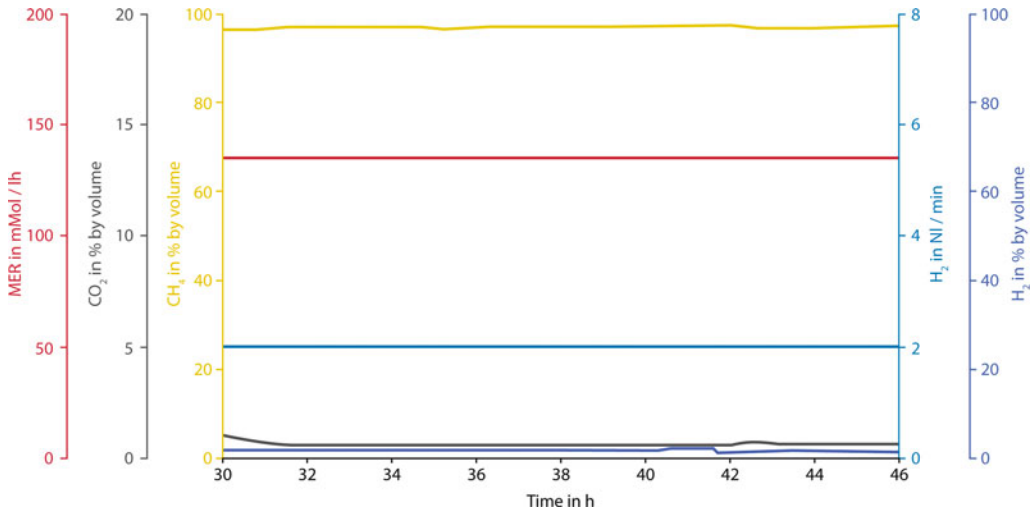



**Fig. 8.34** Gas quality of biological methanation with constant hydrogen and $CO_2$ supply in a 10 liter reactor using pure cultures in Linz [62]

### 8.3.4.2 Reactor Concepts

There are currently two standard processes for implementing biological methanation: reactors using pure cultures or mixed cultures.

#### ▪ Reactors Using Pure Cultures

In this reactor concept, hydrogen and carbon dioxide are supplied to a stand-alone methanation rector under constant process conditions. Thermophile Archaea in pure culture function as bio-catalysts in the reactor.

Besides the educt-gases, hydrogen and $CO_2$, only certain minerals dissolved in water for organism growth must be constantly supplied [50].

Various companies are currently developing methanation technologies. A pioneer in the field since 2007 is Krajete GmbH. At the heart of the process is a specially designed stirred tank reactor. The micro-organisms used (monoculture) to catalyze the reaction are contained in the tank in an aqueous solution. Methane formation occurs in the stirred tank when $H_2$ and $CO_2$ are continually supplied. The educt-gases at the bottom of the reactor are inserted into the fermentation liquid (liquid and biomass) using a stirrer such as in a slurry reactor using the FT process. They are then converted to methane as they pass through the reactor [64].

The product collects in the headspace of the reactor, and is continually released through the exhaust line in the cover plate. Besides the gaseous substrates $H_2$ and $CO_2$, the micro-organisms used here require a small number of other elements (N, S, P, trace elements) to be continually supplied to the fermenter in aqueous salt solutions. Due to this continual supply of liquids and because water is produced by methane formation, to keep the volume constant fermentation liquid must be constantly removed from the reactor. Continual-operation results in a reaction equilibrium. This means that the conversion rates and concentrations of all materials stay constant over time. This applies to the living biomass as well, since it is constantly regenerated.

The thermophile strain of these micro-organisms is sufficiently active for production in temperatures ranging from about 45 to 70 °C. The optimal pH level is 7.0, but in laboratory experiments pH levels ranging from 5.0 to 8.0 were also tolerated [62].

The methane formation rate peaks at 1 mole of methane per liter of fermentation volume per hour, which is equivalent to 22.41 $m^3$ per hour

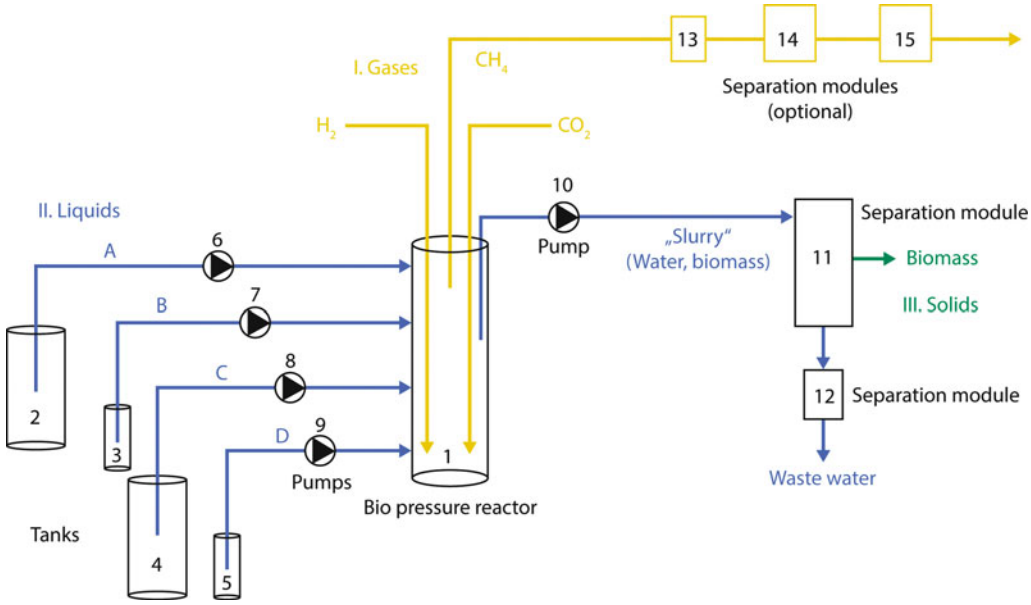



**Fig. 8.35** Concept design of a facility using pure cultures. Ten liter reactor in Linz. Block diagram of a bio-reactor at production scale (1) with facility peripherals. Modules I and II supply gases and liquids. Module III separates and processes the suspension. The biomass is separated in Component 11. Component 12 (which is optional) treats the suspension water so that it can be disposed of as waste water if required. Thirteen and 14 are the water separator and $H_2S$ scrubber used to remove residual moisture and $H_2S$. Component 15 refines the product with a molecular sieve [62]

per cubic meter of reactor volume. Under favorable conditions, over 99% of the hydrogen is converted. If pure educt-gases are supplied, this results in a dry crude gas composition containing at least 96% by volume of $CH_4$, at most 3% by volume of $H_2$, and 1% by volume of $CO_2$.

Since the biological catalyst tolerates secondary components, in theory, crude biogas, processed biogas, automobile gas, and coke oven gas can be methanized directly. Under ideal conditions, the reactor can go from stand-by mode to full-load operation within a few seconds. Technical optimization of the start-up process is critical here. Laboratory experiments indicate that multiple load alternations and long idle periods have no negative effect on the bacteria's productivity. But this has yet to be proven in long-term stability tests at a larger scale.

In addition to methane, water and biomass are formed. About 2% of the carbon produced from the $CO_2$ is absorbed by the biomass. The water generated as well as the biomass must be constantly removed from the process. This results in a flow of waste water containing biomass. In theory, this waste water can be used as a substrate in biogas facilities or for fertilizer. It can also be disposed of using the sewage system and then purified in a waste treatment plant. Treatment requires separating the biomass for composting or combustion, as well as removing certain ions [62].

Figure 8.35 shows the concept design of a facility in Linz as an example.

A gas supply system feeds the educt-gases, hydrogen and $CO_2$, into the bio-reactor (1). The product gas leaves the reactor and is then purified in the other separation modules (13, 14, 15). All water and sulfur is removed so that the gas conforms to the DVGW requirements for gas feed-in.

Additives in salt solutions are fed in from containers (2, 3, 4, 5) by pumps (6, 7, 8, 9). Process water as well as wet biomass are also

siphoned off by a pump (10). They are then separated in the next step (11). Depending on how the waste water is used, the water may be treated in a final step (12).

The basic components of the process is the core reactor (bio-pressure reactor) (1), the containers (2, 3, 4, 5), and the separation modules (11, 12 optional, 13, 14, 15). Other facility components such as mass and volume flow-rate sensors, compressors on the product side, and analytical measurement instruments are not included here. The illustration shows only the reactor and the peripherals required to process the gas flow or the suspension.

The containers (2, 3, 4, 5) are required to supply the suspension. The pumps (6, 7, 8, 9, 10) are used to supply the salt solutions and to remove the process water.

The purification and separation modules (11, 12 optional, 13, 14, 15) are required to process the suspension water or to remove the approximately 500 ppm of $H_2S$ and residual $CO_2$ from the gas flow.

Heat is exchanged through the shell using water as a coolant. By using the biological process for thermal management, the goal here is to minimize energy input for a heating/cooling unit to the point where the unit is only rarely required.

Figure 8.36 shows the design of an experimental reactor using pure cultures.

A number of experiments in laboratory and pilot facilities with reactor volumes of a few liters to a few cubic meters have shown that high gas quality is still found in the headspace of the reactor, even after long idle periods. Methanation of hydrogen and $CO_2$ can also be restarted immediately without any delay or compromise in gas quality [62, 85].

In addition, certain bacteria strains are extremely resistant to foreign materials such as oxygen and stable over long periods, meaning they can be fully reactivated, even after idle periods lasting several weeks [53].

The process has yet to be proven on a large-scale. Mixing the gases with the reactor liquid is a particular challenge here. This may reduce the gas quality as well as increase the energy consumption required for homogenization. Further research is required in this area.



**Fig. 8.36** Ten liter reactor using pure cultures in Linz (source: Krajete GmbH)

### Reactors Using Mixed Cultures

Besides reactors using pure cultures, there are also reactors that use thermophile Archaea in mixed cultures. These mixed cultures are composed of different methanogenic bacteria strains. Here, a supply of minerals dissolved in water is also critical for bacteria growth.

### Mixed Cultures in Bio or Sewage Plants

Unlike pure cultures, mixed cultures are already used in standard processes such as biogas fermentation and sewage treatment. The idea is to use them for methanation as well. By adding hydrogen, methane yield could then be increased in biogas facilities or sewage plants. Since they are also used for biogas or sewage gas production, some of the organisms required are already present in the reactor. But some special methanogenic bacteria strains must be added to the facility to optimize hydrogen conversion.

Since the substrate contained in the fermenter provides the nutrients required for the bacteria, additional minerals must no longer be supplied.

It is typically assumed that increasing hydrogen content in fermentation processes dramatically reduces their productivity, or even halts them entirely [60]. But the methanogenic bacteria in the digestion tank of a sewage treatment plant can not only process a normal hydrogen flow, they can even process $H_2$ volumeflows of up to a hundred times greater [10]. In Schwandorf, experiments implementing this idea were conducted in biogas fermenters and working sewage treatment plants. The results demonstrated that hydrogen fed into a stable fermentation process had no measurable negative effects. Figure 8.36 shows the effect of adding a small quantity of hydrogen, 5 $m^3$/h, to a digestion tank that produces about 36 $m^3$/h of sewage gas in a mixture of 65% by volume of $CH_4$ and 35% by volume of $CO_2$. The results show that, within an hour, 60% by volume can be increased to 63% by volume (blue line) and the portion of $CO_2$ reduced as a result (red line). After a period of time, the hydrogen is completely absorbed, and only very low residual quantities of hydrogen are found in the product gas (green line).

The advantage of mixed cultures is that the existing reactors, power connections, gas infrastructure, and gas utilization methods can be used. The costs for PtG facilities are reduced as a result. A difficulty is the energy consumption required for stirrers to inject gas into the fermenter, and the gas quality levels and gas volumes per reaction volume that can be achieved as a result.

## 8.3.5 Methanol Synthesis

Between 1920 to 1923, at a chemical facility in the central German town of Leuna, the German chemist and university professor, Matthias Pier, developed methanol high-pressure synthesis at an industrial scale to produce methanol as a basic material for the chemical industry. Lignite coal was used as a source material. A fluidized bed process was used to gasify and condition the coal to synthesis gas. Methanol was previously produced solely by simple distillation from wood biomass.

### 8.3.5.1 Basic Principles

#### Chemical Reactions

Methanol can be formed from carbon monoxide and hydrogen (Eq. 8.94) or from carbon dioxide and hydrogen (Eq. 8.97). Both reactions are highly exothermic. As a result, the reactor requires a cooling unit. Boiling-water cooled reactors or synthesis gas return are used to cool the reactor. Another way to cool the reactor is to inject cold synthesis gas:

$$\mathrm{CO} + 2\mathrm{H_2} \leftrightarrow \mathrm{CH_3OH};$$
$$\Delta H_R^0 = -91\,\mathrm{kJ/mol}, \tag{8.94}$$
$$\mathrm{CO_2} + 3\mathrm{H_2} \leftrightarrow \mathrm{CH_3OH} + \mathrm{H_2O};$$
$$\Delta H_R^0 = -49\,\mathrm{kJ/mol}. \tag{8.95}$$

Methanol synthesis is an equilibrium reaction that can be shifted towards methanol by increasing the pressure and temperature. But since the thermodynamic equilibrium does not allow very high conversion rates of synthesis gas, it must be recycled and then fed back into the synthesis. This also requires heat exchangers and compressors. The cycle consists of synthesis, then separation of methanol from water, then return of the remaining synthesis gas. Methanol synthesis uses catalysts based on zinc (Zn), chrome (Cr), or copper (Cu) and occurs at pressures over 50 bar and temperatures ranging from 220 to 380 °C. With current technology, the selectivity is 99.9% and the is efficiency over 70%.

To increase the methanol yield per cycle, the following approaches could be used:

- Adjust the synthesis gas ratio to match the stoichiometry.
- Increase the equilibrium level towards methanol by increasing the pressure and temperature.
- Use new catalysts that function at lower temperatures.

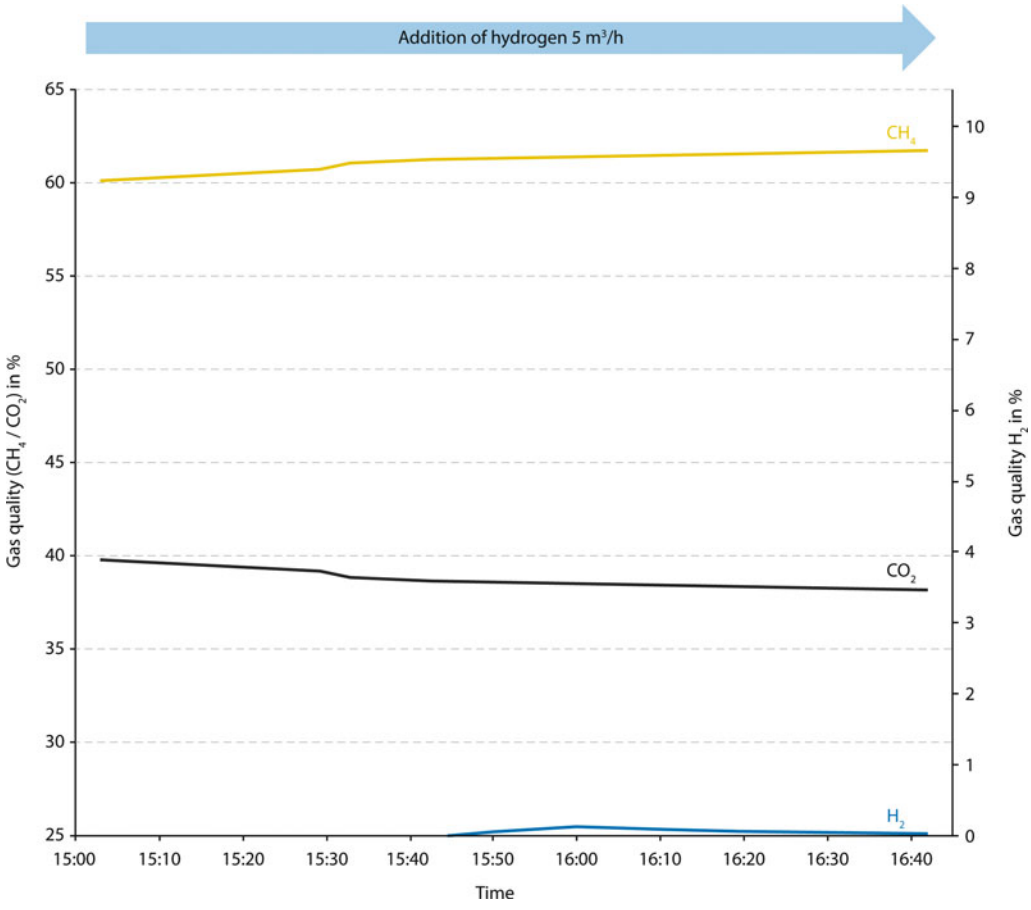



**Fig. 8.37** Increasing methane content in a sewage gas fermenter (digestion tank) by adding hydrogen; results from experiments conducted in Schwandorf [85]

- Extract methanol from the reaction using membranes, absorbers, or condensation to increase the equilibrium level on the product side.

Using $CO_2$ allows synthesis at lower temperatures and with higher selectivity. This means that synthesis gas can be conveniently used in the PtL storage process. But the reaction (Eq. 8.95) also produces water, which then has to be separated off [59].

### Production

There are several established processes for producing methanol (Fig. 8.39):

1. Synthesis of synthesis gas from fossil and biogenic raw materials (commercial facilities).
2. Directly converting methane to methanol.
3. Energy storage processes based on the reaction of carbon dioxide and hydrogen.

For synthesis gas generation, any carbon-based material such as coal, coke, crude oil, methane, or $CO_2$ can be used. Natural gas is currently favored because it contains almost no impurities that damage catalysts, the hydrogen content is high, and the reactions require less energy than with other methods [9, 81]. But the main reason is because natural gas is more cheaply available than biomass or renewable hydrogen.

### 1. Synthesis of Synthesis Gas by Indirectly Converting Methane to Methanol

Methane can be converted using either direct conversion or indirect conversion. With indirect conversion of methane to methanol, synthesis gas is produced by partial oxidation in an intermediary step.

With partial oxidation (Eq. 8.96), methane is partially burned with oxygen at a substoichiometric ratio to produce synthesis gas (see steam-reforming of methane to produce hydrogen in ▶ Sect. 8.1.3.2). The synthesis gas ratio of $H_2$ to CO is 2:1 in this reaction. The waste heat produced must be removed using cooling equipment:

$$\mathrm{CH_4} + \frac{1}{2}\mathrm{O_2} \leftrightarrow \mathrm{CO} + 2\mathrm{H_2};$$
$$\Delta H_R^0 = -35\,\mathrm{kJ/mol}. \qquad \textbf{(8.96)}$$

To produce synthesis gas without consuming additional energy or using special cooling units, exothermic steam-reforming (Eq. 8.96) combined with the strongly endothermic reaction in Eq. 8.97 can be used in what is termed autothermal reforming:

$$\mathrm{CH_4} + \mathrm{H_2O} \leftrightarrow \mathrm{CO} + 3\mathrm{H_2};$$
$$\Delta H_R^0 = +206\,\mathrm{kJ/mol}. \qquad \textbf{(8.97)}$$

The reactions can then occur simultaneously if a mixture of methane, water vapor, and oxygen is used. But since the preferred pressures and temperatures for these reactions vary, it makes better sense to split them up in two steps. Steam-reforming occurs in the first step. Synthesis gas is then produced in the second step from the unconverted methane using partial oxidation.

The final synthesis of methanol from CO and $H_2$ is achieved using Eq. 8.94.

### 2. Synthesis by Directly Converting Methane to Methanol

The other method is to convert the methane directly to methanol using partial oxidation without first converting it to synthesis gas. This reaction is preferred because it eliminates the difficult synthesis gas generation process.

$$\mathrm{CH_4} + \frac{1}{2}\mathrm{O_2} \leftrightarrow \mathrm{CH_3OH};$$
$$\Delta H_R^0 = -126\,\mathrm{kJ/mol}. \qquad \textbf{(8.98)}$$

Pure oxygen is better-suited for methanol synthesis as an oxidizing agent than air because the reaction occurs at high pressures, and it is more expensive to produce air at pressures ranging from 10 to 20 bar than $O_2$.

The challenge with this reaction is handling the products. Methanol together with a small percentage of formaldehyde can continue to oxidize, leading to complete combustion of the methane.

### 3. Renewable Hydrogen and Carbon Dioxide

Another method of producing methanol is through the synthesis from hydrogen and carbon dioxide shown in Eq. 8.95. This process differs from the ones described above because it is not based on fossil or biogenic carbon sources, and as a result, can also be applied with PtL storage technology using wind and solar energy.

The limiting factors of this process are the source materials $CO_2$ and $H_2$. Hydrogen can be produced by electrolysis using electricity generation surpluses when the portion of renewable energy is high. $CO_2$ sources include separation in coal power plants, industrial processes, biogas facilities, air, or $CO_2$ recycling (▶ Sect. 8.3).

The advantages of this process are that the temperature is lower than with methanolization using synthesis gas and the selectivity to methanol is higher. It is also more efficient because endothermic $CO_2$ reduction to carbon monoxide occurs simultaneously with final, exothermic methanol synthesis. This means that the heat produced is immediately consumed.

The challenge with this process is removing the water vapor that results in the product gas to produce pure methanol.

### 8.3.5.2 Reactor Concepts

#### ■ Synthesis Processes

Methanol synthesis processes fall into three categories distinguished by the working pressure [59]:

1. High-pressure synthesis: the high-pressure process was the first process used for methanol synthesis. This process occurs at pressures ranging from 250 to 350 bar and temperatures ranging from 320 to 380 °C. The catalyst is based on zinc chromium oxide ($Zn/Cr_2O_3$). It is not very active, but it is thermally stable and resistant to catalyst poisons such as sulfur compounds. This process is rarely used today because the methanol yield is low and the temperature is difficult to control.
2. Medium-pressure synthesis: this process occurs at temperatures up to 300 °C and at pressures ranging from 100 to 250 bar using $Zn/Cr_2O_3$ or zinc-copper catalysts.
3. Low-pressure synthesis: this process occurs at pressures ranging from 50 to 100 bar and moderate temperatures ranging from 220 to 280 °C. The catalyst is based on copper, zinc, and aluminum oxide ($Al_2O_3$). Once it became feasible to remove sulfur from synthesis gas, low-pressure synthesis became the most common methanol synthesis process. The process eliminates the need for resistant catalysts that work only at high temperatures and pressures. These conditions result in relatively few by-products, and the selectivity for methanol is close to 100%.

#### ■ Reactor Types

As with the FT process, methanol synthesis reactors are either fixed bed reactors or slurry reactors. ▶ Section 8.3.6 describes the basic designs of these reactor types. A fixed bed reactor requires a $H_2$:CO ratio ranging from 2.05 to 2.15 for methanol synthesis, while a slurry reactor requires a ratio of only 1.0.

Table 8.11 compares the operating conditions of various processes for producing synthetic fuel, such as PtL and biomass-to-liquid (BTL).



**Fig. 8.38** Methanol reactor by Linde AG. Source: Linde AG

A practical methanol reactor design is the isothermal reactor built by Linde (Fig. 8.38). This fixed bed reactor has an integrated heat exchanger. The reactor is cooled by removing the sensible heat of the gasses and liquids, as well as the latent evaporation heat of the cooling water. The heat generated by the reaction of the synthesis gas to methanol on the catalyst particles is removed by cooling tube-bundles. The cooling tube-bundles in the Linde reactor are specially designed using a spiral form to prevent thermal stress in the tubes and reactor.

#### ■ Product Treatment

The conditions in the reactor result in a gaseous product stream. After leaving the reactor, high-value hydrocarbons produced as by-products are separated. The quantity of hydrocarbons produced depends on the synthesis gas ratio, the reaction environment, and the type, as well

**Table 8.11** Comparison of the operating conditions of various processes for producing synthetic fuel [59]

| | $H_2$:CO ratio | Pressure in bar | Temperature in °C | Catalyst (basic material) |
|---|---|---|---|---|
| Methanol synthesis | 1–2.15 | 50–300 | 220–380 | Zn/Cr/Cu |
| FT process | 0.85–3 | 1–70 | 120–350 | Fe/Co/Ru/$ZrO_2$ |

as age, of the catalyst. The gas remaining is recycled and fed back into the reactor.

The separated raw methanol is then processed in a distillation column to reduce the water content of the product below 2% by volume. The liquid methanol is then ready for use in relevant applications.

### Use

Globally, about 70% of methanol production is for producing formaldehydes, methyl tertiary butyl ether (MTBE), dimethyl ether (DME), or acetic acid [9, 81]. Methanol is also used as a raw material for producing colors, silicones, and plastics.

Methanol is a general source material used as an energy source, a basic chemical material, or an intermediary product. It has many applications; for example, it is used in the petrochemical industry to produce a range of chemical compounds. Combined with carbon monoxide, methanol can be used to produce acetic acid. Using zeolite catalysts, methanol can also be converted into olefin. Formaldehyde is another chemical compound that can be produced using methanol. It is one of the most important basic materials used by the chemical industry. It is also used in medicines and as a preservative in the cosmetics industry. For many years, it was used as an additive in the textile industry to keep clothing from wrinkling.

In the petroleum industry, it is processed to produce MTBE and then added to fossil gasoline. MTBE is an additive containing oxygen that improves the combustion characteristics of gasoline by increasing the octane. Because the molecule contains oxygen, this additive also reduces harmful emissions. A disadvantage of MTBE and, therefore, of using methanol as well is that MTBE is extremely poisonous, and double-walled tanks must be used to prevent ground water contamination.

In addition, gaseous methanol can be directly processed to produce DME that can be used as a diesel substitute or basic chemical material. Here, methanol is catalytically dehydrogenated, as shown in Eq. 8.99, in a separate reactor at a pressure of 15 bar and temperatures ranging from 250 to 300 °C. The raw DME is separated from the remaining water in a distillation column and then processed to pure DME.

$$2CH_3OH \leftrightarrow CH_3OCH_3 + H_2O. \qquad \textbf{(8.99)}$$

Because of its very high cetane number, DME's characteristics are also brilliantly suited for use in combustion or diesel engines. In Scandinavia, large pilot projects have tested the production of DME from wood, as well as its use in trucks.

DME can also be converted to gasoline using methanol-to-gasoline (MTG). Light alkanes are produced by dehydrogenating DME and are then converted to hydrocarbons with a maximum of 10 carbon atoms. These hydrocarbons can directly replace fossil gasoline in the conventional petroleum sector using the existing infrastructure. The advantages here are similar to those offered by PtG based on methane (▶ Sect. 8.6).

Figure 8.39 gives an overview of how methanol is produced and for which chemical compounds it serves as an intermediary product.

Methanol can also be used as a pure fuel replacement for LNG or liquefied petroleum gas (LPG), or in fuel cells if they are corrosion-resistant. Since using methanol fuel cells at a large scale is currently not economically vi-

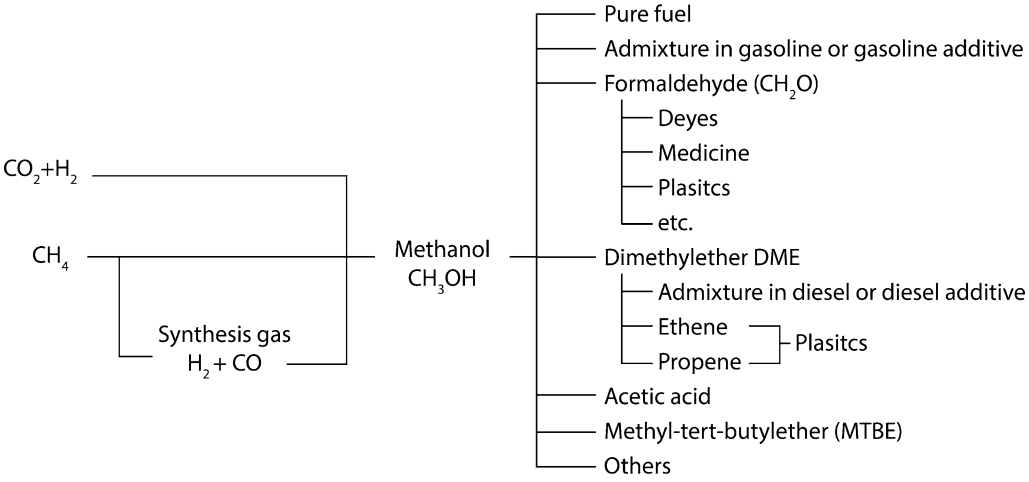



**Fig. 8.39** Overview of methanol production and processing

able, methanol is chiefly used in the energy sector as an additive to conventional fuels.

Ethene (ethylene, $C_2H_4$) and propene (propylene, $C_3H_6$) are important raw materials for producing plastics that can also be produced using methanol. Propene and ethane are typically produced from crude oil. The general term for this process is methanol-to-olefin (MTO) [9].

Here, DME ($CH_3OCH_3$) is catalytically dehydrogenated, producing hydrocarbons and water (Eqs. 8.100 and 8.101)L

$$CH_3OCH_3 \leftrightarrow C_2H_4 + H_2O, \quad \textbf{(8.100)}$$

$$3CH_3OCH_3 \leftrightarrow 2C_3H_6 + 3H_2O. \quad \textbf{(8.101)}$$

To reduce the non-energetic use of crude oil and, therefore, $CO_2$ emissions, methanol from renewable hydrogen and $CO_2$ can be used as a raw material in the chemical industry.

As described in ▶ Sect. 14.3, renewable methanol production was first introduced commercially in Iceland using renewable electricity and $CO_2$ from geothermal sources by the company Carbon Recycling International (CRI).

### 8.3.6 FT Process

In the 1920s, Franz Fischer and Hans Tropsch at the Kaiser-Wilhelm-Institut für Kohleforschung in Mühlheim an der Ruhr invented a process for coal liquefaction. These chemists were the first to use a catalyst for this process. With coal liquefaction, a synthesis gas of carbon monoxide (CO) and hydrogen ($H_2$) is converted into gaseous, liquid, and solid hydrocarbons [59].

The FT process was commercially introduced during the Second World War because of resource shortages. At that time, there were nine facilities in Germany for converting coal. After the war, Fischer-Tropsch fuels were no longer competitive since crude oil was cheaply available again.

But the 1973 oil crisis renewed interested in the FT process. Since then, pilot projects and industrial facilities have been built in a wide variety of locations, particularly in South Africa (coal-to-liquid) and Qatar (gas-to-liquid). In the last twenty years, facilities for converting woody biomass using BTL and wind or solar electricity together with $CO_2$ from PtL have also been built. These facilities have made the process sustainable and established it on a broader raw material base (▶ Sect. 8.7).

### 8.3.6.1 Basic Principles

#### ■ Chemical Reactions

The FT process is a polymerization process that produces mainly gaseous, liquid, and solid hydrocarbons with a range of chain lengths from synthesis gas. The process produces gaseous hydrocarbons ($C_1$–$C_4$), gasoline ($C_5$–$C_{10}$), diesel ($C_{11}$–$C_{18}$), and waxes ($C_{19+}$). Equation 8.102 shows the simple basic equation for the FT process:

$$\mathrm{CO} + 2\mathrm{H_2} \leftrightarrow [-\mathrm{CH_2}-] + \mathrm{H_2O};$$
$$\Delta H_\mathrm{R}^0 = -165\,\mathrm{kJ/mol}. \qquad \textbf{(8.102)}$$

This basic equation can be expanded to produce alcohols (Eq. 8.103), alkenes (Eq. 8.104), or alkanes (paraffins) (Eq. 8.105). These reactions occur at different speeds depending on the catalysts, pressure, and the temperature [59]:

$$n\mathrm{CO} + 2n\mathrm{H_2} \leftrightarrow \mathrm{C}_n\mathrm{H}_{2n+1}\mathrm{OH} + (n-1)\mathrm{H_2O}, \qquad \textbf{(8.103)}$$

$$n\mathrm{CO} + 2n\mathrm{H_2} \leftrightarrow \mathrm{C}_n\mathrm{H}_{2n} + n\mathrm{H_2O}, \qquad \textbf{(8.104)}$$

$$n\mathrm{CO} + (2n+1)\mathrm{H_2} \leftrightarrow \mathrm{C}_n\mathrm{H}_{2n+2} + n\mathrm{H_2O}. \qquad \textbf{(8.105)}$$

In reality the reaction is much more complex, and involves a range of other reactions depending on a variety of different parameters.

The reaction's thermodynamic and kinetic processes are mostly known. The product composition is heavily-dependent on the reaction conditions. The catalyst is a decisive factor. In addition, low temperatures and high pressures result in long hydrocarbon chains, and vice-versa.

The reaction rate is approximately proportional to the square of the hydrogen partial pressure and indirectly proportional to the carbon monoxide pressure [65]. Furthermore, alkanes are more likely to be produced than alkenes.

The FT process is embedded in a process chain for producing hydrocarbons. This process chain is normally composed of four units. These are described in more detail below:

1. Production of synthesis gas ($H_2$ and CO)
2. Gas purification and gas treatment
3. The FT process
4. Treatment of the products

#### ■ 1a. Producing Synthesis Gas from Renewable Electricity and $CO_2$ for Energy Storage and Fuel Production

The relevant method for producing synthesis gas for renewable fuel production uses water electrolysis with renewable electricity (▶ Sect. 8.1.3.1), as well as the reduction of $CO_2$ to CO using a reverse water-gas shift reaction similar to methanization (Eq. 8.91). These processes are discussed in detail in the relevant sections.

#### ■ 1b. Producing Synthesis Gas from Fossil and Biogenic Raw Materials Using Conventional Processes

Besides water splitting and $CO_2$ reduction using renewable energy, synthesis gas can also be produced conventionally through gasification of biogenic and fossil raw materials. These processes are similar to the thermochemical production of hydrogen (▶ Sect. 8.1.3.2), and are discussed in detail in that section.

With gasification, a carbon-based fuel is oxidized to carbon monoxide using partial oxidation by adding an oxidation agent such as oxygen $O_2$, air, or water vapor. This is also called partial burning, because the fuel is not entirely oxidized to $CO_2$. A hydrogen-rich oxidizing agent is used to produce the synthesis gas, which in most cases is water vapor [106].

Equation 8.106 describes the gasification of carbon using water vapor:

$$\mathrm{C} + \mathrm{H_2O} \leftrightarrow \mathrm{CO} + \mathrm{H_2};$$
$$\Delta H_\mathrm{R}^0 = +131\,\mathrm{kJ/mol}. \qquad \textbf{(8.106)}$$

With coal gasification, 25% of the energy contained in the coal is used to meet the requirements of the endothermic reaction described in Eq. 8.106. Another portion of the energy in the coal is used to treat the synthesis gas so that it has the correct stoichiometric ratio of CO to $H_2$ for the FT process. This is achieved by using a water-gas shift reaction (Eq. 8.107) to increase

the hydrogen content. The stoichiometric ratio of hydrogen to carbon monoxide should be 2:1 (Eq. 8.102):

$$\mathrm{CO} + \mathrm{H_2O} \leftrightarrow \mathrm{CO_2} + \mathrm{H_2};$$
$$\Delta H_R^0 = -40.9\,\mathrm{kJ/mol}. \quad (8.107)$$

If biomass is used as a raw material, it must first be treated to produce pure carbon for gasification. Called pyrolytic decomposition, in this process, the biomass is slowly heated up to temperatures of around 500 °C in an airtight vessel. The macromolecules of the biomass are decomposed, producing gases and a solid residue composed mainly of carbon (biocoke). A total of around 80 to 85% is converted into gaseous products such as CO, $CO_2$, $H_2O$, or $CH_3OH$ (methanol). As a result, 15 to 20% remains as raw material for gasification [59, 106, 124].

### 2. Gas Purification and Gas Treatment

Depending on the production process, the synthesis gas may require purification and treatment. The water electrolysis method using renewable energy and the addition of $CO_2$ is comparative easy to handle from a stoichiometric point of view, and depending on the $CO_2$ source, requires only limited gas purification. But synthesis gas from other gasification processes requires significantly more treatment. Synthesis gas contains many accompanying substances such as phenol, ammoniac, hydrogen sulfides, and other undesirable components or catalyst poisons that may hinder the FT process.

In addition, the ratio of $H_2$ to CO is often incorrect and must be adjusted using a water-gas shift reaction, separation of $CO_2$ by PSA, or by adding electrolytic hydrogen. The recycled light hydrocarbons ($C_2$–$C_8$) can be catalytically treated for the FT process using steam-reforming or autothermal reforming [106].

### 3. FT Process Sequence

The FT process is composed of several steps:

1. Adsorption of educts at the catalyst.
2. Formation of intermediary products.
3. Chain polymerization and other transformations of the intermediary products.
4. Desorption of the products.

The third step in the synthesis process is the most important one. Chain polymerization is a chemical reaction in which the same or different monomers add onto a growing polymer chain one at a time.

The chain-growth is generally described by Eq. 8.108:

$$C_n + C_1 = C_{n+1}, \quad (8.108)$$

where $C_1$ is the starting molecule of the growing chain and $n$ the number of carbon atoms. Depending on the starting molecule, there are three different typical mechanisms [65]:

1. $C_1$ contains oxygen: the starting material here is usually pure carbon (C). the carbon is hydrogenated to produce $CH_x$, which can be easily polymerized.
2. $C_1$ contains $H_2$ or $O_2$: the reaction that occurs here to form long-chain hydrocarbons is called polycondensation. By splitting $H_2O$ molecules, the monomers are combined to form polymers.
3. $C_1$ is carbon monoxide: the CO molecule is absorbed and bonds to the catalyst surface. This produces a R–C bond, where R is the catalyst material. The C atom forms a bond with a metal atom in the catalyst and with the carbon atom which bonds the hydrocarbon chain to the catalyst surface.

With a constant molecular weight distribution of Fischer-Tropsch products (ratio between the various long molecule chains), the synthesis follows a formal kinetics of polymerization. It can be divided into two partial reactions, chain-growth ($k_1$), and polymer desorption ($k_2$). Figure 8.40 shows the reaction scheme.

$C_1$ reacts with the hydrocarbon bonded to the catalyst (R–$C_n$), resulting in a larger chain R–$C_{n+1}$, or it completes the chain and is then desorbed to $C_n$. Chain-growth continues to a certain point. The chain length determines whether the chain grows or is desorbed.

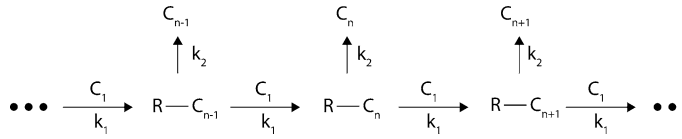



**Fig. 8.40** FT process reaction scheme

The molecular weight distribution of the products is uniquely defined by the chain-growth probability $\alpha$:

$$\alpha = \frac{k_1}{k_1 + k_2}. \tag{8.109}$$

The chain-growth probability is determined by the environmental conditions and the choice of catalyst.

The hydrocarbon distribution is a function of the Schulz-Flory distribution determined by the mass distribution $W_n$ of hydrocarbons with $n$ carbon atoms:

$$W_n = n \cdot \alpha^{n-1} \cdot (1 - \alpha)^2. \tag{8.110}$$

Figure 8.41 shows the mass distribution of hydrocarbons with gaseous hydrocarbons ($C_1$–$C_4$), gasoline ($C_5$–$C_{10}$), diesel ($C_{11}$–$C_{18}$), and waxes ($C_{19+}$).

Methane and waxes can have a selectivity of 100%. Figure 8.42 shows the distribution of products resulting from a FT process with a chain-growth probability of 0.85.

The Fischer-Tropsch products behave according to the law described in Eq. 8.110. But in actual processes, the methane content is usually higher. This is because methane can be produced in two ways; either as a product of polymerization or as a product of direct hydrogenation of CO. The rates of these reaction are primarily determined by the catalyst and the temperature. Hydrogenation should be limited as far as possible.

Catalysts based on the transition metals iron, cobalt, nickel, and ruthenium can be chemically processed to facilitate polymerization. Here, the elements are applied to porous metal oxides. These metal oxides include diatomite, zeolite, or titanium oxide. Zirconium

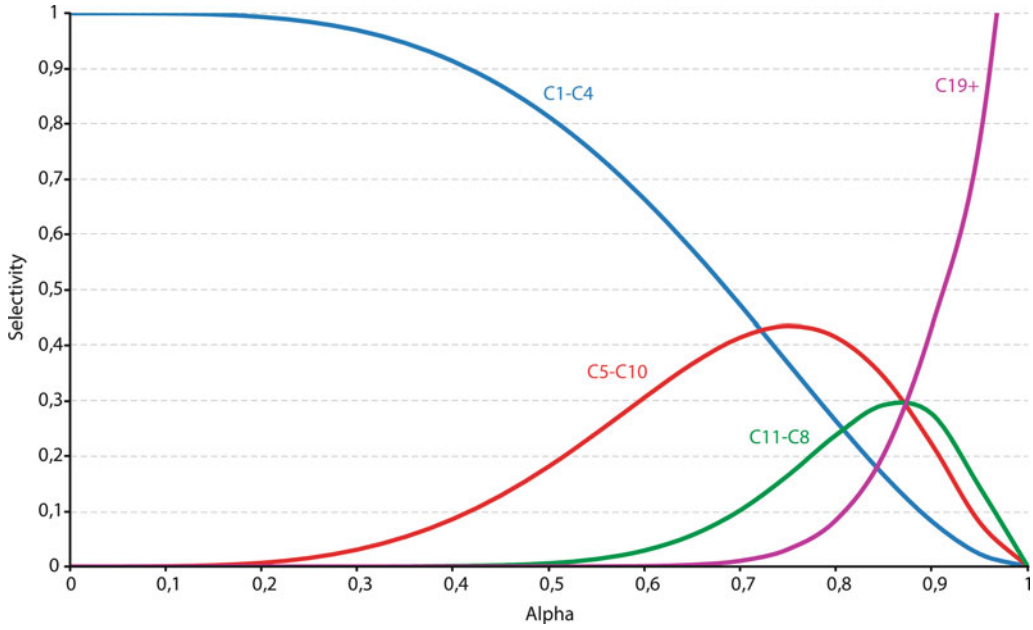



**Fig. 8.41** Probability distribution for Fischer-Tropsch products

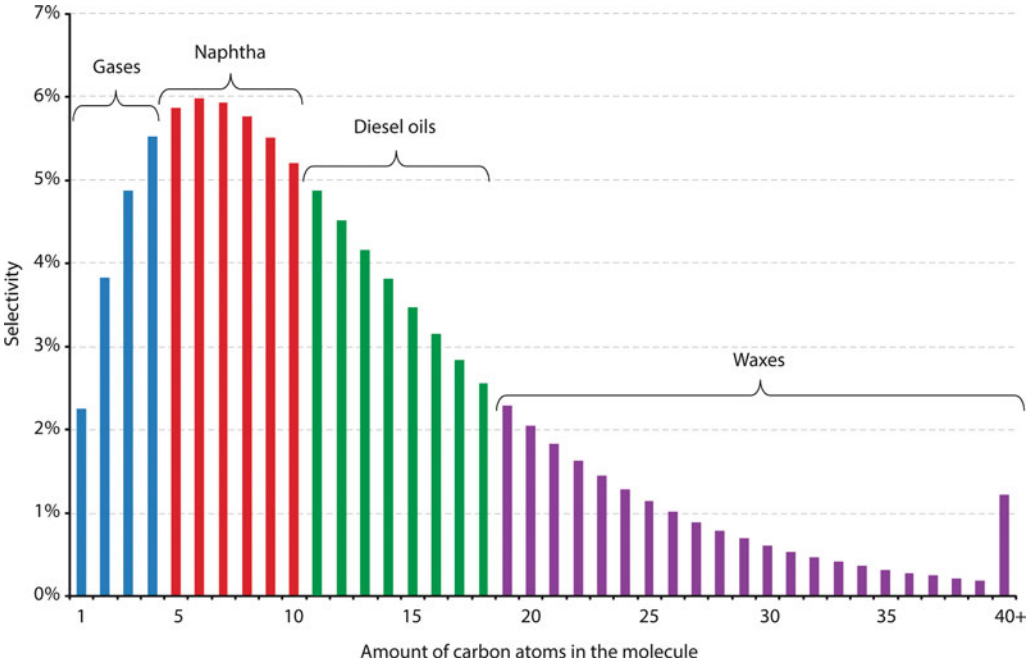



**Fig. 8.42** Distribution of products resulting from a FT process with a chain-growth probability of 0.85

oxide ($ZrO_2$) is also a very effective carrier material for cobalt because the Co-$ZrO_2$ catalyst works at temperatures starting at 160 °C, and liquid hydrocarbons can be produced with a selectivity of 90% at ambient pressures. Only small amounts of methane are produced at the same time. The chain-growth probability $\alpha$ can be estimated at 0.9 with this catalyst.

But methane formation can be minimized, either by chemically modifying the catalyst or by altering the synthesis gas. Adding 1 to 4% of ammoniac ($NH_3$) to the synthesis gas increases the selectivity for $C_{5+}$ and reduces the formation of methane. Removing the $NH_3$ from the synthesis gas afterwards keeps the yield of $C_{5+}$ high without increasing the low methane yield. The Schulz-Flory distribution increases, resulting in a higher $\alpha$ [65].

Simultaneously chemically modifying the catalyst and altering the synthesis gas could theoretically reduce the selectivity for methane to one, and increase the selectivity for liquid hydrocarbons to around 90%. Supplementing Fig. 8.42 with Fig. 8.43 shows the resulting distribution of products. The distribution clearly shifts towards long-chain hydrocarbons. The selectivity for methane production is reduced to a theoretical value of 1%. The selectivity for long-chain growth dramatically increases.

### 4. Product Treatment

After the FT process, the resulting raw products are treated so that they can be used as synthetic fuels.

- Treatment of raw gasoline (naphtha): naphtha can be used as a raw material in the petrochemical industry, or converted to gasoline by isomerizing the molecules [59]. In this process the individual atoms or atom groups in the molecule change their arrangement within the molecule itself.
- Diesel oils from the FT process: Fischer-Tropsch diesel must also be isomerized so that its flow-characteristics at low temperatures conform with the technical requirements for fuels.
- Waxes ($C_{19+}$): using hydrocracking, long-chain hydrocarbons can be saturated to form short-chain hydrocarbons, and the

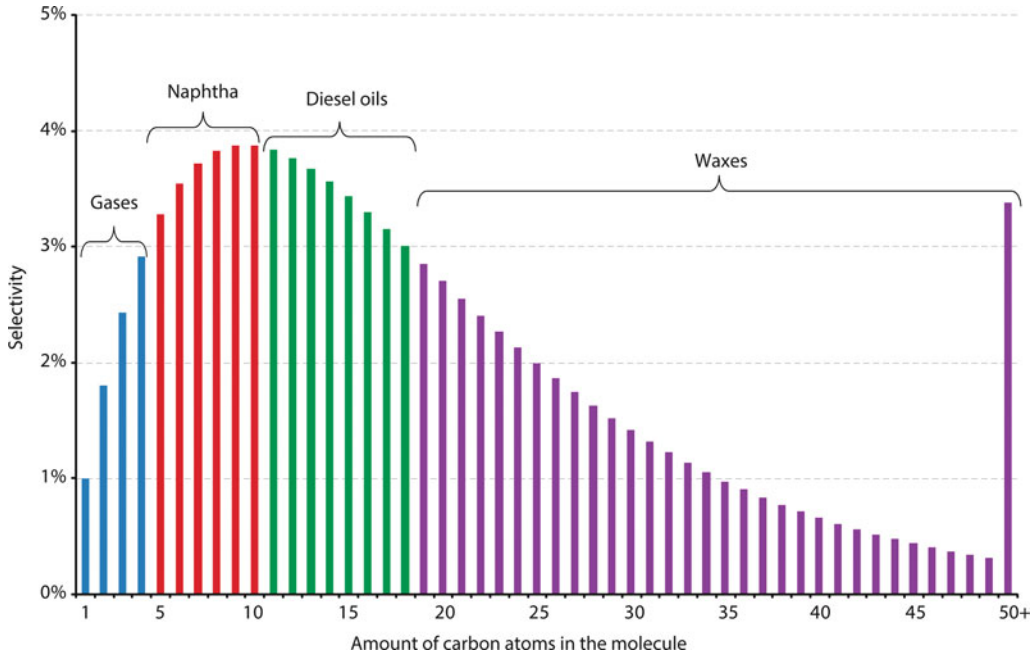



**Fig. 8.43** Distribution of products resulting from an FT process with a chain-growth probability of 0.9

unsaturated particles split off. Hydrogen is released during the process. Hydrocracking of waxes is carried out at relatively low-temperatures so that the chain breaks in the middle. After the break, secondary reactions such as isomerization occur on the fragments. This results in usable synthetic fuels compatible with the infrastructure.

### 8.3.6.2 Reactor Concepts

A major challenge with the FT process is handling the released reaction enthalpy of n $\Delta H_R^0 = -165\,\text{kJ/mol}$. Generally, fixed bed reactors (pipe-bundle reactors) are used, but heat extraction with fluidized bed or slurry reactors is more effective. These three types are briefly described below [59, 106].

- Pipe-bundle reactor: a pipe-bundle reactor is a fixed bed reactor containing up to 25,000 pipes with a diameter ranging from 15 to 25 mm. The synthesis gas flows into the reactor from above and then through the pipes containing the catalyst in the form of a solid but finely granulated fill (Fig. 8.44, left). Because of the small diameter of the pipes, the synthesis gas flows through them at a very high speed. This causes turbulence, resulting in high heat and mass transfer. Water flows around the exterior of the pipes, removing the heat released through evaporation. Other temperature control methods available include using molten salts for latent-heat storage. A disadvantage of this reactor type is that the heat is not evenly distributed, meaning heat dissipation to the water may also be uneven. This may result in the formation of hotspots that could damage the catalyst.
- Fluidized bed reactor: the center of Fig. 8.44 shows the design in an outline of a fluidized bed reactor. The synthesis gas is blown into the reactor from below, picking up the finely granulated catalyst with it. The Fischer-Tropsch products are then extracted. Particular care must be taken not to extract any catalyst particles together with the products. The catalyst is mechanically separated from the product gas flow and falls into the bunker. It is then fed back into the reactor.

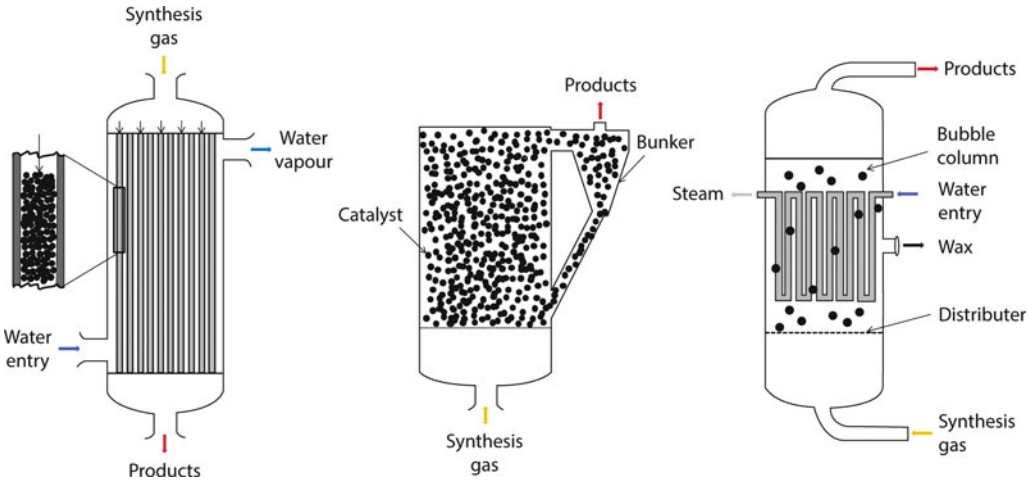



**Fig. 8.44** Designs outlining various reactor types: *left*, pipe-bundle reactor, *center*, fluidized bed reactor, *right*, slurry reactor

- Three-phase reactor: the three-phase reactor (or slurry reactor) consists of a holder and a cooling inductor. The holder is filled with a suspension (slurry) composed of wax and catalyst particles (Fig. 8.44, right). The synthesis gas is fed in from the bottom and then evenly injected into the suspension through a gas distributor. The synthesis gas is converted as it rises through the suspension. Light hydrocarbons, water, and unconverted synthesis gas are released at the reactor exit on top. The heavy hydrocarbons produced are drawn off in the middle of the reactor. Water flows through the cooling coil, removing the heat released through evaporation to cool the reactor. The larger reactor mass makes temperature control easier, but as a result, this reactor takes longer to start-up than a pipe-bundle reactor. This reactor also has yet to be tested at an industrial scale.

All three reactors can be operated in one of two ways [59, 106, 123]:

1. Once-through operation: the synthesis gas is fed through the reactor a single time and, as far as possible, completely converted. The gasses that remain are used to generate heat or for CHP generation.
2. Full-conversion operation: the unconverted synthesis gas is fed back into the reactor and, if applicable, reformed to maximize the fuel yield.

### Catalyst

Only materials that meet the following requirements are suitable as catalysts in the FT process [65]:

- They must have a high mechanical and thermal resistance.
- The gas hourly space velocity should be around 1,000 L/h. This is the ratio of gas volume flow to catalyst volume, and is used to determine the quantity of educt required for a certain retention time in the catalyst volume.
- For economic reasons, the catalyst's selectivity should tend more to liquid hydrocarbons than gaseous hydrocarbons. In a reaction with several products, the selectivity is defined by the proportion of each product in the results. The higher the proportion is, the more the reaction tends towards that product.
- The transition metals iron (Fe), cobalt (Co), nickel (Ni), and ruthenium (Ru) are the elements best-suited for use as catalysts. They have various applications depending on the particular requirements.

**Table 8.12** Overview of catalysts for the FT process

| Material | Pressure | Temperature | Selectivity |
|---|---|---|---|
| Nickel | Ambient pressure | 150–250 °C | Methane |
| Cobalt | Ambient pressure to slightly elevated pressure | 150–250 °C | Linear paraffins[a] |
| Iron | Moderate pressure | 200–350 °C | Olefin[b], paraffins, and hydrocarbon compounds containing oxygen (alcohol) |
| Ruthenium | Very high pressures (up to 1,000 bar) | Low temperatures (100 °C) | Products with high molecular weights |

[a] Paraffin = mixture of alkenes ($C_nH_{2n+2}$) with 18+ carbon atoms.
[b] olefin = alkenes ($C_nH_{2n}$), cycloalkanes, and polyenes.

Table 8.12 compares these catalysts. The selectivity of cobalt and iron are best-suited for cost-effective use. As a result, they are the most common in practice. Because of its high price on the international market, ruthenium is currently not an option for use at an industrial scale.

▶ Section 14.3 describes an example of a PtL facility from the company Sunfire. This facility uses the FT process to produce synthetic fuels.

## 8.4 Storage Media and Holding

Depending on their aggregate state, chemical energy sources can be stored in gaseous, liquid, or solid form. This section discusses the design and function of the containers, technical equipment, and facilities required. The focus here is on storage media in a gaseous state.

### 8.4.1 Gaseous Storage Media

In Germany, construction of the gas infrastructure began in the middle of the 19th century for lighting gas, later called town-gas. After the transition to natural gas in the 1970s, the expansion of the infrastructure continued into the current century, and is still ongoing. From the beginning, a problem was reconciling the basically constant production of gas with the daily and seasonal fluctuations in demand. The solution to the problem was the development of gas storage technology, at first predominantly depressurized gasometers. Today, underground storage facilities with enormous storage capacities are standard.

Similarly, in the transition from fossil to renewable energy sources, storage technologies such as PtG will play an increasingly important role. Currently in its early phases, this shift in technology will also occur over a long period of time. As a result, the following discussion focuses on the storage of renewable gases such as hydrogen (▶ Sect. 8.1.2) or methane (▶ Sect. 8.3.1.2) produced from renewable electricity.

#### 8.4.1.1 Storage Containers

The compressed gas containers discussed in this section were developed to store town gas. In exceptional cases, some of the container types were also used to store pure hydrogen. This means that 'mass storage' here refers to the storage requirements of the town gas era. The current natural gas industry as well as the future energy industry based primarily on renewable energy requires mass storage capacities several orders of magnitude larger.

The first mass storage facilities for town gas were called gasometers. They stored gas at a constant pressure and at variable volumes with slight overpressure. A typical example is

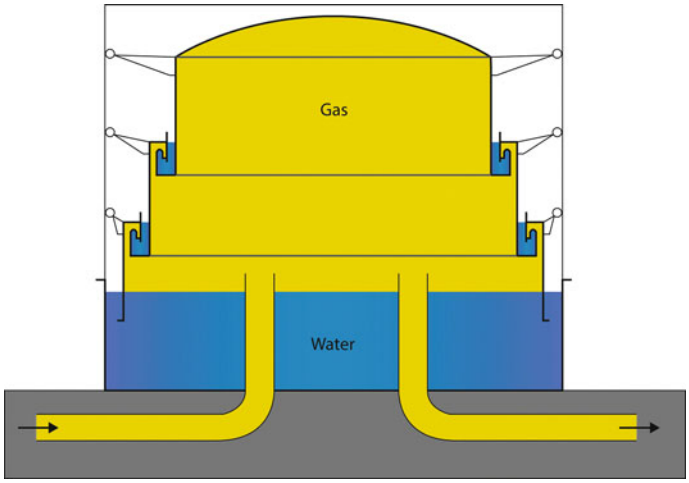



**Fig. 8.45** Gasometer with a telescopic design (source: KBB UT)

the floating bell gasholder. Here the gas-filled storage container was insulated from the atmosphere by a water seal. Later, telescopic gas holders (Fig. 8.45) using the same basic principle significantly increased storage capacities.

The actual storage unit was installed in a supporting structure (Fig. 8.46). Telescopic gas holders were followed by disc-type gas holders that used a flat piston in a cylinder to store gas at low pressures.

Since maintaining the pressure only slightly above atmospheric pressure severely limited storage capacities, scientists soon began to focus on pressurized containers.

### Working Gas and Cushion Gas

Unlike gasometers, in pressurized containers, the gas is held at a constant volume but at variable pressures in a specific range. The usable quantity of gas in this pressure range is called the working gas. The quantity of gas remaining at the minimum pressure is called the cushion gas. The ratio of working gas to cushion gas varies with different pressurized storage methods.

Two gasometers in Germany are also used for hydrogen storage, in Frankfurt-Höchst (Infraserv Höchst) and Gersthofen (CABB GmbH) [115].




**Fig. 8.46** Hoesch gasometer in Westfalenpark, Dortmund

The geometry of spherical gas containers permit significantly higher operating pressures, and as a result, higher energy storage densities (see Table 8.12 and Fig. 8.47). With this design, the specific material consumption requirements for the container are lowest. This is crucial because the investment costs are primarily determined by the material costs.



**Fig. 8.47** Spherical gas container in Aachen (source: FOTOLIA)

**Table 8.13** Typical spherical gas container specifications

| | |
|---|---|
| Sphere diameter | 40 m |
| Maximum pressure | 10 bar |
| Storage capacity | 335,000 m$^3$ ($V_n$) |

**Table 8.14** Specifications of a natural-gas storage facility in Urdorf, Switzerland

| | |
|---|---|
| Pipe diameter | 1,400 mm |
| Depth below ground of the storage pipes | 2 m |
| Total pipe length | 4,140 m |
| Geometric volume | 6,400 m$^3$ |
| Maximum operating pressure | 100 bar |
| Storage capacity | 574,000 m$^3$ ($V_n$) |

Spherical gas containers are currently not used to store pure hydrogen. An exception is the use of cryogenic gas containers for liquid hydrogen in aerospace.

Pipe storage refers to gas pipelines in a serpentine form shallowly buried underground (Fig. 8.48). As an example, Table 8.14 lists the specifications of a natural-gas storage facility in Urdorf, Switzerland.



**Fig. 8.48** Design of a natural gas-pipe storage facility in Urdorf, Switzerland (source unknown)

Unlike underground storage in geological formations, these storage facilities can be installed in practically any region. Since these facilities use conventional steel pipes, compared to spherical gas containers, they can be operated at significantly higher pressures. In addition, the capacity is entirely determined by the total length of pipe. But the geometry of a long cylinder with a small diameter requires far more steel than a sphere with the same geometric volume.

### 8.4.1.2 Underground Gas Storage in Geological Formations

In general, the storage capacity of storage facilities above ground is limited by the economic feasibility of the geometric volume combined with the practical storage pressure. By contrast, underground geological formations per-

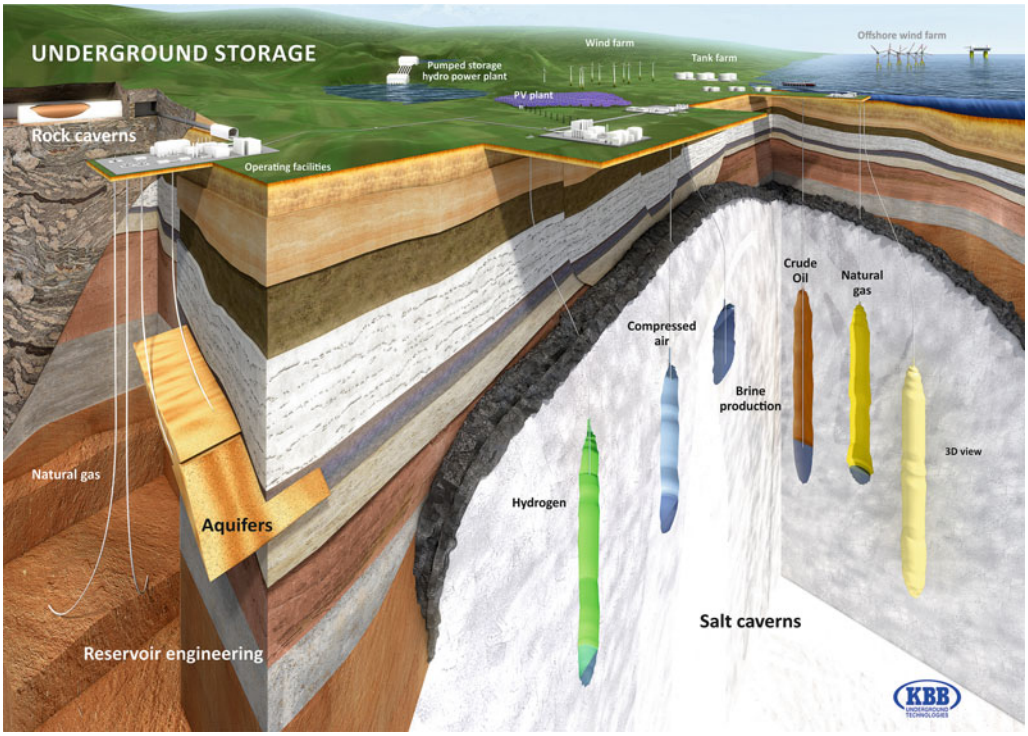



**Fig. 8.49** Gas storage in underground geological formations (source: KBB UT)

mit considerably larger storage volumes at a low cost and also require significantly less land. In addition, storage pressures of up to 200 bar and above can be realistically achieved at greater depths. Since the storage capacity is primarily determined by the product of the volume and the pressure, the dimensions of underground storage are on a different order than above ground. The capacities of the pressurized containers discussed above are typically far below $V_n = 1$ million $m^3$, but the capacities of German underground storage facilities, for example, have a standard volume averaging around 500 million $m^3$.

This explains why, for decades, large quantities of natural gas have been stored almost exclusively underground. Figure 8.49 shows the various underground storage options. In the beginning, depleted gas or oil reservoirs as well as porous, water-carrying formations (aquifers) were used for storage. Artificially constructed salt caverns were later built to supplement these facilities. In the past, porous and salt cavern storage was used to a limited extent for town gas, which is more than 50% hydrogen. In Great Britain and in the American state of Texas, specially designed salt caverns have been effectively used to store pure hydrogen for many years.

All the large-scale gas storage facilities in underground geological formations currently used around the world share the following characteristics:

- In compariosn to containers with walls only a few centimeters thick above ground, large-scale gas storage facilities in underground geological formations have extremely low risk of unintended gas leakage through walls of layers of rock up to several hundred meters thick.
- Very high storage capacity due to large geometric volumes and high operating-pressures.
- Little use of land at ground level.

- Low-specific installation and operating costs compared to gas storage facilities above ground.
- Only feasible where suitable geological formations are available, often meaning the choice of locations is very limited.
- Already succesfully implemented in many industrialized countries, and as a result, likely to be accepted by the public in the future as storage facilities for gasses such as hydrogen or methane produced with renewable energy.

### 8.4.1.3 Salt Caverns

#### Construction

Salt caverns are artificially constructed underground caves in salt rock (Fig. 8.50). In a location where there are adequately large and homogenous salt rock formations underground, a borehole with a diameter of $d < 1\,\text{m}$ is sunk into the salt rock. It is then sealed by steel pipes cemented into the hole. The cavern itself is constructed by a process called solution mining. A major advantage of this approach is that the cavern can be constructed without building expensive shafts or transporting workers and machinery underground. Instead, all the work is done above ground. This is significantly less expensive and time-consuming than conventional mining methods.

To inject water and dissolve the salt rock, two concentric pipes are dropped down the borehole (Fig. 8.51). Water is injected into the inner pipe to dissolve the salt rock. The brine pushed back up to ground level through the ring between the inner pipe and the outer pipe is either used as a raw material or sustainably disposed of in the sea, for example. The brine can be used as a material in chlor-alkali electrolysis to produce chlorine, sodium hydroxide, and hydrogen as described in ▶ Sect. 8.1.3, or to produce evaporated salt.

A protective fluid, or 'blanket' (for example nitrogen), is also injected into the ring area to control the flow of brine to the surface. The spatial dimensions of the cavern can be monitored and adjusted during the process using sonar.

The goal here is the construction of a cavern that best exploits the salt rock available to ensure effective long-term storage for gas. The excellent creep properties of salt rock mean that these caverns are technically impermeable to gases when operating pressures are maintained in the permitted range. But creep here does result in a slight decrease in available volume over time.

When the cavern volume required has been reached, the cavern is tested for leaks, equipped for gas operation, and initially filled with gas. The next step is to test the seal of the access borehole at the surface, which is crucial for safe operation as a gas storage facility. The cavern is then connected to a gas tubing string, and a brine draining string dropped down into the cavern. The draining string allows storage gas to be injected into the cavern through the ring area, pushing the brine up to ground level.

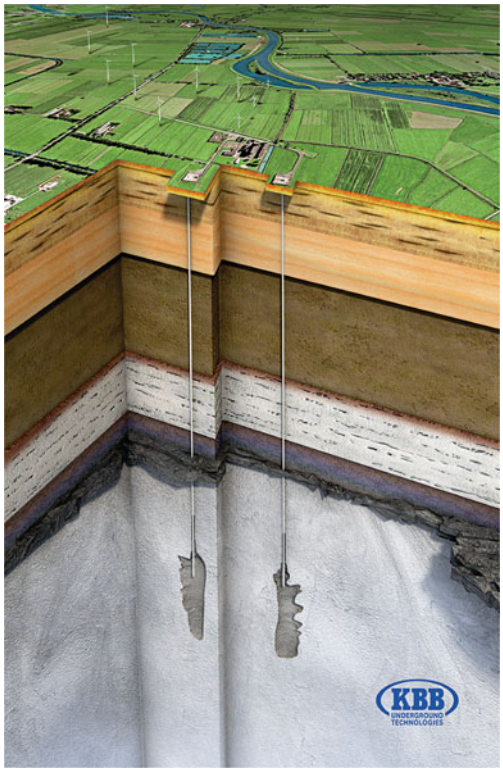



**Fig. 8.50** Gas storage caverns (source: KBB UT)

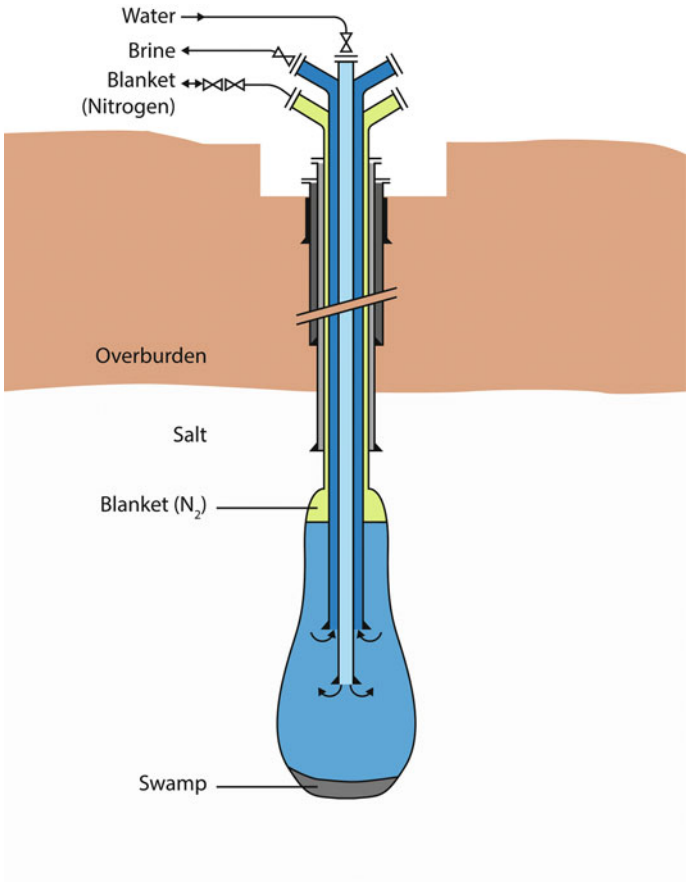



**Fig. 8.51** Solution mining—cavern construction in salt rock (source: KBB UT)

Finally, the draining string is removed with pressure applied, and an underground safety valve installed. If the cavern head at ground level is damaged (in a worst-case scenario), this valve automatically prevents the stored gas from rapidly escaping (blow out).

### Geological and Geotechnical Requirements

The basic disadvantage of underground storage is its reliance on geological formations suitable for storage. The primary requirements for building a gas cavern are:

- The availability of a salt formation with adequate lateral and vertical dimensions.
- A salt formation at least 200 m thick at a depth of around 500 to 2,000 m.
- A salt formation containing a limited portion of insoluble elements.
- An available option for recycling or sustainably disposing of the brine produced (around eight times the cavern volume).

In Germany, geological formations in the North Sea coastal region and central Germany are very well-suited for cavern construction. Due to the lack of suitable salt formations in southern Germany, primarily depleted gas reservoirs are used for storage in that region (▶ Sect. 8.4.1.2).

### Typical Dimensions

Depending on the geological situation, the geometric volume of gas storage caverns typically ranges from several 100,000 $m^3$ up to about 1,000,000 $m^3$. The operating pressure increases in a linear relationship with the cavern depth. Assuming a cavern ceiling at a depth of 1,000 m

**Table 8.15** Specifications for the EWE Vertrieb GmbH Nüttermoor natural-gas storage facility in Ostfriesland [95]

| | |
|---|---|
| Number of caverns | 21 |
| Depth | 950–1,300 m |
| Average individual cave volume (geometric) | Around 400,000 $m^3$ |
| Working gas quantity | 1,319 million $m^3$ |
| Short-term extraction rate | 1.5 million $m^3/h$ |

and a cavern volume of 500,000 $m^3$, the resulting operating pressure would be between 60 and 180 bar.

This means that a single 500,000 $m^3$ cavern has a mass working gas capacity of 4,900 tons for hydrogen or 46,000 tons for methane.

As an example of a large storage facility, below are the specifications for the EWE Vertrieb GmbH Nüttermoor natural-gas storage facility in Ostfriesland (Table 8.15).

#### Experience with Hydrogen-Rich Town Gas Storage

Currently, gas caverns are primarily used to store natural gas. Other storage media include hydrogen, helium, pressurized air, and in the past, town gas with a high hydrogen content.

Town gas is a gas mixture containing high percentages of methane, nitrogen, carbon monoxide, and hydrogen (up to 50% depending on the quality), which was stored in Germany and other European countries primarily in depleted reservoirs, in aquifers, and (to an extent) in salt caverns as well. The highly reactive hydrogen combined with the other gas components, mineral components in the reservoirs, and bacteria sometimes resulted in corrosion of the equipment underground, reduced fluidity in porous reservoirs, and led to changes in the gas composition (for example, formation of hydrogen sulfide—$H_2S$) leading to gas losses.

Bacteria are particularly a problem with aquifer storage. This is because of the large gas-water contact area. Bacteria are less of a problem with depleted gas fields, and only a slight problem in caverns.

Because town gas contains a variety of components, experience with town gas applies only to a limited extent to natural gas/hydrogen mixture storage or pure hydrogen storage [52].

#### Experience with Pure Hydrogen Storage

Based on observations of three small caverns in Teesside in the United Kingdom and two large caverns near Houston, Texas in the USA, scientists now have years of practical experience with pure hydrogen storage. A third cavern is also nearing completion in Texas (Fig. 8.52). Leakage data published for these caverns demonstrate that they are equally as effective as natural gas caverns. For the BMBF project HYPOS, an existing natural gas cavern in Saxony-Anhalt will be converted to a hydrogen cavern by 2020. This cavern will then be Germany's first underground hydrogen storage facility [55].

But in Europe, and particularly in Germany, gaining permission for new hydrogen caverns will require modifications in line with significantly stricter local safety regulations. In particular, the cements, steels, and plastics used must be adequately proven safe for use with hydrogen. To ensure public acceptance of this approach, studies are also planned to scientifically prove that hydrogen can be effectively stored in salt rock without leakage.

### 8.4.1.4 Porous Storage

Porous storage is, by far, the most important form of storage for natural gas supply across the globe. These are natural porous reservoirs sealed off from the surface by gas-tight rock formations.

The reservoirs are accessed by drilling down into the rock. Unlike open caverns, porous reservoirs are a system of small, interconnected pores. This means that several boreholes must be drilled to limit flow channels and so reduce flow-resistance within the reservoir during gas filling or extraction. Horizontal drilling technology developed in recent years can reduce filling and extraction times as well as limit the number of boreholes required.

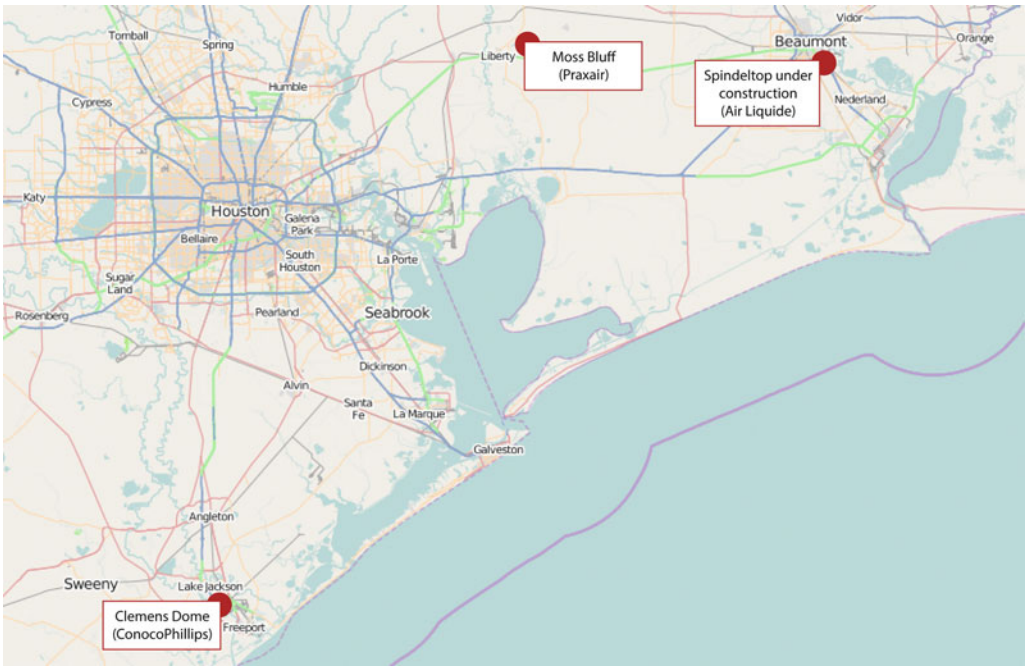



**Fig. 8.52** Hydrogen caverns in Houston, Texas, USA (source: KBB UT)

### Depleted Gas and Oil Reservoirs

The most common porous storage facilities are depleted gas reservoirs (Fig. 8.53). Reservoirs can be conveniently converted into storage facilities if they are suitable for the purpose. If the hydrocarbons that are sealed inside them over geological ages never migrate to the upper strata or to the surface, it would act as proof that they would not leak despite their limited density. Another advantage of these facilities is that the layers of rock above the reservoir sealing it from the surface were already thoroughly studied during exploration and mining. In addition, some pre-existing mining boreholes can be reused for storage operation.

The primary geological and geotechnical requirements that determine if a depleted hydrocarbon reservoir can be used for gas storage are:

- Suitable depth (depth dimensions) so that the operating pressure is compatible with the connected pipeline system.
- The reservoir mechanical characteristics of the formation, i.e., porosity and permeability to gas flow. High porosity and permeability are preferable for storage facilities that are frequently filled and emptied.

In practice, only about 10% of depleted reservoirs are suited for being converted into natural-gas storage facilities [93].

Several other factors must be taken into account when considering if a gas reservoir can be used as a hydrogen storage facility:

- Before being converted into a storage facility, a hydrocarbon reservoir is usually only emptied to a certain percentage (typically 50%); i.e., the storage gas is exposed to residual quantities of various hydrocarbon gases or liquids in the reservoir. This is why depleted oil reservoirs are usually not used for natural-gas storage.
- If a reservoir is used to store hydrogen, it must be assumed that the stored hydrogen will be contaminated by hydrocarbons. If highly-pure hydrogen is required, the hydrogen must be separated above ground after leaving the reservoir at significant expense.

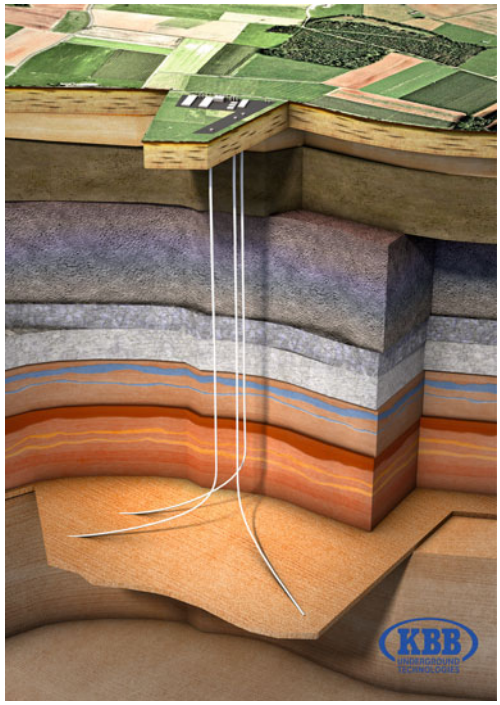



**Fig. 8.53** Gas storage in porous reservoirs (source: KBB UT)

- Since the rock matrix of the reservoir is composed of various minerals and hydrogen is highly reactive, introducing hydrogen may result in chemical reactions. This can lead to hydrogen losses as well as to the formation of reaction products that may degrade the storage facilities flow-characteristics.
- Practical experience has shown that there are also micro-organisms such as bacteria in the reservoirs that may react with the hydrogen as well. This may again result in storage gas losses and compromised flow-characteristics.

The possible reactions between hydrogen and substances or organisms found in reservoirs are currently the focus of extensive research in Germany and internationally. Although salt caverns are in general a better choice for hydrogen storage, the use of porous storage may be essential in the future to adequately meet storage requirements in some regions or countries.

**Table 8.16** Specifications of E.ON Gas Storage GmbH's Bierwang natural-gas storage facility [95]

| | |
|---|---|
| Depth | Around 1,560 m |
| Working gas quantity (natural gas) | 1,450 million $m^3$ |
| Short-term extraction rate | 1.2 million $m^3/h$ |

As an example of a porous storage facility, the specifications of E.ON Gas Storage GmbH's Bierwang natural-gas storage facility in a former gas reservoir are presented below (Table 8.16).

There is some experience with storing hydrogen in Germany, gained from storing hydrogen-rich town gas. But because certain reactions in these facilities involve the carbon monoxide contained in town gas, experience with town gas is applicable here only to a limited extent. Previously, Germany used three depleted hydrocarbon reservoirs to store town gas. These were later converted for natural-gas storage. There was some gas loss and gas quality changes in several of the storage facilities during operation. This resulted from reactions with the carbon monoxide contained in the town gas. When $H_2$ is introduced, CO may be reduced to $CO_2$ and $H_2O$. The $CO_2$ may then result in other reaction products [93].

So far, pure hydrogen has been stored in depleted gas reservoirs only under experimental conditions.

### Aquifer Formations

For decades, aquifer formations have also been extensively used to store large quantities of natural gas. Aquifer formations are natural, porous, and permeable reservoirs that were initially filled with water containing a certain concentration of salt instead of natural gas or crude oil.

If a reservoir of this type is sealed from the surface by a rock layer, and this rock layer is also formed in a dome-like shape, then the aquifer

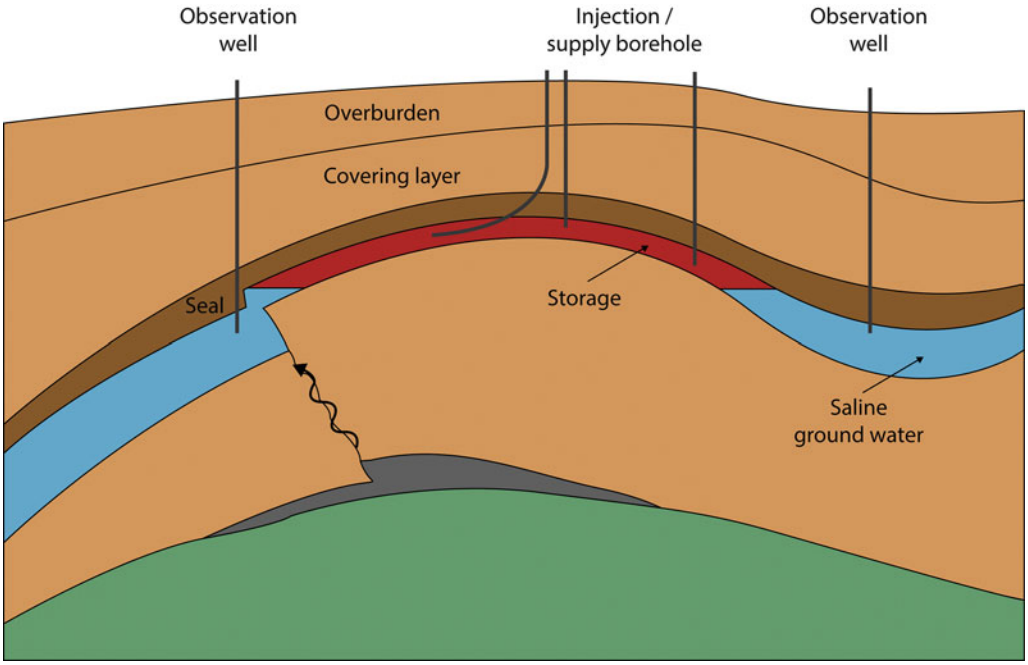



**Fig. 8.54** Gas storage in aquifer formations (source: KBB UT)

can be used to store gas. Here, boreholes are sunk into surface of the formations, and then gas is injected into the holes (Fig. 8.54). The deepest point where gas can be injected is called the spill point.

The primary geological and geotechnical requirements determining if an aquifer formation can be used for gas storage are generally the same as with depleted hydrocarbon reservoirs. These requirements include a dome-like shape at the top of the formation that seals the reservoir from the surface, suitable depth for the storage pressure required, and suitable reservoir parameters providing adequate porosity and permeability. In recent years, several studies have examined whether aquifers could be used for storage or final storage of $CO_2$ (carbon dioxide) from coal power plants. But determining that aquifers can be used to store $CO_2$ a single time is not necessarily the same as determining if they can be used for hydrogen storage, which requires frequent filling and emptying to balance fluctuating renewable energy.

The essential difference between using depleted hydrocarbon reservoirs and aquifers for gas storage is that the geological and technical reservoir characteristics of the aquifers have not been thoroughly studied. This means that it has not been determined if it is sealed off from the surface by the rock above the reservoir. As a result, costly exploration is required just to determine if the formation is suitable for gas storage.

The other factors that must be taken into account when considering if an aquifer can be used as a hydrogen storage facility are basically the same as with depleted reservoirs. The only difference is the lack of fossil hydrocarbon residues that may cause impurities in the hydrogen. Potential reactions between the highly reactive hydrogen and minerals or organisms found in reservoirs are also a problem here. These reactions may result in gas losses, the production of undesirable gases, or other reaction products that could permanently damage the flow channels.

**Table 8.17** Specifications of RWE Gasspeicher GmbH's Kalle natural-gas storage facility in an aquifer formation

| | |
|---|---|
| Depth | Around 2,100 m |
| Working gas quantity (natural gas) | 215 million $m^3$ |
| Short-term extraction rate | 0.45 million $m_3$/h |

**Table 8.18** Specifications of a prototype LRC cavern in Sweden

| | |
|---|---|
| Depth | 130 m |
| Diameter | 40 m |
| Height | 100 m |
| Maximum operating pressure | 230 bar |

Experience with town gas storage has shown that the risk of reactions with bacteria is, in particular, higher with aquifers than with depleted reservoirs or salt caverns. This is because of the large contact area between the gas and water phases.

As an example, the specifications of RWE Gasspeicher GmbH's Kalle natural-gas storage facility in an aquifer formation are presented below (Table 8.17).

Previously in Germany, hydrogen-rich town gas was stored in between eight to 13 aquifer storage facilities. Three of these storage facilities were later shut down. The causes discussed above led to significant gas losses and gas quality changes in several of the storage facilities during operation [93].

So far, pure hydrogen has not been stored in aquifer formations. But there is growing interest in this option, and the reactions between hydrogen and the mineral or biological components found in a range of these facilities are currently being researched.

### 8.4.1.5 Rock Caverns and Abandoned Mines

#### ▪ Conventionally Excavated Caverns (Rock Caverns)

For many years, liquid hydrocarbons have been stored in large, conventionally excavated, non-lined rock caverns in bedrock such as granite. Although the rock has cracks, these caverns can be used for storage. To be suitable for storage, the cavern must be located far beneath the groundwater table. At this depth, minimal quantities of groundwater constantly flow through the cracks into the storage facility, preventing the gas or liquid stored there from escaping through the cracks. The water that collects at the bottom of the cavern must then be pumped out as required.

This hydrodynamic storage concept has so far only been used with gas at high pressure in the Haje natural-gas storage facility in the Czech Republic. Use of this concept to store gases at high pressure has limited potential. Because of the operating pressures required, the storage facilities must be located far underground. As a result, sinking exploration shafts and conventionally excavating tunnels to construct these storage facilities would be extremely expensive. In the case of Haje, cost was a less decisive factor. Apparently, this storage facility was constructed by taking over and expanding existing mining sites that were originally intended as final storage for nuclear waste.

Lined rock caverns, or LRC, offer a more realistic approach to gas storage in bedrock. To store gases at high pressure in rock caverns at shallow depths where the hydrodynamic storage concept does not apply, conventionally excavated caverns are furnished with a gas-tight steel lining.

A prototype LRC cavern has been successfully operated in Sweden for several years. Its basic specifications are presented in Table 8.18.

There are currently plans to build a second lined gas cavern in Innertkirchen, Switzerland. Because of the high-specific construction costs for these storage facilities, they are only relevant for regions such as Sweden or Switzerland, where there are suitable rock formations but no salt formations or reservoirs.

So far, no attempts have been made to store hydrogen in rock caverns.

#### ■ Abandoned Mines

Abandoned mines have been converted for gas storage in only a few cases. The existing, often quite large, cavern volume is an advantage, but sealing off a complex mine system including numerous tunnels and shafts is a major challenge. Another problem is that, just to determine whether the cavern can safely hold gas at high pressure, the shafts first have to be sealed off at great cost. Given the high mobility of hydrogen's very small molecules, this option seems relatively impractical.

### 8.4.1.6 Comparison of Different Gas Storage Technologies

#### ■ Future of Gas Storage in the Gas Economy and for PtG

Storage of natural gas at an industrial scale in underground storage facilities has been an established technology for decades. Since methane is the main component of natural gas, the following discussion applies equally to renewable methane. In the past, storage in natural reserves was more common than in salt caverns. This was because of their enormous capacities, but also because storage was primarily required for balancing a constant supply with seasonally fluctuating demand. The liberalization of the gas economy has increased the demand for commercial storage with the capacity to store or extract large quantities at short notice based on the current gas price. Because the design is significantly better-suited to these requirements than with other storage options, this led to an expansion of storage capacity in salt caverns.

It can be assumed that these high flexibility requirements, i.e., high-turnover frequency at high rates, will remain high for methane and hydrogen storage facilities in the future. This is because the production of these gases will be directly linked to the output of PtG facilities driven by fluctuating wind and Sun energy.

But because salt formations such as oil and gas reservoirs and aquifer formations are very unevenly distributed geographically, there will be a large incentive to exploit all three options to store renewable energy. For example, the inadequate flexibility of porous storage could be somewhat improved by increasing the number of access boreholes. Recently developed rock caverns furnished with a lining, if required, may be another option. But so far, these storage facilities are still in prototype.

The following sections begin with a table comparing the specific characteristics of hydrogen storage options in an evaluation matrix. This is followed by a comparison of their capacities for both renewable gasses.

#### ■ Comparison of Hydrogen Storage Technologies

Table 8.19 evaluates and compares the characteristics of various hydrogen gas storage options in detail. Salt caverns are best-suited for large volume hydrogen storage. But this storage method depends on the availability of suitable salt formations. In addition, proper disposal of large quantities of brine produced during construction is required.

The primary reasons for favoring salt caverns are:

- Salt caverns are technically leak-proof to hydrogen.
- The hydrogen in storage is not contaminated by the host salt rock because it is inert to gases.
- Because of the limited contact area between gas and brine and the high salinity of the brine, experience has so far indicated that biochemical reactions are irrelevant.
- Caverns are very well-suited for high filling and emptying rates—i.e., short charging and discharging durations together with frequent load alternations.

The main reason to consider using porous storage facilities for hydrogen is that the expected future requirements for large volume storage in Europe and across the world cannot be met exclusively by geographically limited salt caverns. Experience with natural-gas storage has shown that large areas can be adequately served

**Table 8.19** Overview of hydrogen gas storage options. ++ Very good or very well-suited, + Good or well-suited, +/− Satisfactory, − Unsatisfactory or poorly suited, −− Bad or not suited

| | Depleted gas reservoirs | Aquifer formations | Salt caverns (field) | LRC |
|---|---|---|---|---|
| Safety | + | +/− | ++ | + |
| Seal | + | +/− | ++ | + |
| Proof of seal | + | +/− | ++ | + |
| Practical experience | +/− | +/− | ++ | − |
| Feasibility | +/− | +/− | ++ | +/− |
| Storage capacity | ++ | ++ | ++ | +/− |
| Flexibility | +/− | +/− | ++ | ++ |
| Contamination of $H_2$ | − | +/− | + | ++ |
| Reactions $H_2$ < > existing components | +/− | − | + | ++ |
| Exploration | ++ | − | + | + |
| Cushion gas content | +/− | − | + | ++ |
| Investment | ++ | +/− | ++ | − |
| Operation | + | + | + | + |



only by a combination of porous and salt cavern storage.

### 8.4.1.7 Current and Future Storage Capacity Potential

#### ▪ Comparison of Hydrogen and Methane Storage Capacities

The following discussion applies only to the situation in Germany. For the sake of simplicity, it is assumed that hydrogen will initially only be stored in caverns and methane in both caverns and porous storage facilities. The storage capacity (working gas volume) data and storage facility numbers in Table 8.20 are based on official statistics from the State Authority for Mining, Energy, and Geology (in German abbreviated LBEG) of Lower Saxony, and were updated at the end of 2012 [66].

To estimate the future potential of renewable gases such as methane and hydrogen, potential storage expansion must be distinguished from already available storage. Already available storage also includes additional storage space made available by the assumed decrease in use of natural gas.

Several studies have estimated the potential for expanding compressed air and hydrogen caverns. These estimates are based on published geological maps that indicate the locations, lateral dimensions, and depths of countless salt formations primarily in northern Germany. Since it is a challenge (even for experts in the field) to determine the storage potential (number of possible caverns, volume, pressure range, and resulting capacity) of each formation using these data, the currently available figures should be generally considered rough estimates. Due to growing interest among policymakers in the actual expansion potential, large studies are currently underway, both in Germany and internationally, to obtain more accurate results.

In general, many suitable salt formations are found in northern Lower Saxony, Saxony-Anhalt, and Schleswig-Holstein. They are less common in Mecklenburg-Western Pomerania

**Table 8.20** German natural-gas storage statistics [66]

| | | Porous storage facilities | Cavern storage facilities | Unit |
|---|---|---|---|---|
| Working gas volume | In operation | 10.6 | 12.1 | Billion $m^3$ ($V_n$) |
| Working gas volume | In the planning or construction phase | 1.0 | 7.2 | Billion $m^3$ ($V_n$) |
| Working gas volume | Total | 11.8 | 19.9 | Billion $m^3$ ($V_n$) |
| Number of storage facilities | In operation | 21 | 29 | Quantity |

and Brandenburg. The farthest south they are found is in the Werra region (northeast Hessen), but with very limited potential. The German Federal Environment Agency's 'Energy Goals 2050' study estimated the expansion potential as 400 salt caverns with a useable working gas volume of 22 billion $m^3$ ($V_n$) [118].

Table 8.21 compares the capacity, power, and annual consumption of gas storage in Germany today (updated 2012 and including storage in the planning and construction phases) with the technical potential for the future (2050). For the sake of simplicity, it was assumed that hydrogen will only be stored in salt caverns and methane in both salt caverns and porous storage facilities. At 106 GW the current average discharging power for gas storage is already quite high. This shows that gas storage already has the capacity to provide enough gas to stabilize the electricity network at all times using PtG and gas power plants.

The total resulting long-term storage capacity for 2050 is presented in Table 8.21. If methane is used as an energy source, then there will be 53 billion $m^3$ of storage capacity or 530 TW h in 2050. If hydrogen is used, then there will be 42 billion $m^3$ or 126 TW h.

By comparison, the currently available estimates for future storage requirements are in the double-digit TW h range. This demonstrates that there is more than adequate storage capacity to meet the requirements for energy transition. Even the currently available capacity is sufficient. There is little additional potential to add to porous storage facilities. If new gas caverns are added, they will be salt caverns.

### 8.4.2 Liquid Storage Media

There is a range of liquid media with characteristics suitable for use in the energy sector. The following sections focus on the most important energy sources today, their characteristics, and how they are stored.

**Table 8.21** Comparison of storage capacities for renewable gasses in Germany—today and in the future with GCVs of 10 and 3 for methane and hydrogen in kW h/$m^3$ [66, 118]

| | Hydrogen | | Methane | |
|---|---|---|---|---|
| Time-frame | 2012+ | 2050 (potential) | 2012+ | 2050 (potential) |
| Capacity in TW h | 60 | 126 | 317 | 533 |
| Average discharging power in GW | | See ▶ Chap. 3 (several values) | 106 | See ▶ Chap. 3 (several values) |
| Annual consumption in TW h/a | | See ▶ Chap. 3 (several values) | 930 | See ▶ Chap. 3 (several values) |

**Table 8.22** Total working gas volumes in cavern and porous storage facilities in 2050

| Working gas<br>Unit | Cavern storage<br>Billion $m^3$ ($V_n$) | Porous storage<br>Billion $m^3$ ($V_n$) | Total<br>Billion $m^3$ ($V_n$) | Total<br>TW $h_{th}$ |
|---|---|---|---|---|
| Hydrogen | 42 | 0 | 42 | 126 |
| Renewable methane | 42 | 12 | 53 | 530 |

### 8.4.2.1 Liquid Gas, LPG, LNG, and CNG

#### Technical Characteristics

Liquid gases includes all gases stored under compression or at low temperatures in liquid form. Liquid gas typically refers to LPG (Liquefied Petroleum Gas), but LPG should not be confused with LNG (Liquefied Natural Gas) or CNG (Compressed Natural Gas). LNG is natural gas cooled to −160 °C at ambient pressure for storage and transport. LNG is 1/600 the volume of natural gas under normal conditions.

The components of liquid gas are saturated ($C_nH_{2n+2}$) or unsaturated ($C_nH_{2n}$) hydrocarbons with $n = 3$ or 4. With LPG, only propane and butane are used:

- Propane ($C_3H_8$)
- Propene ($C_3H_6$)
- Butane ($C_4H_{10}$)
- Butene ($C_4H_8$)
- Methylpropane (isobutane) ($C_4H_{10}$)
- Methylpropene (isobutene) ($C_4H_8$)

LPG is produced as a product of crude oil conversion in refineries, or directly during crude oil and natural gas extraction as an associated gas.

#### Comparison of LPG and CNG

Table 8.23 shows a comparison of LPG and CNG.

#### Storage

Liquefying gases results in significantly higher-specific densities, and as a result, lower geometric storage volumes. Unlike natural gas, methane, or hydrogen, the gases contained in LPG can be liquefied at ambient temperatures and low pressures. This means LPG has a high volumetric energy density but is convenient to handle and requires limited modifications at filling stations. As a result, LPG is more popular than CNG in Germany and other countries.

LPG is stored in small quantities in steel containers. In larger quantities, liquid gas is stored above ground in spherical pressure tanks (▶ Sect. 8.4.1.1), and underground in cavern storage facilities (▶ Sect. 8.4.1.3).

Because its boiling point is −160 °C, liquefying natural gas requires significantly more energy. As a result, natural gas is typically transported in pipelines and stored in gaseous form. Since transport in gaseous form over large distances is very energy-intensive and generally impossible by sea, in these cases, natural gas is

**Table 8.23** Comparison of technical specifications for LPG and CNG

| | LPG | CNG |
|---|---|---|
| Octane | 105–115 (depending on the composition) | 120–140 |
| Storage | Liquid at 8–10 bar and ambient temperatures (400 g fuel/liter) | Gaseous at 200 bar (160 g fuel/liter) |
| $CO_2$ emissions | Reduced by about 15% compared to gasoline vehicles | Reduced by about 25% compared to gasoline vehicles |
| Calorific value | 12.9 kW h/kg | 14.0 kW h/kg |

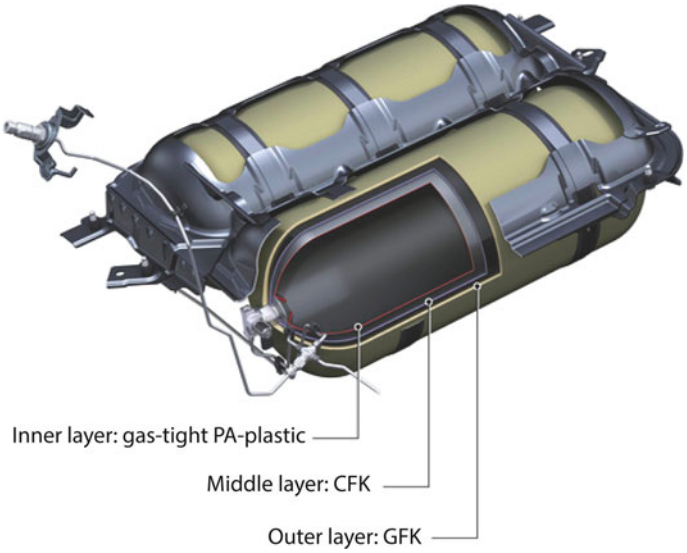



**Fig. 8.55** Gas tank design in the Audi A3 Sportback g-tron. (Source: Audi AG)

liquefied to LNG. It is then evaporated and fed into the natural gas infrastructure at the destination.

LNG is also stored in liquid form under ambient pressure at liquefying terminals for shipping, in special LNG tankers and in specially insulated tanks at destination terminals.

Figure 8.55 shows CNG gas tank design in an automobile as an example.

### 8.4.2.2 Crude Oil

After coal, crude oil is the most popular energy source in the world today (▶ Sect. 1.2). Many fuels and intermediary products currently required for the energy sector and chemical industry are produced from crude oil. Crude oil storage is a form of energy storage.

#### ▪ Technical Characteristics

Table 8.24 lists the components of crude oil together with their boiling points and applications. These components are separated in refineries by a process called fractional distillation which uses the different boiling points of the components.

Since demand for the crude oil components listed here such as gasoline, diesel, kerosene, and so on is higher than their proportional supply in crude oil, they are also produced by converting available higher hydrocarbons using other chemical processes. Cracking, for example, is frequently used. Here, long-chain hydrocarbons are broken by applying high temperatures (▶ Sect. 8.1.2). Depending on the products required, different temperatures, pressures, and catalysts are used.

#### ▪ Transportation

Crude oil is only transported in tanker vessels containing up to 500,000 tons of crude oil by sea, or in pipelines by land (Figs. 8.56 and 8.57). Pipelines are used to unload the oil at ports and for storage. They are also used to safely transport the oil and deliver it to oil consumers. Crude oil pipelines have a power ranging up to 80 GW. In Germany, there are about 2,400 km of pipelines.

Rail, road transport, and inland shipping are only used to distribute crude oil products.

#### ▪ Storage and Storage Technologies

Crude oil is stored in both aboveground storage technologies and underground storage technologies. The technologies most commonly used are floating roof tanks and salt caverns.

In refineries or for commercial use, oil is typically stored in aboveground steel tanks with volumes ranging up to 125,000 $m^3$.

**Table 8.24** Composition of crude oil [75]

| | Boiling point | Number of carbon atoms | Application |
|---|---|---|---|
| Gas | < 20 °C | $C_1$–$C_4$ | Fuel, synthesis gas |
| Light petroleum | 20–90 °C | $C_5$–$C_7$ | Solvent |
| Ligroin | 90–120 °C | $C_7$, $C_8$ | Solvent |
| Gasoline | 100–200 °C | $C_7$–$C_{12}$ | Fuel |
| Kerosene | 200–315 °C | $C_{12}$–$C_{16}$ | Airplane fuel |
| Diesel/heating oil | 250–375 °C | $C_{15}$–$C_{18}$ | Fuels |
| Lubricating oil | > 350 °C | $C_{16}$–$C_{20}$ | Lubrication |
| Paraffin wax | Melting point 50–60 °C | $C_{20}$–$C_{30}$ | Candles |
| Asphalt | Not liquid | | Road construction |
| Residue | Solid | | Solid fuel |






**Fig. 8.56** Oil tanker at a drilling rig. (Source: apfelweile, fotolia)

Figure 8.58 shows the design of a typical floating roof tank. The oil is contained in a steel cylinder topped by a floating roof. Sealed on its outer surface, this piston prevents gaseous crude oil components from escaping into the atmosphere, as well as rain from entering the container.

Unlike in solid roof tanks used in the past, in these modern tanks, there is no area filled with gasses above the liquid level. As a result, the tanks are significantly safer to operate.

The tank has a double outer wall and is enclosed by an additional circular wall. The filling level is determined by the oil column pressure as well as by the level of the floating roof. These tanks are typically up to 70 m in diameter with volumes ranging up to 100,000 $m^3$.

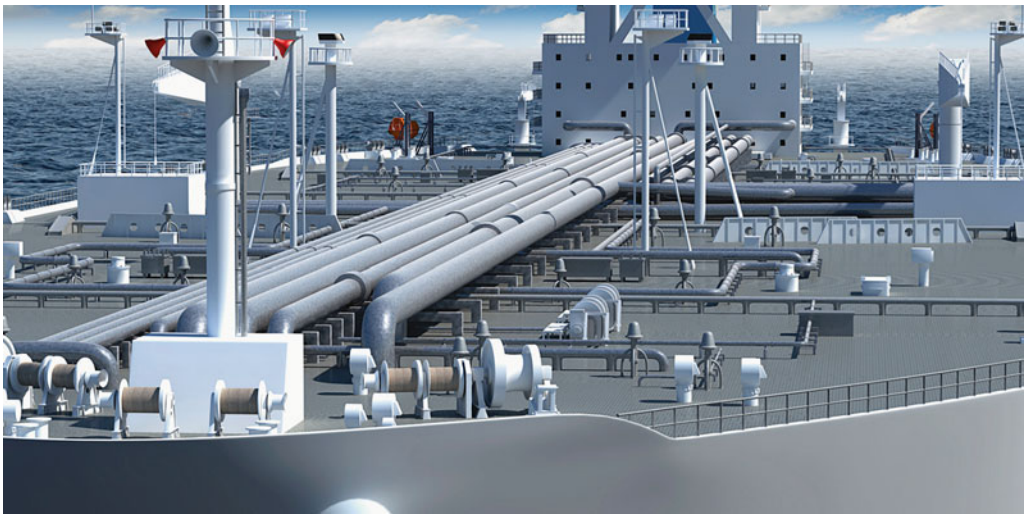


**Fig. 8.57** Dimensions of a large oil tanker. (Source: apfelweile, fotolia)

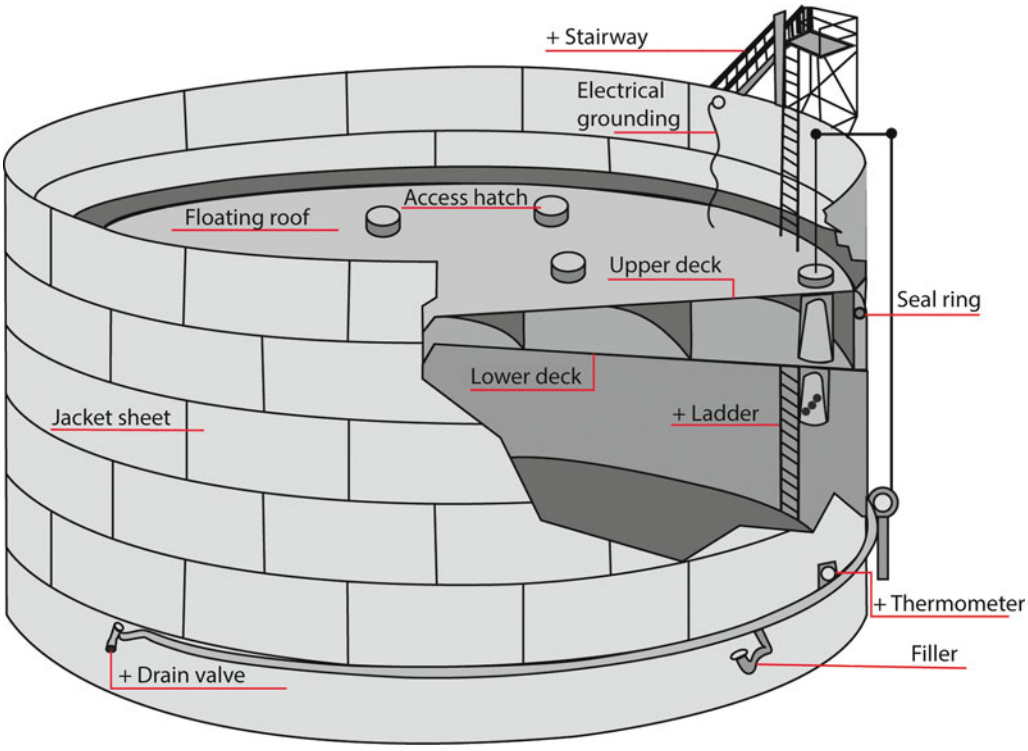



**Fig. 8.58** Floating roof tank for oil storage

Where suitable geological formations are available, underground storage facilities are used to store very large quantities, such as for strategic reserves.

In Germany and the USA (strategic petroleum reserve—SPR), large quantities of crude oil are stored in numerous salt caverns. Salt caverns are well-suited for storage purposes because salt rock is impermeable and inert to oil. Cavern construction costs are also relatively low. Since oil is not compressible, unlike with gas caverns, compression and expansion cannot be used for loading and unloading (filling and emptying or charging and discharging).

This means that brine is often forced to the surface when the cavern is filled with oil. The oil is unloaded using brine, or using water in a strategic reserve. Water can only be used to unload the oil a few times, because dissolution processes increase the cavern's size about 15% each time.

In countries where there are no suitable salt formations, crude oil is also stored in conventionally excavated rock caverns. Since rock such as granite has cracks, the hydrodynamic storage concept described above must be used (▶ Sect. 8.4.1.5). Cavern positioning and other features allow minimal quantities of groundwater to flow into the storage facility, preventing the denser crude oil from escaping through the cracks. The water collects at the bottom of the cavern, which is then pumped out and cleaned. Because of their porosity and issues with biological interaction, porous storage facilities are not suitable for crude oil storage.

German law requires large quantities of crude oil to be stored for emergency use. The quantity of energy stored is equivalent to average net imports over 90 days [26]. A significant portion is stored in salt caverns on the North Sea coast (▶ Sect. 1.2).

In 2009 in Germany, the storage capacity of petroleum storage depots over 1,000 $m^3$ totaled $64.3 \times 10^6$ $m^3$. Almost 65% of this capacity was in external depots such as caverns. Caverns contain 40% of the capacity, meaning they contain the largest portion of storage capacity in Germany [77].




**Fig. 8.59** Diesel filling station for the agriculture and forestry sectors

### Crude Oil Products: Gasoline, Diesel, and Kerosene

The most important crude oil products are gasoline, heating oil, and kerosene. The total capacity of consumer depots over 100 $m^3$ is about $40 \times 10^6$ $m^3$. Smaller depots such as heating oil tanks in private households or filling stations are difficult to track, and are not included in statistics.

In 2010, there were 14,744 filling stations in Germany [77], but there are no numbers on their individual storage capacities. Filling stations aside then, in Germany there is a total available storage capacity for petroleum products of nearly $105 \times 10^6$ $m^3$. As an example, Fig. 8.59 shows a diesel filling station for the agriculture and forestry sectors.

In 2010, demand in Germany for petroleum products was about $106 \times 10^6$ tons. Approximately 34% of the demand was for super or naphtha gasoline, 30% was for diesel fuel, nearly 25% was for light and heavy heating oil, and 8% was for aviation fuels such as Jet-

**Table 8.25** Comparison of the characteristics of ethanol and gasoline [59, 82]

| | Ethanol | Gasoline |
|---|---|---|
| Calorific value | 26.8 MJ/kg | 42.7 MJ/kg |
| Density (at 15 °C) | 0.794 kg/L | 0.72–0.78 kg/L |
| Octane | 107 | 93 |

A1. The remaining demand was for by-products and special products such as lubricants or gasses.

### 8.4.2.3 Biofuels

In 2011, biofuels accounted for 5.5% of fuel consumption in Germany [77]. The three types of biofuels are biodiesel, bio-ethanol, and vegetable oil. Mandatory mixing ratios are regulated by law and described in more detail in ▶ Sect. 13.3.1.

#### ▪ Bio-ethanol

As the name indicates, bio-ethanol is alcohol ethanol derived from a biological source. Alcohols are hydrocarbon derivatives. In alcohols, a hydrogen atom is replaced by an OH group. Called functional groups, they give alcohols their chemical and physical characteristics. In the energy sector, ethanol and methanol can be used as additives in gasoline.

Ethanol or ethyl alcohol's formula is $C_2H_5$-OH. It is produced by alcoholic fermentation followed by distillation using sugary plants, starchy plants, or grains. Bio-ethanol is a first-generation biofuel. Currently efforts are underway to produce second-generation biofuels from biogenic residual materials such as straw or wood scrap (cellulose) that require no negative land-use changes and can be produced cheaply from waste products [127], but the market is not well-developed enough yet [11].

Table 8.25 compares ethanol and gasoline. Additives can increase the octane of conventional fuels so that they burn more efficiently. The calorific value of ethanol is nearly one-third lower than gasoline.

**Table 8.26** Comparison of the characteristics of biodiesel and diesel [59, 82]

| | Biodiesel | Diesel |
|---|---|---|
| Calorific value (typical value) | 37.1 MJ/kg | 43.1 MJ/kg |
| Density (at 15 °C) | 860–900 kg/m$^3$ | 820–845 kg/m$^3$ |
| Cetane number | 51 | 51 |
| Harmful emissions | Around 10% less than diesel | |

#### ▪ Biodiesel

Biodiesel is produced by the transesterification of vegetable oils. In Germany, rapeseed oil is typically used, which can also be burned directly in modified engines. But vegetable oil is converted to biodiesel so that no engine modifications are required. Biodiesel can be used as a pure fuel, or added to mineral diesel at any mixing ratio.

In the transesterification process, a monohydric alcohol (usually methanol) is added to the vegetable fat (fatty acids), which contains only one OH group (hydroxyl group). The resulting product is chemically a fatty acid methyl ester (FAME) or vegetable oil methyl ester (Table 8.26).

#### ▪ Vegetable Oil

Although it could be easily integrated into the energy sector in rural areas and regional economies, energy tax law acts as a disincentive for the use of vegetable oil. As a result, currently it plays only a minor role. If the law is modified, vegetable oil could become more important. Vegetable oil has a large potential for use in agriculture where it could close regional economic circuits (▶ Sect. 13.3.3).

#### ▪ Storage of Raw Material and Biofuels

The storage method depends on the processing status. Oilseed or grains are stored differently than oils or biofuels. To inhibit conversion processes such as auto-oxidation, fat cleavage, or polymerization, storage must ensure that

these processes are not accelerated by exposure to oxygen, light, heat, water, and metal ions. These processes are inhibited by antioxidants contained in the biomass as well, but these antioxidants are consumed over time. As a result, depending on external requirements biomass should not be stored longer than six to twelve months.

Oilseed rape, corn seeds, and cereal grains should be stored at low humidity because, here, dry material losses by oxidation processes are practically negligible. Vegetable oil and biodiesel should ideally be stored in cool, dark, airtight, and rust-free tanks.

In harvested crops containing sugar, the sugar can be quickly consumed by oxidation processes. As a result, they should be processed immediately after harvesting into bio-ethanol. The bio-ethanol can then be stored in tanks as an end product.



#### 8.4.2.4 Methanol and DME

Methanol is the simplest member of the alcohol group, and has the molecular formula $CH_3OH$. Methanol is also called methyl alcohol, and under standard conditions is a colorless, highly poisonous liquid. Its boiling point is about 65 °C and its melting point is about −98 °C. Because it is in the hydroxyl group, methanol is infinitely soluble in water.

Methanol's energy density is about half of gasoline's (Table 8.27). In principal, twice the amount is required to power a car over the same distance. This amount would also be twice the mass because the densities are similar. There is another disadvantage when adding methanol to gasoline. Some materials used in distribution, storage, and in vehicles are incompatible with methanol. Methanol can corrode metals such as aluminum or magnesium. Methanol also affects certain plastics and rubbers, making them brittle or soft.

But methanol has some advantages over gasoline. Methanol's octane is around 100, meaning an air/methanol mixture can be compressed to a smaller volume in the compression stroke of an engine (▶ Sect. 8.5.3.1). In addition, methanol has a higher flame velocity, meaning it burns more cleanly than gasoline. As a result, less than twice the amount of methanol is actually required to produce the same amount of power.

**Table 8.27** Comparison of the characteristics of methanol and gasoline [9, 81]

| | Methanol | Gasoline |
|---|---|---|
| Calorific value | 22.7 MJ/kg | 42.7 MJ/kg |
| Density (at 20 °C) | 0.79 kg/L | 0.72–0.78 kg/L |
| Octane | 100 | 93 |
| Compression ratio | 11:1 | 10:1 |

Because hydrogen bonds are created between the hydrogen and oxygen atoms of neighboring methane molecules, methane's boiling point is higher than gasoline's. Methanol can, therefore, absorb more heat, improving heat dissipation. This means that air-cooling can be used instead of water cooling [9, 81]. With minor modifications, current gasoline engines could also use methanol as a pure fuel. Today, standard engines can already burn gasoline mixtures with a methane content of up to 20% by volume. Currently, up to 3% by volume is permitted in fuel mixtures [73].

Since burning methanol releases virtually no hydrocarbons, nitrous oxide, or particles, methanol used either as an additive or as a pure fuel reduces a vehicle's harmful emissions.

Because it is not soluble in diesel, methanol cannot be used as an additive with diesel. But it can be easily converted to DME by dehydrogenation. DME is a colorless, non-corrosive, non-toxic, environmentally-friendly gas that is usually stored as a liquid under pressure. Because of its cetane number ranging from 55 to 60, DME could be used as a diesel substitute. Conventional diesel has a cetane number of around 51 (Table 8.27). It also burns so cleanly that no post-treatment of the gas is required to comply with emissions limits.

In addition, methanol can be processed into gasoline using the methanol-to-gasoline (MTG) process (▶ Sect. 8.3.5), and then stored in conventional tanks.

**Table 8.28** Comparison of the characteristics of DME and diesel [9, 81]

| | DME | Diesel |
|---|---|---|
| Calorific value | 28.8 MJ/kg | 43.1 MJ/kg |
| Density (at 20 °C) | 0.67 kg/L | 0.84–0.89 kg/L |
| Cetane number | 55–60 | 51 |

### 8.4.2.5 Liquid Hydrogen Carrier Materials (LOHC)

Liquid organic hydrogen carriers (LOHC) can be used to store and transport hydrogen under ambient conditions as a diesel-like liquid with a high energy density. In addition to applications in hydrogen logistics, LOHC combined with hydrogen-production technologies (see ▶ Sect. 8.2) and hydrogen-consumption technologies (see ▶ Sect. 8.5) can be used to create an energy-storage system.

#### ▪ Storage and Extraction with Liquid Hydrogen Carriers

To heteroaromatic carrier-fluid in an exothermic, catalytic hydrogenation reaction.

When energy is required, the hydrogen is released using endothermic catalytic dehydrogenation. Other technologies are then applied to extract and utilize the hydrogen. This means that hydrogenating LOHC releases heat, but dehydrogenating LOHC requires heat.

Ideally, the liquid organic hydrogen carrier is not consumed during these hydrogenation and dehydrogenation processes. It serves solely as a temporary carrier of the chemically bonded hydrogen.

Because of its specific characteristics, the LOHC storage system in both its hydrogenated and dehydrogenated forms can be stored, transported, and handled in large quantities like the other standard liquid fuels (see [113] and ▶ Sect. 8.4.2.2).

#### ▪ Safety

Many inherent system features prevent the hydrogen from being improperly released from the liquid carrier by chance, accident or misuse. These features include the hydrogenated LOHC material, the special catalyst, the adequately high temperature level and the heat source that supplies the heat required by dehydrogenation at this temperature level. Together, all of these elements make the system safer. Fig. 8.60 shows the LOHC system dibenzyltoluene (H0-LOHC)/perhydrodibenzyltoluene (H18-LOHC) with the typical charging- and discharging-process conditions, as well as the quantity of heat released or consumed.

#### ▪ Advantages and Disadvantages

Hydrogen storage using LOHC offers these advantages and possibilities:

- The complexity of handling hydrogen as a gas with its low density, high volatility, and high flammability is replaced by the simpler handling required by a 'diesel-like' energy source in liquid form under ambient conditions, eliminating molecular hydrogen from the transport and storage chain.
- The LOHC system storage density of hydrogen is very high in comparison to molecular compressed storage. This significantly reduces the costs of hydrogen transport and storage.
- Dehydrogenation is an endothermic catalytic reaction. The hydrogen can only be released in special facilities using suitable catalysts by applying heat, preventing it from being improperly released by accident or misuse.
- Hydrogenation is an exothermic catalytic reaction. Heat is released at temperatures ranging up to 200 °C, and can be used for energetic purposes such as heating or steam generation.
- The product released is hydrogen, which can be used for energetic purposes or as a material (for example, in hydrogen filling stations or in the chemical industry).

But hydrogen storage using LOHC is also associated with these disadvantages and problems:

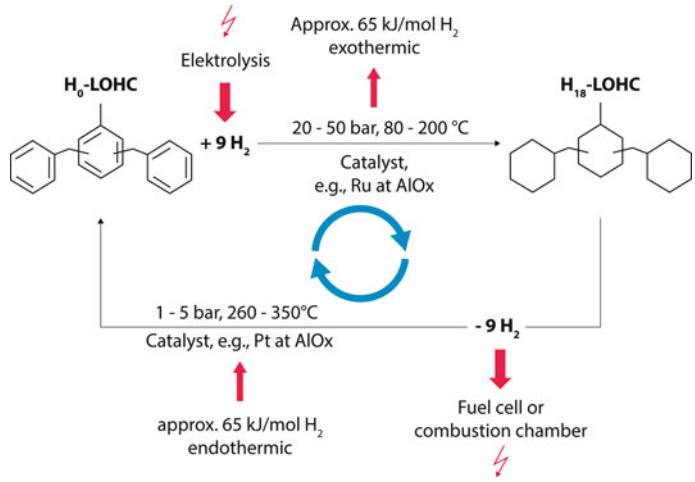



**Fig. 8.60** LOHC system dibenzyltoluene (H0-LOHC)/perhydrodibenzyltoluene (H18-LOHC) with typical charging and discharging process conditions, as well as the quantity of heat released or required [18]

8

- Depending on the application, the heat required for dehydrogenation can be provided by the waste heat from the extraction technology (▶ Sect. 8.5.1), or by burning a portion of the hydrogen released (which reduces the dehydrogenation efficiency to about 73%).
- The chemical processes of hydrogenation and dehydrogenation require using catalysts and a process design that effectively maintain the long-term stability of the materials, as well as the high purity level of the hydrogen released.
- Some LOHC materials (for example toluene) have been designated hazardous materials that require special safety and handling precautions. But toluene has a significantly lower hazard classification than fossil gasoline.
- Fossil raw materials are currently still initially required to produce the LOHC. Synthetic production may be possible in the future, and is preferable.

## 8.4.3 Solid Storage Media

### 8.4.3.1 Coal

Despite having by far the highest specific $CO_2$ emissions in energy supply, coal in the form of brown and hard coal is still Germany's main energy source for electricity supply.

Brown coal currently accounts for 25% of electricity supply. Close to 200 million tons of brown coal are mined annually in four territories. In recent years, the output distribution was 50% in Rheinland, 1% in Helmstedt, 19% in central Germany, and 30% in Lausitz. Large quantities of energy are stored in directly available brown coal (also called exposed coal).

Mining of hard coal is planned to continue in Germany until 2018. Currently, about 10 million tons are mined annually. In addition, Germany imports about 30 million tons of hard coal annually from Russia, the USA, Colombia, South Africa, and Poland. Imported coal is unloaded at seaports in Rotterdam, Antwerp, Wilhelmshaven, Nordenham, and Hamburg. It is then transported by inland shipping or rail to where German power plants are located. In Wilhelmshaven it is transported directly to a power plant by conveyor belts. The seaports also have stockpiles with a storage capacity of up to two million tons used to speed processing, not as a storage warehousing. Two million tons with a calorific value of around eight MW h/ton is equivalent to about 16 TW h of stored energy, 350 times the capacity of pumped-storage. This means that, apart from gas storage with 217 TW h of capacity, coal storage capacity is the largest in Germany. This again demon-



**Fig. 8.61** Stockpile storage at a port of hard coal for electricity generation in a power plant. (Source: Klaus Eppele, fotolia)

strates the crucial role of chemical-energy storage. It also illustrates that, in comparison with other storage, the energy density of chemical-energy storage is by far the highest.

Power plant facilities have coal stockpiles with capacities ranging from several tens of thousands of tons to several hundreds of thousands of tons. These stockpiles are used to allow flexible delivery logistics. They are also used in part to warehouse different types of coal that can only be burned in specific mixtures. Warehousing includes passive and active stockpiles.

Active stockpiles are required for coal deliveries and for coaling the power plant. Only passive stockpiles can be used for long-term storage to compensate for bottlenecks in supply. Most locations do not have passive stockpiles. Many types of coal are not suitable for long-term storage because they are prone to spontaneous combustion. Stockpile fires are a large financial and ecological risk.

In general, coal can be stored in stockpiles, bunkers, or halls (Fig. 8.61). With solid energy sources, stockpiling means storage in the open where it is exposed to the elements. This is a very simple kind of storage easily designed for large quantities. Coal can be stored in conical, longitudinal, and area stockpiles.

- Conical stockpiles: the coal is poured from a fixed-discharge point.
- Longitudinal stockpiles: the stockpile is distributed along one axis at a limited height. This method is used to store several types of coal.
- Area storage: the coal is poured evenly over an area. This is for very large quantities.

Typically, hall storage is used to protect the environment from dust emissions and water contamination. Regulatory authorities require new buildings to include hall storage. An example is the Staudinger coal power plant near Frankfurt. Coal oxidizes when exposed to oxygen, producing heat. This can cause the coal to spontaneously combust. As a result, fire safety systems are also required. These fire safety systems are expensive, because containing fire in halls is significantly more difficult than in the open. This means personnel protection requirements are also high.

In addition to coal storage for energy supply, there are also individual coal stores in households holding similar quantities as pellet stores. Like pellet heating, hard coal heating is supplied by screw conveyors. This results in significant dust emissions (Fig. 8.62).

### 8.4.3.2 Biomass

Biomass storage is typically used to store biomass from harvest until its consumption as



**Fig. 8.62** Household coal store for hard coal heating



**Fig. 8.63** Biomass storage: open-air wood storage



**Fig. 8.64** Example of biomass storage: corn in a mobile silo—front view

an energy source. Producers, distributors, or even consumers can all store biomass. Since with energy crops and wood the time between harvest and consumption often spans months, biomass storage is seasonal storage.

The storage technologies detailed below are used to store biomass.

### Open-Air Storage

- Without weather protection: coarse biomass is piled on palettes or gravel ground. Bulk solids are piled on hard ground insulated from moisture. In both cases, the biomass should be protected from contamination.
- With weather protection: firewood is air-dry and suitable for burning only after six to 24 months of storage. As a result, stored wood is usually piled on ground insulated from moisture and protected from the rain (Fig. 8.63). In addition, there should be adequate ventilation for heat and air moisture produced during storage. This requires placing the woodpiles some distance apart from each other and from the walls of the building. Simple plastic tarpaulins can be used to cover bulk solids such as wood chips or silage of corn or grass (Fig. 8.64). Besides providing weather protection, the tarpaulins also promote anaerobic pre-fermentation of the stored energy crops (Fig. 8.65).

### Building Storage

- Halls: biomass is stored in existing buildings, new buildings, or barns (Fig. 8.66). Good ventilation is required to dry the biomass and to prevent condensation damage to the building. Ideally, the floor of the building should have a drainage system to collect and remove condensation. Bulk



**Fig. 8.65** Example of biomass storage: corn in a mobile silo—plan view



**Fig. 8.67** Example of biomass storage: straw bales in a barn



**Fig. 8.66** Example of biomass storage: wood chips in an open-air barn

solids such as wood chips, hay, or straw also require an edge barrier strong enough to contain the pressure of the piled biomass. Stalk material is also frequently stored in compressed form in bales (Fig. 8.67).

- Containers: these are primarily for bulk solids and stalk material, such as tower silos for wood chips, grass, or corn, for example.

Natural processes that occur while biomass is stored and warehoused that may pose significant storage risks.

- Material losses through biological processes: material losses are minor with wood chippings, stalk material, and logs with proper storage; for example, with spruce there is a relatively small material loss of about 4% over three years. Since plant respiration quickly reduces sugar, storage of raw materials containing sugar is more difficult.
- Self-heating or spontaneous combustion, especially with hay.
- Health risks posed by fungus growth.
- Rewetting.

## 8.5 Extraction Technologies

In addition to storage technologies and storage media, energy storage concepts also require extraction technologies. Like turbines with pumped-storage, combustion technologies are required to convert the energy stored in solid, liquid, and gaseous energy sources into electricity, power, and heat. This section is devoted to these extraction technologies. The systems for gases and liquids are first described,

and then discussed in ▶ Sects. 8.6 and 8.7 as energy storage systems.

### 8.5.1 Electricity Generation Using CHP Generation

CHP generation includes power plants that directly convert mechanical energy into electrical energy, but also exploit the thermal energy produced in the process. In principle, CHP can be electricity or heat-oriented. Ideally, they are electricity-oriented (▶ Sect. 14.1).

#### 8.5.1.1 Fuel Cells

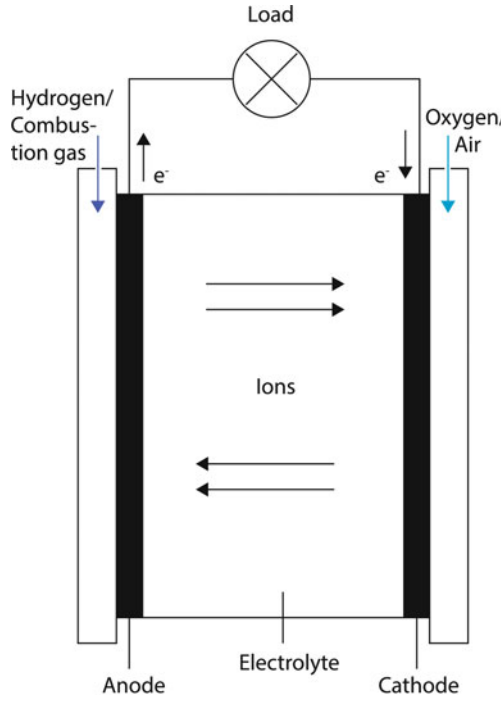
The underlying principle of fuel cells was discovered in 1838. But since handling the fuels and materials required is complex, for many years, electric generators were still more common. As oil and energy prices increased, researchers returned their attention to fuel cells.



■ **Operating Principle**

Fuel cells use reverse electrolysis. ◘ Figure 8.68 shows the basic design of a fuel cell. The fuel cell contains two porous (gas-permeable), catalytically active electrodes. Catalytic means that the electrode material's characteristics reduce the reaction's activation energy. Pure hydrogen or combustion gas containing hydrogen flows around the anode, causing electron release (oxidation). The oxidation agent at the cathode is either pure oxygen $O_2$ or air (around 21% $O_2$ by volume). The electrodes are separated by an electrolyte to control the speed of the chemical reaction. The electrolyte is gas-permeable and ion-conducting to prevent the two gases from intermixing. This could result in an oxyhydrogen reaction and an explosive release of energy [29].

First the hydrogen at the anode releases its electrons, ionizing to $H^+$ ions. Then the released electrons travel through an electrical conductor from the anode to the cathode, where the current can be used by a load. Once they arrive at the anode, the electrons split the oxygen molecules into $O^{2-}$ions. Depending on the type of fuel cell, the $O^{2-}$ions then either travel through the electrolyte to the anode and react there with the $H^+$ ions to form water ($H_2O$), or the reverse (◘ Fig. 8.68).




◘ **Fig. 8.68** Basic fuel cell design [29]

Individual fuel cells are rare. Usually several cells are connected in series in a stack, as with electrolyte cells. Individual cells are typically connected in a bipolar stack. This means that each wall separating the cells functions on one side as a cathode and on the other as an anode (see stack design in ▶ Sect. 8.2.3).

■ **Fuel Cell Types**

The primary criteria that distinguish different fuel cell types are the electrolyte, combustion gas, and operating temperature. These are listed together with the reduction and oxidation agents for the (currently) most common types in ◘ Table 8.29, and are illustrated in ◘ Fig. 8.69 [84].

Since PEM fuel cells are the most common today, they will be discussed here in-depth.

**Table 8.29** Fuel cell types with reduction agent, oxidation agent, electrolyte, and temperature range [84]

| Type | Name | Reduction agent | Electrolyte | Temperature range | Oxidation agent |
|---|---|---|---|---|---|
| AFC | Alkaline fuel cell | $H_2$ | Potassium hydroxide KOH | 20–90 °C | $O_2$ |
| DM-FC | Direct methanol fuel cell | $CH_4O$ | Proton-conducting membrane | 60–130 °C | $O_2$, air |
| MC-FC | Molten carbonate fuel cell | $H_2$, $CH_4$, combustion gas containing $H_2$ | $Li_2CO_3$, $K_2CO_3$ | 600–650 °C | $O_2$, air |
| PA-FC | Phosphoric acid fuel cell | $H_2$ | $H_3PO_4$ | 160–220 °C | $O_2$, air |
| PEM-FC | Proton exchange membrane fuel cell | $H_2$, combustion gas containing $H_2$ | Proton-conducting polymer membrane | 60–120 °C | $O_2$, air |
| SO-FC | Solid oxide fuel cell | $H_2$, $CH_4$, combustion gas containing $H_2$ | Ceramics $ZrO_2/Y_2O_3$ | 800–1,000 °C | $O_2$, air |

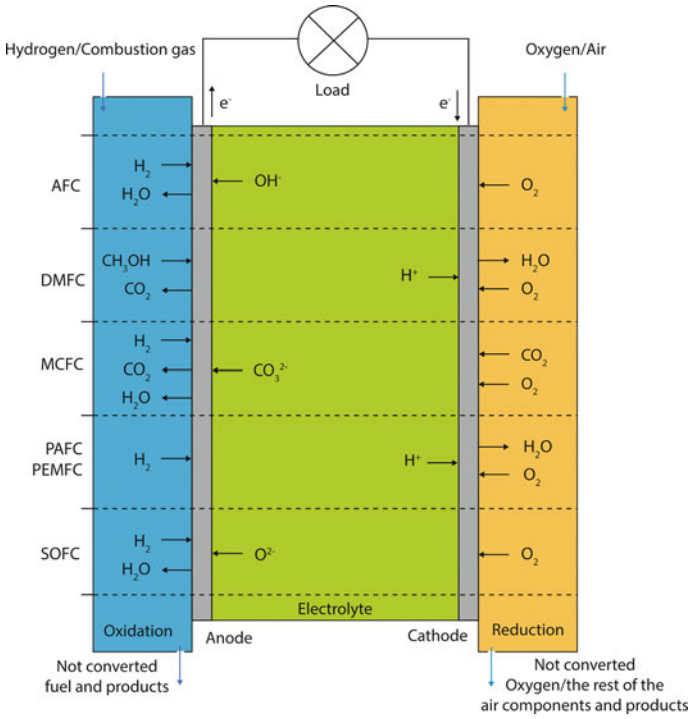



**Fig. 8.69** Reactions and materials with various fuel cell types [84]

The electrolyte is a polymer-based, proton-conducting membrane. The electrodes are usually carbon or metal carriers coated with a platinum catalyst. The advantage of these fuel cells is they can be supplied with air instead of oxygen. In addition, membrane fuel cells have high-energy densities. Problems with this type of fuel include the short service life of the membrane and finding a suitable electrode material.

**Table 8.30** Specifications of a $H_2/O_2$ fuel cell with a liquid and gaseous product

| | Two-phase system: water in liquid form (25 °C, 1 bar) | Gas-phase reaction: water as steam (100 °C, 1 bar) |
|---|---|---|
| Change in enthalpy/Gibbs potential $\Delta G$ | 237.13 kJ/mol | 228.57 kJ/mol |
| Bonding enthalpy $\Delta H$ | 285.83 kJ/mol | 241.82 kJ/mol |
| Thermodynamic efficiency | 83.0% | 94.5% |
| Reversible cell voltage | 1.23 V | 1.18 V |
| Thermoneutral cell voltage | 1.48 V | 1.25 V |

The following reactions occur in a PEM fuel cell:

anode (oxidation):

$$H_2 \rightarrow 2H^+ + 2e^-, \tag{8.111}$$

cathode (reduction):

$$\frac{1}{2}O_2 + 2e^- \rightarrow O^{2-}, \tag{8.112}$$

complete (redox reaction):

$$H_2 + \frac{1}{2}O_2 \rightarrow H_2O. \tag{8.113}$$

## Thermodynamic Principles

The advantage of fuel cells over an oxyhydrogen reaction is that the energy is directly converted from chemical bonding energy to electric energy without first producing thermal energy. As a result the cells are low-noise, low-emission, and highly efficient even under partial-loads. They are not dependent on the energy conversion efficiency of the Carnot limit, and they do not produce large amounts of waste heat as with conventional electricity generation. Conversion is limited only by the change in free enthalpy $\Delta G_R$ (or Gibbs potential) [29]. This means that the theoretical maximum convertible energy is:

$$\Delta G_R = \Delta H_R - T \cdot \Delta S, \tag{8.114}$$

where the formation enthalpy $\Delta H_R$ at 25 °C and 1 bar is −285.83 kJ/mol, which is equivalent to the GCV $H_s$ of hydrogen. As a result:

$$\Delta G_R = -237.13 \frac{\text{kJ}}{\text{mol}}. \tag{8.115}$$

Since the energy actually converted is lower due to the change in entropy, the attainable cell voltage is $U_{rev}$ at 1.229 V. This is below the theoretically attainable maximum voltage $U_{max} = 1.481$ V. The thermodynamic efficiency is determined by the ratio between these two values [28]:

$$U_{rev} = -\frac{\Delta G_R}{z \cdot F}, \tag{8.116}$$

$$U_{max} = -\frac{\Delta H_R}{z \cdot F}, \tag{8.117}$$

$$\eta_{rev} = \frac{|\Delta G_R|}{|\Delta H_R|} = \frac{U_{rev}}{U_{max}} = 0.83 = 83\%, \tag{8.118}$$

with

$z$ – number of electrons per molecule ($z(H_2) = 2$),
$F$ – 96,485 A s/mol as Faraday constant.

Table 8.30 lists the specifications of a $H_2/O_2$ fuel cell with a liquid and gaseous product. As with water electrolysis, steam is significantly more efficient than water (▶ Sect. 8.6.4).

Figure 8.70 shows the characteristic voltage-current density curve for a fuel cell. Also shown are the maximum voltage $U_{max}$ and the reversible voltage $U_{rev}$. In a real fuel cell, other effects occur that reduce the cell's voltage or cause losses.

The voltage losses shown in Fig. 8.70 are defined as follows [29]:

- $\Delta U_D$ are the voltage losses caused by the passage of electrons across the boundary between the electrode and electrolyte.

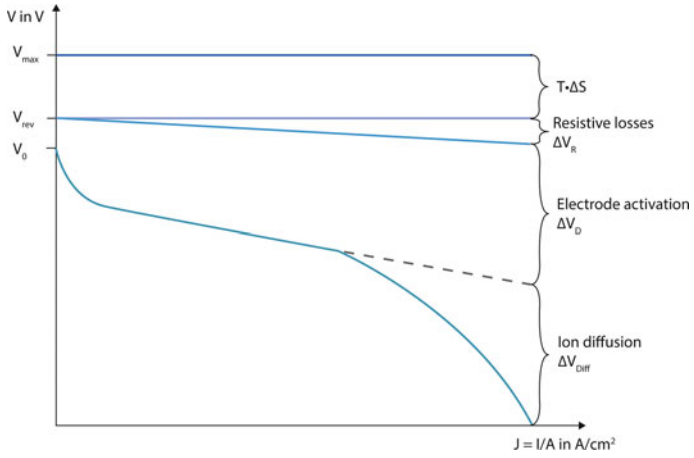



**Fig. 8.70** Characteristic voltage-current density curve for a fuel cell showing losses from internal resistance, passage of electrons across the electrode/electrolyte boundary, and ion diffusion [29]

- $\Delta U_R$ is the ohmic voltage drop caused by the internal resistances of the electrode and the conductor.
- $\Delta D_{Dif}$ are diffusion losses. These are particularly high with high current-densities because, at these levels, hydrogen and oxygen cannot be supplied at the rate the chemical reaction actually requires.

These factors determine the electric efficiency (or voltage efficiency), which is defined by the ratio between a cell's measured voltage $U$ and the theoretical maximum voltage $U_{max}$, taking into account all the losses described:

$$\eta_U = \frac{U}{U_{max}} = \frac{U_{rev} - \Delta U_R - \Delta U_D - \Delta U_{Dif}}{U_{max}}. \quad (8.119)$$

The fuel cell efficiency $\eta_{FC}$ is an overall assessment. It compares the electrical power of the fuel cell, including auxiliary energy, with the power contained in the fuel volume flow:

$$\eta_{FC} = \frac{P_{el}}{\dot{V}_{H_2} \cdot \Delta H_R}. \quad (8.120)$$

This can also be defined as [84]:

$$\eta_{FC} = \eta_U \cdot \eta_I \cdot \eta_{rev} \cdot \eta_{sys} \cdot \eta_B. \quad (8.121)$$

Efficiency $\eta_{rev}$ and $\eta_U$ were previously determined by Eqs. 8.118 and 8.119. The system efficiency $\eta_{sys}$ includes losses from peripherals such as pumps. The combustion efficiency $\eta_B$ is determined by the percentage of hydrogen converted. The electrical power efficiency $\eta_I$ is determined as follows.

Faraday's first law is applied to determine the theoretically required volumetric flow, and so the minimum volumetric flow for the measured electrical power:

$$\dot{V}_{theo} = \frac{I \cdot R \cdot T}{z \cdot F \cdot p} \quad (8.122)$$

with

$I$ – measured current in amps,
$R$ – universal gas constant 8.314 J K$^{-1}$ mol$^{-1}$, temperature of the hydrogen in Kelvin,
$P$ – atmospheric pressure in Pascal.

When multiplied by the number of cells $n$, the result is the system's overall volumetric flow. For the conversion rate $\eta_B$, the result is:

$$\dot{V}_{ges,theo} = \frac{n \cdot I \cdot R \cdot T}{\eta_B \cdot z \cdot F \cdot p}. \quad (8.123)$$

The electrical power efficiency can then be determined using Eq. 8.123 and the measured hydrogen flow volume. This is also termed the Faraday efficiency, or conversion efficiency:

$$\eta_I = \frac{\dot{V}_{ges,theo}}{\dot{V}_{mess}} = \frac{I}{I_{th}}, \quad (8.124)$$

with

$I_{th}$ – theoretical current in amps that would result with the measured fuel volume flow and an ideal fuel cell.
$I$ – measured current in amps.

### ■ Technical Applications

Fuel cells must be maintained in a certain operating temperature-range. In most cases, this means that heat must be dissipated from the cell. PEM fuel cells typically use water-cooling. Equation 8.125 is used to determine the power loss as well as the fuel cell efficiency defined in Eq. 8.120 or 8.121:

$$P_V = \dot{V}_{KW} \cdot \rho_W(T) \cdot c_{p,W}(T) \cdot \Delta T_{KW}. \quad \textbf{(8.125)}$$

The density $\rho_W(T)$ and heat capacity $c_{p,W}(T)$ are temperature-dependent parameters of water. $\Delta T_{KW}$ is the temperature differential between the incoming and outgoing cold-water flow volume $\dot{V}_{KW}$.

According to the first law of thermodynamics, incoming power is equal to outgoing power. So for the system, the result is:

$$P_{zu} = \underbrace{P_{el} + P_V}_{P_{ab}}, \quad \textbf{(8.126)}$$

with

$P_{el}$ – electrical power generated by the fuel cell,
$P_{zu}$ – power added to the system by hydrogen and its calorific value.

These two values are determined by Eqs. 8.127 and 8.128:

$$P_{el} = U \cdot I, \quad \textbf{(8.127)}$$

$$P_{zu} = \dot{V}_{H_2} \cdot \Delta H_{U,H_2}, \quad \textbf{(8.128)}$$

with

$\dot{V}_{H_2}$ – flow volume under normal conditions,
$\Delta H_{U,H_2}$ – lower calorific value of 3.0 kW h/m³.

Fuel cells are not economically viable in today's market, and are only available where subsidized. But fuel cell technology has enormous potential for the future. It uses 'cold' combustion that produces only water, and unlike conventional power plant technology, it is not subject to the Carnot efficiency limit [29].

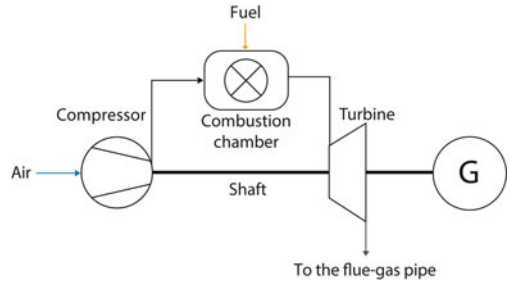



**Fig. 8.71** Design and operation of a gas turbine [39]

### 8.5.1.2 Gas Turbine Power Plants

Energy supply increasingly relies on stationary gas turbines to cover peak loads, for use in steam turbine combination power plants, and more rarely for use in CHP generation. Their rated electrical power ranges from a few kW (micro-gas turbines) to several hundred MW (combined cycle plants). Open gas turbines typically use air and flue gases as working media. The term 'gas turbine' does not refer to the fuel, which may be gaseous, liquid, or solid. Instead, it refers to the gaseous working media. Because of their short start-up times of seven to 15 minutes and their low capital costs, gas turbine power plants are particularly well-suited as peak load power plants. Figure 8.71 illustrates the design and operation of this type of gas turbine [22].

The facility's main components are a fresh air intake, a compressor, a combustion chamber, a turbine, and a generator. The intake air is compressed in the compressor, heated to a temperature of about 1,500 °C in the combustion chamber, and then decompressed in the turbine, releasing enthalpy. This drives a generator connected to the shaft of the turbine, converting mechanical energy into electrical energy.

A gas turbine facility uses the Joule cycle. This cycle is illustrated by the $T$-$s$ diagram in Fig. 8.72.

Gas turbines use a stationary, isobaric heat supply. In an ideal Joule cycle, the process steps are:

- 1 → 2: the air is compressed in a turbo compressor from ambient pressure to high

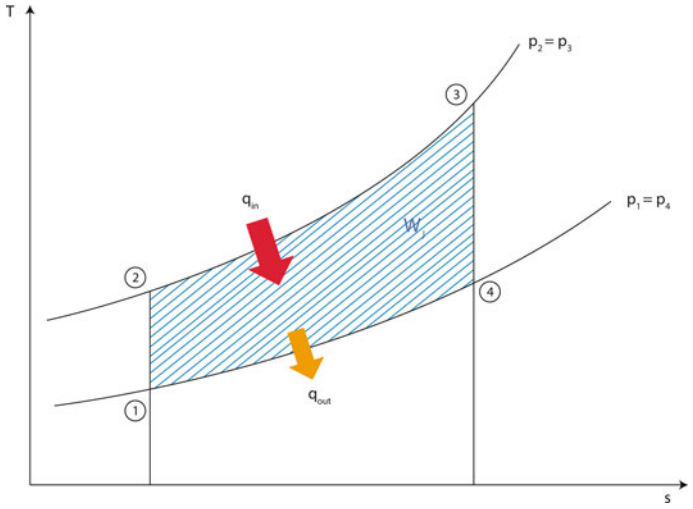



**Fig. 8.72** *T-s* diagram of the Joule cycle

pressure, ideally in isentropic compression. This increases the temperature of the air.

- 2 → 3: The compressed air together with the fuel is passed through the stationary combustion chamber. The resulting air-fuel mixture is combusted. Since the pressure remains the same but the temperature rises, this step is termed isobaric heat supply.
- 3 → 4: The hot flue gas is decompressed in the turbine to ambient pressure. The turbine produces work, driving the generator and the compressor. The temperature then drops, ideally in isentropic decompression.
- 4 → 1: The exhaust is isobarically released into the atmosphere. This releases heat into the atmosphere.

The hatched area in Fig. 8.72 is proportional to the turbine's specific work. It is determined by the difference between the work produced by the turbine and the work consumed by the compressor, and defines the maximum portion that can be converted to electrical energy. In addition, $q_{zu}$ is the heat energy supplied and $q_{ab}$ the heat energy dissipated in the cooling cycle.

In reality, there are losses in the Joule cycle. These losses are caused by, for example, irreversible pressure drops in the turbine, compressor, and flow channels, due to incomplete combustion in the combustion chamber, and due to blade cooling in the turbine and compressor. These losses result in lower turbine capacity and higher compressor capacity. This in turn significantly reduces the effective power, meaning less work is available to the generator [1].

Steam turbines operate at temperatures up to around 650 °C. They are part of a closed water circulation system that constantly vaporizes water, superheats it, and then condenses it again in the cooling cycle.

In gas and steam power plants, steam turbines are exclusively driven by hot steam flows. As a result, they are not exposed to the fuel used in the facility. In contrast, the combustion of a gas-air mixture in gas turbines means they are directly in contact with hot combustion gases. Since temperatures in the turbine can reach 1,500 °C, blade cooling is required. Without cooling, the blade material would quickly wear out and fail [35].

#### 8.5.1.3 Gas and Steam Power Plants

Power plants that combine the principles of a gas turbine and a steam power plant are called gas and steam combination power plants, gas and steam turbine power plants, or combined-cycle gas turbine (CCGT) power plants. Here, the gas turbine functions as a heat source for the steam turbine process.

For economic and thermodynamic reasons, steam power plants currently operate at tem-

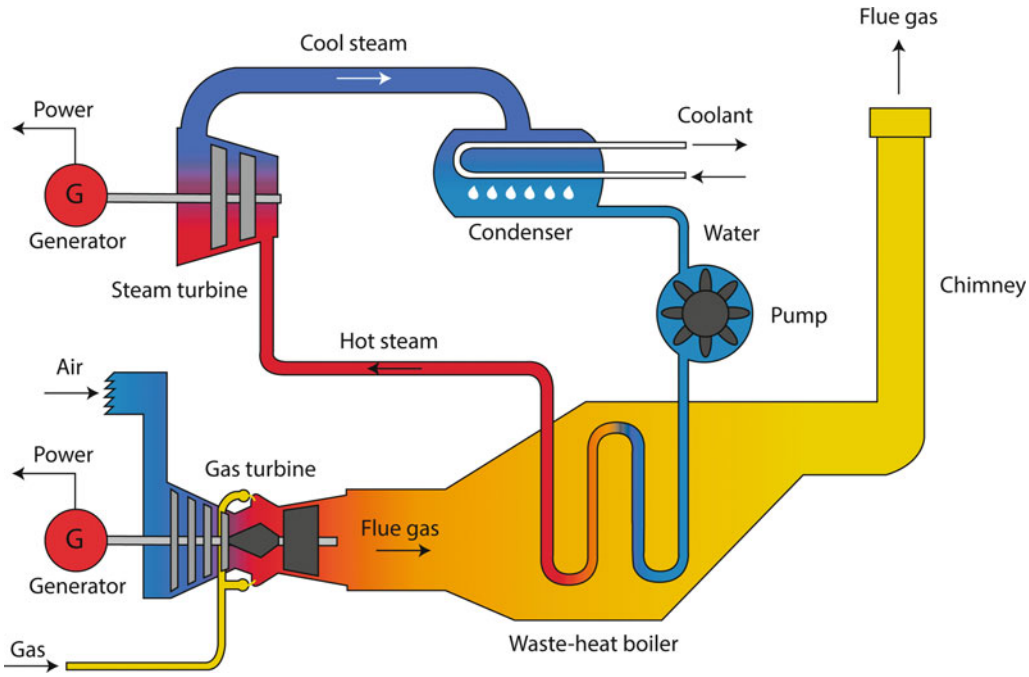



**Fig. 8.73** Design and operation of a CCGT power plant

peratures no higher than 550 to 650 °C. By comparison, in gas turbine power plants the turbine inlet temperatures range up to 1,500 °C, and the exhaust temperatures range up to 550 °C. This means the hot exhaust from the turbine can be exploited by a steam power plant using a heat recovery steam generator. Figure 8.73 illustrates the operation of a CCGT plant [21].

The gas turbine process is the same as the process described in ▶ Sect. 8.5.1.2. In addition, the exhaust is passed through a waste heat steam boiler in a CCGT power plant. There, the flue gas is used to vaporize or superheat the water in the closed steam power process. This heated, vaporous medium is then decompressed and cooled in the steam turbine. Finally, the medium is fully liquefied in a condenser and returned to its original condition using a feed water pump. The cycle then begins again.

CCGT power plants have a high efficiency of 62%. By comparison, gas turbine power plants have an efficiency of only 38%. Similarly, steam turbines have an efficiency of around 35% in CCGT power plants, or 30 to 45% in power plants using purely steam. CCGT power plants can also be constructed more quickly than coal power plants. Gas power plants can use renewable (storage) gas, and even when using fossil gas, have lower specific emissions of $CO_2$ and other exhaust gases than coal power plants. But coal power plants are currently still cheaper to operate. This is because the fuel is cheaper, and emissions trading has been inadequately implemented [1].

### 8.5.1.4 District Heating Plants

A district heating plant (CHP) converts fuel into electricity and heat at the same time using the principle of CHP generation (▶ Sect. 14.1). CHP are typically located where the heat is consumed or where there is a connection to a heating network. Since delivering heat over long distances entails high capital and operational costs, often small, decentralized CHP with small gas turbines or gas engines are directly connected to residential developments or

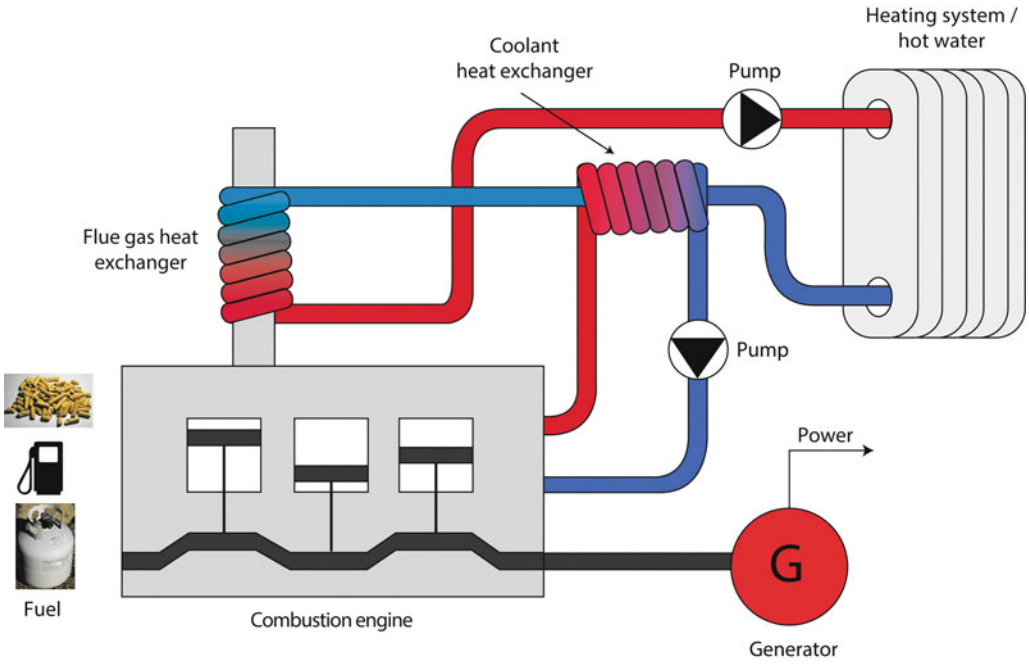



**Fig. 8.74** Design and operation of a district heating plant [39]

other heat consumers. The electrical and thermal energy generated ranges from a few kW to several hundred MW [1]. Figure 8.74 illustrates the design and operation of a CHP [21].

These plants require a combustion engine to drive the generator. The engine can be powered by conventional fuels such as natural gas, biogas, and renewable gas, or by liquid fuels such as vegetable oil. It is theoretically possible to convert hydrogen to electricity in a CHP, as has been done by the company 2 G, for example, but this is rare. Compared to fuel cells, the disadvantage here is the low electrical power efficiency. The major advantages are lower capital costs and longer service life [39].

CHP heat is decoupled on two levels: as engine exhaust heat and as hot flue gas. The electricity produced by the generator is used to supply the power plant building itself, or sold to a network operator and fed into the power network.

District heating plants are generally designed for full-load operation over long periods to ensure cost-effective operation. Extremely detailed heat and electricity consumption data is required to adjust operation so that it aligns correctly with connected consumer demand. As a result, CHP are also equipped with control and regulation devices.

The possible modes of operation, which are described in more detail in ▶ Sect. 14.1, are:

- Heat-driven CHP
- Electricity-driven CHP
- Electricity-oriented CHP (electricity-driven with thermal storage)

### 8.5.2 Building Heating and Cooling Supply

Because gas is easy to distribute, produces relatively low $CO_2$ emissions, and has good combustion characteristics, it is currently used as fuel in low-temperature heating boilers or condensing boilers to generate heat. Gas can also be used in gas engine heat pumps, or to power air-conditioners.

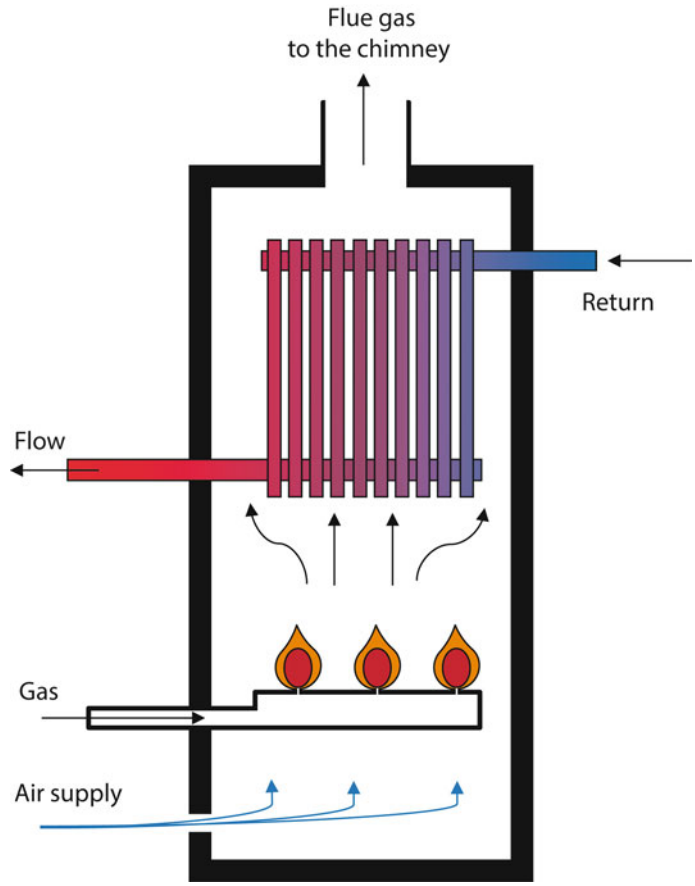



**Fig. 8.75** Design and operation of a low-temperature boiler [83]



These heating and cooling applications can also be powered by stored renewable gas. Like electric heat-pumps and solar-thermal energy facilities, they can then contribute to decarbonizing the heating sector. In this way, they also function as discharge-technologies for renewable gas.

### 8.5.2.1 Gas Heating

Low-temperature boilers (heating boilers) and condensing boilers are currently the most common gas heating systems.

#### ▪ Low-Temperature Boilers

Low-temperature boilers are improved standard boilers that can adjust their flow temperatures to a reference variable such as, for example, the outdoor temperature. By maintaining lower temperatures, compared to standard boilers they have lower stand-by losses, i.e., lower heat losses from the pipeline to the ambient air. Because the flow-temperature is lower, they can also be used to supply larger radiators or surface heating in walls and floors.

Figure 8.75 shows the general design of a low-temperature boiler [21, 83]. The gas enters the boiler at supply pressure and mixes with the air. The gas is then combusted when the pilot flame is ignited by an ignition spark. The exhaust is passed through a heat exchanger, transferring the heat to the heating water and hot-water supply water. Finally, the cooled exhaust is released through a chimney.

#### ▪ Condensing Boilers

In addition to the net calorific value (NCV), condensing boilers also exploit the GCV of the

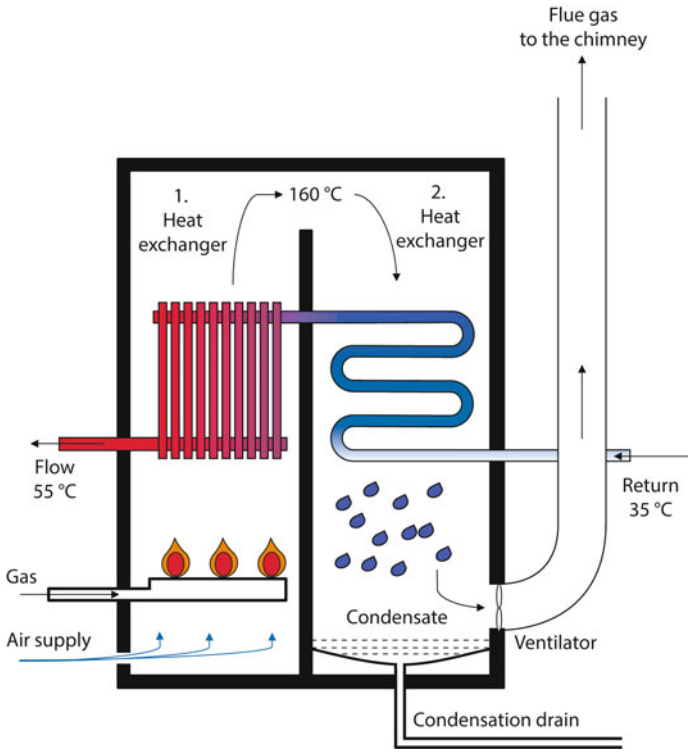



**Fig. 8.76** Design and operation of a condensing boiler [83]

gas to achieve even higher efficiency. These facilities can achieve a 107% thermal efficiency in relation to the NCV.

Condensing boilers are designed like low-temperature boilers, except a second heat exchanger is used to condense the exhaust. In normal facilities, this condensation heat is released unused into the environment through the chimney. It can be used instead to increase the temperature of the heater return flow (Fig. 8.76). Condensing boilers are best-suited for heating systems with low heater return flow-temperatures.

Compared to low-temperature boilers, these boilers achieve a better energy yield by exploiting the condensation heat, which ranges from 5 to 9%. Since the boilers have a lower surface temperature, and as a result, radiate less heat, losses are also reduced by 1%. In addition, exhaust losses are reduced by up to 8%. In total, this increases the efficiency by 14 to 18% in comparison with conventional gas heating [21, 83].

The water produced requires two additional pieces of equipment. First, a drain for the average 1.0 to 1.5 liters of condensation produced per $m^3$ of natural gas. Second, the $CO_2$ in the exhaust reacts with the condensation water to produce carbonic acid ($H_2CO_3$). In small facilities, this is not an issue. But in larger facilities, a neutralization unit is required to prevent wastewater and ground water contamination.

### 8.5.2.2 Gas Heat Pumps

Heat pumps are typically assumed to be electric heat-pumps, i.e., heat pumps powered by electricity. But heat pumps can also be powered by gas. These pumps are called gas heat pumps. Gas heat pumps can be heat pumps driven by gas engines, absorption heat pumps, or recently developed adsorption heat pumps (also called zeolite heating appliances) [12].

#### ▪ Heat Pump Efficiency

The temperature of the heat source (ambient heat) and the flow-temperature on the heat-

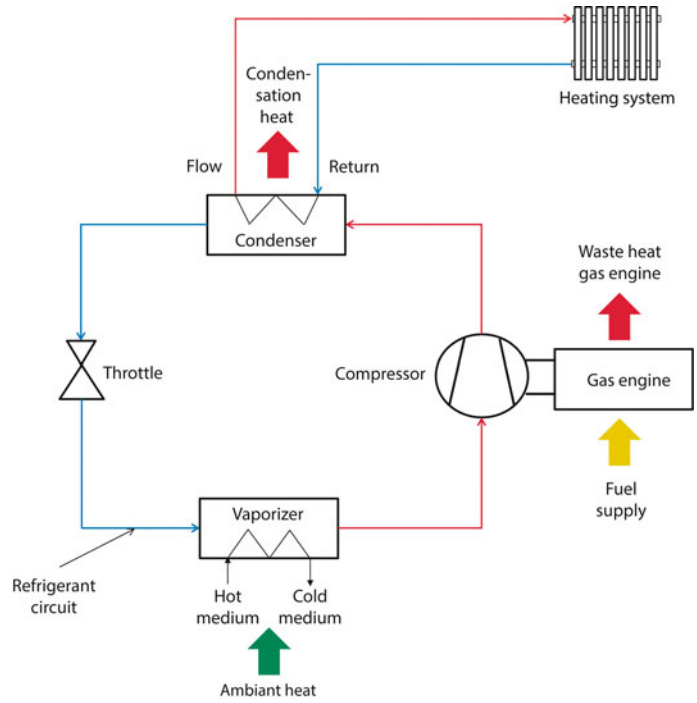



**Fig. 8.77** Design and function of a gas-powered heat pump [12]



ing side are decisive in determining heat pump efficiency. The smaller the difference between these two temperatures, the less energy the compressor consumes, thus balancing the difference.

The coefficient of performance $\varepsilon_{HP}$ is required to calculate heat pump efficiency. A heat pump's coefficient of performance is determined by the ratio of the heating capacity produced by the heat pump $\dot{Q}_{use}$ and the heat pump's consumption of power in the form of electrical power or combusted chemical power $P_{in,gas}$. The smaller the temperature-difference between the heat source and the heating, the higher the coefficient of performance. With gas heat pumps, the following relationship applies:

$$\varepsilon_{HP} = COP = \frac{\dot{Q}_{use}}{P_{in,gas}}. \qquad (8.129)$$

By this definition, a heat pump's efficiency may be a value larger than one. For example, if the coefficient of performance is 3.5, then 3.5 times the power supplied by the gas engine is converted into usable heating capacity.

Another important variable is the annual performance factor, or seasonal coefficient of performance (SCOP) (Eq. 8.130). This factor is used to estimate the heat pump's economic efficiency. To determine its value, heat pump operation must be observed over a long period of time, ideally for a year. The annual performance factor is defined by the ratio between the quantity of heat produced $Q_{HP}$ and the energy consumed $W_{el}$ of $W_{chem}$ per year. The energy consumed includes fuel as well as auxiliary energy for pumps, control, and other elements.

$$SCOP = \frac{Q_{HP}}{W_{el/chem}}. \qquad (8.130)$$

### ■ Gas-Powered Heat Pumps

Gas-powered heat pumps operate like electric heat-pumps, except the compressor is powered by a gas engine instead of an electric motor. An advantage of this technology is that waste heat from the engine can be fed into the heating circuit.

Figure 8.77 illustrates the design and function of a gas-powered heat pump. Depending

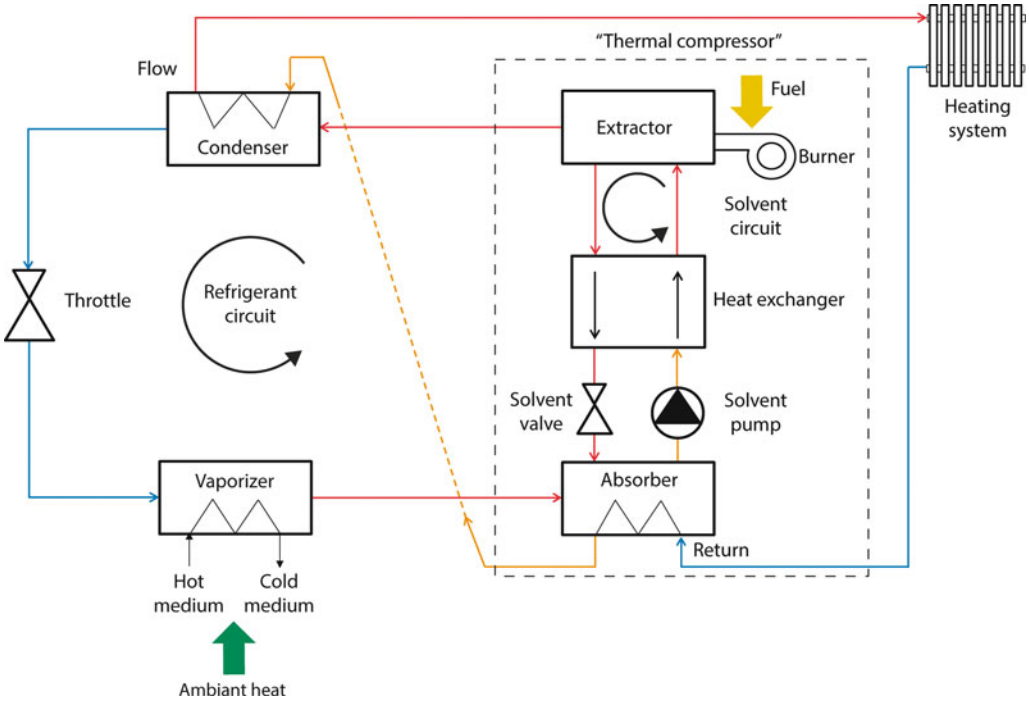



**Fig. 8.78** Design and operation of an absorption heat pump [12]

on the operating method, ambient heat is extracted from the ground, from the ground water, or from the outside air. The vaporizer functions like a heat exchanger. It uses the extracted ambient heat to change a circulating coolant into the gaseous phase. The gas is then compressed in a compressor, increasing the temperature of the coolant. Finally, the compressed gas is cooled and liquefied in a second heat exchanger; the condenser. The heat exchanger also transfers the energy released by condensation (condensation heat) to the water in the heating circuit. The pressurized liquid coolant is decompressed in an expansion valve (throttle) so it can be fed back into the vaporizer, closing the circuit [12, 21].

### ■ Absorption Heat Pumps Using Gas

Unlike gas-powered heat pumps, absorption heat pumps use a thermal condenser instead of a compressor [12, 21]. A thermal condenser includes an absorber, a solvent pump, a heat exchanger, an extractor, and a burner fired by gas (Fig. 8.78).

After leaving the vaporizer, the gaseous coolant (for example lithium bromide) is absorbed in a solvent (typically water) in the absorber. The absorption capacity of the solvent increases together with the pressure, but falls together with the temperature. The same effect can be observed with mineral water. Gaseous $CO_2$ is absorbed in water. Since the pressure drops when the bottle is opened, a portion of the dissolved gas escapes.

In the absorber, heat is produced by absorption and by condensation of the solvent returning from the extractor. The heat is absorbed by the hot water, raising the temperature of the water at the condenser inlet. The solvent is pressurized by the pump, and then heated in the heat exchanger by the solvent return.

In the extractor, the enriched solvent is heated further by the gas burner, expelling the absorbed coolant. In the heat exchanger and solution valve, the coolant is decompressed again

to absorber pressure and then fed back into the absorber.

Next the coolant is fed into the condenser where it is condensed, releasing condensation heat into the heating cycle. The coolant is then fed back into the vaporizer through an expansion valve, and the cycle starts again from the beginning.

All components are powered by thermal energy except the solvent pump. But the pump-power is low in comparison to the power of the thermal compressor.

### ■ Adsorption Heat Pumps

Like absorption heat pumps, adsorption heat pumps use a coolant and heat exchangers. Energy is added by burning gas with thermal energy instead of mechanical energy, as is the case in electric engine or gas engine heat pumps [12]. Adsorption heat pump technology has been relatively recently developed, and can use the following media:

| | |
|---|---|
| Fuel: | gas |
| Low-temperature heat: | solar or ambient heat |
| Sorbent for adsorption of the coolant: | zeolite |
| Coolant: | water (steam) |

Adsorption heat pumps work on the same principle as all other heat pumps. In the first step, the coolant (for example, water) is vaporized in the vaporizer. In the process, it absorbs low-calorific heat supplied by the environment or a solar collector. But instead of using a compressor to produce the low pressures required, this pressure is produced by adsorption (accumulation) of the water vapor on zeolite.

Zeolite is a non-toxic, non-flammable, and ecologically harmless mineral such as crystalline silicate which has a very large surface-area, even in a very confined space. As a result, it can absorb large quantities of water vapor (see thermochemical-energy storage in ▶ Sect. 10.6). The heat produced by adsorption on the zeolite block is collected and used for heating purposes. This phase lasts until the zeolite block is saturated.

In the second step of desorption, the water vapor stored on the zeolite block is expelled by applying heat. The heat required is produced by burning gas, and supplied by the same heat exchanger that previously collected the useful heat from the block in the first adsorption step. The water vapor condenses on the heat exchanger in the condenser (which functioned as the vaporizer in the first step). The condensation heat can then again be used for heating purposes. The water can also then be used again for adsorption, and the process starts again from the beginning.

Since low-temperature levels of 3 °C or above are adequate, a solar facility or ambient heat can supply the activation energy for adsorption.

But the activation energy for desorption requires temperatures of around 120 °C. A gas-fired condensing boiler can be used for this purpose. The water circulates at pressures ranging from 5 mbar and 200 mbar to minimize the evaporation and condensation of energy.

Zeolite gas adsorption heat pumps can be used wherever conventional heat pumps are used. This technology developed relatively recently and has a very simple design. Unlike in compression heat pumps, no small moving parts are required. Besides the heat exchanger or vaporizer and condenser, only pumps for the coolant (that transport the heat at the same time) are required.

But this type of heat pump is, in principle, simply an improved gas-fired condensing boiler technology. Manufacturer specifications indicate that with these heat pumps, 80% of the heat produced for heating or hot water is still produced by burning gas, and only 20% from ambient or solar energy.

**Definition**

Absorption vs. adsorption: *ab*sorption forces a material *into* a liquid or solid. *Ad*sorption *accumulates* gases or liquids onto the surface (boundary layer between the two phases) of a solid. A 'sorption

heat pump' is used for both technologies: absorption and adsorption heat pumps.

### 8.5.2.3 Sorption Refrigeration Machines

Since heat pumps function on the same principle (left running cycle process) as a refrigerator, sorption heat pumps can also be designed as sorption refrigeration machines. The process is the same as described in ▶ Sect. 8.5.2.2.

But the purpose is different. Heat pumps supply as much heat as possible. Refrigeration machines are designed to absorb as much low-temperature heat as possible to provide cooling on-site.

Cooling is 'produced' in the vaporizer, where a coolant (for example, water) is vaporized at a low pressure. The cold produced by the vaporizer's heat exchanger can then be transported by a suitable coolant (for example, water) to where cooling is required [12].

Indicated by $\varepsilon_{RM}$, the facility's efficiency is larger than one and defined by Eq. 8.131 as the benefit (extracted heat capacity $\dot{Q}_{out}$) over the consumption (supplied capacity $P_{in,gas}$):

$$\varepsilon_{RM} = \frac{\dot{Q}_{out}}{P_{in,gas}}. \qquad (8.131)$$

## 8.5.3 Mobility and Transport

Combustion engines are the 'discharging technologies' for chemical-energy storage in the transportation sector. Despite continuous improvements, for decades, the operating principle has remained the same. Conventional engines can run on gas from PtG, biogas, or fuels from PtL or biofuels. The following sections briefly describe the (currently) most common combustion engines.

Fuel cells also function as discharging technologies for the transport sector when the electricity they produce is used by electric drive engines. The use of this technology to generate electricity is explained in detail in ▶ Sect. 8.5.1.1.

### 8.5.3.1 Gasoline Engines and the Four-Stroke Principle

Besides gasoline, gasoline engines can also use methane, ethanol, or hydrogen for fuel. This means that this conventional technology can be used as a discharging technology for renewable gas, and for synthetic fuels in general.

Conventional gas engines operate on the four-stroke principle. ◘ Figure 8.79 illustrates the process in simplified form [72]. Four-stroke engines are also called Otto cycle engines after their inventor, the German engineer, Nicolaus August Otto.

- **First-Stroke: Intake**

During intake, the outlet valve is closed and the inlet valve is open. The piston travels down, drawing air or a gas mixture in. In carburetor engines, the gas mixture composed of fuel and air is drawn into the carburetor earlier. In standard modern gasoline engines with direct injection, in the first-stroke only air is drawn in and the fuel directly injected. The air flow is monitored and fuel supplied at the air-fuel ratio $\lambda = 1$. This means that the amount of air in the mixture is precisely the amount theoretically required for combustion. Depending on operating conditions, the mass of the gas mixture intake or air intake can be regulated by a throttle valve. When the piston has traveled to its lowest point, the inlet valve closes. The second-stroke follows.

- **Second-Stroke: Compression and Ignition**

The piston travels up, compressing the gas mixture. The kinetic energy required is supplied by the rotational movement of the piston driven by flywheel energy storage on the piston itself, or on the other pistons on the same motor shaft. During compression, both the inlet and outlet valves are closed. Compression causes the temperature to rise to around 400 to 500 °C, vaporizing most of the fuel particles. Shortly before the end of the second-stroke, the compressed gas mixture is ignited by a spark.

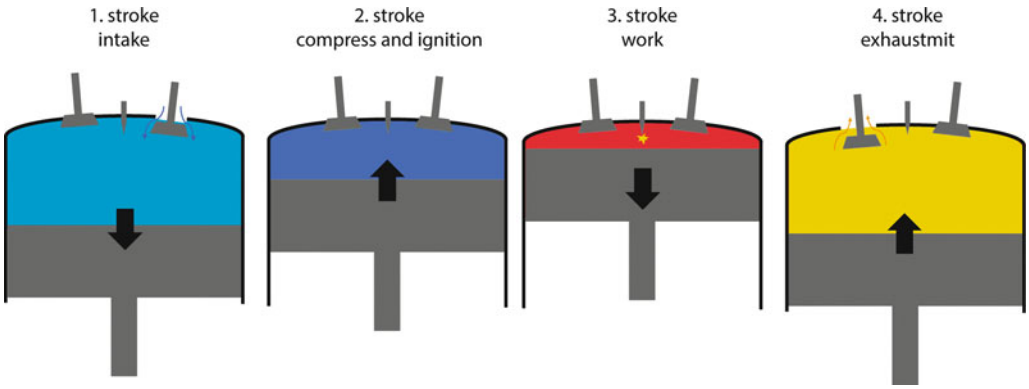



**Fig. 8.79** Four-cycle gasoline engine operation



#### Third-Stroke: Work

In the power-stroke, after the piston starts to descend again the gas mixture spontaneously combusts, reaching temperatures over 2,000 °C and pressures up to 120 bar. The materials used, therefore, must be strong enough to withstand these conditions. The piston is driven down to its lowest position, performing mechanical work. The combusted gas cools, and the pressure falls to a few bar. At the end of the third-stroke, the outlet valve opens.

#### Fourth-Stroke: Exhaust

During exhaust, the piston, driven by the flywheel on the piston itself or on the other pistons on the same motor shaft, travels back up. This forces the exhaust out through the outlet valve. The cycle then starts again from the beginning.

### 8.5.3.2 Diesel Engines

As with two or four-cycle engines, there are a variety of diesel engine designs. Most are four-cycle engines used primarily in motor vehicles, locomotives, ships, heavy-duty machines, or diesel generators. The diesel engine was invented in 1893 by Rudolf Diesel. His goal was to achieve the thermodynamic optimum in a thermal engine using local fuels such as vegetable oil.

When constantly operated at rated power, the most efficient design is the two-stroke diesel engine. This engine is used in ships or power plants. The four-stroke engine is better-suited for frequent load alterations.

Diesel engines also operate on the four-stroke principle illustrated in Fig. 8.79 [72]. But the ignition process and operating parameters differ from gasoline engines. In a diesel engine, there is no external ignition of the gas mixture. Instead, the mixture spontaneously combusts. Only air (or a mixture of air and exhaust in newer designs) enters during intake, and is then compressed. During compression, the temperature of the air increases to around 700 to 1,000 °C. Just before the piston reaches its highest point (end of the second-stroke), fuel is injected into the diesel engine in preparation for the third-stroke (power). Since the temperature of the compressed air exceeds the ignition temperature of diesel, after a short ignition delay the fuel spontaneously combusts. This means that injection, mixture, and combustion are partially simultaneous. In the third-stroke during fuel combustion, the temperature ranges from 1,500 to 2,500 °C and the pressure reaches up to 150 bar.

In gasoline engines, air intake and fuel supply are regulated by a throttle valve. Diesel engines are regulated for quality instead, meaning the fuel quantity injected depends on the engine performance requirements. Diesel engines are more efficient than gasoline engines because the compression is higher, and because throttle losses under partial-loads are elimi-

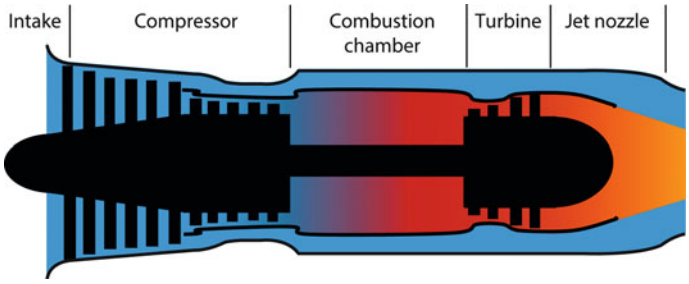



**Fig. 8.80** Design and operation of a jet engine together with the temperatures in the individual components

nated. As a result, fuel consumption is lower. The air-fuel ratio $\lambda$ ranges from 1.1 to 10.

#### 8.5.3.3 Turbines and Jet Engines

Unlike on land where power is applied to the road surface using friction to move the vehicle forward, in the air, forward momentum is achieved by accelerating air in the opposite direction of travel. In aviation, jet engines are used for this purpose [14]. Here, forward momentum is created by thermally accelerating ambient air. The air is drawn into the engine, mixed with fuel, and combusted. It then becomes a propulsion jet that collides with air at a lower speed, producing thrust power.

There are many kinds of jet engines. These include gas turbines, ramjets, combined gas turbine and jet engines, pulsejet engines, and turbo rocket engines. All are based on Newton's third law, *action = reaction*.

A simple design common today is the turbo-jet engine. This engine has an intake, a compressor, a combustion chamber, a turbine, and a jet nozzle (Fig. 8.80). The compressor, combustion chamber, and turbine are the core components of a jet engine, and are together referred to as the gas generator. These engines offer the advantages of moderate efficiency and low noise levels even at lower speeds.

Ambient air is drawn into the gas turbine through the intake and then compressed in the compressor. Unlike in rocket engines, the oxygen required for combustion comes from the air. As a result, this type of turbine engine is called an 'air-breathing' engine.

The compressed air is mixed with fuel in the combustion chamber and the gas mixture combusted. The hot gas expands in the turbine, releasing a large amount of its energy. The turbine powers the compressor as well as peripherals such as a generator for the on-board power supply. Most of the energy released by the fuel is used for these purposes. The energy remaining is used to produce thrust. The combusted gas mixture expands further in the jet nozzle until it is at about ambient pressure. The expanding gas produces a flow velocity of 600 to 900 m/s or higher in the jet nozzle. To increase performance, an afterburner can be installed after the turbine to additionally heat and accelerate the gas. This increases thrust by 30 to 70%, but also increases fuel consumption by 80 to 120%. As a result, afterburners are not used in commercial aviation [70].

Today, jet engines are fueled almost exclusively by kerosene (Jet-A1). Biofuels and synthetic fuels could also be used in jet engines. But switching fuels requires building an international consensus, because planes fly over long distances and infrastructure components must be standardized across the globe. Although vegetable fuels and BTL are suitable fuels for aviation and have also been tested, their potential here is limited [127]. As a result, synthetic fuels from potentially unlimited sources such as wind energy, solar energy, and hydropower using PtL should be the focus for aviation in the future (▶ Sect. 8.7).

## 8.6 The Storage System PtG

At this point, previously described elements shall be combined to form a complete stor-

age system, which consists of storing technology (see ▶ Sects. 8.2 and 8.3), storage medium (▶ Sect. 8.4), and extraction technology (▶ Sect. 8.5). The storage system PtG (electricity to gas) is presented in the following section.

For gaseous energy sources, focus is mainly on storage systems based on PtG, because they offer the greatest potential. This potential is based on their capability of using existing infrastructure and substituting conventional energy sources in the transport, power, and heat sector.

In general, two PtG concepts have to be differentiated based on the characteristics of their energy sources: hydrogen ($H_2$) and methane ($CH_4$). Their deployment, as well as the extraction technologies used, make the main difference. In addition, there is the optional methanation stage. In the following, basic concepts of PtG are explained. The specific application for decarbonization and some projects are presented in ▶ Chaps. 13 and 14.



### 8.6.1 The Beginnings of PtG

#### ▪ Energy Storage Demand in Dynamic Simulations—Hydrogen and Biomass

In the course of expansion of renewable energies in Germany—mostly wind and PVs—calls for energy storage grew ever louder since the early 2000s.

While considering the annual balance sheet has been sufficient for a long time, which is based on only one value for wind and solar power generation, dynamic simulations of a power system containing a large percentage of renewable energies (▶ Chap. 3) have detected and revealed a large storage and balance demand. This demand could not be supplied by conventional German storage technologies, such as pumped-hydro, battery power plants, or compressed air storage (CAS). Caverns exclusively for hydrogen storage have been considered as the sole solution [89, 121]. Since there is no infrastructure for hydrogen and a very limited potential for hydropower buildout, purely renewable energy systems depend on bioenergy as balancing energy.

#### ▪ The Combined Power Station at the ISET Kassel—Now Fraunhofer IWES

In the 1990s, Enßin, Füller, Hahn, Rohrig, and their colleagues at the institute for solar energy supply technology (ISET) in Kassel built a database for feed-in from wind turbines as part of the 250-MW-measuring program. Since the early 2000s, this data has been used for wind forecasts and the construction of a virtual power plant in the form of a wind turbine cluster [30–32]. The project, called the 'Combined Power Station' (◘ Fig. 8.81) resulted from their work and was able to prove that, at any point of time, power supply based on 100% renewable energies was possible in Germany at a scale of 1 to 10,000, measured at the necessary energy supply and demand. To achieve this goal, wind turbines of Enercon GmbH, PV plants of Solarworld AG, and biogas plants of Schmack Biogas GmbH were combined and controlled in real time according to German load profile. Only power storage was simulated as the pump-storage plant Goldisthal. In this way, it was possible to rebut presumptions that purely renewable power systems were not able to provide a stable power supply [68].

Reinhard Mackensen's analyses showed that the expansion of renewable energies to its full extent would mainly be based on wind power and PVs, and thus would require major balancing measures in the form of storage capacities or stored biomass. It is not possible to provide these balancing measures by expanding pump-storage plants, nor can enough biomass be produced on the available areas [68, 69]. The core problem was to realistically upscale installed biomass and storage capacity by a factor of 10,000. One approach of the ISET was to interconnect the power and gas sector, and thus be able to store wind and solar energy in the form of hydrogen in the natural gas grid. It would then be possible to flexibly reconvert it into electricity via gas turbines and cogeneration plants [127].

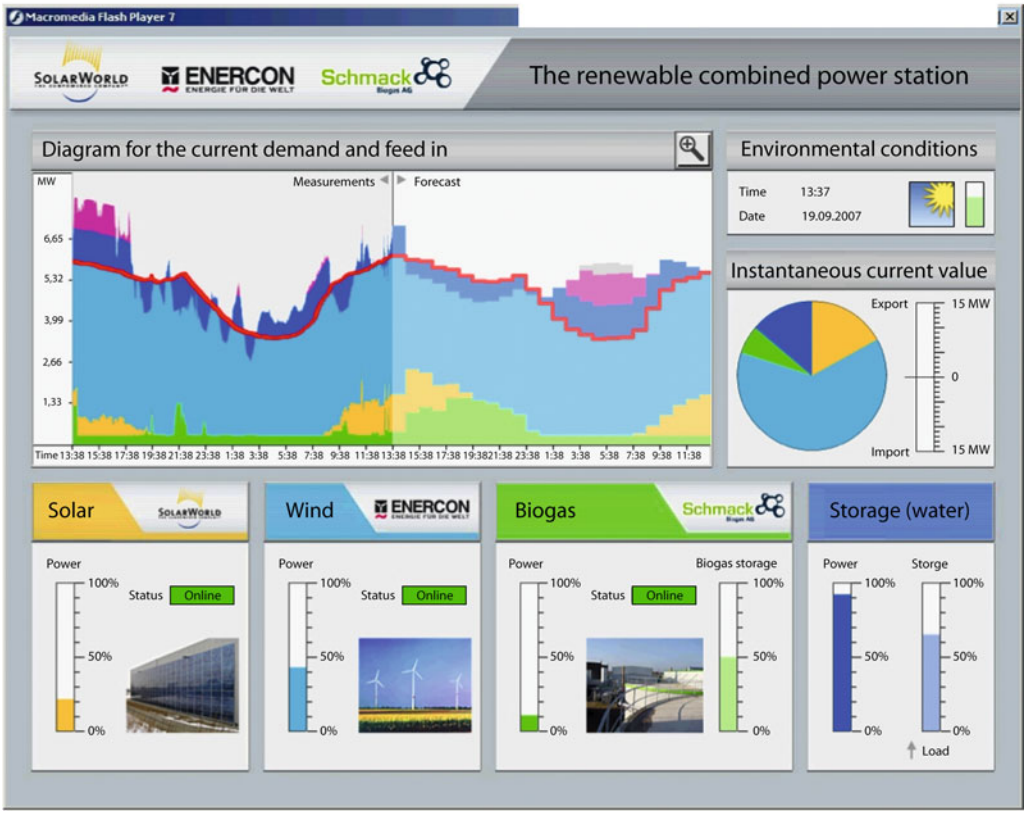



**Fig. 8.81** Combined power station at the ISET (source: Mackensen, ISET)

### Methanol Production from $CO_2$ and Biomass Gasification at the ZSW Stuttgart

In the 1990s, Andreas Bandi, Thomas Weimer, Michael Specht, and their colleagues at the Center for Solar Energy and Hydrogen Research (ZSW) in Stuttgart developed a synthesis to produce methanol from atmospheric $CO_2$ and solar energy. A small-scale pilot plant was set up, which extracted $CO_2$ from the air by means of adsorption and electro dialysis. It then chemically reacts $CO_2$ to methanol using hydrogen from solar powered electrolysis. Following this, the technical feasibility of $CO_2$-recycling to produce methanol was successfully proven [5, 97, 98, 128]. In the 2000s, research at the ZSW concerning hydrogen and chemical energy sources focused on biomass gasification. They developed a process of their own (the absorption enhanced reforming process) to produce a hydrogen-rich gas from biomass via two coupled fluidized bed reactors [99, 102, 128].

### The First Coupled Power and Gas Grid in the WBGU-Bioenergy Report

By the middle of the 2000s, the potential, as well as its limitations, of biomass became clear. The increase in food prices in 2008 got the 'food-versus-fuel debate' going and brought up the question of to which degree biomass can and should be energetically used [33, 88]. The WBGU-Bioenergy Report shows that, while bioenergy is very well-suited to balance fluctuating wind and solar energy, the necessary sustainable potential is not available. Both authors, Jürgen Schmid and Michael Sterner of the ISET Kassel, came to the conclusion that, because of its scarcity, bioenergy is best integrated into the existing natural gas grid via fermentation, gasi-

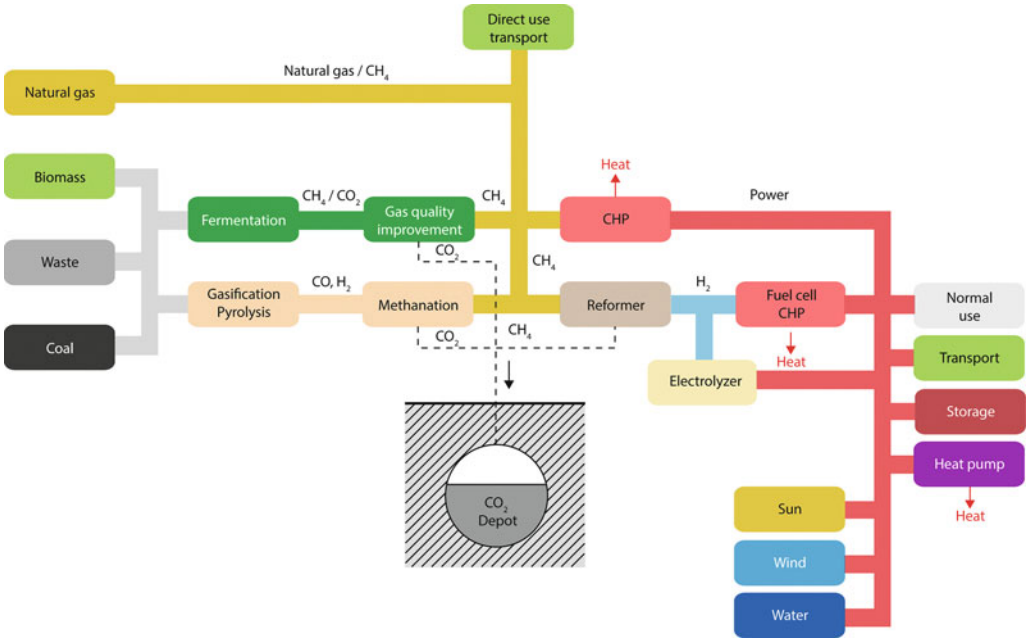



**Fig. 8.82** Coupling of electricity and gas system via electrolysis in the WBGU Report on bioenergy [127]

fication, and methanation [111, 127]. In this way, existing transport and storage capacities can be used, and thus provide energy to all sectors via power plants, cogeneration plants, gas cars, and gas heating. In addition, it is possible, on the one hand, to separate $CO_2$ and establish an actual $CO_2$ sink, and on the other hand, to integrate fossil coal, which will last a long time, in a climate-friendly way.

In the end, this integrated energy system consisted of an electricity and a gas system, which were coupled via gas power stations and cogeneration plants on the one hand, and an electrolyzer which produced hydrogen for fuel cells, on the other (Fig. 8.82). Schmid and Sterner presented this system along with the combined power station at the 16th European Biomass conference [92, 110]. Michael Specht and his colleagues from the ZWS Stuttgart presented their paper on chemical energy conversion of biomass [5]. Having the accordant background, he produced the idea of improving the possibility of integration of hydrogen into the natural gas grid by using the Sabatier reaction. As shown in Fig. 8.82, the syngas $CO_2$ from coal and biomass is used for methanation.

## Patent, Studies, and Projects Concerning PtG

At this point, both institute's preliminary work was merged together and the PtG concept was elaborated on. In 2009, this lead to a patent application [101] and a doctoral thesis on PtG, which made the concept of chemically storing energy from wind and solar plants well-known and put it into context with energy transition [107]. As another consequence, the first PtG plant for methanation of $CO_2$ in Germany was developed in Stuttgart by order of Waldstein, the founder of SolarFuel GmbH [34, 100].

In addition, different pilot projects were launched. While studies were carried out for E-On, Greenpeace Energy, and Audi AG in Kassel, hardware was refined in Stuttgart. Both activities paved the way for the realization of pilot projects and the publication of the new concept (see ▶ Sects. 14.3 and [108]).

In energy economy, this concept was made well-known by a number of associations (▶ Chap. 3): the research papers by the Fraunhofer IWES (formerly ISET), on which the Long-Term Scenario of the Federal Environment Ministry (BMU) is based [79], the

report published by the German Advisory Council on the Environment (SRU, [103]), the Federal Environment Agency's 'UBA Energy Goals 2050' [118] and the VDE ETG Storage Study [122]. So far, the greatest PtG project has been realized by Audi AG and fuels 1,500 vehicles with $CO_2$-neutral gas (▶ Sect. 14.3).

## 8.6.2 PtG Hydrogen

The storage system, PtG hydrogen (PtG-$H_2$), uses electricity surplus from renewable energies (▶ Chap. 3) to produce hydrogen. Hydrogen can potentially be used in several different ways, e.g., as an admixture in the natural gas grid or it can be used energetically at a different point of time and place if filled in a compressed hydrogen tube trailer. The following stages are experienced:

- Storing:
  Storing technologies (▶ Sect. 8.2):
  - AEL
  - Proton exchange membrane electrolysis (PEMEL)
  - HTES
- Storage:
  Storage media (▶ Sect. 8.4):
  - Gas grid
  - Cavern storage
  - Gas and oil deposits
  - Aboveground storage
- Extraction:
  Extraction technologies (▶ Sect. 8.5):
  - Fuel cell
  - Gas turbine, combined cycle plant, cogeneration plant
  - Gas heating, gas hat pump, refrigeration machines
  - Fuel cell vehicles (FCV), rocket propulsion
  - Material use

### ■ Possible Plant Concepts

High-quality natural gas in Germany is composed of 96% by volume methane, 1 vol% $CO_2$, 2 vol% nitrogen ($N_2$), and 1 vol% hydrocarbons such as propane and butane [49]. According to the DVGW (German Technical and Scientific Association for Gas and Water) the admixture of 1.5% hydrogen is possible. Higher blending quotas cause research needs and adjustment requirements for certain applications, such as gas turbines, porous storage, or natural gas tanks in vehicles, which are limited to 0–4%. For this reason, PtG hydrogen storage systems differ in regard to the way hydrogen is used after electrolysis.

In this book, the use of hydrogen is distinguished between material (1) and energetic. Furthermore, energetic use can be divided into use in an infrastructure exclusively for hydrogen (2) and use in pre-existing gas infrastructure (3). There is a clear presentation of how hydrogen can be used in ◘ Fig. 8.83.

### 8.6.2.1 Material Use

In this section, options for use of hydrogen described in ▶ Sect. 8.1.2 are completed by the description of a PtG hydrogen storage system with the objective of material use.

An industrial plant or a refinery with a great need for hydrogen can be attached directly to a PtG-$H_2$ plant (◘ Fig. 8.84). Since most industrial applications need constant supply, the system includes a hydrogen tank as a buffer. Hence, requirements for PtG-$H_2$ systems are a location with great availability of renewable energy sources and a suitable consumer of $H_2$.

In addition, the integration of green hydrogen into petroleum refineries is shown in ▶ Sect. 13.3.2.

**Example**

There is great climate protection potential in the reduction of iron through the application of the direct reduction process (DRP) rather than the $CO_2$-intensive blast furnace process. The DRP uses hydrogen to withdraw oxygen from the ore ($Fe_2O_3$). Pig iron and water are results of this reaction. Another advantage of the DRP is the content of less than 1% carbon in the pig iron. After the blast furnace process, up to several percent carbon have to be removed in order to meet DIN (German Institute for Standardization)

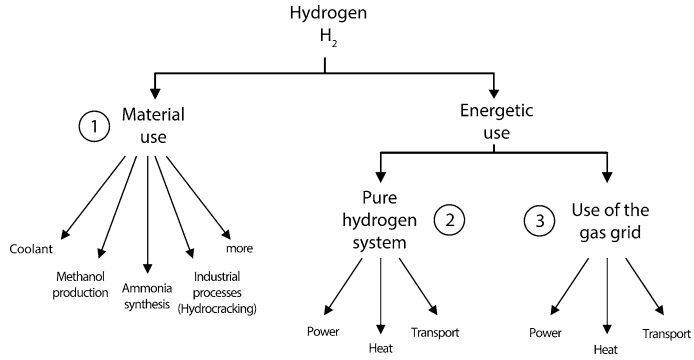



**Fig. 8.83** Overview of the possible uses of hydrogen

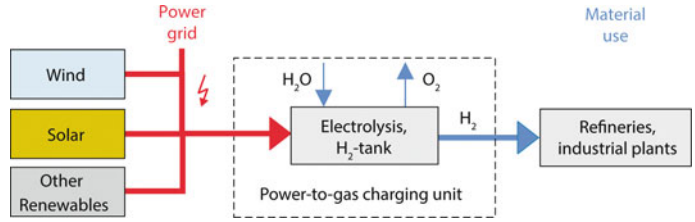



**Fig. 8.84** Schematic representation of a PtG system for material use of hydrogen

norms, according to which pig iron, the starting product for steel, has to contain less than 2% carbon.

### 8.6.2.2 Energetic Use via Hydrogen Infrastructure

When, in the future, a hydrogen economy has been established, it will be possible to use hydrogen directly in a hydrogen-only system (Fig. 8.85). Regions with already-existing suitable hydrogen storage and lines are eligible starting points as well as regions with a high density of consumers in chemistry parks. This is researched in the course of the BMBF project 'HYPOS' for eastern Germany, which examines wind-PV-hydrogen hybrid parks and hydrogen test fields, including Germany's first hydrogen storage [55]. Storage options for short-term storage are, along with hydrogen lines, aboveground $H_2$ tanks. Long-term storage can be realized in gas caverns. Porous storage is not suitable for hydrogen storage because of microbiological hydrogen sulfide emergence, which results in corrosion (▶ Sect. 8.4.1.4).

In times of deficits due to fluctuating renewable energies, this system reconverts hydrogen to electricity via specially adapted gas turbines or fuel cells, and thus acts as electricity storage. In this case, an independent hydrogen infrastructure provides seasonal balance for times of both low winds and sunshine hours.

In addition, hydrogen can be used in the field of heat supply or for transport when sold at hydrogen stations.

Realization is obstructed by high costs for the expansion of an independent hydrogen infrastructure and high prices for hydrogen extraction technologies, such as FCV, fuel cell cogeneration plants, and reconversion units.

Integration of hydrogen into $H_2$ mobility, including transport and distribution infrastructure, is additionally shown in ▶ Sect. 13.3.2.

### 8.6.2.3 Energetic Use via Admixture to Natural Gas and Use of Existing Gas Infrastructure

From today's point of view, an independent hydrogen infrastructure is only financially reasonable in some regions with a great demand for hydrogen, and for industrial consumers, and suitable existing storage facilities such as cavern storage.

Matters are different when hydrogen is added to natural gas using the existing gas in-

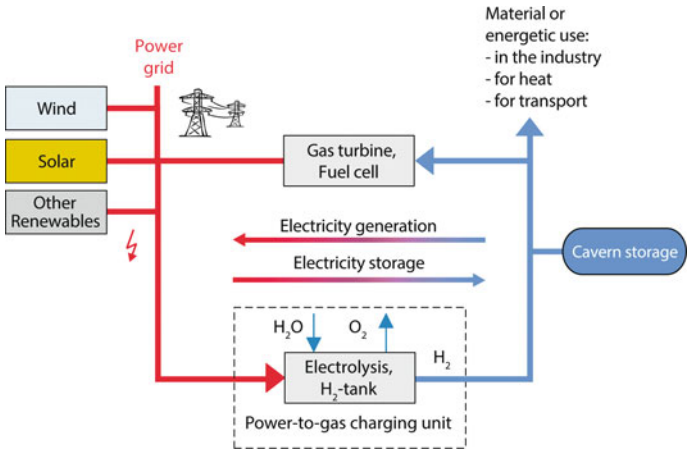



**Fig. 8.85** Energetic use of hydrogen in a hydrogen-only infrastructure

frastructure. The gas grid is expanded over all of Germany and there are high-capacity cross-border interconnections. Furthermore, state-of-the-art consumers, which only need slight adaptions to higher hydrogen percentages, can be used in all energy sectors. These pre-existing technologies make development of new ones redundant.

The challenge here is hydrogen tolerance of specific components (Fig. 8.95). In this field, there are research needs and adjustment requirements to increase the technically possible blending quota of 1–2% by volume (see [49] and ▶ Sect. 8.6.5.1).

In a PtG hydrogen storage system, surplus electricity is used for water splitting in an electrolyzer (Fig. 8.86). In order to prepare hydrogen produced in this manner for feed-in to the gas infrastructure, it is fed to a gas storing unit, including a compressor. In consideration of hydrogen tolerances shown in Fig. 8.95, from that point on, usage is possible in all kinds of ways: reconversion to electricity, heat, transport or material use.

When used for seasonal balancing, the mixture of hydrogen and natural gas can be stored in all gas storages up to a blending quota of 1% hydrogen (other than pure hydrogen). Along with salt cavities, porous storage is an option. Buffering on a short-term scale is possible in aboveground gas storages. Furthermore, the gas mixture can be brought to all consumers in households, businesses, and industries via the gas grid. Among others, possible applications are gas engines, condensing gas boilers, gas heat pumps, gas stoves, gas tools, gas-based materials, or reconversion to electricity for peak-load supply.

### 8.6.3 PtG Methane

In addition to electrolysis, there is another storing technology, methanation, in the PtG methane (PtG-$CH_4$) storage system (▶ Sect. 8.3). Hydrogen and carbon dioxide ($CO_2$) are reacted biologically or chemically to methane ($CH_4$) and water ($H_2O$) [107].

The main advantages of this system are easier compressibility, storage, transport, and usage due to higher-energy density of methane. Disadvantages result from the additional procedural step, which needs $CO_2$, causes waste heat, and therefore reduces efficiency of the overall process. Among others, intelligent heat concepts can compensate for this disadvantage by using waste heat for vaporization in HTES (see ▶ Sects. 8.2.6 and 8.6.4).

A PtG-$CH_4$ system can be composed of the following components:

- Storing:
  Storing technologies (▶ Sect. 8.2):
  - Electrolysis
    – AEL

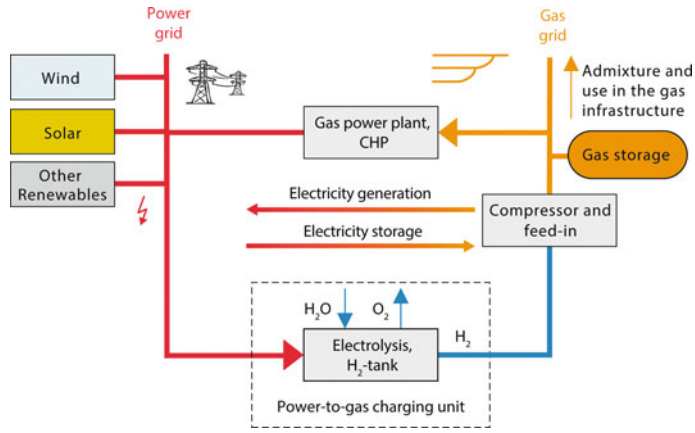



**Fig. 8.86** Schematic representation of hydrogen use in the existing gas infrastructure

- Proton exchange membrane electrolysis (PEMEL)
- HTES

- Methanation (▶ Sect. 8.3):
  - Chemical Methanation
  - Biological Methanation

- Storage:
  Storage media (▶ Sect. 8.4):
  - Gas grid
  - Cavern storage
  - Gas and oil deposits
  - Aboveground storage
- Extraction:
  Extraction technologies (▶ Sect. 8.5):
  - Fuel cell
  - Gas turbine, combined cycle plant, cogeneration plant
  - Gas heating, gas hat pump, refrigeration machines
  - Gas vehicles, ships, airplanes
  - Material use

### ■ Possible Plant Concepts

In the field of PtG-$CH_4$, there are different concept categories which are all based on the concept shown in Fig. 8.87 [107].

Bidirectional interconnection of power and gas grids in order to store renewable energies is the general idea of PtG (▶ Sect. 8.6.1). Electricity-surpluses power water splitting. In the process of methanation, the produced hydrogen and $CO_2$ are reacted to methane. This requires one of several different possible sources of $CO_2$, such as carbon capture and storage (CCS), biogas plants, sewage plants, atmospheric $CO_2$, industrial processes, or conventional power plants. Renewable methane can be temporarily stored in gas storage or fed into the gas grid. Once there, it can be reconverted to electricity via gas turbines, cogeneration plants, etc., or be used in the heat and transport sector.

What differs between each concept are the $CO_2$ sources and how they are integrated into the process of methanation.

#### 8.6.3.1 Atmospheric $CO_2$

Methane produced with atmospheric $CO_2$ and renewable electricity is $CO_2$-neutral (Fig. 8.88). It is possible to decrease the content of $CO_2$ in the atmosphere by connecting the combustion process with a CCS system.

There are different ways to extract $CO_2$ from the air:

- Adsorption
- Absorption
- Condensation
- Membrane separation

Since the concentration of $CO_2$ in the atmosphere is only ca. 400 ppm or 0.4 ‰, every one of these processes is energy-intensive. Therefore, pure $CO_2$ sources should be used in order to increase efficiency and profitability of PtG plants.

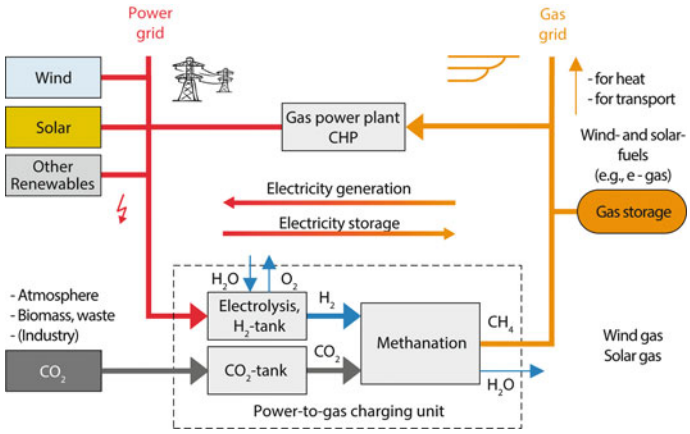



**Fig. 8.87** Basic concept of PtG methane [107]

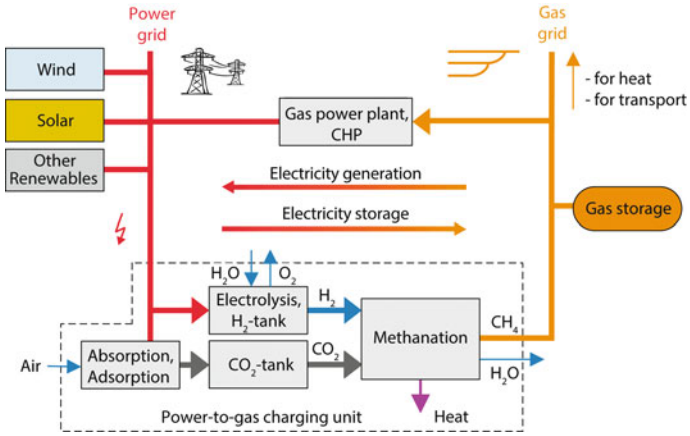



**Fig. 8.88** PtG methane using atmospheric $CO_2$ [107]

This system is given its raison d'être by regions worldwide, which offer a great potential of renewable energies but are far from consumers. Since air is the only source of $CO_2$ in these regions, this system makes it possible to use their potential and decrease their dependence on natural gas imports [107].

Two of the four above-named extraction technologies are very energy-intensive: condensation requires considerable cooling of the air, and membrane separation requires a very high pressure to extract $CO_2$ from the air. These processes are standardly applied in air separation units (ASU) for industrial extraction of nitrogen, oxygen, and noble gases such as argon [98]. From today's point of view, with respect to effort and losses, technologies based on absorption and adsorption are favored.

### Absorption Process

An alkaline solution, such as sodium hydroxide (NaOH), potassium hydroxide (KOH) or calcium hydroxide ($Ca(OH)_2$), absorbs $CO_2$ from the air and reacts to a carbonate like sodium carbonate ($Na_2CO_3$). Now an acid can dissolve $CO_2$ from the carbonate.

In order to restore acid and alkaline solution, an electrodialysis with bipolar membranes is carried out. In this electrochemical process, protons ($H^+$) and hydroxide ions ($OH^-$) are being separated by an electric field. These ions are produced by splitting water, which in turn is activated by a bipolar membrane.

According to laboratory test by the ZSW Stuttgart, absorption and electrodialysis (when put together) require 2.28 MW h per ton $CO_2$ [5, 98]. In practice, this value is higher.

### ■ Adsorption Process

The adsorption process uses a batch procedure in which first $CO_2$ is adsorbed and then emitted, and thus made available, when supplied with low calorific heat. Adsorption processes, such as the pressure swing adsorption, are standard in gas preparation and purification technologies. The advantage is that low-temperature heat from different processes (e.g., electrolysis, CHP, and possibly synthesis also) can be used for desorption.

**Example**

The Climeworks company produces and runs a commercially available demonstration plant capable of extracting atmospheric $CO_2$. One cycle takes up to six hours. First of all, air is conducted through the adsorption chamber where $CO_2$ adheres to cellulose granulate. It takes three hours, before enough $CO_2$ is accumulated. After another three hours at 95 °C and reduced pressure, the desorption phase completes the cycle. Under these conditions, it is possible to extract 99.5% pure $CO_2$ from the cellulose with a vacuum pump. It is possible to extract 80% of all $CO_2$ molecules from the air with this plant using a sorbent. In absolute numbers, this means 800 $m^3$/h air and 4 kg/d resp. 1,000 kg/a $CO_2$ [42, 43, 132].

In the future, ca. 1,000 t $CO_2$/a with a composition of 99.9% $CO_2$, 30 ppm $O_2$, and 20 ppm $H_2O$ will be achievable on a 100 $m^2$ area. Energy input is between 200 and 300 kW h electricity per ton $CO_2$, mainly for the fan, and between 1,500 and 2,000 kW h/t $CO_2$ for low calorific heat (supply temperature: 105 °C, return temperature: 95 °C) mainly for desorption. Costs for extraction are expected to decrease in the future to about 200 €/t from today ca. 800 €/t with an expenditure of ca. 30 €/t for electricity and heat [41].

This demonstration plant was installed at the beginning of 2013 and proved its suitability for daily use under different environmental conditions. It is planned that the demonstration plant will work in co-operation with Audi, which provides $CO_2$ for the PtG plant in Werlte (see [4] and ▶ Sect. 14.2.2.2).

## 8.6.3.2 $CO_2$ from Biogas Treatment Plants

### ■ Principle

This concept's base material for $CO_2$ is biomass or waste, which has been fermented in a digester. Depending on dwelling time and the kind of digester, the purified biogas can contain up to 45% $CO_2$. For a lot of technical applications, the inert $CO_2$ is obstructive, which is why biogas is purified to natural gas quality (> 96% $CH_4$) prior to feed-in into the natural gas grid. For this reason, the purified biogas is called biomethane and can be stored, distributed, and used in all fields of application via a gas grid. Using the existing gas infrastructure has many advantages: pre-existing technology can be applied and, contrarily to on-site conversion to electricity, waste heat can be used more specifically. This makes exploitation of biogas more efficient.

Processes for gas separation are adsorption, absorption, chemical absorption, membrane separation, or cooling [8].

In combination with PtG, very pure extracted $CO_2$ which is normally blown into the atmosphere can be used for methanation instead. Together with electricity surpluses and hydrogen, it is reacted to methane. When there is no sufficient electricity surplus for hydrogen production or when hydrogen buffers are empty, $CO_2$ can simply be stored and used when needed (◘ Fig. 8.89).

### ■ Advantages

The great advantage of coupling these processes is a more efficient use of resources and energy: in this system, waste heat produced by methanation can entirely be used for fermentation or treatment procedures. By using $CO_2$, a naturally bound resource, methane production of a biogas treatment plant can be almost doubled if PtG is applied. Additionally, the climate-damaging methane slip of treatment plants can be avoided.

### ■ Biomass Gasification Variant

Instead of a digester, a gasification plant can be used for solid biomass. When supplied with

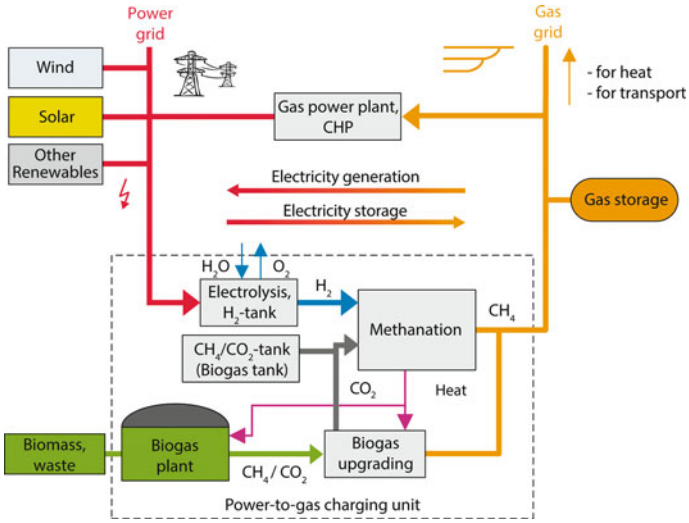



**Fig. 8.89** PtG methane using $CO_2$ from biogas treatment or biomass gasification [107]

heat and oxygen, carbon-hydrate compounds are split into CO, $H_2$, $H_2O$, $CH_4$, and $CO_2$. This gas mixture is catalytically reacted to methane after purification and conditioning. A PtG plant can provide this process with oxygen and hydrogen and increase its gas yield by using surplus electricity.

### 8.6.3.3 $CO_2$: A Component of Gas from Biogas and Gas Purification Plants

#### Principle

Direct methanation of biogas or sewage gas is possible, even without previous $CO_2$ separation (Fig. 8.90). Both gases consist of 50–60% methane, 40–50% of $CO_2$, and small amounts of accompanying substances. This gas is conducted from the digester to methanation, where $CO_2$ from bio or sewage gas and renewable hydrogen can react to high-percentage methane.

By connecting a biogas plant to a PtG system, which also eliminates the additional energy expenditure for biogas treatment, it can produce twice as much methane.

#### Advantages of Biological Methanation

This process can be realized both chemically and biologically. Biological methanation in particular seems suitable in this case, because the necessary bacterial strains are already contained in biogas and sewage treatment plants (▶ Sect. 8.3.3.2). Additionally, parts of the infrastructure of pre-existing biogas and sewage treatment plants can be used, and thus save investment cost. This includes premises, electrical installations and, if applicable, bio or sewage gas utilization (conversion to electricity, gas grid, etc.). In combination with municipal infrastructure in particular (e.g., transport fleet), on-site PtG at a sewage treatment plant is very promising.

Along with integration into existing biogas or sewer-gas plants, another possibility is methanation in pure cultures. This has the advantage of increasing conversion rates at reduced dwelling time, because bacterial strains can be treated more specifically.

### 8.6.3.4 $CO_2$ from Flue Gas Emitted by Coal Power Stations

#### Principle

The main shortcoming of today's coal usage is its $CO_2$ emission. In light of worldwide coal reserves at this time, concepts for separation, sequestration, and storage (carbon capture and storage—CCS) are being developed and put to the test [107]. It is far more realistic to use $CO_2$ from coal power stations energetically or materially (CCU) rather than store it in potentially leaky formations underground. There are

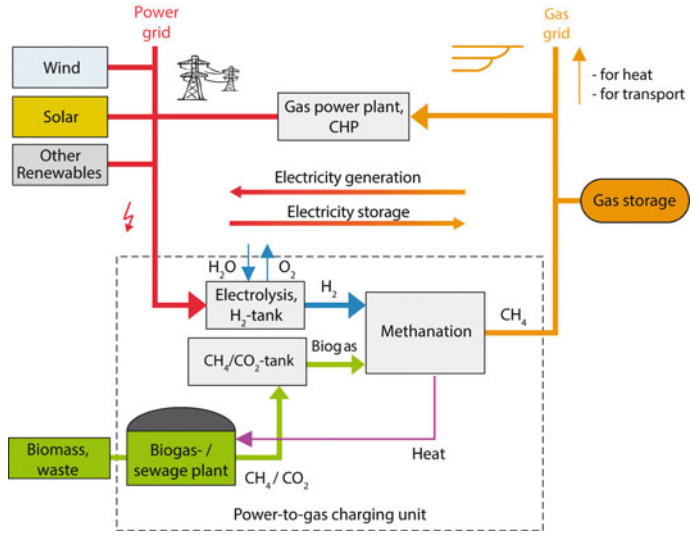



**Fig. 8.90** PtG methane directly reacting a $CH_4/CO_2$ mixture from biogas or gas purification plants [107]

8

different processes for separating carbon dioxide from waste-gases of combustion processes: in a downstream separation of waste-gas after combustion, during the gasification stage before combustion for combined cycle plants using coal gasification or during combustion in a pure oxygen atmosphere (oxyfuel combustion process, Fig. 8.91).

### ▪ Oxyfuel Combustion Process

Since one product of water electrolysis is pure oxygen, a different process seems most attractive. If electrolysis cannot provide enough oxygen, an air separation unit can. This is more energy-intensive and decreases the overall system's efficiency. Taking everything into account, this process may still be more advantageous than energy-intensive downstream separation.

### ▪ Allocation of Emissions

The allocation of $CO_2$ emissions is quite a challenge. On the one hand, $CO_2$ is disposed of by the power plant, but on the other hand, it is not emitted until the combustion of methane, whose production is based on renewable energies. For this reason, the concept is climate-neutral at best. Clear allocation of emissions to coal power stations or gas consumers is required. Otherwise, emissions can be outsourced from the power sector to the heat and transport sector, where the emissions trading law does not apply. So-called 'green washing' of coal power plants is to be avoided.

It is of great importance for this concept that coal power stations are not operated above their must-run limit when methanation is in progress in times of great wind and solar feed-in. In this way, energetically pointless conversion of a chemical energy source to an electrical one following reconversion (so-called 'chemical short-circuit') can be avoided. Renewable feed-in is mainly there to replace fossil power plants. Electrolysis must not be supplied with electrical energy by fossil power plants (▶ Sect. 14.3).

## 8.6.3.5 $CO_2$ Recycling from Gas Power Stations and Other Sources

### ▪ Principle

In order to create a closed carbon cycle, the oxyfuel combustion process can be applied to the combustion of produced methane in gas power stations. This requires spatial proximity of storing and extraction technology, because pure oxygen from electrolysis is needed for clean burning, whose only product gases are carbon dioxide and water. Thus, produced $CO_2$ can be recycled to methane and, therefore, the carbon cycle is closed and climate-neutral.

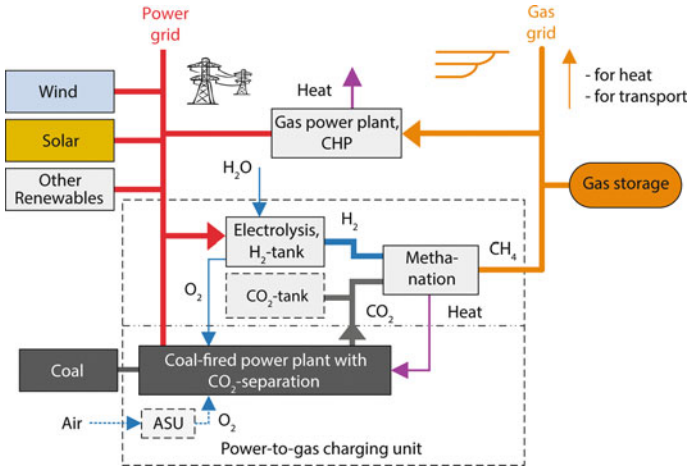



**Fig. 8.91** PtG methane using $CO_2$ emitted by coal power stations via an oxyfuel combustion process [107]

### Other Sources

Another possibility is the use of fossil $CO_2$ from energy-intensive industrial plants, such as steel works, paper mills, or cement plants. They supply their high energy-consumption for process heat (possibility of waste heat integration) through combustion of fossil energy sources. This source of $CO_2$ is very favorable, because they also allow reduction of material and non-energetic $CO_2$ emissions. Further sources are waste-gases from engine test benches or special industrial processes (▶ Sect. 8.3.1.2).

## 8.6.4 Efficiency, Potentials, $CO_2$ Emissions, and Costs

### 8.6.4.1 Efficiency Increases Due to Integration of HTES

Irrespective of which specific process is applied to produce a specific end product, all production variants for synthetic carbon-hydrates have one thing in common: while production of hydrogen is an endothermic reaction at the beginning, during the exothermic synthesis of hydrogen and carbons to carbon-hydrates, such as methane, methanol, gasoline, diesel, kerosene or waxes, parts of previously supplied electrical energy is released in the form of heat.

It is this thermodynamic fundamental principle efficiency losses are based upon for production of synthetic carbon-hydrates, compared to pure hydrogen production. These losses can only be compensated for through the reintegration of waste heat that is released during the process.

One way to achieve this is to vaporize feedwater and supply, thus producing vapor to steam electrolysis (HTES). Now, electrical energy only has to supply the NCV instead of the GCV, which it has to provide for water electrolysis.

This thermodynamic saving of 16% electrical energy by recuperating waste heat allows the production of synthetic carbon-hydrates with an efficiency similar to pure hydrogen production.

These two process chains are compared in Figs. 8.92 and 8.93. The thermodynamic maximum efficiency is 84% for each one, which equals the difference between the GCV and NCV of hydrogen ($NCV_{H_2}/GCV_{H_2}$-ratio). Efficiency rates expected in practice are between ca. 65–79%.

### 8.6.4.2 Efficiency Rates of PtG Systems

A complete PtG system contains

- Transformer ($\eta = 90\%$)
- Electrolyzer ($\eta = 70\%$)

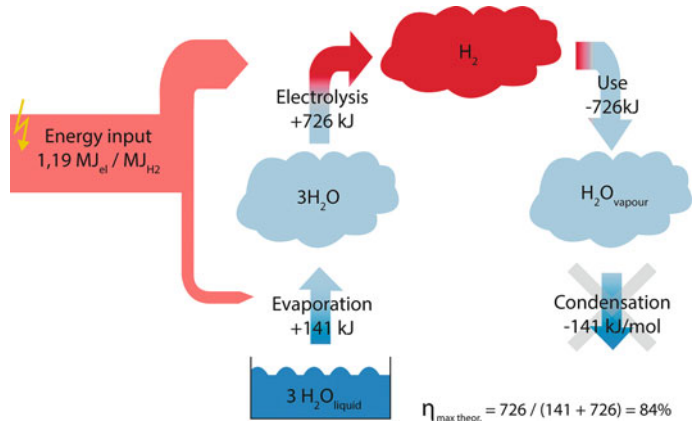



**Fig. 8.92** HTES for hydrogen production from steam without recuperation of waste heat from syntheses (source: Sunfire GmbH)

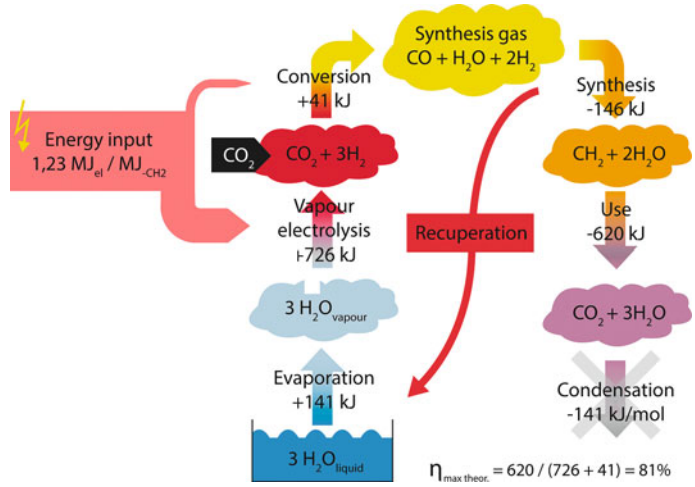



**Fig. 8.93** HTES for carbon-hydrate production from steam and $CO_2$ with recuperation of waste heat from syntheses for the vaporization of water. Similar efficiency rates as pure hydrogen production (source: Sunfire GmbH)

8

- Methanation ($\eta = 82.5\%$)
- Compression and gas storage ($\eta = 97\%$)
- An extraction technology, which can vary depending on the energy service

These average efficiency rates result in different overall efficiency rates (Table 8.31). Efficiency of pure PtG hydrogen storage systems are ~ 5–12% higher than systems with methanation, because of the missing interim step.

### 8.6.4.3 Potentials for Energy Storage

Other than the power-grid, the gas grid offers enough transmission and storage capacity. In gas storage, there is a chemical resp. thermal storage capacity of 217 TW h with considerable potential for expansion (▶ Sect. 8.4.1.7). Thus, stored gas can provide some 120 TW h electricity, or 20% of Germanys gross power consumption, and fill all major gaps in renewable energy supply if reconverted efficiently via sufficient combined cycle plants at an efficiency rate of 60%.

For systems including methanation, this capacity is completely available. For feed-in of hydrogen, respective limits have to be considered. Assuming an average tolerance of 1–2%, there is 2–4 TW h storage capacity for hydrogen. However, this value is purely theoretical, because it is based on the assumption that hydrogen is evenly distributed over Germany. Many gas grid flows vary with the season. In reality, mainly hydrogen caverns are suited for hydrogen storage (▶ Sect. 8.4.1).

**Table 8.31** Efficiency chains for different PtG storage systems (own depiction, based on [108], completed by recuperation of waste heat from synthesis for HTES)

| Path | Overall efficiency (%) | Boundary condition |
|---|---|---|
| *PtG* | | |
| Power-to-hydrogen | 54–79 | Compression to 200 bar (gas storage) |
| Power-to-methane | 49–78 | |
| Power-to-hydrogen | 57–80 | Compression to 80 bar (long-distance and transport lines) |
| Power-to-methane | 50–78 | |
| Power-to-hydrogen | 64–84 | No compression |
| Power-to-methane | 51–79 | |
| *Power sector* | | |
| Power-to-hydrogen-to-power | 34–51 | Conversion to electricity via fuel cell |
| Power-to-methane-to-power | 30–38 | Combustion in combined cycle plant (60%) |
| *Transport sector* | | |
| Power-to-hydrogen-to-motor power | 38–53 | Use in fuel cell (60%) |
| Power-to-gas-to-motor-power | 24–49 | Reconversion via combined cycle plant and use of electric vehicle (80%) |
| Power-to-methane-to-motor power | 18–37 | Combustion in gasoline engine (35%) |
| *Heat sector* | | |
| Power-to-methane-to-heat-and power | 43–68 | CHP (45% heat, 40% power) |
| Power-to-methane-to-heat | 53–84 | Condensing boiler (105%) |

For comparison, pump-storage plants have a storage capacity of 0.04 TW h. If, theoretically, all 42 M existing cars in Germany were electric vehicles with a capacity of 20 kW h each and on the grid at the same time, they could provide 0.42 TW h storage capacity. This calculation is realistically based on the assumption that half of the cars can be used to balance deficits. At a discharge-rate of 60 GW, they could stabilize the power-grid for some 7 h. Extraction of all gas storage would suffice, at the same rate, for 2,000 h or three months. This comparison makes clear what a huge storage potential PtG has (Fig. 12.2).

Along with storage capacity, the gas grid supplies a well-expanded transport and distribution network. While typical transmission lines limit transmissions to 3.5 GW (two 380 kV three-phase systems), the long-distance trans-Europe natural gas pipeline can transport gas equal to some 70 GW.

This means that the coupling of the power and gas grid does not only make storage of great amounts of energy possible, it also allows their spatial separation during storing and usage of renewable methane. This is a unique selling proposition of PtG.

### 8.6.4.4 $CO_2$ Emissions of PtG

- **Potential to Decrease $CO_2$ Emissions with Renewable Electricity Only**

Two things are of importance for the climate impact of PtG storage systems: the source resp. supply of electricity and the substituted energy source.

**Table 8.32** Emissions of fossil energy sources and PtG storage systems in g $CO_2$eq per energy unit (kW h) and per energy service resp. in g $CO_2$eq per km mileage at a very moderate consumption of 40 kW h/100 km (ca. 4 L Diesel/100 km); based on 100% combustion, conversion losses included. Reference system 2010. Gray electricity mix emissions: 546 g $CO_2$eq/kW h. [56]

| Energy source | g $CO_2$eq/kW $h_{th}$ combustible | g $CO_2$eq/kW h energy service | g $CO_2$eq/km mileage | Energy service |
|---|---|---|---|---|
| Fossil systems | | | | |
| Lignite | 404 | 1,161 ($\eta = 0.35$) | | Power |
| Hard coal | 339 | 902 ($\eta = 0.38$) | | |
| Natural gas | 202 | 411 ($\eta = 0.49$) | | |
| Natural gas | 202 | 224 ($\eta = 0.9$) | | Heat |
| Heating oil | 266 | 296 ($\eta = 0.9$) | | |
| Diesel | 266 | | 106 | Transport |
| Natural gas | 202 | | 81 | |
| PtG systems (efficiency of electricity to gas: 60%) | | | | |
| Lignite—gas | 1,935 | 3,949 ($\eta = 0.49$) | | Power |
| Gray electricity—gas | 950 | 1,857 ($\eta = 0.49$) | | |
| Windgas | 33 | 68 ($\eta = 0.49$) | | |
| Lignite—gas | 1,935 | 2,050 ($\eta = 0.9$) | | Heat |
| Gray electricity—gas | 950 | 1,011 ($\eta = 0.9$) | | |
| Windgas | 33 | 37 ($\eta = 0.9$) | | |
| Lignite—gas | 1,935 | | 774 | Transport |
| Gray electricity—gas | 950 | | 364 | |
| Windgas | 33 | | 13 | |

The first point is extensively discussed in ▶ Sect. 14.3. It can be said that only renewable, $CO_2$-free electricity is environmentally-friendly and has a decreasing effect on emissions. Gray electricity from coal, or gas for hydrogen or methane production, is not only energetically absurd, but also frequently causes the emissions that conventional hydrogen or methane causes. This is revealed even by a simplistic greenhouse gas balance: if cheap lignite electricity (1,161 g $CO_2$eq/kW h) is converted to methane at an efficiency of 60% (1,935 g $CO_2$eq/kW h) and reconverted to electricity via combined cycle plant at an efficiency of 60%, storage electricity with 3,225 g $CO_2$eq/kW h is produced (Table 8.32). This is almost eight times the amount of fossil power of natural gas.

The same applies for transport: at a thrifty consumption of 40 kW h/100 km (ca. 4 L diesel or 0.4 kW h/km), a vehicle fueled by lignite PtG emits 774 g $CO_2$eq/km, which is six times more than fossil diesel (126 g $CO_2$eq/km).

In spite of this negative environmental balance, lignite electricity is being considered as a possibility for supplying PtG because it is currently the cheapest power on the market. At this point, opposing goals of economy and ecology, as discussed in ▶ Chap. 1, become clear.

### Potential to Decrease $CO_2$ Emissions and a Question of Which Energy Source Can be Substituted

The second point regarding the climate impact of PtG is the question of which order fossil energy sources are substituted. It is essential, if the federal government's goals are to be achieved and climate protection is to be further established, to substitute all fossil energy sources with renewable energies, renewable fuels, and energy storage in all sectors. First, the procedure of substitution should remove emission-rich energy sources, such as coal and subsequently low-emission energy sources, e.g., natural gas.

As shown in ◘ Table 8.32, substitution of lignite and hard coal in the power sector is the first choice from a climate protection point of view. As a first step, coal is replaced by wind-Sun and water-power. In the second step, it is replaced by energy storage such as PtG. Since PtG is only deployed in rare times during deficits of renewable energies, efficincy losses are acceptable.

Substitution of gasoline and diesel fuels makes sense, as long as they cannot be replaced by direct usage of renewable electricity in electric vehicles.

An extrapolation of the potential to decrease $CO_2$ emissions from one single plant to all of Germany is only possible if surplus quantities are taken into account (▶ Chap. 3). As a rule, it can be said that:

- The deployment of renewable electricity is a basic prerequisite.
- The more $CO_2$ intensive a substituted energy source, the greater the reduction potential.

## 8.6.4.5 Costs of PtG

### Market Conditions

Hydrogen produced by steam-reforming of natural gas causes production costs of 3–4 €-¢/kW h, natural gas costs of 2–3 €-¢/kW h at the stock market, and gray electricity costs between 1 and 6 €-¢/kW h [27]. Surplus electricity for even smaller prices is only available for a very small number of hours, which shows how difficult it is for PtG to competitively convert power to gas.

### Economic Efficiency

PtG is a very young energy technology, and it cannot be realized economically today. Investment costs for new plants are between 2,500 and 5,000 €/kW, and operating costs are mainly subject to electricity prices, which vary between 0 €-¢/kW h (very rare) and 9 €-¢/kW h (average price for wind-power).

◘ Figure 8.94 shows the results of an elaborated cost calculation which were made in the course of the project, 'Energy Storage Concepts' for PtG hydrogen and PtG methane. These results are shown as a range from optimistic (low investment and operating costs, low interest rates and low risk) to pessimistic expectations (high investment and operating costs, high interest rates and high risk). All assumptions can be seen in detail in [49].

Economically competitive production of renewable hydrogen or methane requires more than 7,000 h electricity supply at 0 €-¢/kW h without further levies. From today's point of view, this scenario seems more than unlikely.

Only after a concept with electricity supply costs of 5 €-¢/kW h in base-load operation (more than 7,000 h) has been developed, e.g., sail-powered energy (▶ Sect. 8.8), will it be possible to supply hydrogen for 8–17 €-¢/kW h and methane for 13–24 €-¢/kW h. If levies for $CO_2$ or prices for natural gas were to increase, renewable gases could be an economical and sustainable alternative, even for higher costs.

It becomes clear that hydrogen can only be produced economically in the most optimistic case, which means almost constant electricity supply at stock market prices or below can be used. But this means that something else other than surpluses of wind or solar energy must be used, because they occur only very rarely and not on a constant basis. If gray electricity is used, the product gas is the same as fossil gas concerning disadvantages in the $CO_2$ balance and marketing (▶ Sect. 8.6.4.4). In many places in Germany, feed-in management is used

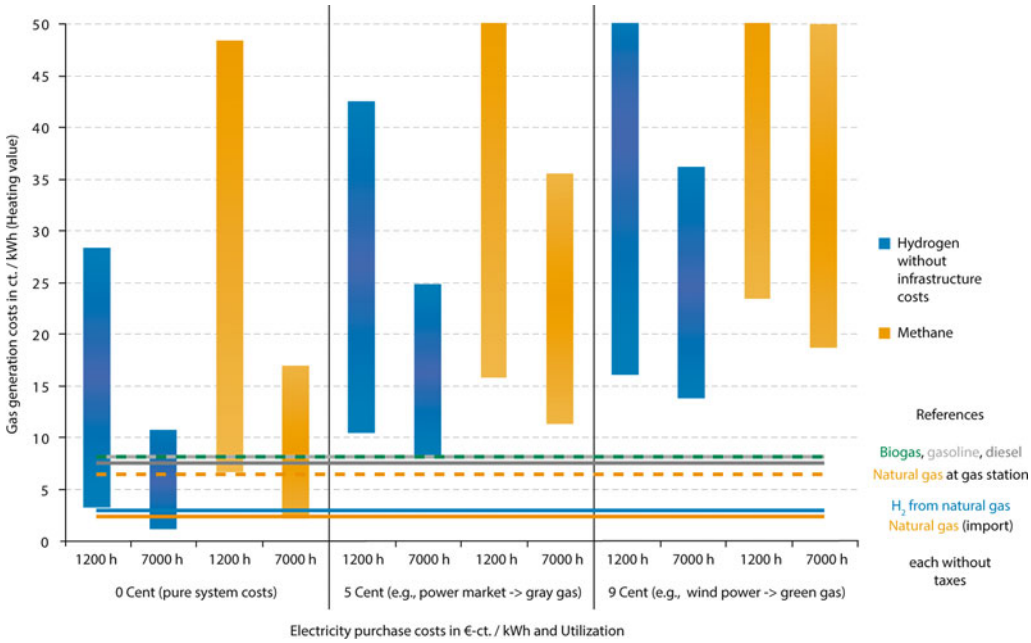



**Fig. 8.94** Range of gas production costs in €-¢/kW h for PtG hydrogen and PtG methane for different electricity prices and full-load hours in the DVGW project, 'Energy Storage Concepts'. Hydrogen paths are represented in blue, methane in orange, each in a range from optimistic to pessimistic. Electricity supply is plotted from 0 €-¢/kW h (plant costs only) over an average value for stock market prices (5 €-¢/kW h) to electricity supply by a wind-power plant (9 €-¢/kW h), each for different periods of use and utilization time (the year has 8,760 h). Reference costs for gases and fuels made with fossil and biogenic energy are depicted as dashed lines (adapted from [49])

to curtail surpluses. At the moment, the absolute value is within limits: in the past year, only ca. 1 ‰ of Germany's energy consumption has been curtailed (▶ Chap. 12).

A basic rule for PtG is: only if electricity supply is mainly renewable (more than 80%), the produced gas has the privilege of being equal to biogas. This simplifies the connection of the PtG plant to the gas grid and the gas's benchmark is increased from 2–3 €-¢/kW h (fossil natural gas) to 7–8 €-¢/kW h (bio-natural gas).

If the stored gas is reconverted to electricity via a gas power station, it leads to generating power costs some two times higher because of the complete electricity storage chain.

From today's point of view, market entry seems most likely in the field of fuels for transport or resources for the chemical industry, because the price level is higher in there than in the electricity and heat market.

Other legal frameworks concerning PtG, such as multiple-crediting as biofuels, is discussed in ▶ Sect. 14.3.

### ▪ Hydrogen vs Methane

On the one hand, a PtG hydrogen storage system does not require a methanation unit and, therefore, saves on efficiency and costs. On the other hand, costs are not assessable for the adaption of plants incompatible to hydrogen in the gas infrastructure or setting up a hydrogen infrastructure. For this reason, the exhaustion of hydrogen admixture quotas of 1–2%, including downstream methanation, is favorable from today's point of view for long-term storage with PtG. More information can be found in the gas grid development plans [36].

## 8.6.5 Advantages and Disadvantages of Hydrogen and Methane

### 8.6.5.1 PtG Hydrogen

A PtG hydrogen storage system is favorable due to reasons related to efficiency and costs, as long as admixture limits of hydrogen are not exceeded or hydrogen can be stored and used locally. It has to be preconceived that, for small natural gas flows, admixture limits are reached very quickly and storage has to be applied in order to level hydrogen feed-in.

Unlike for methane and natural gas, there are no comprehensive solutions suitable for the mass. Fuel cell technology has long been subject to research in auto-industry and heat supply, while technologies ready for the market are merely announced time and again. Furthermore, market entry is only possible if subsidized by companies or the public purse (and even then, market entry is possible in small quantities only). It is also yet to be seen, if fuel cells will be come out on top of e-mobility, conventional powertrains, electric heat-pumps, and alternative renewable heating systems based on wood and the Sun.

When adding hydrogen to the natural gas, changing fuel properties of the gas mixture have to be taken into account. For one thing, the volumetric calorific value decreases by some 7% depending on the natural gas quality if 10% by volume hydrogen is added. This has to be compensated for by an increased quantity to be supplied, which in turn requires adaption of, for example, compressors.

The adaption of the natural gas infrastructure to higher admixture quotas is associated with the need for research and high costs.

Figure 8.95 shows which components are particularly affected and the existence of need for adaption and research.

It has to be taken into account that, in the transport sector, natural gas must not contain more than 2% by volume hydrogen, because higher concentrations may cause embrittlement of steel tanks in CNG vehicles. But also, for reconversion to electricity, high shares of $H_2$ are problematic: gas turbines are only operational for admixture quotas between one and 3% by volume, as specified by the manufacturer, because of changing combustion characteristics (increased flame velocity, different temperature, etc.). For this reason, even cogeneration plants (which are, according to the manufacturer's data, hydrogen-tolerant up to 25%) are, in practice, operated with only 15%.

In general, it is assumed that the admixture limit for hydrogen in the natural gas grid is 1–1.5%. High local feed-in of hydrogen may cause problems if the natural gas load flow is low, because limits are exceeded locally. Additionally, there are some industrial gas applications which use gas as a 'flaming tool' (e.g., drying in the porcelain and glass industry). Fluctuating gas quality can have a strong influence on the product quality [49].

Since conditions and requirements in long-distance and distribution gas grids vary strongly, both locally and regionally, each possibility for the feed-in of the additive gas hydrogen has to be checked individually.

According to the FNB's (long-distance grid operators) gas grid development plans, increasing the admixture limit from today's 1–1.5 to 10% requires the replacement of all compressors, which costs 3.6 billion € in the long-distance grid alone [36].

Advantages and disadvantages of feed-in of hydrogen into the gas grid verses PtG methane are compared in Table 8.33.

### 8.6.5.2 PtG Methane

The storage system PtG methane has certain advantages compared to the hydrogen system and other long-term storage systems, but it also has disadvantages.

The systems advantages are obvious. It is possible to integrate renewable methane in today's energy infrastructure without any problem since it has the same quality and it can fully replace natural gas ('replacement gas'). Unlike hydrogen, the use of renewable methane is uncritical regardless of admixture quotas for

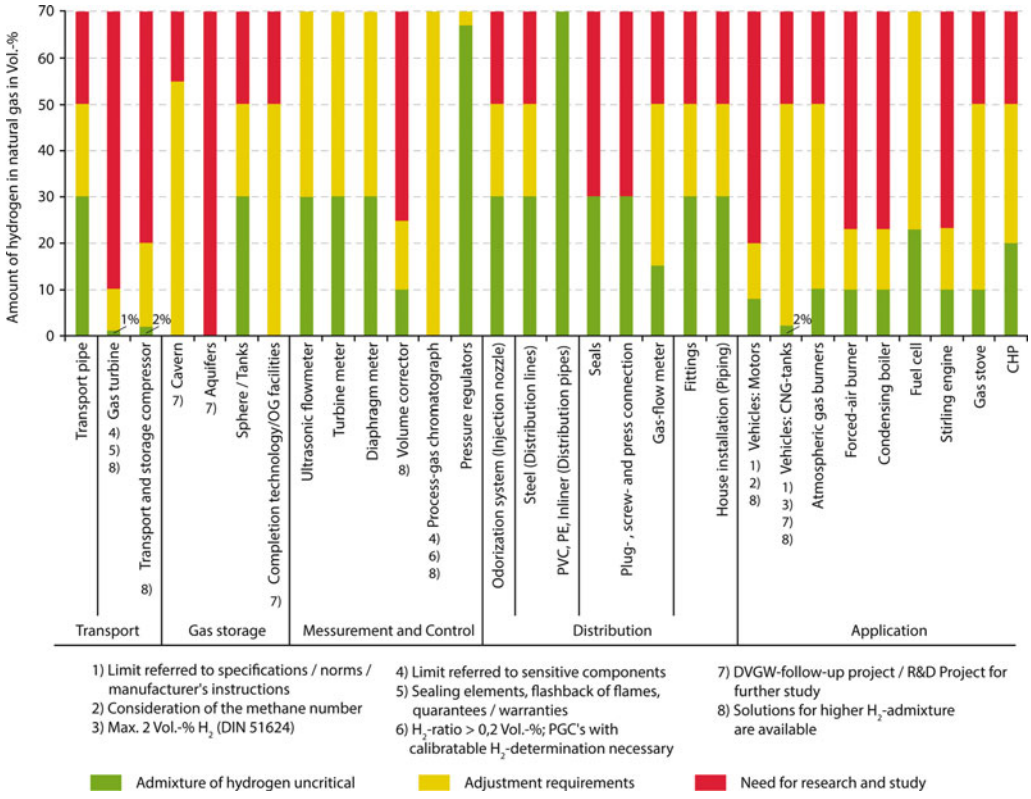



**Fig. 8.95** Hydrogen tolerance of specific components of the gas infrastructure [49]

gas turbines, porous storage, distribution lines, seals, and applications, such as combustion engines or gas stoves.

Furthermore, infrastructure for transport, storage, and application technology already exists across the board. This means that there are long-used state-of-the art applications in every energy sector and in the chemical industry (▶ Sect. 8.5).

Another advantage is the higher volumetric energy density of methane compared to hydrogen, which makes smaller storage systems possible and saves cost and space. With reference to one standard cubic meter, the calorific value of methane is 3.3 times the calorific value of hydrogen.

The cost situation of this storage system requires a differentiated review. Up to the admixture limit of hydrogen, a system without methanation is more economical, because they operate without $CO_2$ supply and methanation units. As soon as that limit is reached, it is more cost-efficient to store renewable energy in the form of methane instead of adapting the German infrastructure to a higher admixture quota of hydrogen.

A disadvantage of PtG methane is its need for $CO_2$ supply. Efficiency losses of the overall process reflect the additional expenditure. But on the other hand, the extraction and storage of atmospheric $CO_2$ is a possibility to reduce its concentration in the air using the energy system itself (▶ Sect. 8.9). In the long-run, $CO_2$ extraction from the air might become a necessity in fighting global climate change anyway and, therefore, it will be cheaply available. Critically, it is important to operate PtG with a closed carbon cycle.

**Table 8.33** Advantages and disadvantages of a PtG storage system with hydrogen and methane

| | Hydrogen | | Methane | |
|---|---|---|---|---|
| | Advantages | Disadvantages | Advantages | Disadvantages |
| Efficiency | | | | |
| Storing technology | 54–84% | | Equal | 49–79% |
| Storage | Equal | | Equal | |
| Extraction technology | Equal | | | |
| Feed-in into the gas grid | | Additive gas: today's admixture limit 1–1.5%; max. 2% by Volume | Replacement gas: no limit | |
| Infrastructure | | Largely non-existent, no affordable and fully-developed application technology | Existing infrastructure including application technologies, usable to the full extent | |
| Transport | | | | |
| Storage | | | | |
| Application | | | | |
| Material demand, climate impact and plant operation | Independent of $CO_2$, therefore more flexible siting (except for usage of atmospheric $CO_2$ for methanation) | Additional hydrogen storage necessary for fluctuating load flow of natural gas | Possible $CO_2$ sink if operated in CCS mode | Necessity of a $CO_2$ source, continuous methanation is based on upstream hydrogen production |
| Energy density (specific calorific value at 0 °C and 1.013 bar or space requirement for storage) | | 3.0 kW h/m$^3$ | 10.0 kW h/m$^3$ Three times more, smaller storage system possible | |
| Transformation costs | Cheaper than methane up to the admixture limit | Storing: Electricity—$H_2$ Storage Extraction: $H_2$—electricity Transport, Storage | | Only storing and additional methanation and $CO_2$ supply vs hydrogen |

## 8.7 The Storage System PtL

### The Importance of PtL in Energy Transition

The most common and oldest form of PtL or power-to-solid (PtS) storage system is biomass. For billions of years, solar energy has been stored in biomass (especially sugar and starch) through photosynthesis. Biomass serves as 'short-term storage' for living organisms. But it can also be converted to 'long-term storage' as fossil energy sources in the Earth's crust, where it can be stored for millions of years (▶ Chap. 1). Since the Earth's available biomass potential is inadequate to sustainably meet energy and fuel demands, it cannot entirely replace fossil energy sources. Instead, this process must be synthetically replicated using PtG and PtL.

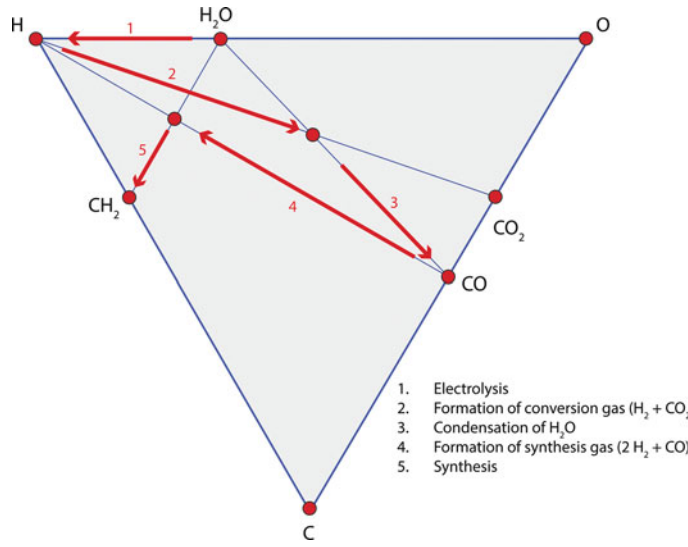



**Fig. 8.96** Conversion of water and $CO_2$ into liquid hydrocarbons (diesel and kerosene) demonstrated in a C–H–O system using electrolysis and the FT process



Gas in the form of hydrogen or methane is essential for decarbonizing the energy sector, but replacing high-energy density liquid or solid fossil energy sources is also crucial. At least in the foreseeable future, electric batteries will not be used for applications requiring fuels with high gravimetric and volumetric energy densities (such as aviation, shipping, heavy-duty machines, and long-haul freight trucking), and will use hydrogen only to a limited extent. Methane is an attractive option for shipping heavy-duty machines and trucking, but aviation will continue to rely on liquid hydrocarbons.

Suitable PtL target products are synthetic fuels such as methanol, gasoline, diesel, kerosene, wax, and DME (▶ Sect. 8.4.2.4).

PtL basically relies on carbon integration. The carbon can be supplied by gasifying biomass (▶ Sect. 8.3.6.1) or by $CO_2$. ▶ Section 8.3 describes the various $CO_2$ sources and how they are utilized by energy storage.

### ▪ Syntheses in a C–H–O System

The production of methane or other hydrocarbons begins with the production of hydrogen. The hydrogen is then synthesized with carbon from $CO_2$ to produce methane or other hydrocarbons. The example in ◘ Fig. 8.96 illustrates how these processes can also be demonstrated in a C–H–O system (▶ Sect. 8.1.1).

The conversion of $H_2O$ and $CO_2$ into liquid hydrocarbons PtL using electrolysis, conversion, and in this case, the FT process, can be described as follows.

In the first step, $H_2O$ is electrolyzed to $H_2$ (and $O_2$). In the second step, $H_2$ is mixed with $CO_2$ to form a conversion gas, and the $CO_2$ reduced to CO. The $H_2O$ formed as a result in then condensed out in the third step. In the fourth step, CO is mixed with additional $H_2$ to form synthesis gas. This gas reacts in a (Fischer-Tropsch) process to form hydrocarbons, here shown as $CH_2$. If the $H_2O$ formed is then separated (step five), the result is a statistically distributed mix of various n-paraffins. These can be processed using modern refinery processes to produce conventional fuels, combustibles, or chemicals.

As with PtG and the existing gas infrastructure, this method can be used to produce a renewable replacement for fossil crude oil compatible with the existing fuel infrastructure.

With chemical methanation using the Sabatier reaction, steps two, four and five all occur in the Sabatier reactor. The water is condensed out in an intermediary step (multi-step reactor concept), or after the Sabatier reaction is completed.

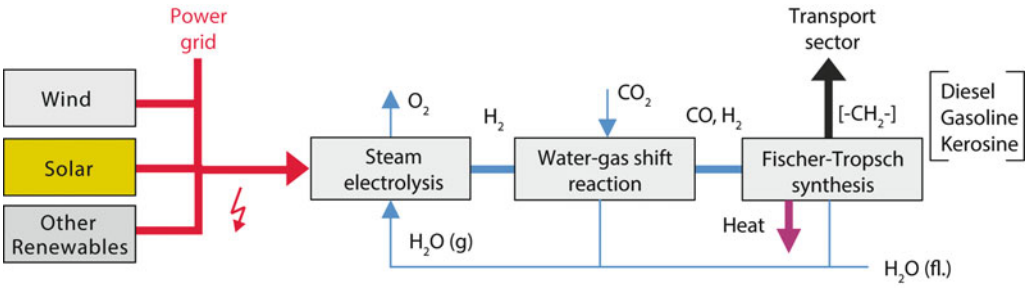



**Fig. 8.97** Design of a PtL storage system using the FT process to produce liquid fuels for aviation

### 8.7.1 PtL for Producing Fischer-Tropsch Liquid Fuels

PtL storage systems follow these steps:

- Charging:
  Charging technologies (see ▶ Sects. 8.2 and 8.3.6):
  - AEL
  - Membrane electrolysis (PEMEL)
  - HTES
  - FT process
- Storage:
  Storage types (▶ Sect. 8.4):
  - Aboveground petroleum storage
  - Pipelines and filling stations
- Discharging:
  Discharging technologies (▶ Sect. 8.5):
  - Airplane turbines
  - Cogeneration plants, gas turbines, combined cycle plants, diesel generators
  - Gasoline engines, diesel engines, all conventional modes of transportation
  - Fuel cells after reforming or with methanol that can be produced by PtL
  - Material use

During conversion, the reverse water-gas shift reaction (Eq. 8.3) uses hydrogen to convert $CO_2$ to carbon monoxide. This reaction is an endothermic side-reaction in existing steam-reforming facilities that produce hydrogen from natural gas. This reaction occurs at high temperatures with nickel catalysts (▶ Sect. 8.1.3.2).

The conversion unit used in the PtL process has a design similar to a steam reformer. The primary differences are the importance of the reverse water-gas shift reaction, and how the energy required is supplied. In steam reformers, the thermal energy is typically supplied by burning natural gas. With PtL, electric heating is used. Eventually fuels will not be burned, and instead will be produced by coupling with electrical energy.

Adequately high temperatures above 700 °C are essential to ensure that basically only CO and $H_2$, and no methane, are fed into the FT process that follows. Methane is inert, and as a result, a carrier gas that causes losses. This means that this synthesis has a significantly different focus compared to methanation or methanolization.

Liquid fuels based on the FT process can be used for basically all applications. But in the current environment, it is especially well-suited for use in aviation. Figure 8.97 shows the design of an example PtL storage system.

### 8.7.2 PtL for Producing Methanol

Currently, methanol is typically produced using fossil raw materials such as methane or coal. But to decarbonize the energy sector successfully, renewable alternatives are urgently required in the transportation sector. Methanol sustainably produced from renewable energy using a PtL/methanol storage system could play a crucial role here. It could also be used in the chemical industry as a raw material for $C_1$ chemistry, replacing fossil energy sources (see ▶ Sects. 8.3.5 and [9]).

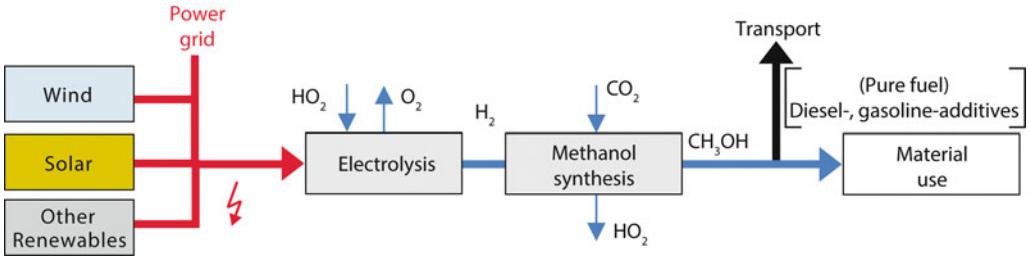



**Fig. 8.98** Design of a PtL/methanol storage system

The components included in a PtL/methanol storage system can be combined as required:

- Charging:
  Charging technologies (see ▶ Sects. 8.2 and 8.3.5):
  - AEL
  - Membrane electrolysis (PEMEL)
  - HTES
  - Methanol synthesis
- Storage:
  Storage types (▶ Sect. 8.4):
  - Aboveground petroleum storage
  - Pipelines, filling stations
- Extraction:
  Discharging technologies (▶ Sect. 8.5):
  - Material use
  - Gasoline engines
  - Gas turbines, combined cycle plants, cogeneration plants
  - Heat pumps, refrigeration machines
  - FCV, turbine power

Figure 8.98 shows the design of a methanol storage system. These systems differ from others primarily by their use of methanol. The advantage of methanol over the gaseous energy sources, hydrogen and methane, is its volumetric energy density. As a result it is easier to handle, particularly in energy logistics (loading and unloading tanks, etc.).

Two advantages methanol synthesis has over the FT process is its higher selectivity and energy conversion efficiency. Methanol storage systems produce a uniform energy source. The FT process produces an entire range of liquid fuels from various hydrocarbons and with various chain lengths that require a separate fuel preparation step (for example, hydrocracking). In addition, the energy source methanol can be used for non-energetic applications in the chemical industry.

Unlike with PtG methane, there is no closed, existing storage infrastructure that can be used to distribute the product to consumers. But methanol is more efficient to produce, and in some areas, compatible with the petroleum infrastructure. Today, single-digit gasoline methanol mixtures are commonly available. These mixtures offer a simple solution for meeting biofuel quotas and increasing the portion of renewable energy in the transportation sector. A disadvantage of methanol is its high toxicity. But it is water-soluble and easier to degrade microbiologically than crude oil. This means that, together with LNG (from PtG), methanol is also a suitable energy source for shipping.

In addition, automobile engines can be modified to run on pure methanol, or gasoline containing a high percentage of methanol. If fuel cells become more established in the future, they could also be easily modified to run on methanol in the electricity, heating, and transport sectors.

### 8.7.3 Efficiency, Costs, and Early Markets

As described above, the components of the PtL process are electrolysis, conversion, and synthesis. Conversion is only required if synthesis

is based on CO, and if it has not already occurred with HTES (▶ Sect. 8.2.2.3). CO is required by the Fischer-Tropsch synthesis specifically (▶ Sect. 8.3.6). Methanol synthesis can also use $CO_2$ (▶ Sect. 8.3.4).

### ■ Efficiency

The efficiency primarily depends on the type of electrolysis used. As shown in ▶ Sect. 8.6.4, using steam electrolysis can dramatically reduce sensible heat losses from exothermic synthesis.

As a result, coupling HTES with steam and fuel synthesis can increase efficiency by 65 to 70%. If, by comparison, alkaline or PEM electrolysis is used (see ▶ Sects. 8.2.2.1 and 8.2.2.2), efficiency increases only by 55 to 60% [90].

Because the reaction produces less waste heat, based on thermodynamic principles, methanol synthesis is more efficient than methane synthesis. The overall efficiency for large facilities ranges from 75 to 80% [73].

### ■ Costs and Early Markets

With electricity supply costs at 5 €-ct./kW h and an efficiency of about 70% (ratio of the NCV of $CH_2$ to the electrical energy supplied), the assumed costs of Fischer-Tropsch products using PtL are 10 to 15 €-ct./kW h of chemical energy, although facility size also plays a key role in determining costs [80].

PtL facilities are expected to gain market access when existing refineries are converted. These could then recycle $CO_2$, and gradually convert to using renewable hydrocarbons marketed in Europe in accordance with biofuel quota regulations. Since this would allow refinery processes to integrate Fischer-Tropsch products directly, the technical advantage here is that no additional product treatment would be required at Fischer-Tropsch facilities.

Fischer-Tropsch waxes provide another market for PtL. These synthetic n-paraffins are very pure, straight-chain hydrocarbons that can be used in the cosmetics industry and other fine chemical processes in the chemical industry. The prices on these markets are significantly higher than on the fuel market. The prices on the electricity and heating markets are even lower than on the fuel market. As a result, PtL products will be launched in several markets at once [80].

There is already a global market for methanol. If methanol is produced from methane, then where site conditions are equivalent, power-to-methanol (PtM) is technically preferable to the PtG process. Since the value of methanol also exceeds natural gas, it is better-suited for the market. It is currently available today as a fuel mixed with gasoline at up to 3% by volume. Using biofuel regulation incentives to establish PtM makes good sense [73]. But the first facilities have already been built even in the absence of government incentives. A facility in Iceland currently produces competitively priced methanol from geothermal energy and fossil $CO_2$. Since the facility uses a fossil $CO_2$ source, the product should be classified as fossil methanol. These first PtL facilities are described in detail in ▶ Sect. 14.3.

## 8.8 Ocean Fuels as Further Development of PtG and PtL

The **problem** with **PtG** and **PtL** is that, under current conditions, they are generally not **economically viable**. In the future, unsustainable or technically infeasible fossil and nuclear energy generation will be eliminated. Since renewable energy sources such as hydropower, geothermal energy, and biomass are limited in their **potential**, energy transition will rely heavily on **wind** and **PV power**.

These **fluctuating** sources with **low full-load hours** or surpluses are not well-suited to technologies in the **chemical industry** that, for economic and technical reasons, are implemented on an industrial scale, requiring a **constant supply** of electricity around the clock of 8,760 hours a year.

The previous chapters demonstrated that **chemical-energy storage** will be

a **crucial component** of energy transition. This section examines how renewable sources could **constantly and sustainably supply the energy required** by this storage under conditions that the **public would accept**.

### 8.8.1 Raw Materials and Fuels from the Ocean—Issues of Potential and Acceptance

#### ■ Wind and Solar Energy Offer the Largest Renewable Potential

$CO_2$-neutral energy sources produced from renewable energy are required to ensure a secure, environmentally-friendly supply of energy. Some renewable sources such as biomass, geothermal energy, hydropower, or tidal power have limited potential or public acceptance, and as a result cannot be expected to meet the global demand for electricity, heating, and fuels. The two highest-yield renewable energy sources are wind and solar energy. Their potential exceeds global demand many times over. But their temporal availability means storing energy from these sources is essential for consistent and secure supply.

Economical utilization of the primal energy sources, from the Sun and wind, is limited to PV and wind energy facilities. As a result, in the future, these facilities will be the largest primary energy sources. As energy sources, they depend on technical or regulatory factors determining the area available for these facilities, and on the acceptance of this type of energy generation by communities in those areas.

#### ■ Rationale for Using Energy from the Ocean

Fossil fuel shortages and anthropogenic climate change (▶ Sect. 1.3) are the driving forces behind energy transition. Energy transition will be achieved by both increasing energy efficiency and by exploiting renewable energy sources. Atomic energy is not an option for a range of reasons. These include issues with atomic waste disposal, proliferation of nuclear technology, risks of a maximum credible accident (MCA) caused by internal as well as external factors or by a terror attack, availability of accessible fissile material, effects of uranium mining (particularly in developing countries), and public acceptance, which are all factors to consider in relation to its potential as an energy source. Exploring renewable energy potential is a more reasonable alternative (◘ Fig. 8.99).

#### ■ The Neglect of Mobility and Chemical Basic Materials in Energy Transition

The areas of mobility and basic materials in the chemical industry have been neglected in energy transition.

Both areas are extremely heavily-dependent on crude oil and natural gas, and alternatives in both areas are expensive or rare. Biofuels or biomass-based raw materials hold some promise, but have limited potential because of their competing uses in the food sector, for example [2].

Electro-mobility has significant potential in the transport sector. This is because it is three to four times more efficient than conventional mobility when regenerative braking is used. The problem is that battery technologies limit how far these vehicles can be driven. Wind and solar fuels could solve this problem by providing an energy source with a higher-energy density. The advantage of these fuels is that they can be conveniently transported and stored, and consumption can be centralized or decentralized.

For chemical basic materials, many so-called biorefinery concepts have been discussed and researched. These concepts are based on the storage process, photosynthesis, and like bioenergy require the use of land area. As with wind-fuels, concepts have been developed to use $CO_2$ as a raw material with wind energy as an energy supplier. Integration of wind-hydrogen into crude oil treatment in refineries has also been discussed (▶ Sect. 8.1).

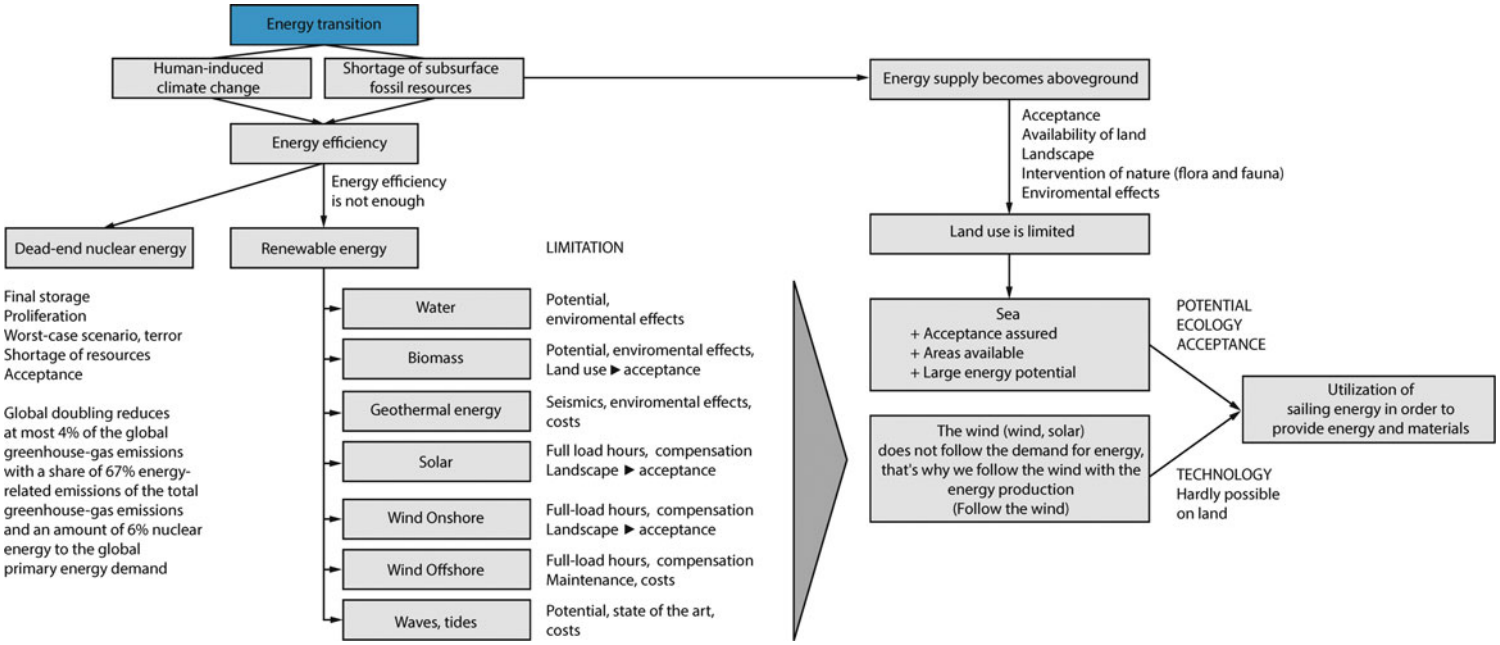



**Fig. 8.99** Reasons for generating and storing synthetic fuels as well as electricity-based raw materials from the ocean

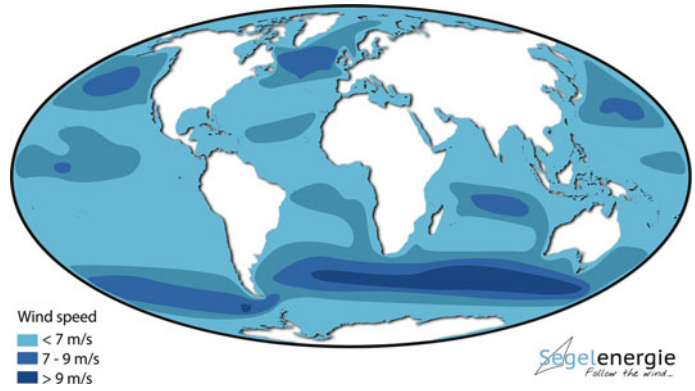



**Fig. 8.100** The large wind potential in the ocean: average wind speeds 10 m above the ocean surface



### The Global Ocean Wind Potential Solution

Biomass-based solutions are currently the focus in the transition to sustainable fuels and raw materials. But biomass potential is inadequate to supply both areas, and its efficiency of 0.5 to 2% (from solar energy to biomass using photosynthesis) results in an extremely low energy yield per unit of area [2, 127].

By comparison, an analysis of global renewable energy potential demonstrates the impressive advantages of ocean wind:

- About 71% of the Earth's surface is covered by ocean.
- The best and largest wind potential is in the ocean.
- The renewable energy potential in the ocean remains basically unused.
- The acceptance of energy use in the ocean is higher than of technologies located near residential areas (no 'not in my backyard' issues). But this acceptance requires that the construction of offshore wind power facilities do not favor large corporations at the expense of smaller operators or regional groups.
- Depending on the technology used, the impact on the environment is low compared to biomass, fossil energy, nuclear energy, or other energy forms.

Besides deep geothermal energy, algae cultivation, and tidal or ocean current power plants, as shown in Fig. 8.100, ocean wind power has the greatest potential.

### Limits of Conventional Offshore Wind Energy

The primary difference between wind power on land and in the ocean is that facility utilization is higher in the ocean, but maintenance, installation, and logistics are more expensive. Besides wind, offshore facilities must also withstand stresses such as ice and wave exposure. As a result, they must be designed for greater dynamic loads.

There is currently a range of foundation technologies used for erecting wind energy facilities in a variety of water depths:

- Shallow depth (around 10 to 25 m):
  - Gravity foundation (heavyweight foundation)
  - Single-pile foundation (monopile)
- Midwater depth (around 20 to 50 m):
  - Three-pile foundation (tripile)
  - Three/four-leg foundations (tripod and quadropod)
  - Lattice tower concepts (jacket)
  - Suction-pile foundation (bucket foundation)

Another significant difference from onshore technology is wind energy facility accessibility. To ensure easy and safe access for maintenance personnel, offshore wind energy facilities must be equipped with ship landings or helicopter pads. In addition, the facilities can only be accessed by ships during daylight hours when waters are calm.

The facility operating control system is equipped with reliable remote control technology. The facilities are also equipped with redundant peripherals, sensors, and machine condition monitoring systems to detect errors early. Hoists and cranes are installed on the facilities for replacing components (gearboxes, generators, bearings, and transformers) during maintenance and repair. Another significant difference with onshore facilities is that offshore facilities must be built to withstand a humid environment and constant exposure to high levels of salt. The facility parts are specially coated to protect against corrosion and wear. To ensure electrical and electronic operational reliability, the machine cabin is hermetically sealed [17].

Conventional offshore wind power facilities can only be used in shallower waters. Since shallow waters are usually near the coast, these facilities should be used to feed electricity into the network and not to generate fuel. Connecting to the electricity network eliminates the problem of logistics. But the largest wind potential is farther out in the ocean where a cable connection is typically not cost-effective.

The following discussion, therefore, examines two alternative options for producing and storing energy from the ocean together with their advantages and disadvantages.

### 8.8.2 Floating Wind Platform Option

#### Operating Principle

Wind energy from the ocean can be converted to electrical energy on large, floating platforms holding several wind energy facilities, or by several free-standing wind energy facilities anchored deep in the ocean floor and connected together to form a wind park. Floating platforms have a robust design that can tolerate rough ocean conditions. They can withstand extreme weather situations, and are easy to access. At least during installation, electrical energy storage technology requires personnel on-site. Electrical energy storage also requires different operational concepts for maintenance and logistics.

Floating wind power platforms can be constructed in water depths exceeding 50 m. These facilities are classified by their floating bodies and their moorings.

- Individual facilities on buoys (spar/spar buoy type)
- Facilities with semi-submersible floating bodies (semi-submersible type)
- Tension-leg platforms (TLP, standard for offshore oil and gas platforms)
- Pontoon and hybrid types

Some concepts have a modular design so that they can be preassembled in shipyards. But some concepts require the wind converter to be assembled on the platform, or facilities to be connected together to form a wind park in the ocean. This increases capital costs and the time required for installation. Platforms with semi-submersible floating bodies can be assembled in a shipyard together with their wind converters, and then tugged to the installation-site. The ORECCA project provides a good overview of this technology and its potential [120].

Maintaining stability in this consistently harsh environment as well as in stormy weather is a complex problem. During storms, facilities anchored by chains sink deeper into the water to improve their stability by actively taking on ballast water or by increasing downthrust. In combination with the long cantilever of the tower, the large weight of the wind converter generates high-dynamic torque when loaded on the platform or floating body. As a result, the machine cabin cannot exceed a maximum deflection angle and acceleration (typically $\alpha_{\text{vertical}} < 3\text{–}4°, a < 2\,\text{m/s}^2$) [126].

The floating bodies are made of robust, reinforced concrete, or if possible, of steel. The floating bodies can have either a rigid or a flexible design. Rigid floating bodies (spar type) use their buoyancy to hold the wind power facility above water, and a deep weight to equalize its motion. Flexible, semi-submerged structures pump ballast water in and out of several tanks integrated into the floating body, shift-

ing the center of gravity to compensate against wind and wave power. But the stability of these structures depends on the mooring system as well as the floating body. Depending on the design, the platform's stability in the water, drift, and rotation on a vertical axis may pose additional problems. Chains are cheap but do little to contain motion caused by wind and waves, or to prevent rotational and rolling motions. Mooring the platform with several tight tethers (tendons, TLP concept) effectively prevents swaying. As a result, this design is frequently used in the oil and gas extraction industry.

Due to the floating body's deep draft, spar-type floating wind energy facilities in the multi-megawatt class can only be used in depths exceeding 100 m. Since they are less stable, they cannot be used with platforms that generate fuel. With large facilities carrying several wind converters, the costs of mooring in relation to capacity is lower.

Because of their stability in the water, semi-submersible concepts and tension leg platforms are the best options here. Despite their high costs compared to cheaper buoy concepts that have already been implemented, projects currently in planning or construction use these designs. For each project, costly simulations of construction unit demand and dynamic structure behavior are also required [20, 37, 105, 130].

Figure 8.101 shows a platform design concept with a semi-submersible floating body for generating methanol as an electricity fuel using three wind converters. Based on the WindSea concept [130], the platform uses one upwind and two downwind wind turbines for a total power of 10.8 MW. The sides of the triangular platform are 81 m long. The distance between the turbines is 103 m. The platform has a load capacity of about 9,600 tons. With an average facility use of 4,350 hours and an assumed efficiency of 26%, the facility can produce 4.2 million tons (11,660 MW h) of methanol. Logistically, transporting this quantity of methanol to land would require 21 trips per year.

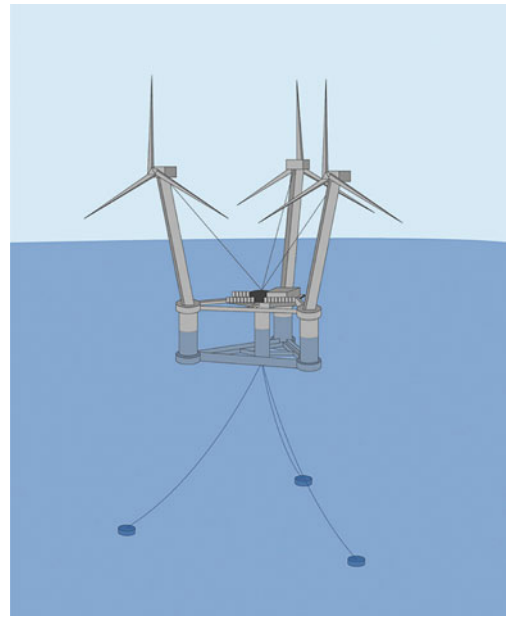


**Fig. 8.101** Floating, semi-submerged platform for producing the electricity fuel methanol using three wind converters (based on the WindSea concept [130])

### Potential and Efficiency

Floating wind power facilities in deep waters could allow significantly more sites in the ocean with good wind conditions to be exploited without conflicting with shipping. The major advantages of floating wind power platforms are high-achievable electrical power and good facility utilization in the ocean. The theoretical potential in deep ocean areas is adequately large to feed electricity into the network as well as generate synthetic fuels. In European waters, suitable locations are concentrated in the northern part of the North Sea, the Irish Sea, and off the coast of France and Portugal (Fig. 8.100). In the part of the North Sea in German territory, the use of floating wind energy facilities is either not necessary or not possible due to shallower waters (maximum 60 m deep).

### Costs

Since no floating wind parks have been constructed to date, reliably estimating their costs

is difficult. Finding the correct balance between wind park power, fuel production capacity, storage capacity on the platform, and capital or operational costs for the components is a challenge. Concepts with low facility power are best-suited for research and development. But because of high-technology and personnel costs, under current conditions, such smaller facilities are unlikely to be cost-efficient. Over the long-term however, very large structures or wind parks could be a viable, cost-effective option with adequate potential for generating synthetic fuels or basic materials for the chemical industry (such as methanol).

#### ■ Advantages and Disadvantages

The concept has the following advantages:

- Exploitation of the large, renewable energy potential in the ocean.
- Unlike conventional offshore wind power, this technology allows the enormous potential in deep waters to be exploited.
- Excellent wind conditions result in high facility-utilization.
- Wind fuel parks with high-installed capacities could be built if suitable designs are developed.
- Cheaper design and higher automation results in lower personnel costs than with mobile ocean fuel platforms such as energy ships.

But implementing the concept also has disadvantages:

- Together with their anchoring systems, for many concepts, a minimum water depth of 100 m is required. As a result, the facilities must often be located far from the coast.
- As with conventional offshore energy, this offshore facility technology is expensive. In addition, access to the facilities depends on the weather, and the wind converters and platforms must be able to sustain extreme mechanical stress.
- All concepts require systems to compensate for wind and wave motion.
- With the exception of TCP platforms for crude oil and natural gas, there is practically no previous experience with floating wind-platforms.

### 8.8.3 Sail-Powered Energy Option

#### ■ Solution to the Central Problem with PtG

Under current economic conditions, operating PtG facilities is typically cost-effective only if facility utilization is very high. Among regenerative sources, base-load can only be supplied by hydropower, and its potential is already largely exhausted in Europe. The full-load hours of wind and PV facilities that generate electricity range between 600 and 4,000 hours. Facility utilization adequate for cost-effective energy generation can currently only be achieved by operating fossil and nuclear energy facilities. But this has a negative effect on the quality and value of the energy stored, because it is then no longer regenerative and competes with conventional energy. In addition, increasing facility utilization makes little sense because the stored energy is then converted into electricity and the electricity simultaneously stored.

These two core problems with PtG can be solved by using the sail-powered energy concept.

#### ■ Operating Principle

Sail-powered energy is a combined wind/hydropower storage system implemented as an energy ship.

A sail system sets a ship in a motion (◘ Fig. 8.102). A turbine in the water then converts a part of the ship's kinetic energy into electricity. Fixed to the ship, the turbine uses a flow machine (rotor or propeller) to drive a generator that produces electricity. Alternatively, electricity can be directly generated from the wind flow as well. The electricity is then electrochemically converted together with water and $CO_2$ (using PtG or PtL) into a storable form of energy [109].

Energy ships can continuously exploit the large wind potential in the ocean to produce renewable fuels with high-energy densities, such as hydrogen, methane (natural gas), methanol,

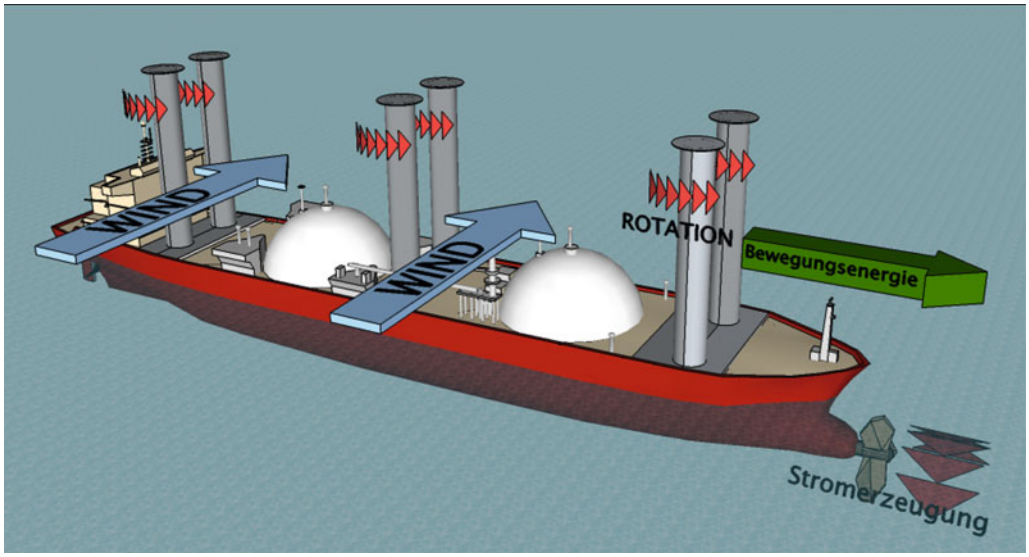



**Fig. 8.102** Operating principle of sail-powered energy—example of an energy ship using a sail rotor [109]



and (over the long-term) diesel or jet fuel as well.

### Potential and Efficiency

The current regenerative portion of fuel consumption (5.5% in 2011) is equivalent to 34.5 TW h. This requires planting 2.4 million hectares of energy crops and using about 90,000 tractors, or sailing about 2,200 energy ships in the ocean, each with a power of five MW.

The following is an example of how the energy path efficiency may be calculated.

- The mechanical motion of wind (wind power) is converted (100% starting point) to constant translational motion (mechanical energy and traction power).
- A portion of the traction power is required to overcome hull resistance. This resistance is determined by the length of the ship, the cruising speed, and other factors such as wave size (energy remaining: 75 to 90%).
- The current of the ocean water relative to the motion of the ship at the hull is converted by a turbine (Betz's coefficient) into mechanical rational energy (energy remaining: 34 to 45%).
- The mechanical energy is converted into electrical energy using an electric motor (or a gearbox and power electronics), and then supplied to a PtG or PtL facility (remaining energy: 25 to 40%).
- Finally the electric energy is converted into an electricity fuel or basic material for the chemical industry using various technical processes (see ▶ Sects. 8.2 and 8.3). This means that 5 to 30% of the original wind energy stored can be stored in a chemical energy source.

The overall efficiency of this process is low in comparison to the utilization rate of fossil fuels in vehicles with conventional combustion engines. But the potential and costs of implementing this technology are also relevant factors.

Directly converting wind flow into rotational and electrical energy increases efficiency by eliminating the conversion step. But a disadvantage is that the mechanical components on deck are exposed to the wind and higher levels of stress.

### Reducing Costs by Route Optimization

Constant facility utilization is a decisive factor in reducing costs with PtG. This can be achieved by optimizing the energy ship route to avoid storms, hazardous areas, wind lulls, or areas where winds are low.

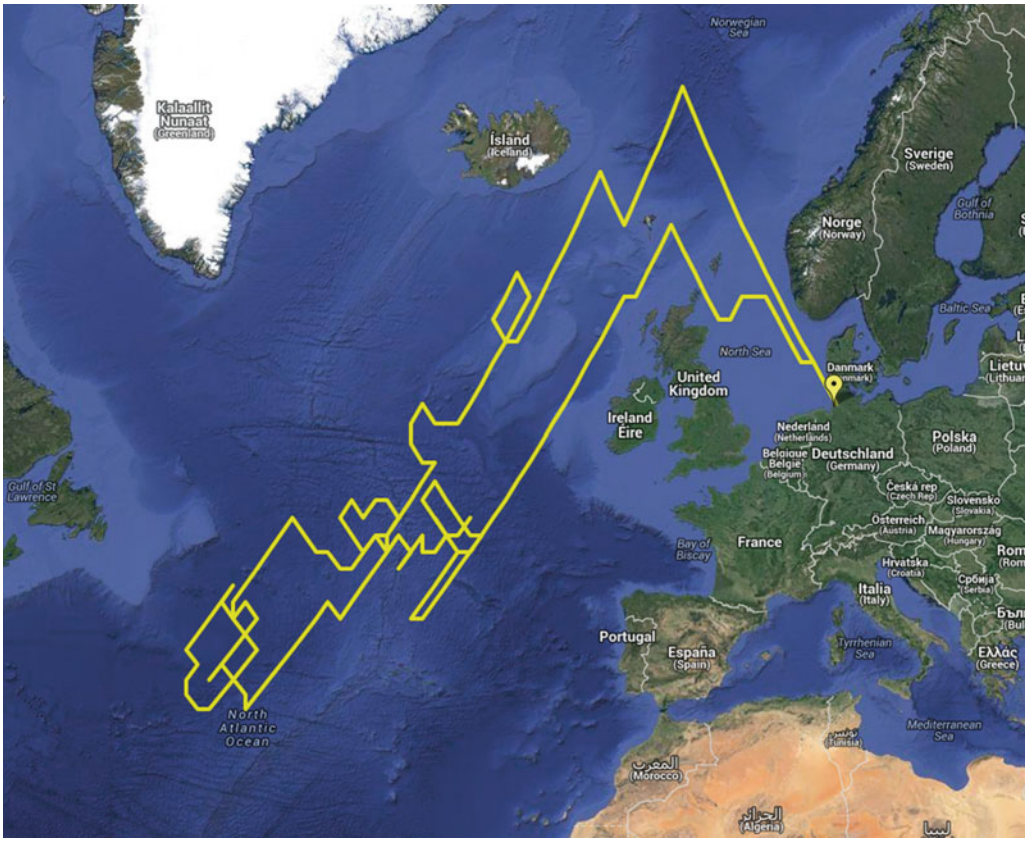



**Fig. 8.103** Energy ship route optimization—example of a three-month voyage, starting and ending in Cuxhaven in northern Germany, and sailing into the North Atlantic

Figure 8.103 shows a possible route for a three-month voyage, starting in Cuxhaven in northern Germany and sailing into the North Atlantic.

Using intelligent routing and precise steering, the energy ship can be effectively guided to areas with steady winds. Energy ship navigation relies on GPS technology as well as satellite and computer-assisted weather forecasting. The goal of computer-assisted route optimization is to maximize energy generation while minimizing risk to the energy ship.

Optimizing the route requires dividing the route into several sections. This is because energy yields are easier to calculate in smaller sections than across a long journey. Each section is then assigned an energy yield. The route in Fig. 8.103 was planned as a round-trip. The starting point is the same as the ending point. Where there are various delivery or transfer points in the ocean, other types of routes can be planned. A range of parameters determines the route taken by the ship, and as a result, the energy yields of the individual route sections. These include ambient conditions such as the wind direction and wind strength in various locations, wave direction and height, ocean current direction and strength, air pressure, air temperature, humidity, and precipitation. Weather conditions are determined using meteorological data, and ocean conditions using hydrological data. Other parameters include container filling levels on board and facility utilization. All parameters are determined in time

intervals for an area or geographical field. They are used as primary or secondary variables in the mathematical calculations and optimization.

By comparison, initial calculations have, for example, determined an average wind speed of 12 m/s at a particular stationary facility location where there is also a risk that extreme weather conditions may endanger fuel facilities. By using route optimization, an average wind speed of 15 m/s can be achieved. Since wind power is determined by the wind speed to the third power, this amounts to doubling the energy potential. In addition, weather extremes can then be avoided by a mobile fuel facility in the form of an energy ship.



### Advantages and Disadvantages

The concept has the following advantages:

- Exploitation of the large, renewable energy potential in the ocean.
- Sail-powered energy is a combination of proven, tested technologies: wind power using sail technologies, ship building, flow machines, and process technology are all well-developed processes and technologies. Since only the combination is new and not the individual technologies themselves, the risk of malfunctions is minimal.
- The meteorological and geographical conditions in the ocean result in significantly higher wind speeds than on land. Energy ships can also set their course to follow high-yield wind areas. This can result in very high facility-utilization with renewable energy. Initial route optimization calculations indicate a facility utilization of 7,000 hours. This means wind could be used as a base-load to generate fuels and chemically raw materials.
- Maintaining energy ships is easier than maintaining ocean platforms. This is because they can be docked in protected harbor areas for maintenance.
- Ocean fuels can typically be fed into existing supply routes, and also transported, distributed, and consumed. For example, hydrogen or methane gas could be fed into the North Sea gas network. In the case of methane gas or liquid hydrocarbons, the existing vehicle technologies and tank infrastructure could also be used. In addition, methanol is a raw material which is essential to the chemical industry today, and that could be renewably generated using this method.
- These 'green ships' could also create new jobs while stimulating the marine, mechanical engineering, and facility engineering sectors. Constructing and maintaining energy ships would be a sustainable use of the existing shipyard infrastructure. The facilities could be mass produced because they do not require modifications for various geographical or meteorological conditions (wind, solar, biogas, etc.).

Despite these advantages, this concept also faces certain challenges:

- Ship operation is very similar to chemical industry facility operation. Unlike in wind power and solar facilities, shift operation on ships requires personnel to be constantly on-site. As a result, large energy ships are required for cost-effective operation. Increasing automation would reduce these costs.
- Testing a pilot ship is very costly. Shipping approvals are required before testing.

## 8.9 $CO_2$ Reduction by Energy Systems PtG, PtL, and Ocean Fuels

To conclude this chapter, this section presents a sustainable, technically realistic vision of a hypothetical energy system based on energy from wind, Sun, and hydropower using power-to-heat (PtH), PtG, PtL, and ocean fuels for a renewable energy supply (see Fig. 8.104 based on [107]).

The can optionally use bioenergy and geothermal energy. By extracting, using, recycling, and storing $CO_2$ from the air, the system could renewably reduce global $CO_2$ emissions,

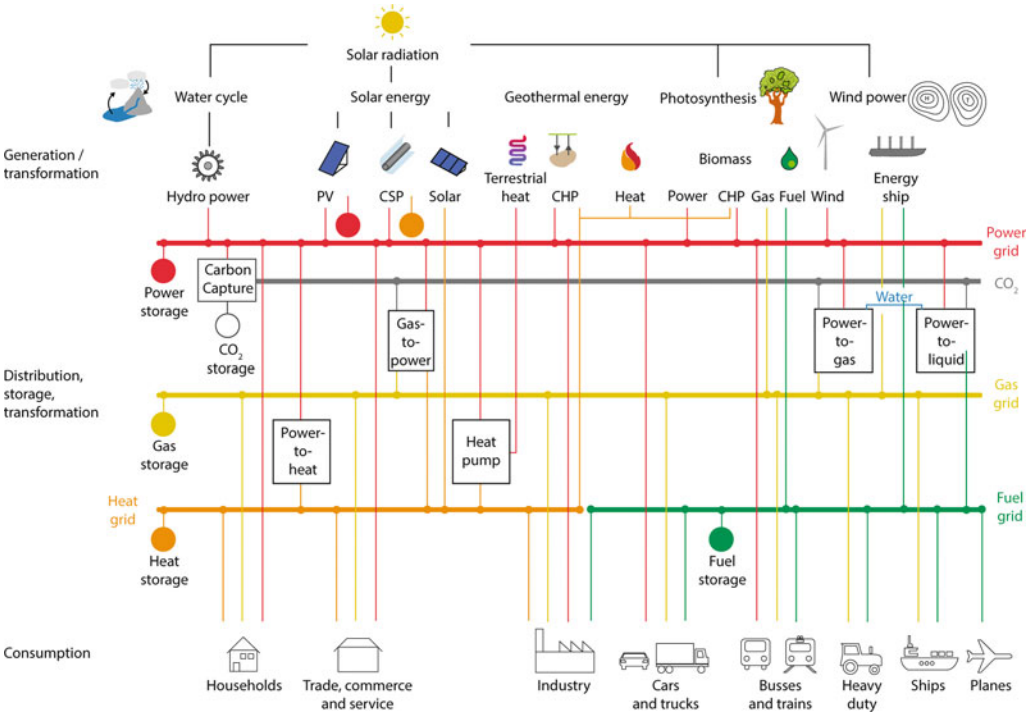



**Fig. 8.104** Energy system for electricity, heating, mobility, and the chemical industry using PtH, PtG, and PtL that reduces $CO_2$ emissions by using $CO_2$ as the central component of chemical-energy storage [107]

while meeting energy requirements at the same time.

Energy demand can be met by exploiting renewable energy sources, implementing various energy storage options, and applying intelligent controls, as well as by cross-sectoral coupling of the electricity, gas, fuel, and heating networks. Primary gas can be produced from hydrogen and $CO_2$ from the air. This gas can then be used by CHP, gas turbines, gas heat pumps, or fuel cells to supply electricity and heating. Waste heat from PtG or PtL is exploited by the system. All fuels for road, rail, air, and ship transportation are produced using this source. Depending on specific requirements, these fuels include methane, methanol, diesel, or kerosene. Basic materials for the chemical industry are also produced using this source. Most individual mobility is powered by electricity. It is also technically feasible to power trucking and bus transportation with electricity. Electric heat-pumps and geothermal energy supplement supply in the heating sector.

In this energy system, biomass is freely available for producing food and feed. Wood and plants are used as materials to supply products that were previously produced in the chemical industry using crude oil and natural gas.

## 8.10 Summary

- Studying the **C–H–O system** is extremely useful for understanding the **history of fossil and biogenic energy storage** as well as the **new processes PtG and PtL**.
- **Hydrogen** is a **chemical energy source** that can be produced in a variety of ways. The most common process worldwide for producing hydrogen is steam-**reforming**

**using natural gas** at prices ranging from 3 to 4 €-ct./kW h. Most hydrogen is currently consumed in the petrochemical industry to **produce ammoniac and methanol, or to hydrogenate hydrocarbons**.

- **Water electrolysis** was discovered in England and Germany in **1800**. The supervising scientist, von Ritter, immediately recognized the **link to photosynthesis**, hypothesizing that the 'warming and shining element of sunshine' was released in the process.
- **Water electrolysis** is a critical component here. There are **three types** of water electrolysis. **AEL**, the most common and currently cheapest type, membrane **electrolysis**, and **HTES** with a range of advantages (efficiency, partial-load performance) as well as disadvantages (particularly costs and service life).

  Since only small quantities of **hydrogen** can currently be integrated into the **energy infrastructure**, processing hydrogen further at a higher cost makes good sense. A variety of syntheses can be used to **convert hydrogen together with $CO_2$ to methane, methanol, diesel, gasoline, or kerosene**, making it easier to store, transport, and consume. This **solves** the **chicken or egg** dilemma with hydrogen, since there is ample $CO_2$ available for syntheses.
- **Biological methanation** is more robust and milder than chemical methanation, but only suitable for **small, decentralized** processes. Chemical methanation is a long-proven technology available **on an industrial scale**.
- The implementation of **methanol synthesis and the FT process** is similar to the use of chemical methanation in modern chemical reactors. Using these processes, renewable energy can be produced or stored in the form of liquid hydrocarbons.
- There is more than **adequate storage capacity in the gas infrastructure** to meet the requirements of **energy transition**. Even the currently available capacity is sufficient for this purpose. Although there is little additional potential with porous storage, gas caverns in the form of salt caverns offer significant potential.
- **The existing infrastructure** is also **adequate for liquid and solid chemical storage media**. Large quantities of energy carriers can be stored in this infrastructure, particularly in the petroleum sector. This infrastructure can also be exploited using PtL and the natural storage process, photosynthesis.
- **LOHC** can be used to **store and transport hydrogen** under ambient conditions as a **diesel-like liquid** in the existing petroleum infrastructure. The long-term stability and cost of this new technology can also be improved. Unlike with hydrogen storage in caverns, **storage efficiency levels drop by up to 30%** when the heat required for LOHC dehydration is generated by burning a portion of the hydrogen released.
- Except for fuel cells, all **discharging technologies for chemical-energy storage are commercially available** today without subsidies. These include gas condensing boilers, gas and steam power plants, diesel engines, and jet engines for aviation.
- **PtG hydrogen** can also be integrated as a material, and directly used in refineries. But constructing a **pure hydrogen infrastructure would be expensive**. Gas turbine, gas storage, and other modern technologies currently limit feed-in of hydrogen as an **additive gas** in the natural gas network to 1 to 1.5%, or to a **maximum of 2%**. As a result, extensive use of the gas infrastructure for seasonal long-term storage is **only viable with methanation**.
- The **storage potential** that can be exploited with **PtG-methane** is **enormous**. If gas storage is discharged using 60 GW combined cycle plants, Germany's electricity demand could be met for **three months** from **gas storage** alone. By comparison, if all vehicles in Germany were converted to electricity and then fed into the electricity network, they would meet demand for a maxi-

mum of seven hours at the same discharge-rate.

- Another **major advantage of PtG** is that it can be used for both **temporal and spatial balancing (storage and transport)**. This **feature is unique** to this technology.
- By recuperating high-caloric waste heat from chemical syntheses for steam generation, thermodynamic savings allow synthetic carbohydrates such as synthetic fuels to be produced with an efficiency similar to pure hydrogen production.
- The use of **renewable electricity** is a **basic prerequisite** for **reducing $CO_2$** using PtG. The more $CO_2$-intensive the energy source substituted, the greater the reduction potential. The use of gray electricity counteracts the climate protection benefits of PtG. In the extreme case of **lignite coal**, reconversion of storage gas to electricity at about 3,200 g $CO_2$eq is **more than eight times the amount as with fossil power from natural gas**. In the transport sector at about 3,200 g $CO_2$eq, it is **over seven times the amount as with fossil diesel** fuel. Only the use of **windgas and wind-fuels** based on wind, solar, and hydropower **reduces emissions**.
- Currently, PtG can only be cost-effective in an optimistic scenario with **constant electricity supply** at about 0 to 1 €-ct./kW h. But even in this scenario, operating hours exceeding 4,500 exclude PtG as a storage option. Currently, market entry seems most likely in the areas of transport fuels or raw materials for the chemical industry. This is because the prices on these markets are significantly higher than on the electricity or heating markets.
- For reasons of **efficiency and cost**, as long as gas network **admixture limits** are not exceeded or hydrogen can be stored and used locally, **hydrogen from PtG is a better choice**. For technical and economic reasons, in all other cases, **methanation is preferable**. This is because it allows the **gas infrastructure to be fully utilized**.
- Using **PtL**, renewable energy can be integrated into the aviation, shipping, freight trucking, and heavy-duty machine sectors **without competing with food and feed sectors**. **Fischer-Tropsch fuels** include **electricity kerosene** that is particularly well-suited to aviation. **Methanol** and LNG are appropriate for shipping. In addition, **methanol** has a **high selectivity** with the **best conversion levels among synthetic fuels**. As a result, it is suited for use as a **fuel for individual transport**. Because they can close regional economic circuits, **vegetable fuels** are particularly well-suited for use in **heavy-duty machines** such as tractors.
- The areas of **mobility and basic materials in the chemicals industry** have been neglected in energy transition. Both areas are **extremely heavily-dependent on crude oil and natural gas**, and alternatives are expensive or rare. With its large, untapped wind potential, the ocean may offer a solution. About **71% of the Earth's surface** is covered by ocean. The best and **largest wind potential** is in the ocean. The **acceptance** of energy generation in the ocean is **higher** than of technologies located near residential areas.
- There are two concepts for producing fuels and raw materials in the ocean. One option is **sail-powered energy** or energy harvesting in the ocean using **energy ships** as mobile, route-optimized wind-hydropower fuel facilities. The other option is **floating electricity fuel platforms**. The flexible energy source methanol is well-suited for both options. Both concepts use energy storage as a simple way to avoid the logistical problems associated with conventional offshore technologies. It remains to be seen which fuel and raw material production concepts will eventually prevail. But there is **no shortage of ideas** for how to utilize and store renewable energy.
- An energy system based on wind, Sun, water, and air is technically feasible. In combi-

nation with $CO_2$ storage, this system could even actively protect the environment by reducing $CO_2$ levels in the atmosphere.

## References


1. Allelein H-J (2010) Energietechnik. Systeme zur Energieumwandlung; Kompaktwissen für Studium und Beruf, 5th edn. Vieweg + Teubner, Wiesbaden
2. Anton C (ed) (2013) Bioenergie: Möglichkeiten und Grenzen. Halle (Saale) (Stellungnahme)
3. Atkins PW, Bär M, de Paula J (2006) Physikalische Chemie, 4th edn. Wiley-VCH, Weinheim
4. Audi (2014) Aus der Luft gegriffen. http://audi-dialoge.de/magazin/technologie/01-2014/104-aus-der-luft-gegriffen. Accessed 10 Mar 2014 (Audi AG)
5. Bandi A (1995) CO2 recycling for hydrogen storage and transportation. Electrochemical CO2 removal and fixation. Energy Convers Manag 36
6. Bayer M (2000) Entwicklung alternativer Elektroden und Aktivierungskonzepte für die alkalische Hochleistungselektrolyse. Universität Ulm (Dissertation)
7. BayLfU (2004) Biogashandbuch Bayern – Materialienband. BayLfU, Augsburg
8. Beil M (2008) BiogasMAX. Biogasaufbereitung zu Biomethan. 6. Hanauer Dialog, Kassel, Hanau (Tagungsband)
9. Bertau M, Offermanns H, Plass L, Schmidt F, Wernicke H-J (eds) (2014) Methanol. The basic chemical and energy feedstock of the future. Springer, Heidelberg, Berlin, New York
10. Bischofsberger W (2005) Anaerobtechnik. Springer, Heidelberg, Berlin, New York
11. BMU (2012) Erneuerbare Energien in Zahlen. Nationale und internationale Entwicklung. Bundesministerium für Umwelt, Naturschutz und Reaktorsicherheit, Berlin
12. Bonin J (2012) Handbuch Wärmepumpen. Planung und Projektierung, 2nd edn. Beuth Praxis. Beuth, Berlin
13. Bott M, Thauer RK Proton-motive-force-driven formation of CO from CO2 and H2 in methanogenic bacteria. Eur J Biochem 168:407–412
14. Bräunling WJG (2009) Flugzeugtriebwerke. Grundlagen, Aero-Thermodynamik, ideale und reale Kreisprozesse, thermische Turbomaschinen, Komponenten, Emissionen und Systeme, 3rd edn. VDI-Buch. Springer, New York
15. Brian D. James, George N. Baum, Julie Perez, Kevin N. Baum (2009) Technoeconomic Analysis of Photoelectrochemical (PEC) Hydrogen Production. Final Report – DOE Contract Number: GS-10F-009J, Arlington, Virginia
16. Brinner A (2013) Elektrolyse – Basics IV. Stuttgart
17. Brückl O (2013) Wind- und Wasserkraft. Regensburg (Vorlesungsskript)
18. Brückner N, Obesser K, Bösmann A, Teichmann D, Arlt W, Dungs J, Wasserscheid P (2014) Evaluation of Industrially Applied Heat-Transfer Fluids as Liquid Organic Hydrogen Carrier Systems. ChemSusChem 7:229–235
19. Mittlestadt C, Willey J, Stone R, Riffle J, Rowlett J, Daryaei A (2016) High Temperature, High Pressure Electrolysis
20. Casale C, Lembo E, Serri L, Viani S (2010) Preliminary Design of a Floating Wind Turbine Support Structure and Relevant System Cost Assessment. Wind Eng (34):29–50
21. Cerbe G (2008) Grundlagen der Gastechnik. Gasbeschaffung, Gasverteilung, Gasverwendung, 7th edn. Hanser, München (mit 133 Tafeln, 102 Beispielen, 66 Aufgaben)
22. Chubb TA, Nemecek JJ, Simmons DE (1978) Application of chemical engineering to large scale solar energy. Sol Energy 20(3):219–224. https://doi.org/10.1016/0038-092X(78)90100-7
23. Czeslik C, Seemann H, Winter R (2010) Basiswissen physikalische Chemie, 4th edn. Studienbücher Chemie. Vieweg + Teubner, Wiesbaden
24. DVGW (2008) G 260: Gasbeschaffenheit. Bonn
25. eawag (2013) Stoffwechsel der Mikroorganismen. Dübendorf, Schweiz
26. EBV (2013) Logistik und Bestände. http://www.ebv-oil.org/cms/cms2.asp?sid=60&nid=&cof=60. Accessed 18 Dec 2013 (Erdölbevorratungsverband)
27. EEX (2014) EEX ist die führende Energiebörse in Europa. http://www.eex.com/de#/de. Accessed 14 Feb 2014 (European Energy Exchange AG)
28. Elsner N (1982) Grundlagen der technischen Thermodynamik, 3rd edn. Vieweg, Braunschweig [u. a.] (Mit 20 Tab)
29. Elsner M (2013) Praktikum Brennstoffzellen. Regensburg (Versuchsanleitung)
30. Enßlin C, Füller G, Hahn B, Hoppe-Kilpper M, Rohrig K (1993) The Scientific Measurement and Evaluation Programme in the German 250 MW Wind Programme. European Wind Energy Conference, Kassel
31. Ernst B (2003) Entwicklung eines Windleistungsprognosemodells zur Verbesserung der Kraftwerkseinsatzplanung. Universität Kassel (Dissertation)
32. Ernst B, Hoppe-Kilpper M, Rohrig K, Scheibe M (2004) Zeitreihen der Windeinspeisung und deren statistische Analyse – Zusatzuntersuchung im Rahmen der dena-Netzstudie. Energiewirtschaftliche Planung für die Netzintegration von Windenergie in Deutschland an Land und Offshore bis zum Jahr 2020, Kassel
33. FAO (2008) The State of Food and Agriculture 2008: Biofuels – Prospects, Risks and Opportunities. FAO, Rome

34. Fichtner N (2011) Aus Wind mach Gas mach Strom. Vor drei Jahren hatten zwei Wissenschaftler eine gute Idee. Bald könnte sie das deutsche Energiesystem revolutionieren. Financial Times Deutschl 10
35. FIZ Karlsruhe (2010) Grundbegriffe. Der Unterschied zwischen Dampf- und Gasturbine. http://kraftwerkforschung.info/quickinfo/grundbegriffe/der-unterschied-zwischen-dampf-und-gasturbine/. Accessed 9 Sept 2013
36. FNB (2014) Netzentwicklungsplan Gas 2012 – 2014. http://www.fnb-gas.de/de/netzentwicklungsplan/netzentwicklungsplan.html. Accessed 13 Feb 2014 (Vereinigung der Fernleitungsnetzbetreiber Gas e.V)
37. FOWC (2013) Fukushima Floating Offshore Wind Farm Demonstration Project. Fukushima Offshore Wind Consortium (http://www.fukushima-forward.jp)
38. Franz B, Franz S, Riedel E (eds) (2009) 1x1 der Gase. [physikalische Daten für Wissenschaft und Praxis], 4th edn. Air Liquide Deutschland, Düsseldorf
39. Gailfuß M (2013) Allgemeine Erläuterungen. http://www.bhkw-infozentrum.de/all_erl.html. Accessed 20 Dec 2013 (BHKW Infozentrum)
40. Gardiner M (2012) Fuel Cells and Hydrogen Enabling Large Scale Renewable Energy. IPHE Hydrogen for Energy Storage Workshop, Sevilla
41. Gebald C (2013) CO2 Supply through Direct Air Capture. Conference on CO2 as Feedstock for Chemistry and Polymers. Essen
42. Gebald C, Wurzbacher JA, Tingaut P, Zimmermann T, Steinfeld A (2011) Amine-Based Nanofibrillated Cellulose As Adsorbent for CO2 Capture from Air. Environ Sci Technol 45(20):9101–9108. https://doi.org/10.1021/es202223p
43. Gebald C, Wurzbacher JA, Tingaut P, Steinfeld A (2013) Stability of Amine-Functionalized Cellulose during Temperature-Vacuum-Swing Cycling for CO2 Capture from Air. Environ Sci Technol 47(17):10063–10070. https://doi.org/10.1021/es401731p
44. Geitmann S (2012) Energiewende 3.0. Mit Wasserstoff und Brennstoffzellen, 3rd edn. Hydrogeit-Verl, Oberkrämer (Sachbuch)
45. Gerthsen C (2010) Gerthsen Physik, 24th edn. Springer-Lehrbuch. Springer, Heidelberg [u. a.]
46. Götz M (2013) Methanisierung im Dreiphasen-Reaktor. Innovationsforum PGP, Leipzig
47. Hamann CH, Vielstich W (2005) Elektrochemie, 4th edn. Wiley-VCH, Weinheim
48. Hasegawa N, Yoshida T, Tsuji M, Tamaura Y (1996) Integrated carbon recycling system for mitigation of CO2 emissions utilizing degraded thermal energy. Energy Convers Manag 37(6-8):1333–1338. https://doi.org/10.1016/0196-8904(95)00342-8
49. Henel M, Köppel W, Mlaker H, Sterner M, Höcher T (2013) Entwicklung von modularen Konzepten zur Erzeugung, Speicherung und Entwicklung von modularen Konzepten zur Erzeugung, Speicherung und Einspeisung von Wasserstoff und Methan ins Erdgasnetz. Abschlussbericht DVGW-Projekt G1-07-10, Leipzig
50. Hey B (2012) Power-to-Gas als Möglichkeit zur Speicherung eines Energieüberangebots und als Bestandteil eines flexiblen Demand Side Managements. HAW Hamburg (Masterthesis)
51. Hiller H, Reimert R, Marschner F, Renner H-J, Boll W, Supp E, Brejc M, Liebner W, Schaub G, Hochgesand G, Higman C, Kalteier P, Müller W-D, Kriebel M, Schlichting H, Tanz H, Stönner H-M, Klein H, Hilsebein W, Gronemann V, Zwiefelhofer U, Albrecht J, Cowper CJ, Driesen HE (2006) Gas Production Ullmann's Encyclopedia of Industrial Chemistry. Wiley-VCH Verlag GmbH & Co. KGaA, Weinheim, Germany
52. Höcher T (2013) Erfahrung mit Wasserstoff in Stadtgas-Untergrundspeichern. Innovationsforum PGP, Leipzig
53. Hofstetter D (2013) Einsatz der biologischen Methanisierung in der Foulum-Demonstrationsanlage in Dänemark. Power-to-Gas: Integration von Biogasanlagen & Biologische Methanisierung, Dänemark
54. Holze R (1998) Leitfaden der Elektrochemie. Teubner-Studienbücher: Chemie. Teubner, Stuttgart, Leipzig
55. HYPOS (2014) Hydrogen Power Storage & Solutions East Germany. http://www.hypos-eastgermany.de/. Accessed 14 Mar 2014 (BMBF)
56. Icha P (2013) Entwicklung der spezifischen Kohlendioxid-Emissionen des deutschen Strommix in den Jahren 1990 bis 2012. Climate Change 07/2013, Dessau-Roßlau
57. Jensen JO, Bandur V, Bjerrun NJ, Jensen SH, Ebbesen S, Mogensen M, Trophoj N, Yde L (2008) Pre-Investigation of Water Electrolysis
58. Kaltenmeier K (1988) Untersuchungen zur Kinetik der Methanisierung von CO2-reichen Gasen bei höheren Drücken. Universität Karlsruhe (Dissertation)
59. Kaltschmitt M, Hartmann H, Hofbauer H (eds) (2009) Energie aus Biomasse. Grundlagen, Techniken und Verfahren, 2nd edn. Springer, Dordrecht, Heidelberg, London, New York, NY
60. Kämpfer P, Weißenfels WD (2001) Biologische Behandlung organischer Abfälle. Springer, Berlin
61. Kopyscinski J, Schildhauer TJ, Biollaz SMA (2010) Production of synthetic natural gas (SNG) from coal and dry biomass – A technology review from 1950 to 2009. Fuel 89(8):1763–1783. https://doi.org/10.1016/j.fuel.2010.01.027
62. Krajete A (2013) Biological Methanation for Intermittent Power Storage. 2. OTTI Power-to-Gas Konferenz Regensburg, Regensburg

63. Krajete A (2013) Biological Methanation for Intermittent Power Storage. 2. OTTI Power-to-Gas Konferenz Regensburg, Regensburg
64. Krajete A et al (2012) Archaea Microorganisms for Bilogical Power Storage. Stationäre Energiespeicher für Erneuerbare Energien, Karlsruhe
65. Kutas G, Lindberg C, Steenblik R (2007) Biofuels – At What Cost? Government Support for Ethanol and Biodiesel in the European Union. International Institute for Sustainable Development (IISD), Genf (2007 Update)
66. LBEG (2013) Erdöl und Erdgas in der Bundesrepublik Deutschland 2012. Hannover
67. Miles MH, Kissel G, Lu PWT, Srinivasan S J Electrochem Soc 123:332–336
68. Mackensen R, Rohrig K, Emanuel H (2008) Das regenerative Kombikraftwerk. Kassel (Abschlussbericht)
69. Mackensen R (2011) Herausforderungen und Lösungen für eine regenerative Elektrizitätsversorgung Deutschlands. Universität Kassel (Dissertation)
70. Mayhew T, McCracken P (2013) Tokelau. Renewable Energy Project (Case Study)
71. McCrary JH, McCrary GE, Chubb TA, Nemecek JJ, Simmons DE (1982) An experimental study of the CO2 x CH4 reforming-methanation cycle as a mechanism for converting and transporting solar energy. Sol Energy 29(2):141–151. https://doi.org/10.1016/0038-092X(82)90176-1
72. Merker GP, Schwarz C, Teichmann R (2012) Grundlagen Verbrennungsmotoren. Funktionsweise, Simulation, Messtechnik, 6th edn. ATZ/MTZ-Fachbuch. Vieweg + Teubner, Wiesbaden
73. Meyer-Pittroff R (2012) Chemische Energiespeicherung mittels Methanol. Silicon-Fire-Technologie wandelt Elektrolysewasserstoff und Kohlendioxid in Methanol um. BWK Vdi-Springer-Verlag 64(9):36–39
74. Moore WJ, Hummel DO, Trafara G (1986) Physikalische Chemie, 4th edn. De Gruyter, Berlin
75. Mortimer CE, Müller U (2010) Chemie. Das Basiswissen der Chemie, 10th edn. Thieme, Stuttgart
76. Munk K (2008) Taschenbuch der Mikrobiologie. Thieme, Stuttgart
77. MWV (2011) Jahresbericht Mineralölzahlen 2010. Berlin
78. Niess UM (2004) Die Demethylierung von Dimethylselenid ist eine adaptive Antwort des Archaeons Methanococcus voltae auf Selenmangel. Philipps-Universität Marburg (Dissertation)
79. Nitsch J, Pregger T, Sterner M, Wenzel B (2012) Langfristszenarien und Strategien für den Ausbau der erneuerbaren Energien in Deutschland bei Berücksichtigung der Entwicklung in Europa und global. Bundesmin. für Umwelt Naturschutz und Reaktorsicherheit, Berlin (Schlussbericht BMU – FKZ 03MAP146)
80. Ohlshausen C (2013) Komponenten für Power-to-Gas / Power-to-Liquid. Power-to-Gas: Integration von Biogasanlagen & Biologische Methanisierung. Regensburg
81. Olah GA, Prakash, Surya GK, Goeppert A (2009) Beyond oil and gas. The methanol economy, 2nd edn. Wiley-VCH, Weinheim
82. Paul N, Kemnitz D (2007) Biokraftstoffe. Pflanzen Pflanzen Rohstoffe Produkte, 3rd edn. Gülzow
83. Pistohl W (2007) Handbuch der Gebäudetechnik: Planungsgrundlagen und Beispiele. Heizung, Lüftung, Beleuchtung, Energiesparen, 6th edn. vol 2. Werner, Köln
84. Quaschning V (2011) Regenerative Energiesysteme. Technologie – Berechnung – Simulation, 7th edn. Hanser, München
85. Reuter M (2013) Power-to-Gas: Biological methanization; first at a municipal sewage plant. 8th International Renewable Energy Storage Conference, Berlin
86. Rönsch S, Ortwein A (2011) Methanisierung von Synthesegasen – Grundlagen und Verfahrensentwicklungen. Chem Ing Tech 83(8):1200–1208. https://doi.org/10.1002/cite.201100013
87. Rönsch S, Matthischke S, Müller M, Eichler P (2012) Dynamische Simulation von Reaktoren zur Festbettmethanisierung. Leipzig (Workshop „Fließschemasimulationen in der Energietechnik" 2012)
88. Sachs JD (2008) Surging food prices mean global instability. Misguided policies favor biofuels over grain for hungry people. Scientific American Magazine May:2
89. Sauer DU (2006) The demand for energy storage in regenerative energy systems. First International Renewable Energy Storage Conference (Eurosolar IRES I), Gelsenkirchen
90. Schaloske MC, Schott B (2012) Energieträger der Zukunft. Potentiale der Wasserstofftechnologie in Baden-Württemberg. Stuttgart
91. Schmack D (31. Juli 2013) Projekt Power-to-Biogas. Email, Schwandorf
92. Schmid J, Sterner M (2008) Bioenergy in future energy systems. Proceedings of the International Conference '16th European Biomass Conference & Exhibition' of EUBIA in Valencia 16
93. Schmitz S (2011) Einfluss von Wasserstoff als Gasbegleitstoff auf Untergrundspeicher. Berlin
94. Schulz A (2005) Selektive Methanisierung von CO in Anwesenheit von CO2 zur Reinigung von Wasserstoff unter den Bedingungen einer PEM-Brennstoffzelle. Universität Karlsruhe (Dissertation)
95. Sedlacek R (2013) Untertage-Gasspeicherung in Deutschland. Underground Gas Storage in Germany. Erdöl Erdgas Kohle 129(11):378–388
96. Smolinka T, Günther M, Garche J (2011) Stand und Entwicklungspotential der Wasserelektrolyse

zur Herstellung von Wasserstoff aus regenerativen Energien. Freiburg im Breisgau (Kurzfassung des Abschlussberichtes NOW-Studie)
97. Specht M (1998) Comparison of the renewable transportation fuels, liquid hydrogen and methanol, with gasoline – energetic and economic aspects. Energy conversion and management:23
98. Specht M, Bandi A, Elser M, Heberle A, Maier CU, Schaber K, Weimer T (2000) CO2-Recycling zur Herstellung von Methanol. Stuttgart (Endbericht)
99. Specht M, Marquard-Möllenstedt T, Sichler P, Zuberbühler U (2006) Der AER-Prozess: Neues thermochemisches Biomasse-Vergasungsverfahren mit flexiblen Edukt- und Produktströmen. Beiträge zur DGMK-Fachbereichstagung "Energetische Nutzung von Biomassen". DGMK, Hamburg (Tagungsbericht/Deutsche Wissenschaftliche Gesellschaft für Erdöl, Erdgas und Kohle, Bd 2006,2.)
100. Specht M, Zuberbühler U, Koppatz S, Pfeifer C, Marquard-Möllenstedt T (2008) ransfer of Absorption Enhanced Reforming Process (AER) from Pilot Scale to an 8 MW Gasification Plant in Guessing, Austria. Proceedings of the International Conference '16th European Biomass Conference & Exhibition' of EUBIA, Valencia 16
101. Specht M, Sterner M, Stuermer B, Frick V, Hahn B (2009) Renewable Power Methane – Stromspeicherung durch Kopplung von Strom- und Gasnetz – Wind/PV-to-SNG (Deutsches Patent DE 10 2009 018 126.1)
102. Specht M, Sterner M, Brellochs J, Frick V, Stuermer B, Zuberbühler U, Waldstein G (2010) Speicherung von Bioenergie und erneuerbarem Strom im Erdgasnetz. Storage of Renewable Energy in the Natural Gas Grid. Erdöl Erdgas Kohle 126(10):342–346
103. SRU (2011) Wege zur 100% erneuerbaren Stromversorgung. Erich Schmidt, Berlin (Sondergutachten)
104. Statista (2014) Importabhängigkeit und Selbstversorgungsgrad Deutschlands bei ausgewählten Rohstoffen im Jahr 2008
105. Statoil (2014) Hywind – The floating wind turbine. http://www.statoil.com/. Accessed 11 Mar 2014 (Statoil ASA)
106. Sterner M (2007) Technical Analysis and Assessment of Biomass-to-Liquid Technologies. Institut für Energetik und Umwelt und Carl-von-Ossietzky Universität Oldenburg, Leipzig, Oldenburg (Masterthesis at the German Biomass Research Centre Leipzig)
107. Sterner M (2009) Bioenergy and renewable power methane in integrated 100% renewable energy systems. Limiting global warming by transforming energy systems. Renewable Energies and Energy Efficiency vol 14. Kassel University Press, Kassel
108. Sterner M, Jentsch M (2011) Energiewirtschaftliche und ökologische Bewertung eines Windgas-Angebotes. Kassel (Gutachten für Greenpeace Energy)
109. Sterner M, Raith T (2013) Segelenergie – Follow the wind. Ein neues Konzept zur Gewinnung von Stromkraftstoffen auf hoher See. http://segelenergie.de/. Accessed 13 Feb 2014 (FENES – Forschungsstelle für Energienetze und Energiespeicher)
110. Sterner M, Schmid J (2008) Electromobility – an efficient alternative to conventional biofuels to put biomass on the road. Proceedings of the International Conference '16th European Biomass Conference & Exhibition' of EUBIA in Valencia 16
111. Sterner M, Schmid J (2009) WBGU Gutachten – zukunftsfähige Bioenergie und nachhaltige Landnutzung. In: Faulstich M, Mocker M (eds) Biomasse & Abfall. Emissionen mindern und Rückstände nutzen. Dorner PrintConcept GmbH, Sulzbach-Rosenberg, pp 23–38
112. Stiller C (2014) Nutzung von konventionellem und grünem Wasserstoff in der chemischen Industrie. In: Töpler J, Lehmann J (eds) Wasserstoff und Brennstoffzelle. Technologien und Marktperspektiven. Springer, Berlin, Heidelberg
113. Teichmann D, Arlt W, Freymann R (2011) A future energy supply based on Liquid Organic Hydrogen Carriers (LOHC). Energy Environ Sci 4(8):2767–2773
114. Thomm M (2006) Archaea. Regensburg
115. Tietze V, al. Stolten D et al (2013) Transition to Renewable Energy Systems. Near-Surface Bulk Storage of Hydrogen, 1st edn. Wiley-VCH, Weinheim
116. Töpler J, Lehmann J (eds) (2014) Wasserstoff und Brennstoffzelle. Springer, Berlin, Heidelberg
117. Trost T, Horn S, Jentsch M, Sterner M (2012) Erneuerbares Methan: Analyse der CO2-Potenziale für Power-to-Gas Anlagen in Deutschland. Z Energiewirtsch 36(3):173–190. https://doi.org/10.1007/s12398-012-0080-6
118. UBA (2010) 2050: 100% erneuerbarer Strom. Energieziel 2050. Umweltbundesamt, Dessau-Roßlau
119. Universität Ulm (2010) Die elektrolytische Leitfähigkeit. http://www.uni-ulm.de/fileadmin/website_uni_ulm/nawi.inst.251/Didactics/elekleit/html/index041.html. Accessed 4 Sept 2013 (Universität Ulm)
120. Vannuci D (2011) Technologies – State of the Art. Offsshore Renewable Energy Conversion platforms – Coordination Action. http://www.orecca.eu/ (Orecca Project)
121. VDE (2009) Energiespeicher in Stromversorgungssystemen mit hohem Anteil erneuerbarer Energieträger. http://www.vde.com/de/fg/ETG/Arbeitsgebiete/V1/Aktuelles/Oeffentlich/Seiten/Energiespeicherstudie-Ergebnisse.aspx. Accessed 29 Dec 2013 (VDE)
122. VDE ETG (2012) Energiespeicher für die Energiewende. Frankfurt am Main

123. Vogel A (2006) Synthetische Biokraftstoffe: Eine Analyse vorhandener Konzepte: Innovationsforum "Stoffumwandlung in Gase im Bereich der Energieverfahrenstechnik". Institut für Energetik und Umwelt (IE), Leipzig
124. Vogel A (2007) Dezentrale Strom- und Wärmeerzeugung aus biogenen Festbrennstoffen: Eine technische und ökonomische Bewertung der Vergasung im Vergleich zur Verbrennung. Technische Universität Hamburg-Harburg, Hamburg-Harburg, Leipzig (Dissertation)
125. Voigt JH (1800) Magazin für den neuesten Zustand der Naturkunde mit Rücksicht auf die dazugehörigen Hülfswissenschaften. Voigts Magazin für den neuesten Zustand der Naturkunde, Weimar
126. Wang CM, Utsunomiya T, Wee SC, Choo YS (2010) Research on floating wind turbines: a literature survey. Ies J Part A: Civ Struct Eng 3(07):267–277
127. WBGU (2008) Welt im Wandel: Zukunftsfähige Bioenergie und nachhaltige Landnutzung. WBGU, Berlin (Hauptgutachten 2008)
128. Weimer T (1996) Methanol from atmospheric carbon dioxide a liquid zero emission fuel for the future. Energy Convers Manag 37
129. Wenske M (2012) Wasserstoff – Herstellung per Elektrolyse. Dauerthal
130. Windsea (2014) About WindSea. http://windsea.com/sfiles/07/1/file/ (Windsea)
131. Winter C-J, Nitsch J (1989) Wasserstoff als Energieträger. Technik, Systeme, Wirtschaft, 2nd edn. Springer, Berlin
132. Wurzbacher JA, Gebald C, Steinfeld A (2011) Separation of CO2 from air by temperature-vacuum swing adsorption using diamine-functionalized silica gel. Energy Environ Sci 4(9):3584. https://doi.org/10.1039/c1ee01681d
133. Yoshida T, Tsuji M, Tamaura Y, Hurue T, Hayashida T, Ogawa K (1997) Carbon recycling system through methanation of CO2 in flue gas in LNG power plant. Energy Convers Manag 38:443–S448. https://doi.org/10.1016/S0196-8904(96)00308-1
134. Zuberbühler U, Specht M (2013) Power-to-Gas, Experience with demo and pilot plants, up to 99% methane. 8. International Renewable Energy Storage Conference – Session Power-to-Gas, Berlin

# Mechanical Energy Storage

*Ingo Stadler, Franz Bauer, Marcus Budt, Eduard Heindl, and Daniel Wolf*

**9.1 Gaseous Media – 484**
9.1.1 Compressed Air Energy Storage Power Plants – 484
9.1.2 Renewable, Emissions-Free CAS Processes – 492
9.1.3 Compressed Air Energy Storage Volumes – 502
9.1.4 Conclusion – 505

**9.2 Liquid Media – 506**
9.2.1 Pumped-Storage Plants – 506
9.2.2 Innovative Concepts for Storing Potential Energy in Liquid Media – 510

**9.3 Solid Media – 533**
9.3.1 Flywheel Storage Facilities – 533
9.3.2 Mechanical Stored Energy Systems – 546

**9.4 Summary – 556**

**References – 557**

**Electronic supplementary material** The online version of this chapter (https://doi.org/10.1007/978-3-662-55504-0_9) contains supplementary material, which is available to authorized users.

© Springer-Verlag GmbH Germany, part of Springer Nature 2019
M. Sterner, I. Stadler (Eds.), *Handbook of Energy Storage*, https://doi.org/10.1007/978-3-662-55504-0_9

**Overview**

Chemical-energy storage systems use caverns, porous storage facilities, tanks, and storage rooms to store chemical energy sources. Caverns, caves, and reservoirs can also be used to store gaseous media such as air, liquid media such as water, and solid media such as rock.

The principles of mechanical energy storage are based on classical Newtonian mechanics, or in other words on fundamental physics from the eighteenth and nineteenth centuries. As a result, these types of storage are typically divided into two categories; storage of kinetic and potential energy, or storage of 'pressure energy'.

In this chapter, storage media is categorized by its aggregate state, and described by its function and application: first compressed air energy storage and then conventional electricity storage—pumped-storage plants. The chapter continues with a discussion of innovative methods of storing potential energy using water as a medium. These include artificially constructed pumped storage, pumped storage in the open sea, dam storage on rivers, pumped storage on heaps in repurposed mining areas, underfloor or underground pumped storage, and surface mine storage.

The chapter concludes with a description of classical and modern flywheel energy storage systems. This age-old technology is then compared with a new concept: mechanical stored energy exploiting both pumped storage and change in the potential energy of rocks or large boulders.



## 9.1 Gaseous Media

### 9.1.1 Compressed Air Energy Storage Power Plants

Ambient air is ideally suited for use as an energy storage medium because it is freely available regardless of location across the globe. Unlike water, air can be compressed. This means that energy can be stored in ambient air using pressure differences. Ambient air is already widely used in industrial applications as an energy source. It is used in a range of processes, including drilling, pressing, and cleaning among many other processes. Compressed air is particularly well-suited for use as an energy source in explosive environments such as coal mines. For industrial use, compressed air is produced almost exclusively by decentralized compressors. In Germany, about 16 TW $h_{el}$ is used to produce compressed air for industrial use, or approximately 2.5% of Germany's electricity demand [46].

Unlike electrical energy or natural gas, compressed air is not an established energy source for general energy supply. But pressurized air is widely used to store electrical energy. The breakthrough came in 1979 with the Huntorf compressed air energy storage power plant. It was the first power plant of its kind, and is still in operation today [24]. The term 'compressed air energy storage' is applied to compressed air storage (CAS) for general energy supply as well as to compressed air energy storage power plants. The abbreviation CAES is also widely used.

#### 9.1.1.1 Background and Pilot Facilities

- **History of Energetic CAS**

The idea to use ambient air for mechanical and then electrical energy storage was first proposed in the 1940s [7]. In 1948, F.W. Gay submitted his patent, 'Means for Storing Fluids for Power Generation', to the United States patent office [20]. But energetic CAS attracted little academic or commercial interest until the 1960s. This is primarily because there was virtually no demand for additional energy storage at an industrial scale to supplement pumped-storage plants. But the situation gradually changed in the 1960s with the introduction of nuclear power plants and the growing use of higher-yield lignite coal power plants to meet base-load demand. This also added an economic incentive to store cheap base-load electricity in low-load hours, i.e., at

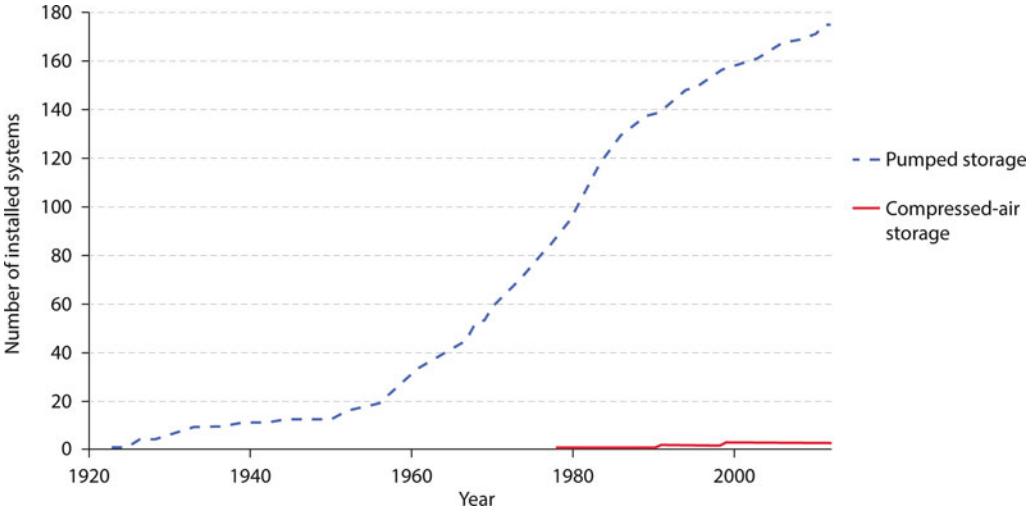



**Fig. 9.1** Number of installed pumped storage and CAS power plants worldwide

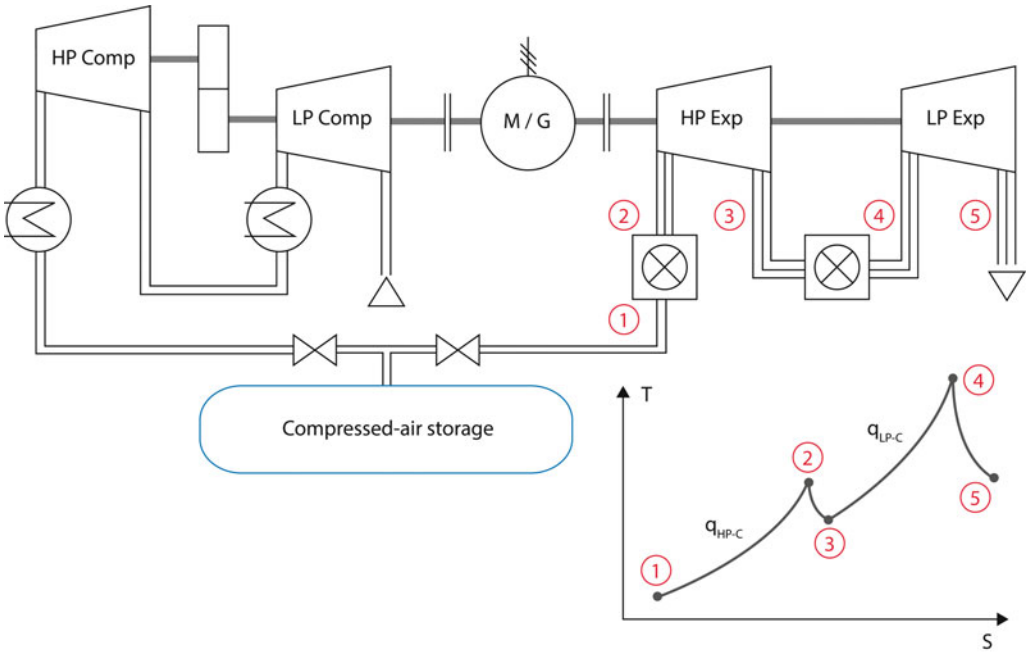



**Fig. 9.2** Simplified schematic design of the Huntorf compressed air power plant with a *T*-*s* diagram of the expansion process

night and on weekends, for use during peak-load hours. Where feasible, this was achieved by building pumped-storage plants. The diagram in Fig. 9.1 illustrates the rapid expansion of pumped-storage plants in the 1960s and 1970s.

### Huntorf CAS Power Plant

As a result, in 1969, the energy supply company Nordwestdeutsche Kraftwerke (NKW—today E.ON Kraftwerke) decided to build a compressed air power plant. The storage plant was

designed to temporarily store cheap base-load from nuclear power plants, as well as provide black-start capability to the northern German electricity network [36]. The design also took advantage of local geological formations suitable for storing compressed air at an industrial scale. The northern German lowlands contain salt layers at a suitable depth (around 500 to 1,500 m) for constructing underground caverns. These caverns can be used to cheaply store compressed air.

It took the company nine years to build the CAS power plant and bring it online. The technical terminology also differed from the terminology used today. The power plant operator, NKW, named the plant ASSET, short for 'air storage system energy transfer'. This terminology emphasized the actual use of the storage power plant from the point of view of an energy supply company [24]. Similarly, the technology development company, BBC (today General Electric and Ansaldo), used the name 'gas turbine air storage peaking plant'. This terminology emphasized that, from an engineering point of view, a CAS power plant was based on the technology of an open gas turbine power plant.



Figure 9.2 shows a schematic design of the Huntorf storage power plant. The process includes two compression (comp) and two expansion (exp) units arranged on a shaft and connected by switchable couplings to a motor generator (M/G).

Only the high-pressure compressor (HP-comp) sits on its own shaft, connected by a gearbox to the main shaft. In Fig. 9.3, the HP-comp and gear box are shown in the foreground, and the low-pressure compressor (LP-comp) in the background.

During the compression process, air in the low and HP-comps is intercooled and compressed up to an outlet pressure of 72 bar. The air has to be cooled again before it can be stored in the salt cavern. Since the Huntorf facility uses a diabatic process, all recooled compression heat is released into the atmosphere.

Figure 9.4 shows an exterior view of the storage power plant. The compressed air is stored in two dedicated solution-mined salt caverns with a total capacity of 310,000 $m^3$, located about 700 m below ground. In Fig. 9.4, only the cavern supply line is shown as a bright horizontal line directly under the power plant. Two separate caverns were constructed in Huntorf to ensure availability. If one cavern requires repairs, the power plant can still continue to operate using the other cavern. During operation, the pressure ranges from 46 bar (no storage) to 72 bar (full storage). In exceptional conditions, the power plant can also safely operate at pressures below 46 bar.

During the discharging process, the compressed air is released from the cavern at a controlled constant pressure of 42 bar and then fed into the high-pressure combustion chamber ([24] and point (1) in Fig. 9.2). After leaving the high-pressure combustion chamber,

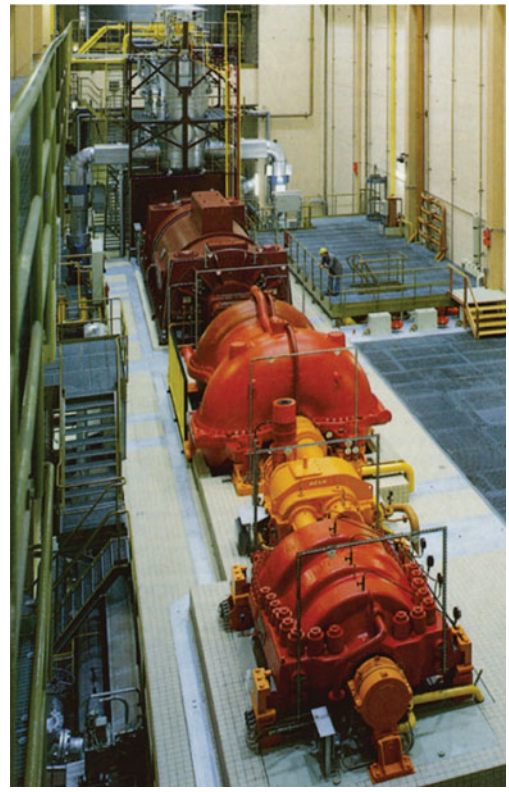


**Fig. 9.3** Interior view of the CAS power plant in Huntorf (source: E.ON Kraftwerke GmbH)



**Fig. 9.4** Exterior view of the CAS power plant in Huntorf (source: E.ON Kraftwerke GmbH)

the hot combustion gases are decompressed to about 10 bar in the high-pressure turbine used as a steam turbine derivative. At this pressure-level the air is reheated using additional heat from firing natural gas, and then decompressed in the low-pressure turbine. The design of the low-pressure step is based on gas turbine technology. After 28 years of operation, in 2006 the expansion string required a retrofit. The inlet temperature of the high-pressure turbine (see point (2) in Fig. 9.2) was reduced from 550 to 490 °C. In the low-pressure element, the inlet parameters was increased from 10 to 13 bar/945 °C (see point (4) in Fig. 9.2). As a result of the retrofit, the facility's electrical discharging power increased from 290 to 321 MW.

In recent years, the Huntorf facility has often been used to provide minute-reserves. In addition, the storage power plant can participate in reactive power control. When the storage power plant is not charging or discharging, synchronized condenser operation can also be used for this purpose. Here, both couplings are opened and the generator runs in parallel to the network with no load.

As the first facility of its kind, the CAS power plant in Huntorf introduced several technological innovations. These include [47]:

- CAS in underground solution-mined salt caverns.
- A high-pressure combustion chamber for gas turbines.
- A high-pressure gas turbine with quick start functionality.
- An engine-to-generator power ratio of 1:5 in a single component.

Despite introducing so many innovations at the same time, the facility has been reliable [45, 47].

### Developments in the USA

The success of the Huntorf project also stimulated interest in compressed-air energy-storage systems (CAES) technology in the USA [17]. At the end of the 1970s, a large research program was launched, aimed at developing and implementing energetic CAS for energy supply [4]. The focus of the project was on two areas:

- Determining the long-term stability criteria of underground reservoirs used for CAS.
- Developing and assessing sophisticated CAES concepts to reduce the use of fossil energy sources in discharging.

A demonstration CAES program was also launched at the same time as the research program. Both the research and demonstration programs were funded by the US Department of Energy (DOE) and managed by the Pacific Northwest National Laboratory (PNNL). The research program determined that diabatic CAES, such as the storage power plant in Huntorf, were technically feasible and could be implemented in the near future. As a result,

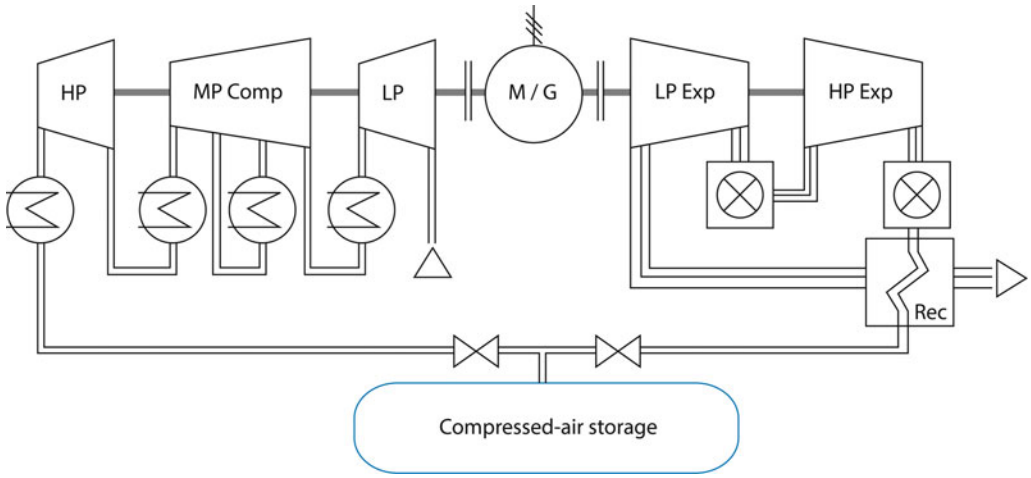



**Fig. 9.5** Simplified schematic design of the McIntosh compressed air power plant

the Electric Power Research Institute (EPRI) was tasked with developing and promoting diabatic CAES. The focus of research on sophisticated CAES concepts was then shifted to successfully implementing diabatic CAES in the USA. In the research program, PNNL also determined that diabatic CAES—i.e., CAS power plants with internal intermediate storage of compression heat using no additional heat for discharging—is the most promising type of sophisticated CAES concept [58]. By contrast, EPRI identified a CAES hybrid using both additional heat and intermediate storage of compression heat as the most promising type of sophisticated concept [22].

The demonstration project resulted in the decision to partner with the energy supply company, Soyland Power Co-Operative Inc., to construct a diabatic CAES [42]. Contracts for the 220 MW facility had already been signed when the energy supplier unexpectedly backed out of the project. The cancelation of the project was officially explained as a response to unanticipated moderate increases in electricity demand [4]. In addition to the slower pace of increase in electricity demand, cheaper sources of energy for covering peak loads had also become available to the supplier. These factors resulted in the decision to cancel the construction of the storage power plant [7].

### McIntosh

Later, the first CAS power plant in the USA was built in 1991 by the Alabama Electric Co-Operative (AEC) at the McIntosh power plant facility in Alabama [44]. As in northern Germany, in Alabama, the compressed air could be stored in underground salt caverns. Unlike in Huntorf however, in McIntosh, only one large salt cavern is used. As the schematic design in Fig. 9.5 shows, the basic constellation of components with the machinery arranged on a main shaft and a central motor-generator closely resembles the design of the Huntorf facility [10, 40].

The primary improvement on the Huntorf storage power plant is the integration of an exhaust recuperator (Rec). During the expansion phase (or storage discharge), the recuperator uses the hot exhaust gases from the low-pressure turbine (around 370 °C) to preheat the compressed air before it enters the high-pressure combustion chamber. Figure 9.6 shows a T-s diagram illustrating the expansion process in the McIntosh power plant (black line). For comparison, the same process in the Huntorf facility without recuperation is shown on the diagram as a gray line (the process before the retrofit at Huntorf is on the left, and the process after is on the right).

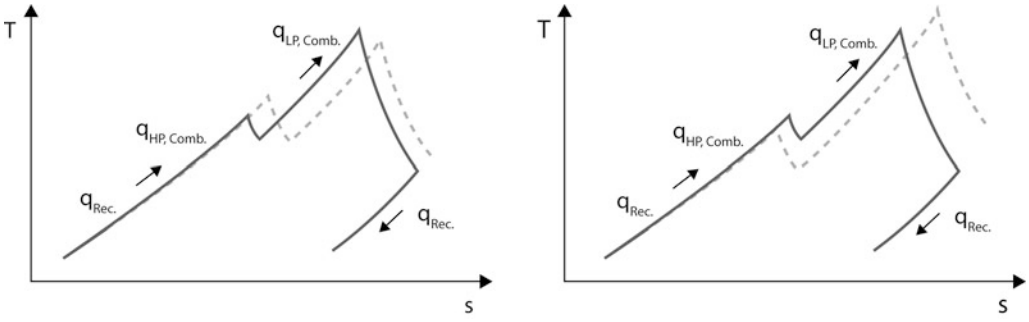



**Fig. 9.6** $T$-$s$ diagram of the expansion process at McIntosh (*black line*) and at Huntorf (*gray line*) before (*left diagram*) and after (*right diagram*) the retrofit

The illustration demonstrates that, at McIntosh, the air was heated between points (1) and (2) by cooling the hot exhaust gases in the recuperator $q_{\text{Rec}}$. Additional heat from firing natural gas is used to increase the temperature to 490 °C before the air enters the turbine. This demonstrates that using an exhaust recuperator results in less natural gas consumption, increasing the efficiency of the discharging process. The Huntorf process uses no exhaust recuperation, and as a result, consumes more fuel. The McIntosh facility requires 1.17 kW h of natural gas to produce a kW h of electrical energy, and the Huntorf facility requires 1.6 kW h.

But as the two diagrams in Fig. 9.6 show, the low-pressure inlet temperature in the Huntorf process (gray line) was brought below the McIntosh process (black line) temperature by the retrofit. The inlet temperature of the high-pressure turbine was also increased to 70 °C above the McIntosh temperature, significantly increasing the electrical power to 31 MW.

Table 9.1 summarizes the relevant technical specifications of the two storage power plants.

A striking difference here is that the McIntosh facility's cycle-efficiency level of 54% is significantly higher than the Huntorf facility's at 42%. This is primarily due to the use of a recuperator at the McIntosh facility. Increases in individual component efficiency are of only secondary importance. Closer examination of the operating regime of the McIntosh power plant explains the emphasis on increased efficiency in the design. The power plant was intended for load shifting involving large quantities of electricity on a weekly cycle which, for economic reasons, requires a high level of efficiency [44]. Huntorf, by contrast, has a two-hour discharging duration and was intended only for use over short periods during times of high prices (peak hours). This means it operates more as a reserve power plant than as a load shifting facility handling large volumes. As a result, high-efficiency is of secondary importance. Since high starting reliability and availability are much more important here, the facility design reflects these requirements [6].

### ▪ Current Projects

The storage power plant in McIntosh increased interest in the technology among other American energy suppliers, including the Tennessee Valley Authority and the Hawaiian Electric Co. But no serious plans to build another CAS power plant resulted [18]. In 2001 a CAES project was announced with the plan to use the decommissioned limestone mine in Norton, Ohio to store compressed air [51]. This mine could provide a gigantic storage volume of about 10 million $m^3$. But extraction mines are typically not gas-tight, and are therefore suitable for storing compressed air only in exceptional cases as a result. A turbine power of 2 GW over a duration of two days would be required to continually discharge this enormous reservoir. The power was to be provided

**Table 9.1** Relevant technical parameters of the McIntosh and Huntorf compressed air power plants [13, 33, 37, 40, 47]

| | | Huntorf | McIntosh |
|---|---|---|---|
| Power plant | Facility operator | E.ON Kraftwerke | PowerSouth Electric Corp. |
| | Cycle-efficiency level[a] | 0.42 | 0.54 |
| | Energy consumption for 1 kW $h_{el}$ discharging work | 0.8 kW $h_{el}$/1.6 kW $h_{gas}$ | 0.69 kW $h_{el}$/1.17 kW $h_{gas}$ |
| | Storage volume (dischargeable work) | 560 MW h | 2,640 MW h |
| | Duration of planning—construction—start-up | 1969–1978 | 1988–1991 |
| Compression | Compressor manufacturer | Sulzer (now MAN Turbo) | Dresser-Rand |
| | Max. el. power consumption | 60 MW | 50 MW |
| | Max. air mass flow | 108 kg/s | Around 90 kg/s |
| | Compressor units | 2 | 3 |
| | Loading duration (with full load) | Around 8 h | Around 38 h |
| Storage | Cavern construction company | KBB | PB-KBB |
| | Cavern pressure range | 46–72 bar | 46–75 bar |
| | Cavern volume | 310,000 $m^3$ | 538,000 $m^3$ |
| Expansion | Turbine manufacturer | BBC (now Alstom) | Dresser-Rand |
| | Max. el. power output | 321 MW | 110 MW |
| | Control range | 100–321 MW | 10–110 MW |
| | Discharging duration (with full load) | Around 2 h | Around 24 h |
| | Start-up duration (normal/emergency) | 14/8 min | 12/7 min |
| | Max. air mass flow | 455 kg/s | 154 kg/s |
| | High-pressure turbine entry parameters | 41.3 bar/490 °C | 42 bar/538 °C |
| | Low-pressure turbine entry parameters | 12.8 bar/945 °C | 15 bar/871 °C |
| | Exhaust temperature | 480 °C | 370 °C (before recuperator) |

[a] With diabatic CAES using additional heat from firing natural gas, the cycle-efficiency level given should not be considered the AC/AC efficiency as with pure energy storage. ► Section 9.1.1.2 explains the definition of the cycle-efficiency level.

by nine 300 $MW_{el}$ gas turbines from Alstom (type ET11NM) [55], but the plan has yet to be implemented. In December 2006, Alstom withdraw its commitment to supply the technology due to a shortage of internal resources. Dresser-Rand then submitted an alternative offer to pro-

vide the turbomachinery technology [129]. In November 2009, the American energy supplier, FirstEnergy Generation Corp., sold the rights to the Norton project. In addition to the project in Norton, Ohio, other CAS power plants are currently planned in the USA. The energy supplier, PG&E in California, plans to build an over 300 $MW_{el}$ diabatic CAS power plant with a storage volume of 10 full load hours. Porous rock formations there are under consideration for use as storage volumes. The power plant is expected to go on-line in 2021. Plans on the east coast of the USA hold less promise. The energy supply company NYSEG is planning a facility with a power ranging from 100 to 300 $MW_{el}$. Solution-mined salt caverns will be built for storage volume. But the project was halted in 2012 because conditions in the energy sector made the investment economically unfeasible [52]. In addition to the projects in the USA, there are also plans to build diabatic CAS power plants in Europe as well. One example is a 135 $MW_{el}$ facility planned in Larne, Northern Ireland. The plant will have a discharging duration of six to eight hours and use underground salt formation to store the compressed air [19]. There are also plans to build an adiabatic CAS facility with internal thermal storage that requires no additional heat, and as a result, releases no emissions. These projects are discussed in detail below in ▶ Sect. 9.1.2.1

### 9.1.1.2 Efficiency of Diabatic and Adiabatic CAS

#### ■ Diabatic CAES

In the previous section, the cycle-efficiency level of the CAS plant in Huntorf was given as 42%, and of the facility in McIntosh as 54%. The two cycle-efficiency levels are comparable, and show that the McIntosh CAES is more efficient than the Huntorf facility. But these cycle-efficiency levels cannot be directly compared with those of other storage technologies discussed in this book. This is because a fundamental characteristic of diabatic CAS power plants is that they are not a type of purely electric storage. Instead, they are a type of hybrid facility that combines a power plant and a storage facility. This is particularly obvious when it is taken into account that a diabatic CAS power plant yields more electric energy during the discharging process than it absorbs during the charging process. Because of the first law of thermodynamics, this is inconceivable with pure storage. A diabatic CAES can yield more electric work during discharging than it absorbs during charging because natural gas is fired during discharging. As a result, the diabatic CAES cycle-efficiency level definition applied here counts as consumption of both the electric energy required for compression $E_{ein,el}$ and the thermal energy from fired natural gas required for expansion $E_{ein,th}$ (lower-calorific value). With pure storage processes, the dischargeable electric work $E_{aus,el}$ is defined as the output:

$$\eta_{zyk} = \frac{E_{out,el}}{E_{in,el} + E_{in,th}}. \tag{9.1}$$

The cycle-efficiency levels given for Huntorf and McIntosh were calculated using this definition. These calculations can be illustrated as follows using McIntosh as an example.

The McIntosh CAES consumes 0.69 kW h of electric energy $E_{in,el}$ and 1.17 kW h of thermal energy $E_{in,th}$ to yield one kW h of electric energy:

$$\eta_{zyc} = \frac{E_{out,el}}{E_{in,el} + E_{in,th}} = \frac{1}{0.69 + 1.17} = 0.54. \tag{9.2}$$

In concrete terms, firing natural gas increases the enthalpy of the working gas, and so increases its capacity to perform work. In this case, external heat fed into the expansion process is converted into work. When the turbine inlet temperature is increased, the power yield increases but the efficiency level remains the same. This is demonstrated by the definition of thermal efficiency for a gas turbine process (Joule cycle):

$$\eta_{th\ Joule} = 1 - \left(\frac{p_0}{p_{max}}\right)^{\frac{(\kappa-1)}{\kappa}}. \tag{9.3}$$

According to Eq. 9.3, the ratio of maximum turbine outlet pressure $p_0$ to turbine inlet pressure $p_{max}$, as well as the isentropic exponent $\kappa$ determine the thermal efficiency. Since $\kappa$ is a chemical property and cannot be modified when air is the working medium ($\kappa = 1.4$), the efficiency level can only be influenced by changing the pressure ratio. The greater the pressure ratio, the greater the thermal efficiency level. This can be achieved by:

- Increasing the pressure ratio.
- Using the exhaust heat to preheat the air before it enters the combustion chamber with an exhaust recuperator (see McIntosh).
- Repeatedly intercooling the air during the compression process.
- Increasing the isentropic compressor and turbine efficiency levels.

9

#### ▪ Adiabatic CAES

The cycle-efficiency level definition presented above (Eq. 9.1) takes into account that diabatic CAES use both a storage and power plant process. As a result, by definition, the efficiency of this process cannot be directly compared with pure storage processes in batteries or pumped-storage plants, for example. Despite this, scientists have continued to search for a valid definition of the cycle-efficiency level which would be comparable with the efficiency of pure storage processes. But direct comparisons with pure storage processes have so far failed to produce any meaningful results [56]. There are, however, CAS processes that are also pure storage processes. These processes require no additional heat whatsoever. Adiabatic CAES are the most well-known of these types of processes. Here, the cycle-efficiency level is simplified to:

$$\eta_{cyc} = \frac{E_{out,el}}{E_{in,el}}. \tag{9.4}$$

With this kind of CAES, the cycle-efficiency level can be directly compared with other pure storage technologies such as batteries and pumped storage. The cycle-efficiency levels of adiabatic CAES typically range from 55 to 75%.

### 9.1.1.3 Classification

Besides diabatic and adiabatic CAES processes, there are also other processes for energetic CAS. Here it is helpful to first systematically sort these processes into classes. Using the CAES cycle-efficiency level definitions presented above, the processes can first be divided into those with additional heating and those without:

- Processes with external additional heat: diabatic.
- Processes without external additional heat: adiabatic, isothermal, etc.

The process temperature can also be used to sort the processes into smaller categories. As shown in Fig. 9.7, diabatic CAES have the highest process temperatures ranging from 500 to 140 °C, adiabatic CAES the second-highest ranging from 90 to 700 °C, and isothermal CAES have the lowest ranging from 20 to 90 °C.

In addition, air can be stored in liquid form if it is cooled to temperatures below −196 °C. But these facility concepts are not categorized as CAS. Instead, these facilities are categorized as liquid air energy storage (LAES). The following section describes in further detail the characteristics of adiabatic CAES, isothermal CAES, and LAES.

## 9.1.2 Renewable, Emissions-Free CAS Processes

Converting a diabatic CAS power plant to a pure storage system requires eliminating the use of external energy sources to preheat the air before expansion. This means storing the compression heat produced by the process and feeding it back into the air before expansion. Adiabatic CAES, isothermal CAES, and LAES all use this technique. Unlike diabatic CAES, all of these processes are emissions-free (when the emissions produced to generate the storage electricity are ignored). But these processes have not been implemented on an industrial scale, and are either still in the research and de-

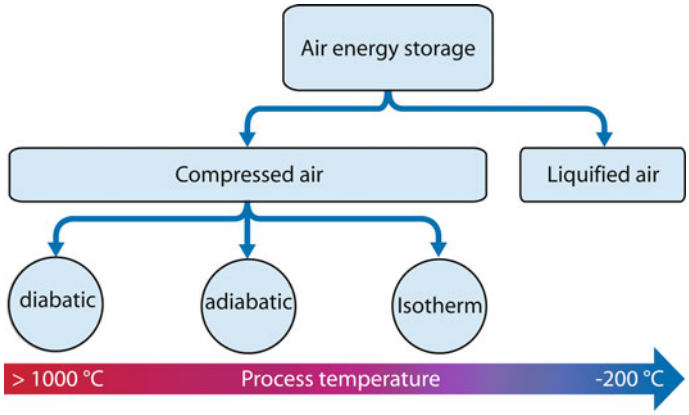



**Fig. 9.7** Classification of compressed air energy storage by process temperature

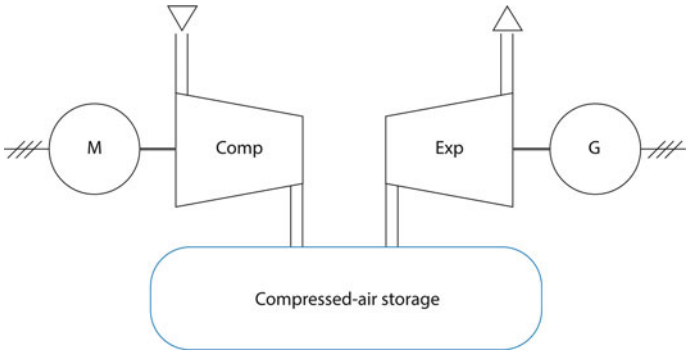



**Fig. 9.8** Simplified schematic design of an uncooled CAS facility

velopment phase or currently being tested in demonstration projects. This section discusses these processes in further detail.

### 9.1.2.1 Adiabatic CAS

Uncooled compressed air energy storage (U-CAES) is the simplest way to utilize compression heat. In this process, the air is heated to a very high temperature determined by the storage pressure, and then stored in this heated state. As a result, there is no need whatsoever to heat the compressed air later (Fig. 9.8).

Problems with this concept include the high temperatures reached in the higher compression steps, and problems with designing a CAS facility so it can withstand these temperatures. In combination with the storage pressures required, these problems can present difficult and complex challenges. The U-CAES concept is currently in the experimental stage [28, 37].

Because of these challenges, the vast majority of adiabatic concepts separate CAS from thermal storage. Here, the storage medium is repeatedly cooled between the steps in the compression process. Unlike with CAES (D-CAES), the thermal energy is stored in thermal-energy storage (TES) instead of released into the environment. It is later reused to preheat the compressed air (Fig. 9.9).

#### ▪ Excursus: Thermal Storage Suitable for Use in CAS Facilities

The most important component of an A-CAES facility is the thermal storage unit that eliminates the need for additional fossil fuel heat as in diabatic facilities. As a result, this component is crucial in determining the storage facility's discharging power as well as its cycle-efficiency. The choice of thermal storage technology is determined by a range of parameters, and also largely determines the design of the other components of the system. In addition, the thermal storage unit determines much of the investment costs and, therefore, the economic efficiency

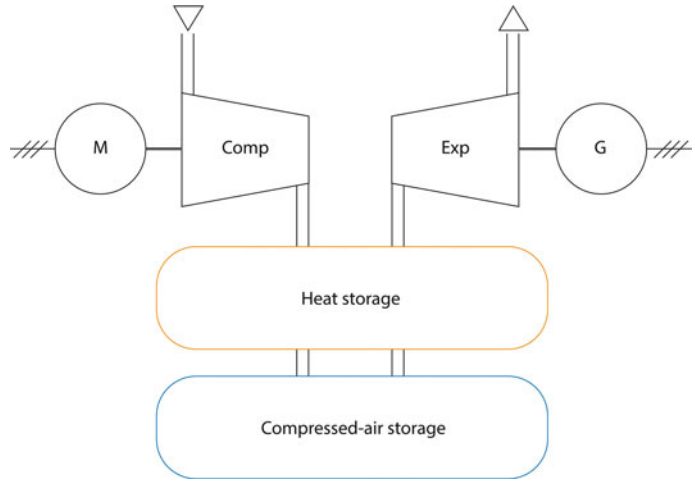



**Fig. 9.9** Simplified schematic design of an adiabatic compressed air energy storage (A-CAES) facility

of the overall system. Depending on the technology used, thermal storage system costs can account for up to 20% of total investment costs for an A-CAES [39]. As a result, the thermal storage used must be both technically feasible and cost-efficient.

The general technical requirements for thermal storage used in an adiabatic CAS facility are as follows:

- Cooling of the compressed air to the lowest possible outlet temperature during the charging process.
- Heating of the compressed air to the highest possible outlet temperature during the discharging process.
- Low variation in the temperature of the outlet air from thermal storage.
- Low pressure loss.
- Low idle period losses.

A variety of thermal storage technologies can meet these requirements. Figure 9.10 summarizes the viable options. As indicated there, the available technologies can be broadly categorized by how the air comes into contact with the thermal storage medium. Systems either use direct contact or indirect contact. Direct contact increases the pressure of the thermal storage medium as necessary. Indirect contact does not increase the storage medium's pressure.

The systems can also be more narrowly categorized by the thermal storage medium used. The media are categorized by their aggregate state as gaseous, liquid, or solid. Liquid and solid storage media have a higher thermal capacity, and are therefore preferable.

The gaseous media listed here should only be used for thermal storage under pressure when additional advantages result. An example here would be combining thermal storage and CAS in a single unit so that a separate thermal storage unit is no longer required (see U-CAES, ▶ Sect. 9.1.2.1).

With a solid storage medium, compressed air can be brought into direct contact with the medium in the thermal storage unit. A pressurized container with a rock or ceramic-structure filling can be used in these types of systems. With both types of fillings, there must be enough space within the storage material to allow the compressed air to flow through it (Fig. 9.11). This ensures effective heat transfer between the air and the solid storage medium. These kinds of thermal storage units have been used as regenerators for decades in steel mills, but at much lower pressures than in a CAS facility.

In this kind of thermal storage or regenerator, thermal layering is used to obtain the air outlet temperatures required. This means that, in a vertical flow regenerator like the one shown

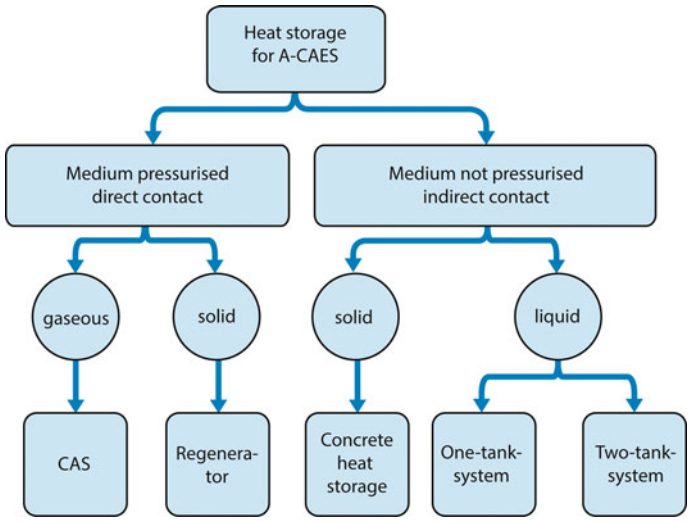



**Fig. 9.10** Classification of thermal storage types used in adiabatic CAS

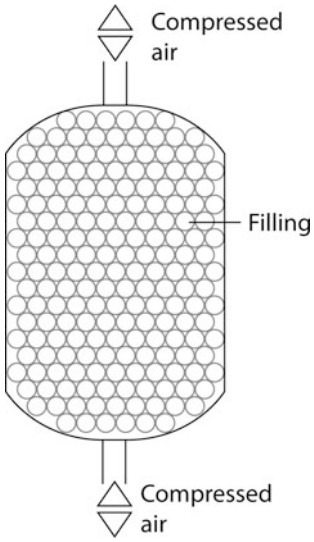



**Fig. 9.11** Vertical flow regenerator with direct contact between the compressed air and solid thermal storage medium

in Fig. 9.11, horizontal layers at varying temperatures are formed. If the regenerator is fully charged, for example, then the temperature of the storage medium at the upper inlet is approximately the same as the air inlet temperature. At lower levels, the temperature increasingly falls until the solid material at the lower outlet is at the air outlet temperature.

The use of regenerators in A-CAES is currently the subject of a number of studies to determine which solid material should be used and how it should be constructed [15, 23, 25, 26, 60].

In the second technology approach shown in Fig. 9.10, the storage medium is not under pressure in the storage unit. The compressed air is fed in through pipelines that physically wall off the air from the thermal storage medium. But in these kinds of heat transfer systems, heat transfer is reduced by thermal resistance in the pipe material.

Solids that can encase the heat exchanger are an excellent choice here. Special storage units using concrete to encase the pipes have been developed for use in A-CAES. Similarly, liquids can be used as thermal storage media by placing the heat exchange pipes vertically in the liquid as shown in Fig. 9.12. But since liquid storage media can typically be pumped, they can also be fed through the heat exchanger and then stored in an external container. As in the regenerators described above, in these kinds of one-tank systems (Fig. 9.12) temperature-layering is unavoidable. But with liquids, there is a risk that the layering of the storage medium could be destroyed by mixing. As a result, the inlet and outlet design is particularly important in systems using pumped liquid media. An al-

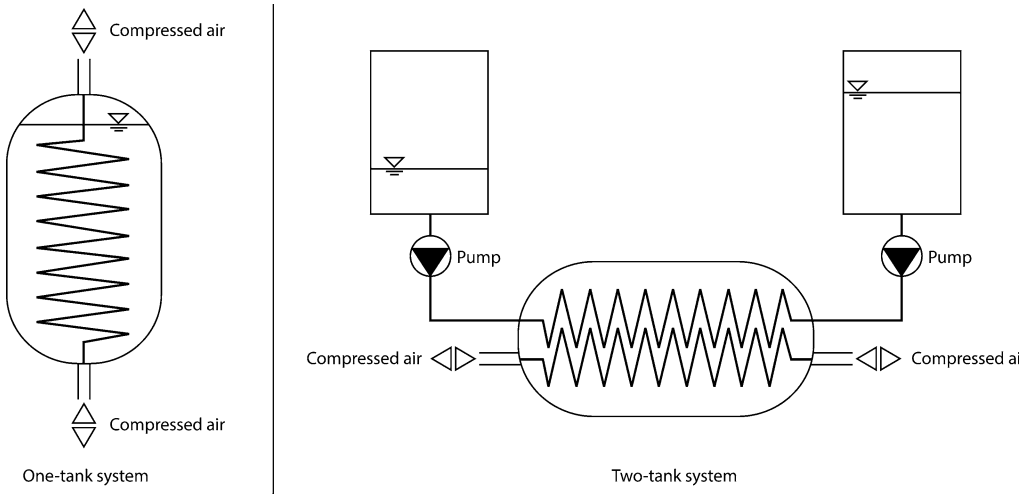



**Fig. 9.12** Thermal storage systems with indirect contact between the compressed air and liquid thermal storage medium



ternative is the two-tank system (Fig. 9.12). Here, warm and cold storage media are kept in separate containers. This system results in no temperature-layering, eliminating the problem of the liquid mixing in the container.

### Adiabatic CAS Designs

Between 2003 and 2007, an EU project developed an advanced adiabatic compressed air energy storage (AA-CAES) concept (▶ Sect. 9.4). In this concept the air intake is compressed by an axial compressor to 2 bar, cooled down once, and then raised to a final pressure of 62 bar by radial machines (Fig. 9.13).

During the process, the temperature of the air is raised to around 620 °C. The hot air is then fed through a TES used as a direct flow regenerator. Solid material fill is used as the storage medium, explaining why the TES shown here is also described as fill bed storage. The air sheds some of its thermal energy by flowing through the TES. It is then fed at temperatures ranging from 30 to 50 °C into the CAS and stored there. The system also features an emergency cooler placed between the TES and CAS. This ensures that the temperature of the compressed air does not exceed the temperature tolerated by the underground salt caverns used in this case. Further information about the use of underground caverns and other methods of storing compressed air can be found in ▶ Sect. 9.1.3. During discharging, the compressed air is removed from the cavern and fed through the TES in the opposite direction. The air is heated by flowing through the TES, and then fed into the expander at a temperature of 600 °C and a pressure of 55 bar. The air is expanded to atmospheric pressure in the expander without any additional heating (Fig. 9.14)

This adiabatic CAS concept results in cycle-efficiency levels ranging up to 70% [35]. Due to the high temperatures and the thermal stresses they cause, the facility requires 15 minutes to reach its rated power after start-up.

The thermal storage technology used in the AA-CAES project facility has significant advantages. These include the low-specific costs of the fill material (gravel, ceramic, and so on), high-specific storage density, and high cycle-efficiency. But because the TES is directly impacted, it must be specially designed to withstand the high temperatures and pressures in the system. The compressors used must be able to withstand high temperatures as well. Since there is currently no demand for compressors of this sort, compressors sold today can only withstand temperatures of up to 400 °C. As a result, major advances are required in both

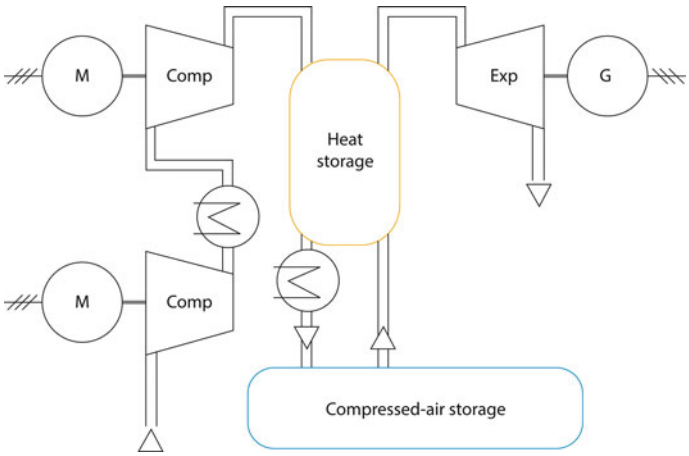



**Fig. 9.13** Simplified schematic design of an adiabatic high-temperature CAS facility using the AA-CAES concept

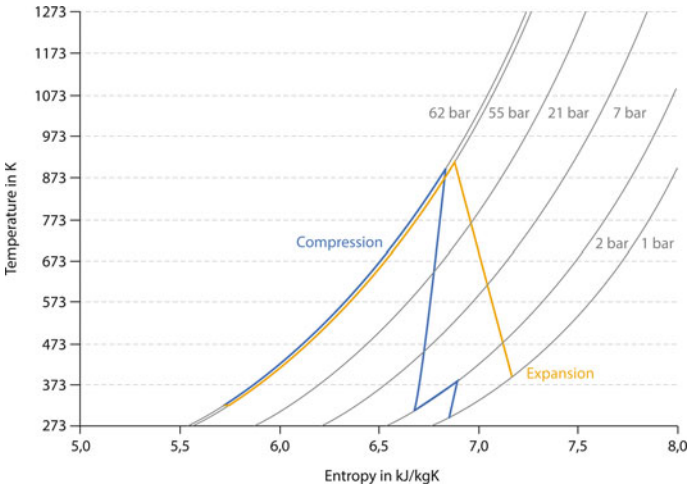



**Fig. 9.14** *T*-*s* diagram of an adiabatic high-temperature CAS facility

areas. The ADELE project, a collaboration between science and the industrial sector, has been working on building a pilot facility since 2010 [48, 49].

Other concepts focus on eliminating these requirements by reducing the storage temperatures. This would allow compressors currently available on the market to be used. But at the same storage pressure, frequent intercooling of the compressed air would be required. This would increase the facility complexity, because then it would also be necessary to use two thermal storage units connected in series, however, this would allow compressors currently on the market to be used. The process configuration has little effect on the cycle-efficiency, because the cycle-efficiency of adiabatic CAS facilities is chiefly determined by how fully the compression heat is utilized, and not by the absolute storage temperature [8].

Figure 9.15 shows a block diagram of an A-CAES with storage temperatures of nearly 400 °C [58]. Two direct-flow TES are used, meaning the compression heat is transferred to a thermal storage medium during compression at two points.

In the facility in Fig. 9.15, ambient air is intercooled once after the first compression step, and then compressed to a medium pressure level. At the outlet of the second compression step, the air reaches a temperature of around 400 °C. This outlet temperature is compatible

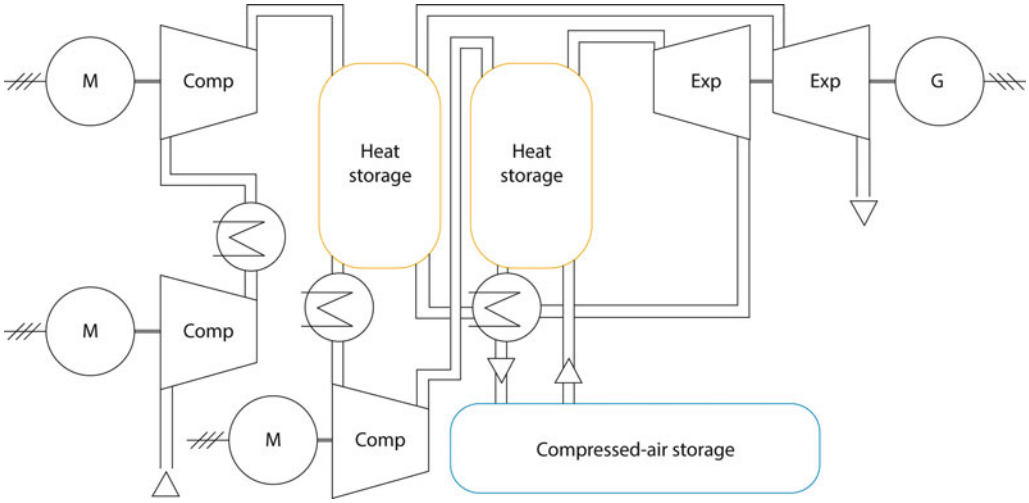



**Fig. 9.15** Simplified schematic design of an adiabatic, medium-temperature CAS facility



with compressors available on the market today. After releasing compression heat in the first TES, in a second compression step the compressed air is brought up to the required storage pressure. In this second compression step, the air again reaches temperatures ranging around 400 °C. As a result, it can also charge the second TES. A two-step expansion process with two preheating steps to temperatures of around 380 °C in the two TES is used to discharge the storage facility. With this kind of facility layout, the cycle-efficiency does not vary significantly from a facility with one TES and significantly higher storage temperatures. Since the thermal stresses are just as high, the start-up time also remains the same [58].

Currently under study are facility layouts with even lower storage temperatures that could use currently available standard components in the compressors, expanders, and TES [8, 9]. Four-step thermal storage systems are required with temperatures ranging from 80 to 200 °C.

Figure 9.16 illustrates a facility of this type. By distributing compression over six compression steps, each including intermediate heat transfer to a liquid storage medium, the compression outlet temperature can be significantly reduced in comparison to one or two-step facilities using the same storage pressure. Since temperatures are low, storage media used for a range of other applications, such as water or thermal oil, can also be used here. In addition, these media can be used in two-tank thermal storage systems since (depending on the process status) they can be pumped. Simple pipe-bundle heat exchangers, for example, can then be used in these cases to transfer the heat from the compressed air to the storage medium. The discharging process also requires several steps, repeatedly preheating the compressed air up to the low storage temperature [14].

This concept results in cycle-efficiency levels ranging around only 56% below the other facilities described here. But since these facilities can be started up in five minutes, they could serve different segments of the market. Figure 9.17 illustrates the design of a facility of this sort [14].

A number of heat exchangers remove the compression heat produced after each individual compression step, and then return it to the compressed air after each expansion step. On the left side of the illustration, the air is drawn in from the ambient air and then compressed to the storage pressure using (in this facility) an eight-step radial compressor. On the right side, the storage volumes are connected to the high-

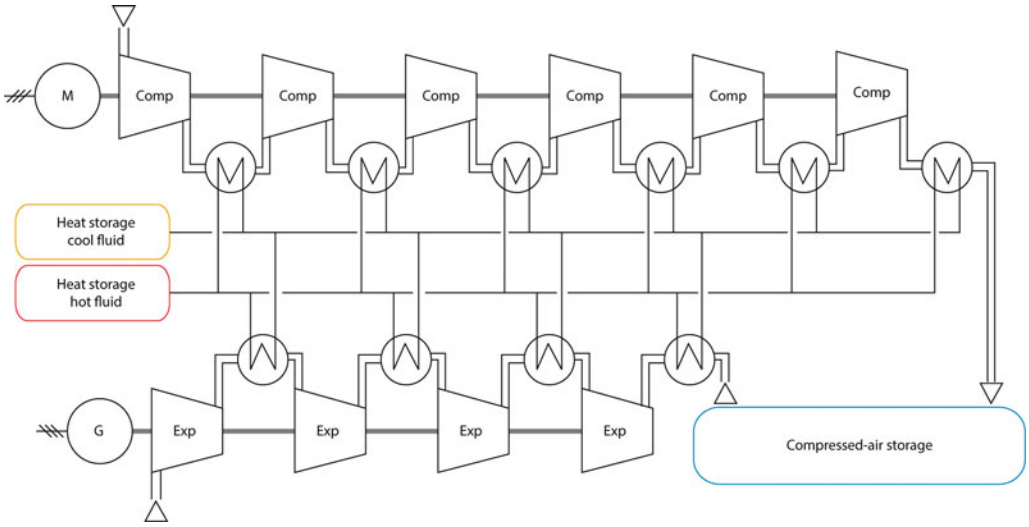



**Fig. 9.16** Simplified schematic design of an adiabatic low-temperature CAS facility

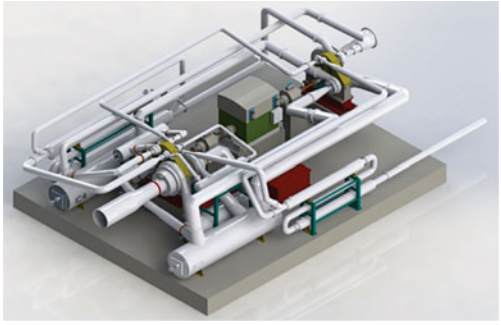


**Fig. 9.17** CAD model of an adiabatic low-temperature CAS facility (LTA-CAES®) [14]

pressure outlet pipe. To discharge the storage, the compressed air flows in the opposite direction back through this pipe. It is then expanded to ambient pressure by the four-step radial expander also on the right-side of the illustration (Fig. 9.16).

### 9.1.2.2 Isothermal CAS

Unlike CAES concepts that store the compression heat produced and then use it during expansion, isothermal concepts limit the change in temperature during the pressure change phases. The ideal result here would be no temperature increase during compression and no temperature drop during expansion—in other words, a thermodynamically isothermal change-of-state. The advantage of this kind of change-of-state is that all the energy fed into to the compressor is available for changing the air pressure. In the ideal case then, heating the medium results in no losses. This means that isothermal compression has particular advantages for electric-energy storage. But in fact nearly all industrial scale compression processes attempt to approximate an isothermal change-of-state by repeatedly intercooling the compressed gas. Adiabatic CAES concepts with low storage temperatures basically do the same. But with each intercooling, additional temperature and pressure losses occur in the heat exchangers used.

As a result, isothermal compressed air energy storage (I-CAES) concepts attempt to eliminate these additional losses by approximating an isothermal change-of-state in the compressor or expander itself. Since the heat must be removed from, or added to, the air in equilibrium with the compression heat produced, the speed of the change-of-state is decisive. Thermal flows adequate for this purpose can only be generated if the state of change is

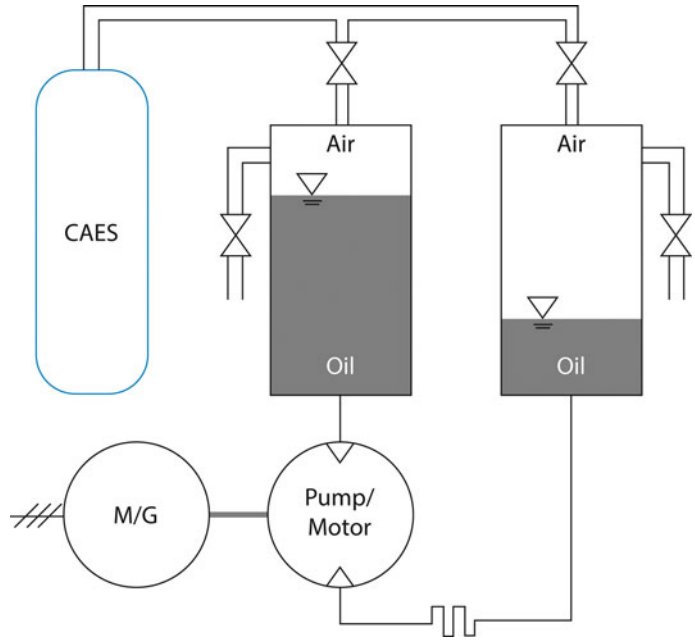



**Fig. 9.18** Simplified schematic design of an isothermal CAS facility



slow enough. Besides, by slowing the speed, an isothermal process can be more closely approximated by improving the heat exchanges and reducing the amount of compression heat produced.

Because the speed if so decisive, isothermal CAS systems typically use reciprocating engines. These engines have good efficiency levels even at slower speeds. Using the largest reciprocal engines available and running them slowly effectively limits the volumetric flow. This also limits the potential power of each individual unit to around 2 MW. As a result, this module size is common in the concepts currently under development. The facility power can be increased by connecting several modules together [53].

Isothermal CAS facilities were tested extensively in 2006 [32]. The primary purpose of these tests was to ensure that the compression heat produced was successfully absorbed and then returned to the compressed air during expansion. Here, engines were used that operated on the same principle as reciprocal engines, but which used a fluid column (such as oil) to compress or expand the air instead of a piston. This means that the energy was converted by a hydraulic engine, which is more efficient than a pneumatic engine (Fig. 9.18). At the same time, the fluid column absorbs part of the compression heat produced. The heat transfer here is especially effective since the air and fluid come into direct contact.

Building on this concept, the goal of current research is to improve heat transfer by adding components in the piston chamber of a conventional reciprocal engine [21, 53].

But these modifications are limited by the heat transfer surface area available. Since the piston chamber has a limited volume, little space is available for additional components. In fluid columns, the surface area of fluid that can be used for heat transfer is limited by the diameter of the piston chamber.

Scientists are currently working on overcoming these limits. One approach is to spray water into the piston chamber, increasing the surface area available for heat transfer. Here very small water drops are formed whose surface area is very large in relation to their volume. This significantly improves heat transfer from the air to the water. Adding water also im-

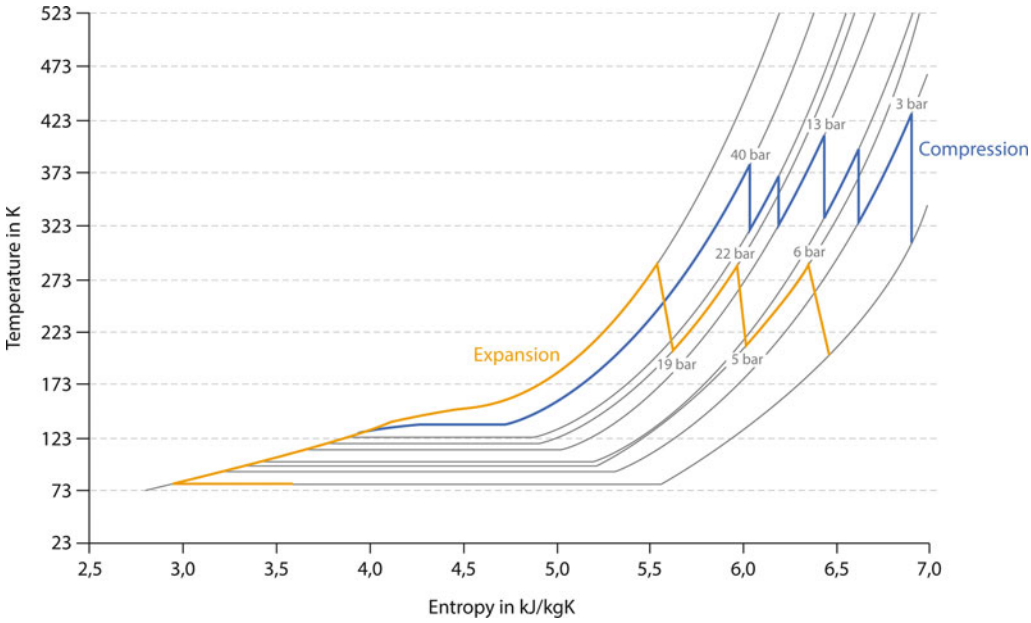



**Fig. 9.19** *T-s* diagram of a LAES facility without additional heating

proves the air's heat capacity, further minimizing the change in temperature. The compressed air and water produced are stored either separately or together after compression, depending on the concept. To achieve a similar effect during expansion, the water is then sprayed back into the piston chamber [10, 53].

### 9.1.2.3 LAES

The LAES concept is based on the Linde process for liquefying air. This common industrial process can also be used for electric-energy storage because electric energy is absorbed from the network to operate the compressor during air liquefaction. As with all the CAES processes described above, this means that the electricity is first converted into potential energy in the compressed air. The ambient air intake is compressed to 70 bar in several steps and repeatedly intercooled (Fig. 9.19).

But here, the cold, compressed air is then expanded before being fed into the storage volume. Using the counterflow principle, during expansion the air temperature falls so low that it enters a liquid state. Air in a liquid state has a higher-energy density, and can be stored in insulated tanks at ambient pressures. The energy density of liquid air is about ten or twenty times higher than the energy density of the compressed air in the concepts described above. Unlike with most industrial scale CAES facilities, this means that the facilities are not geographically limited to areas that offer suitable CAS volumes, such as salt caverns (▶ Sect. 9.1.3). To extract the stored electric energy, the air is warmed to ambient temperatures so that it returns to a gaseous state. The pressure of about 40 bar produced as a result can be exploited in several expansion steps. Because the temperature of the vaporized air during expansion is very low (around 10 °C), the system can also utilize low-temperature waste heat (< 90 °C) that is otherwise difficult or impossible to exploit. This significantly increases the otherwise rather low cycle-efficiency level. Figure 9.20 shows the T-s diagram of a process without additional heating. This process has a cycle-efficiency level of around 30%. These facilities have start-up times of less than ten minutes [31].

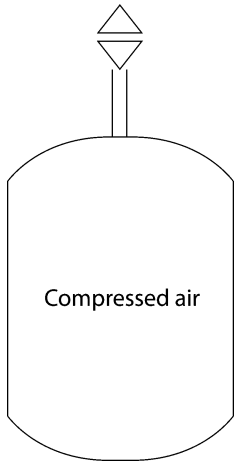



**Fig. 9.20** Isochoric gas storage volumes

### 9.1.3 Compressed Air Energy Storage Volumes



A crucial component of CAS power plants as well as all CAS facilities is the storage volume used to store the compressed air. Besides primarily determining the compressed air system's storage capacity, this component also has a significant effect on the design of the other system components. There are two types of storage volumes.

#### ■ Isochoric Storage Volumes

Isochoric CAS maintains a constant volume (Fig. 9.20). This means that during loading and unloading, the pressure of the gas stored continually changes.

A conventional gas cylinder is a simple example of an isochoric storage volume. It has a defined volume and a maximum permitted cylinder pressure. When the gas cylinder is opened, the gas held under pressure escapes and the cylinder pressure falls over time. For use in a blowtorch, for example, the gas must be kept at a constant pressure. But this pressure is typically far below the pressure of the gas cylinder. This means that the primary reason the cylinder pressure is so high is to reduce the amount of space required to store the gas. As a result, most gas cylinders have a pressure regulator as well. This reduces the current pressure in the cylinder to the constant operating pressure required. The isochoric storage volumes used at the Huntorf and McIntosh CAS power plants operate on the same principle. Depending on the load state, both facilities operate at storage pressures ranging from 45 to 75 bar. Before expansion in the gas turbine, the compressed air is released from the CAS at a controlled constant turbine inlet pressure of 41 bar. This is to accommodate the combustion chamber's maximum permitted pressure load. Systems without combustion chambers can ignore this pressure limit. As a result, they operate on both the compression and expansion side at varying pressures.

#### ■ Isobaric Storage Volumes

Isobaric CAS maintains a constant pressure over the entire loading and unloading process. This is achieved using hydraulic compensation balancing the compressed air in storage with a fluid. When compressed air is pushed into the container, it comes into direct contact with the fluid and pushes it back. The fluid then escapes into another container. If the difference in elevation is adequate, this balancing container can be maintained at ambient pressure. This means that the fluid column determines the pressure in the CAS (Fig. 9.21).

#### ■ Construction Design

Isochoric and isobaric storage volumes can be built either aboveground or underground. Overground storage volumes can be constructed using containers or pipes made of steel or composite materials. Spherical containers made of other materials such as concrete are also an option. The key characteristics of aboveground storage volumes are as follows.

Advantages:

- Generally feasible in any geographical location
- Permits large pressure differences

Disadvantages:

- High-specific capital costs
- High space requirements, even for moderate storage volumes

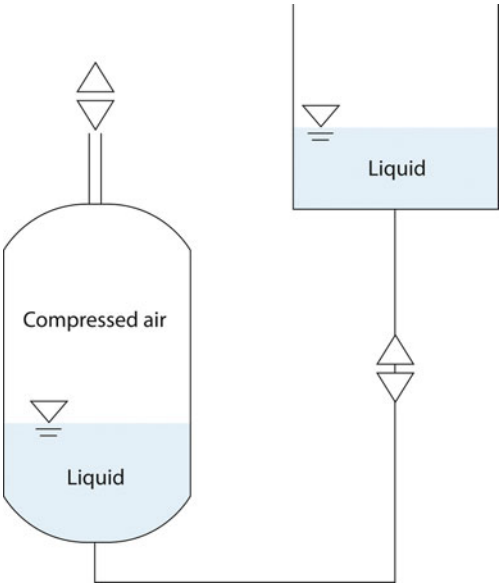



**Fig. 9.21** Isobaric CAS with hydraulic compensation

- Frequent pressure and safety inspections required

There are several different basic types of underground storage volume designs. The primary requirements for an underground cavern suitable for use as storage with a CAES power plant is that it can withstand the pressure range used by the plant over the long-term, and that it is (or can be) made gas-tight. A secondary requirement is low enough flow-resistance in porous reservoirs to allow sufficiently high loading and unloading rates. In addition, exposure of the original geological environment to the oxygen in the compressed air must not trigger any chemical or biological reactions.

Solution-mined salt caverns make especially practical storage volumes. This is because they feature:

- Long-term stability, even with large fluctuations in pressure, as well as high $\Delta p/\Delta t$ gradients typical of CAES facilities.
- Minimal flow-resistance within the storage volume, allowing high loading and unloading rates.
- Exceptionally gas-tight.
- Low-specific costs.

But since, especially in many regions outside Germany, salt formations are not available, scientists have focused on finding alternative solutions. Depleted oil/natural gas reservoirs are certainly very large, but there are major risks associated with exposing the residual oil or gas to compressed air. Porous groundwater-bearing reservoirs or aquifers are a preferable solution. The porous space is similar in structure to a sponge. The flow-rates required for compressed air can be ensured by adding a large number of access boreholes or using reach-drilling where necessary. A critical factor is the potential reactions between the oxygen in the air at high partial pressure and the mineral components in the reservoir, because oxidation may then reduce the oxygen content of the unloaded compressed air. Reactions with microorganisms in the reservoir are also a risk and, in the worst case scenarios, may cause clogging in the pore matrix.

In the USA, tests were performed on these caverns in the 1980s [4, 57]. They demonstrated that oxygen reacts with reservoir rock, reducing the oxygen content of the compressed air. In addition, the volume flows required could only be achieved by adding a significant number of additional access boreholes. Overall development costs with aquifer use were also shown to be significantly higher than with salt caverns. The primary cost driver here was the geological exploration required to judge the capacity and impermeability of the formation. Even with exploration, choosing a suitable location is still highly risky.

Another option is abandoned mines, some of which have enormous volumes. But since extraction mines were not originally designed to store compressed air, proving their stability and impermeability is a major challenge. Underground storage volumes share the following characteristics.

Advantages:

- Low aboveground space requirements
- Low-specific capital costs

Disadvantages:
- Only feasible where suitable geological formations are available
- Geologically limited pressure differences apply

The Huntorf and McIntosh CAS power plants use solution-mined salt caverns as isochoric storage volumes [44, 45]. The primary advantage of salt caverns is that, for decades, they have been used to store seasonal natural gas reserves, strategic oil reserves, and to a limited extent, compressed air. Since engineers have extensive experience with constructing these caverns, the technology is extremely well-developed. In addition, salt rock can be assumed to be technically gas-tight, meaning there are only negligible pressure losses over the technically applicable time periods. The greater the layer-depth of a gas cavern, the greater the permitted range of maximum to minimum pressures, and the greater the energy content by volume. In practice, feasible layer-depths range from 600 to 1,400 m. A unique characteristic of salt rock is that the material flows under pressure (similar to the ice in a glacier), especially at higher temperatures. The solidity of the rock decreases at higher temperatures as well. As a result, the compressed air injected into the cavern must be cooled to a temperature around 50 °C or below.

Construction of a salt cavern with brine shuttle ponds to create an isobaric storage volume was planned for a CAS power plant in the USA, but neither it nor the power plant was finally built [43]. Some current concepts also use isobaric storage volumes of this sort [41].

Salt caverns have many advantages, however, many regions simply do not have suitable salt formations. As a result, scientists have focused on finding alternative solutions. The use of other geological formations without salt stone has been tested but not implemented. Porous groundwater-bearing aquifer structures are one option. These are porous layers of rock sealed from the surface by gas-tight rock layers. Tests on aquifer structures were performed in the early 1980s, mostly in the USA [5, 101]. These tests showed that volume-flows typical of salt caverns could only be achieved by adding a significant number of additional access boreholes to reduce flow-resistance in the pore matrix. A more serious problem was that oxygen reacts with reservoir rock in the cavern, reducing the oxygen content of the compressed air. In addition, overall development costs with aquifer use were determined to be significantly higher than with salt caverns. The main reason was the geological exploration required to judge the capacity and impermeability of the formation.

Even with exploration, choosing a suitable location is still highly risky. After extensive geological exploration and model analyses in the USA, the Dallas Center (Iowa) aquifer structure was chosen for the construction of a compressed storage power plant [29]. But after the first boreholes were drilled, tests determined that the volume flow required could not be achieved and the plan was abandoned [50].

Since there is a shortage of salt formations in Japan, scientists there focused on using conventionally excavated tunnels and shafts as underground storage volumes. The challenge with these caverns is ensuring that they are gas-tight. In an abandoned zinc mine in Kamioka, a volume of 200 $m^3$ at a depth of 1,000 m was sealed off using concrete [130]. But since no other measures were taken to seal the volume, it was not fully gas-tight. In another location in Japan, a volume of 1,600 $m^3$ was sealed off with an inner rubber lining and successfully tested with pressures up to 80 bar [138].

The use of abandoned mines for CAS was also studied in Europe. In Germany, these facilities have extremely limited potential because of their high permeability [13]. In Switzerland, the use of tunnel sections is currently under study [2].

Unlike existing conventionally excavated caverns, these volumes would be specifically constructed for gas-tight storage. Lined rock cavern (LRC) technology is the latest innovation in underground cavern storage. A storage volume of this kind in Scandinavia has been successfully used for commercial storage

of natural gas for the last ten years. Especially in regions without salt rock, LRC could become a viable alternative for storing hydrogen or compressed air [133]. Another promising approach to building isobaric volumes is underwater storage facilities. Scientists are currently developing structures installed on the seabed that store the compressed air in direct contact with the water around it. Flexible containers and balloons anchored to the seabed are also under study. In these facilities, the compressed air is physically separated from the water around it by a thin container casing [42]. An advantage of both system types is that the water around the facility exerts a constant pressure determined by the depth of the storage facility.

#### Storage Capacity

From a technical point of view, all the storage types described above could be constructed in virtually any size. But depending on the capital costs, the benefits vary in different application areas. An important factor is that the storage capacity of a CAS facility is determined by both the geometric volume as well as the storage pressure. In what follows, the various storage types are generally categorized by their geometric volume. This is because the permitted storage pressure is determined by a range of boundary conditions. As a rule of thumb, the storage density can be assumed to range from 1.8 to 9 kW h/$m^3$.

Solution-mined salt caverns with geometric volumes exceeding 150,000 $m^3$ have very low-specific capital costs. This is because the costs to enlarge the cavern are low once solution mining has begun. With smaller salt caverns, the high start-up capital costs of drilling dominate. This dramatically increases the specific capital costs. Depending on the cavern depth, the maximum pressure can range up to 200 bar. The CAES expansion potential in Germany using salt caverns has been estimated at a geometric volume of 200 million $m^3$ [5]. Depending on the facility type, this is equivalent to a storage capacity of 600 to 900 GW h.

High costs for deep drilling are also a disadvantage with aquifer storage facilities. Although there are no costs for creating the underground storage volume, with these storage facilities, a significant number of additional access boreholes are required to achieve charging and discharging capacities comparable with solution-mined salt caverns. As a result, aquifer storage is best-suited for very high storage capacities requiring moderate charging and discharging capacities.

Other underground caverns typically requiring significant investment to seal them and ensure they are gas-tight are better-suited for moderate storage volumes (up to 150,000 $m^3$). The same is true for underwater storage volumes and aboveground pipe storage facilities often used to store natural gas.

There are several cylindrical pressurized containers in operation that contain volumes up to 200 $m^3$ at pressures up to nearly 200 bar. Smaller volumes can be stored using a number of gas cylinders or gas cylinder racks (up to 0.15 $m^3$ and 300 bar per cylinder).

### 9.1.4 Conclusion

Network-connected electric storage can, in general, be used for a wide range of applications. But not all technologies are equally suited to the various applications. Clearly, compressed air energy storage is not generally appropriate for certain applications. These are primarily applications requiring very fast reaction times. Examples here include compensating for flickering or voltage fluctuations in the network and ensuring uninterruptible power supply (UPS). The following specifies which application areas best suit the air energy storage technologies described in this section.

#### Application Areas by Type of Compression and Expansion Technology Used

Because they use standard gas turbines, currently existing and planned CAS power plants require a certain amount of minimum power. As a result, the uses of this

technology are similar to the uses of gas turbine power plants. With adequate storage volumes, these power plants are useful for temporally shifting large quantities of energy and providing network services such as minute-reserves. They can also provide reactive power control and black-start capability at the network level.

- The A-CAES concepts currently under discussion are suited for use in the same application areas. Because they use turbomachinery technology comparable with the technology used in D-CAES, facilities with high storage temperatures, they have practically the same start-up characteristics. Due to their faster start-up times, A-CAES concepts with low storage temperatures can also serve the secondary balancing energy market (required reaction time < 5 min) [14]. The LAES concepts described above have similar start-up characteristics.
- Smaller A-CAES can be used to compensate for generation and consumption peaks, or to secure stand-alone networks. Since most of the concepts use turbomachinery technology, A-CAES typically requires a minimum power in the megawatt range. As a result, they are best-suited for use with large, fluctuating suppliers (for example wind parks) or large consumers (for example industrial facilities) [12].
- I-CAES facilities could be easily integrated into these applications areas as well. But by using reciprocating engines, I-CAES facilities could also be used for lower power applications (< 1 MW) and remain efficient. As mini-CAES, they could also potentially be used for storage in households.

#### Application Areas by Type of Storage Volume Used

- As with the various machine types, there are also ideal application areas for the storage volumes used. The storage capacities that suit the various storage volume types from a technical and economical point of view were discussed above in ▶ Sect. 9.1.3. In general, large storage volumes are best-suited for shifting large quantities of energy for load balancing at a central location in the network. Typically these kinds of volumes (for example salt caverns) are in any case geographically fixed. Because of their geographical flexibility, moderate volumes are best-suited for decentralized network support applications, or generation and consumption optimization. Because of their limited storage capacity, very small volumes on the scale of gas cylinder racks are best-suited for end consumer use in areas such as self-consumption optimization and self-sufficient electricity supply.

## 9.2 Liquid Media

### 9.2.1 Pumped-Storage Plants

Hydropower has been used as an energy source for thousands of years. Starting in the 3rd century B.C., hydropower was used in China to operate mechanical tools [61]. In Germany, pumped-storage technology was first used to store energy at the turn of the 20th century [63].

This section discusses pumped storage and pumped-storage power plants. The storage and power capacities of these types of power plants currently are by far the largest. No other storage technology even comes close in scale. Pumped storage is also a tried and tested technology that is still being improved today with new machine components, for example. As a result, its contribution is critical is transitioning energy supply to renewable energy sources [62, 63].

#### Pumped-Storage Plants

Pumped-storage plants (or pumped-storage power plants, or simply pumped storage) includes an upper and lower reservoir. Typically these reservoirs are artificially constructed. The upper reservoir is a separate reservoir with no or negligible natural intake. The lower reservoir can either flow into a river or be self-contained. Pumped-storage plants are chiefly used to store electric energy during low-load

times and generate electricity during peak-load times. They are also used to keep the power system frequency stable and to provide reactive power control, which is called synchronized condenser operation. Without natural water intake, pumped-storage plants are considered pure energy storage (electricity storage), and not a renewable energy source [64].

When the network requires energy, for example to cover peak loads, the generator in the machine house generates electricity that is then fed into the public network using a transformer. The generator is driven by the turbine, which is in turn driven by flowing water. A surge tank is used to balance rapid pressure changes during electricity generation start-up or shutdown. During low-load times, surplus energy from the network is used to pump the water from the lower reservoir to the upper reservoir. The upper reservoir is generally designed to allow full load operation for at least three to five hours. With larger storage reservoirs, the water reservoir is adequate to generate power for an entire weekend. Since pumped-storage facilities are high-pressure facilities and drop-heights can far exceed 50 m, Francis and Pelton turbines are used in these facilities. The choice of turbine is determined by the required power, the drop-height, and the flow-rate [63].

- **Storage Power Plants**

Storage power plants also exploit the potential energy of altitude differences. Here the upper reservoir is formed by damming a river. This means the upper reservoir has a natural intake. This intake is typically adequate to supply the upper reservoir's storage requirements. If not, water can be pumped to the upper reservoir just as in a pumped-storage power plant [65]. Depending on the storage volume and intake, storage power plants are categorized as daily, weekly, seasonal, and annual storage facilities [66]. Since the drop-heights are on average small, Kaplan and propeller turbines are used in these facilities. Based on the drop-height and the turbine type, storage power plants are classified as high-pressure or medium-pressure facilities. But there is a gray area between high-pressure and medium-pressure facilities [65]. Besides electricity generation, storage power plants are also used to supply cities, agriculture, and the industrial sector with water, to regulate water levels for shipping, and to protect against flooding. Supported by a computer system, the dam also filters out waste or floating debris, and prevents fish from entering the turbines [61].

Storage power plants are considered a renewable energy source. At the same time, they are a form of primary energy storage.

#### 9.2.1.1 Basic Principles

The energy used by hydropower plants to generate electricity is a kind of potential energy called energy of position. This is the difference in energy between a higher position and lower position (see ◘ Figs. 9.22 and [63]).

Since the upper reservoir is above the lower reservoir, it has a higher potential energy. This energy is also called work capacity. It is calculated from the storage content $V$, the density of water, the force of gravity, the effective drop-height $\Delta h$, and the total efficiency $\eta_{\text{total}}$.

$$E = V \cdot \rho \cdot g \cdot \Delta h \cdot \eta_{\text{total}}, \tag{9.5}$$

with

$E$ – potential energy,
$V$ – volume,
$g$ – gravitational acceleration ($g = 9.81\ \frac{\text{m}}{\text{s}^2}$),
$\rho$ – density of water ($\rho \approx 1{,}000\ \frac{\text{kg}}{\text{m}^3}$),
$\Delta h$ – effective drop-height,
$\eta_{\text{total}}$ – total efficiency.

If $Q$ is the outflow, the power is then given by:

$$\begin{aligned} P &= \dot{E} = \dot{V} \cdot \rho \cdot g \cdot \Delta h \cdot \eta_{\text{total}} \\ &= Q \cdot \rho \cdot g \cdot \Delta h \cdot \eta_{\text{total}}, \end{aligned} \tag{9.6}$$

with

$P$ – power,
$\dot{E}$ – time derivative of the potential energy,
$\dot{V}$ – time derivative of the volume,
$Q$ – outflow/flow-rate.

The outflow (also called the flow-rate) is the volume of water that flows through the pressure pipeline over a specific unit of time.

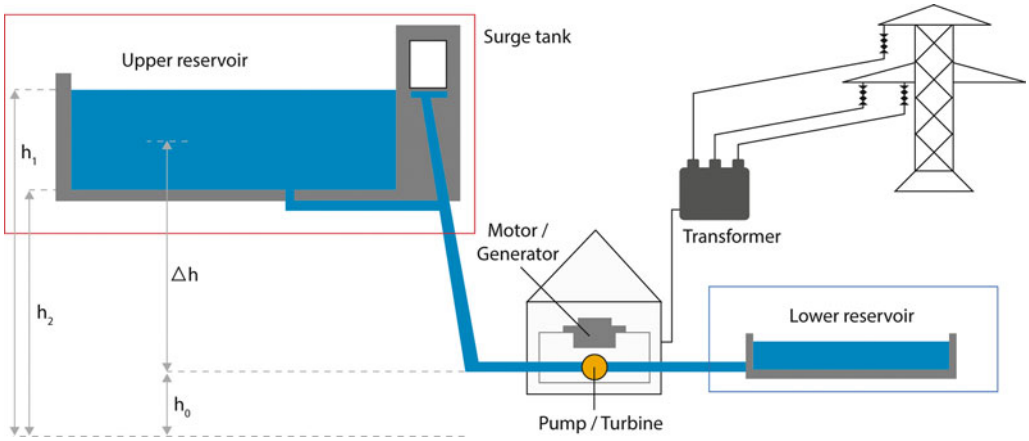



**Fig. 9.22** Upper reservoir/lower reservoir relationship



The effective drop-height shown in Fig. 9.22 is calculated from the mean height of the storage reservoir floor and the water surface subtracted by the height of the lower reservoir. This figure is proportional to the work capacity as well as to the power.

$$\Delta h = \frac{h_1 + h_2}{2} - h_0, \tag{9.7}$$

with

$h_0$ – lower reservoir height,
$h_1$ – storage reservoir surface height,
$h_2$ – storage reservoir floor height.

### 9.2.1.2 Parameters

The key parameters of pumped power plants and storage power plants are:

- Efficiency
- Losses
- Energy density
- Power density
- Full load hours

The efficiency is the ratio between the electric energy yield or the electric power and the supplied electric energy or electric power. The losses that determine the efficiency level are illustrated in Fig. 9.23 using a pumped-storage plant as an example.

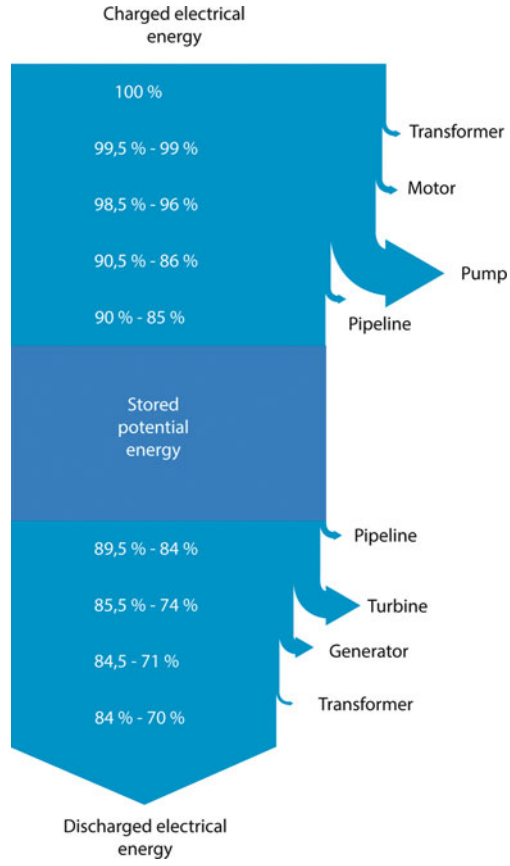



**Fig. 9.23** Losses/efficiency

The supplied electric energy is always larger than the electric energy recuperated. With pumps and turbines, losses occur in the transformer, the generator or motor, the turbine or pump, and the pipeline. The total efficiency of a generator or pump is calculated by multiplying the partial efficiencies:

$$\eta_{\text{total}} = \eta_{\text{P}} \cdot \eta_{\text{T,P}} \cdot \eta_{\text{G,M}} \cdot \eta_{\text{Trans}}, \tag{9.8}$$

with

$\eta_{\text{P}}$ – pipeline efficiency,
$\eta_{\text{T,P}}$ – turbine/pump efficiency,
$\eta_{\text{G,M}}$ – generator/motor efficiency,
$\eta_{\text{Trans}}$ – transformer efficiency.

Modern pumped-storage plants have efficiency levels ranging up to 83% [63]. The energy density, i.e., the ratio of the potential energy to the volume of pumped water, is calculated as follows:

$$w = \frac{m \cdot g \cdot \Delta h}{V} = \rho \cdot g \cdot \Delta h, \tag{9.9}$$

with

$w$ – energy density,
$m$ – mass.

Due to the extremely large volume, the energy density is very small and in the same range as capacitor energy density.

The power density is the ratio of the electric power to the volume. Because water density is higher, water turbines have higher power densities than gas or steam turbines [65].

#### ■ Service Life

Pumped power plants and storage power plants generally have a very long service life. But they require regular maintenance and repairs. Because of the large volumes of water, the machine components are exposed to significant dynamic, mechanical, and thermal stress. The storage reservoir and the dam are exposed to the elements, causing severe strain. Water level fluctuations and temperature changes are also important factors. The water exerts enormous pressure on the concrete walls. Potential energy and efficiency losses of up to 10% are caused by water losses through leaks in the upper reservoir. Water evaporation and seepage are negligible [63].

The service life of the Goldisthal pumped-storage plant, for example, has been estimate at 80 to 100 years. Two weeks of maintenance and repairs are scheduled each year. Extensive inspections are performed over two to three months every five years, or over six months every 15 years [66].

The Vianden power plant is another example of long service life with pumped power plants and storage power plants. No ageing or wear was detected at the facility for over 40 years after it went into operation. In addition, the problems found at that time could be eliminated by undertaking extensive repairs. Shorter inspections were performed every two to three years (over two to three weeks) and general inspections every ten to 15 years (over about 26 weeks). These inspections effectively ensured the facility's excellent availability and reliability [67].

Examples of practical applications for pumped-storage plants in Germany and across the world are discussed in ▶ Sect. 13.1.2.

### 9.2.1.3 Costs

The construction costs for hydropower facilities vary extremely widely. They are determined by the size of the reservoirs and the machine components, by the country or location, and by whether the facility is constructed from scratch or a converted existing facility. As a result, few general statements about cost can be made. The specific capital costs of constructing a large new facility with a power of 20 MW in Spain were 440 €/kW. But this facility is an exception. Construction costs for small power plants (500 kW to 10 MW) in Germany and Switzerland range from 1,000 €/kW for a converted facility, to 1,500 €/kW for a renovated facility, to between 4.000 and 5,000 €/kW for a new facility. Compared to new facilities, converted and renovated facilities are relatively cheap options

for increasing the yield and power capacities of older existing facilities. Construction costs are lower for larger facilities. For example, overall costs for the Goldisthal pumped-storage plant were below 600 €/kW [66].

Construction costs for a pumped-storage power plant can be reduced by up to 30% by using a powerful Francis turbine that functions as both a turbine and a pump [63].

#### 9.2.1.4 Conclusion

- Pumped power plant and storage power plant technology is the most extensively tried and tested form of energy storage at an industrial scale. As a result, it is critical for electricity storage (pumped-storage power plants) and for primary energy storage (storage power plants). These facilities can store energy surpluses (preferably from renewable energy sources) in low-load times and reconvert them to electricity in peak-load times.
- In addition to storing and generating energy, secondary benefits of this technology include good, fast controllability, flood protection, and water supply for cities and the industrial sector. These facilities also have a high-efficiency level of up to 83%, and long service lives.
- But they do have some disadvantages as well. Constructing reservoirs and damming rivers has a severe impact on the environment. Plant plans and plant construction projects often prompt criticism, protests by environmental activists, and public opposition campaigns. As a result, protecting the environment must be a key priority in their design [10]. Although this technology's potential is largely exhausted in Germany and cannot be significantly expanded there, resources across Europe, for example in Norway, Sweden, and the Alps, could be used to store energy from neighboring countries. But this would require extensive expansion of the European network [61].

## 9.2.2 Innovative Concepts for Storing Potential Energy in Liquid Media

### 9.2.2.1 Artificially Constructed Pumped Storage

Artificially constructed pumped-storage facilities are pumped-storage plants that exploit an artificially constructed difference in elevation between the upper and lower reservoirs. The advantage of artificially constructed pumped storage is that they can be built in regions that lack the geological features required for pumped storage—e.g., in flat or windy regions.

There are a variety of approaches to designing artificially constructed pumped storage. Figure 9.24 shows the form of artificially constructed pumped storage that is easiest to construct. The earth is excavated to construct the lower reservoir, and is then used to build a wall to contain the upper reservoir. The round form minimizes the excavation required and shortens transport distances in the facility. This artificially constructed pumped storage concept was developed by Matthias Popp, but the idea has yet to be implemented. All estimates given here come from Popp's publications.

The artificially constructed pumped storage concept can also be applied offshore. In deep water the design is reversed. The interior reservoir functions as the lower reservoir and the ocean as the upper reservoir. In regions with high evaporation rates the lower reservoir would fall somewhat. Fig. 9.25 shows a sec-

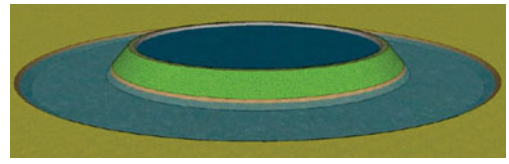


**Fig. 9.24** Artificially constructed pumped storage—model design [68]



**Fig. 9.25** Offshore pumped storage in deep water [68]

tional view of an offshore pumped-storage facility of this kind [68].

Shallower waters would permit construction of a walled off, elevated upper-reservoir. Here, the ocean functions as the lower reservoir. Figure 9.26 shows an offshore pumped-storage facility of this kind. With only one walled off reservoir, a major advantage of the offshore design is its small footprint. Plenty of water is always available, and the risk of flooding inhabited land if a leak occurred is eliminated.

Another option would be to use and expand natural or existing artificially created differences in elevation, such as abandoned surface mines where the elevation difference is too small for conventional pumped storage. Figure 9.27 shows a facility that uses existing differences in elevation in a non-circular design [68].

### Operating Principle

The operating principle of artificially constructed pumped storage is the same as with conventional pumped storage. Electricity surpluses are stored by pumping water from the lower reservoir into the upper reservoir. When electricity demand is high, the water is fed back down to the lower reservoir through a turbine connected to a generator. The electric energy produced is then fed into the network using a transformer.

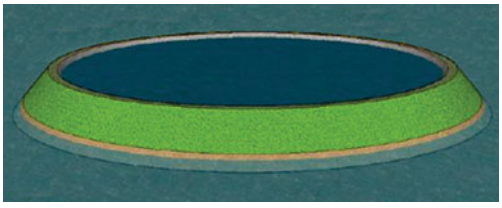


**Fig. 9.26** Offshore pumped storage in shallow water [68]

### Efficiency

The efficiency of artificially constructed pumped storage varies little from the efficiency of conventional pumped storage.

### Storage Capacity and Energy Density

The storage capacity is determined by the mass of water that can be stored in the upper reservoir, the difference in elevation between the upper and lower reservoirs, and the fluctuations in the water levels of the upper and lower reservoirs [82]. Since gravity at the Earth's surface is $g = 9.81\,\mathrm{m/s^2}$ and the density of water is $\rho_W = 1{,}000\,\mathrm{kg/m^3}$, if the average drop-height is $h_{FRWS}$ and the volume of water exchanged is $V_A$, then the potential energy stored by the water in the upper reservoir is:

$$E_{RWS} = g \cdot \rho_W \cdot h_{FRWS} \cdot V_A. \tag{9.10}$$

In an idealized circular wall design, the volume of water exchanged $V_A$ is given by:

$$V_A = \frac{\pi}{3} \cdot h_{level} \cdot \left( r^2_{Wall\ upper} + r_{Wall\ upper} \cdot r_{Wall\ lower} + r^2_{Wall\ lower} \right), \tag{9.11}$$

and is equivalent to the volume calculation of a truncated cone.

The radii $r_{Wall\ upper}$ and $r_{Wall\ lower}$ are determined by the slope angle $\alpha_{Slope}$, the fluctuation in the water level of the upper reservoir $h_{Level}$, the freeboard height $h_{Freeboard}$, and the crown width $b_{Crown}$ of the wall in Fig. 9.28, and given by:

$$r_{Wall\ upper} = \frac{d_{Wall} - b_{Crown}}{2} - b_{Wall\ upper} \tag{9.12}$$

and

$$r_{Wall\ lower} = \frac{d_{Wall} - b_{Crown}}{2} - b_{Wall\ lower}, \tag{9.13}$$

where $b_{Wall\ upper}$ and $b_{Wall\ lower}$ can be calculated using the trigonometric functions of

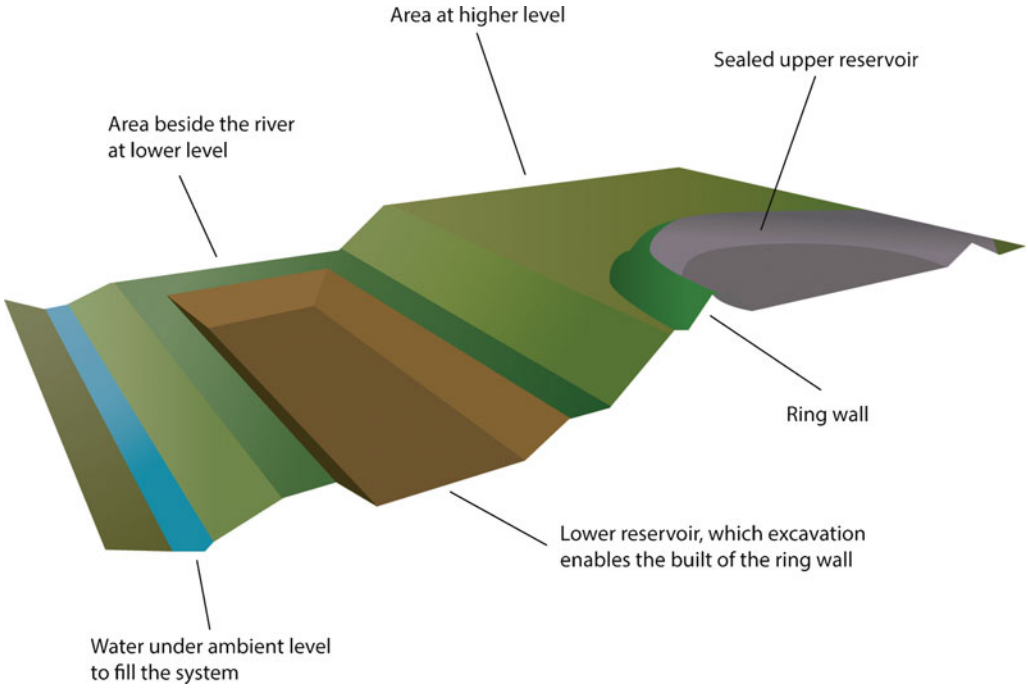



**Fig. 9.27** Artificially constructed pumped storage—alternate form [81]

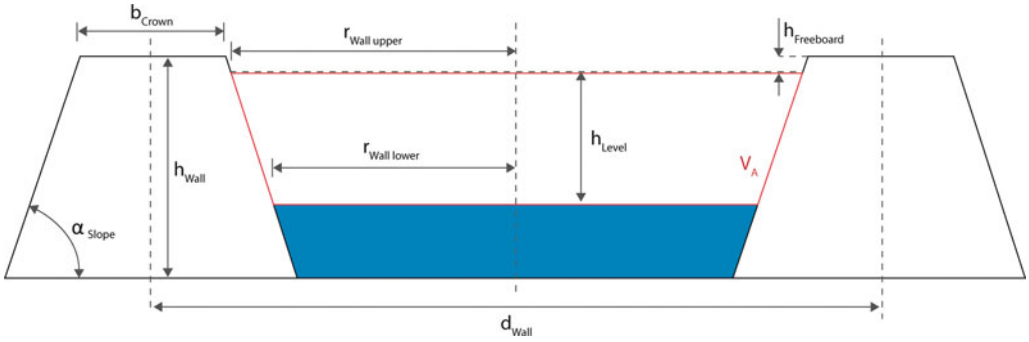



**Fig. 9.28** Sectional view of a circular wall containing an upper reservoir inside

a right-angled triangle (Fig. 9.29),

$$\tan\alpha = \frac{h_{\text{Freeboard}}}{b_{\text{Wall upper}}}$$

$$\rightarrow b_{\text{Wall upper}} = \frac{h_{\text{Freeboard}}}{\tan\alpha_{\text{Slope}}}, \quad (9.14)$$

$$\tan\alpha = \frac{h_{\text{Freeboard}} + h_{\text{Level}}}{b_{\text{Wall lower}}}$$

$$\rightarrow b_{\text{Wall lower}} = \frac{h_{\text{Freeboard}} + h_{\text{Level}}}{\tan\alpha_{\text{Slope}}}. \quad (9.15)$$

Combining these, the radii are defined by:

$$r_{\text{Wall upper}} = \frac{d_{\text{Wall}} - b_{\text{Crown}}}{2} - \frac{h_{\text{Freeboard}}}{\tan\alpha_{\text{Slope}}} \quad (9.16)$$

and

$$r_{\text{Wall lower}} = \frac{d_{\text{Wall}} - b_{\text{Crown}}}{2} - \frac{h_{\text{Freeboard}} + h_{\text{Level}}}{\tan\alpha_{\text{Slope}}}. \quad (9.17)$$

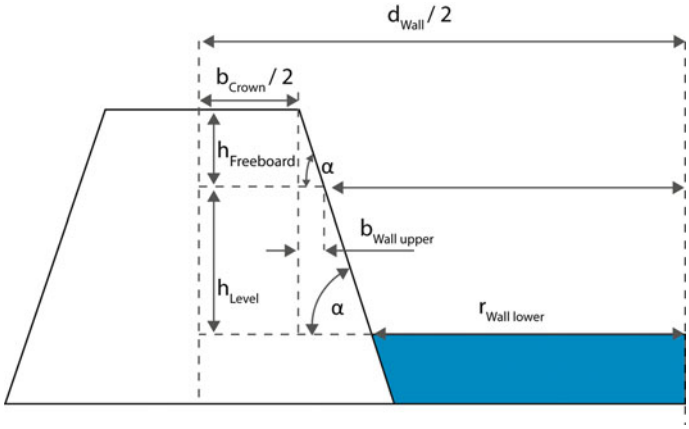



**Fig. 9.29** Radii calculations

Table 9.2 shows energy density, exchanged volume of water, and storage capacity in relation to average drop-height, fluctuation in the water level, and wall diameter.

The table shows storage capacity as gross capacity and as net capacity, taking into account losses through reconversion to electricity. The energy density is defined by how much energy per cubic meter of water is stored. It is determined by the wall height, and is approximately the same as with conventional pumped-storage plants.

With artificial pumped storage designed like the one shown in Fig. 9.24, the geometric relationships result in a dramatically increased capacity. For example, doubling the diameter quadruples the water surface area. Doubling the average drop-height at the same time doubles the energy capacity (Table 9.2). Doubling the level difference between the upper and lower reservoirs doubles the volume of water exchanged. In total, doubling all the parameters increases the storage capacity 16-fold. But since the excavation volume required to build the wall increases only eightfold, the specific excavation volume falls. If only the exterior diameter is doubled, then the storage capacity increases eightfold [82].

Figure 9.24 lists the specifications of an artificial pumped-storage facility designed as in Table 9.3 with an average power over 30 days of 10 GW [68].

**Table 9.2** Gross/net capacity, energy density, and volume of water exchanged for various storage facility sizes with drop-heights, water levels, and diameters incremented by a multiple of two

| | | | | |
|---|---|---|---|---|
| Average drop-height in m | 100 | 200 | 400 | 800 |
| Water level fluctuation in m | 25 | 50 | 100 | 200 |
| Wall diameter in km | 2 | 4 | 8 | 16 |
| Slope angle in ° | 32 | | | |
| Freeboard height in m | 2 | | | |
| Exchanged volume of water in km$^3$ | 0.08 | 0.62 | 4.93 | 39.44 |
| Energy density in kW h/m$^3$ | 0.27 | 0.55 | 1.09 | 2.18 |
| Gross capacity in GW h | 20.94 | 335.49 | 5,371.88 | 85,982.86 |
| Net capacity $\eta_{Re} = 90\%$ in GW h | 18.84 | 301.94 | 4,834.69 | 77,384.57 |

**Table 9.3** Example of an artificial pumped-storage facility designed as in Fig. 9.42, with an average power over 30 days of 10 GW [68]

| Upper reservoir | | Lower reservoir | | Overall system | |
|---|---|---|---|---|---|
| Height above the surrounding environment | 440 m | Internal diameter | 11.0 km | Volume of water exchanged | 7.00 $km^3$ |
| Diameter | 9.6 km | External diameter | 22.2 km | Space requirement | 400 $km^2$ |
| Water surface area | 73.0 $km^2$ | Water surface area | 290.0 $km^2$ | Water fill | 37.00 $km^3$ |
| Slope angle | 32° | Water level fluctuation | 25.0 m | Storage capacity | 7.0 TW h |
| Water level fluctuation | 100 m | Water depth | 34.5 m | | |
| Wall volume | 9.54 $km^3$ | | | | |

Figure 9.30 shows the storage capacities of various facility sizes with similar construction costs using existing differences in elevation, as well as of offshore designs. If natural differences in elevation are available, then even storage facilities with small radii may be economically viable. The smaller the difference in elevation, the larger the diameter must be to achieve the specific parameters required. With an average drop-height of around 200 m, the highlighted storage sizes result in a specific excavation volume of 2.3 to 2.4 $m^3$/kW h, a specific storage capacity of 4.5 to 6.5 kW h/$m^2$, and estimated specific construction costs of 5,000 €/kW or around 15 €/kW h [83].

## Excavation Volumes

The lower reservoir is dimensioned so that the amount of earth excavated to build it is adequate to construct the wall for the upper reservoir [68]. Table 9.3 shows that the amount of earth excavated to construct the wall is well within the standard range for surface mining. In operation since 1978,

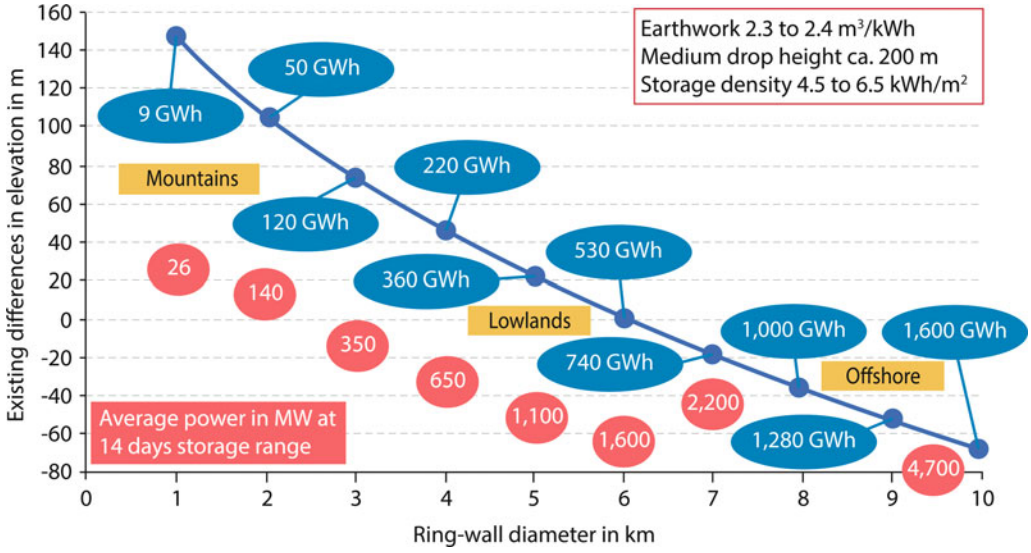



**Fig. 9.30** Storage capacities of artificial pumped-storage facilities with similar construction costs using various existing differences in elevation [83]

**Table 9.4** Excavated volumes for various wall sizes

| | | | | |
|---|---|---|---|---|
| Wall height in meters | 200 | 400 | 800 | 1,600 |
| Wall diameter in km | 2 | 4 | 8 | 16 |
| Crown width in meters | 15 | | | |
| Slope angle in ° | 32 | | | |
| Wall volume in $km^3$ | 0.399 | 3.117 | 24.636 | 195.879 |

Germany's largest surface mine in Hambach excavates around 0.3 $km^3$ of earth annually. About 18.6 $km^3$ of earth will be excavated there by the time the mine is shut down in 2040 [84].

The volume excavated $V_{Wall}$ is determined by the height $h_{Wall}$, the slope angle $\alpha_{Slope}$, the crown width $b_{Crown}$, and the diameter $d_{Wall}$ of the wall, and given by:

$$V_{Wall} = h_{Wall} \cdot \left( b_{Crown} + \frac{h_{Wall}}{\tan \alpha_{Slope}} \right) \cdot \pi \cdot d_{Wall}. \quad (9.18)$$

The volume required can be reduced by using a natural or existing difference in elevation [82]. Table 9.4 shows the wall volumes and demonstrates, as discussed above, that doubling the diameter increases the volume of the wall eightfold, and the capacity 16-fold.

Artificially constructed pumped storage can be compared with convention pumped storage by the specific excavated volume per kilowatthour stored $\nu_{Exc.RWS}$:

$$\nu_{Exc.RWS} = \frac{V_{Wall}}{E_{RWS}}. \quad (9.19)$$

For the example in Table 9.3, the resulting specific excavated volume is $\nu_{Exc.RWS} = 1.36\,m^3/kW\,h$. By comparison, the pumped-storage plant in Goldisthal has a specific excavated volume of $\nu_{Exc.Goldisthal} = 0.72\,m^3/kW\,h$ [85].

### Space Requirements

The storage facility design determines its space requirements. An artificial pumped-storage facility with the design shown in Fig. 9.24 and the dimensions shows in Table 9.3 would require a contiguous area of 400 $km^2$. In a densely populated country like Germany, such a large area would be difficult to find. To avoid population displacement and facilitate the choice of location, the form can be altered and the storage facility integrated into locally available natural features. This then increases the volume of excavation required [86]. Surface mines are not an option here. German surface mines (active or decommissioned) are spread across an area exceeding 1,000 $km^2$ [68]. Table 9.5 shows the space requirements of circular artificial pumped-storage facilities with various diameters.

$$A_{Total.RWS} = \frac{\pi}{4} \cdot {d_{Outer}}^2 \quad (9.20)$$

The storage capacity per square meter increases as the diameter increases, and is calculated from the stored energy $E_{RWS}$ and the total area of the storage $A_{Total.RWS}$:

$$e_{RWS} = \frac{E_{RWS}}{A_{Ges.RWS}}. \quad (9.21)$$

As a result, the example in Table 9.3 has a specific storage capacity of $e_{RWS} = 17.5\,kW\,h/m^2$. By comparison, the pumped-storage plant in Goldisthal has a specific storage capacity of $e_{Goldisthal} = 15.5\,kW\,h/m^2$ [14].

These calculations do not apply to offshore facilities. Since only the upper reservoir wall must be built, they require significantly less space.

### Water Requirements

An artificially constructed pumped-storage facility's water requirements are determined by

**Table 9.5** Space requirements by outer diameter of the lower reservoir

| Outer diameter in km | 10 | 15 | 20 | 25 |
|---|---|---|---|---|
| Space requirements in km² | 78.54 | 176.71 | 314.16 | 490.87 |

**Table 9.6** Capital costs and specific costs for the example described in Table 9.4

| | |
|---|---|
| Capacity in GW h | 7 |
| Costs in millions of € | 40,341 |
| Specific costs per kW h in €/kW h | 6.04 |
| Specific costs per kW in €/kW h | 4,034 |

the volume of the upper reservoir $V_{Upper}$, the fill level of the lower reservoir $V_{Lower}$, and the volume of water exchanged $V_A$.

The example in Table 9.3 requires 37 km² of water. By comparison, Lake Constance has a water volume of 48 km² [87]. To fill the reservoir for the first time, the facility must be located near a large source of water such as a river that can provide water during flooding [82]. Filling such an enormous volume could take several years. Water requirements do not pose a problem for offshore facilities.

9

### Construction, Costs, and Cost Efficiency

Building an artificially constructed pumped-storage facility requires no new or innovative technology. The upper reservoir can be erected using bucket-wheel excavators common in surface mining. Conveyor belts transport the excavated earth to a spreader that piles the material up to form a wall. The interior of the wall is then sealed [86].

Previously completed projects suggest that building an artificially constructed pumped-storage facility with the dimensions described in Table 9.9 is entirely realistic. For example, the Nurek Dam in Tajikistan has a height of 300 m. Argentina has a dam 224 km long, one of the longest ever built. The Kariba reservoir in Africa has a dam water volume of 180 km³. Similar projects in Germany have also shown that construction at this scale is technically feasible using modern surface mining methods.

The costs of the storage facility described in Table 9.3 have been roughly estimated by Popp using a calculation tool at around 40 billion euro [83]. This figure takes into account costs for purchasing the land, expanding the infrastructure, excavating the reservoir, building the wall, sealing the upper reservoir, and filling the facility with water, as well as the costs for pumped-storage technology, monitoring systems, and the network connection. With a storage capacity of 7 TW h, the resulting specific costs per stored kilowatt-hour are around 6 €/kW h. The specific costs per installed kilowatt of power is about 4,000 €/kW. By comparison, constructing a new pumped-storage plant in Germany incurs specific costs of 4,000 to 5,000 €/kW [66]. Costs vary enormously depending on the size and design of the artificially constructed pumped-storage facility (Table 9.6).

### Hybrid Artificially Constructed Pumped-Storage Facilities

Artificially constructed pumped-storage sites are also suitable for generating renewable electricity. Photovoltaic (PV) facilities could be installed on the surface of the wall that faces the sun, and in windy regions, wind power facilities could be installed on the wall and around the lower reservoir. Figure 9.31 shows an illustration of a hybrid artificially constructed pumped-storage facility of this kind with the dimensions described in Table 9.7.

In addition, the bodies of water and the difference in elevation of the wall could be used to attract tourism. The water level fluctuations of 20 m in the lower reservoir do not pose any problem for recreational use. This is because the level changes very slowly. In the Edersee in Hesse, for example, the level fluctuates up to 30 m without affecting recreational use. There, visitors can access floating islands connected to the mainland by footbridges [83, 86].



**Fig. 9.31** Illustration of a hybrid artificially constructed pumped-storage facility [83]

Figures 9.32, 9.33, and 9.34 show offshore storage facilities with sunken interior reservoirs. The form and size of the wall sealing off the interior reservoir differs in each of these designs. Larger areas constructed using land-fill could be used for residential developments or for the industrial sector. The water surface of the interior reservoir could be used for floating PV facilities or floating solar-thermal energy power plants as in Fig. 9.33.

Belgium plans to build the first facility of this type using an offshore concept with an interior lower reservoir. The facility would use the ocean as the upper reservoir and have a wall shaped like a horseshoe 3.5 km in diameter (Fig. 9.35) to seal off the lower reservoir [89].

### 9.2.2.2 Spherical Tank Pumped Storage

Energy storage with spherical tank pumped storage uses basically the same principle as conventional pumped-storage plants. A hollow, concrete spherical tank is installed deep under the water on the ocean floor. This volume is used as the lower reservoir. The ocean functions as the upper reservoir. When there are electricity surpluses, water is pumped out of the spherical tank. When electricity is required, water under pressure from the ocean above is allowed to flow back into the spherical tank, powering a turbine. Here, a pump turbine is used. The storage facility's only connection is a cable to carry the electricity. Figure 9.36 shows the

**Table 9.7** Specifications for a hybrid artificially constructed pumped-storage facility with 2,000 wind power facilities installed on the wall and in the region, as well as PV facilities installed on roofs in the region [86]

| Upper reservoir | | Lower reservoir | | Overall system | |
|---|---|---|---|---|---|
| Height above the surrounding environment | 215 m | Internal diameter | 6.7 km | Volume of water exchanged | 1.39 $km^3$ |
| Diameter | 6.0 km | External diameter | 11.4 km | Space requirements | 100 $km^2$ |
| Water surface area | 29.0 $km^2$ | Water surface area | 66.8 $km^2$ | Storage capacity | 0.7 TW h |
| Slope angle | 32° | Water level fluctuation | 20.0 m | Average power | 2.0 GW |
| Water level fluctuation | 50 m | | | Peak power | 3.2 GW |
| Wall volume | 1.46 $km^3$ | | | | |

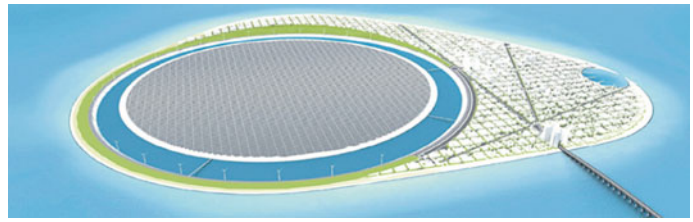


**Fig. 9.32** Offshore hybrid artificially constructed pumped-storage facility with wind power and PV facilities as well as residential housing on areas created by landfill [88]



**Fig. 9.33** Offshore hybrid artificially constructed pumped-storage facility with wind power and solar-thermal energy facilities as well as residential housing on areas created by land-fill [88]

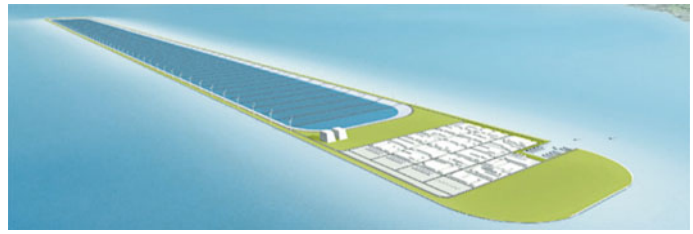


**Fig. 9.34** Offshore hybrid artificially constructed pumped-storage facility with wind power facilities and areas created by land-fill used by the industrial sector [88]



operating principle of a spherical tank pumped-storage facility [90].

This energy storage concept was developed by the StEnSea project. Short for 'stored energy in the sea', StEnSea is a joint project of the Fraunhofer-Institut für Energiewirtsachaft und Energiesystemtechnik and Hochtief AG [90, 92].

The advantage of this concept is that it exploits the difference in pressure between the water surface and the seabed, meaning that there is no need to construct upper and lower reservoirs at different elevations. Figure 9.37 shows a storage facility of this type in its charged and discharged states.

### Efficiency

A spherical tank pumped-storage facility's efficiency ranges from 80 to 85% [90, 92]. Efficiency losses are caused by losses in the transformer $\eta_{Tr}$, the motor or generator $\eta_{M,G}$, and the pump or turbine $\eta_{P,T}$. Since the facility is placed directly in the ocean, unlike with conventional pumped-storage facilities there are



**Fig. 9.35** Planned artificially constructed pumped-storage facility off the coast of Belgium [89]

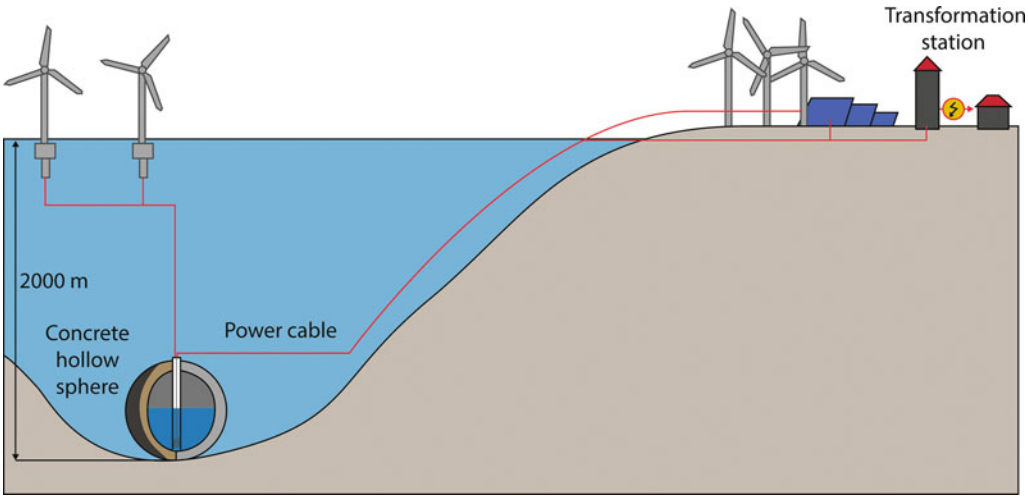



**Fig. 9.36** Operating principle of an underwater pumped-storage facility [91]

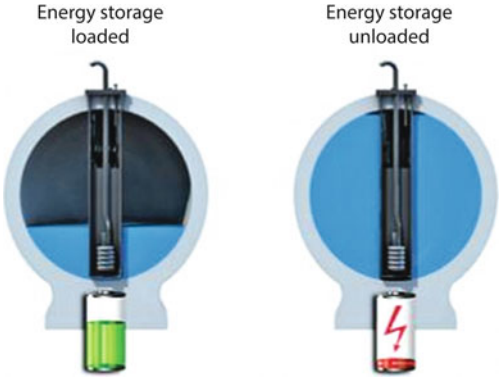



**Fig. 9.37** Storage facility filling levels in charged and discharged states [92]

no pipeline losses. Self-discharge losses are also eliminated.

### Storage Capacity, Energy Density, and Cost Efficiency

The storage capacity of a spherical tank installed on the seabed is determined by both its depth and volume. Since gravity is $g = 9.81\,\mathrm{m/s^2}$ and the density of water is $\rho_W = 1{,}000\,\mathrm{kg/m^3}$, if the depth is $T_{Sphere}$ and the volume of water exchanged is $V_{Sphere}$, then the potential energy stored by the water in the spherical tank pumped storage $E_{KPS}$ is:

$$E_{KPS} = g \cdot \rho_W \cdot T_{Sphere} \cdot V_{Sphere}. \qquad (9.22)$$

It should be kept in mind that the spherical tank is only emptied nearly to a vacuum, reducing the storage capacity. The spherical tank volume is determined by the interior diameter $d_{Sphere}$ and is given by:

$$V_{Sphere} = \frac{1}{6} \cdot \pi \cdot {d_{Sphere}}^3. \qquad (9.23)$$

The pressure $p_{Sphere}$ is determined by the spherical tank's depth, the density of water, and gravity, and is given by:

$$p_{Sphere} = g \cdot \rho_W \cdot T_{Sphere}. \qquad (9.24)$$

Table 9.8 shows the energy density, pressure, volume, and storage capacity of spherical tanks by depth and diameter.

Doubling the installation depth doubles the storage capacity. If the diameter is doubled as well, then the volume increases eightfold and the capacity increases 16-fold. If the diameter only is doubled, then the storage capacity increases eightfold.

This means that a facility of 230 spherical tanks 40 m in diameter installed at a depth

**Table 9.8** Storage capacity of spherical tank pumped-storage facilities by depth and diameter

| | | | | | |
|---|---|---|---|---|---|
| Depth in m | 200 | 400 | 800 | 1.600 | 3.200 |
| Pressure in bar | 19.62 | 39.24 | 78.48 | 156.96 | 313.92 |
| Energy density in kW h/m$^3$ | 0.55 | 1.09 | 2.18 | 4.36 | 8.72 |
| Diameter in m | 20 | 40 | 80 | 160 | 320 |
| Volume in m$^3$ | 4,188 | 33,510 | 268,082 | 2,144,660 | 17,157,284 |
| Capacity in MW h | 2.28 | 36 | 584 | 9,350 | 149,000 |

of 400 m would have a storage capacity of 8.5 GW h. This is equivalent to the storage capacity of the Goldisthal pumped-storage plant [64].

### Construction, Application, and Location

Because a concrete spherical tank 20 m in diameter weighs several thousand tons, it cannot be built on land and must be constructed at sea [90]. In addition, the spherical tank's design must be exceptionally robust to withstand the high pressures at great depths. The pump turbine's water inlet must also be kept free of foreign objects such as mussels [91].

A single spherical tank has only a small storage capacity. Several hundred spherical tanks must be constructed and combined in a single facility to achieve a higher storage capacity. This means that producing the tanks must be efficient and cost-optimized. Hard substrate surfaces are required to install the tanks on the seabed.

In case of emergency and for maintenance purposes, a method of bringing the tanks back up to the surface is required. Inflatable belts could be used to achieve this. Figure 9.38 shows a facility with several spherical tank pumped-storage units [90, 92].

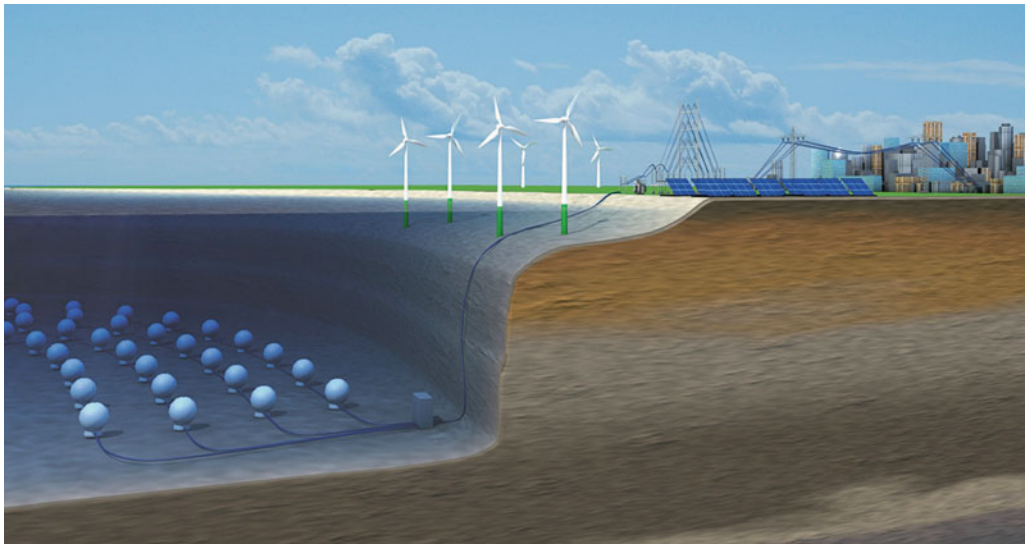


**Fig. 9.38** Example installation of a spherical tank pumped-storage facility on the seabed composed of several tanks [92]

There are few geographical requirements. The site must be at a sufficient depth, and the area must be large enough for a facility of several hundred spherical tanks. This concept is, therefore, feasible across the globe. The North Sea and Baltic Sea coasts are excluded, because the ocean is not deep enough there for cost-effective operations. With depths ranging from 600 to 800 m and an area of several thousand square kilometers, the Norwegian trench is the first choice for a German facility. Another advantage of this site is its proximity to existing or planned offshore networks, as well as existing wind power facilities [90].

Since the storage facility is installed deep beneath the ocean, there is no visible change to the landscape or environment. Compared to conventional pumped-storage plants, generally the impact on the environment is minor.

But since the storage capacity here is low, these facilities are not suitable for balancing weekly or monthly fluctuations. In the near future, there are plans to build and operate a pilot facility of this type at a depth of 100 m under the sea. The idea is to install the first spherical tank pumped-storage facility on the seabed in the coming years [90].

### 9.2.2.3 Dam Storage

Fig. 9.39 shows Germany's waterways. They are divided among seven administrative areas: north, northwest, west, central, east, southwest, and south. Dammed and naturally flowing rivers or canals that are partially or wholly inaccessible to vessel traffic are distinguished from lakes here [94].

#### ▪ Operating Principle

Fig. 9.40 shows how German federal waterways are used for pumped storage. Individual storage is distinguished here from storage chains. With dam storage, a barrage in the form of locks or a ship-lift separates the upper reservoir from the lower reservoir, creating the difference in elevation between them [94]. When there are electricity surpluses, water is pumped from the lower reservoir into the upper reservoir. When electricity is required, the water is fed back down to the lower reservoir through a turbine connected to a generator, generating electricity. The principle is therefore the same as with conventional pumped-storage plants.

#### ▪ Efficiency

The efficiency of dam storage facilities is comparable with conventional pumped-storage plants, and as a result, with mechanical stored energy systems as well.

#### ▪ Storage Capacity and Location

The total length of waterways usable for energy storage in Germany is 1,340 km. The total drop-height is 611 m divided among 64 dams with drop-heights under 38 m [94].

The storage capacity of waterways is determined by the difference in elevation between the upper and lower reservoirs, as well as by the volume of water exchanged. Since gravity is $g = 9.81\,\mathrm{m/s^2}$ and the density of water is $\rho_W = 1{,}000\,\mathrm{kg/m^3}$, if the average drop-height is $h_{FSSS}$ and the volume of water exchanged is $V_{ASSS}$, then the potential energy stored by the water in the upper reservoir $E_{SSS}$ is:

$$E_{SSS} = g \cdot \rho_W \cdot h_{FSSS} \cdot V_{ASSS}. \qquad (9.25)$$

The volume of water exchanged $V_{ASSS}$ is limited by the waterways themselves. These waterways are primarily used for shipping. The normal water level of a canal is typically 4 m high, with fluctuations up to 25 cm. Pumping the water back and forth must not cause water levels to fall below or exceed normal levels. This is because high water levels reduce clearance under bridges and may cause damage to dams. Low water levels may cause problems by dangerously reducing the water depth [96].

The volume of exchanged water $V_{ASSS}$ can be roughly determined from the length $l_K$, width $b_K$, and potential water level fluctuation $h_{PK}$ of the canal:

$$V_{ASSS} = l_K \cdot b_K \cdot h_{PK}. \qquad (9.26)$$

Table 9.9 lists the canals and locks that could be used for storage together with their differences in elevation.

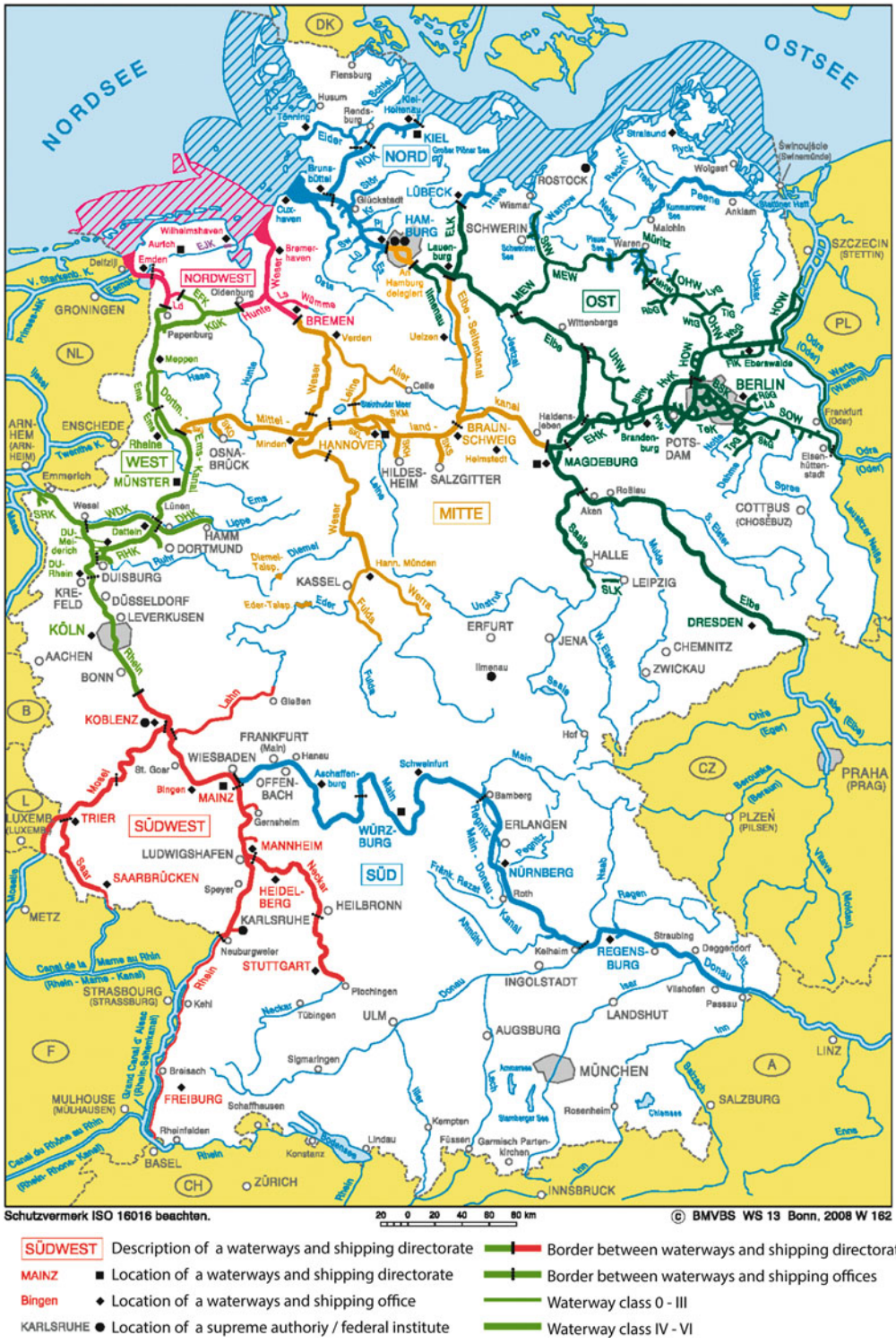



**Fig. 9.39** General map of German federal waterways [95]

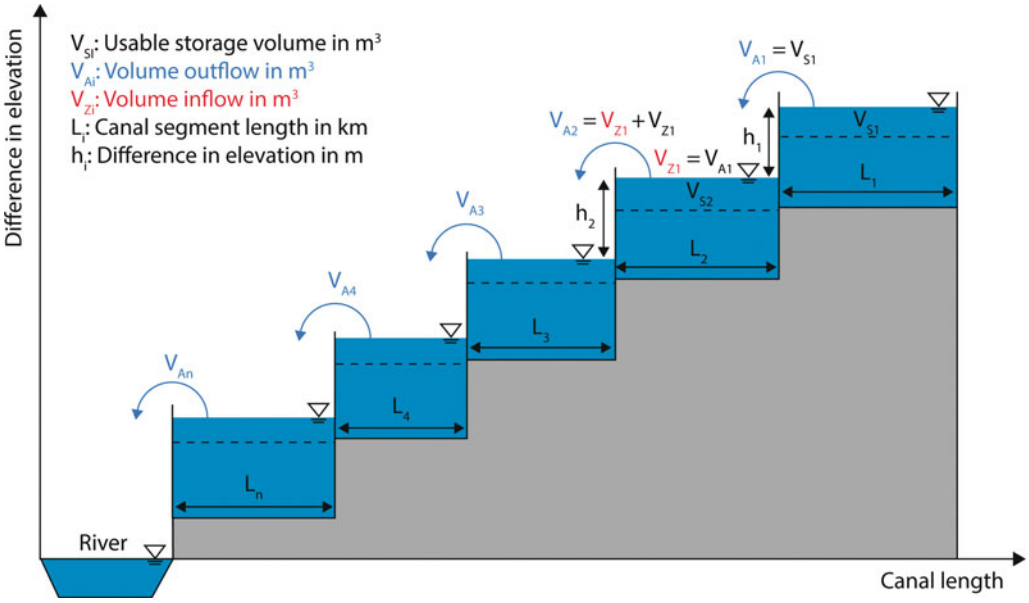



**Fig. 9.40** Operating principle of individual pumped storage and pumped-storage chain facilities on German federal waterways [94]

**Table 9.9** Relevant canals that could be used for energy storage [94]

| Administrative area | Name | Length in km | Locks | ∑ drop-height in m |
|---|---|---|---|---|
| Central | Elbe-Seitenkanal (ESK) | 115 | 2 | 61 |
| South | Main-Donau-Kanal (MDK) | 171 | 16 | 243 |
| Central | Mittellandkanal (MLK) | 326 | 3 (14)[b] | 43 (133)[b] |
| East | Havel-Oder-Wasserstraße (HOW)[a] | 135 | 4 | 46 |
| West | Wesel-Datteln-Kanal (WDK) | 60 | 6 | 44 |
| West | Rhein-Herne-Kanal (RHK) | 45 | 5 | 35 |
| West | Dortmund-Ems-Kanal (DEK)[c] | 226 | 10 (15)[b] | 68 (79)[b] |
| North | Nord-Ostsee-Kanal (NOK) | 99 | 2 | 10 |
| East | Elbe-Havel-Kanal (EHK) | 55 | 2 | 9 |
| East | Spree-Oder-Wasserstraße (SOW)[a] | 130 | 6 | 23 |
| West | Datteln-Hammeln-Kanal (DHK) | 47 | 2 | 7 |
| East | Finowkanal (FiK) | 32 | 12 | 36 |

[a] Waterways consisting of lakes or dam-regulated rivers and canals that could be cost-effectively used for pumped storage in individual dam sections but not for storage chains.
[b] With branch canals and secondary canals.
[c] Including dam-regulated river sections.

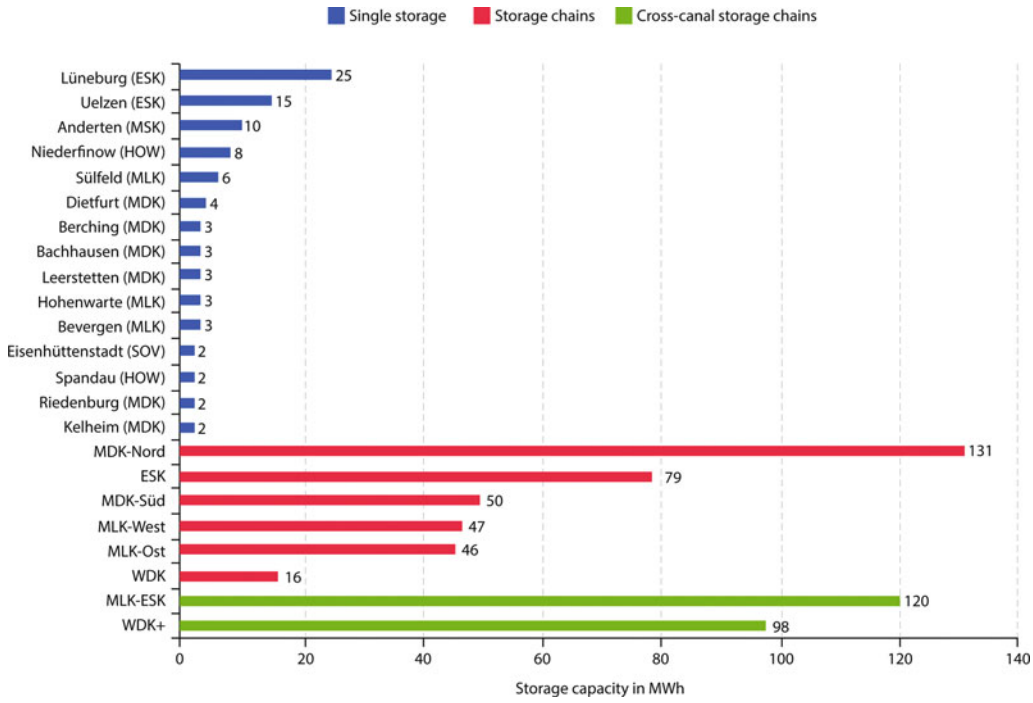



**Fig. 9.41** Energy storage potential on German federal waterways for individual storage facilities, storage chains, and cross-canal storage chains [94]

Figure 9.41 shows the storage capacity of usable German federal waterways for individual storage, storage chains, and cross-canal storage chains. It should be kept in mind that the total storage capacity is not determined by the sum of all the individual storage and storage chain capacities. This is because some canal sections would be counted more than once in the total sum [94].

The individual storage facility with the highest storage capacity of 25 MW h is at the Lüneburg ship-lift on the Elbe-Seiten-Kanal (Fig. 9.42). The storage chains and cross-canal storage chains with the highest capacities are on the northern section of the Main-Donau-Kanal (MDK-Nord), the cross-canal storage chain on the Mittellandkanal and the Elbe-Seitenkanal (MLK-ESK), and on the Wesel-Datteln-Kanal including the West German canal intersection (WDK+) [94].

Optimal exploitation of these individual storage facilities, storage chains, and cross-canal storage chains would result in a total storage potential of around 400 MW h [94].

### Construction and Applications

Dam storage facilities require no construction because they use previously constructed upper and lower reservoirs. As a result, they enjoy high public acceptance. The machine houses and pumps have already been installed as well. The machine components just have to be upgraded for turbine operation. The costs differ for individual storage facilities and chain storage. In principle, all locks used for turbine operation must be upgraded. With chain storage, there are higher additional costs for water management.

Since dam storage has a storage capacity of around 400 MW h, it can be used as hourly storage. These facilities can also be used as virtual power plants to provide balancing energy [94]. The total capacity is rather low. But because the infrastructure at the locks has already been



**Fig. 9.42** Individual storage facility with the highest storage capacity at the Lüneburg ship-lift with a drop-height of 38 m [97]

built, these facilities are easily accepted by the public and entail limited environmental impact. The costs are also negligible.

### 9.2.2.4 Repurposed Mining Areas

There are generally three types of repurposed mining areas:

- Underfloor storage or underground pumped storage-facilities.
- Surface mine pumped-storage facilities.
- Pumped storage-facilities on heaps.

#### ▪ Operating Principle

The operating principle of pumped-storage facilities installed on heaps, surface mines, and underground is the exactly same as with artificially constructed or conventional pumped-storage plants.

#### ▪ Efficiency

The efficiency of these three types of storage facilities in mining areas is comparable with pumped-storage plants.

#### ▪ Storage Capacity and Energy Density

The storage capacity of these three types of repurposed mining area facilities depends on the drop-height and the volume of water exchanged. Since gravity is $g = 9.81\,\mathrm{m/s^2}$ and the density of water is $\rho_W = 1{,}000\,\mathrm{kg/m^3}$, if the average drop-height is $h_{FBBS}$ and the volume of water exchanged is $V_{BBS}$, then the potential energy stored by the water in the upper reservoir $E_{BBS}$ is:

$$E_{BBS} = g \cdot \rho_W \cdot h_{FBBS} \cdot V_{BBS}. \quad (9.27)$$

The average drop-height varies by storage type. The drop-height of pumped-storage on heaps ranges from 50 to 150 m [98], of underground pumped-storage from 500 to 1,500 m [99], and of surface mine pumped-storage from 100 to 400 m [98].

The storage system energy density is determined by the drop-height and calculated as follows:

$$w_{BBS} = g \cdot \rho_W \cdot h_{FBBS}. \quad (9.28)$$

Table 9.10 shows the drop-heights and resulting energy densities of heap, strip mine, and underground pumped-storage facilities.

#### ▪ Heap Pumped-Storage

Heap pumped-storage facilities are installed on slag heaps in rock or lignite coal mining areas. The upper reservoir is located directly on the slag heap and the lower reservoir at ground level or below (Fig. 9.43). The storage capacity is determined by the dimensions and strength of the heap. PV and wind-power facilities could be installed on the heaps as well [69, 99].

In Germany there are a total of 20 locations that could be used for heap pumped-storage

**Table 9.10** Drop-heights and resulting energy densities of storage facilities in repurposed mining areas

| Storage type | Underground pumped-storage | Strip mine pumped-storage | Heap pumped-storage |
|---|---|---|---|
| Drop-height in m | 500–1,500 | 100–400 | 50–150 |
| Energy density in kW h/m$^3$ | 1.36–4.09 | 0.27–1.09 | 0.14–0.41 |

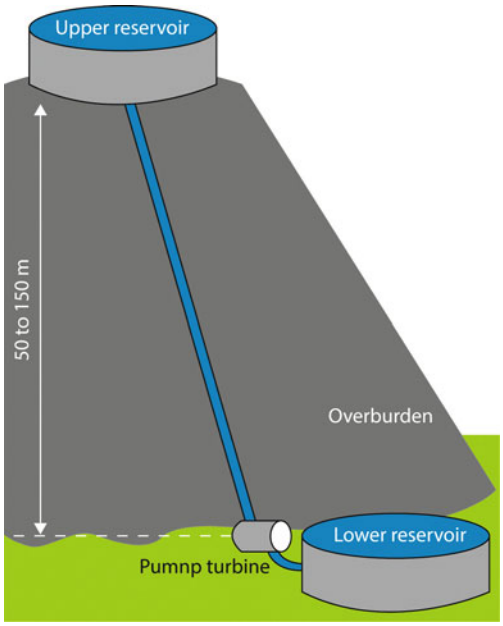



**Fig. 9.43** Heap pumped-storage operating principle [98]

**Table 9.11** Specifications of the Sundern heap combined pumped-storage plant planned near Hamm, Westphalia [102]

| | |
|---|---|
| Exchanged volume of water in m$^3$ | 600,000 |
| Average drop-height in meters | 50 |
| Storage capacity in MW h | 81.75 |
| Installed power in MW | 10 |
| Water-discharge over six hours in m$^3$/s | 27.78 |
| Energy density in kW h/m$^3$ | 0.14 |
| Wind-power facilities (power in MW) | 3 (6) |

**Table 9.12** Storage capacity and specific costs for the Suldern heap pumped-storage facility

| | |
|---|---|
| Storage capacity in MW h | 81.75 |
| Specific costs per kW h in €/kW h | 733.9 |

combination power plants. There are 71 heaps with adequate drop-heights in the Ruhr district, but only eight of them have adequate volumes. These eight have a total storage potential of 2,200 MW h. Figure 9.44 shows a map of heaps located in North Rhine-Westphalia [100].

RAG Montan Immobilien and RWE Innogy completed a feasibility analysis to determine whether the heap in Hamm, Westphalia, could be used for a pumped-storage plant combined with wind power facilities [100]. Figure 9.45 shows the heap as it stands today together with an illustration of the heap with upper and lower reservoirs as well as three wind power facilities.

Table 9.11 lists the specifications of the plant storage facility planned. The volume of water exchanged in the upper reservoir is 600,000 m$^3$, and the average drop-height is 50 m. The table also shows the potential installed-power of the storage facility when discharged over six hours.

Because of the small drop-heights and limited volumes of water exchanged, heap pumped-storage facilities have low storage capacities. But they could be a convenient, decentralized storage solution for some consumers.

Cost-effective operation requires maximizing the number of cycles. Table 9.12 shows the specific costs per kilowatt-hour of storage capacity. Capital costs are in the range of 60 million euros [102].

Even after the upper reservoir has been constructed, 70% of the heap is still available for other uses [102]. The heap could be opened to




**Fig. 9.44** Map of heaps located in North Rhine-Westphalia [100]




**Fig. 9.45** The Sundern heap today and illustrated as a heap pumped-storage facility [100, 101]

the public and hiking paths could be provided, or observation points looking out on the upper reservoir, for example [102].

The impact on the environment is minor. Since the heap holding the upper reservoir already exists, there is no impact on an untouched natural landscape [103]. The construction of a lower reservoir alone is less likely to lead to conflicts with local residents.

RAG Montan Immobilien and Steag New Energies have also commissioned a feasibility analysis of the Luisenthal heap location in Saarland [99].

### Underfloor or Underground Pumped-Storage Facilities

Instead of using a mountain or hill to create the difference in elevation between the upper and lower reservoirs like a conventional pumped-storage plant, underfloor or underground pumped-storage facilities use the shafts of hard coal or ore mines, for example. The upper and lower reservoirs are both underground, although the upper reservoir can be constructed above ground where space is available. In the best case scenario, it can also be constructed on an elevated slag heap. The drop-heights of repurposed mining areas range from 500 to 1,500 m [69, 99].

In Germany, there are 100 mines that could be used for underfloor pumped-storage facilities. The total storage potential if all of these mines were used would amount to around 20 GW h. The mines with the largest capacities are located in the Harz region, the Erzgebirge, Siegerland, and in the Lahn-Dill region [104].

The Energy Research Center of Lower Saxony has completed a study entitled 'Wind Energy Storage by the Reuse of Abandoned Mines', examining the reuse potential of two abandoned mines located in Bad Grund in the Harz region and Pöhla in the Erzgebirge (Table 9.13).

### Underfloor Pumped-Storage Facility Construction

The costs of construction vary from mine to mine. Figures 9.46 and 9.47 show how costs

**Table 9.13** Pumped-storage facility specifications for the Bad Grund site in the Harz region and the Pöhla site in the Erzgebirge [105]

| Location | Bad Grund | Pöhla |
|---|---|---|
| Drop-height in meters | Around 700 | Around 600 |
| Exchanged volume of water in $m^3$ | Around 240,000 | Around 282,000 |
| Energy density in kW h/$m^3$ | 1.91 | 1.64 |
| Storage capacity MW h | 400 | |

may differ. Currently flooded mines must first be drained, increasing costs. An underfloor storage facility generally requires three shafts: the main shaft, an escape shaft, and a shaft for the network connection (Fig. 9.48). Depending on the mine and the condition of the shafts available, it may be necessary to build these shafts [105].

Because of their geometry, repurposing existing caverns makes little sense. This means that the storage sections must be excavated for construction. Drilling and blasting are the preferred methods for this type of excavation [105].

The costs of underground construction can be reduced and the drop-height increased by constructing the upper reservoir aboveground where possible, or by using an existing water reservoir if available. The earth excavated to construct the lower reservoir and the shafts could then be used to build the upper reservoir. At the Bad Grund site, upper reservoir construction accounted for 16.4% of the total investment costs, and at the Pöhla site this was 17.2% [105].

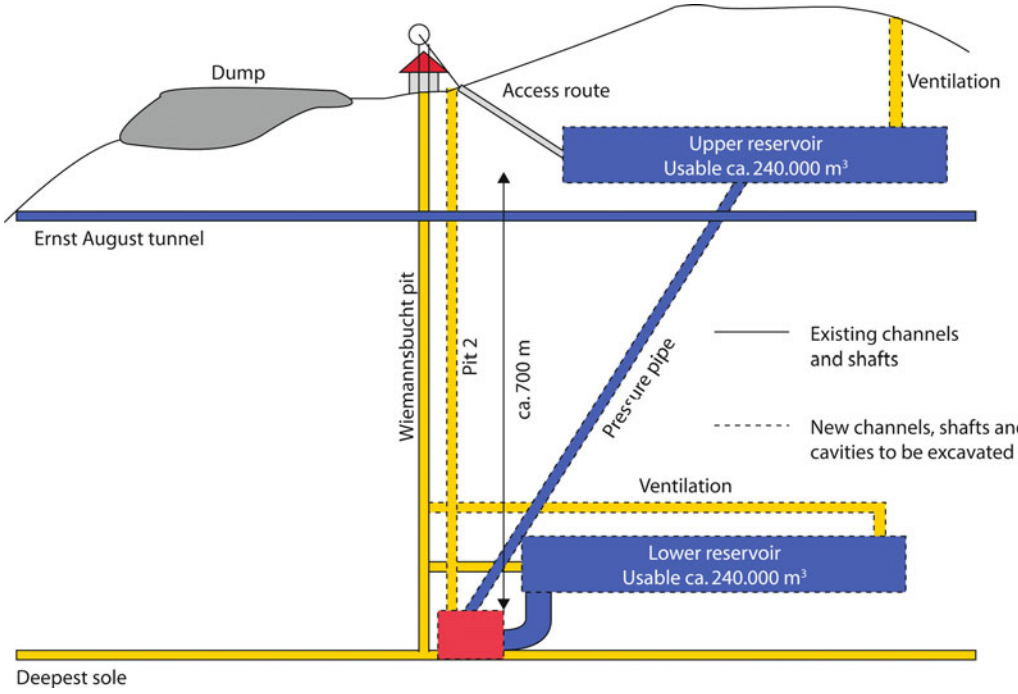



**Fig. 9.46** Underfloor pumped-storage facility at Bad Grund in the Harz region [105]

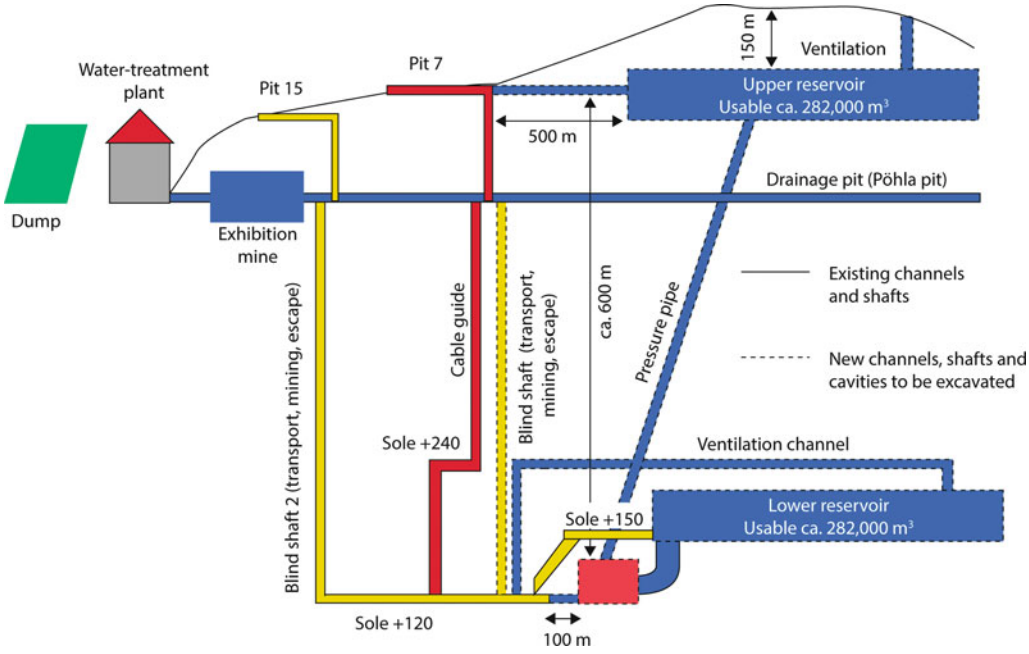



**Fig. 9.47** Underfloor pumped-storage facility at the Pöhla site in the Erzgebirge [105]

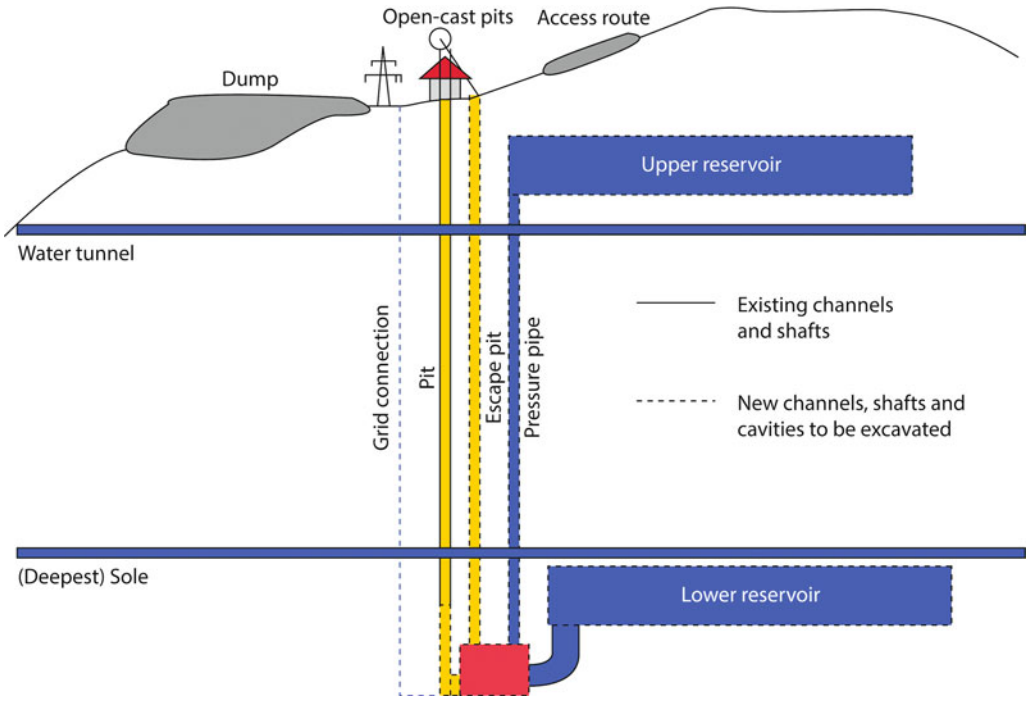



**Fig. 9.48** Underfloor pumped-storage facility concept [105]

**Table 9.14** Breakdown of costs (together with percentage share of total costs in parentheses) for each line item at the Bad Grund and Pöhla sites [105]

| Location | Bad Grund (total costs in %) | Pöhla (total costs in %) |
|---|---|---|
| Underground construction in millions of € | 109.71 (60.41) | 112.12 (53.74) |
| Network connection in millions of € | 20.33 (11.19) | 27.22 (13.04) |
| Infrastructure in millions of € | 1.97 (1.09) | 4.10 (1.97) |
| Machine technology in millions of € | 47.18 (25.98) | 58.18 (27.89) |
| Miscellaneous costs in millions of € | 2.40 (1.33) | 7.03 (3.36) |

A disadvantages of locating the upper reservoir above ground is that longer shafts are required, thus increasing costs. In addition, public acceptance may pose more of a problem with an upper reservoir that visibly impacts the environment [105].

When an existing water reservoir is used as an aboveground upper reservoir in particular, sealing off the storage reservoir to reduce water contamination that may shorten machine component service life makes good sense.

In addition, a horizontally constructed pressure shaft requiring shorter cable lengths improves cost-efficiency [105]. As with conventional pumped-storage plants, maintenance and repair costs with underfloor storage facilities are high [69].

### Costs and Cost Efficiency

Table 9.13 shows the drop-height, volume of water exchanged, energy density, and storage capacity for these two facilities.

The capital costs of the two sites studied are comparable in scale (Table 9.14), but the breakdown of costs vary considerably. This shows that there are no general rules for construction costs or cost-efficiency, and that each potential mine-site must be considered separately.

Table 9.14 shows how costs differed at the two sites. The costs for each line item (together with the percentage share of total costs in parentheses) are listed in the breakdown of costs [105].

Both underground storage facilities have a storage capacity of 400 MW h. Each facility also has a specifically-installed power of 100 MW. The specific costs of 1,816 €/kW for the Bad Grund site is the arithmetic mean of the two extreme scenarios. These specific costs result in total capital costs of 181.6 million euro. The model mine facility at the Pöhla site has specific costs of 2,086 €/kW. These specific costs result in total capital costs of 208.6 million euro [105].

Capital costs are higher with underfloor pumped-storage facilities than with conventional pumped-storage plants [105]. Use of geothermal energy could provide an additional source of revenue. Temperatures ranging above 40 °C are quite common in mines [98].

### Surface Mine Storage Facilities

Open surface mines are another option for repurposed mining areas. Open surface pumped-storage facilities are similar to heap pumped-storage facilities. The upper reservoir is constructed at ground level, or in the best case on a slag heap within the surface mine to increase the drop-height. There are two possibilities for the lower reservoir. Either the strip mine pit can be used as the lower reservoir after the mine has been decommissioned (Fig. 9.49), or the lower reservoir can be constructed on the surface mine's lowest level as a sealed cavern (Fig. 9.50). An advantage of the second option is that the cavern and piping system can be installed while the surface mine is still in operation. It also guarantees a specific drop-height. As is common with depleted surface mines, after construction, the pit can be filled with surface mining slag or with water [69, 99].

**Table 9.15** Technical and economic parameters for the Bad Grund and Pöhla sites [105]

| Location | Bad Grund | Pöhla |
|---|---|---|
| Storage capacity MW h | 400 | |
| Installed power in MW | 100 | |
| Specific costs in €/kW | 1,816 | 2,086 |
| Capital costs in millions of € | 181.6 | 208.6 |

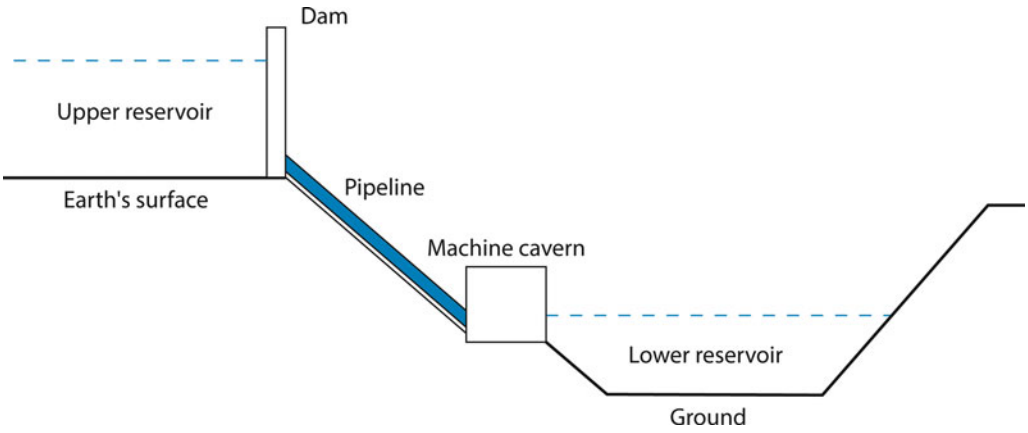



**Fig. 9.49** Lower reservoir for strip mine pumped-storage built in the strip mine pit

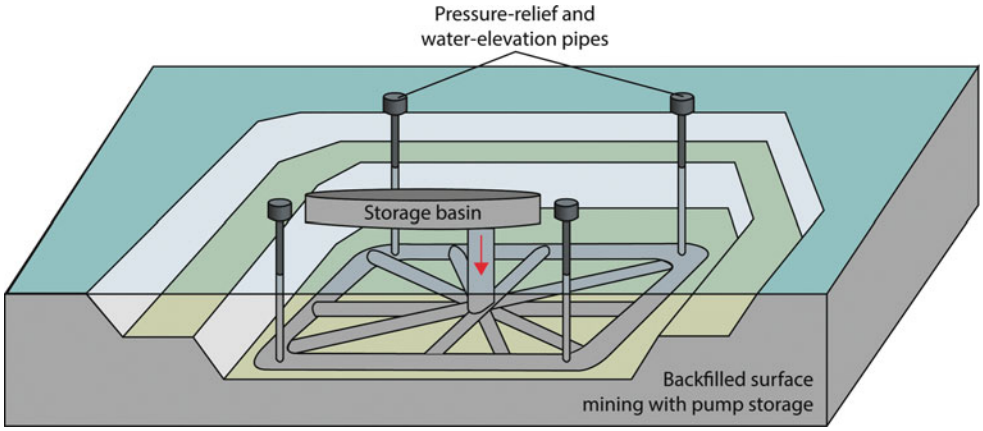



**Fig. 9.50** Lower reservoir for underfloor pumped-storage built under the strip mine pit [107]

The storage capacity is determined by the maximum effective volume of water exchanged and the drop-height. Figure 9.51 shows the water-management planning concept for the Lausitz regions in central Germany. Together the two regions have 68 pit lakes with a total volume of 4,511 km$^2$. Assuming that a tenth of the total volume of these pit lakes can be used for pumped-storage facilities, the average drop-height would be 80 m and the total storage capacity:

$$E_{\mathrm{BBS}} = \frac{g \cdot \rho_{\mathrm{W}} \cdot h_{\mathrm{FB}} \cdot V_{\mathrm{Oberb.}}}{10}, \qquad (9.29)$$

or approximately 98.3 GW h [106].

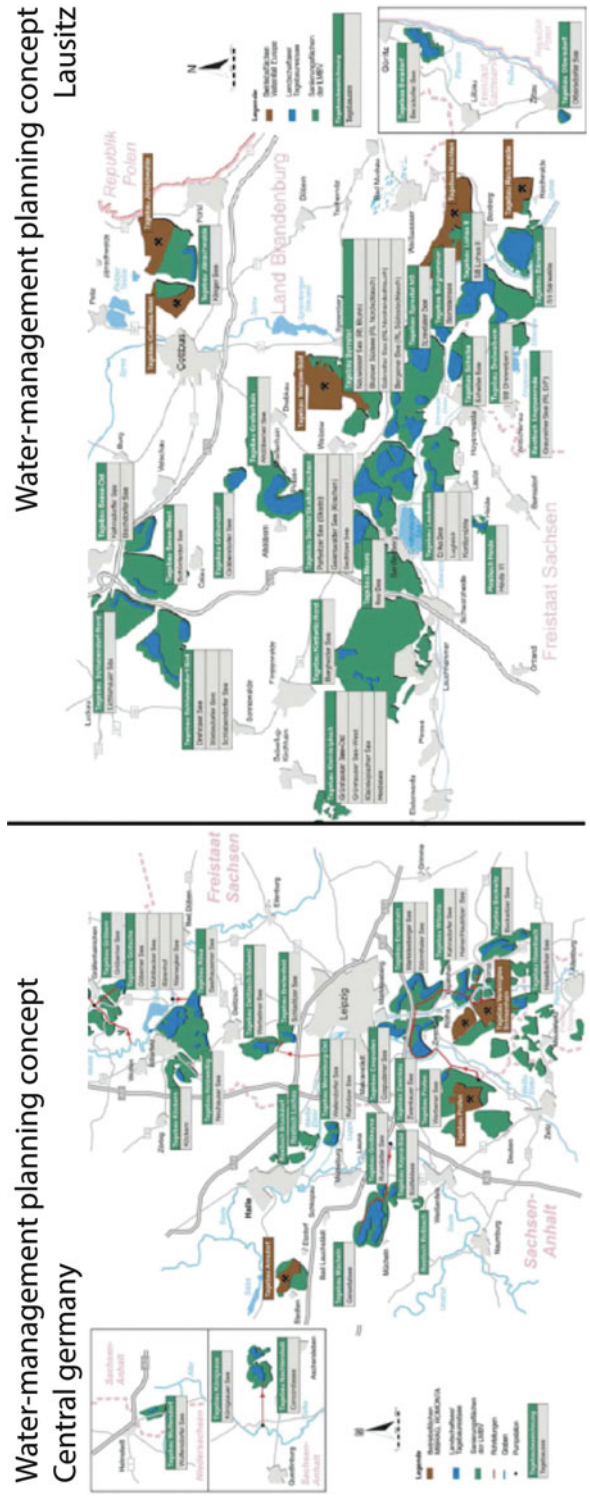



**Fig. 9.51** Water-management planning concept for the Lausitz regions in central Germany [106]

The costs of these storage facilities are less than for conventional pumped-storage plants because the lower reservoir is already constructed. In addition, the plant can be constructed as part of a plan to use the site for other purposes [106].

If a surface mine pit has already been flooded and opened to the public as a local recreational area, then any plan to convert it for use as a pumped-storage facility could face public opposition and be difficult to implement [104].

Another option is to connect two surface mine pits at different elevations. This would eliminate the need to construct an upper reservoir as well [99].

The underfloor storage concept shown in Fig. 9.50 could also be implemented in coastal regions (Fig. 9.52). Here, a sealed cavern submerged in the ocean serves as the lower reservoir. The upper reservoir is placed on a high cliff [98].

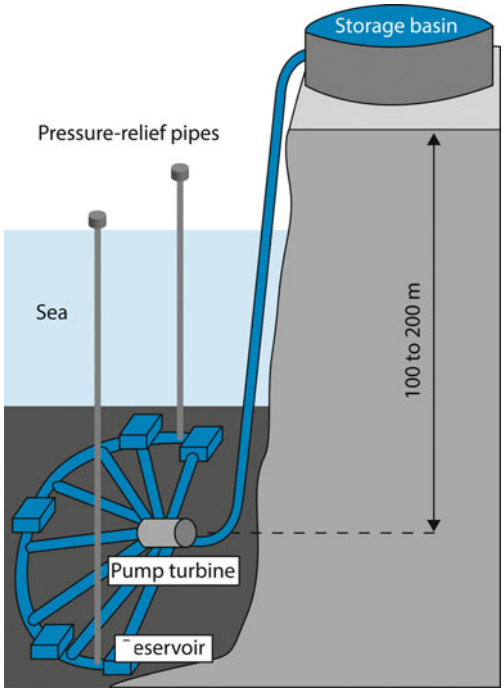



**Fig. 9.52** Underfloor surface mine storage concept implemented in regions with high coastal cliffs and steep drop-offs into the ocean at the coast [98]

#### 9.2.2.5 Conclusion

- Energy storage using differences in the potential of liquid media has a long history. At least in the area of electric energy supply, it remains the most commonly used form of energy storage. This is particularly true of the storage technology discussed in the first part of this chapter: pumped-storage plants.
- The second part of the chapter discusses alternatives to pumped-storage plants that use the same operating principle, but without some of the disadvantages of conventional pumped-storage. These concepts are currently in the planning, research, or pilot-plant stages.
- Pumped-storage plants require specific geographical conditions with large differences in elevation, and as a result, are generally found in mountainous regions. The artificially constructed pumped-storage facility concept would allow pumped-storage plants to be built in level areas as well. No large structures are required by spherical tank pumped-storage facilities, because these facilities use the pressure differences in a high-water column (the ocean). Dam storage facilities and repurposed mining area facilities use existing infrastructure for the purpose of energy storage.

## 9.3 Solid Media

### 9.3.1 Flywheel Storage Facilities

Mass moment of inertia has been used in machines since around 6,000 B.C. The Chinese, and later, the Mesopotamians were the first to use this technology. To build a centrifugal mass, they placed a small, rotating disc with a hole in its center on a stick. The centrifugal mass was made of wood, stone, clay, metal, glass, or bone. This simple flywheel design was used to manufacture yarn. The threads were bound directly to the spindle, and then spun into yarn. Another early use of flywheels from around

4,000 B.C. was in pottery wheels. Because keeping a much heavier mass stationary without heavy friction poses a greater challenge, pottery wheels were invented later. The first pottery wheels were made of wood with a stone bearing. The existence of these pottery wheels has been proven by pottery finds from this period. By examining the pottery, scientists can determine if the pieces were made on a pottery wheel using centrifugal force or by hand. Archaeological evidence indicates that use of the wheel for transportation was discovered after the discovery of flywheel 'machines' [113].

In the centuries that followed, the number of kinds of pottery wheels grew. A particularly remarkable discovery came from India. Here, archaeologists discovered a pottery wheel with a centrifugal mass made out of a composite of clay and bamboo rings connected to the axle by wood spokes. This fiber-composite centrifugal mass was the first true flywheel.



Pottery wheels were turned by hand or by foot. The pottery wheel could rotate steadily at speeds up to 100 1/min for several minutes. A pottery wheel found in Mesopotamia is estimated to have had an energy content of 0.14 W h.

These results could only be achieved with the use of a well-functioning bearing. In most cases a needle bearing placed in a bearing shell made of stone, porcelain, or wood held the axial load. The disc was precisely constructed so that it would self-stabilize, or it was stabilized by a slide bearing. The bearing was partly lubricated using vegetable oils, animal fats, or bitumen.

With the later invention of crank-driven spinning machines and manual mills, the centrifugal mass became a key component of many other machines. The asymmetrical driving motion of these machines required a centrifugal mass to produce an even mechanical motion. In the Middle Ages, water and wind-mills used large centrifugal masses to even the shaft power and varying load conditions in these machines.

Then in the 17th century, Galileo Galilei discovered the law of the inertia of masses. Even though it had been in use for thousands of years, until Galileo, philosophers and natural scientists had been unable to explain the phenomenon of mass inertia.

With the Industrial Revolution and the invention of the steam engine in the 18th century, flywheels became increasingly important in engineering. Flywheels were first used as pottery wheels to store energy, but beginning with the steam engine and continuing until the 20th century, they were used primarily as inert mass to equalize rotary motion. In many cases, the pulley and the flywheel were actually the same component in the machine, and performed both functions simultaneously. Over time, steam-engines grew in size. The size of the flywheel grew as well, until existing wheels made of cast iron were no longer strong enough to withstand the centrifugal force without shattering [113].

Flywheels used to transfer piston power to the drive train were also essential in the development of the combustion engine in the 19th century. Working separately but in the same period, Carl de Laval and Sir Parsons designed, built, and patented the first steam turbines for generating electricity. Their revolutionary flywheel designs increased the permitted rotation speeds of flywheels significantly [110].

The first flywheel developed specifically for energy storage was invented in 1883 by John A. Howell. Made of steel, it had a mass of 160 kg and a diameter of 45 cm. After accelerating up to 21,000 1/min, it was capable of powering a 1.5 km torpedo at an average speed of 55 km/h for quite a distance through the water.

The first Ilgner transformers were built in the early 1920s. Using the same principle as the Leonard transformer, these transformers had a rotary current motor coupled to a flywheel that permitted continued operation during engine failures or load surges. These transformers are frequently used in steel mills and in hoists.

Before dry batteries were commercially available, flywheels were also used in the toy industry. They were often found in toy cars, yo-yos, spinning tops, and so on.

The first modern flywheel was designed by the Swiss company Oerlikon in 1950. They built

the first mobile flywheel energy storage system for use on short-distance buses (gyrobus). The unit stored 9.15 kW h, and together with brake energy recuperation, could power the bus over a distance of 3.5 km. The bus stops were equipped with public electricity network connections for recharging the storage unit.

The steel gyrobus flywheel was sealed in a hydrogen atmosphere to reduce air friction losses. The flanges and shaft ends were also specially engineered. To prevent the flange from placing stress on the flywheel, an elastic design was used for these components.

The company MFO used the same technology to build a gyrolocomotive for the Lorraine iron-ore mine, also called the 'mines de Saint Pierremont', in 1954. The gyrolocomotive was operational at the mine in Gonzen until it closed in 1966. Three more gyrolocomotives were sold by MFO in 1955 to South Africa for use in a goldmine near Johannesburg. After the Gonzen mine was restored for tourism, the gyrolocomotive was brought back as a ride for visitors touring the decommissioned mine.

In 1973, Richard F. Post published a design for a car using a flywheel drive concept. By this time fiber-composite materials had been developed which allowed significantly higher rotational speeds, more than balancing out for the reduced mass. Post suggested that, like gyrobuses, these flywheel automobiles storing 30 kW h of electric energy could recharge at electricity filling stations. One charge could power the car at 100 km/h for a distance of around 320 km. Since the vacuum-sealed flywheel had a magnetic bearing system, the car would remain charged for several months when idle. But this concept has been largely forgotten in recent years [108].

In 1974, a stationary flywheel energy storage facility was installed at the Max-Planck-Institut in Garching. This facility was crucial for supplying the energy required by fusion experiments conducted there in later years. This flywheel energy storage facility has four separate forged steel disks that rotate on a single shaft, generating a power of 155 MW for a period of 10 to 15 seconds. By shortening and carefully planning the operating time-frames, even with air resistance losses of 650 kW at 1,650 1/min, no vacuum seal was required.

At about the same time, Boeing Vertol Co. in Philadelphia was commissioned by the United States Department of Transportation to develop a rapid transit system powered by flywheel energy storage. The plan was to use an innovative, modern magnetic bearing system and a vacuum seal in the flywheel design. Called the Concept Train (ACT 1), the train was successfully tested in 1975. But the train was never used for public transportation because of a lack of electric rails.

In 1978 MAN was commissioned by the German Federal Ministry for Research and Technology to design a stationary flywheel energy storage facility. The plan was to use this facility to store brake energy from downhill slopes on Stuttgart regional train lines. The flywheel energy storage facility concept produced by the study had a capacity of 36 kW h, falling only somewhat short of the 50 kW h flywheel energy storage facility requested by the ministry. In the concept, a vertically positioned, steel flywheel weighing 5 tons rotated in an air environment at a pressure of 10 mbar and a speed of 2,800 1/min. But the concept was never implemented.

The first hybrid cars with combined combustion and electric engine drive using intermediate flywheel energy storage were tested in mid-1984 at Kaiserslautern University. Initial trials indicated fuel savings of around 3 L/100 km in city traffic using these cars. The engine can be shut off when idle or in a zero-load state, and then quickly restarted using the flywheel when power is required.

In an entirely different context, flywheel energy storage can also be used in combination with renewable energy. The Rutherford Appleton Laboratory in the United Kingdom is researching the use of flywheel storage in combination with wind energy. For the study, researchers have built a stand-alone test facility, including a wind-power facility generating 45 kW, a diesel electricity generator, and a flywheel energy storage facility. The flywheel en-

ergy storage facility is used as a buffer to bridge wind lulls. It is also used to avoid frequently starting and stopping the diesel electricity generator. Because the flywheel energy storage facility's short switching times range in the milliseconds, power fluctuations in the system are effectively eliminated.

But the major breakthrough in flywheel energy storage technology came in the late 1990s. Maximizing the quantity of energy stored required lighter flywheel masses. This in turn required developing new materials with extraordinarily high-tensile strengths. By using fiber materials, higher rotation speeds could finally be achieved. The low weight of these fiber discs could increase flywheel energy storage up to 1,000%. For example, a steel disc weighing 1 ton rotating at speeds ranging from 1,500 to 3,000 1/min stores the same quantity of energy as a fiber-composite disc weighing only 10 kg rotating at speeds ranging from 12,000 to 24,000 1/min. But since air resistance at speeds over around 500 1/min are significantly higher, fiber-composite disc must be sealed in a hydrogen environment or in a vacuum.

Finally, in 2004, the Braunschweig Technical University, in collaboration with the German Aerospace Center (Deutsches Luft- und Raumfahrtzentrum, DLR), made an important advance. Their goal was to develop a flywheel energy storage facility with an energy density of 56 W h/kg. This was achieved by significantly improving the reluctance motor. Reluctance motors are fast-responding, low-loss energy converters that are particularly well-suited for use in flywheel energy storage facilities.

#### 9.3.1.1 Physical Principles

In simple terms, flywheel energy storage can be understood as a single mass point $m$ rotating around a fixed axis at a distance $r$ and an angular velocity $\omega$.

The orbital speed $v$ is then determined by the distance $r$ and the angular velocity $\omega$:

$$v = r \cdot \omega. \tag{9.30}$$

By considering a single mass point $m$ on the orbit $r$ (Fig. 9.53), the kinetic energy is given by:

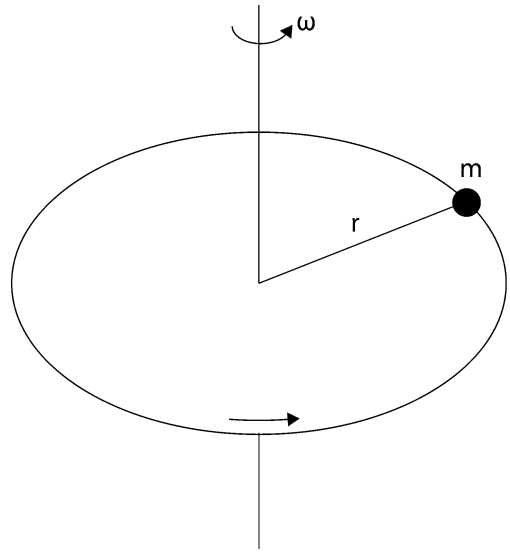



**Fig. 9.53** Orbit

$$E_{\text{kin}} = \frac{1}{2} m v^2 \tag{9.31}$$

or

$$E_{\text{kin}} = \frac{1}{2} m (r\omega)^2. \tag{9.32}$$

This formula also contains another quantity from kinetics; the mass moment of inertia, or simply the moment of inertia $J$. This is given by the mass $m$ of a body multiplied by the radius $r$ to the axis of rotation squared:

$$J = m r^2. \tag{9.33}$$

The kinetic energy of the orbiting body $E_{\text{kin}}$ can then be determined by inserting this quantity in the equation:

$$E_{\text{kin}} = \frac{1}{2} J \omega^2. \tag{9.34}$$

To determine the result for an extended body, the body can be distributed across a number of $n$ mass points. This means that each mass point of the mass $\Delta m_i$ is at a certain distance $r_i$ from the axis of rotation (Fig. 9.54). It should be kept in mind that each mass point has the same angular velocity $\omega$, but is not necessarily

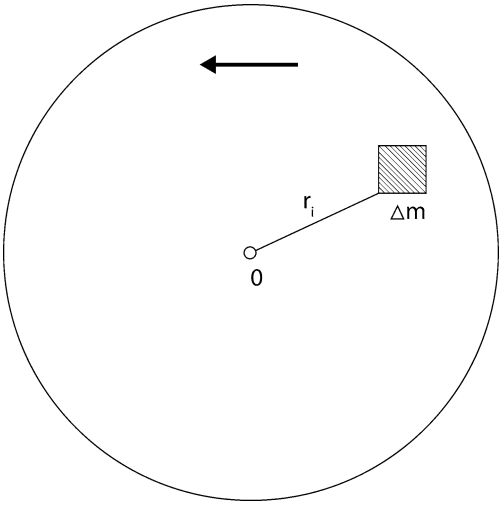



**Fig. 9.54** Rotating mass

the same distance r from the axis of rotation. As a result, the rotational energy $E_{\text{rot}}$ of a body is given by the sum of the kinetic energy $E_{\text{kin}}$ of the individual mass points:

$$E_{\text{rot}} = \sum_{i=1}^{n} E_{\text{kin}} = \frac{1}{2}\left(\sum_{i=1}^{n} \Delta m_i r_i^2\right)\omega^2, \tag{9.35}$$

$$E_{\text{rot}} = \frac{1}{2} J \omega^2. \tag{9.36}$$

Since the rotational energy and the kinetic energy $m/2 \cdot v^2$ of a body have a linear relationship, in formal terms, they are entirely equivalent. In both cases, a body with the mass $m$ is set in motion against its inertia. But it should be noted that the mass moment of inertia $J$ determines the rotational energy. This allows the spatial distribution of the body volume and the mass to be taken into account [116].

#### ▪ Calculating the Moment of Inertia

As indicated above, the total mass moment of inertia is given by the sum:

$$J = \sum_{i=1}^{n} r_i^2 \Delta m_i. \tag{9.37}$$

In many cases, the sum can only be estimated using elementary means. Preferably, a differential equation is used to determine the finite mass $\Delta m_i$. The body is considered to have a total volume $v$:

$$J = \int_{[v]} r^2 dm. \tag{9.38}$$

Many books include tables listing the mass moment of inertias for frequently occurring or simple geometric forms [116].

### 9.3.1.2 Materials

Technical innovations in the last 20 years, including fiber-composites, have resulted in new applications for flywheel storage. The new generation of flywheels delivers high-energy ffdensities in a compact design. The characteristics and energy densities of the various materials used (Table 9.16) show how widely they differ. There is a particularly large contrast between metallic rotors and rotors made of fiber-reinforced plastic. Because fiber-reinforced plastics have higher specific strengths, the same mass with lower density results in higher energy content.

#### ▪ Shattering Characteristics

Most rotational energy storage facilities currently in use have a steel flywheel. Disadvantages of steel include its low-energy density and the safety precautions required in case the flywheel shatters. Since circumferential speeds can reach 500 m/s during operation, a storage facility that is not properly secured could be lifted several meters into the air by a shattering steel flywheel. Repeated testing of the flywheel at excessive speeds is no guarantee that the flywheel may not fail (as shown in Fig. 9.55) at some point over its entire service life. As with turbines, this means that safety precautions are essential in these facilities. The facilities must be regularly maintained and inspected so problems are detected early on. Fiber-composite flywheels operate at higher maximum rotational speeds, but the risks in case of failure are no greater than with steel fly-

**Table 9.16** Comparison of energy densities (Source: VDI [111])

| Material | Tensile strength in N/mm² | Density in kg/m³ | Specific strength in kN m/kg | Maximum circumferential speed in m/s | Potential energy density in kJ/kg |
|---|---|---|---|---|---|
| Steel | 1,300 | 7,800 | 167 | 410 | 106 |
| Titanium | 1,150 | 5,100 | 225 | 570 | 143 |
| GFK | 1,300 | 1,900 | 680 | 820 | 335 |
| CFK | 6,300 | 1,546 | 2,470 | 1,570 | 1,570 |

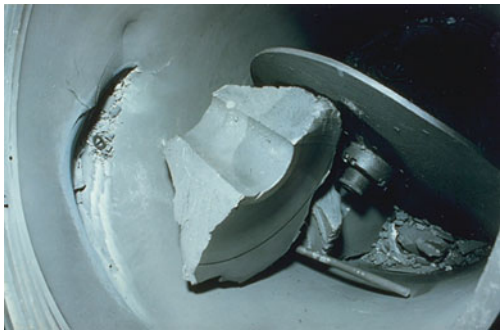


**Fig. 9.55** Steel rotor fracture pattern [112]



**Fig. 9.56** Fiber-composite rotor fracture pattern [112]

wheels. When a metal rotor fails, it shatters into large fragments. These fragments then hit the housing wall at high speeds with enormous energy, causing severe damage. A plastic rotor can be designed so that it shatters into a large number of extremely small particles with relatively small energies that hit the housing wall in an evenly distributed pattern (Fig. 9.56). As a result, the housing of a flywheel energy storage facility with a fiber-composite rotor can have a significantly more compact design [111].

#### 9.3.1.3 Flywheel Energy Storage Facility Design

Fig. 9.57 shows the design of a flywheel energy storage facility. The key component that stores energy is the flywheel, usually rotating in a vacuum or a gas environment. This minimizes air resistance losses. The flywheel is connected to the housing by a bearing. A flywheel energy storage facility is coupled with an electric machine (motor/generator). If the facility is connected to the network, then a frequency converter is used to permit electricity feed-in at all times at network frequency.

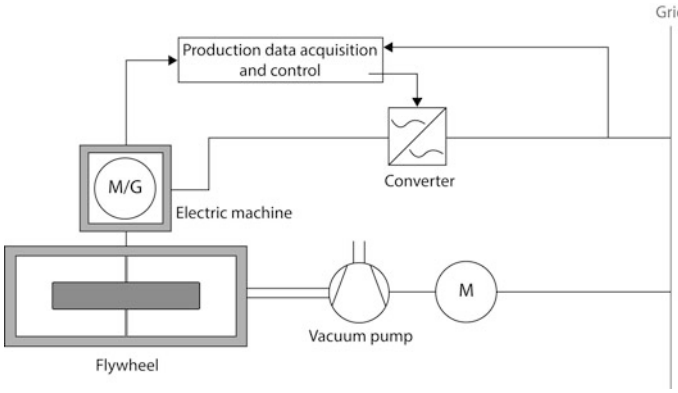
#### 9.3.1.4 Flywheel Designs

A flywheel stores energy as rotational energy. If a material is used that stretches elastically under centrifugal force, then the flywheel also stores potential energy. But with conventional flywheels made of steel or fiber-reinforced plastics with little elasticity, this potential energy is negligible. As explained above, the energy stored is given by:

$$E_{\text{kin}} = \frac{1}{2} J \omega^2. \tag{9.39}$$

The mass moment of intertia $J$ is determined by the flywheel form and the density of the material used. The energy stored is limited by the maximum permitted rotation speed, which is in turn determined by the material used.

**Fig. 9.57** Design




The various flywheel forms and materials are best compared using mass-specific energy density as a criterion. To determine the energy density, the stress within the disc must be considered first.

This is calculated using a differential equation for an infinitesimally small volume element together with its deformation conditions, the equilibrium conditions, and Hook's law. The effective forces include the weight force, the centrifugal force, and the drive torque during acceleration or deceleration. In addition, other factors such as temperature/pressure differences and gyroscopic moment may apply. Centrifugal force is a decisive factor because the flywheel is rotating at high speeds. As a result, the relationship of these mutually-dependent elements of the stress tensor $\sigma_i$ can be described as follows:

$$\{\sigma_i\} = \rho\omega^2 r_a^2 \{k_i(r, \varphi, z)\} \tag{9.40}$$

$\rho$ – density,
$r_a$ – external radius of the flywheel,
$k_i$ – function determined by the flywheel form and the cylinder coordinates $r$, $\varphi$ and $z$.

Applying the strength hypothesis, the equivalent stress $\sigma_v$ can be calculated from the individual components of the multi-axial stress state. This corresponds to the equivalent stress of a uniaxial equivalent stress:

$$\sigma_v = f(\sigma_i) \text{ with } i = 1 \text{ to } 6. \tag{9.41}$$

After determining the largest equivalent stress in the flywheel, this quantity is compared with the material's permitted load. The fatigue strength and resulting safety requirements must be taken into account when calculating a material's permitted load. To simplify the calculation, this value can be excluded from the strength hypothesis, resulting in the following equation:

$$\sigma_{\text{permitted}} = \sigma_{v\max} = \rho\omega^2 r_a^2 \max\{f(k_i)\}. \tag{9.42}$$

In the next step, the equation is solved for $\omega^2$ and Eq. 9.35 then applied:

$$E = \frac{J}{2\rho r_a^2 \max\{f(k_i)\}} \sigma_{\text{permitted}}. \tag{9.43}$$

If both sides are divided by $m$, the result is:

$$\frac{E}{m} = \frac{1}{2}\frac{J}{m r_a^2}\frac{1}{\max\{f(k_i)\}}\frac{\sigma_{\text{permitted}}}{\rho}. \tag{9.44}$$

Now the first part of the equation can be summarized in a single factor. This new factor is called form-factor $K$, and is determined exclusively by the form of the flywheel, and not by its material or dimensions:

$$K = \frac{1}{2}\frac{J}{m r_a^2}\frac{1}{\max\{f(k_i)\}}. \tag{9.45}$$

This form-factor is a value between 0 and 1 which describes the uniformity of the flywheel stress. A form-factor of 1 is possible only in theory. This would mean that the stress was precisely the same at every point of the flywheel. To determine the overall equation for the mass-specific energy density $E/m$, Eq. 9.45 must be inserted into Eq. 9.44:

$$\frac{E}{m} = K\frac{\sigma_{\text{permitted}}}{\rho}. \tag{9.46}$$

The mass-specific energy density can then be used to make an estimate for the flywheel. The flywheel form and material can now be used to calculate the mass required for a specific energy content.

Early flywheels used in the first steam-engines were built as wheels with spokes. With this design, the entire mass was located at the outer edge of the wheel. The wheel was connected to the hub by a number of spokes. The

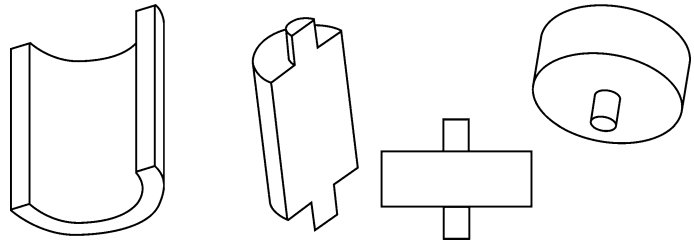


**Fig. 9.58** Alternative flywheel designs

large mass at the outer edge of the wheel ensures a large mass moment of inertia. A disadvantage is that the connection between the hub and the wheel is weak, limiting the maximum rotation speed. The material in this area quickly reaches its maximum permitted load limit.

Other designs in the form of a cylinder or massive disc are more compact (Fig. 9.58). Here, there is less stress at the edge and more at the center. A flywheel designed as a thin disc results in an approximately biaxial equivalent stress. Increasing, the disc thickness results in radial and tangential tensile stress, as well as compressive stress. This reduces the flywheel's strength and, therefore, the maximum rotation speed.

As mentioned at the beginning of this section, stress in rotating materials was first studied by Carl Gustav de Laval in the 19th century, but his focus was on the geometry of turbine design. His design of a turbine propeller that equally distributed all material stresses laid the groundwork for later advances in flywheel disc geometry. His theory's turbine propeller design would have a form-factor of 1. But the product of the rotation speed and the radius in his design must be infinite, a requirement that under real conditions can never be met.

Under real conditions, the stress drops at the edges. This means that, in reality, a rim must be added around the disc to increase the stress. This in turn increases the strength of the disc. Form-factors ranging up to 0.95 can be achieved with this design. With massive flywheels, it should be noted that adding a central borehole doubles the tangential stress at the edge of the borehole.

If modern fiber-reinforced plastics are used, the strength is around 20 times higher in the fiber direction as it is perpendicular to the fiber. As a result, a different form of geometry is required than that used with a steel wheel. The ideal form is a thin ring. But still, radial stresses cause the fibers to reach their load limit before the maximum permitted load in the fiber direction has been reached.

Modern fiber-reinforced plastic flywheels are often made from many thin rings inserted into each other. With this process, care must be taken to ensure that interplay among the individual rings does not result in radial stresses. For this reason, the rings are decoupled from each other by spring elements or elastic separators.

To reduce radial stresses, the individual rings can also be inserted into each other using a conical design. This creates compressive stresses in the flywheel that reduce radial tensile stresses during operation [109, 112].

### ▪ Material Characteristics

Depending on their behavior under load conditions, the materials used are classified as either isotropic or anisotropic. Steel is an isotropic material whose load condition best suits a disc form (form-factor 0.95). Specific strength is often used as a criterion to compare difference materials. This is determined by the quotient of a material's tensile strength and density. As shown in Table 9.16 above, the major difference with earlier kinetic energy storage systems is the materials used. Steel rotors were often designed in forms that ensured safety if they shattered, but reduced the power. In addition, these rotors required regular inspections for cracks using non-destructive testing methods.

For many years, high-tensile steel was the material most frequently used for rotors in-

stalled in flywheel energy storage facilities. It is still used today in most stationary facilities. The steel casting process is well-suited for manufacturing small flywheel discs with uniform strength. But it works far less well for thicker flywheels. Here, inclusions degrade the quality of the steel, thus reducing the strength.

Larger flywheel discs can be manufactured from forged steel. Hardened and tempered steel made of 36NiCrMo16 for example has a yield strength of 1,050 N/mm$^2$, and can tolerate very large loads [114]. But using this material for turbine manufacture is about 2.7 times more expensive by volume than using S235JR steel. In addition, the material chosen must have a high fatigue strength to withstand the alternating charging and discharging cycles [114].

Modern flywheel storage facilities use rotors made out of anisotropic materials, for example. These are particularly common in mobile facilities. They have higher specific energy contents at lower masses than steel flywheels. This also significantly reduces the risks associated with flywheel failure.

Aside from fiber-reinforced plastics, hardened and tempered steels are the most important materials in flywheel manufacture. Fiber-reinforced plastics include glass fiber-coated plastics (GfK), carbon fiber-coated plastics (CfK), and aramid fiber-reinforced plastics (AFK). Epoxy resins are combined with the various fibers to manufacture these materials, which are also called matrixes [112].

#### 9.3.1.5 Bearing Types and Bearing Arrangement

Designing the flywheel bearing is one of the most difficult aspects of building a flywheel energy storage facility. During operation, the bearing must withstand large loads as well as equalize imbalances and gyroscopic moments with the weight of the rotor. In addition, new fiber-reinforced plastics continually increase the maximum permitted rotation speeds, thus in turn increasing the demands on the bearing. To achieve acceptable levels of efficiency, friction losses in the bearing and rotor must also be kept to an absolute minimum. As a result, rotors are often sealed in a vacuum or gas-filled atmosphere. This places additional demands on the bearing lubrication. Finally, the bearing should have as long a service life as possible to minimize maintenance costs.

- **Rolling Bearings**

Rolling bearings have limited applications with large flywheels. As the size of the bearing increases, the maximum rotation speed falls and bearing friction increases. But with larger diameter flywheels, the load capacity alone increases. Large flywheel loads rotating at higher speeds shorten bearing service life. An advantage of these bearings is that they are mass-produced, and as a result, cheaply available. By defining a work cycle and determining the utilization times, it can be estimated if the service life of a particular rolling bearing will be adequate. Since oil mist lubrication cannot be used in a vacuum, circulating oil lubrication is required for adequate lubrication. Circulating oil lubrication also effectively cools the bearing.

- **Slide Bearings**

In slide bearings, two parts in rubbing contact (the shaft and the bearing shell) are separated by an intermediate medium. There are two types of slide bearings: hydrostatic and hydrodynamic.

In hydrostatic slide bearings, an external oil pump produces the oil pressure required to bear the load. With this system, power losses are causes by pump and friction losses. An advantage here is that basically any load can be placed on the bearing (assuming that the oil pump produces an adequate oil pressure for maintaining a lubricant film) at any rotation speed without resulting in wear.

Hydrodynamic slide bearings create the lubricant film that bears the load by using the relative motion between the shaft and the bearing shell. This bearing passes through three friction stages. Static friction is followed by mixed friction, which then turns to fluid friction as the rotation speed increases. Since they have no load or rotation speed limits, hydrodynamic slide bearings are often used in steam turbines.

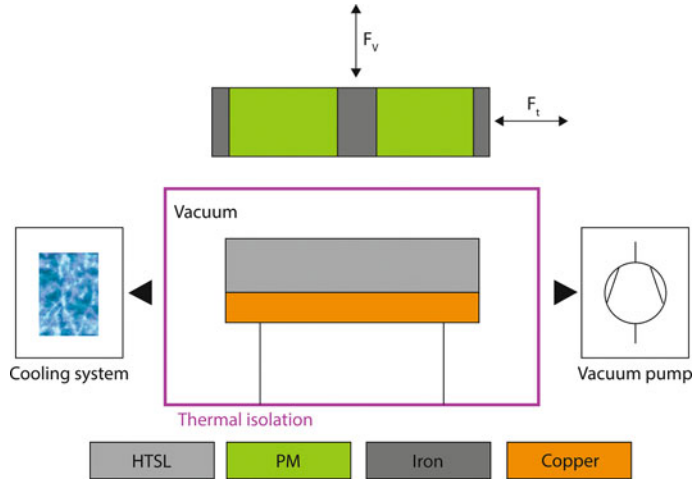



**Fig. 9.59** Magnetic bearing

This type of bearing is not suitable for use with flywheel energy storage. The large number of charging and discharging cycles would repeatedly expose the bearing to static friction, greatly accelerating the aging process [115].

### Magnetic Mearings

Magnetic bearings stabilize moving bodies using magnetic force without any contact. Here the loads placed on conventional bearings can be reduced or completely eliminated. The advantages of this type of bearing are as follows.

- Wear-free, because there is no rubbing between the shaft and the bearing seat.
- No additional lubrication is required, making the bearing ideal for use in a vacuum.
- Tolerates very high rotation speeds, which are limited only by the strength of rotor.
- Requires practically no maintenance, reducing costs. Additional electricity costs to operate the active magnetic coils and for the cooling system are offset by the long service-life of the bearing.

The disadvantages of this type of bearing are the purchase price and the significantly larger mounting space required. In addition, safeguards must be put in place in case the magnetic field fails. Emergency bearings (or safety bearings as they are termed in bearing engineering) are required that can adequately withstand the impact and load of the rotor until it stops, or the enormous acceleration that may result from failure of the shaft at high rotation speeds.

### Bearing Types

There are two general types of bearings: passive and active bearings.

Active bearings:

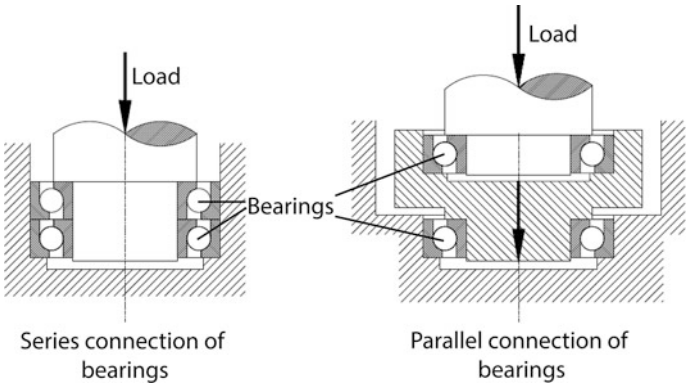
- Adjustable bearing parameters (damping, stiffness)
- Electronic imbalance compensation
- Precise positioning of the rotor in the air gap
- Monitoring of all bearing parameter
- Minimal vibrations

Passive bearings:

- Superconducting magnetic bearings—SMB (require cooling)
- Magnetic force bearings to support conventional bearings
- Minimal vibrations

Modern SMB or high-temperature superconducting bearings (HTSB) are manufactured using superconductors. The process applies the Meissner-Ochsenfeld effect and Lenz's law, which determines the direction of an electric current produced by electromagnetic induction. Figure 9.59 shows the design of a superconducting magnet, including electronic monitoring and cooling systems. A vacuum pump is

**Fig. 9.60** Bearing




also a key component of many flywheel energy storage facilities.

There are two types of cooling systems. The bearing can be cooled using a cooling medium such as liquid nitrogen, hydrogen, or helium. This type of cooling is only feasible if tanks to supply the medium are located nearby, or if units to produce the cooling media are installed. But a cooling unit can also be used to cool the bearing. The advantage here is that the bearing is then a closed system that requires no external operating materials. For this reason, a cooling unit is the best choice for bearing cooling. For real applications, low-temperature superconductors require temperatures ranging from 60K to 77 K. Newly developed materials that are superconducting above 77 K (HTSB) offer an energy-saving alternative [117].

### ▪ Bearing Arrangement

The flywheel shaft can be horizontally or vertically positioned. If it is horizontally positioned, then the weight force and any imbalances are uniformly distributed across the bearing. A disadvantage of this positioning is that the weight force produced bending moments. In addition, high-pulsating tensile stresses may occur.

With vertical positioning, axial bearings as well as radial bearings are required to absorb the weight force. One or two additional radial bearings are also required to guide the rotor and ensure any imbalances are absorbed. There are several possible options here.

Axial bearings:
- Hydrostatic slide bearings
- Magnetic bearings
- A combination of several rolling bearings

Radial bearings:
- Rolling bearings in roller or ball design (in modern facilities, rolling bearings use highly durable ceramic rolling elements with good wear characteristics)
- Magnetic bearings

By connecting them in series (Fig. 9.60, left), a single axial rolling bearing can be used to distribute the load over several bearings. Similarly, two or more bearings can be connected in parallel (Fig. 9.60, right). Bearings of the same or of different design can be used here.

Several flywheels can also be connected together to increase the energy content of a flywheel energy storage facility. The dimensions of the flywheel facility are then only slightly larger, and the use of several small flywheel discs improves bursting characteristics. But it should be kept in mind that horizontal shaft positioning puts an additional load on the axial bearing. The MAN study showed that, with a vertical shaft, distributing the load over several flywheels increases the service life of the bearing [118].

## 9.3.1.6 Charging and Discharging the Storage Facility

An electric machine and a converter are required to charge and discharge a flywheel en-

ergy storage facility. To discharge, the electric machine converts the mechanically stored energy into electric energy. To charge, it converts the electric energy into mechanical energy. In the process, heat is produced by friction and electricity losses. The following electric machines can be used.

### ■ Direct Current Machine

A direct current machine can be operated as a generator or an electric motor. A rotor with an armature winding turns in a fixed magnetic field installed in a massive housing. Because the rotation of the motor alters the magnetic field, a commutator is periodically used to reverse the polarity. To use electricity from, or feed electricity into, an alternating current network, power electronics are required. If a converter is used, generation peaks may put a severe strain on the sliding contacts. Even if the converter is capable of handling high power levels, with a large number of pole pairs sparking, it causes such extensive wear on the sliding contacts that converters should not be used in facilities intended for fast energy supply.



### ■ Asynchronous Machines

Three-phase asynchronous induction machines can also be operated as a motor or as a generator. The motor has a fixed component called the stator with a rotor inside, which is also called the inductor. The inductor is mounted on a shaft, and can move freely. There are two types of inductors, squirrel-cage inductors and inductors using coils. In a squirrel-cage inductor, non-ferrous metal rods are set into a sheet iron pack. The sheet iron pack is made of many iron sheets only a few millimeters thick and insulated from each other. The inductor rods are inserted into grooves in the sheets. Die-cast aluminum is poured into the grooves in the pack after the sheets have been stacked.

When the asynchronous machine is operating as a motor, the rotation speed of the inductor is always slower than the rotating field at the coil. This speed differential is called slip. If an asynchronous machine is coupled with a flywheel storage facility to resolve the frequency on the public electricity network, then sharp changes in the rotation speed of the inductor are required. This is because the inductor turns somewhat slower during motor operation and somewhat faster during generator operation.

### ■ Synchronous Machines

Three-phase synchronous induction machines have a variety of designs. These fall into two main categories: internal and external-pole machines. Each main category then contains two smaller categories: salient or solid-pole machines. All the machines have a stator, a rotor, and an excitation device. The stator has three-phase windings spaced 120 electrical degrees apart. These windings are called U, V, and W, and can be wired in a star or triangle connection. The stator design is the same as in an asynchronous machine. The machine is first synchronized to the network using a power inverter. The power converter can then be bypassed during synchronous operation. The synchronous machine operates at exactly the same frequency as the network voltage applied from this point on. Even in the case of a power failure, the mass of the rotor prevents an abrupt stop. The voltage generated is then at a frequency equivalent to the rotation rate.

### ■ Reluctance Machines

A reluctance machine is an electric motor that generates torque in the rotor using reluctance force alone. In electric motors with magnetic exciters, this is primarily due to the Lorentz force. The advantage of a reluctance machine is that it requires neither permanent magnets nor electric windings on the rotor. As a result, practically all components prone to wear such as slip-rings or brushes are eliminated.

Compared to magnetically excited electric motors, reluctance machine torque is low. This means that a larger reluctance machine is required to generate the same torque as an asynchronous motor. Another disadvantage is that the machine generates a pulsating torque, especially at lower starting pole numbers. Generator operation requires the use of capacitors. The

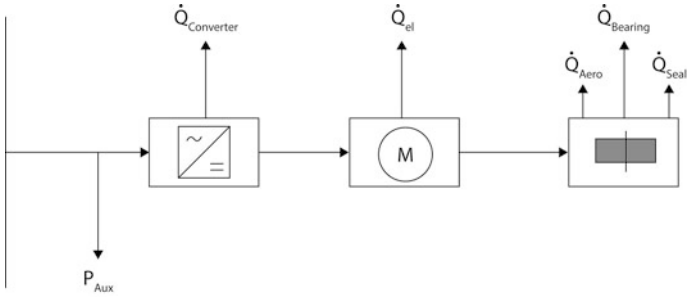



**Fig. 9.61** Flywheel energy storage facility losses

robust construction of the rotor ensures that reluctance machines can effectively withstand short-term overloads and high rotation speeds. Because of their simple design, they can be cheaply manufactured in large numbers.

### Dynamic Processes

Electric energy is mechanically stored when the flywheel is charged during acceleration. In this phase, the mechanical moment is positive. Conversely, discharging the flywheel energy storage system results in negative mechanical moment. The generated mechanical power $P_{\text{mech}}$ here is proportional to the angular velocity $\omega$ and the moment $M$:

$$\pm M_{\text{mech}} = J \cdot \ddot{\varphi} = J \cdot \dot{\omega} \text{ with } \frac{d\varphi}{dt} = \omega, \tag{9.47}$$

$$P_{\text{mech}} = M_{\text{mech}} \cdot \omega = J \cdot \dot{\omega} \cdot \omega. \tag{9.48}$$

The stored or extracted energy $E_{\text{sp}}$ over a certain time period is determined by calculating the integral of the power over this time period:

$$E_{\text{sp}} = \int_{t_1}^{t_2} P_{\text{mech}} dt = \int_{t_1}^{t_2} J \cdot \omega \cdot \dot{\omega} dt, \tag{9.49}$$

$$= J \int_{\omega_1}^{\omega_2} \omega \cdot d\omega dt = \frac{1}{2} J \left(\omega_2^2 - \omega_1^2\right). \tag{9.50}$$

The rotation speed of the flywheel mass is limited by the material's maximum permitted load. This in turn limits the charging and discharging process. The rotation speed is additionally reduced to extend the service life of the flywheel. It must also be taken into account that the maximum power input is additionally limited by the electric components and the flywheel shaft.

### Charging and Discharging Losses

Equation 9.43 only partially accounts for this mechanical system. Further losses are caused by friction in the bearings $M_{\text{L}}$ or friction from the seals $M_{\text{D}}$. Depending on the internal housing pressure, air friction $M_{\text{Aero}}$ may also cause loss torque (Fig. 9.61). Taking these factors into account alters Eq. 9.42 to:

$$\sum M = \pm M_{\text{mech}} - M_L(\omega) - M_{\text{Aero}}(\omega) - M_D(\omega) = J \cdot \dot{\omega}. \tag{9.51}$$

To formulate the differential equation for energy storage in a flywheel subject to friction, the angular velocity must be included as well:

$$\frac{dE}{dt} = \pm P_{\text{mech}}(\omega) - P_L(\omega) - P_{\text{Aero}}(\omega) - P_D(\omega). \tag{9.52}$$

Other losses include energy consumption by the peripherals. Depending on the flywheel energy storage facility design, peripherals may include control electronics for cooling the bearing, a low pressure pump to supply oil with rolling bearings or a high-pressure pump with hydrostatic bearings, a direct current power supply with electromagnetic bearings, a vacuum pump to maintain a vacuum in the housing, and a cooling unit for other electronic facility components.

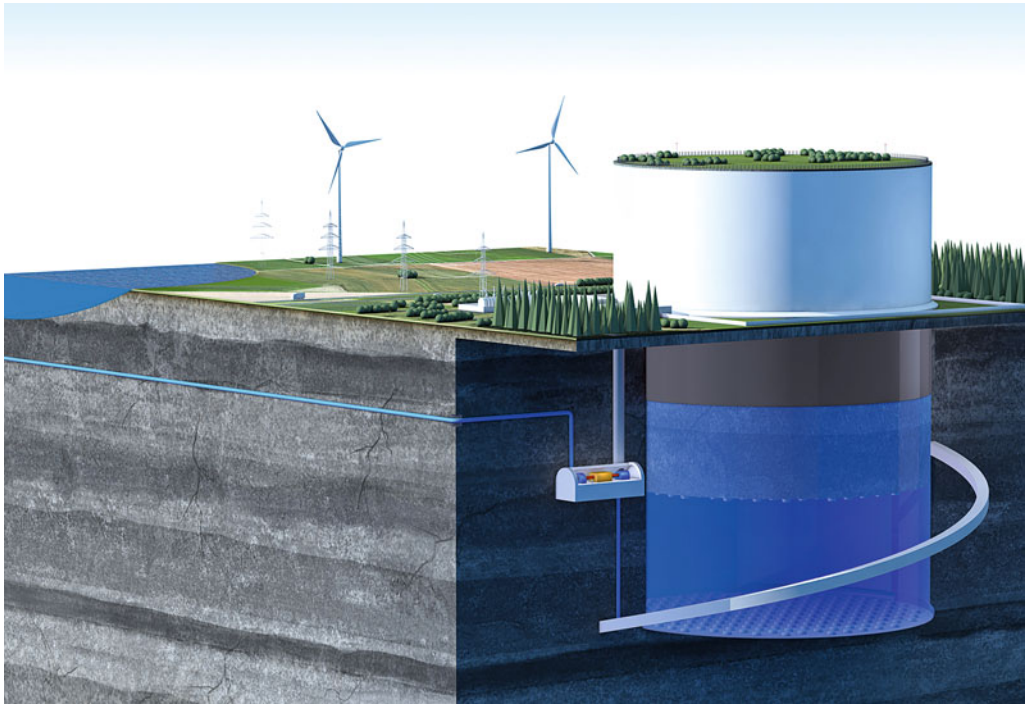


**Fig. 9.62** Basic operating principle and the hydraulic rock storage system



### 9.3.2 Mechanical Stored Energy Systems

Mechanical stored energy systems use a liquid medium such as water to change the potential energy of a solid medium such as rock. They are similar to pumped-storage facilities in that they use turbines and pumps. They are currently categorized as a form of electricity storage (▶ Chap. 2).

#### 9.3.2.1 Basic Operating Principle and the Hydraulic Rock Storage System

Fig. 9.62 illustrates the operating principle of a mechanical stored energy system. To charge the system, water under pressure is forced by electric pumps under an exposed rock cylinder. The hydraulic force raises the rock cylinder, storing electricity in the form of potential energy. The level of pressure required is determined by the mass of the exposed rock cylinder, and ranges from 21 to 103 bar [124].

To discharge the facility or reconvert the energy to electricity, the rock cylinder is allowed to sink and the water under pressure fed through a turbine connected to a generator. The electric energy produced is then fed into the electricity network using a transformer.

A unique characteristic of this electricity storage system is that it uses rock to store potential energy at a density many times higher than the energy density of water. This results in higher storage capacities. With this concept, water is used only as a hydraulic liquid [125].

This hydraulic rock storage system concept developed by Eduard Heindl has yet to be implemented. All estimates given here come from Heindl's publications.

The following sections describe the system's technical parameters.

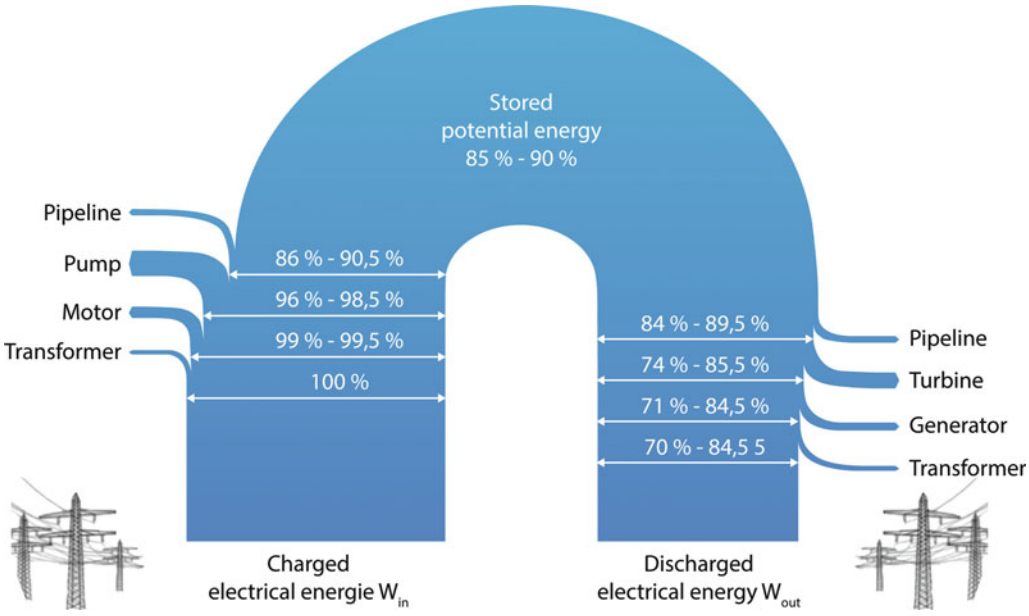



**Fig. 9.63** Mechanical stored energy system efficiency [121, 122, 134, 135]

### Efficiency

Mechanical stored energy system efficiency is comparable with pumped-storage plant efficiency. This is because the machine components used are in fact identical (Fig. 9.63; [121, 122, 134, 135]). The efficiency is determined by the efficiency of the transformer $\eta_{Tr}$, the motor or generator $\eta_{M,G}$, the pump or turbine $\eta_{P,T}$, and the piping $\eta_R$:

$$\eta_{ges} = \eta_{Tr} \cdot \eta_{M,G} \cdot \eta_{P,T} \cdot \eta_R. \quad (9.53)$$

### Energy storage volume and capacity

The quantity of energy stored by a mechanical stored energy system is determined by the mass of the rock that forms the cylinder and the mass of water that can be pumped into the cavern under the cylinder (Fig. 9.64; [137]). Assuming the stone density $\rho_G$ is 2,600 kg/m$^3$, i.e., equivalent to the density of the Earth's continental crust [127], and gravity at the Earth's surface is $g = 9.81\,\mathrm{m/s^2}$, then the potential energy $E_Z$ of a cylinder with a volume of $V_Z$ elevated to height $h_Z$ is:

$$E_Z = g \cdot \rho_G \cdot V_Z \cdot h_Z. \quad (9.54)$$

The volume $V_Z$ of the cylinder is determined by the radius $r_Z$ and height $l_Z$:

$$V_Z = \pi \cdot {r_Z}^2 \cdot l_Z. \quad (9.55)$$

Since the system floats on water, the center of gravity of the rock mass must be maintained above the sealing line to prevent the cylinder from tipping or tilting. As in ship construction, the buoyancy principle [126] applies. The cylinder can only be raised to the sealing line at the middle of the cylinder, or to a maximum height of [70, 124]:

$$h_Z = l_Z/2. \quad (9.56)$$

The cylinder's potential energy $E_Z$ is given by:

$$E_Z = g \cdot \rho_G \cdot \pi \cdot {r_Z}^2 \cdot \frac{l_Z}{2}. \quad (9.57)$$

The stored energy $E_Z$ is reduced by the potential energy losses $E_W$ of the water with a density of $\rho_W = 1{,}000\,\mathrm{kg/m^3}$, which is pumped from the surface water source under the cylinder, and which has a center of gravity at a height of $\vec{r}_S$

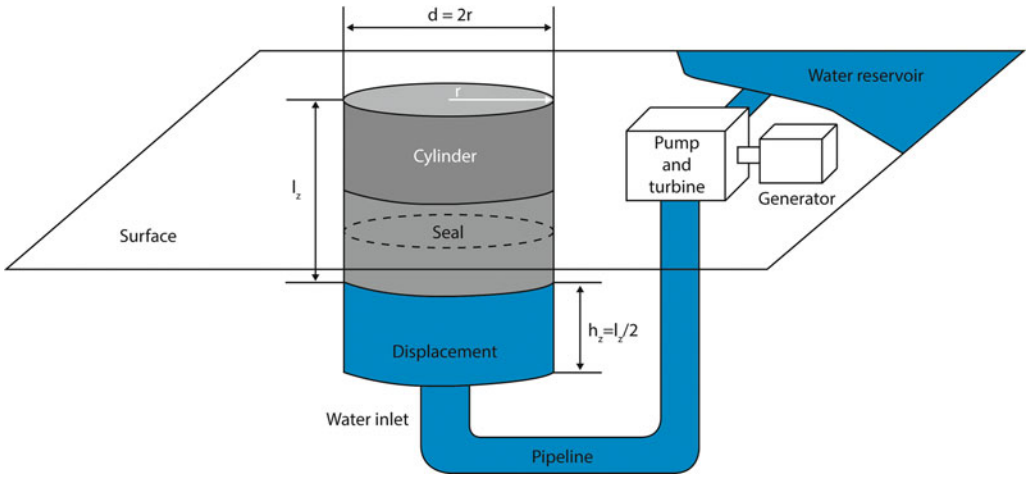



**Fig. 9.64** Mechanical stored energy system design and operating principle [137]

and a volume of $V_{H,}$:

$$E_W = \vec{r}_S \cdot g \cdot \rho_W \cdot V_H \cdot h_Z. \tag{9.58}$$

The volume $V_H$ of the displacement area is determined by the radius $r_Z$ and height $l_Z$ of the cylinder, and is given by:

$$V_H = \pi \cdot {r_Z}^2 \cdot \frac{l_Z}{2}. \tag{9.59}$$

The water in the displacement area is between the depths of $l_Z$ and $l_Z/2$. Its center of gravity $\vec{r}_S$ is determined by the following formula:

$$\vec{r}_S = -\frac{\left(l_Z + \frac{l_Z}{2}\right)}{l_Z}. \tag{9.60}$$

Combined, the potential energy losses of the water are given by:

$$E_W = -\frac{\left(l_Z + \frac{l_Z}{2}\right)}{l_Z} \cdot g \cdot \rho_W \cdot \pi \cdot {r_Z}^2 \cdot \left(\frac{l_Z}{2}\right)^2. \tag{9.61}$$

The potential energy stored by the mechanical stored energy system $E_{LES}$ is therefore given by:

$$E_{LES} = g \cdot \rho_G \cdot \pi \cdot {r_Z}^2 \cdot \frac{{l_Z}^2}{2} - \frac{\left(l_Z + \frac{l_Z}{2}\right)}{l_Z} \cdot g \cdot \rho_W \cdot \pi \cdot {r_Z}^2 \cdot \left(\frac{l_Z}{2}\right)^2. \tag{9.62}$$

The sum result is:

$$E_{LES} = \left(\rho_G \cdot l_Z^2 - \frac{3}{4} \cdot l_Z^2 \cdot \rho_W\right) \cdot \frac{g \cdot \pi \cdot r_Z^2}{2} = \frac{g \cdot \pi \cdot r_Z^2 \cdot l_Z^2}{2} \cdot \left(\rho_G - \frac{3}{4} \cdot \rho_W\right). \tag{9.63}$$

If Eq. 9.63 is used to calculate the capacity for a mechanical stored energy system with a very large radius $r_Z = 250\,\text{m}$ and a very great height $l_Z = 500\,\text{m}$, the result is an approximate theoretical storage capacity of $E_{LES} = 125\,\text{GW h}$. In addition, Eq. 9.63 shows that doubling the radius and the height results in a 16-fold increase in the quantity of stored energy $E_{LES}$ [126]. If only the height or radius is doubled, then there is a four-fold increase in storage capacity. This means that the theoretical storage capacity ranges in the terawatt hours.

**Table 9.17** Theoretical gross and net storage capacities for various facility sizes where $l_Z$ is equal to $2r_Z$

| | | | | | |
|---|---|---|---|---|---|
| Radius in m | 50 | 75 | 100 | 125 | 250 |
| Pressure in bar | 21 | 31 | 41 | 52 | 103 |
| Gross capacity in GW h | 0.2 | 1.0 | 3.0 | 8.0 | 125 |
| Net capacity $\eta_{Re} = 90\%$ in GW h | 0.18 | 0.9 | 2.7 | 7.2 | 112.5 |

Even subtracting energy losses required for reconversion to electricity, the storage capacity is, in theory, adequate to cover Germany's electricity requirements for a day [134]. To illustrate the dramatic increase in storage capacity when the radius and height are doubled, Table 9.17 shows the gross and net storage capacities for various facility sizes where $l_Z$ is equal to $2r_Z$ [124].

In practice, the rock cylinder concept has yet to be implemented. The cylinder used at the test facility at the University of Innsbruck has a diameter of 2.3 m, a height of 6 m, and a weight of 40 tons (▶ Sect. 9.3.2.3).

### ▪ Pressure

Pressures within a mechanical stored energy system vary depending on the facility size and state of charge (SOC). A good indication of the maximum pressure level in the pump and turbine is the pressure $p_D$ at the seal. When the storage facility is fully charged, this point is at the same elevation as the pump or the turbine if they are located at ground level (Fig. 9.65, left).

The pressure of the rock cylinder on the water is given by:

$$p_Z = g \cdot \rho_G \cdot l_Z. \tag{9.64}$$

The pressure of the water on the rock cylinder varies as the water column in the displacement area changes. It depends on the height $h_Z$ to which the rock cylinder is raised, and is given by:

$$p_W = g \cdot \rho_W \cdot (l_Z - h_Z)\,. \tag{9.65}$$

The lower the position of the cylinder, the lower the pressure at the seal. This is because the water column working against the cylinder rises at the same time. The pressure resulting at the seal is given by:

$$p_D = p_Z - p_W = g \cdot (\rho_G \cdot l_Z - \rho_W \cdot (l_Z - h_Z))\,. \tag{9.66}$$

If the pump and turbine are placed 50 m below ground level (Fig. 9.65, right), then the pressure is given by:

$$p_T = g \cdot (l_Z \cdot \rho_G + \rho_W \cdot (50\,\text{m} - h_Z))\,. \tag{9.67}$$

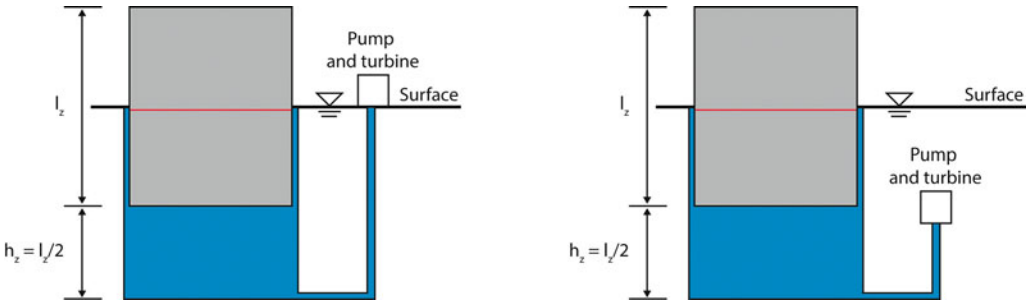



**Fig. 9.65** Pressure in a mechanical stored energy facility with pump and turbine placed at ground level and below ground level

**Table 9.18** Theoretical specific storage capacities for various facility sizes with $l_Z$ equal to $2r_Z$

| Radius in m | 50 | 75 | 100 | 125 | 250 |
|---|---|---|---|---|---|
| Surface area in $m^2$ | 7,854 | 17,671 | 31,416 | 49,087 | 196,350 |
| Specific storage capacity in kW h/$m^2$ | 25.20 | 56.71 | 100.83 | 157.48 | 629.84 |

## Space Requirements

The theoretical space requirements of a mechanical storage energy facility can be roughly determined by calculating the surface $A_Z$ of the exposed cylinder:

$$A_Z = \pi \cdot {r_Z}^2. \tag{9.68}$$

A mechanical storage energy facility with a radius of $r_Z = 125\,\text{m}$, a height of $l_Z = 250\,\text{m}$, and a capacity of around 8 GW h has, according to Eq. 9.68, a surface area of $A_Z = 0.049\,\text{km}^2$. By comparison, the upper reservoir of the largest existing German pumped-storage plant in Godisthal has a capacity of 8.5 GW h and a surface area of 0.55 $\text{km}^2$ [136].

A better reference value for comparison is storage capacity in relation to surface area. This value expresses the amount of energy stored per square meter of surface area. The storage capacity $e_{LES}$ depends on the radius and height of the system, and is given by:

$$e_{LES} = \frac{E_{LES}}{A_Z} = \frac{g \cdot l_Z^2}{2} \cdot \left(\rho_G - \frac{3}{4} \cdot \rho_W\right). \tag{9.69}$$

As a result, the capacity for a mechanical stored energy system with a theoretical radius of $r_Z = 250\,\text{m}$ and a height of $l_Z = 500\,\text{m}$ would be $e_{LES} = 630\,\text{kW h/m}^2$. By comparison, the real pumped-storage plant in Goldisthal has a specific storage capacity of $e_{Goldisthal} = 15.5\,\text{kW h/m}^2$ [14].

Table 9.18 shows the theoretical specific storage capacities and theoretical space requirements for various facility sizes, where again, $l_Z$ is assumed to be equal to $2r_Z$.

This means that the theoretical specific storage capacity for a mechanical energy storage system with a radius of $r_Z = 50\,\text{m}$ and a height of $l_Z = 100\,\text{m}$ is 1.6 times higher than the real pumped-storage plant in Godisthal. The storage facility requires a large water source nearby to supply water during charging, and to take in water during discharging. If not, an adequately-sized reservoir must be built to handle the water exchange. This would dramatically increase the amount of space required.

There is also little space available and few suitable locations for large storage lakes in densely populated countries [132].

## Water Requirements

Pumped-storage systems often require large quantities of water. The volume of water required is determined by the volume of the displacement area $V_H$ which varies based on the radius and the height of the cylinder, and is calculated using Eq. 9.59.

According to Eq. 9.59, a theoretical mechanical energy storage system with a radius of $r_Z = 250\,\text{m}$ and a height of $l_Z = 500\,\text{m}$ requires 0.05 $\text{km}^3$ of water when fully charged.

Since this value is difficult to compare, the energy per cubic meter of water stored can be considered instead. The energy density of a mechanical energy storage system is determined by the volume of the displacement area filled with water and the total amount of energy stored:

$$w_{LES} = \frac{E_{LES}}{V_H} = g \cdot l_Z \cdot \left(\rho_G - \frac{3}{4} \cdot \rho_W\right). \tag{9.70}$$

Applying the theoretical dimensions indicated above, a radius of $r_Z = 250\,\text{m}$ and a height of $l_Z = 500\,\text{m}$ results in an energy density of $w_{LES} = 2.52\,\text{kW h/m}^3$. Table 9.19 shows the theoretical energy densities, water requirements, and specific volumes for various facility sizes where $l_Z$ equals $2r_Z$. The real pumped-storage plant in Goldisthal has an energy den-

**Table 9.19** Theoretical energy densities, water requirements, and specific volumes for various facility sizes where $l_Z$ equals $2r_Z$

| Radius in m | 50 | 75 | 100 | 125 | 250 |
|---|---|---|---|---|---|
| Water requirements in $m^3$ | 392,699 | 1,325,359 | 3,141,593 | 6,136,000 | 49,087,000 |
| Rock cylinder mass in millions of tons | 2.04 | 6.89 | 16.34 | 31.91 | 255.25 |
| Specific volume in $m^3$/kW h | 1.963 | 1.325 | 1.047 | 0.767 | 0.397 |
| Energy density in kW h/$m^3$ | 0.51 | 0.75 | 0.96 | 1.30 | 2.52 |

sity of $w_{\text{Goldisthal}} = 0.71\,\text{kW h/m}^2$ [135]. This is equivalent to about two-sevenths of the energy density of a theoretical mechanical energy storage system. This difference is due to the fact that water is used only as a hydraulic liquid and not as a storage medium in mechanical-energy storage systems [124].

The inflow and outflow quantities are determined by the power of the pump and turbine. Table 9.20 shows the theoretical outflow quantities with various requirements, i.e., daily, weekly, and monthly balancing for various sizes of mechanical storage energy systems (again with $l_Z$ equal to $2r_Z$). This means that a theoretical mechanical storage energy facility with a radius of $r_Z = 250\,\text{m}$, a height of $l_Z = 500\,\text{m}$, and a turbine power of 736 MW would require 81.2 $m^3$/s of water over an operating period of a week. The real pumped-storage plant in Goldisthal with an installed turbine power of 1,060 MW requires eight full load hours to output all the energy in storage, which amounts to a water-discharge of 416.67 $m^3$/s [135].

### Construction, Costs, and Cost-Efficiency

A location with stable rock where a firm cylinder can be exposed is generally required to build a mechanical energy storage system. For safe construction and operation, rock with even layers and limited fissures is preferable but not required. Steep cliffs of compact sandstone and limestone located at the coast would work well. But granite is the most stable form of rock, and forms cliffs up to 1,200 m high. Facility construction would rely primarily on mining processes, permitting an approximate estimation of costs. But since a storage facility of this type has never been built, these estimates remain theoretical. The following sections describe the potential design and estimated costs of a hydraulic rock storage system with a theoretical radius of $r_Z$ =125 m and a resulting theoretical storage capacity of 8 GW h.

### Tunnel System

The construction and operation of a mechanical storage energy system would be facilitated by an access tunnel spiraling around the installation (Fig. 9.66) and providing access to heavy vehicles. A tunnel with a gradient $\alpha$ would have a length $L$ of:

$$L = 2 \cdot \frac{r}{\sin \alpha}. \tag{9.71}$$

The estimated costs of the tunnel are 2,100 € per meter of tunnel. For a mechanical energy storage system with a 125 m radius and a 10% gradient, this would amount to estimated costs of 3.2 million €. The cylinder is accessed through several short branches off the spiral tunnel.

### Exposing the Cylinder Wall

The cylinder wall can be exposed by digging a deep ditch down to the base of the cylinder. The ditch would have a width of four meters after digging. Its size is then reduced at a later stage. Precise blasting is required to loosen the rock (Fig. 9.67). The rock is then removed using a cribbed chute and transported to the surface up the sloped tunnel. This material can then be used to construct a water reservoir if required.

The surface of the piston and cylinder are exposed during the digging of the ditch. De-

**Table 9.20** Theoretical water outflow as well as turbine and pump-power for various facility sizes ($l_Z$ equal to $2r_Z$)

| Radius in m | 50 | 75 | 100 | 125 | 250 |
|---|---|---|---|---|---|
| Water outflow over 8 h in $m^3/s$ | 13.64 | 46.02 | 109.08 | 213.06 | 1,704.41 |
| Water outflow over 168 h in $m^3/s$ | 0.65 | 2.19 | 5.19 | 10.15 | 81.16 |
| Water outflow over 720 h in $m^3/s$ | 0.15 | 0.51 | 1.21 | 2.37 | 18.94 |
| Turbine/pump 8 h in MW | 25.04 | 124.25 | 376.98 | 966.25 | 15,458.75 |
| Turbine/pump 168 h in MW | 1.19 | 5.91 | 17.94 | 46.01 | 736.13 |
| Turbine/pump 720 h in MW | 0.28 | 2.03 | 4.18 | 10.74 | 171.76 |





**Fig. 9.66** Mechanical energy storage tunnel system in spiral form with optional shaft

pending on the type of stone, shotcrete and sealing foil secured by rock bolts can be used to seal and waterproof the cylinder and the piston. The surface at the seal area can be finished with concrete, preferably by slip-forming, facilitating the installation of rolled bellows.

Initial estimates indicate that this method of cylinder-wall construction, including the cribbed chutes and surface finishing of the cylinder and piston, would cost around 1,400 € per square meter.

Given the cylinder wall $A_S$, then:

$$A_S = 4 \cdot \pi \cdot r^2. \tag{9.72}$$

As a result, the cylinder wall could cost around 266 million €.

### Separating the Base-Plate

Mining processes can be applied to separate the base-plate. Parallel galleries are opened under the piston and are separated by a gallery-width from each other. These remaining columns temporarily support the piston (Fig. 9.67).

The excavated galleries are sealed off above and below so that they are watertight. Concrete columns are then built inside the galleries that will later support the entire weight of the piston. In the next step, the remaining sections are removed and sealed so they are watertight as well. The piston and cylinder bases are now exposed and sealed watertight (Fig. 9.69).

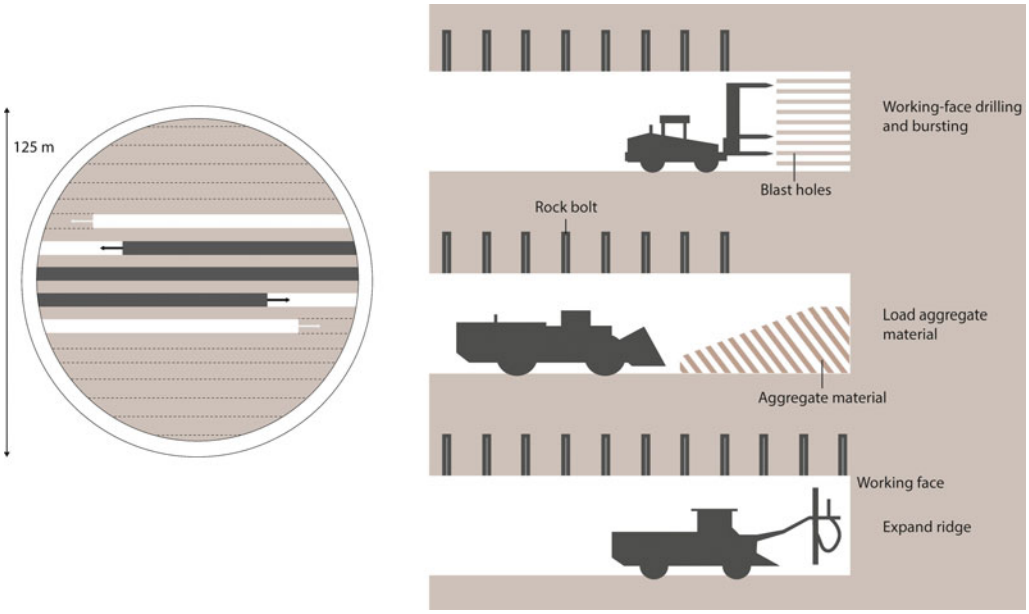



**Fig. 9.67** Mining process applicable for separating the base-plate: overhead view of the gallery layout (*left*), side-view of blasting inside the galleries and roof construction (*right*)

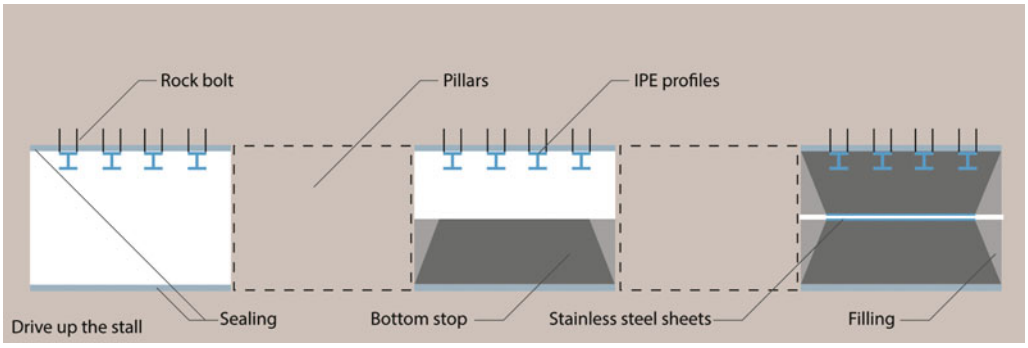



**Fig. 9.68** Detail of base-area construction

The area separated is given by:

$$A_{\text{Base plate}} = \pi \cdot r^2. \tag{9.73}$$

At an assumed cost of 2,500 € per square meter, including construction and sealing, this would amount to costs of around 124 million €.

## ■ Seal

The seal is a critical component of mechanical stored energy construction. It is subject to two contradictory requirements. The seal gap must be as narrow as possible so that the force on the seal is not excessive. But the seal gap cannot be constructed with precise accuracy across a distance of several 100 m. In addition, the seal and surfaces must be accessible to workers and machines so that they can be properly maintained. Otherwise, even the smallest malfunction could result in a total loss of the facility.

One solution to this problem would be a rolling diaphragm seal inserted in a relatively narrow gap 20 cm wide. The membrane material is similar to conveyer belt material,

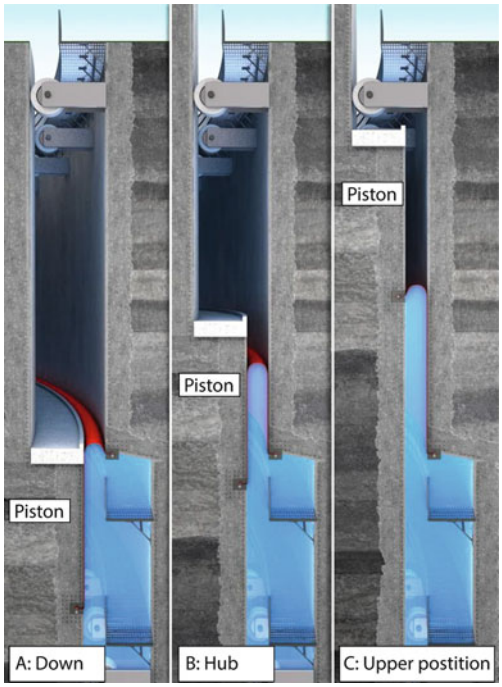



**Fig. 9.69** Rolling diaphragm seal placed in the narrow gap created when the cylinder rises

and could effectively withstand forces resulting from pressures of 50 bar or more. Conveyer belts are additionally reinforced with steel cords running along their length. Access to the seal during construction and for maintenance could be provided by offsetting it from the piston and cylinder radius (Fig. 9.69).

An advantage of this seal concept is that it automatically keeps the piston centered in the middle of the cylinder. If the piston drifts from the center, the bellows bulge. This increases the pressure area on one side, forcing the piston back into the center.

As the piston rises, the bellows unfold. This reduces the length of the seal sheeting to half the distance traveled by the cylinder.

The area $A_D$ of the seal is given by:

$$A_D = \pi \cdot r^2. \tag{9.74}$$

The specific costs of the seal depends on the pressure. This is because higher pressures require stronger steel cords in the interior of the rubber sheeting. Estimates range around 200 €/m$^2$. The costs of a seal for a 8 GW h storage facility would then be around 10 million €.

### 9.3.2.2 Gravity Power Storage System

Another theoretical mechanical stored energy concept is called the gravity power storage system.

Unlike the hydraulic rock storage system described in ▶ Sect. 9.3.2.1, the dimensions of the gravity power system are small. The storage principle is also slightly different, since it uses the same principle as the power tower system (▶ Sect. 9.3.2.3).

With the gravity power, power tower, and hydraulic rock storage systems, electricity is converted to potential energy and stored by raising a load (piston) placed in a cylinder filled with water. But unlike in the hydraulic rock storage system, here, the energy is stored by guiding the water from the upper pump volume to the lower storage volume. When the piston is in the upper area of the cylinder, the electricity storage facility is charged. To discharge the system, the direction of the flow is reversed. The piston sinks, powering a turbine. This converts mechanical potential energy into mechanical kinetic or electric energy.

This theoretical gravity power concept has an assumed diameter of 30 to 100 m and a shaft depth of 500 to 1,000 m. The piston would be half the height of the shaft (250 to 500 m).

This concept has a number of advantages over pumped-storage facilities:

- The facility is completely underground and barely visible from outside; only the transformer housing is visible above ground, meaning the public is likely to easily accept the facility.
- The space requirements are lower, reducing the impact on the environment.
- Since a particular geological topography is not required and choice of location is flexible, approval and construction times may be shortened.

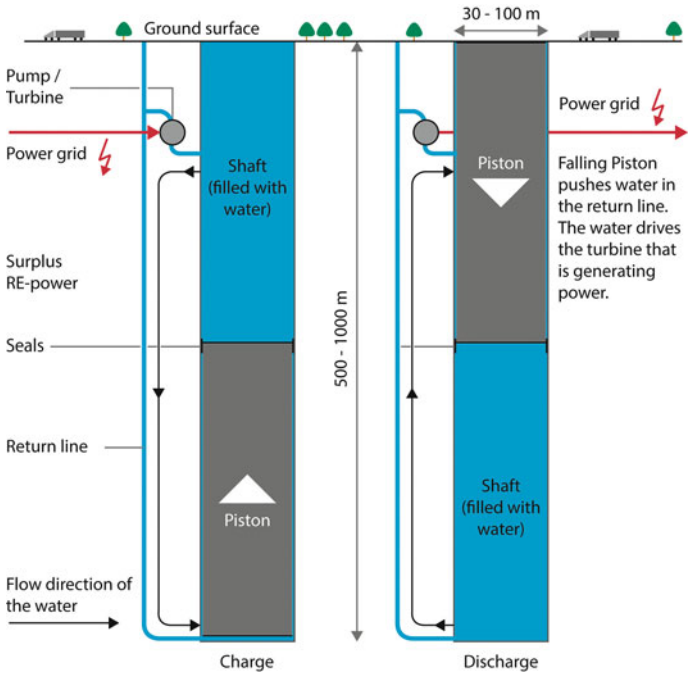



**Fig. 9.70** Operating principle of a gravity power type mechanical energy storage facility during charging and discharging [123]

Depending on geological conditions, the piston can either be cut whole from the rock on-site (rock piston type) or built from the excavated earth using reinforced concrete. The shaft and piston are cladded in reinforced concrete. The piston is additionally encased in stainless steel.

The gravity power modules have a high level of efficiency > 80%, and could be competitive with short-term electricity storage facilities. The power is scalable depending on the geological conditions.

The facility is filled with the water required for operation before its first use. The shaft can then be sealed. No additional water supply is required.

During the storage process, the water above is pumped down into the shaft, raising the piston. To discharge the facility, the piston pressure is used to drive the turbine. Water is fed back up, and the piston sinks.

A flexible seal is required to build up pressure without allowing the water to mix. Since the piston moves very slowly, friction at the seal is assumed to be negligible.

### 9.3.2.3 Power-Tower Storage System

Concluding this discussion of theoretical mechanical stored energy concepts, this section describes the only mechanical energy storage facility design that has been tested to date: the power-tower storage system. This storage system type was developed and tested at the University of Innsbruck. Two experimental power-tower models are currently in operation (PT1 and PT2). A third facility (PT3) is in the planning stages.

Figure 9.71 (left) illustrates the operating principle, which is practically identical to the gravity power system (▶ Sect. 9.3.2.2).

The power-tower can be constructed above ground in the form of a tower, or below-ground in shafts. The pump turbines can also be arranged in a variety of ways. They can be installed externally or integrated into the piston [131].

Figure 9.71 (right) shows the existing Power-Tower 2 facility with the pump turbine integrated into the load. The cylinder is 6 m high and has an inside diameter of 2.3 m. The

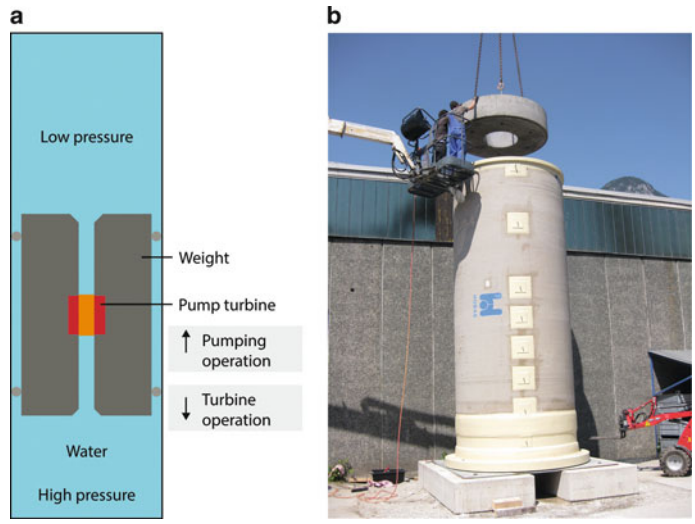



**Fig. 9.71** Operating principle and the existing experimental mechanical energy storage facility 'Power-Tower 2' at Innsbruck University, Austria

piston weighs 40 tons. This experimental model has a charging and discharging power of 4 kW and a storage capacity of 0.2 kW h.

The advantages of the power-tower system are similar to the advantages of pumped-storage facilities, and include [120]:

- High efficiency levels (> 80%)
- Robust technology
- Long service life
- Basically infinite number of charging cycles
- Theoretically unlimited scalability
- No impact on the environment when built underground

But a disadvantage of the power-tower system is its relatively low-energy density. As with the hydraulic rock storage system, the density can only be increased by significantly increasing the facility dimensions.

A theoretical storage capacity of 10 MW h would require a power-tower to be a 100 m high and 30 m wide [119]. This would result in very high capital costs, seriously reducing the facility's cost-efficiency. Researchers at Innsbruck University believe that constructing a power-tower system with dimensions exceeding 100 m is infeasible.

They argue that increasing the number of facilities and choosing locations with suitable geology for convenient construction are better strategies for realistically reducing costs.

They are also designing spring constructions to increase the pressure in the lower reservoir. This would increase the energy density of the storage system [131]. But since the facility uses robust technology, operating costs are low. To increase storage capacity, several smaller power tower mechanical energy storage facilities could be arranged in clusters. Since the individual power-towers could then be activated or deactivated separately, this would also allow a finer calibration of the amount of energy charged and discharged.

## 9.4 Summary

- **Energy storage in mechanical form** using **rotating solid masses** has been used **for thousands of years**. Flywheel masses still **play a key role in modern energy supply**. **Every turbine and every electric generator** in a conventional power plant is **a flywheel mass energy storage device**. As a result, they are crucial for the **stability of electricity supply**. Generally, flywheel storage facilities are characterized by a capability to supply **high levels of power within**

**a short period of time**. But the **quantity of energy** they store is generally **low**.

- The aim of mechanical stored energy concepts **using solid media** is to achieve **higher energy densities**. As with pumped-storage plants, these concepts are based on **changing the elevation** of **large masses** (here large boulders, for example).
- Mechanical stored energy facilities, would probably have the **largest total installed powers and store the greatest quantities of energy among energy storage systems worldwide**. This is certainly true if **only electric energy supply** is considered. **TES systems** are discussed below in ▶ Chap. 10. These facilities are often ignored, but in fact they are the **most widely distributed form of electric-energy storage overall**. For example, practically **every building** is equipped with a **hot water tank**.

## References

1. AA-CAES (2007) Advanced Adiabatic Compressed Air Energy storage. http://cordis.europa.eu/ (Abschlussbericht, Auftrag ENK6-CT-2002-000611)
2. ALACAES SA (2013) the AA-CAES technology. http://www.alacaes.com/
3. K (1985) Underground Storage: A CAES Prerequisite, Präsentation auf: Compressed Air Energy storage Plants (MiniCAES) regional conference, Chicago, Illinois, p 6
4. Allen RD, Doherty TJ, Kannberg LD (1985) Summary of Selected Compressed Air Energy storage Studies. Pacific Northwest Laboratory, Richland, WA, p 112
5. Auer J (2012) Moderne Stromspeicher: Unverzichtbare Bausteine der Energiewende. http://www.dbresearch.de/PROD/DBR_INTERNET_DE-PROD/PROD0000000000284196.PDF
6. BBC (1986) Operating Experience With the Huntorf Air-Storage Gas Turbine Power Station. Brown Boveri 73(6):12
7. Berk B, Hurwitch JW, Schuller CR (1983) CAES and UPH Technologies: An Uncertain Future. Undergr Space 7:342–346
8. Budt M, Wolf D, Prümper H-J (2012) LTA-CAES – A Low-temperature approach to Adiabatic Compressed Air Energy storage. Innostock 2012 – The 12th International Conference on Energy storage, Lleida
9. Buffa F, Kemble S, Manfrida G, Milazzo A (2013) Exergy and Exergoeconomic Model of a Ground-Based CAES Plant for Peak-Load Energy Production. Energies 6:1050–1067
10. Collins S (1993) Commercial options for energy storage multiply. Power 137(1):55–57, McGraw-Hill, New York
11. Crotogino F, Hübner S (2008) Energy storage in Salt Caverns/Developments and Concrete Projects for Adiabatic Compressed Air Energy storage and for Hydrogen Storage. Solution Mining Research Institute – Spring 2008 Technical Conference, Porto, Portugal, p 14 (28–29 April 2008)
12. Dämgen U (2013) Neuer Entwicklungsansatz bei Druckluftspeichern. BWK – Das Energiefachmagazin 1(2):70–74
13. Dengel AJ, Fliß T (2009) Druckluftspeicher zur Energiespeicherung in stillgelegten Salzbergwerken und zur Stabilisierung der Grubenhohlräume. BMU, p 140 (Abschlussbericht TP2/TP3, Forschungsbericht 032767A)
14. Doetsch C, Budt M, Wolf D, Kanngießer A (2012) Adiabates Niedertemperatur-Druckluft-speicherkraftwerk zur Unterstützung der Netzintegration von Windenergie (Abschlussbericht)
15. Dreißigacker V, Müller-Steinhagen H, Zunft S (2009) Thermo-mechanical investigation of packed beds for the large-scale storage of high temperature heat. Effstock 2009 – Thermal Energy storage for Energy Efficiency and Sustainability (11th International Conference), Stockholm, Sweden, p 8
16. Eckroad S, Gyuk I, Mears L, Gotschall H, Kamath H (2003) EPRI-DOE Handbook of Energy storage for Transmission and Distribution Applications. Palo Alto, CA, p 512 (EPRI-DOE Bericht Nr. 1001834)
17. Eldridge FR (1976) Wind Energy Conversion Systems Using Compressed Air Storage. The MITRE Corporation, McLean, VA, p 27
18. Elliott T (1995) Electric-energy storage hinges on three leading technologies. Power 139(8):42–45, McGraw-Hill, New York
19. Gaelectric (2012) Gaelectric Energy storage – Project CAES – Larne, NI Presentation to Larne Borough Council. Larne. http://www.gaelectric.ie/wp-content/uploads/GES_LBC_Presentation_05032012.pdf (p. 12.)
20. Gay FW (1948) Means for Storing Fluids for Power Generation. US Patent Nr. 2433296, p. 8.
21. GeneralCompression (2013) Verfügbar unter: http://www.generalcompression.com/
22. Gillhaus A, Crotogino F, Hubner S (2006) Verbesserte Integration großer Windstrommengen durch Zwischenspeicherung mittels CAES. Aachen
23. Glendenning I, Chew PE, Grant R, Glanville R, Moye MH (1979) Technical and Economic Assessment of Advanced Compressed Air Storage (ACAS) Concepts. CEGB – Central Electricity Generation Board,

England for EPRI – Electric Power Research Institute, Palo Alto, CA, p 519
24. Herbst CH, Hoffeins H, Stys ZS (1978) Huntorf 290 MW Air storage System Energy Transfer (ASSET) Plant Design, Construction and Commissioning. American Power Conference, Chicago, IL, p 17
25. Hobson MJ, Bahadur S, Driggs CL, James DC, Sangermano JC, Gerhardt JC, Hinkel RC, Hresko KA, Galola MK (1981) onceptual Design and Engineering Studies of Adiabatic Compressed Air Energy storage (CAES) with Thermal Energy storage. Acres American Incorporated for Pacific Northwest Laboratory, Richland, WA, p 216
26. Jakiel C, Zunft S, Nowi A (2007) Adiabatic compressed air energy storage plants for efficient peak load power supply from wind energy: the European project AA-CAES. Int J Energy Technol Policy 5(3):10
27. Kalhammer FR, Schneider TR (1976) Energy storage. Annu Rev Energy 1:311–343
28. Kentschke T (2004) Druckluftmaschinen als Generatorantrieb in Warmluftspeichern. TU Clausthal, Institut für Tribologie und Energiewandlungsmaschinen, p 201 (Dissertation)
29. King M, Moridis G (2009) Technical Feasibility of Compressed-Air Energy storage in an Aquifer Storage Vessel. EESAT 2009 – Electrical Energy storage Applications and Technologies, Seattle, WA, p 6
30. Laing D, Lehmann D (2008) Concrete storage for solar thermal-power plants and industrial process heat. 3rd International Renewable Energy storage Conference (IRES 2008), Berlin, p 6
31. The Centre for Low Carbon Futures (2013) Liquid Air in the energy and transport systems – Opportunities for industry and innovation in the UK (Vollständiger Bericht)
32. Lemofouet S, Rufer A (2006) Hybrid Energy-storage system Based on Compressed Air and Super-Capacitors with Maximum Efficiency Point Tracking (MEPT). Ieee Trans Ind Electron 53(4):1005–1115
33. LightSailEnergy (2013) Technology. http://www.lightsail.com/tech/
34. Marchese D (2008) Norton Energy storage: CAES Resiliency in Uncertain Markets. Compressed Air Energy storage (CAES) Scoping Workshop, Columbia University, New York, NY, p 14
35. Marquardt R, Moser P, Hoffmann S, Pazzi S, Klafki M, Zunft S (2008) AA-CAES – Opportunities and challenges of advanced adiabatic compressed-air energy storage technology as a balancing tool in interconnected grids. 40. Kraftwerkstechnisches Kolloquium 2008, Dresden, p 14
36. Mattick W, Haddenhorst HG, Weber O, Stys ZS (1975) Huntorf – The World's First 290-MW Gas Turbine Air-Storage Peaking Plant. American Power Conference. vol 37, pp 322–330
37. Abd-El Fattah ME-SF (2005) Uncooled Compressed Air Storage for Balancing of Fluctuating Wind Energy. TU Clausthal, Institut für Elektrische Energietechnik, p 180 (Dissertation)
38. Nakayama A, Yamachi H (1999) Thermodynamic analysis of efficiency and safety of underground air energy-storage system vol 3. Kobe University, pp 247–254 (Bericht des Research Center for Urban Safety and Security)
39. Nakhamkin M, Marshall R, Swensen E (1988) Thermal Energy storage for Advanced Compressed-Air Energy storage Plants. Gibbs & Hill Inc., New York. Bericht aus, p 142 (erstellt für: EPRI, AP-5844)
40. Nakhamkin M, Andersson L, Swensen E, Howard J, Meyer R, Schainker R, Pollak R, Mehta B (1992) AEC 110 MW CAES plant: status of project. Asme J Eng Gas Turbines Power 114:695–700
41. Nielsen L, Leithner R (2009) Dynamic Simulation of an Innovative Compressed Air Energy storage Plant – Detailed Modelling of the Storage Cavern. Wseas Trans Power Syst 4(8)
42. Pimm AJ, Garvey SD, Drew RJ (2011) Shape and cost analysis of pressurized fabric structures for subsea compressed air energy storage. Proceedings of the Institution of Mechanical Engineers, Band 225, Teil C: Journal Mechanical Engineering Science
43. PNNL (1982) Technology Assessment Report for the Soyland Power Cooperative, Inc.; Compressed-air energy-storage system (CAES), PNNL Pacific Northwest Laboratory, Richland, WA, p. 106
44. Pollak R (1994) History of first U.S. Compressed Air Energy storage CAES plant 110MW 26h, Band 2: Construction, EPRI: Palo Alto, CA, p. 202
45. Quast P (1981) The Huntorf Plant: Over 3 Years Operating Experience with Compressed Air Caverns. KBB Kavernen Bau- und Betriebs-GmbH, p 11
46. Radgen P, Blaustein E (2001) Compressed Air Systems in the European Union – Energy, Emissions, Savings Potenzial and Policy Actions. LOG_X Verlag, Stuttgart, p 162 (Forschungsbericht)
47. Radgen P (2008) 30 Years Compressed Air Energy storage Plant Huntorf–Experiences and Outlook. 3rd International Renewable Energy storage Conference (IRES 2008), Berlin, p 18
48. RWE power (2010) ADELE–Der adiabate Druckluftspeicher für die Elektrizitätsversorgung. http://www.rwe.com/web/cms/mediablob/de/364316/data/364260/59668/rwe-power-ag/klimaschutz/adele/Broschuere-ADELE.pdf (Brochüre)
49. RWE power (2010) ADELE–Ein Speicher für grünen Strom. http://www.rwe.com/web/cms/mediablob/de/514008/data/365478/1/rwe/innovation/projekte-technologien/energiespeicher/projekt-adele-adele-ing/Flyer-Sechs-Fragen-zum-Projekt-in-Stassfurt.pdf (Brochüre)
50. Schulte RH, Critelli N Jr., Holst K, Huff G (2012) Lessons from Iowa: Development of a 270 Megawatt Compressed Air Energy storage Project in Midwest Independent System Operator – A Study for

the DOE Energy. Storage Systems Program, Sandia Report SAND2012-0388
51. Smith D (2001) The first CAES merchant. Mod Power Syst 21(9):21–25
52. Staubly RK, Pedrick GA (2012) Seneca Compressed Air Energy storage (CAES) Project – Final Phase 1 Technical Report. http://www.smartgrid.gov/document/seneca_compressed_air_energy_storage_caes_project (p. 66)
53. SustainX (2013) Technology. http://www.sustainx.com/technology-isothermal-caes.htm
54. Terashita F, Takagi S, Kohjiya S, Naito Y (2005) Air-tight butyl rubber under high pressures in the storage tank of CAES-G/T system power-plant. J Appl Polym Sci 95(1):173–177
55. Tuschy I, Althaus R, Gerdes R, Keller-Sornig P (2004) Entwicklung der Gasturbinen in der Luftspeicher-Technologie. VGB Powertech 4(2004):84–87
56. Tuschy I Druckluftspeicherkraftwerke als Option zur Netzintegration erneuerbarer Energiequellen: Ein Vergleich der Konzepte. 40. Kraftwerkstechnisches Kolloquium 2008, Dresden, p 12
57. Wiles LE, McCann RA (1983) Reservoir Characterization and Final Pre-Test Analysis in Support of the Compressed Air Energy storage. Pacific Northwest Laboratory, Richland, WA, p 62 (Pittsfield Aquifer Field Test in Pike County, Illinois)
58. Wolf D (2011) Methods for Design and Application of Adiabatic Compressed Air Energy storage Based on Dynamic Modeling, Dissertation Ruhr-Universität Bochum, urn:nbn:de:0011-n-1546519, ISBN: 978–3-87468-264-0
59. Zaloudek FR, Reilly RW (1982) An Assessment of Second-generation Compressed Air Energy storage Concepts. Pacific Northwest Laboratory, p 82
60. Zunft S, Tamme R (2003) Entwicklung thermischer Speicher für adiabate Druckluftspeicherkraftwerke. Das Projekt AA-CAES. DLR – Deutsches Zentrum für Luft- und Raumfahrt e.V, Stuttgart, p 1
61. http://www.thema-energie.de. Accessed 13.02.2013
62. http://www.neueenergie.net/index.php?id=657&tx_ttnews[tt_news]=4508&tx_ttnews[backPid]=621&cHash=614afaa09f. Accessed 31.01.2013
63. Mosonyi E (2009) Wasserkraftanlagen. Heidelberg, Springer Verlag (p.: 27–42, 55, 76, 114–117, 675–688.)
64. Quaschning V (2009) Regenerative Energiesysteme. Hanser, München
65. Zahoransky R (2010) Energietechnik. Vieweg+Teubner, Wiesbaden
66. Czisch G (2005) Szenarien zur zukünftigen Stromversorgung (p.: 99–111, 409–411.)
67. http://www.seo.lu/de/Hauptaktivitaeten/PSW-Vianden/Unterhalt. Accessed 11.12.2012
68. Popp M (2010) Speicherbedarf bei einer Stromversorgung mit erneuerbaren Energien. Springer, Berlin Heidelberg
69. Schmidt M (2013) Auf dem Weg zum Nullemissionsgebäude. Springer, Wiesbaden (p.: 318, 324–325)
70. Heindl E (2013) Hydraulic Hydro-Storage for grid scale energy storage, Hochschule Furtwangen 09. März 2013 p.: 3–6, 9–12. Heindl Internet AG . Accessed 05. Januar 2013
71. http://lageenergiespeicher.de
72. Heindl E (2013p) Präsentation „Der Lageenergiespeicher" Lehrertage. Universität Regensburg (p.: 1, 24, 27, 38, 40)
73. Klett Verlag GmbH E http://www2.klett.de/sixcms/list.php?page=geo_infothek&article=Infoblatt+Schalenaufbau+der+Erde. Accessed 12 Apr 2013
74. Neupert U, Euting T, Kretschmer T, Notthoff C, Ruhlig K, Weimert B (2009p) Energiespeicher. Fraunhofer IRB Verlag, pp 131–136
75. Heindl E (2012p) Forschungsbericht „Der Lageenergiespeicher als Baustein der Energiewende". Hochschule Furtwangen (p.: 3–4, 6)
76. Alber M (2000) Advance rates of hard rock TBMs and their effects on project economics. Tunn Undergr Space Technol 15(1):55–64
77. Wijk G (1991) Rotary drilling prediction. Int J Rock Mech Min Sci Geomech Abstr 28(1):35–42
78. Graniteland.com C & H Steimel GbR http://www.graniteland.com/infos/production/quarry-equipment. Accessed 2011
79. Stahlbroker – LAXACON GmbH http://www.stahlbroker.de. Accessed 2011
80. Alibaba.com Hong Kong Limited http://german.alibaba.com/product-gs/hdpe-waterproof-geomembrane-452569482.html. Accessed 2011
81. Popp M (2012) Ringwallspeicher für die Energiewende. Spektrum Wiss (2):84–87 (Prof. Dr.-Ing. Matthias Popp. Accessed 22. April 2013)
82. http://www.ringwallspeicher.de
83. http://www.poppware.de
84. Power RWEAG http://www.rwe.com/web/cms/de/60012/rwe-power-ag/standorte/braunkohle/hambach. Accessed 3 May 2013
85. VDE Verband der Elektrotechnik Elektronik Informationstechnik e.V., Bericht: „Exkursion in das Pumpspeicherwerk Goldisthal" p.: 3–12
86. Popp M (2012p) Präsentation „Ringwallspeicher: ein essentieller Beitrag der Geotechnik zur Energiespeicherung Geotechnik-Tag. Technische Universität München (p.: 14–16, 22)
87. Internationale Gewässerschutzkommission für den Bodensee http://www.igkb.de/html/seedaten/index.html. Accessed 3 May 2013
88. Paludan Architects G http://www.greenpowerisland.dk/. Accessed 4 May 2013

89. ZEITONLINE GmbH http://blog.zeit.de/gruenegeschaefte/2013/01/24/belgien-plant-mega-insel-als-stromspeicher. Accessed 22 Apr 2013
90. Bayerischer Rundfunk http://www.br.de/radio/bayern2/sendungen/notizbuch/energiespeicher-kugelspeicher-100.html. Accessed 4 May 2013
91. Frankfurter Allgemeine Zeitung GmbH http://www.faz.net/aktuell/technik-motor/umwelt-technik/in-der-tiefe-der-meere-hohlkugeln-speichern-ueberschuessigen-windstrom-1608012.html. Accessed 4 May 2013
92. Aktiengesellschaft HOCHTIEF http://www.berichte.hochtief.de/gb12/57.jhtml#fn1. Accessed 4 May 2013
93. Heise Medien Gruppe GmbH & Co. KG http://www.heise-medien.de/presse/Technology-Review-ueber-Untersee-Stromspeicher-1793860.html. Accessed 24 May 2013
94. Stenzel P, Bongartz R, Kossi E (2013) Potenzialanalyse für Pumpspeicher an Bundeswasserstraßen in Deutschland. Energiewirtsch Tagesfr 63(3):54–57
95. Wasser und Schifffahrtsverwaltung des Bundes http://www.wsv.de/service/karten_geoinformationen/bundeseinheitlich/pdf/w162.pdf. Accessed 10 May 2013
96. Verein Deutscher Ingenieure e.V. http://www.vdi-nachrichten.com/artikel/Schifffahrtskanaele-werden-dezentrale-Pumpspeicher/50772/2. Accessed 10 Jan 2013
97. Schiffshebewerk Lüneburg http://www.schiffshebewerk-scharnebeck.de/Schiffshebewerk000-kl.JPG. Accessed 14 May 2013
98. ZEITONLINE GmbH http://www.zeit.de/2010/48/Pumpspeicherkraftwerk. Accessed 4 May 2013
99. Forschungszentrum Jülich GmbH STE Preprint 04/2012 „Energiespeicher". http://www.fz-juelich.de/SharedDocs/Downloads/IEK/IEK-STE/DE/preprint_04_2012.html
100. Innogy GmbH RWE Präsentation „Integrierte Energiekonzepte auf Halden". http://www.tuev-nord.de/cps/rde/xbcr/SID-562D0207-AF98295B/tng_de/schramm.pdf
101. Heidjann GmbH & Co.KG http://www.stromauskunft.de/blog/forschung/windparks-und-pumpspeicherkraftwerke. Accessed 24 May 2013
102. WAZ NewMedia GmbH & Co. KG, http://www.derwesten.de/wirtschaft/oekostrom-von-bergehalde-id6500796.html. Accessed 29 May 2013
103. Innogy GmbH RWE Flyer „Energiepark Halde Sundern". https://www.rwe.com/web/cms/de/1241776/rwe-innogy/presse-news/mediencenter/informationsmaterial
104. Süddeutsche Zeitung http://www.sueddeutsche.de/wissen/erneuerbare-energie-windstrom-aus-dem-bergwerk-1.1018995. Accessed 7 Nov 2012
105. Erlei M, Dimmig A-K, Neumann C (2011) Forschungsbericht „Windenergiespeicherung durch Nachnutzung stillgelegter Bergwerke". Energie-Forschungszentrum Niedersachsen (p.: 771–802, 840–856)
106. Schulz D (2009) Präsentation „Speicherpotenziale von Pumpspeicherwerken in Tagebaurestlöchern ehemaliger Braunkohlereviere". Forum Netzintegration, Deutsche Umwelthilfe, Berlin, pp 4–15
107. Universität Duisburg-Essen http://www.uni-due.de/geotechnik/forschung/upw.shtml. Accessed 19 May 2013
108. Khammas AAW Buch der Synergie. http://www.buch-der-synergie.de/c_neu_html/c_10_06_e_speichern_schwung_nahverkehr.htm. Accessed 1 Aug 2013
109. cand.-Ing. Florian Strößenreuther: Machbarkeitsstudie und Konzept einer stationären Schwungradanlage zur dezentralen, verbraucherorientierten Energiespeicherung
110. Deutsches Museum Meisterwerke aus dem Deutschen Museum Band IV. http://www.deutsches-museum.de/sammlungen/ausgewaehlte-objekte/meisterwerke-iv/turbine/. Accessed 8 Aug 2013
111. Dipl.-Ing. Wolfgang Bärwald (DLG) Regelung von Reaktionsrädern. http://www.dlr.de/os/desktopdefault.aspx/tabid-7148/11932_read-29205/. Accessed 28 July 2013
112. Burg P Schnelldrehendes Schwungrad aus faserverstärktem Kunststoff. http://www.aspes.ch/publications/diss.pdf. Accessed 26 July 2013
113. Tischner H Die Erfindung des Rads. http://www.heinrich-tischner.de/33-ge/kultur/rad-erf.html. Accessed 8 Aug 2013
114. Wittel H, Muhs D, Jannasch D, Voßiek J Roloff/Matek Maschinenelemente Tabellenbuch, 19th edn. Vieweg+Teubner
115. Wittel H, Muhs D, Jannasch D, Voßiek J Roloff/-Matek Maschinenelemente Normung, Berechnung, Gestaltung, 19th edn. Vieweg+Teubner
116. Lindner Physik für Ingenieure, 18th edn.
117. Gutt H-J, Komarek P, Kasper E Schwung-Energiespeicher-System mit supraleitenden Magnetlagern. http://elib.uni-stuttgart.de/opus/volltexte/2002/1087/pdf/3-8322-0167-x_dok.pdf. Accessed 5 Aug 2013
118. Zwerenz W, Schauberger H Stationäre Schwungrad-Energiespeicheranlage SSB
119. Aufleger M (2015) Powertower. Bayerischer Energiedialog, München

120. Aufleger M, Neisch V (2015) POWERTOWER – Energie speichern, wo sie erzeugt wird. http://www.powertower.eu/index.html (Universität Innsbruck)
121. Dünkel W (2006) Pumpspeicherwerk Goldisthal – 1.060 MW-Kavernenkraftwerk. Bericht – Exkursion in das Pumpspeicherwerk Goldisthal/Thüringer Wald, Kassel
122. Giesecke J, Mosonyi E (2009) Wasserkraftanlagen. Planung, Bau und Betrieb, 5th edn. Springer (s.l)
123. Gravity Power (2014) Technology. http://www.gravitypower.net/technology-gravity-power-energy-storage/. Accessed 14 Oct 2015
124. Heindl E (2013) Hydraulic Hydro-Storage for grid scale energy storage. Furtwangen
125. Heindl Energy Der Lageenergiespeicher. http://www.heindl-energy.com/de/der-lageenergiespeicher/uebersicht.html
126. Heindl Energy Idee und Funktion. http://www.heindl-energy.com/de/der-lageenergiespeicher/idee-funktion.html. Accessed 13 Oct 2015
127. Klett Verlag (2012) Infoblatt Schalenaufbau der Erde. Erdkruste, Erdmantel, Erdkern und ihre physikalischen Eigenschaften. https://www.klett.de/alias/1011308. Accessed 23 Oct 2015
128. LightSailEnergy (2013) We Store Energy in Compressed Air. LightSailEnergy. http://www.lightsail.com/. Accessed 29 Dec 2013
129. Marchese D (2008) Norton Energy Storage: CAES Resiliency in Uncertain Markets. New York
130. Nakayama A, Yamachi H (1999) Thermodynamic analysis of efficiency and safety of underground air energy storage system. Kobe
131. Neisch V, Klar R, Aufleger M (2012) Powertower – Hydraulischer Energiespeicher. Graz
132. Neupert U (2009) Energiespeicher. Technische Grundlagen und energiewirtschaftliches Potenzial. Fraunhofer-IRB-Verl, Stuttgart
133. Tengborg P, Johansson J, Durup JG (2014) Storage of highly compressed gases in underground Lined Rock Caverns – More than 10 years of experience. Tunnels for a better Life, Brazil
134. Popp M (2010) Speicherbedarf bei einer Stromversorgung mit erneuerbaren Energien. Springer, Berlin, Heidelberg
135. Quaschning V (2009) Regenerative Energiesysteme. Technologie – Berechnung – Simulation, 6th edn. Hanser, München (mit 271 farbigen Bildern, 113 Tabellen und einer DVD)
136. Quast P (1981) The Huntorf Plant: Over 3 Years Operating Experience with Compressed Air Caverns
137. Schmidt M (2013) Auf dem Weg zum Nullemissionsgebäude. Grundlagen, Lösungsansätze, Beispiele. Springer, Dordrecht
138. Terashita F, Takagi S, Kohjiya S, Naito Y (2005) Airtight butyl rubber under high pressures in the storage tank of CAES-G/T system power plant. J Appl Polym Sci 95(1):173–177. https://doi.org/10.1002/app.20815

# Thermal Energy Storage

*Ingo Stadler, Andreas Hauer, and Thomas Bauer*

**10.1 Thermal Storage System Characteristics – 565**

**10.2 Storage Technologies – 567**
10.2.1 Sensible-Thermal Storage – 567
10.2.2 Latent-Thermal Storage – 568
10.2.3 Thermochemical-Thermal Storage – 568
10.2.4 Thermophysical Properties and Material Requirements – 571

**10.3 Thermodynamic Principles – 571**
10.3.1 Thermal Energy – 571
10.3.2 Heat Transfer – 572
10.3.3 Thermal Insulation – 573

**10.4 Sensible TES – 574**
10.4.1 Storage Materials – 574
10.4.2 Storage Systems Using Solid Storage Media – 576
10.4.3 Storage Systems Using Liquid Storage Media – 581

**10.5 Latent TES – 588**
10.5.1 Characterization of Latent-Thermal Storage Materials – 590
10.5.2 Latent-Thermal Storage Materials – 591
10.5.3 Heat-Transfer Concepts – 597
10.5.4 Conclusion – 600

**10.6 Thermochemical-Energy Storage Systems – 601**
10.6.1 Storage Materials for Thermochemical Processes – 602
10.6.2 Designs – 604
10.6.3 Conclusion – 606

**Electronic supplementary material** The online version of this chapter (https://doi.org/10.1007/978-3-662-55504-0_10) contains supplementary material, which is available to authorized users.

© Springer-Verlag GmbH Germany, part of Springer Nature 2019
M. Sterner, I. Stadler (Eds.), *Handbook of Energy Storage*, https://doi.org/10.1007/978-3-662-55504-0_10

10.7 Costs – 607

References – 608

### Overview

**TES** could play a crucial role in the transition to a renewable and efficient energy supply. The heating and cooling sector is Europe's largest energy consumer. Contributing up to 50% of consumption, the sector is an even larger consumer than the transport and electricity sectors. As cross-sectoral technology, TES could also be a key element in improving the flexibility and efficiency of the industrial process heat and the power generation sector, e.g., with concentrated solar power (CSP) plants.

Three basic systems are used for TES technology. The best-known system is sensible-heat storage, such as buffer storage used in heating facilities. Thermal energy can also be held in latent-heat storage or thermochemical storage systems. This chapter describes the characteristics of these three technologies in detail.

The term 'thermal-energy storage' also includes heat and cold storage. Heat storage is the reverse of cold storage. Heat storage absorbs energy during charging, and cold storage releases energy in the form of heat during charging. If the energy stored is at a temperature below ambient temperatures, the system is called cold storage. If the temperature level is above ambient temperatures, the system is called heat storage.

These range in duration from short-term to seasonal storage. They also range in temperature level, from domestic water heating to high-temperature storage. Furthermore, for electricity generation (solar-thermal power plants), there are different heat transfer fluids such as water, steam, gases, and molten salts. In addition, heat storage is divided between mobile applications and stationary applications.

## 10.1 Thermal Storage System Characteristics

This section discusses the various application areas and characteristics of TES systems.

### ■ Temperature Range

Temperature is a decisive characteristic of TES systems. The temperature at which a TES system is charged and discharged generally determines its application area. The various temperature-levels of application areas of TES systems are as follows.

*High-temperature applications* require temperatures ranging from 300 to 1,400 °C. In the renewable-energy area, solar-thermal power plants are the primary applications in this range. To ensure continual electricity generation, even during the night when there is no sunlight, large storage systems using molten salt at temperatures ranging up to 560 °C are charged during the day and then discharged at night. Thermal storage systems could also be included in *compressed-air energy storage* (CAES) systems to raise their efficiency from about 50% of CAES to about 70% with advanced adiabatic compressed-air energy storage (AA–CAES) systems, with maximum temperatures of about 600 °C. Existing industrial process heat examples with temperatures well above 1,000 °C include solutions in the steel industry, the glass industry, and industrial air-purification systems. The steel industry has been one of the earliest applications. Even today, so-called hot-blast stoves or Cowper stoves that preheat the blast of a steel furnace are commercially utilized.

*Process heat* at temperatures ranging from 100 to 250 °C is chiefly used to generate steam for industrial processes. These processes include, for example, pasteurization and sterilization. Steam-accumulator technology (also called 'sliding-pressure water storage', or 'Ruths'), which is a state-of-the-art technology used for thermal storage, is used in process-heat applications. 'Displacement storage' or 'thermocline' storage systems can also be utilized for pressurized water. Hot and cold water are combined within one vessel to supply pressurized water up to 180 °C (about 30 bar).

The temperature of thermal storage for *heating* in buildings ranges from 25 °C for surface-heating systems (underfloor heating) to 90 °C for radiators with small surfaces. For hygienic reasons, temperatures above at least 60 °C are required for warm-water supply in households and businesses.

Cold storage in the *cooling and air-conditioning* area typically requires temperatures ranging from 5 to 18 °C. Food is generally cooled to temperatures ranging from 5 to 8 °C. Air-conditioning ranges from 6 to 18 °C. Food freezing is an additional area, requiring temperatures below −18 °C.

### ■ Heat-Transfer Fluid (HTF)

TES systems differ widely, not only in terms of the temperature level, but also in terms of the heat carrier, which is also known as the HTF. HTFs may be of the single-phase type (e.g., water, air, thermal oil, molten salt) or the two-phase type with a condensation and evaporation process in the system (e.g., water/steam). The storage material and heat carrier might be identical (e.g., water). In the simpler direct-storage concept, an additional volume of hot working fluid to store heat is used. Many working fluids cannot be directly stored; the energy must be transferred to a separate storage medium. Here, two different media (as a heat carrier and storage medium) are utilized. This concept is usually referred to as the indirect storage concept. Indirect storage concepts require sufficient heat-transfer rates and the minimization of temperature gradients from the HTF to the storage medium. A separate HTF and storage medium may be used for the following reasons:

1. The HTF is expensive (e.g., synthetic thermal oil).
2. The HTF has a low volumetric energy density (e.g., gas, steam).
3. The HTF is pressurized (e.g., steam, water, thermal oil), whereas the larger storage volume is at (or closer to) ambient pressure for economic reasons.
4. The HTF is incompatible with the storage medium.

For *indirect storage concepts*, the storage medium and the HTF may be in direct contact (e.g., ceramics as storage medium with air as the heat carrier in the steel industry). In some cases, *direct contact* of the heat carrier and storage material is not economic or feasible, such as if the heat carrier is pressurized (e.g., steam) or incompatible with the storage medium. In this case, a design with *indirect contact* of the carrier and the storage medium can be utilized. The indirect contact can be realized by an external heat exchanger or an embedded heat exchanger in the storage volume [50].

### ■ Thermal Losses

Important aspects of thermal losses include the TES temperature level, thermal insulation, surface-to-volume ratio (or size), environmental conditions (e.g., temperature, wind speed), number of charge/discharge cycles per year, and operation time at nominal temperature. Typically, the aspect of thermal insulation versus thermal losses is economically optimized. TES systems can have low thermal losses. For example, molten salt tanks with efficiencies of up to 99% have been constructed.

### ■ Number of Tanks

The number of tanks, or storage blocks, is another classification criterion. The single-tank concept is characterized by various zones with charged and discharged storage material. An example is a sensible-heat storage system with hot and cold zones (e.g., a water tank). Alternatively, storage systems can utilize two tanks. For example, a sensible-heat storage system with molten salt consists of two individual tanks at different temperatures and fluid levels. The two-tank concept allows for a decoupling of the thermal capacity (storage volume of the two tanks) and the thermal power (additional external heat exchangers).

### ■ Long/Short-Term Storage

As with all energy storage technologies, a key characteristic of TES systems is the span of time between charging and discharging. Short-term storage applies to storage over a duration ranging from several minutes to a few days. Long-term storage holds energy over a duration ranging from weeks to a year.

It should be noted that short-term storage systems typically have higher charging and discharging capacities than long-term storage

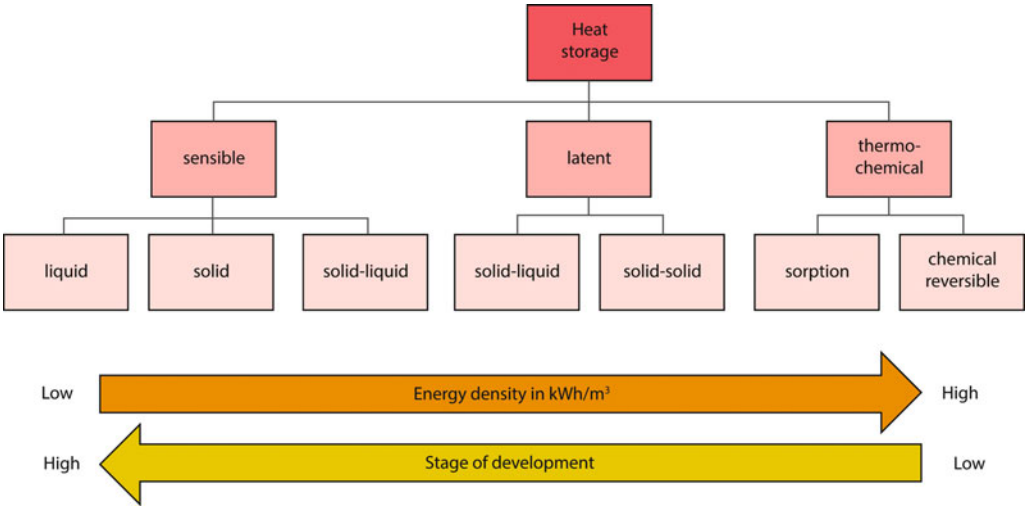



**Fig. 10.1** Overview of various TES technologies

systems, but they store smaller quantities of energy.

### Centralized/Decentralized Storage

Location within the energy system is also an essential criterion for characterizing an energy storage system. Storage systems are classified as centralized or decentralized. There are no official or unambiguous definitions of these terms, so they can only be defined by examples. Large solar-thermal power plants have large molten salt-storage facilities located inside the power plant. These storage facilities can be termed centralized storage facilities. Buffer storage for heating in a single-family house or latent-heat ice storage for air-conditioning in office buildings are typical examples of decentralized storage facilities. The closer the storage is to the consumer, the more decentralized it is.

### Stationary/Mobile Storage

Stationary-energy storage systems are installations fixed to a particular location. These are distinguished from mobile storage systems. Since energy density is a crucial factor here, typically these are latent-heat storage or thermochemical storage systems. The energy is stored in containers at the charging location if, for example, the energy cannot be exploited there. The stored energy is then transported to the consumer.

## 10.2 Storage Technologies

Thermal energy can be stored in a variety of ways. This section explains the terms sensible, latent, and thermochemical thermal storage (Fig. 10.1).

### 10.2.1 Sensible-Thermal Storage

Sensible storage of thermal energy requires a perceptible change in temperature. A storage medium is heated or cooled. The quantity of energy stored is determined by the specific thermal capacity ($c_p$-value) of the material. Since, with sensible-energy storage systems, the temperature differences between the storage medium and the environment are often larger than with other types of storage, the thermal insulation used is crucial.

Because water has a high-specific thermal capacity as well as other advantages such as environmental friendliness, easy availability, and

low cost, many sensible-thermal storage systems use water.

Typical applications for this kind of storage are in heating systems for buffer storage. But sensible-thermal storage systems are also used for medium- and long-term (seasonal) storage. If water is used as a heat-carrier medium here, it can be modified for frost protection by adding alcohols. If required, it can also be replaced by another material. Solid materials such as gravel or iron oxide rock, for example, can be used in sensible-thermal storage facilities.

Compared to latent or thermochemical thermal storage systems, sensible-thermal storage facilities have lower energy densities if a limited temperature-range is considered. But sensible-thermal storage technology is standardized and significantly lower in price.

### 10.2.2 Latent-Thermal Storage



Latent-thermal storage systems store the energy required for a phase change together with sensible heat. In practice, most technologies use a phase change from solid to liquid. This phase change usually entails a volume change of about 10%. This must be taken into account in the system design. The transition or melting enthalpy is a significant factor.

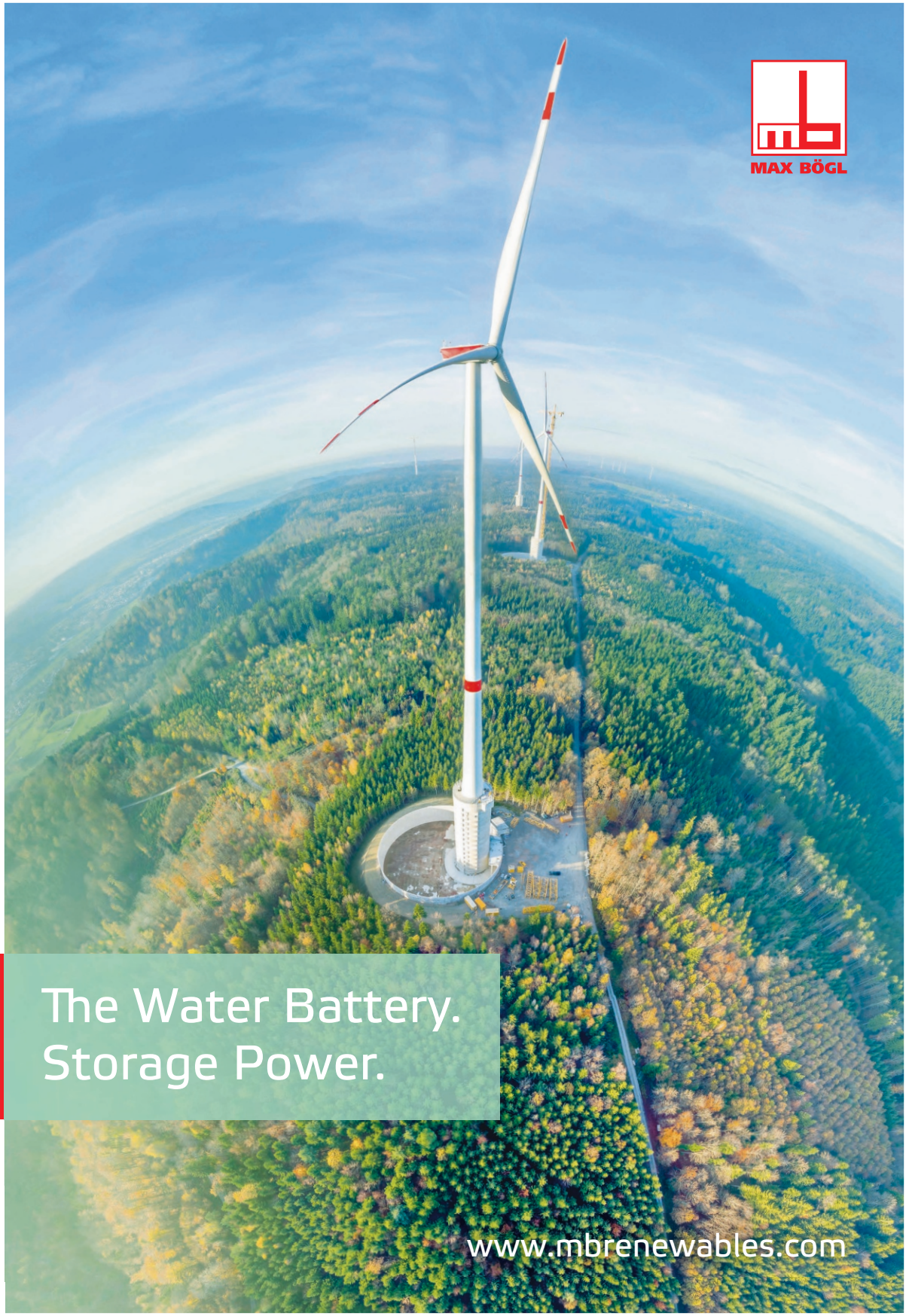
The phase change from liquid to gas entails a large change in volume that is difficult to manage. As a result, it is rarely used. There are theoretically three kinds of storage systems of this type. The first option is isochoric storage. Here, the pressure rises together with the temperature and, as a result, together with the evaporating temperature. The second option is isobaric storage. Since this requires a large condensation chamber, in practice this option is not used. The third option is storage in an open system at ambient pressure using the phase change from liquid to gas. This type of storage is actually a kind of chemical storage, so it is discussed in the section under adsorption [23].

Latent storage has several advantages over sensible storage. Significantly more thermal energy can be stored at smaller temperature-differences than with sensible storage. This means that these systems have higher energy densities. In addition, the temperature remains constant over a longer time during charging and discharging. As a result, phase-change materials (PCM) integrated into the building structure, with melting temperatures ranging from 20 to 25 °C, can be used (for example). This keeps room temperatures in the comfortable range, since it takes longer to make the room too cold or too hot. Because of their high storage capacities, the design of latent-thermal storage facilities can be significantly more compact. The melting temperatures of the various types of materials used range from −40 °C to well over 1,000 °C.

An interesting option that is particularly useful for transporting thermal energy is slurries, which are also called phase-change slurries (PCS). The advantage of slurries is that they can always be pumped, regardless of their aggregate state. This is achieved by adding the PCM to a carrier-fluid with a low solidification temperature. Alternatively, only a part of the PCM's thermal capacity is used so that an adequate liquid phase remains. Slurries are used for building air-conditioning, and are also used in industrial facilities. Here, ice slurries may be used.

### 10.2.3 Thermochemical-Thermal Storage

Strictly speaking, the term thermochemical-energy storage refers to chemically reversible reactions where the reaction products can be separated and stored over a long period. This separation eliminates storage losses. During discharging, an exothermic reaction then releases the stored energy. Thermochemical-energy storage systems permit very high energy storage densities, but have been rarely implemented in practice. This is because the technology is largely still in the research and development phase.


MAX BÖGL
The Water Battery.
Storage Power.
www.mbrenewables.com

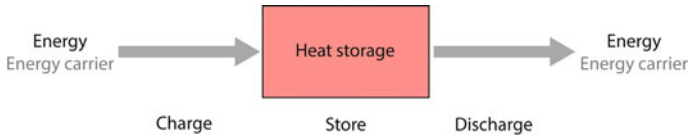



**Fig. 10.2** Energy storage processes

Sorption storage facilities are also often categorized as thermochemical storage systems. Research on sorption storage is current focused on utilizing industrial waste heat. This technology is particularly well-suited for industrial drying processes. Absorption and adsorption processes are more physical than chemical. But since it is common practice, sorption storage systems are categorized as thermochemical-energy storage systems in this chapter.

### 10.2.4 Thermophysical Properties and Material Requirements

The following requirements should be met by heat storage materials for sensible, latent, and thermochemical TES:

1. Large gravimetric storage capacity (high heat capacity, latent heat, or heat of reaction)
2. Large volumetric storage capacity (high density and gravimetric values listed above)
3. Long service life, non-toxic, non-flammable, no explosive phases, simple in handling (e.g., hygroscopy)
4. Non-corrosive with respect to the containment, the heat exchanger and heat transfer, enhancement structures (e.g., fins), utilization of inexpensive structural materials
5. Ability to undergo charging/discharging cycles without losses in performance and storage capacity over many cycles (high cycling and thermal stability)
6. Suitable material costs, high availability
7. High thermal diffusivity and thermal effusivity values (high heat transfer rates)
8. Small density change versus temperature (e.g., to minimize thermomechanical stress)

## 10.3 Thermodynamic Principles

### 10.3.1 Thermal Energy

TES systems increase their energy content (charging) by adding energy or an energy carrier. They then store this energy content over a specific period of time with as little loss as possible (storing), and release the energy or energy carrier when required (discharging). Discharging reduces the storage system's energy content (Fig. 10.2).

Thermal energy—heat and cold—is not a state variable describing the system condition, but a process variable that applies only during changes of state or processes (Fig. 10.3). This is particularly true for storage capacity (or energy storage density), i.e., the stored thermal energy in relation to the mass or volume of the storage facility.

This means that a storage facility does not contain a certain quantity of heat or cold, but rather that it contains the thermodynamic potential to transfer a quantity of heat or cold to another medium (Fig. 10.4).

As a result, the term 'energy consumption' is incorrect from a physical point of view. This is because no energy is consumed; it is simply converted into another form. Similarly, the term 'energy storage' is not strictly correct because, although it may no longer be usable, the

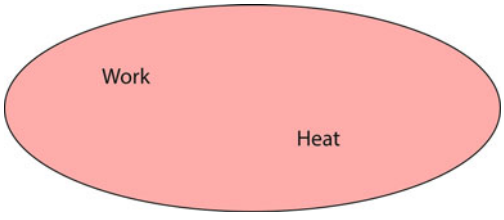



**Fig. 10.3** Process variables

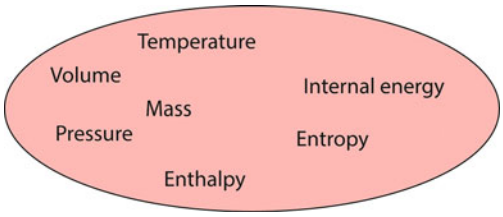



**Fig. 10.4** State variables

energy certainly remains unchanged. In what follows, the term exergy is used to describe the portion of energy that, without limit under ambient conditions, can be converted into other forms of energy. The greater the difference between the storage temperature and the ambient temperature, the greater the exergy content and the significance of the heat. The term anergy is used here to describe the portion of energy that is released into the environment and is no longer usable as a result. If the charging, storing, and discharging processes of a TES system causes losses, the anergy content rises and the energy content falls. But the sum of the anergy and exergy content remains the same. Equation 10.1 shows how the exergy content is calculated:

$$E_{\text{Exergy}} = Q \cdot \frac{T_S - T_U}{T_S} = Q \cdot \left(1 - \frac{T_U}{T_S}\right). \tag{10.1}$$

This demonstrates that the exergy content is determined by the quantity of heat $Q$, the storage temperature $T_S$, and the ambient temperature $T_U$. This fraction is equivalent to the Carnot efficiency limit, referring to the maximum useful work contained in the heat. For the sake of simplicity, in the following discussion, the terms energy storage, quantity of heat, and so on will be in reference to their common dictionary definitions.

### 10.3.2 Heat Transfer

There are three types of heat transfer: convection, heat radiation, and heat conduction.

Convection refers to the transport of particles carrying thermal energy in a flowing fluid. As a result, it is also called heat flow. For example, gravity heating systems transport the heat from thermal storage to radiators by circulating water, and so use convection. This type of convection is also called natural or free convection. With forced convection, the particles are transported by mechanically driving a fluid using pumps or ventilators (such as circulating pumps in warm-water heating). Convection also occurs at the exterior of the radiators. Air near the radiators is heated and expands. It then rises, and cold air replaces it from below. The fluid can be driven by temperature, density, concentration, or pressure differences within the system.

Heat radiation is electromagnetic radiation released by materials due to their temperature. With TES, heat radiation is in the infrared range. At higher temperatures, the heat radiation's maximum radiation shifts towards shorter wavelengths. Heat radiation does not depend on the material. According to the Stefan-Boltzman equation, it is determined by the temperature $T$, the surface area $A$, the emissivity $\varepsilon$ of the radiating body, and the Stefan-Boltzmann constant $\sigma = 5.67 \times 10^{-8}\,\mathrm{W\,m^{-2}\,K^{-4}}$:

$$\dot{Q} = \frac{\partial Q}{\partial t} = \varepsilon \sigma A T^4. \tag{10.2}$$

Since there is (more) heat radiation from a warm medium to a cold medium and (less) heat radiation from a cold medium to a warm medium, a lower temperature difference results. Enameling, anodizing or coating metal objects such as radiators can increase the emission of infrared radiation and, as a result, the heat radiation.

Heat conduction refers to the transfer of kinetic energy between neighboring atoms or molecules in solid materials or resting fluids without any material transport. The flow of heat is caused by the difference in temperature, meaning the heat flows from a warm medium to a cold medium. The heat flow through the object is primarily determined by the tempera-

ture difference between the warm surface ($T_2$) and the cold surface ($T_1$), the surface area $A$, the thickness $d$ of the body, and the heat conductivity $\lambda$. Heat conductivity depends on the material and the temperature and is given in W/(m K). Radiators are made out of metals with high heat conductivities so that the maximum quantity of heat is transferred from the warm water to the air in the room.

$$\dot{Q} = \frac{\lambda}{d} A \, (T_2 - T_1) \, . \tag{10.3}$$

### 10.3.3 Thermal Insulation

With sensible-thermal storage, thermal insulation is crucial for reducing thermal losses. Latent and thermochemical-thermal storage systems also require insulation, but it plays a less essential role. This is because the temperature differences between the thermal storage and the environment are smaller, or because insulation is only required during the charging and discharging processes.

Equation 10.4 shows the relationship between the temperature difference and thermal losses in a storage system:

$$Q_{\text{losses}} = U \cdot A \cdot (T_{\text{S}} - T_{\text{U}}) \, . \tag{10.4}$$

Key factors for thermal insulation are the surface area $A$, the storage temperature $T_{\text{S}}$, the ambient temperature $T_{\text{U}}$, and the overall heat-transfer coefficient $U$. This last coefficient determines the power-per-Kelvin temperature difference transferred through a square meter of area, and is given in units of W/(m$^2$ K). For $n$ layers, it is determined as follows:

$$U = \frac{1}{\frac{1}{\alpha_i} + \frac{s_1}{\lambda_1} + \frac{s_2}{\lambda_2} + \ldots + \frac{s_n}{\lambda_n} + \frac{1}{\alpha_a}} . \tag{10.5}$$

Equation 10.5 demonstrates that the heat-transfer coefficient is determined by the heat conductivity $\lambda$, the layer thickness $s_i$ of the materials, and the heat-transfer coefficient $\alpha$. This is a proportional factor that describes the intensity of thermal transfer at a boundary. The heat transfer coefficient is not a material constant. Instead, it is determined by the flow speed, the kind of fluid, the geometric relationships, and the surface properties.

**Table 10.1** Heat conductivity of various materials at room temperature

| Material | Heat conductivity $\lambda$ in W/(m K) |
|---|---|
| Water | 0.562 |
| Air (78% nitrogen, 21% oxygen) | 0.026 |
| Vacuum | 0 |
| Glass | 0.76 |
| Concrete | 2.1 |
| Iron | 80 |
| Copper | 400 |
| Aluminum | 235 |
| Diamond | 1,000–2,500 |
| Silver | 430 |
| Polyurethane (PUR) | 0.021–0.035 |
| Wool/cork | Around 0.035 |

Tables 10.1 and 10.2 list the material constants for a number of materials.

Higher levels of insulation can be achieved by replacing the insulation material with a vacuum (as in a double-walled thermos, for example). At pressures below 0.001 mbar, thermal losses are almost exclusively caused by heat radiation alone. Vacuum insulation is often used where the design cannot accommodate thick insulation.

To reduce heat radiation, as well vacuum insulation, powder or fiber insulating material can also be used. These types of super-vacuum insulation reduce heat conductivity to levels ranging from 0.01 to 0.003 W/mK. This means that their insulating capacity is five to ten times greater than that of conventional insulating materials.

**Table 10.2** Heat-transfer coefficients of various materials at room temperature

| Material | Thickness in cm | Heat-transfer coefficient $U$ in W/(m² K) |
|---|---|---|
| Concrete | 25 | 3.3 |
| Aerated concrete | 40 | 0.16–0.21 |
| Brick | 24 | 1.5 |
| Brick + composite thermal system (PUR) | 30 | 0.3 |
| Solid wood | 20.5 | 0.5 |
| Single-glazed window | – | 5.9 |
| Double-glazed window | – | 3 |
| Passive house standard window | – | 0.5–0.8 |
| Polystyrene | 2 | 1.7 |
| Polystyrene | 10 | 0.35 |

## 10.4 Sensible TES



Sensible heat is absorption or release of heat that results in a perceptible change in temperature. The storage medium used is heated or cooled. The relation between the quantity of heat $Q$ and the temperature is given by the following equation:

$$Q = m \cdot c_p \cdot (T_2 - T_1)\,. \tag{10.6}$$

The quantity of heat is determined by the temperature difference, the mass $m$ and the specific thermal capacity $c_p$. These physical characteristics determine the amount of heat that must be added to a kilogram of mass to elevate its temperature by one Kelvin. Table 10.3 shows the $c_p$ values for a range of storage materials. A high-specific thermal capacity is preferable with thermal storage. This is because less material is then required to store a specific quantity of energy, and the thermal storage facility is more compact in design.

Compared to latent or thermochemical storage systems, sensible-thermal storage facilities have lower energy densities. The energy density is limited by the specific thermal capacity and the maximum permitted temperature difference. The temperature difference is determined by application boundary conditions, or by the temperature range of the medium's phase change (for unpressurized water, between 0 and 100 °C).

An advantage with liquid sensible-storage media is the transferability and the realization of high charging and discharging capacities. The thermal power level is determined by the pump-power and, in some cases, by the heat exchanger power. But with solid storage media, very high temperatures can be stored. In comparison with the other two thermal storage technologies, sensible-thermal storage systems have relatively low capital costs. They are also the farthest developed and established systems on the market (e.g., unpressurized and pressurized water storage, thermal masses in buildings, regenerators in process industry, and molten-salt storage for CSP plants).

### 10.4.1 Storage Materials

The choice of a storage material is determined by the following:

- The system operating temperature.
- The suitability of the material for thermal transport.
- The suitability of the material for transport and storage.

**Table 10.3** Temperature ranges, thermal capacities, densities, and application areas for various materials [1, 2]

| Medium | Temperature range | Specific thermal capacity | Volumetric thermal capacity | Density | Applications |
|---|---|---|---|---|---|
| Unit | °C | kJ/(kg K) | kJ/(m³ K) | kg/m³ | |
| Water | 0–100 | 4.19 | 4,175 | 998 | Domestic water, heating facilities |
| Sand, gravel, rock | 0–800 | 0.71 | 1,278–1,420 | 1,800–2,000 | Soil thermal storage |
| Granite | 0–800 | 0.75 | 2,062 | 2,750 | Soil thermal storage |
| Concrete | 0–500 | 0.88 | 1,672–2,074 | 1,900–2,300 | Thermally active components |
| Brick | 0–1,000 | 0.84 | 1,176–1,596 | 1,400–1,900 | |
| Iron | 0–800 | 0.47 | 3,655 | 7,860 | Storage material for solar storage systems |
| Thermal oil | 0–400 | 1.6–2.1 | 1,360–1,620 | 850–900 | |
| Gravel-water fill | 0–100 | 1.32 | 2,904 | 2,200 | Soil thermal storage |
| Molten salts | 150–450 | 1.3 | 1,725–1,970 | 2,243–2,561 | Concentrating solar-thermal power plant |
| Sodium | 100–800 | 1.3 | 750–925 | 975–1,203 | |

- The availability and price of the material.
- The environmental friendliness of the material.

The characteristics of materials used in sensible-thermal storage systems are listed in Table 10.4. In addition to the specific thermal capacity, the volumetric thermal capacity is frequently also given for building applications. This is because, here, the weight matters less than the spatial volume required. The volumetric thermal capacity of non-porous solids typically ranges from 1.5 to 6 MJ/(m³ K).

The medium most frequently used in sensible-thermal storage systems is water. Water has the following characteristics [3]:

- Available practically everywhere in large quantities.
- Cheap.
- Easy to transport.
- Environmentally-friendly because it is non-toxic, non-aggressive, non-flammable, and non-combustible.
- Easy to handle (engineers have extensive experience of working with water, and workmen are familiar with the technology).
- High-specific thermal capacity (4.219–4.185 kJ/(kg K)).
- Low thermal conductivity (0.562–0.560 W/(m K)).
  - Hinders thermal exchange between hot and cold water.
  - Layering: warm water can be directly drawn off from the upper storage area with no additional heating required.
- Various densities at various temperatures.
  - Possibly layering.
- Relatively low viscosity ($1.792–1.003 \times 10^{-6}$ m²/s).
  - Very good thermal-transport medium enabling high charging and discharging capacities.
- Very good solvent properties.
- With domestic water heating, water functions as a heat carrier and heat storage

medium, as well as a product required for consumption.

The primary applications for water as a storage material are buffer storage and heating facilities. These systems balance short-term (several hours/days) differences between the heat generated and consumed. Other application areas for water are medium-term (weeks/months) to seasonal-thermal storage (summer/winter) at temperatures between 0–100 °C. Seasonal storage is often used to store solar heat and for building heating. Combined with local heating, these storage systems often supply enough solar heat to cover 50% of the total heat required by a building for heating and for domestic warm water.

Since vapor pressure increases strongly at temperatures above 100 °C, this also increases the pressure requirements for the container. This in turn increases the cost of the storage system. As a result, thermal oil is typically used for temperatures exceeding 100 °C. But thermal oil has a significantly lower thermal conductivity (around 0.1 W/(m K)) and a lower thermal capacity than water. By combining thermal oil with rock fill that has a higher thermal capacity, the storage capacity can be increased. This also reduces the quantity of relatively expensive thermal oil required. Another alternative is molten salts. Molten nitrate salts can be used at temperatures ranging up to 560 °C.

At very high temperatures, solid storage systems made out of ceramics (regenerator-type storage) or iron oxide rock (storage heaters) are used.

For the most part, over long periods, heat and cold are stored underground. The following types of storage are generally used:

- Aquifer storage facilities
- Cavern storage facilities
- Geothermal-probe storage facilities
- Geothermal-collector storage facilities
- Gravel/water or soil/water storage facilities

The various designs for sensible energy storage system are discussed in the following sections. For the purposes of this discussion, the storage systems are classified according to the aggregate state of the storage medium. First, storage systems using solid storage media are discussed. Following that, storage systems using liquid storage media are discussed. The discussion concludes with a description of storage systems that use both solid and liquid storage media.

## 10.4.2 Storage Systems Using Solid Storage Media

This section describes six kinds of storage systems with basically similar designs and functions. In the cases of geothermal probes, geothermal ground collectors, and foundation storage, a solid storage medium (soil and concrete) is indirectly charged and discharged by a heat-carrying fluid. Night storage heating also uses a solid storage medium (iron oxide rock), but here the heat is transferred by an electric heating element.

### 10.4.2.1 Geothermal-Probe Storage Systems

Geothermal-probe storage systems use soil or rock as a storage medium. Geothermal probes are commonly used with water-saturated clay rock, due to this having a high thermal capacity and low permeability. With higher groundwater-flow rates, the heat would be quickly carried away [16].

The heat is transferred by a U-pipe or coaxial heat-transfer pipe (often made of polyethylene) inserted 20–150 m into a vertical borehole. The diameter of the borehole ranges from 10 to 15 cm. Drilling at a depth below 100 m requires mining permits in Germany [3].

Since polyethylene is a relatively poor thermal conductor (0.4 W/(m K)), this limits the heat-transfer capacity. The heat-transfer capacity can be increased by filling the drilling tube with a bentonite-cement-sand mix [5].

A water-antifreeze mixture passed through the pipe at a rate of about 0.5 to 1 m/s is used as a heat carrier. This creates a turbulent flow,

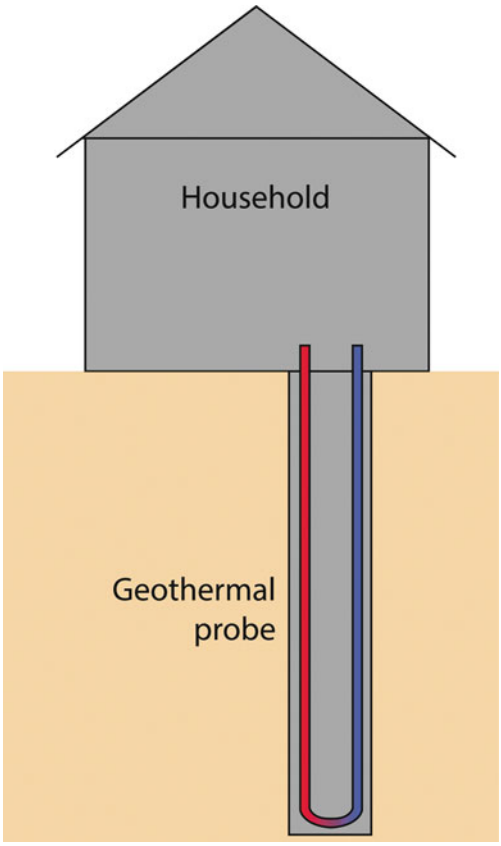



**Fig. 10.5** Geothermal probe

increasing the heat transfer. Heat conduction is typically used to indirectly charge and discharge the system.

By connecting several geothermal probes in a probe field, soil can be used as a storage mass. The distance between the probes can range from 1.5 to 12 m. In general, geothermal probe fields have no structures built above them. They can have storage volumes exceeding 50,000 $m^3$. The storage temperature typically ranges from 40 to 80 °C.

Geothermal-probe storage systems can be used as both heat and cold storage facilities by installing a reversible heat pump. They are most efficient at low-temperature ranges and low-flow temperatures (such as 35 °C for underfloor heating) (see Figs. 10.5 and [1]).

### 10.4.2.2 Geothermal Ground-Collector Storage Systems

Geothermal ground-collectors are installed near the surface in loose soil at depths ranging from about 1 to 2 m. As a result, they are subject to seasonal temperature fluctuations [6]. As with geothermal probes, geothermal ground collectors also use soil as a storage medium. A heat-carrier fluid (water-antifreeze mixture) flows through horizontal plastic pipes with a diameter of about 25 mm [16]. The pipes are coupled to a heat pump so that the geothermal energy can be used for heating. For cooling, excess heat is transferred from the building to the soil. The individual pipe sections are less than 100 m long to limit the pump-power required [7].

Geothermal ground collectors require a large area for installation. For residential buildings, geothermal ground collectors typically require an area equal to two times the living space in the building supplied with heat. In addition, structures cannot be built above these facilities, the pavement over them cannot be too thick, and they have limited applications where deep roots penetrate the ground [8]. Another disadvantage is that laying the pipe requires costly pit excavation.

Table 10.4 lists the thermal extraction capacities with various ground types. The table shows that more heat can be extracted from moist ground types than from dry ground types.

**Table 10.4** Extraction capacities with various ground types using geothermal ground collectors

| Ground properties | Thermal extraction capacity in W/$m^2$ |
|---|---|
| Dry, sandy | 10–15 |
| Moist, sandy | 15–20 |
| Dry, loamy | 20–25 |
| Moist, loamy | 25–30 |
| Groundwater-bearing | 30–35 |

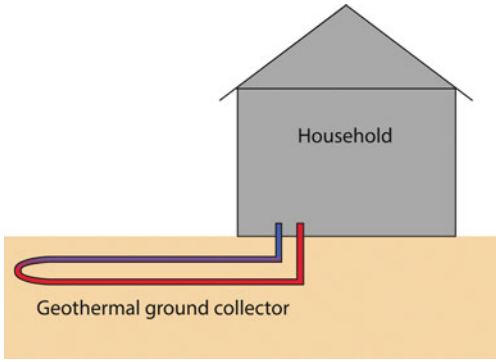



**Fig. 10.6** Geothermal ground collector

Since geothermal ground collectors typically do not come into direct contact with groundwater, in Germany and other European countries they can be built without a specific permit (see Figs. 10.6 and [9]).

### 10.4.2.3 Foundation Storage

Foundation storage design resembles geothermal-probe system design. Here, a heat-carrier medium flows through plastic pipes that are connected to the building's foundation reinforcements. The foundation structure functions as a heat exchanger. Since it is a thermally active component, it also functions as a storage mass together with the surrounding soil. This means that the system is indirectly charged and discharged [3].

The storage system is typically insulated on all sides and frequently used in combination with solar-thermal facilities. Here, the foundation storage system stores surplus solar energy in the summer and then discharges it using a heat pump in the winter months [10].

The plastic pipes are generally connected to the reinforcements by cable ties. The pipe sections are individually operated so that the system can continue to function even if one component fails [1].

Unlike geothermal probes or geothermal ground-collector systems, structures can be built over foundation storage systems (Fig. 10.7). Depending on the foundation, the system design can vary in regards to details such as:

- Energy piles: pile foundation used as the foundation structure (Fig. 10.8).
- Foundation absorber: base-plate used as the foundation structure.
- Diaphragm wall used as the foundation structure.

In theory, the system can provide heating supported by a heat pump, as well as provide cooling supported by a refrigeration machine. Temperatures in the soil range 4–20 °C. Lower temperatures should be avoided to prevent cracks from forming in neighboring concrete structures.

### 10.4.2.4 Thermally Active Components

Thermally active components can be used to store thermal energy in the foundation of a building, as well as in the building itself. This use of thermally active components is also frequently called thermal-component activation or concrete-core activation.

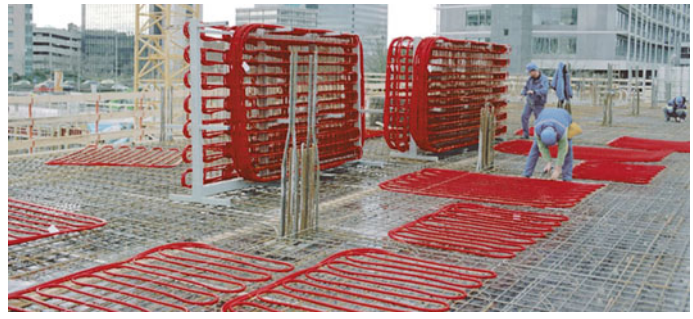


**Fig. 10.7** Foundation storage system

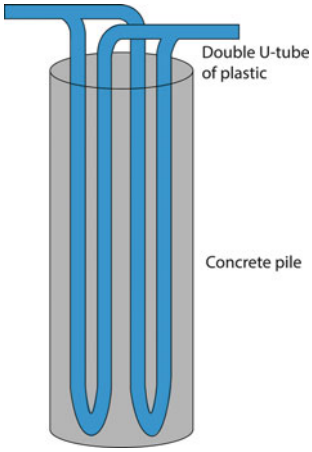



**Fig. 10.8** Energy pile

The building's concrete components, such as the ceilings, walls, or floors, function here as storage masses. The components are charged and discharged by water flowing through tube coils integrated into the core of the concrete. Underfloor heating is the most common form for this system.

The temperature of the components is generally kept in a range between 18 and 35 °C. At temperatures under 18 °C, the building may no longer be comfortable for the occupants inside, and condensation may form on the activated components. Massive buildings can store energy over long periods of time. The carriers then react to temperature fluctuations, keeping room temperatures relatively constant. Thermally active components can be used for both heating and cooling purposes (see Figs. 10.9 and [1]).

### 10.4.2.5 Storage Heaters

Storage heaters are also a form of energy storage in a sensible-thermal storage system (Fig. 10.10). Unlike all the other sensible-energy storage systems discussed here, storage heaters do not use a heat-carrier medium for charging. Instead, the heat is directly stored by converting electricity into heat using a heating element that is then stored in iron oxide rock.

Storage heaters absorb electric energy, convert it into heat, and then store it in their core. The heater then releases the heat into the room over a longer period of time. In the past, energy-supply companies offered electricity at cheaper rates at night to supply night-storage heaters. In the future, the loading process could be dictated by other factors, such as the availability of renewable energy from wind-power surpluses. In theory, temperatures in any range could be stored by converting electricity to heat. In practice, temperatures significantly higher than those required for room heating (up to 600 °C) are stored.

Storage heaters can be designed so that the release of heat is not controllable. With this design, the storage core is completely enclosed in weak thermal insulation. The heat is released by convection and radiation. But in practically, in all storage heaters found in Germany, the heat release is automatically controlled. The heat release is controlled by a ventilator. Cold air drawn in by the ventilator flows upwards and then spreads out. A portion of the air passes through the storage shaft and is heated as a result. This partial flow may exit the storage core at very high temperatures. As a result, the hot



**Fig. 10.9** Thermally active components



**Fig. 10.10** Section of a storage heater

air is mixed with the other partial flow that passes directly to the outlet opening through a bypass damper without being heated.

The most frequently used storage media are iron oxide rock and magnesite (also called by its brand name, Feolit) [12]. The storage medium must have a high storage capacity, as well as the capacity to quickly release the heat stored when required, i.e., the medium's thermal conductivity must be as high as possible.

Magnesite is a ceramic material made of iron oxide and magnesium. Its specific thermal capacity is determined by temperature. At room temperature, its specific thermal capacity is around 0.245 W h/(kg K) and, at a temperature of 600 °C, around 0.34 W h/(kg K). Another advantage of magnesite is that its thermal conductivity is determined by temperature. At 200 °C, the thermal conductivity is around 9.3 W/(m K), and at 600 °C, it is around 5.8 W/(m K). This means that the thermal conductivity doubles at lower temperatures, permitting high heat extraction, even with small low-temperature differences [13].

### 10.4.2.6 High-Temperature Regenerator-Type Storage

This storage type allows the highest storage temperature levels of up to 1,600 °C, avoiding the problem of the high vapor-pressure of liquid media [51]. The maximum application temperature depends on the specific material. Ceramics are typically utilized. Also, in spite of their relatively low-specific heat, these typically inorganic solids may still achieve high storage densities, where the operating conditions exhibit large temperature spreads. This is often the case with applications that use gases as the HTF.

Regenerators, also called regenerative heat exchangers, comprise a storage inventory that is heated and cooled through an intermittent heat transfer between a hot and a cold fluid. The storage is operated in counterflow: during charging, the hot fluid enters the storage module at the 'hot' end, and during discharging the flow direction is reversed and the cold fluid enters at the 'cold' end.

Existing industrial examples include solutions in the steel industry, glass industry, and in industrial air- purification systems. The steel industry was one of the earliest applications. Even until today, so-called hot blast stoves or Cowper stoves that preheat the blast of a steel furnace, are commercially utilized. To provide heat over longer time periods, two or three stoves are used in an alternating operation (Fig. 10.11). Sintered refractory bricks in hexagonal shapes are a common inventory choice. The temper-



**Fig. 10.11** Regenerator (or Cowper) for sensible-heat storage in solids

ature in the upper part of the stove can be as high as 1,300–1,600 °C. Heat rates are in the range of 100–300 MW [53]. Regenerative thermal oxidizer (RTO) systems are applied to purify air from volatile organic compounds through an exothermic process taking place inside the regenerator unit. This process oxidizes the organic solvents at elevated temperatures in the range 800–1,000 °C. The internal heat transfer between the hot cleaned gas and the incoming cold gas is achieved through the intermittent storage of the heat in the regenerator's ceramic inventory, allowing an almost autothermal plant operation with heat-recovery efficiencies of up to 95% and more. Commercial implementations of RTO have a typical volume of up to 600 $m^3$ [52].

In recent years, there has been increased interest in regenerator-type storage for various power plant applications, including combined-cycle plants, CSP plants, and advanced AA-CAES plants for utility-scale electricity storage. In this context, the technology has been further developed for increased performance and lower costs. In particular, regenerator storage based on a packed-bed inventory has been looked at. While it is less common today, it can further reduce investment costs and avoid the scalability issues of previous designs.

### 10.4.3 Storage Systems Using Liquid Storage Media

The following section discusses storage designs using a liquid storage medium. A major advantage of these systems is that, in most applications, the storage medium functions as a heat-carrier medium at the same time. This permits very high thermal power levels to be achieved.

The most frequently used material is water. Although cavern storage systems play only a minor role with TES, there are many applications for heat and hot water storage in earth basins and tanks made of steel, concrete, or plastic. This section also discusses cold storage at temperatures ranging from 0 to 20 °C.

#### 10.4.3.1 Hot Water Storage in Steel, Concrete, or Plastic Containers

This section discusses the storage types most frequently used for storing sensible-heat energy. The storage medium is water. The temperature ranges up to 95 °C. These storage systems are typically used in small- to medium-sized heating systems as buffer storage to balance supply over short periods. Larger models are used to integrate local or district-heating networks to balance supply over longer periods.

Steel, concrete, or plastic containers are used to store warm or hot water. In larger storage systems, water-tight, reinforced concrete is increasingly used in place of steel-plate containers. Due to the low levels of injected oxygen, warm water for domestic use is typically stored in corrosion-resistant materials such as steel, coated steel, or copper. In sealed hot-water or buffer systems with very low levels of injected oxygen, unprocessed and uncoated steel can be used [1]. The use of glass fiber-reinforced plastics is a more recent development [15].

These storage systems can be installed aboveground, underground, semi-recessed, or in buildings [3, 16]. A good surface-to-volume ratio is preferable to minimize thermal losses. As a result, larger storage systems have proportionally lower thermal losses. This means that spherically-shaped storage facilities would be best, but for a range of reasons, they are rarely built in practice. Building and erecting a spherical storage facility is difficult. Because of layering in the water, the contact area between the hot and cold water should also be minimized to avoid heat conduction that could destroy the layering. For these reasons, cylindrical warm and hot-water storage facilities that can also tolerate overpressure are generally used. With these storage facilities, the typical ratio of height to diameter ranges from 2:1 to 5:1 [1]. Insulating materials include foam materials, mineral wool, glass foam, and glass wool.

Warm- and hot-water storage systems use both direct and indirect contact charging and discharging concepts. With direct charging, the

heat-storage medium also functions as the heat carrier: there is no hydraulic separation. The warm water produced is fed into the storage facility at the top. It then remains at the top because of its higher temperature and lower density. It can also be extracted from there if required. These systems are called stratified storage systems. An example of this kind of system is a buffer storage facility filled with hot water. When heating is required, water is extracted from the buffer storage and fed through a pipe network to areas where heat is released (radiators and heating coils). The advantages of direct charging and discharging are the simple design and lack of internal storage components.

With indirect storage charging, the heat is transferred to the storage medium by a heat exchanger. This design is used in heat-supply systems when different fluids are used for heat transport and for thermal storage. Here, heat in the upper part of the storage facility is transferred to the warm water circuit by a heat exchanger [1]. Tank-in-tank storage systems that use three different heat carriers are one example of this kind of system (Fig. 10.12). In solar collector circuits, a water-alcohol mixture is used to protect against freeze and frost. The heat is transferred from the mixture to the hot water in a tank by a heat exchanger. This tank contains a second tank filled with domestic warm water. An advantage of indirect charging and discharging is that it prevents corrosion, contamination, and loss of storage material. This is because the storage components are sealed systems with no storage-material contact with the environment.

Small- to medium-sized storage facilities (0.1–200 $m^3$) frequently use cylindrical pressurized containers with two convex bottoms. Larger storage facilities (up to around 50,000 $m^3$) typically use similar containers with flat bottoms. The facilities are insulated by using foam filler between the steel wall and the cover panel, or by inserting insulation panels. Thermal insulators with high diffusion resistance should be used so that the insulator functions as a moisture barrier as well. Soft foam molding made of synthetic rubber (EPDM) is frequently used. Polyurethane is normally used for the joints and seams.

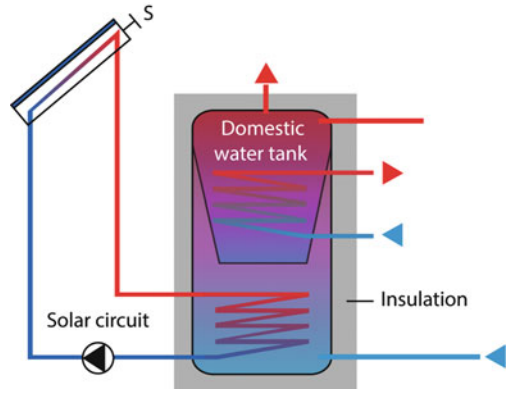



**Fig. 10.12** Tank-in-tank thermal storage system

Containers made of glass-fiber reinforced plastics (GFRP) are smaller in size than steel containers. Currently, several 1,500 $m^3$ GFRP tanks are available. GFRP tanks with capacities up to 6,000 $m^3$ will be available in the future. GFRP tanks are made of various types of glass mixed with unsaturated polyester and vinyl resins. Rigid polyurethane foam (RPF) is often used as a thermal insulation material.

Concrete, reinforced concrete, or prestressed concrete containers are also used to store warm water and occasionally cold water. In newer storage facilities, high-strength and ultra-strength concrete can be used to seal the system as well, thus eliminating the need for additional cladding.

## Cold-Water Storage Facilities

Cold-water storage facilities store water at temperatures ranging from 0 to 20 °C. Cold-water storage facilities are connected to the central refrigeration of a cold-water system.

The design of this type of storage system is similar to the design of warm- and hot-water storage systems. Cold-water storage systems also frequently use steel containers because of their high mechanical load capacity and impermeability. In addition, they are easily formed and welded.

Cold-water storage facilities can be constructed aboveground, underground, and in buildings. In general, these systems are directly charged and discharged. Since they are typically used for short-term storage, they have high charging and discharging capacities. As in warm-water storage facilities, water layering also occurs in cold-water storage facilities. But because the temperature and density-differences are so small, diffusers are required for flow control to maintain the layering. The typical feed and return temperatures in cold-water storage systems are 6–12 °C [3].

### Caverns

Caverns are underground and artificially constructed (for example, when mining ore or for salt extraction) or naturally occurring (for example, from erosion) caves filled with water to serve as energy sources or sinks. These systems are directly charged and discharged.

Caverns cannot be artificially sealed or thermally insulated, meaning the surrounding layers of earth must be highly stable and dense. Rock layers made of granite, gneiss, magmatic rock, or other highly stable sediments are suitable for storage applications.

Caverns can be used for both short-term and long-term storage, but very few cavern storage systems currently in operation around the world use water as a storage medium. Most of these facilities are in Scandinavia. Because of their high fixed costs, caverns are best-suited as large storage facilities. This reduces the ratio of the one-time facility development and construction costs to the storage volume [3]. Cavern storage facilities are more frequently used for gas storage (natural gas and hydrogen).

## 10.4.3.2 Warm Storage and Hot-Water Storage in Earth Basins

A major advantage with underground hot-water thermal storage is that the storage medium is water, an inexpensively available material with a high storage capacity that is comparably easy to handle [14].

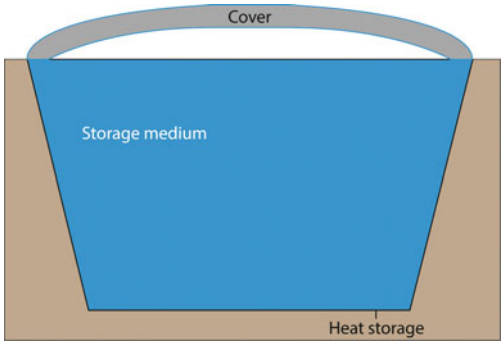



**Fig. 10.13** Design of a hot-water thermal storage facility with self-supporting cover

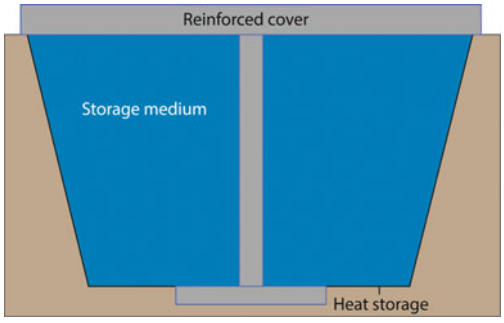



**Fig. 10.14** Design of a hot-water thermal storage facility with reinforced cover

Thermal storage with reinforced or self-supporting covers can withstand higher loads, such as vehicle or pedestrian traffic (Fig. 10.13). Floating covers cannot support these loads, but they are less expensive. Thermal storage with reinforced or self-supporting covers are also easier to access in case maintenance is required (Fig. 10.14).

Storage facilities with reinforced covers can be constructed in any size, but the feedthroughs required in the floor and ceiling may result in leaks and thermal bridges. Together with the more complex foundation, this may make construction a greater challenge overall.

Floating covers are simple, inexpensive, and suitable for any storage size, but they increase the difficulties of charging and discharging (Fig. 10.15).

Currently, planning and constructing earth basins with self-supporting covers is very ex-

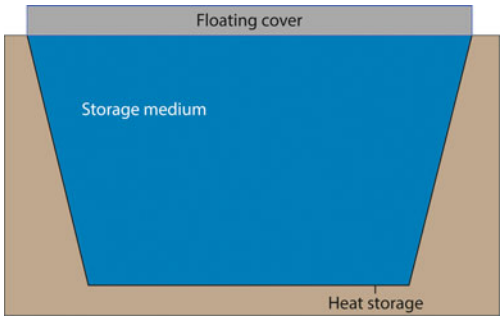



**Fig. 10.15** Design of a hot-water thermal storage facility with floating cover

pensive and complex. In addition, storage volumes and storage surface areas are limited [14].

#### 10.4.3.3 Aquifer Storage Facilities

In aquifers, water is fed into a cave of loose or solid rock located in soil, and then stored there. Aquifers are sandwiched between either watertight aquitards or aquicludes at both the top and bottom. Types of aquifers include [3]:

- Porous aquifers: sand and gravel
- Fractured aquifers: sand, limestone, and basalt
- Karst aquifers: limestone

The water-saturated soil is accessed through one, or often several, separate boreholes. Natural groundwater flow determines where these well systems can be installed.

For charging, warm or cold water is fed into a 'warm' or 'cold' borehole. The storage capacity of the water and soil are used to store the energy. Operation requires water to be extracted from one of the boreholes. The water is then pumped by a well system through a heat exchanger to another borehole. The heat exchanger transfers the heat to a secondary circuit or extracts heat from a secondary circuit. This permits heat or cold to be stored and then resupplied at a later time. This also means that the system is directly charged and discharged [16]. Filtering, chemical water conditioning, and system-pressure maintenance are all managed aboveground. This storage system can be charged with solar-thermal energy in the summer, for example, at operating temperatures well over 50 °C.

Aquifer storage systems are used for long-term storage. They store surplus heat in the summer and resupply it in the winter months. Coupled with heat pumps or sorption refrigeration machines, aquifer storage systems can generally also be used for heating and cooling buildings.

Aquifer storage systems are typically at depths of 100–500 m. The space between the boreholes generally ranges between 50–300 m [1]. Most of these projects are located in Scandinavia, the Netherlands, or Belgium. The typical storage size ranges from 5,000–200,000 $m^3$. In Germany, geological conditions suitable for these systems are located in the Alpine foothills and in northern Germany. A building with an aquifer storage system has been built in Rostock, for example. The Reichstag building in Berlin also uses aquifer storage [18]. In the Reichstag building, around 77% of the energy stored is reutilized (or 67% when pump energy is taken into account). With cold storage, the ratio is about 93% (or 88%) [19].

Besides thermal losses, silting of the heat exchanger and pumps may also cause problems. Depending on the soil type, iron deposits in the pipes may also be an issue [16].

Aquifer storage system construction (Fig. 10.16) requires a permit from local water authorities to feed water underground.

#### 10.4.3.4 Earth Basins

Earth-basin thermal storage systems are categorized by storage material. Gravel-water thermal storage facilities and soil thermal storage facilities using a sand-water mixture can be constructed in virtually any location [20].

After the earth basin is excavated, drainage mats are laid to prevent surface water from seeping into the wall layers below. Other components of the walls include a protective membrane, sealing layers, thermal insulation, and a moisture barrier.

The volumes of the facilities constructed so far range from around 100 to 10,000 $m^3$ [21].

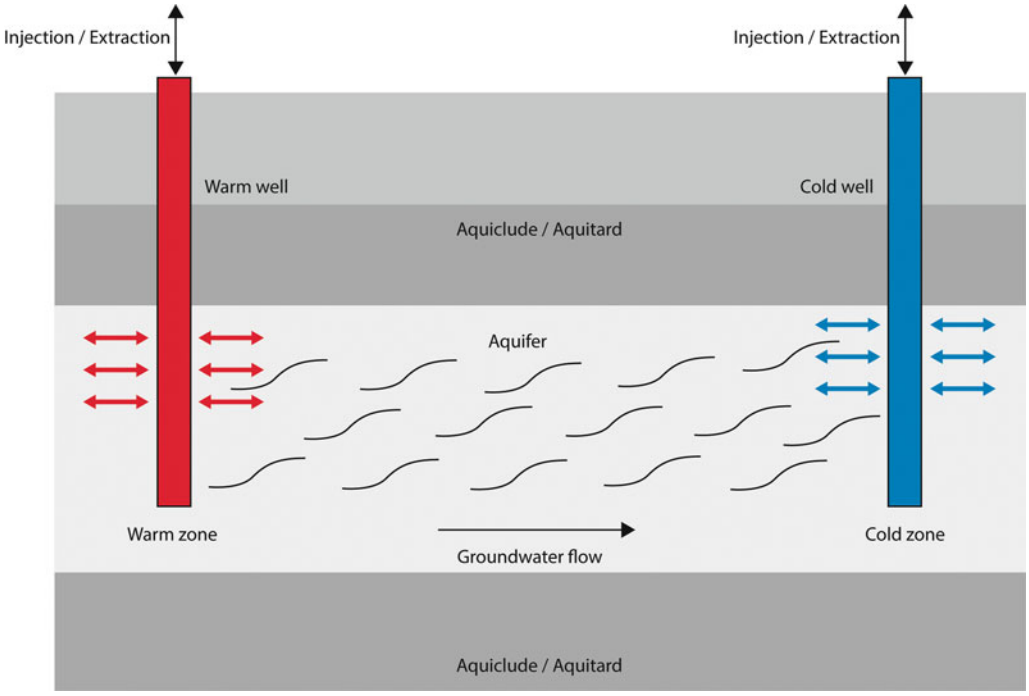



**Fig. 10.16** Aquifer storage system

Earth basins can be indirectly charged using a heat-carrier medium fed through plastic pipes. They can also be directly charged and discharged by pumping water through vertical and horizontal gravel pathways [1]. In both cases, the heat-carrier medium used (water) and the soil (gravel and sand) serve to store the thermal energy (Fig. 10.17). Because of the thermal insulation materials used, maximum storage temperatures are limited to about 85 °C [22].

### 10.4.3.5 High-Temperature Storage Systems

At higher-temperature levels storage media include pressurized water, molten salts, mineral oil, and liquid sodium.

#### Steam Accumulators and Displacement Storage for Pressurized Water

Steam accumulator technology (also called the 'sliding pressure water storage' or 'Ruths') is a state-of-the-art technology in terms of thermal storage used in process heat applications. Steam accumulators are charged by condensation of steam fed into the pressurized liquid volume. During the discharge process the pressure in the storage vessel is decreased and saturated steam is extracted. Since water is used both as a storage medium and heat transfer fluid, high discharge rates and short reaction times are possible (Fig. 10.18). Hence, buffer storage operation with a high thermal power is feasible.

Steam accumulators use sensible-heat storage in pressurized saturated-liquid water, and the capacity is defined by the volume of the pressure vessel. The storage capacity corresponds to the variation of sensible energy of the liquid volume. While a larger decrease of pressure is advantageous in relation to the volumetric storage capacity, the acceptable pressure variation might be limited by efficiency considerations and process requirements. The maximum operation temperature is limited by the critical point of saturated water (374 °C,

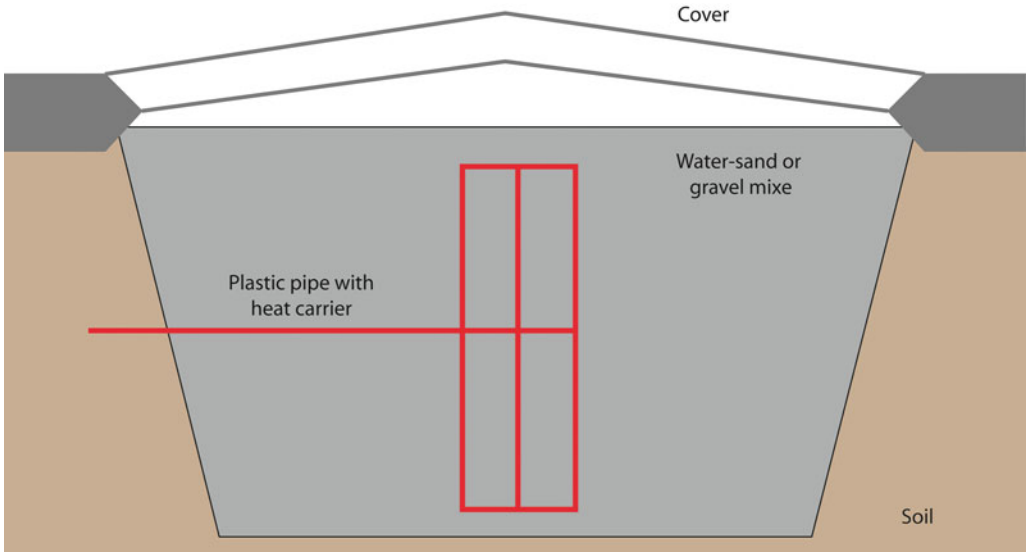
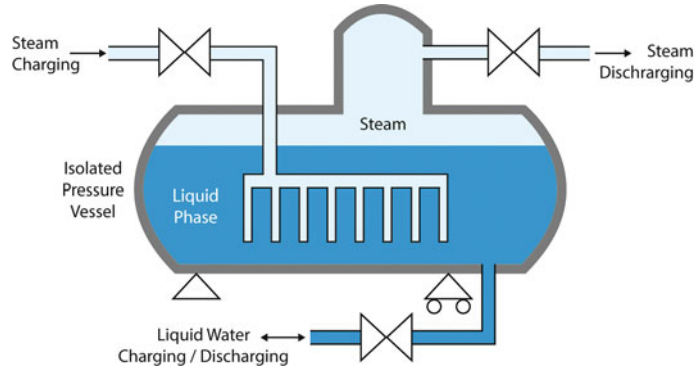



**Fig. 10.17** Earth-basin thermal storage facility

**Fig. 10.18** Scheme of a steam accumulator for sensible-heat storage in pressurized water (source DLR)




221 bar). The costs are dominated by the pressure vessel. Hence, typical systems operate at a maximum temperature of 250 °C and with an upper pressure limit of 40 bar [51, 54].

Ruths storage systems can equalize and cover variations of steam or pressurized-water demand or supply. Steam accumulators may supply heat to industrial steam grids, cover peak power, supply batch processes, or be used in combination with steam turbines or cogeneration. There are several processes that employ steam accumulators, such as in the mineral, pulp and paper, food, textile, and chemical industries.

For pressurized water, '**displacement storage**' or 'thermocline' storage systems can also be utilized. Hot and cold water are within one vessel. The hot, less dense water is in the upper part, whereas the cold water is in the lower part. A temperature transition zone will form between cold and hot parts. This zone will move up and down during charging and discharging. The outlet temperature will stay practically constant, almost until the end of the discharge. In order to achieve good stratification, preferably a tall, vertical cylindrical vessel is utilized. Typical displacement storages supply pressurized water up to 180 °C (about 30 bar). Large-scale



**Fig. 10.19** Two-tank molten-salt system in the solar-thermal power plant Andasol 3 (DLR has a permission for this picture)

displacement storage systems are commercial products in the district-heating sector [51].

## Molten-Salt Storage Systems

Similar to residential unpressurized hot-water storage tanks, high-temperature heat (170–560 °C) can be stored in molten salts by means of a temperature change. Nitrate salts, known from their application as fertilizers, are used as a storage medium. These salts are solid at room temperature and liquid at higher temperatures. High-temperature properties are similar to water in terms of the volumetric storage density, viscosity, and transparency. The major advantages of molten salts are low costs, high thermal stabilities and low vapor-pressures. The low vapor-pressure results in storage designs without pressurized vessels (Fig. 10.19). In general, there is experience of using molten salts within a number of industrial applications related to heat treatment, electrochemical reactions, and heat transfer. The application of salts requires the consideration of the lower temperature limit defined by the melting temperature. One aspect of molten salts is unwanted freezing during operation. Freezing must be prevented in the piping, the heat exchanger, and in the storage tanks. Hence, auxiliary heating systems are often installed. The thermal stability of the molten salts defines the upper-temperature limit. Salt mixtures, rather than single salts, have the advantage of a lower melting temperature. These mixtures can have similar thermal-stability limits to the single salts of the mixtures. Hence, salt mixtures can have a larger temperature-operation range compared to single salts. For solar-thermal power plants (also called 'concentrated solar-power'—CSP plants), alkali nitrate salt mixtures are the preferred candidate fluids for TES. Typically, a non-eutectic salt mixture of 60 wt% sodium nitrate and 40 wt% potassium nitrate is utilized. This mixture is commonly called solar salt. The minimum operation temperature of solar salt is typically set to 290 °C (limited by the liquidus temperature of about 250 °C). The maximum operation temperature is 560 °C, as defined by the thermal stability. The TES system consists of a cold (e.g., 290 °C) and a hot (e.g., 560 °C) unpressurized tank. For a temperature-difference of 250 K, the storage density of the medium reaches a value of about 200 kW h/m$^3$. Currently, there are commercial solar-thermal power plants with molten-salt storage units up to 5,000 MW h (Solana from Abengoa in the US). In 2015, the installed molten-salt storage capacity in CSP plants was larger than 30,000 MW h, and the grid-connected molten-salt storage power, expressed as electrical power, was 1,500 MW$_{el}$. For the CSP application, typical storage capacities range from 3 to 15 h. At the time of writing, typical storage costs range between 20–75 €/kW h depending on parameters, such as

capacity and power as well as the temperature-difference between hot and cold tanks.

The research on storage components aims to replace the two tanks by a single tank with stratification over the height. There are three defined zones in the tank: cold zone (at the bottom), mixing zone (in between), and a hot zone (at the top). Some systems operate without filler material (thermocline concept), and some systems utilize additional filler materials within the liquid-volume (thermocline-filler concept). This filler can improve stratification and minimize effects from free convection and conduction, which can destroy the thermocline zone. In addition, overall capital costs can be reduced by the replacement of an expensive liquid with an inexpensive filler material.

### Other High-Temperature Liquids

Mineral, synthetic, or silicon oils are suitable for short-term thermal storage. Mineral oil can be used at ambient pressures up to about 300 °C. Synthetic oils are thermally stable up to 400 °C, but at higher temperatures they have to be pressurized, which is often uneconomic. The flammability and the price of mineral oil are disadvantages of oil systems. Potentially, an inexpensive filler material, such as cast iron or natural stone, could store thermal energy and replace some thermal-oil volume. Applications considered are conventional and solar-thermal power plants. Liquid sodium is seldom used as a storage medium. Although this material has excellent thermal conductivity and can be used over a wide range of temperatures, safety measures are also required to prevent powerful exothermic reactions with water, for example.

#### 10.4.3.6 Conclusion

- Compared to latent or thermochemical storage systems, sensible-thermal storage facilities are the most advanced in development. This means that there is less potential for further development and cost-reductions than with the two other types of storage. Nevertheless, sensible-thermal storage systems continue to be improved (for example, through reduced thermal losses or improved layering) as new application areas are found [1].
- High-temperature TES is a cross-sectoral technology that is utilized, not only in the industrial process heat sector, but also in other application fields such as solar-thermal power plants. Molten-salt storage recently became fully commercial in large-scale, solar-thermal power plants. Hence, recent high-temperature TES developments can be transferred to the industrial process heat and conventional power sectors. The transfer of commercial TES technologies and new high-temperature TES approaches in a R&D stage also result in possibilities for reduced investment costs, simpler system integration, higher energy densities, and adaption to specific HTFs or new temperature levels.
- Recent power-to-heat (PtH) installations combined with hot-water TES show the potential for coupling of the electricity and heat sectors for further integration of volatile, renewable electricity generation. In the future, heat-pump systems and high-temperature TES will offer additional efficient solutions in this field.
- Because of the economic boundary conditions, in the foreseeable future, seasonal storage of solar heat will only be implemented using large water storage facilities. There are two ways this situation could be changed: by developing innovative insulation concepts that adequately reduce the costs for this application, or by using layered loading units that directly charge the facility by storing the heat-carrier fluid in the appropriate temperature layer.

## 10.5 Latent TES

To determine the heat stored $Q_{\mathrm{Lat}}$ in a latent-thermal storage facility, the enthalpy of melting $\Delta H_{\mathrm{ls}}$ with the phase change from solid to liquid

must be added to Eq. 10.6:

$$Q_{\text{Lat}} = \int_{T_1}^{T_2} mc_p dT + \Delta H_{\text{ls}} = \overline{T}\Delta S_{12} + T_{\text{ls}}\Delta S_{\text{ls}} \approx \overline{T}\,(\Delta S_{12} + \Delta S_{\text{ls}}) > Q_{\text{Sens}} = \int_{T_1}^{T_2} mc_p dT. \tag{10.7}$$

The phase change occurs at a temperature $T_{\text{ls}}$ with an accompanying change of entropy $\Delta S_{\text{ls}}$. The equation shows that, assuming a phase change at temperatures between $T_1$ and $T_2$, with small changes in temperature, a latent-thermal storage facility can store more heat than a sensible-thermal storage facility.

Under what conditions then does it make sense to use latent TES? Water is the standard storage medium for sensible heat, as well as latent cold. In the past, for example, blocks of ice from a frozen lake were cut to size and then stored in cellar vaults until summer to provide cooling for food.

Water is plentiful, inexpensive, environmentally-friendly, and has a high-specific thermal capacity $c_p$, but it can only be used in temperatures ranging from about 5–95 °C with ambient pressure. The following example shows that, in some temperature ranges, a PCM may have advantages over sensible-thermal storage.

As a general rule:

$$\Delta q^{\text{PCM}} = c_p^{\text{PCM}} \cdot \Delta T + \Delta h. \tag{10.8}$$

Since the specific thermal capacity of a PCM in the solid phase is generally not the same as in the liquid phase, three terms determine the thermal energy stored in a latent-thermal storage facility:

$$\Delta q^{\text{PCM}} = c_{p,\text{solid}}^{\text{PCM}} \cdot \Delta T_{\text{solid}} + \Delta h + c_{p,\text{liquid}}^{\text{PCM}} \cdot \Delta T_{\text{liquid}}. \tag{10.9}$$

The heat stored in a sensible-thermal storage facility (in this case a water storage facility) is defined as follows:

$$\Delta q^{\text{water}} = c_p^{\text{water}} \cdot \Delta T, \tag{10.10}$$

with the following material data:

$$c_p^{\text{water}} \approx 4.2\,\frac{\text{J}}{\text{g}\cdot\text{K}},$$
$$c_p^{\text{PCM}} \approx 2.1\,\frac{\text{J}}{\text{g}\cdot\text{K}} \text{ and } \Delta h \approx 150\,\text{J/g},$$

where the average specific thermal capacity is $c_p^{\text{PCM}}$ (average over solid and liquid phases), and $\Delta T$ the overall temperature difference.

As a result:

$$\frac{\Delta q^{\text{PCM}}}{\Delta q^{\text{water}}} = \frac{c_p^{\text{PCM}}}{c_p^{\text{water}}} + \frac{\Delta h}{c_p^{\text{water}} \cdot \Delta T}, \tag{10.11}$$

$$\frac{\Delta q^{\text{PCM}}}{\Delta q^{\text{water}}} \approx 0.5 + \frac{35.7\,\text{K}}{\Delta T}. \tag{10.12}$$

In this example, the storage capacity of a latent-thermal storage facility with a temperature-difference smaller than 70 K exceeds the storage capacity of a sensible warm-water storage facility.

A PCM with an enthalpy of melting of 250 J/g (about the average enthalpy of melting for salt hydrates) increases the potential temperature-difference by 120 K. This means that, in regards to material, the storage density of a PCM-storage system is superior to that of a warm-water storage system. This difference is particularly relevant when the application limits the usable temperature-difference.

As a result, latent-thermal storage systems are very well-suited for cold storage. Building cooling typically uses systems with temperature-differences around 6 K. But building heating and warm-water supplies usually use systems with temperature-differences ranging 20–50 K or more. For cold storage at around 0 °C, water is the standard PCM because of its very high melting enthalpy of 334 J/g (Table 10.5).

Figure 10.20 illustrates the basic relationship discussed here between the temperature and the quantity of heat stored. PCM 2 in

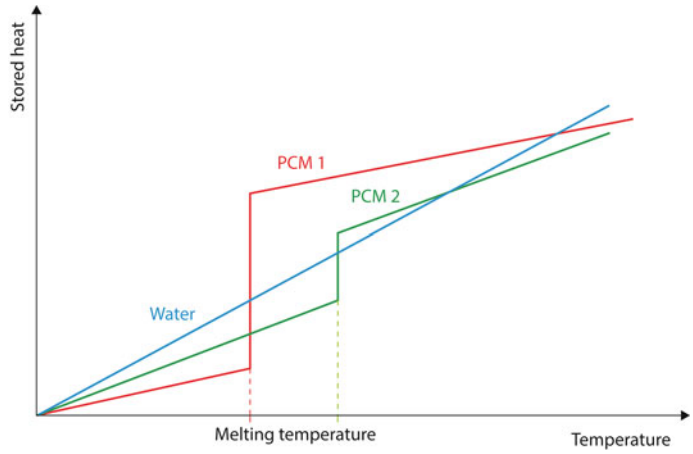



**Fig. 10.20** Quantity of heat stored in relation to temperature

green has a lower enthalpy of melting than PCM 1. As a result, it should only be used with smaller temperature-differences. With larger temperature-differences, the thermal capacity of water compensates for the melting enthalpy of the PCM. In the diagram, the gradient of the line is equivalent to the thermal capacity.

10

- **Properties**

A major advantage of PCM-storage systems is that they can store large quantities of energy with small temperature-differences. This means that the exergy losses of storage are lower than with sensible storage concepts because adding energy does not also increase the temperature-difference with the environment. But the system is technically difficult to implement. Depending on the material used, separation, undercooling, and unmanageable volume changes may result. Inadequate heat transfer resulting in low capacity is also often a problem. Design solutions must be found here to ensure the storage system complies with the parameters required. As a result, PCM-storage systems are often more expensive than comparable sensible-storage systems.

### 10.5.1 Characterization of Latent-Thermal Storage Materials

The standard method for characterizing a PCM is differential scanning calorimetry (DSC). Here, a small sample (5–10 mg) is placed in a crucible. This crucible is then placed together with an empty crucible (control) in a symmetrical measuring cell and subjected to a defined temperature program. Two methods of measurement are used. Dynamic measurement with temperature ramps of typically 2 K/min or stage measurement with the temperature varied in steps until thermodynamic equilibrium is reached. The heat flow is calculated from the temperature difference between the temperature sensors under the two crucibles (see Figs. 10.21 and 10.22). An enthalpy-temperature diagram can then be produced using this data.

Figure 10.23 shows the typical result of a dynamic DSC measurement with a heating and cooling rate of 2 K/min. The hysteresis here is fairly slight. This is because the substance measured is pentadecane, which is an alkane. The linear heating curve at low temperatures and the cooling curve at high temperatures indicates a relatively constant specific thermal

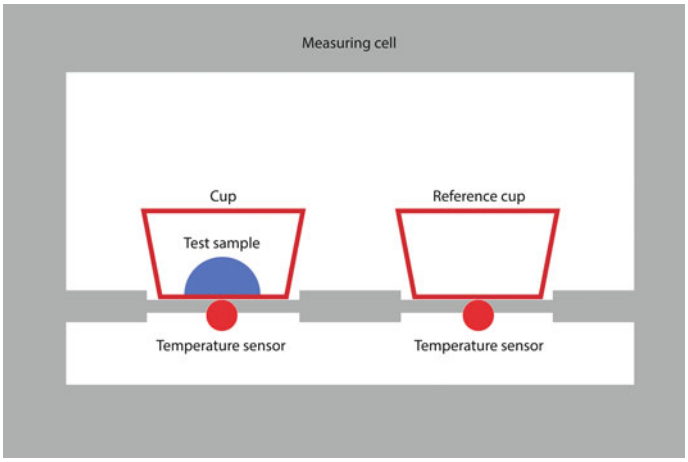



**Fig. 10.21** Symmetrical measuring cell with test and control crucibles, as well as temperature sensors under the crucibles



**Fig. 10.22** DSC Q 2000

capacity. But with pentadecane, the two phase-changes are unusual. The first phase-change with lower enthalpy is equivalent to a solid-solid phase change. The second phase-change at 5–15 °C indicates a solid-liquid phase change.

The T-history method can also be used to characterize a PCM. In this procedure, two identical containers, one filled with the PCM tested and the other with a control substance, are subjected to a quick change in ambient temperature. The reactions of the samples are then used to produce a temperature-time diagram. The control substance is required to determine the thermal capacity and transition enthalpy afterwards [27]. Figure 10.24 shows the measurements that result from using this procedure. The results indicate that the PCM tested has a melting range instead of a discrete phase-change temperature. The solidification and melting temperatures differ. This effect is called hysteresis, and it ranges up to 10 K with some materials. There is also evidence of undercooling as described above with salt hydrates.

### 10.5.2 Latent-Thermal Storage Materials

There are a range of materials suitable for thermal storage over a phase change. Figure 10.25 gives an overview of the various classes of materials together with their melting temperatures and melting energies. In practice, a phase change from solid to liquid is most commonly used. Despite the high phase-change enthalpy, a phase change from liquid to gas entails a large

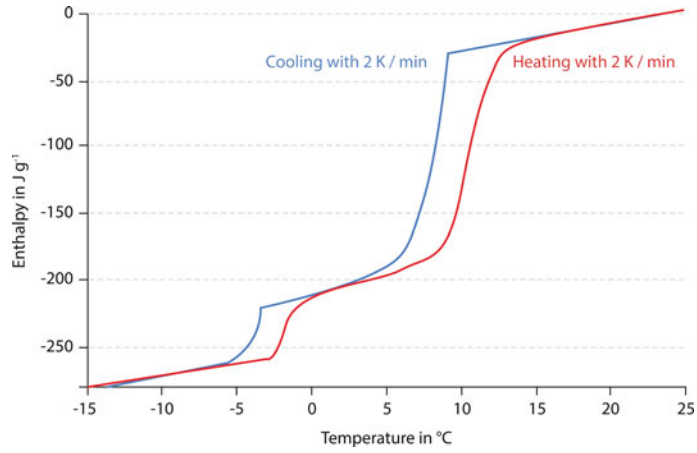



**Fig. 10.23** Enthalpy-temperature diagram resulting from a dynamic DSC measurement

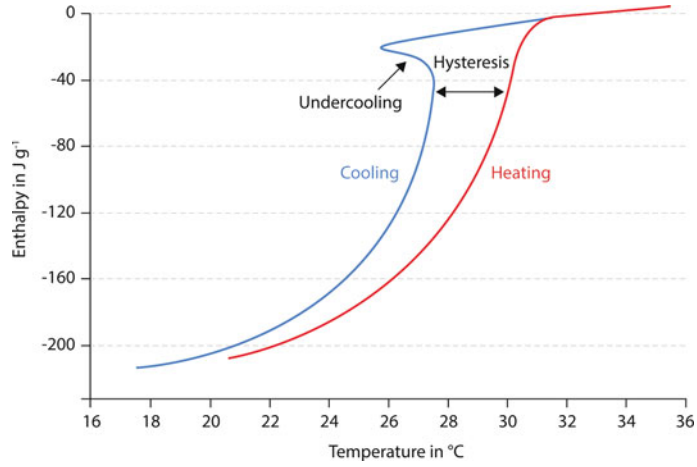



**Fig. 10.24** Typical T-history measurement of the PCM calcium-chloride hexahydrate

10

change in volume that is difficult to manage. As a result, it is rarely used.

With some material classes, cooling of the liquid phase may result in undercooling. Here, the melt cools below the melting range without crystallizing: the sample is then in a metastable state. When crystallization is triggered, the material crystallizes and the phase-change enthalpy is released. The material also warms to levels at or below the crystallization temperature, which (in a material without hysteresis) is equivalent to the melting temperature. The actual maximum temperature reached is determined by the extent of the undercooling when crystallization is triggered and by the thermal losses to the environment during crystallization.

Not all materials are suitable for use as PCMs. The following lists the required criteria for a PCM material [24].

- Physical criteria:
  - High phase-change enthalpy and specific thermal capacity
  - Suitable melting temperature
  - Good thermal conductivity
  - Reproducible phase-change
  - Manageable undercooling
- Technical criteria:
  - Physical and chemical stability
  - Low vapor-pressure
  - Manageable change in volume
  - Low corrosion with construction materials

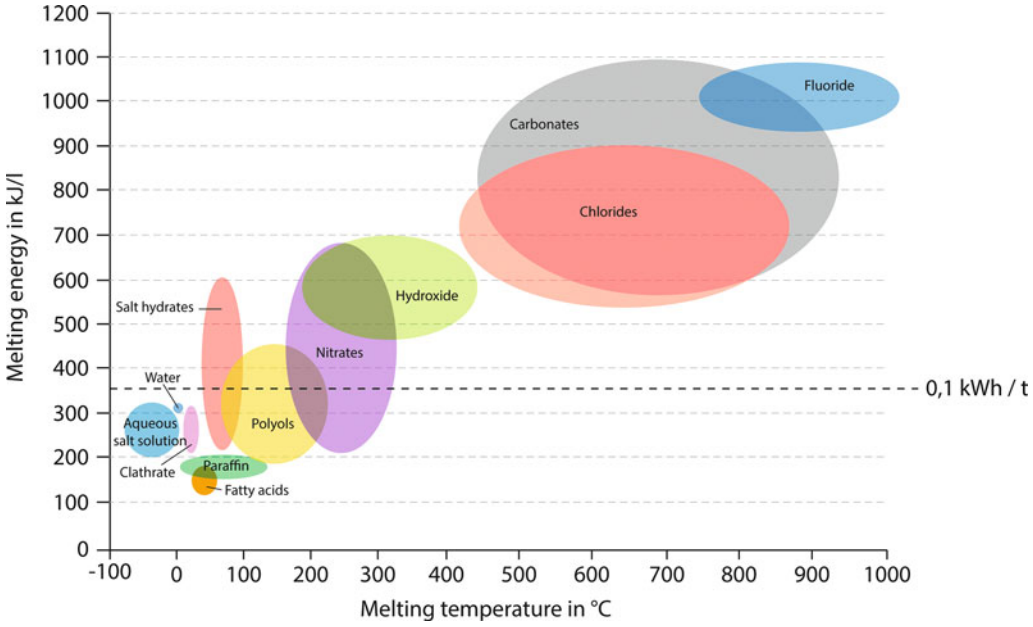



**Fig. 10.25** PCM material classes

- Suitable melting and solidification characteristics; cycle stability
- Economic criteria:
  - Low in price
  - Easily available
  - Environmentally-friendly; low toxicity

For example, water matches these criteria. Because of its melting temperature, water is generally used for air-conditioning.

Table 10.5 shows a selection of various materials, together with their melting enthalpies and melting temperatures.

Besides water, the salt hydrate and paraffin material classes are most frequently used in practice in latent-thermal storage systems. As a result, they are described in greater detail in the following section.

### 10.5.2.1 Salt-Hydrates

Salt-hydrates are salts bonded to water in fixed stoichiometric proportions (Fig. 10.26). Even slight changes in the stoichiometric concentration alters the transition enthalpy of a salt hydrate. As a result, one criterion for the use of salt hydrates as PCMs is a constant water content over the entire service life. Another problem with using salt-hydrates is incongruent melting. Several phases are formed during melting that then separate because of their varying densities. This means that the thermal capacity falls as the number of cycles increases. To counteract this effect and ensure higher cycle stability, the salt-hydrate tanks can be stirred. Macro- or micro-encapsulation or borax injections can also be used to increase stability [24, 25].

An additional challenge with using many salt-hydrates is their strong tendency to undercool. This means that, in practice, the stored heat is released at lower temperatures, or possibly not at all. But as in the case of pocket heaters, undercooling may also be desirable and useful. By adding inorganic solids, nucleation can be accelerated, reducing the tendency to undercool [26]. But this also reduces the specific storage capacity.

These technical problems aside, salt-hydrates have notably high volume-related, inherent storage density and good thermal

**Table 10.5** Characteristics of various PCMs

| Class of material | Material | Molecular formula | Melting temperature in °C | Melting enthalpy in kJ/kg | Thermal conductivity in W/m²K | Density in kg/m³ |
|---|---|---|---|---|---|---|
| Eutectic salt water mixture | Water/sodium chloride | $H_2O$/NaCl | −21 | 222 | – | 1,165 (liquid 20 °C) |
| Water | Water | $H_2O$ | 0 | 334 | 0.597 (liquid 20 °C) | 998 (liquid 20 °C)<br>917 (solid) |
| Salt hydrate | Calcium chloride hexahydrate | $CaCl_2 \cdot 6H_2O$ | 29 | 171 | 0.54 (liquid 39 °C) | 1,562 (liquid 32 °C) |
| | Disodium hydrogen phosphate Dodecahydrate | $Na_2HPO_4 \cdot 12H_2O$ | 35–40 | 280 | 0.476 (liquid) | 1,442 (liquid) |
| | Sodium sulfate penthahydrate | $Na_2S_2O_3 \cdot 5H_2O$ | 48 | 187 | – | 1,670 (liquid) |
| | Sodium acetate trihydrate | $Na(CH_3COO) \cdot 3H_2O$ | 58 | 226 | – | 1,280 (liquid) |
| | Magnesium nitrate hexahydrate | $Mg(NO_3)_2 \cdot 6H_2O$ | 89 | 149 | 0.49 (liquid 95 °C) | (liquid) |
| | Magnesium chloride hexahydrate | $MgCl_2 \cdot 6H_2O$ | 117 | 165 | 0.57 (liquid 120 °C) | (liquid) |
| Salts | Sodium nitrate | $NaNO_3$ | 307 | 172 | 0.51 (liquid) | 1,900 (liquid) |
| | Potassium nitrate | $KNO_3$ | 333 | 266 | 0.5 (liquid) | 1,900 (liquid) |
| | Lithium nitrate | $LiNO_3$ | 254 | 360 | 0.6 (liquid) | 1,800 (liquid) |

**Table 10.5** (Continued)

| Class of material | Material | Molecular formula | Melting temperature in °C | Melting enthalpy in kJ/kg | Thermal conductivity in W/m²K | Density in kg/m³ |
|---|---|---|---|---|---|---|
| Salt mixture | Sodium nitrate + potassium nitrate | $KNO_3/NaNO_3$ | 222 | 100 | 0.5 (liquid) | 1,900 (liquid) |
| | Lithium nitrate + sodium nitrate | $LiNO_3$–$NaNO_3$ | 194 | 265 | 0.5 (liquid) | 1,900 (liquid) |
| Paraffin | Octadecane | $C_{18}H_{38}$ | 28 | 245 | 0.15 (solid) | 777 (liquid) |
| Fatty acid | Lauric acid | $CH_3(CH_2)_{10}COOH$ | 43 | 178 | 0.15 (liquid 50 °C) | 870 (liquid 50 °C) |
| | Myristic acid | $CH_3(CH_2)_{12}COOH$ | 58 | 186 | – | 861 (liquid 55 °C) |
| Sugar alcohol | Erythritol | $C_4H_5(OH)_6$ | 120 | 340 | 0.32 (liquid 140 °C) | 1,300 (liquid 140 °C) |
| PEG | PEG 6000 | $HO\text{-}[CH_2\text{-}CH_2\text{-}O]_n\text{-}H$ | 60 | 190 | | 1,085 (liquid 70 °C) |



**Fig. 10.26** Separated Glauber salt ($NaSO_4 \cdot 10H_2O$); above: saturated aqueous solution; center: Glauber salt; below: anhydrous sodium sulfate

conductivity in comparison to paraffins. They are also cheaper than paraffins.

### 10.5.2.2 Paraffins

Paraffins are organic mixtures made of saturated hydrocarbons produced by distilling crude oil. They are primarily composed of long-chain alkanes. The melting point can be adjusted as required by varying the chain length. Paraffins are used commercially for thermal storage at temperatures ranging from −5 to 120 °C. Since paraffin mixtures are composed only of paraffins with various chain lengths, they melt congruently and have a high cycle stability. In addition, unlike metals, paraffins are ecologically safe and non-corrosive. They pose no health hazard and show only a tendency to undercool with micro-encapsulation.

A disadvantage of paraffins is their combustibility. This prevents their use in some environments. In comparison to salt-hydrates, they are also expensive and have a very low ther-

mal conductivity of around 0.2 W/(m K). In addition, a phase change may produce volume changes ranging up 20% [26].

The most important criterion for choosing a PCM is its phase-change temperature. This can be adjusted as required by mixing alkane chains of various lengths. But mixing pure/commercial paraffins usually reduces the phase-change enthalpy and increases the melting range. Using commercial paraffins has a similar effect. They are frequently used because of their low cost. For these reasons, the exact characteristics of these materials must be carefully considered. The RAL PCM certificate (RAL-GZ 896; ▶ http://www.pcm-ral.de) determines quality and testing specifications useful in this regard.

#### 10.5.2.3 Anhydrous Salts

The cations are mainly alkali (e.g., Li, Na, K) and alkaline earth (e.g., Ca, Mg) metals. The anions that are considered include nitrates, nitrites, hydroxides, bromides, carbonates, chlorides, sulfates, and fluorides. Many anhydrous salts are miscible, and this results in a large variety of potential single salts and salt mixtures (binary and ternary systems). For temperatures up to 350 °C, in particular, alkali-metal nitrates and nitrites and their mixtures are suitable PCMs if requirements such as handling and steel compatibility are taken into account. In CSP-technology development, direct steam generation in the absorber tubes has sparked interest in latent-heat storage systems. The latent-heat system acts as a steam-storage system for the two-phase heat-carrier water/steam. The melting temperature for candidate PCMs is between 120 °C and 340 °C. Here, the application of storage concepts using sensible-heat storage is usually not cost-effective. For two-phase heat carriers, sensible-heat storage systems have a low energy efficiency or large exergy due to the large temperature gradients between the storage media and HTF. In a latent-heat storage system, both the PCM and the heat carrier undergo a phase change at about the same temperature. Hence, it is possible to avoid larger temperature-differences between water/steam and PCM. Additionally, it is feasible to provide steam storage solutions for the process-heat sector.

#### 10.5.2.4 Composite Materials

In their pure form, PCM often have low thermal conductivity or they separate as the number of cycles increase. There are a range of potential solutions to this problem. This section discusses several concepts.

To increase the thermal conductivity of a PCM, for example, a graphite matrix can be impregnated with PCM. ZAE Bayern used this method to increase the thermal conductivity by a factor of 8 to 100, by adding only 10% by volume of graphite to the PCM.

To prevent poor thermal conductivity and stability in large PCM units, especially with PCM made of several components, the units are frequently encapsulated in smaller units. Plastic and metal containers can be used, as can bags made of plastic-metal composite materials. An advantage of this type of encapsulation is that it hermetically seals the PCM, preventing material exchange with the environment. This is particularly useful if salt-hydrates are used. PCM in this form can also be used to conveniently upgrade existing thermal storage systems. This is because it is compact enough to fit easily into storage tanks. To avoid problems caused by the change in volume, air is frequently encapsulated together with the PCM (see ◘ Figs. 10.27 and 10.28).

Besides macro-encapsulation, PCM can also be processed using micro-encapsulation. Regardless of its actual phase-state, micro-encapsulated PCM behaves like a powder. The advantage of this kind of encapsulation is that it makes the material easier to handle. It can be conveniently added to plasterboard or textiles, for example. Because the encapsulation is small and contains little PCM, mechanical damage to the encapsulation results in the loss of only very small quantities of PCM. Among others firms, BASF commercially produces micro-encapsulated PCM. The PCM pellets have a diameter ranging from 2 to 20 μm and are made

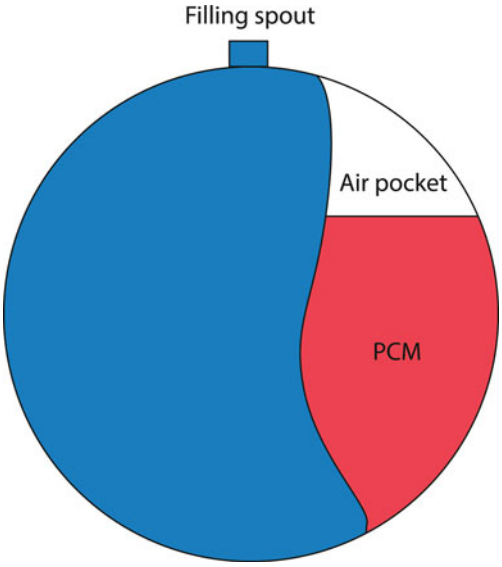



**Fig. 10.27** Macro-encapsulated paraffin



**Fig. 10.28** Micro-encapsulated paraffin. (Source: BASF SE)

of paraffin coated with acrylic. The product is typically used in combination with building materials required for passive building cooling. Micro-encapsulated PCM can be blended with colors, plasterboard, etc. Depending on the material, these building materials can range between 20–40% by weight of PCM.

Adding PCM to porous structures is another process used to increase thermal conductivity and stability. Wood-fiber board can be impregnated with PCM, for example. Paraffins can also be integrated into plastic matrixes. An advantage of these composite materials is that, like encapsulated PCM, they can be used in storage facilities as fill.

Fraunhofer IFAM in Dresden is currently researching binding PCM in a metal matrix. Here fiber or wire structures, as well as infiltrated metallic foams, are used to improve thermal conductivity. With these processes, balancing the ratio of PCM to carrier-substance is crucial. This is because increasing the proportion by volume of PCM increases the storage capacity, but it reduces the thermal conductivity [28].

### 10.5.3 Heat-Transfer Concepts

Heat-transfer concepts for latent storage materials are primarily optimized to maximize thermal capacity. Various technical approaches can be used to improve the heat transfer.

This section discusses the various heat-transfer concepts. Broadly speaking, heat transfer may be either passive or active. With passive heat-transfer, free convection alone moves the PCM, and the heat-carrier fluid does not come into contact with the storage medium. The heat transfer occurs at a defined surface (heat exchanger). This type of heat transfer may produce melt fronts that have negatively influences the heat-transfer resistance. Figure 10.29 shows examples of simple passive storage-system designs.

With active heat-transfer, the storage material is also kept in motion by an agitator. Here, a distinction is drawn between indirect and direct-heat-transfer. With indirect charging, the PCM does not come into contact with the heat-carrier fluid; with direct charging, the heat-carrier fluid flows through the storage medium, and no heat exchanger is required.

Based on these heat-transfer concepts, the heat is transported across system boundaries. The thermal capacity of this type of storage system can be increased by installing internal, heat-conducting structures. But in general, the capacity is low.

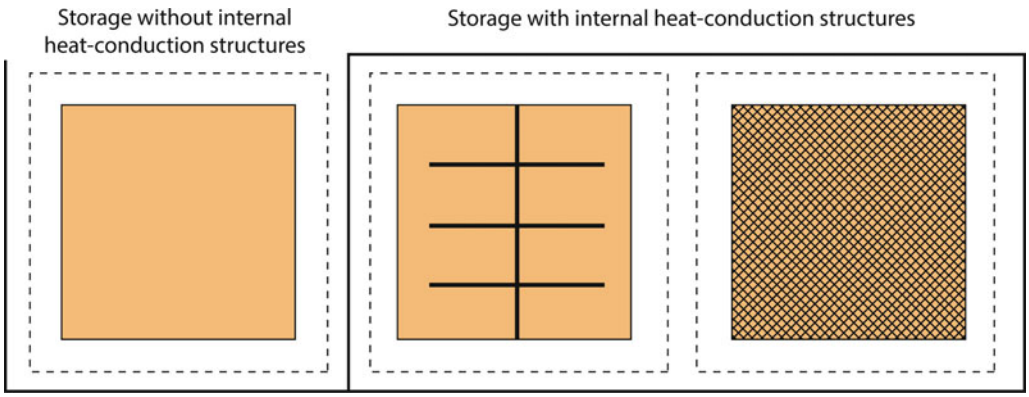



**Fig. 10.29** Simple storage systems with and without internal heat-conducting structures

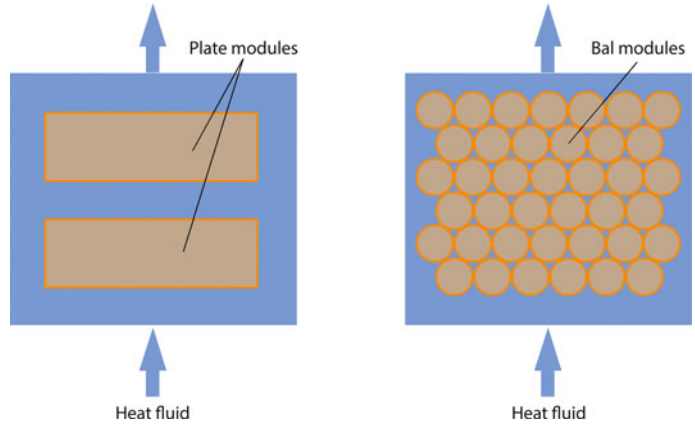



**Fig. 10.30** Module storage system; *left*: plate modules; *right*: ball modules (nodules)



Storage systems of this kind are typically inexpensive. Since no peripherals are required, they also have high storage densities. In addition, with these sealed systems, there is no material exchange with the environment. As a result, the system is protected against contamination, corrosion and storage-material losses. Freezing packs, as well as macro- and micro-encapsulated PCM systems, use this heat transfer concept.

The charging and discharging capacity of these storage systems can be increased by using a modular design (Fig. 10.30). Here, macro-encapsulated PCM can be used as fill in the storage system. The advantage of this approach is that the PCM can be simply and flexibly integrated into systems with a range of tank geometries. The heat-carrier fluid flows through the storage system and the PCM fill. The overall capacity of this kind of storage system is increased by the large contact area. But frequently, the flow through the various modules is uneven. This means that the heat transfer is not consistent across all the individual modules. The additional encapsulation material required also reduces the share of PCM in the storage system, lowering the specific power and capacity. Figure 10.30 illustrates the basic design of this concept. Modular storage systems are common in Japan. Because of the high peak-hour electricity prices there, cold for air-conditioning is often stored at night. In addition to fills, PCM plates installed in ventilation ducts use this heat-transfer concept, as well.

The simplest form of passive charging is frequently used in sensible-storage systems. Here,

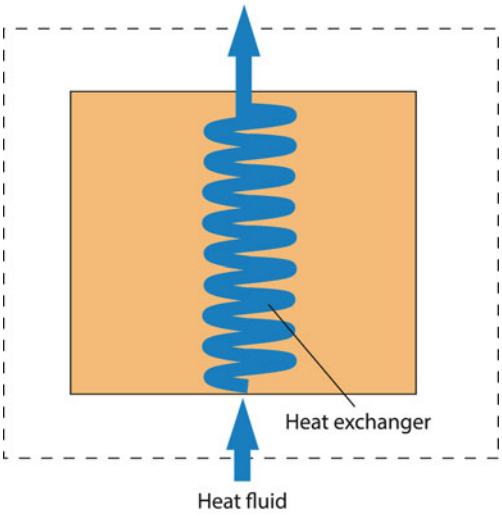



**Fig. 10.31** Storage system with internal heat exchanger

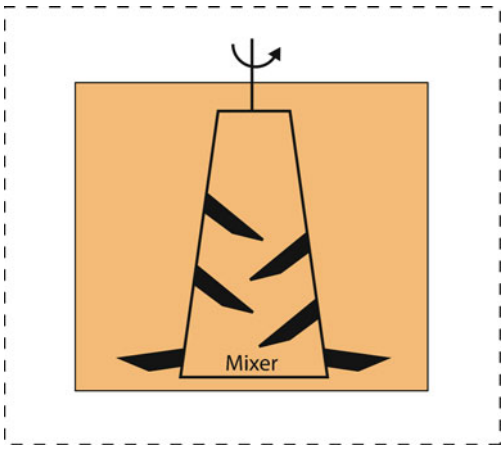



**Fig. 10.32** Active, indirect storage system with internal agitator

a heat exchanger with a geometry specifically designed for the PCM is integrated into the storage system. The thermal conductivity characteristics as well as the capacity and power required generally determine the heat-exchanger geometry. The advantage of this concept is that a high share of storage material (exceeding 90%) can be installed. The disadvantages of this are melt-front formation, increasing heat-transfer resistance, and a tendency to separate with salt-hydrates. Fig. 10.31 shows the basic design of a storage system of this type.

Storage systems with an internal agitator and an integrated heat exchanger (Fig. 10.32) use indirect, active heat-transfer concepts. The advantage here is reduced separation with salt-hydrates, for example, thus increasing cycle stability. Constant agitation prevents the formation of a solidification front with poor heat-transfer coefficients; this ensures consistent power consumption and power output. But the overall efficiency is reduced by the motor's additional power consumption.

A solution here is to use the agitator as a heat exchanger as well. A separate heat exchanger would lower the share of storage material, reducing the storage system's thermal capacity. Another option is to rotate the entire tank so that an internal agitator is no longer required.

Direct-contact storage systems use active, direct-heat-transfer concepts. Here the heat-carrier fluid flows through the storage material, mixing it at the same time. This process can prevent separation of the individual components, particularly with salt-hydrates. The heat-carrier fluid's retention time can be adjusted to match the PCM's heat-transfer coefficients by altering the storage system's geometry as well as the density difference required between the two materials. But not all heat transfer fluids can be used here because the materials are in direct contact and could mix with each other. Since no heat exchanger is required, direct-contact storage systems are compact and have high capacities. But regulating these systems is difficult, and the PCM cannot be permitted to solidify completely. This condition reduces the capacity. Complete solidification of the PCM, permitting storage of sensible heat, is only possible with major technical alterations (for example, by installing a bypass). But because the contact area is reduced, this also reduces the capacity. Figure 10.33 shows the basic design of a direct-contact storage system.

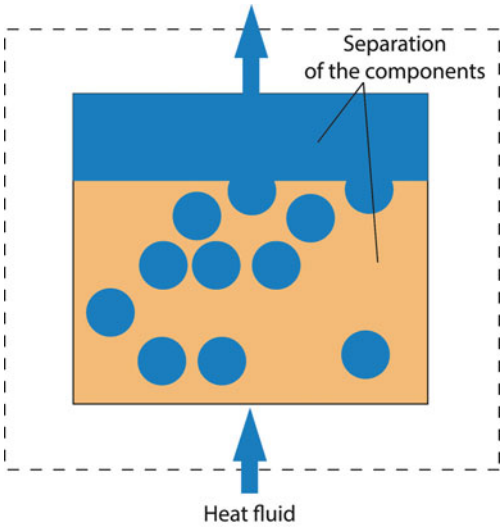



**Fig. 10.33** Direct-contact storage system

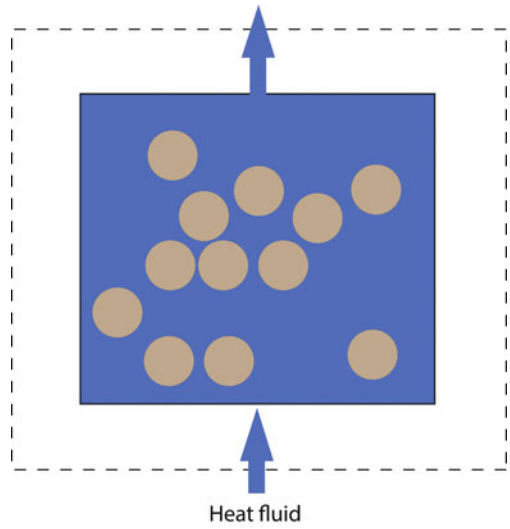



**Fig. 10.34** Slurry storage system



Another storage concept that allows the heat-carrier fluid and PCM to come into contact is slurries. Slurries can still be pumped even when the PCM has solidified. This means that slurries can be used to store thermal energy and distribute heat or cold at the same time. They are generally termed PCS in these applications. Slurries can be produced in a variety of ways. With ice slurries, the heat-carrier fluid and PCM used are made of the same substance. Emulsions containing substances of varying hydrophilicity combined with emulsifiers can also be used. In addition, micro-encapsulated PCM can be proportionally added to the heat-carrier fluid to ensure the mixture can still be pumped. But in this case, care must be taken to prevent the pump from damaging the encapsulation.

The share of PCM in slurries typically ranges from 20 to 40%, or in exceptional cases, up to 60%. The lower the share of heat-carrier fluid, the greater the viscosity. Higher viscosities require greater pump-power. This in turn increases costs.

Because the substances are transported in a composite and the temperature levels that result remain relatively constant, these systems have lower exergy losses than conventional concepts. This means that slurry storage systems may have very high capacities.

Figure 10.34 shows the basic design of a slurry storage system.

### 10.5.4 Conclusion

- Phase-change material research is focused on identifying new materials that **maximize melting enthalpy** at the melting temperatures required by various applications [30–33]. The primary areas of applications are **heating and air-conditioning of residential and office buildings**.
- Material research and material development is focused on within this chapter in relation to determining the causes of undercooling and determining the processes that trigger crystallization [34]. A current focus of research for applications in buildings are solid-solid changes as well as phase changes where the material remains form-stable.
- **Latent-thermal storage** component research and development is primarily focused on **improving heat transport to maximize thermal capacity during**

**charging and discharging**. Researchers are also investigating **passive storage systems** for air-conditioning (also called passive cooling). Here, PCM (macro- or micro-encapsulated) is installed in rooms requiring cooling. The PCM absorbs heat when the temperature rises, cooling the room to a certain degree as a result. When temperatures fall below the melting point at night, the PCM solidifies again. It is then ready to cool the room again the next day.

- **Active concepts with PCM movement** rather than passive concepts allow for separation of thermal power and capacity, as well as constant charge and discharge power. This concept has been successfully developed for slurry type cold storage using artificial ice but is still under development for higher temperatures.

## 10.6 Thermochemical-Energy Storage Systems

Thermochemical-energy storage systems use the reaction energy from reversible chemical processes or physical surface reactions. They have particularly high-energy densities. The reversibility of the process is a key factor here. In addition, the energy is stored as reaction energy, not heat. As a result, there are no thermal losses during charging. Technically at least, this would permit very long storage durations. But for economic reasons, thermochemical storage systems are rarely feasible. When the reaction partners are recombined during discharging, an exothermic reaction releases the stored energy.

The following discussion divides thermochemical-energy storage systems into three categories: chemically reversible processes, adsorption storage systems, and absorption storage systems.

With TES systems, ideally an endothermic and reversible dissociation of a condensed compound $AB$ results in two reaction products: a condensed reaction product $A$ and a condensed reaction product $B$ in gaseous form. The abbreviations s, l, and g are used to indicate the various aggregate states of the reactants, i.e., solid, liquid, and gaseous:

$$AB(\mathrm{s,l}) \leftrightarrow A(\mathrm{s,l}) + B(\mathrm{g}). \qquad \textbf{(10.13)}$$

The reaction products can be easily separated because they are in different aggregate states. This also permits the products to be stored without losses or risk of reverse reactions. But the energy storage density is reduced by the volume required to store gases. This problem can generally be solved by condensing the gaseous phase, or by using an 'open' system that releases the gaseous components into the atmosphere and then reabsorbs them from the atmosphere when required.

### ■ Chemically Reversible Processes

In principle, thermochemical-energy storage systems can use any reversible chemical reaction. The decisive criterion here is the equilibrium temperature at which the products and educts are at thermodynamic equilibrium. Storage-system discharge (exothermic reaction) occurs at a temperature below the equilibrium temperature. But charging (endothermic reaction) must occur at higher temperatures.

### ■ Adsorption Storage Systems

Adsorption is the physical accumulation of molecules (adsorbate) on the surface of a usually porous adsorbent. Unlike with chemical reactions, there is no defined equilibrium temperature. The heat released is determined by the varying binding energies at the accumulation sites in the adsorbent and, as a result, not constant. The storage density of an adsorption storage system is determined by the adsorbate's evaporation enthalpy, the binding forces between the adsorbate and the adsorbent, and by the lift in charge between the charging and discharging temperatures.

### ■ Absorption Storage Systems

Unlike adsorption using accumulation, with absorption, a molecule is intercalated into the

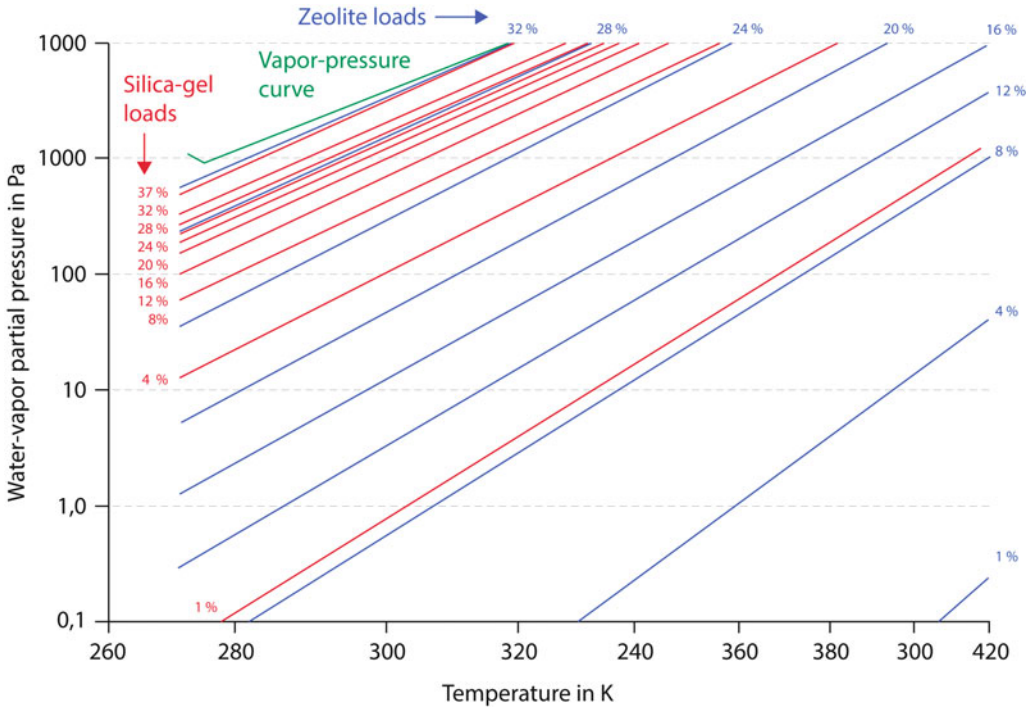



**Fig. 10.35** Isosteres diagram for silica gel/water and zeolite/water

absorbent phase. In this process, the absorbate is a soluble material dissolved into a solvent (absorbent). Strictly speaking, since no chemical processes occur, absorption is not a chemical process. Instead, it is a dilution process. Absorbents are liquids (for example, salt solutions that can absorb water vapor), but adsorbents are solid, microporous materials.

The energy storage density with absorption is determined by the molar mass of the absorbate, the affinity and aggregate state of the absorbent, and the absorbate.

### 10.6.1 Storage Materials for Thermochemical Processes

Storage materials applicable for thermochemical processes also fall into three categories: materials for chemically reversible reactions, adsorption materials, and absorption materials.

The reactions that occur in thermochemical storage systems can be categorized by their reaction equilibriums. These equilibriums are generally determined by the pressure and temperature. With a particular substance combination, such as magnesium oxide and water, a certain reaction equilibrium is reached at a specific temperature and vapor partial-pressure. These equilibriums are termed:

- Isotherms (curves at the same temperature)
- Isobars (curves at the same pressure)
- Isosteres (curves at the same water content)

Figure 10.35 shows the curves at the same water content. The maximum content is obtained when the isosteres approach the vapor curves. The air is then saturated with vapor. These conditions maximize the water content. The content for silica gel is 37%, and for zeolite it is 32%. With adsorption systems of this type, it should be noted that the increase in isosteres varies by the water content. This is generally not the case with chemical reactions.

**Table 10.6** Materials for chemically reversible reactions

| Reaction type | Equation | Equilibrium temperature (1 bar) in °C | Energy storage density in kW h/kg |
|---|---|---|---|
| Salt-hydrate | $MgSO_4 \cdot 7H_2O \Leftrightarrow MgSO_4 + 7H_2O$<br>$CaCl_2 \cdot 2H_2O \Leftrightarrow CaCl_2 \cdot H_2O + H_2O$ | 122<br>174 | 0.463<br>0.091 |
| Hydroxide | $Mg(OH)_2 \Leftrightarrow MgO + H_2O$<br>$Ca(OH)_2 \Leftrightarrow CaO + H_2O$ | 268<br>521 | 0.372<br>0.373 |
| Carbonate | $CaCO_3 \Leftrightarrow CaO + CO_2$<br>$BaCO_3 \Leftrightarrow BaO + CO_2$ | 896<br>1,497 | 0.463<br>0.298 |
| Metal hydride | $MgH_2 \Leftrightarrow Mg + H_2$ | 293 | 0.834 |
| Catalytic reactions | $SO_3 \Leftrightarrow SO_2 + 0.5O_2$ | 767 | 0.340 |
| Steam reformation | $CH_4 + H_2O \Leftrightarrow CO + 3H_2$ | 687 | 1.672 |

**Table 10.7** Adsorption materials

| Adsorbent | Maximum content in $kg_{H_2O}/kg_{adsorbent}$ | Adsorption enthalpy in kW h/$kg_{H_2O}$ | Energy density in kW h/$kg_{adsorbent}$ |
|---|---|---|---|
| Zeolite 13X | 0.32 | 0.964 | 0.308 |
| Silica gel desiccant beads | 0.37 | 0.758 | 0.280 |

The diagram also shows that obtaining lower contents (equivalent to the charging process when used for storage) at a constant pressure requires significantly higher temperatures with zeolite than with silica gel. But discharging zeolite also results in greater temperature lifts.

### 10.6.1.1 Chemically Reversible Reactions

Storage materials for chemically reversible reactions vary by their equilibrium temperatures at ambient temperatures and by the quantity of energy converted in the reaction. These parameters are shown in Table 10.6.

The energy storage densities listed here are based on the mass of the reactants, and they indicate the maximum achievable levels. The reaction of barium carbonate to barium oxide results in the highest temperatures, ranging up to 1,497 °C. The theoretically highest energy storage density results from the steam-reforming of methane and water to carbon monoxide and hydrogen. In the ideal case, the density here is 1.672 kW h/kg. But practically implementing reactions of this type in TES systems still requires extensive further development and research.

### 10.6.1.2 Adsorption

Adsorption processes are classified as a type of thermochemical storage reaction. The most common adsorbents are zeolite and silica gel. Table 10.7 shows the maximum water content and energy density for a range of materials. Also, the energy storage densities listed here indicate the maximum achievable levels.

A key criterion for adsorbents in adsorption processes is the specific surface area of the material. The more water that can be collected on the surface, the greater the quantity of energy that can be stored. Table 10.8 shows various adsorption materials with their specific surface areas in $m^2$ per gram.

But the achievable discharging temperature is determined by the specific adsorption enthalpy or by the binding energy (adsorption

**Table 10.8** Materials for adsorption and their surface areas

| Adsorbent | Chemical molecular formula | Specific surface area in $m^2/g$ |
|---|---|---|
| Aluminum oxide | $Al_2O_3$ | 100–400 |
| Adsorber resins | For example styrene | 100–800 |
| Silica gel | $SiO_2$ | 500–800 |
| Carbon molecular sieve | C (as anthracite) | 500–1,000 |
| Zeolite | $Al_2O_3$, $SiO_2$ | 800–1,200 |
| Activated carbon | C | 800–2,000 |

**Table 10.9** Absorption materials

| Absorbent | Absorbate | Absorption enthalpy in $kJ/mol_{absorbate}$ | Molar mass in $g/mol_{absorbate}$ | Energy storage density in $kW\,h/kg_{absorbate}$ |
|---|---|---|---|---|
| $H_2O(l)$ | LiBr(s) | 49.04 | 86.85 | 0.157 |
| $H_2O(l)$ | $NH_3(g)$ | 34.18 | 17.03 | 0.558 |
| $H_2O(l)$ | $H_2SO_4(l)$ | 95.28 | 98.08 | 0.270 |

10

enthalpy minus the evaporation enthalpy). This means that, under some circumstances, certain adsorbents can absorb very large quantities of water. Since the water bonds very loosely to the adsorbent, the quantity of usable heat discharged by the storage system is relatively small.

#### 10.6.1.3 Absorption

Table 10.9 lists various absorbents together with their molar masses, absorption enthalpies, and theoretical energy storage densities. Absorbents, in general, have fairly low binding energies. This results in smaller temperature lifts during discharging than with solid adsorbents.

### 10.6.2 Designs

Compared to latent-thermal storage systems, thermochemical storage facility designs are significantly more complex. In addition to heat exchange, materials must also be exchanged. Furthermore, the materials must be separated or exchanged at the same time as when heat is added or removed. The challenge here is to develop compact storage facility designs that maximize the heat- and material-transfer efficiencies. Broadly speaking, there are two tapes of thermochemical-energy storage facility design: sealed and open systems.

Sealed systems are generally airless systems with a vacuum seal that permit gaseous components of any kind to be used. Very low pressures in the vacuum are required for the reaction. But the gaseous components must be stored in the system after the charging process. The components B can be condensed to reduce the volume required for storage. Figure 10.36 shows the basic design of a condenser of this type.

For the reverse reaction, the components B must be vaporized again. This evaporation process requires ambient heat and largely determines the usable energy or power of the storage facility.

If they are thermally charged, sealed systems can provide heat by releasing the reaction enthalpy in the reactor, or provide cold by absorbing evaporation heat in the condenser. With the material combination of zeolite/water, for example, the cold produced by the condenser can result in the formation of ice.

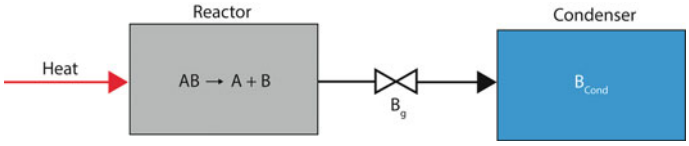



**Fig. 10.36** Gas-component condenser design

In open systems, these components must be present in the atmosphere. They are released during charging and then reabsorbed during discharging.

Various designs can be used with open systems. Because they are the simplest and least costly, fixed bed designs are the most common. The adsorbent is in the form of a fill here. The adsorbate (usually water vapor) flows through it at ambient pressures (Fig. 10.37). Other reactor designs exchange a mass flow of solid or liquid sorbent with the adsorbate flow. The advantage of these reactors is that power and storage capacity are decoupled. The power is determined by the size of the reactor, but the capacity is determined by the size of the sorbent storage container. In practice, these types of reactors are typically used only with liquid-reaction combinations. With adsorption storage systems using solid zeolite, for example, the resulting mechanical strain makes transporting the zeolite into the reactor a major challenge.

With open adsorption systems, no storage at all is required for the gas components B inside the storage system. Ideally, they are components of the atmosphere that can be temporarily stored in the ambient air. This increases the energy storage density by the share of volume subtracted (which was used to store the gas components). But it should be kept in mind that discharging an open adsorption storage system requires that an adequate concentration of the gaseous components B be available in the atmosphere (Fig. 10.38).

The zeolite/water system is the most commonly used type of open, adsorption storage design. This is more a physical process than a chemical reaction. The operating principle of this storage system is based on the adsorption of water vapor by electrostatic forces in the micro-porous zeolite (Fig. 10.39). This process functions as the discharging process in the storage system. Here, adsorption enthalpy is released in the form of heat.

Additional heat is required to charge the storage system. This heat releases the water collected on the zeolite and then vaporizes it. The vapor produced can be released into the atmosphere using air as a carrier medium, thus eliminating the need for temporary storage. But

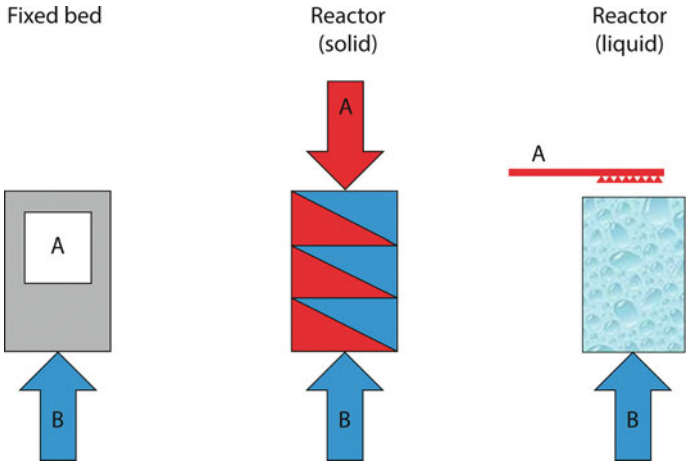



**Fig. 10.37** Various open, thermochemical storage facility designs

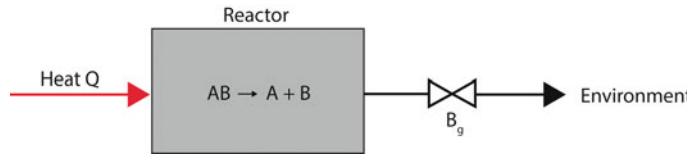



**Fig. 10.38** Atmospheric-gas component design

an adequately humid flow of air must be available to discharge the storage system. As a result, this thermal storage system is particularly well-suited for drying processes. This process is already used in many modern dishwashing machines.

### 10.6.3 Conclusion

- **Research on efficient thermochemical storage system design** is currently focused on developing new storage materials. The goal here is to maximize the reaction enthalpy (or sorption enthalpy) at the temperatures required. Research on **sorption storage systems** is focused on optimizing currently-used adsorbents [42] as well as developing new adsorbent classes, such as AlPOs, SAPOs, and MOFs [43, 44]. Scientists in Germany and other countries are also researching liquid- and solid-adsorbent combinations (called **composite materials**) [45]. Besides sorption processes, researchers are investigating other chemical reactions applicable for **high-temperature**



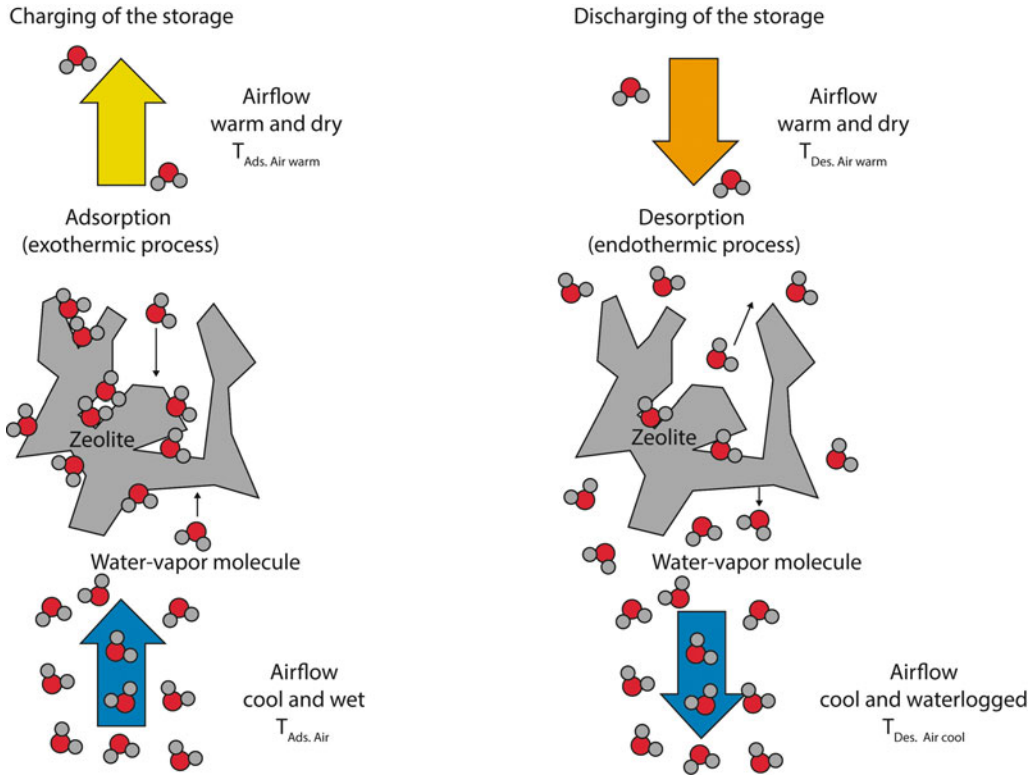



**Fig. 10.39** Zeolite/water storage system

**applications and seasonal-thermal storage** [46, 47].

- **The relevant material combinations** are also being tested to determine their **stability** and **ageing mechanisms** under application conditions.
- Besides storage materials, another important area of research is thermochemical storage-system **reactor design**. The goal here is to optimize the thermal capacity, while ideally also reducing costs, for example, by minimizing the auxiliary energy required [48, 49]. Modeling tools are being developed for the various storage reactor types to evaluate their potential benefits.

## 10.7 Costs

As with all storage technologies, cost is a crucial factor in determining their feasibility. To draw comparisons across technologies, the specific capital costs given in euros per unit of storage capacity €/kW h are used.

The costs of TES systems are often largely determined by the costs of the storage materials. But with most storage systems and in particular with latent and thermochemical storage systems, the costs of the heat exchanger or exchange surfaces far exceed the cost of the storage materials. As a result, few general statements about costs can be made.

In addition, the application and the number of cycles per unit of time it requires are decisive factors in determining the cost efficiency of a TES system. The sensible-storage systems for seasonal storage of solar heat described in this chapter range from one to 1.5 cycles per year. This means that extremely inexpensive materials, such as water and low-cost storage containers made of concrete, for example, can be used. A thermal storage facility utilizing industrial waste heat goes through several cycles per day. As a result, the facility may be significantly more expensive. Latent or thermochemical storage systems can be used with these applications to reduce costs.

### ■ Sensible-Thermal Storage Systems

Sensible-thermal storage systems are the least expensive technology available for storing thermal energy. The storage materials used (water, stones, soil etc.) are usually very inexpensive and easily available in large quantities almost everywhere. But the containers used here require good insulation, thus significantly increasing the overall costs.

The largest sensible-thermal storage facilities in Germany are seasonal hot-water storage facilities with volumes ranging from 5,000 to 10,000 $m^3$ and specific capital costs ranging from 0.5 to 3 €/kW h. Geothermal-probe storage systems range more widely in price. Since they are largely determined by local conditions, costs may range from 0.1 €/kW h all the way up to 10 €/kW h. System costs of molten-salt storage is in a range from 20–50 €/kW h.

### ■ Latent-Thermal Storage Systems

Currently, latent-thermal storage systems are significantly more expensive than sensible-thermal storage systems. This is because of the expensive storage materials required, the comparably complex construction design (heat transfer), the current state of research and the low level of market penetration. Frequently, these storage systems are made to order. The storage facility and heat transfer geometry are then tailored to the customer's specific needs for storage capacity and power. The physical characteristics of the PCM used are also taken into account.

Costs for PCM storage facilities generally range from 10 to 50 € per kW h of storage capacity, but they can also be much higher. The advantage of micro-encapsulated PCMs is that no peripherals are required to effectively store heat. In many cases, the costs of micro-encapsulated PCMs used for passive building cooling can be amortized over only five years because the heating and cooling costs of the building are eliminated. The price of micro-encapsulated PCMs is currently around 10 €/kg [29].

Using water as a PCM to store latent cold has been standard for many years (for exam-

ple in Japan), and it costs about the same as sensible-thermal storage.

### ■ Thermochemical-Energy Storage Systems

With thermochemical-energy storage systems, the price of the storage materials is similar to the price of PCMs. But the materials additionally must be processed (e.g. into pellets), and reactors are also complex and expensive. The reactors are also complex and expensive. Since these complex reactor designs combine material and heat exchange, they are the primary cost drivers with thermochemical storage systems. Additional peripherals, such as condensers or humidifiers, may also be required. Depending on the design and the operating conditions (vacuum or ambient pressure), thermochemical-energy storage systems range in cost from 8 to 100 €/kW h.



## References


1. Fisch N (2005) Wärmespeicher, 4th edn. TÜV-Verlag. ISBN 3-8249-0853-0
2. Baum S (2011) Langzeitausgleich erneuerbarer Energie mittels Energiespeicherung in Wasserstoff. FH Köln
3. Urbaneck T (2012) Kältespeicher. Oldenbourgh Verlag. ISBN 978-3-486-70776-2
4. Gintars D (2010) Erdwärme für Bürogebäude nutzen. BINE Informationsdienst. FIZ, Karlsruhe, Eggenstein-Leopoldshafen
5. Meier F (2010) Erdgekoppelte Wärmepumpen für Neubauten. BINE Informationsdienst. FIZ, Karlsruhe, Eggenstein-Leopoldshafen
6. http://www.waermepumpen.info/erdwaermepumpe/erdkollektor
7. http://www.heiz-tipp.de/ratgeber-312-dimensionierung_erdkollektor.html
8. http://www.energiesparhaus.at/energie/wp-erdkollektor.htm
9. http://www.bosy-online.de/Erdkollektoren.htm
10. http://www.enregis.de/auftritt/daten/pdf/Referenz-Oldenburg-2012.pdf
11. Dimplex (2004) Projektierungs- und Installationshandbuch. Ausgabe V, April
12. Borstelmann P, Rohne P (1989) Handbuch der elektrischen Raumheizung. Hüthig Buch Verlag GmbH, Heidelberg
13. Moditz H (1975) Elektrische Raumheizung. Springer, Wien – New York
14. Ochs F, Heidemann W, Müller-Steinhagen H, Koch H, Lichtenfels A (2007) Heißwasser-Erdbecken-Wärmespeicher mit freitragender Abdeckung für solare Nahwärmesysteme. ITW Stuttgart, Pfeil und Koch Ingenieurgesellschaft, DLR Stuttgart, Ingenieurbüro Lichtenfels, Keltern
15. http://www.abwaermeatlas-sachsen.de
16. Verein Deutscher Ingenieure (1994) Energiespeicher – Energiespeicher – VDI Berichte 1168, 3-18-091168-9
17. Stieglitz R, Heinzel V (2012) Thermische Solarenergie. Springer, Berlin Heidelberg https://doi.org/10.1007/978-3-642-29475-4_8
18. Friedrich U (2007) Aquifer speichert Überschusswärme aus Heizkraftwerk. BINE Informationsdienst. FIZ, Karlsruhe, Eggenstein-Leopoldshafen
19. Friedrich U (2003) Aquifer für das Reichstagsgebäude. BINE Informationsdienst. FIZ, Karlsruhe, Eggenstein-Leopoldshafen
20. Ochs F, Heidemann W, Müller-Steinhagen H (2007) Langzeit-Wärmespeicher für solare unterstützte Nahwärmesysteme. ITW Stuttgart
21. Ochs F, Heidemann W, Müller-Steinhagen H, Koch H (2006) Erdreich/Wasser-Erdbecken-Wärmespeicher mit direktem Beladesystem. ITW Stuttgart, DLR Stuttgart, Pfeil und Koch Ingenieurgesellschaft, Stuttgart
22. Schneider B (2009) Schulsanierung mit solarer Nahwärme verknüpft. BINE Informationsdienst. FIZ, Karlsruhe, Eggenstein- Leopoldshafen
23. Mehling H (2008) Heat and Cold storage with PCM. Springer, Berlin Heidelberg
24. Mehling H (2001) Latentwärmespeicherung: „Neue Materialien und Materialkonzepte". b ZAE Bayern Abteilung Energieumwandlung und -speicherung, Garching
25. Scheffknecht G (1988) Ein Beitrag zur Dynamik des Latentwärmespeichers. VDI Verlag GmbH, Düsseldorf
26. Ebert H-P (2006) FORSCHUNGSNETZWERK LWSNet: GRUNDLAGENASPEKTE IN DER AKTUELLEN PCM-FORSCHUNG. Bayrisches Zentrum für Angewandte Energieforschung e.V., p 167
27. http://www.zae.uni-wuerzburg.de/files/pcm_thist.pdf (1 Apr 2013)
28. Meinert J Zellulare Metalle und Verbundwerkstoffe zur Optimierung des Be- und Entladeverhaltens thermischer Energiespeicher, Fraunhofer-Institut
29. http://www.eor.de/fileadmin/eor/docs/aktivitaeten/asue_eor_14_02_2006/Unterlagen/01_ASUE_PCM-Grundlagen+Wirtschaftlichkeit-A4.pdf (30 June 2013)
30. L8 Paksoy H (2007) Thermal Energy storage for Sustainable Energy Consumption: Fundamentals, Case Studies and Design, Springer Verlag, ISBN 978-1402052880

31. Zalba B, Marin JM, Cabeza LF, Mehling H (2002) Review on thermal energy storage with phase change: materials, heat transfer analysis and applications In. Appl Therm Eng 23:251–283
32. Acem Z, Lopez J, Del Barrio EP (2010) KNO3/NaNO3 – Graphite materials for thermal energy storage at high temperature: Part I. – Elaboration methods and thermal properties In. Appl Therm Eng 30:1580–1585
33. Gschwander S, Schossig P (2006) Phase Change Slurries as heat storage material for cooling applications In Ecostock – 10th International Conference on Thermal Energy storage
34. Günther E, Mehling H, Hiebler S (2007) Modeling of subcooling and solidification of phase change materials. Model Simul Mater Sci Eng 15:879–892. https://doi.org/10.1088/0965-0393/15/8/005
35. Alkan C, Günther E, Himpel M, Hiebler S (2012) Complexing Blends of Polyacrylic acid-Polyethylene glycol and Poly(ethylene-co-acrylic acid)-Polyethylene glycol as Shape Stabilised Phase Change Materials. Energy Convers Manag J 64:364–370
36. Entwicklung neuartiger PCM, formstabiler PCM und PCM-Verbundmaterialien mit verbesserter Wärmeleitfähigkeit (ENFoVerM), Projekt wird gefördert vom Bundesministerium für Wirtschaft und Technologie (BMWi) unter FKZ 0327851D, 2009–2013
37. Whitman CA, Johnson MB (2012) White, Mary Anne; Characterization of thermal performance of a solid–solid phase change material, di- n -hexylammonium bromide, for potenzial integration in building materials. Thermochim Acta 531:54–59. https://doi.org/10.1016/j.tca.2011.12.024
38. Hauer Vorlage
39. Thermische Energiespeicher zur Effizienten Nutzung erneuerbarer Energien/Überschusswärme und ihre Umsetzung in Thüringen, LEG Thüringen mbH, Abteilung Akquisition, Technologie und internationale Kontakte, Bereich Technologiemanagement
40. BINE Projektinfo 02/01
41. Bayerisches Landesamt für Umwelt (LfU)
42. Schumann K, Brandt A, Unger B, Scheffler F (2011) Bindemittelfreie zeolithische Molekularsiebe der Typen LTA und FAU. Chem Ing Tech 83(12):2237–2243
43. Henninger S, Schmidt F, Henning H-M (2010) Water adsorption characteristics of novel materials for heat transformation applications. Appl Therm Eng 30(13):1692–1702
44. Jänchen J, Ackermann D, Weiler E, Stach H, Brösicke W (2005) Calorimetric investigation on zeolites, AlPO4's and CaCl2 impregnated attapulgite for thermochemical storage of heat. Thermochim Acta 434(1):37–41
45. Gordeeva LG, Aristov YI (2012) Composites 'salt inside porous matrix' for adsorption heat transformation: a current state-of-the-art and new trends, International Journal of Low- Carbon Technologies
46. van Essen VM, Zondag HA, Gores JC, Bleijendaal LPJ, Bakker M, Schuitema R, van Helden WGJ, He Z, Rindt CCM (2009) Characterization of MgSO[sub 4] Hydrate for Thermochemical Seasonal Heat Storage. J Sol Energy Eng Asme 131(4):41014–42009
47. Kato Y, Takahashi R, Sekiguchi T, Ryu J (2009) Study on medium-temperature chemical heat storage using mixed hydroxides. Int J Refrig 32(4):661–666
48. Krönauer A, Lävemann E, Hauer A (2012) Mobile Sorption Heat Storage in Industrial Waste Heat Recovery. 12th International Conference on Energy storage. Lleida, Spain (16.-18.05.)
49. Beek TJJ van, Rindt CCM, Zondag HA (2012) Performance analysis of an atmospheric packed bed thermo-chemical heat storage system. Proceedings of the 12th International conference on Energy storage (Innostock 2012), 16–18 May 2012, Lleida, Spain
50. Bauer T, Steinmann W-D, Laing D, Tamme R Thermal energy storage materials and systems Annual Review of Heat Transfer, Chapter 5, S 131–177
51. Beckmann G, Gilli PV (1984) Thermal Energy Storage: Basics, Design, Applications to Power Generation and Heat Supply. Springer
52. Cabeza LF (ed) (2015) Advances in thermal energy storage systems. Methods and applications. Woodhead Publishing Series in Energy vol 66. Elsevier, Amsterdam
53. Laing D, Zunft S Using concrete and other solid storage media in thermal energy storage (TES) systems Advances in Thermal Energy Storage Systems – Methods and Applications, S 65–86
54. Steinmann WD, Eck M Buffer storage for direct steam generation Solar Energy, Bd 80, S 1277–1282

# Load Management as an Energy Storage System

*Ingo Stadler and Fabian Eckert*

**11.1 Special Characteristics of Demand Response Compared to Other Energy Storage Systems – 615**

**11.2 Demand Response in Households and Cross-Application Technologies – 616**
11.2.1 Storage Heaters – 616
11.2.2 Electric Hot Water Supply – 618
11.2.3 Electric Cooling – 620
11.2.4 Heating Circulation Pumps – 623
11.2.5 Ventilation Facilities – 624
11.2.6 Washing Machines, Clothes Dryers, and Dishwashers – 625

**11.3 Industrial Applications of Demand Response – 626**

**11.4 Summary of German and European Demand Response Potential – 630**
11.4.1 Demand Response Potential in Germany – 630
11.4.2 Demand Response Potential in Europe – 630
11.4.3 Comparison of Various DSM Studies – 631

**11.5 Developments and Trends – 632**
11.5.1 Load Shedding Utilization in Industry – 632
11.5.2 Future Technical and Economic Potential – 632
11.5.3 Guaranteed Capacity and Renewable Energy Integration – 633
11.5.4 Potential to Reduce Network Expansion and Annual Peak-Load – 634

**Electronic supplementary material** The online version of this chapter (https://doi.org/10.1007/978-3-662-55504-0_11) contains supplementary material, which is available to authorized users.

© Springer-Verlag GmbH Germany, part of Springer Nature 2019
M. Sterner, I. Stadler (Eds.), *Handbook of Energy Storage*, https://doi.org/10.1007/978-3-662-55504-0_11

11.6 Summary – 634

References – 635

## Overview

► Chapters 6 to 9 focused on storage systems that store electric energy in a range of forms, and then release the energy again as electric energy. ► Chapter 10 discussed the use of thermal-energy storage (TES) systems for thermal management.

This chapter examines management methods. These methods use processes that typically convert electric energy into another form of final energy that can also be stored. This form of energy is often thermal energy. But unlike with the systems discussed in previous chapters, here the energy stored is not converted back into electricity. Instead, the energy is used and stored in the same form.

From the point of view of the energy supply system, these management methods perform exactly the same function as energy storage systems. This chapter discusses load-management in general, then potential uses of load-management, and finally, current trends.

Scientists use a wide variety of terms to describe methods for managing energy requirements. These include load-management, demand-side management (DSM), demand response, and demand-side bidding. There is currently no general or consistent definition.

The International Energy Agency's (IEA) report, 'Implementing Agreement on Demand-Side Management Technologies and Programmes', uses the two terms DSM und demand-side bidding. DSM is defined as actions that affect energy efficiency in general, and change energy consumption over the long-term.

By contrast, demand-side bidding is defined as a process that affects the short-term flexibility of electricity consumers, and as a result, actively helps balance electricity generation and consumption. Individual demand-side bidding actions which increases load flexibility are categorized under the more general term of demand response. This means that demand response is the more precise term. The German definition for the term 'load-management' covers actions that fall under the definition of demand response in English.

### Why Discuss Demand Response in a Book About Energy Storage?

Energy storage systems decouple electricity production (or the production of other energy sources) from electricity demand (or from other types of energy demand). But with electric energy supply, decoupling cannot be achieved by storing electricity alone.

**Shifting electricity demand to times when electricity is generated by wind or solar power, for example, serves exactly the same purpose as energy storage.**

As a result, an analysis of demand response belongs in a book about energy storage. Discussions of load shifting often focus on shifting the use of applications such as washing machines, dryers, or dishwashers to a different time. But load shifting in households requires consumer co-operation, making it an exception. In addition, no energy storage is involved here (unless people waiting longer for their clean laundry, for example, is considered a form of storage).

Most load shifting processes include energy storage, even if no electric-energy storage is used. Consumers convert electricity into various forms of final energy—frequently heat or cold—which are in fact easier and cheaper to store than electricity. For example, a refrigerator stores thermal energy and remains cold even if the electricity is turned off. This means that it makes no difference from the user's perspective when precisely the refrigerator consumes electric power to generate cold. This is the other reason why demand response belongs in a book about energy storage:

**Most load shifting processes store final energy that is not reconverted back into electricity, but is instead used in that same form at a later time.**

Demand response is a logical consequence of renewable energy supply within an energy

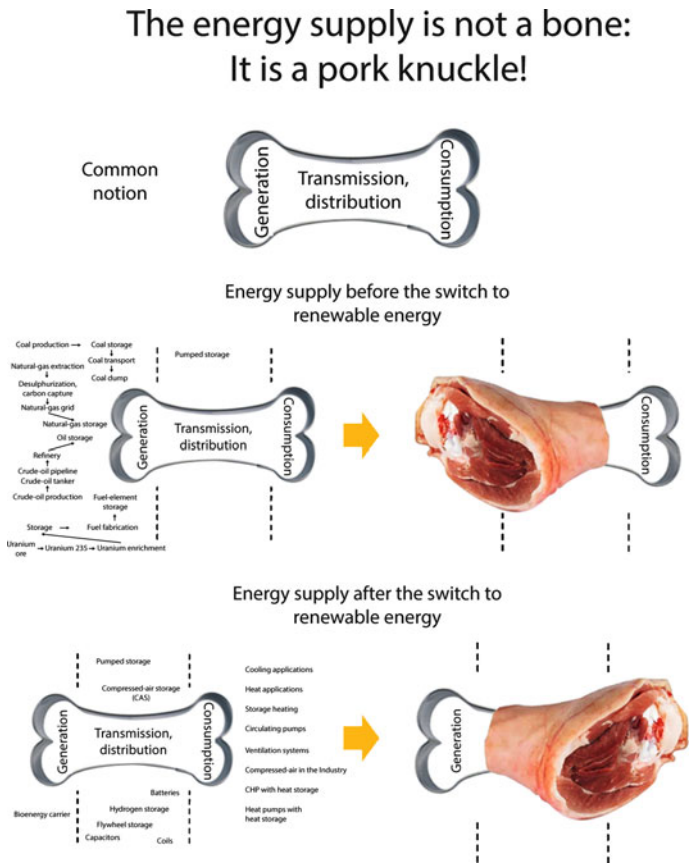



**Fig. 11.1** The conversion from supply-side management to DSM

supply system dominated by fossil and nuclear energy sources. This phenomenon is metaphorically illustrated in Fig. 11.1.

It is often wrongly assumed that non-renewable electricity supply requires no energy storage (apart from a few pumped-storage power plants). This would mean that electricity would always be generated 'just in time' to meet demand (see the bone in Fig. 11.1, below). In reality, the energy supply system is not initiated by power plants. The energy supply system also includes logistical operations worldwide that supply the power plants. These operations in turn require a range of storage processes (▶ Chap. 1).

Coal does not just fall into a power plant straight out of the mine. For example, hard coal is mined in Australia and then stored in coal stockpiles on freighter ships at the Rotterdam harbor, then later stored on inland ships. Following that the coal is stored in coal stockpiles at the power plant before finally being used to produce electricity 'just in time'. Similar processes are used in Russia to store extracted natural gas until the gas finally reaches underground salt caverns in Germany for storage. It is then (much later) converted into electricity (and heat) in a gas power plant 'just in time'.

Nuclear energy is a special case. Between the time uranium ore is mined in Canada and used in German nuclear power plants, for example, many temporary storage processes are used. But the case of nuclear energy is unique, because nuclear fuel must also be stored as radioactive waste for many years after it stops producing electricity.

Metaphorically speaking then, energy supply is more like a knuckle of pork than a bone. The meat on the knuckle is stored energy. In an energy system based on fossil and nuclear en-

ergies, the meat (the stored energy) is on the left side, meaning previous to electricity generation.

Renewable energy supply largely eliminates this kind of storage. Wind and sunshine cannot be stored before use to generate electricity. The only renewable energy sources that can be handled like fossil energy sources are bioenergy and storage water. These two sources of electricity supply can be stored before they are used to generate electricity. Otherwise, renewable energy must be stored as secondary energy. ▶ Chapters 6 to 10 describe these processes in detail. Typically the energy stored here is converted back into electricity at a later time (incurring conversion losses).

An alternative would be to reverse the existing system. The knuckle of pork would then be turned so that the meat (the stored energy) is on the right side of the system, meaning after electricity has been consumed. Here, the energy is stored after the electricity has been consumed. This means that final energy is stored. This has the advantage of eliminating the conversion process at the end, together with the conversion losses. This is what occurs with demand response. This chapter describes these energy storage processes in detail.

## 11.1 Special Characteristics of Demand Response Compared to Other Energy Storage Systems

### ■ Investment Costs

The most significant advantage of demand response in comparison to other energy storage systems is the lower storage capacity investment costs. In fact, there are no costs. This is because demand response only uses preexisting processes. For example, cold storage is not built for the purpose of storing energy. It is built to store perishable goods. But by chance, cold storage has a thermal storage capacity that permits it to run more electrically powered refrigeration units when there are surpluses of electricity from wind and Sun.

But demand response still involves costs. These costs just do not apply to the storage capacity itself.

### ■ Communication Technology Integration

There are a large number of energy storage systems like these that could help support the integration of renewable energy. But this requires communicating when they should provide that capacity and for how long, as well as whether they should charge or discharge. So although there are countless existing storage systems of this type and no investments in storage capacity is required, communication technology must be installed to integrate these storage systems into energy supply management.

A key factor for demand response then is the increasing number of energy service providers who bill their customers by remotely reading energy meters. In the future, all households will be networked by communication technology in this way. This is precisely what is required for successfully implementing demand response. The Italian energy supplier ENEL is a pioneer in this area. In Italy, 30 million conventional electricity meters have been replaced by remotely readable electronic meters. Besides reducing administrative costs, these meters are used to limit capacity during peak-load times, simplify tariff or provider changes, and remotely turn off power for unpaid accounts. This means that, like these unpaid accounts, the storage systems described in this chapter could be turned on and off remotely using the same system.

### ■ Households vs. the Industrial Sector

There is enormous potential for load shifting in all electricity application areas. But exploiting this potential may make more sense in some areas than in others.

Industrial applications are frequently favored over households, for example, because the load shifting capacities there are much greater. Since communication technology must be installed in both cases and the costs are roughly

the same, industrial processes are clearly a better choice. But it must also be taken into account that not all industrial processes can be used as energy storage processes. This means that determining the economic advantages of industrial processes also requires considering the resulting costs of halting production.

Another factor is the absolute potential. The potential per facility and per property is significantly higher with industrial applications. But since there are a very large number of households, in households the absolute total potential is significantly higher. In other words, the connected electric load of a cold storage facility is many times higher than that of a refrigerator. But there are so many refrigerators in use that the total potential of all private refrigerators far exceeds the potential of all cold storage facilities.

### ▪ The Capacity-Time Dilemma

In comparison to other energy storage systems, demand response has impressive potential. The available capacity is so high that no other storage would be required in demand response time periods. This means that the only limiting factors are the time periods. Most processes allow shifting across time periods, ranging from minutes to a few hours. Practically none of these processes allow shifting for longer than a day, and then only by using additional thermal storage, for example.

The following section discusses the potential in households together with cross-application technologies used in many buildings.

## 11.2 Demand Response in Households and Cross-Application Technologies

### 11.2.1 Storage Heaters

Night storage heaters were already integrated into the electric energy supply system long before the recent enormous increase in renewable energy generation. They were developed in the 1960s to increase utilization and efficiency with power plants that are difficult to regulate. This shows that, in terms of their capability to cover an electric load profile, nuclear plants, lignite coal plants, and wind power facilities all share the same characteristics. They cannot be regulated to suit a particular load profile, or can be but only with difficulty. Storage heaters can be used to balance generation and demand in these cases.

Night storage heaters absorb electric energy during low-load times, convert it into heat, and store it in their core. The heater then releases the heat into the room gradually over the rest of the day. Night storage heaters are individual space heaters. This means that heating an entire apartment with storage heaters requires a heater in each room.

In terms of primary energy use and ecological efficiency, the use of electric energy for heating purposes is a poor choice. But this is only if the electricity is generated in condensation power plants by firing coal. If surplus electricity generated by renewable energy sources is stored in storage heaters, then using electricity for heating is a good choice. By integrating large quantities of renewable energy into the supply network, storage heaters could be extremely useful.

Since electric storage heaters are widespread, have a large storage potential, and cannot be conveniently converted to warm water heating for example, these heaters will remain in use for a long time to come. But instead of only being charged at night, now they can be charged whenever there are wind power or solar electricity surpluses.

There are three types of electric room heaters: direct heaters, storage heaters, and heat pumps. Only storage heaters can be used for demand response (with technical modifications, for example, hot-water storage). Storage heaters include storage heater appliances, underfloor storage heaters, and central heating. Most are storage heater appliances (> 95%) [2].

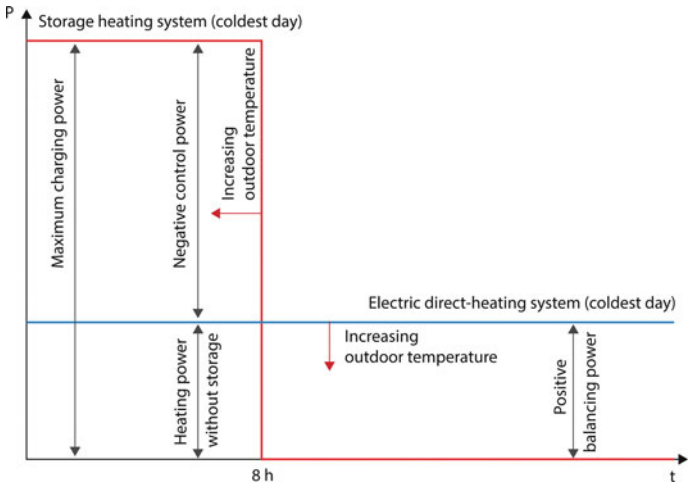



**Fig. 11.2** Positive and negative balancing energy supplied by storage heaters

In 1996, 2.5 million night storage heaters were in use across Germany [3]. Most of these (2.37 million) were in households. About 8% of households in the former West Germany and 3% of households in the former East Germany used night storage heating [4]. In total, storage heaters consumed close to 27 TW h of electricity in 1996 [3]. The installed capacity rose from about 10 GW in 1970 to nearly 40 GW in 1995. By incentivizing the use night storage heaters, energy supply companies succeeded in balancing the load profile to a significant extent. But over the last 40 years, the load profile in summer months has remained essentially the same.

This means that about 27 TW h of electricity-shifting potential was stored in storage heaters and then released over a longer period in the form of heat. In comparison, the electricity generated by pumped water in all the pumped-storage power plants without natural intake in Germany amounted to only 3.7 TW h in 1996. As a result, storage heaters stored more than seven times the amount of electricity than pumped-storage power plants.

Since pumped-storage power plant utilization is limited when compared to storage heaters, the efficiency of pumped-storage facilities is also about 70% lower. The efficiency of storage heaters can approach 100% when the storage heaters are not overloaded so that they overheat the space. When storage heaters are correctly managed, the statistical self-discharge of the storage heaters is released as useful heat. As a result, it does not reduce the efficiency. Storage heaters are discussed in detail in ▶ Chap. 10.

Figure 11.2 shows that storage heaters support positive and negative load balancing, or supply positive and negative balancing energy. Storage heaters should be compared with direct electric heating, i.e., with heating that uses the same 'fuel' but does not store thermal energy. The blue line in Fig. 11.2 indicates the constant power consumption of direct heating in relation to the outside temperature. It increases as the outside temperature falls. The red line indicates the power consumption of storage heaters.

The demand response potential of storage heaters can be calculated using the installed storage heater capacity data in Germany, and by using research determining how they are operated. The negative balancing energy that can be supplied by a storage heater is equal to the connection capacity of the storage heater minus the power consumption of a direct heater [1].

Discharging storage heaters without consuming electricity is equivalent to saving electricity by not using direct electric heating. As a result, the energy level of an assumed direct heater is exactly equal to the positive balancing energy supplied by a storage heater.

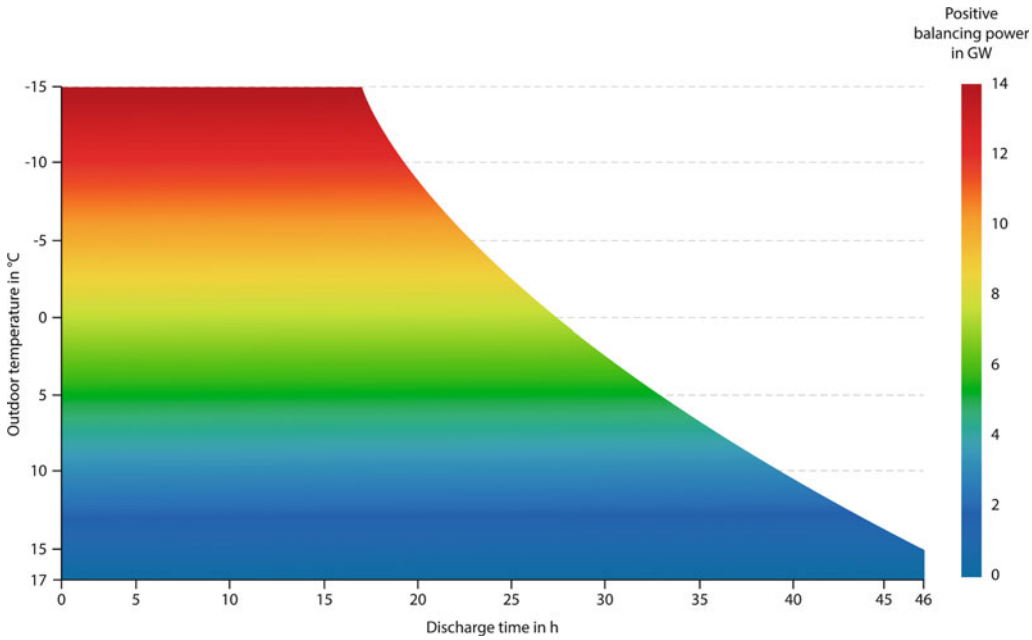



**Fig. 11.3** Positive balancing energy determined by the energy level and duration of installed storage heating in Germany and compared to outside temperature

11

In Germany, the amount of positive balancing energy supplied during peak times is 14 GW (Fig. 11.3). This means that the positive balancing energy is at its highest point when the outside temperature is lowest. It falls steadily until the temperature rises up to where no room heating is required. The negative balancing energy potential is discussed in [1].

### 11.2.2 Electric Hot Water Supply

Just as storage heaters provide room heating using electricity, electric hot water supply uses electricity to heat cold water for bathing, showering, hand washing, dish washing, etc. Similar to electric storage heaters, electric hot water appliances can also be used to shift electric load, increasing the cost-efficiency of network or power plant operation.

If the electric hot water supply appliance has integrated storage, the storage is charged during low load times (especially during the night) to compensate for the decrease in load. Appliances without storage still function to balance the load. This is because hot water demand-peaks (mornings, evening, and weekends) are at different times than load peaks in the industrial sector. But appliances without storage cannot be used for active demand response.

Unlike hot water supply using gas, oil, or district heating, the advantage of electric hot water supply is that it distributes electric energy in the building virtually without losses, and generates heat directly at the location where it is consumed. This means that long hot water pipes or circulation pipes that result in high losses are not required. Electric resistance heaters convert close to 100% of the electric energy used into heat. But when upstream losses incurred by electricity generation in power plants is taken into account, the primary energy consumption is significantly higher. Depending on the length of the transport pipes, hot water heaters are still quite efficient in terms of primary energy.

There are a wide range of processes used to heat water with electricity. As a result, not all hot water supply appliances are suited for use with demand response. Appliances not connected to the water supply include immersion heaters, kettles, and coffee machines. They are only used exactly when the hot water is required. They have no storage capacity, and so cannot be used for demand response.

There are three groups of appliances connected to the water supply: boilers, continuous-flow heaters, and storage facilities. Boilers heat water once. Each time hot water is required, the appliance must be turned on again. The water is usually supplied right after it is heated. Boilers are called open appliances and are constantly filled with water. When cold water flows in, hot water is pressed out through an overflow pipe. Boilers used to be uninsulated. Today, boilers are insulated and usually custom-made for the application required. Boilers have limited uses with demand response. Boiling water appliances typically installed in kitchens are also a kind of boiler. They generally have a volume of five liters, or in special cases, up to 50 liters. They are also not suitable for demand response [5].

Continuous-flow heaters are compact and sealed hot water appliances with very high heating powers ranging from 12 to 27 kW. They can supply hot water to one or several taps. Their very high powers allow the water to be adequately heated as it flows through the appliance, eliminating the need for storage. Although there are many continuous-flow heater types, none of them can be used for demand response because they do not include storage [5].

Hot-water storage facilities are hot water appliances that use electric resistance heating to heat cold water. The hot water can then be stored by the appliance in a thermally-insulated container over long periods with only negligible losses. Storage volumes here typically range from five to 1,000 liters. Losses fall as the storage content increases and the ratio of surface area to volume changes. Because of these losses and the long storage intervals, only large storage facilities of this type are suitable for demand response [5].

In an efficiency analysis of electric hot water supply in households, a European Commission SAVE project estimated the total number of appliances in several member states. According to the study, electricity consumption in Europe for electric hot water supply was about 87 TW h (based on 1997 data). Electricity consumption for electric hot water supply amounted to about 15% of household consumption in the European Union (EU) [5].

In Germany, the study determined that hot water was produced using electricity in 15.2 million of a total of 34.6 million households. This is equivalent to 43.9%. About a third of all hot water appliances installed in Europe are located in Germany. Process heat consumption in households amounted to 123 TW h in 2003 [8]. About 49 TW h of this heat was produced using electricity. This includes consumption for electric cooking, hot water supply, and other electric appliances. The study determined that hot water supply amounts to 15 TW h of the total [8–10].

In the trade, industry, and services (TIS) sector, electricity consumption for process heat was 32.5 TW h. Here, 40% of the process heat was used for hot water supply [7]. This is equivalent to a consumption of 13 TW h. This means that, in total, Germany consumes 28 TW h of electricity for electric hot water supply.

But Germany is an exception in terms of how water is supplied. In Europe, central hot water supply is standard, but in Germany only 4 million of over 15 million households have central electric hot water supply [6]. Assuming that a fourth of the electricity consumed for hot water supply can be used for demand response, 7 TW h is then available for load shifting each year.

Figure 11.4 illustrates the operating principle of demand response with electric hot water appliances. The horizontal line indicates the electric power consumption of the many uncoordinated storage appliances. Since only the energy consumption of storage appliances is considered here, the consumption can be repre-

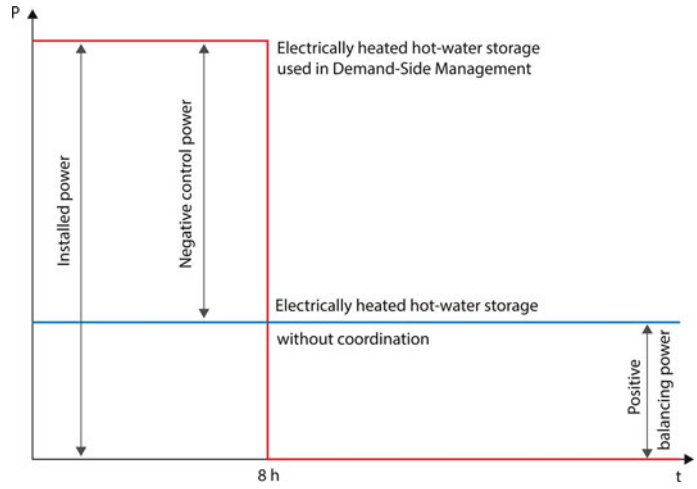



**Fig. 11.4** How hot-water storage appliances integrated into demand response provide balancing energy

sented as linear. If continuous-flow heaters are included as well, then fluctuating consumption over the day must be taken into account.

Hot water appliances with empty storage that have been integrated into demand response can be charged with electric power when required, providing negative balancing energy. If the storage is full, no electric power is consumed. Instead, the average power consumption of the uncoordinated storage appliances is used to provide positive balancing energy.

The size of the freestanding tank used is determined by the maximum daily demand for hot water. This means that the electric power consumption can be shifted 24 hours or longer when daily consumption is lower than the maximum. The total storage capacity of hot-water storage appliances suitable for demand response amounts to about 44 GW h, with a maximum positive balancing energy of 800 MW [1].

Electrically powered hot-water storage appliances can provide negative balancing energy when the storage is not fully charged. Here, water is heated using electric energy and then stored. Since these appliances are designed for use during low tariff times, their storage can be completely charged within eight hours. The resulting negative balancing energy supplied adds up to about 5 GW [1].

### 11.2.3 Electric Cooling

Technical generation of cold is essential in many areas of daily life. Cold is produced in private households in refrigerators and freezers. It is also required across the entire food supply chain, from producing, to distribution, to storage in refrigerators. In addition, cold is critical in many industries, especially in the chemical industry. Cold is also increasingly required to air-condition buildings.

Because refrigerated or frozen goods have a thermal capacity, storage capacity is an inherent feature of almost all cold applications. This storage capacity means cold applications are extremely well-suited for use with demand response. This is because refrigerators can be shut off for a certain period of time without allowing the temperature of the cooled medium to rise above permitted levels.

A recent study [11] determined that the total energy demand for technical cold generation in 1999 was 77,000 GW h. Of this total demand, 66,000 GW h was met with electricity, and 11,000 GW h without electricity. Cold generation therefore accounts for 14% of total electricity demand. Table 11.1 shows how the energy demand for technical cold generation in Germany is distributed.

**Table 11.1** Energy demand for technical cold generation in Germany [11]

| | Total energy demand in GW h/a | | | Primary energy in GW h/a | Total cold in GW h/a |
|---|---|---|---|---|---|
| | Electric | Not electric | Total | | |
| Food | 48,050 | 3,071 | 51,121 | 153,909 | 108,058 |
| Industrial cold | 6,845 | 0 | 6,845 | 20,795 | 5,255 |
| Air-conditioning | 9,705 | 7,776 | 17,481 | 50,349 | 48,548 |
| Other | 1,579 | 65 | 1,644 | 4,981 | 3,066 |
| **Total** | **66,179** | **10,912** | **77,091** | **230,034** | **164,927** |

**Table 11.2** Use of cold in the food supply area [11]

| | Total energy demand in GW h/a | | | Primary energy in GW h/a | Total cold in GW h/a |
|---|---|---|---|---|---|
| | Electric | Not electric | Total | | |
| Production | 19,616 | 0 | 19,616 | 59,436 | 54,929 |
| Transport | 0 | 3,071 | 3,071 | 8,316 | 7,751 |
| Distribution | 9,805 | 0 | 9,805 | 29,708 | 19,146 |
| Households | 18,630 | 0 | 18,630 | 56,449 | 26,232 |
| **Total** | **48,050** | **3,071** | **51,121** | **153,909** | **108,058** |

The food refrigeration area includes the production, transport, distribution, storage, sale, and home refrigeration of foodstuffs. The results of the study on the use of cold to refrigerate food shows that the greatest energy consumption is concentrated at the beginning and end of the food supply chain, i.e., for food production in small or large industrial facilities and for home refrigeration. The consumption is about the same in these two areas in terms of both total energy and primary energy consumption. The second largest area of consumption is distribution and storage. This area consumes about half the combined energy of the two areas at the ends of the food supply chain. Energy consumption for producing cold is lowest in the area of food transport (Table 11.2).

Cold required to produce food is not considered here for use with demand response, although the large amount of electricity consumed in this area would appear to make it an attractive option. This is because some processes in this area have very narrow timeframes—for example, milk must be cooled from 35 to 5 °C within three hours after the milking process. But some food production processes may still be suited for use with demand response.

All commercial uses of cold are included under the categories of distribution and storage. Although supermarkets dominate here, a range of other commercial uses of cold account for close to 10 GW h of the total (Table 11.3).

Cooling and freezing appliances in the household cooling area account for 18.6 TW h. Compared to estimates found in other sources, the estimate here is low. In another source, total electricity consumption for refrigerators and freezers in private households is estimated at a 25.6 TW h [12]. In a third source, (see [13] referring to [14, 15]) electricity consumption in this area is estimated at 83 PJ (23 TW h).

**Table 11.3** The use of cold in food distribution and storage [11]

| Food distribution and storage | Total energy demand in GW h/a | Primary energy demand in GW h/a | Total cold demand in GW h/a |
|---|---|---|---|
| Supermarkets | 6,294 | 19,071 | 13,182 |
| Restaurants | 984 | 2,981 | 1,801 |
| Ice-cream shops | 118 | 358 | 173 |
| Snack bars | 198 | 600 | 322 |
| Cafeterias | 248 | 752 | 399 |
| Hotels | 375 | 1,136 | 725 |
| Youth hostels | 001 | 3 | 2 |
| Beverage retail | 351 | 1,065 | 497 |
| Pharmacies | 33 | 99 | 49 |
| Gas stations | 498 | 1,510 | 675 |
| Cold storage facilities | 704 | 2,133 | 1,321 |
| **Total** | **9,805** | **29,708** | **19,146** |



The previous section focused exclusively on food cooling, which accounts for just 73% of the electricity used for cooling. Within the food area, only the areas of food retail and private households were included. This excludes the area of food production, which accounts for 41% of the food area. In addition, air-conditioning, the food industry, and other areas offer some potential for demand response.

Household cooling appliances include a housing, a component for containing the coolant, and a cooling unit. These appliances are categorized by their temperature ranges as refrigerators (+5 °C), freezers (−18 °C), or combined refrigerator/freezers (between +5 °C and −18 °C). Freezers are better insulated than refrigerators and typically have an electric heater or a high-pressure pipe in the coolant circuit to prevent the door seal from freezing shut. In combination refrigerator/freezers, heat at two different temperature-levels is removed.

Depending on where they are installed, household cooling appliances are classified among several climate ranges [17]. Depending on the ambient temperature, the cooling load of appliances in the climate range SN ranges from 18 to 100%. This means that these refrigerators generally operate with partial-loads [16]. Since these conditions require refrigerators to have oversized capacities, they can be used for demand response.

A refrigerator's warming behavior and, as a result, its storage capacity is largely determined by its content. This is because modern refrigerators have basically no thermal capacity. Studies have shown that an empty refrigerator warms to indoor temperatures approximating ambient temperatures just 20 minutes after being shut off. Refrigerators with integrated phase-change materials (PCM) designed to bridge compressor shut-off periods of several days are manufactured as niche products [18–23].

The following discussion assumes a temperature range from +2 °C to +7 °C. It should be noted that increasing the permitted temperature to +10 °C nearly doubles the shut-off times.

In addition to the numerically determined relationship between the shut-off time and the refrigerator's filling level, the positive balanc-

ing energy is also determined by the length of time it is available. The resulting positive balancing energy is about 1.5 GW. The maximum negative balancing energy would result if the temperature of the refrigerated items in all refrigerators is +7 °C, and all refrigerators turn on their compressors at the same time. This capacity amounts to about 4.3 GW.

Other cooling appliances used in private households are freezer compartments and freezer chests. Compared to refrigerators, the storage times are significantly shorter here. There are two reasons for this. One reason is that the temperature difference between the freezer and the ambient temperature is significantly higher. This means that the quantity of heat input into the freezer is larger. The second reason is that the thermal capacity of water is reduced by about half when it is frozen into ice. This drop in thermal capacity is about the same with foodstuffs. The following discussion assumes a temperature range from −18 °C to −12 °C. The positive balancing energy here amounts to around 1.4 GW [1].

In addition to refrigerators and freezers in private households, another group of cold applications that may have potential is refrigerators and freezers used in food retail. Supermarkets are a particularly relevant category in this group. This is because the largest portion of their energy consumption by far (73%) is used to technically generate cold [24].

An extremely wide variety of cooling appliances are used in supermarkets. These include refrigerated cases, refrigerated shelves, freezer islands, freezer compartments, refrigerated rooms, and freezer rooms. These appliances also fall into two categories: plug-in units and racks of refrigerator or freezer appliances. With plug-in appliances, the refrigeration units are integrated into the appliance. With racks, several cooling appliances are cooled using a coolant circuit connected to a centrally located compressor.

Using the same method of calculation as was applied above with refrigerators and freezers in households, the positive balancing energy of cooling appliances in food retail amounts to 1.1 GW. The negative balancing energy is 2.8 GW [1].

### 11.2.4 Heating Circulation Pumps

Unlike electric storage heaters, hot water heating facilities have no storage unit. In addition, they do not use electricity to produce heat. The heat is generally produced by burning natural gas or oil, or brought into the building from a district heating system.

Despite this, hot water heaters can be used for demand response. Buildings heated by hot water heating have thermal capacity, i.e., heat stored in the building structure. When the heating is shut off, the room temperature does not immediately drop. Instead, temperatures remain comfortable without any heating supply over a specific period of time determined by the building standard. Figure 11.5 shows the relationship between room cooling and wall construction.

Since the heat is generated from natural gas and oil, the electric energy that can be used for demand response is limited to the auxiliary energy. This energy is used to transport the heat from the boiler where it is produced (or from the transfer station if district heating is used) to where the heat is released in the rooms by radiators or underfloor heating. Electric energy is used to power circulation pumps that pump hot water through the heating circuit, distributing the water.

Since with hot water heating (the most common form of heating in Germany) only the auxiliary energy can be used for demand response, it may at first seem that the amount of energy involved is negligible. But actually, circulation pumps are among the largest consumers of electricity in private households. In Germany, circulation pumps consume about 15 TW h of electricity, or 3.5% of Germany's total consumption. This means that circulation pumps in total consume the same amount of electricity as the German railway together with all of the nation's trams [25].

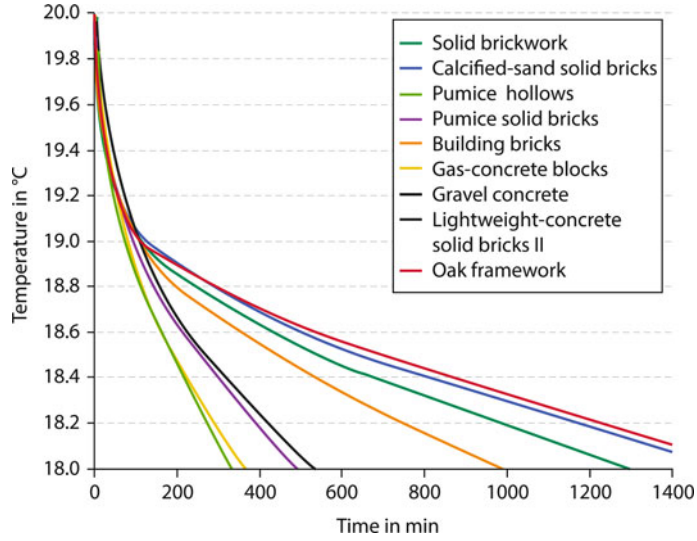



**Fig. 11.5** Room temperature curves with nine different wall types and 12 cm mineral wool insulation, assuming a fixed temperature curve in the wall, an outside temperature of 0 °C, and an indoor temperature of 20 °C

The capacity available for demand response is entirely determined by the circulation pumps, but the duration that the capacity is available is determined by the structure of the building and its storage capacity.

Modern hot water heating is typically regulated by a method based on a heat curve. The heat curve determines the set point of the flow temperature, and as a result, the heating capacity in relation to outside temperature – assuming the heating medium flow is constant.

This means that with normal operation in a heated room, the network curve is constant if the room temperature is constant. The flow through the radiators does not change, even if the outside temperature changes. The heating capacity is adjusted as required by changing the hot water temperature. As a result, with normal operation, a radiator's operating point remains constant. The thermostat reduces the inlet pipe diameter only when changes occur that cannot be detected by the outdoor temperature sensor (heat input by solar radiation or increased interior heating loads). The result is a steeper network curve. An unregulated pump reduces the flow, but increases the fall in pressure. A variable speed pump that maintains a constant pressure difference $\Delta p$, for example, would in this case reduce the flow without increasing the pressure. This reduces the pump's power consumption.

To determine the potential of hot water heating for demand response, the following factors must be taken into account: the annual electric energy consumption by circulation pumps in Germany, the number of circulation pumps in operation in Germany or the level of installed capacity, and the duration of time that circulation pumps are in operation. Combined with the annual load curve of the outside temperature, the heating duration in relation to the heating threshold temperature can then be determined. During a heating season, this results in a positive balancing energy of 2.3 GW over the period of time determined by the thermal insulation.

Circulation pumps can only provide positive balancing energy. Either the heating facility is in operation together with the circulation pump, and the circulation pump can be shut off for a certain period of time, or the heating facility is shut off and it makes no sense to activate the pump for demand response if no heating is supplied.

### 11.2.5 Ventilation Facilities

Ventilation facilities create or maintain air conditions in a room or a building that ensure peo-

ple's comfort or are critical for production processes. The criteria for these requirements may vary widely. They include supplying fresh air or oxygen, removing harmful substances by cleaning the air-supply, maintaining a comfortable temperature or humidity, removing heat, maintaining the pressure to prevent air exchange, and controlling room noise levels.

A ventilation facility by itself does not store electric energy. But in combination with a room or building filled with air, a ventilation facility can be used to store electricity.

Here, the storage medium is the air. The state of charge (SOC) in this electric storage system is indicated by the air quality. If the air quality is good, than the storage system is full. This means that the ventilation system can be shut off—or run at lower power—until the air quality sinks to the permitted limit. The storage system is then discharged, and the ventilation facility must be turned on again to raise the air quality in the space.

So by utilizing the room's air capacity to maintain a certain level of quality without air-renewal, ventilation facilities can be used for load shifting. They can then function as electric-energy storage systems.

A number of studies determined the energy consumption of electric drives or ventilators in Germany and/or Europe [26–28]. The following discussion uses the results of the SAVE project, 'Market Study for Improving Energy Efficiency for Fans', funded by the European Commission. This study determined that in 1997 in Germany, ventilators with powers ranging from 1 to 500 kilowatts consumed 43,217 GW h. Of the total consumption, 43% was in the industrial sector, 5% in transport, and 52% in tertiary areas. The energy consumption of ventilators in Europe was 197 TW h.

The same study estimated the technical energy savings potential at 10 to 15%, and the realistic potential at 3.5 to 8.3%. Taking into account the predicted increases in ventilator power, the study estimated that in Europe, ventilator consumption in 2020 would be 220 TW h if energy saving measures were taken, or 290 TW h if no energy saving measures were taken.

The study then used reference facilities and modeling to determine the potential shut-off times for ventilation facilities, as well as the positive (6 GW) and negative (16 GW) balancing energy that would result [1].

### 11.2.6 Washing Machines, Clothes Dryers, and Dishwashers

This category is an exception. This is the only technology group which does not rely on storage to influence the load curve. Instead, demand response in this category relies on users to change their behavior and, as a result, shift the electric load.

This is the only area where electricity consumers actually become aware of the requirements of demand response. They then alter their washing, drying, or cleaning habits to suit the needs of the electric energy supply system. All the other methods of demand response discussed here rely on the inherent storage capacity of an electric application to shift the electric load.

This method of demand response therefore depends on consumer awareness. But since the extent of this awareness may vary considerably, there is some doubt whether the 'storage potential' discussed in this section could actually be realized, even with automated appliances.

To determine the load shifting potential in private households that can be achieved by changing consumer behavior, the electricity consumption in households must first be examined in closer detail.

Total electricity consumption in German households amounted to 139.1 TW h in 2003. Table 11.4 shows how this electricity consumption was allocated among various electricity applications [12].

Except for stoves, lighting, and televisions, all the categories here can be used for demand response. This amounts to 58% of consump-

**Table 11.4** Electricity consumption in 2003 (RH: room heating, PH: process heat, ME: mechanical energy, LI: lighting, I&C: information and communication) [12]

| Appliance | Consumption in TW h/a | | | | | |
|---|---|---|---|---|---|---|
| | RH | PH | ME | LI | I&C | Total |
| Storage heating | 20.7 | 0.0 | 0.4 | 0.0 | 0.1 | 21.2 |
| Electric stoves | 0.0 | 15.0 | 0.1 | 0.1 | 0.1 | 15.3 |
| Hot water | 0.0 | 14.9 | 0.0 | 0.0 | 0.1 | 15.0 |
| Lighting | 0.0 | 0.0 | 0.0 | 14.8 | 0.0 | 14.8 |
| Refrigerators | 0.0 | 0.1 | 13.1 | 0.0 | 0.1 | 13.3 |
| Freezers | 0.0 | 0.1 | 12.2 | 0.0 | 0.1 | 12.3 |
| Washing machines | 0.0 | 4.4 | 1.4 | 0.0 | 0.1 | 5.8 |
| Clothes dryers | 0.0 | 2.7 | 0.9 | 0.0 | 0.0 | 3.6 |
| Dishwashers | 0.0 | 4.4 | 1.4 | 0.0 | 0.0 | 5.8 |
| Televisions | 0.0 | 0.0 | 0.0 | 0.0 | 10.2 | 10.2 |
| Direct heating | 4.0 | 0.0 | 0.2 | 0.0 | 0.0 | 4.2 |
| Other | 0.0 | 3.5 | 10.5 | 0.4 | 3.2 | 17.6 |
| Total | 24.6 | 45.2 | 40.2 | 15.2 | 13.9 | 139.1 |



tion, or annually around 81.2 TW h. Direct electric heating can be shifted to at least the same extent as circulation pump load. Cold (refrigerators and freezers), storage heating, and hot water supply were discussed in the previous sections. Washing machine, clothes-dryer, and dishwasher consumption can be altered by changing consumer behavior. The total consumption here amounts to 15.2 TW h.

A recent study examined in detail the load profile of household electricity consumption in Germany [29]. Using the individual consumption levels of these appliances, Fig. 11.6 shows the daily load profile for the three load groups; washing machines, clothes dryers, and dishwashers.

Assuming maximum flexibility in these three load groups, Fig. 11.6 shows the resulting load profile. This is also the maximum achievable positive balancing energy.

## 11.3 Industrial Applications of Demand Response

As previously discussed in this chapter, the load-management potential of a single industrial facility is larger than the potential of a single unit in the household area. Assuming that the costs for installing the communication technology are roughly the same in both areas, the costs of exploiting the potential are then significantly lower in industry. For this reason, it can be assumed that the potential in industry will be exploited first, even if the total potential in households is significantly greater.

It should be kept in mind that with large industrial facilities, flexible load-management for demand response is available only for very limited time periods. Since the investment costs for these production facilities are high, they are

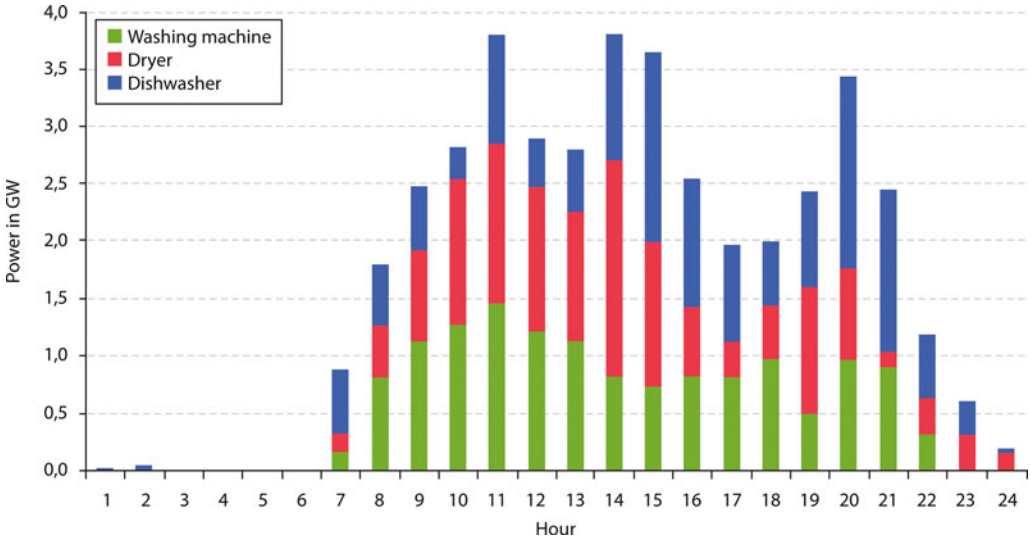



**Fig. 11.6** Standardized daily energy consumption or load profile for washing machines, clothes dryers, and dishwashers. The load profile is equivalent to the theoretically achievable positive balancing energy

fully utilized for as many hours as possible. This means that the margins available for shifting operations over time are very narrow. In addition, starting up and shutting down production processes may alter the quality of the products or incur additional costs [30].

Table 11.5 shows which industries are suitable for demand response, and which of their processes can be used for load shifting. Table 11.6 shows the energy consumption of various industries, the frequency of potential load shifting, the shifting duration, the quantity of energy that can be shifted, and the maximum capacity.

Basically, three electrolysis processes are used in chlor-alkali electrolysis. The amalgam process and the membrane process allow capacity reductions, but the diaphragm process does not. This is because the diaphragm would be destroyed. In [30], the load-management potential of ten German chlorine producers was estimated at 730 MW (see [30] and Table 11.6).

Air separation requires the air to be compressed and then liquefied by cooling. In this process, the air is reduced by rectification to its components, nitrogen, oxygen, and argon. Only the compressors can be operated at partial-loads. Here, [30] estimates the load shifting potential at 170 MW (Table 11.6).

In aluminum production, bauxite is first converted into alumina ($Al_2O_3$) using the Bayer process. The alumina is then reduced to pure aluminum using electrolysis. The electricity required ranges from 12.9 to 17 W h/t. The load shifting potential in the aluminum industry is estimated to be 275 to 325 MW (Table 11.6; [30]).

For copper production, a copper concentrate with a concentration of 30% is typically supplied. This is then mixed with sand and melted at temperatures above 1,200 °C to form copper matte and iron silicate slag. Blister copper is then produced from the copper matte using a converter. Oxygen is removed using reduction with natural gas. The material is then cast into anode plates that has a copper content ranging up to 99.5%. In a last step, the material is electrolytically refined to a purity exceeding 99.99%. This last step can be used for load-management. The load shifting potential is estimated to be at 5 to 7.5 MW [30]. With zinc production, a load shifting potential of 25 MW is assumed (Table 11.6).

**Table 11.5** Industrial applications of demand response [30]

| Industry | Applications | Type of load change |
|---|---|---|
| Chlorine industry | Electrolysis | Partial-load operation with reduced power consumption |
| Aluminum industry | Electrolysis | Shut-off of individual lines |
| Copper industry | Electrolysis | Shut-off of individual lines |
| Zinc-lead industry | Electrolysis | Shut-off of individual lines |
| Steel industry | Electric arc furnaces | Production planning, furnace shut-off |
| Paper industry | Pulp and thermomechanical pulp production | Shut-off of grinders or refiners |
| Cement industry | Cement and raw milling | Power consumption shut-off or reduction |
| Chemical industry | Air separation | Partial-load operation with reduced power consumption |
| Mining industry | Water control | Power consumption shut-off or reduction |
| Water supply industry | Pumping | Power consumption shut-off or reduction |
| Timber industry | Saw mills, milling machines | Production planning |
| Cross-section technology industry | Milling, pumping, compressors, air-conditioners, and cooling units | Shut-off or partial-load operation for certain periods |



Several processes in paper manufacture can be used for demand response, particularly in the production of chemical and mechanical pulp. Here the wood is ground on a grindstone or thermochemically shredded using a refiner. These processes consume large quantities of electricity, and can be interrupted for short (and sometimes longer) periods. Another application that consumes a large quantity of electricity is waste-paper recycling. The paper is dissolved in water and then shredded using pulpers. This process can also be used for load-management. The potential here for load shifting is estimated to be 400 MW (Table 11.6; [30]).

Steel production primarily uses two processes: the blast furnace process and the electric steel process. This last process consumes large quantities of electricity and can be used for load-management. Electric arc furnaces are used to melt the steel. Graphite electrodes conduct the electric current, creating an electric arc that can be applied to the metal. After the melting process, the furnace is tipped over and emptied into a pan. Given adequate lead-time, the start of the process can be shifted, or the melting process briefly interrupted. The load shifting potential here is estimated to be 400 MW (Table 11.6; [30]).

Cement production passes through four processes: mining the raw material, preparing the raw material, firing the raw material into clinker, and grinding the clinker into cement. The grinding processes are particularly well-suited for load-management. Crushers and mills that consumer large quantities of electricity can be shut off when required. In cement plants, 70 to 80% of the electricity is consumed by motor applications. The load shifting potential here is estimated to be 90 to 235 MW (Table 11.6; [30]).

**Table 11.6** Estimates of potential uses of demand response across industries [30]

| Sector | Application | Electricity consumption in TW h | Activations per year | Max. duration in hours | Shiftable energy in GW h | Max. capacity shift in MW h |
|---|---|---|---|---|---|---|
| Raw materials chemistry | Chlorine electrolysis (membrane & Hg) | 8.8 | 40 | 4 | 117 | 730 |
| | Air separation | 5 | 40 | 4 | 27 | 170 |
| Non-ferrous metals | Aluminum electrolysis | 10.5 | 40 | 4 | 48 | 300 |
| | Copper/zinc electrolysis | 1.1 | 40 | 4 | 5 | 30 |
| Paper | Pulp production | 3.5 | 365 | 2 | 292 | 400 |
| Metal manufacture | Electric steel (electric arc furnaces) | 6.8 | 40 | 4 | 30 | 400 |
| Rock and soil | Cement and raw milling | 3.2 | 365 | 3 | 394 | 180 |
| Total | | 38.9 | | | 913 | 2,210 |

### Excursus: Industrial Compressed Air Utilization

Energy has been stored in the form of compressed air for many years. Currently there is discussion of using compressed air storage (CAS) power plants for balancing low-load and peak-load times. Here the energy stored must be converted several times. Electric energy powers a compressor that compresses the air before it is stored. Later, the air is decompressed in a turbine, for example, converting the energy into mechanical energy. Finally, the mechanical energy is then used to generate electricity in a generator. The number of conversion steps increases losses, resulting in a relatively low overall level of efficiency. Adiabatic CAS power plants with TES currently in development are not expected to be much more efficient (see ▶ Chaps. 9 and 10).

For demand response, another possibility would be to store compressed air in industrial facilities where it would not require reconversion into electricity, but could be used directly as compressed air. Generating compressed air consumes more electricity than any other area in industry.

Besides electricity, compressed air is the most frequently used energy carrier in industry and trades. In the EU, around 315,000 air compressors with powers ranging from 10 to 300 kW are currently in use. About 72% of these facilities have connection capacities below 100 kW. Only 28% have a power ranging between 110 and 300 kW. In EU countries as well as across the world, electricity consumption in industry and trades is largely determined by the use of electric motors for power. In the EU, the electricity consumption for motor applications is estimated at 800 TW h. High-consumption motor applications include compressed air generation, ventilators, and pumps. Compressed air generation accounts for 80 TW h of the total consumption. In Germany, compressed air generation consumes 14 TW h annually [38].

The CAS process in industry is a form of energy storage with practically no energy loss which could be used for demand response. In addition, CAS is far more efficient than the use of compressed air storage power plants for load shifting. But the compressed air containers required are expensive. As a result, energy storage at pressures typically used in industry is not cost-effective. A solution here could be to increase the pressure level. But the additional energy consumption required to further compress the air would essentially cancel out the advantages. Another alternative would be to operate the compressors at variable speeds, and supply balancing energy by varying the pressure level within the permitted limits. Conservatively estimated, this could result in a balancing energy-potential exceeding 200 MW.

## 11.4 Summary of German and European Demand Response Potential



### 11.4.1 Demand Response Potential in Germany

Demand response potential is found in two areas: TIS or households. In [36], the technical and economic potential of DSM for load shifting in Germany is broken down by sector, and then again by application (Fig. 11.7)

The cement industry, chlorine production, and paper manufacturing are particularly well-suited for demand response. The potential for load increases in these areas is estimated at 850 MW, and for load-reductions, at 1,600 MW. In the household sector and the TIS area, heat applications with high potential, such as night storage heating or electric hot water supply, offer significant potential. Households also have the largest total potential. Besides heat applications, household applications such as clothes-washing, clothes-drying, and dishwashing have a high potential for load increases. But as discussed earlier in this chapter, demand response with these applications relies on changes in consumer behavior, not on energy storage.

The potential for load increases in the household sector is estimated at 11,750 MW, and the potential for load decreases at 3,150 MW. In the TIS area, this potential is estimated at 4,000 MW and 1,700 MW, respectively.

The cross-sectoral potential of air-conditioning can also be considered, but its use depends on outdoor temperatures. Since air is used as a storage medium here and air's storage capacity is small, with longer-shifting durations, undercooling (extended load increases) or overheating (extended load-reductions) in buildings may result. These effects are incompatible with the function of air-conditioning. This means that air-conditioning is not suitable for shifting over longer periods. But air-conditioning will gain in importance in coming years. This is because its potential will increase, and because the use of air-conditioning is typically linked with increased solar radiation. This increased radiation is also associated with surpluses from photovoltaic (PV) facilities. These surpluses can therefore be absorbed by air-conditioning.

In total then, the potential for load decreases across all sectors in Germany is about 6,400 MW, and the potential for load increases is about 16,600 MW. The potential for load increases is typically higher, because several hours of load can be shifted to one hour.

### 11.4.2 Demand Response Potential in Europe

The potentials for the same applications in a range of European countries are shown in [36] (Table 11.7). In some countries, the potential is lower than in Germany. In total, the potential for load decreases is about 24,000 MW, and the potential for load increases is about 41,000 MW.

This means that the scale of the potential is relevant for European network operations. As a result, it should be taken into account in

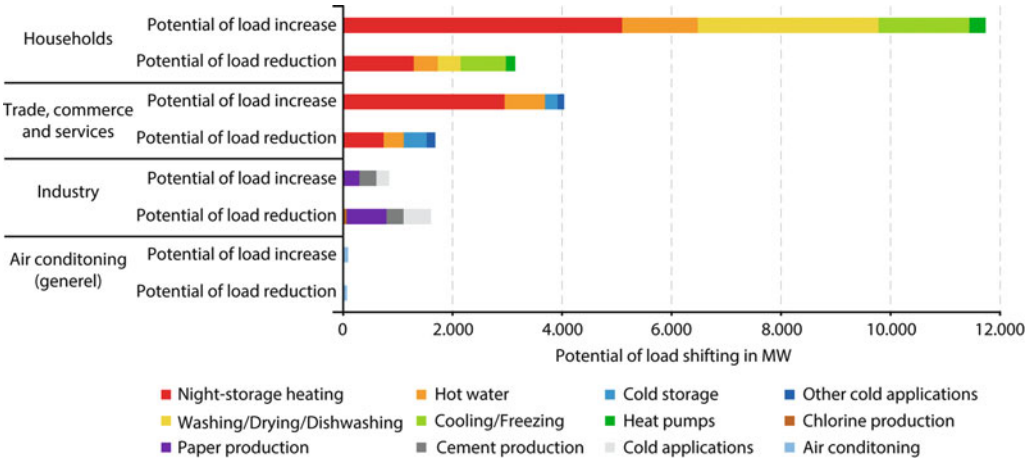



**Fig. 11.7** DSM potential for load-reductions and load increases in individual sectors, broken down by application [36]

**Table 11.7** Technical and economic potential of DSM in selected European countries [36]

| | Belgium | Finland | France | Italy | Poland | Spain |
|---|---|---|---|---|---|---|
| Load decreases in MW | 310 | 2,160 | 2,920 | 1,680 | 640 | 1,850 |
| Load increases in MW | 700 | 820 | 6,200 | 2,940 | 1,150 | 2,280 |

capacity balances and in calculations of guaranteed capacity for the energy union. This is because load-management allows the reduction of must-run capacity.

### 11.4.3 Comparison of Various DSM Studies

The load-management potential in Germany has been examined by these studies:

- 'Dena-Netzstudie II – Integration erneuerbarer Energien in die deutsche Stromversorgung im Zeitraum 2015–2020 mit Ausblick auf 2025 (Grid study on integrating renewables into German electricity supplies between 2015 and 2020)' from the German Energy Agency [32]
- The VDE-ETG 'Demand-Side Management' study [34]
- The IAEW RWTH Aachen study in the ET [36]

A major difference among these studies is that the estimated potential of night storage heating in households and trades is very high in Dena-Netzstudie II. Another difference is the type of potential assessed. The study commissioned by the VDE estimates the theoretical potential in Germany. Dena-Netzstudie II examines the technical potential, and the study supervised by the IAEW at RWTH Aachen focuses on the technical and economic potential, which is the lowest potential. The VDE study also distinguishes between winter and summer, i.e., it includes air-conditioning in summer, and night storage heating, heat pumps, and increased hot water demand in winter.

But because of (existing) night storage heating, all the studies assign the largest potential to the household and TIS sectors. The potential for load decreases is exceeded by the potential for load increases in all of the studies as well (Fig. 11.8).

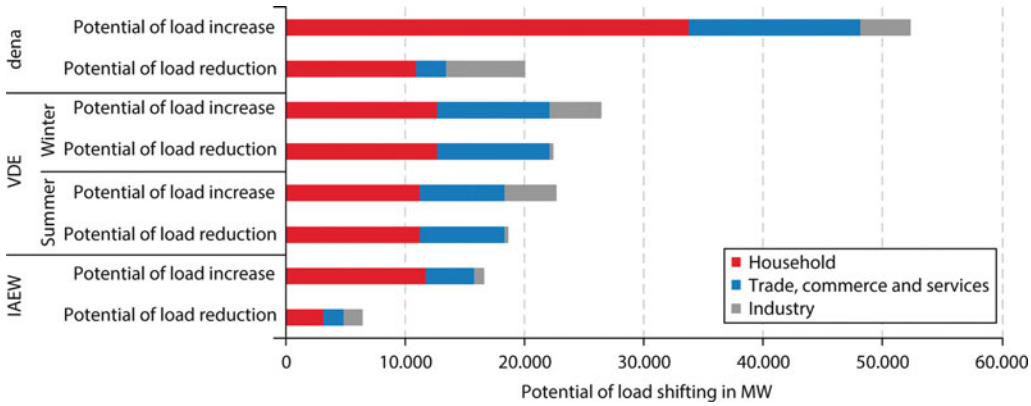



**Fig. 11.8** Comparison of various studies of load-management potential in the household, TIS, and industry sectors [33, 35, 36]

## 11.5 Developments and Trends

Increasing shares of renewable energy in energy generation and the elimination of conventional power plants will result in gaps in energy supply. New concepts are required to bridge these gaps. Load-management could effectively help reduce the guaranteed capacity required from Germany's power plant portfolio as well as integrate renewable surpluses, thus reducing the costs of the German electricity system.

### 11.5.1 Load Shedding Utilization in Industry

The German Interruptible Loads Ordinance (abbreviated AbLaV in German) offers compensation for load shedding, or for providing industrial facilities for load shedding. This ordinance is a first step towards implementing load-management. Figure 11.9 shows deliveries of interruptible loads broken down by balancing zone and quantity of energy. The date, 20 March 2015, is of particular interest. On that day, there was a solar eclipse. This is clearly reflected in the number of deliveries on that date. The quantity of energy totaled 360 MW h spread across 15 deliveries.

### 11.5.2 Future Technical and Economic Potential

Because of the number of factors involved, estimating the future technical and economic potential for the years 2020 or 2030 is a challenge. Since the focus ranges from theoretical potential to technical and economic potential, the results of the relevant studies cannot, in general, be compared.

Because a large number of new consumers will be added to the electricity sector (electric heat-pumps, electro-mobility, and air-conditioning) that have only a minor impact on electricity consumption today, the potential for load-management will generally increase in the future.

From now until 2020, the potential will be higher in winter than in summer. But according to the VDE-ETG study [34], this trend will be reversed by the simultaneous increase in air-conditioning and improved efficiency in the heating sector. If load-management is fully implemented by 2030, then the minimal load could be increased by a factor of 2.7. This would smooth out the residual load, resulting in minimal shut-downs of thermal and renewable energy facilities. This load-smoothing effect can also be observed in simulations of future energy systems.

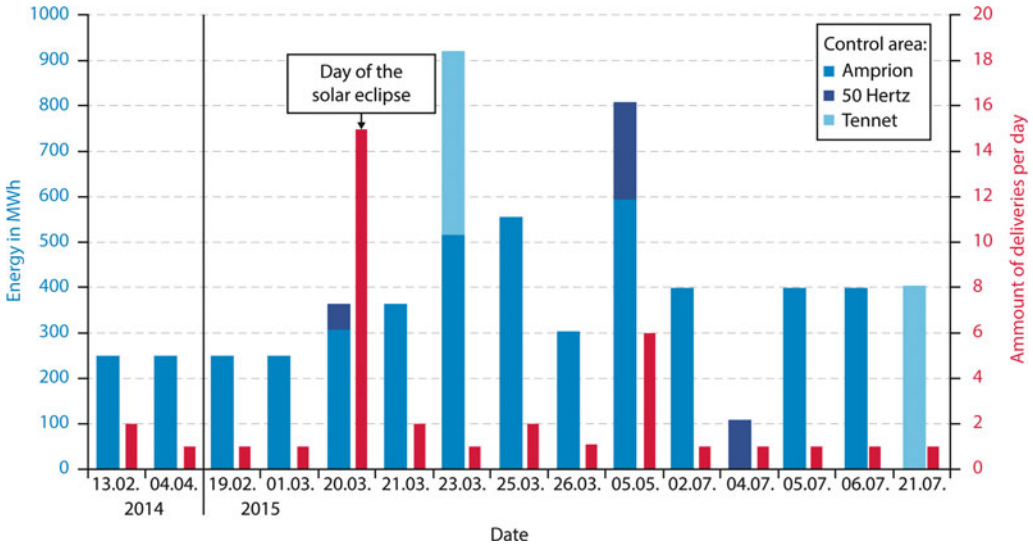



**Fig. 11.9** Quantity of energy and number of deliveries per day in various balancing zones [37]

If all industrial production capacity is utilized for load-management, the resulting theoretical storage capacity of 77 GW h would exceed the capacity of all German pumped-storage plants combined (40 GW h). But not all of this capacity can actually be used, because storage filling levels in the facilities are determined by production requirements. Available storage capacity in industry could be expanded under the appropriate conditions.

Even if the electricity network is expanded, in Germany, electricity surpluses from renewable energy will still play a minor role in 2020. As a result, load-management will also be of minor importance until that time. But as with power-to-gas (PtG), the conditions permitting full utilization of load-management should be in place as early as possible. This is to ensure that the energy system can then rely on this cost-effective form of flexibility when the time comes.

With high shares of renewable energy, load-management varies substantially by the time of day. This and other parameters limit its overall potential. As a result, only 47% of load decreases and 18% of load increases included in the IAEW study's total estimate of the technical and economic potential can actually be exploited. This is primarily due to seasonal and time-of-day limitations [36].

### 11.5.3 Guaranteed Capacity and Renewable Energy Integration

Load-management can supply guaranteed capacity, as well as significantly reduce guaranteed capacity demand at peak-load times. In addition, load-management can improve the utilization of renewable energy surpluses, increase the energy efficiency of the existing power plant portfolio, and ensure the portfolio is more cost-efficient.

In households and TIS alone, by 2030, load-management could integrate 42 TW h of renewable energy annually; the equivalent of 20,000 MW onshore wind power facilities [33]. But this potential is primarily at the transmission network level. The majority of surpluses requiring integration come from PV and wind facilities at levels ranging up to 110 kV. By 2020, 80% of available renewable energy could be regionally exploited by shifting 20% of the load. This would also reduce the need for network

expansion to accommodate peak loads. If the planned network expansion is assumed, then by 2030, renewable energy supply will exceed the load by a large margin. With a 100% share of renewable energy for electricity supply, the share of energy that can be used locally by load shifting sinks to 15%. As a result, short- and long-term storage as well as feed-in management will be absolutely essential [34].

### 11.5.4 Potential to Reduce Network Expansion and Annual Peak-Load

Load-management could be used to reduce the maximum (positive) residual load. The residual load is equal to the consumption (load) minus the renewable generation. Positive residual load results from renewable energy deficits, and requires conventional power plants to cover the remaining electricity demand. Negative residual load results from renewable energy surpluses. Currently, negative residual load results only in scattered network areas when renewable energy feed-in is high and load is low.

Negative load periods will become more frequent as the share of renewable energy increases. Load-management can be used to reduce these periods. Smoothing residual load results in improved utilization of cheap base-load power plants. Smoothing also reduces the use of expensive peak load power plants. This is because the maximum residual load is reduced by DSM (by up to 1,800 MW according to [35]). Another advantage here is that reducing residual load reduces the conventional power plant portfolio. This can in turn reduce guaranteed capacity. When base-load generation is dominated by carbon energy, then a disadvantage of using flexibility options such as DSM is increased $CO_2$ emissions. But the solution to this problem is not to avoid flexibility options such as DSM or storage. Instead, the value of $CO_2$ in the EU emissions trading system (ETS) should be adjusted to compensate.

## 11.6 Summary

- This chapter discussed a **range of processes** that have the **same effect** on the energy supply system **as energy storage**, and in fact often store energy.
- They differ from all other forms of energy storage discussed here in that they are all **existing processes** that could provide **storage capacity without requiring any investment**. They can be activated at costs far below those required by other energy storage systems previously described. Their **theoretical potential** is **so large** in comparison with the available capacity that they could meet the entire demand. But this is true only **for periods ranging from minutes to a few hours**, and in exceptional cases, up to a day. In addition, some technical applications can be used only at certain times of day or in certain seasons. As a result, the energy storage systems described in ▶ Chaps. 6 and 10 **are essential for bridging longer periods**.
- Demand response could make **a significant contribution to energy transition by smoothing residual load** and **reducing the annual peak load**. This would **reduce guaranteed capacity** supplied by fossil power plants, as well as **reduce network expansion requirements** by increasing regional utilization of renewable energy. **More renewable energy** could then be integrated into the energy system, **increasing environmental benefits while reducing costs to consumers**.
- **Conditions for access to load-management** in industry are similar to conditions in other markets such as the balancing energy market. But **the requirements are complex**, and there are currently **few incentives** to participate. The **AbLaV is a first step** towards implementing load-management. But it must be modified to ensure **load-management is profitable over the long-term**, and widely adopted as a result.

## References

1. Stadler I Demand Response – Nichtelektrische Speicher für Elektrizitätsversorgungssysteme mit hohem Anteil erneuerbarer Energien. ISBN 3-86624-092–99
2. Borstelmann P, Rohne P (1989) Handbuch der elektrischen Raumheizung. Hüthig Buch Verlag, GmbH, Heidelberg
3. Vereinigung Deutscher Elektrizitätswerke – VDEW e.V. (1998) Raumwärmemarkt – Strategie-Optionen deutscher Stromversorger. Verlags- und Wirtschaftsgesellschaft der Elektrizitätswerke m.b.H. – VWEW, 1. Ausgabe
4. ¸http://www.umweltlexikon-online.de/fp/archiv/RUBenergie/Elektrospeiherheizung.php
5. Kuhrwahl H, Wölfle W (1998) ABC der Elektro-Warmwasserversorgung. Energie-Verlag GmbH, Heidelberg (ISBN 3-87200-684-3)
6. Lechner H , et. al. (1998) Analysis of Energy Efficiency of Domestic Electric Storage Water Heaters. Study for the Directorate General for Energy (DG XVII) of the Commission of the European Communities, Contract No. SAVE-4.1031/E/95-013, Final Report, ISBN 3-901381-59-7
7. Enquete Kommission Nachhaltige Energieversorgung „Nachhaltige Energieversorgung unter den Bedingungen der Globalisierung und der Liberalisierung", Schlussbericht
8. Geiger B, Nickel M, Wittke F (2005) Energieverbrauch in Deutschland: Daten, Fakten, Kommentare. Bwk – Das Éneng Fachmag 57(1):2
9. VDEW (2004) Endenergieverbrauch in Deutschland 2002. VDEW Projektgruppe Nutzenergiebilanzen
10. ISI, DIW, GfK, IfE (2004) Energieverbrauch der privaten Haushalte und des Sektors Gewerbe, Handel, Dienstleistungen (GHD). Projektnummer 17/02, Abschlussbericht an das Bundesministerium für Wirtschaft und Arbeit
11. Steimle F, Bruckmann O, Mai M, Elsenheimer F, Schikora H, Schrey R, Jahn K, Kruse H, Heidelck R, Benda U, Blömer M, Bobst E, Vollmer D, Sussek W (2002) Energiebedarf bei der technischen Erzeugung von Kälte in der Bundesrepublik Deutschland. Statusbericht Des Dtsch Kälte- Klimatechnischen Vereins (22)
12. Geiger B, Nickel M, Wittke F (2005) Energieverbrauch in Deutschland – Daten, Fakten, Kommentare. Bwk Das Energie-fachmagazin 1/2
13. Enquete Kommission Nachhaltige Energieversorgung „Nachhaltige Energieversorgung unter den Bedingungen der Globalisierung und der Liberalisierung", Schlussbericht
14. http://www.ag-energiebilanzen.de
15. http://www.hea.de
16. Philipp J (2002) Optimierung von Haushaltskühlgeräten mittels numerischer Modellierung. TU Dresden (Dissertation)
17. DIN EN 153: Methoden zur Messung der Aufnahme elektrischer Energie und damit zusammenhängender Eigenschaften für netzbetriebene Haushalt-Kühlgeräte, Tiefkühlgeräte, Gefriergeräte und deren Kombinationen. Deutsche Norm
18. Setterwall F Advanced Thermal Energy storage through Application of Phase Change Materials and Chemical Reactions - Feasibility Studies and Demonstration Projects. International Energy Agency (IEA), Energy Conservation through Energy storage, Annex 17
19. NAPS Refrigerator for Vaccine Storage. NAPS Systems Oy, Finland, http://www.napssystems.com
20. Ewert MK, Bergeron DJ, Foster RE, LaFleur O Photovoltaic Direct-Drive, Battery-Free Solar Refrigerator Field Test Results. NASA Johnson Space Center, Houston, Texas, USA
21. Toure S, Fassinou WF (1999) Cold Storage and Autonomy in a three compartments photovoltaic solar refrigerator: experimental and thermodynamic study. Renew Energy 17
22. Ewert MK, Agrella M, Frahm J, Bergeron DJ, Berchowitz D Experimental Evaluation of a Solar PV Refrigerator with Thermoelectric, Stirling and Vapor Compression Heat Pumps
23. Informationsdienst BINE (2002) Latentwärmespeicher. Fachinformationszentrum, Karlsruhe (Themen Info IV/02)
24. Hoppe, Brier, Nägele Rationelle Energieverwendung beim Kühlen und Gefrieren. ISBN 3-88122-706-7
25. Brandt G Stromsparende Heizungsumwälzpumpen. Seminar-Dokumentation, Impuls Programm Hessen
26. Radgen P (2001) Market Study for Improving Energy Efficiency for Fans. SAVE Programme (Project XVII/4.1031/Z/99-313. Final Report. ISBN 3-8167-6137-2. Juli)
27. Enquete Kommission Nachhaltige Energieversorgung „Nachhaltige Energieversorgung unter den Bedingungen der Globalisierung und der Liberalisierung", Schlussbericht
28. Almeida AT, et.al. (2000) Improving the penetration of energy efficient motors and drives. Final Report. European Commission. SAVE 4.1031/Z/96-044
29. Prior D (1997) Nachbildung der Energiebedarfsstrukturen der privaten Haushalte - Werkzeug zur Bewertung von Energiesparmaßnahmen. VDI Fortschrittsberichte, vol 6. VDI Verlag, Düsseldorf (Nr. 379)
30. Klobasa M (2007) Dynamische Simulation eines Lastmanagements und Integration von Windenergie in ein Elektrizitätsnetz auf Landesebene unter regelungstechnischen und Kostengesichtspunkten. ETH Zürich (Diss ETH Nr. 17324)

31. VDI-Gesellschaft (2002) Druckluft: Erzeugung, Aufbereitung, Verteilung, Anwendung und Planung. VDI Verlag GmbH, Düsseldorf (VDI-Berichte 1681)
32. DENA (2011) dena-Netzstudie II. Berlin
33. Deutsche Energie-Agentur (2015) Marktentwicklung Lastmanagement in Deutschland. Berlin
34. ETG-Task Force Demand Side Management (06/12) Demand Side Integration-Lastverschiebungspotentiale in Deutschland, Frankfurt
35. Grote F, Drees T, Budkke J, Moser A (2013) Einfluss des Demand Side Managements auf den Kraftwerkseinsatz in Europa. Energiewirtsch Tagesfr 12:32–36
36. Grote F, Drees T, Budkke J, Moser A (2013) Einfluss des Demand Side Managements auf den Kraftwerkseinsatz in Europa. Energiewirtsch Tagesfr 12:32–36
37. Hauck H (11.08.15) Abschaltungen gemäß AbLaV. E-Mail
38. VDI-Gesellschaft (2002) Druckluft: Erzeugung, Aufbereitung, Verteilung, Anwendung und Planung

# Comparison of Storage Systems

*Michael Sterner and Martin Thema*

**12.1 Overview of Technical and Economic Parameters – 640**

**12.2 Application Areas Determined by Storage Capacity and Discharging Duration – 640**
12.2.1 Electric-Energy Storage Systems—Capacitors and Coils – 647
12.2.2 Electrochemical-Energy Storage Systems—Batteries – 647
12.2.3 Mechanical-Energy Storage Systems—Pumped-Storage, CAS, and Flywheel Storage – 648
12.2.4 Thermal-Energy Storage Systems—Thermal Storage – 648
12.2.5 Chemical-Energy Storage Systems—Power-to-X (PtX) – 649
12.2.6 Load-Management – 650

**12.3 Comparison of Costs, Efficiency Levels, and Energy Densities – 650**
12.3.1 Comparison of All Storage Systems by Cost, Efficiency, and Energy Density – 650
12.3.2 Comparison of Electricity Storage Systems Costs by Cycle Duration – 653

**12.4 Strengths, Weaknesses, and Stages of Development – 655**
12.4.1 Energy-Storage System: Stages of Development – 655
12.4.2 Strengths and Weaknesses of the Various Technologies – 655

**12.5 Cost-Reduction Potential with Batteries and PtX – 656**
12.5.1 Cost Trends and Potential with Lithium Batteries – 656
12.5.2 Cost-Reduction Potential with PtG – 662

**Electronic supplementary material** The online version of this chapter (https://doi.org/10.1007/978-3-662-55504-0_12) contains supplementary material, which is available to authorized users.

© Springer-Verlag GmbH Germany, part of Springer Nature 2019
M. Sterner, I. Stadler (Eds.), *Handbook of Energy Storage*, https://doi.org/10.1007/978-3-662-55504-0_12

12.6 Future Potential and Public Acceptance of Energy Storage Systems – 665

12.7 Summary – 669

References – 670

## Overview

There are several approaches to classifying energy storage systems (see ► Chaps. 1 and 2). Storage systems are used in a large number of different technologies at various stages of development, and in a wide range of application areas (see ► Chaps. 3 to 5). This chapter compares the capabilities of the different storage systems using the following criteria:

- Storage capacity
- Discharging time
- Energy density
- Application fields and areas
- Capital costs
- Efficiency and cycle life
- Market maturity and technology availability

This comparison of storage systems also provides a convenient overview of the various storage systems and their capabilities.

## The Unit of Electric Energy

In order to compare energy storage systems the criteria of comparison must be determined first. This is closely related to the question of how energy storage systems are classified (► Chap. 2). Energy systems can be compared by their technical characteristics, function, application areas, markets, installation sites, or operating time-frames.

Generally speaking, all-inclusive comparisons of energy storage systems are practically impossible. Energy storage systems often differ fundamentally from each other because they function on different physical principles. For example, in a bilayer capacitor (electric), energy is stored basically directly on the surface. As a result, no conversion steps are required to supply it to an electric energy system. In conventional energy sources such as coal, crude oil, or gas, the energy is stored in chemical bonds. This means that, to supply the energy to an electric energy systems, conversion steps are required. Batteries use an electro-chemical process that combines these characteristics. Mechanical storage systems such as pumped-storage plants (PSP) or flywheel-energy storage generate electric energy from large quantities of potential and kinetic energy using a number of conversion steps. With thermal storage systems, the energy is stored via temperature differences, phase-changes, or chemical bonds. Directly comparing any of these forms of energy poses a significant challenge.

The following example demonstrates the fundamental differences between these forms of energy (electric, electro-chemical, chemical, mechanical, and thermal energy) by comparing the values of a kilowatt-hour of electric energy and of thermal energy.

### Example

One kilowatt-hour (1 kW h) is equivalent to 3.6 megajoules (MJ) of energy. To carry a washing machine (90 kg) to the top of a mountain 4,000 m high, or a sack of potatoes (50 kg) to the top of Mount Everest requires exactly that same amount of energy: one kilowatt-hour (see Eqs. 12.1, 12.2, and 12.3).

By definition:

**Mass:** – $m = 90\,\text{kg}, 50\,\text{kg}$
**Energy:** – $E = 3.6\,\text{MJ}$
**Force of gravity:** – $g = 9.81\,\text{m/s}^2$
**Height to be determined:** – $h$

Solution:

$$E_{\text{pot}} = m \cdot g \cdot h, \tag{12.1}$$

$$h_{\text{mountain,washing machine}} = \frac{E_{\text{pot}}}{m_{\text{washing machine}} \cdot g} = \frac{3.6\,\text{MJ}}{90\,\text{kg} \cdot 9.81\,\text{m/s}^2} = 4{,}080\,\text{m}, \tag{12.2}$$

$$h_{\text{mountain,sack of pototatoes}} = \frac{E_{\text{pot}}}{m \cdot g} = \frac{3.6\,\text{MJ}}{50\,\text{kg} \cdot 9.81\,\text{m/s}^2} = 7{,}340\,\text{m}. \tag{12.3}$$

The same amount of energy is required to heat 34 liters of water to 25 Kelvin (25 °C) using an electric heating element. This quantity of energy is sufficient to heat about a quarter of a bathtub of water to a comfortable bathing temperature of 35 °C if the cold water supplied is at 10 °C (Fig. 12.1).

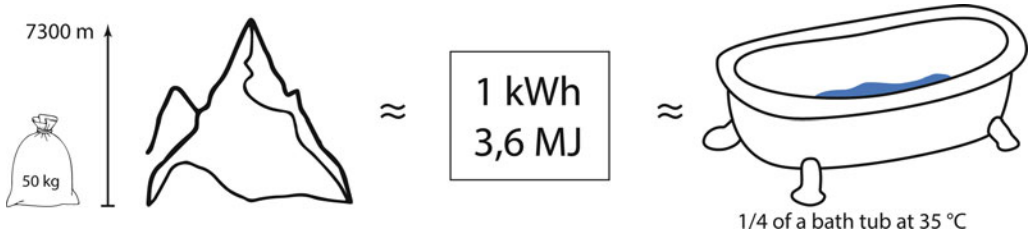



**Fig. 12.1** A kilowatt-hour is required to carry a sack of potatoes (50 kg) to the top of Mount Everest. The same amount of energy is required to heat a quarter of the water in a bathtub to a comfortable bathing temperature

By definition:

**Thermal energy:** – $Q = 3.6\,\mathrm{MJ}$
**Thermal capacity of water:** – $c_\mathrm{w} = 4.182\,\mathrm{kJ/kg\,K}$
**Temperature difference:** – $\Delta T = 25\,\mathrm{K}$ (bath water temperature: 35 °C, cold water temperature: 10 °C)

To be determined:

**Mass:** – $m$

Solution:

$$Q = c_\mathrm{w} \cdot m_\mathrm{water} \cdot \Delta T, \tag{12.4}$$

$$m = \frac{Q}{c \cdot \Delta T} = \frac{3.6\,\mathrm{MJ}}{4.182\,\frac{\mathrm{kJ}}{\mathrm{kg\,K}} \cdot 25\,\mathrm{K}} = 34\,\mathrm{kg} = 34\,\mathrm{L}. \tag{12.5}$$

12

Obviously, various of forms of energy have various values. Mechanical and electric energy are 100% exergy, but the thermal energy in 35 °C water is almost entirely anergy. Equation 12.6 shows that, unlike anergy, exergy can be converted into any other form of energy:

$$\text{Energy} = \text{exergy} + \text{anergy}. \tag{12.6}$$

Since electric energy is exclusively exergy and a 'high-quality' form of energy that can be comparably easily converted into other energy forms, it will be used here as the standard for all storage technologies.

## 12.1 Overview of Technical and Economic Parameters

Table 12.1 lists all the parameters defined or derived in ▶ Chap. 2, and then described in Part III for the technologies in ▶ Chaps. 6 to 11. Because the levels of development differ (▶ Sect. 12.4.1), the parameter ranges vary substantially in some cases as well. To provide a better overview, averages calculated from the figures commonly found in reference works were used here instead. These figures were collected from around 70 sources. The technologies are compared using these figures in the remainder of the chapter.

## 12.2 Application Areas Determined by Storage Capacity and Discharging Duration

The comparison in Fig. 12.2 of existing storage facilities in Germany by their discharging duration $t_\mathrm{aus}$ and storage capacity $W$ demonstrates how widely the characteristics and application areas of different storage technologies vary. This kind of comparison is also called a Ragone chart.

In this double-logarithmic diagram, discharging duration $t_\mathrm{aus}$ up to about a year is on the vertical axis and storage capacity $W$ on the horizontal axis. As references, the average annual electricity consumption of a two-person household, a town of 100 inhabitants, a city the size of Regensburg with 150,000 inhabitants, and a large city the size of Berlin with 3.5 million inhabitants is also shown.

The circled areas indicate where the various existing facilities in operation today are found. The diagram shows that most storage technolo-

**Table 12.1** Overview of averages of essential technical and economic parameters for a range of storage technologies [1, 3, 7–17, 19–25, 27–31, 33–40, 42–50, 54, 55, 59, 61, 62, 64, 66]

| Technology (today) | Technical | | | | | | Costs | | |
|---|---|---|---|---|---|---|---|---|---|
| | Energy density | | Efficiency | Self-discharge | Service life | | CAPEX | | OPEX fix |
| | Gravimetric | Volumetric | | | Cycle life | Service life over time | | | |
| | W h/kg | kW h/m³ | % | %/day | Cycles | a | €/kW h | €/kW | €/kW h |
| **Electrical energy storage** | | | | | | | | | |
| Capacitors (DLC) | 0.1–10 | 10 | 90–95 | 0.004–0.013 | 1 million | 10 | 5,150–12,000 | 125–300 | n/a |
| Coils (SMES) | 1 | 10 | 92 | 10–12 | > 1 million | 30 | 13,570–75,670 | 300–915 | n/a |
| **Electrochemical energy storage systems** | | | | | | | | | |
| *Low-temperature batteries* | | | | | | | | | |
| Lead-acid batteries | 25–40 | 25–65 | 74–89 | 0.17 | 203–1,500 | 10 | 90–355 | 200–490 | 0.16–0.76 |
| Nickel batteries | 55–75 | 60–105 | 71 | n/a | 350–2,000 | n/a | 385–1,100 | 385–1,100 | n/a |
| Lithium batteries | 110–190 | 190–375 | 90–97 | 0.008–0.041 | 3,500–20,000 | 15 | 140–180 | 100–200 | 0.13–0.76 |
| *High-temperature batteries* | | | | | | | | | |
| Sodium batteries | 100–165 | 155–255 | 72–81 | n/a | 2,500–8,250 | 17 | 265–645 | 285–1,075 | 0.07–0.76 |
| *Batteries with external storage* | | | | | | | | | |
| Redox-flow batteries | 16–41 | 20–60 | 70–79 | 0.3 | 7,000–15,000 | 17.5 | 250–700 | 710–1,790 | n/a |

**Table 12.1** (Continued)

| Technology (today) | Technical | | | | | | Costs | | |
|---|---|---|---|---|---|---|---|---|---|
| | Energy density | | Efficiency | Self-discharge | Service life | | CAPEX | | OPEX fix |
| | Gravimetric | Volumetric | | | Cycle life | Service life over time | | | |
| | W h/kg | kW h/m³ | % | %/day | Cycles | a | €/kW h | €/kW | €/kW h |
| **Chemical energy storage systems** | | | | | | | | | |
| *Conventional chemical energy storage systems* | | | | | | | | | |
| Liquid gas, liquefied petroleum gas, LPG | 12,870 | 6,770 | – | n/a | – | – | n/a | – | – |
| Heating oil-/crude oil storage | 11,830 | 10,315 | 99.9 | n/a | – | n/a | n/a | – | – |
| *Biofuels* | | | | | | | | | |
| Bioethanol | 7,410 | 5,850 | – | n/a | – | – | n/a | – | – |
| Biodiesel | 10,305 | 8,985 | – | n/a | – | – | n/a | – | 0.0002 |
| *Power-to-gas—storage types* | | | | | | | | | |
| Cavern storage facilities (methan) | 14,300 | 1,100 | 99 | n/a | n/a | n/a | n/a | n/a | n/a |
| Cavern storage facilities (hydrogen) | 34,000 | 350 | 95 | n/a | n/a | n/a | n/a | n/a | n/a |
| porous storage facilities (methan) | 13,450 | n/a | n/a | n/a | n/a | n/a | n/a | n/a | n/a |
| *Charging technologies* | | | | | | | | | |
| Alkaline electrolysis (AEL) | – | – | 61–79 | n/a | – | 25–30 | – | 760–1,050 | n/a |
| Membrane electrolysis (PEM, PEMEL) | – | – | 67–82 | n/a | – | 10–20 | – | 675–1,350 | n/a |

**Table 12.1** (Continued)

| Technology (today) | Technical | | | | | | Costs | | |
|---|---|---|---|---|---|---|---|---|---|
| | Energy density | | Efficiency | Self-discharge | Service life | | CAPEX | | OPEX fix |
| | Gravimetric | Volumetric | | | Cycle life | Service life over time | | | |
| | W h/kg | kW h/m$^3$ | % | %/day | Cycles | a | €/kW h | €/kW | €/kW h |
| **Chemical energy storage systems** | | | | | | | | | |
| *Charging technologies* | | | | | | | | | |
| High temperature electrolysis (HTES) | – | – | 94 | n/a | – | 2 | – | 2,000 | n/a |
| Membraneless electrolysis | | | 85–90 | n/a | | n/a | | n/a | n/a |
| Chemical methanation | – | – | 80 | n/a | – | n/a | – | 800–1,000 | n/a |
| Biological methanation | | | 80 | n/a | – | n/a | – | 650 | 0.04 |
| *Discharging technologies* | | | | | | | | | |
| Combined heat and power (CHP) | | | 85 | | – | 30 | – | 350–1,000 | n/a |
| Fuel cells | | | 43–53 | | – | n/a | – | 2,305 | 47 |
| Gas turbines | | | 35–38 | n/a | – | 25 | – | 400 | n/a |
| Gas and steam power plants | | | 35–65 | | – | 30 | – | 750 | 0.205 |
| *Power-to-gas—overall process* | | | | | | | | | |
| Power-to-hydrogen (compr. 200 bar, storage) | | | 54–72 | n/a | – | – | – | n/a | n/a |
| Power-to-methan (SNG, compr. 200 bar, storage) | | | 49–64 | | | | | | |

**Table 12.1** (Continued)

| Technology (today) | Technical | | | | | | Costs | | |
|---|---|---|---|---|---|---|---|---|---|
| | Energy density | | Efficiency | Self-discharge | Service life | | CAPEX | | OPEX fix |
| | Gravimetric | Volumetric | | | Cycle life | Service life over time | | | |
| | W h/kg | kW h/m$^3$ | % | %/day | Cycles | a | €/kW h | €/kW | €/kW h |
| **Chemical energy storage systems** | | | | | | | | | |
| *Power-to-gas—overall process* | | | | | | | | | |
| Power-to-hydrogen (compr. 80 bar, transport) | | | 57–73 | | | | | | |
| Power-to-methan (SNG, compr. 80 bar, transport) | | | 50–64 | | | | | | |
| Power-to-hydrogen (atmospheric) | | | 64–77 | | | | | | |
| Power-to-methan (atmospheric) | | | 51–65 | | | | | | |
| Power-to-hydrogen-to-power (el. gen. at $\eta = 0.6$ & compr. 80 bar) | | | 34–44 | | | | | | |
| Power-to-methan-to-power (el. gen. at $\eta = 0.6$ & compr. 80 bar) | | | 30–38 | | | | | | |
| Power-to-hydrogen-to- CHP (40% power, 45% heat, compr. 80 bar) | | | 48–62 | | | | | | |
| Power-to-methan-to-CHP (40% power, 45% heat, compr. 80 bar) | | | 43–54 | | | | | | |
| Power-to-methan with HTES | | | 75 | | | | | | |
| Power-to-liquid with HTES | | | 65 | | | | | | |

**Table 12.1** (Continued)

| Technology (today) | Technical | | | | | | Costs | | |
|---|---|---|---|---|---|---|---|---|---|
| | Energy density | | Efficiency | Self-discharge | Service life | | CAPEX | | OPEX fix |
| | Gravimetric | Volumetric | | | Cycle life | Service life over time | | | |
| | W h/kg | kW h/m³ | % | %/day | Cycles | a | €/kW h | €/kW | €/kW h |
| **Mechanical energy storage systems** | | | | | | | | | |
| Pumped storage plants | 0.3–1.4 | 0.35–1.1 | 70–82 | 0–0.5 | 12,800–33,000 | 40–100 | 40–180 | 550–2,040 | 0.08 |
| *Compressed air energy-storage (CAES)* | | | | | | | | | |
| Diabatic | | 2–7 | 40–55 | 0–10 | 8,620–17,100 | 40 | 40–80 | 340–1,145 | 0.01–0.26 |
| Adiabatic | | 2–8 | 60–68 | n/a | – | n/a | n/a | 600–800 | n/a |
| Isothermal | | 25 | 95 | n/a | – | n/a | n/a | n/a | n/a |
| Liquid air energy storage | | 120–200 | n/a | n/a | – | n/a | n/a | n/a | n/a |
| Flywheel storage systems | 5–90 | 210 | 83–93 | 72–100 | > 1 million | n/a | 650–2,625 | 125–275 | 1 |
| **Thermal storage systems** | | | | | | | | | |
| Sensible thermal storage systems | 10–50 | 100–300 | 45–75 | n/a | 5,000 | n/a | 0.2–8 | 80–130 | 0.1 |
| Latent thermal storage systems (PCM) | 49–97 | 113 | 75–90 | n/a | 5,000 | n/a | 15–50 | 80–160 | 0.1–0.5 |
| Thermochemical energy storage systems (TCS) | 120–960 | 120–250 | 80–100 | n/a | 3,500 | n/a | 8–100 | n/a | n/a |
| District heating storage systems | n/a | 350 | n/a | n/a | n/a | n/a | n/a | n/a | n/a |

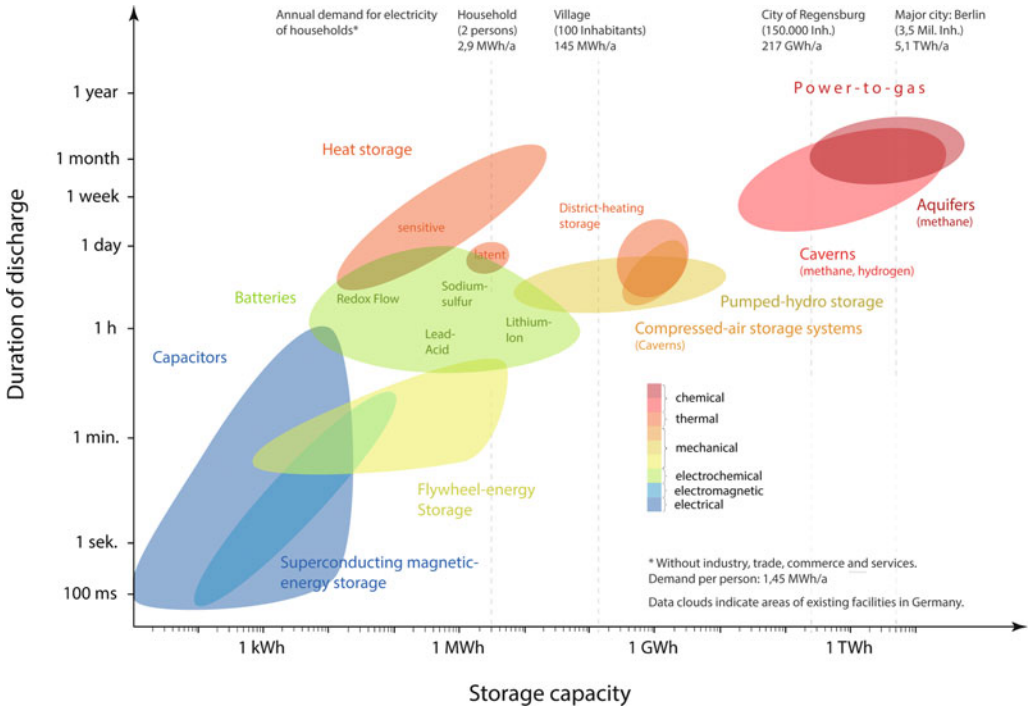



**Fig. 12.2** Storage types compared with storage capacity and discharging duration (Ragone chart): the *circled areas* indicate German facilities which have existed since 2013

12

gies are in the short-term storage range of $t_{dis} <$ 24 hours. Far fewer are in the long-term storage area.

Short-term storage systems:

- Capacitors, coils (all purely electric-energy storage systems)
- Flywheel storage systems
- Batteries (all electro-chemical energy storage systems)
- Latent-thermal storage systems
- Compressed air storage (CAS) systems
- Some sensible-thermal storage systems or district-heating storage systems
- Most PSP

Long-term storage systems:

- Cavern storage (power-to-gas—PtG—using hydrogen and methane)
- Porous storage (PtG only using methane)
- Many sensible-thermal storage systems, some district-heating storage systems
- Some PSP

Only chemical-energy storage systems (cavern and porous storage using PtGs) are at the same scale and in the same range as fossil energy stored in the form of coal or natural gas.

This shows that for energy transition, sufficient storage capacity with adequate discharging durations is available. This also means that there is no 'storage problem' with renewable energy, as is often assumed.

The following sections discuss the storage capacities, discharging durations, and energy densities of the various technologies together with their application fields and areas. The discussion starts with the smallest storage capacities and discharging durations (electric-energy storage systems), and ends with the largest (chemical-energy storage systems). Load-management is a special case and is discussed at the end.

### 12.2.1 Electric-Energy Storage Systems—Capacitors and Coils

Because they store low quantities of energy in the kilowatt-hour range and have extremely short discharging durations ranging from milliseconds to seconds, electric-energy storage systems such as capacitors and coils are only used in niche areas (Fig. 12.3). One example is ensuring voltage quality in electricity networks.

Superconducting-magnetic energy storage (SMES) requires cooling to temperatures near absolute zero. This is technically extremely difficult. As a result, this technology is only used in short-term and high-capacity storage systems that supply electric energy at very short notice and for short durations [20]. These systems can relieve strain on the electricity network by absorbing and balancing large peak loads.

In hybrid systems, in combination with batteries for example, bilayer capacitors are used to extend battery life or as drive boosters in the transport sector (Fig. 12.3). A major advantage of these systems is the long cycle life exceeding a million cycles.

### 12.2.2 Electrochemical-Energy Storage Systems—Batteries

Electro-chemical storage systems or battery storage have capacities in the range of several megawatt-hours. They have discharging durations of up to a day, and can be used as short-term storage systems.

A number of different battery technologies are used in a wide variety of applications. These range from consumer batteries in the milliwatt range to battery parks in the megawatt range used as storage power plants. These systems are limited to applications in the electricity and transport sectors (Fig. 12.4).

Because of the difficulties involved in handling hot and often liquid components, high-temperature batteries such as sodium-sulfur batteries can only be used in stationary applications. The power and capacity of batteries with external storage such as redox flow batteries can be easily scaled. They are currently used in stationary applications, but they could also be used in the future for fuel supply.

Many low-temperature batteries such as lead, nickel, or lithium batteries use fully-

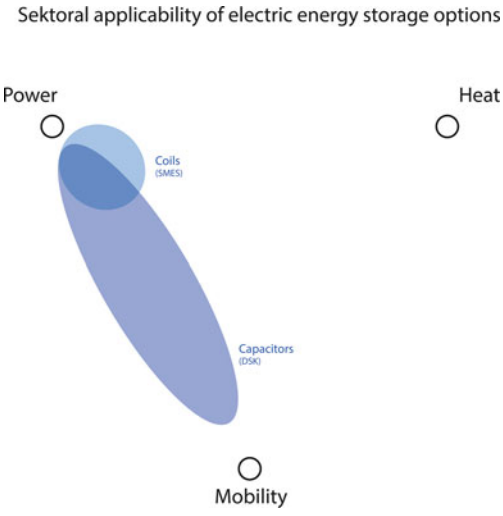



**Fig. 12.3** Application areas for electric-energy storage systems, such as capacitors and coils in the electricity, heating, and transport sectors

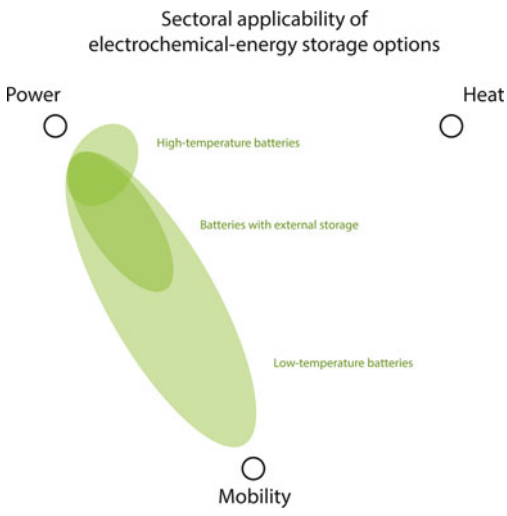



**Fig. 12.4** Electro-chemical energy storage application areas in the electricity, heating, and transport sectors

developed and perfected technologies. These batteries are essential components of uninterruptible power supply (UPS) systems in crucial infrastructure facilities such as power plants and hospitals (lead-acid and nickel batteries in particular). Outside the electricity sector, these systems are currently used for 'power storage' to supply short-term balancing energy, and increasingly in electro-mobility.

### 12.2.3 Mechanical-Energy Storage Systems—Pumped-Storage, CAS, and Flywheel Storage

Mechanical-energy storage systems that use pumped-storage or CAS differ significantly from flywheel storage. In the short-term range, the capacity and power of flywheel storage systems fall between electric storage systems and batteries. They have considerably higher capacities, but only slightly longer discharging durations than electric storage systems. There are a range of application areas for flywheel-energy storage systems. They are used as phase shifters to provide short-circuit capacity in the electricity network, for example, or for recuperating braking energy in the transport sector.

CAS systems have somewhat lower capacities than PSP over durations of a day. Like pumped-storage systems, CAS systems are bound to specific geographical sites, generally in northern Germany where caverns are located. They can be used to supply positive and negative balancing energy in the electricity sector. Because of their geographical concentration in Germany, they are often collectively termed 'pumped-storage north'.

Each pumped-storage facility has several gigawatt-hours of storage capacity, resulting in an enormous quantity of total storage potential. The facility dimensions depend on location conditions, and vary widely. They are typically used to supply or absorb balancing energy, and in some cases, for phase-shifting. Some PSP are also used to balance generation. Historically, most PSP have operated as short-term

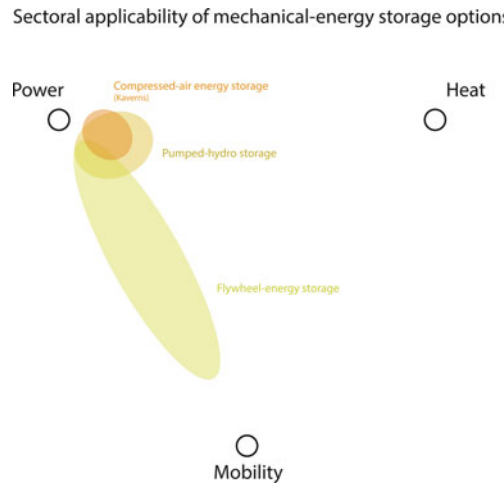



**Fig. 12.5** Mechanical-energy storage application areas in the electricity, heating, and transport sectors

storage facilities for balancing fluctuations over the day (day/night) with medium discharging durations ranging from six to eight hours. But some pumped-storage facilities are used for long-term storage with discharging durations of several days (Fig. 12.5).

### 12.2.4 Thermal-Energy Storage Systems—Thermal Storage

Thermal-energy storage systems include buffer systems in households having a few kilowatt-hours of capacity, seasonal storage systems in smaller local heating networks, and district heating systems with capacities in the gigawatt-hours. Latent and thermos-chemical thermal storage systems are generally used in niche applications, such as room air-conditioning (phase-change materials—PCM) or for thermal management in dishwashers (zeolite).

Various charging technologies can also be used to integrate them into the electricity and heating sectors (Fig. 12.6). For example, daily storage systems as well as electricity-oriented combined heat and power (CHP) generation facilities or heating plants can be used to buffer intermittently available heat from solar-

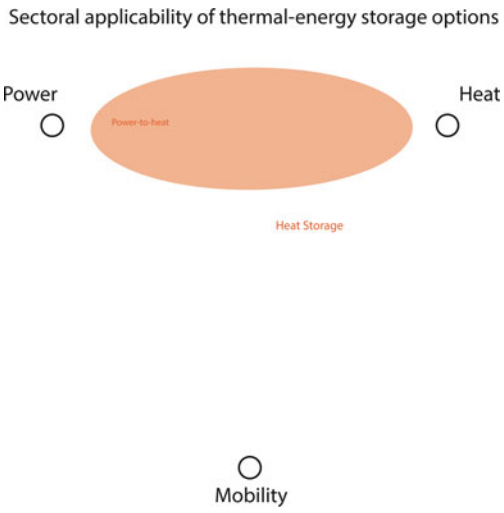



**Fig. 12.6** Thermal-energy storage application areas in the electricity, heating, and transport sectors

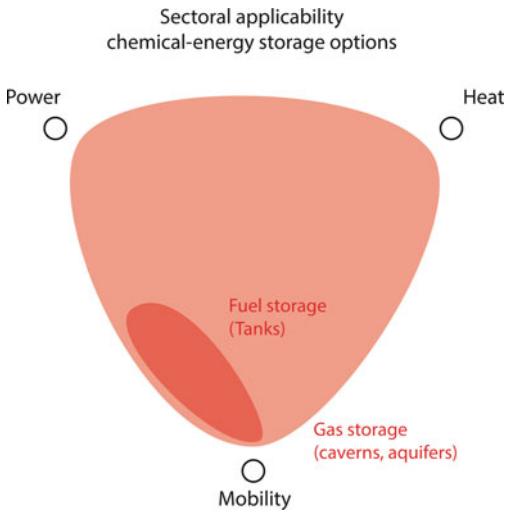



**Fig. 12.7** Chemical-energy storage application areas in the electricity, heating, and transport sectors

thermal power plants. These same facilities can also absorb electricity surpluses from the electricity network using storage stoves, electric resistance heating (power-to-heat—PtH), or electric heat-pumps. In the transport sector, they are used only for special applications. An example is the use of PCM materials for engine block preheating.

The most common application by far is buffer storage in households—mainly for fossil energy, but in the future increasingly for solar heat, bioheat, and geothermal energy.

### 12.2.5 Chemical-Energy Storage Systems—Power-to-X (PtX)

Chemical-energy storage in the form of biomass, coal, and gas is crucial for the current energy generation system. It will also be an essential component of the future renewable energy system. With each facility ranging in the terawatt-hours, chemical-energy storage has by far the largest capacity. It is also the only option for seasonal energy storage using the charging technology PtG in combination with the existing gas infrastructure for storing and converting gas into electricity.

Energy stored in the form of hydrogen or methane can be used by all three sectors—electricity, heating, and transport (Fig. 12.7). There is already a large existing infrastructure for transporting, distributing, and exploiting methane in gas-fired boilers and CHP in the heating sector; in gas vehicles and gas ships (liquefied natural gas—LNG) in the transport sector; and in gas turbines, combined-cycle gas turbine plants (CCGT), and CHP in the electricity sector. The infrastructure for hydrogen is still under development, and currently only available in chemistry parks. Surplus energy from renewable energy sources can be temporarily stored in the gas network or in gas storage facilities, and then supplied to other locations when demand is higher.

Only chemical-energy storage can combine energy storage and energy transport at this scale. The transmission capacity of a large gas pipeline is about ten times greater than that of a high-voltage transmission line. There is also significantly greater public support for expanding the gas network than for expanding the electricity network. But electricity transmission

is more efficient than converting electricity into gas and then transporting the gas. Expansion costs and operations could be minimized by synchronizing the two networks. The strengths and weaknesses of electricity networks and gas networks complement each other quite well.

Another option with chemical-energy storage is to convert electricity into basic chemical materials (methanol) or liquid fuels (power-to-liquid—PtL). These liquid fuels would be particularly useful in transport segments requiring high-energy densities such as aviation.

### 12.2.6 Load-Management

Load-management is not directly a storage technology, but it can serve some storage functions. Precisely activating and shedding loads can result in effects similar to the effects of storage, but at much lower costs. For example, positive and negative balancing energy can be supplied by activating or deactivating loads at the correct moment, temporally shifting electricity demand as a result.

Depending on which technology is regulated (for example, cooling units, heat pumps or storage units in electric vehicles, and machinery), load-management could be implemented in the three sectors: electricity, heating, and transport (Fig. 12.8). With the exception of electric trains, electro-mobility is still a minor element of the transport sector. As a result, the potential for load-management here is currently limited. But large connection capacities could be achieved in the heating sector by fully exploiting storage stoves, electric heat-pumps, and PtH for load-management.

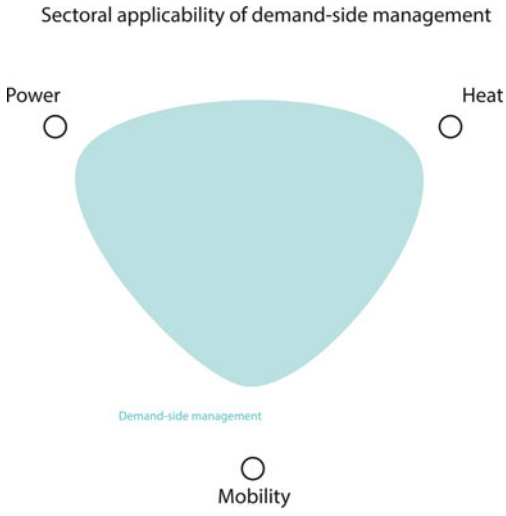



**Fig. 12.8** Load-management application areas in the electricity, heating, and transport sectors

## 12.3 Comparison of Costs, Efficiency Levels, and Energy Densities

Based on the previous section's discussion of the various technologies, this section briefly compares the relevant technical parameters with the economic parameters. Figure 12.9 compares the volumetric energy density $w_V$, efficiency $\eta$, and specific capital costs $k_0$ of the various storage technologies discussed in this book.

### 12.3.1 Comparison of All Storage Systems by Cost, Efficiency, and Energy Density

These three parameters have been chosen from a range of important parameters. Other parameters are also relevant. These include the parameters for storage systems listed in Table 12.1 and defined in ▶ Chap. 2. Among these are the storage capacity $W$ in W h and the discharging duration $t_{dis}$ in hours discussed in ▶ Sect. 12.2. Cycle life is also a decisive factor for the cost-effectiveness of storage systems. As a result, the following are only descriptive statements. They are based solely on capital costs, and do not take fully into account the cycle life. This means that this illustration considers just three of many important characteristics that significantly im-

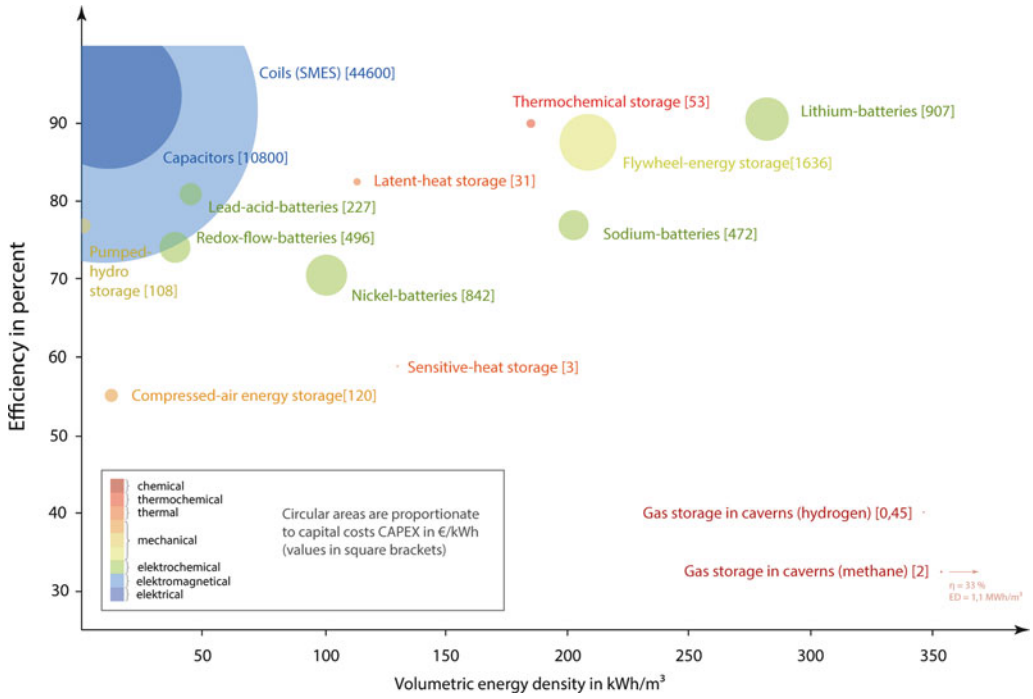



**Fig. 12.9** Capital costs compared to energy density and efficiency for various storage technologies. The $y$-axis here starts at 30%. Methane-cavern storage located on the $x$-axis is actually off the scale

pact the cost-effectiveness and usefulness of a storage system.

The efficiency of a technology indirectly affects its resource consumption. Due to resource shortages, climate change, and environmental risks, efficient technologies are preferable to less efficient solutions, as long as other crucial parameters such as environmental friendliness (for example, toxicity), cost, and soft criteria such as public acceptance do not prohibit their use.

Another key factor with many applications is the storage system's volumetric energy density (in kW h/m$^3$). Technologies with low volumetric energy densities cannot be used for mobile applications or applications where space is limited. This is why it has been chosen as the second parameter in this comparison.

The third parameter is cost of facility construction in relation to the capacity (specific capital costs $k_0$). Aside from the cycle life and the fixed as well as variable operating costs, these are the most important factors determining cost-effectiveness.

Other parameters from Table 12.1 such as reaction time, service life, and cycle life are also referred to in the following discussion.

### Electric-Energy Storage Systems

The large circles for electric-energy storage systems (capacitors and coils) stand out in Fig. 12.9. This is because of their high-efficiency levels and high costs. Because of their very low volumetric energy densities, they are located in the upper left.

With energy technology, extremely fast reaction times result in dramatically higher costs. At 12,000 to over 62,000 € per installed kilowatt-hour, the specific capital costs for capacitors and coils are over ten times higher than for all other available storage technologies. In addition, the highest efficiency levels come with the lowest volumetric energy densities, primarily because so little energy is stored. But the

cycle lives of electric-energy storage systems are over a million, exceeding all other storage technologies. As a result, in special applications with a high number of cycles, they may be cost-efficient (Table 12.1). This demonstrates how limited the applications are for this technology: the technology is appropriate for applications that efficiently store electricity over very short periods of time and release it extremely quickly.

### Electro-Chemical Energy Storage Systems

Because the energy densities of batteries vary considerably, they are distributed across the entire graph with efficiency levels ranging from 70 to 95%.

In comparison with other storage systems, the capital costs of the electro-chemical storage systems considered here (lead-acid, redox flow, nickel, sodium, and lithium batteries) fall somewhere in the middle, and range from about 230 to 950 €/kW h. The various battery types primarily differ in terms of their volumetric energy densities. This is because the theoretical energy density of a battery is determined by where the elements used in the battery are located in the voltage series (▶ Sect. 7.1).

With efficiency levels exceeding 90%, lithium batteries are the most efficient. Their volumetric energy densities of around 270 kW h/m$^3$ also make them particularly compact storage systems. But compared to other batteries such as lead-acid batteries, they have the highest specific costs. Most battery storage systems have a cycle life ranging from 760 to 1,200 cycles. The exception here is redox flow technology, because in these batteries, the charge is stored separately in an external storage unit and they have cycle lives of around 5,000 cycles.

### Mechanical-Energy Storage Systems

Mechanical-energy storage systems vary widely in terms of their efficiency, energy density, and capital costs.

Flywheel-energy storage systems have superior efficiency levels and energy densities. But like lithium batteries, they also have the highest costs in their group. Similar to electric storage systems but unlike other technologies with similar energy densities, they can be used for applications in the millisecond to minute range.

Pumped-storage is a fully-developed technology with low capital costs per installed unit of power. But at levels of around 75%, the efficiency of pumped-storage is only average compared to other storage systems. The volumetric energy density is very low, and increases only marginally as the difference in elevation between the upper and lower reservoirs rises. As a result, the system is bound to a few selected geographical sites. The advantage of this system is its potential storage capacity, which is the largest among short-term storage systems.

The capital costs of CAS systems are basically the same as for pumped-storage systems. But the slightly larger energy densities with this system cannot compensate for the low efficiency levels below 55%. This is because the CAS systems currently in use rely on fossil energy in the form of natural gas. In addition, conventional CAS systems can only be built where caverns are found. An exception is isothermal CAS using a combination of pneumatics and hydraulics. These smaller, modular systems could be used for decentralized applications. But the technology is still mostly in the development phase.

All mechanical-energy storage systems have a high-cycle life, and as a result, higher efficiency levels. Pumped-storage systems, for example, have very long service lives exceeding 80 years. Some existing facilities are over 100 years old.

### Thermal-Energy Storage Systems

Thermal storage systems have the lowest costs. With costs of only around 2 €/kW h, the circle for sensible-thermal storage systems such as buffer storage and district heating is particularly small on the graph. These systems are the only ones with costs comparable to chemical storage systems. But as with chemical storage using PtG, they lose a large amount of the energy stored through self-discharge. As a result, they have efficiency levels of only 60%.

Latent-thermal storage systems and thermochemical storage systems are more efficient, but they also cost more. The volumetric energy densities of thermal storage systems are only average, and range between 130 and 170 kW h/m$^3$. Thermochemical storage systems have the highest efficiency levels and energy densities. This again confirms that chemical bonds have the greatest potential for energy storage.

### ■ Chemical-Energy Storage Systems

Chemical-Energy storage systems such as cavern storage have very low pure storage costs, ranging from around 0.5 to 2 €/kW h. The circles for hydrogen and methane are very small on the graph. Storage of methane (natural gas) using PtG has the highest volumetric energy density of all the storage technologies discussed in this book: about 1,100 kW h/m$^3$. This circle is not to scale on the graph. The energy density of hydrogen storage in caverns is also quite high at around 350 kW h/m$^3$.

But because the electricity must be converted into hydrogen or methane and then compressed to working pressures, these systems have low efficiency levels and high costs. This is not taken into account in ◘ Fig. 12.9.

Aside from maintenance required by peripherals, cavern storage systems have unlimited service lives.

### ■ Summary

Energy storage systems are used by a range of application areas with various efficiency, energy density, and cost requirements. This means that the options for effectively comparing energy storage systems using different technologies are limited.

## 12.3.2 Comparison of Electricity Storage Systems Costs by Cycle Duration

◘ Figure 12.10 shows the range of electricity-shifting costs for a kilowatt-hour with the three most common electricity storage systems according to [58]: pumped-storage, battery power plants using lithium technology, and PtG using methane.

### ■ Assumptions

The costs include:

- Capital costs for the storage system (in relation to energy in €/kW h and in relation to power in €/kW).
- Capital costs for facility construction (annuities, interest).
- Costs of storage losses.

Other factors include the frequency of storage use, service life, and specific self-discharge. The figures used are taken from ▶ Sect. 12.1. The range of costs is determined by all of these factors together with the varying cycle durations. For all storage systems, one kilowatt-hour of storage per cycle was used as the comparison criterion. The electricity purchase costs were assumed to be neutral at 0 €/kW h. This means that only the costs for temporally shifting the electricity were taken into account.

Since the charging unit is the same as the discharging unit with lithium-ion batteries and PSP, these costs are only incurred once. The total costs in relation to capacity for battery storage systems are about 1,000 €/kW h, but for porous storage systems only about 0.1 €/kW h. With PtG technology, both the charging unit for electrolysis and methanation as well as the discharging unit for reconversion to electricity must be taken into account. Based on electricity generation costs at a gas power plant, these costs were set according to [58] at 8.65 cents per discharged kilowatt-hour. These costs are in addition to capital costs determined by the cycle life.

### ■ Merit Order of Electricity Storage Systems

In a specific cycle duration range, each of the electricity storage systems PSP, lithium-ion batteries, and wind gas have a different cost advantage distinct from the others.

- The optimally cost-effective cycle duration for battery storage systems is under an hour. These facilities can react to very quick

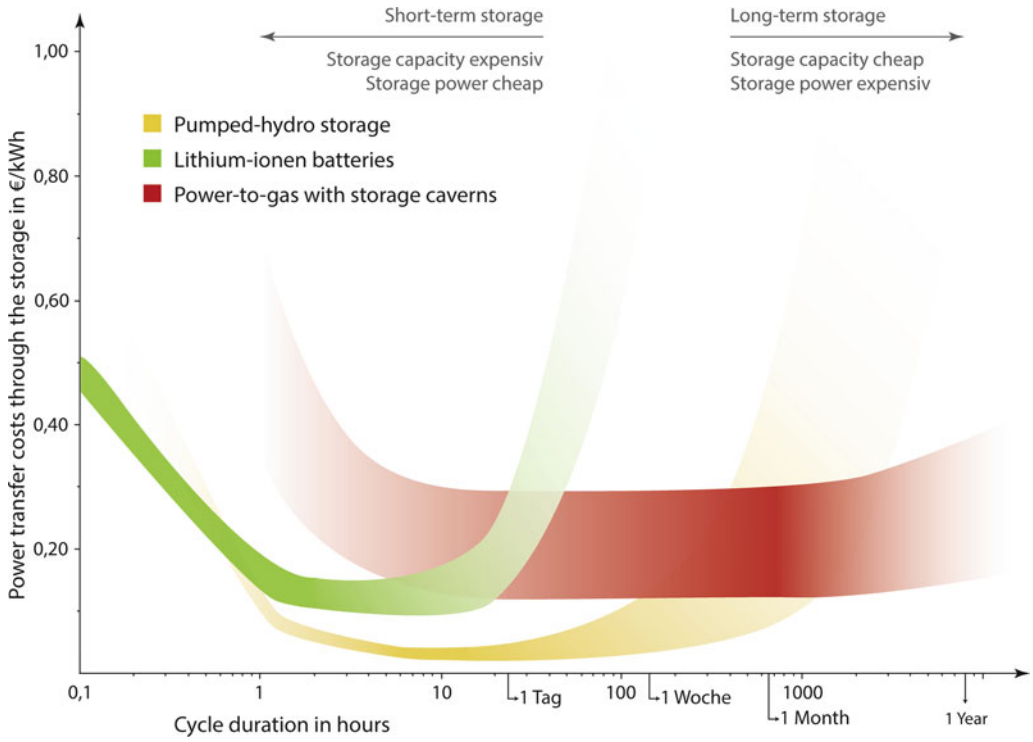



**Fig. 12.10** Comparison of costs for one kilowatt-hour of storage, taking into account cycle duration with PSP, battery power plants using lithium technology, and PtG using methane in cavern storage [58]

12

load changes, and as a result, stabilize the electricity network over the very short-term (voltage quality, voltage maintenance, short-circuit capacity supply, instantaneous reserve (IR), primary balancing power—PBP).

- PSP are the cheapest electricity storage systems for cycle durations ranging from about an hour to several days. Historically, these systems have been cycled daily. They are increasingly used by the reserve and balancing energy markets. A very small number of PSP in Austria can also be cycled weekly. Similar to batteries with durations above several hours, for geological and financial reasons, the cost curves for PSP result in very high expenses with durations above a month. As a result, PSP is not relevant at these durations.
- PtG is the cheapest electricity storage system for cycle durations ranging from about a week to a month. This is because their capital costs in relation to energy are by far the lowest, and because they have negligible self-discharge rates. Storage capacities at this scale would be unaffordable with battery power plants, and geologically impractical with PSP. Gas storage systems can be operated in partial cycle durations in the short-term range. But because PtG is about half as efficient, in this range it is significantly more expensive than batteries or pumped-storage. Since electrolyzers have short reaction times, short-term surpluses could still be absorbed by PtG for long-term storage without efficiency losses.

## Summary

Greater focus on short-term storage increases the emphasis on cost for power while reducing the emphasis on cost for capacity. Even under

**Table 12.2** Technology readyness level (TRL) [41]

| | | |
|---|---|---|
| TRL 1 | Basic research | Study and analysis of the operating principle |
| TRL 2 | Basic researchFeasibility studies | Analysis of the technology application |
| TRL 3 | Feasibility studiesTechnology development | Testing the functionality of the technology |
| TRL 4 | Technology development | Test set-ups in the laboratory |
| TRL 5 | Technology developmentDemonstration | Test set-ups in the application environment |
| TRL 6 | DemonstrationSystem development | Prototypes in the application environment |
| TRL 7 | System development | Prototypes in operation |
| TRL 8 | System developmentStart-up, operation | Qualified system with proven functionality in the application area |
| TRL 9 | Start-up, operation | Qualified system proven through successful operation |

the currently prevailing cost structure, at durations under an hour, battery storage systems are preferable to established pumped-storage systems. As costs for battery storage fall, they will become even more attractive for durations up to several hours. But for durations ranging from 6 to 12 hours, pumped-storage will remain the cheapest form of daily storage.

The opposite holds when the focus is on long-term storage. Here PtG is particularly cost-effective. This is because it is the only long-term storage technology that can process large quantities of energy over the long-term, and store it cheaply over long periods with practically no losses. In comparison to pumped-storage and battery power plants, PtG is the cheapest form of long-term electricity storage [58].

This means that these three technologies and their costs complement each other.

## 12.4 Strengths, Weaknesses, and Stages of Development

### 12.4.1 Energy-Storage System: Stages of Development

One method of describing the development levels of various technologies is the 'technology readiness levels' (TRL) classification system described in Mankins 1995 [41]. This system determines levels of development ranging from technology in the basic research phase to technology currently in operation (Table 12.2).

Figure 12.11 shows the readiness levels of all the energy storage options discussed in this book. The levels were determined by conducting specialist interviews and surveys. A large number of storage technologies are already qualified systems proven through successful operation, and classified as level TRL 9. Technologies such as lithium batteries, PtH, and latent-thermal storage are at level 8. Chemical methanation is between levels 7 and 8. Coils are currently the least developed technology. They have only been studied as test set-ups and prototypes in the application environment. All the other systems are at levels ranging from system development to start-up.

### 12.4.2 Strengths and Weaknesses of the Various Technologies

Most storage technologies could still be improved. The only fully perfected technologies are PSP, some electrochemical-storage systems such as lead-acid batteries, sensible-thermal

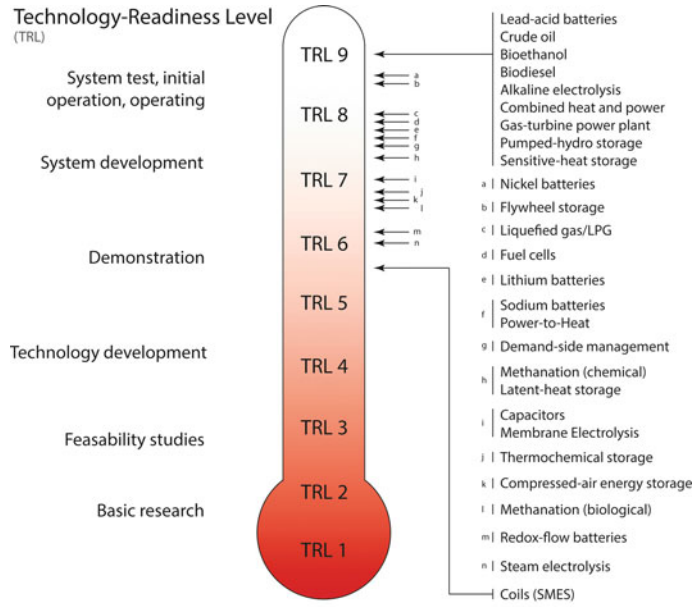



**Fig. 12.11** Technology readiness of various energy storage systems

12

storage systems, and caverns or porous storage for methane gas.

As summarized in Table 12.3 based on [20], and using the information found in Table 12.1 as well as in information the technology chapters in Part III, each technology has its advantages and disadvantages or strengths and weaknesses.

## 12.5 Cost-Reduction Potential with Batteries and PtX

The current focus of storage development and research is on batteries and PtX. This section analyzes cost trends and potentials with these technologies. The discussion takes into account current developments and assumes a future learning curve. Lithium batteries are used as an example from the battery technologies covered in ▶ Chap. 7. PtG is used as an example from the chemical storage technologies defined as PtX in ▶ Chap. 8.

### 12.5.1 Cost Trends and Potential with Lithium Batteries

#### ▪ Current Cell Price Trends

Led by electro-mobility and battery power plants, in the last five years, costs for lithium-battery storage systems have fallen significantly. From 2007 to 2016, prices for lithium-ion cells dropped almost 60% (Fig. 12.12). This is equivalent to an annual price reduction of around 6.5% [67].

In addition, current studies assume that cell prices for lithium-ion batteries will fall below 200 €/kW h in the next five years. The cost per unit of usable storage capacity is largely determined by the number of cells and the storage size (MW or kW range).

**Table 12.3** Strengths and weaknesses of various storage technologies based on [20] and summarized using information found in Table 12.1 as well as information found in the technology chapters in Part III

| Technology | Strengths and possibilities | Weaknesses and obstacles |
|---|---|---|
| **Electric-energy storage systems** | | |
| Capacitors | – Very high-efficiency<br>– High power capacity<br>– Long cycle life<br>Suitable for applications with extremely high-reaction time requirements (for example, voltage quality) | – Low-energy density<br>– High costs per installed unit of energy<br>– Storage batteries can be used for high power applications |
| Coils (SMES) | – High power capacity<br>– High-cycle life<br>– New superconducting materials<br>– Suitable for supplying decentralized short-circuit capacity | – Enormous cooling requirements<br>– Expensive materials required for superconductors<br>– High costs (measurement electronics, cooling)<br>– Security requirements (low temperatures, strong magnetic fields)<br>– Inadequately tested<br>– High-specific capital costs |
| **Electrochemical-energy storage systems** | | |
| *Low-temperature batteries* | | |
| Lead-acid batteries | – Best established battery technology<br>– Cheap battery system with short amortization periods<br>– Energy and power densities suitable for stationary applications<br>– Very safe compared to lithium or sodium batteries<br>– No complex cell management required<br>– Tried and tested worldwide<br>– In use for 150 years<br>– Fully automated bulk production could decrease costs<br>– No site-specific conditions required<br>– Many manufacturers worldwide<br>Cheap storage system for stand-alone networks | – Asymmetric charging and discharging capabilities<br>– Damaged by deep-discharging<br>– Long idle periods in low states of charge<br>– Good temperature management required<br>– Battery room ventilation required<br>– Limited cycle life<br>– Less competitive as costs for lithium batteries fall<br>– Limited lead deposits available |
| Nickel batteries | – Very long cycle and service lives (low dendrite formation)<br>– High-energy density<br>– Suitable for high power area applications<br>– Suitable for use with consumer applications and hybrid vehicles<br>– Can be used at low temperatures and under extreme environmental conditions<br>– Tolerant of deep-discharge and different states of charge | – High nickel costs<br>– Less competitive as costs for lithium batteries fall |

**Table 12.3** (Continued)

| Technology | Strengths and possibilities | Weaknesses and obstacles |
|---|---|---|
| **Electrochemical-energy storage systems** | | |
| *Low-temperature batteries* | | |
| Lithium batteries | – Highest-energy density<br>– Highest efficiency<br>– High power capacity<br>– Bulk manufacture reduces price<br>– No special site requirements<br>– Suitable for stationary and mobile applications (battery parks and electro-mobility)<br>– Greatest potential among batteries for cost-reduction and broad use<br>– Development of new active materials | – No inherent safety mechanism (thermal-runaway)<br>– Expensive battery management system required for safety and long service-life<br>– Individual cell monitoring<br>– Manufacture (packaging) and cooling required<br>– Fast-charging capability<br>– Limited service life at charges outside 30 to 70%<br>– High costs<br>– Low public acceptance because lithium disposal required<br>– Limited lithium reserves |
| *High-temperature batteries* | | |
| Sodium batteries | – High-energy density<br>– Long cycle- and service-lives<br>– Many existing stationary facilities<br>– Many expired patents, new manufacturers<br>– No local requirements<br>– Cheap materials (sodium and sulfur)<br>– Almost unlimited supply of materials | – High costs for heating and cooling<br>– Thermal losses<br>– High self-discharge with longer idle periods<br>– Safety hazards caused by high-operating temperatures<br>– Few manufacturers<br>– Competes with lead-acid and Li-ion batteries<br>– Safety issues (fire)<br>– Sodium must be isolated from elements in the environment (particularly water) |
| *Batteries with external storage* | | |
| Redox flow batteries | – Independently scalable energy and power<br>– Storage container physically separate from reaction cell<br>– High-cycle life<br>– Different redox pairs can be used<br>– New material combinations continually developed—no shortage of resources<br>– Improvements in materials could result in efficiency levels up to 90% and lower costs<br>– Independent of location<br>– Many expired patents, increasing competition<br>– Cost-effective, particularly with high capacity to power ratios (4:1 to 10:1) | – Low-energy density<br>– Acidic liquids cause leakage<br>– Expensive storage media<br>– Pump-maintenance costs<br>– Pump-electricity consumption<br>– Legal problems obtaining permits for the use of large quantities of acid |

**Table 12.3** (Continued)

| Technology | Strengths and possibilities | Weaknesses and obstacles |
|---|---|---|
| **Chemical-energy storage systems** | | |
| *Conventional chemical-energy storage systems* | | |
| Liquid gas/liquefied petroleum gas (LPG)<br>Crude oil | – Fully-developed technology<br>– High-energy density<br>– Available infrastructure<br>– Available application technology | – All fossil energy source disadvantages (climate change, environmental risks, import dependency, limited resources, etc.) |
| *Biofuels* | | |
| Bio-ethanol<br>Biodiesel | – Well-developed technology<br>– Available infrastructure<br>– High-energy density<br>– Available, affordable vehicle technology | – Large areas required for production<br>– Competes with food and feed production<br>– Limited sustainability |
| *PtG* | | |
| Hydrogen storage | – Only option for long-term storage aside from methane<br>– Low space requirements<br>– Very large quantities of energy can be stored<br>– High-energy density<br>– Limitless supply of water<br>– Alternative to biogas (land use and monocultures)<br>– Hydrogen can be used in all energy sectors<br>– The liquid hydrogen carrier-material (LOHC) can be used in the existing liquid-fossil energy source infrastructure | – High costs<br>– Low efficiency<br>– A third of the storage density of methane<br>– No hydrogen turbines<br>– Competes with other long-terms storage systems (for example hydro-power in Scandinavia) and flexibility options<br>– Competes for cavern storage with compressed air, oil, natural gas, or $CO_2$<br>– Direct feed-in of hydrogen into the natural gas network limited to a 2% maximum<br>– Costly construction of hydrogen infra-structure required (transport, distribution, applications) |
| Methane storage | – Only option for long-term storage aside from hydrogen<br>– Low space requirements<br>– Very large quantities of energy can be stored<br>– Very high-energy density<br>– Higher-energy density means lower costs in relation to energy compared to hydrogen storage<br>– Energy storage and transport possible using gas infrastructure<br>– Very large storage capacities<br>– Alternative to biogas (land use and monocultures)<br>– Limitless supply of water<br>– Flexible utilization in all energy sectors with existing, affordable end applications | – $CO_2$ source required or $CO_2$ must be extracted from the air<br>– High costs or additional costs for methanation and $CO_2$ supply<br>– Low efficiency<br>– Competes with other long-terms storage systems (for example, hydro-power in Scandinavia) and flexibility options<br>– $CO_2$ methanation technology minimally developed |

**Table 12.3** (Continued)

| Technology | Strengths and possibilities | Weaknesses and obstacles |
|---|---|---|
| **Mechanical-energy storage systems** | | |
| PSP | – Fully-developed, established technology<br>– Very long service-life<br>Low self-discharge<br>– Good efficiency<br>– Large potential in Norway and Sweden<br>– Low storage costs<br>– Some plants can also be used for long-term storage | – Very low-energy density<br>– Geographically limited<br>– High capital costs<br>– Slow return on investment<br>– Only large facilities are cost-effective<br>– Long authorization procedures<br>– High standard of environmental requirements<br>– Increasing competition with other storage systems (battery parks in particular)<br>– Not always accepted by the public |
| Compressed air energy storage (CAES) | – Relatively low costs for the storage units (caverns)<br>– No space required at the Earth's surface<br>– Long service lives of the storage units (caverns), compressors, and turbines<br>– Low self-discharge<br>– Good correlation between high-wind areas and cavern locations<br>Promising new decentralized concepts (for example isothermal, or using hydraulics) | – Geographically limited<br>– Geological requirements (gas-tight, etc.)<br>– High capital costs<br>– Low efficiency<br>– Only two pilot facilities in operation and no adiabatic power plants<br>– Slow return on investment<br>– Competes for cavern storage space with hydrogen, oil, natural gas, and $CO_2$<br>– Increasing competition with other storage systems (battery parks in particular) |
| Flywheel storage | – High-efficiency<br>– High-energy density<br>– Fast-charging capability<br>– Low maintenance costs<br>– Long service-life<br>Potential applications for UPS, short-circuit capacity, and mobility | – Vacuum chamber required<br>– Safety risks (rotating masses)<br>– Cooling system for superconducting magnetic bearing<br>– High self-discharge<br>Competing technologies |
| **Thermal-energy storage systems** | | |
| Sensible-thermal storage (buffer storage, district-heating storage) | – Cheap storage units<br>– Established, proven, simple technology<br>– Many facilities in operation<br>– Often used with solar energy<br>– Required for geothermal energy, heat pumps, and increasing CHP flexibility<br>– Potential applications with district heating, heating networks, and long-term storage | – Only average efficiency<br>– High self-discharge in stand-by mode |



The usable storage capacity is determined by the given rated capacity multiplied by the permitted depth of discharge (DOD). Not all systems have the same DOD. Lead batteries can be discharged only to about 50%. Lithium batteries show minimal wear when discharged to 20% of the state of charge (SOC), i.e., to a DOD of 80%. Some manufacturers integrate charging

**Table 12.3** (Continued)

| Technology | Strengths and possibilities | Weaknesses and obstacles |
|---|---|---|
| Latent-thermal storage (PCM) | – High-efficiency<br>– Low capital costs<br>– High-energy density<br>– Potential use with air-conditioning and specialized applications<br>– Large development and research potential | – Not established<br>– Only average energy density |
| Thermochemical storage | – Very high-efficiency<br>– Low capital costs<br>– Could be used with specialized applications, thermal transport with zero losses, and long-term storage<br>Large development and research potential | – Not established |

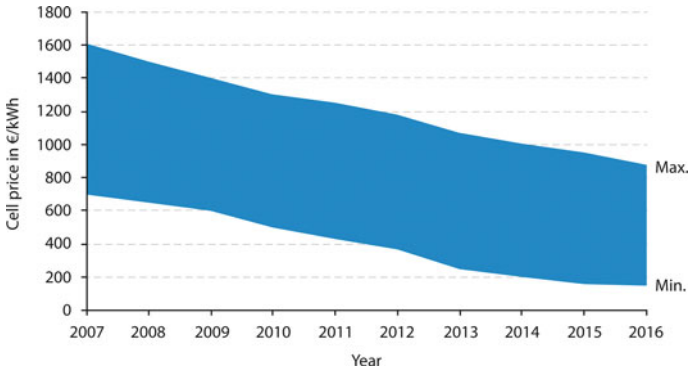



**Fig. 12.12** Change in lithium-ion cell prices from 2007 to 2016 [67]

and discharging limits into their battery systems, and then specify the DOD as 100%. In reality, this is equivalent to a DOD intrinsic to the system of at most 70 to 80%.

In addition, the following distinctions are crucial in comparing the prices and costs of battery storage systems:

**Cell:** – individual cells.
**Battery pack:** – several cells including safety technology (usually a battery management system).
**Battery system:** – 1-x battery packs connected together, including peripherals and monitoring (power inverter, user interface, energy-management system, etc.).

With energy technology, costs are also typically distinguished from prices (excluding/including dealer margins and installation costs).

As a result, here battery power plants are discussed separately from household battery storage systems. In addition, peripherals, transport, service, installation costs for household battery storage systems, and consumption charges for the power converter are all included in costs [53].

### Battery Power Plants/Large Battery Storage Systems

Costs for large battery storage systems above 1 MW (also called battery power plants) currently range between 1,000 and 1,200 €/kW [60]. For example, total costs for the 5 MW WEMAG/Younicos AG power plant were around 6.5 million € including a 1.3 million € grant from the German Federal Ministry for the Environment [63]. This means that the costs for the power plant were 1,300 €/kW. Since cell prices have fallen since then, today

this battery power plant could be built without the grant.

### Household-Battery Storage/Household Storage

Driven by falling prices and the KfW Bank incentive program, there is currently growing interest in Germany in household-battery storage systems with small capacities in the kW h range. The incentive program funded around 23,550 facilities by the end of 2016 [55].

**Example**

Currently, prices for household-battery storage systems vary widely by size and manufacturer. The average cost of a battery system including the system and installation costs is around 1,800 €/kW h [26, 60]. For example, the American company Tesla advertises a price of 360 €/kW h for a 10 kW h module and around 450 €/kW h for a 7 kW h module (assuming an exchange rate of 1.1 USD = 1 EUR) [56]. But these are only the wholesale prices for the costs of the battery block including the battery management system. These costs exclude the costs of the power inverter, installation, dealer margins, and other components. The power converter alone increases the costs of the Tesla system to around 750 €/kW h [26, 32].

The full costs for the 7 kW h module for PV household storage are estimated at 10,600 $, or 9,640 €:

- Battery block: 3,500 $
- Power converter: 2,000 $
- Energy manager: 500 $
- Measuring equipment: 400 $
- Color display: 500 $
- Installer/reseller margins: 1,800 $
- Installation costs: 1,900 $

The estimated installation costs are high because the system is composed of many individual components. In this example, the system price is around 1,377 €/kW h of installed storage capacity, about 25% lower than German system prices.

But a more precise comparison of costs would also take into account the costs for one kW h of stored energy, which in turn requires taking into account the DOD, the cycle life, and the service life. These last three factors are decisive for calculating costs.

Tesla offers a ten year guarantee on its battery blocks. If used for daily cycling with a PV system, this would amount to a total of 3,650 cycles. Tesla estimates the cycle life at 5,000 cycles. A simple comparison of the manufacturer specifications demonstrates that, from this point of view, costs are largely determined by service life and cycle life (Table 12.4).

### Development of Costs and Energy Densities with Lithium Batteries

Figure 12.13 shows the development of technical and economic parameters for lithium technology until 2050, as predicted in a study. The study assumed that there would be a breakthrough in Li-air or Li-sulfur around the year 2025. Since system costs are largely determined by cell costs, the costs given here are based on the cell cost figures.

The costs discussed in the standard literature apply to lithium-ion batteries for electromobility. These costs can also be applied to stationary systems [2]. According to these predictions, energy densities will be up to 300 W h/kg and cell prices relatively low for lithium-ion batteries by 2025. Assuming a breakthrough in new cell technologies, increased energy densities with modern lithium-based batteries will range from 700 to 1,000 W h/kg. Cell costs will also sink accordingly. In addition, service lives exceeding 15 years are predicted by 2050.

## 12.5.2 Cost-Reduction Potential with PtG

### Potential Cost-Trends with an Assumed Learning Curve

Capital costs for PtG using hydrogen or methane were determined by reviewing the relevant literature and from the survey of specialists conducted by the Forschungsstelle für Energienetze und Energiespeicher (FENES)

**Table 12.4** Comparison of electricity-shifting costs with a German household storage system (Sonnenbatterie GmbH) and an American household storage system (Tesla) (source: manufacturer specifications)

| | Sonnenbatterie eco | Tesla Powerwall |
|---|---|---|
| Installed storage capacity | 8 kW h | 7 kW h |
| DOD | 100% | 80% |
| Usable storage capacity (= installed storage capacity multiplied by DOD) | 8 kW h | 5.6 kW h |
| Cell alterations (end of life capacity losses) | -15% | -15% |
| Cycle life | 10,000 | 5,000 |
| End customer price (net price without installation) | 11,300 € (1,413 €/kW h usable capacity) | 7,900 € (1,411 €/kW h usable capacity) |
| Electricity-shifting costs (= specific end customer price divided by aging multiplied by cycle life) | 16.6 ct/kW h | 33.2 ct/kW h |

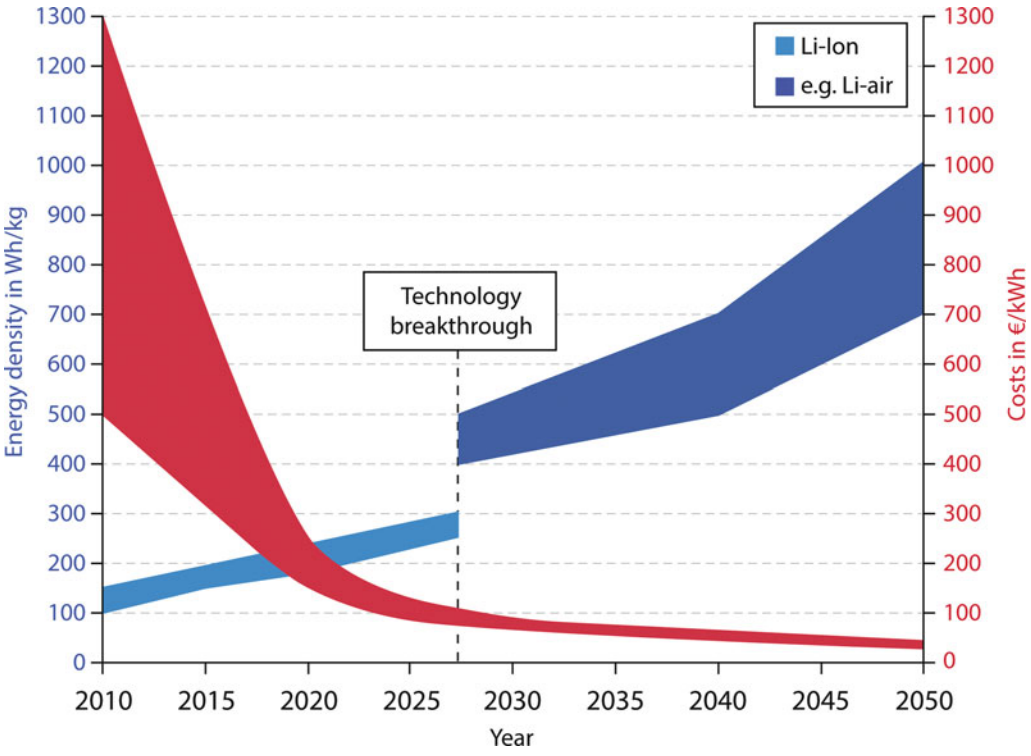



**Fig. 12.13** Development of technical and economic parameters for lithium batteries until 2050 [65]

(Table 12.5). Costs per installed unit of charging power (power) are distinguished from fixed operating costs (work), i.e., fixed costs per unit of stored energy. With PtG using methane, electrolysis and methanation together determine the costs for a charging unit.

**Table 12.5** Current spread of capital costs for PtG in the 100 kW to megawatt range [51]

| | Hydrogen ($H_2$) | | Methane ($CH_4$) | |
|---|---|---|---|---|
| | Min. | Max. | Min. | Max. |
| Power price in €/kW | 1,000 | 3,000 | 2,000 | 4,000 |
| Work price in €/kW h | 0.3 | 0.6 | 0.1 | 0.2 |

A crucial difference here is that with hydrogen, only cavern storage can be used for long-term storage. With methane, large porous storage can also be used. Since caverns must always be artificially constructed, the fixed costs for hydrogen are higher. Hydrogen can also be stored in aboveground pressurized containers. But since the quantities are small and the costs significantly higher, this method is not considered here (▶ Sect. 8.4).

The cost spread shown here was used as a basis for estimating future cost trends for installed power. The method used here assumed a specific learning curve: a reduction in capital costs by a certain percent each time the facility capacity doubled. For example, costs for photovoltaic (PV) drop significantly by 20% each time the global installed power doubles [18]. By contrast, costs fall for other fully-developed technologies with wide market acceptance only by single-digit percentages.

With chemical process engineering, an average and realistic learning curve results in reductions of 13%. This rate is about equal to the average rate for a progressive technology, such as PV, and above the conservatively estimated rate of 5% [6].

Based on this learning curve, the current cost spread shown in Table 12.5, and the maximum or minimum installed power with PtG for the predicted years, the power price for a facility in the years 2025 and 2035 could be determined (Fig. 12.14).

This shows that market developments will largely determine the validity of one of the chief arguments against PtG high costs. These two factors are mutually dependent. If the market is too small, then there are no investments in mass production and costs remain high. This is why economically important technologies such as PV have always received start-up funding. In the case of PtG a limited-time reduction in electricity costs would be an adequate incentive.

Costs are expected to fall dramatically after market entry and then even out at a low level.

### Cost-Reduction Potential of Using PtG in the Electricity System

Another study conducted by the Forschungsstelle für Energienetze und Energiespeicher (FENES) and Energy Brainpool on behalf of Greenpeace Energy determined that PtG has the potential to significantly reduce costs in a purely renewable energy system [58].

In the study, a trend scenario extending to 2050 that conservatively excluded alternative flexibility options examined two different electricity systems:

- Without PtG (wind gas): generation gaps are covered using gas power plants driven by natural gas, incurring costs for the gas as well as the $CO_2$ certificates. Compensation is paid for renewable electricity surpluses but they are not utilized, resulting in a renewable energy share of only 86%.
- With PtG (wind gas): compensation for renewable surpluses are purchased for 0 to 35 €/MW h, stored as wind gas, and then used by gas power plants to cover generation gaps without requiring $CO_2$ certificates. The electricity system is 100% renewable.

Additional costs are required at the beginning, but an electricity system with PtG would be cheaper than a fossil-based system by around 2035. According to the study, this would result in savings ranging from 12

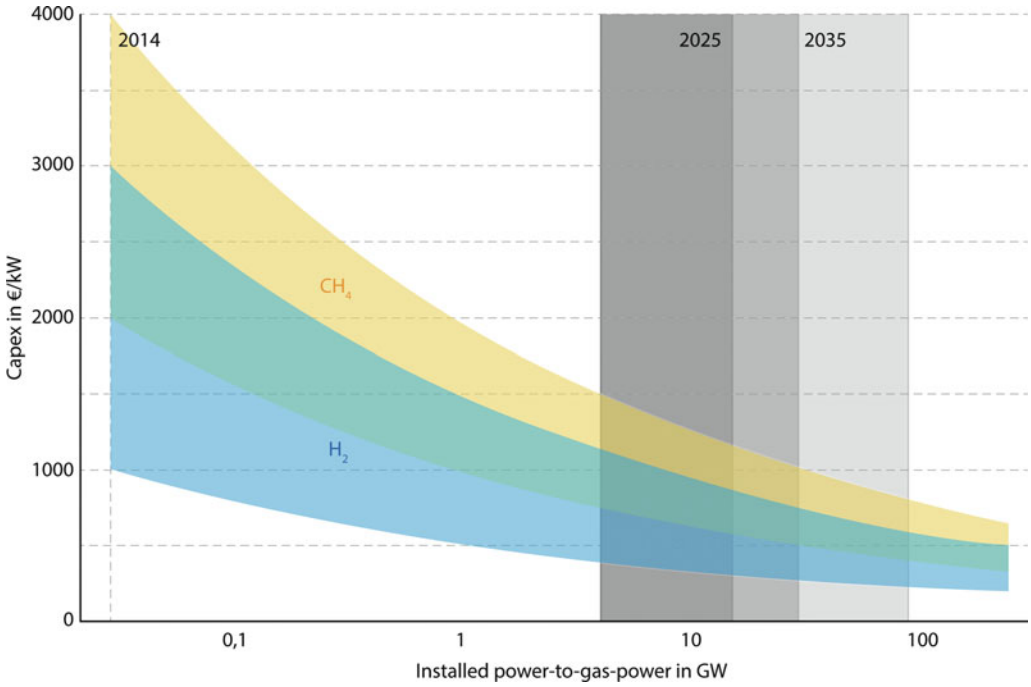



**Fig. 12.14** Comparison of cost trends for PtG using hydrogen (*blue*) and PtG using methane (*yellow*), assuming a realistic cost-reduction of 13% per doubling of the installed power. Based on the installed power given in [52], the shaded areas are the cost spreads for the years 2025 and 2035 [57]

to 18 billion € by 2050, depending on the rate of compensation for renewable electricity (Fig. 12.15). Given the boundary conditions assumed, these figures should be considered as maximums. But they still demonstrate that PtG could dramatically reduce costs.

## 12.6 Future Potential and Public Acceptance of Energy Storage Systems

### ▪ Energy Storage—The Achilles' Heel of Energy Transition

Energy transition depends on the utilization and expansion of wind and solar energy. These are the only sustainable energy sources with adequate technical and economic potential.

The central challenge with these energy sources is maintaining and storing the energy required. Fluctuations in wind and solar energy can be minimized but not eliminated in a large-scale electricity network. Depending on the weather, generation gaps of up to three weeks can be expected. These gaps cannot be covered, even if the facilities are massively oversized.

Ideally designed network expansion and load-management would also not be adequate to cover the gaps all across Europe. If no long-term storage is available, electricity generation would be forced to rely on fossil electricity generation such as gas turbines during these periods. This means that the Achilles' heel of sustainable energy supply is energy storage, ensuring that energy supply from these forms of energy is temporally and spatially balanced.

### ▪ Greater Public Acceptance of Energy Storage than of Other Elements in Energy Transition

The central challenges are communicating the goals of energy transition to the public as well as

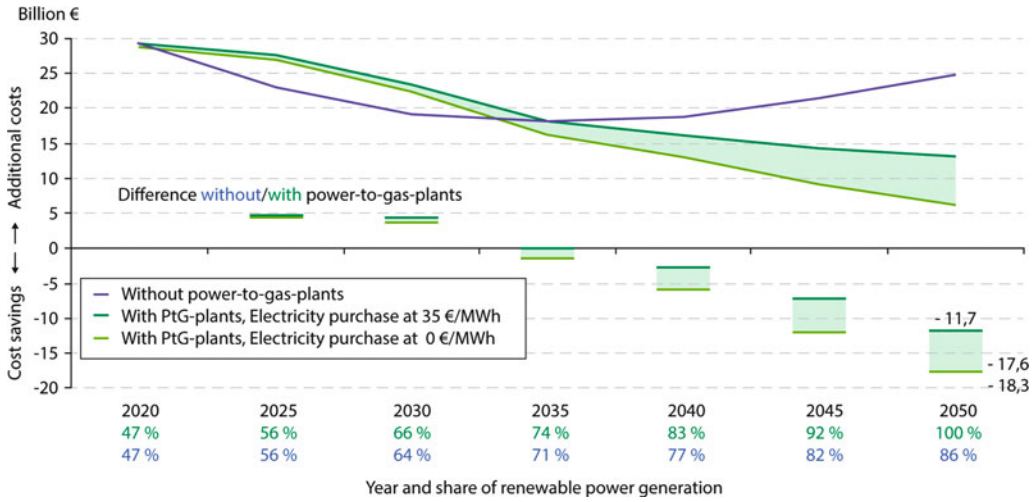



**Fig. 12.15** Costs for electricity generation with increasing shares of renewable energy in an electricity system (assumed compensation costs for electricity from wind/PV surpluses ranging from 0 to 35 €/MW h) with and without PtG (wind gas) facilities together with the cost differences between the two system alternatives. In this figure, the two scenarios are compared, taking only the different costs into account. In the system without PtG facilities, these costs are electricity costs for natural gas power plants and for curtailing wind and PV facilities. In the system with PtG facilities, these costs also included the capital and operating costs for wind gas facilities [58]

promoting public participation and acceptance. The specific issues are building new wind and solar facilities together with new power lines. Unlike these fundamental components of energy transition (with the exception of pumped-storage), energy storage enjoys wide public acceptance. This means that storage could play a crucial role when technically or economically preferable options are unavailable or cannot be implemented.

12

### Use of Short-Term Storage Systems Such as Pumped-Storage or Battery Parks

The largest daily fluctuations in PV can be balanced by using short-term storage. Suitable daily storage systems include large-scale pumped-storage and battery systems, ranging from household batteries to battery parks. CAS is another technically feasible option. But regenerative CAS requires a coherent heating concept. This concept is currently in the research and trial phases. As a result, this system will probably not be economically feasible in the near future. Capacitors, coils, or flywheel storage systems could be used in niches such as voltage quality, reactive power control, or short-circuit capacity. But short-term storage systems can only bridge supply gaps for short periods, and are not a replacement for long-term storage such as weekly or seasonal storage.

### Use of Long-Term Storage Such as PtG

In the past, energy sources with high-energy densities—i.e., fossil and nuclear energy sources—performed the function of long-term storage. But the potential of these sources is limited over the long-term, and they are associated with other problems. To protect the environment the use of fossil fuels must be minimized, and nuclear energy is no longer viable in some countries because of negative public opinion. The same is true for nuclear fusion, which shows little promise of becoming an economically viable option for energy supply anytime soon. This means that nuclear technology is not a solution to the problem of long-term storage, or a replacement for fossil fuels.

Scandinavian hydropower could be a solution for Europe, but public acceptance for

the electricity network expansion required is no higher there than in Germany. In addition, many of the storage water-power facilities would have to be converted to pumped-storage facilities mixing fresh and salt water. This presents significant technical and ecological challenges. The only national solution available in Germany is the exploitation and development of the existing natural-gas storage system by using PtG. This could supply 1,500 to 3,000 times the capacity of all German pumped-storage with a reconversion to an electricity rate of 28 to 60%. Storage of pure hydrogen is technically feasible, but the large amounts of energy required to pressurize the hydrogen makes it a less attractive option in this regard. In addition, hydrogen infrastructure is currently only available in the chemical industry. For these reasons, the percentages of hydrogen in gas turbines, gas power plants, CHP, gas-fired boilers, gas storage systems, and gas measuring or transport systems are currently in the single-digit range.

Methanization could solve some of the problems associated with the direct storage and use of hydrogen. The currently available natural gas infrastructure could then be used together with its storage systems, transport pipelines, and gas applications. In addition, the energy density of methane gas as an energy source is three times that of hydrogen.

### ■ Energy Storage Driven by Mobility

In the short- or medium-term, the electricity sector will not demand large quantities of storage. The opposite is true for mobility. Here, there will be a growing demand for sustainable fuels and alternative drive systems in the medium-term. Mobility is extremely heavily-dependent on crude oil, and alternatives are expensive or rare. Biofuels hold some promise but have limited potential because of their competing uses in the food sector.

### ■ Development of Batteries Driven by Electro-Mobility and Second-Life

Electro-mobility is promising because regenerative operation here is three to four times more efficient than conventional drive systems. Electro-mobility could drive further development of battery technologies such as lithium batteries. This could result in dramatic cost-reductions, making the use of lithium batteries attractive for stationary applications in battery parks supplying short-term storage to the electricity sector.

A particularly promising area here is second-life battery use. After their first use for several years in electro-mobility, batteries are reused for electricity storage at a significantly lower cost. Since the cost burden is distributed and reduced, second-life creates business opportunities. The final result is double the battery use.

This double use could even coincide with the battery's use for electro-mobility. The battery could be simultaneously used for a stationary application such as storing household solar electricity, for example. This means that over the long-term, instead of two-battery storage systems (cellar and car) households may require only a single electric car battery that can also be discharged for stationary purposes. Hybrid or overhead-cable electric truck concepts are also currently being studied for long-distance trucking. Electrification of the transportation chain would also drive the development of electro-chemical energy storage systems.

### ■ PtG and PtL Driven by Synthetic Fuels

One problem with electro-mobility is that battery technologies currently limit how far electric vehicles can be driven. But emission standards will become increasingly strict in the future, making the use of fossil fuels with conventional combustion engines largely impractical. Wind and solar fuels (synthetic fuels) could solve this problem since they are low-emission, $CO_2$-neutral energy sources with higher-energy densities. The advantage of these fuels is that they can be conveniently transported and stored, and consumption can be centralized or decentralized. These energy sources would be particularly well-suited for the long-distance trucking and heavy-duty ma-

chine segments. Current battery technology alone cannot be used for aviation, shipping, or to power tractors and hydraulic machines such as bulldozers.

This means that technical solutions are required to convert renewable electricity into chemical energy sources. PtG and PtLs are two leading technologies in this area. A technical challenge with implementing these conversion facilities is flexibly operating components such as the electrolysis and methanization units. An economic challenge is developing sustainable electricity sources with adequate utilization levels. Full load hours with stationary wind and solar facilities range from only 600 to 4,000 hours; too low in comparison to conventional chemical facilities (around 8,500 hours). In addition, there is little public acceptance for the wind and solar energy expansion that is required just for the electricity sector. Mobility would require additional facilities in similar or even higher numbers. This is because the production and consumption of synthetic fuels requires enormous conversion losses.

### ■ Innovative Synthetic Fuels from the Ocean.



The utilization of remotely-located hydropower or geothermal energy could solve this problem. But the location of these energy sources limits their potential. A new concept for meeting this challenge is to produce synthetic fuels in the ocean. Across the globe, the largest wind energy potential is in the ocean. But this potential remains almost completely untapped. Public acceptance for utilizing this energy is higher than with technologies located near inhabited areas. Depending on the technology used, the impact on the environment is also comparatively low. Technology could be developed for producing these wind-fuels using wind-platforms and sail-powered energy. Sail-powered energy combines wind, hydropower, and storage technologies. Sail-powered energy can continuously convert wind energy into chemical-energy sources that can be stored and then supplied using the existing infrastructure. A disadvantage of this new technology is the high cost, although the significance of cost is relative to the scarcity of resources. But from a strictly technical point of view, synthetic fuels produced on land and in the ocean would solve the problem of limited resources.

### ■ Thermal Storage and Integrating the Heating Sector are Practical Choices

Although electrochemical and chemical-energy storage systems have potential for the future, thermal storage has the most immediate potential. In the current phase of energy transition, exploiting this form of storage is technically and economically the most practical choice. The advantages are obvious. This form of storage can provide flexibility for CHP generation, give the electricity system overall more flexibility by facilitating load-management, and integrate electricity surpluses using PtH, heat-storage stoves, or electric heat-pumps.

### ■ Power-to-Chemicals (PtC) as a Long-Term Solution in the Chemical Industry

Besides affecting the energy storage systems discussed in this book, the growing scarcity of resources also threatens the supply of raw materials for the chemical industry. Most of these materials are derived from oil and natural gas. Energy storage systems and charging technologies using PtC could provide a long-term solution to this problem. Here, renewable electricity is used as primary energy to produce basic materials for the chemical industry, such as methane, methanol, and polymers from easily available raw materials such as water and $CO_2$.

### ■ Summary

The future of energy storage has yet to be determined. But energy storage will be as crucial to energy supply in the future as it is today. That means that energy storage will play a crucial role going forward. Public acceptance for energy storage is generally high, and poses a problem only in isolated cases. There are also a wide range of innovative energy storage technologies available.

## 12.7 Summary

- **Sufficient storage capacity** is available for **energy transition**. This means that **there is no 'storage problem'** with renewable energy, as is often assumed.
- **Energy storage systems** often **differ fundamentally from each other** because they function on different physical principles. This means that the options for effectively comparing energy storage systems using different technologies are limited.
- The majority of storage technologies are **fully-developed and tested**.
- The crucial parameters determining the **cost-effectiveness** and application of a storage system are its **capital costs, efficiency, energy density**, and **cycle life**.
- **Capacitors** and **coils** have the **highest efficiency**, but they also have the **highest specific capital costs**, the lowest-energy densities, and the shortest charging or discharging durations. As a result, they are only suitable for applications requiring many cycles.
- In many respects, **batteries** fall somewhere **in the middle**. They are used as **short-term storage systems** in the transport sector. Besides conventional **lead-acid batteries**, **lithium batteries** have the greatest potential. A particularly **promising** area here is ***second-life*** use of batteries in the electricity and transport sectors. This **distributes costs**, making the use of batteries in both sectors **more competitive**. The **cost of lithium batteries will fall** as the technology is further developed and penetrates new markets. This means that **household-battery storage systems** and **battery power plants** are precursors of **exponential growth** in this area.
- **Pumped-storage** is the **only established, industrial scale technology in the short-term storage area** with **good efficiency levels**, **acceptable costs**, and large capacities. But **public acceptance** poses a problem for constructing new facilities.
- Because of their low efficiency levels and energy densities, **conventional CAS systems** currently play only a **minor role**. But promising, **innovative approaches** to exploiting this technology **are in development**.
- **Flywheel storage systems** have **high-efficiency levels** and **energy densities**. They are suitable for supplying **short-circuit capacity**, for **UPS applications**, and for brake-energy recuperation in the **transport sector**.
- **Chemical energy systems** such as **PtG** are the **backbone** of current and future energy supply. They have by far the **highest comparable energy densities** and storage capacities. Only chemical-energy storage systems (cavern and porous storage using PtG) are on the same scale and in the **same range** as fossil energy stored in the form of coal or natural gas.
- Among all energy storage systems **with acceptable efficiency levels** and energy densities, **thermal storage systems** are **the cheapest**. They can be very **conveniently integrated** into renewable electricity supply. They also can provide **flexibility** for **CHP** as well as **couple the electricity and heating sectors**, facilitating the **expansion of renewable energy**.
- In the **merit order** of **electricity storage systems**, the **cheapest storage** technologies complement each other: **lithium-battery storage systems** for cycle durations up to an hour, **pumped-storage** for durations up to several hours, and **PtG** for periods exceeding a week. The crucial factors here are the capital costs related to unit of power or energy, the cycle duration, and the self-discharge rate.
- For **short-term storage** of electricity, the **capital costs** for **power** are decisive. For **long-term storage**, the capital costs for **storage capacity** are decisive.
- **Lithium-battery storage systems** and **PtG** have the **greatest cost-reduction potential**.

- In the **transport sector** as well, **stricter emissions standards** will result in an **increased demand** for **new storage systems such as batteries or synthetic fuels**.
- As it is today, **energy storage** will **be crucial** to energy supply in the future. That means that energy storage will play **a crucial role** going forward.
- Public **acceptance** for energy storage **is** generally **high**.
- There are also a **wide range of innovative energy** storage technologies available.

## References


1. Antrekowitsch H (2013) Wasserstoff. Rahmenbedingungen, Stand der Technik, Potential, Leoben
2. Aundrup T, Beck H-P, Becker A et al (2015) Batteriespeicher in der Nieder- und Mittelspannungsebene. Anwendungen und Wirtschaftlichkeit sowie Auswirkungen auf die elektrischen Netze, Frankfurt
3. Bieber M (2011) Compressed Air Energy Storage. VDI Wissensforum Energiespeicher, Düsseldorf, München
4. Bieber M, Marquardt R, Moser P (2010) The ADELE Project – Development of an Adiabatic CAES Plant Towards Marketability. 5th International Renewable Energy Storage Conference, Bonn, München
5. Braess H-H (2011) Vieweg Handbuch Kraftfahrzeugtechnik, 6th edn. ATZ-MTZ Fachbuch. Vieweg & Teubner, Wiesbaden
6. Breyer (2015) Kostendegression in der chemischen Verfahrenstechnik (mündlich)
7. Brody R (2012) Isothermal CAES: Fuel-Free, Site-Flexible Compressed Air Energy Storage for Renewables Integration and T&D Substitution. VDI Wissensforum Stationäre Speichermöglichkeiten, Düsseldorf
8. Buffa F, Kemble S, Manfrida G, Milazzo A (2013) Exergy and Exergoeconomic Model of a Ground-Based CAES Plant for Peak-Load Energy Production. Energies 6(3):1050–1067. https://doi.org/10.3390/en6021050
9. von Burg P (1998) Moderne Schwungmassenspeicher – eine alte Technik in neuem Aufschwung. Gelsenkirchen
10. Chen H, Cong TN, Yan W, Tan C, Li Y, Ding Y Progress in electrical energy storage system: A critical review. Prog Nat Sci 19(3):291–312
11. Crotogino F, Donadei S (2011) Zukünftige Nutzung von Gaskavernen und Umwandlung gasförmiger Medien in elektrische Energie. VDI Wissensforum Energiespeicher, Düsseldorf, Hannover
12. Doetsch C, Budt M, Wolf D, Kanngießer A (2012) Adiabates Niedertemperatur-Druckluftspeicherkraftwerk zur Unterstützung der Netzintegration von Windenergie. Oberhausen (Projektbericht)
13. Eurosolar (Hrsg) (2012) Electrical energy storage technologies and the built environment. 7th International Renewable Energy Storage Conference (IRES 2012).
14. Ewert M (2011) Flexibilität durch Wärmespeicherung in konzentrierenden Solarkraftwerken. egeb Forum Energie, Düsseldorf
15. Fay P (2011) BHKW-Check. Frankfurt am Main
16. Feddeck P (2001) Thermochemische Speicher. Eggenstein-Leopoldshafen
17. FNR (2013) Basisdaten Bioenergie Deutschland. Fachagentur Nachwachsende Rohstoffe (FNR), Gülzow-Prüzen
18. Fraunhofer ISE (2014) Aktuelle Fakten zur Photovoltaik in Deutschland. Freiburg
19. Freund S (2012) Entwicklung von adiabaten Druckluftspeicherkraftwerken. VDI Wissensforum Stationäre Speichermöglichkeiten für erneuerbare Energien
20. Fuchs G, Lunz B, Leuthold M, Sauer DU (2012) Technologischer Überblick zur Speicherung von Elektrizität. Überblick zum Potential und zu Perspektiven des Einsatzes elektrischer Speichertechnologien. Im Auftrag der Smar Energy for Europe Platform GmbH (SEFEP). RWTH Aachen (Institut für Stromrichtertechnik und Elektrische Antriebe (ISEA) http://www.sefep.eu/activities/projects-studies/Ueberblick_Speichertechnologien_SEFEP_deutsch.pdf)
21. Geitmann S (2012) Alternative Kraftstoffe. Erdgas & Flüssiggas – Biodiesel & Pflanzenöl – Wasserstoff & Strom – Womit fahre ich am besten? GRIN Verlag GmbH, München
22. Geitmann S (2012) Energiewende 3.0. Mit Wasserstoff und Brennstoffzellen; Sachbuch, 3rd edn. Hydrogeit-Verl, Oberkrämer
23. Giesecke J, Mosonyi E, Heimerl S (2009) Wasserkraftanlagen. Planung, Bau und Betrieb, 5th edn. Springer, Heidelberg
24. Graf F, Bajohr S (2009) Erzeugung von SNG aus ligninreicher Biomasse. Énerg | Wasser-praxis 2009(4):10–16
25. Graß C (2012) Dezentrale Erzeugung von Biodiesel. Möglichkeiten, Wirtschaftlichkeit, Qualitätssicherung. Fachtangung Biokraftstoffe für die Landwirtschaft. Berlin
26. Habi R (2014) Der Stromspeicher-Check: Wie günsitg ist Teslas Powerwall wirklich? http://green.wiwo.de/der-stromspeicher-check-wie-guenstig-ist-teslas-powerwall-wirklich/. Accessed 7 July 2015

27. Hauer A, Specht M, Sterner M (2010) Energiespeicher – Steigerung der Energieeffizienz und Integration erneuerbarer Energien. FVEE Themen 2010. Forschen für das Zeitalter der erneuerbaren Energien, pp 110–114
28. Hauer A, Hiebler S, Reuß M (2013) Wärmespeicher, 5th edn. BINE-Fachbuch. Fraunhofer IRB Verl, Stuttgart
29. Höflich B, Kreutzkamp P, Peinl H, Völker J, Kühne M, Kuhn P, Tzscheutschler P, Hermes R, Krahl S, Meisa K (2012) Analyse der Notwendigkeit des Ausbaus von Pumpspeicherwerken und anderen Stromspeichern zur Integration der erneuerbaren Energien. Berlin
30. H-Tec Systems (2013) Wasserstoff-Erzeugung mit PEM-Elektrolyse. Lübeck
31. nternational Electrotechnical Comission (2011) Electrical Energy Storage. White Paper, Genf
32. Ketterer B, Karl D, Möst S (2009) Lithium-Ionen-Batterien: Stand der Technik und Anwendungspotential in Hybrid-, Plug-in Hybrid- und Elektrofahrzeugen
33. Klell M (2005) Wasserstoff. Allgemeines – Erzeugung – Verteilung – Speicherung – Anwendung. Graz
34. Kötz R (2002) Doppelschichtkondensatoren. Technik, Kosten, Perspektiven. Siebentes Kasseler Symposium Energie-Systemtechnik, pp 138–149
35. Krassowski J (2012) Power-to-Gas-Technlogien als Baustein in einem regenerativen Energiesystem. Ansätze zur Systemintegration. Das Energieversorgungskonzept für die Hansestadt Stendal als strategischer Modellansatz. Oberhausen
36. Kruck C (2008) Integration einer Stromerzeugung aus Windenergie und Speichersystemen unter besonderer Berücksichtigung von Druckluft-Speicherkraftwerken. Universität Stuttgart (Dissertation)
37. LaMonica M (2013) Abri's Battery. A tiny startup called Ambri wants to transform our energy system with massive liquid-metal batteries. http://www.technologyreview.com/featuredstory/511081/ambris-better-grid-battery/
38. Laubach J, Wülbeck H-F (2003) Die Wettbewerbsfähigkeit von großen Laufwasserkraftwerken im liberalisierten deutschen Strommarkt. Stuttgart (Endbericht (Langfassung))
39. Leonhard W, Buenger U, Crotogino F, Gatzen C, Glaunsinger W, Huebner S, Kleimaier M, Koenemund M, Landinger H, Lebioda T, Sauer DU, Weber H, Wenzel A, Wolf E, Woyke W, Zunft S (2008) Energiespeicher in Stromversorgungssystemen mit hohem Anteil erneuerbarer Energieträger. Bedeutung, Stand der Technik, Handlungsbedarf. VDE, Frankfurt am Main
40. Mahnke E, Mühlenhoff J (2012) Strom Speichern. Renews Special, vol 57. Berlin
41. Mankins JC (1995) Technology Readiness Levels. A White Paper, Washington, D.C.
42. Mauch W, Mezger T, Staudacher T (2009) Anforderungen an elektrische Energiespeicher. Stationärer und mobiler Einsatz. München
43. Neuhoff M (2013) Energiespeicher/Energiebereitstellung für Elektrofahrzeuge – Alternativen zur Lithium-Ionen Batterie und deren Fertigung. http://wiki.zimt.uni-siegen.de/fertigungsautomatisierung/index.php/Energiespeicher/_Energiebereitstellung_f%C3%BCr_Elektrofahrzeuge_%E2%80%93_Alternativen_zur_Lithium-Ionen_Batterie_und_deren_Fertigung
44. Pehnt M, Höpfner U (2009) Wasserstoff- und Stromspeicher in einem Energiesystem mit hohen Anteilen erneuerbarer Energien. Analyse der kurz- und mittelfristigen Perspektive. Heidelberg (Kurzgutachten)
45. Sauer DU (2010) Energiespeicher für ein stabiles Stromnetz 14. Fachkongress Zukunftsenergien, Aachen
46. Schnumberger W, Janßen H, Wittstadt U (2004) Wasserspaltung mit Strom und Wärme. Jahrestagung des Forschungsverbunds Sonnenenergie. FVS Themen, Berlin
47. Smolinka T, Günther M, Garche J (2011) Stand und Entwicklungspotential der Wasserelektrolyse zur Herstellung von Wasserstoff aus regenerativen Energien. Freiburg im Breisgau (Kurzfassung des Abschlussberichtes NOW-Studie)
48. Sterner M (2009) Bioenergy and renewable power methane in integrated 100% renewable energy systems. Limiting global warming by transforming energy systems. Renewable Energies and Energy Efficiency, vol 14. Kassel University Press, Kassel
49. Sterner M, Gerhardt N, Saint-Drenan YM, von Oehsen A, Hochloff P, Kocmajewski M, Jentsch M, Lichtner P, Pape C, Bofinger S, Rohrig K Energiewirtschaftliche Bewertung von Pumpspeicherwerken und anderen Speichern im zukünftigen Energieversorgungssystem. http://www.fvee.de/fileadmin/politik/IWES_Gutachten-Pumpspeicher.pdf (Fraunhofer Institut für Windenergie und Energiesystemtechnik (IWES) Kassel)
50. Sterner M, Jentsch M (2011) Energiewirtschaftliche und ökologische Bewertung eines Windgas- Angebotes. Gutachten für Greenpeace Energy, Kassel
51. Sterner M, Moser A, Thema M, Eckert F, Schäfer A, Drees T, Rehtanz C, Häger U, Kays J, Seack A, Sauer DU, Leuthold M, Stöcker P (2014) Stromspeicher in der Energiewende. Untersuchung zum Bedarf an neuen Stromspeichern in Deutschland für den Erzeugungsausgleich, Systemdienstleistungen und im Verteilnetz. Berlin (Studie)
52. Sterner M, Thema M, Eckert F, Moser A, Schäfer A, Drees T, Rehtanz C, Häger U, Kays J, Seack A, Sauer DU, Leuthold M, Stöcker P (2014) Stromspeicher in der Energiewende. Untersuchung zum Bedarf an neuen Stromspeichern in Deutschland für den

Erzeugungsausgleich, Systemdienstleistungen und im Verteilnetz. S, Berlin (Studie)
53. Sterner M, Eckert F, Thema M, Bauer F (2015) Der positive Beitrag dezentraler Batteriespeicher für eine stabile Stromversorgung. Regensburg/Berlin/Hannover
54. Stöver B, Rehfeldt S, Alekseev A, Stiller C (2013) Process Engineering and Thermodynamic Evaluation of Concepts for Liquid Air Energy Storage. Liquid Air Energy Storage (LAES): A Flexible and widely applicable medium-therm large-scale energy storage concept. München
55. Strauch N (2013) Einsatz von Energiespeicher-Technologien in Inselsystemen mit hohem Anteil erneuerbarer Energien. Berichte aus der Energietechnik. Shaker, Aachen
56. Tesla Motors (2015) POWERWALL. Tesla Stromspeichersystem. http://www.teslamotors.com/de_DE/powerwall (Tesla Motors)
57. Thema M, Sterner M, Eckert F, Lenck T, Götz P (2015) Bedeutung und Notwendigkeit von Windgas für die Energiewende in Deutschland. Hamburg, Regensburg
58. Thema M, Sterner M, Eckert F, Lenck T, Götz P (2015) Bedeutung und Notwendigkeit von Windgas für die Energiewende in Deutschland. Hamburg, Regensburg
59. Tiedemann A, Srikandam C, Kreutzkamp P, Roth H, Gohla-Neudecker B, Kuhn P (2008) Untersuchung der elektrizitätswirtschaftlichen und energiepolitischen Auswirkungen der Erhebung von Netznutzungsentgelten für den Speicherstrombezug von Pumpspeicherwerken. Berlin (Kurz: NNE- Pumpspeicher)
60. Unnerstall T (2015) Speicher als Baustein für den Ausgleich von Erzeugungs- und Verbrauchsschwankungen. Berlin
61. VDE ETG (2012) Energiespeicher für die Energiewende. Frankfurt am Main
62. Wagner U (2012) Speichertechniken für die zukünftige Energieversorgung. http://www.dlr.de/tt/Portaldata/41/Resources/dokumente/ess_2012/Wagner_Energiespeicher_zuk_nftige_Energieversorgung.pdf (Deutsches Zentrum für Luft- und Raumfahrt)
63. WEMAG AG (2014) Geschäftsbericht 2013. Schwerin
64. Wenske M (2011) Stand und neue Entwicklungen bei der Elektrolyse. DBI-Fachforum Energiespeicherkonzepte und Wasserstoff, Berlin
65. Wohlfahrt-Mehrens M (2011) Energiespeicher für die Elektromobilität: Stand der Technik und Perspektiven. Baden-Württemberg
66. Wolf D (2011) Methods for design and application of adiabatic compressed air energy. Ruhr-Universität Bochum (Dissertation)
67. Wollersheim O (2014) Profitabilität stationärer Stromspeichertechnologien. 4. VDI-Fachkonferenz. Energiespeicher für die Energiewende 2014, Raunheim

# Energy Storage Integration and Applications

Contents

Chapter 13 Storage Integration in Individual Energy Sectors – 675

Chapter 14 Storage Integration for Coupling Different Energy Sectors – 757

# Storage Integration in Individual Energy Sectors

*Michael Sterner, Ingo Stadler, Fabian Eckert, and Martin Thema*

**13.1 Integration in the Electricity Sector – 676**
13.1.1 Function and Purpose of Storage in the Electricity Sector – 676
13.1.2 Pumped-Storage Plants and Storage Power Plants – 683
13.1.3 Flywheel Storage Facilities – 695
13.1.4 Battery Power Plants – 697
13.1.5 Decentralized Battery Storage Systems in Houses and Districts – 699
13.1.6 Stand-Alone Networks with Renewable Energy and Storage Systems – 708
13.1.7 Thermal Storage in Solar-Thermal Power Plants – 721

**13.2 Integration in the Heating Sector – 725**
13.2.1 Thermal Storage for Solar-Thermal Energy – 726
13.2.2 Latent and Sorption Storage Systems in Buildings and Households – 733
13.2.3 Forest-Wood Used as Chemical Storage for Heating Supply – 736

**13.3 Integration in the Transportation Sector – 741**
13.3.1 Biofuel Mixtures and the Use of Vegetable Oil – 741
13.3.2 Integration of Hydrogen in the Transportation Sector – 745
13.3.3 Integration of Flywheel Storage Systems in Short-Distance Public Transportation – 747

**13.4 Summary – 749**

**References – 752**

**Electronic supplementary material** The online version of this chapter (https://doi.org/10.1007/978-3-662-55504-0_13) contains supplementary material, which is available to authorized users.

© Springer-Verlag GmbH Germany, part of Springer Nature 2019
M. Sterner, I. Stadler (Eds.), *Handbook of Energy Storage*, https://doi.org/10.1007/978-3-662-55504-0_13

**Overview**

How is energy storage integrated and currently implemented in the electricity supply, heating supply, and mobility sectors? This chapter provides both theoretical and practical answers to that question. The chapter focuses on the integration of renewable energy. Cross-sectoral energy storage systems that link the electricity, heating, and mobility sectors are discussed in ▶ Chap. 14.

This chapter focuses on storage integration in the electricity sector. After considering stand-alone networks, the chapter uses practical examples to analyze the various storage applications in the European network. The chapter concludes with a discussion of storage integration in the heating and transportation sectors.

## 13.1 Integration in the Electricity Sector

### 13.1.1 Function and Purpose of Storage in the Electricity Sector

The application areas for energy storage in the electricity sector can be classified in several ways.

1. By application area:
   - In the European network
   - In stand-alone networks
2. By network and voltage level:
   - Transmission network vs. distribution network
   - 380 kV, 220 kV vs. 110 kV, 10/20 kV, 400 V
3. By market:
   - Electricity trade:
     - Spot markets (intraday—continuous trade, day-ahead—auction trade)
     - Derivative markets (contingent and non-contingent forwards; exchange vs. over the counter, or OTC, options, forward transaction, futures, etc.)
     - In some cases future capacity markets
   - Reserve markets (especially balancing power and balancing energy):
     - Primary, secondary, tertiary balancing power (minute-reserves)
     - Long-term balancing of generation and demand
   - Self-consumption optimization (households, trade, the industrial sector)

Storage integration and applications in the electricity sector are similarly diverse. As discussed in this section, they are traditionally classified by function and purpose.

#### ▪ Storage vs. Function and Purpose

Storage facilities have a range of applications and purposes in the electricity sector. They can be used to serve a single function alone, or to serve several functions at the same time. The more functions and segments a storage facility can simultaneously serve, the greater its cost-effectiveness.

Figure 13.1 provides an overview of the functions and applications of storage systems in the electricity sector that are studied in this book.

Cross-sectoral applications of various storage systems are discussed in detail in ▶ Chap. 14. The following sections briefly describe applications for balancing supply and consumption, as well as system service applications. Several examples of pure electricity storage are then discussed.

#### 13.1.1.1 Supply-Balancing and Arbitrage

The primary function of electricity storage is to balance surpluses and deficits in the load and supply curves. Price differences on the electricity markets drive arbitrage transactions. Aside from on reserve markets where quantities are limited, the greatest potential for storage application is in this area.

This means that storage systems generate the largest revenues when the difference between expensive peak electricity (high de-

| Possible applications of differnet storage technologies | | Generation balance | | System services | | | | | | | | | | | | | | |
|---|---|---|---|---|---|---|---|---|---|---|---|---|---|---|---|---|---|---|
| | | | | Operational management | | Frequency stability by active power control | | | | | | | Voltage stability and -quality | | Security of supply and rebuilding | | | |
| | | | | | | tran-sient | Control- and reserve power | | | | | | | | | | | |
| | | Spot markets (stock market and off market OTC trade) | Futures markets (stock market and off-market OTC trade) | Network-congestion management (redispatch, partly used for voltage stability) | Ramping (high rates of power change) | Spinning reserve (immediate frequency stabilization) | Primary control power (pos. and neg. coupled) | Pos. * Secondary control power | Neg. | Pos. * Tertiary control power (minute range) | Neg. | Long-term reserve (Wind or permanent reserve) | Supply of short-circuit power (dynamic voltage stability, Fault-Ride-Through) | Supply of reactive power (static voltage stability) | Ability to do a black start | Uninterruptible power supply | Contribution to securing the supply of power (especially reduction & protection of peak load inter alia reduction of must-run capacities) |
| Electrical energy storage | Double-layer capacitor (DLC) | | | | | | | | | | | | | | | | | |
| | Coils (SMES) | | | | | | | | | | | | | | | | | |
| Electrochemical energy storage | Lead-acid batteries | | | | | | | | | | | | | | | | | |
| | Nickel batteries | | | | | | | | | | | | | | | | | |
| | Lithium batteries | | | | | | | | | | | | | | | | | |
| | Sodium batteries | | | | | | | | | | | | | | | | | |
| | Redox-flow batteries | | | | | | | | | | | | | | | | | |
| Chemical energy storage | Power-to-gas-power - charging technology electrolysis | | | | | | just neg. | | | | | just neg. | | | | | | |
| | Power-to-gas-power - discharging technology gas plant | | | | | | | | | | | | | | | | | |
| | Power-to-gas-heat - power-to-gas-to-heat | | | | | | just neg. | | | | | just neg. | | | | | | |
| | Power-to-gas,power-to-liquid - electricity fuels | | | | | | just neg. | | | | | just neg. | | | | | | |
| | Power-to-chemicals - chemical basic materials | | | | | | just neg. | | | | | just neg. | | | | | | |
| Mechanical energy storage | Pumped hydro-power plants | | | | | | | | | | | | | | | | | |
| | Compressed-air storage | | | | | | | | | | | | | | | | | |
| | Flywheel-energy storage | | | | | | | | | | | | | | | | | |
| | Potential energy storage | | | | | | | | | | | | | | | | | |
| Thermal energy storage and DSM | Electric heat pump | | | | | | just neg. | | | | | | | | | | | |
| | DSM (Demand response integration) general | | | | | | just neg. | | | | | | | | | | | |
| | Power-to-heat - E-heater, WW, local -,district-,process heat | | | | | | just neg. | | | | | | | | | | | |

Very well-suited | Well-suited | Basically suited / research needs | Not suited or application not possible

* the shutdown of loads could provide positive control power by the „release of power" (on the balance sheet)

**Fig. 13.1** Overview of the functions and applications of storage systems in the electricity sector

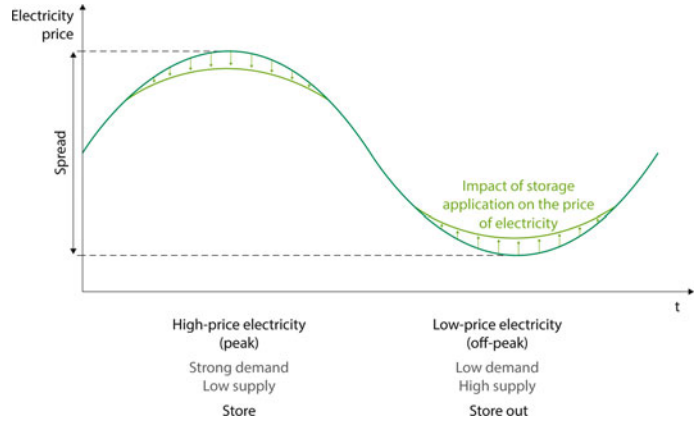



**Fig. 13.2** Application of electricity storage for supply-balancing driven by the electricity market (arbitrage transactions)

mand, low supply; also called peak prices) and cheap electricity (low demand, high supply; also called off-peak prices), or the electricity price spread (Fig. 13.2), is greatest, and when the fluctuations between peak and off-peak are the most frequent and dramatic.

In a storage cycle driven by the electricity market, the price difference between the discharged electricity sold and the charged electricity bought minus efficiency losses determines the revenue, and the amount of coverage provided. Increasing renewable energy electricity rollovers on the spot market has dramatically reduced electricity prices on the exchange. Because of increased photovoltaic (PV) electricity feed-in, classic peak electricity prices during the day are rare. This has significantly reduced the electricity price spread. In some cases, the spread has been too small to cover the operating costs of existing amortized pumped-storage power plants. This situation will be reversed as wind and PV facilities are expanded, resulting in high prices for discharging in times of little wind and Sun, and low prices for charging in times of wind and Sun electricity surpluses.

The structure of the wholesale electricity market is divided into two areas. In Germany the largest quantity of electricity is traded off the exchange, typically in bilateral contracts in OTC trade. A smaller amount is traded on exchanges such as the European Energy Exchange (EEX) [49, 70]. Spot and derivative markets are used in both cases.

- Off-exchange OTC trade (outside market)
  Spot market (physical settlement)
  Derivatives market (forwards, options, typically standardized products; physical and financial settlement)
- Power exchange
  Spot market (physical settlement)
  Derivatives market (forwards, options, standardized products; typically financial settlement)

The following sections briefly describe the spot and derivative markets on the power exchange.

### Spot Market

The trading venue for short-term electricity deliveries in central Europe is the EEX spot market in Paris (EPEX SPOT). It serves Germany, France, Austria, and Switzerland. Here, electricity is offered in MW trade units—or MW h trade units since the trading period is always an hour—on the intraday (sale on day of delivery) and day-ahead markets (sale on the day before delivery). The trading terms and electricity products for peak-load, base-load, and hourly contracts are continually revised and are described in [25].

### Derivative Market

Long-term delivery contracts, derivative contracts, and futures are negotiated on the derivative markets. Here, the delivery periods are measured in months, quarters, and years. The

capacities and delivery durations are defined in energy packages traded as block units [49]. The volume on the derivate market is significantly higher than on the spot market.

Natural gas, coal, and $CO_2$ certificates are also traded on the EEX energy exchange in addition to electricity.

The second primary market for energy storage in the electricity sector is the balancing power market that provides the system service of frequency control.

### 13.1.1.2 Providing System Services

#### The Role of System Services in Electricity Supply

System services are essential for consistent, safe, and stable electricity supply. They reliably maintain voltage, frequency, and load in the electricity network in an acceptable range, or compensate for disturbances in the network.

This means that system service products are always required when the electricity system is at risk of exiting the range of safe operation.

The most important system services are frequency control, voltage control, and restoring power supply. These system service products have typically been supplied by fossil power plants, pumped-storage plants, and by adjusting operational resource utilization by means of controllable local network stations or reactive power control facilities. Currently, and in the future, energy storage systems will play an increasingly important role in providing system services.

The Dena 2030 system service study, 'Sicherheit und Zuverlässigkeit einer Stromversorgung mit hohem Anteil erneuerbarer Energien' by TU Dortmund/ef.Ruhr, described in detail the role of system services in energy supply systems with large shares of renewable energy [60].

The German 'Verordnungsermächtigung zu Systemdienstleistungen' (§ 64, see [17]) laid the groundwork for the 'Verordnung zu Systemdienstleistungen durch Windenergieanlagen' (SDLWindV, [17]), which came into effect on July 3, 2009. These regulations require wind energy facilities to provide system services by reducing their real power within a minute or by contributing to voltage control, for example. Implementing these options requires upgrading the communications technology in network operator control rooms as well as regulatory changes to market access conditions. Other renewable energy facilities and energy storage systems unaffected by the ordinance could also currently serve these functions.

#### Frequency Control Using Balancing and Reserve Power

The network frequency in AC voltage and three-phase networks is a reference variable that correlates with the balance between generation and consumption. To avoid critical deviations from the nominal frequency (50 Hz in the European network) resulting in vibration effects in loads or suppliers on the network that my cause an emergency shut-down, the network is designed to maintain the frequency within a tolerance range of $\pm 0.01$ Hz. This means that positive and negative balancing energy or balancing power is required to maintain the balance between supply and consumption.

Depending on how quickly and for how long the balancing energy is required, it is termed instantaneous reserve (IR), primary balancing power (PBP), secondary-balancing power (SBP), or tertiary balancing power (or minute-reserve power—MRP) (see Table 13.1 and Fig. 13.3).

IR is supplied by mechanical-energy storage systems (flywheel-energy storage). This is kinetic energy stored in rotating facility components (such as turbines, synchronous machines, wind-power facility rotors), magnetic energy stored in synchronous machine coils, or electric energy stored in converter capacitors. These intrinsic reserves can counter the effects of a disturbance in the network in fractions of a second. They maintain the frequency until the automatically activated PBP takes over, which is fully started up and available after 30 seconds at most.

The SBP then takes over as soon as possible from the PBP so that balancing power remains

**Table 13.1** Balancing power supply over time after a disturbance in the network. Request or initiation type, and period of time the type of balancing power must be available

| | Request/initiation | Time until full availability after disturbance | Required availability duration |
|---|---|---|---|
| IR | Intrinsic | Instantaneous | Around 30 s |
| PBP | Automated | Max. 30 s | 15 min |
| SBP | Automated | Max. 5 min | 15 min |
| MRP | By telephone/automated | Max. 15 min | Around 45 min |

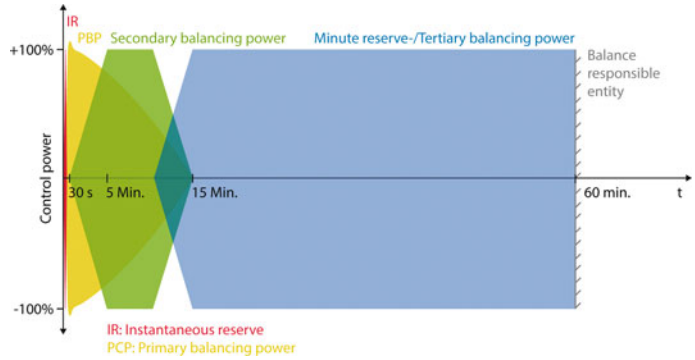



**Fig. 13.3** Balancing energy supply over time in an electricity system after a frequency deviation

available to handle the disturbance. The SBP starts up after 30 seconds at most, and is available at full power after five minutes at most. Within 15 minutes after the disturbance is detected, the minute-reserves take over, providing the balancing energy required. Transmission network operators allocate the minute-reserves in 15-minute intervals either automatically or by telephone for at most an hour per disturbance. During this period, slower alternative power plant capacity compensates for generation gaps or absorbs generation surpluses.

Energy storage systems combined with power electronics have a range of versatile applications on the balancing power market. Battery power plants can provide positive or negative balancing power, for example. Pumped-storage and compressed air storage systems can also serve these functions. Capacitors and coils are particularly useful for providing positive balancing power in the primary balancing energy and IR areas. Power-to-heat (PtH—thermal storage) and power-to-gas (PtG—gas storage, electrolysis) are particularly well-suited for providing negative balancing power.

### Using Reactive Power to Maintain Voltage Levels and Voltage Quality

Transmission network and distribution network operators are responsible for maintaining the voltage within their network area in a permissible range. This means that they must ensure that short-circuits do not cause voltage drops, for example. Locally balanced reactive power control and adequate short-circuit capacity are essential for ensuring protective systems are activated in time [60].

Short-circuit capacity at a connection point in the electricity network is capacity that can be absorbed during a short-circuit from the upstream network when no protective systems respond and no technical facilities are damaged.

As a metric for this capacity, a theoretical value linking values that, in reality, never occur at the same time is used. Stress on electric facilities, circuit-breaker switching capacity, and

network reactions can be quantified using this metric [60].

Historically, short-circuit capacity was provided by rotating masses in (conventional) generation facilities. Until now, power electronics and the control of decentralized renewable energy facilities were not adequately developed for this purpose. Even if they were, network operators were often unwilling to integrate them into their systems or their communication technology prevented easy integration.

Today, short-circuit capacity can be conveniently provided by decentralized renewable energy generation facilities as well as various storage technologies using fast-control technology and adapted power electronics. This process is called fault ride-through.

A second crucial component of voltage maintenance is balanced reactive power control. This is supplied by local facilities (power plants, decentralized generation facilities, compensation measures) in each network section. Energy storage systems can also supply reactive power. Pumped-storage plants and rotating masses (flywheel-energy storage, phase-shifters) have been used for this purpose for many years. But discharging units with generators (such as gas turbines for PtG), battery storage systems, and all other storage systems coupled to the network by converters could also be modified for the same purpose.

In Germany, there is currently no market for reactive power. In addition, energy storage systems can only provide this service over the natural network monopolies. Like redispatch and generation recovery (black-start capability), this is a market component that could be organized regionally. This is because all three problems are regional, and the service could be provided by some energy storage types.

#### 13.1.1.3 Network Operations and Other Market or System Contributions

Network operators are responsible for managing network operations and for ensuring secure network operation free of disruptions. Network operators ensure compliance with limit values by continually monitoring and controlling the network and large consumption or generation facilities.

Network operators monitor network data and take actions within regulatory guidelines, such as network access conditions and legal provisions to adjust generation and consumption as required. Operating resources such as controllable local network transformers (CLNT) can be flexibly implemented to stabilize operations. Another option is contractual utilization of services to stabilize network operations, such as storage-plant use or redispatch to prevent network congestion.

- **Network Congestion Management and Network Load Relief—Redispatch**

Electricity surpluses are usually caused by congestion in the electricity network. Congestion is remedied by modifying existing power plant utilization planning (dispatch) over the short-term. This is termed power plant redispatch.

Redispatch is also used at the transmission network level for voltage maintenance. It is a component of network congestion management. Network operators use network congestion management to prevent electricity network overloads [60]. For this purpose, power plants (both renewable and conventional) can be curtailed, shut down, or reallocated.

The German Renewable Energy Law (Erneuerbare-Energien-Gesetz, EEG) regulation guarantees feed-in for all the energy produced by renewable energy generation facilities [18]. If network congestion causes a wind power facility to be curtailed or shut down, for example, the network operator must reimburse the facility operator for the losses incurred.

But this may have unintended consequences, because it is often cheaper to curtail renewable energy and pay for the losses than to shut down slow fossil power plants.

As shares of renewable energy increase, this problem will grow in significance. The fundamental question will then become whether renewable energy should be allowed to marginalize fossil energy.

### Role in Operations, Guaranteed Capacity, and Must-Run Capacity Reduction

In the future, energy storage systems will play a crucial role in electricity network operations. They will contribute to the perpetuation of renewable energy by balancing generation or forecasts, and will also contribute to quicker gradient control. As a result, they will relieve the transmission and (in particular) the distribution networks, increase supply security, contribute to guaranteed capacity, and reduce fossil must-run capacity. Currently there is no market in Germany for some of these services provided by storage that contribute to technical supply security. But these products and markets could be created in Germany as they have in other countries.

System services provided by storage systems in both centralized and decentralized facilities will play a crucial role for network operations over the short- and long-term [60]. They will also have a significant financial impact.

### Uninterruptible Power Supply (UPS)

Another storage system application that can also contribute to operations is UPS. In critical infrastructure facilities such as hospitals, data centers, communications centers, and police stations, during network failures, battery-based energy storage systems have typically been used for many years to ensure supply for crucial security and survival facilities. Aside from supporting network stability in some countries, until now, this was the primary application area for electricity storage systems.

### Long-Term Reserves—Wind or Persistent Reserves

With seasonally fluctuating renewable energy, long-term reserves (wind or persistent reserves) will also play an increasingly important role in ensuring reliable operations over longer periods. In systems with high shares of renewable energy, seasonal surpluses can be converted into chemical energy sources and stored to balance seasonal shortages at other times.

### Generation Recovery and Black-Start Capability

Locally contained disturbances are normally the responsibility of the distribution network operator. But if they spread into a larger-scale power failure (black-out), the transmission network operator is responsible for restoring supply as quickly as possible. Following a previously determined plan and supported by the distribution operators, the transmission network operator first successively establishes smaller stand-alone networks. These are then synchronized and coupled with each other. In the beginning, these partial networks require black-start capable power plants that can start up on their own power without any external energy supply. Battery systems are also used here to start up larger power plants. Historically, pumped-storage plants have been used for this purpose. In the future, other storage power plants such as battery power plants or gas power plants with gas storage fed by PtG will also be used.

### Capacity Market vs. Flexibility Market vs. Balancing Power Market

In Germany, capacity markets have been discussed as a method for ensuring technical supply security. The existing balancing power market is, in principal, a kind of capacity market. But it was designed for large power plants in base-load operation, and historically has a strong supply-side bias. This has gradually changed over recent years. But in a system with large shares of renewable energy, the tendering criteria specifying weekly delivery periods are outdated. Since wind-power and PV facility forecasts range from at most one to three days depending on the weather, the criteria blocks these facilities from accessing the market. Establishing flexibility markets to meet the increasing demand for flexibility has also been considered.

All three problems could be solved by modifying the existing balancing power market to meet these five requirements:

- Technology neutrality.
- Market-based pricing.
- Gradient capacity guidelines in the prequalification conditions.
- Contribution to secure supply.
- Integration of renewable energy facilities and the consumer side (load-management or demand-side integration) with shorter delivery periods and smaller lot sizes.

If these simple requirements are met, energy storage systems together with renewable energy facilities could access new markets. The enormous potential on the consumer-side (▶ Chap. 11) that remains untapped due to lack of incentive could also find market access.

### 13.1.2 Pumped-Storage Plants and Storage Power Plants

Pumped-storage plants and storage power plants are hydropower plants that use the potential energy of water at various altitudes to generate and store energy. By retaining water at a higher altitude, they create a specific storage capacity. Pumped-storage plants differ from pure storage power plants, because they can absorb and charge energy from the electricity network by pumping water that has already been used back up from the lower reservoir or river bed to the upper reservoir.

Proven over decades, pumped-storage is currently the best-established, most efficient, and cheapest form of large-scale electricity storage over short periods. But environmental sustainability and public acceptance present challenges for building new, large-scale pumped-storage facilities.

#### ■ Pumped-Storage for Balancing Supply from Wind and Solar Energy

Pumped-storage plants and storage power plants can be quickly started up and shut down within one to three minutes, depending on the facility type. As a result, they can be used to balance large power fluctuations in the network. The Goldisthal pumped-storage plant requires only 75 seconds to go from an idle state to turbine operation, for example. As ◘ Fig. 13.4 shows, this means that pumped-storage can be used to balance forecast errors and store feed-in peaks from renewable energy in high-consumption periods by means of arbitrage.

The graph compares the energy fed in from PV facilities in the Amprion network on 29 October 2010 with the operation of Schluchseewerk AG pumped-storage plants in the same period. In high-consumption periods in the morning and evening, the pumped-storage plants discharged if there was no feed-in from PV. During the day, PV yield exceeded forecast by as much as 400 MW. The pumped-storage plants compensated for the imbalance by charging at full capacity.

#### ■ System Services Provided by Pumped-Storage

Because they can be easily controlled, i.e., quickly switched from pump to turbine operation, pumped-storage plants are also used for reactive power control and frequency maintenance. Large rotating masses in turbine and generator facilities supply IR and contribute to supply security.

In addition, pumped-storage plants and storage power plants are black-start capable. This means that they can start up independently from the electricity network, and even in the case of a complete network failure, provide energy to other power plants for start-up.

Because of their high flexibility and quick reaction times in supplying and absorbing capacity, pumped-storage plants typically meet the high pre-qualification requirements for supplying SBP products.

#### ■ PBP Provided by Hydraulic Short-Circuit

To supply positive balancing energy at the same time as negative balancing energy, and as a result, PBP, besides pumping water back into the storage reservoir, pumped-storage plants can also use a hydraulic short-circuit (◘ Fig. 13.5).

The pump set's feed rate usually cannot be regulated, and as a result always requires

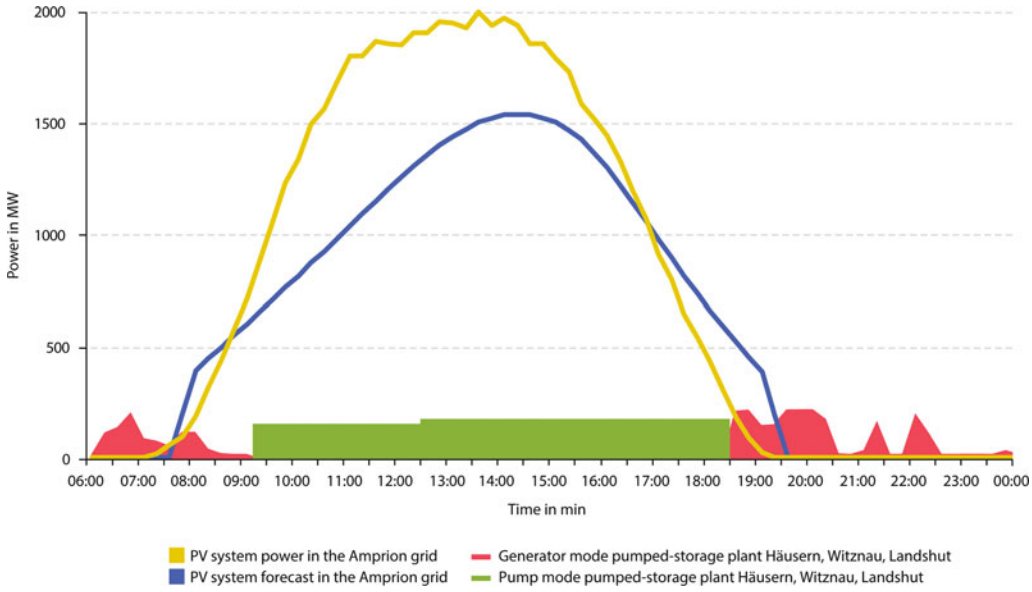



**Fig. 13.4** Machine use by Schluchseewerk AG pumped-storage plants in Häusern, Witznau and Waldshut, Südbaden to balance forecast errors and store solar energy surpluses in low-consumption periods with little solar electricity compared to solar energy forecasts and feed-in in the Amprion network area (source: Schluchseewerk AG)

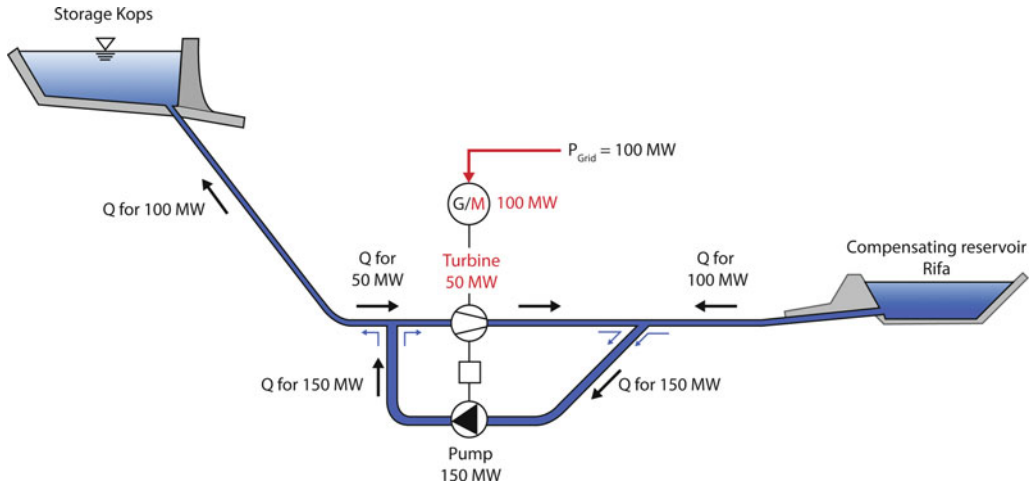



**Fig. 13.5** PBP supplied by pumped-storage using a hydraulic short-circuit, taking Vorarlberger Illwerke AG's Kopswerk II facility as an example. The pump can be indirectly controlled by the turbine's power control connected to the pump (source: Vorarlberger Illwerke AG)

the same power. To create a hydraulic short-circuit, the pump set is directly coupled with the turbine. By opening the turbine set throttles, mechanical power is converted into electrical power at the same time as the pumps consume the power, partially compensating for the pumps' consumption. This means that the water is basically pumped in a circle, and energy is 'eliminated' in the short-circuit. This makes little sense from a technical point of view, but



**Fig. 13.6** Pump set at Vorarlberger Illwerke AG's Kopswerks II facility. The pump set is coupled with the generator (above, through the ceiling) to create a hydraulic short-circuit (source: Vorarlberger Illwerke AG)

can be profitable when sold effectively on the balancing power market. By flexibly shifting the operating point in this way, the power plant can continually adjust to the demand for balancing power. This means that the system is also fully capable of supplying balancing power in the negative power range, i.e., when there are power surpluses in the network.

Figure 13.5 illustrates pump operation to provide balancing power in Vorarlberger Illwerke AG's Kopswerk II power plant. Here, 100 MW of negative balancing power is required. This means that 100 MW must be removed from the network. The pump-power is 150 MW. The coupled turbine supplies 50 MW of power. As a result, exactly 100 MW of electricity is drawn from the network [77]. Figure 13.6 shows the actual design of the coupled turbine and pump sets.

Not all pumped-storage plants and storage power plants are equally well-suited for this purpose. Depending on geographical and technical conditions, various factors may play a more or less important role. The following sections describe several power plants in Germany.

#### 13.1.2.1 Pumped-Storage Plants in Germany

Germany currently (2014) has around 40 pumped-storage facilities with a pumped-storage capacity of 7 GW and a storage capacity of around 40 GW h.

A selection of German pumped-storage plants are shown in the illustrations below. There are also smaller pumped-storage plants with powers ranging from 0.5 to 120 MW. These include the Geehsthacht power plant. This plant has no separate lower reservoir, and is directly connected to the Elbe River. The Langenprozelten pumped-storage plant is a special case. It is used exclusively to supply electricity to the Deutsche Bahn during peak-load times.

- **Goldisthal Pumped-Storage Plant (Thuringia)**

Currently, the largest pumped-storage plant in Germany in the Goldisthal facility in Thuringia (see Table 13.2 and Fig. 13.7). The facility went into operation in 2004 with a power of 1,060 MW. The plant's storage can meet demand for eight full load hours and has a work capacity of 8,480 MW h.

- **Atdorf Pumped-Storage Plant**

Schluchseewerk AG plans to build the Atdorf pumped-storage plant in the Black Forest with a power of 1,400 MW and a work capacity of 13 GW h (Table 13.3). It would be the biggest pumped-storage plant in Germany, surpassing the Goldisthal PSP [67].

From design to implementation, new construction takes about ten years. The plants have a service life ranging from 60 to 100 years, or even longer. As a result, pumped-storage plants are very long-term investments with high quality and maintenance requirements.

**Table 13.2** Profile: Goldisthal pumped-storage plant

| | |
|---|---|
| Turbine power | 1.06 GW |
| Storage capacity/work capacity | 8.48 GW h |
| Discharging duration | 8 h (at full load) |
| Start-up | 2004 |
| Control area | 50 Hz (eastern Germany, Berlin, and Hamburg) |
| Drop-height | Around 300 m |
| Upper reservoir storage volume | Around 12 million $m^3$ |
| Lower reservoir storage volume | Around 18.9 million $m^3$ |
| Operator | Vattenfall |



**Fig. 13.7** Upper reservoir of the Goldisthal pumped-storage plant with a storage volume of around 12 million $m^3$ of water (source: Vattenfall Europe AG)



### Herdecke Pumped-Storage Plant

RWE's Herdecke pumped-storage plant replaced the Koepchenwerk power plant in 1989. Named after an energy pioneer from the Ruhr district and built in 1927, the old plant was demolished after a serious mechanical breakdown. The new power plant uses the upper and lower reservoirs used by the old facility (see Table 13.4 and Fig. 13.8). The old Koepchenwerk was one of the two first large-scale pumped-storage plants constructed in Germany. The other was the Niederwartha pumped-storage plant on the Elba river. At the time, these power plants were exclusively used

**Table 13.3** Profile: Atdorf pumped-storage plant [67]

| | |
|---|---|
| Turbine power | 1.4 GW |
| Storage capacity/work capacity | 13 GW h |
| Discharging duration | 9 hours |
| Authorization (expected) | 2016 |
| Expected start-up | – |
| Control area | TransnetBW (Baden-Württemberg) |
| Drop-height | Around 600 m |
| Upper reservoir storage volume | 9 million $m^3$ (Hornbergbecken I) |
| Lower reservoir storage volume | 9 million $m^3$ (Haselbecken) |
| Operator | Schluchseewerk AG |
| Investment volume | Around 1.6 billion € |

**Table 13.4** Profile: Koepchenwerk pumped-storage plant [65]

| | |
|---|---|
| Turbine power | 153 MW |
| Start-up time to turbine operation | 75 s |
| Pump-power | 153 MW |
| Storage capacity/work capacity | 590 MW h |
| Discharging duration | 3.8 h |
| Start-up | 1989 |
| Control area | Amprion |
| Drop-height | Around 150 m |
| Upper reservoir storage volume | 1.6 million $m^3$ |
| Operator | RWE |

to improve the utilization of thermal power plants [65].

Pumped-storage plants are still used today to optimize power plant portfolio utilization by enhancing electricity value in arbitrage transactions. To avoid increasing $CO_2$ emissions in the electricity mix by using flexibility options such as pumped-storage, higher priced $CO_2$ certificates ranging from 30 to 70 €/ton for $CO_2$ disposal are required. It should be kept in mind that, since the service life of a PSP is very long, in energy transition, pumped-storage will primarily be used to store and enhance the price of renewable energy.

### ▪ Bleiloch and Hohenwarte 1 Pumped-Storage Plant

The Bleichloch and Hohenwarte 1 pumped-storage plants are on two of five dams in the Saale (Saale cascade) in Thuringia (Fig. 13.9). They were constructed in the early and mid-20th century. With storage volumes of around 200 million $m^3$ and powers of 80 and 63 MW, these two power plants operated by Vattenfall




**Fig. 13.8** RWE AG's Koepchenwerk Herdecke pumped-storage plant with 153 MW in the Amprion network (source: RWE Power AG)

Europe are at about the same scale. Hohenwarte 1 supplies an average of 74 GW h of electricity a year.

13

#### ▪ Säckingen Pumped-Storage Plant

Schluchseewerk AG's Säckingen pumped-storage plant is a classic high-pressure facility with a drop-height of about 400 m. Figure 13.10 shows the power plant's 160 m long, 23 m wide, and 33 m high turbine hall. At an altitude of 400 m, the Eggberg reservoir contains about 2.1 million $m^3$ of water able to power six full load hours (Fig. 13.11). Storage reservoirs on the Rhine are used as a lower reservoir. As in a conventional pumped-storage plant, the water from these reservoirs is pumped back up to the upper reservoir. Natural intake accounts for about 18% of generation. The turbines can start up from an idle state to full power within 90 seconds, making these facilities among the most flexible pumped-storage plants in operation [66].

#### ▪ Wehr Pumped-Storage Plant

At 630 m, the Wehr power plant in Baden-Württemberg has by far the largest effective drop-height among German pumped-storage plants. This drop-height is achieved by using the Hornberg reservoir 1,000 m above. The power plant has a discharging power of 910 MW and is also operated by Schluchseewerk AG (Fig. 13.12).

### 13.1.2.2 Pumped-Storage Plants and Storage Power Plants Worldwide

#### ▪ Hydropower as the Most Commonly Used Source of Renewable Energy Worldwide and as an Energy Storage System

Because of the available potential, in many countries, the share of hydropower in relation to total energy demand is many times higher than in Germany. In 2012, the share of hydropower worldwide was 6.4% of primary energy (▶ Chap. 1). Without counting



**Fig. 13.9** Bleilochtalsperre river dam on the Saale in Thuringia used by the Vattenfall Europe for pumped-storage (source: Vattenfall Europe AG)




**Fig. 13.10** Turbine hall at the Säckingen cavern power plant (source: Schluchseewerk AG)

pumped-storage plants, the installed power of hydropower plants worldwide in 2012 was 990 GW supplying 16.5% of global electricity demand. The most hydropower (23%) was generated in China. Over half of newly installed hydropower plants were located in China in 2012, with 1.5 GW from pumped-storage plants and 3.6 GW under construction [62].

In Europe, Norway is a special case. Here nearly all electricity supply relies on hydropower. In Austria and Switzerland as well, hydropower plants powered by water resources in the Alps supply more than 50% of electric energy.

The technical expansion potential in Asia, Africa, and Latin America is also very high. Expansion could supply regions with electricity that have never had access to electricity. But the ecological and socio-cultural effects of large-scale hydropower projects (Three Gorges Dam, Itaipú) often cause serious problems for the local population and environment. Because of these projects, millions of local inhabitants were resettled against their will and lost their homes. The reservoirs destroyed cultural treasures and ecologically vital areas. As a result, new hydropower and pumped-storage plant projects should carefully consider non-technical factors to minimize harm to the local population and the environment.

### ■ Pumped-Storage as the Most Commonly Used Electricity Storage Technology with the Greatest Growth Worldwide

In 2012, pumped-storage worldwide totaled 138 GW. The greatest capacities were 45 GW



**Fig. 13.11** Eggberg reservoir (upper reservoir) at the Säckingen pumped-storage plant (source: Schluchseewerk AG)



**Fig. 13.12** Machine hall at the Wehr pumped-storage plant (source: Schluchseewerk AG)

in Europe, around 26 GW in Japan, around 22 GW in the USA, and 20.3 GW in China. Across the globe in 2012, 3 GW of new pumped-storage capacity went into operation. Countries such as Indonesia plan to add 3 GW of capacity. Spain plans to expand capacity to around 9 GW, China from 20.3 to 30 GW. This means that the pumped-storage market is the largest growing market for electricity storage. The market is mainly served by the largest manufacturers: Alstrom, Andritz, IMPSA, and Voith Hydro [62].

Updated geographical information system (GIS) evaluations have been used to estimate pumped-storage potential in the European Union (EU). With a maximum difference of 5 km between the upper and lower reservoirs, realizable potential in Europe is estimated at 10 TW h. Of this total potential, 40% is located within the EU [37].

Table 13.5 lists the rated powers of pumped power plants and storage power plants in Europe together with their storage capacity, annual electricity generation, and utilization. In Europe, German pumped-storage plants have the greatest annual turnover.

### Vianden (Luxemburg) Pumped-Storage Plant

The Vianden pumped-storage plant in Luxemburg is one of Europe's largest (see Table 13.6 and Fig. 13.12). Part of the lower reservoir is in Germany, and the peak electricity it generates is fed into the German transmission network. The electricity consumed to operate the pumps is also drawn from the German transmission net-

**Table 13.5** Overview of power, capacity, and annual electricity generation for pumped-storage power plants in European countries in 2011 [28, 37]

| Country | Rated power in MW | Capacity in GW h | Annual electricity generation in GW h |
|---|---|---|---|
| Belgium | 1,307 | 8 | 1,217 |
| Bulgaria | 864 | 2 | 765 |
| Germany | 6,777 | 39 | 6,099 |
| France | 6,985 | 184 | 5,074 |
| Greece | 699 | 21 | 264 |
| United Kingdom | 2,744 | 33 | 2,895 |
| Ireland | 292 | 2 | 0 |
| Italy | 7,544 | No information | 2,539 |
| Croatia (2010) | 293 | No information | 106 |
| Lithuania | 900 | 49.3 | 564 |
| Luxemburg | 1,096 | 6.1 | 1,069 |
| Norway | 1,326 | 11,000 | 406 |
| Austria | 3,365 | 125 | 3,504 |
| Poland | 1,406 | 11 | 422 |
| Portugal | 1,029 | 107 | 564 |
| Rumania | 92 | No information | 218 |
| Sweden | 99 | No information | 122 |
| Switzerland | 1,817 | 369 | 1,746 |
| Slovakia | 916 | 3.7 | 368 |
| Slovenia | 180 | No information | 143 |
| Spain | 5,260 | 1,530 | 2,275 |
| Czech | 1,147 | 6.7 | 701 |

Albania, Denmark, Estonia, Finland, Latvia, Lichtenstein, Malta, Holland, Turkey, Hungary, Cyprus, and the city states have no installed pumped-storage power plants, and so are not listed.
There is no data available for Bosnia and Herzegovina, Iceland, Russia, Ukraine, and Belarus.

work. A new eleventh machine set with an additional 190 MW of pump-power and 195 MW of turbine power has further increased this flexible power plant's capacity [71].

### Bath County Pumped-Storage Plant (USA)

The Bath County power plant in northern Virginia near the West Virginia border in the USA went into operation in 1985. With a 3 GW discharging power, it is the most powerful pumped-storage plant in the world. It uses six 510 MW Francis turbines (Table 13.7) [20].

### Malta Pumped-Storage Plant (Austria)

The Malta pumped-storage plant is Austria's most powerful pumped-storage plant

**Table 13.6** Profile: Vianden pumped-storage plant [71]

| | |
|---|---|
| Turbine power | 1,096 MW |
| Pump-power | 850 MW |
| Turbine/pump work capacity | 4,630/6,240 MW h (around 4 h/7 h) |
| Start-up | 1964 |
| Drop-height | Around 280 m |
| Upper reservoir storage volume | 6.8 million $m^3$ |
| Lower reservoir storage volume | 6.8 million $m^3$ |
| Operator | Société Électrique de l'Our (SEO) |



**Fig. 13.13** The Vianden pumped-storage plant in Luxemburg on the river Our bordering Germany and Luxemburg. The river is used as the lower reservoir (source: Société Électrique de l'Our)



**Table 13.7** Profile: Bath County pumped-storage plant [20]

| | |
|---|---|
| Turbine power | 3 GW |
| Start-up | 1985 |
| Upper reservoir storage volume | 44 million $m^3$ |
| Lower reservoir storage volume | 34.5 million $m^3$ |
| Drop-height | Around 380 m |
| Operator | Allegheny Power System, Dominion |

**Table 13.8** Profile: Malta pumped-storage plant (Austria) [86]

| | |
|---|---|
| Turbine power | 120 MW |
| Pump-power | 116 MW |
| Storage capacity/discharging duration | 76 GW h/26 days |
| Start-up | 1979 |
| Drop-height | 198 m |
| Operator | Verbund AG |



**Fig. 13.14** Upper stage of the Malta pumped-storage plant in Austria with a 26 day discharging duration and the characteristics of a long-term storage facility (source: Verbund AG)

(Table 13.8) [86]. With a discharging duration of 633 hours or 26 days, it has the longest discharging duration in Europe and the characteristics of a long-term storage facility. The power plant has a power of 116 MW and generates 618,400 MW h of energy annually. It can store 200 million $m^3$ of water in its upper reservoir (Kölnbrein storage facility). The water is pumped from a pre-storage reservoir with several intakes, and from the river Möll into the storage reservoir [86].

Figure 13.3 shows the Malta upper stage. It went into operation in Austria in 1979. Construction lasted from 1971 to 1977.

### ■ Three Gorges Dam Storage Power Plant (China)

The Three Gorges Dam in China is the world's largest hydropower plant (Table 13.9). The plant currently has a power of 18.2 GW and generates 85 TW h annually, which is a ninth of China's total electricity generation.

The plant effectively generates electricity and prevents flooding. But it also displaced entire cities and regions with millions of inhabitants, negatively impacting the local environment and culture. Years after the project's completion, the plant continues to cause serious problems. It has significantly disrupted the natural flow of the Yangtze River. Upstream provinces suffer from water shortages and reduced river navigability. Landslides are a problem at the reservoir [21, 30]. As a result, the plant is frequently a target of criticism.

### ■ Itaipú (Brazil/Paraguay)

The Itaipú power plant on the border between Brazil and Paraguay was built between 1975

**Table 13.9** Profile: Three Gorges Dam [3]

| | |
|---|---|
| Turbine power | 18.2 GW |
| Annual generation | 84.7 TW h/year |
| Utilization | Around 4,650 FLH |
| Waterway | Yangtze |
| Resettlement | 1.3 million people, 1,600 factories |
| Official/unofficial costs | 21/39 billion € |
| Start-up | 2009 |

**Table 13.10** Profile: Itaipú [88]

| | |
|---|---|
| Turbine power | 14 GW |
| Annual generation | 98.6 TW h |
| Utilization | Around 7,050 FLH |
| Waterway | Paraná |
| Start-up | 1984 |

**Table 13.11** Profile: Aswan Dam [26]

| | |
|---|---|
| Turbine power | 2.1 GW (12 Francis turbines) |
| Storage volume | 135 to 169 billion $m^3$ |
| Waterway | Nile |
| Resettlement | 100,000 people |
| Start-up | 1970 |
| Investment volume | Around 2.2 billion euro |



and 1991. It was expanded to its current power of 14 GW in 2004 (Table 13.10). In 2013, the power plant generated 98.6 TW h of electric energy, covering 75% of Paraguay's electricity demand and 16.9% of Brazil's [44]. A High-voltage direct current (HVDC) transmission line runs directly from Itaipú to São Paulo, supplying the greater São Paulo and Rio de Janeiro areas with hydropower.

The power plant is a joint project of Brazil and Paraguay. The energy generated from the Río Paraná river on their shared border supplies both countries. Each country owns half of the power plant. But since Brazil requires significantly more energy, it buys and imports energy from Paraguay.

### Aswan Dam (Egypt)

The Aswan Dam in southern Egypt created one of the largest artificial water volumes in the world by damming the Nile, the enormous Lake Nasser (Table 13.11).

The goals of the project were to generate electricity as well as improve navigability, irrigate agricultural areas, develop new industries, and supply drinking water. But the plant also reduced nutrient levels in the water, dramatically reducing the fish populations in the Nile

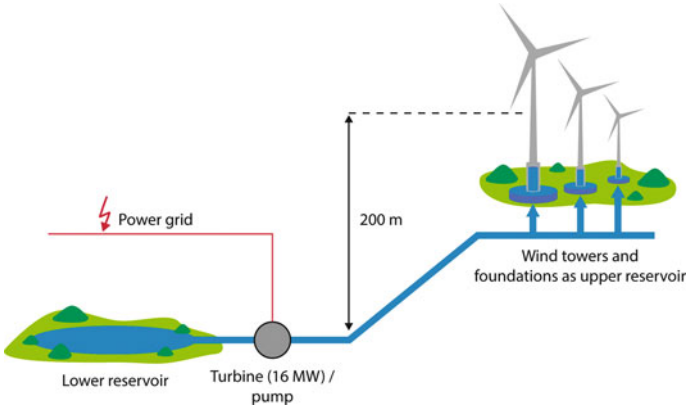



**Fig. 13.15** Basic design of the Gaildorf green electricity storage plant, a combined wind and pumped-storage plant. The bases and towers of the wind-power facilities are used as upper reservoirs [51]

and even in the Mediterranean. Some cultural assets were moved including the famous temples of Abu Simbel. But others were sunk in the Nile [26]. The plant also impacted the aquatic ecology of the Nile. Since the building of the dam, the Nile's fertile silt can no longer fertilize the fields downstream. In the 1970s, a large alkaline electrolysis (AEL) plant was also built at the dam to produce hydrogen for ammonia synthesis and fertilizer production (▶ Chap. 8).

#### 13.1.2.3 Special Combined Wind and Pumped-Storage Plant—The Gaildorf Green Electricity Storage Plant

In Baden-Württemberg near Gaildorf, four 5.0 MW wind power facilities are currently under construction that will be combined with pumped-storage to create a green electricity storage plant (Fig. 13.15). The base of each wind energy facility will be used as a water reservoir. These active reservoirs will be located in the lower sections of the wind turbines. The wind turbines are located in a passive reservoir or exterior reservoir that can hold most of the 40,000 $m^3$ of water contained in each tower. These special turbine bases will also increase the tower height by 40 m.

As in a pumped-storage plant, water will be pumped from a lower reservoir with a 160,000 $m^3$ storage capacity into the turbine bases using wind-electricity. The electric storage capacity will be 70 MW h [51].

The powerhouse will be connected to the storage bases by a polyethylene (PE) pressure pipeline. This pipeline can be flexibly laid along existing paths. As a result, the pumped-storage facility can be easily integrated into the landscape without major modifications. By using flexible machine-technology including several variable-speed pump turbines, the power plant can supply balancing power as well as store energy. The construction and machinery of this green electricity storage plant is completely standardized and modular in design. Using precast concrete components and pre-assembled machinery, the plant is largely prefabricated.

The project is funded by 7.15 million euros from the German Federal Ministry for the Environment, Nature Conservation and Nuclear Safety's environmental innovation program.

### 13.1.3 Flywheel Storage Facilities

Besides standard electricity storage technology using pumped-storage, other mechanical-energy storage systems are used for special applications. Because of their technical characteristics, flywheel storage facilities are used in the following areas:

- As stand-by storage to handle network fluctuations, short-term interruptions, network filtering, or frequency and voltage regulation.
- As energy reserves for load peaks or power-up and start-up processes.



**Fig. 13.16** Twenty MW flywheel storage facility used for frequency stabilization in the state of New York (source: Beacon Power LLC)

#### 13.1.3.1 Balancing Network Fluctuations

The commercially sized Beacon Power flywheel storage facility with 20 MW of buffering capacity is used in the state of New York by the New York Independent System Operator (NYISO) for frequency regulation. In operation since 2011, the storage facility is connected to a 115 kV distribution network. Previously, generators powered by fossil fuels or hydropower generators were used to balance network frequency fluctuations. Flywheel storage facilities with reaction times in the milliseconds are now used to balance network fluctuations more quickly.

The Stephentown facility uses 200 flywheels that complete between 3,000 and 5,000 full load cycles annually (Fig. 13.16). Tests in New England have shown that the system can complete 150,000 charging/discharging cycles without any losses in charging capacity. The tests proved the mechanical durability of this technology. The mechanical efficiency exceeds 97% and the electrical efficiency is around 85% [9].

The company is building other facilities at the same scale in Pennsylvania and smaller facilities in Massachusetts. No data about capital costs is available.

#### 13.1.3.2 UPS Facilities

Because they supply energy quickly and are cheap to maintain, flywheel storage facilities are suitable for stationary applications such as UPS facilities. The company Piller manufactures UPS facilities with powers ranging up to 2.4 MW and storage capacities ranging from 6 to 21 MW (1.7 to 5.8 kW h). The discharging durations at full power are short, ranging from 2.5 to 8.8 seconds.

The advantage of these facilities over conventional USP facilities is the high-power density. This reduces the space required. In addition, unlike batteries the facilities require no air-conditioning. The cost savings in comparison to battery parks are determined by the capital costs and the cycle life. The batteries must be changed in USP facilities using battery systems every five to ten years. Flywheel storage facilities have longer service lives. But the initial capital costs are significantly higher because of the costs for manufacturing the flywheels [57].

#### 13.1.3.3 Short-Term High-Power Energy

Special experiments in plasma physics require large powers up to 300 MW and energy quantities in short cycles that cannot be absorbed by the public electricity network. The Max Plank Institute uses several flywheel storage facilities to handle the strong alternating loads produced by fusion power plant research.

Cern, the European Organization for Nuclear Research in Switzerland, also uses this technology in its particle research facility. The facility uses one of the largest particle accel-



**Fig. 13.17** WEMAG/Younicos AG battery power plant in Mecklenburg-Western Pomerania using lithium-ion batteries (simulated exterior view). (Source: Younicos AG)

erators in the world to investigate the basic principles of the universe.

### 13.1.4 Battery Power Plants

Around the world for many years, battery power plants have been used to regulate electricity networks. In unstable network regions and primarily for conventional energy supply, they are used to ensure network quality or balance differences between generation and consumption.

For energy systems in transition, battery parks or battery power plants can help integrate fluctuating renewable energy by taking over system service, replacing fossil must-run capacity, and contributing to supply security.

#### ■ Europe's Largest Commercial Battery Power Plant Located in Germany

Battery parks can also be used in regions with very high renewable energy surpluses. In 2014, Europe's largest commercial battery power plant was completed. The plant is located in a very windy region of northeast Germany (see Fig. 13.17, 13.18, and Table 13.12). This joint venture of the battery company Younicos AG and the public utility WEMAG will serve here as an example of this facility type.

This battery power plant supplies positive and negative balancing power as a system service on the primary balancing energy market. The plant balances short-term network fluctuations and receives compensation at a capacity price. The facility's power electronics also allow it to meet transient requirements (fault ride-through/IR).

Although the facility is a pilot project, the plant is intended and expected to operate at a profit for over 20 years. The manufacturer Samsung SDI offers a 20-year guarantee on its batteries when operated with software and battery management from Younicos AG. Besides pumped-storage and storage water-power plants, in Germany, conventional power plants



**Fig. 13.18** Internal view of the WEMAG/Younicos AG battery power plant in Mecklenburg-Western Pomerania using lithium-ion batteries. (Source: Younicos AG)

**Table 13.12** Profile: WEMAG/Younicos AG battery power plant in Mecklenburg-Western Pomerania

| | |
|---|---|
| Capacity | 5 MW h |
| Power | 5 MW |
| Cell manufacturer | Samsung SDI |
| Cells installed | 25,600 cells |
| Guaranteed service life | 20 years |
| System service | Primary balancing energy |
| Co-operating partners | WEMAG, Younicos AG |
| Funding | 1.3 million € grant from the German Federal Ministry for the Environment |



primarily supply balancing power. As a result, combining battery power plants of this type with renewable energy could reduce greenhouse gas emissions.

The power plant is controlled by the network frequency. If the frequency falls below the standard frequency of 50 hertz, the power plant discharges to help maintain the frequency. If the frequency rises above a threshold value above the standard frequency, then the power plant charges. The batteries are only half-charged and discharged to allow latitude for supplying positive or negative balancing energy whenever required.

**Table 13.13** Profile: GVEA/Saft AG battery power plant using nickel cadmium batteries in Alaska, USA [23, 40, 83]

| | |
|---|---|
| Capacity | 6.75 MW h |
| Power | 27 MW (short-term max. 46 MW) |
| Capital costs at time of construction | 35 million USD |
| Manufacturer | Saft (cells), ABB (power electronics) |
| Cells installed | 13,760 cells, Ni-Cd |
| Dimensions and weight of batteries | 120 × 26 m, 1,300 tons |
| Service life | 20 years (with 100 full load and 500 partial cycles) |
| System service/application | USP, incoming and outgoing active and reactive power |
| Co-operating partners | Golden Valley Electric Association, Saft, ABB |
| Start-up | August 2010 |

#### North America's Largest Commercial Battery Power Plant

The world's largest nickel cadmium storage facility went into operation in 2010. It was built by ABB and Saft AG for the GVEA in Golden Valley, Fairbanks in Alaska (Table 13.13). The facility supports the network and ensures UPS for a stand-alone network in that location. The system weighs around 1,300 tons and contains 13,760 individual nickel cadmium cells connected in four strings. The system's power is 27 MW at a capacity of 6.75 MW h. This means that the system can supply 27 MW of power for 15 minutes. In exceptional circumstances, the system can deliver a power of 46 MW over a short duration of seven minutes. The nickel cadmium batteries have a service life of 20 years with 100 full load cycles and 500 partial cycles.

Installation of the storage required an investment of 35 million USD. This was equivalent to 36.4 million € in 2013 (adjusted for inflation). Assuming that a third of the total costs (around 12.2 million €) were incurred for the storage facility alone, then the resulting specific capital costs are 452 €/kW or 1,807 €/kW h [83].

Other sources give the costs as 250 USD/kW and 900 USD/kW h, with these figures referring to the costs in the year of installation. Adjusting for inflation, the resulting specific costs are 260 €/kW or 936 €/kW h [80].

The system reduces supply congestion by 65% and can be operated in several modes [23]:

- For voltage stabilization using reactive power control in continuous or overload operation.
- For frequency stabilization (with IR as the primary operating mode).
- For automatic scheduling of instantaneous power supply during voltage-drops on transmission lines or generators in the region.
- For balancing large, predictable load fluctuations by using load-management.

## 13.1.5 Decentralized Battery Storage Systems in Houses and Districts

### 13.1.5.1 Innovations and Trends

Household batteries are an established electricity storage technology. Falling costs have created new markets for this technology, allowing it to be used for a wider range of applications (see [24] and ▶ Sect. 12.5).

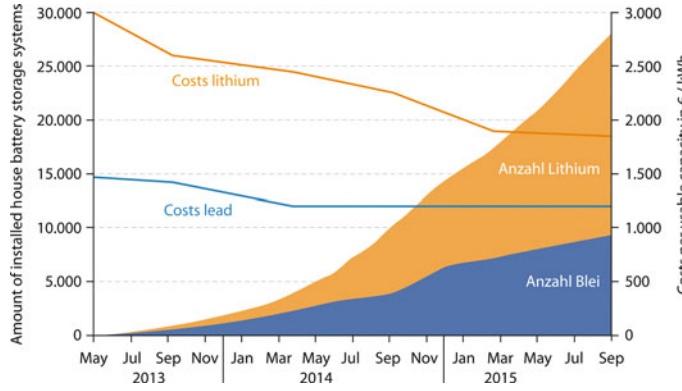



**Fig. 13.19** Comparison of the number of installed household-battery storage systems and costs for usable capacity with lithium and lead since the start of the KfW promotion program

Voltage maintenance, network structure overload, inadequate short-circuit capacity, and asymmetrical network loads are already challenges in the current transitional system. In the future, these problems will become more acute. Battery storage systems could be an answer (▶ Sect. 13.1.1).

### Battery Technology and Application Innovations

Intense efforts in the auto-industry have resulted in improved cell technology, the development of new materials, significant reductions in battery storage costs, and new as well as larger production capacities. Other areas have benefitted from these developments. These include UPS, off-grid systems, and battery storage for network stabilization or optimizing self-consumption. This last application is particularly relevant for many PV system operators because of falling lithium-ion battery prices and the increasing price differential between electricity costs and EEG feed-in compensation.

Particularly for intelligent control of decentralized generation (which includes weather forecasting, self-consumption, and overall system optimization), battery systems are increasingly important as integral components of building technology.

Between 2009 and 2012, system prices dropped by 30%. They will continue to drop going forward [38]. The construction of large production facilities such as Tesla's Gigafactory, for example, will also reduce costs (▶ Sect. 12.5). With a planned output of 35 GW h/a by 2020, the factory will supply both the transport sector and stationary energy storage facilities [14].

### Increasing Number of Installed Household-Battery Storage Systems

At the same time, in recent years the number of decentralized household batteries installed in Germany has significantly increased as well. This has been largely driven by the KfW banking group's storage promotion program. Figure 13.19 shows the trend for household batteries using lithium and lead. The costs for usable capacity with lead batteries has basically remained the same, but prices for lithium systems have fallen significantly. This is primarily the result of longer cycle lives with lithium-ion batteries. Since it can be reasonably assumed, based on the discussion above, that this trend will continue in the future, over the long-term, lead batteries will exit the household-battery storage market. Besides rising electricity prices, soft factors such as contributing to energy transition and a general interest in storage technology are decisive factors here in the decision to buy [46].

Storage users are also focused on maximizing self-consumption from PV facilities and increasing self-sufficiency. When battery storage systems are used purely for self-consumption optimization and priority is given to solar electricity charged in the morning, then PV feed-in peaks into the network result once the maximum state of charge (SOC) is reached. In this

case, the use of storage places additional burdens on the network instead of relieving it from stress. Battery storage systems can also be charged with electricity from the network. If they are charged in a pool in times of high electricity consumption, then this use of storage increases stress on the local network as well [47].

#### ▪ Requiring Operation That Benefits the System

For these reasons, it is essential to ensure storage system use benefits the network and the system, resulting in synergetic advantages for both storage and network operators. A (battery) storage system or a generation facility serves the system when its behavior promotes the larger goal of increasing the overall system's flexibility. This also means that storage system use optimally balances fluctuating supply with electricity demand, minimizing residual load fluctuations.

The battery storage system capabilities mentioned above primarily apply to the low and medium-voltage levels of the distribution network. But they could also be extended to the higher voltage levels. Like pumped-storage systems then, besides participating in arbitrage transactions for balancing generation they could also take over many system services. These services could also make storage operation more profitable. In Germany, the first facilities with powers in the range of several MW and capacities in the range of several MW h have already been installed (▶ Sect. 13.1.4).

For regulatory reasons, individual battery storage systems are currently not permitted on the balancing energy market. A solution here is to connect many smaller facilities into a larger virtual storage system. This is called pooling. Other generation and consumption facilities could also be combined with battery storage systems and then operated together as a virtual power plant.

**Example of Household-Battery Storage Systems Used as a Virtual Swarm Power Plant for Supplying PBP**

The Nuremberg municipal utility group and the distribution network operator, N-Ergie, partnered with the Siemens subsidiary Caterva for the SWARM pilot project. For the project, about 60 individual 21 kW h and 20 kW battery storage systems were equipped with mobile phone modules and connected in a swarm. The results was Germany's first virtual power plant composed of household-battery storage systems pre-qualified for supplying primary balancing energy. Caterva alone is responsible for the participation on the balancing power market, so no additional burdens are placed on the homeowners [22].

The system's storage capacity is 20 kW h. Of this total, 4 kW h is reserved for homeowner PV self-consumption optimization, and16 kW h for the distribution network operator's swarm operations. Caterva developed the control software and the battery system. N-Ergie handled the prequalification including the legal framework. It also connected the swarm to the operation control center.

#### ▪ Compensating for System Services

The compensation for these additional system services in the electricity system has yet to be determined. But adequate compensation for private operators is required when private property (battery storage) is used for a common purpose (stable electricity supply). Such use must also not disadvantage private operators. Compared with other electricity system components, electricity storage is an extremely flexible element that can be added at short notice to compensate for unexpected developments such as delayed network expansion.

### 13.1.5.2 Increasing Self-Sufficiency

Batteries are frequently used to increase household self-sufficiency. But even an infinitely large battery combined with a PV facility limited to the size of the roof of the house cannot make a household completely self-sufficient. The only exceptions are households with large PV facilities and/or very low energy consumption (◘ Fig. 13.20).

Household-battery storage systems are also used to increase the cost-efficiency of PV facilities. The differential between market price or

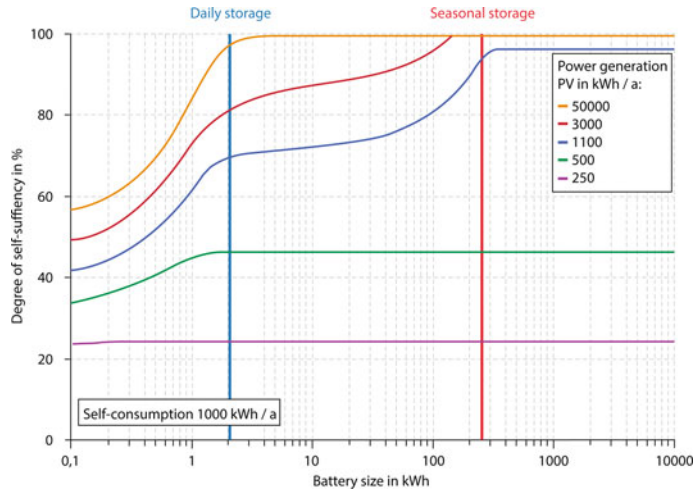



**Fig. 13.20** Level of self-sufficiency as a function of battery size and annual PV yield [89]

feed-in compensation and energy supplier electricity prices is increasing steadily. As a result, the financial advantages of self-consumption are also steadily increasing. Without storage, energy consumption can typically only be reduced by about 30% if quality of life and daily routines remain the same. With a battery system, consumption can be reduced by around 60 to 65% [73].

Figure 13.20 shows the level of self-sufficiency by battery size and PV electricity generation. Two aspects are particularly worth noting here. On the one hand, after a certain point, increasing battery capacity does not significantly increase self-sufficiency. This point is reached when the battery stores more than is required for daily consumption. The optimal size is 2 kW h storage capacity per 1,000 kW h consumption [89].

On the other hand, a very large storage system can be used as seasonal storage to store electricity surpluses in summer for winter consumption. But this requires a battery capacity exceeding 100 kW h. These batteries are not financially viable for private households in the current environment.

This means that full self-sufficiency is only possible if summer surpluses are transferred to the dark months of winter using a battery, or if the PV facility is large enough to supply adequate energy even in winter. Both systems are very costly, or can only be implemented at significant additional costs.

### 13.1.5.3 Stabilizing the Electricity Network

The following sections analyze the technical potential of decentralized battery storage and then describe which options are available today and could be implemented over the medium-term.

#### ▪ Maximizing Self-Consumption of Solar Electricity

Maximizing self-consumption of solar electricity using a battery storage system means covering self-consumption as far as possible with electricity self-generated directly on-site. Since solar electricity fluctuates dramatically depending on weather conditions, battery storage systems are used here for buffering. They generate financial rewards for operators by arbitrage between the EEG promoted feed-in compensation for PV facilities and the end customer electricity price including all surcharges.

Four standard procedures are applied here [10, 46]:

1. Direct charging
   Solar electricity is first consumed on-site. When generation exceeds consumption, the solar electricity is charged. When supply falls short, it is discharged. A disadvantage with this procedure is feed-in peaks with

steep gradients. When the Sun is shining brightly, these peaks occur around noon once the storage system is fully charged. But a large number of different facilities of various capacities limits this effect. This is because the facilities then do not tend to feed-in all at the same time, distributing the feed-in more widely [33, 34].

2. Delayed charging
   With delayed charging, a control unit is used to partially store the solar electricity generated over the day in the battery until a pre-defined SOC, and partially feed it into the network. This prevents high feed-in peaks.
3. Peak shaving
   Compared to the preceding two procedures, this procedure places the least burden on the network. Here, PV generation feed-in peaks above 60% of the PV generator power are charged. This means that network-critical noon-time peaks from PV generation are absorbed, but the priority of self-consumption is secondary.
4. Forecast-based charging
   This procedure is a combination of the three previous procedures. A load and weather forecast determines at what time of day charging relieves stress on the network. After direct charging, this procedure results in the highest self-consumption, while serving the network at the same time. If PV feed-in power is reduced to 70% of the installed capacity or even lower in the future, this procedure would result in the lowest levels of curtailed energy [10, 46].

Figure 13.21 shows the basic differences between the four procedures. Together with the of the Network Technology/Network Operation Forum (Forum Netztechnik/Netzbetrieb; FNN) technical guidelines for connections, the current methods for maximizing self-consumption including peak shaving are a start towards benefitting the network and the system. Maximizing self-consumption can also help maximize the amount of renewable energy beneficially integrated into the system. But still, important aspects of system optimization are ignored. One example is when a battery storage system is charged with solar electricity, but at another location in the distribution network an electricity deficit results in supply by conventional power plants. In the reverse case, in a network area with many wind-power facilities, too few consumers and too little transport capacity may lead to curtailments when the decentralized battery storage systems are full.

To better satisfy these criteria for optimizing the network and the system, in addition to the current network situation, self-consumption systems with PV storage should integrate consumption and weather forecasts into their operation. Decentralized system solutions that fulfill these requirements and benefit the system without higher-level control are already available on the market. These solutions used what is termed forecast-based charging.

Self-consumption systems should also be capable of moderating or ramping steep gradients when electricity is drawn from the network, as well as when electricity is fed into the network. This would stabilize the behavior of these systems from the network point of view. In addition, the use of storage cannot be permitted to perpetuate conventional power plant operation, and as a result, increase $CO_2$ emissions from energy supply.

### Voltage Maintenance and Voltage Quality

General voltage maintenance and voltage quality requirements are discussed in ▶ Sect. 13.1.1.2. Decentralized battery storage systems are capable of supplying reactive power control. This application is permitted under FNN guidelines, but no compensation is provided.

The transition to converter-based generation such as wind and PV has resulted in increasing shortages of reactive power control. This is because converters disconnect from the network in case of a disturbance, typically worsening the problem. In the future, battery storage systems could reverse this trend by collectively supplying short-circuit capacity at the medium-voltage level.

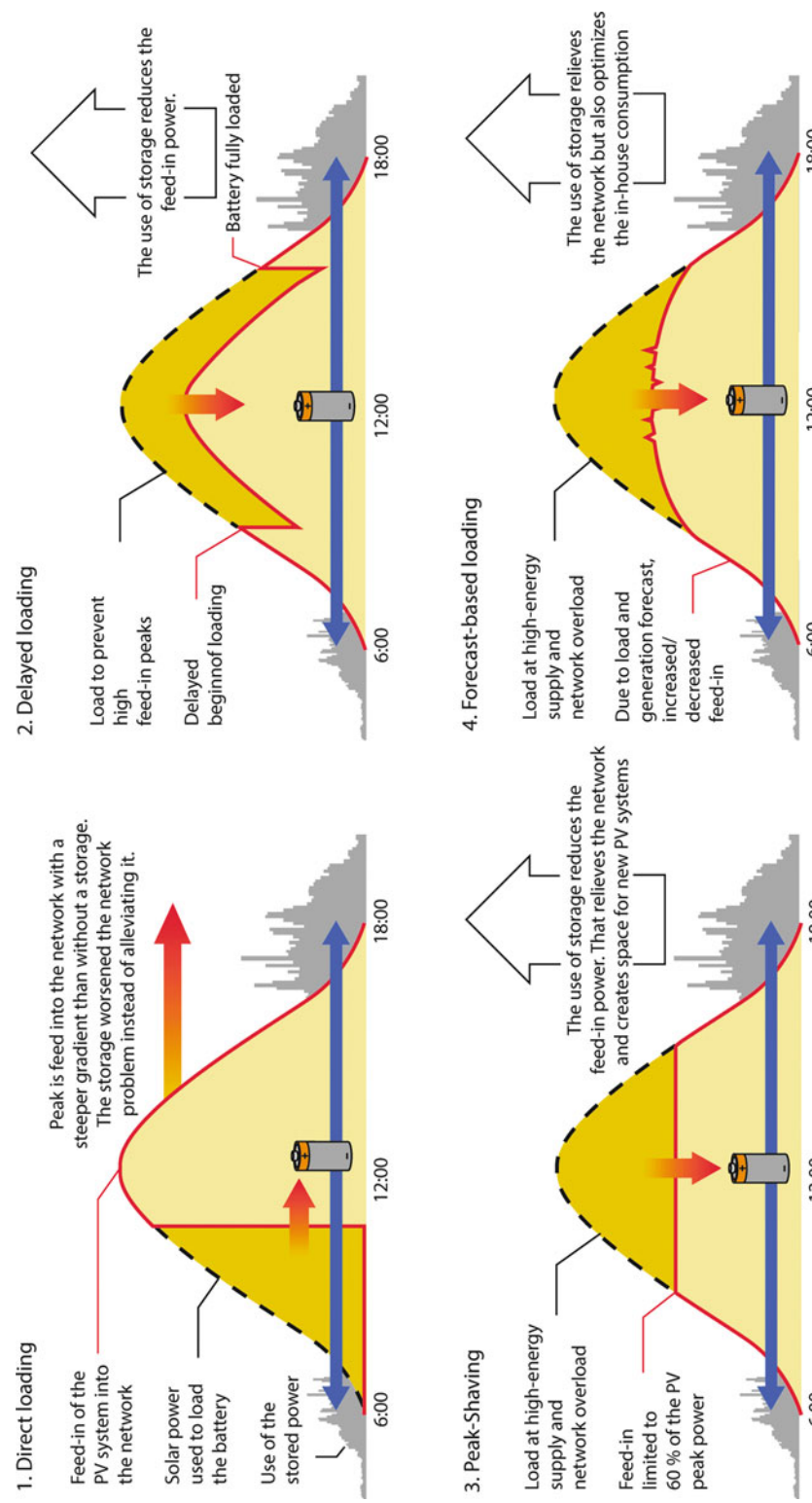



**Fig. 13.21** Comparison of four different battery storage procedures: direct charging, delayed charging, peak shaving, and forecast-based charging as a reliable approach to storage operation benefitting the system [10, 46, 61]

Local storage together with real power reduction could counteract voltage increases in the distribution network caused by renewable feed-in. It has been shown that storage use generally increases shares of integrated renewable energy [33, 92].

### ■ Network Operations—Gradient Control and Network Congestion Management

In the current electricity system, battery storage plays only a negligible role in ensuring secure network operation free of disruptions. Specific generation units can also be shut off or turned on to ease network congestion (power plant redispatch). In the future, batteries could be used at targeted overloaded points on the network to ease congestion situations, as well as to prevent the curtailment of renewable suppliers, for example. In the future, according to [61], in specific cases battery use could be more cost-efficient than curtailing.

Peak-load control by larger consumers using decentralized battery storage systems could reduce electricity demand peaks, reducing stress on the network, and as a result economically optimizing operations.

Steep gradients in residual load caused by fluctuating renewable energy feed-in are increasingly a problem in network operations. Particularly at the generation site, decentralized battery storage systems can counteract gradients in generation power by charging or discharging during quick changes in load.

In special cases, battery storage could be a cheaper flexibility option for the distribution network than conventional network expansion. When voltage problems coincide with overload problems and target grid planning diverges from currently permissible network expansion, voltage problems are effectively unnecessary.

### ■ Balancing and Reserve Power—Frequency Maintenance by Real Power Control

Because of their quick reaction times in the millisecond range, battery storage systems are ideally suited for supplying balancing power in a range up to minutes. This means that they can supply IR [61]. Such systems are already operating profitably in the PBP area. One example is the Younicos battery power plant (▶ Sect. 13.1.4). But they have not been shown in practice to be profitable in the SBP and minute-reserve areas (▶ Sect. 13.1.1), and they will not be profitable in these areas unless costs fall dramatically. Increasing the supply duration negatively impacts their use in the secondary and minute-reserve markets as well. This is because battery storage prices are primarily determined by capacity costs (€/kW h) [27].

Calculations by the German Energy Agency (Dena) have shown that by 2033, PBP supplied by hydraulic and thermal power plants will no longer fully meet the demand [61]. In the future, as thermal power plant availability falls, battery storage could be an economical solution for ensuring a decentralized supply of PBP [61]. But to fulfill the requirements for participating on the balancing energy market, decentralized battery storage systems must be connected in a swarm (pool).

#### Example of a Household-Battery Storage System with PtH Used as a Large Storage System for SBP and Minute-Reserves

The company Deutsche Energieversorgung in partnership with the company SENEC offers type Storage G2 lead batteries with a usable capacity of 8.2 kW h and a storage power of 2.5 kW. These units can be combined by central coordination to create a virtual, dynamic large storage system.

Using this 'economic grid' concept, SBP and minute-reserves are supplied to charge and discharge the battery storage system, or to operate a heating rod (PtH). The electricity removed is also supplied to the operators at no cost. This amounts to up to 800 kW h of electricity for the household and up to 2,500 kW h for the heating rod. Besides the batteries and the heating rods, information and communication technology such as relays, meters, and routers must be installed. The provider promises customers that the system will be amortized in this way in the course of less than ten years, and guar-

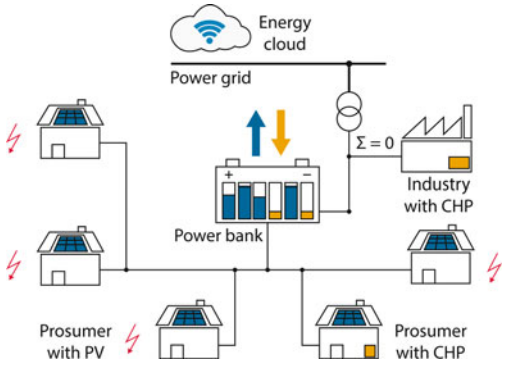



**Fig. 13.22** District-battery storage system using the electricity bank concept developed by ads-tech and MVV [54]

antees it for the same period. The homeowner contractually grants power of attorney for prequalification (ÜNB, VNB, balancing group manager) to SENEC. The company then operates the decentralized components as a pool for SBP and minute-reserves [19].

**Example of a District-Battery Storage System Used as an Electricity Bank**

The battery system manufacturer, ads-tech, together with the Mannheim public utilities, MVV, developed the electricity bank concept. Here, several lithium batteries are combined in a container to store surplus energy from decentralized generation from PV and district heating plants. Storage occurs at the low-voltage network level.

The electricity bank functions like a normal bank. When surpluses from PV or CHP of a prosumer (simultaneous consumer and generator of energy) occur, they are 'deposited' into the electricity bank account. Then when there are deficits, they are 'withdrawn' (Fig. 13.22). Households only require a metering box with a cellular connection to be installed.

Unlike in the SENEC and CATERVA examples, here the storage system is a district-storage system that is centrally located instead of in the consumer's house. This facilitates maintenance (24-hour access) reduces costs (MW h instead of kW h) and permits the electricity bank to participate in the balancing power markets during idle periods. As a result, this concept represents a promising new business model for public utilities [54].

### ■ Supply Security and Recovery

In the current electricity system, black-start capable pumped-storage plants are particularly crucial for supply recovery. But battery storage systems could also serve this purpose. Adequate available power and storage capacity as well as suitable control mechanisms are the only requirements here. If small, decentralized storage systems contribute to supply recovery, a reconnection process after black-outs must also be established. With appropriate power electronics and interfaces, wind parks, gas turbines, and district heating plants using battery storage systems could also be modified to provide black-start capability. This is because nacelle rotation, rotor blade pitch, and excitation voltage for example can be set without network availability [61].

In addition, battery storage systems could also potentially be used to increase the guaranteed capacity of generation facilities. In the case of foreseeable short-term load peaks triggered by price fluctuations, battery storage systems could be charged in advance for supplying guaranteed capacity to cover these consumption peaks. In the current environment, it is not cost-effective to maintain a battery storage system fully charged over a long period for this purpose.

Battery storage systems—particularly lead battery systems—are standard technology for UPS, and are used to bridge short supply gaps or permit the controlled shut-down of sensible loads. Other cell technologies, such as lithium-ion technology, are also beginning to be used for this purpose.

### ■ Balancing Generation on Spot Markets—Exchange and OTC

From a technical point of view, battery storage systems are capable of participating in electricity markets. As prices fall, these systems will probably become an attractive option for short-term balancing of wind and PV feed-in fore-

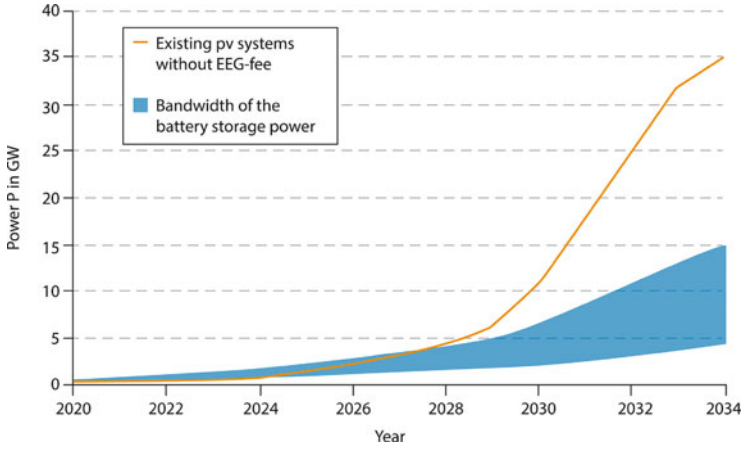



**Fig. 13.23** Cumulative power of PV facilities with EEG incentives and the range of battery storage capacities until 2034 [79]

casting errors on the power exchange's intraday spot market and in off-exchange trade.

Currently, participation of battery storage systems on conventional power markets is not economically viable. Assuming electricity prices remain constant, in the future, prices for battery storage systems must fall significantly if they are to participate in the spot markets [27].

### 13.1.5.4 Potential Household-Battery Storage System Trends

There are about 20,000 household-battery storage systems currently installed in Germany. Assuming each facility has a power of 3 to 4 kW, their cumulative power is 45 to 80 MW.

#### ▪ Price Difference Between Electricity Costs and PV Electricity as an Incentive

By all accounts, market development will be highly dynamic. This is because intermediary storage of electricity from PV facilities was not cost-effective until now. This changed when the EEG compensation for PV facilities sank below price levels for electricity drawn from the network. The cost difference between self-generated electricity and electricity from the network is expected to grow in the future. Combined with falling costs for battery cells, storing electricity on-site will then become profitable for a larger group of consumers.

EEG incentives for a large number of PV facilities will expire in 2029. As a result, household-battery storage system capacity could grow to 15 GW. This is because most installed PV systems continue to deliver over 80% of their rated power, even after 20 years, and can have service lives ranging from 30 to 35 years.

Figure 13.23 shows the number of existing PV facilities without EEG incentives and the range of installed storage capacities [79]. The numbers for existing facilities without EEG incentives were determined under the assumption that currently installed facilities will no longer have EEG incentives after 20 years. Most PV facilities in Germany were installed between 2009 and 2011. As a result, there is a steep rise in installed battery capacity starting in 2030. Facility storage capacity was assumed to be 4 kW across the board. The range of storage capacities reflects the range of powers for the existing facilities that will no longer have EEG incentives. These powers will range from a minimum of 5% to a maximum of 30% of the installed PV-rated power. It was also assumed that by 2030 around 700,000 PV facilities combined with storage would be installed [79].

#### ▪ Peaks in PV Feed-In into the Network Despite Storage Use

A transmission network operator's simulations, including around 7.5 million household storage facilities, have shown that despite the use

of storage, peaks in PV feed-in into the network will occur in summer. This is because in summer most storage facilities are full, while in winter they tend to be empty. This means that with smaller storage systems, no reduction in peak feed-in can be expected in summer. But it can also be assumed that the use of battery storage systems in stationary and mobile applications will smooth the load profile overall. This factor should be taken into account in network simulations.

For commercial reasons, there could be a large number of such battery storage systems that would end up in the electricity system. This would then significantly affect electricity network operations. As a result, as discussed above they should be operated so that they benefit the network and the system.



**Fig. 13.24** The Earth at night—the regions with electricity are visibly illuminated. (Source: [M] 1xpert, fotolia)

### 13.1.6 Stand-Alone Networks with Renewable Energy and Storage Systems

The first electric networks were stand-alone networks. The continental networks were created in the last century by combining these stand-alone networks. Stand-alone networks still exist today in industrialized countries. For example, primarily in remote regions such as the Alps, solar home systems are used. These systems include a PV facility, a control unit including loads, and a battery storage facility. Off-grid generation facilities such as these can also use wind-power facilities.

But the greatest potential for stand-alone systems is in rural regions lacking electricity, as well as on hundreds of thousands of islands across the globe. The following discussion focuses on three islands with a high share of renewable energy that have storage systems.

#### 13.1.6.1 Background and Potential

In industrialized countries, a constant supply of electricity is taken for granted. However, less than half the world has access to electricity supply. These regions are typically rural areas far from distribution networks (Fig. 13.24). Around 1.3 billion people or a fifth of the world population has direct access to electricity supply [58].

Stand-alone networks are the only way to supply these remote areas and islands, which do not have access to the electricity and gas networks, with electricity. Often fossil fuels such as diesel are shipped into these area over great distances to power generators that supply electricity.

Since existing stand-alone networks depend on large shipments of fossil energy sources, increasing fuel prices and falling renewable energy prices will make transitioning to renewable sources an attractive option. In addition to cost, economic criteria such as independence from fossil imports or environmental issues are also crucial factors for stand-alone networks with storage systems.

- **Competition of PV with Diesel Generators as a Driver for Storage Systems**

PV facilities are already cost-efficient in many regions lacking electricity supply. But high subsidies for fossil diesel and lack of access to the technology as well as the maintenance infrastructure often stand in the way.

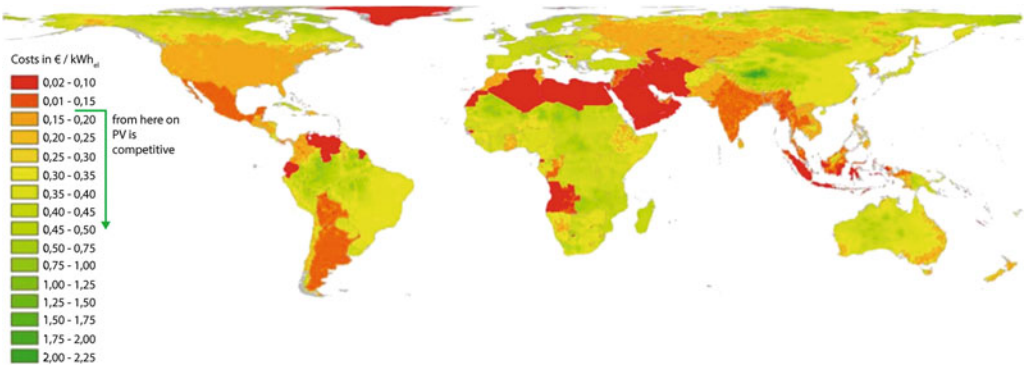



**Fig. 13.25** Electricity generation costs using diesel in various countries. Areas with domestic oil reserves and high diesel subsidies are in *red* [58]

Electricity generation costs in diesel-powered stand-alone networks across the globe currently range from 0.02 to 2.60 €/kW h, i.e., from 0.2 to 26 € per liter of diesel. This wide price-spread is the result of subsidies for this fossil fuel, transport over large distances to remote areas, and fuel scarcities. At electricity generation costs above 0.25 €/kW h (2.5 € per liter of diesel), there is an economic incentive to use PV facilities in stand-alone networks. As Fig. 13.25 shows, this is especially the case in sunny regions with high diesel prices [58].

In these regions, PV systems would have an amortization period of less than four years and could deliver savings of up to 2.25 €/kW h. This means that there is major potential for expanding renewable stand-alone networks with storage in these areas.

#### ▪ Technical Implementation of Renewable Stand-Alone Networks Using Storage Alone

Since wind and weather as well as electricity-demand fluctuate dramatically on an island, ensuring network stability poses an extremely difficult technical challenge. Besides information and communication technology as well as an energy-management system, pure renewable energy supply is out of the question without storage.

A stand-alone network includes the components detailed in Table 13.14.

The design and combination of these stand-alone network components are as varied as the islands and regions themselves. Meteorological conditions as well as regional requirements differ widely. Comparing the industrialized American island state Hawaii with the undeveloped east African island of Zanzibar, for example, demonstrates these contrasts.

Using existing or planned stand-alone networks as examples, the following discussion examines the various renewable energy and energy storage system options. Methods of system control and financial aspects are also considered.

### 13.1.6.2 Storage Integration on the Island Graciosa in the Azores

The Portuguese island Graciosa belongs to the Azores archipelago in the Atlantic Ocean. It has an area of around 70 $km^2$ and about 4,500 inhabitants. Younicos AG is building a stand-alone electricity supply system here for the energy supplier EDA, using battery storage and a very high share of wind and solar energy. The power purchasing agreement (PPA) has already been signed [32, 84].

#### ▪ Existing Electricity Supply System

The average annual electricity demand on the island is about 14 GW h. The largest peak load is about 3 MW. Currently, 85% of electricity de-

**Table 13.14** Stand-alone system components

| | |
|---|---|
| Generation unit(s) | PV and wind-power facilities, possibly a back-up generator powered by diesel or biofuels, rarely hydropower facilities |
| Energy storage systems | Typical battery storage system, rarely others such as PtG facilities, for example |
| Energy-management system | Facility control technology integrated in the control room |
| Consumers | Households, trade, and possibly the industrial sector |

mand is met using fossil fuels, and about 15% by wind-power facilities. The diesel generators have a total power of 4.2 MW and at 11.9 GW h a utilization of at least 2,800 hours. Each year, 4 million liters of fossil fuel are shipped to the island for the diesel generators.

### Planned Electricity Supply System

The share of renewable energy in the electricity supply system will be increased from (currently) 15% to between 60 and 70%, or up to 100%. The plan is to use fixed-tilt PV facilities with a power of 1 MW. In addition, six Enercon E44 wind-power facilities with a specific power of 900 kW (in total 5.4 MW) will be used. Besides a single transmission line to the wind part, no additional network expansion is required. The remaining 30 to 40% of electricity demand will be met by about three 1 MW back-up generators using fossil fuel. In the future, the generators will be renewably powered by vegetable diesel produced by pyrolysis using renewable electricity. The back-up generators will only be used in the rare instances when there is no wind or solar electricity available, and the battery storage system is in a low SOC.

### Storage Use

To ensure stable network operations, balance generation, and to supply all necessary system services, a battery park is integrated into the system. A 1.5 MW lithium-ion system with a capacity of 1.5 MW h will be used as what is termed a power battery. A high-temperature sodium-sulfur system with a total power of 1.2 MW and a capacity of 8.5 MW h will be used as what is termed an energy battery for balancing over several hours. With a moderate number of cycles under adequate control, it has an average service life of 15 years. The battery system has a quick AC reaction time below 100 ms.

Figure 13.26 illustrates the planned system.

### Control and Energy Management

One of the greatest challenges with building a stand-alone network based on renewable energy is control. The system was required to ensure supply at a quality that meets EN50160 requirements.

There were also different requirements for central and decentralized monitoring units (Fig. 13.27).

A central controller optimizes network operations and ensures balanced generation. It is also tasked with battery management and maintaining long-term supply security. Because of the storage capacity of the batteries, these processes are not time-sensitive.

The decentralized controllers ensure network stability by balancing capacity. They independently take these stabilizing measures as required. With durations ranging from microseconds to seconds, these measures ensure stable network operations by decoupling the electricity networks from the communication media networks.

EN50160 requires maintaining adjustment limits determined by the service quality standards for frequency and voltage control. The primary limiting parameters here are the tolerances and qualitative requirements. High-performance computers in the battery converter control electronics performing this con-

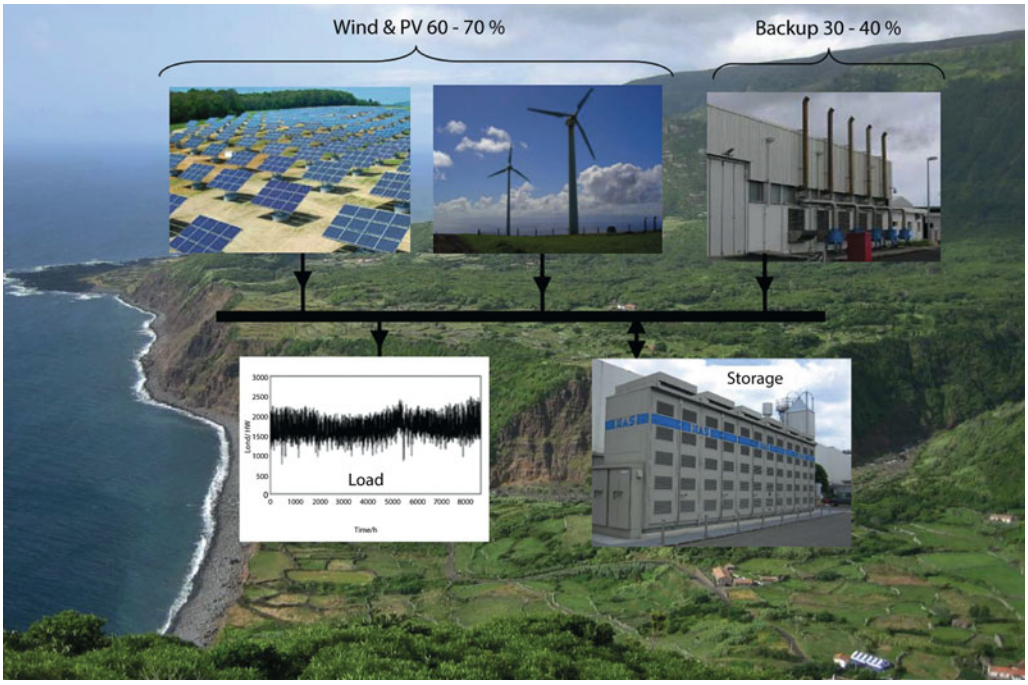



**Fig. 13.26** Renewable electricity supply system including battery storage on the island of Graciosa [87]

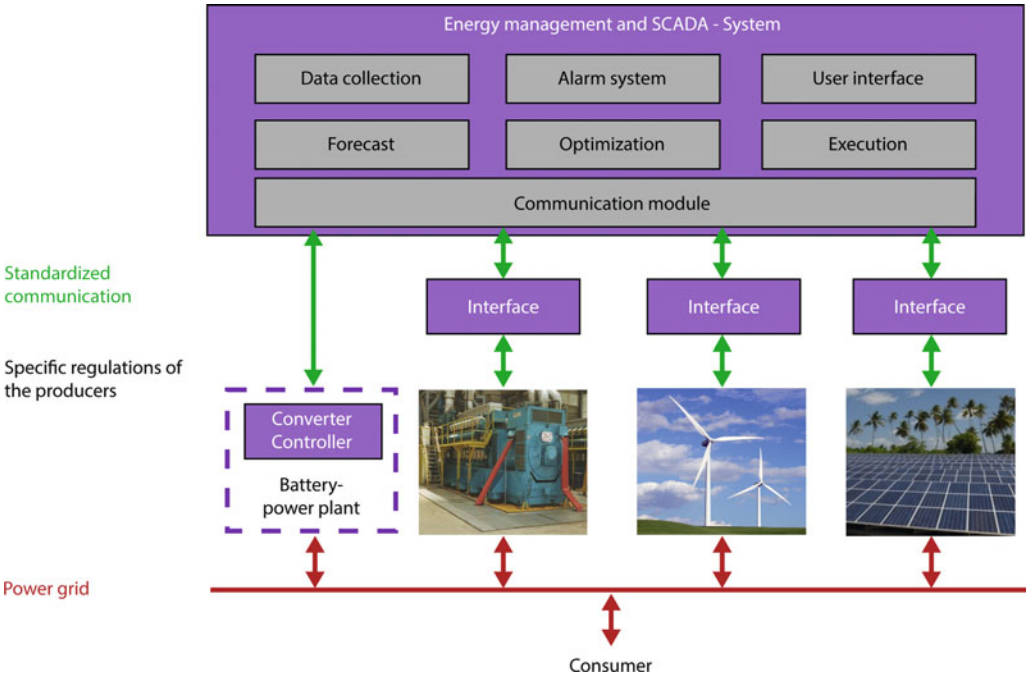



**Fig. 13.27** Control of the stand-alone system on Graciosa. (Source: Younicos AG)

trol task. These computers quickly and accurately monitor the network state.

The queries permit the converters to shut down all required points in the power quality area. This means that, unlike with rotating masses, the network frequency is not modified by slowing or accelerating the machine. Here, the battery power control algorithm is modulated instead. In a system using 100% renewable energy and with the fluctuations that result, these intelligently controlled storage systems can maintain frequency and voltage in the ranges required.

The decentralized control units use frequency performance curves, and can be operated in parallel as voltage sources in accordance with EN50160. As a result, the renewable power plant park can be conveniently expanded at a later time.

The network frequency is the command variable and the controlled variable. Frequency deviations can be detected by monitoring the battery SOC or discharge. These deviations are then used to control the reaction of the other components of the stand-alone network. Supplier and loads are intelligently balanced as a result, minimizing losses in the system. Even if IT communications between the decentralized components and energy management fail, stabile network operations can be maintained by using the frequency as the communication medium.

Adequate short-circuit capacity supply as a safeguard in case of a network failure is another EN50160 requirement. Fast battery inverter control can modulate short-circuit current, maintaining compliance with standards and protecting the converter from overvoltages.

Figure 13.28 shows test operations using a model of the stand-alone system at a scale of 1:3 in Berlin. The system, together with battery system 1 (lithium-Ion) and 2 (sodium-sulfur), quickly balances out network fluctuations.

#### Cost-Efficiency

Capital costs for the entire projects are around 25 million €. In addition to the storage systems, this includes the wind-power and PV facilities, the monitoring and control system, the electricity transmission lines, the land, financing costs, and project development costs. There are additional annual maintenance costs amounting to the usual 2% of capital costs (▶ Chap. 2). Over a period of 20 to 25 years, the stand-alone system can annually supply about 8.5 GW h of electric energy. This means the system can ensure a cost-efficient, sustainable energy supply.

### 13.1.6.3 Storage Integration on the North Sea Island of Pellworm

A second stand-alone network is the SmartRegion Pellworm on the North Sea island of Pellworm in Schleswig-Holstein's Wattenmeer National Park. With an area of 37.44 km$^2$, Pellworm has 1,180 inhabitants in 560 households [69].

#### Previous Electricity Supply

Pellworm Island has a long history of decentralized energy supply. In 1983, a solar power plant with a peak power of 300 kW was built on the island. Three wind-power facilities with a total power of 100 kW were added in 1992 to create a hybrid power plant. Operated by E.ON Hanse Wärme GmbH, the hybrid power plant currently has an installed electric power of 1,072 kW with 772 kW from PV facilities and 300 kW from wind-power facilities. In addition to the hybrid power plant, there are also a large number of wind, solar, and biomass facilities as well as a community-owned wind park on the island of Pellworm. Two 20 kV undersea cables connect the island to the mainland, allowing compensation for power surpluses and congestion.

For the SmartRegion Pellworm innovation study, details of all the suppliers and consumers on the island of Pellworm were compiled and assessed. The study concluded that electricity generation exceeded electricity consumption at least three-fold (Table 13.15). A large portion of the capacity (11.9%) and energy yield (6.3%) was supplied by the hybrid power plant. Four-

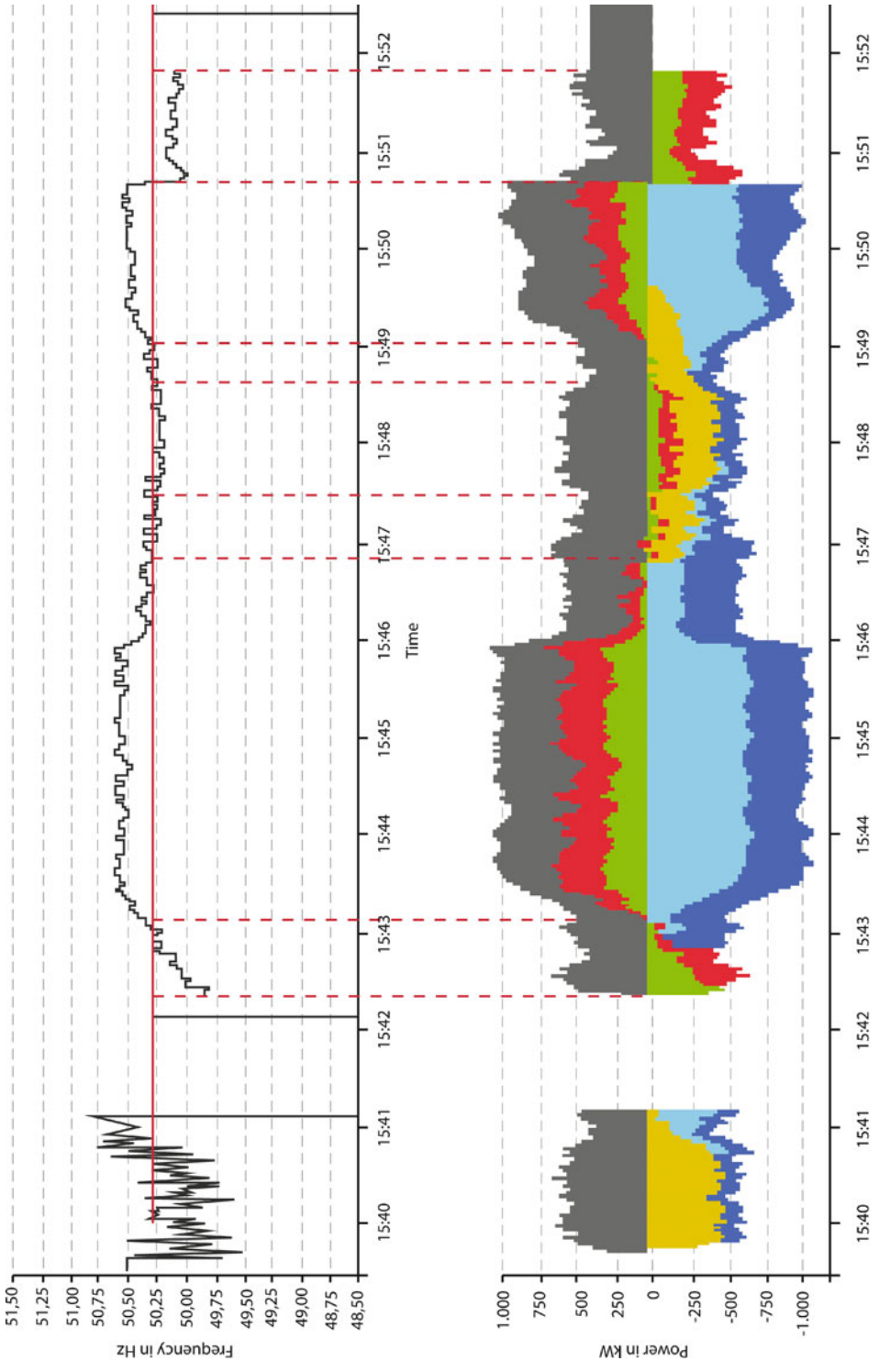



**Fig. 13.28** Test operation for frequency maintenance using a 1:3 scale model of the system on the island of Graciosa [84]

**Table 13.15** Planned annual renewable energy electricity supply based on real supply data from 2011 [11, 69]

| Generation unit | Installed power in kW | Quantity of energy feed-in in 2011, in MW h/a | Number of full load hours in hours per year |
|---|---|---|---|
| Hybrid power plant Wind | 330 | 946 | 2,868 |
| Hybrid power plant PV | 772 | 745 | 965 |
| Wind Grüner Deich 1+2 | 400 | 1,082 | 2,705 |
| Wind Schütting | 225 | 693 | 3,080 |
| Pellworm wind park | 4,800 | 13,866 | 2,889 |
| Biogas facility | 530 | 4,463 | 8,422 |
| Private PV facilities | 3,404 | 3,740 | 1,099 |
| **Total** | **10,461** | **25,535** | **2,441** |
| **Consumption unit** | **Number of meters** | **Annual energy consumption in MW h per year** | |
| Households | 731 | 3,275 | |
| Businesses | 185 | 1,179 | |
| Special agreements | 57 | 815 | |
| Heat storage stoves | 148 | 1,498 | |
| Electric heat-pumps | 20 | 179 | |
| Farming | 15 | 123 | |
| **Total** | **1,156** | **7,069** | |

13

teen percent of the energy generated was used to for heating [69].

To actively involve the local population in the study, the study also surveyed opinions on the generation facilities and the expansion of the electricity network. The results of the survey showed that more than two-thirds of the participating households felt that expanding the intelligent electricity network was a good idea.

### New Electricity Supply

The goal of the SmartRegion Pellworm project is to maximize the quantity of renewable electricity used for self-consumption on the island of Pellworm, thus reducing electricity consumption from the mainland. The project was also designed to yield insights on transitioning a network towards a renewable electricity supply, which could potentially be applicable to other regions also.

To achieve these goals, storage systems will be integrated into the system to absorb surplus electricity and then release it when required. The network will also be intelligently expanded (smart grid) to ensure network stability. Suppliers, consumers, and network components will be coupled so that they could react to deviations concertedly. In addition, new technologies such as CLNT will be installed [69, 72].

Figure 13.29 shows a snapshot of generation, transport, storage, and consumption on the island, using dat available online.

The renewable energy facility parameters for the planned electricity supply based on real supply data from 2011 and compared to consumption are shown in Table 13.15 [11, 69].

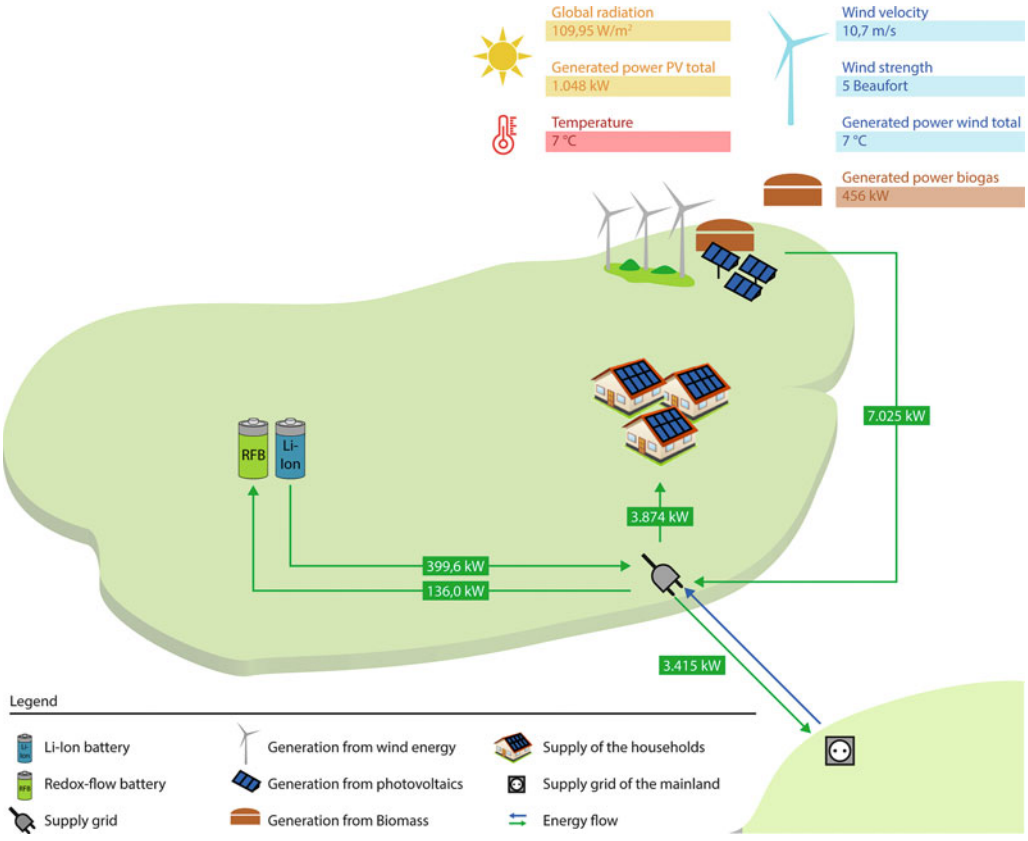



**Fig. 13.29** Current feed-in, consumption, and weather data for the SmartRegion Pellworm [72]

## Storage Use

On Pellworm, two short-term storage systems are used as what are termed a power battery and an energy battery [72].

A redox flow battery is used to store surplus energy over longer periods with minimum losses so that it will be available during periods of little wind or Sun. Vanadium salts stored in various tanks are used as an electrolyte. This allows the redox flow battery power to be dimensioned independently. It has a charging and discharging power of 200 kW and a storage capacity of 1,600 kW h. As a result, this short-term storage system has a discharging duration of 8 hours.

A lithium-ion battery is used as a power battery to balance fluctuations and supply greater power. Here many lithium-ion cells are connected together to form a larger unit (battery pack) placed in a container together with the battery management system. This battery pack has a total storage capacity of 560 kW h. The maximum charging capacity is 560 kW, and the maximum discharging capacity is 1,100 kW. This means that the battery container can be charged or discharged in 30 minutes.

In addition to the redox flow and lithium-ion batteries, there are 11 households with existing installed PV household battery systems on Pellworm. These systems fall in two categories. The smaller systems have a storage capacity of 6 kW h and a power of 4.5 kW. The larger household storage systems have a storage capacity of 9 kW h and a power of 10.5 kW, more than double the smaller systems. Pellworm's energy-management system can oper-

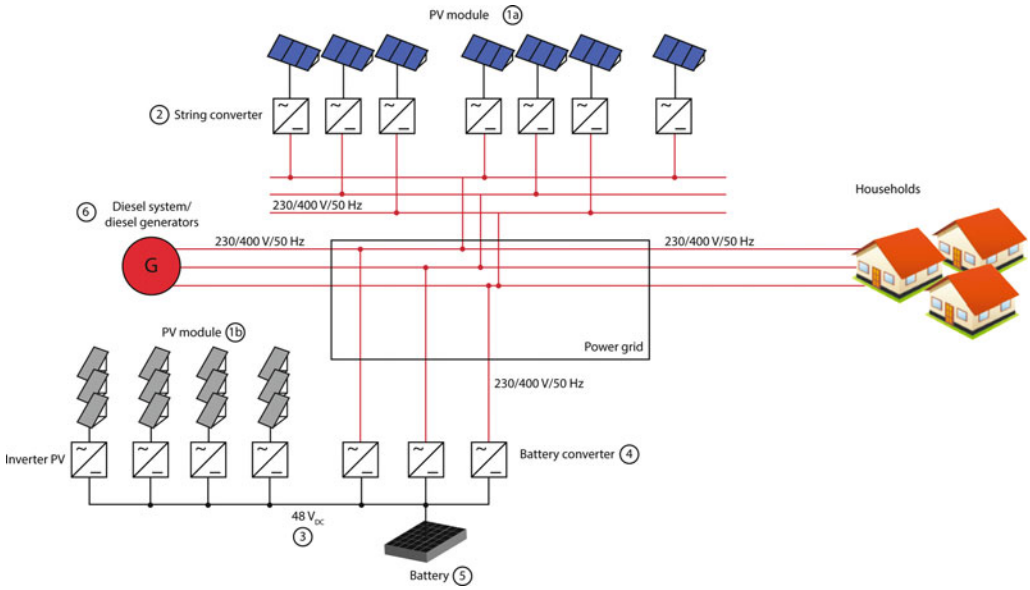



**Fig. 13.30** Integrated energy-management system in the Pellworm SmartRegion [11]

ate these 11 household storage systems as a virtual storage system for hourly storage with a capacity of 80 kW h and a power of 80 kW.

The utilization of these battery systems depends heavily on the application field and the operating strategy. They can be used for various purposes, including balancing generation on the electricity market, relieving stress on the network by network congestion management, increasing self-consumption, or a combination of all three of these (▶ Sect. 13.1.1)

Heat storage stoves are used as flexible loads for load-management (PtH). The electric heat stored can be used to heat living spaces as and when required. A module is used to forecast heating requirements. This permits more renewable electricity to be integrated while ensuring heating requirements are met at all times. Electric vehicles will be integrated into this virtual storage system in the future as well.

### ■ Control and Energy Management

Two CLNT keep the voltage constant at 400 V during load fluctuations. Load increment switches in the transformers adjust the transformer ratio as required. The power electronics in the Li-ion battery are used to supply balancing power and reactive power control. They are also used to provide system services for network stabilization [72].

All suppliers, consumers, and storage systems are equipped with intelligent meters and communication technology so that feed-in, consumption, and network quality can be monitored in real time (Fig. 13.30).

All data for assessing and establishing energy plans and forecasts are collected together in the intelligent energy-management system. The energy forecasts take into account weather data (wind strength, wind direction, global radiation, temperature, and precipitation), consumption and generation data, historical data, and special dates such as holidays or events. Central control combined with forecasting allows the system to react to load fluctuations caused by meteorological conditions or facility failures.

### ■ Cost-Efficiency

Since the Pellworm SmartRegion project is an innovation project, cost-efficiency is not the top priority. The focus is on gathering insights with

**Table 13.16** Previous electricity supply statistics for the three atolls [50]

| Atoll | Peak load in kW | Electricity consumption in kW h/a | Diesel consumption in liters/year |
|---|---|---|---|
| Fakaofo | 51.2 | 255,100 | 60,290 |
| Atafu | 38.0 | 201,800 | 47,692 |
| Nukunonu | 36.7 | 219,400 | 52,018 |
| Gesamt | – | 676,300 (gross), around 655,000 (net) | Around 160,000 |

integrating renewable energy into an existing network that could be applicable in other regions as well. The project has an investment volume of almost 10 million €. Of the total, the German Federal Ministry for the Environment provided 4 million € for this flagship project.

### 13.1.6.4 Storage Integration on the Pacific Island of Tokelau

The Tokelau archipelago is a territory of New Zealand about 500 kilometers north of Samoa in the South Pacific Ocean that consists of three atolls—Atafu, Nukunonu, and Fakaofo. Around 1,400 people live here on 12 $km^2$ of land area. There are also no airports and docks for larger ships in Tokelau. All imported products (including diesel) must be shipped on small boats and unloaded by hand. Diesel spills have repeatedly resulted due to accidents during unloading at sea. These spills had a negative impact on the fragile island environment (reefs, etc.).

The tropical island has a humid climate. With an average solar radiation of 2,000 kW h $m^{-2}$ $a^{-1}$, use of PV is an obvious choice [45].

The island's maximum elevation is only five meters above sea-level. As a result, Tokelau is threatened by rising sea levels and has an existential interest in protecting the climate and expanding renewable energy use.

#### ■ Previous Electricity Supply

Before the energy transition on Tokelau, energy was generated almost exclusively by diesel generators. Over 160,000 liters of diesel was required to meet the annual electricity demand of 655 MW h. All households on this tropical island are connected to the electricity network and supplied with electricity at all hours. To save electricity and avoid large load peaks, the Tokelau government outlawed air-conditioners and electric stoves.

The entire electricity infrastructure was modernized and upgraded in 2005. New generators, power plant buildings, and power cables ensured higher efficiency and greater security of supply. Since each atoll has an independent electricity network, Tokelau has three fully decoupled systems [50].

Table 13.16 shows the annual consumption data in the electricity sector for each atoll, and that electricity consumption is nearly equally distributed across the three atolls. The atolls also have very similar load profiles. The load ranges from 20 to 25 kW at night, and rises slightly to 25 to 30 kW during the day. This means electricity consumption is fairly constant. But after 6 pm, consumption rises dramatically by up to about 50% to a load peak ranging from 30 to 40 kW (20 h), and then falls linearly back down to 20 to 25 kW. The following discussion treats the electricity networks on the three atolls as a single network.

#### ■ New Electricity Supply

In 2010, the government of Tokelau became determined to upgrade Tokelau's electricity supply as part of one of the Tokelau Renewable Energy Projects (TREP). With the goal of making Tokelau energy supply sustainable, diesel imports for electricity generation were minimized and a PV system, including battery storage, was installed. An average 90% of Tokelau's

**Table 13.17** New electricity generation system statistics by cluster for all 28 clusters in Tokelau [50]

| | Cluster | Tokelau in total |
|---|---|---|
| PV module power (1) | 33.1 kW | 930 kW |
| String transformer power (2) | 21.0 kW | 588 kW |
| Battery charger power (3) | 9.6 kW | 269 kW |
| Battery transformer power (4) | 13.5 kW | 380 kW |
| Battery storage capacity (5) | 288 kW h | 8.1 MW h |

electricity demand would now be met by a combination of PV and batteries. The remaining 10% would now be met by the existing diesel generators. This project was successfully completed in October 2012 [50].

The new electricity supply system was designed in clusters. Table 13.17 shows the statistics for these clusters. Figure 13.31 shows the schematic design of a cluster. A total of 28 identical clusters were installed in Tokelau.

Here, a portion of the energy generated by the PV modules (1a) is fed directly into the electricity network using string transformers (2). The remaining PV electricity (1b) is transformed to 48 V DC (3) and then either temporarily stored in the batteries (5), or fed into the network using the battery transformers (4) depending on the network situation. If PV electricity generation or battery-bank energy is inadequate, then the diesel system (6) is switched on. The diesel generators then run at their optimal operating point independent of current power requirements. This means that the generators supply a certain amount of power, and any power left over is stored in the newly installed batteries.



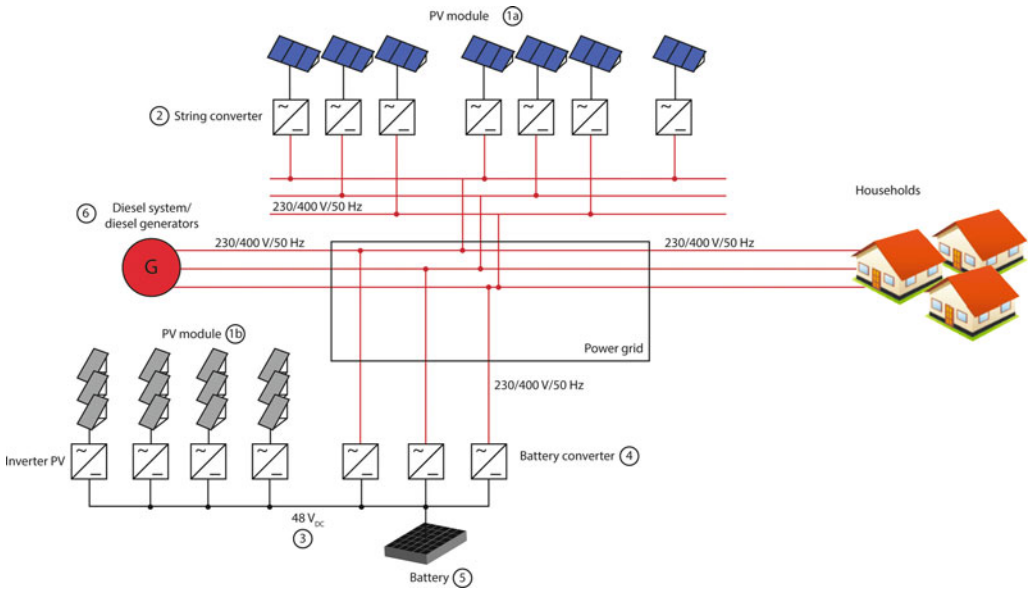



**Fig. 13.31** Cluster design in Tokelau

### Storage Use

To meet around 90% of annual electrical energy demand with PV electricity, even in areas with very high solar radiation such as Tokelau, temporary storage is required. Ideally, the electricity storage system is charged with surplus PV electricity during the day and then discharged at night.

In Tokelau, 1,344 batteries with a total storage capacity of 8,063 kW h were installed for this purpose. Because of their low cost, durability, reliability, safety, and low-maintenance requirements, lead-acid cells were chosen here. But they are more sensitive to deep-discharging. As a result, they are discharged to a maximum of 60%. In the rare cases when the state-of-charge (SOC) falls below this level, the diesel generator is manually switched on. If no diesel is available or the generator malfunctions, then at SOC levels below 30%, the batteries are disconnected from the network to prevent permanent damage. Under normal conditions, the total battery capacity available is adequate to meet Tokelau's electricity demand for between one and three days. With good charging management, the service life of lead batteries is about nine years [50].

### Control and Energy Management

Frequency and voltage tolerance maintenance or control is one of the challenges of energy transition. But this is not a high priority in Tokelau, because there are very few consumers sensitive to voltage and frequency.

In the cluster design used in Tokelau, the battery transformers are responsible for system control.

Each cluster has three battery transformers. One is the master transformers for the cluster, and the other two are its slaves (Fig. 13.31). All the clusters are connected together by a multi-cluster (MC) box. This allows them to control the frequency and voltage. The battery SOCs are also monitored. Here, electricity generation from PV modules is curtailed or, in rare cases when the SOC falls below 60%, an alarm indicates that the diesel generator must be manually switched on [50].

### Cost-Efficiency

Besides the environmental factors, rising diesel prices in coming decades is a major reason for transitioning from fossil electricity generation to renewable energy. Table 13.18 shows the results of an economic comparison between a fossil and renewable electricity generation system covering a project duration of 25 years. Since a diesel network already exists, no additional investment is required here.

With the PV system, the transformers and batteries have to be replaced twice within 25 years. The diesel generator does not need to be replaced because it is rarely used. With electricity generation from diesel alone, due to high utilization, the generators must be replaced once in the same period.

The largest single-cost item is for the batteries (Table 13.18). The goal here is to maximize battery life with good charging management [50].

The comparison shows that the decisive factor is savings on diesel costs. The comparison makes the conservative assumption that diesel prices will remain the same for the next 25 years, resulting in an annual saving of 540,000 € from the conversion. But if diesel costs increase by 3% annually, then the savings reach 1.2 million € per year.

Figure 13.32 shows the expenses for both generation systems over the project period. Both systems have the same incomes. The illustration conservatively assumes diesel prices remain constant.

With the diesel system, expenses increase almost linearly because the determining factor here is the annual constant cost of diesel. Because they are so low in comparison to the costs for fuel, the costs for replacing the diesel generator after 13 years are not a factor.

Because of the initial investment costs of around 5 million €, the starting point with the PV battery system is very high. But primarily due to the 540,000 € in savings for diesel costs, the annual expenses here are lower than with the diesel system. As a result, the expenses curve is significantly less steep. The costs for replacing the transformers once (point 1 in

**Table 13.18** Comparison of electricity generation costs with a PV battery system and a diesel system over a 25-year period [50]

| | PV battery system | Diesel system |
|---|---|---|
| Capital costs | 5,070,000 € | – |
| Annual diesel purchasing costs | 60,000 € | 600,000 € |
| Annual maintenance and repair costs | 33,000 € | 69,000 € |
| Transformer replacement costs (1) | 600,000 € | – |
| Battery replacement costs (2) | 2,250,000 € | – |
| Diesel generator replacement costs | – | 126,000 € |
| Annual electricity generation | 775,000 kW h | 775,000 kW h |
| **Electricity generation costs** | **0.81 €/kW h** | **0.9 €/kW h** |

The figures here were converted from New Zealand dollars to euros (exchange rate at the end of 2013: 1.00 NZD = 0.60 €).

Fig. 13.32) and replacing the batteries twice (point 2 in Fig. 13.32) are also much more significant.

But the PV battery system is still superior, not only in terms of environmental and public policy, but also in purely economic terms. Start-

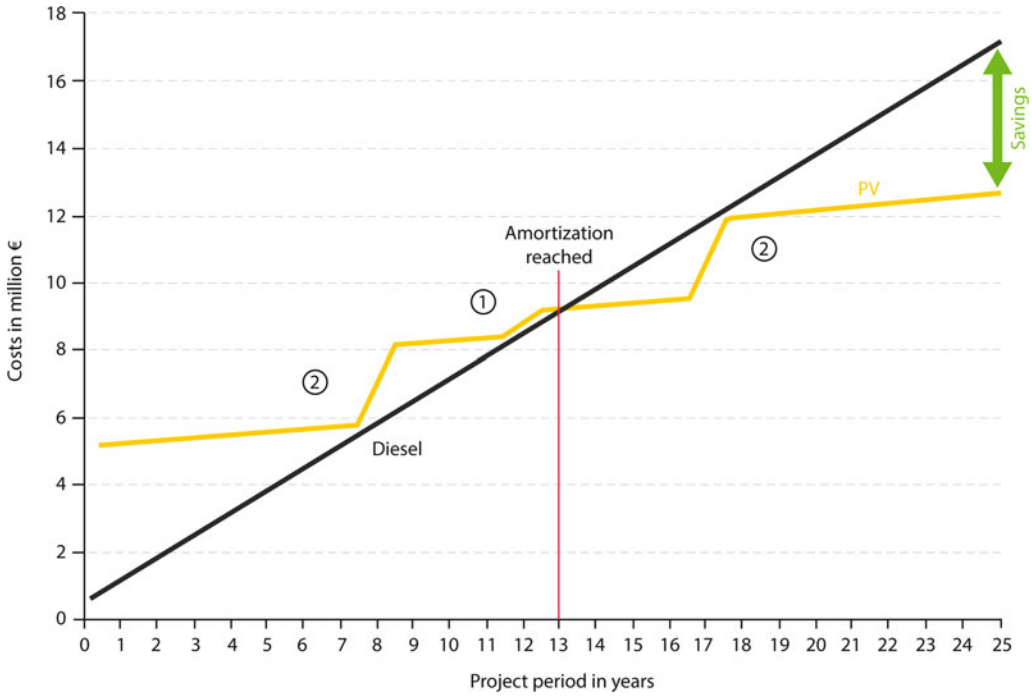



**Fig. 13.32** Comparison of financial costs for a PV system and a diesel system over the project period of 25 years (author's illustration based on [50])



**Fig. 13.33** New electricity generation in Tokelau

ing in the thirteenth year of operation, expenses for the diesel system exceed expenses for the PV battery system. These savings generate an economic advantage. This advantage is also clearly reflected in the electricity generation cost calculations (Table 13.18).

#### Challenges and Outlook

In the months with the least sunshine between November 2012 and February 2013, 88% of the load in Tokelau could be met by PV and batteries. Because of hardware problems, during this period 8% of the PV modules were not connected.

Taking account of this unused PV capacity and including the sunny months, renewable energy can be expected to meet 90% of the load all year, achieving the project's goal (Fig. 13.33).

The remaining 10% of annual electricity demand is currently still met by diesel generators. To ensure that electricity demand can be met 100% sustainably, in the future, diesel should be replaced with the local biofuel concentrated coconut oil [50].

### 13.1.6.5 Comparison of Stand-Alone Systems

Table 13.19 compares these three examples of storage integrated into stand-alone networks.

Remarkably, per capita electricity demand is thirteen times higher on Pellworm than in Tokelau. This is because of the contrasting climates and living standards. The largest storage capacity are found on the islands farthest from the mainland: Tokelau.

It is also worth noting that storage dimensions are significantly smaller on Graciosa than in Tokelau. This is due to wind power use on Graciosa and a higher share of remaining diesel generation.

In Tokelau, costs and durability alone determined the choice of battery technology. The Pellworm and Graciosa systems use a mixture of power batteries for balancing short-term fluctuations or network stabilization, and energy batteries for balancing electricity fluctuations over several hours.

The Graciosa stand-alone network was financed with private capital entirely, while the Pellworm system was financed with 40% government financing, and the Tokelau system was financed with about 80% low-cost loans provided by the government.

Implementing these renewable stand-alone networks yielded valuable insights that could be applicable to energy transition on land, i.e., to the continental network.

## 13.1.7 Thermal Storage in Solar-Thermal Power Plants

Solar-thermal power plants convert solar radiation into electric energy using a thermal cycle and thermal storage to buffer solar energy. Collectors absorb solar radiation and convert it into heat. In temperate climates, solar-thermal energy is primarily used to generate hot water and contribute to heating. In countries with high levels of direct solar radiation, this energy can be concentrated to produce very high

**Table 13.19** Comparison of key statistics for the stand-alone networks described here

| | Graciosa | Pellworm | Tokelau |
|---|---|---|---|
| Location | Azores | North Sea | Pacific |
| Surface area in km$^2$ | 70 | 37 | 12 |
| Inhabitants | 4,500 | 1,180 | 1,400 |
| Electricity demand per capita in MW h a$^{-1}$ cap.$^{-1}$ | 3.1 | 6.0 | 0.47 |
| Previous electricity supply | | | |
| Energy sources | Diesel, wind | Undersea cable, wind, PV, biogas | Diesel |
| Quantity of fuel in liters/year | 4,000,000 | – | 160,000 |
| Peak load in kW | 3,000 | 1,156 | 115 |
| Electricity consumption in MW h/a | 14,000 | 7,069 | 655 |
| Planned, implemented new electricity generation | | | |
| Renewable energy sources | Wind, PV, vegetable oil | Wind, PV, biogas | PV, vegetable oil |
| Installed power in kW | Wind 5,400<br>PV 1,000 | Wind 5,725<br>PV 2,742<br>Biogas 520 | PV 930 |
| Renewable energy in MW h | 8,500 | 22,290 | ~ 590 |
| Target for load covered by renewable energy | 70–90% (100%) | 60% | 90% (100%) |
| Electricity storage | | | |
| Storage type | Sodium-sulfur battery<br>Lithium-ion battery | Redox flow battery<br>Lithium-ion battery | Lead-acid battery |
| Storage capacity in MW h and storage power in kW | 8.5 MW h/1.2 kW (NaS)<br>1.5 MW h/1.5 MW (Li) | 1.6 MW h/0.2 MW (RF)<br>0.64 MW h/0.64 MW (charging) or 1.18 MW (discharging) | 8.1 MW h/0.38 MW |
| Cost-efficiency | | | |
| Capital costs in millions of € | 25 (purely private investment) | 10 (4 million in government funding) | 5.15 (4.2 million in government loans) |
| Fuel cost savings in millions of €/year | 3.0–3.4[a] | – | 0.55 |

[a] Based on a diesel price of 35 to 40 €-ct./kW h and including existing wind-power facilities.



temperatures. This permits electricity generation using a steam power process.

One advantage of solar-thermal power plants over PV is that the solar generated heat can be stored. Since heat is easier to store than electricity, energy storage systems in solar-thermal power plants are cheaper to build. Ex-

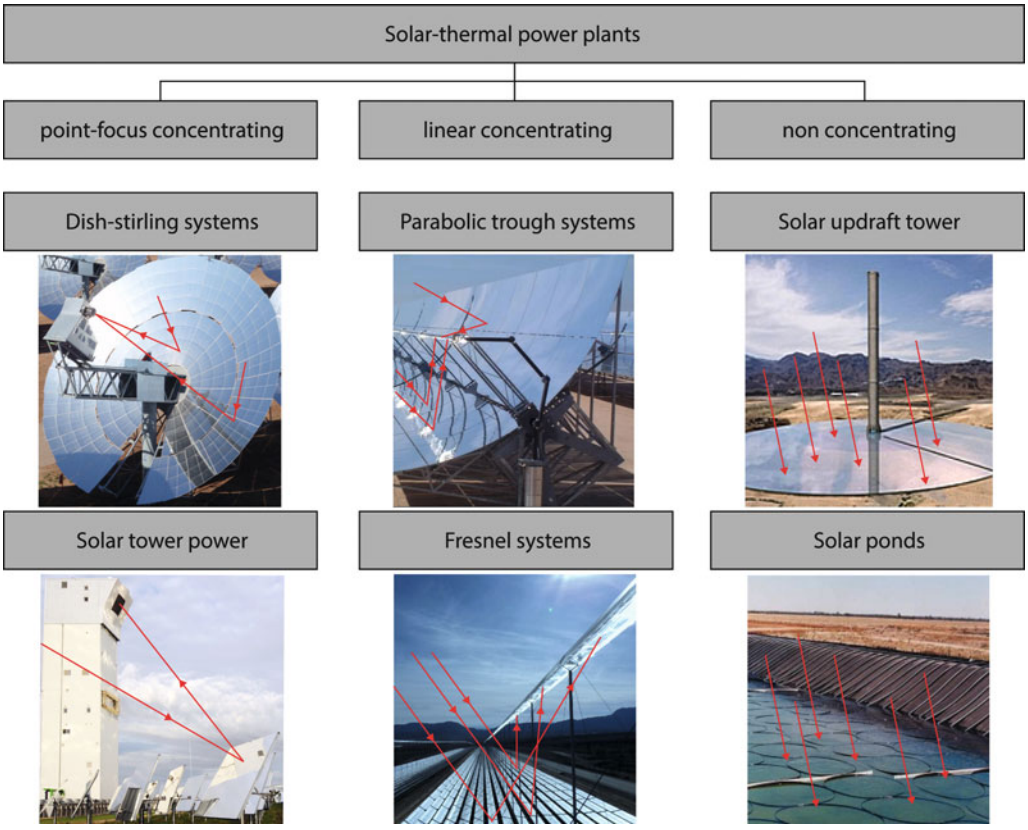



**Fig. 13.34** Overview of solar-thermal power plants used for electricity generation [81]

panding thermal storage facilitates electricity generation planning.

### 13.1.7.1 Operating Principle of Solar-Thermal Power Plants

There are two types of solar-thermal power plants: concentrating facilities and non-concentrating facilities. Concentrating facilities include linear concentrating systems such as parabolic trough or Fresnel power plants, as well as point focus concentrating systems such as tower power plants and dish-Stirling systems. To operate these facilities, solar radiation must be concentrated. Here, reflecting surfaces that track the Sun are used to concentrate solar radiation. The concentrated light is then directed into an absorber where it heats a heat-carrier medium. There are also solar-thermal power plants that operate without concentrating solar radiation. They are called non-concentrating facilities. These include solar updraft towers (Fig. 13.34).

The following sections explain the use of thermal storage in solar-thermal power plants.

### 13.1.7.2 Thermal Storage in Parabolic-Trough Power Plants

- **Operating Principle of Parabolic-Trough Power Plants**

Parabolic-trough power plants are a kind of concentrated solar-thermal facility. These power plants use reflectors made of parabolic mirrors. The mirrors are positioned on the north-south axis. Positioning them on this axis allows the mirrors to track the Sun from east to west. The solar radiation is concentrated on a focal line; the absorber pipe. As a result,



**Fig. 13.35** Salt tanks used as thermal storage facilities in the solar-thermal power plant Andasol I near Guadix, Spain. (Source: DLR)

these facilities are line-focused systems. A heat-carrier medium flowing through the absorber pipe (usually a synthetic or heat-resistant oil) is then heated to temperatures up to 400 °C. The oil then releases the heat through a heat exchanger in a classic steam power process.

#### ■ Use of Thermal Storage in Practice

Europe's first parabolic-trough power plants were built in the province of Granada in the south of Spain. The three facilities there, Andasol 1, 2, and 3, have a combined collector area exceeding 1.5 million $m^2$ and were built by the German company, Solar Millennium AG [74, 81].

To store surplus heat, each of the three facilities is equipped with a two-tank thermal storage system. Each system contains a mixture of around 30,000 tons of potassium and sodium nitrate salts. At night, the mixture can also supply heat for the steam power process (Fig. 13.35). The salt can be kept warm in the tanks over several weeks. In sunny months, these solar-thermal power plants can operate practically around the clock. The three power plants can supply about a half million people with solar electricity, saving about 450,000 tons of $CO_2$ annually in the current Spanish electricity mix (Table 13.20).

### 13.1.7.3 Thermal Storage in Solar-Tower Power Plants

#### ■ Operating Principle of Solar-Tower Power Plants

Solar-tower power plants have hundreds or even thousands of individual mirrors arranged in a field around a tower. The mirrors, which are also called heliostats, can track the Sun on two axes and focus solar radiation on dot-shaped receivers at the top of the tower. As a result, these solar-thermal facilities are spot-focused systems. The focused solar radiation heats the receivers. The receivers then release the heat into an ambient air flow. The air can reach temperatures ranging from 650 to 850 °C. It is then used to vaporize water to drive a steam turbine cycle [59, 81].

#### ■ Use of Thermal Storage in Practice

The PS10 power plant operated by Abengoa Solar is the first commercial solar-tower power plant. The facility was built near the city of Sevilla in Spain, and went into operation in 2007. Here, a total of 624 heliostats concentrate solar radiation on a tower 115 m high. The power plant also has a thermal storage system with four tanks that can bridge turbine operation when there is no solar radiation for

**Table 13.20** Data for the Andasol 1, 2, and 3 power plants [74]

| | Andasol 1 + 2 | Andasol 3 |
|---|---|---|
| **Solar field** | | |
| Solar field size | 510,120 $m^2$ | 497,040 $m^2$ |
| Number of parabolic mirrors | 209,664 | 204,288 |
| Number of absorber pipes, each 4 m long | 22,464 | 21,888 |
| Annual direct solar radiation | 2,136 kW h/$m^2$ per year | 2,136 kW h/$m^2$ per year |
| Efficiency level of the solar field | Around 70% peak efficiency, around 50% yearly average | Around 70% peak efficiency, around 50% yearly average |
| Storage capacity of the thermal storage system | 28,500 tons of salt for 7.5 VLh | 30,000 tons of salt for 8 VLh |
| **Power plant** | | |
| Turbine power | 49.9 MW | 49.9 MW |
| Annual operating hours | Around 3,500 VLh | Around 3,700 VLh |
| Calculated net electricity volume | 150 GW h | 165.41 GW h |
| Efficiency level of the entire facility | Around 28% peak efficiency, around 15% yearly average | Around 28% peak efficiency, around 15% yearly average |

**Table 13.21** Data for the PS10 solar-thermal tower-power plant in Spain [1]

| | |
|---|---|
| Electrical power | 11 MW |
| Annual electricity generation | 23 GW h |
| Number of heliostats each with a surface area of 120 $m^2$ | 624 |
| Tower height | 115 m |
| Thermal storage capacity | 20 MW h |
| Capital costs | 35 million € |

30 minutes at full power or 50 minutes at half power (see Table 13.21 and [1]).

The Gemasolar power plant in Spain is another example of a tower power plant that uses thermal storage. This facility has a liquid-salt storage system with a storage capacity of 15 hours, permitting the power plant to supply base-load when solar radiation is adequate. The facility uses 8,500 tons of liquid sodium and potassium nitrate salt heated to 565 °C and stored in a two-tank liquid storage system (Table 13.22). A notable difference here is that the liquid salt is used as the heat carrier, and as a result, also flows through the receiver. This means that no heat-carrier medium such as oil is required to transport the heat in addition to the liquid salt [75].

## 13.2 Integration in the Heating Sector

Heat and cold storage are fundamental components of the heating and cooling sector. ▶ Chapter 10 describes the individual technologies used in detail.

Figure 13.36 gives an overview of the various thermal storage types used in households,

**Table 13.22** Data for the Gemasolar solar-thermal tower-power plant in Spain [75]

| | |
|---|---|
| Electrical power | 19.9 MW |
| Annual electricity generation | 110 GW h |
| Number of heliostats each with a surface area of around 100 $m^2$ | 2,650 |
| Tower height | 140 m |
| Thermal storage capacity | 15 h, heat carrier: salt |

the heat carriers they use, and whether they can be used directly or directly for bivalent heating.

## 13.2.1 Thermal Storage for Solar-Thermal Energy

Solar-thermal energy refers to the conversion of solar energy into heat energy. In buildings, solar energy can either be used passively or actively.

### Passive Use of Solar Radiation for Room Heating and Lighting

Passive use of solar energy is applied exclusively for building heating and lighting. Here, solar radiation enters the building through the windows, warming or lighting the interior. With passive use, optimal building positioning and heat-retaining or insulating materials reduce the consumption of fossil energy.

Solar radiation from the upper areas of the windows is directed onto the bright ceiling of

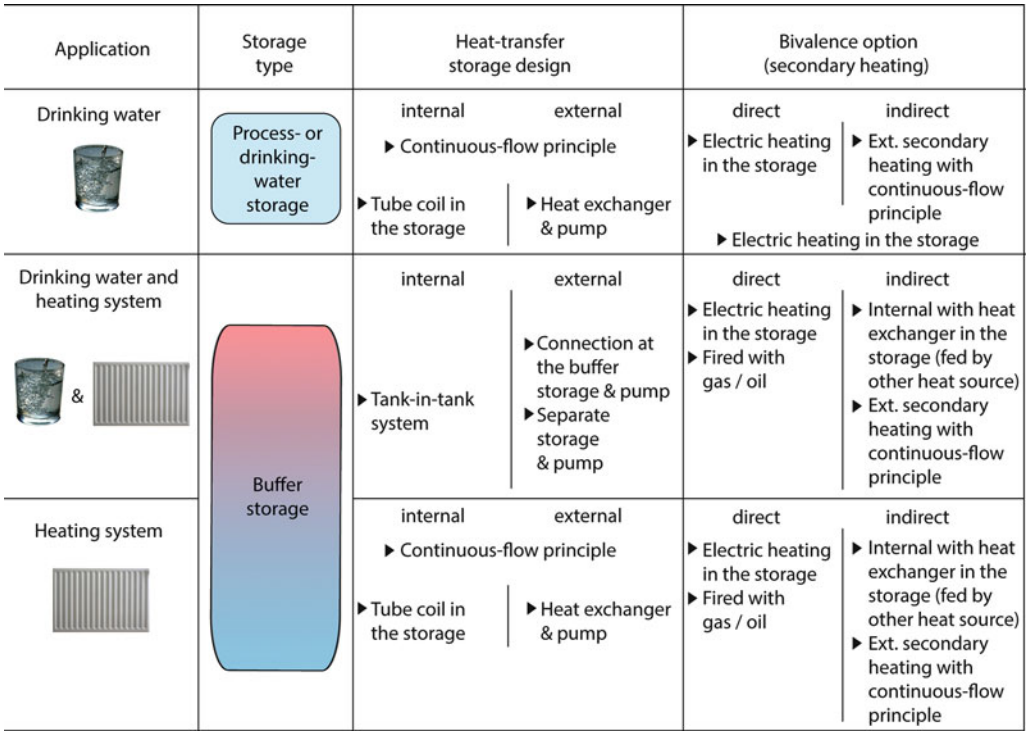



**Fig. 13.36** Overview of the integration of various thermal storage systems in a range of applications [81]

the interior and then reflected diffusely into the room. This increases the temperature in the room while significantly reducing electricity costs for lighting. Combined passive microprism and micro-lens sheets are used here to direct the light [48, 53].

#### ■ Active Use of Solar Radiation Using Collectors

With active use, collectors absorb solar radiation and then release it into a heat-carrier medium. The principle here is the same as with solar-thermal power plants. A circulation pump transports the heat from the collector to a buffer storage system. The thermal storage system compensates for fluctuations in solar radiation.

#### ■ Short- and Long-Term Thermal Storage

Households typically have hot-water storage systems. These are either short- or long-term thermal storage systems. Short-term thermal storage can supply heat for only a few hours, bridging supply for a day. In many cases a solar facility combined with a thermal storage system alone can ensure hot water supply from transition period to transition period, i.e., from spring to autumn.

Seasonal storage systems are required to store solar heat from summer until winter. Here, thermal storage absorbs heat in times of surplus and then releases it to the user when required. Active use of solar energy can be used to heat drinking water and service water or contribute to heating. The two types of use can be combined as well.

The following discussion focuses on the use of solar energy to heat drinking water and support heating in combination with storage, especially with hot-water storage. For the operating principles of the individual solar collectors, refer to the literature [13, 81].

### 13.2.1.1 Operating Principle of Solar Facilities

With gravitation-driven or thermo-siphon facilities and forcible circulation systems, the operating principle depends on the type of heat transport.

#### ■ Gravitation-Driven or Thermo-Siphon Facilities

Thermo-siphon facilities require no pumping unit. The heat transport is driven entirely by the physical fact that warm water is lighter than cold water, and rises as a result. This means that the thermal storage system is located above the solar collector. When the water in the thermal storage system cools, it sinks to the bottom. It then flows through the return pipe back into the collector, where it is heated again by solar radiation (◘ Fig. 13.37).

Thermo-siphon facilities also fall into two categories: single and double-circuit facilities. ◘ Figure 13.37 shows how they differ. In a single-circuit facility, the drinking water flows directly through the collector. The heated water is then fed into the storage system. This means that, unlike in a double-circuit facility, a thermal exchanger is not required.

In a double-circuit facility, the water heated in the collector is contained in a separate circuit; the solar circuit. The heat in the solar circuit is then transferred to the service water in the thermal storage system by a heat exchanger. This means that the solar circuit is separate from the service water, thus improving water hygiene.

Because the water circulates very slowly in northern regions, thermo-siphon facilities have a very low efficiency. As a result, gravity-driven facilities are rarely used in central Europe. The advantages of these systems are that they do not consume electricity and are cheaply available. Since no pump and control technology is required, they are also very low-maintenance [81].

They are ideally suited for use in tropical countries. As a result, these simple, highly durable systems are common in Africa, Latin America, and Asia.

#### ■ Forcible Circulation Systems

Since the thermal storage system is installed above the solar collector, thermo-siphon facili-

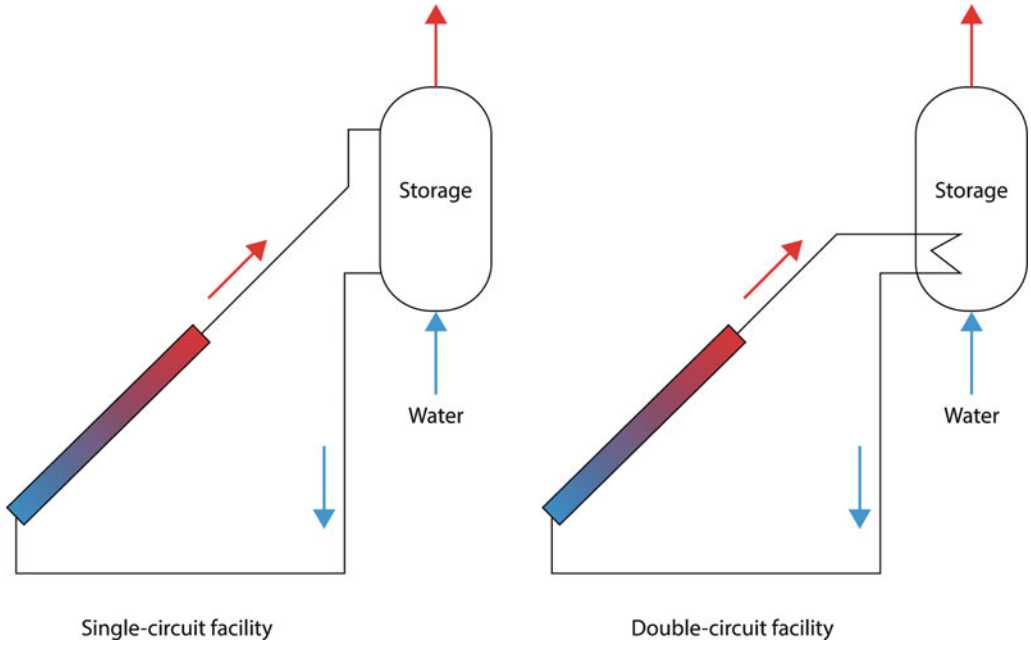



**Fig. 13.37** Design and operating principle of a single-cycle thermo-siphon facility: drinking water flows directly through the collector (*left*); double-cycle facility: a heat-carrier medium flows through the collector. The heat in the heat-carrier medium is transferred to the drinking water in the thermal storage system by a heat exchanger (*right*) [81]



ties can only be used in countries without winter and frost. In areas with frost, the hot-water storage system is kept in the building. Here, water circulation must be forced by an electric pump. These facilities are called forcible circulation systems. There are two types of forcible circulation systems. As with thermo-siphon systems, the facilities have either an open or closed cycle.

In facilities with an open cycle, the collector cycle is directly connected to the service water cycle. The service water flows directly through the collector, absorbing heat from solar radiation. But this facility concept is not suited for year-round operation in central or northern Europe because the water can freeze in the pipes and collectors. As a result, in these regions a closed cycle is always used. Here the solar cycle and the service cycle are kept separate. The solar cycle contains a heat-carrier medium containing antifreeze.

Since the temperature difference between the collector and the thermal storage system is sometimes too small to significantly heat the service water, constant pumped circulation is not required. As a result, the circulation pump is regulated by a controller. Temperature sensors on the collector and the thermal storage system monitor the temperature difference between these two points. When the temperature difference exceeds a pre-determined value, the controller switches on the circulation pump. This pre-determined value typically ranges from 5 to 10 °C. When the temperature difference falls below this pre-determined value, the pump shuts off again. Correctly setting the controller is essential for achieving high-efficiency levels [59, 81].

#### 13.2.1.2 Buffer Storage Systems for Small Solar Facilities

A well-designed solar facility can fully meet hot water demand in the summer months. Over

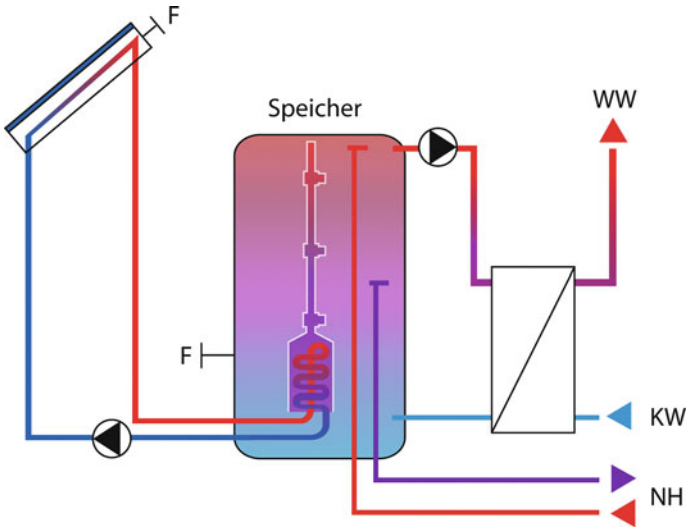



**Fig. 13.38**
Temperature-layering in a centralized storage system for supplying hot water [81]

a full year, it can meet around 60% of all service water demand. But efficient operation requires adjusting the facility to suit the water demand. The key component in a solar-thermal facility is the hot-water storage system. There are several types of storage systems used for this purpose [15].

### ■ Layering Processes in Storage Systems

Temperature-layering in storage systems increases their efficiency with solar-thermal applications. Temperature-layering is the natural result of the varying density of water at different temperatures. Warmer water has a lower density. As a result, heated water rises to the top of the storage system where it can be fed out for consumption. Fresh water then enters the storage system in the lower area. This means that there are several different temperature-levels within a hot-water storage system. The higher and narrower the thermal storage system is, the more pronounced these temperature levels become.

The heat absorbed from the solar collectors is fed in to the coldest area of the hot-water storage system. Temperature-layering ensures that the temperature difference between the collector and the storage system is greatest here, and that the heated water is always fed in to the thermal storage system in the right place (Fig. 13.38).

Efficient use of the storage system for supplying hot water requires stabilizing these temperature-layering processes. Turbulence caused by feeding water in or out of the tank should be minimized. Turbulence makes temperature-layering unstable, mixing the water and reducing the storage system's efficiency.

Figure 13.38 shows temperature-layering in a conventional centralized storage system supplying hot water by using a heat exchanger to warm fresh water. Secondary heating is required for year-round operation. These systems can also be designed to supply both drinking water and hot water.

### ■ Centralized Storage Systems

The use of centralized storage systems to supply either drinking water or hot water is a standard application for thermal storage. When solar heat is inadequate, conventional heating is used to secondarily heat the water to the required temperature (Fig. 13.39).

Heating water heating is very similar to drinking-water heating. But here, cheaper tank systems are used to store the heating water. Stainless steel containers are not required, for example. The growth of Legionella is also not a concern.

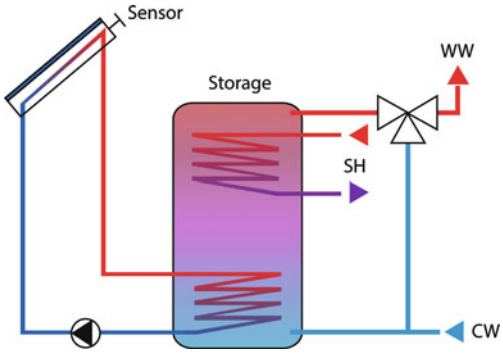



**Fig. 13.39** Centralized storage system for heating drinking water using a mixing valve and with optional secondary heating [81]

Both concepts are used for solar heating of service water. Particularly in smaller living units, these systems can significantly reduce heating supplied by burning fuels or from other sources [81].

#### Combined Storage Systems

These systems combine drinking-water heating with additional heating support. The collector surfaces and storage units are larger than in simple drinking-water storage systems. Combined storage systems can use a continuous-flow process or a dual storage design.

With the dual storage design, the first storage tank is contained within the second storage tank. This system is also often referred to as a tank-in-tank system. The interior tank containing drinking or service water is enclosed in the heating water tank. The storage facilities are relatively expensive. As a result, they are rarely used [16].

#### Dual Storage Systems

Dual storage systems include a drinking or service water storage unit, and an additional buffer storage unit for the heating facility. The storage units are connected in series. This means that the service water and the heating water are contained in two separate storage units. The service water storage unit has first priority.

Dual storage systems are used when space limitations exclude the use of a large storage system. In spaces where the ceiling is too low or the door too narrow, two smaller storage units can be installed in place of a large hot-water storage system. This system also allows an existing facility to be expanded if the storage capacity is no longer adequate [56].

### 13.2.1.3 Seasonal-Thermal Storage Systems for Large Solar Facilities

#### Large Solar Facilities in Local Heating Networks

Besides thermal storage systems in households to supply service water and support heating, there are also larger solar-thermal facilities combined with seasonal-thermal storage systems integrated into local heating systems.

The solar collectors are installed on the roofs of selected residential buildings. Water transported in underground pipes is usually the heat-carrier medium. The solar heat is transported over a solar network to a heating plant, and then stored in a large seasonal-thermal storage system typically either partially or fully underground. Hot water is secondarily heated using conventional heating if necessary, and then distributed to the buildings in the network as required.

District heating networks also use large thermal storage systems for buffering.

#### Design

There are four seasonal-thermal storage system designs: hot water, gravel/water, geothermal probe, and aquifer-thermal storage systems (▶ Chap. 9). The design is largely determined by the geology and hydrogeology underground. Building law provisions are also a crucial factor, since aquifer and geothermal-probe thermal storage systems require detailed underground evaluations. Thermal losses from these storage systems can be minimized with good thermal insulation, permitting their use as seasonal-energy storage systems.

#### Hot-Water Thermal Storage Systems

Hot-water thermal storage systems can be used regardless of geological conditions. They can

**Table 13.23** Overview of hot-water storage system projects [85]

| Project | Storage volume in $m^3$ | Construction costs in € | Construction costs related to useable volume in €/$m^3$ |
|---|---|---|---|
| Rottweil (1995) | 600 | 271,950 | 453 |
| Friedrichshafen (1996) | 12,000 | 1,351,650 | 113 |
| Hamburg (1996) | 4,500 | 960,500 | 213 |
| Ilmenau (1997/98) | 300 | 140,500 | 468 |
| Hannover (2000) | 2,750 | 665,000 | 242 |

also be built in smaller sizes. These storage systems are generally made of reinforced concrete, and some are fully or partially built into the ground. They are often built underground for aesthetic reasons, particularly in residential areas. To minimize thermal losses, the container walls are covered with additional thermal insulation. In addition to the side walls, the bottom and cover are insulated as well.

There are several projects in Germany using large hot-water thermal storage system (Table 13.23). Two are described here as examples.

A pilot facility was built in 1995 in Rottweil. This thermal storage system has a 600 $m^3$ container, partially above ground. The cylindrical container is 5 m high and has an inside diameter of 13 m. The thermal insulation made of mineral wool is between 20 and 30 cm thick. The thermal storage system is used as a short-term storage system in combination with a district heating plant. The design of the Rottweil project can also be used for long-term storage systems.

Another example is the facility in Friedrichshafen. A hot-water storage system was built in 1996 to supply a residential development with solar heat. The residential development has eight buildings with 586 apartments. The development has a total of 39,500 $m^2$ of residential space. The thermal storage system storage volume is 12,000 $m^3$. Solar collectors with a surface area of around 5,400 $m^2$ supply the solar energy used to heat the water. The solar collectors are used to heat the service water to temperatures ranging from 40 to 90 °C.

### ▪ Gravel/Water-Thermal Storage Systems

A mix of gravel or sand with water is used in these thermal storage systems as the heat storage medium. The system is placed in an Earth basin covered in materials impermeable to water and vapor and then filled with gravel or sand and water. The system is loaded and unloaded, either by dual-wells or by tube coils inside the storage system. The gravel filling makes this thermal storage system self-supporting. This means that, theoretically, unlimited storage sizes are possible. But the thermal capacity of gravel or sand is significantly lower than of pure water. As a result, thermal storage systems of this type are larger than hot-water storage systems with the same thermal capacity.

In Eggenstein-Leopoldshafen, a collector surface area of 1,600 $m^2$ together with a 4,500 $m^3$ gravel/water-thermal storage system are used to supply heat to a school and sports center. The thermal storage system is insulated on the side walls with 50 cm of expanded glass granulate and on the cover with 90 cm of foam glass gravel. The thermal storage system is also sealed water-tight with 2.5 mm of plastic sheeting. Construction of this storage system was completed within three months for 550,000 € [85].

### ▪ Aquifer-Thermal Storage Systems

This type of storage system uses groundwater-bearing layers in the earth called aquifers

for underground-thermal storage. Aquifer-thermal storage systems are typically accessed by two boreholes and include two underground caverns.

One cavern is filled with warm water, the other with cold water. To load this thermal storage system cold water is fed out of one aquifer, heated, and then fed into the other aquifer. To unload the storage system, the water is fed back in the other direction. In summer, cold water can also be fed out of the aquifer to air-condition buildings using existing heating cycles. This type of thermal storage system cannot be thermally insulated. The constructions costs are significantly lower than for other types of seasonal-thermal storage.

In Rostock-Brinckmannshöhe, a residential development was built in 1999/2000 which included 108 apartments and an aquifer storage system. Solar collectors with a total surface area of 1,000 $m^2$ were installed on all eleven roofs of the residential complex. The aquifer accessed by two boreholes is located underneath the property. In summer, water at a temperature of 10 °C is fed out of the cold aquifer and then heated in the solar collectors.

The hot water is then fed into the warm aquifer for seasonal storage. In winter, the water is fed back in the other direction. The warm water can be fed out whenever required. At the start of the unloading process, the discharge temperature is around 45 °C. Since the temperature falls over the duration of the heating period, an additional heat pump with a heating power of 100 kW is also integrated into the system. The heat pump meets heat requirements when there is insufficient seasonal-thermal storage system or solar energy. This thermal storage system can shift around 63% of the solar heat stored in the ground to the winter months [4, 39, 68].



### ■ Swimming Pools and Bathing Facilities

Energy costs for heating swimming pools with electricity or fossil energy sources are typically very high. Solar-thermal energy is therefore a particularly attractive option for heating swimming pools. As a result, many swimming pool operators are transitioning their energy supply to this low-cost alternative. Large temperature-differences are not required to heat a swimming pool. But this is offset by the larger quantity of water that is heated.

This means that solar facilities with large flow volumes are required to heat swimming pools. The temperature level is relatively low. Swimming pool absorbers have a very simple, durable, and cheap design. They use black mats or tubes which are mainly made of cheap plastics. Unlike residential solar collectors, these absorbers have no thermal insulation or glass covering. As a result, reflection losses caused by a glass covering are completely eliminated. Convection losses are low since the system operates only at low temperatures. The system has a relatively high-efficiency with this application. Since the swimming pool water is fed directly through the absorber, the facility requires no heat exchanger of any kind [76].

Solar-thermal energy is best-suited for heating open-air pools used only in summer. In these months, heating requirements can be met exclusively by a solar-thermal facility. But solar heating is not suitable for swimming pools that operate year-round. The heat supply is insufficient to heat these large quantities of water to an adequate temperature in spring and autumn. As such, using solar facilities to heat open-air pools has a decisive advantage. The solar energy and visitor number curves largely coincide.

**Example**

The indoor bathing facility in Azuqueca de Henares near Madrid is an example of this solar energy application. Solar collectors with a surface area of 347 $m^2$ can meet up to 70% of the pool's annual energy costs. Solar energy is used to provide heat for a 1,250 $m^2$ swimming pool, a whirlpool, and 16 showers.

The Wöhrdbad in Regensburg is another example of this use of solar energy to heat an open-air pool. This open-air pool is open daily from May through to September and has two separate pools, a 50 m long exercise pool and a non-swimmer pool. A solar facility with 1,000 $m^2$ of solar collectors has been in op-

eration at this open-air pool since 1993. Over the entire summer, all heating requirements for both pools can be met by this facility without any additional heating. Only the shower water is heated with gas heating.

Solar collectors that heat swimming pools are also used as energy storage systems by private pool owners. An open-air pool with a water surface area of 20 $m^2$ requires a collector area of 20 $m^2$ to supply adequate energy from the Sun. In summer, no additional water heating is required, reducing costs as well as $CO_2$ emissions [31, 76].

- **Large Thermal Storage System Applications in Solar Houses**

In a solar house, at least 50% of the energy required to heat the rooms comes from the Sun. These houses offer superb living comfort while minimizing heating costs. The goal here is to meet the majority of heating requirements with renewable energy to end reliance on fossil fuels.

Drinking water and combination storage systems are primarily used to supply hot water and support room heating. But in a solar house, the focus is on supplying primary energy from the Sun for building heating. Here, solar energy is stored in large water tanks integrated into the house and in massive brick walls. As a result, heating requirements can be met using solar energy practically year-round. In the winter months, small log or pellet ovens supply additional environmentally-friendly heating.

The large thermal storage system can be used to temporally shift the larger supply of solar heat available in summer to meet the larger household heat requirements in winter. The large water tank can be integrated into the living area of the house or buried in the ground.

- **The First Apartment-Buildings in Europe Heated Entirely by Solar Energy Using a Large Solar Storage System**

The first apartment-building in Europe heated entirely by solar energy was built in Bern, Switzerland. The building includes eight apartments and was completed in 2007 (Fig. 13.40).



**Fig. 13.40** First apartment-building in Europe heated entirely by solar energy in Bern, Switzerland. (Source: Jenni Energietechnik AG)

With 1,230 $m^2$ of floor space, the building's heating demand is 9.8 kW. The building has 300 $m^2$ of solar collectors and a 205,000 liter solar storage system. As shown in Fig. 13.41, the storage system is equally large.

This building is supplied exclusively by solar energy. By using a large buffer storage system, no additional heat sources besides the solar facility are required.

The solar center in Kienberg, Upper Bavaria, is an office and exhibition building which was completed in 2007 and has 466 $m^2$ of floor space. The building required 9 kW of heating power and has an annual heating demand of 11.1 MW h. The 107 $m^2$ of solar collectors are oriented to the south. The 25,400 liter buffer storage system is 8.5 m high and has a diameter of 2 m. Up to 90% of the building's demand can be met by solar energy using this storage system. A pellet boiler can optionally be used for secondary heating [64].

## 13.2.2 Latent and Sorption Storage Systems in Buildings and Households

### 13.2.2.1 Building Air-Conditioning Using Latent-Thermal Storage Systems

In addition to standard and simple sensible-thermal storage, latent-thermal storage is now increasingly used in buildings also.



**Fig. 13.41** Storage system of an apartment-building heated entirely by solar energy in Bern, Switzerland. (Source: Jenni Energietechnik AG)

### Passive Cooling Using Phase-Change Materials (PCM)

Since their walls have substantial thermal storage capacity, massively built buildings maintain a pleasantly cool interior, even when temperatures outdoors are high. Lightweight buildings typically require active cold generation using compression or adsorption chillers, for example (▶ Sect. 8.5). This results in additional primary energy consumption and high electricity costs during peak-load times.

Passive cooling systems using PCM are an alternative to conventional air-conditioning in lightweight buildings. These systems can behave like massive walls by storing the latent heat of a phase-change, typically a solid-liquid phase-change. The PCM store heat generated by solar radiation and internal sources within the building during the day. At night, the materials use the adequately and freely available cold in the environment to release the heat stored during the day. The PCM is then prepared to absorb heat again the following day (Fig. 13.42).

Either free or forced convection can be used to transport heat to the PCM. Systems with free convection use PCM storage elements (such as macro-encapsulated PCM, Fig. 13.43 left) in the walls or ceilings, or special plaster mixed with PCM. Forced convection systems use additional fans with low electricity requirements or separate PCM-storage systems directly integrated into the air-conditioning system.

With passive cooling systems using PCM, the melting temperature $T_m$ of the PCM chosen must suit the application temperature range. The melting temperature $T_m$ must be far enough below the room temperature during the day to ensure that the PCM melts. But the $T_m$ must also be far enough above the ambient temperature at night to ensure that the PCM fully crystalizes. Depending on the location, in Europe, PCMs with melting temperatures ranging from 20 to 30 °C are used.

To determine the thermal storage capacity of a PCM, the enthalpy curve, i.e., the change in enthalpy at temperature $h(T)$, must be precisely calculated. Commercial PCM often include additives or are composite materials. This ensures melting temperatures ranging over several degrees Celsius. Because PCM passive

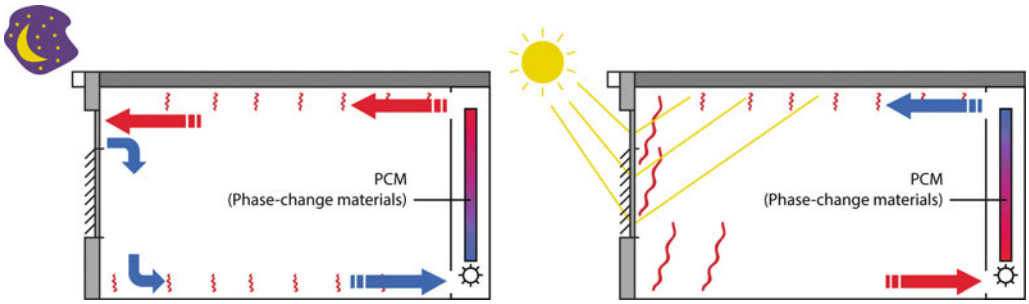



**Fig. 13.42** Cold storage in PCM at night (*left*), and cooling the building interior on the following day (*right*) [91]

cooling systems operate in narrow temperature ranges, temperature measurement errors of only 1 °C can result in significantly reducing their usable thermal capacity [91].

Other PCMs for building air-conditioning and other applications are currently in the research and development phase.

### 13.2.2.2 Washing Machines with Thermochemical-Energy Storage Systems

Thermochemical-energy storage systems are also used in appliances, such as in adsorption washing machines using zeolite.

Zeolite pellets have an extremely high-specific surface area, ranging from 800 to 1,000 $m^2/g$ and a pore size below 1 nm. These pores adsorb water molecules. When the water is intercalated, energy is released. This energy can then be collected during desorption. Zeolite pellets can adsorb up to 30% of their weight in water. Zeolite is used in cleaning and drying cycles in washing machines [55].

#### ▪ Operating Principle

During the cleaning cycle, zeolite heated to 240 °C by a heating coil is forced to release (desorb) the water intercalated the last time the dishwasher was run (Fig. 13.44). Although it is more energy-intensive than a cleaning cycle without zeolite, this process saves water. This is because part of the water used to clean, moisten, and warm the dishes was saved the last time the washing machine was run. In addition, the drying cycle consumes practically no additional energy.

The drying phase only requires energy for a fan. The fan blows the air containing water from the washing and rinsing cycles through the zeolite. The zeolite then adsorbs the water.



**Fig. 13.43** PCM storage element (*left*) installed in the ceiling of a meeting room (*right*) [91]

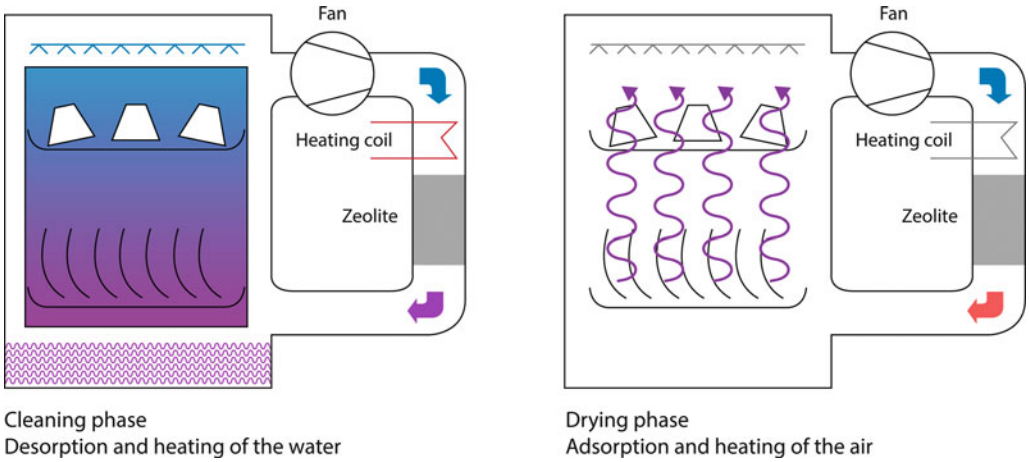



**Fig. 13.44** Operating principle of a washing machine using a thermochemical-energy storage system [55]

This adsorption releases heat. This heat is then absorbed by the dry air. This dry, hot air is then passed over the dishes so that it can absorb the water from them. This process quickly dries the dishes, completely removing even small drops of water on plastic dishes or small pools of water left at the bottom of containers. During adsorption, the humidity falls from 100% to around 10%. This also means that no annoying hot vapor is released by the washing machine when it is opened at the end of the cycle.

Using this storage system can significantly reduce energy consumption, and as a result, reduce household $CO_2$ emissions [55].

## 13.2.3 Forest-Wood Used as Chemical Storage for Heating Supply

### 13.2.3.1 Large Climate Protection and Heating Supply Potential

Wood is the largest form of energy storage in Germany. The quantity of solar energy stored in forests by photosynthesis in Germany and around the world is enormous. Reforestation and forestry in general results in the absorbance of $CO_2$. Compared to other methods, this approach to climate protection is also very cheap (▶ Chap. 1). In Germany, wood absorbs on average 18 tons of $CO_2$ $ha^{-1}$ $a^{-1}$ [6].

In all future energy scenarios, biomass is crucial. But energy crops compete with food and feed crops. In addition, energy crops are typically used by biogas facilities to generate electricity or as biofuels for transport. In Germany, 10% of heating supply relies on renewable energy sources, and almost all of them rely on wood (see ▶ Chaps. 3 and 4).

#### ▪ Large Wood Supply with Underestimated Growth

According to the 2002 National Forest Inventory, there is around 3,400 million cubic meters of wood in Germany. Since each cubic meter is equivalent to 200 liters of heating oil, this is equivalent to around 680 billion liters or 4.3 billion barrels of heating oil, i.e., 500% of Germany's annual oil consumption [6].

About a third of the wood, or around 1 billion cubic meters, is in Bavaria. Bavaria is Germany's largest state, and also has the largest forest area. Compared to the first National Forest Inventory in 1988, the supply of wood increased significantly by 23% in 2012. One reason is improved growing conditions. Climate change has extended the growing period by about four weeks, increased nitrogen emissions,

and raised atmospheric $CO_2$ levels. In addition, forest soil nutrient levels have significantly improved since the use of hay was discontinued after World War Two. A hundred years ago, annual growth per hectare was 4 to 6 $m^3$. Today growth averages 12 to 14 $m^3\ ha^{-1}\ a^{-1}$. The difference between the quantity of wood supply and the quantity harvested is also significant. The quantity of wood harvested does not included timber under 7 cm in diameter, which is about 10% of the total supply.

Depending on the owner, wood consumption varies considerably. The latest National Forest Inventory found that only 61% of growth in Bavaria was consumed [6]. This means that a large amount of stored renewable energy in Germany's forests is potentially available for heating supply. This untapped potential is primarily in private forests, in small private forests in particular. In Bavaria, about 12 to 15 million harvested cubic meters from all forest ownership types are currently used. The potential is 1.5 to 2 times higher.

### Large Low-Cost Heating Potential

Wood can be used as a material or as an energy source (Fig. 13.45):

- Material use:
  - Timber for furniture, building structures, etc.
  - Industrial wood such as paper wood to produce paper or chipboard
- Use as an energy source for heating and electricity:
  - Firewood, logs
  - Pellets
  - Wood chips

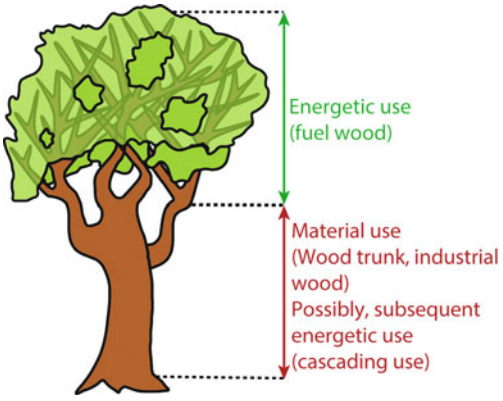



**Fig. 13.45** Uses of wood

In Africa and Asia, wood is primarily used as an energy source. In Europe and North America, harvested timber is primarily used as a material (▶ Sect. 1.1).

But increasing, oil and gas prices have stimulated the use of wood for energy in Europe. Using the energy stored in wood for heating is particularly relevant here.

Wood chip prices have doubled in the last 10 years, and pellet prices have also increased by over 50%. But prices for both products are still lower than heating oil or natural gas prices. Pellet prices are currently one-third lower than heating oil prices (2015) and 20% below natural gas prices. Wood chips are over 50% lower than heating oil and natural gas prices. Heating oil and natural gas prices are also subject to global fluctuations in price, but wood products are typically traded locally. As a result, wood product prices are more stable (Fig. 13.46).

Wood is also a domestically produced renewable resource that could be used to reduce fossil energy source imports. As the following example demonstrates, the potential of forest-wood used as a form of solar-energy chemical storage for heating is enormous.

**Example**

In Bavaria, one cubic meter ($m^3$) of wood grows each second. The forest area is 2.56 million hectares, and the growth 12 to 14 $m^3\ ha^{-1}\ a^{-1}$.

How much growth is there per year?

How many tons of $CO_2$ are absorbed by the forest each year, in total and per inhabitant?

At 200 liters/$m^3$, what is the growth's equivalent in heating oil? If the growth was used entirely to supply energy, how much could the heating-oil consumption in Bavaria be reduced? At a heating oil price of 90 €-ct./liter, how much is this quantity of energy then worth in total and per inhabitant?

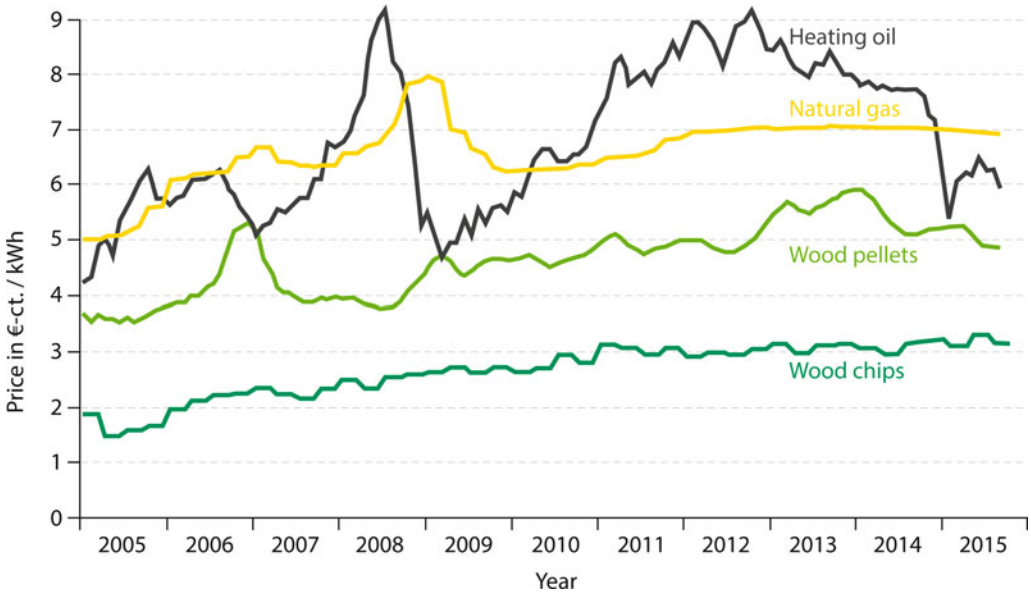



**Fig. 13.46** Prices for heating oil, natural gas, wood pellets, and wood chips over previous years (source: Carmen e. V.)

The Bavarian forest is seen as an energy storage system. What is its charging power using photosynthesis?

By definition:

**Calorific value of wood:** – around 2,000 kW h/m$^3$, equivalent to around 200 liters of heating oil/m$^3$ (mixture of hard and soft wood)
**Population of Bavaria:** – 12.56 million
**Heating-oil consumption of Bavaria:** – around 6,000 million liters/year (2011)

Solution:

**Growth (conservative):** – $E_{\text{wood}} = 2.56 \times 10^6 \text{ ha} \cdot 12 \frac{\text{m}^3}{\text{ha a}} = 30.72 \text{ million } \frac{\text{m}^3}{\text{a}}$

**$CO_2$ absorption by growth:** – $m_{CO_2} = 2.56 \times 10^6 \text{ ha} \cdot 18 \frac{\text{t}}{\text{ha a}} = 46 \text{ million } \frac{\text{t}}{\text{a}}$

**$CO_2$ absorption per inhabitant:** – $m_{CO_2,\text{EW}} = \frac{46 \text{ million } \frac{\text{t}}{\text{a}}}{12.56 \text{ million}} = 3.7 \frac{\text{t}}{\text{a}}$ per capita

**Heating oil equivalent:** – $E_{\text{wood-equiv.}} = 30.72 \times 10^6 \frac{\text{m}^3}{\text{a}} \cdot 200 \frac{\text{L}}{\text{m}^3} = 6{,}144 \text{ million } \frac{\text{L}}{\text{a}}$

**Heating oil share:** – $\frac{E_{\text{wood-equiv.}}}{E_{\text{heating oil}}} = \frac{6{,}144}{6{,}000} = 102\%$

**Equivalent worth in money:** – $k_{\text{wood}} = 6{,}144 \text{ million } \frac{\text{L}}{\text{a}} \cdot 0.9 \frac{€}{\text{L}} = 5.53 \text{ billion } €$

**Equivalent worth in money per inhabitant:** – $k_{\text{wood,inhabitant}} = \frac{5.53 \text{ billion } €}{12.56 \text{ million}} = 440 \frac{€}{\text{a}}$ per capita

**Charging power of the forest:** – $P_{\text{solar-wood,chg}} = 30.72 \times 10^6 \frac{\text{m}^3}{365 \cdot 24 \text{ h}} \cdot 2{,}000 \frac{\text{kW h}}{\text{m}^3} = 7{,}014 \text{ MW}$

This means that the forest has a power over 7,000 MW and charges 5,508 MW—more energy than all the atomic power plants operating in Bavaria in 2013 combined.

If 30 to 50% of forest growth is used for heating energy using wood heaters, this would reduce fossil heating-oil consumption by 2 to 3 billion liters and reduce $CO_2$ emissions by about 14 to 23 million tons a year.

Material use should be prioritized over energetic use to ensure cascade use. About 50% of harvested wood is used as timber, typically as a raw material for construction and building maintenance. A smaller amount is also used for paper and as industrial wood.

Another positive effect is the creation of regional economic circuits. This is particularly important in rural areas as demographics change.

### 13.2.3.2 Increasing Growth by Balancing Forest and Game

Under normal circumstances, and with the proper balance between forest and game, wood is a raw material that grows naturally. But be-

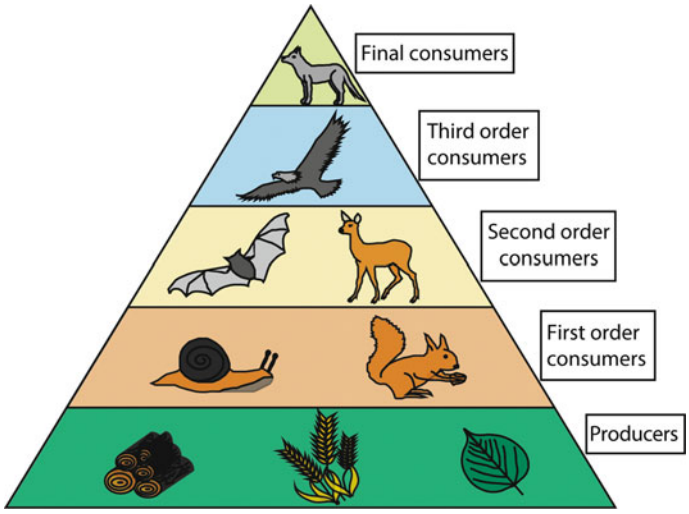



**Fig. 13.47** The food pyramid in the forest

sides the forestry sector, there are other stakeholders in forest use. Hunters require healthy populations of forest game. In addition, forests are increasingly used for leisure activities focused on certain aspects of life in the forest.

In the past, various producers and consumers maintained the natural balance in the forest's food pyramid (Fig. 13.47). But the final consumers at the top of the pyramid (such as wolves, lynxes, and bears) were then educed in number by expanding settlements and hunting. As a result, artificial hunting by humans of the consumers farther down in the pyramid (such as red deer and wild boar) was required to replace these natural hunters above. Until several centuries ago, hunting was reserved for the nobility. Today in Europe hunting is a middle-class hobby or occupation.

The lack of natural enemies and deliberate feeding dramatically increased the population of second and third-tier consumers. If game populations are not maintained at natural levels, then deer and red deer require more food, costing producers in the forest. This has led to conflicts between forest owners and hunters in the past, and remains a problem today. When game populations are high, the animals chew on growing young tree saplings. As such, game browsing reduces forestry results. As a result, forest owners view game browsing as property damage that should be compensated for by hunters. Since natural growth requires intensive work and takes many years, many forest owners put up fences and grow other plants as obstructions.

Putting up fences is very costly. A single hectare contains from 2,000 to 7,000 plants at 50 to 120 €-ct. each and 400 m of fencing at 8 €/m. Adding 50 €-ct. per plant for planting labor, depending on the tree type, costs per hectare can reach up 10,000 €. Figure 13.48 illustrates the problem. No raw material grows in the open forest, but in protected forests it grows naturally.

To address this problem, the following forestry and hunting regulations have been introduced [5].

- Varied and healthy game populations are to be maintained at a level compatible with their natural living conditions.
- Permitted commercial farming, forestry, and fishing should be affected by game as little as possible.
- In particular, hunting should generally permit the natural restocking of local tree types without additional protections.
- To the greatest extent possible, the forest should have priority over game and be maintained or restocked naturally.
- Forest security, health, and resources should be continually protected and strengthened.



**Fig. 13.48** Natural restocking vs. tree cultivation and fencing. Costly and labor-intensive fencing is required to restock the forest. A negative example from Lower Bavaria

Forest owners periodically measure game gnawing levels to assess forest conditions and natural restocking [7]. These assessments are used to determine the shooting quotas agreed on by the forest owner associations and the hunters. These quotas are enforced in some areas but not in others. Since forest owners are allowed to hunt on their own property only if they own a very large contiguous forest area over 80 hectares, the forest owner associations lease hunting on their properties over very long periods, ranging from 9 to 12 years [2].

If the forest and game are well-balanced, then the forest restocks itself with high yields. Healthy forest restocking can reduce harvesting periods from 80 or 100 years to 10 or 20 years, significantly increasing the yield. As the old, mature trees are gradually removed, natural regeneration under the continued shelter of the old trees results in stable and diverse restocking (Fig. 13.49). Material or energetic use of the increased yield then results in profits. Healthy forests also counter climate change. Increased growth results in increased climate protection at no additional cost. Mixed and naturally restocked forests more effectively resist climate change, better protect against flooding, and promote biodiversity.

In addition, a balanced game population reduces the number of accidents involving animals that cause injuries and damage. There are around 200,000 accidents caused by wild deer a year in Germany, and this accounts for a fifth of the game slain. The damages caused by these accidents amounts to about 500 to 600 million €. About 3,000 people are injured as well. An LMU Munich analysis of accident statistics and game browsing forest conditions demonstrated a strong correlation between game browsing and accidents caused by game [42].

Experience has shown that in areas with a high number of accidents caused by game, the number of accidents falls dramatically when hunting kills are increased by permitting forest owners to hunt on their own hunting grounds. This means that balancing game populations increases road safety as well as promotes forest growth [2].

### ■ Positive Aspects of Natural Restocking

Natural restocking has many advantages.

- Energy, climate, and environment:
  - Higher yield, more energy
  - More cost-free climate protection
  - Forests that better resist climate change
  - More cost-free flood protection
  - More biodiversity
- People and animals:
  - Fewer accidents caused by game
  - Fewer injuries and less damage
  - Better animal protection

Since mixed hardwood and fir restocking is especially valuable for forests, the environment,



**Fig. 13.49** Natural restocking by correctly balancing forest with game. The forest grows back on its own. A positive example from Lower Bavaria

and safety, Bavaria pays a 1,000 € per hectare subsidy for this type of restocking.

But this additional storage and energy potential can only be exploited with the full cooperation of all participants, including the government administration, hunting associations, and forest owners. For forest owners in particular, cultivating and profitably exploiting forests together with the other stakeholders requires a strong commitment.

The potential of forests to absorb $CO_2$ and store energy is routinely underestimated. Forests in Germany and across Europe offer an enormous potential supply of heating based on stored solar energy, which is a potential that should be effectively exploited.

## 13.3 Integration in the Transportation Sector

In practically all vehicles, energy storage has been integrated into the transportation sector in the form of batteries for over a century for 'black-start' capability and on-board electricity supply. As a result, the following discussion focuses exclusively on the integration of energy storage in the transportation sector in relation to renewable energy. ▶ Section 14.3 examines the coupling of the electricity and transportation sectors by electro-mobility and synthetic fuels using cross-sectoral storage systems.

### 13.3.1 Biofuel Mixtures and the Use of Vegetable Oil

#### 13.3.1.1 Potential and Environmental Impact

Like forest wood, biofuels are energy sources charged by the process of photosynthesis using solar energy, water, and air. Some, such as vegetable oil or bio-ethanol, can be used by vehicles with special combustion engines in their pure form. They can also be converted for use in conventional engines as biodiesel. Woody biomass can also be converted into biofuels by biomass gasification (biomass-to-liquid (BTL), etc., ▶ Sect. 8.3). But thermochemical conversion entails the logistical challenge of gathering raw materials spread over large areas for wood gasification and fuel synthesis in one particular location.

BTL is a second-generation biofuel process still mainly in the research phase, but fossil fuels mixed with biodiesel and bio-ethanol that inte-




**Fig. 13.50** Filling station with E10 fuel, a mixture of fossil fuel with 10% biofuels. (Source: Tom Bayer, fotolia)

grate renewable energy into the transportation sector are already standard (Fig. 13.50).

### Available Area and Residual Materials

The potential for integrating biofuels into the transportation sector is largely determined by the amount of land available for energy crops. Biofuels can be produced primarily from two sources:

- Energy crops
- Residual or waste materials (including cascade use)

Energy crops include rapeseed for biodiesel, grains for bio-ethanol, and vegetables for vegetable oil or biogas production. In Germany, around 2 million hectares from close to 12 million hectares of farmland are used for energy crops. If population levels fall and yield per hectare increases for all crop types, then the potential area available could expand. But this land is not only required for biofuels. These areas are also used for biogas production by the gas and electricity sectors, or for biological raw materials by the industrial sector.

So in the future, biofuels can only contribute to energy supply for mobility. This is because even in optimistic scenarios, the area available is inadequate to replace petroleum fuels entirely. Besides electro-mobility and synthetic fuels, importing energy crops or related products is also an option. But here, the use of biofuels has environmental benefits only if they are produced without harming the environment, such as by clearing rain forests or converting natural reserves to farmland [90].

Producing biofuels from residual or waste materials poses far less of a risk to the environment. This is because, unlike energy crops, these materials do not compete with food or feed crops.

### Environmental Impact

▶ Section 8.4.2 describes the characteristics of biofuels, explains how they are produced, and compares them to fossil fuels. This section examines the environmental aspects of various biofuels.

Generally speaking, biofuels made from residual or waste materials have a better greenhouse gas balance than energy crops. This is because they result in no indirect emissions from land-use changes [36, 78, 90].

- Vegetable oil has a positive energy balance, i.e., the energy expended for production is smaller than the energy content of the raw material, thus reducing $CO_2$ emissions. In addition, vegetable oil is highly biodegradable. Since sustainable farming of vegetable oil has the potential to reduce $CO_2$ emissions by over 80%, vegetable oil is the most environmentally-friendly biofuel of all.
- With an output/input ratio of 3:1, biodiesel has a positive energy balance as well. In addition, biodiesel is only slightly hazardous to water, while conventional diesel is classified as a water pollutant [29].

- Although bio-ethanol production is very energy-intensive, more energy is stored by photosynthesis in bio-ethanol than is consumed in its production. Bio-ethanol is also easily biodegradable.
- Wood, residual, and waste materials can be converted into fuels by biomass gasification or pyrolysis. It has a higher potential to reduce $CO_2$ emissions than first-generation biofuels, and its hectare yield is also higher [29].

The environmental impact of biofuels made from energy crops is primarily determined by the farming method, the land-use changes it requires, and the fossil energy sources it replaces [78]. Compared to biofuels, synthetic fuels produced using renewable electricity from wind, solar, and hydropower have a significantly higher hectare yield, and offer substantially greater potential to reduce $CO_2$ emissions.

### 13.3.1.2 Mixtures and Integration

#### Policy Framework

The EU's goal is to increase the share of renewable energy in all member countries to 10% by 2020. But since biofuels are more expensive than fossil fuels, achieving this goal requires additional measures. As a result, the EU permitted its member states to exempt biofuels from the petroleum tax. Biofuels were at first tax-free. Then from 2006 to 2012, the tax was raised in steps. Bio-ethanol is an exception and remained tax-free until 2015.

The Biofuel Quota Act determining the mixture of biofuels required in conventional fuels as well as their taxation came into effect in Germany on January 1, 2007. This law requires that biofuels make up a defined percentage of the petroleum industry's total annual sale of fossil gasoline and diesel fuels. Biodiesel and bio-ethanol are almost exclusively used to meet these quotas. The goal of the law is to reach a level of 8% by 2015 [12].

Vegetable oil fuels have the best environmental balance and the lowest conversion losses of all biofuels. But technically they can only be easily integrated into the farming and trucking sectors. Biodiesel and bio-ethanol have only limited potential in the individual transport sector, but they have larger potential in the farming sector. As in previous times when a third of the land farmed was traditionally reserved for growing oats to 'fuel' the horses, a third of land farmed today could be used to grow enough energy crops to entirely replace fossil diesel for farming. Farming machinery cannot be driven by electricity using battery storage, and must be powered by energy sources with higher energy densities as a result. Synthetic fuels will probably be too expensive for this purposes, and used mainly in aviation instead. But tractors could use vegetable oil fuels.

Under the old petroleum tax law until 2006, vegetable oil fuels benefitted from a tax exemption of around 47 €-ct/liter. This made vegetable oil a financially attractive alternative to fossil fuels. In the transition to the new energy tax law, this exemption was gradually reduced. By 2013, vegetable oil fuels only benefitted from a net tax exemption of around 2 €-ct/liter. Producing vegetable oil production requires a permit to operate as an energy company together with a customs warehouse, a customs warehouse certificate, and a sustainability certification. This means that decentralized production and consumption of vegetable oil is economically unfeasible if it is fully taxed. As a result, many decentralized vegetable oil mills closed after the energy tax law changed. But adjusting the law could potentially increase the integration of domestic vegetable oil in the transportation sector.

Special regulations for the farming and forestry sectors included higher levels of tax relief, although they were still relatively low. But a tax exemption of about 45 €-ct/liter came into effect in 2013, making vegetable oil an attractive alternative again in this area.

#### Technical Integration

In addition to the policy issues, there are also technical requirements for integrating biofuels. Here, a range of approaches and measures could be taken. Stored biofuels could be inte-

grated into the transportation sector as pure fuels or in mixtures together with conventional fuels. The factors here vary by fuel type.

- Vegetable oil (such as rapeseed oil): since the characteristics of pure vegetable oil differ from diesel, vegetable oil can only be used in modified combustion engines. Vegetable oil has a higher viscosity. This makes cold-starting conventional diesel engines at lower ambient temperatures using vegetable oil a problem. These engines can be modified in two ways. With a one-tank system, vegetable oil alone is used for fuel. The engine is modified so that it can cold-start using vegetable oil. With a two-tank system, conventional diesel is used to start the engine and vegetable oil to run it once an adequate operating temperature is reached.
- Biodiesel: biodiesel is produced by the transesterification of vegetable oil, and like PtG, can be used by the existing infrastructure. Automobile manufacturers authorize certain models for biodiesel after ensuring that no plastic vehicle parts such as seals will be adversely affected. Many models cannot be used with biodiesel, particularly those with particle filters. As a result, a maximum of 7% is permitted in mixtures. Biodiesel accounted for nearly 4% of fuel consumption in 2011, and like vegetable oil, its use is falling [8]. This is also the result of the annual increase in taxes on biodiesel since 2006. Biodiesel is currently taxed at the full petroleum tax rate.
- Bio-ethanol: like biodiesel, bio-ethanol can be mixed with conventional gasoline and used in unmodified engines. Since alcohol has a higher octane than gasoline, in small amounts it can even improve the combustion characteristics of gasoline fuels. Currently, a maximum of 5% is permitted in mixtures. No vehicle modifications are required below this level. Vehicles must be authorized by the manufacturer to use what is called E10, i.e., a mixture of 10% ethanol. In general, most new vehicles are now authorized for E10 (Fig. 13.50). Flexible-fuel vehicles (FFV) available from a range of manufacturers are capable of operating on various fuel mixtures containing up to 85% ethanol. Bio-ethanol is not available because it cannot be used for cold start-ups. Because of the introduction of E10, bio-ethanol is the only major biofuel with a growing market share. Since FFV have become more common, the number of filling stations offering E85 has grown to over 300 in 2013. This could result in an increase of the number of consumers of this fuel [8].
- Biomethane: unlike the other biofuels described here, biomethane corresponds 1:1 to its conventional equivalent, natural gas. As with PtG, all natural gas vehicle can use biomethane without any engine modifications. With over 900 filling stations offering biomethane, it is significantly easier to find than E85 (300) or hydrogen (less than 10). But natural gas vehicles have only a small market share [29]. In addition, pure biomethane is available at 100 filling stations in Germany. Biomethane can be produced by fermentation or by biomass gasification.
- BTL: with gasification, biomass is decomposed at high pressures and temperatures to produce synthesis gas. This is then used in synthesis gas processes such as methanol synthesis (▶ Sect. 8.3.4) or the Fischer-Tropsch process (FT process) (▶ Sect. 8.3.5). By integrating this process into refineries, second-generation biofuels can be produced which have the same characteristics as conventional diesel or gasoline. This means that they can be used in the existing infrastructure and in existing vehicles with any preparation or modifications.

If these technical and regulatory requirements are met, biofuels could be integrated into the transportation sector as a form of stored solar energy that promotes recycling and decarbonization.

## 13.3.2 Integration of Hydrogen in the Transportation Sector

### 13.3.2.1 Hydrogen Use in Oil Refineries

For larger consumers in the chemical industry, hydrogen is produced on-site by an industrial gas company facility or purchased from suppliers. ▶ Section 8.1.3 describes hydrogen production in detail.

Annual global hydrogen demand is rising, primarily driven by rising demand from refineries. This is because they increasingly process heavy oils (long-chain hydrocarbons), and because of higher purity requirements for crude oil products.

Besides basic materials for the chemical industry, refineries primarily produce fuels (◘ Fig. 13.51). This means that the integration of hydrogen into refinery processes is more closely related to electricity fuel production. But since it is also categorized as a material use, it will be discussed here. ▶ Section 8.6.2 described natural gas mixtures produced using PtG. An indirect but extremely practical method of integrating hydrogen into the transportation sector that also requires little modification to the distribution infrastructure or vehicles is adding hydrogen by hydrocracking (◘ Fig. 13.51).

Hydrocracking is a process for converting heavy crude oil or bitumen (for example tar sand oil) in refineries to petroleum products. These raw materials are increasingly used because of the dwindling supply of sweet oil. Since hydrogen is added during hydrocracking, the portion of alkanes ($C_nH_{2n+2}$) is very high. Heavy, long-chain hydrocarbons are split using catalysts at temperatures of around 500 °C and at hydrogen pressures up to 200 bar [41].

The general reaction formula (see Eq. 13.1) is:

$$C_NH_{2N+2}+H_2 \rightarrow C_nH_{2n+2}+C_nH_{2m+2} \quad \textbf{(13.1)}$$

with

$$N = n + m.$$

#### ▪ Opportunities for Integrating Renewable Hydrogen

The use of hydrogen produces no $CO_2$ emissions. This means that if $CO_2$ certificate prices in European emissions trade rise, then the industrial sector will have a financial interest in using green hydrogen. There is a linear relationship between the added value of hydrogen and the price of $CO_2$ certificates. As a result, doubling the certificate price doubles the value added by hydrogen. In 2014, prices ranged from 5 to 7 €/$tons_{CO_2}$, meaning the value added by hydrogen was 0.1 €/kg. But this added value is generally too low to position green hydrogen as an economically attractive alternative in the transportation sector [82].



**◘ Fig. 13.51** Refineries that replace hydrogen produced using natural gas with renewable hydrogen produced using PtG can then use hydrocracking to indirectly integrate hydrogen into the transportation sector by producing synthetic fuels. (Source: Marco2811, fotolia)

Another reason hydrogen may become an attractive option for some companies is that it reduces $CO_2$ emissions from manufacturing. That could create an entirely new industrial sector offering climate-neutral products for an additional fee. It is also a way to integrate hydrogen that does not require incentives. Currently in niche markets such as perfume manufacture, for example, raw material prices play a secondary role in consumer pricing, and customers are willing to pay more for 'green' products.

#### 13.3.2.2 Hydrogen Use in Hydrogen Mobility

Besides directly integrating green hydrogen into oil refineries to increase the share of biofuels in the transportation sector, the hydrogen economy could theoretically be further developed and expanded. In Germany, hydrogen pipelines currently exist only in stand-alone hydrogen networks in the Ruhr district serving the chemical industry in Halle and Bitterfeld. These pipelines are also operated by only two companies (Air Liquide and Linde).

The Hypos project in eastern Germany includes plans to expand the hydrogen network by converting a natural gas cavern to a hydrogen cavern. There are also plans to directly integrate a wind and PV park producing hydrogen into a chemical park [43].

13

##### ■ Transport and Distribution

Depending on the quantity, distance to the consumer, and requirements on the hydrogen, the following transport and distribution methods can be used [82]:

- Pipelines: pipelines are used where the gas company and consumers are near each other (for example, in a chemistry park) or if consumers are highly concentrated in a single region. Depending on the material used, pipelines are operated at pressures ranging from 40 to 70 bar.
- Liquid tank trucks: large quantities (35,000 to 40,000 N $m^3$) can be distributed over large distances up to 1,000 km using special liquid tank trucks. The disadvantage here is that liquefying hydrogen requires a considerable amount of energy, ranging from 0.9 to 1.2 kW h of electricity per cubic meter. Energy is also required to cool the liquid hydrogen during transport and storage. This considerably reduces the efficiency of producing and distributing the hydrogen.
- Truck trailers: between 3,000 and 6,000 N $m^3$ of hydrogen can be transported on trailers in pressurized containers at 200 bar. The trailer can be exchanged with an empty tank on-site, or the contents transferred to a preinstalled tank. The advantage of compression is that it requires less energy than liquefaction. The disadvantage is that only relatively small quantities of hydrogen can be transported using this method. This means that transport is generally profitable only over short distances.
- In smaller quantities, hydrogen is transported in pressure cylinders of various sizes.

##### ■ Use of Hydrogen

PtG can convert green electricity surpluses into green hydrogen. In addition to direct consumption, the hydrogen can also be combined with $CO_2$ to produce methane or other synthetic fuels for a variety of applications in the energy infrastructure (▶ Chap. 8). Depending on the application, the level of greenhouse gas savings determines if substituting fossil fuels with synthetic fuels makes sense. The quantity required and the cost-effectiveness are factors here as well.

The greatest potential for $CO_2$ reductions, according to [82], are in the transport sector and in the industrial sector. Fuel cell vehicles (FCV) have significantly higher efficiency levels than normal combustion engines. In addition, diesel and gasoline have significantly higher $CO_2$ emissions per unit of energy yield than fossil natural gas, for example, which can be replaced by producing electricity or by producing renewable methane. This means that, in the transport sector, 1 kW h of hydrogen could replace between 1.5 and 2.2 kW h of energy from fossil sources. Although current hydro-

**Table 13.24** Comparison of the environmental benefits and potential benefits with various applications ([82] and author calculations)

| | Energy source replaced | Potential substitution, fossil kW h to hydrogen kW h | $CO_2$ emission reductions in g $CO_2$eq per therm. kW h | Market potential | Cost-efficiency | Obstacles |
|---|---|---|---|---|---|---|
| PtG | Natural gas | 0.8–1 | 208–585[a] | High | Very low | Few incentives, $CO_2$ source; low electricity surpluses; $H_2$ tolerances |
| Conversion to electricity via combined cycle plants | Natural gas | 1 | 260 ($\eta = 0.90$) | Very high | Very low | Modifying gas turbines for higher $H_2$ concentration |
| Manufacturing | Natural gas | 1.31 | 350 | High | Low | None |
| Transportation (FCV) | Gasoline, diesel, natural gas | 1.5–2.2 | 465–680[b] | Currently low/very high in the future | Low | Few vehicles, limited infrastructure |

[a] Natural gas 234 g $CO_2$eq per therm. kW h, efficiency of the heating sector 90%, electricity sector 60%, transportation sector 40%.
[b] Gasoline 311 g $CO_2$eq per therm. kW h, diesel 316 g $CO_2$eq per therm. kW h.

gen demand in this sector is still very small, the demand is expected to increase significantly (▶ Sect. 5.2.3). Since there are no efficiency losses due to reforming, 1 kW h of hydrogen can replace up to 1.31 kW h of energy from fossil sources in the industrial sector [82].

But despite these advantages, renewable hydrogen is still not currently cost-effective in either of these areas. Table 13.24 summarizes the results.

Additional potential could result from policies imposing quotas. Biofuel quotas or greenhouse gas reduction requirements, for example, could increase the value of renewable gases such as hydrogen or methane compared to fossil fuels. This would make these gases a financially attractive alternative, thus integrating them into the market.

### 13.3.3 Integration of Flywheel Storage Systems in Short-Distance Public Transportation

There are a number of approaches to integrating flywheel storage systems in short-distance public transportation (▶ Chap. 9). They cannot be easily integrated into buses. This is because the buses must first be converted to electric drive. In addition, the flywheel requires significant space and reduces driving performance. In the 1950s, Switzerland introduced a flywheel bus (the 'Gyrobus'). These problems do not apply to rail transport. As a result, the following section focuses on the integration of flywheel storage systems in short-distance public rail transportation.

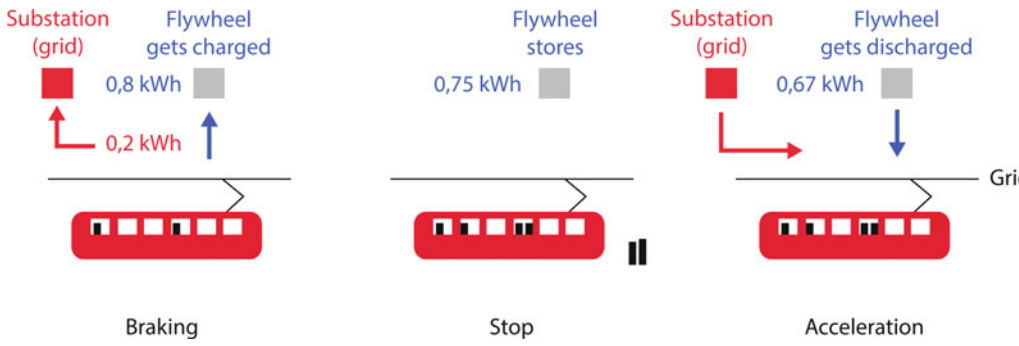



**Fig. 13.52** Use of a flywheel-energy storage system to recover tram braking energy [63]

### Examples of Flywheel Storage Systems in Public Transportation

In Zwickau, flywheel storage technology was used in the tram system. Because of their weight, flywheels can be used to store brake energy in trams. Since overloads may result, electricity peaks produced by recovering braking energy cannot always be fed back into the electricity network. These power-peaks can be charged into stationary flywheel storage systems and then discharged when a tram is accelerating. In Zwickau, this storage technology resulted in 200 MW h of energy savings, or savings of 20 to 30% [63].

Another example is the Freiburger Verkehr AG's (VAG) flywheel storage facility which has operated in test mode since early 2013. Here, energy is normally fed back into the tram electricity network each time a tram brakes. This means that in Freiburg, on a track with less traffic, the braking energy of one tram can only be used if another tram requiring braking energy for acceleration happens to be nearby. As a result, the VAG uses a flywheel-energy storage system to recover braking energy on a remote stretch of Line 1. The system saves about 250 MW h of energy a year and reduces $CO_2$ emissions by 145 tons [35].

### Effects of Flywheel Storage Systems in Short-Distance Transportation

A flywheel storage facility can deliver energy savings. For each tram braking, 0.2 kW h of energy is fed back into the network. This amounts to 20% of the braking energy. Starting from a stop requires 1.77 kW h of electricity per start (Fig. 13.52).

A flywheel storage system is used to store 0.8 kW h of the lost braking energy per braking for this purpose. After efficiency losses, 0.75 kW h is actually stored. This means that the energy required to accelerate is reduced to 1.1 kW h. As a result, 38% less energy is consumed per operating cycle. Taking into account electricity consumption for heating, additional components, and so on, in total, the electricity network supplies 20 to 25% less energy to the tram.

An additional 5% of savings can be achieved by connecting the energy storage system between two substations. A substation is a transformer station used to supply the tram system with electricity from the public electricity network.

### Stationary Flywheel-Energy Storage Facility Design

Figure 13.53 shows the flywheel storage facility for the tram in Zwickau. This compact facility has no special requirements for the installation location. All the required components are contained in the facility. The system can be connected to the electricity network by a grid connection, or operated independently using a self-supply unit.

**Example**

The potential cost and energy savings resulting from integrating flywheel storage systems in short-distance public rail transportation can be

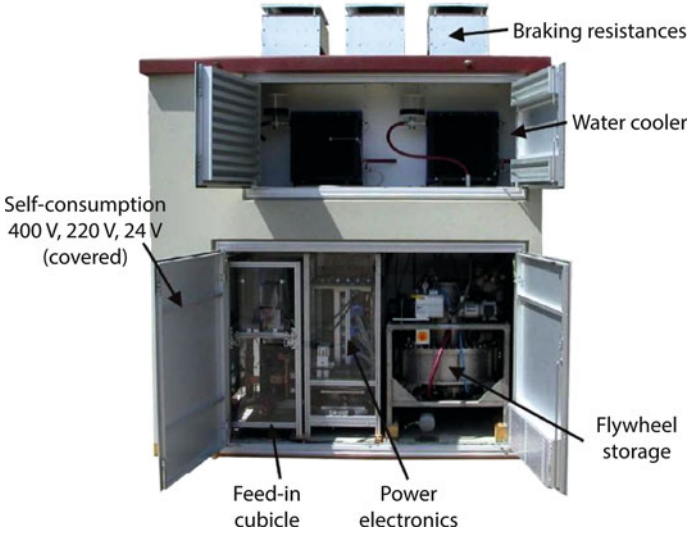



**Fig. 13.53** General view of the flywheel storage facility built for the tram in Zwickau [63]

demonstrated by using a Munich subway line as an example.

The network has 95 km of track with 576 trains running about 140 times on each route. The trains weigh between 50 and 160 tons [52]. The 750 V electric engines on these trains drive the train during acceleration, or function as generators during braking. This braking energy is currently not used except to drive another train at the same time where possible.

The U1 line has 15 stops and runs 121 times in each direction. The trains weigh 62 tons. The average speed is about 36 km/h. If the train accelerates between stations to a speed of 72 km/h then, ignoring wind resistance and friction, the kinetic energy of the train during braking is:

$$E = \frac{1}{2} \cdot m \cdot v^2 = 12.6\,\text{MJ} = 3.44\,\text{kW h}.$$

This means that the daily quantity of braking energy on the U1 line is:

$$E_{\text{ges}} = 3.44\,\text{kW h} \cdot 15 \cdot 2 \cdot 121 = 12{,}503\,\text{kW h}.$$

Assuming that the braking energy is not used, a flywheel storage system could charge the energy released and discharge it during acceleration. The U1 line would then require 15 facilities with a capacity of 4.2 kW h each to maintain a top speed of 80 km/h.

In practice the facilities have a recovery rate of 40%, of which 80% can be fed back in. This means that the overall efficiency is 32%. Applying these results to the example in Fig. 13.52 where nearly 1.1 kW h was recycled using the flywheel storage system, this suggests that savings on the line U1 could amount to around 4,000 kW h a day. If electricity costs are 10 €-ct/kW h, then this is equivalent to savings of 400 € a day or more than 100,000 € a year. Investments for the flywheel storage system could be quickly amortized, with cost, energy, and $CO_2$ savings continuing to grow over time.

## 13.4 Summary

- There are a wide range of options for integrating storage systems into the electricity sector in a **variety of applications**. The more functions and segments a storage facility can simultaneously serve, the greater its **cost-effectiveness**.
- Storage system operation delivers the greatest benefits when the **electricity price difference** between charging and discharging is largest, and **price fluctuations** the most frequent.

- Besides participating in these arbitrage transactions, storage systems are extremely well-suited for supplying **system services**, and in particular for participating on the **balancing power markets**.
- Many electricity storage systems are also uniquely positioned to provide **black-start** capability, contribute to quicker **gradient control**, and increase **guaranteed capacity**. But they are currently **undercompensated** for performing these system-relevant functions.
- The functions of the **capacity market** (guaranteed capacity), the balancing power market (frequency maintenance), and the **flexibility market** could all be integrated into the existing **balancing power market**. But this can only be achieved by ensuring **technology neutrality**, **increasing market** orientation, implementing **gradient capacity** guidelines, and contributing to **guaranteed capacity**. With shorter delivery periods and smaller lot sizes, **renewable energy facilities** and the **consumer side** must be better integrated.
- In combination with renewable energy, **electricity storage systems capable of supplying PBP** such as battery parks or pumped-storage facilities could **replace fossil power plants**. This would **stabilize the operation of the electricity supply system** while **reducing $CO_2$ emissions** at the same time.
- Proven over decades, **pumped-storage** is currently the **most established**, **most efficient**, and **cheapest form** of **large-scale electricity storage over short periods**.
- Pumped-storage capacity in Europe could potentially be expanded. But **environmental sustainability** and **public acceptance** present challenges for building new, large-scale pumped-storage facilities.
- Pumped-storage plants are still used today to optimize power plant portfolio utilization by enhancing electricity value in **arbitrage transactions**. To avoid **increasing $CO_2$ emissions** in the electricity mix by using flexibility options such as pumped-storage, higher priced **$CO_2$ certificates** ranging from **30 to 70 €/ton** for $CO_2$ disposal are required. It should be kept in mind that since the service life of a PSP is very long, in energy transition, pumped-storage will primarily be used to store and enhance the price of renewable energy.
- Besides batteries and hot-water storage systems, pumped-storage is the most commonly used storage technology around the world. **Pumped-storage facilities** are the **most commonly used electricity storage technology** (around 140 GW) with the greatest growth worldwide.
- In a small number of cases, **flywheel storage systems** are used for **network stabilization** and in special research project applications.
- **Battery parks** can provide **system services** across the board. **Multiple use** of battery parks, including participation on various markets, is a **currently cost-effective** approach to integrating renewable energy on the distribution network level.
- In the future, **battery storage systems in co-operation** could **supply balancing power** to the electricity system network instead of conventional power plants, as is common today. **Battery power plants** are already **cost-effective** in the PBP area.
- **Battery storage systems** can be designed for **black-start capability**. As a result, they could contribute to **supply recovery** in combination with wind parks, gas turbines, and district heating plants. Within limits, **battery storage systems** can **increase** the **guaranteed capacity fluctuating power generators**.
- **Currently, falling costs have created new markets** for **household-battery storage** outside the electricity market. This **is driven by increasing price differences** between **electricity consumption costs** for household customers and the **EEG incentives** for solar energy, or by the elimination of EEG incentives for old PV facilities starting in 2020.

- **PV self-consumption systems** should be operated to **benefit the network and system** by integrating consumption and weather forecasts, taking into account the network situation, and optimizing the overall system. These and other measures would minimize **local and, to a lesser extent, global residual load fluctuations**.
- **District-battery storage systems** could be used at targeted overloaded points **to prevent** the **curtailment** of renewable suppliers and **ease critical network situations**. They could also be used to reduce maximal electricity demand by ramping steep gradients in residual load, thus **relieving the network**.
- By **increasing self-consumption, battery storage systems** in combination with many other storage systems can generally **contribute to system stability**, thus in turn **increasing their cost-effectiveness**.
- In contrast to market-driven use, use of battery storage systems to serve and **actively stabilize** the network **cuts distribution network expansion costs**.
- **Extreme conditions** due to **high fossil fuel prices** as well as **very high shares of renewable energy** in the electricity system are both possibilities with **stand-alone networks**. As a result, implementing renewable stand-alone networks can yield **valuable insights** applicable to energy transition on land, i.e., to **the continental network**.
- In addition, many **stand-alone projects** using energy storage systems **can be cost-effective**. **Challenges** here include the **logistics**, the varying **legal implications** of implementation, and successfully transferring or **maintaining** the systems.
- **Thermal storage systems** in **solar-thermal power plants** extend power plant operation even in times of low solar radiation. Since heat is easier to store than electricity, energy storage systems in solar-thermal power plants are **cheaper** to build. Expanding thermal storage facilitates electricity generation planning but does not increase base-load operation. This is because most thermal storage systems can only bridge periods under 10 hours.
- In combination with **thermal storage systems**, a well-designed **solar facility** can fully meet **hot water requirements** in the **summer months**. Over a full year, a solar facility can meet around 60% of all service water demand.
- **Sensible-thermal storage systems** can be used as **cheap, long-term storage systems** for solar heating supply in **single-family households and apartment-buildings** with solar facilities. Since the technology is easy to integrate, housing plans should include these facilities in their design.
- Climate change will increase **air-conditioning** requirements. Passive cooling systems using PCM are an alternative to conventional air-conditioning in lightweight buildings. These systems can behave like massive walls by storing the latent heat of a phase-change, typically a solid-liquid phase-change.
- **Thermochemical-sorption storage systems** can be used in **dishwashers** to significantly reduce energy consumption as well as increase **user comfort**.
- There is a **large supply of wood** in Germany, and its **growth is underestimated**. In terms of quantity and area, in **Germany the greatest amount of energy is stored by forests** using photosynthesis. In addition, forests have the potential to sustainably absorb large quantities of $CO_2$ and supply substantial quantities of heat. In addition to direct energetic use of wood, **cascade use** also makes good sense. The growth of wood In Bavaria alone is adequate to meet the annual consumption of **heating oil**. Energetically, the forest has more charging power than all the atomic power plants operating in Bavaria combined.
- **Wood's storage potential** is an **economically attractive** option for **supplying heat**. Wood chip prices have doubled in the last ten years, and pellet prices have also increased by over 50%. But prices for both products are still significantly lower than

heating oil or natural gas prices. Wood is also a **domestically produced renewable resource** that could be used to reduce fossil energy source imports and **stimulate regional economies**.

- **Potential** energy and $CO_2$ storage could be **significantly increased** by **natural forest restocking**. This requires a **functioning balance** between **forest and game**, as well as the full commitment of the government administration, hunting associations, and forest owners. For energy supply, the climate, and the environment, the **advantages of natural restocking** are higher yields, more **stored** energy, increased **climate protection** at no additional cost, forests better **protected** against climate change, **greater flooding protection** at no additional cost, and improved **biodiversity**. Natural restocking also **reduces** the number of **accidents** involving animals that cause **injuries and damage**. In addition, animals are better protected in thicker forests. Natural restocking is incentivized by attractive state subsidies.
- Like wood, **biofuels** are **stored solar energy sources**. They could be produced in adequate supply to achieve **sustainable mobility**, and decarbonize the transportation sector. But they will at first be used in mixtures with other renewable fuels, or in combination with electro-mobility. Fuels produced from residual or waste materials are better for the environment than energy crops.
- Farming machinery cannot be driven by electricity using batteries or hydrogen, or only at too great an expense. This means that **vegetable oil** is **particularly important** in farming, because it is practically the **only storage alternative** available. Current **regulations discourage** the use of vegetable oil in Germany even though the **advantages** are **obvious**. Technically it is relatively easy to integrate, and it use could stimulate regional economies.
- Technically, **bio-ethanol** and **biodiesel** are easier to integrate than vegetable oil. They are also promoted by current regulations. In general, biofuels can be conveniently integrated into the transportation sector to **promote recycling**.
- **Hydrogen** can be relatively **easily integrated** into existing **refinery processes**, and can be used in the transportation sector to earn 'super-credits' for fulfilling **biofuel quotas**. In addition, hydrogen could be **profitably** exploited in the **material product cycle**. If hydrogen can be integrated on-site, then additional conversion steps are not required.
- Although integrating **hydrogen** into a dedicated **hydrogen infrastructure** has significant ecological and technical benefits, it is **currently not economically feasible**.
- Pilot projects have shown that **flywheel storage systems** used in **short-distance public rail transportation** can effectively reduce costs, energy consumption, and $CO_2$ emissions.



## References


1. Abengoa Solar (2014) PS10, the first solar power tower worldwide. http://www.abengoasolar.com/web/en/nuestras_plantas/plantas_en_operacion/espana/PS10_la_primera_torre_comercial_del_mundo.html. Accessed 03.2014 (Abengoa Solar.)
2. Ammer C, Vor T, Knoke T, Wagner S (2010) Göttinger Forstwissenschaften. In: Der Wald-Wild-Konflikt. Analyse und Lösungsansätze vor dem Hintergrund rechtlicher, ökologischer und ökonomischer Zusammenhänge, vol 5. Univ.-Verl. Göttingen; Niedersächsische Staats-und Universitätsbibliothek, Göttingen, Göttingen
3. Aßmann J, Uhlenbrock K (2011) Infoblatt Drei-Schluchten-Staudamm. Projektdaten, Planung, Bau, Probleme. http://www2.klett.de/sixcms/list.php?page=geo_infothek&node=Drei-Schluchten-Staudamm&miniinfothek&article=Infoblatt+Drei-Schluchten-Staudamm. Accessed 13 July 2013
4. Bauer D, Marx R, Nußbicker-Lux J, Ochs F, Heidemann W, Müller-Steinhagen H (2010) German central solar heating plants with seasonal heat storage. Sol Energy 84(4):612–623. https://doi.org/10.1016/j.solener.2009.05.013
5. Bayerische Staatsregierung (2005) Waldgesetz für Bayern. BayWaldG, München

6. Bayerisches Staatsministerium für Ernährung, Landwirtschaft und Forsten (2002) Vorrat, Zuwachs und Nutzung. Die zweite Bundeswaldinventur 2002. LFW Wissen, München
7. Bayerisches Staatsministerium für Ernährung, Landwirtschaft und Forsten (2012) Forstliches Gutachten zur Situation der Waldverjüngung 2012. München
8. BDBe (2013) E85 – Mobil mit bis zu 85% Bioethanol. http://www.bdbe.de/bioethanol/e85/. Accessed 8 Apr 2014 (Bundesverband der deutschen Bioethanolwirtschaft e. V.)
9. Beacon (2014) Operating Plants. http://www.beaconpower.com. Accessed 5 Mar 2014 (Beacon Power LLC)
10. BINE Informationsdienst (2015) Akkus im Niederspannungsnetz für mehr PV-Erträge. http://www.bine.info/newsuebersicht/news/akkus-im-niederspannungsnetz-fuer-mehr-pv-energie/ (BINE Informationsdienst)
11. Blank T (2014) Informationen zur Smart-Region Pellworm. E.ON, Essen (Email)
12. BMAS (2006) Bundesgesetzblatt Jahrgang 2006 Teil I Nr. 62. Bonn
13. Bollin E (2008) Automation regenerativer Wärme- und Kälteversorgung von Gebäuden. Komponenten, Systeme, Anlagenbeispiele, 1st edn. Studium Technik. Vieweg, Wiesbaden
14. Callman G (2015) Tesla Stationary Storage: Tools for the Electrical Grid. Energy Storage Europe 2015, Düsseldorf
15. DENA (2013) Deckung des Warmwasserbedarfs. http://www.thema-energie.de/heizung-warmwasser/heiztechnik/solarwaerme/deckung-des-warmwasserbedarfs.html. Accessed 7 Oct 2013 (Deutsche Energie-Agentur)
16. DENA (2013) Kombianlagen. http://www.thema-energie.de/energie-erzeugen/erneuerbare-energien/solarwaerme/einsatzmoeglichkeiten/kombianlagen.html. Accessed 7 Oct 2013 (Deutsche Energie-Agentur)
17. Deutscher Bundestag (2009) Verordnung zu Systemdienstleistungen durch Windenergieanlagen. Bonn (Systemdienstleistungsverordnung (SDLWindV))
18. Deutscher Bundestag (2011) Gesetz zur Neuregelung des Rechtsrahmens für die Förderung der Stromerzeugung aus erneuerbaren Energien. Bonn (Erneuerbare-Energien-Gesetz (EEG))
19. DEV und SolarInvert GmbH (2014) Econamic Grid Broschüre
20. Dominion (2014) Bath County Pumped Storage Station. https://www.dom.com/about/stations/hydro/bath-county-pumped-storage-station.jsp. Accessed 14 Mar 2014 (Dominion Generation)
21. dpa (2010) Millionen Menschen müssen umsiedeln. Nachdem bereits eine Million Menschen dem Bau des Drei-Schluchten-Damms in China weichen mussten, sollen nun weitere vier Millionen folgen. http://www.sueddeutsche.de/panorama/drei-schluchten-damm-millionen-menschen-muessen-umsiedeln-1.344584. Accessed 17 May 2010 (Süddeutsche.de)
22. Dunker R (2015) Das Caterva Energiespeichersystem (ESS)
23. Dvorak P (2011) Battery stores 40 MW for Fairbanks, Alaska emergencies. http://www.windpowerengineering.com/design/electrical/battery-stores-40-mw-for-ankorage-emergencies/. Accessed 13 Feb 2014 (Windpower Engineering & Development)
24. Echternacht D (2015) Stromspeicher in der Nieder- und Mittelspannungsebene. Frankfurt
25. EEX (2014) EEX ist die führende Energiebörse in Europa. http://www.eex.com/de#/de. Accessed 14 Feb 2014 (European Energy Exchange AG)
26. Ellrich M (2012) Infoblatt Nasser-Stausee (Assuan-Staudamm). Informationen rund um den Nasser-Stausee in Ägypten
27. Energietechnische Gesellschaft im VDE (2015) Batteriespeicher in der Nieder- und Mittelspannungsebene. Anwendungen und Wirtschaftlichkeit sowie Auswirkungen auf die elektrischen Netze. Studie der Energietechnischen Gesellschaft im VDE (ETG), Frankfurt am Main
28. Eurelectric (2011) Pumpstore – Developed and potential. http://www.eurelectric.org/factsfolders/factsfolder.asp?FolderID=5236. Accessed 1 Apr 2014
29. FNR (2007) Biokraftstoffe – Pflanzen, Rohstoffe, Produkte, 3rd edn. FNR
30. Focus (2011) Drei-Schluchten-Damm: Folgeschäden und Folgekosten. http://www.focus.de/wissen/klima/klimaprognosen/drei-schluchten-damm-folgeschaeden-und-folgekosten_aid_629078.html. Accessed 19 May 2011 (Focus)
31. Frahm T (2013) Pool Solarheizungen. http://www.solaranlagen-portal.com/solarthermie/nutzung/pool. Accessed 8 Oct 2013 (solaranlagen-portal.com)
32. Franzen E (2013) Inselnetze. Regensburg (E-Mail von Younicos)
33. Fraunhofer ISE (2012) AP2: Effekte und Auswirkungen im Verteilnetz. Abschätzung und Einordnung von energiewirtschaftlichen, ökonomischen Abschätzung und Einordnung von energiewirtschaftlichen, ökonomischen und anderen Effekten bei der Förderung von objektgebundenen elektrochemischen Speichern. Foliensammlung zu AP2, Freiburg
34. Fraunhofer ISE (2012) AP2: Effekte und Auswirkungen im Verteilnetz. Abschätzung und Einordnung von energiewirtschaftlichen, ökonomischen Abschätzung und Einordnung von energiewirtschaftlichen, ökonomischen und anderen Effekten bei der Förderung von objektgebundenen elektrochemischen Speichern. Foliensammlung zu AP2, Freiburg

35. Freiburger Verkehrs AG (2013) Innovationsprojekt „Schwungradspeicher" wird bei der Freiburger Verkehrs AG erprobt. Freiburg im Breisgau
36. Fritsche UR, Wiegmann K (2008) Ökobilanzierung der Umweltauswirkungen von Bioenergie- Konversionspfaden. WBGU, Berlin (Expertise für das WBGU-Hauptgutachten „Welt im Wandel: Bioenergie und nachhaltige Landnutzung„)
37. Gimeno-Gutiérrez M, Lacal-Arántegui R (2013) Assessment of the European potential for pumped hydropower energy storage. A GIS-based assessment of pumped hydropower storage potential. EUR, Scientific and technical research series, vol 25940. Publications Office, Luxembourg
38. Goldie-Scot L (2015) 2015 Global Energy Storage Market Overview. Energy Storage Europe. Energy Storage Europe VDE Financial Dialogue, Düsseldorf
39. GtV (2013) Energie speichern mit Geothermie. http://www.geothermie.de/wissenswelt/geothermie/technologien/energie-speichern-mit-geothermie.html. Accessed 7 Oct 2013 (GtV Bundesverband Geothermie e.V.)
40. GVEA (2014) Battery Energy Storage System (BESS). http://www.gvea.com/energy/bess. Accessed 6 Feb 2014
41. Haack D (2012) Klimakonferenz Smart grid. SmartRegion Pellworm, Flensburg
42. Hothorn T, Brandl R, Müller J, Merenlender AM (2012) Large-Scale Model-Based Assessment of Deer-Vehicle Collision Risk. PLoS ONE 7(2):e29510. https://doi.org/10.1371/journal.pone.0029510
43. HYPOS (2014) Hydrogen Power Storage & Solutions East Germany. http://www.hypos-eastgermany.de/. Accessed 14 Mar 2014 (BMBF)
44. IHDI (2014) Consumption increases and Itaipu beats 2012 record. https://www.itaipu.gov.br/en/press-office/news/consumption-increases-and-itaipu-beats-2012-record. Accessed 20 Mar 2014 (Usina Hidreléctrica de Itaipu)
45. Isaka M, Mofor L, Wade H (2013) Tokelau. Renewable energy opportunities and challenges in the Pacific Islands region. Abu Dhabi
46. Kairies K-P, Magnor D, Sauer DU (2015) Wissenschaftliches mess- und Evaluierungsprogramm Solarstromspeicher. WMEP PV-Speicher. International Renewable Energy Storage Conference (IRES), Düsseldorf
47. Kays J, Seack A, Haebler J, Rehtanz C (2014) Evaluation of Storage Systems in Distribution Networks by Means of an Agent Based Simusation System. Wroclaw
48. Klammt S, Neyer A, Müller HFO (2012) Redirection of sunlight by microstructured components – Simulation, fabrication and experimental results. Sol Energy 86(5):1660–1666. https://doi.org/10.1016/j.solener.2012.02.034
49. Konstantin P (2013) Praxisbuch Energiewirtschaft. Springer, Berlin, Heidelberg
50. Mayhew T, McCracken P (2013) Tokelau. Renewable Energy Project (Case Study)
51. Naturstromspeicher GmbH MBS (2015) Naturstromspeicher Gaildorf, Sengenthal
52. MVG (2014) U-Bahn, Bus und Tram für München. Technische Daten. http://www.mvg-mobil.de/ueberuns/fahrzeuge/technik.html. Accessed 10 Feb 2014 (Münchner Verkehrsgesellschaft mbH)
53. Neyer A, Müller HFO, Klammt S Effiziente Lichtumkehrvorrichtung mit zweiseitiger prismatischer und linsenartiger Oberflächenstrukturierung (Deutsches Patent Nr. DE 10 2008 055 857)
54. Ossenbrink R (2014) „Strombank" puffert die lokale Erzeugung. Sonne Wind und Wärme. http://www.sonnewindwaerme.de/photovoltaik/strombank-puffert-lokale-erzeugung
55. Paintner K (2012) Nutzung offener Sorptionsspeicher in Hausgeräten. OTTI Kolleg – Anwenderforum Thermische Energiespeicher. Neumarkt i. d. Oberpfalz
56. Philipps R (2013) Solarthermie Zweispeichersysteme. http://www.321-sun.de/solarthermie/solarthermie-speicher/zweispeichersysteme/. Accessed 7 Oct 2013 (321-sun.de)
57. Piller (2013) Energiespeicher. Powerbridge – kinetischer Energiespeicher. http://www.piller.com/205/energy-storage. Accessed 20 Mar 2014 (Piller Power Systems)
58. Pleßmann G, Erdmann M, Hlusiak M, Breyer C (2014) Global Energy Storage Demand for a 100% Renewable Electricity Supply. Energy Procedia 46:22–31. https://doi.org/10.1016/j.egypro.2014.01.154
59. Quaschning V (2011) Regenerative Energiesysteme. Technologie – Berechnung – Simulation, 7th edn. Hanser, München
60. Rehtanz C, Greve M, Häger U, Hilbrich D, Agricola A (2014) dena-Studie Systemdienstleistungen 2030. Voraussetzungen für eine sichere und zuverlässige Stromversorgung mit ho- hem Anteil erneuerbarer Energien. Berlin
61. Rehtanz C et al (2014) dena-Studie Systemdienstleistungen 2030. Sicherheit und Zuverlässigkeit einer Stromversorgung mit hohem Anteil erneuerbarer Energien. Berlin
62. REN21 (2013) Renewables 2013 – Global Status Report. REN21 Sekretariat, Paris
63. rosetta Technik GmbH (2006) Energiespeicher für das Straßenbahnnetz. Roßlau (Stand 08/06)
64. Rubeck P (2013) Sonnenhäuser. Solarzentrum Kienberg. http://www.sonnenhaus-institut.de/solar-haeuser.php5?p=Solarzentrum+Kienberg. Accessed 8 Oct 2013 (Sonnenhaus-Institut e.V.)
65. RWE (2014) PSW Herdecke. http://www.rwe.com/web/cms/de/1439312/rwe-power-ag/standorte/wasserkraft/rwe-wasserkraftwerke/psw-herdecke/. Accessed 13 Feb 2014 (RWE Power AG)

66. Schluchseewerk AG (2014) Das Kavernenkraftwerk Säckingen. http://www.schluchseewerk.de/standorte/hotzenwaldgruppe/kraftwerk-saeckingen/. Accessed 24 Feb 2014 (Schluchseewerk AG)
67. Schluchseewerk AG (2014) Neubauprojekt Pumpspeicherkraftwerk Atdorf. http://www.schluchseewerk.de/index.php?id=174. Accessed 24 Feb 2014 (Schluchseewerk AG)
68. Schmitt B, Vajen K, Jordan U (2008) Integration of Solar Heating Systems for Process Heat Generation in Breweries. EUROSUN 2008 – 1st international congress on heating, cooling and buildings, Kassel
69. Schütt R (2012) Dezentrale Energieversorgung am Beispiel der Insel Pellworm. Braunschweig
70. Schwill J, Sämisch H (2014) Spotmarkt (EPEX SPOT). http://www.next-kraftwerke.de/wissen/strommarkt/spotmarkt-epex-spot. Accessed 3 Feb 2014 (Next Kraftwerke)
71. SEO (2014) PSW Vianden. Technische Daten. http://www.seo.lu/de/Hauptaktivitaeten/PSW-Vianden/Anlagen/Technische-Daten. Accessed 26 Mar 2014 (Société Electrique de l'Our)
72. SHN AG Energie-Region mit Zukunftsanschluss. SmartRegion Pellworm. http://www.smartregion-pellworm.de/home.html Accessed 19. Dezember 2013
73. SMA (2013) Planungsleitfaden SMA Smart Home. Die Systemlösung für mehr Unabhängigkeit. Kassel
74. Solar Millennium AG (2013) Die Parabolrinnen-Kraftwerke Andasol 1 bis 3 – Die größten Solarkraftwerke der Welt. Erlangen
75. solarserver (2011) Solarthermie der Zukunft: Gemasolar, das Solarturm-Kraftwerk von Torresol Energy mit Flüssigsalz-Speicher. http://www.solarserver.de/solar-magazin/anlage-des-monats/solarthermie-der-zukunft-gemasolar-das-solarturm-kraftwerk-von-torresol-energy-mit-fluessigsalz-speicher.html. Accessed 8 Oct 2013 (Heindl Server GmbH)
76. solarserver (2012) Schwimmbad-Heizung mit Solarthermie ermöglicht regeneratives Sportvergnügen. http://www.solarserver.de/solar-magazin/nachrichten/archiv-2012/2012/kw29/schwimmbad-heizung-mit-solarthermie-ermoeglicht-regeneratives-sportvergnuegen.html. Accessed 8 Oct 2013 (solarserver.de)
77. Spannagel J (2013) Evaluation von Maschinenüberholungen in Speicherkraftwerken im energiewirtschaftlichen Kontext. Ostbayerische Technische Hochschule (Bachelorarbeit)
78. Sterner M (2009) Bioenergy and renewable power methane in integrated 100% renewable energy systems. Limiting global warming by transforming energy systems. Renewable Energies and Energy Efficiency, vol 14. Kassel University Press, Kassel
79. Sterner M, Moser A, Thema M, Eckert F, Schäfer A, Drees T, Rehtanz C, Häger U, Kays J, Seack A, Sauer DU, Leuthold M, Stöcker P (2014) Stromspeicher in der Energiewende. Untersuchung zum Bedarf an neuen Stromspeichern in Deutschland für den Erzeugungsausgleich, Systemdienstleistungen und im Verteilnetz. Berlin (Studie)
80. Steward D, Saur G, Penev M, Ramsden T (2009) Lifecycle Cost Analysis of Hydrogen Versus Other Technologies for Electrical Energy Storage. Golden
81. Stieglitz R, Heinzel V (2012) Thermische Solarenergie. Grundlagen, Technologie, Anwendungen. Springer Vieweg, Berlin (Lehrbuch)
82. Stiller C (2014) Nutzung von konventionellem und grünem Wasserstoff in der chemischen Industrie. In: Töpler J, Lehmann J (eds) Wasserstoff und Brennstoffzelle. Technologien und Marktperspektiven. Springer, Berlin, Heidelberg
83. Tillmetz W (2010) Überblick elektrochemische Energiespeicher. Ulm
84. Triebel C (2012) Regelung eines Inselnetzes im MW-Bereich mit Hilfe stationärer Speicher. VDI Wissensforum Stationäre Energiespeicher, Karlsruhe
85. Universität Stuttgart (2013) Solar unterstützte Nahwärme. Heißwasser-Wärmespeicher. http://www.itw.uni-stuttgart.de/abteilungen/rationelleEnergie/technik/heisswasserws.php. Accessed 7 Oct 2013 (Universität Stuttgart)
86. VERBUND (2014) Pumpspeicherkraftwerk Malta Oberstufe. http://www.verbund.com/pp/de/pumpspeicherkraftwerk/malta-oberstufe. Accessed 16 Mar 2014
87. Voight A (2012) Graciosa Project Overview. Berlin
88. Voith (2014) Itaipú, Brasilien. http://www.voith.com/de/maerkte-branchen/branchen/wasserkraft/large-hydro-kraftwerke/itaipu_main-9768-9768.html. Accessed 10 Mar 2014
89. Waffenschmidt E (2014) Dimensioning of Decentralized Photovoltaic Storages with Limited Feed- in Power and their Impact on the Distribution Grid. Energy Procedia 46:88–97. https://doi.org/10.1016/j.egypro.2014.01.161
90. WBGU (2008) Welt im Wandel: Zukunftsfähige Bioenergie und nachhaltige Landnutzung. WBGU, Berlin (Hauptgutachten 2008)
91. Weinleder H (2011) Abschlussbericht PCM. Demoprojekt: Report ZAE 2. Würzburg
92. Weniger J, Bergner, Joseph, Tjaden, Tjarko, Kretzer J, Schnorr F, Quaschning V (4–2015) Einfluss verschiedener Betriebsstrategien auf die Netzeinspeisung räumlich verteilter PV-Speichersysteme, Bad Staffelstein

# Storage Integration for Coupling Different Energy Sectors

*Michael Sterner, Ingo Stadler, Fabian Eckert, Norman Gerhardt, Christian von Olshausen, Martin Thema, and Tobias Trost*

**14.1 Coupling of the Electricity and Heating Sectors – 758**
14.1.1 Increasing the Flexibility of CHP Using Thermal Storage and Heating Networks – 758
14.1.2 Integration of Electric Heat-Pumps Using Thermal Storage and Heating Networks – 764
14.1.3 Integration of PtH Using Thermal Storage and Heating Networks – 768
14.1.4 Battery Storage vs. Load Shifting vs. Thermal Storage—An Example – 774

**14.2 Coupling of Power and Transport Sectors – 776**
14.2.1 Electro-Mobility – 776
14.2.2 Electric Fuels – 780

**14.3 Coupling of the Power and Gas Sectors: PtG – 785**
14.3.1 PtG in the Context of the Energy Supply System – 785
14.3.2 Development of PtG in Germany and Neighboring Countries – 788

**14.4 Summary – 801**

**References – 803**

**Electronic supplementary material** The online version of this chapter (https://doi.org/10.1007/978-3-662-55504-0_14) contains supplementary material, which is available to authorized users.

© Springer-Verlag GmbH Germany, part of Springer Nature 2019
M. Sterner, I. Stadler (Eds.), *Handbook of Energy Storage*, https://doi.org/10.1007/978-3-662-55504-0_14

**Overview**

**Electricity is becoming the primary source of energy**, a trend that is particularly apparent through the **coupling** of the **electricity sector** with **other energy sectors**.

In addition to the established **links** between the **electricity and heating sectors** using combined heat and power (CHP), which is supplemented by electric heat-pumps and power-to-heat (PtH), other new links are also emerging. These links are manifesting in the form of **electro-mobility** and **electric fuels** in the **electricity and transport sectors**; and in the **electricity and gas sector** they are appearing in the form of **power-to-gas (PtG)**. The production of **basic chemical materials** such as methanol or polymers using electrical energy, water, and $CO_2$ will also play a role in the future. However, the latter will not be dealt with explicitly here. Instead we will consider in detail other aspects of electricity as a primary energy source and its integration and application for energy storage.

## 14.1 Coupling of the Electricity and Heating Sectors

The expansion of renewable energy means that it is becoming increasingly important to link the three major energy sectors—namely, electricity, heating, and transport. Storage systems play an important role for balancing temporary mismatch between supply and demand. The 'electricity storage problem' is partly resolved here by using thermal storage, which provides the electricity system with cost-effective flexibility. This chapter will consider the following issues in detail:

- CHP
- The integration of electric heat-pumps
- The integration of PtH to supplement ▶ Chap. 11

▶ Chapter 11 deals with in detail the integration of household appliances and systems for supplying heating and cooling as part of load-management. That chapter considers the following points which will not be dealt with in any detail in this section apart from PtH for the heating supply:

- Load-management in households using:
  - Storage heating systems
  - Electrical hot water supply
  - Electrical cooling generation
  - Heating system circulating pumps
  - Ventilation systems
  - Washing machines, driers, dishwashers
- Load-management in the industrial sector

### 14.1.1 Increasing the Flexibility of CHP Using Thermal Storage and Heating Networks

This section provides an overview of CHP. It also describes how CHP can be used more efficiently to integrate renewable energy when it is combined with thermal storage and heating networks.

#### 14.1.1.1 CHP as the Traditional Method for Coupling of the Electricity and Heating Sectors

■ **Basic Principle of CHP**

CHP is the classic example of the coupling of the electricity and heating sectors using thermal storage.

Conventional thermal power plants convert their fuel to electricity with high thermal losses. The average electrical efficiency is about 38% and the waste heat is released into the environment through a cooling tower. In comparison, modern combined-cycle power plants (CCPP) have an efficiency of more than 60% with lower thermal losses.

Using CHP, electrical and thermal energy are utilized simultaneously and the efficiency of the energy conversion is increased to as much as 90%. However, 'power loss' is standard, except in the case of CHP technologies or gas turbines with waste heat boilers. This reduces the ratio between power and heat and thus the exergetic efficiency of the process [1]. CHP plants can be operated using either fossil fuels

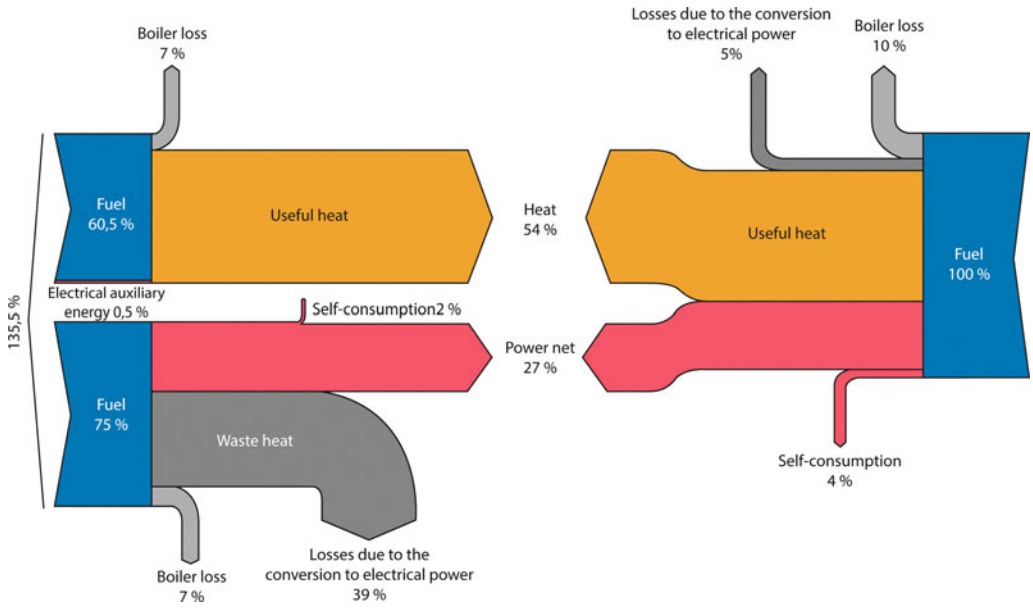



**Fig. 14.1** Separate generation of useful electrical and thermal energy compared to coupled generation, adapted from [32]

such as coal, heating oil, and natural gas or with renewable fuels such as biogas, biomethane, renewable methane, sewage gas, plant oil, wood, and wood gas. The most commonly used fuel continues to be natural gas.

When comparing CHP plants and condensation power plants with the same supply functions, it is critical how much of the heating fraction of the peak load boiler is made up of district heating and which alternative heat generation technology is used for balancing in the case of condensation power plants.

For the example of a decentralized system without a heating network shown in Fig. 14.1, CHP (right) has considerably better efficiency advantages compared to the combination of a condensation power plant and a gas boiler (left). For coupled generation of electricity and heat, a total of 100% fuel is converted to useful energy of 54% heat and 27% electricity. In contrast, for separate generation, a total (60.5 + 75)% of fuel is applied to produce the same quantity of useful energy as for coupled generation. This can save up to one-third of the primary energy. However, the primary energy savings could be considerably lower if other reference plants are selected [32].

### ■ Potential Applications for CHP Plants

The electrical and thermal output range of CHP plants is very broad and ranges from a few kilowatts to several hundred megawatts. CHP plants have a correspondingly large field of application. CHP can be used as a supply solution almost everywhere that heat is required: whether for local or district heating networks, for process heat in the industrial sector at temperatures of up to 500 °C, or even for decentralized private use. Thermal storage systems act as a buffer to reconcile differences in heat supply and demand. Economically suitable applications are primarily those where there is high heat consumption with a simultaneous need for electricity (for example, in densely populated areas and industrial plants). District heating systems frequently serve apartment-buildings and commercial complexes and, to some extent, industrial parks [32].

CHP plants are, however, usually not profitable for single homes or duplexes. Only mini-

CHP plants are economically suitable for single plants in apartment complexes. Local heating networks are one option for connecting new urban regions and can, in the medium-term, be combined to form a district heating network. As part of the expansion of CHP using biomass, rural local heating networks have been frequently constructed—for example, in the form of biogas plants in villages and rural communities—despite a low population density.

### Designing and Sizing CHP Plants

CHP plants are designed and dimensioned differently in relation to their specific area of application. The dimensioning of a CHP plant is a key determinant of its cost-effectiveness. The different modes of operation are described in ▶ Sect. 8.5.1.4. Ultimately, every project, and therefore every design, is individual.

Traditionally, an emphasis has been placed on ensuring a CHP plant is neither over-dimensioned nor under-dimensioned [32]. However, the expansion of renewables has encouraged new approaches in this regard. Over-dimensioned plants can exploit the potential of thermal storage more efficiently and enable considerably higher CHP contributions to district heating, meaning that the use of heating boilers can be greatly reduced. This achieves improvements in primary energy factors, which are economically relevant when considering the requirements of the German Energy Saving Ordinance (EnEV) for connecting new buildings to an existing or new heating network [23].

### Example of Denmark and the Netherlands

When discussing the expansion of CHP plants, Denmark and the Netherlands are often compared to Germany. In the Netherlands, CHP currently makes up around 30% of the electricity supply and in Denmark more than 50%. However, CHP expansion in both these countries has taken very different paths. In Denmark the district heating market in particular has driven and shaped the development of CHP. Unlike Germany, Denmark has an organically developed, nation-wide heating network infrastructure, even in smaller communes with low building density in which the networks have lower inlet temperatures well below 90 °C, making them suitable for complementary heat generators as well as open-air solar-thermal energy and heat pumps. In contrast, industrial CHP dominates in the Netherlands [13].

### Summary of Various CHP systems

There are a range of different CHP systems such as:

- Heating plants using combustion engines with an electrical output of 2–20 MW for district heating networks that are highly flexible and have reasonable investment costs.
- Gas turbine heating plants with waste heat boilers.
- Gas turbines/steam turbines/heating plants (CCPP with heat utilization).
- Steam/heating plants based on coal, wastes, and sewage sludge as well as wood. A special form that utilizes wood are ORC plants.
- CHP plants with a steam boiler and steam motor.
- CHP plants with a Stirling engine or fuel cells.

A detailed description of how the different types of plant function will not be given here. Instead, reference will be made to [32].

### Limited Potentials for CHP in Summer

Particularly in the summer months, the consumption of heat is not high enough because there is no need for heating. In the case of biogas CHP plants, the heat often goes unused making the efficiency of the CHP plants very low. Seasonal-thermal storage that stores the thermal energy from the summer months in readiness for the cold months of the year helps here. However, because of the heat losses and the low-temperature level, other technologies such as solar-thermal energy or geothermal energy are more suitable (▶ Sect. 4.5).

For a special type of CHP, called combined cooling, heat and power (CCHP), air-

conditioning buildings in summer is an interesting area of application. Using heat-driven refrigerators, the annual utilization period for CHP can be increased considerably [32]. Thermal refrigerators include absorption, adsorption, diffusion, and steam jet cooling systems as described in ▶ Sect. 8.5.2. However, in practice, it is usually the case that the natural gas fuel is too expensive and, therefore, the CHP heat is too valuable to use for cooling energy. In recent years, compression refrigerators have also achieved considerable gains in efficiency while prices have fallen. Therefore, niche applications for industrial waste heat or solar-thermal energy appear to be the only economical applications for heat-driven refrigerators.

#### ■ Local Heating vs. District Heating

In major heating plants, electricity and heat are cogenerated, yet optimal heat utilization onsite is often not possible. To transport the heat, the water is routed to the consumer through a network of well-insulated pipelines as part of a local or district heating network. The heat is then released in a transfer station located at the end-consumer site. In most cases, the customer's heat transfer system includes a heat exchanger that separates the district heating cycle from the consumer cycle. Only in the rarest of cases is the district heating cycle directly coupled to major consumers. The losses are in the range 6–20% [40].

Local and district heating systems cannot be clearly differentiated. There is no uniform definition for distinguishing between a smaller 'local heating' network and a larger 'district heating' network. The term 'local heating' generally describes small and decentralized heating networks. District heating, on the other hand, refers to larger networks with very long transport pipelines. From a technical point of view, however, there is no fundamental difference between local and district heating. For this reason, the term district heating will be used in most cases for simplification. Like the gas network, a heating network also represents an energy storage system, one containing admittedly low amounts of energy. This differentiates these two networks from the electricity network, which for purely physical reasons is not an energy storage system (apart from minimal capacitive and inductive amounts).

### 14.1.1.2 Use of Thermal Storage in Electricity-Based CHP to Integrate Renewable Energy

#### ■ Heat-Driven vs. Electricity-Driven vs. Electricity-Based Modes of Operation

CHP plants feature two modes of operation: heat-driven and electricity-driven. The conventional mode of operation is heat-driven as plants that are designed to be heat-driven are generally the most economical. Under this form of operation, CHP generation is determined by the heat load, with electricity being the by-product. Because electricity is also generated at times when it is not required, heat-driven CHP plants are referred to as 'must-run' units. This type of unit unnecessarily increases the reservoir demand in the electricity sector (▶ Chap. 3). This can be alleviated by using electricity-driven and electricity-based modes of operation.

**In the electricity-based mode of operation, the CHP plant is operated based on the needs of the electricity network while also covering heat demand. Unlike the electricity-driven mode of operation, any surplus heat is not dissipated but is instead stored. Thermal storage systems decouple the temporal fluctuations in electricity and heat demand.**

In the future, it will become increasingly important to temporally decouple the electricity and heat production of CHP plants. In some cases, heat-driven CHP plants are not switched off even when electricity prices are low, and therefore act as a barrier to the integration of renewable electricity. This is not usually because of technical reasons however, because the plants have supplemental electrical heating power that can take over the heat supply at low electricity prices. This is the case when there is a high feed-in from renewable energy with

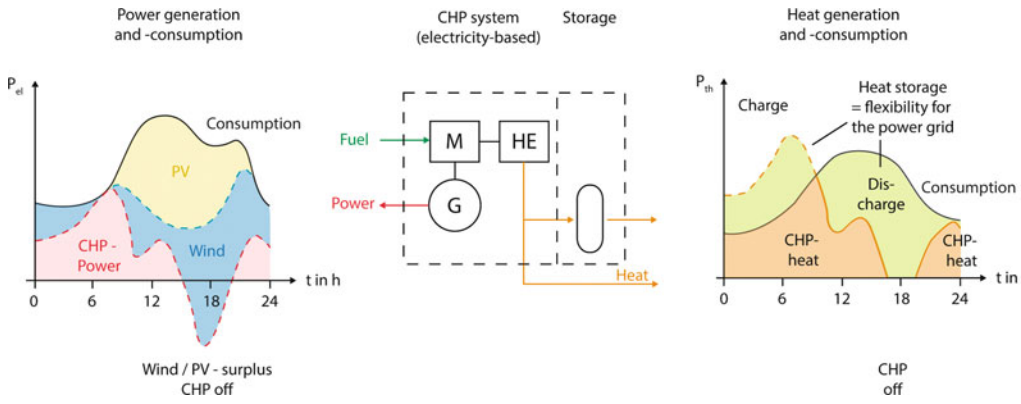



**Fig. 14.2** Combination of CHP and thermal storage to increase the flexibility of the CHP plant and energy storage

no coverage of the marginal costs of the CHP. However, this reduces the efficiency of the heat supply.

In addition to heat-driven CHP plants, there are plants that have a must-run nature as a result of the energy economy's legal framework. These include industrial CHP plants for on-site electricity generation and CHP in the lower capacity classes, which usually receive fixed subsidies based on the 'usual price' as defined by the Combined Heat and Power Act (Kraft-Wärme-Kopplungsgesetz; KWKG). Again, this case also acts as a barrier to the integration of renewable energy.

For electricity-based operations, the higher electrical output is also increased by the thermal output. At the same time, so much heat can be produced that it can no longer be entirely fed into the district heating network apart from on cold days [24].

Thermal storage systems with a wide variety of designs enable heat generation to be decoupled from heat demand, and in this way compensate economically for the lack of flexibility in power generation.

## Flexibility Using Thermal Storage and Additional Components

CHP plants become a flexible system when combined with thermal storage, peak-load boilers, electrode boilers, and/or large-scale heat pumps. This allows the heat supply and the operation of the CHP plant to be adjusted to the requirements of the power system, including fluctuating wind and solar power [3].

Thermal storage plays a particularly important role in this regard (Fig. 14.2). The surplus heat can be stored with minimal technical effort. The costs of thermal storage systems are considerably lower than those of electricity storage systems, even when combined with the costs of over-dimensioning of the plant output. By using thermal storage, heat generation is decoupled from electricity generation. The CHP plant can, therefore, respond more flexibly to load fluctuations [4].

## Flexibilization of the Sandreuth Heating Plant Using Thermal Storage and an Electrode Boiler

In the Nuremberg suburb of Sandreuth, N-Ergie Kraftwerke GmbH operates a heating plant with an electrical capacity of 225 MW and a thermal capacity of 462 MW, predominantly based on natural gas. Unlike other straight heating plants, the Sandreuth heating plant stores the heat in a district heating network to which more than 60,000 heat customers are connected. The network has a connected load value of 913 MW with a thermal output of about 1.15 TW h and a route length of 311 km.

To increase the flexibility of the heating plant within the district heating network, it was expanded in 2014 by adding a large thermal

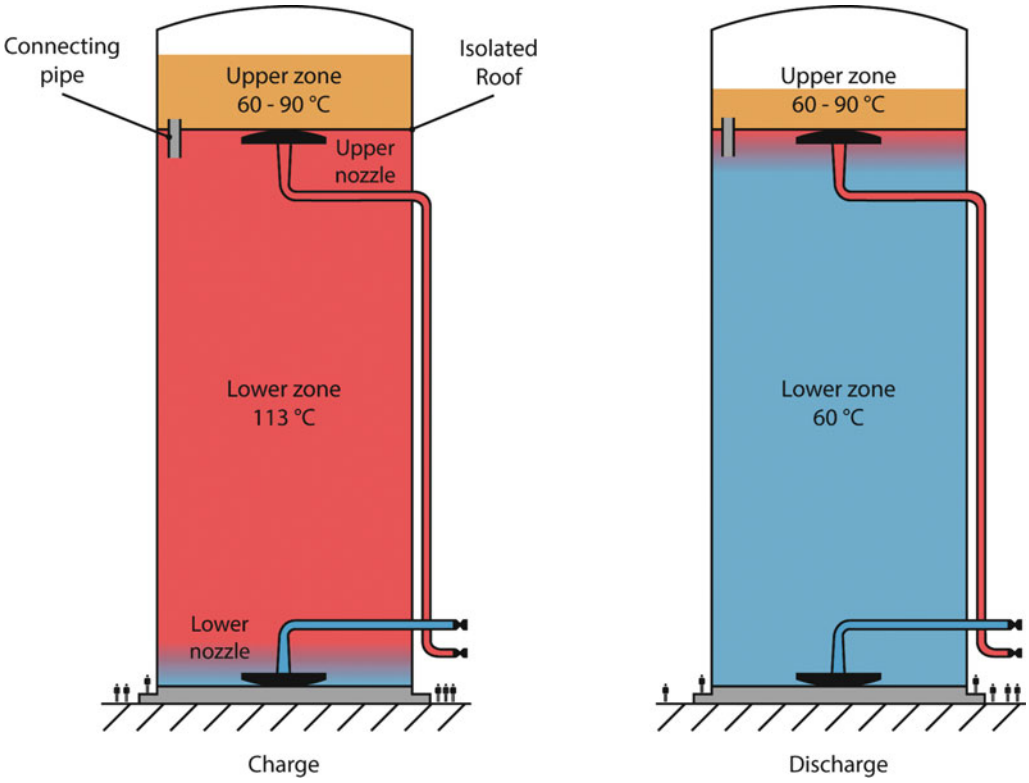



**Fig. 14.3** Principle of action of the thermal storage system in the Sandreuth heating plant with a thermal injection and withdrawal rate of 94 MW (source: adapted from N-Ergie Kraftwerke GmbH)

storage system of 94 MW and two electrode boilers of 25 MW each.

Prior to this, electricity generation had been rigidly coupled with heat generation. As a result, on the one hand, electricity produced from natural gas had been inefficiently fed into the electricity network at times when there was low power demand or an oversupply of renewable electricity, and thus led to low electricity prices. On the other hand, when electricity prices were high and the feed-in from renewable energy was low—for example, in summer—the heat-sink for the CHP plant was unavailable. Both these drawbacks can now be eliminated by the addition of the thermal storage system:

- When the demand for electricity is low, the power generation is restricted and the heat demand is covered by the thermal storage system.
- When the demand for electricity is high, the power generation is increased and surplus heat is buffered in the thermal storage system.

The thermal storage system was installed as an atmospheric two-zone storage system that has a storage capacity of 1,500 MW h with a maximum temperature of 113 °C. Evaporation of the water at temperatures above 100 °C in the lower zone inhibits the pressure of the 60–90 °C heated water in the upper zone. This type of installation is novel in Germany (Fig. 14.3).

The storage system was designed with a height of 70 m to be able to supply the district heating network with the necessary pressure even when the heating plant is switched off on weekends in the summer months. With a di-




**Fig. 14.4** Thermal storage system of the Sandreuth heating plant in Nuremberg for flexibilization of the CHP plant including PtH with a height of 70 m (source: N-Ergie Kraftwerke GmbH)

ameter of about 26 m, this produces a storage volume of 33,000 $m^3$ of water (Fig. 14.4).

As part of the PtH expansion, two Parat electrode boilers were also installed (Fig. 14.4) that are directly connected to the generator of the gas turbine to avoid emissions for end consumers. From the business perspective of the operator, this makes sense, yet from a macroeconomic perspective, it is not advantageous to use natural gas to generate electricity so that this electricity can be used to generate heat.

The primary purpose of the electrode boilers is their use in the negative secondary and minute-reserve market, which offers additional flexibility to the electricity supply system (▶ Sect. 13.1). The economic investment in this flexibilization with thermal storage and PtH amounts to about €17 million, of which 20% is funded by the CHP Act [42].

Figure 14.4 shows the dimensions of the thermal storage system in its environment. This large-scale thermal storage system was clad with a special facade made of trapezoidal sheets in order to harmonize its visual appearance with the skyline of Nuremberg. The grounds are equipped with a retaining wall to mitigate any leaks. The storage system was constructed piece by piece from steel parts in a special spiral assembly process. It has 50-cm thick heat-insulation (Fig. 14.4).

## 14.1.2 Integration of Electric Heat-Pumps Using Thermal Storage and Heating Networks

Heat pumps avoid the emissions associated with fossil fuel heating systems, provided they are operated using renewable energy.

### 14.1.2.1 Combination of Heat Pumps and Heat Sources

Low-temperature sources are required to operate heat pumps. Stored thermal energy can be drawn from the soil, water, or air and used for space heating and hot water. The heat source that is used determines the type of heat pump [8]:

- Soil: brine-to-water heat pumps with geothermal probe or geothermal ground collectors
- Water: water-to-water heat pumps that use ground water
- Air: air-to-water heat pumps with an absorber system for ambient air

The choice of heat source is highly-dependent on the geological conditions at a particular site and the available budget: the lowest operating costs with the greatest efficiencies are associated with brine-to-water heat pumps with geothermal energy probes; however, they also have the highest investment costs. In contrast, an air-to-water heat pump has low investment costs but also the highest operating costs, par-



**Fig. 14.5** Facade and 50-cm thick heat-insulation of the Sandreuth thermal storage system, added for flexibilization of the CHP plant and for use for PtH (source: N-Ergie Kraftwerke GmbH)

ticularly in winter when air with an external temperature of minus 10–20 °C is supposed to be used as a heat source. Geothermal energy with a constant temperature of plus 10 °C has the advantage here.

Geothermal probes and geothermal ground collectors are also used as thermal storage systems and are described in ▶ Sect. 10.4.2.

In ▶ Sect. 8.5.2, the principles of action of the various types of heat pumps are explained in more detail. Similar to gas-powered heat pumps, there are also electrically-operated compression heat pumps as well as absorption and adsorption heat pumps, which are simply referred to as electric heat-pumps below.

#### 14.1.2.2 Combination of Heat Pump and Solar Arrays or Photovoltaic Systems (PV Systems)

- **Coupling of Heat Pumps with Thermal Solar Arrays**

From a technical perspective, heat pumps can be easily combined with thermal solar arrays. This means that in summer, a large part of the hot water requirement can be covered. Similarly, in transition seasons, a part of the heating requirement can also be covered. Several possible uses are plausible here. A solar array can heat a hot-water storage system, which can also be charged by the heat pump when necessary. Space heating is provided solely by the heat pump in this case. The regulation of the heat pump is intended to prioritize the solar heat generation so that as little electricity as possible is needed. In summer, the hot water requirement can be covered solely by the solar array over several months.

There is also the option of connecting the solar-thermal array on the source side of the heat pump. The solar heat is thus used as either the sole heat source for the heat pump or as a supplement. In this case, solar energy in summer can contribute to regeneration of the soil, and the soil can be used as a heat source and thermal storage system [6].

The question remains here as to whether the additional investment costs for the solar array can be recouped by the efficiency gains of the heat pump. Because heat pumps themselves are a capital-intensive technology, a cost-effective system design also requires a relatively high load.

- **Coupling of Heat Pumps with PV Systems and Thermal Storage**

PV systems primarily generate electrical energy. Surplus solar electricity can be stored in electrical storage systems (i.e., batteries) or in thermal systems such as buffer storage systems. The latter storage option is possible by combining a PV system with a heat pump or a heating rod (PtH), which always has thermal storage available.

This combination can increase the profitability of the entire system because the on-site consumption of cheap solar electricity increases as a result of the requirements of the heat pump. Because heating energy requirements and solar radiation run counter to one another across the seasons, the effect is reduced primarily to providing hot water and secondarily to supplementary heating in spring and fall. As described in ▶ Sect. 4.5.2, a very large storage system relative to the shiftable electricity load is required for flexibilization of the heat pump due to its performance figures. Using on-site PV electricity generation, there is also an incentive to considerably increase the temperature of the thermal storage system, whereby the efficiency suffers because of larger temperature differences.

The potential for PV electricity to cover the heat demand without optimized use is between 10% and 30% for newly constructed plants, and between 5% and 20% for older plants. For heat pumps optimized for self-generated electricity, increases of about 15% can be achieved. In actual applications, greater increases are possible.

#### 14.1.2.3 Integration of Heat Pumps, Thermal Storage Systems, and Ice Storage Systems in Households, Businesses, and the Industrial Sector

- **Heat Pumps in Households, Businesses, and District Heating Systems**

Heat pumps are installed almost exclusively in individual buildings. Their use in recent years has declined because of increasing taxes and duties on electricity purchase costs, and their use is restricted to newly constructed buildings which are subject to different efficiency requirements as a result of the EnEV. In the commercial sector, a heat pump can also be used in summer for cooling, which improves cost-effectiveness and efficiency. In individual buildings, radiant floor heating and the building's mass can be used as thermal storage for the flexible use of the system (▶ Sect. 4.5.2).

Additional flexibilization options include thermal storage and the over-dimensioning of system output. The flexibilization measure that is currently standard as part of load-management is for the distribution system operator to switch off the heat pumps twice a day for three hours. This relieves stress on the distribution system. The first heat pumps will also be pooled in virtual power plants so that they can be used flexibly in the electricity market [7].

Households and businesses also dominate the district heating sector. In Denmark, a few networks already use large heat pumps, which are the next step in efficiency after electrode boilers. This is possible in Denmark because of the low inlet temperatures for district heating. In Germany, a reduction in the temperature of district heating is conceivable in principle over the long-term, and this may create additional application options while increasing the flexibility of heat pump operation [27].

- **Heat Pumps Combined with Ice Storage and Solar Arrays for Heat and Cooling Supply**

The use of ice storage systems combined with solar arrays, heat pumps, and thermal storage is also promising and is technically feasible at the moment, although capital intensive (◘ Fig. 14.6). Such systems are appropriate for households and larger building complexes. Ice storage systems use the latent heat of water for energy storage. It consists of one container with water and two heat exchangers. The container has a volume of several cubic meters and is usually embedded in the soil.

A special solar collector provides the building with space heating and hot water using a salt-to-water heat pump together with buffer storage. If the heat demand cannot be covered by the ambient solar heat, the heat pump draws heat from the ice storage system until the water is completely frozen. This phase-change is reversed when feeding into the ice storage system when surplus solar energy is used to melt the ice. In this way, solar energy can be saved over longer periods by freezing and melting the water [41]. As an alternative to using solar col-

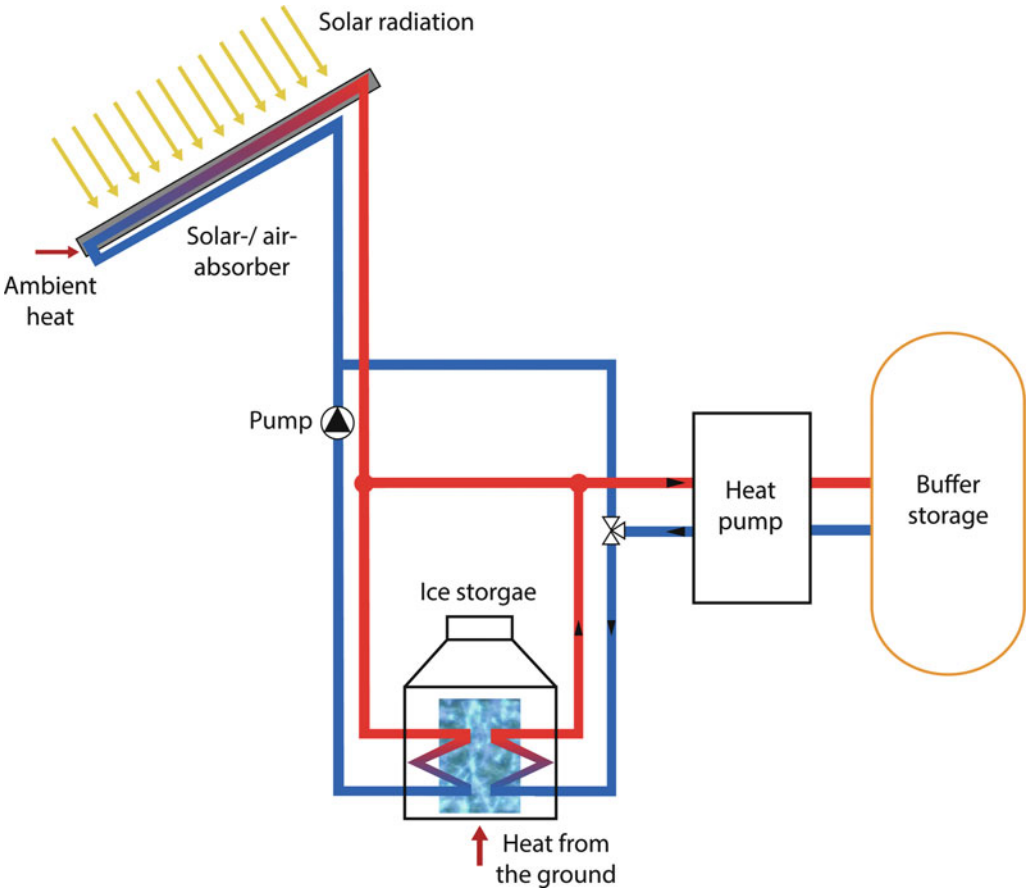



**Fig. 14.6** Combination of a heating and cooling system comprising of an ice storage system, solar array, heat pump, and buffer storage, adapted from [41]

lectors, the system can be operated solely with a PV system.

**How Much Latent Heat is There in 10 m³ of Water?**

When water is frozen, latent heat is released which can be used for heating purposes. Water is a highly suitable phase-change material (PCM) thanks to its very high enthalpy of fusion of 334 kJ/kg and easy handling. It has a density of 1 kg/L. Therefore, when 10 m³ of water is frozen or melted, this produces a storage capacity of 928 kW h:

$$\Delta Q_{\text{Water}} = m_{\text{Water}} \cdot \Delta h_{\text{S,Water}}$$
$$= 10{,}000\,\text{kg} \cdot 334\,\frac{\text{kJ}}{\text{kg}}$$
$$= 3{,}340\,\text{MJ} = 928\,\text{kW h}.$$

The quantity of energy corresponds to about 100 L heating oil with a heating value of 10 kW h/L.

Another advantage of this system is that it can be used for cooling systems and air-conditioning, which will become increasingly important as the effects of climate change are felt and the electricity network is placed under additional strain (▶ Chap. 3). Simply using a water cycle—without operating the heat pump—moves water through the ice storage system and starts to melt the ice. This cools the water down and transfers the cold through the existing piping system into the rooms of the house.

Ice storage systems are not a new technology but have been used since the start of the

20th century in dairies and breweries and have been discussed as an option for building air-conditioning [29].

- **Heat Pumps in the Industrial Sector**

On the one hand, there is a high demand for process heat of less than 100 °C in the industrial sector. On the other hand, there is major potential for industrial waste heat at a low-temperature level. Where both factors are present at a single site, large heat pumps lend themselves to improving the efficiency and cost-effectiveness of heat supply. The current state-of-the-art technology allows inlet temperatures of about 80 °C. Further increases, albeit small, are still technically possible [27].

## 14.1.3 Integration of PtH Using Thermal Storage and Heating Networks

The basic features of PtH are described in ▶ Chap. 4. This section deals with the integration of PtH in households, businesses, and the industrial sector. In this connection, a distinction must be made between the rapid growth in on-site power consumption and PtH from a system perspective.

### 14.1.3.1 Integration of PtH in Households and Businesses

- **Incentive for Self-Consumption of Electricity from PV Systems in Households**

It is becoming increasingly popular for the operators of PV systems to use the electricity they generate themselves. The renewable energy feed-in tariff for electricity fed into the network is still currently higher than the cost of procuring natural gas. In certain cases, however, it already makes economic sense for households to only feed their PV-generated electricity into the public grid once their electricity and heat demand is covered through maximum utilization of solar electricity. In such cases, small systems can be economical, even without a renewable energy feed-in tariff. Hot water demand can be covered using cost-effective hot water heat pumps with solar electricity. However, solar energy is not usually sufficient to also heat living spaces. The necessary long-term storage of heat for this purpose is still too expensive. In this case, supplemental heating can be provided by conventional heat generators.

- **Heating with PV for Self-Consumption**

There are several options available for utilizing the surplus electricity produced from PV systems, such as storing the electricity in batteries. Domestic battery storage is still quite expensive, however, and rarely cost-effective in Germany (▶ Sect. 14.1.4).

For this reason, exploiting surplus electricity from PV systems is of interest for hot water and supplemental heating because existing thermal storage systems with cost-effective heating rods can be retrofitted very easily, from a technical point of view (◘ Fig. 14.7). For this application alternative, a control and regulation unit is of critical importance as a supplement component to the PV system, thermal storage, and heating rods. An optional component is a domestic battery storage system. The microcontroller of the regulation unit measures the output parameters of the power inverter, battery storage, and electricity demand and controls the output electronics of the heating rod as required.

This regulation of the plant ensures that the electricity that is generated by the PV system is first consumed directly in the household itself to minimize the electricity drawn from the grid. Only when no electricity is required and when PV electricity is available is surplus (if any) stored in batteries for subsequent self-consumption, or converted into thermal energy using the heating rod or heat pumps in the thermal storage. This allows savings in fuel to generate heat, and also reduces costs and emissions. The potential of this technology is estimated to lie in the gigawatt range [31].

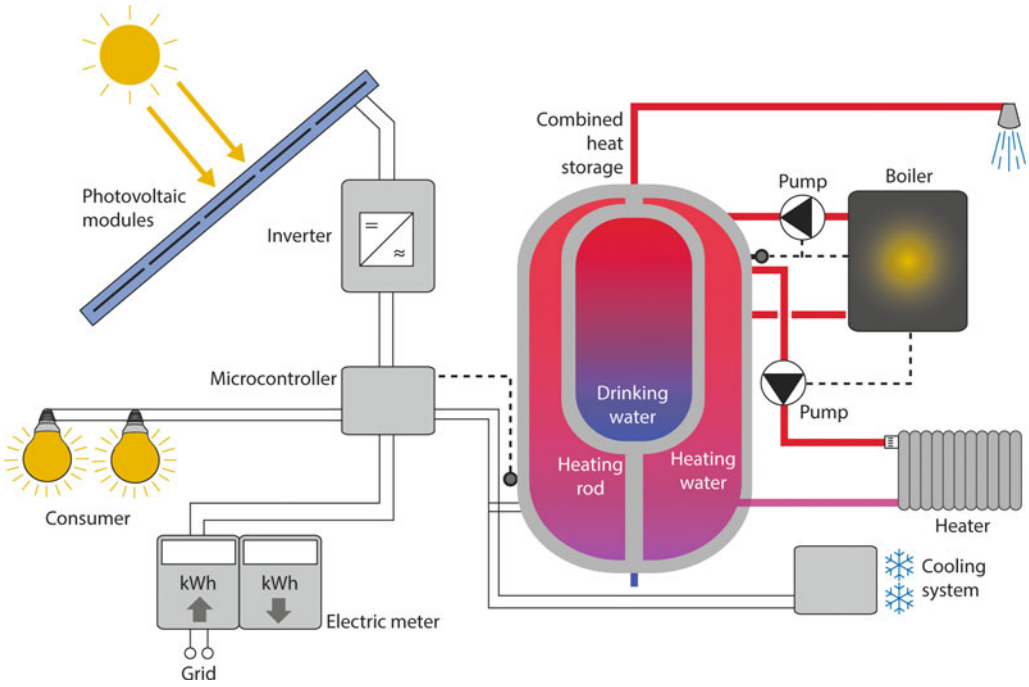



**Fig. 14.7** Schematic diagram of the integration of PtH in buffer storage systems in a household, adapted from [31]

### Photo-Thermal Energy as an Economical Use of Solar Electricity for Hot Water

PtH in the form of heating rods and heat pumps for the supply of hot water is of particular interest. A new term, photo-thermal energy, is introduced here, which is derived from the term solar-thermal energy.

**Definition**

Photo-thermal energy is the supply of heat for hot water and space heating using PtH (heating rods or heat pumps) that utilizes electricity generated by a PV system.

There are circumstances in which the supply of hot water using PV electricity and a heating rod or heat pump in connection with buffer storage is more cost-effective than using a conventional boiler or a solar-thermal system.

Photo-thermal energy has the following advantages over solar-thermal energy:

- Lower investment costs.
- Lower maintenance requirements.
- Power can be utilized for electricity, heat, and electro-mobility.
- Lower energy costs because, as well as providing hot water, the high costs associated with purchasing electricity are reduced.
- Less surplus energy in summer and, therefore, a greater utilization rate for solar energy.

For supplemental heating, however, solar-thermal energy can be more economical and beneficial than photo-thermal energy, particularly when the system's design incorporates a PV heating rod.

Photo-thermal energy is primarily cost-effective for supplying hot water from late spring and through the summer to early fall. What is critical in this case is the efficiency of the conventional heating system during this heating-free period. This efficiency is very low

when heating the daily hot water supply because the system only operates for short periods in partial-load operation, and in doing so, all components first have to be brought to operating temperature. Heating systems with high heating power can only achieve efficiencies of 35% when providing hot water only [39]. The following sample calculation shows the consequence of the efficiency:

**Example**

The renewable energy feed-in tariff for PV systems less than 10 kW in size was 12.35 ct/kW h in August 2015. The heating oil price at the same time was a low 58 ct/L incl. VAT or 5.8 ct/kW h with a heating value of about 10 kW h/L. Without taking into account the low investment costs for a heating rod and its control, the efficiency determines above which point producing hot water with solar electricity is more cost-effective than the feed-in:

$$\eta_{\mathrm{WW}} = \frac{5.8}{12.35} = 47\%.$$

The sale of solar electricity means that the operator of a PV system is considered a company. According to the current legal situation, this means that self-consumption is considered a benefit in kind, which must be treated as taxable for VAT purposes. Adversely, the legislature proposes that the basis used to calculate the value-added tax is the avoided purchased electricity, including pro-rata basic fees. With a net electricity price of 23 ct/kW h, the value-added tax that is payable per kW h is 4.37 ct, simplified without pro-rata basic fees. This means that the renewable energy feed-in tariff plus 4.37 ct/kW h is the threshold of cost-effectiveness. The efficiency of conventional heating systems that solely provide hot water would, therefore, have to be even worse for the use of photo-thermal energy to be economical.

$$\eta_{\mathrm{WW}} = \frac{5.8}{12.35 + 4.37} = 35\%.$$

However, this is only a snapshot at a point when oil prices were low and the renewable energy feed-in tariff was more than 12 ct/kW h. Both factors will certainly change in future.

Figure 14.8 shows a comparison of the cost-effectiveness of various solutions for providing hot water based on PVs and solar-thermal energy. The share of the electricity demand covered by solar is 60% for all solutions. Systems greater than 10 kW in size are not considered because the 2014 Renewable Energy Sources Act (Erneuerbare-Energien-Gesetz, EEG) has a reduced renewable energy surcharge for self-consumption, which reduces cost-effectiveness. When the solutions are compared to the feed-in of renewable energy only, we find the following:

- In the current market situation, solar-thermal energy is barely worthwhile.
- PVs for hot water, the self-consumption of electricity, and EEG feed-in have the best values in connection with larger systems.
- For smaller systems, a solely photo-thermal system is the most cost-effective option because there is no need to install a power inverter. Furthermore, the tax disadvantages of the renewable energy feed-in tariff and self-consumption of electricity are avoided.
- As the size of the PV system increases, unused surplus must be expected, just as for solar-thermal energy. For this reason, plants without renewable energy feed-in are no longer competitive.

### Design of PtH Systems for Hot Water in Households

The dimensioning and selection of the individual components are highly-dependent on the size of the PV system installed. Experience shows that a photo-thermal system can meet hot water demand over the course of a year. If the system is also to be used to heat living areas, the limits of its capacity will be reached. To provide both hot water and space heating requires a very large PV system, including overproduction in summer and seasonal-thermal storage with a water volume of up to 120 $m^3$. The volume of water storage necessary makes this option of little interest economically, and

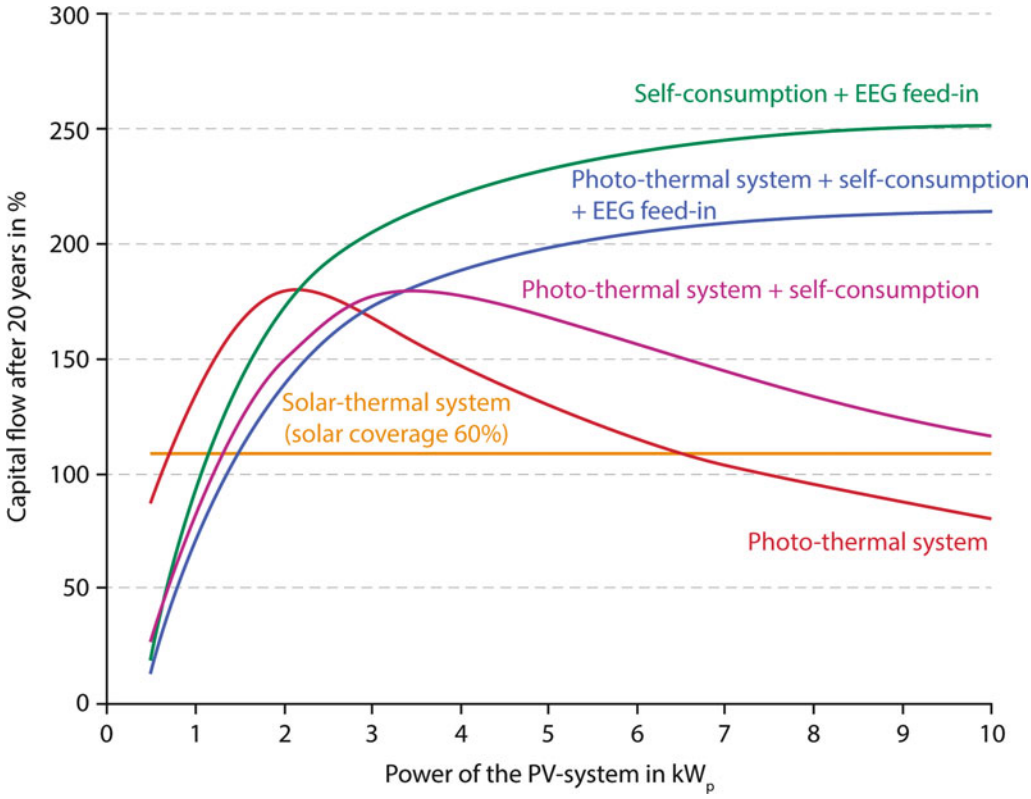



**Fig. 14.8** Economic comparison of various systems to utilize solar energy for hot water and electricity, depending on the size of the PV system, with a capital flow over a period of 20 years, adapted from [30]

it may also be unfeasible due to space limitations on site. One solution is to use a hybrid collector made up of a combination of PV and solar collectors to increase the efficient use of space. However, this option is expensive. The most cost-effective solution is a combination of a PV system and a heat pump instead of a heating rod to raise the utilization efficiency of the electricity. Such PV hot water pumps, including buffer storage, are available starting at €2,000.

### ■ PtH from a Total System Perspective

Like self-consumption, PtH has tremendous potential for integrating the surplus electricity produced from renewable energy sources (▶ Sect. 4.7).

The coupling of PV systems with heat generation can make financial sense for many homeowners, even if it appears inefficient from a macro-economic perspective, as long as directly utilized solar electricity can replace $CO_2$-intensive coal electricity. Nevertheless, electricity produced on-site is not considered surplus electricity from a network or market perspective. Furthermore, households consider such energy generation more valuable than electricity from the public grid, because it fosters energy-independence. With a view to the coupling of the electricity and heating sectors, the expansion of heat-driven PV and PtH in general will generate major interactive effects that will be relevant for thermal storage in the future.

Full coverage of the heat demand using PtH does not make sense, at least when using heating rods. This is because exclusively using electrical heating in winter would, in the worst scenario, lead to a large numbers of households

with simultaneous high demand, which would make network stability difficult to plan, increase peak loads, and thus unnecessarily push up the economic costs of covering peak loads (e.g., gas turbines).

For this reason, heating rods should only be used in households as supplemental heating (bivalent heating). For supplying heat for households there are other, in some cases more efficient, renewable energy alternatives such as heat pumps, wood heating, solar arrays, and gas-fired condensing boilers based on renewable natural gas.

There are also very promising applications in the industrial sector and in district heating, as well as in combination with efficient heat generation systems such as mini-CHPs when a minimal proportion of heat demand is covered by PtH.

### 14.1.3.2 Integration of PtH in Industrial Applications and Process Heat

#### ▪ PtH from an On-Site Power Supply Perspective

The incentives for industrial companies to generate electricity on-site using PV depends on the individual exemption rules. Energy-intensive industrial companies are exempt from many taxes and duties. Furthermore, unlike CHP, PVs cannot provide assured output so that grid access charges can be avoided. Accordingly, there is usually little incentive for direct heat generation using solar electricity. However, the situation is different for manufacturing firms or companies in sectors without reduced EEG surcharges as a result of the Renewable Energy Sources Act.

#### ▪ PtH from a Total System Perspective

The industrial sector has a high demand for high-temperature process heat. To meet this demand, there are very few technological alternatives apart from CHP systems and gas heating plants. Both applications can be combined with electric heating plants. This produces hybrid systems that can adapt extremely efficiently to the requirements of the electricity market when there is surplus electricity produced from renewable sources or gaps in supply.

From today's perspective, PtH on an industrial scale is only economically feasible in the balancing power market.

#### ▪ Incorporation of an Electrode Boiler into Existing Industrial Heating Cycles

The implementation of PtH in existing heating and steam cycles in the industrial sector will be described here by way of example. Electrode boilers are an established technology that can be used for this type of application. With the intelligent integration of electrode boilers into process heat systems, short-term power surpluses can be used to produce negative balancing energy in the form of hot water or steam, thus replacing fossil fuel energy.

The prerequisites for use in the balancing power market are suitable plant locations with heat-sinks that can be used year-round and a nearby connection to the electricity network that has adequate reserve electrical capacity.

Electrode boilers are the predominant technology used here (◘ Fig. 14.9). The following criteria are important when selecting the site:

- A prerequisite for the steam network is an ability to absorb 5–20 MW of saturated steam across the whole year into a non-critical part of the network where it can be put to meaningful use. The electrode boiler can supply hot water and/or saturated steam with a maximum pressure of 30 bar at a temperature of 230 °C and ramp up to full load within 30 s. Accordingly, the boiler could, in principle, also provide negative primary balancing power (PBP), but this is not yet accepted in the balancing power market. There are less stringent requirements for the secondary-balancing power (SBP) market: full power must be provided within 5 minutes and the available capacity must be specified on a weekly basis.
- For the power connection, there should be unused reserve capacity at the medium-voltage level, which is equal (at a minimum) to the 5 W capacity of the boiler (another




**Fig. 14.9** Design of an electrode boiler for industrial implementation of PtH

condition of the current balancing power market).

- Water treatment is also required for operation. The boiler requires water with a conductivity of 60 μS/cm (see the conductivity measurement of water in ▶ Sect. 8.1) for which a small dose of limestone is added at the start. The steam produced does not have any conductivity, meaning no further additives are required for ongoing operation. The non-vaporizing substances in the water can become concentrated, which is why some of the water must be repeatedly withdrawn from the boiler. The quality of the drinking water determines the level of this blowdown or elutriation.

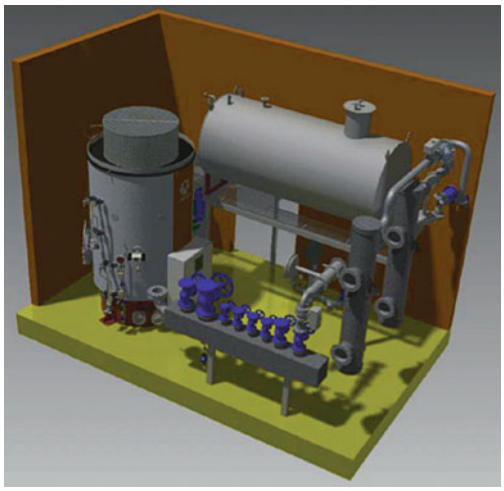


**Fig. 14.10** Schematic diagram of the construction of a PtH plant in the form of an electrode boiler for use in the balancing power market (source: Parat)

The total PtH system includes the following components (Fig. 14.10):

- Construction engineering: foundation, pipeline routes, etc.
- Electrical engineering: power transformer as required including transformer cell, MS switching station, medium- and low-voltage cabling, auxiliary power supply, cable routes, measurement and protection technology.
- Boiler technology: electrode boiler including peripherals such as heating cycle pumps, fittings and pipes on the boiler, safety valves, control cabinet, conductivity meter.
- Control engineering: measurement and control technology and instrumentation for the new system including emergency shut-down, status, and readiness signals.
- Hydraulics: connection of steam, water, and compressed air on the feed-water side to the existing plant, pipelines for heat retention for the boiler, overpressure valves, drainage, sampling including heat meter for steam generation and reference.

The Norwegian manufacturer, Parat, already has three different PtH systems operational or

in planning in Germany, all of which are used in the SBP market.

- Two 25 MW electrode boilers for a 70-m hot-water storage system for N-Ergie Kraftwerke GmbH in Nuremberg as part of the district heating network (▶ Sect. 14.1.1.2).
- Two 20 MW electrode boilers in the Infraserv GmbH industry park in Höchst near Frankfurt to feed into the 16-bar steam network at approximately 200 °C (stand-by: 12 bar, 200 °C; losses in stand-by due to insulation about 20 kW).
- Two 10 MW electrode boilers in a paper factory near Berlin.

### 14.1.4 Battery Storage vs. Load Shifting vs. Thermal Storage—An Example

**Why is the Coupling of the Electricity and Heating Sector so Critical for the Success of a Cost-Effective Energy Transition?**

To answer this question, we must consider the costs that arise when shifting a kilowatt-hour of electrical energy from one point in time to another. One obvious and easily understandable option is to use this kilowatt-hour to charge a battery and to discharge it at a later point. This option is examined in the first example below.

As an alternative to charging a battery, shiftable loads can draw more current and then store the final energy in the form of cold, such as in a refrigerator, for example. When the battery discharges, these loads would then not draw any current. The shift effect regarding the current is the same. This option is examined in the second example below.

Instead of feeding the electricity into a battery, the third alternative is to operate a heat pump, and then feed the heat that is generated into a hot-water storage system. When the battery is discharged, the heat pump is not operating and the building is heated with heat from the thermal storage system. Again, the shift effect regarding the current is the same. This option is examined in the third example. All of the examples are based on one storage cycle per day and an interest rate of 5%.

**First Case: Battery Storage**

With assumed investment costs of €350/kW h for a small lithium-ion battery with a service life of 20 years, this produces an annuity of:

$$\begin{aligned} A_{\mathrm{Bat}} &= K \cdot \frac{(1+i)^n \cdot i}{(1+i)^n - 1} \\ &= \frac{€350}{\mathrm{kW\,h}} \cdot \frac{(1+0.05)^{20} \cdot 0.05}{(1+0.05)^{20} - 1} \\ &= 28.1 \, \frac{€}{\mathrm{kW\,h\,a}}. \end{aligned}$$

With a maximum depth of discharge (DOD) of 80%, this gives the following costs for each temporally shifted kilowatt-hour $K_{\mathrm{v,Bat}}$ of:

$$\begin{aligned} K_{\mathrm{v,Bat}} &= 28.1 \, \frac{€}{\mathrm{kW\,h\,a}} \cdot \frac{\mathrm{a}}{365\,\mathrm{d}} \cdot \frac{\mathrm{d}}{1} \cdot \frac{1}{0.8} \\ &= 9.6 \, \frac{€\text{-ct}}{\mathrm{kW\,h}}. \end{aligned}$$

**Second Case: Load Shifting**

A recent study calculated the load shifting potential for a representative single-family dwelling that does not use electricity for heating and hot water as low; namely 2.14 kW h/d (refrigeration units, circulating pump, several household appliances). Investment costs are not available here for the storage capacity but the cost factors for communication technology, with only a small adjustable load, include a smart-meter (€300 in the pilot stage, later allocated on a pro-rata basis at €100) and in-house communication system (€100 in the pilot stage and €3 per terminal device with, e.g., Zigbee standard). With a service life of 25 years, this produces an annuity of:

$$\begin{aligned} A_{\mathrm{DSM,Pilot}} &= K \cdot \frac{(1+i)^n \cdot i}{(1+i)^n - 1} \\ &= (€300 + 3 \cdot €100) \\ &\quad \cdot \frac{(1+0.05)^{25} \cdot 0.05}{(1+0.05)^{25} - 1} \\ &= 42.57 \, \frac{€}{\mathrm{a}} \end{aligned}$$

or

$$A_{\text{DSM,Series}} = K \cdot \frac{(1+i)^n \cdot i}{(1+i)^n - 1}$$
$$= (€100 + 3 \cdot €3) \cdot \frac{(1+0.05)^{25} \cdot 0.05}{(1+0.05)^{25} - 1}$$
$$= 7.73 \frac{€}{\text{a}}.$$

This gives costs $K_{\text{v,DSM,Pilot}}$ or $K_{\text{v,DSM,Series}}$ for each temporally shifted kilowatt-hour of only:

$$K_{\text{v,DSM,Pilot}} = 42.57 \frac{€}{\text{a}} \cdot \frac{\text{a}}{365\,\text{d}} \cdot \frac{\text{d}}{2.14\,\text{kW h}}$$
$$= 5.45 \frac{€\text{-ct}}{\text{kW h}}$$

or

$$K_{\text{v,DSM,Series}} = 7.73 \frac{€}{\text{a}} \cdot \frac{\text{a}}{365\,\text{d}} \cdot \frac{\text{d}}{2.14\,\text{kW h}}$$
$$= 0.99 \frac{€\text{-ct}}{\text{kW h}}.$$

If the same calculation is carried out for a single-family dwelling with an electrical heating system, there are considerably higher shiftable quantities of energy available. The same study calculated these quantities to be 96 kW h/d [34]. For the same costs for the communication system, this produces costs in this case of $K_{\text{v,DSM,Pilot}} = 0.1\,€\,\text{ct/kW h}$ or $K_{\text{v,DSM,Series}} = 0.02\,€\,\text{ct/kW h}$.

**Third Case: Thermal-Energy Storage (TES)**

If heat is generated electrically, e.g., by using resistance heating or, more efficiently, using a heat pump, then storing heat in a hot-water storage system in order to discharge it at a later time, the costs for the storage system also drops. If costs of €800 are assumed for buffer storage with 300 L capacity, at a useable temperature difference of 55 K, the specific heat of water of 4.19 kJ/kg K and density of 1,000 kg/m$^3$, the specific storage costs would amount to:

$$e_{\text{Hot water}} = 4.19 \frac{\text{kJ}}{\text{kg K}} \cdot 55\,\text{K} \cdot 1{,}000 \frac{\text{kg}}{\text{m}^3} \cdot \frac{1\,\text{h}}{3{,}600\,\text{s}}$$
$$= 64 \frac{\text{kW h}}{\text{m}^3}.$$

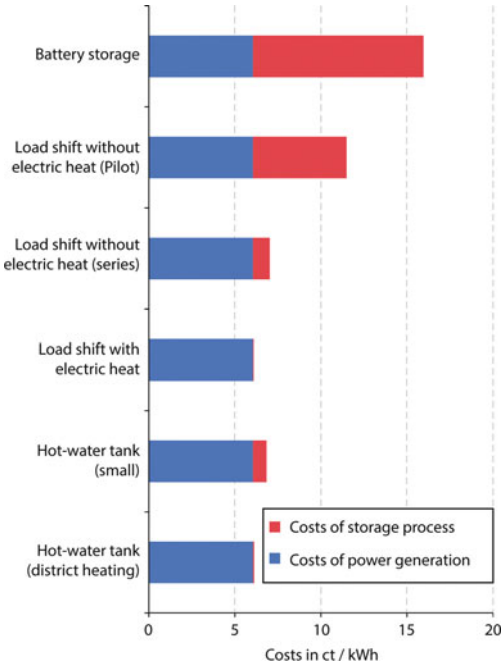



**Fig. 14.11** Comparison of the storage costs for different alternatives with and without coupling of the power and heating sectors using a household as an example

This gives specific storage costs of:

$$k_{\text{v,Hot water}} = \frac{€800}{300\,\text{L}} \cdot \frac{1{,}000\,\text{L}}{\text{m}^3} \cdot \frac{\text{m}^3}{64\,\text{kW h}}$$
$$= 41.66 \frac{€}{\text{kW h}}.$$

With a service life of 25 years also, this produces an annuity of:

$$A_{\text{Hot water}} = 41.66 \frac{€}{\text{kW h}} \cdot \frac{(1+0.05)^{25} \cdot 0.05}{(1+0.05)^{25} - 1}$$
$$= 2.96 \frac{€}{\text{kW h a}}$$

and costs $K_{\text{v,Hot water}}$ for each shifted kilowatt-hour of:

$$K_{\text{v,Hot water}} = 2.96 \frac{€}{\text{kW h a}} \cdot \frac{\text{a}}{365\,\text{d}} \cdot \frac{\text{d}}{1}$$
$$= 0.8 \frac{€\text{-ct}}{\text{kW h}}.$$

If the same calculation is carried out with large district heating systems with volumes of several

thousand cubic meters and considerably lower specific costs, the costs for the shifted kilowatthouyr $K_{v,Districtheat}$ are well below 0.1 € ct/kW h.

Figure 14.11 shows the importance of the coupling of power and heat, and thus its importance for cost-effective integration of renewable energy as a fundamental part of energy transition. Adjustments between electricity generation and power demand—that is, energy storage—is imperative. With assumed electricity generation costs of 6 € ct/kW h, electricity becomes many times more expensive after being stored in the battery, while this same process is barely noticeable when the power and heating sectors are coupled with TES. Even a considerable decline in the cost of battery storage systems does not change this fundamental fact.

## 14.2 Coupling of Power and Transport Sectors

Electro-mobility offers a range of possible solutions for coupling the power and transport sectors which will be discussed in more detail with examples below. Overhead line vehicles and electric rail transport are not considered in this context because they lack an integrated storage system, which means they do not help to balance mismatch between power supply and demand.

14

### 14.2.1 Electro-Mobility

Road-based electric vehicles are being discussed as a key solution for the development of sustainable mobility, in part because they enable the direct coupling of the power and transport sectors (▶ Chap. 5). However, it is essential that electric vehicles are intelligently incorporated into the energy system and that renewable energy is used to charge the vehicles.

#### 14.2.1.1 Drive Concepts

Figure 14.12 shows the essential alternative drive concepts which can be either partly or completely electrically operated. These include hybrid electric vehicles (HEV) with no external power connection, plug-in hybrid electric vehicles (PHEV), range-extended electric vehicles (REEV), pure battery electric vehicles (BEV), and fuel cell electric vehicles (FCEV). The individual concepts differ essentially in the different dimensioning of the electrical power train and the overall vehicle architecture.

Hybrid vehicles predominantly consist of a conventional combustion engine that is supplemented by an electric motor. The battery to drive the electric motor is charged by recovering braking energy (recuperation) and by the combustion engine while accelerating. In some instances, this allows short distances to be traveled using electricity alone. However, hybrid vehicles lack an external power connection to charge the battery. A battery vehicle, on the other hand, is operated solely by an electric motor that stores the energy required in the traction battery of the vehicle. The battery is charged through the electricity network and through braking energy recovery. PHEV and REEV are, in simplified terms, mixed forms of hybrid and battery vehicles that overcome the distance limitation associated with a pure battery vehicle.

The fundamental construction of a plug-in hybrid vehicle corresponds to that of a hybrid vehicle, but with a different component design and the possibility of charging the battery with an external power connection. In the case of REEV, the propulsion is purely electrical, but if required, a modified combustion engine is used to charge the battery. External charging of the battery is also planned, analogous to the plug-in hybrid. For FCEV, the power to drive the electric motor is generated directly in the vehicle by a fuel cell that converts energy stored chemically in the form of hydrogen into electrical energy.

The drive concepts described here differ with a view to vehicle architecture, component design, and fuels used. Accordingly, their broader adoption will have divergent repercussions on the power sector.

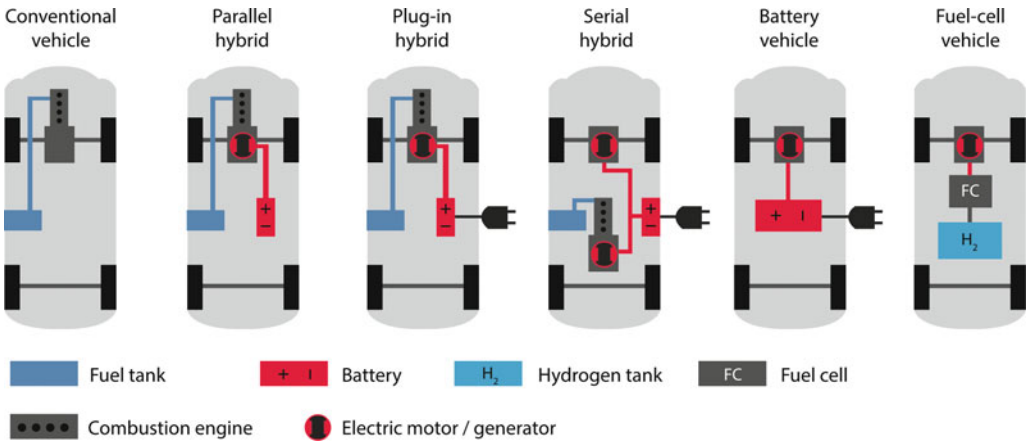



**Fig. 14.12** Summary of current and future key drive concepts in the automobile sector

As part of the National Electro-mobility Platform (an advisory board to the German government) a number of flagship projects have been established to analyze various issues and to prepare for the broader adoption of electro-mobility [26]. The issues to be analyzed include:

- Battery technology
- Propulsion technology
- Light-weight construction
- ICT and infrastructure
- Recycling
- Vehicle integration

Automobile manufacturers in the US, such as Tesla Motors, are approaching the development of electro-mobility progressively and are planning for production on a large scale. A decline in battery costs is expected as a result of such mass production.

### 14.2.1.2 Infrastructure and Charging Concepts

#### Infrastructure

The establishment of comprehensive and needs-based infrastructure to generate, store, and distribute alternative fuels will be a considerable determinant of the success of the particular fuel options.

The National Electro-mobility Platform envisages a total of 1.2 million charging points by 2020 to charge electric vehicles. Of these charging points, 85% will be in the private sphere, 9% in the semi-public sphere, and 6% in the public sphere. Over 7,000 charging points have been installed in Germany thus far [26]. There are a range of options here from a technical perspective:

- Conventional conductive charging using plugs and a charging cable
- Inductive charging using charging coils
- Changing the battery

Installing such infrastructure will be associated with major upfront investment costs as well as considerable ongoing operational costs. While the charging of electric vehicles by households is of course possible, charging infrastructure in the public sphere will also be necessary.

What should not be underestimated here is the electricity required to heat the charging columns to prevent the formation of condensation that could damage the electronics. The heating output can be up to 300 W per column, which adds up to 360 MW when summed up using 1.2 million charging points. A further disadvantage is the high cost of installation: the EU has suggested that 150,000 charging stations would be needed which would have a price tag of €750 million. The technology for billing the charging energy to the customer comprises the largest share of costs, but there are also costs associated with maintenance and repairs.



**Fig. 14.13** Electric vehicle charging with a mobile electricity meter in the charging cable on a light mast with integrated system socket. Source: Ubitricity GmbH, Robert Lehmann

There are a number of innovative concepts in this area, such as integrating the charging points into existing infrastructure. Furthermore, integrating the metering and billing technology into a special charging cable carried in the vehicle could reduce the infrastructure of the charging point to a minimum. The costs for the charging station would fall in this case to €500 instead of €5,000 for an on-site charging column. The additional charges for the special charging cable are about €100 according to the manufacturer and concept developer, Ubitricity [15].

Simple system sockets mounted on the wall or existing street lamps can be used as charging points. The latter concept has already been demonstrated in various cities such as Berlin (Fig. 14.13).

The charging strategies that would be used to couple the power and transport sectors are also crucial. Two possible charging strategies to connect electric vehicles to the energy supply system are presented below.

- **Unidirectional Charging**

The term unidirectional charging, also known as grid-to-vehicle (G2V), refers to the withdrawal of electrical energy from the electricity network with subsequent storage in electric vehicles. This strategy involves both controlled and uncontrolled charging. With uncontrolled unidirectional charging, the vehicle battery is charged directly when connected to the electricity network. By contrast, with controlled charging, a control signal indicates when charging should ideally take place. This allows charging to be preferred when renewables feed-in is high or delayed when there are grid bottlenecks.

- **Bidirectional Charging**

Compared to unidirectional charging, bidirectional charging (vehicle-to-grid—V2G) also feeds electrical energy from the vehicle battery back into the public electricity network. In this way, electro-mobility becomes a valuable electricity storage system for the power sector.

The implementation of V2G charging requires a communications and charging infrastructure designed specifically for this purpose. Ancillary services for the electricity network could also be carried out using the vehicles. This concept is purely theoretical at the moment because there is no corresponding business model and almost all suppliers of electric vehicles do not permit bidirectional charging or the access to the battery that is required for this process. This is because manufacturers fear the lifetime of the battery will be reduced by the additional stress and the external influence of the network operator and/or the customer.

#### 14.2.1.3 Possible Development of Electro-Mobility up to 2050

In the long-term, battery storage systems will enjoy ever greater rates of adoption. The key drivers of market growth for battery storage systems are electro-mobility and PV systems that use battery storage to increase on-site consumption.

The essential drivers for positive development are fixed $CO_2$ thresholds for vehicles and increasing electricity purchase costs for domestic customers and/or removal of the renewable energy feed-in tariff. Both applications (i.e., electro-mobility and PV with battery storage) will benefit from the fall in costs for battery storage.

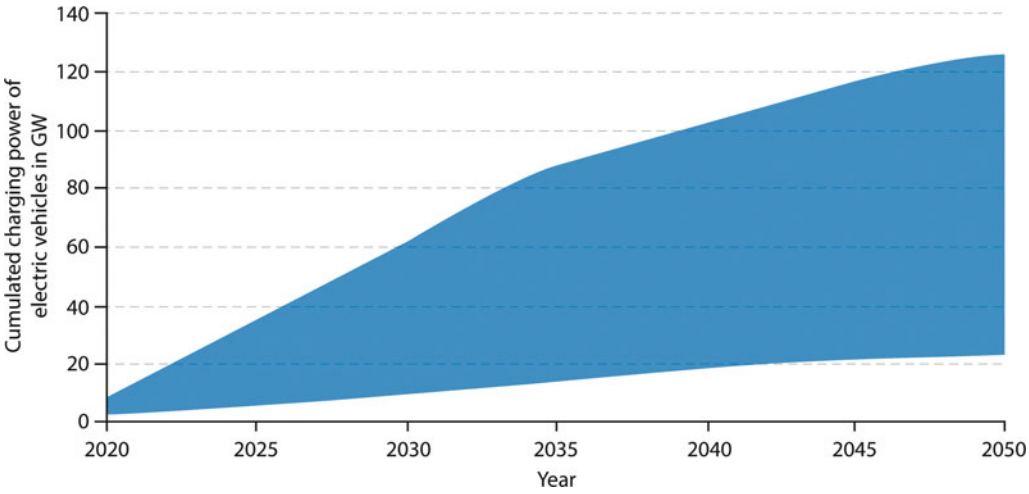



**Fig. 14.14** Possible development in the cumulative charging power from the electricity network for electric vehicles by 2050, adapted from [38]

Solutions to re-use old batteries in a productive way are also being explored. In collaboration with outside partners, Daimler has established the first battery power plant in Lünen near Dortmund based on discarded rechargeable batteries from about 1,000 Smart cars. The 13 MW power plant is being used to provide PBP to the grid. At the end of their serviceable life, the batteries are recycled by a company located on-site.

In the electro-mobility sector, the number of vehicles increased from about 4,000 in 2012 to about 16,000 in 2015. According to [38], the connected loads of battery-based electric vehicles will cover a range from a minimum of 23 up to 126 GW by 2050 (Fig. 14.14).

This assumes that the numbers of vehicles in Germany will be a constant 43.9 million by 2050. It is also assumed that the minimum connected load for every million electric vehicles is 3 GW.

The range indicated for the capacity in Fig. 14.14 is the result of various scenarios. The lower figure is based on the conservative assumption that the combustion engine will continue to dominate the market until 2050. The upper figure results from a scenario that assumes that the combustion engine will be completely driven out of the market by 2050. The rise in the numbers of electric vehicles will make the use of demand-side management (DSM) essential in the future.

**Example**

If there are 1 million electric vehicles on German roads by 2020 in accordance with the objective of the federal government, this will produce a connected load of about 3 GW with a storage capacity of 60 GW h, assuming a storage capacity of 60 kW h per vehicle. With vehicle numbers of 10–45 million, the connected load increases to 30–135 GW with a capacity of 600–2,700 GW h. It is expected that there will be an increase in the peak load in the evening hours at about 6:00 pm when commuters return home. If only 50% of the vehicles are connected to the network, this produces a power bandwidth of 1.5–67.5 GW.

The example shows that grid operators must consider the charging of electric vehicles in order to prevent excessive demand spikes and network overloads. For this reason, sensible infrastructure measures and charging concepts are required, as described in ▶ Sect. 14.2.1.2.

### 14.2.2 Electric Fuels

In addition to the direct use of electricity as an energy carrier for road transport, there is also the option of storing electricity in the form of chemical energy and consequently feeding this energy into the transport sector as a fuel. In this context, experts are discussing gaseous and liquid fuels as options for areas of the transport sector in which the direct use of electricity is difficult. Examples of the familiar storage concepts PtG and power-to-liquid (PtL) are discussed below in the context of the transport sector (see ▶ Sects. 8.6 and 8.7).

#### 14.2.2.1 HafenCity Hydrogen Fueling Station in Hamburg

Since mid-February 2012 the energy supplier Vattenfall has been operating a hydrogen fueling station in Hamburg. This system was constructed as part of the Clean Energy Partnership (CEP), a consortium of automotive, petroleum, energy, and technology companies that is focused on expanding hydrogen infrastructure. The project is funded by the national Hydrogen and Fuel Cell Technology innovation program run by various German ministries. The aim is to ensure the competitiveness of hydrogen and fuel cell technology [25].

Hydrogen can be centrally produced and distributed by pipeline or tanker. Alternatively, it can be produced and refueled on location in a decentralized fashion (▶ Sect. 5.3). Both approaches are implemented in Hamburg; about half of the hydrogen is generated directly at the fueling station using electrolysis. Certificates for renewable energy is purchased for the electricity drawn from the grid. The remainder is supplied externally. Hydrogen can be stored and refueled either in liquid form at very low-temperatures or in gaseous form at very high pressure. In Hamburg the hydrogen is stored in gaseous form at a pressure of 800 bar.

In 2013 seven fuel cell hybrid buses were operated using the fueling station by the Hamburg transit company Hochbahn (◘ Fig. 14.15). In addition to hydrogen fuel cells, the buses also have lithium-ion batteries that enable regenerative braking as well as providing additional energy for starting acceleration. A total of 1,435 L or 35 kg of hydrogen at 350 bar is used to fuel the buses. The efficiency of the fuel cell system is about 60%, which leads to a consumption of between 8 and 10 kg per 100 km [20]. Fuel cell vehicles (FCV) from different manufacturers are currently undergoing testing.

In a further expansion stage, a total of 20 line buses can be operated with a capacity of 750 kg per day.

#### 14.2.2.2 Methane Generation for Long-Distance Mobility in Lower Saxony

In the industrial PtG plant operated by Audi AG in Werlte, Lower Saxony, water treated in an alkaline electrolyzer is cleaved into hydrogen and oxygen (▶ Sect. 8.2). The three electrolyzers each have an electrical power of 2 MW, giving a total of 6 MW. The maximum 6.3 MW total power capacity is the result of the additional electrical loads needed to operate the system (◘ Fig. 14.16). The hydrogen that is generated is placed into intermediate storage in a storage system for up to one hour and then compressed to 10 bar for the subsequent methanation step [14].

The gas is converted to methane in a chemical methanation plant (◘ Fig. 14.17). The tube-bundle reactor operates as a fixed-bed reactor with stepped gas addition in normal operation at a pressure of 5–10 bar and a temperature range of 200–350 °C (▶ Sect. 8.3). In a single step process, a methane quality of > 90 vol% $CH_4$ is achieved using a nickel catalyst. The reactor is kept at operating temperature in stand-by and has a warm start time of 5–10 minutes. The pre- and post-rinsing of the reactor is carried out with inert gas; in stand-by mode it is filled with hydrogen. The educt-gases are desulfurized to remove any sulfur compounds that damage the catalyst. The product-gases are dried and prepared before being fed into the gas network. The reactor is thermally managed using wall cooling with molten salt as a latent-




**Fig. 14.15** Hydrogen fueling station HafenCity with the fuel cell and battery vehicle 'Sauberbus' (source: Hamburger Hochbahn AG)



**Fig. 14.16** Two of the three alkaline electrolyzers from McPhy Energy Deutschland GmbH, Berlin, each with 2 MW electrical connected load to generate hydrogen for methanation in the Audi e-gas plant in Werlte, Lower Saxony

thermal storage system and to use the waste heat to operate the biogas plant and the biogas purification plant, particularly for separating $CO_2$ from the raw biogas [14, 19].

Biogas from an adjacent residue biogas plant is used as the carbon dioxide source.



**Fig. 14.17** Chemical methanation plant to implement the Sabatier process for harvesting electric fuel in the Audi e-gas plant in Werlte (source: Audi AG)



**Fig. 14.18** Amine washes for biogas preparation in the waste biogas plant in Werlte. In this plant carbon dioxide is separated off from the biogas to be fed into the gas network as biomethane. The separated $CO_2$ is then used in the methanation plant in the Audi e-gas plant, source: Audi AG

The waste heat produced from the electrolysis and the methanation is used in the processing plant for sanitizing the residue biomass as well as separating the carbon dioxide in the amine washes (Fig. 14.18). Biogas can also be fed into the methanation reactor without any preparation [14, 19].

According to forecasts from the operator, the plant produces up to 1,000 t of methane each year, which can be fed into the natural gas network, stored, transported, and then used at a different site as an electric fuel for long-distance mobility. This quantity allows the refueling of about 1,500 Audi A3 Sportback g-tron, assuming each vehicle is driven 15,000 km annually (see Fig. 14.19 and [2]).



**Fig. 14.19** The renewable gas that is generated is used as fuel for long-distance mobility in Audi vehicles such as the A3 Sportback g-tron (source: Audi AG)

The project was the result of the development of PtG technology in Stuttgart and Kassel by ZSW Stuttgart, Fraunhofer IWES, and SolarFuel GmbH (now ETOGAS GmbH) (▶ Sect. 8.6). The world's first industrial PtG plant was established in 2013 by Audi AG together with the partners listed above and EWE AG, MAN Diesel & Turbo, and MT Biomethan GmbH. The accompanying research was funded by the German Environmental Ministry.

The plant was built with the aim of promoting carbon-neutral long-distance mobility and electro-mobility in general. Renewable $CO_2$ from the natural carbon cycle is used and renewable electricity is utilized to operate the plant. As part of the Audi e-fuels strategy, the production of ethanol and diesel from water, solar energy, and $CO_2$ using micro-organisms is also being investigated in a research facility in New Mexico [2].

### 14.2.2.3 Methanol Production for Gasoline Admixture in Iceland

A plant operated by Carbon Recycling International (CRI) in the city of Grindavik on the Iceland peninsula Reykjanes produces cost-effective methanol with the help of renewable energy (Fig. 14.20).

The George Olah carbon dioxide to renewable methanol plant is named after the winner



**Fig. 14.20** The George Olah carbon dioxide to renewable methanol plant operated by CRI in Grindavik, Iceland (source: CRI)

of the Nobel prize in chemistry, George Olah. It was constructed between October 2009 and late 2011 and opened in April 2012. The company operated a pilot plant in August 2007 that produced 1 L methanol per day [9, 10, 35].

Iceland is a special site in this regard because about one-third of its electricity is generated from geothermal plants and two-thirds from hydropower. The production of renewable methanol can be reproduced in a similar manner anywhere that has geothermal, wind, hydro, or solar energy available, and where $CO_2$ from the atmosphere is used.

The plant produces renewable hydrogen using the Icelandic power mix with alkaline electrolysis (AEL) for methanol synthesis. The methanation takes place at a lower temperature and lower pressure compared to steam-reforming; that is, the reactions take place in a low-pressure synthesis (▶ Sect. 8.3.3). The tube-bundle reactor used works with a nickel-based catalyst.

The plant generates 1.7 million liters of methanol per year in base-load operation from about 40 GW h geothermal electricity, which corresponds to an energy volume of about 8.7 GW h and a plant efficiency of about 22% [9, 10].

The production of the plant was ramped up in the fall of 2014 from an annual 1.7 million L methanol per year to 5 million L, which equates to about 2.5% of Iceland's fuel consumption [35]. Following expansion, the nominal electrical output of the electrolytic plant rose to 5 MW, and the plant now removes about 4,500 t of fossil $CO_2$ from the soil every year. In the EU member states, Norway, Iceland, and Switzerland, up to 3% methanol may currently be added to gasoline or E10. The limit in Iceland will be raised by 2020 to 10% [5]. The advantages or drawbacks of methanol and its properties are described in more detail in ▶ Sect. 8.4.2.

PtL is referred to as emission-to-liquid (ETL) in this plant because fossil $CO_2$ is converted to liquid fuels or key chemicals using renewable energy.

The pilot project in Grindavik will provide information about the distribution and logistics of methanol in Europe and Iceland. CRI will be constructing another plant in the near future which is aiming to generate up to 50 million L methanol for the European region [9, 10].

#### 14.2.2.4 Diesel Production Using Fischer-Tropsch Synthesis in Dresden

As part of the 'Sunfire' project funded by the German Ministry of Education and Research (Bundesministerium für Bildung und Forschung, BMBF), a total of ten partners worked together between 2012 and 2015 to realize PtL technology using high-temperature steam electrolysis. The most important results of the project are:



**Fig. 14.21** HTES in the Sunfire PtL plant in Dresden (source: Sunfire GmbH)

1. Development and operation of the first steam electrolysis prototypes with an electrical input power of about 10 kW working under up to 30 bar pressure. This corresponds to a hydrogen output of a little over 3 $m^3$/h. The steam is generated by using the waste heat from the Fischer-Tropsch synthesis and the efficiency of the process can be increased to about 65–70%.
2. Construction and operation of a PtL plant that can produce one barrel (159 L) of Fischer-Tropsch raw product per day using $CO_2$ and $H_2$. The Fischer-Tropsch synthesis is carried out at about 20 bar and a temperature range of 200–230 °C in a tube-bundle reactor. Cobalt is used as the catalyst. The reactor is thermally managed using boiling water cooling, which in turn provides the steam for the steam electrolysis (see point 1).

In addition to the problems associated with developing the individual components (RWGS conversion and steam electrolysis under pressure, see Fig. 14.21), a fundamental challenge was to link the various components to each other and to balance continuous process technology as part of flexible output operation. The theory behind the technology and the interaction of the two components is described in detail in ▶ Sect. 8.7.

The key data for the plant are as follows:

- Project name: Sunfire Fuel 1
- Electrical power: 190 kW
- Fuel production $CH_2$ (diesel): 9 kg/h
- $CO_2$ source: tank with green $CO_2$ and validation of the Oxyfuel $CO_2$ from the Vattenfall power plant site 'Schwarze Pumpe'
- Charging technology: high-temperature electrolysis (HTES, ▶ Sect. 8.3)
- Storage technology: fuel tank
- Withdrawal technology: vehicles in road transport and chemical raw materials in refineries

The plant was commissioned in November 2014 by the Minister of Education and Research, Johanna Wanka. In April 2015 the Minister's official car was refueled with the first liters of the Fischer-Tropsch fuel derived from $CO_2$ and $H_2O$. A range of tests, including some conducted by Audi AG, indicated that the quality of the fuel corresponded to the high quality of Fischer-Tropsch products.

At the same time that the Fuel 1 plant was being commissioned, Sunfire GmbH developed a reversible fuel cell (▶ Sect. 8.2.5) for the US company Boeing with 120 kW electrolysis input power. The plant was successfully tested in July 2015. In addition to demonstrating the feasibility of the reversibility on an industrial prototype scale, this development primarily



**Fig. 14.22** Reverse water-gas shift reactor in the Sunfire Fuel 1 test plant for producing electric fuels using Fischer-Tropsch synthesis via PtL (source: Sunfire GmbH)

demonstrated the scalability of the technology. Figure 14.22 shows the reverse water-gas shift reactor in the Sunfire Fuel 1 plant.

## 14.3 Coupling of the Power and Gas Sectors: PtG

### 14.3.1 PtG in the Context of the Energy Supply System

#### 14.3.1.1 PtG as an Interface Between Energy Sectors

Over the last 15 years, the proportion of renewable energy making up the German power supply has risen dramatically. In the future, wind power and PVs will play a pivotal role in this mix. While they have the greatest potential of all forms of renewable energy, they are also plagued by the largest fluctuations and are highly-dependent on the weather. Wind power and PVs alone are therefore not capable of ensuring high security of supply. Ensuring security of supply will depend on many factors as the feed-in from renewables increases, including the construction of power plants with flexible modes of operation, effective load-management, grid expansion, and energy storage. PtG is one of the most promising technologies because gas has the largest available storage capacity in Germany and the existing gas infrastructure can be readily integrated (▶ Sect. 8.6).

By coupling energy networks and systems in the electricity, heating, and transport sectors, PtG can help to stabilize the supply of energy while mitigating other problem areas, such as the trade-off between food or fuel that is associated with biofuels. PtG can also make the production of raw materials for the chemical industry a renewable process using power-to-chemicals (PtC).

■ **Brief Description of PtG**

PtG, windgas, or e-gas (electric renewable gas) all refer to technical processes for mimicking natural photosynthesis in plants [36, 37]. Plants developed photosynthesis over millions of years to enable the storage of energy over long periods. Despite its efficiency of about 1%, which is relatively low compared to energy technology, photosynthesis has proven successful in evolution. Using solar energy, carbon dioxide ($CO_2$) and water ($H_2O$) are converted in two steps to carbohydrates ($C_6H_{12}O_6$) with oxygen ($O_2$) being released in the process (▶ Sect. 1.1).

The first step, the cleavage of water, is mimicked in PtG using electrolysis. Several types of electrolysis are theoretically possible, including alkaline, membrane, pressure, and HTES. All three procedures still require further research and development to deal with the issue of intermittent conversion using renewable energy (▶ Sect. 8.2).

During the second step of photosynthesis, hydrogen reacts with carbon dioxide, which is ideally removed from the atmosphere. Unlike plants, PtG generates methane ($CH_4$) as its final product. There are currently two possible processes available for methanation: chemical and biological methanation. Biogenic and fossil energy pathways are used as $CO_2$ sources (▶ Sect. 8.3).

The hydrogen that is generated can be fed directly into the natural gas network depending on the site of the plant and the flow-rate at the

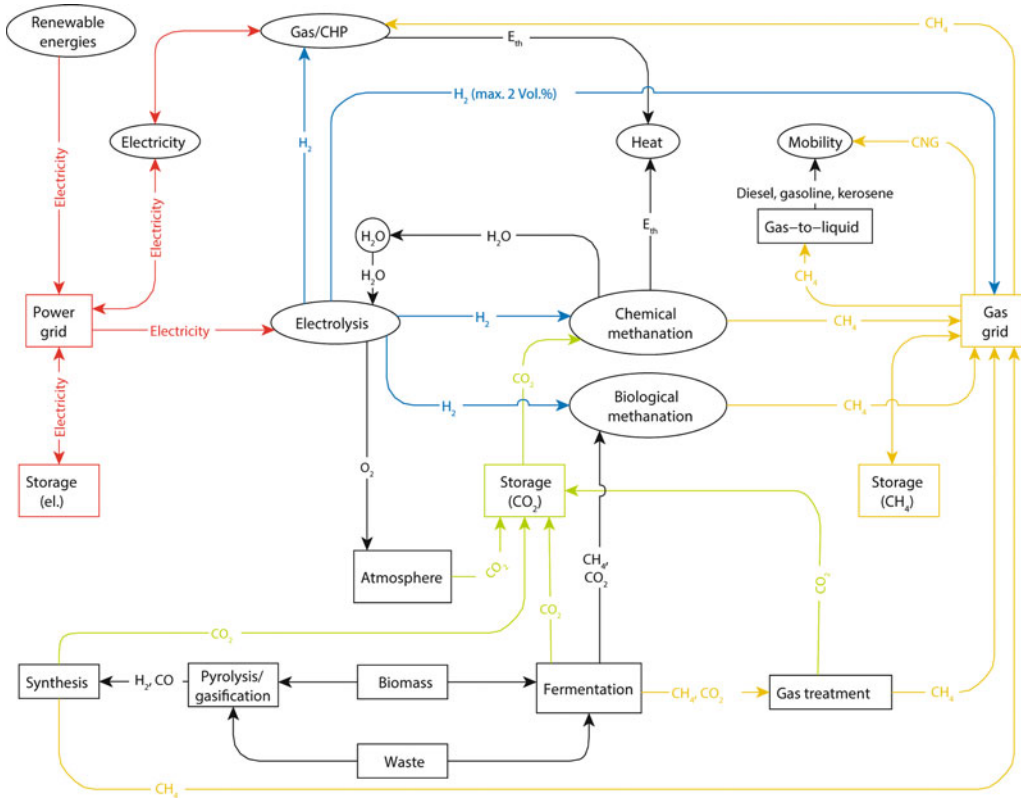



**Fig. 14.23** Multi-functional integration options for PtG in the energy system. Electricity, heating, and transport sectors are coupled together

node point while adhering to current hydrogen feed-in limits [18].

14

## Diverse Integration Options for PtG for Coupling the Energy Sectors

For coupling the electricity and gas networks in the energy system, the following options are currently available (Fig. 14.23):

- Hydrogen or methane are generated with (surplus) energy from the electricity network using electrolysis and an optional methanation process.
- Depending on the application, carbon dioxide (e.g., from gas processing in sewage and biogas plants or from the atmosphere) can be fed into the cycle, which provides a beneficial use for the $CO_2$.
- Large quantities of this energy can be stored temporarily in the gas network and accessed later in a manner that is decoupled from the electricity network.
- The path towards greater mobility is possible using the gas network, meaning that the power and transport sectors can be coupled (▶ Sect. 14.2.2).
- By reconverting the gas to electricity in thermal power plants (e.g., gas turbines, combined cycle technology power plants, CHP plants) or fuel cells, the utilization moves in the opposing direction. As a rule, additional heat is released, which in turn enables coupling to the heating sector (▶ Sect. 14.1).

### 14.3.1.2 Opportunities, Risks, and Framework

#### Risks Associated with PtG

The technologies behind PtG, electrolysis, and methanation are well-established. However, the changed demands placed on energy technology in combination with the expansion of renewable energy have created a need for new innovations and cost-reductions. It would also be expedient to integrate the technology into the goals and implementation plans of the clean-energy transition in its early stages so that the technology can be refined in terms of cost-reductions while also ensuring expectations remain realistic [28].

Another risk associated with this technology is the *greenwashing* of conventional energy generation. The $CO_2$ source for methanation is irrelevant for the carbon footprint of the PtG process, which is climate-neutral in and of itself. Nevertheless, PtG should not be considered to be a sink for emissions from fossil power plants because the emissions ultimately remain with the user of the fossil fuel and, even after carbon capture and use (CCU), the $CO_2$ returns to the atmosphere when the product is combusted [36].

There is also a risk that chemical energy carriers such as coal will be used to generate electricity that is then used to create another stored energy carrier such as hydrogen or methane. While this use of PtG technology would be highly counterproductive in relation to environmental goals, it would also produce high-energy losses, meaning it is unlikely to be cost-effective. A similar risk exists with regards to the upgrading of nuclear power using PtG. In the heat market it makes more sense in these cases to convert the electricity from conventional generation to heat directly via PtH in a heating rod. Aside from these PtG variations, numerous efficient and renewable heat supply concepts are available.

#### Opportunities Associated with PtG

The risks mentioned above are, however, contrasted by a range of opportunities. For one, the existing natural gas infrastructure, including pipelines, storage systems, power plants, CHP systems, furnaces, heating systems, and vehicles, can generally be operated unchanged with methane and to a limited degree with hydrogen, with no need for major conversions.

Similar to the power network, the gas network offers enormous existing and technically proven storage capacities. In the heating sector, wind-based PtG could provide up to 50% of German households with a climate-neutral energy carrier. A heat supply system based on PtG is a technically practical option for renewable heat supply (without the risk of monocultures, as may be the case with biogas), particularly for rented homes where renters cannot convert the heating system or install insulation. Ideally, CHP plants should be used to generate heat from windgas [37].

The transport sector can also use methane from renewable energy sources as a carbon-neutral energy carrier. This will expand vehicle ranges (thanks to its high-energy density) while also reducing the pressure on food production that results from biofuels. Lastly, this technology can minimize the import dependencies associated with natural gas and the transport bottlenecks in the power sector. The transmission capacity of gas in pipelines compared to electricity in overhead lines is about one order of magnitude higher. If the gas network is used like the electricity network as a transmission network, network bottlenecks and the costs of redispatch can be reduced.

#### Legal Framework for PtG

If the legal framework is intelligently implemented and misuse is avoided, the advantages of the technology will prevail, and PtG, including the links it creates between the power and gas networks, can develop into a cornerstone of clean-energy transition.

If the charging technology PtG is used to optimize the use of power plants, it stabilizes the most cost-effective form of energy in the merit order of the power market, which at present is predominantly electricity derived from lignite coal. Likewise, electricity purchased for PtG plants from the balancing power

market is, by definition, stored as 'gray power'. In both cases, considering the current power mix, the carbon footprint of the gas that is generated is more negative than that of fossil natural gas, thus obviating an essential component of its macro-economic and environmental benefit (▶ Chap. 2). The current practice of using green power certificates to trace accountability does not eliminate this dilemma either, because the generation of renewable electricity is both temporally and spatially separated from the storage, and therefore does not alleviate network congestion, nor does it contribute to the necessary integration of fluctuating renewable energy. This is an underlying problem for all flexibility options, and not only for PtG.

A core aim of the PtG concept is to enable the storage of surplus fluctuating renewable energy, such as wind and solar energy, in order to alleviate mismatches between supply and demand [33, 36]. The full economic and environmental benefits of PtG will only be achieved if the technology is harnessed in line with this aim. Exemptions from regulatory surcharges should be linked to these criteria and to operations that are beneficial to the energy networks.

To ensure that only surplus power is processed in PtG rather than a stored chemical energy carrier, the electricity price for the PtG plant should be less than the marginal costs of the most cost-effective fossil power plant in the merit order [21, 22].

The price for surplus electricity can be shaped by supply and demand in accordance with the same principles as the energy-only market (EOM). The supply is formed by cheap surplus electricity from renewable energy that costs less than the marginal costs associated with fossil power plants. The demand is generated from PtG plants and other flexibility options such as PtH, load-management, flexible power plants, flexible CHP plants, or short-term storage systems that compete for cheap surplus electricity on a technology-neutral footing. The technology-neutral design of this market for surplus electricity is important to ensure that the negative economic effects can be avoided (such as an increase in greenhouse gas emissions from the electricity sector resulting from technology-specific preference for a more inefficient and more cost-intensive technology). Whether such a market function for flexibility should also be implemented in the existing EOM must be discussed [21, 22].

If the use of the energy takes place in a sector other than the electricity sector (heating, transport, and the industrial sector), then PtG represents an end customer from the perspective of the electricity sector, and grid operators should take advantage of this fact when performing load-management. PtG only acts as an electricity storage system if the stored energy is supplied to the electricity sector in a system that converts gas to power. This reconversion to electricity can take place in various ways (e.g., gas-fired power plants, CHP, or fuel cells).

In the short- to medium-term, it makes sense to allow exemptions to end customer charges using a suitable reduction that requires certain criteria to be met so that a market can mature and the technology can be tested, even if PtG does not act as an electricity storage system.

In the long-term, PtG must be appropriately incorporated in the costs of decarbonization of other sectors. If electricity becomes a primary energy source and aids other sectors, such as the heating and transport sectors and the chemical industry in their decarbonization process, and these sectors benefit economically to a suitable degree from this, the electricity sector should not bear the costs alone. Instead, the costs and benefits should be equitably distributed across all those sectors that benefit.

## 14.3.2 Development of PtG in Germany and Neighboring Countries

### 14.3.2.1 Summary of the Development

PtG is an essential part of energy transition and also in terms of providing future long-

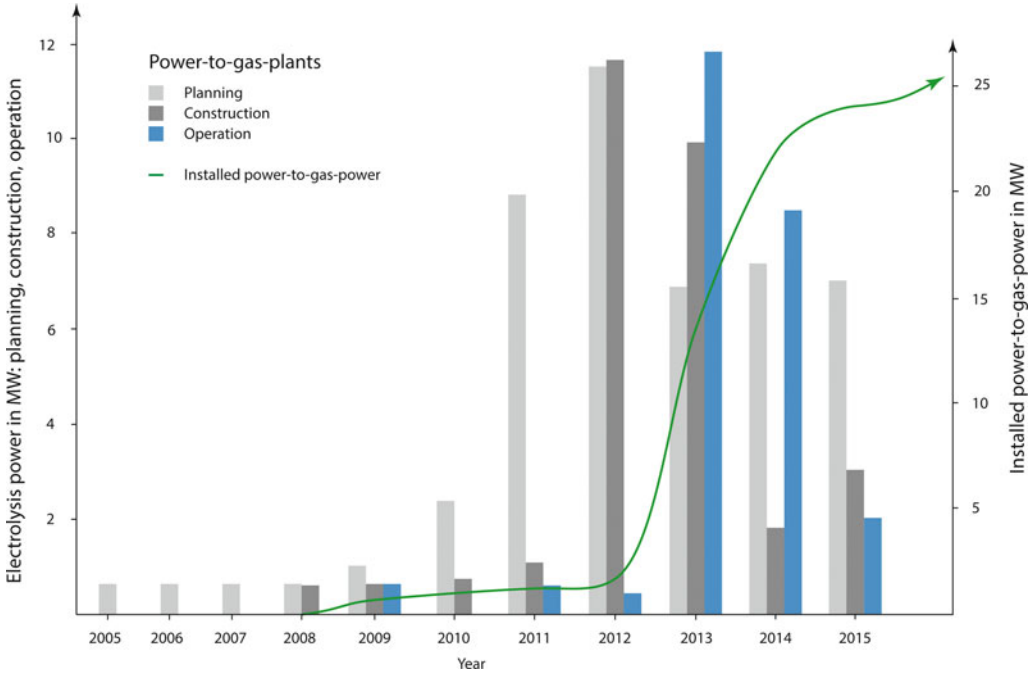



**Fig. 14.24** The development of PtG plant capacity in Germany: cumulative capacity of the plants that were in planning, under construction, or commissioned in the particular year, as well as the cumulative installed capacity over time. (Source: Enertrag AG)

term storage needs (▶ Chap. 2), to supply gas heat pumps and CHP plants with renewable gas (▶ Chap. 4), and to replace energy-dense fuels and raw materials in the chemical industry (see ▶ Chaps. 5 and 7).

To make this technology fit for a broad range of energy technology applications in the near future, there have been a number of projects running over the last decade, as highlighted in the summary of PtG pilot plants in Germany in Fig. 14.24 and Table 14.1. Plants have also been set up in Austria, Spain, France, Italy, Denmark, Argentina, the US, and South Korea.

### Development and Plants up to 2015

The subject of the hydrogen economy has long been discussed. In 2005 Enertrag came to the conclusion that a chemical energy carrier such as hydrogen is the only industrial option for long-term storage in Germany. The company consequently started planning a hybrid power plant in Prenzlau, which has been in operation since 2011. The concept of linked methanation and feeding into the existing gas network was added in 2009, which also, as a result of the reactor catastrophe in Fukushima, led to a breakthrough in 2011 in PtG technology in science and research [36]. In 2011 just under 20 MW of PtG capacity was in planning, with the installed electrolysis output in the pilot plants for this technology set to rapidly increase to about 13 MW by 2013. The installed electrolysis capacity in PtG projects was just under 25 MW in 2015 (Fig. 14.24). Table 14.1 shows a (by no means exhaustive) summary of the most relevant PtG projects. One reason behind the flattening of the trend in PtG expansion from 2014 onwards is that the major projects that started in 2011 onwards are currently gathering information. In addition, the current unstable regulatory framework means that large project volumes are being held back.

**Table 14.1** Summary of selected completed, ongoing, and planned PtG projects around the world as of the start of 2016. Other major EU projects are in planning (adapted from [11, 12])

| Project and site | Company and partners | Date of commissioning, project start | El. power in kW | $H_2$ production rate in N $m^3/h$ | $CH_4$ production rate in N $m^3/h$ |
|---|---|---|---|---|---|
| Argentina | | | | | |
| Hychico, Comodoro | Hychico | 2008 | ND | 120 | – |
| Denmark | | | | | |
| P2G-Foulum, Foulum | E.ON, Erdgas Zürich, Elektrizitätswerk der Stadt Zürich (EWZ), NEAS, Aarhus University, Danish Energy Agency (EUDP) | 2013 | 250 | 50 | – |
| BioCat, Copenhagen | Electrochaea.dk ApS, Audi AG, Hydrogenics Europe, BIOFOS, HMN Gashandel, NEAS Energy, Insero Business Services | 2016 | 1,000 | 200 | 50 |
| Germany | | | | | |
| BioPower2Gas, Allendorf (Eder) | MicrobEnergy GmbH (Viessmann), EnergieNetz Mitte GmbH, EAM EnergiePlus GmbH, Ingenieurbüro CUBE Engineering GmbH, Institut dezentrale Energietechnologien (IdE) gGmbH, Jühnde bioenergy village | 2015 | 300 | 60 | 15 |
| Methanation am Eichhof, Bad Hersfeld | Fraunhofer IWES, ZSW Stuttgart, SolarFuel GmbH, ETOGAS | 2012 | 25 | 6 | 4 |
| H2BER, Berlin | Total, Enertrag, Linde AG, McPhy Energy, 2G Energietechnik | 2014 | 500 | 230 | – |
| PtG Berlin-Schöneberg | NBB netzgesellschaft Berlin Brandenburg GmbH & Co. KG | 2014 | 7 | 1 | – |
| Hydrogen Research Center Cottbus | Enertrag, Total, Vattenfall, Deutsche Bahn | 2012 | 145 | 30 | – |
| PtG Emden | Emden/Leer University of Applied Sciences | 2013 | 312 | 60 | 14 |
| Etzel hydrogen cavern storage | IVG Caverns GmbH | 2013 | 2,000–6,000 | 1,000 | – |
| WindGas Falkenhagen | E.ON Gas Storage GmbH, E.ON edis AG, E.ON New Build & Technology GmbH | 2015 | 2,000 | 360 | – |
| Strom-zu-Gas, Frankfurt/Main | Thüga | 2014 | 300 | 60 | – |

**Table 14.1** (Continued)

| Project and site | Company and partners | Date of commissioning, project start | El. power in kW | $H_2$ production rate in N $m^3$/h | $CH_4$ production rate in N $m^3$/h |
|---|---|---|---|---|---|
| Germany | | | | | |
| H2Move, Freiburg | Fraunhofer ISE | 2012 | 16 | 6 | – |
| RH2-WKA, Grapzow | WIND-WASSERSTOFF-projekt GmbH & Co. KG, National Organization for Hydrogen and Fuel Cell Technology (NOW), HaasEngineering, Architekturbüro Karten Klünder, Hydrogenics, Senergie GmbH, Drehpunkt | 2013 | 1,000 | 210 | – |
| Hydrogen fueling station HafenCity in Hamburg | Vattenfall Europe AG | 2013 | 850 | 180 | – |
| PtG Hamburg-Reitbrook | E.ON Gas Storage GmbH, E.ON Hanse AG, Hydrogenics GmbH, SolviCore GmbH & Co. KG, Fraunhofer Institute for Solar Energy Systems (ISE), German Aerospace Center (DLR) | 2014 | 1,000 | 265 | – |
| H2Herten, Herten | AHG mbH | 2013 | 280 | 30 | – |
| Ibbenbüren pilot plant | RWE Deutschland AG, CERAM HYD, Westnetz GmbH | 2013 | 150 | 20 | – |
| HELMETH, Karlsruhe | Karlsruhe Institute of Technology (KIT), Polytechnic University of Turin, Sunfire GmbH, European Research Institute of Catalysis, Ethos Energy, National Technical University of Athens, Deutscher Verein des Gas- und Wasserfaches e. V. | 2016 | 30 | – | 3.9 kg/h |
| Mainz Energy Park | Stadtwerke Mainz AG, Linde AG, Siemens AG, RheinMain University of Applied Sciences | 2014 | 6,000 | 1,000 | – |
| $CO_2$RRECT, Niederaußem | Bayer Technology Services, Bayer Material Science, RWE, Siemens | 2013 | 300 | 50 | 1.25 |
| Hybrid power plant, Prenzlau | Enertrag AG, FH Stralsund, TU Braunschweig, German Hydrogen and Fuel Cell Association | 2011 | 600 | 120 | – |
| Power gap filler, Reußenköge | GP Joule, H-Tec Systems | 2015 | 200 | 40 | – |
| PtG am Eucolino, Schwandorf | MicrobEnergy GmbH | 2013 | 108 | 21.3 | 5.3 |

**Table 14.1** (Continued)

| Project and site | Company and partners | Date of commissioning, project start | El. power in kW | $H_2$ production rate in N $m^3$/h | $CH_4$ production rate in N $m^3$/h |
|---|---|---|---|---|---|
| Germany | | | | | |
| Microbial methanation, Schwandorf | MicrobEnergy GmbH, Zweckverband Verbandskläranlage Schwandorf Wackersdorf | 2015 | 275 | 30 | 7.5 |
| Biogas booster, Straubing | MicroPyros | 2014 | ND | ND | 0.4 |
| PtG Stuttgart | EnBW Regional AG, National Organization for Hydrogen and Fuel Cell Technology (NOW), Clean-Energy-Partnership (CEP) | 2013 | 400 | 60 | – |
| SolarFuel-Alpha plant, Stuttgart | Center for Solar Energy and Hydrogen Research Baden-Württemberg (ZSW), SolarFuel GmbH, Fraunhofer IWES | 2009 | 25 | 4 | 2.4 |
| Stuttgart | ZSW, Enertrag AG, ETOGAS GmbH | 2014 | 370 | 90 | – |
| Stuttgart | ZSW, ETOGAS GmbH, Fraunhofer IWES | 2012 | 250 | 50 | 12.5 |
| e-gas plant, Werlte | Audi AG, EWE AG, MT BioMethan GmbH, ETOGAS GmbH | 2013 | 6,000 | 1,300 | 300–340 |
| France | | | | | |
| Myrte, Corsica | University of Corsica (Project Manager), Areva Renewables, CEA | 2009 | 110 | 23 | ND |
| Italy | | | | | |
| Ingrid FCH JU project, Puglia | Seven co-operating partners | ND | 1,000 | 200 | ND |
| The Netherlands | | | | | |
| P2G project, Rozenburg | DNV Kema, Stedin.net, Resort Wonen, Gemeente Rozenburg | 2012 | 7 | ND | 2 |
| Switzerland | | | | | |
| PtG Rapperswil | Erdgas Obersee, Audi, Climeworks | 2015 | 25 | 4 | 1 |

Companies of varying size and from diverse sectors are involved in the ongoing pilot projects: the automotive industry, energy suppliers, windfarm operators and project developers, electrolyzer manufacturers, research institutes, global players, and a number of municipal works.

A broad range of experience is being gathered from plants with electrical power between 25 kW and 6 MW for the electrolysis. These plants utilize a wide range of different technical approaches. For example, alkaline and membrane electrolyzers are being tested and refined as is methanation based on chemical and biological means. The operating status of the plants ranges from research and development through to planning and construction phase to test and ongoing operation. The projects focus on trialing hydrogen technology and feeding hydrogen into the electricity network. Some projects have already been completed.

#### ▪ Project Goals

The foregoing projects have diverse goals. From a technical perspective, the projects involve the refinement and testing of various electrolysis and methanation techniques and prototypes. The aim is to optimize efficiency, runtime, or dynamic operation and to test various modes of operation such as optimization after gas production, base-load operation, and peak-load operation. Another aim of many of the projects is to demonstrate that the technology is suitable as a dynamic network component that can cope with the steep power gradients of renewable energy feed-in. On the whole, the technical aims relate to enhancing operations, integrating production into energy markets (e.g., participating in the balancing energy market), demonstrating a process chain, upgrading plant systems, and/or preparing for large-scale implementation.

From a business perspective, cost structures are being improved and value-adding chain are being optimized using production concepts that extend from individual components all the way up to the overall design of the plant. Appropriate business models are being developed with the goal of preparing for the commercialization phase. Technical and regulatory challenges associated with the construction and operation of PtG plants are also being explored.

Environmental aspects are being taken into account by quantifying the green hous gases (GHG) abatement contributions of the projects. Lastly, economic aspects are also playing a role, including field tests to determine the adaptability of the existing power market design and studies to evaluate macro-economic benefits.

#### ▪ Current Status of the Projects

Some projects will be examined in more detail below. Current information about projects can be found at the German Energy Agency's strategy platform 'Power-to-Gas' (www.powertogas.info), the DVGW innovation offensive (www.dvgw-innovation.de), and on the author's homepage (▶ www.power-to-gas.de).

### 14.3.2.2 PtG Plants (Hydrogen)

#### ▪ Hybrid Power Plant, Prenzlau, and Greenpeace Energy eG

The hybrid power plant in Prenzlau integrates wind turbines, electrolysis, aboveground hydrogen storage, a biogas plant, and power and heat generation using CHP. The power plant also offers direct marketing of the hydrogen that is produced for transport and used in the industrial sector via the filling of tankers.

The 600 kW alkaline electrolyzer, designed and constructed by Enertrag, converts surplus power into hydrogen at 120 $m^3$/h, which is in turn stored in pressure tanks (◘ Fig. 14.25). From here, the hydrogen can either be used directly for industrial purposes or in FCV, or it is fed back into the network when the feed-in from renewable energy is low. Biogas from a biogas plant is admixed and converted in two CHP plants that have a hydrogen tolerance of 15%. To increase the efficiency, the waste heat from electricity production is fed into a district heating network. Flexible operation and the potential for providing positive and negative balancing power are also being investigated.




**Fig. 14.25** Hybrid power plant, Prenzlau, operated by Enertrag AG in which a self-manufactured alkaline electrolyzer produces windgas for customers of Greenpeace Energy eG and feeds it into the gas network. The gas can also be stored temporarily in steel tanks and filled into tankers or combusted in the existing gas CHP plant after being added to biogas (source: Enertrag AG)

The foundation stone of the plant was laid in 2009 and the plant was inaugurated and started its test phase in October 2011. It has been in operation since the start of 2013, and in 2014 hydrogen was fed into the natural gas network for the first time to supply about 8,000 customers of the green power and windgas distributor, Greenpeace Energy eG.

Greenpeace Energy eG is the first energy supplier to promote PtG with its pro-Windgas tariff, which used direct marketing with its customers to encourage the use of 100% renewable energy supply as part of energy transition by developing important storage technology. The company offers a gas that satisfies environmentally stringent criteria, such as no emissions and which, unlike biogas, is produced without large-scale livestock farming or intensive agriculture [17].

### ▪ WindGas Falkenhagen

In August 2013 E.ON SE started operating a pilot plant in Falkenhagen to convert electricity from wind energy to hydrogen (Fig. 14.26). The site of the plant between Berlin and Hamburg was selected because of the high wind resource in Brandenburg and the proximity to gas infrastructure. The demonstration plant is intended to replicate the entire process chain from fluctuating wind power generation to the renewable hydrogen being fed into the network. The alkaline electrolyzer from Hydrogenics in Belgium has a nominal power of 2 MW and produces 360 $m^3$/h hydrogen. The efficiency, referring to the combustion value of the entire chain, is 66%. The plant was the first one to feed hydrogen into the German transmission network. It is operated by an E.ON subsidiary. The partners include E.ON edis AG, E.ON New Build & Technology GmbH, as well as Swissgas AG, which purchases a part of the hydrogen and sells it on the Swiss market.

### ▪ PtG Demonstration Plant in Frankfurt

Thüga AG has set up and operates the first PtG plant that feeds hydrogen into the gas distribution network as a consortium of municipal works with 12 project partners (Fig. 14.27). A PEM electrolysis system from the English manufacturer ITM Power with a nominal power of 315 kW, which can be ramped up to 385 kW in cases of excess load, has been operating in Frankfurt since 2013. In the process, it generates 60–70 $m^3$/h hydrogen with an expected plant efficiency of 4.9–5.2 kW h/$m^3$ and a gas quality of 99.8 vol% pure hydrogen. Using a gas pressure regulating and metering station and a mixing plant, this flow of hydrogen will be added to a gas distribution network flow of 3,000 $m^3$/h natural gas that is constant throughout the year. It is not necessary to compress the hydrogen because it is released from the electrolysis unit at 3.2 bar. The gas limits such as 3 vol% oxygen are readily satisfied. Along with the aim of gathering information about the technology and the costs, the addition of a methanation unit is also planned. Because of the decentralized standard and the local situation, biological methanation and a biomass composting plant in the immediate vicinity as the source of $CO_2$ are options here [14].

### ▪ Regenerative Balancing Power Plant $RH_2$-WKA in Grapzow

The $RH_2$ Werder/Kessin/Altentreptow wind farm was constructed as a wind farm with hydrogen storage and is one of the largest on-




**Fig. 14.26** PtG pilot plant operated by E.ON SE in Falkenhagen, between Berlin and Hamburg, with a nominal electrical power of 2 MW as the first plant to feed hydrogen into the high-pressure natural gas network (source: E.ON SE)

shore wind farms in Germany with a capacity of 140 MW. $RH_2$ stands for regenerative hydrogen. An alkaline electrolyzer with a capacity of 1 MW generates 200 $m^3$/h hydrogen, primarily to cover the on-site power needs of the wind farm. The wind farm is intended to be operated towards to the distribution system as an autonomous carbon-free 'balancing' power plant, which is the primary purpose of the wind/hydrogen plant. The plant was inaugurated in late 2012 and has been in the test phase since 2013. In other project stages, local consumers will be supplied with electricity, heat, hydrogen, and oxygen. The construction of a local heating network, a system to feed hydrogen into the gas network, and the construction of an electric-charging station for electro-mobility are planned for this purpose.

### ■ Mainz Energy Park

From 2015 onwards, the municipal works Stadtwerke Mainz AG plans to store surplus electricity from adjacent wind turbine generator systems in the gas network in the Mainz Energy Park where it will supply energy that is decoupled from surpluses. Hydrogen will also be filled into tankers and optionally used at a fueling station. In this context, innovative technologies such as PEM electrolysis will be trialed on an industrial scale of 6 MW. The hydrogen production will be fixed at a maximum production volume of 1,000 $m^3$/h. Partners in the research project include Linde AG, Siemens AG, and RheinMain University of Applied Sciences.

### ■ Etzel $H_2$ Cavern Storage

Because of their large storage capacity, salt caverns are of particular interest for storing hydrogen. Salt caverns near the existing gas storage systems of IVG Caverns GmbH in Etzel in northern Germany will be operated in conjunction with PtG plants, and a range of utilization pathways such as feeding into the gas network



**Fig. 14.27** The PtG demonstration plant operated by Thüga AG in Frankfurt with a nominal power of 315 kW (source: Thüga AG)

and use in the industrial sector, mobility, and the heat market will be tested and exploited. The aim is to realize a pilot and demonstration plant for large-volume storage of surplus wind electricity in salt caverns in the form of hydrogen. For this purpose, an electrolyzer with a connected load of 2–6 MW will be constructed to produce 1,000 $m^3$/h.

### ■ PtG Demonstration Plant in Hamburg-Reitbrook

In Hamburg-Reitbrook a prototype of a 1 MW PEM electrolyzer from the manufacturer, Hydrogenics GmbH, will be tested by E.ON Gas Storage GmbH on a megawatt scale. The production of 265 $m^3$/h will be scientifically monitored by Fraunhofer ISE and the German Aerospace Center (Deutsches Luft- und Raumfahrtzentrum, DLR). The field test will enable trialing of the input power range and the infrastructure and development of business models.

### ■ Hydrogen Fueling Station, HafenCity, in Hamburg

The alkaline electrolyzer in the hydrogen fueling station of Vattenfall Europa AG generates a maximum of 180 $m^3$/h. It will be used by Hamburg Hochbahn AG, the major transit company in Hamburg, and will be funded by the Ministry of Transport (▶ Sect. 14.2.2.1).

### ■ BTU Hydrogen Research Center in Cottbus

Brandenburg University of Technology (BTU) in Cottbus is refining pressure-electrolysis technology in the Chair of Power Plant Technology. A corresponding research center was opened in 2012 along with a pressure electrolyzer with 145 kW electrical power and 20–30 $m^3$/h was commissioned. High-pressure electrolysis has the advantage of the construction type being more compact and the product-gas not having to be compressed for storage, which is an additional high-energy process. The facilities associated with the electrolysis such as feed water treatment, nitrogen supply, gas purification and drying, and cooling will also be researched more extensively, as will storage of the product-gas. The focus is on the adaptability of the electrolysis in response to highly fluctuating feed-in in terms of its function as a network balancing component.

### ■ Hychico PtG Plant with Hydrogen Reconversion to Electricity in a Gas Turbine

In the Hychico PtG plant in Comodoro Rivadavia (Chubut province) in Argentina, wind power is converted in two electrolyzers to produce a hydrogen production rate of 120 N $m^3$/h. The hydrogen that is generated is mixed with natural gas and reconverted in a gas turbine with a $CH_4$ content of up to 42%, whereby the turbine can be operated under peak load with a $H_2$ content of up to 27%. After optimizing the turbines, the operator expects a higher proportion of hydrogen in the combustion gas to be possible. By adding the

**Table 14.2** PtG hydrogen storage systems in operation described in detail as of the start of 2016, adapted from [11, 12]

| Project | Injection | Storage | Withdrawal |
|---|---|---|---|
| Hybrid power plant Prenzlau (Enertrag AG and Greenpeace Energy eG) | AEL | Aboveground Tank; gas network | Fuel cell in motor vehicles; CHP for power and heat generation |
| Hychico | PEMEL | ND | Gas turbine |
| E.ON PtG Falkenhagen | AEL | Gas transmission network | Heat, mobility, chemistry, power generation |
| Thüga AG PtG demonstration plant in Frankfurt | PEMEL, planned addition of methanation | Gas distribution network | Open |
| $RH_2$-WKA wind farm | AEL | Aboveground Pressure tank | On-site electricity supply, heat, mobility |
| PtG demonstration plant, Hamburg Reitbrook | PEMEL | Gas network | – |
| Hydrogen fueling station HafenCity in Hamburg | AEL | Tanker, pressure tank | Bus transport, vehicles |
| Hydrogen Research Center in Cottbus | AEL, pressure electrolysis | Aboveground Pressure tank | Fuel cell for reconversion to electricity |

AEL = alkaline electrolysis, PEMEL = PEM electrolysis.

hydrogen, the emission values for $CO_2$, CO, and $NO_x$ were also improved.

#### Large-Scale Hydrogen Reconversion to Electricity in Fuel Cell Power Plants

To convert stored hydrogen into electricity, fuel cells are one option in addition to CHP plants and gas turbines (▶ Sect. 8.5.1.1). These can also be combined to form industrial units as demonstrated by the largest fuel cell power plant with a capacity of 59 MW in Hwasung, South Korea. The power plant generates electricity and feeds the resulting waste heat into a district heating network. In the US state of Connecticut, a large power plant park with 63.3 MW of fuel cell power is currently in planning [16].

#### Other Research and Development Plants

In addition to the plants described above, there are other research and development plants that are in planning or which are already operational in the area of hydrogen such as $H_2$Herten, RWE Ibbenbüren, NBB Berlin-Brandenburg, Stadtwerke Emden, EnBW Stuttgart, ZSW Stuttgart, Fraunhofer ISE Freiburg, and the Berlin-Brandenburg Airport, which are listed in Table 14.2.

Table 14.2 summarizes the PtG plants for hydrogen located in Germany that were operational in 2014 and indicates their most important properties as energy storage systems.

### 14.3.2.3 PtG Plants (Methane)

Table 14.3 summarizes the existing PtG plants for methane in Germany in 2014. Their backgrounds and properties as energy storage systems are described below.

#### Twenty-Five Kilowatt Alpha Plant in Stuttgart

ZSW Stuttgart and its partner, Fraunhofer IWES, decided that its first realization of the concept of PtG will be carried out in collaboration with SolarFuel GmbH. On behalf of the company newly founded by Gregor Wald-

**Table 14.3** PtG methane storage systems operating in Germany and adjacent countries, adapted from [11, 12]

| Project | Injection | $CO_2$ source | Storage | Withdrawal |
|---|---|---|---|---|
| Alpha plant in Stuttgart and am Eichhof | AEL | Atmosphere, biogas | Pressure tank | Mobility, CHP |
| Beta plant in Stuttgart | AEL | $CO_2$ bottles | Pressure tank | Mobility, vehicles |
| Audi e-gas plant in Werlte | AEL | Biogas | Gas network | Mobility, vehicles |
| BioPower2Gas in Allendorf (Eder) | | Biomethane plant | Gas network | From the natural gas network |
| Power-to-biogas in Schwandorf | PEMEL | Sewage treatment gas | Gas network | CHP |
| PtG in Eucolino | AEL | Biogas | Gas storage; natural gas network | CHP |
| DVGW EBI three-phase reactor | Gas bottles | Raw biogas | – | – |
| Krajete process (AT) | Gas bottles | Raw biogas | – | – |
| PtG Foulum project (DK) | Gas bottles | Raw biogas | – | CHP |
| $CO_2$RRECT | PEMEL | Lignite-fired power plant Niederaußem | – | Substance utilization |

AEL = alkaline electrolysis, PEMEL = PEM electrolysis.

stein, ZSW Stuttgart constructed the first PtG methane plant in 2009 (Fig. 14.28). This allowed demonstration of the technical feasibility of the patented PtG concept and acquisition of other information about $CO_2$ methanation; an area that had been largely unexplored in the energy sector [33]. Fraunhofer IWES sounded out the incorporation of the plants into the energy economy in associated research about optimal operating strategies and concepts for high rates of utilization of the plants in wind farms, while also examining the network relevance using a forecast comparison.

This alpha plant is made up of two containers and uses air as the $CO_2$ source. The first container has a washer for $CO_2$ uptake in a wash solution and an electrodialysis unit that removes the $CO_2$ from the wash medium. The second container has an alkaline electrolyzer with an electrical connected load of 25 kW. The hydrogen is converted into methane in a chemical fixed-bed reactor in tubes with external wall cooling and this methane can be used to refuel vehicles with a Fuel Maker. Because the focus for this plant was on demonstrating the technology, there was no process optimization and,



**Fig. 14.28** PtG pilot plant in 25 kW scale at ZSW in Stuttgart (source: ZSW Stuttgart)



**Fig. 14.29** PtG research plant on a 250-kW scale in ZSW in Stuttgart (beta plant) (source: ZSW Stuttgart)

as a result, the efficiency of the plant for converting PtG is 40%.

### Two-Hundred-and-Fifty Kilwatt Beta Plant in the 'Power-to-Gas' Joint Project

A second plant was constructed in Stuttgart by the same consortium with funding provided by the German Ministry for the Environment. This was a plant with 250 kW capacity (Fig. 14.29). This plant is also a research plant. The provision of balancing energy, load dynamics, optimization potentials, the plant's viability in the energy economy, various $CO_2$ sources, and possible upscaling into the megawatt range are being investigated. Two different fixed-bed reactors (tube bundle and plate reactor) for chemical methanation are being trialed and compared. The results from the Audi e-gas plant in Werlte will also be used. The plant delivers 50 $m^3$/h hydrogen that is converted using the two different pathways of chemical methanation to produce a gas power of about 12.5 kW (LHV), which corresponds to a product gas flow of 12.5 $m^3$/h. The gas is made up predominantly of methane.

### BioPower2Gas, Allendorf (Eder)

As part of the BMWi 'Energetic Biomass Utilization' research program, a PtG plant with biological methanation is being investigated in the 'BioPower2Gas' project in terms of its long-term stability, ability to be integrated into a biomethane plant, and the achievement of a stable gas quality that can be fed into the network. The aim is to ensure a reliable and flexible mode of operation. Investigations into balancing energy operation and fluctuating input qualities for educts and environmental conditions are also being carried out. A balancing, verification, and certification procedure for the SNG that is produced opens up new business models for participation in the biofuel market. The green gas will be sold to Audi AG.

The plant has 300 kW electrolysis power and has been operational since the start of 2015, generating 60 N $m^3$/h hydrogen and 15 N $m^3$/h methane. The plant is the first in Germany to feed SNG, generated using biological methanation into the natural gas network without additional processing.

### Audi e-gas Plant in Werlte

The e-gas plant operated by the automotive company Audi is described in more detail in ▶ Sect. 14.2.2.2.

### Power-to-Biogas in the Joint Sewage Treatment Plant in Schwandorf

Biological methanation is being used in a sewage treatment plant for the first time in Schwandorf in Bavaria. At the joint sewage treatment plant in Schwandorf, MicrobEnergy GmbH from the Viessmann Group operates a PEM electrolyzer from Proton with a power of



**Fig. 14.30** Power-to-biogas plant operated by MicrobEnergy GmbH (Viessmann Group) with a PEM electrolyzer (*middle*), mixing plant (*front left*), and digestion tower (*back left*) near an old power plant site (source: MicrobEnergy GmbH)

275 kW (maximum), which generates 30 $m^3$/h hydrogen (Fig. 14.30). This is imported to the digestion tower of the sewage treatment plant using various technologies where it is converted to methane by the specially adapted micro-organisms in the tower. The requirements for the purity of the hydrogen are very low. The research work is supported by the Bavarian Ministry of Economics. The partners include Verbundkläranlage Schwandorf and OTH Regensburg, which carry out both the analysis and evaluation of the technical, economic, and environmental parameters of the plant, while also developing business models for the technology and identifying its economic role. Other project results are mentioned in ▶ Sect. 8.3.3.

### ■ PtG in Eucolino

Trials of biological methanation in pure cultures are being carried out at the same site operated by MicrobEnergy GmbH. A biogas plant is used as the $CO_2$ source and the biogas that is generated is made up of 52% methane and 48% carbon dioxide. Micro-organisms convert $H_2$ and $CO_2$ to pure methane in the process. The electrolysis power is 108 kW with a maximum of 21.3 $m^3$/h hydrogen being generated. This hydrogen means the biogas fermenter is able to produce 5.3 $m^3$/h methane. The plant is designed for discontinuous hydrogen production.

### ■ Methanation am Eichhof

The Stuttgart 25-kW methanation plant was brought to Bad Hersfeld to the Fraunhofer IWES for testing with biogas from a biogas plant. The biogas contains only about 60% methane and normally the gas requires processing to ensure natural gas quality. Using direct methanation, this processing can be omitted. The tests were successfully completed and have also shown that the catalyst used in the plant is deactivated very quickly as a result of contamination by sulfur compounds.

### ■ DVGW Three-Phase Reactor at the Engler-Bunte Institute (EBI)

A laboratory reactor with a three-phase reactor for trialing chemical methanation is being investigated by the DVGW at the EBI in Karlsruhe in collaboration with a number of partners. The special technology generates a maximum of 1 $m^3$/h methane and is explained in ▶ Sect. 8.3.3.

### ■ Krajete Process in Austria

The 10 liter bio-reactor which implements biological methanation in Linz is described in more detail in ▶ Sect. 8.3.3.

### ■ PtG Foulum and PtG BioCat Projects in Denmark

The first Danish pilot plant PtG Foulum was operated from July to November 2013 and uses raw biogas from anaerobic fermentation as a carbon dioxide source as well as hydrogen from bottles in order to trial biological methanation on a pre-commercial scale. A stirred tank reactor of 10,000 L capacity that was filled to a maximum filling level of 4,500 L with a pure culture of the micro-organism *methanothermobacter thermautotrophicus* was used (Fig. 14.31). Over more than 3,200 h operating time, various operating parameters for the biological methanation were tested. Although the stirred tank reactor was not optimized, had low stirring force, and could only be operated under atmospheric pressure, $CO_2$



**Fig. 14.31** Stirred tank reactor with a capacity of 10,000 L for biological methanation in Denmark, realized and operated by Electrochaea.dk (source: Electrochaea.dk)

conversion rates of up to 95% were measured. The bio-catalyst proved to be very robust and also accepted raw biogas containing up to 2,000 ppm $H_2S$ as the $CO_2$ source, and also survived several incidents of contamination with $O_2$. It could also be demonstrated that the biological system can be actively controlled and many characteristics of the micro-organisms can be specifically modified to create optimal environmental conditions for the methanation. The gas that was generated was converted in a CHP plant on-site to electricity and heat.

The plant was developed and operated by the Danish company, Electrochaea.dk, and was located in the Biogas Research Center of the University of Aarhus in Foulum, Denmark. The project was funded by the EUDP and supported by the University of Aarhus, Erdgas Zurich, EWZ, NEAS Energy, and E.ON.

The PtG Foulum project demonstrated that biological methanation itself functions efficiently in a stirred tank reactor not intended for this purpose and can be directly operated with biogas. As part of the PtG Biocat project, which is funded by up to 55% by the Danish government, a new plant was established in 2016 based on optimized bio-reactors.

The plant has an electrical charging power of 1 MW and is located on the grounds of a waste water treatment plant in Avedøre, Denmark. It will also be used for frequency stabilization in the electricity network. The project partners are Hydrogenics, Audi AG, NeasEnergy, HMN Naturgas, BioFos, and Insero.

The hydrogen is obtained using a refinement of alkaline water electrolysis. The $CO_2$ used is from raw biogas or in purified form from biogas. The high-quality methane gas that will be generated is fed directly into the gas network.

### ■ $CO_2$RRECT

$CO_2$RRECT is an abbreviation for '$CO_2$ reaction using regenerative energies and catalytic technologies', and is a merger between a range of partners from business and science that have been inspired by the PtG concept. The Niederaußem lignite-fired power plant will act as the $CO_2$ source. Unlike other projects, this project will not focus on using the gas for energy purposes but instead it will be used as a raw material. A diverse range of methods and catalysts for converting the $CO_2$ will be investigated in order to generate carbon monoxide or formic acid (HCOOH) as an intermediate product to manufacture chemicals or polymers. The project can also be evaluated as a PtC study.

## 14.4 Summary

- The **coupling of electricity and heat** is the most **cost-effective way** to **integrate renewable energy**. The temporal decoupling of electricity generation and consumption by storing energy in batteries generates much higher costs compared to linking the electricity and heating sectors using TES.

- Power-oriented CHP plants can be an economical flexibility option if the power generation systems, heat-sinks, and thermal storage are optimally tailored to one another.
- Storing energy produced by surplus heat in local and district heating networks is a state-of-the-art process and has been trialed in many countries. PtH harnesses opportunities for using existing infrastructure (analogous to PtG in the gas network).
- The **combination of heat pumps, solar-thermal energy, heat and cold storage** has major potential in all areas of **heat and cold supply**.
- The potential of PtH as a means of **integrating PV electricity** is enormous. The design of PtH must involve a **bivalent heating element** in order to avoid a disadvantageous increase in the annual peak load of the power system.
- PtH in industrial processes is considerably more cost-effective to implement than PtG, with the same benefits for the electricity sector in relation to load-management and balancing power. If **natural gas** is replaced by **PtH**, the process is also **more efficient** than PtG.
- **Photo-thermal energy** is **more economic and requires less maintenance** than **solar-thermal energy** and allows **more efficient utilization of solar energy** for power, heat, and transport with **minimal surpluses**.
- **Small photo-thermal energy systems** for hot water are economic, even **without the renewable energy feed-in tariff**, while **larger systems** are of interest for the **combination of hot water, self-consumption of electricity, and renewable energy feed-in**.
- In **electro-mobility** the first intrinsic coupling of the power and transport sectors is imminent. This requires **electrification of the drive train**, the construction of **charging infrastructure**, and **reductions in the costs of the components**, particularly the **batteries**, which can be achieved by **mass production of electric vehicles**.
- Due to the predominance of **unidirectional charging**, electric vehicles will only be accessible for improving load-management in the electricity sector. Only when **bidirectional charging** becomes available will battery storage in electric vehicles **also be accessible to the electricity sector**. However, the estimated storage capacities are low (i.e., they are approximately ten times that of pumped-storage plants at maximum).
- Electric fuels have major potential to reach areas of the transport sector, where direct use of electricity has proven difficult. **Gaseous and liquid fuels** such as diesel and gasoline for **long-distance mobility**, **buses**, and **aviation** are already being produced in pilot projects.
- PtG is a cornerstone of clean-energy transition because of its role in **long-term storage to safeguard the power supply**, as **gas storage for heat supply**, and as **energy-dense fuel and raw material for transport and the chemicals industry**. The technology links many areas of the energy supply system.
- The opportunities associated with PtG include the ability to **harness the existing gas infrastructure** (including end-user devices such as gas-fired boilers, gas vehicles, and gas-fired power plants). **Gas mobility** is one of the first markets that has emerged for PtG. There is also a bridge to the chemical industry because **methane is an important raw material** in this sector.
- There are **risks** associated with **counterproductive trends**. The original idea of **using surplus wind and solar electricity** can lead to **greater utilization of coal or nuclear power** because of the economic pressure to ensure continuous operation of a PtG facility. Specifically, PtG could lead to one stored energy carrier (e.g., coal) being converted into another stored energy carrier, thus producing considerably higher carbon emission. This would be environmentally counterproductive. The technology also allows for the practice of **greenwashing**.

- Because of such risks, a clear **regulatory framework** is required to prevent misuse. A temporal and quantitatively limited **exemption from end-consumer charges** makes sense. However, to promote adoption of the technology, there needs to be a clear **link from PtG** and other flexibility options that **surplus electricity from renewable sources** and **operation is beneficial to the network** over the long-term.
- When coupling sectors, one sector (e.g., the electricity sector) cannot bear the costs associated with decarbonization for other sectors (e.g., the chemicals industry, heat, or transport sectors). Therefore, **all technologies** that use electricity as the primary energy for other sectors must also be appropriately involved in **financing the electricity sector using surcharges** as principle end consumers.
- The basic idea behind the invention of PtG is to enable the **storage of surplus fluctuating renewable energy in order to reconcile mismatch between power supply and demand**. The economic and environmental benefits of PtG can only be fully realized if the technology is harnessed in line with this aim.
- To ensure that only **excess power supply** are processed using PtG, the **electricity price** paid by a PtG plant should be **below the marginal cost of the most cost-effective fossil power plant** in the merit order.
- A number of **pilot and demonstration plants** in Germany and Europe have confirmed the technical feasibility of PtG.
- **Biological methanation** has proven to be considerably **more robust** than chemical methanation in terms of **pollutants in the educt-gas** (e.g., sulfur compounds).
- The key challenges for the future development of PtG include **increasing the operational flexibility of PtG plants in a way that supports clean-energy transition**, **reducing the costs of the components**, and **enabling continuous operation with new power procurement concepts**.

## References

1. AGFW (2009) AGFW-Regelwerk – Arbeitsblatt FW 308. Zertifizierung von KWK-Anlagen – Ermittlung des KWK-Stromes. Bundesanzeiger-Verl.-Ges, Köln (Bundesanzeiger, 61, 145a.)
2. Audi (2013) Energiewende im Tank. http://www.audi.de/content/de/brand/de/vorsprung_durch_technik/content/2013/08/energiewende-im-tank.html. Accessed 10 Feb 2014 (Audi AG)
3. Beer M (2011) Potenzial funktionaler Speicher mit flexibler Kraft-Wärme-Kopplung. Energiewirtsch Tagesfr 61(12):8–10
4. Beer M (2011) Wärmespeicher. Mehr Freiheitsgrade für KWK. München
5. Bertau M, Offermanns H, Plass L, Schmidt F, Wernicke H-J (eds) (2014) Methanol. The basic chemical and energy feedstock of the future. Springer, Heidelberg, Berlin, New York
6. Braungardt S, Günther D, Miara M, Wapler J (2013) Elektrisch angetriebene Wärmepumpen. Aktuelle Ergebnisse aus Forschung und Feldtests. BINE-Info, Eggenstein-Leopoldshafen, Freiburg
7. Bruckner T, Götz M, Böttger D, Kondziella H (2013) Potential von Power-to-Heat in der Regelzone von 50 Hertz. 3. VDI-Fachkonferenz Energiespeicher für die Energiewende 2013, Mainz
8. Büttner W, Fritzer T (2013) Erdwärme – die Energiequelle aus der Tiefe. Augsburg
9. Chemical Technology (2013) George Olah CO2 to Renewable Methanol Plant, Reykjanes, Iceland. http://www.chemicals-technology.com/projects/george-olah-renewable-methanol-plant-iceland/. Accessed 10 Feb 2014 (Net Resources International)
10. CRI (2014) First Commercial Plant. http://www.carbonrecycling.is/. Accessed 10 Feb 2014 (Carbon Recycling International)
11. DENA (2014) Strategieplattform Power-to-Gas. http://www.powertogas.info/. Accessed 10 Feb 2014 (DENA – Deutsche Energie-Agentur GmbH)
12. DVGW (2013) Power-to-Gas-Landkarte. Power-to-Gas Demo-Projekte in Deutschland. http://www.dvgw-innovation.de/presse/power-to-gas-landkarte/. Accessed 10 Feb 2014 (Deutscher Verein des Gas- und Wasserfaches e.V.)
13. Erdmann G, Dittmar L (2010) Technologische und energiepolitische Bewertung der Perspektiven von Kraft-Wärme-Kopplung in Deutschland. Berlin
14. Estermann T (2014) Entwicklung eines Konzeptes zur Erweiterung der Thüga-Power-to-Gas-Demonstrationsanlage um eine Methanisierungseinheit. Development of a concept to expand the Power-to-Gas demonstration plant of the Thüga group about a methanation unit. OTH, Regensburg (Bachelorarbeit)
15. Etspüler M (2014) Stromtanken an der Laterne. VDI Nachrichten 2014(3)

# Supplementary Information

Epilogue – 806

Index – 807

© Springer-Verlag GmbH Germany, part of Springer Nature 2019
M. Sterner, I. Stadler (Eds.), *Handbook of Energy Storage*, https://doi.org/10.1007/978-3-662-55504-0

# Epilogue

**Evolution = Revolution**
We possess the technology for the energy transition
So don't waste time in fake-news discussion
By not giving climate change the attention it deserves
Instead complete the green revolution with endless reserves

For what would we be without the environment – our natural basis of life?
Without – not a single economy could ever survive!
How dare we lose that ground,
we can't fail to keep the world spinning around.

We have all necessary knowledge in our hands,
The challenge is clear – everyone understands,
For not by words, by actions you will know us,
But still – we are caught on the "economy first" bus,

Driven by profit, economic growth and short-term thinking,
Focused on money, not on generation linking,
Humans are meant for cooperation instead of competition,
Cleary all connected in unity, not meant for division.

But the economization of life,
Drives us not to affluence but to strife,
If we have no more natural space to live in,
we'll cross swords, and no longer fit in.

Things are not fixed, they are always in transformation,
There is still time left to act, all is in connection,
If we do our part – the rest will be done.
As we say for ages: "Thy will be done!".

The universe is 14 billion-years old,
Entirely unique in its mold.
Its knowledge inhabits each of us, each cell,
in flesh and blood, our breath, in every spell.

Nature leads the way, planting ideas as well as seeds,
And pushing the spiral dynamics, crying out for deeds,
The Earth is begging: "I can't handle it anymore",
So let's go, what are we waiting for?

Michael Sterner

# Index

## A


Abandoned mine 410, 411
Absorption
– enhanced reforming process 443
– heat pumps using gas 437
– storage system 601
AC voltage measurement 351
Accumulation 438
Accumulator 242
Acid constant 349
Activated carbon 197
Active materials 281, 289
Adsorption
– heat pump 438
– storage systems 601
Adsorptive glass mat 257
Advanced adiabatic compressed air energy storage 496
Agitator 597
A h capacity 242
Air
– conditioning 74, 76
– electrode 262
– separation unit 449, 452
– traffic 167
Air-breathing engine 441
Air-conditioner 157
Air-fuel ratio 441
Alkaline
– zinc-manganese dioxide system 263
Alkanes 370
Aluminum production 627
Ambient heat use 142
Ampere hours efficiency 239
Ampere's law 218
Anergy 572, 640
Anhydrous salt 596
Animal power 12
Anion 196
Annual curve 89
Annual peak load reduction 634
Annuity investment costs 45
Anode 203, 236, 343
– oxidation 428
Anolyte 321
Antimony poisoning 254
Antimony-free effect 259
Apartment building heated entirely by solar energy 733
Aquifer 403, 406, 503, 584, 732
– formations 408
Arbitrage transaction 676
Arc process, electricity-based 184
Archaebacteria 381
Arrhenius equation 302
Artificially constructed pumped storage 510
– construction 516
– cost efficiency 516
– costs 516
– efficiency 511
– excavation volumes 514
– hybrid 516
– operating principle 511
– space requirements 515
– storage capacity 511
– water requirements 515
Asynchronous induction machine 544
Atmospheric carbon dioxide ($CO_2$) 448
Autothermal reforming 390
Auxiliary energy 429
Aviation 441, 668, 743
– fuel 171
Avogadro constant 7, 235


## B


Balanced reactive power control 681
Balancing 87, 502, 676, 706
– forest and game 738
– power market 682
Base load power plant 94, 128
Battery 24, 175, 647, 652
– application innovations 700
– cost reduction potential 656
– decentralized storage 699
– design 242
– electric vehicle 176
– management system 306, 315
– parks 124, 666, 697
– power plant 46, 127, 697
  – costs 661
  – in Germany 697
  – in North America 699
– secondary 26
– second-life 667
– self-sufficiency 701
– size 702
– state 243
– storage 130, 653, 774, 778
  – balancing and reserve power 705
  – beyond the electricity market 131
  – costs 661
  – gradient control 705
  – network congestion management 705
  – network operations 705
  – supply security and recovery 706
  – voltage maintenance 703
  – voltage quality 703
– technology 700
– vehicle 181
Bell gasholder 401
Bilayer capacitor 647
Binding energy 603
Bio pressure-reactor 387
Biocoke 395
Biodiesel 13, 419, 741, 744
Bioenergy 104, 442, 443, 474
– potential 9
Bioethanol 13, 179, 372, 419, 743, 744
Biofuel 13, 167, 171, 174, 178, 179, 419
– available area 742
– environmental impact 741, 742
– global use 13
– integration 743
– mixtures 741, 743
– potential 741
– Quota Act 743
– residual materials 742
– storage 419
– technical integration 743
Biogas 75, 84, 141, 143, 450, 451, 781
– production surpluses 152
– storage 118
– treatment plants 371
Biogenic
– energy 15
– waste 141
Bio-inspired catalyst materials 340

Biomass 4, 5, 141, 146, 386, 442, 461
– electricity generation
– flexible 118
– inflexible 118
– from waste materials 72
– gasification 443
– variant 450
– pyrolysis 338
– storage 11, 423
– in buildings 424
– open-air 424
Biomass-to-liquid 744
Biomethane 450, 744
Bipolar electrode 315, 321
Bitumen 745
Bivalent heating 772
Black smoker 381
Black start capability 682
Blow out 405
Bode plot 264, 267
Bog 12
Boiler 619
Boiling water cooling, 784
Bonding enthalpy 428
Boost charge process 275
Boundary 573
Braking energy 213, 748
Brine shuttle pond 504
Brown coal 13, 422
Buffer storage 74, 582
– centralized storage system 729
– combined system 730
– dual storage system 730
– for small solar facilities 728
Building
– cooling supply 433
– heating supply 433
– mass 157
Burning gas 438
Butane 445
Butler-Volmer equation 238, 250

## C

C1 carrier 382
Cadmium
– electrode 262
– hydroxide 263
Calvin cycle 5
Capacitor 24, 192, 194, 647
– aging 210
– applications 212
– breakdown 211
– charge current 200
– charging 199
– discharging 200
– electrostatic 195
– energy density 207
– energy loss 205, 207
– estimating the service life 211
– fundamental features 192
– self-discharge 206
– service life 209, 211
– stored energy 194
– temperature influences 210
– use in wind turbines 213
– voltage 199
Capacity
– charge storage 193
– installed 60, 61
– market 682
Capital
– costs 45
– interest 46
Car sharing 176
Carbon
– capture and use 787
– cycle 14, 15
– dioxide ($CO_2$) 337
– absorption 5
– atmospheric 448
– biogenic 371
– capture and storage 448
– certificate prices 745
– concentration 9
– emissions 16, 148, 453, 457
– from biogas treatment plants 450
– from flue gas 451
– from power plants or manufacturing facilities 372
– gas from biogas and gas purification plants 451
– gas purity 384
– gas quality 384
– methanation 374
– recycling 373
– recycling from gas power stations 452
– separation from air 372
– storage in the oceans 15
– synthesis 5
– uptake 798
– electrodes 288
– hydrate production 454
– monoxide 12, 337
– oxide (CO) methanation 373
Carbonate 449
Carbonic acid 435
Carotinoid 6
Cascade use 738
Catalyst 375, 377
Catalytic hydrogenation reaction 421
Cathode 203, 236, 343
Catholyte 321
Cavern 33, 583
– conventionally excavated 410
– storage 73
– underground 504
– supply line 486
Cell
– design 242
– polarization 237
Cellulose 419
Cement production 628
Centralized thermal storage 148
Chain polymerization 395
Charge
– current 200
– storage 193
Charging
– bidirectional 778
– concepts 777
– duration 41
– efficiency 41
– end voltage 298
– power 37, 92
– unidirectional 778
Chemical
– energy storage 649, 653
– methanation plant 780
– potential 233
– sector 183, 187
– short circuit 452
– synthesis 369
Chlor-alkali electrolysis 336, 404, 627
Chloride ion 254
Chlorine 336
– combustible gas 336
Chlorophyll 6
Chloroplast 4
C–H–O system 327, 462
Chromophore 6
Circulation pump 624
Climate
– change 17, 18, 740
– anthropogenic 15, 17
– protection 124, 148, 736
Clothes dryer 625
Coal 422, 614
– firing 616
– liquefaction 393
– power plant surpluses 152
– storage 422
Cobalt 283
Coefficient of performance 154, 436

Coffee bag cell 295, 296
Coil 294, 647
Cold-water storage 582
Colza plant 13
Combined cycle power plants (CCPP) 758
Combined gas and steam power plant 431
Combined heat and power 13, 157
– Act (KWKG) 762
– basic principle 758
– flexibility 758
– generation 141, 152, 426, 432, 668
– limited potentials in summer 760
– plant
  – designing 760
  – sizing 760
– potential applications 759
Combined wind and pumped storage plant 695
Combustion
– chamber 430, 441, 502
– engine 439
– gas 426
Comparison of storage systems 639
Composite material 596
Compressed air 484, 495, 502
– energy storage 493
  – adiabatic 492, 493, 496
  – classification 492
  – construction design 502
  – cycle efficiency level 491
  – diabatic 491
  – isothermal 499
  – power plant 484, 485, 487, 488, 504, 629
  – renewable, emissions-free processes 492
  – thermal storage 493
  – uncooled 493
  – volumes 502
– industrial utilization 629
Compressed gas container 400
Compressed natural gas 414
Compressor 430, 436, 441, 459, 484, 496, 629
Concentration cell 236
Concrete 495, 576
– spherical tank 520
Condensation
– heat 437
– power plant 759
Condensing boiler 435
Conducting salt 288
Conduction 572
Conductivity
– meter 351
– molar 348
– specific 348
Constant
– voltage charging 298
Continuous
– current 219
– flow heater 619
Controllable local network transformers 130
Convection 572
Conversion losses 668, 743
Converter 543, 661, 703
Coolant
– circuit 622
– pump 365
Cooling
– electric 620
– passive systems 734
– requirements 139
Cooper pairs 215
Copper 290, 627
Copper plate 90, 120
Corrosion rate 254
Cost analysis 88, 90
Cost/benefit analysis 106
Coulomb 192
Coupled power and gas grid 443
Coupling
– of heat pumps with photovoltaic systems and thermal storage 765
– of heat pumps with thermal solar arrays 765
– of the electricity and heating sectors 758
– of the power and gas sectors 455, 785
– of the power and transport sectors 776
Cracking 415
Cross-sectoral coupling power-to-heat 147
Crude oil 33, 415
– products 418
– storage 415
– technical characteristics 415
– transportation 415
Cryogenic gas container 402
Crystallization 592
Current interrupt device 294
Curtailing 96, 100
Cycle
– efficiency 89, 94
– number 42

# D

Daily storage 648, 666
Dam storage 509, 521
– efficiency 521
– location 521
– operating principle 521
– storage capacity 521
DC voltage 718
Debye-Hückel-Onsager theory 348
Decarbonization 131, 184, 462, 788
– of the heating sector 142
Decentralized
– battery storage 699
– thermal storage 149
Deep geothermal energy 72, 79
Deficits 455
Deforestation 11
Demand response 613
– capacity-time dilemma 616
– communication technology integration 615
– households versus industry 615
– in cross-application technologies 616
– in households 616
– in industry 626
– investment costs 615
– potential
  – in Europe 630
  – in Germany 630
Demand side management 71, 87
– economic potential 64
– technical potential 64
Derivative market 678
Dielectric 193, 206
– flashover 310
Diesel
– engine 440
– fuel 418
– oil 397
– production using Fischer-Tropsch synthesis 783
Difference in elevation 510, 652
Differential scanning calorimetry 590
Diffusion coefficient 291
Digestion tank 388
Dimethyl ether (DME) 392, 420
Dipole 193
Direct
– current machine 544

– electric heating 617, 626
– reduction process 445
Direct-contact storage 599
Discharge
– current 202
– voltage 201
Discharging
– duration 42
– efficiency 41
Disc-type gas holder 401
Dish-Stirling system 723
Dispatch 681
Displacement storage 586
Dissociation 601
District battery storage 706
District heating 761, 766
– network 156
– plant 432
  – satellite CHP 152
– storage 156
Double-layer capacitor 195, 196, 198
– determining the efficiency 207
– use in the transport sector 214
Drinking water 694, 727
Drive concept 168, 776
Drive technology 174
Dynamic Simulation 442


# E


Earth
– atmosphere 18
– basin 584
– surface 468, 511
Economic development 69, 169
Educt gas 371
Efficiency improvement 145
Electric
– conductivity 237
– cooling 620
– energy 639
  – storage system 647, 650
  – technical and economic parameters 640
– engine 535
– field 192
  – strength 347
– fuel 780
– heat pump 147, 154, 157
  – integration 764
  – monovalent 154
– hot water supply 70
– mobility 74, 76
– motor 544, 776
– vehicle 77
  – with range extender 177
Electrical
– current flow 346
– energy 24
  – storage 192
Electricity 35
– additional storage 106, 108
– as primary energy 146, 175
– demand 59, 101
– generation 75
  – costs 93
  – direct 57
  – in Europe 99
  – time series 99
– import 83
– market model 125
– mix 59, 65, 66
  – in the future 60
  – in the present 59
– modeling 99
– negative prices 56
– network 30, 53
  – fluctuations 62
  – stabilization 702
– price spread 678
– purchase costs 653
– reconversion 119
– renewable 146, 171
– sector 676
– storage 26, 30
  – comparison of costs by cycle duration 653
  – in the energy transition 126
  – long-term requirements at the transmission network 128
  – merit order 653
  – requirements at the transmission network level 130
  – requirements for system services 131
– supply
  – costs 457, 465
  – system service 679
– surpluses 53, 112, 125, 148, 373
  – dynamic simulation to determine 61
  – markets 55
  – networks 55
  – unexploited 108
Electrification
– of mobility 175
– of traffic 171
Electrochemical
– cells 235
  – energy and efficiency 239
  – side reactions 239
– energy
  – converter 240
  – storage 230, 240, 647, 652
– impedance analysis 237
– process 232, 346
– voltage window 288
Electrode 205, 232
– boiler 762
  – Incorporation into existing industrial heating cycles 772
– electrochemical reactions 235
– equilibrium 233
– negative 252
– polarization 237
– positive 253
– potential 232, 234
– reaction zone 238
– resistances 351
Electrodialysis 372, 449
Electrolyser 85
Electrolysis 335
– atmospheric 352
– block 359
– cells 354
  – kinetic effects 344
– conductivity 346
– coolant pump 365
– facility
  – components serving the entire system 361
  – downstream components 361
  – increase in overall efficiency 368
  – upstream components 361
– heat exchanger 366
– membrane-less 358
– peripherals 360
– piping system 364
– pressurized 352
– reversible 357
– type 354
– waste heat 362, 367
  – calculations 362
  – design 362
  – economic efficiency 368
  – effects 368
Electrolyte 195, 205, 241, 426
– calculating charges 347
– electrical conductivity 241
– liquid 286
– solution
  – calculating ion mobility 347
Electrolyte-gas mixture 345
Electrolytic conductivity measurement 350
Electrolyzer 174, 360

Electromagnetic radiation energy 333
Electromobility 103, 167, 173, 175, 180, 466, 667, 776, 777
– possible development 778
Electron 5
– donor 382
Electroneutrality principle 236
Electronics 777
Elementary charge 192
Emission-to-liquid 783
Energy
– balance 76
  – evaluation 83
– battery 715, 721
– biogenic 15
– carrier 24, 571
– changing the forms of storage 17
– $CO_2$ reduction 474
– conversion chain 33
– converter 24
  – electrochemical 240
– crops 9, 742
– demand of a decarbonized transport sector 182
– density 40, 207
– distribution 76
– efficiency 20, 121
– form 33
– fossil 13, 15, 91
  – significance of storage 20
– from the ocean 466
– Germany's system in 2050 149
– losses 39, 206
– market 55
– mechanical 71
– mix 171, 185
  – in the transport sector 172
– natural 4
– nuclear 15
– parameters 36, 37
– plant 12
– primary requirements 145
– renewable 4, 17, 19, 71, 96, 111, 174
  – expansion 101
  – feed-in management 93
  – integration 633
– renewable guaranteed capacity 633
– requirements
  – in households 142
  – manufacturing 145
  – trade, industry and services 144
– rotational 538
– ship 471, 474
– solar 4, 466
– storage 24
  – centralized systems 44
  – charging 24
  – charging process 219
  – chemical 35, 36, 327, 649, 653
  – classification 33
  – costs 96
  – cross-sectoral systems 26, 28, 29
  – cycle life 42
  – decentralized systems 44
  – definition 24
  – discharging 24
  – discharging process 220
  – driven by mobility 667
  – dual-use systems 44
  – economic classification 45
  – efficiency 40
  – electrochemical 34, 230, 240, 652
  – electromagnetic 35
  – electrostatic 35
  – fixed systems 45
  – for the energy transition 86
  – future potential 665
  – geopolitical purpose 33
  – in batteries 230
  – in the electricity sector 676
  – in the transportation sector 741
  – loading 24
  – long-term systems 44
  – mechanical 34, 36, 484, 648, 652, 679
  – mobile systems 45
  – natural 4
  – parameters 36, 242
  – physical purpose 30
  – primary systems 26
  – public acceptance 665
  – purely magnetic 35
  – secondary systems 26
  – sectoal systems 26
  – short-term systems 43
  – spatial classification 44
  – stages of development 655
  – subcategories 25
  – superconducting electromagnetic systems 214
  – superconducting magnetic system 216, 219
  – supply systems 33
  – thermal 36, 648, 652
  – thermochemical 568, 601
  – through the ages 4
  – unloading 24
– supply
  – development 169
  – heat sector 59
  – power sector 58
  – transport sector 59
– throughput costs 92
– transition 20, 56, 123, 131, 167, 665
  – chemical basic materials 466
  – global 17
  – mobility 466
Enthalpy-temperature diagram 590
Equilibrium
– concentrations 234
– voltage 231
Equivalent
– circuit 203, 206
– conductivity 348
– mass 235
Ethanol 419
Ethyl alcohol 419
Ethylene carbonate (EC) 287
Etzel $H_2$ cavern storage 795
European
– domestic market 114
– electricity generation 99
– transmission network 103, 127
Euryarchaeota 381
Exergy 572, 640
Exfoliation 288
Exhaust recuperator 488
Expansion
– optimization in Europe 107
– planning for Germany 100
Extraction technology 60, 425
Extractor 437

# F

Faraday constant 230, 234
Faraday's law 429
Farmland 742
Fault ride-through 681
Federal Environment Agency
– renewable energies from renewable sources 69
– UBA 100% study 69
Federal waterways 521
Feed water treatment 796
Feedback effect 258
Feolit 580
Fiber
– composite disc 536

– structure
  – electrode 270
  – technology 271
Fiber-reinforced plastics 541
Filling 494, 597, 605
Final consumer 739
Final energy 57
– consumption 57
– demand 59
Fire wood 11
Fischer-Tropsch process 393, 462, 464, 784
– catalysts 399
– chain-growth probability 396
– chemical reactions 394
– product treatment 397
– reactor concepts 398
– sequence 395
Fixed bed reactor 377, 391
Flexibility 92
– demand 53
– market 682
– options 55, 125, 128, 131, 143
– requirements 125
Float charging voltage 274
Floating
– body 469
– cover 583
– wind platform (operating principle) 469
– wind power facility
  – costs 470
  – efficiency 470
  – potential 470
Flow cells 240
Fluidized bed reactor 398
Flywheel energy storage 533, 648, 652, 695
– balancing network fluctuations 696
– bearing arrangement 541, 543
– bearing types 541, 542
– charging 543
  – losses 545
– design 538
– discharging 543
  – losses 545
– dynamic processes 545
– housing 538
– in public transportation 748
– material characteristics 540
– materials 537
– physical principles 536
– shattering characteristics 537
– stationary facility 748
Food refrigeration 621
Forecast 716
– error 683
Forest 11
Formaldehyde 392
Fossil
– energy 15, 91
  – carriers 172
  – industry 327
– fuel 14, 178
– heating supply 140
Foundation storage 578
Four-stroke principle 439
Fractional distillation 415
Free reaction enthalpy 237
Freezer compartments/chests 623
Freight traffic 169, 176
– development 169
– developments 172
Friction losses 541
Fuel
– cells 240, 426, 784
  – as discharging technologies for the transport sector 439
  – electric vehicle 776
  – hybrid bus 780
  – operating principle 426
  – technical applications 430
  – thermodynamic principles 428
  – types 426
  – vehicle 177
– costs 109
– oil-based 167
– renewable 171
– storage 28
– strategy 168
– supply development 169
Full hybrid 177
Full load hours 471


## G


Gaildorf green electricity storage plant 695
Galvani potential 232
Gas 28
– boiler 759
– cavern 405
– cylinder 502
– engine 432, 436
– generator 441
– heat pump 125, 149, 157, 435
  – efficiency 435
– heating 434
– hourly space velocity 399
– infrastructure 400, 446
– mobility 178
– network 787
– pipeline 402
– power plant 127
– purification plant 451
– quality 459, 794
– reservoirs 407
– station 174
– storage 37, 82, 150, 448
  – above ground 403
  – capacity 83
  – fill levels 84
  – technologies 411
– turbine 78, 432
  – power plant 430
Gaseous media 400, 484
Gas-fired boiler 125, 149, 649
Gasifying 462
Gasoline 397, 418
– engine 439
Gasometer 400
Gas-powered heat pump 436
Gassing voltage 255
Generation
– peaks 92
– recovery 682
– situation 105
Generator operation 544
Geothermal
– energy 104, 474, 530, 577
– ground-collector storage system 577
– power 83
– probe storage system 576
German Energy Saving Ordinance (EnEV) 760
German energy system in 2050 124
German Interruptible Loads Ordinance 632
Gibbs
– energy 237, 239
– potential 428
Gibbs-Helmholtz equation 341
Global
– irradiance 13
– solar radiation 6
– warming 17
Glucose photosynthesis 4
Goals for the heating sector 139
Goldcap 212
Graphite 282
– electrode 284
– felts 314
– redox potential 283
Gravel/water thermal storage 731
Gravitation-driven facility 727
Green hydrogen 746

Green ship 474
Greenhouse gas
– emission 17
– reduction 747
Greenwashing 373, 787
Grey electricity 28, 456, 457
– surplus 63
Grid
– corrosion 253
– electrode 246
Grid-to-vehicle 778
Gross electricity
– consumption 93
– generation 60
Gross primary production 7
Groundwater 584
Gyrobus 747

# H

Haber-Bosch process 184
Half cell 247
Hall storage 423
Hard coal 13, 388, 422, 614
– power plant 95
Head lead 246
Healthy forest 740
Heap pumped storage 525
Heat
– curve 624
– exchanger 366, 599
– load profile 157
– production 75
– pump 74–76, 142, 144
  – and heat sources 764
  – and solar arrays or photovoltaic systems 765
  – combined with ice storage and solar arrays 766
  – efficiency 436
  – expansion 143
  – in businesses 766
  – in district heating systems 766
  – in households 766
  – in industry 768
– radiation 572
– seal joint 295
– storage 27, 36, 66
  – latent potential 157
  – sensible systems 155
  – solar-thermal plant 27
  – thermochemical potential 157
– supply 761
– transfer 572, 597
  – active 597
  – passive 597
Heating
– boiler 434
– capacity 436, 624
– circulation pumps 623
– coil 735
– element 639
– energy carrier 146
– load 158
– mix 140
– modernization 158
– oil 418
– plant Sandreuth 762
– requirements development 139
– rod 765
– sector 725
  – decarbonization 142
  – goals 139
  – paradigm shift 146
  – storage potential 155
  – surpluses 151
  – transition 142
– supply
  – fossil 140
  – renewable 141
– with photovoltaics for self-consumption 768
Heavy duty machine 440, 668
Helmholtz double layer 196
Helmholtz plane 196, 203
High energy cell 299
High heating load 159
High-pressure
– compressor 486
– turbine 487, 489
High-temperature
– battery 303, 647
– electrolysis 182, 453
– storage system 585
Hot water
– buffer tank 30
– requirements 140
– storage 581, 619, 729
  – in earth basins 583
– supply 769
  – electric 618
– thermal storage 730
Hotspot 377, 380
Hot-water storage 581
Hourly storage 118
Household
– battery storage 662, 700, 705, 707
– cooling appliance 622
Hybrid
– bus 171
– capacitor 198
– car 171
– power plant Prenzlau 793
– vehicle 776
Hychico power-to-gas plant in Argentina 796
Hydration 196
Hydraulic short circuit 683
Hydro power 506, 688
– plant
  – Aswan Dam (Egypt) 694
  – basic principles 507
  – costs 509
  – Itaipú (Brazil/Paraguay) 693
  – Three Gorges Dam (China) 693
Hydrocarbon reservoir 407
Hydrocracking 745
– of waxes 398
Hydrogen 96, 442, 458, 649
– as energy source 329, 330
– bonds 420
– cavern 406
– cost efficieny 457
– distribution 746
– economy 328
– electrode 234
– energetic use 446
– extraction technologies 446
– formation (standard electrode potential) 343
– fuel cells 240
– fueling station Hafencity in Hamburg 780
– global production 333
– mobility 177
– parameters 330
– production 333, 454
– properties 330
– reconversion to electricity 796
  – large-scale 797
– renewable 745
– storage 406, 407
  – capacities 412
  – technologies 411
  – using LOHC 421
– transport 746
– use 746
  – in hydrogen mobility 746
  – in oil refineries 745
hydrogen
– pipeline 746
Hydrogenase 382
Hydrogen-rich town gas storage 406
Hydropower 15, 72, 79, 121

Hysteresis losses 222

## I

Ice storage 74, 155
Immobilized electrolyte 268
Increase in temperature 489
Individual
– space heater 616
– transport 174
Indoor air pollution 12
Induced voltage 218
Inductance 221
Induction 218
Industrial
– revolution 4
– wood 11, 737
Inert gas 361
Infrastructure 777
Inland shipping 415
Installed capacity 60
Integration of power-to-heat
– in businesses 768
– in households 768
– in industrial applications 772
– in process heat 772
Intercalation
– electrode 291
– stages 292
Intergovernmental Panel on Council Change 19
Investment 92
– costs 92, 102, 106
  – for short and long-term storage 103
Ion
– calculating forces 346
– electrode 232
– transport 346
Iron chrome redox flow cell 318
Iron-oxide rock 580
Isothermal reactor built by Linde 391

## J

Jet
– engine 441
– fuel 472
– nozzle 441
Joule cycle 430, 491

## K

Kerosene 418, 441
Kirchhoff's second law 201
Kohlrausch's square root law 349

## L

Land area 466
Land use changes 11
Large battery storage system (costs) 661
Large solar facility 730
Large thermal energy storage in solar houses 733
Large-surface electrode 246
Latent heat
– accumulator 74
– storage 157
Latent thermal energy storage 568, 588, 653
– building air-conditioning 733
– cold storage 589
– costs 607
– materials 590, 591
Law of induction 218
Layered oxides 301
Leach circuit 361
Lead-acid battery 245
– aging mechanisms 259
– basic reactions 247
– cell voltage 247
– charging 255
– design 245
– discharging characteristics 249
– equilibrium 247
– mole balance 247
– sealed 257
– side reactions 251
– storage capacity 247
Lenz's law 542
Light energy 340
Lignite electricity 456
Lignocellulosic plant 372
Linde process 501
Lined rock cavern 504
Liquefied
– petroleum gas 414
Liquid
– air energy storage 492
– electrolyte 286
– gas 414
– media 506
  – storing potential energy 510
– organic hydrogen carrier (LOHC) 421
  – advantages and disadvantages 421
  – extraction 421
  – safety 421
  – storage 421
– storage media 413
Lithium
– battery 280, 652, 700
  – application areas 293
  – cell prices 656
  – cell safety 301
  – cell voltage 283
  – charging and discharging 297
  – cost trends 656
  – costs 662
  – designs 293
  – dimensions 296
  – discharging characteristics 298
  – electrochemical stability window 286
  – electrode design 296
  – electrode material conductivity 291
  – electrolyte 286
  – energy densities 662
  – operating method 297
  – operating principle 281
  – performance characteristics 297
  – potential 656
  – self-discharge 300
  – service life 300
  – temperature characteristics 299
– bromide 437
– cobalt oxide 281
– hexafluorarsenate 288
– hexafluorphosphate 288
– ion cells 280
– ion polymer cells 286
– perchlorate 288
Load
– duration curve 90
– management 103, 108, 613, 632, 650, 758
  – as energy storage system 613
– shedding utilization in industry 632
– shifting 613, 630, 774
Local heating 761
– network 730
Long-distance
– transportation 151
– trucking 667
Long-term
– reserve 682
– storage 129, 666, 727
  – climate protection 94

– costs 96
– power-to-gas 82
– with little cycle efficiency 87
Low heating load 159
Low pressure turbine 487, 488
Lower reservoir 506, 686
Low-temperature
– battery 647
– boiler 434
– heating 148, 160

# M

Macroencapsulation 596
Magnesite 580
Magnetic
– bearing 542
– excitation 218
– field 544
– strength 218
Mainz Energy Park 795
Manganese dioxide electrode 262
Mass moment of inertia 533
– calculating 537
MATLAB 76
Mechanical energy storage 71, 484, 546, 648, 652, 679
– construction 551
– efficiency 547
– energy storage volume 547
– exposing the cylinder wall 551
– gravity power storage system 554
– hydraulic rock storage system 546
– operating principle 546
– power tower storage system 555
– pressure 549
– seal 553
– separating the base plate 552
– space requirements 550
– tunnel system 551
– water requirements 550
Meissner-Ochsenfeld effect 215, 542
Melting temperature 568, 593, 734
Membrane
– electrode assembly 355
– electrolysis 355
– expansion vessel (MEV) 152
– fuel cells 427
Metal oxide 396
Methanation 369, 447, 460, 783
– biological 370, 380, 451
– basic principles 381
– reactor concepts 385
– chemical 370, 373, 375
– $CO_2$ source requirements 376
– reactor concepts 376
– use 377
– waste heat utilization 376
Methane 83, 386, 442, 447, 457, 458, 649, 787
– as energy source 369
– combustion 452
– gas 9, 96
– generation for long-distance mobility 780
– reaction 338
– renewable 178
– storage 149
– capacities 412
Methanogenesis 380, 381
– biological reactions 382
Methanol 420, 463
– product treatment 391
– production 389
– for gasoline admixture 782
– synthesis 388, 390, 465, 783
– chemical reactions 388
– reactor concepts 391
– reactor types 391
– synthesis process 391
– use 392
Methanol-to-gasoline (MTG) 392
Methanol-to-olefin (MTO) 393
Methyl alcohol 420
Methyl tertiary butyl ether (MTBE) 392
Micro gas turbine 430
Micro hybrid 176
Microencapsulation 596
Mild hybrid 177
Mineral oil 588
Mixed cultures 387
– in bio or sewage plants 387
Mobility 439
– demand 185
– needs 169
– strategy 168
Modelling 76
Molten carbonate fuel cell 240
Molten-salt storage 587
Monovalent electric heat pump 154
Monthly storage 118
Mooring 469
Must-run
– capacity 63, 65, 682
– unit 63

# N

$Na_2S_5$ 309
Nafion 314, 316
Naphtha 336
– gasoline 418
Nation Renewable Action Plans (NREAP) 111
Natural gas 14, 33, 167, 178, 446, 459
– as energy source 370
– steam reforming 375
– storage 406, 410
Natural restocking 740
Need for hot water 70
Negative
– electrode 252
– load period 634
Nernst equation 231, 234, 255, 309, 315, 316, 342
Net primary production 7
Net Transfer Capacity (NTC) 120
Network
– congestion 112, 681
– delayed expansion 106, 110
– development
– European plan 107
– European model 125
– expansion 103, 120
– frequency 712
– balancing and reserve power 679
– load relief 681
– operation 681
– simulation 105, 112
– overloads 779
– reduced expansion 634
Nickel
– battery 262
– foam 271
– hydroxide 263, 264
– oxyhydroxide 263, 264
Nickel-cadmium battery 263
– application areas 273
– cells 264
– characteristics 272
– designs 273
– electrolyte 268
– negative electrode 267
– positive electrode 264
– standby parallel operation 274
– technologies for alkaline cells 269
– water decomposition during charging 276

Nickel-metal hydride battery 277
– applications 279
– chemical reactions 277
– negative storage electrode 277
Nickel-zinc cell 262
Night storage heating 28, 153, 616
Nuclear
– energy 15, 615
– power plant surpluses 152

# O

Ocean fuel 465, 474
Off-grid generation facility 708
Offshore wind 79, 83
– capacity 121
– energy 72, 105, 468
Ohmic
– losses 215, 344
– resistance 351
Ohm's law 350
Oil 14, 20, 33
One tank system 495
Onshore wind 79
– capacity 121
– energy 71, 105
Open-circuit voltage 236
Operating costs 45, 106
Organic Rankine cycle (ORC) 28
Ostwald's dilution law 350
Otto cycle engine 439
Overvoltage 250
Oxidation 14
Oxidization of organic substances 254
Oxyfuel
– combustion process 452
– concept 373
Oxygen electron-hole recombination cycle 257
Oxyhydrogen 329

# P

Paper manufacture 628
Parabolic trough power plant 723
Paradigm change 186
Paraffin 595
Parameter range 640
Partial
– currents 238
– oxidation 337, 390
Passenger traffic developments 171
Passive cooling 734
PCM-storage properties 590
Peak
– load power plant 128
– oil 14
Peat 9, 12
PEM electrolysis *see* Membrane electrolysis
Peripheral 25
Permanent magnet 35
Permittivity 193
Peroxosulfuric acid 255
Persistent reserve 682
Petroleum
– products 418
– tax 743
Peukert coefficient 250
Peukert's law 247
Phase-change
– material 157
  – passive cooling 734
– slurry 568
Phosphoric acid electrolyte fuel cell 240
Photon 7
Photosynthesis 4, 5, 340
– artificial 328
– core equation 6
– efficiency 6
– gross 5
– microorganisms 340
– natural 328
– net 5
– real efficiency 7
– theoretical efficiency 7
Photo-thermal energy 769
Photovoltaics 99
– as a driver for storage systems 708
– battery system 719
– electricity
  – peaks 707
Pipe
– bundle
  – heat exchanger 498
  – reactor 398
– storage 402
Piping 547
Planck constant 7
Plate
– capacitor 194
– reactor 378
Plug-in hybrid 177
– electric vehicle 776
Pocket plate cells 269
Point model 90, 121
Polarization 250, 350
Polyacrylonitrile 286
Polyethylene 289, 576
– glycol 286
Polymer electrolyte 286
Polysulfide
– anion 309
– bromide redox flow cell 318
– salt 306
Polyvinylidene fluoride 286
Pooling 701
Population development 69, 169
Porous storage 73, 403, 406
Positive electrode 253
Potassium hydroxide solution 268
Potential difference 195
Power
– battery 715
– caused generation supluses 94
– consumption
  – framework conditions 69
  – in the transport sector 71
  – industry 75
  – of industry and business, trade and services 71
  – of private households 70
  – saving potential 70
– density 208
– inverter 221
– market 55
– parameters 37
– plant
  – deployment modelling 62
  – European expansion planning 100
  – European use 100
  – portfolio's flexibility 102
  – solar-thermal 20, 100, 104
  – thermal 93
– presupposed consumption 70
– sector 58
– supply 53, 64
  – flexibility 91
  – in the future 75
  – renewable 82
  – uninterruptible 682, 696
Power-to-chemicals 668
Power-to-gas 141, 147, 157, 184, 329, 441, 666
– as an interface between energy sectors 785
– as long term storage 82
– beyond the electricity market 131
– $CO_2$ emissions 455
– costs 457
– development 788
– economic efficiency 457

– effect on the electricity generation system 111
– efficiency rates 453
– facility
  – full load hours 113
  – market-based potential 111
  – significance of location 112
– hydrogen 445, 459
  – material use 445
  – storage system 447
– in the electricity system 664
– legal framework 787
– market conditions 457
– methane 447, 459
  – absorption process 449
  – adsorption process 450
  – plant concepts 448
– opportunities 787
– patent 444
– plant
  – hydrogen 793
  – methane 797
  – with hydrogen reconversion to electricity 796
– potentials for energy storage 454
– projects 444
– reducing costs by route optimization 472
– risks 787
– studies 444
Power-to-heat 28, 143, 145, 147
– for hot water in households 770
– from a total system perspective 771, 772
– from an on-site power supply perspective 772
– potential capacity 159
Power-to-liquid 28
– costs 464
– for producing methanol 463
Power-to-X 20, 181, 649
– $CO_2$ sources 371
– cost reduction potential 656
Pressure 502, 549
– swing
  – absorption 376
  – adsorption 450
Primary
– balancing power by hydraulic short circuit 683
– battery 240
– energy 57
  – calculation 59
  – savings 759
  – supplies 19
Primordial bacteria 381
Process
– heat 71, 140, 145, 619
– temperature 492
– waste heat 362
Product gas 361
Propane 445
Proprietary electricity generation 154
Propylene carbonate 289
Protective system 680
Proton 5
– exchange membrane 355
Provision of control power 85
Pseudocapacitance 196
Pseudocapacitor 198
Pulp wood 11
Pump
– current 67
– operation 685
– turbine 517, 555, 695
Pumped power plant
– costs 509
– parameters 508
– service life 509
Pumped storage 66, 106, 121, 652, 666
– as short term storage 82
– facility 648
– for balancing supply from wind and solar energy 683
– plant 25, 26, 42, 455, 506, 617, 683
  – Atdorf 685
  – Bath County (USA) 691
  – Bleiloch 687
  – Goldisthal 685
  – Herdecke 686
  – Hohenwarte 687
  – in Germany 685
  – Malta (Austria) 691
  – Säckingen 688
  – Vianden (Luxemburg) 690
  – Wehr 688
– power 66
– system services 683
Pure
– battery electric vehicle 776
– cultures 385
– fuel 419, 744
Pyrolysis 337, 338
Pyrolytic decomposition 395

# Q

Quench
– detection 217
– protection 217

# R

Radial compressor 498
Radiation energy
– electromagnetic 5, 333
Radiator 434, 572, 582
Ragone chart 243, 640
Rail traffic 172
Ramping 703
Range extender 177
Range-extended electric vehicle 776
Rape 179
Rated capacity 660
Raw
– biogas 371
– timber 11
Reaction entropy 231
Reactor 604
Reciprocating engine 500
Recuperation 214, 776
Recuperator 366
Redispatch 56, 99, 110, 681
Redox
– electrode 232
– flow battery 314, 647
  – application areas 322
  – cell design 314
  – charging and discharging 319
  – circuit diagram 320
  – current-voltage characteristic 319
  – efficiency 320
  – electromobility 322
  – energy density 320
  – environment 323
  – power density 320
  – recycling 323
  – safety 323
  – service life 322
– potential 283
– reaction 235
Reduction of system temperatures 142
Reference hydrogen electrode 231
Refrigeration 76
Refrigerator 622
Regenerative balancing power plant 794
Regenerator 494
Region's Network Scenario 75

Regrowing wood 72
Reluctance machine 544
Renewable
– electricity 146, 171
– energy 17, 71, 96, 111, 174, 615
  – feed-in behaviour 78
  – guaranteed capacity 633
  – integration 633
– fuel 171
Repowering 73
Repurposed mining areas 525
– efficiency 525
– operating principle 525
– storage capacity 525
Reserve power 90
Residual load 55, 61, 85, 94, 103
– base load 79, 81
– determination 89
– evaluation 79
– overall load 79, 82
– time series 99
Resource
– consumption 184
Ressource
– scarcity 17, 18
Reversible solid oxide cell 358
Rock cavern 410, 418
Rolling bearing 541
Room heating 140
Rotational energy 537, 538
Route optimization 473
Run-of-river plant 83

## S

Sabatier reaction 372, 373, 462
Safety vent 294
Sail powered energy 471
– efficiency 472
– operating principle 471
– potential 472
Salt
– cavern 404, 411, 418, 488, 503
  – storage 403
– hydrate 593, 599
– rock 404
Sankey diagram 368
Schulz-Flory distribution 396
Seal 460, 545, 549
Seasonal energy storage 648, 727, 730
Secondary
– battery 240, 259
– heating 729, 730
Sector coupling 25, 28, 143
Security of supply 78
– ensured power 85
Sediment 583
Self-consumption 702
– of electricity in households 768
Self-discharge 41, 206, 259
Self-inductance 218
Self-sufficiency 701
Semiconductor 292
Semi-fuel cells 240
Sensible thermal energy storage 567, 574, 652
– costs 607
– storage material 574
Series connection 543
Shaft 528, 555
– power 534
Shale
– gas 18
– oil 18
Shipping traffic 172
Short circuit 313
– capacity 680, 712
Short-distance
– bus 535
– public transportation 747
Short-term
– high-power energy 696
– storage 66, 129
  – climate protection 94
  – costs 96
  – pump storage 82
  – thermal 727
  – with high cycle efficiency 87
Shutdown 290, 632
Silica 603
Silicon oil 588
Silver/silver oxide electrode 262
Simulation of operation over the year 88, 90
Sinter cells 269
Slide bearing 541
Sliding-pressure water storage 565, 585
Slurry 568, 600
– reactor 391, 399
SMES system
– applications 223
– efficiency 221
– losses 221
Sodium
– polysulfide 303
– sulfur accumulator 306
– sulfur battery 303, 647
  – capacities 311
  – charging and discharging 308
  – cycles 311
  – efficiency 311
  – electrodes 303
  – electrolyte/separator 304
  – energy 311
  – forms 307
  – hazards 313
  – heating system 305
  – module sizes 307
  – power 311
  – safety 313
  – service life 311
– tetrasulfide 310
– trisulfide 310
Soil 576, 584, 764
Solar
– battery 260
– circuit 727
– cooling 155
– electricity
  – maximizing self-consumption 702
  – peak shaving 703
– energy 4, 466
  – active use 727
  – passive use 726
  – storage 9, 10
  – surpluses 152
– facility
  – operating principle 727
– gas 150
– heat 733
– house 733
– tower plant 724
– updraft tower 723
Solar-thermal
– energy 770
  – bathing facilities 732
  – concentrated 338
  – swimming pools 732
– power plant 27, 721
  – operating principle 723
– storage 141, 149
Solid
– electrolyte interface 289
– oxide fuel cell 357
– polymer electrolyte 355
– storage media 422, 533
Solution mining 404
Solvation sheath 196
Sorption
– refrigeration machine 439
– storage 571
Space heating 70, 71
Spherical gas container 401
Spherical tank pumped storage 517
– application 520

– construction 520
– efficiency 518
– location 520
– storage capacity 519
Spill point 409
Splitting water 5
Sponge lead 245
Spot market 678
Stacks 354
– design 359
  – bipolar 359
  – monopolar 359
Stand-alone electricity supply 709
Stand-alone network 708
– background 708
– comparison 721
– potential 708
– technical implementation 709
State of charge 625
Steam 428, 772
– accumulator 565, 585
– electrolysis 339, 357, 784
– engine 13, 534
– generation 773
– reforming 336, 457, 463
– turbine 431
Steel production 628
Stirred tank reactor 385
Stokes' drag 287
Storage
– additional requirements 106
– annuity investment costs 96
– avoidung generation peaks 92
– capacity 39
– container 400
– costs 102
– cycle 37, 40
– demand 53, 64
  – definition 54
  – dynamic simulation to determine 61
  – effect of demand side management 64
  – for biofuels 180
  – for conventional fuels 179
  – for electric drives 180
  – for synthetic fuels 180
  – import/export 64
  – in chemical industry 183
  – in Germany 56, 89
  – in the chemical sector 167
  – in the study of the Fraunhofer ISE 181
  – in the transport sector 167, 178
  – minimum generation 63
  – operating reserve 67
  – parameters 53
– deployment at renewable energies 65
– duration 41
– economic simulation 99
– efficiency level 41
– electrochemical 647
– heater 28, 579, 616
– hourly 118
– hydrodynamic concept 410, 418
– integration
  – for coupling different energy sectors 758
  – in individual energy sectors 676
  – on the island Graciosa in the Azores 709
  – on the North Sea island of Pellworm 712
  – on the Pacific island of Tokelau 717
– isobaric volumes 502
– isochoric volumes 502
– long-term simulation 107
– losses 37, 39
– medium-term simulation 105
– minimal requirements in the European network 113
– monthly 118
– network-based requirements 110
– of biofuels 419
– of raw material 419
– power plant 507, 683, 688
  – costs 509
  – parameters 508
  – service life 509
– requirements 98
  – at the transmission network level 127
  – balancing effects 100
  – detailed study of Germany 108
  – developments 153
  – for crude oil, coal, and gas 153
  – for linking electricity and heating 153, 154
  – for solar facilities 154
  – heating supply 139
  – in a climate goal scenario 147
  – in the climate protection scenario 126
  – in the electricity sector 125
  – SRU scenarios 122
– reservoir 507, 530
– Roadmap project 98, 104, 110
  – methodological approach 98
– solar-thermal 141, 149
– temporal classification 42
– thermal 153
– unit 24
– use in the heating area 148
StoRES (storage for renewable energy sources 115
Storing technology electrolysis 352
Strength hypothesis 539
Substitution method 16
Sufficiency 172
Sulfatation 260
Sulfate crystal 256
Sulfuric acid 255
Sun 4
Supercap 35, 192, 195
– actual charging/discharging curves 205
– applications 212
– charging behavior 202
– family structure 198
– power density 208
– rapid charging processes 204
– service life 211
– structure 198
– use in wind turbines 213
Supercapacitor *see* Supercap
Superconducting magnetic energy storage (SMES) 647
Superconduction 214
Superconductor 35, 214
Supply
– balancing 676
– security 19, 90
– temperature 450
Surface mine
– pit 533
– storage 530
Surge tank 507
Surplus 81
– market-based 110
– of electrical power 53
Sweet oil 745
Switch bounce 205
Synchronized condenser operation 507
Synchronous induction machine 544
Synthesis gas 184, 333, 338, 390
– gas purification 395
– production 394

Synthetic
– fuel 150, 168, 171, 174, 175, 177, 180, 667
– from the ocean 668
– natural gas 373
– oil 588
System
– service 679
– compensation 701
– products 679
– temperature reduction 142

## T

Tafel line 250
Tank-in-tank storage system 582
Tantal disulfide 281
Telescopic gas holder 401
Temperature
– difference 567, 573, 623, 728
– sensor 590, 728
Tendon 470
Ternary electrolyte 268
TES system *see* Thermal energy storage
Thermal
– insulation 573
– power plant 93
– runaway 301
– sensor 306
Thermal energy storage 103, 153, 493, 571, 648, 652, 668, 762, 774, 775
– caverns 583
– centralized/decentralized storage 567
– for large solar facilities 730
– for solar-thermal energy 726
– forcible circulation systems 727
– high-temperature regenerator 580
– in electricity-based CHP 761
– in parabolic trough power plants 723
– in solar tower power plants 724
– in solar-thermal power plants 721
– long/short-term storage 566
– requirements
– development 151
– stationary/mobile storage 567
– technologies 567
– temperature range 565, 566
– thermal losses 566
– thermally active components 578
– using liquid-storage media 581
– using solid storage media 576
Thermochemical
– energy storage 568, 601, 735
– absorption 604
– adsorption 603
– chemically reversible processes 601, 603
– costs 608
– designs 604
– materials 602
– water splitting 338
Thermocline storage 586, 588
Thermodynamics 333
– chemical 233
– of water splitting 340
Thermophile archaea 387
Thermo-siphon facility 727
T-history method 591
Three phase reactor 379, 399
Time constant 199
Time series forecast 99
Titanium sulfide 281
Tower power plant 723
Town gas 338
Transformer 453, 469, 507, 518, 546, 716, 719
– station 748
Transition
– metal oxide 301
– scenario 123
Transmission network 105, 130
– congestion 105
Transport sector 76, 186, 439, 510, 709, 741, 776
– developments 167
– electrification 175
– energy carriers 168
– hybridization 175
– infrastructure 168
– necessary power-to-X capacities 183
– objectives 167
– paradigm change 175
– storage demand 178
Transposition process 291
TREMP process 377
Truck traffic 172, 176
Tube
– bundle reactor 378
– electrode 246
Turbine 441
Turbo jet engine 441
Two tank system 496
Two-zone MAN reactor 375

## U

UBA study 79
Undercooling 592
Underfloor pumped storage 527
– construction 527
– cost efficiency 530
– costs 530
Underground storage 402, 527
– geological and geotechnical requirements 405
– volume 503
Unloading capacity 94
Upper reservoir 506, 686
Uranium 466
Usable energy 59
Utilization rate 472

## V

Vacuum pump 450, 542, 545
Value 465, 639
van der Waals forces 196
Vanadium 322
– bromine redox flow cell 318
– cell 316
– pentoxide 317
– redox flow cell 322
Vapor
– curve 602
– partial pressure 602
– to steam electrolysis 453
VDE-ETG study 73, 86
– data input 89
– methodology 87
– modelling 89
Vegetable oil 419, 741, 743, 744
– energy balance 742
Vehicle 745
Ventilation facility 624
Virtual swarm power plant 701
Volta potential 232
Voltage
– level 680
– quality 680

## W

Warm-water storage 37, 581
– in earth basins 583
Washing machine 625
– adsorption machine using zeolite 735
– with thermochemical energy storage systems 735
Waste heat 571, 781

– boiler 758
Water
– circulation system 431
– cycle 767
– electrolysis 335, 340, 343, 352, 362
– losses 509
– splitting 5
  – thermochemical 338
  – thermodynamics 340
Water-gas shift reaction 338, 394
Waterway storage capacity 521
Wax 453
Wheatstone bridge circuit 351
Wind
– energy 72, 83, 99, 466
– gas 150
– global potential 468
– power 78, 329
– reserves 682
– speed 468, 474
– surplus 119
– turbine
  – capacitor 212
  – cluster 442
  – supercap 213
Wind-hydrogen system 118
Wood 9
– chip 424, 737
– heating supply potential 736
– pellets 738
– sustainable use 11
– used as chemical storage 736
– uses 737
Working gas volume 412

## X

Xanthophylle 6

## Z

Zeolite 438, 603, 735
– catalyst 392
– gas adsorption heat pumps 438
Zinc
– bromine cell 318
– cerium cell 319
– electrode 262
Zinc/bromine cell 322